Conference & Symposium Papers 26/P

UNEDITED PAPERS

Proceedings of an international conference
held in Monaco, 25–29 October 2004
organized by
the International Atomic Energy Agency
and co-sponsored by the
Abdus Salam International Centre for Theoretical Physics,
International Hydrological Programme of UNESCO,
Intergovernmental Oceanographic Commission of UNESCO and the
Commission Internationale pour l'Exploration Scientifique
de la Mer Méditerranée

Isotopes in Environmental Studies

Aquatic Forum 2004

IAEA
International Atomic Energy Agency

UNEDITED PAPERS

Proceedings of an international conference
held in Monaco, 25–29 October 2004
organized by
the International Atomic Energy Agency
and co-sponsored by the
Abdus Salam International Centre for Theoretical Physics,
International Hydrological Programme of UNESCO,
Intergovernmental Oceanographic Commission of UNESCO and the
Commission Internationale pour l'Exploration Scientifique
de la Mer Méditerranée

Isotopes in Environmental Studies

Aquatic Forum 2004

IAEA
International Atomic Energy Agency

The originating Section of this publication in the IAEA was:

IAEA Marine Environment Laboratory, Monaco
International Atomic Energy Agency
4, Quai Antoine 1er
MC 98000 Monaco

ISOTOPES IN ENVIRONMENTAL STUDIES
IAEA, VIENNA, 2006
IAEA-CSP-26
ISBN 92–0–111305–X
ISSN 1562–4153

© IAEA, 2006

Printed by the IAEA in Austria
February 2006

FOREWORD

A better understanding of key processes in the aquatic environment, responsible for its future development and its protection, were at the forefront of the IAEA's International Conference on Isotopes in Environmental Studies – AQUATIC FORUM 2004 convened in Monaco from 25 to 29 October 2004, which was the most important gathering of the year of isotope environmental scientists. The conference was organised by the IAEA's Marine Environment Laboratory in cooperation with the Intergovernmental Oceanographic Commission (IOC) of UNESCO, the International Hydrological Programme (IHP) of UNESCO, the Commission Internationale pour l'Exploration Scientifique de la Mer Mediterranée (CIESM), and the Abdus Salam International Centre for Theoretical Physics (ICTP). The conference was hosted by the Principality of Monaco. Over 320 experts from 60 IAEA Member States and 6 international organizations delivered 185 oral presentations in 6 plenary and 31 parallel sessions and made 130 poster presentations.

Members of the Scientific Advisory Committee of the Conference were: R.F.C. Mantoura, IAEA-MEL, Monaco; P.K. Aggarwal, IAEA, Vienna; A. Aureli, IHP, Paris; M. Boisson, CSM, Monaco; F. Briand, CIESM, Monaco; K.R. Sreenivasan, ICTP, Trieste; U. Unluata, IOC, Paris. The Scientific Secretary of the Conference was P.P. Povinec.

The conference reviewed the present state of the art isotopic methods for investigation of the aquatic environment. The main conference subjects considered were: (i) behaviour, transport and distribution of isotopes in the aquatic environment; (ii) climate change studies using isotopic records in the marine environment; (iii) groundwater dynamics, modelling and management of freshwater sources; (iv) important global projects, such as WOCE, WOMARS, SHOTS, GEOTRACES; (v) joint IAEA-UNESCO submarine groundwater investigations in the Mediterranean Sea, the Southwest Atlantic and Pacific Oceans; (vi) new trends in radioecological investigations, concentrating on the protection of marine biota against radioactive contamination; (vii) transfers in analytical technologies from bulk analyses to particle and compound specific analyses of environmental samples; (viii) development of new isotopic techniques, such as AMS and ICPMS, and their successful applications in environmental studies; and many other exciting topics which were presented and discussed during the Conference.

Four workshops were held simultaneously:

- ATOMS-Med Workshop - development of a project proposal for oceanographic investigations in the Eastern Mediterranean.
- El Niño - Research Co-ordination Meeting of the new IAEA Coordinated Research Project investigating climate change using isotopic records in the marine environment.
- CELLAR Workshop - Collaboration of European Low-Level Underground Laboratories.
- GSI Workshop on Groundwater- Seawater Interactions in coastal zones, organized in cooperation with the IAPSO Commission on Groundwater-Seawater Interactions.

These proceedings contain papers presented during the conference in oral and poster sessions. Several papers presented orally during the conference have been submitted by the authors for publication in a special issue of the Journal of Environmental Radioactivity book series, published by Elsevier. It is hoped that these publications will contribute to the research in isotopes in environmental studies, which will make the use of isotopes more widespread, and will further stimulate work in this exciting field.

The IAEA officers responsible for this publication were P.P. Povinec and J.A. Sanchez-Cabeza of the IAEA Marine Environment Laboratory.

CONTENTS

OCEANS AND SEAS

OCEANS AND SEAS - POSTERS

MEDITERRANEAN SEA

ISOTOPIC STUDIES

ISOTOPIC STUDIES – POSTERS

ISOTOPE HYDROLOGY

ISOTOPE HYDROLOGY – POSTERS

GROUNDWATER-SEAWATER INTERACTIONS

RADIOECOLOGY

RADIOECOLOGY – POSTERS

BIOMONITORS

BIOMONITORS – POSTERS

ATMOSPHERE

ATMOSPHERE – POSTERS

RADIONUCLIDE STUDIES OF SEDIMENTS

MODELLING

MASS SPECTROMETRY

QUALITY ASSURANCE

OPENING STATEMENT

S.A.S. le Prince Souverain de Monaco Albert II

Distinguished Guests,
Ladies and Gentlemen,

We are very pleased to welcome you in Monaco for Aquatic Forum 2004, the second Conference on Applications of Isotopes in Environmental Studies. We all know the importance of the protection of the marine environment for sustainable development and economy of coastal states, like Monaco. Sadly, this environment has been under continuous threats from development, tourism, urbanisation and demographic pressure. The semi-enclosed Mediterranean sea is challenged by new pollutant cocktails, problems of fresh water management, over-fishing, and now increasingly climate change impacts.

Monaco has a long history in the investigation of the marine environment. Prince Albert 1er, was one of the pioneers in oceanographic exploration, organizer of European oceanographic research and founder of several international organizations including the Musée Océanographique.

We are very proud that the International Atomic Energy Agency established in 1961 its Marine Environment Laboratory in Monaco, the only marine laboratory in the United Nations system. Their first purpose-built facilities, dedicated to marine research, launched a new era in the investigation of the marine environment using radioactive and stable isotopes as tracers for better understanding of processes in the Oceans and Seas, addressing their pollution and promoting wide international cooperation. We are pleased that the Government of the Principality of Monaco has been actively engaged in these developments and is continuously supporting activities of the Monaco Laboratory.

We are also proud that the International Hydrographic Bureau has its Headquarters in Monaco. Monaco is also hosting the Commission Internationale pour l'Exploration Scientifique de la Mer Méditerranée (CIESM), whom I have the honor to have chaired since 2001. I am very delighted to follow closely the works of the Commission funded by the 23 member states who support the work of a large scientific network of 500 institutes and over 2500 researchers, united by a commitment to promote marine science for the protection of the Mediterranean Sea and its coastal communities.

We should also mention that our Centre Scientifique de Monaco (CSM) – Observatoire Océanographique Européen, established in 1960, is well known for investigations of coral ecology and geochemistry, which are now under risk from Climate Change, and which I am sure you will discuss in detail during this conference.

I would like to extend my congratulations to all the scientists involved in the essential work of protecting the marine environment who have gathered here in Monaco. I wish you a scientifically exciting and socially enjoyable week in Monaco.

OPENING STATEMENT

Werner Burkart
Deputy Director General
Head of the Department of Nuclear Sciences and Applications
International Atomic Energy Agency, Vienna

Monseigneur,
Excellence, Monsieur le Ministre d'Etat,
Monsieur le Directeur Général CIESM,
Messieurs les Représentants des Organismes Internationaux,
Mesdames, Messieurs,

On behalf of the Director General of the International Atomic Energy Agency, and on my own behalf, I wish to extend a warm welcome to all participants in this International Conference on Isotopes in Environmental Studies – Aquatic Forum 2004. The long history of support to marine science under the patronage of the Royal Family of the Principality of Monaco makes it very fitting that this Conference should take place here.

I also wish to thank our joint organisers of the Conference, the Commission Internationale pour l'Exploration Scientifique de la Mer Mediterranee, UNESCO's Intergovernmental Oceanographic Commission and the International Hydrological Programme, and the UNESCO/IAEA Abdus Salam International Centre for Theoretical Physics.

The role of the UN system in ensuring international peace, security and socio-economic development has never been more relevant or important. As recent international events have demonstrated, the IAEA, often called the 'nuclear watchdog' of the UN system, plays a critical role in the area of nuclear non-proliferation security. But in the dawn of this new century, there are other significant dangers adding to global insecurity and instability that the Agency is also addressing. These include, among other things, energy production, food and agriculture, human health, *water resource management*, and of course, the marine and terrestrial environments.

Our marine environment and water resource programmes aim to increase the knowledge base and scientific capacity of Member States for the management of marine and freshwater resources and protection of the environment.

This is the second international conference organised by the Agency in Monaco on isotopic environmental studies, the previous one having been held in 1998 at the occasion of the opening of the new premises of the IAEA-Marine Environment Laboratory. The new Laboratory has played an even greater role in promoting the use of both radioactive and stable isotopes as powerful tools for a better understanding of processes in the marine and terrestrial environments.

It would be extremely presumptuous of me to talk about the importance of the marine environment and resources while here in Monaco. And I don't intend to do so. But I think it is worth reviewing some of the facts.

Oceans are two thirds of the surface area of the Earth. Oceans are an essential part of the history of human development. Mastery of the seas facilitated integration of civilizations across the globe – civilizations that were once kept apart by the oceans. Today, nearly half of the world's population lives within 60 km of a coastline – and it is growing by the day! Some 14 of the 15 largest mega-cities around the world are coastal.

The Monaco Laboratory has pioneered the detection and oceanographic and marine ecological tracking of radioactivity in the sea, originating from past nuclear tests, submarine accidents and

Chernobyl inputs into the ocean. More recently, the Monaco Laboratory has played a lead role in the unique application of radiotracers and isotopes to fingerprint sources of marine pollution, to track harmful algal blooms, to date deep water masses and sediments and to budget the ocean's carbon cycles and climate change.

These novel results and techniques are transferred through IAEA Training Programmes, many in collaboration with our UN partners, to Member States resulting in a global network of marine environmental competence.

Globally, coastal zones are stressed by population growth. Population pressures include increased solid waste production, polluted urban runoff, and loss of green space and wildlife habitat. Excess nutrient loadings lead to harmful algal blooms, which are a threat to human health and to the coastal resources. Isotopes and nuclear techniques offer unique advantages for diagnosing the health of the ocean and tracing the marine ecosystem.

The potential effects of climate change have great implications for human development. The Earth's freshwater resources are limited, with less than one hundredth of one percent of all water on Earth being freshwater that is accessible for human consumption. That's like one liter in ten thousand liters!!

"Greed, for the lack of a better word, is a good thing". This was Hollywood's description of the essential human values of the 1980s. When used in the context of water, however, greed is not a good thing. As Mahatma Gandhi said nearly 60 years ago, "there is enough water in the world for human need, but not enough for human greed."

While strides have been made in the last thirty years, more than a billion people still lack access to safe drinking water. Desalination in a Greenhouse World is increasingly important. I am glad to see that the Conference is addressing issues related to both the marine and terrestrial environments, because the hydrological cycle on the Earth, and thus freshwater supply, is deeply inter-twined with the climate system, which in turn is linked with the atmosphere and the ocean.

The changes in climate in recent years have led to growing concerns over the effects of climate on natural resources and sustainable development. The El Niño Southern Oscillation phenomena observed in the Pacific Ocean have had significant impacts on ecology, society and economics. The current changes in the marine environment and in climatic conditions can be understood through historical records in corals and sediments. One of the most important parameters in determining the climate on the Earth is the temperature record of the ocean. It is believed that surface seawater temperature and its coupling with atmospheric processes is the most important phenomenon in the long-term climate record. I believe that results obtained using nuclear and isotopic techniques, which will be presented during this Conference, will further help to understand past climate changes on the Earth.

The Conference will address many of these and other issues and will provide an important forum for evaluating the state of the marine and freshwater environments. An ambitious Conference Programme is before you, and I am sure that you will find it most informative, timely and valuable. The Conference, with almost 400 participants coming from 78 Member States and 7 international organizations, I am sure, will lead to a clear vision for further investigations and fruitful international collaborations. I would look forward to the outcome of your deliberations.

I wish you a successful and enjoyable Conference, and a pleasant stay in Monaco and the Cote d'Azur.

OPENING STATEMENT

R.F.C. Mantoura
Director
International Atomic Energy Agency
Marine Environment Laboratory, Monaco

Monseigneur,
Excellence, Monsieur le Ministre d'Etat,
Monsieur le Directeur Général du CIESM,
Distinguished Guests,
Dear Colleagues,
Ladies and Gentlemen,

Welcome to Monaco and to the International Conference on Isotopes in Environmental Studies – Aquatic Forum 2004. We are very pleased that almost 400 participants from 78 countries and 7 international organizations gathered in Monaco at the second conference in this series to discuss recent trends in isotopic environmental studies.

The International Atomic Energy Agency's Marine Environment Laboratory in Monaco has been engaged for over 40 years in investigations of radionuclides in the marine environment. The establishment of the Marine Laboratory in Monaco was triggered in the late fifties by necessity to investigate the impact of atmospheric nuclear weapons testing on the marine environment. The Laboratory started its operation in 1961 in the famous Monaco Oceanographic Museum as IAEA's International Laboratory of Marine Radioactivity. In 1988 the Laboratory moved to larger, but still temporary premises in the Monaco Football Stadium and incorporated in its mission non-radioactive contamination of the marine environment, a fact which was also reflected in 1991 when the Laboratory changed its name to the Marine Environment Laboratory. In 1998 the Laboratory moved to the present permanent premises dedicated to marine research at Quai Antoine 1er along the Port Hercule.

Our Laboratory is highly appreciative for over forty years of support provided by the Government of the Principality of Monaco, and of their growing interest in contamination studies and preserving the marine environment for future generations, a trend which is also demonstrated by the generous support the Government has provided for the organisation of this Conference.

From its beginning the Laboratory has been engaged in studying marine processes using radionuclides as tracers. Actually this line of research started almost simultaneously with the operation of the Laboratory, as the first pioneering work on application of ^{226}Ra as an oceanographic tracer was published by Koczy in 1958 in the Proceedings of the Geneva Conference on Peaceful Uses of Atomic Energy. Of course, early investigations were greatly limited by the techniques available for sampling and analysis of radionuclides in the marine environment. For example, water sampling has evolved from the simple reversing Nansen bottle to the present robotic systems based on ROVs (Remotely Operating Vehicles) and AUVs (Autonomous Underwater Vehicles), and other sophisticated sampling technologies, which use satellite views of sea areas for the optimisation of sampling. Analytical investigations started with the development of simple radiochemical methods and Geiger gas counters, but at present they have entered into an age of robotic radiochemical technologies, sophisticated detectors working on line with powerful computers, often operating underground to improve sensitivity, and in specific applications such as underwater radionuclide monitoring, operating continuously with satellite data transmission. Furthermore the philosophy of radionuclide analysis has dramatically changed from the concept of counting decays to the concept of counting atoms using highly sensitive mass spectrometers working with low energy ions (e.g. Thermal Ionisation Mass Spectrometry – TIMS, Inductively Coupled Plasma Mass Spectrometry – ICPMS, Resonance

Ionisation Mass Spectrometry (RIMS), or accelerated ions to levels of tens or hundreds of MeV in Accelerator Mass Spectrometry (AMS) systems. In other aquatic applications, simplistic laboratory radiotracer experiments with organisms and sediments carried out in small, static aquaria have evolved into larger, mesocosm studies where the many aquatic variables can be controlled in order to better simulate the natural environment and generate more realistic results.

This evolution from simple analytical and experimental techniques to the present sophisticated state-of-the-art technologies has been accompanied by a considerable change in the philosophy of oceanic research as well. We have moved from single institutional investigations carried out until the seventies, to global international oceanic projects, represented first by the GEOSECS programme, and later by the WOCE, the JGOFS and other programmes, including new projects currently under preparation such as the GEOTRACES. I am pleased to mention that the Monaco Laboratory has also carried out, in collaboration with over 30 laboratories, a large scale programme called WOMARS – Worldwide Marine Radioactivity Studies, results of which have recently appeared in a special issue of Deep Sea Research II. And in collaboration with several Japanese institutes we have just launched a new project – Southern Hemisphere Ocean Study (SHOTS) which should contribute to better understanding of circulation processes in the Southern Ocean that play a dominant role in the Earth's climate.

Both radioactive and stable isotopes have been used as powerful tools for a better understanding of processes in the aquatic and terrestrial environments. However, from the hundreds of isotopes available in nature, only relatively few have been applied in environmental studies because of several reasons, for example availability of sensitive analytical techniques or lack of appropriate physical half-lives radiotracers, but more often it is simply due to a lack of new ideas for their utilisation. Therefore, there is a lot of work in front of us to undertake in order to realise new ideas in isotopic aquatic research for better understanding and protecting our environment.

This Conference is addressing issues related to both the marine and terrestrial environments, underscoring the global character of our science that requires regional and international cooperation. The Conference will therefore provide inputs to Inter-Agency sponsored regional and global environmental programmes which will improve our collaboration in future. In this respect I am sure that during the Conference you will have ample opportunity to interact with leading experts in the field and to discuss future trends in environmental isotopic studies.

Along these lines several specialised workshops will be organised during the Conference, namely the:

- ATOMS-Med (Atomic Techniques for Observing Marine Systems) workshop – which will review the present understanding of the Eastern Mediterranean Basin and will prepare a proposal for a new joint project;
- Research Coordination Meeting of the Coordinated Research Project "Nuclear and Isotopic Studies of the El Niño Phenomenon in the Ocean" carried out by the Monaco Laboratory in collaboration with twelve institutes from Australia, France, Indonesia, Israel, Jordan, Monaco, New Zealand, Peru and USA;
- Workshop on groundwater-seawater interaction studies in coastal zones, including presentation of joint results from sampling missions in Sicily and Brazil, obtained in the framework of the Coordinated Research Project "Nuclear and Isotopic Techniques for the Characterization of Submarine Groundwater Discharge in Coastal Zones" carried out jointly by the Monaco Laboratory and the IAEA's Isotope Hydrology Section, and in cooperation with UNESCO's Intergovernmental Oceanographic Commission and the International Hydrological Programme, as well as ten laboratories in Brazil, France, India, Italy, Japan, Slovenia, Russian Federation, Turkey and USA;
- Workshop on underground laboratories organised jointly with the Collaboration of European Low-level Underground Laboratories (CELLAR).

The Conference also documents the active collaboration of several UN and regional agencies in the aquatic environmental studies, in that it is organised jointly by the IAEA, the Commission Internationale pour l'Exploration Scientifique de la Mer Mediterranee (CIESM), UNESCO's Intergovernmental Oceanographic Commission and International Hydrological Programme, and the UNESCO/IAEA Abdus Salam International Centre for Theoretical Physics. This joint collaboration confirms that coordinated international efforts are necessary for studying environmental changes, climate variability and contamination of the aquatic environment which occur on global or regional scales and having impacts over similar scales. I am pleased that this Conference is co-sponsored by these organisations and further cooperation of these agencies will undoubtedly help to widen the impact of our activities and to involve more scientists working in joint, multi-institutional projects.

Finally, I wish you all a scientifically-interesting and rewarding Conference, and a very pleasant stay in Monaco.

CLIMATE CHANGE

Interannual to decadal climate variability in the Pacific and Indian Oceans revealed by isotopic studies of corals

Dunbar, R., D. Fleitmann, D. Mucciarone

Geological and Environmental Sciences,
Stanford University, Stanford CA,
United States of America

Instrumental records of past variability in climatically important regions of the tropical Indian and Pacific Oceans are relatively scarce and short. Multi-century reconstructions of past climate change in these areas are now being made available through the isotopic and chemical analysis of coral skeletons collected from both the surface ocean and deep sea. Here we present a brief synthesis of multi-century trends in ocean climate as revealed by coral archives. In general, these records are consistent with century-scale trends towards a warmer tropical ocean with greater near-equatorial rainfall and greater ENSO variability in more recent decades. Very limited deep sea coral data reveal larger than expected variability in thermocline conditions during the past several centuries. Sufficient data is now available to allow comparisons of Pacific ENSO variability with records of the Monsoon from the Pacific Basin over timescales extending back at least 150 years. The last half of this talk is used to describe a new synthesis derived from East Africa coral records.

We present a monthly resolution stable isotopic record acquired from several large living coral heads (Porites) from the Malindi and Watamu Marine Reserves, Kenya (3°S, 40°E). The annual chronology is precise and is based on exceptionally clear high and low density growth band couplets. The record extends from 1696 to 1996 A.D., making it the longest coral climate record from the Indian Ocean and one of the longest available worldwide. We have analyzed the uppermost portion of 8 separate coral cores. This upper section, used for calibration purposes, provides estimates of signal fidelity and noise in the climate recording system internal to the colony. Coral $\delta^{18}O$ at this site primarily records SST; regression of monthly coral $\delta^{18}O$ vs. SST yields a slope of -0.26‰ $\delta^{18}O$ per °C, and $\delta^{18}O$ explains well over 50% of the variance in SST. Additional isotopic variability may result from changes in seawater $\delta^{18}O$ due to local runoff or regional evaporation/precipitation balance, but these changes are likely to be small because local rainfall $\delta^{18}O$ is not strongly depleted relative to seawater and salinity gradients are small. The coral record indicates a clear warming trend of about 1.5°C that accelerates in the latest 20th century, superimposed on strong decadal variability that persists throughout the record. In fact, $\delta^{18}O$ values in the 1990s exceed the 300 year envelope (they are lower) and correspond with apparently unprecedented coral bleaching in coastal East Africa. The decadal component of the Malindi coral record reflects a regional climate signal spanning much of the western equatorial Indian Ocean. In general, East African SST and rainfall are better correlated with Pacific ENSO indicators than with the Indian Monsoon at all periods (inter-annual through multi-decadal) but the correlation weakens after 1975. One dramatic new result we report here is a strong indication of a major cool and dry period from 1750-1820 A.D. This is the single largest multi-decadal anomaly of the past 300 years and correlates perfectly in time with the historically and anecdotally defined Lapanarat Drought. Our results indicate a strong link between multi-decadal tropical cold SST anomalies and far-reaching continental droughts in East Africa.

Interannual-decadal SST variations are strongly coherent with ENSO indices and other ENSO-sensitive coral records on decadal and interannual time scales. The decadal component of the Malindi coral record reflects a regional climate signal spanning much of the western equatorial Indian Ocean. Previous work has argued that this component likely reflects a monsoonal influence. However,

decadal variance in both Malindi and Seychelles coral records is more strongly coherent with ENSO indices than with the India or East Africa rain indices. The coherency of both coral records with Pacific indicators suggests instead that Indian Ocean variability reflects decadal ENSO-like variability originating in the Pacific. These records don't correlate significantly with the Pacific Decadal Oscillation implying a dominant role for the tropical Pacific (as opposed to extra-tropical regions) as a source of regional decadal variability in the western Indian Ocean. This work confirms that the tropical Pacific can act as an agent forcing decadal climate variability over a very large spatial scale on Earth. We conclude by examining the time-varying relationship between ENSO and the monsoons using available coral records from the Pacific and Indian basins.

Use of coral skeleton as environmental archives: the biological basis

Allemand, D., C. Ferrier-Pagès, P. Furla, S. Puverel, S. Reynaud, É. Tambutté, S. Tambutté, D. Zoccola

Centre Scientifique de Monaco,
Monaco

"There has never been any doubt that corals write valuable information into their skeletons it is their language that has remained blurry and ambiguous" [1].

Paleoceanographers derive information about past environmental conditions from stable isotopes and other tracer records held with geological structures. The skeletons of hermatypic corals are particularly useful for high-resolution studies of tropical paleoceanic environments as they provide an unaltered record of the chemical and physical conditions that existed in the seawater when they were formed. However, these structures do not result from pure chemical $CaCO_3$ precipitation but from highly-regulated biological activities of living organisms. Indeed, trace elements and isotopes were shown to vary widely between and within species [2] or to correlate well with coral growth or extension rates [3]. It was therefore suggested that environmental factors are not completely controlling isotope and trace element signatures in coral skeletons but that biological factors were also important [4]. Furthermore, most of reef-building corals harbor photosynthetic symbionts which stimulate by an unknown mechanism coral calcification, a process called light-enhanced calcification. Consequently, one must consider the effects of these biological activities on the distribution and fractionation of tracers to make correct inferences on climate at the time of skeleton formation. It is, therefore, necessary to understand the physiological mechanisms which control both biomineral formation and carbon supply to the photosynthetic symbiont, called “vital effects”. This paper will present an up-to-date review of the biological control of the biomineralization process in corals which will allow an optimization for the use of coral skeletons as environmental archives.

By using the branched scleractinian coral, *Stylophora pistillata* as a model organism, we have shown that coral skeleton formation results from two biological processes: regulation of the ion concentrations at the site of biomineralization and secretion of macromolecules, called organic matrix, regulating crystallization. Both processes are very rapid and need carrier proteins and various enzymes mainly located within a thin cell layer surrounding the skeleton, called the calicoblastic epithelium. Two major enzymes achieving transepithelial calcium transport have already been characterized as well as some aspects of the sources for carbon supply. Organo-mineral interactions and role of organic matrix will be also presented.

REFERENCES

[1] BARNES, D.J., LOUGH, J.M., Coral skeletons: storage and recovery of environmental information, Global Change Biology **2** (1996) 569-582.

[2] ROSENTHAL, Y., BOYLE, E.A., SLOWERY, N., Temperature control on the incorporation of magnesium, strontium, fluorine and cadmium into benthic foraminiferal shells from Little Bahama Bank: prospects for thermocline paleoceanography, Geochim. Cosmochim. Acta **61** (1997) 3633-3643.

[3] DE VILLIER, S., NELSON, B.K., CHIVAS, A.R., Biological controls on coral Sr/Ca and $\partial^{18}O$ reconstructions of sea surface temperatures, Science **269** (1995) 1247-1249.

[4] COHEN, A.L., LAYNE, G.D., HART, S.R., LOBEL, P.S., Kinetic control of skeletal Sr/Ca in a symbiotic coral: implications for the paleotemperature proxy, Paleoceanogr. **16** 1 (2001) 20-26.

Radiocarbon in corals: a tracer of past changes in the carbon cycle and climate

Druffel, E.R.M.

University of California,
Irvine, California,
United States of America

Radiocarbon in annual and monthly bands of coralline aragonite reflects the $^{14}C/^{12}C$ ratio of the dissolved inorganic carbon (DIC) in surface ocean water that surrounds the coral. The growth rates of massive corals vary from 0.4 to 2.5 cm/yr, and many species grow to several meters in diameter. Therefore, time histories of radiocarbon can be reconstructed for periods of several centuries from corals that grew in tropical and subtropical locations (30N to 30S). Radiocarbon in the surface ocean is controlled mainly by physical processes such as upwelling and lateral transport, which are in turn controlled by climatic variables such as wind speed. Thus, past records of climate are obtained from high precision radiocarbon measurements of banded corals. Radiocarbon time histories for the Pacific and Atlantic Oceans reveal interannual, decadal and centennial variability of past climate.

The exchange rate of CO_2 between the atmosphere and surface ocean (90 Gt C/yr) is large compared to the net transport of anthropogenic CO_2 into the ocean (~2 Gt C/yr [1]). About one-third of this net CO_2 emission is centered in the mid- and eastern tropical Pacific due to enhanced upwelling of subsurface waters that contain high pCO_2 values. Thus, variability of the upwelling rate in this region of the world ocean could significantly change the net transport of anthropogenic CO_2 into the ocean.

Changes observed in surface ocean radiocarbon during the past few centuries will be evaluated in term of their implications for past changes in the carbon cycle.

REFERENCES

[1] SABINE, C., ET AL., The oceanic sink for anthropogenic CO_2, Science **305** (2004) 367-371.

Holocene climate variability along the Antarctic Peninsula and linkage with a terrestrial paleoclimate record from South America

Dunbar, R.[a], A. Ravelo[b], A. Leventer[c], E. Domack[d]

[a] Geological and Environmental Sciences,
Stanford University,
Stanford, California,
United States of America

[b] Marine Science Program University of California,
Santa Cruz, California,
United States of America

[c] Geology Department,
Colgate University,
Hamilton, New York,
United States of America

[d] Geology Department,
Hamilton College,
Clinton, New York,
United States of America

The Antarctic Peninsula is highly sensitive to climate change and is currently experiencing rapid and unusual warming. Here we examine Holocene variability as seen in a multi-tracer stable isotopic study using a 50 m sedimentary section spanning the past 12,000 years from the wqest coast of the Antarctic Peninsula. In our synthesis, we make use of the Palmer Deep ODP site 1098 drill core. These sediments comprise the first high resolution, continuous, Late Pleistocene through Holocene sediment record from the Antarctic continental margin. We analyzed biogenic opal, organic C and N concentrations, and $^{13}C/^{12}C$ and $^{15}N/^{14}N$ isotopic ratios of sedimentary organic matter every 2.5 cm downcore (1600 samples, sample interval of about 7 years). We interpret the main changes in these downcore parameters as indicating substantial variability in productivity. We note that 1) that the lowest productivity of the Holocene occurred during the past 1.5 kyrs BP, 2) Holocene variability in productivity is large, about a factor of 3, 3) A mid-Holocene productivity maximum is coeval with many mid- and low-latitude Holocene paleoclimate records, and 4) evidence is strong for solar forcing via both total irradiance and precessional effects. Given the modern link between sea ice and net annual primary production along the Antarctic margin, it seems likely that episodes of enhanced productivity, both during the middle Holocene and during centennial productivity peaks were associated with reduced ice cover. We explore several mechanisms by which sea ice cover might respond in an fashion consistent with our observations: 1) reduced westerly winds (less evaporative cooling), 2) South Pacific gyre spin-up (less pole-equator T contrast), 3) more local warm deep water upwelling. It is possible that the basic ENSO dynamic we know from studies of interannual variability in the tropical and North Pacific also regulates climate change at decadal to millennial timescales in the South Pacific. In this regard, we note that the strongest Southern Oscillation atmospheric pressure anomaly in the Southern Ocean is in the Bellingshausen/Amundsen seas, upwind from our Antarctic Peninsula study site. We see temporal coherence between a rapid mid-Holocene excursion at site 1098 and a similarly rapid 85 m lowering of the level of Lake Titicaca, at 14°S in the South American Altiplano, again suggestive of a Pacific Ocean control. Comparison with other Antarctic margin

paleoclimate records from East Antarctica and the Ross Sea as well as with terrestrial records from Australia and New Zealand generally shows heterogeneity across longitudes and coherence across latitudes. However, convincing conclusions along these lines are still difficult because of problems in comparing chronologies at sub-millennial timescales between marine records, ice cores, and terrestrial records.

High-resolution bomb pulse radiocarbon records from corals, spanning the Central and Southeastern Pacific Ocean

Warren Beck, J.[a], T. Correge[b], G. Burr[a]

[a] NSF-Arizona AMS Facility,
University of Arizona,
Tucson, Arizona,
United States of America

[b] Institut de Recherche pour le Developpement, (IRD ex ORSTOM),
Nouméa,
New Caledonia

Pacific ocean radiocarbon levels have significantly increased during the last half century as a result of atmospheric nuclear testing, mainly in the 1950s and 1960s. Ambient oceanic radiocarbon levels are recorded in corals living in the surface mixed layer. Several high resolution coral radiocarbon records are presented from the central and eastern south Pacific Ocean, spanning Christmas Island (2°N, 157°W), the Marquesas (8°S, 140°W), and Easter Island (27°S, 109°W). These three records span the bomb-pulse period, at a typical resolution of approximately 3-6 samples per year.

The Record from Christmas Island shows large inter-annual variability whose variations strongly correlate with ENSO. This correlation is due in part to horizontal advection of surface waters in the equatorial Pacific, but is also controlled by variable vertical fluxes of radiocarbon depleted waters entering the mixed layer from the thermocline. Thus, this radiocarbon record may be used as a proxy for ENSO timing and intensity. The Marquisas record shows less interannual variability, though this record is at lower resolution. The Easter Island record shows the least amount of interannual variability. The total amplitude of the bomb pulse is largest at Easter Island (~225 ‰), intermediate at Christmas Island (~175‰), and lowest at the Marquesas (~155‰). As expected, Pre-bomb pulse radiocarbon levels were lowest near the equator (Christmas at ~-65‰) due to the influence of radiocarbon–depleted waters upwelled from the thermocline, and highest at Easter Island (~-43‰), which is close to the center of surface convergence in the southern hemisphere sub-tropical gyre. Radiocarbon levels reached nearly +200‰ at the peak of the bomb pulse at Easter Island, but only achieved levels of ~90‰ at the Marquesas, and ~110‰ at Christmas Island.

Glacial climate transitions in the Southern Hemisphere - new insights from cosmogenic ^{10}Be in rocks and ^{14}C in tree-rings

Fink, D.

ANSTO Environment,
Menai, NSW,
Australia

The study of global climate change recorded and archived in corals, tree-rings, glacial deposits, ocean sediments and ice cores reveals a complex scale of variations ranging from major glacial cycles (100,000 years), millennial (1,000 years) timescales and even decadal changes (ie ENSO). 'Global patterns' of climate cycles are inferred principally from Northern Hemisphere records and modelling approaches. For the major glacial-interglacial cycles this seems to be reliable – however data is now emerging that on the millennial scale of climate change particularly over the Last Glacial-Interglacial Transition (20,000 to 10,000 years ago) and through the Holocene, things are not so simple, let alone 'global'. Critical questions are now being asked as to the synchronicity, intensity and mode of abrupt climate patterns across Earth's hemispheres. However, with a paucity of Southern Hemisphere studies, answers are not readily available.

Long-lived cosmogenic radioisotopes, such as ^{10}Be, ^{14}C, ^{26}Al and ^{36}Cl, are produced by cosmic ray bombardment of Earth's atmosphere and lithosphere. The measurement by Accelerator Mass Spectrometry of concentration profiles of these radioactive 'clocks' and 'tracers' in climate archives is emerging as key parameters to provide the essential chronological frameworks and rates of climate processes to address these vexing questions.

This talk will present 2 examples of cosmogenic isotopes in the study of Southern Hemisphere climate change records. The first relates to application of in-situ produced ^{10}Be and ^{26}Al in glacially transported surface rocks to determine the chronology of glacial cycles in Tasmania and New Zealand during the last deglaciation. The Younger Dryas (YD) is a major short term and intense climatic reversal towards colder temperatures occurring between 11,500-12,800 cal year BP superimposed on the last deglaciation. Its presence has now been identified in most, if not all, of the northern hemisphere archives of late Quaternary climate change. Recently, investigations have centered on searching for a cooling reversal coeval with the YD chronozone in Southern Hemisphere archives. The implications of such an appraisal are significant as a positive outcome directly supports the presence of a global triggering mechanism coupled with climate change synchronicity across the equator.

The second deals with a detailed comparison in the variations of atmospheric radiocarbon recorded in tropical tree rings from Thailand to that in mid-latitude Huon Pine tree-rings from Tasmania during the Little Ice Age (LIA) from ~1600-1800 AD. Such a study allows a better understanding of the mechanisms that control regional ^{14}C atmospheric concentration offsets in terms of atmospheric mixing and the role of the Asian monsoon during periods of known Northern Hemisphere climate cooling such as occurred in the LIA.

Century-to-decade scale modulation of ENSO Recorded by postglacial laminated sediments from the Peru continental margin

Skilbeck, G.[a], M. Gagan[b], I. Goodwin[c], M. Watson[a], D. Fink[d]

[a] Department of Environmental Sciences,
University of Technology, Sydney,
Broadway, Sydney NSW,
Australia

[b] Research School of Earth Sciences,
Australian National University,
Canberra ACT,
Australia

[c] School of Environmental and Life Sciences,
University of Newcastle,
Callaghan NSW,
Australia

ANSTO-Environment,
Menai NSW,
Australia

Cores collected from three sites on the continental margin of Peru during ODP Leg 201 recovered >5 m of LGM-recent sediment. At Site 1227 Holocene sediments are absent, but a well preserved early last glacial-interglacial transition (LGIT) section spanning ~17,200-15,900 cal yrBP is present. The sediments are predominantly diatomaceous oozes with subtle dark and light laminations which may be annual in origin. The chronology of drill-core at this site is well-constrained by five bulk sediment ^{14}C dates that define a linear sedimentation rate of ~270 cm/ka [1].

In contrast, Holocene sediments are well-represented at Sites 1228 and 1229. Sedimentation rates over this period suggest the Holocene can be subdivided into two regimes. The older period spans the early and middle Holocene (~10,000 yrBP to ~2,800 yrBP) during which time the sedimentation rate was relatively slow at 4-6 cm/ka. However, we cannot exclude the possibility of unconformities in this part of the stratigraphic section, and this rate should therefore be considered a minimum. From ~2,800 yrBP to the present day, the chronology at both sites is well defined by multiple ^{14}C ages that allow us to confidently define linear sedimentation rates of 70-100 cm/ka [1]. At both sites, the late Holocene appears to be stratigraphically complete.

In order to investigate an El Nino origin for the laminae on this part of the Peru shelf, we have undertaken two independent lines of study. First, high-resolution (0.1 mm per pixel) scanned colour images were analysed for all of the cores. For the early LGIT and the late Holocene, the chronological model indicates that sub-annual layers can be resolved, where present. Accordingly, we have used the red colour intensity band from the scanned images to carry out time series analysis of ENSO-band (2-8 year) variability. Analysis of Hole 1228B shows two cyclicity peaks in the ENSO band over the past 10 ka. One of these, at a peak period of 5.3 yr, dominates over the last 3 ka, with the overall Holocene pattern very similar to that shown by Rodbell et al. [2], Moy et al. [3], and Riedinger et al. [4]. In contrast, spectral analysis of ENSO band data from Hole 1227B, shows a strong decadal variance peaking at 16.5 and 22.5 yr and only weak variance in the ENSO band (4.7 yr). In addition, there is a

well-developed oscillation in the variance of these data with cyclicity of about 110 yr which we believe is similar to that proposed by [5].

We have sought to test that the laminations do indeed contain a climate signal by undertaking several geochemical and mineralogical studies. The sediments are dominantly diatomaceous oozes, but contain other minor components, including terrigenous sediment and organic matter. We analysed $\delta^{13}C$ of bulk organic matter, $\delta^{18}O$ of planktonic foraminifer tests, organic carbon content, carbonate content, and terrigenous sediment (quartz/feldspar) percentages of representative dark and light laminae in upper part of Hole 1227B. Our hypothesis is that El Nino events will produce warmer and wetter conditions (lower foraminiferal $\delta^{18}O$) and increased terrestrial sediment input (increased quartz and feldspar and lower $\delta^{13}C$ of organic matter). At the same time, the bulk organic carbon and carbonate data will reflect a decline in water-column productivity driven by the suppression of upwelled nutrients during El Niño events. Taken together, our preliminary analyses indicate that the dark laminae represent periods of warmer sea surface temperatures and increased terrestrial runoff associated with El Nino events.

Independent time series and geochemical analysis of LGM-Holocene sediments from the Peru continental margin indicate the presence of an El Nino/La Nina climate signal preserved in alternating dark and light laminae. Time-series analysis of long (>1000 yr), stratigraphically continuous sequences from the late Holocene and the early LGIT reveal decadal (~15-20 yr) and century (~110 yr) scale modulation of ENSO climate variability.

We would like to thank Dennis Mather and the staff at The Australian Institute of Nuclear Science and Engineering (AINSE) for grants supporting radiocarbon dating in this project (Nos 02/169 & 04/139), and the Australian ODP Office for their assistance in providing funds for collection and analysis of material.

REFERENCES

[1] SKILBECK, C.G., FINK, D., "Radiocarbon dating and sedimentation rates for Holocene-Late Pleistocene sediments, eastern equatorial Pacific and Peru continental margin", Controls on microbial communities in deeply buried sediments, eastern equatorial Pacific and Peru margin (D'HONDT, S.L., JØRGENSEN, B.B., MILLER, D.J., et al. Eds), Proc. ODP, Scientific Results [CD-ROM] 201: College Station TX (Ocean Drilling Program) (submitted).

[2] RODBELL, D.T., SELTZER, G.O., ANDERSON, D.M., ABBOTT, M.B., ENFIELD, D.B., NEWMAN, J.H., An ~15,000-year record of El Niño-driven alluviation in southwestern Ecuador, Science **283** (1999) 516-520.

[3] MOY, C.M., SELTZER, G.O., RODBELL, D.T., ANDERSON, D.M., Variability of El Niño/Southern Oscillation activity at millennial timescales during the Holocene epoch, Nature **420** (2002) 162-165.

[4] RIEDINGER, M.A., STEINITZ-KANNAN, M., LAST, W.M., BRENNER, M., A ~6100 14C yr record of El Niño activity from the Galapagos Islands, J. Paleolimnology **27** (2002) 1-7.

[5] TUDHOPE, A.W., CHILCOTT, C.P., MCCULLOCH, M.T., COOK, E.R., CHAPPELL, J., ELLAM, R.M., LEA, D.W., LOUGH, J.M., SHIMMIELD, G.B., Variability in the El Nino-Southern Oscillation through a glacial interglacial cycle, Science **291** 5508 (2001) 1511-1517.

Invasion of anthropogenic CO_2 recorded in stable isotopes of planktonic foraminifera from the northern Gulf of Aqaba, Red Sea

Al-Rousan, S.[a], J. Pätzold[b], S. Al-Moghrabi[a,c], G. Wefer[b]

[a] Marine Science Station,
Aqaba,
Jordan

[b] Fachbereich Geowissenschaften,
Universität Bremen,
Bremen,
Germany

[c] Aqaba Special Economic Zone Authority,
Aqaba,
Jordan

The stable carbon isotopic composition of the planktonic foraminifera *Globigerinoides sacculifer* and *Globigerinoides rubber* (white) and sedimentary organic matter from the northern Gulf of Aqaba have been investigated to estimate changes in del $^{13}C_{DIC}$ in surface waters during the last 1000 years. The high sedimentation rates at the core sites (about 50 cm/k.y.) provide high temporal resolution (10 years). Recent sediments at the top of the cores reflect conditions younger than 1950s.

The del^{13}C records of the planktonic foraminifera from three multicores display similar trends, showing a uniform and consistent pattern before the 1750s, and a gradual decrease of approximately 0.63‰ over the last two centuries (Fig. 1). This decrease seems to track the decrease of del$^{13}C_{DIC}$ in surface waters, which is mainly caused by the increase of anthropogenic input of ^{13}C-depleted CO_2 into the atmosphere [1].

Similarly, a trend toward lighter values of the carbon isotopic composition of sedimentary organic matter (del$\delta^{13}C_{org}$) during the last 200 years supports the interpretation obtained from the planktonic foraminiferal del^{13}C. Furthermore, direct measurements of seawater show that δ^{13}C of the dissolved inorganic carbon (DIC) in the northern Gulf of Aqaba has decreased by about 0.44‰ during the period 1979-2000. The average annual decrease is 0.021‰, which is similar to that recorded globally [2, 3].

The δ^{13}C values of planktonic foraminifera combined with organic matter δ^{13}C from marine sediments are good indicators for reconstructing past changes in atmospheric CO_2 concentrations from the northern Gulf of Aqaba.

REFERENCES

[1] BEVERIDGE, N.A.S., SHACKLETON, N.J., Carbon isotopes in recent foraminifera: A record of anthropogenic CO_2 invasion of the surface ocean, Earth Planet. Sci. Lett. **126** (1994) 259-273.

[2] QUAY, P.D., TILBROOK, B., WONG, C.S., Oceanic uptake of fossil fuel CO_2: Carbon-13 evidence, Science **256** (1992) 74-79.

[3] SONNERUP, R.E., QUAY, P.D., McNICHOL, A.P., The Indian Ocean ^{13}C Suess effect, Global Biogeochem. Cycles **14** (2000) 903-916.

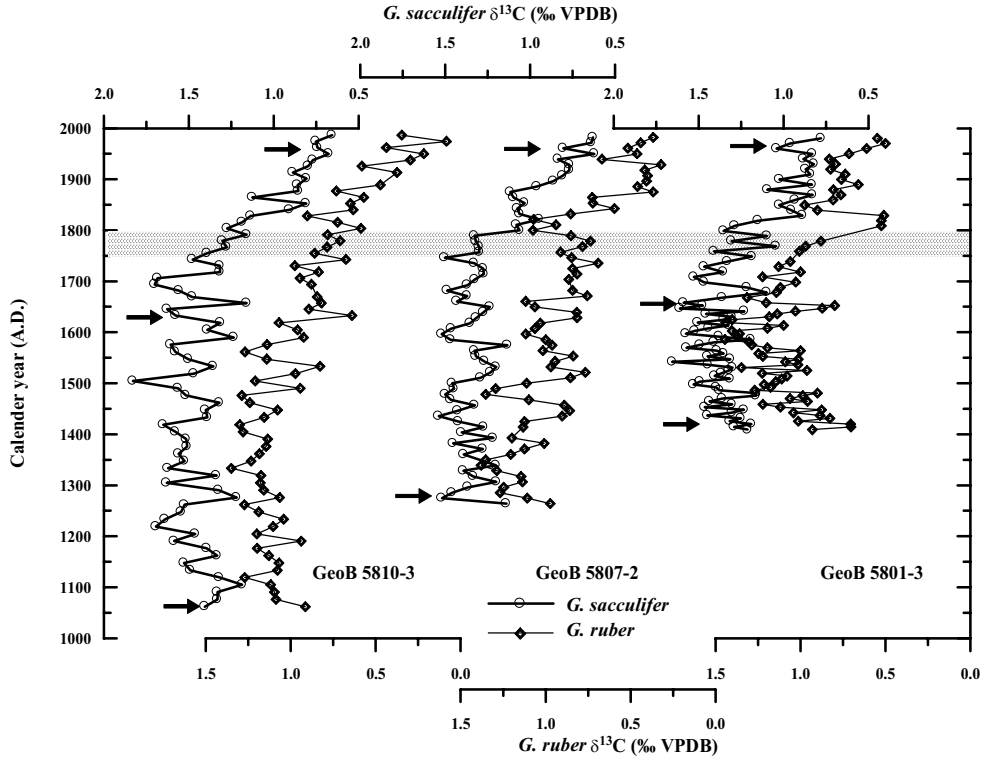

FIG. 1. Stable carbon isotope composition (del^{13}C) of the planktonic foraminifera G. sacculifer and G. ruber, over the last 1000 years from three multicores (GeoB 5810-3, GeoB 5807-2 and GeoB 58013) collected in the northern Gulf of Aqaba, Red Sea. The arrows represent the calibrated ^{14}C radiocarbon age positions. The grey bar indicates the transition zone between the pre-industrial and industrial periods.

Effect of pCO_2 and temperature on the boron isotopic composition of the zooxanthellate coral *Acropora sp.*

Reynaud, S.[a], N. Hemming[b], A. Juillet-Lecrlerc[c], P. Gattuso[d]

[a] Centre Scientifique de Monaco,
Av. Saint Martin,
Monaco

[b] Queens College,
School of Earth and Environmental Sciences,
Flushing, New York,
United States of America

[c] Laboratoire des Sciences du Climat et de l'Environnement,
Laboratoire mixte CNRS-CEA,
Gif-sur-Yvette,
France

[d] Laboratoire d'Océanographie,
CNRS-Univ. Paris VI,
Villefranche-sur-Mer,
France

We have used a unique coral culture procedure, which allows the manipulation of seawater temperature and pCO_2, in order to assess the effects of these variables on the uptake and fractionation of boron isotopes in corals. Corals are important archives for geochemical proxies such as oxygen (O) and carbon (C) isotopes, trace elements, and more recently, boron isotopes. Boron isotope uptake in carbonates is controlled primarily by *p*H. Since a decrease in ocean *p*H can be interpreted as an increase in pCO_2, several studies sought to apply the boron isotope paleo-*p*H proxy to determinations of past atmospheric CO_2. Corals should provide an ideal material for recording the paleo-*p*H of surface water. As with any promising new proxy, it is necessary to understand the controls on boron uptake.

We cultured nubbins of a branching scleractinian coral *Acropora* sp, using a single mother-colony. 4 conditions have been simulated: 430 µatm-25.3°C (referred as "normal pCO_2, normal temperature"), 446 µatm-28.2°C ("normal pCO_2, high temperature"), 712 µatm-25.1°C ("high pCO_2, normal temperature") and 738 µatm-28.3°C ("high pCO_2, high temperature"). The light level used in our experiment corresponds to *in situ* light levels measured at 5-6 meters depth with a 12:12 photoperiod. The *p*H in seawater is a function of total alkalinity (*TA*) and CO_2 concentration. Since the seawater used in this experiment had a known and constant *TA* (2.604 ± 0.004 meq kg^{-1}), we only changed the seawater *p*H to get a fixed value of pCO_2. The regulation obtained during this experiment mimicked the shift in pCO_2 that would occur within one century.

Multiple analyses of the boron isotopic composition (2-7 replicates per sample) were performed in order to ensure accurate results. External reproducibility is typically better than ± 0.5 per mil (2 SD). In this experiment we did not measure the boron isotopic composition of the Mediterranean seawater since it has been shown that it is constant, and equal to 40.26‰. The external precision carbon isotopes from aragonite, estimated using an internal standard, is 0.22‰ (2 SD). The internal reproducibility of the mass spectrometer was 0.1‰. The reproducibility of carbon isotope measurements from seawater was ± 0.14‰ (2SD).

Our results indicate that $\delta^{11}B$ in corals is primarily driven by changes in seawater pH and is not affected by temperature. For corals cultured at "normal pCO_2", the $\delta^{11}B$ of the skeleton is 24.0 ± 0.2‰ at 25°C and 23.9 ± 0.3‰ at 28°C. The values of $\delta^{11}B$ measured for corals cultured at higher pCO_2 were lower: 22.5 ± 0.1‰ and 22.8 ± 0.1‰ at 25 and 28°C, respectively. The $\delta^{13}C$ values of the skeleton are also a function of the pCO_2 treatment. Corals exposed to normal pCO_2 exhibit higher $\delta^{13}C$ values (–2.81 ± 0.13 and –2.75 ± 0.16‰, respectively for normal and high temperature) than corals exposed to high pCO_2 (-4.21 ± 0.17 and -4.14 ± 0.14‰, respectively for normal and high temperature). We observed a positive $\delta^{13}C$ -$\delta^{11}B$ correlation in the samples.

Interpretations presented here and in other studies using boron isotopes depend on knowing the *p*K value for the distribution of the aqueous boron species, and the δ value for the isotopic offset between the two aqueous boron species. These issues do not affect our interpretation of the data. Our major conclusion indicates a lack of buffering by the coral. Although competing effects of respiration, photosynthesis, and carbonate ion effect could make the interpretation of the $\delta^{13}C$-$\delta^{11}B$ co-variation difficult, this experiment should allow the use of corals for studying past changes in ocean chemistry. Changes in pH of surface ocean water that result from changes in atmospheric pCO_2 can be recorded in corals.

Our data on the boron isotope composition of cultured coral samples are consistent with the interpretation that corals do not significantly alter ambient seawater. It is remarkable that the measured values are close to theoretical predictions. Further, we have found that the boron isotopic composition of corals is not temperature dependent over the temperature range corals typically grow.

Predictability of paleogene climate and primary productivity of the Eastern Central Atlantic

Arkaah, A.B.[a], M. Kaminski[b], N. Ogle[c], L. Apaalse[d], D. Atta-Petters[a], G. Wiafe[a], A.K. Armah[a]

[a] University of Ghana,
Legon,
Ghana

[b] University College,
London,
United Kingdom

[c] Queen's University of Belfast,
Belfast,
Northern Ireland,
United Kingdom

[d] Ghana National Petroleum Cooperation,
Ghana

Benthic foraminiferal samples were obtained from 1620 ft to 3270 ft from unwashed cuttings obtained from the South Tano field, offshore Ghana, and were used to predict Paleogene climate and primary productivity of the Eastern Central Atlantic using the Analytical Precision 2003 mass spectrometer.

Samples of epifaunal benthic foraminifera of and Lenticulina spp and Eponides spp for the Upper Paleocene and Lower to Middle Eocene respectively, served as principal sources of biogenic carbonate for the determination of $\delta^{18}O$ and $\delta^{13}C$ of their host water. Average $\delta^{18}O$ values of -1.55‰, -3.01‰ and -1.77‰, were recorded for the Late Paleocene, Early Eocene and Middle Eocene, respectively, while average paleoprimary productivity levels inferred from $\delta^{13}C$ values of -2.30‰, -8.71‰ and -6.42‰, were recorded for the Late Paleocene, Early Eocene and Middle Eocene, respectively. Average paleotemperatures inferred from $\delta^{18}O$ of 23.20˚C, 29.17˚C and 24.10˚C were obtained for the Late Paleocene, Early Eocene and Middle Eocene, respectively

The highest paleotemperature of 36.69˚C was recorded at 2310 ft in the Early Eocene while the lowest paleotemperature of 15.64˚C at 1860 ft was recorded in the Middle Eocene. The highest paleoprimary productivity level of -1.13‰ was recorded at 3270 ft in the Late Paleocene and the lowest paleoprimary productivity level of -11.83‰ was recorded at 1830 ft in the Middle Eocene .

The studies indicate that the Early Eocene was the warmest, least productive and least oxygenated while the Late Paleocene showed optimum oxygen and climate conditions with the highest primary productivity levels. Low circulation system in the Early Eocene could account for low primary productivity levels from the highest temperature range and least oxygenation.

The Early and Middle Eocene were generally warmer than the Late Paleocene, however, two bioevents which occurred in both the Early and Middle Eocene indicate glacial conditions within this interglacial interval. These two "Ice ages" were marked by the highest oxygen levels (between 0.4‰ and -0.5‰) corresponding with the lowest primary productivity levels (between -11.40‰ to -11.90‰) and associated least temperatures below 20˚C to 15˚C.

Paleoclimate and paleoprimary productivity of the Eastern Central Atlantic during the Paleogene were poorly correlated. However a regression model of the second order polynomial predicted the paleoclimate and paleoprimary productivity of the Eastern Central Atlantic during the Paleogene at 64.96% coefficient of determination.

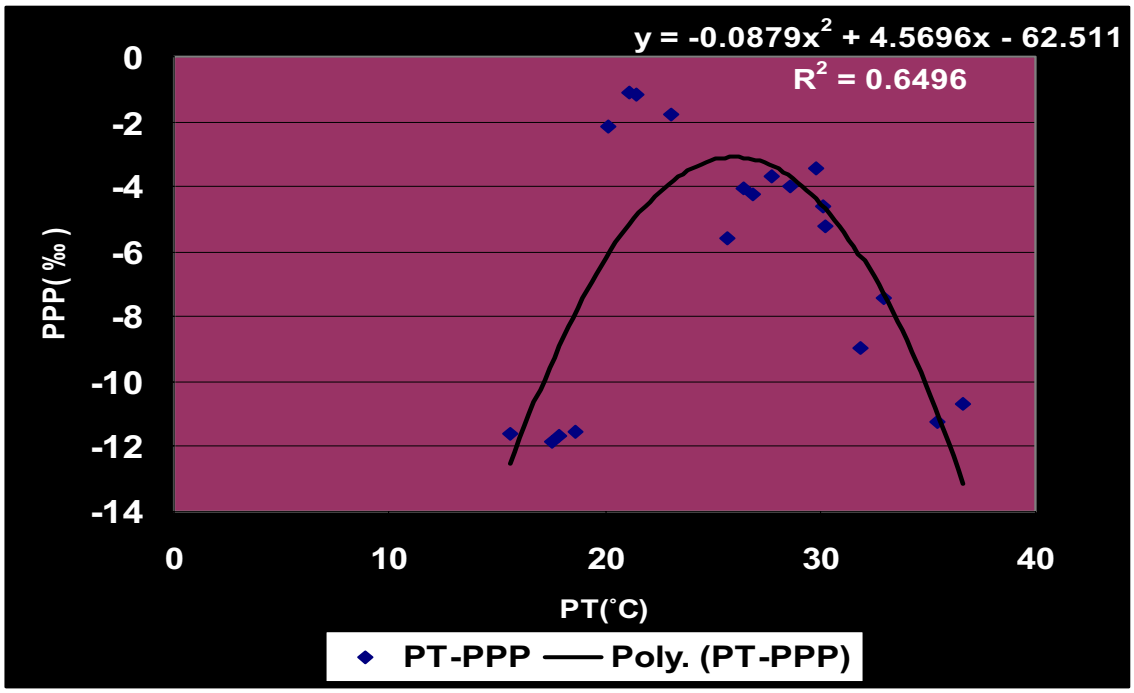

FIG. 1. Regression model for paleotemperatures and paleoprimary productivity levels.

Isotopic composition of perennial cave ice as a proxy for palaeoclimate: the Focul Viu ice cave, Bihor Mts., Romania

Fórizs, I.[a], Z. Kern[b], B. Nagy[b], Zs. Szántó[c], L. Palcsu[c]

[a] Laboratory for Geochemical Research,
Research Centre for Earth Sciences,
Hungarian Academy of Sciences,
Budapest,
Hungary

[b] Department of Physical Geography,
Eötvös Un,
Hungary

[c] Institute of Nuclear Research,
Hungarian Academy of Sciences,
Debrecen,
Hungary

For predicting the climate change in the near future we have to understand the climate changes that happened in the past. Several methods and tools have been developed or are under development for palaeoclimate reconstruction – among them environmental isotopes play an outstanding part –, but none of them can reveal perfectly the past changes in the climate.

One of the most classical method is the utilization of the isotopic composition of ice sheets where the ice formation is continuous, e.g. on Greenland [1] or Antarctica [2]. Ice formation takes place in rock caves as well, where usually not the whole year precipitation is represented in the ice, and in this way the ice formation and its isotope composition is very sensitive for the climate change. So far little research has been devoted to the role of cave ice in palaeoclimatology. Yonge and MacDonald [3] found that ice caves in permafrost and non-permafrost zones behave quite differently, so the relation between the stable isotope composition of cave ice layers and climate parameters should be studied in different climate zones.

Perennial ice block of about 14 meter vertical thickness and estimated volume of 12 000 m^3, including subfossil wood, can be found in the Focul Viu Ice Cave, Bihor Mountains, Romania at 1120 m elevation a.s.l. on a karstic highland under temperate climate. The annual mean temperature of the highland area is about 7°C. The cave ice forms mainly from drip water in springtime, when the temperature of the ice and the rock wall is below freezing point in the cave and over freezing point on surface.

Using a manual corer cca. 7 m long ice core was taken from the ice block situated in the main hall of the cave, from which more than 150 $\delta^{18}O$ measurements were made representing different increments. Near-surface samples were taken from the upper surface and the side wall of the ice block for tritium, $\delta^{18}O$ and δD measurements. The tritium content indicates 1.9 cm/year short-term growth rate for the ice, while the long-term growth rate based on radiocarbon ages of two wood samples from the ice block at 6.7 m and 11.1 m depth is 0.85 cm/year. Long-term growth rate include periods when the ice "growth-melt" balance was zero or negative.

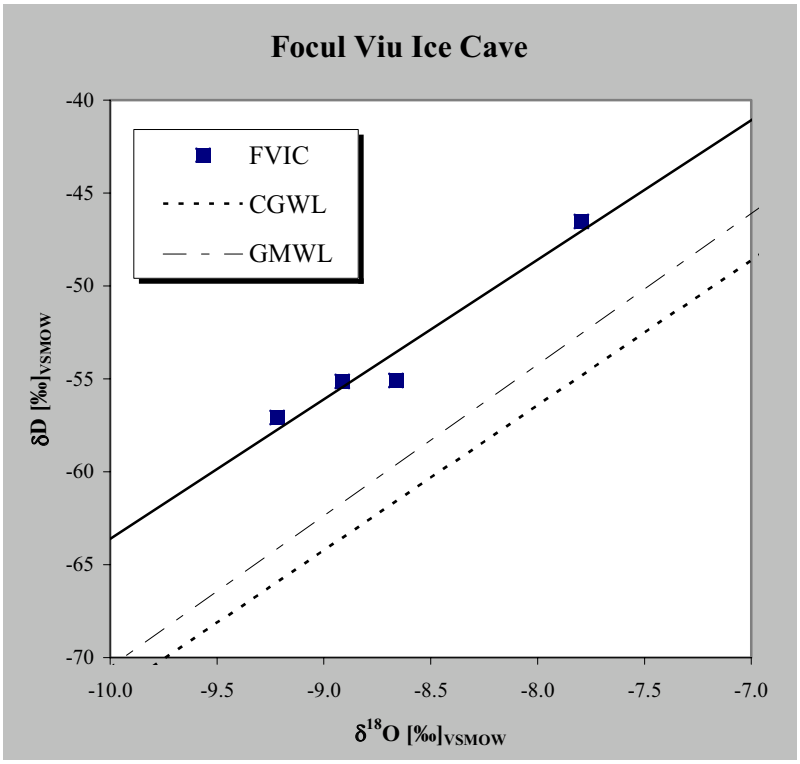

FIG. 1. The δD-$\delta^{18}O$ diagram showing the "ice water line of the Focul Viu Ice Cave" (FVIC), the "ground water line of the Carpathian Basin" (CGWL), and the "global meteoric water line" (GMWL).

The $\delta^{18}O$ values along the vertical section varies between -8.19‰ and -12.3‰ vs. VSMOW. If we accept the observation made by Yonge et al. [4] that the $\delta^{18}O$ value of seepage water in caves is usually the same as the annual mean $\delta^{18}O$ value of the local precipitation and does not show seasonal variation to be right for the Focul Viu Ice Cave, then the above $\delta^{18}O$ variation indicates about 9 °C difference between the minimum and maximum annual mean surface air temperatures during the period represented (about 850 years) by the ice core studied.

The average *d*-excess of the cave ice is 15.7‰, which indicates that either the Mediterranean or the continental component of the local precipitation is considerable. This is well demonstrated by the relative position of the water line of the cave ice in comparison to the groundwater line of the Carpathian Basin and the global meteoric water line on Fig. 1.

REFERENCES

[1] GROOTES, P.M., STUIVER, M., Oxygen 18/16 variability in Greenland snow and ice with 10^3 to 10^5-year time resolution, J. Geophys. Res. **102** (1997) 26455-26470.

[2] PETIT, J.R., JOUZEL, J., RAYNAUD, D., BARKOV, N.I., BARNOLA, J.M., BASILE, I., BENDER, M., CHAPPELLAZ, J., DAVIS, M., DELAYGUE, G., DELMOTTE, M., KOTLYAKOV, V.M., LEGRAND, M., LIPENKOV, V.Y., LORIUS, C., PEPIN, L., RITZ, C., SALTZMAN, E., STIEVENARD, M., Climate and atmospheric history of the past 420,000 years from the Vostok ice core, Antarctica, Nature **399** (1999) 429-436.

[3] YONGE, C.J., MACDONALD, W.D., The potential of perennial cave ice in isotope palaeoclimatology, Boreas **28** (1999) 357-362.

[4] YONGE, C.J., FORD, D.C., GRAY, J., SCHWARCZ, H.P., Stable isotope studies of cave seepage water, Chem. Geol. (Isotope Geoscience Section) **58** (1985) 97-105.

CLIMATE CHANGE - POSTERS

Climate changes in the eastern Equatorial Pacific: results from multiproxy study of IMAGES Core MD02-2529

Ivanova, E.V.[a], L. Vidal[b], L. Beaufort[b], G. Leduc[b]

[a] Shirshov Institute of Oceanology RAS,
Moscow,
Russian Federation

[b] CEREGE, Europole de l'Arbois,
Aix en Provence,
France

Sediment Core MD02-2529 (08°12.5' N, 84° 07.5' W, 1619 m) was retrieved on the Cocos Ridge during IMAGES VIII MONA cruise [1]. The rather shallow depth of the core (1619 m) results in better preservation of planktic foraminifers and coccoliths, especially during glacial stages and terminations, than generally found in the Equatorial Pacific. This provides us with the material for detailed stable isotope and micropaleontological study. On the other hand, the site is located below the Costa Rica dome. In this area the thermocline depth and related upwelling are strongly influenced by the ITCZ meridional migrations and by the ENSO dynamics. The northernmost ITCZ position in the summer produces a cyclonic activity off Costa Rica inducing a dome like structure of the thermocline which shoals significantly. During El Nino years, the thermocline is deep, inducing a strong decrease of the oceanic primary production. Therefore, the studied core is ideally located to monitor past variations of ITCZ migration and ENSO dynamics in the Eastern Equatorial Pacific. We analyzed planktic foraminifers and coccolithophores assemblages, oxygen and carbon isotope ratio of planktic (*Globigerinoides ruber* and *Neogloboquadrina dutertrei*) and benthic (*Cibicidoides wuellerstorfi*) foraminifers, grain size distribution and several dissolution indexes. The obtained oxygen isotope stratigraphy allow us to distinguish five oxygen-isotope stages (MIS 1-5, according to standard abbreviation) in the upper 15 m of the core, and to estimate a mean sedimentation rate of about 13cm/1000years. The amplitude of glacial to interglacial variability between MIS 2 and 1 for the surface-dwelling *G. ruber* reaches 2‰.

Quantitative study of planktic foraminifers and coccolithophores demonstrates pronounced temporal variability. Glacial planktic foraminiferal assemblages differ significantly from those during interglacials by lower content of warm-water surface-dwelling foraminifers and enhanced content of so-called upwelling species (previously investigated in the Oman upwelling in particular by [3]). The presence of deep-dwelling *Globorotalia inflata*, a common species of Recent assemblages in the eastern margins of subtropical gyres, may point to advection of cooler waters during MIS 2. These features of foraminiferal assemblages are in line with glacial to interglacial seasonal and mean-annual sea-surface temperature variations of 2-4°C estimated by modern analogue technique.

The end of MIS 2 is characterized by an increased preservation of calcareous microfossils, followed by enhanced dissolution from the end of Termination I to Holocene. In the coccolith assemblages, the relative abundance of the deep photic zone species *Florisphaera profunda* varies significantly. The species considered as a low-productivity indicator, in particular in low-latitude Indo-Pacific [2] demonstrates lowest values, i.e. points to higher productivity in MIS 6, late MIS 2 and Termination I. This finding is corroborated by an increased abundance of planktic and benthic foraminifers during the late MIS 2, and enhanced content of *Globorotalita glutinata* associated with relatively low value of *G. ruber* during the Termination I. The first of two species is known to prey mainly on fresh organic matter while the second is frequent in oligotrophic waters. Changes in subsurface water structure are

studied by considering the oxygen isotope gradient between surface-dwelling *G. ruber* and thermocline-dwelling *N. dutertrei* records in order to explore regional paleoceanographic variability versus global forcing. Enhanced marine productivity at the end of MIS2 and at the beginning of Terminaton I can be explained by changes in the wind stress and ITCZ migration. It also implies stronger La Nina's and weaker or less frequent El Nino's during the glacials of the last climatic cycle. Moreover, the Costa Rica Dome pattern seems to be generally opposite to areas under the influence of the California current over the same time period.

REFERENCES

[1] BEAUFORT, L., IVANOVA, E., VIDAL, L., et al., MD 126, IMAGES VIII/ MONA Cruise Report (IPEV, Les rapports de campagnes a la mer), Ref. OCE/2002/03, 452 pp.

[2] BEAUFORT, L., DE GARIDEL-THORON, T., MIX, A.C., PISIAS, N.G., ENSO-like forcing on oceanic primary production during the Late Pleistocene, Science **293** (2001) 2440-2444.

[3] IVANOVA, E., SCHIEBEL, R., SINGH, A.D., SCHMIEDL, G., NIEBLER, H.-S., HEMLEBEN, CH., Primary production in the Arabian Sea during the last 135,000 years, Palaeogeogr. Palaeoecol. Palaeoclim. **197** (2003) 61-82.

Reconstructing sedimentation history from radionuclides (^{210}Pb, ^{137}Cs, ^{241}Am) and the recognition of geodynamic events in Lakes Puyehue and Icalma (Chilean Lake District, Northern Patagonia)

Magand, O.[a], F. Arnaud[b], E. Chapron[c], M.-A. Mélières[a], X. Boës[d]

[a] Laboratory of Glaciology and Geophysics of Environment (LGGE),
UMR CNRS 5183,
Grenoble,
France

[b] PBDS, UMR CNRS 8110, UST Lille 1,
Laboratory of Geodynamics of Alpine Ranges (LGCA),
UMR CNRS 5025,
University of Savoie,
France

[c] Renard Centre of Marine Geology,
University of Gent,
Belgium

[d] Clays and Paleoclimate Research Unit,
University of Liege,
Belgium

In this paper, we present a multidisciplinary study of four sediment cores from lakes Puyehue (PU) and Icalma (ICA) aiming at 1) assessing the rhythm of sedimentation and 2) evidencing and calibrating the fingerprint of most important geodynamic events historically known in the surrounding area. This study was the very first step of a currently running multidisciplinary study of holocene-long cores taken on the studied sites during the 2002 "ENSO Chile" survey. Two short cores were taken in each lake, one directly submitted to flood input from the main tributary (PU-I and ICA-II) and one located in a more distal sedimentary environment (PU-II and ICA-I).

The establishment of age-depth relationship was made particularly hard by the intense volcanic and seismic activity affecting the studied area - one of the most tectonically active in the world - and was only made possible through the crossing of a wide panel of chronological indicators. Our approach hence couples radiometric and sedimentological investigations allowing both to wisely interpret the radiometric profiles and in turn to refine the age-depth relationship through the recognition of historically-known events. It consists first in the recognition of potential 'instantaneous deposits' thought to be responsible of major disturbances of the radionuclide profiles [1]. Subsequently the triggering mechanisms of these levels (i.e., earthquake, volcanic eruption or flood event) is sedimentologically determined. Following [1], and once their 'instantaneity' is established, the particular levels are removed from the radionuclide profiles in order to reconstruct the undisturbed evolution of ^{210}Pb as a function of continuously deposited sediment thickness (Fig. 1). Thereafter, both CFCS and CRS ^{210}Pb dating models were applied to the reconstructed profiles and the position of the maximum activity of artificial ^{137}Cs and ^{241}Am was noted, establishing thus independent radionuclide chronologies (Fig. 2). Once dated, the age of instantaneous sediment deposits were confronted to the age of main events susceptible to have triggered them. Particular attention was then paid to the main tectonic manifestations, such as the huge earthquake which hit the surrounding region of Valdivia

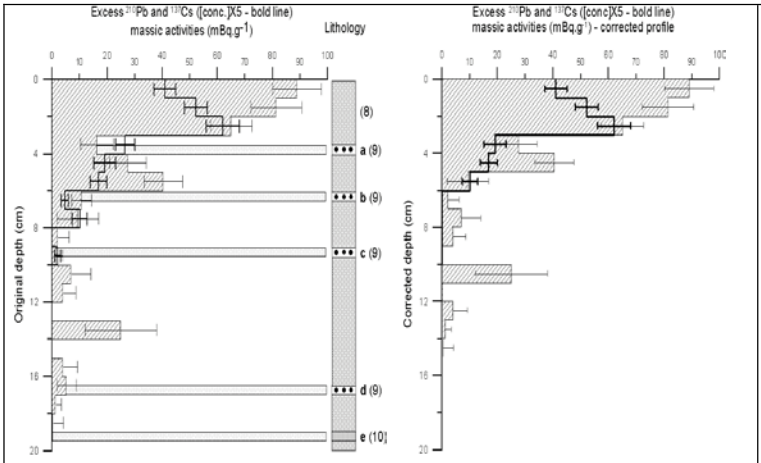

FIG. 1. Example of radionuclide data processing in core ICA-II.

Left : Original profile coupled with lithology and instantaneous deposits (a, b, c, d and e). (8) dark brown silts; (9) sandy tephra deposits; (10) yellowish fine grained layer.

Right: Corrected profile after subtracting the thicknesses of sedimentary events (shaded area).

(including Lake Puyehue) in 1960 and whose magnitude of 9.5 is the strongest ever recorded in the world. When it was possible - i.e., in core PU-II - varve-counting was performed on embedded thin sections [2], providing an annually-resolved control on radiometric chronologies.

After crossing the whole set of chronological information in both lakes, it appears that, amongst the four studied cores, only two (ICA-II and PU-II) were accurately dateable through ^{210}Pb method whereas three ones yield valuable information from the artificial radionuclides ^{137}Cs and/or ^{241}Am. This points the difficult use of ^{210}Pb geochronology in such a disturbed geological setting and emphasizes the absolute necessity of independent control on this kind of geochronological tool.

ACKNOWLEDGEMENTS

Financial support from the French ministry of research and ACI Climate Change is acknowledged. Field work in Chile was possible through the Belgian SSTC research project EV/12/10B led by M. De Batist, N. Fagel and A. Berger.

REFERENCES

[1] ARNAUD, F., LIGNIER, V., REVEL, M., DESMET, M., BECK, C., POURCHET, M., CHARLET, F., TRENTESAUX A., TRIBOVILLARD, N., Flood and earthquake disturbance of ^{210}Pb geochronology (Lake Anterne, North French Alps), Terra Nova, **14-4** (2002) 225-232.

[2] BOES, X., ARNAUD, F., MAGAND, O., DE BATIST, M., FAGEL, N., Thickness variation of sediment lamination in Puyehue Lake (Lake District, Southern Chile) during the last millennium: a regional southern hemisphere record of El Niño ? Geophys. Res. Abs. **6** (2004) 04243.

OCEANS AND SEAS

Bomb-radiocarbon: distribution, inventory, and change

Key, R.M.

A.O.S. Program,
Princeton University,
Princeton, New Jersey,
United States of America

During the 1990s an unprecedented number of oceanic radiocarbon measurements were made as part of the World Ocean Circulation Experiment (WOCE). The samples were analyzed using both large volume beta counting and small volume accelerator mass spectrometry. The number of WOCE radiocarbon samples is approximately 10 times larger than measured during the GEOSECS survey in the 1970s. A new technique was developed to separate the natural and bomb produced radiocarbon components. This procedure is based on the strong linear correlation between radiocarbon and potential alkalinity that is found in intermediate to abyssal waters worldwide. The primary benefit of the potential alkalinity separation method over the previously used silicate method is that it is applicable at all latitudes.

While still sparse relative to hydrographic or nutrient measurements, the new data are sufficient to produce three dimensional objective maps. These maps confirm the major GEOSECS findings, but add considerable detail. As an example, in the deep Pacific the northward abyssal flow is clearly defined as a western boundary current which flows adjacent to the island arc system while the return southward deepwater flow at approximately 2500 m is broad and appears to divide into two tongues in the southern hemisphere. Global integration of the natural radiocarbon yields an inventory of 1.8 x 10^{30} atoms with an uncertainty of approximately 15%.

At the time of GEOSECS, the measured and bomb radiocarbon signals were always highest at the ocean surface. While this was generally true for WOCE, some regions of the Pacific and Indian Oceans showed highest concentrations below the surface in the upper thermocline. This change is due to a decrease in the atmospheric source combined with mixing and upper ocean circulation. In general the radiocarbon penetration depth increased, however the change is relatively subtle for most regions. In the Atlantic, a small increase was found in North Atlantic Deep Water as far south as the Lesser Antilles (15°N latitude).

Global integration of the bomb radiocarbon gives an inventory of 3.1 x 10^{28} atoms. This total is only marginally higher than earlier estimates using the GEOSECS data. Modeling results imply that the earlier inventory calculations were high by approximately 25%. Since the earlier measurements were of the same quality as the WOCE data, this implies that the earlier inventory estimates were biased simply due to a lack of data. The new inventory estimate is consistent with estimates based on atmospheric models and measurements. The highest column inventories are found in the North Atlantic, but high inventories are also found near the formation regions for North Pacific Intermediate Water and in the southern hemisphere associated subduction of Antarctic Intermediate Water and Subpolar Mode Water (Figure 1). Changes in these southern water masses can be traced on isopycnal surfaces almost to the Equator.

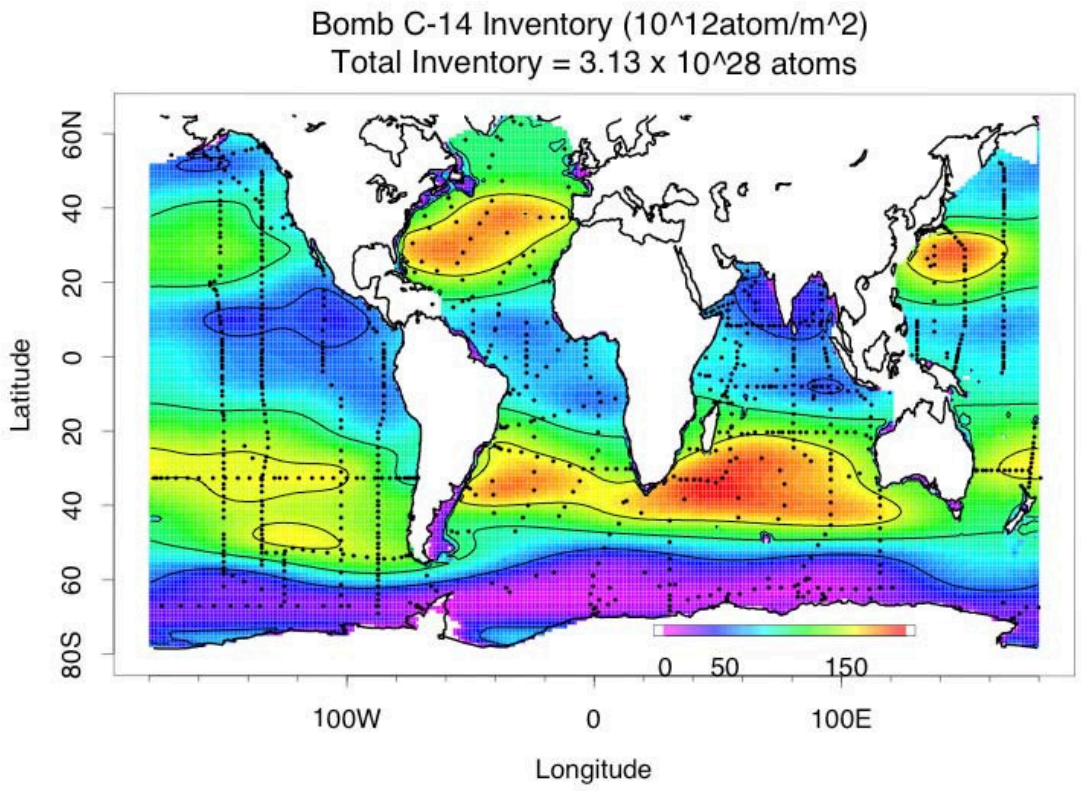

FIG. 1. Bomb C-14 inventory based on GEOSECS and WOCE data. Highest inventories are observed in the North Atlantic, in the regions of formation of North Pacific Intermediate Water and in the southern hemisphere. **See ANNEX I, p. 659 for colour version of figure.**

Distribution of tritium (^{3}H) in the Southern Ocean: Implications for formation rates, circulation patterns and mean residences of major water masses

Schlosser, P.[a,b], B. Newton[a], A. Spieler[a]

[a] Lamont-Doherty Earth Observatory of Columbia University,
Palisades,
New York,
United States of America

[b] Department of Earth and Environmental Engineering,
Department of Earth and Environmental Sciences,
Columbia University,
New York,
United States of America

Tritium is a well-studied tracer for processes in the hydrosphere, including the oceans, continental surface waters and groundwater. The main portion of the tritium signals observed in the modern environment is due to its production during nuclear weapons tests, most of which were conducted in the 1950s and early 1960s. Most of the so-called bomb tritium was produced in the northern hemisphere resulting in a large north/south gradient in the oceanic tritium concentrations. This asymmetric oceanic tritium distribution with very low concentrations in the Southern Ocean requires tritium measurements in the mTU range to achieve sufficient resolution for application of tritium as tracer. Such low detection limits can only be achieved through mass spectrometric measurements of tritium by the ^{3}He ingrowth method.

Over the past two decades high-precision tritium measurements based on the ^{3}He ingrowth method were obtained from several sections in the Southern Ocean. Most of the sections are located in the Atlantic sector (Weddell Sea). The sections show that the surface waters in the Southern Ocean near the Antarctic continents are only ca. 100 mTU (0.1 TU). The deep waters have varying concentrations reaching from the detection limit of ca. 5 mTU to ca. 80 mTU in bottom waters near the formation areas of new Antarctic Bottom Water. The surface concentrations increase towards the north to concentrations of several hundred mTU.

We present distributions of tritium in the Southern Ocean and discuss the information that can be derived from them with respect to formation, circulation and mean residence of major water masses in the Southern Ocean. The interpretation is based on analysis of the tritium sections in the context of hydrographic properties, as well as on simple time-dependent mass balances or box models.

Average ^{3}H, ^{90}Sr, ^{137}Cs and $^{239,240}Pu$ concentrations in surface waters of the Atlantic Ocean — WOMARS collaboration

Povinec, P.P.[a], A. Aarkrog[b], K.O. Buesseler[c], R. Delfanti[d], K. Hirose[e], G.H. Hong[f], T. Ito[a], H.D. Livingston[a], H. Nies[g], V.E. Noshkin[h], S. Shima[i], O.Togawa[a]

[a] IAEA, Marine Environment Laboratory,
Monaco

[b] Risoe National Laboratory,
Roskilde,
Denmark

[c] Woods Hole Oceanographic Institution,
Woods Hole, MA,
United States of America

[d] ENEA Marine Environment Research Centre,
La Spezia,
Italy

[e] Meteorological Research Institute,
Tsukuba,
Japan

[f] Korea Ocean Research and Development Institute,
Ansan, Seoul,
Korea, Republic of

[g] Federal Maritime & Hydrographic Agency,
Hamburg,
Germany

[h] Lawrence Livermore National Laboratory,
Livermore, CA,
United States of America

[i] Japan Marine Science Foundation,
Mutsu,
Japan

Abstract. Sources of anthropogenic ^{3}H, ^{90}Sr, ^{137}Cs and $^{239,240}Pu$ in the Atlantic Ocean, their concentrations in surface waters for the periods of 1991-1995 and 1996-2000, and average concentrations for 2000 are presented and discussed. The highest radionuclide concentrations have been observed in the Irish Sea due to discharges from the Sellafield reprocessing facility, and in the Baltic Sea due to the Chernobyl accident. The obtained results represent the most complete dataset on levels of radionuclides in the Atlantic Ocean surface waters. They can be used as the reference source so that any further contributions from nuclear reprocessing plants, radioactive waste dumping sites, nuclear bomb test sites and possible nuclear accidents can be identified.

1. Introduction

The IAEA-MEL's Radiometrics Laboratory in Monaco, in collaboration with several marine institutes, carried out in 1994 – 2003 a research project on Worldwide Marine Radioactivity Studies (WOMARS), with the primary objective to develop an understanding of the present open ocean distribution of anthropogenic radionuclides in the water column and sediment [1].

The programme was designed with the intention of reviewing the sources which have introduced anthropogenic radionuclides to the world's oceans, and contributing to scientific knowledge of the processes which affect radionuclide distributions. Four anthropogenic radionuclides - ^{3}H, ^{90}Sr, ^{137}Cs and $^{239,240}Pu$ have been chosen as the most representative of anthropogenic radioactivity in the marine environment.

The radioactive contamination of the Atlantic Ocean originates from three main sources: (i) global fallout, due to nuclear weapons testing in the atmosphere (1945 – 1980), which represents a dominant source on the global scale; (ii) nuclear reprocessing in western Europe notably Sellafield in the UK

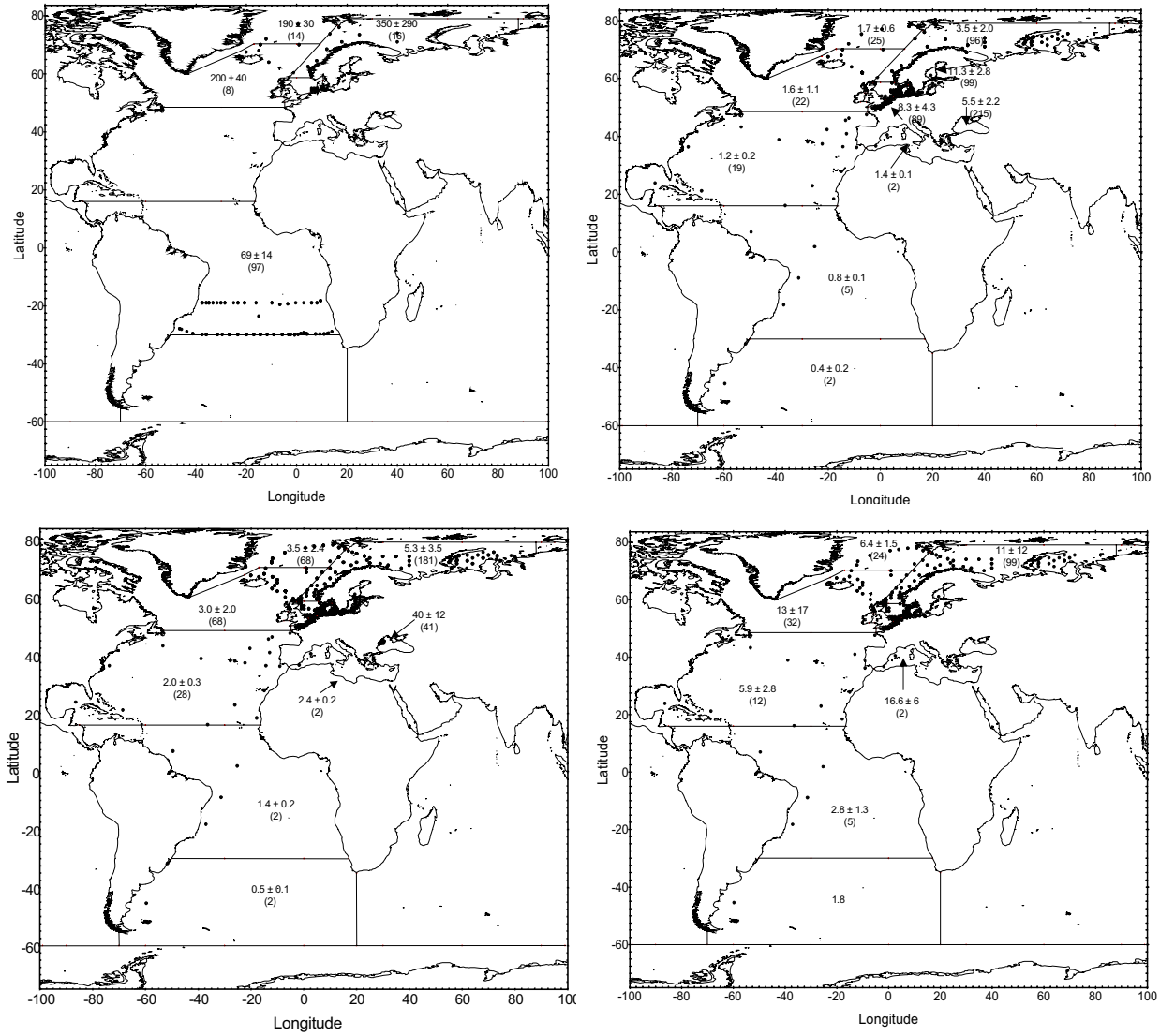

FIG. 1. ^{3}H, ^{90}Sr, ^{137}Cs (all in mBq/L) and $^{239,240}Pu$ (in μBq/L) in surface waters in the latitudinal boxes of the Atlantic Ocean (1991-1995), decay-corrected to 01.01.2000 (the number of results is given in parentheses; dots represent the sampling sites).

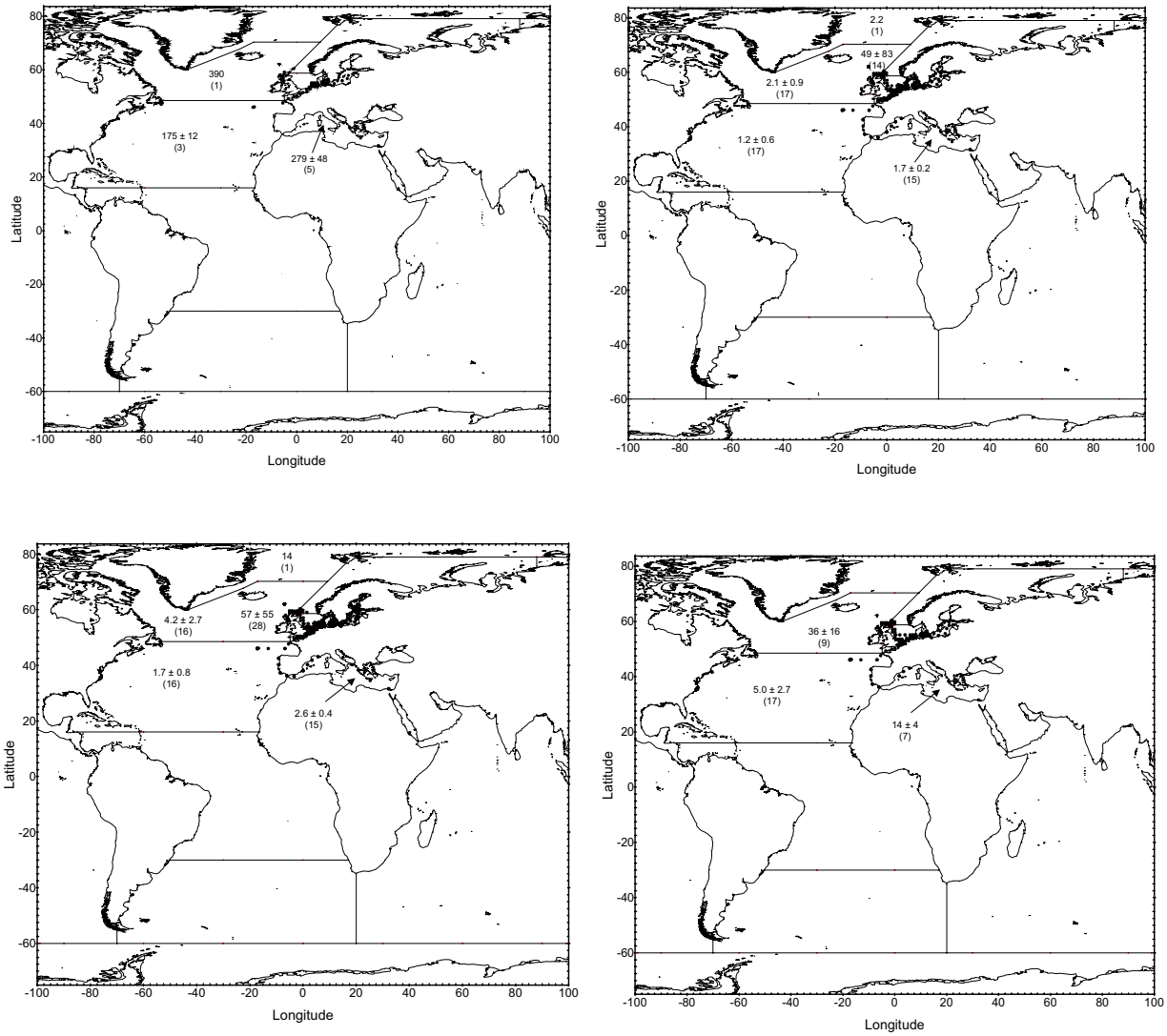

FIG. 2. ^{3}H, ^{90}Sr, ^{137}Cs (all in mBq/L) and $^{239,240}Pu$ (in μBq/L) in surface waters in the latitudinal boxes of the Atlantic Ocean (1996-2000), decay-corrected to 01.01.2000 (the number of results is given in parentheses; dots represent the sampling sites).

and Cap de la Hague in France (the maximum discharges to the sea took place from 1970 to 1985); and (iii) the Chernobyl accident in the Ukraine in 1986. In contrast to the Pacific Ocean [2], the Atlantic has not received local fallout from nuclear weapons testing to any significant extent.

In addition to these sources, nuclear power stations, fuel production facilities, nuclear research facilities, and dumping of low-level radioactive waste in the deep NE Atlantic Ocean may contribute to the contamination of the immediate environment. The discharges or releases from these sources are not detectable in the open marine environment.

In the Arctic Ocean additional potential sources exist, such as dumped radioactive waste in the Kara and Barents Seas, discharges by Ob and Yenisey rivers, discharges from nuclear activities on the Kola peninsula, the sunken nuclear submarine "Komsomolets", and plutonium contamination at the Thule (Greenland) accident site.

Due to the inputs from reprocessing and Chernobyl, the NE Atlantic shows higher concentrations of anthropogenic radionuclides than any other part of the world ocean. Furthermore the variation in radionuclide concentrations is higher than seen elsewhere. This should be taken into account when

quoting average radionuclide concentrations in marginal seas such as the Baltic Sea, the Black Sea, the North Sea, and especially, the Irish Sea.

2. Results and discussion

The Atlantic Ocean with marginal seas was divided into boxes (Fig. 1) in which average radionuclide concentrations in surface waters were were estimated using data stored in the IAEA's Global Marine Radioactivity Database (GLOMARD) [3, 4].

The maps of the distributions and average concentrations for ^{3}H, ^{90}Sr, ^{137}Cs and $^{239,240}Pu$ in Atlantic surface water for the period 1991-1995 and 1996-2000 are shown in Figs. 1 and 2, respectively. The radionuclide data were decay corrected (except for $^{239,240}Pu$) to 01. 01. 2000. Unfortunately, for the south Atlantic Ocean, the radionuclide data are very sparse, therefore a proper evaluation has not been possible. All radionuclide data show a latitudinal effect in their distribution, with growing concentrations from the south to the north.

^{3}H concentrations varied from ~70 mBq/L in the South Atlantic to ~350 mBq/L in the Barents Sea. The average ^{3}H concentration in the Mediterranean Sea was ~280 mBq/L. ^{90}Sr concentrations varied from ~0.4 mBq/L in the South Atlantic to ~3 mBq/L in the Barents Sea. The highest average concentrations for 2000 were estimated for the Irish Sea (~50 mBq/L), Baltic Sea (~10 mBq/L), the English Channel (~4 mBq/L) and the North Sea (~4 mBq/L), resulting from discharges from Sellafield and Cap de la Hague. ^{137}Cs concentrations varied from ~0.5 mBq/L in the South Atlantic to ~5 mBq/L in the Barents Sea. The highest average concentrations for 2000 were estimated for the Irish Sea (~60 mBq/L), the Baltic Sea (~60 mBq/L), the Black Sea (~25 mBq/L), the North Sea (~7 mBq/L), the English Channel (~4 mBq/L) and the Mediterranean Sea (~3 mBq/L).

$^{239,240}Pu$ concentrations varied from ~2 μBq/L in the South Atlantic to ~11 μBq/L in the Barents Sea. The highest average concentrations for 2000 were estimated for the Irish Sea (~500 μBq/L), the North Sea (~ 15 μBq/L), the Mediterranean Sea (~14 μBq/L), the English Channel (~13 μBq/L), the Black Sea (~5μBq/L) and the Baltic Sea (~3 μBq/L).

3. Conclusions

Average ^{3}H, ^{90}Sr, ^{137}Cs and $^{239,240}Pu$ concentrations in Atlantic surface waters for the year 2000 have been established. The highest concentrations have been observed in the Irish Sea due to discharges from the Sellafield reprocessing facility, and in the Baltic Sea due to the Chernobyl accident. The present radionuclide concentrations are controlled by radioactive decay (with the exception of $^{239,240}Pu$) and by oceanographic processes.

The obtained results represent the most complete dataset on levels of radionuclides in the Atlantic Ocean surface waters. They can be used as the reference source so that any further contributions from nuclear reprocessing plants, radioactive waste dumping sites, nuclear bomb test sites and possible nuclear accidents can be identified.

ACKNOWLEDGEMENTS

Financial support provided by the Government of Japan is highly acknowledged. The International Atomic Energy Agency is grateful for the support provided to its Marine Environment Laboratory by the Government of the Principality of Monaco.

REFERENCES

[1] WORLDWIDE MARINE RADIOACTIVTY STUDIES (WOMARS), IAEA-TECDOC-1429, IAEA, Vienna (2005).

[2] POVINEC, P.P., AARKROG, A., BUESSELER, K.O., DELFANTI, R., HIROSE, K., HONG, G.H., ITO, T., LIVINGSTON, H.D., NIES, H., NOSHKIN, V.E., SHIMA, S., TOGAWA, O., ^{90}Sr, ^{137}Cs and ^{239,240}Pu concentration surface water time series in the Pacific and Indian Oceans – WOMARS results, J. Environ. Radioact. **81** (2005) 63-87.

[3] GLOBAL MARINE RADIOACTIVITY DATABASE (GLOMARD), IAEA-TECDOC-1146, IAEA, Vienna (2000).

[4] POVINEC, P.P., HIROSE, K., HONDA, T., ITO, T., SCOTT, E.M., TOGAWA. O., Spatial distribution of ^{3}H, ^{90}Sr, ^{137}Cs and ^{239,240}Pu in surface waters of the Pacific and Indian Oceans – GLOMARD database, J. Environ. Radioact. **76** (2004) 113-137.

Radionuclides as tracers of water masses in the Southern Ocean - ANTARES IV results

Lee, S-H.[a], P.P. Povinec[a], J. Gastaud[a], B. Oregioni[a], L. Coppola[b], C. Jeandel[b], U. Morgenstern[c], Z. Top[d]

[a] Marine Environment Laboratory,
International Atomic Energy Agency,
Monaco

[b] Laboratoire d'Etudes en Geophysique et Oceanographie Spatiales,
Toulouse,
France

[c] Institute of Geological and Nuclear Sciences,
Lower Hutt,
New Zealand

[d] University of Miami,
Miami,
United States of America

Abstract. Water samples collected during the ANTArctic RESearch (ANTARES) IV expedition, carried out in January-February 1999 in the Sub-Antarctic Frontal System in the Southern Indian Ocean, were analyzed for anthropogenic ^{3}H, ^{90}Sr, $^{239,240}Pu$ and ^{241}Am. The results have shown that the distribution of radionuclides in the Southern Ocean is controlled by the water fronts. ^{3}H data show higher concentrations at the surface layer, and gradually decrease with depth, but significant levels of ^{3}H are observed at bottom waters, attributable to intrusion of Antarctic Bottom Water (AABW) into the region.

1. Introduction

The Southern Ocean has been of interest to many research groups due to its key role in the regulation of CO_2 levels, biological productivity, biogenic fluxes, oceanographic processes and its important role in the global climate [1, 2]. The dominant physical control of the biogeochemical distribution of tracers in the Southern Ocean is the banded structure of the Antarctic Circumpolar Current (ACC). North of the ACC, there is a single narrow band (only about 200 km wide) of frontal zone along the shelf edge, where 80% of the ACC transport is concentrated. This frontal zone is formed by the confluence of the Subantarctic Front (SAF) and Subtropical Front (STF). The sampling area of the present study is located in the Crozet Basin (northwest Kerguelen Plateau and east of Crozet Plateau) in the confluence of several fronts: Agulhas Front (AF), STF and SAF (Fig. 1). The most predominant current affecting the circulation in the Crozet Basin is the Agulhas Return Current (ARC), characterized by warm and saline water, extending eastward into the basin.

Only limited information on anthropogenic radionuclides in the Southern Ocean has been available. This paper describes the results obtained from ANTArctic RESearch (ANTARES) IV cruise, concentrating on the distribution of ^{3}H, ^{90}Sr, $^{239,240}Pu$ and ^{241}Am in surface and deep waters of the Southern Ocean. The ANTARES IV cruise was carried out in January-February, 1999, on board of the R/V Marion Dufresne. Surface and water profile seawater samples were collected and analysed following published procedures [3, 4].

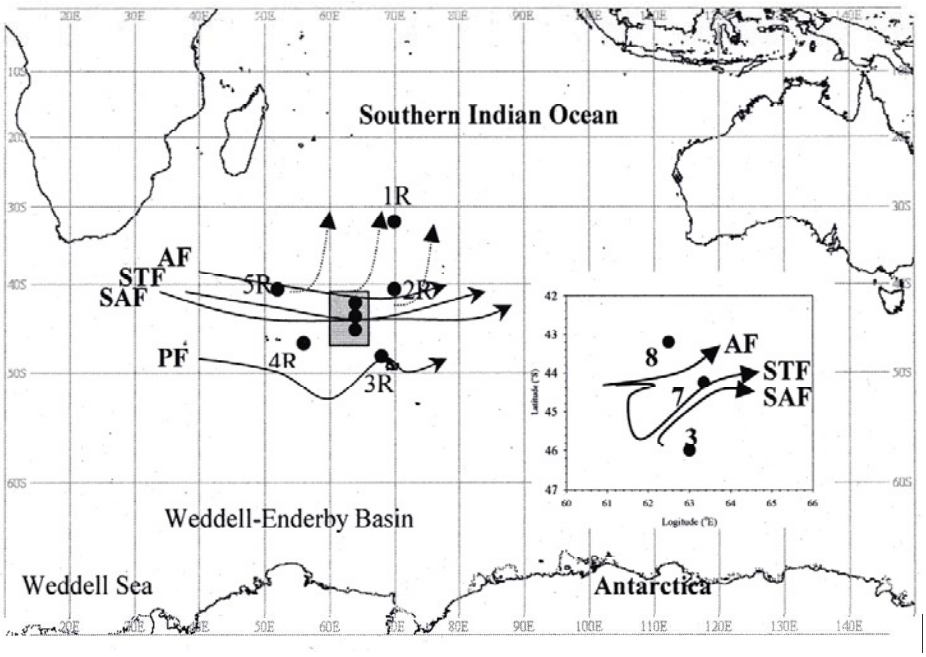

FIG. 1. Map of the study area for ANTARES IV cruise in the Southern Indian Ocean conducted aboard the R/V Marion Dufresne in 1999, and the main water fronts (Stations 3, 7 and 8 represent seawater profile sampling).

2. Results and discussion

The distribution of ^{3}H, ^{90}Sr, $^{239,240}Pu$ and ^{241}Am in surface waters reveals a strong latitudinal variation defined by the water fronts. The surface ^{3}H and ^{90}Sr concentrations are slightly increasing southwardly from 32°S, showing peak concentrations at around 41°S (AF). These tendencies change remarkably from the south of 43°S, where the STF dominates, and where decreasing radionuclide levels were observed. $^{239,240}Pu$ also shows increasing levels from 32° to 41°S, and then a decline down to 46°S, however, Station 3R situated at the most south site at 48°S shows almost by a factor 5 higher $^{239,240}Pu$ concentration than Station 3 situated at 46°S. ^{241}Am is not fully copying the $^{239,240}Pu$ distribution (as it would be expected, because of its similar particle reactive behaviour), showing a peak at 41°S (Stations 2R and 5R), and a minimum at 43°S (Station 8), however, increasing levels were then observed at Stations 7, 3, 4R (in contradiction with the $^{239,240}Pu$ record) and at Station 3R. The fronts in the latitudinal bend of 40-48°S are acting as strong barriers, preventing mixing of water masses between them, so that the concentrations of radionuclides are well preserved in each of the frontal zones.

^{3}H profiles are distinctly classified by STF (Station 7) and SAF (Station 3), and this feature is outstanding in the upper layer of 600 m. ^{3}H concentrations at Stations 3 and 7 are showing a subsurface maximum (at around 100 m), preserving up to 500 m water depth, and then a rapid decrease to 1000 m. Although the top ^{3}H profiles at Stations 3 and 7 are similar in shape, ^{3}H concentrations in the upper layer of Station 7 are two times higher than those at Station 3.

Negligible amounts of ^{3}H appear between 1000 and 2500 m water depth, however, higher levels are observed at bottom waters at both stations. ^{3}H concentration largely decreases below the 1000 m depth, at which Circumpolar Deep Water (CDW) appears, providing the main contribution to the deep-water circulation and ventilation north of 40°S. The depletion of ^{3}H content in the CDW in the STF and SAF fronts (Stations 3 and 7) may be related to the intrusion of North Atlantic Deep Water (NADW), which is known to be the most important contributor to CDW, characterized by salinity maximum and nutrient minima [5].

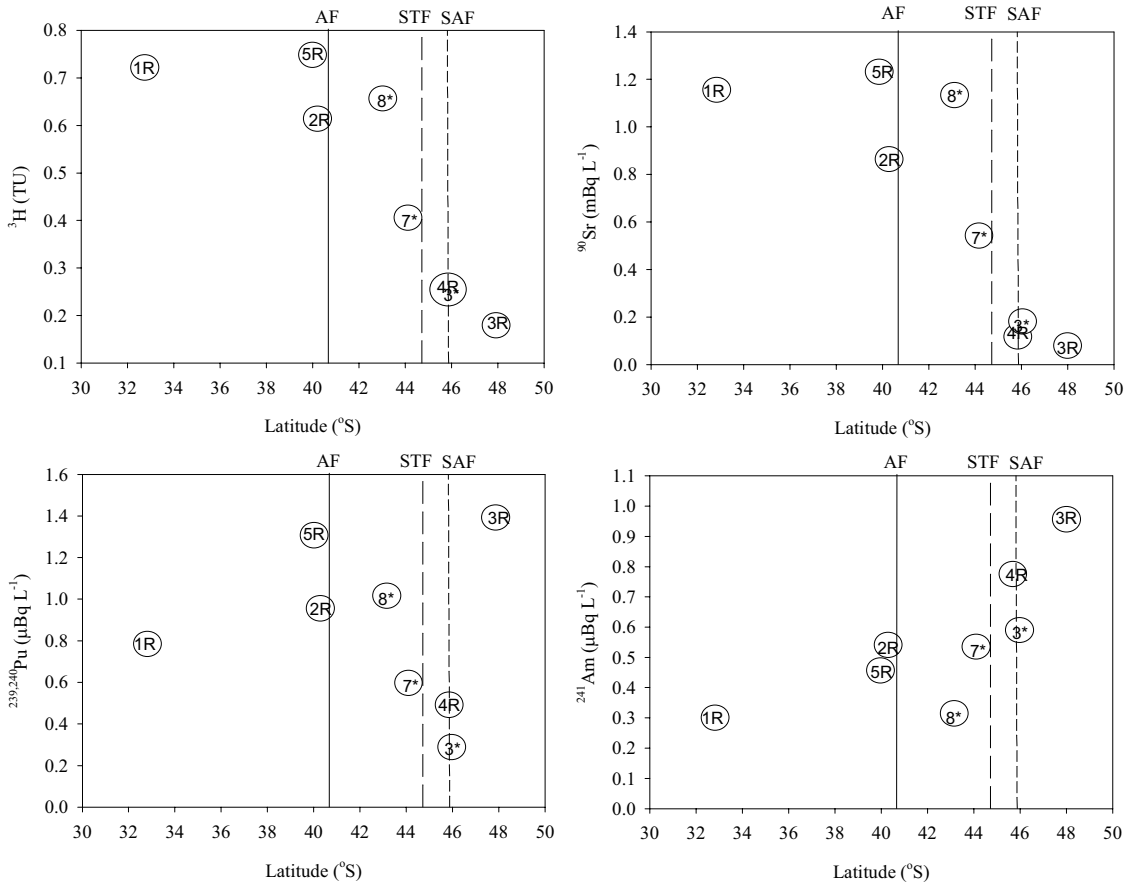

FIG. 2. Radionuclide concentrations in surface waters as a function of latitude (vertical lines represent water fronts).

Higher ^{3}H concentrations have been observed in bottom waters at Stations 3 and 7. This phenomenon has also been found in the Weddell Sea [6]. In general, the bulk of ^{3}H in the water column exist near surface due to the atmospheric input. A contribution by injection of Antarctic Bottom Water (AABW) might be considered as possible source. Below the CDW, the salinity and temperature decrease but oxygen increases, indicating a presence of AABW [7]. Higher ^{3}H levels observed in the bottom layers of SAF (Station 3) and STF (Station 7) could be explained as waters formed previously in the Weddell Sea surface water when ^{3}H levels were higher. Michel [8] reported for 1975-76 in the Weddell Sea 1 TU and 0.5-0.7 TU in surface and bottom water, respectively, and Haine et al. [9] estimated the transport time of surface water from the Weddell Sea to deep waters in the Crozet-Kerguelen Gap using CFCs, as 23 ± 5 years. Hence, 1 TU observed by Michel [8] in 1975-76 in Weddell Sea surface water may become of 0.27 TU in 1999 in deep waters in the Southern Ocean, what is in agreement with ^{3}H levels found at Stations 3 and 7.

3. Conclusions

The Indian sector of the Southern Ocean is a key region for the comprehension of the exchange of water masses between Antarctica and Equatorial regions, playing important role in better understanding of oceanographic processes and the global climate change. The observed distribution of radionuclides in the Crozet Basin, where different water fronts meet in a relatively small area, may therefore be regarded as a useful contribution to oceanographic studies using anthropogenic radionuclides as a complementary approach for tracing water masses in the ocean.

ACKNOWLEDGEMENTS

The authors thank the Captain and the crew of the R/V Marion Dufresne for their help during the ANTARES IV expedition. Colleagues participating in water sampling and pre-treatment of samples are highly acknowledged as well. The Agency is grateful for the support provided to its Marine Environment Laboratory by the Government of the Principality of Monaco.

REFERENCES

[1] TALJAARD, H.A., VAN LOON, H., Climate of the Indian Ocean south of 35°S (VAN LOON, H., Ed.) Climates of the Oceans, Elsevier, Amsterdam (1984) 505-601.

[2] MICHEL, E., LABEYRIE., L., DUPLESSY, J.-C., GORFTI, N., LABRACHAERIE, M., TURON, J.-L., Could deep Subantarctic convection feed the world deep basins during the last glacial maximum? Paleoceanography **10** (1995) 927-942.

[3] LEE, S.H., GASTAUD, J., LA ROSA, J.J., LIONG WEE KWONG, L., POVINEC, P.P., WYSE, E., FIFIELD, L.K., HAUSLADEN, P.A., DI TADA, L.M., SANTOS, G.M., Analysis of plutonium isotopes in marine samples by radiometric, ICP-MS and AMS techniques, J. Radioanal. Nucl. Chem. **248** (2001) 757-764.

[4] LA ROSA, J.J., BURNETT, W., LEE, S-H., LEVY, I., GASTAUD, J., POVINEC, P.P., Separation of actinides, cesium and strontium from marine samples using extraction chromatography and sorbents, J. Radioanal. Nucl. Chem. **248** (2001) 765-770.

[5] YOU, Y., Dianeutral mixing, transformation and transport of the deep water of the Indian Ocean, Deep-Sea Research I **46** (1999) 109-148.

[6] BAYER, R., SCHLOSSER, P. Tritium profiles in the Weddell Sea. Marine Chemistry **35** (1991) 123-136

[7] BOSWELL, S.M., SMYTHE-WRIGHT, D., HOLLEY, S.E., KIRKWOOD, D., The tracer signature of Antarctic Bottom Water and its spread in the Southwest Indian Ocean: Part II - Dissolution fluxes of dissolved silicate and their impact on its use as a chemical tracer, Deep-Sea Res. I **49** (2002) 575-590.

[8] MICHEL, R.L., Tritium distributions in Weddell Sea water masses, J. Geophys. Res. **83** (1978) 6192-6198.

[9] HAINE, T.W.N., WATSON, A.J., LIDDICOAT, M.I., DICKSON, R.R., The flow of Antarctic bottom water to the southwest Indian Ocean estimated using CFCs, J. Geophys. Res. **103** (1998) 27637-27654.

Temporal variation of ^{137}Cs distribution and inventory along 165ºE in the North Pacific from the 1960s to the present

Aoyama, M.[a], K. Hirose[a], K. Komura[c], K. Nemoto[b]

[a] Meteorological Research Institute,
Japan Meteorological Agency,
Ibaraki-ken,
Japan

[b] Japan Meteorological Agency,
Climate and Marine Department,
Ibaraki-ken,
Japan

[c] Kanazawa University,
Low Level Radioactivity Laboratory,
Kanazawa,
Japan

An enhanced observation of ^{137}Cs along 165 deg. E in the North Pacific Ocean was conducted in 2002. The primary objective of this enhanced observation is to develop an understanding of the present open-ocean distribution of radionuclides in the water column in this region. Relatively large numbers of ^{137}Cs concentration data [1] are available in this interested area since 1960s, then we are able to do a study on the temporal variation of ^{137}Cs distribution and inventory. Recent progress of ^{137}Cs measurements in seawater at an underground laboratory at Ogoya [2] made it possible to determine the ^{137}Cs concentration using small volume seawater samples.

The samplings in 2002 were carried out during two cruises by R/V Ryofu-maru operated by Japan Meteorological Agency. Among the stations between 49ºN and 6ºS along 165ºE, seawater samples shallower than 1000 m were collected at 20 stations. An average horizontal spacing was 350 km and vertical spacings were 100 m or less at each station. Sample volumes ranged from 10 to 20 liters. Deeper water samples were collected at 8 stations. Vertical spacings varied from 200 to 500 m and sample volumes varied from 20 liter to 100 liter for deeper seawater samples. A preliminary result of ^{137}Cs concentration along 165ºE for shallower layers is shown in Fig. 1.

^{137}Cs rich water was seen between 40ºN and 15ºN as shown in Fig. 1. The highest ^{137}Cs inventories were observed at latitudes between 30ºN and 40ºN in the North Pacific in the 1960s corresponding to the pattern of global fallout in this region [3]. The body of global fallout of ^{137}Cs in 2002 is, however, within the subtropical gyre where a maximum ^{137}Cs concentration was observed around 20ºN, the southern edge of the subtropical gyre, and in the 200–500 m layer. This finding supports the idea that the body of global fallout has been captured within the subtropical gyre during these four decades.

Southward transport also can be seen around 200 m depth between 20ºN and equator in Fig. 1. Aoyama et al. already showed that southward transport of ^{137}Cs had been caused an increase of ^{137}Cs inventory at the lower latitude of 10 – 20ºN in the 1970s and 1980s [3]. Hirose and Aoyama also reported that shorter apparent half-residence time of ^{137}Cs concentration in surface seawater occurred at the higher latitude in the North Pacific while longer apparent half-residence time of ^{137}Cs concentration occurred in the Equatorial Pacific [4]. These suggest that the southward transport of ^{137}Cs is an important process to regulate the temporal variation of inventory of ^{137}Cs and concentration of ^{137}Cs in surface water in the Equatorial Pacific.

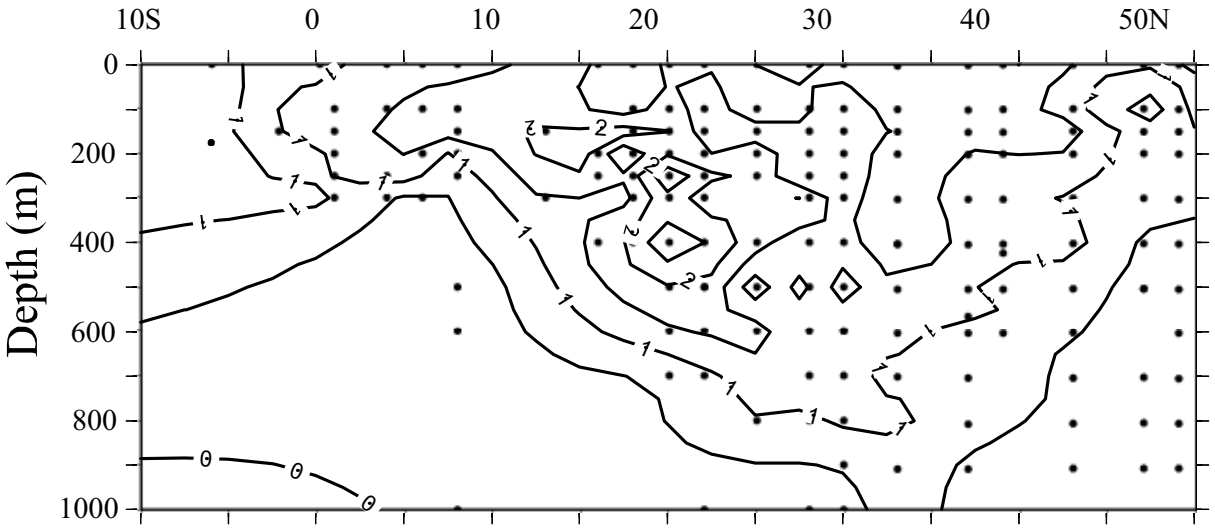

FIG. 1. Section of ^{137}Cs concentration (Bq m^{-3}). Dots show positions of sample. Measurements of about sixty samples at the southern part in this section have not yet been completed.

REFERENCES

[1] AOYAMA, M., HIROSE, K., Artificial radionuclides database in the Pacific Ocean: HAM database, The Scientific World **4** (2004) 200-215.

[2] KOMURA, K., Ogoya underground laboratory for the measurement of extremely low-level environmental radioactivity, (Int. Conf. Radioact. in the Environment, 2002, Monaco).

[3] AOYAMA, M., HIROSE, K., Temporal variation of ^{137}Cs water column inventory in the North Pacific since the 1960s, J. Environ. Radioact. **69** (2003) 107-117.

[4] HIROSE, K., AOYAMA, M., Analysis of ^{137}Cs and $^{239,240}Pu$ concentration in surface waters of the Pacific Ocean, Deep-Sea Res. II **50** (2003) 2675–2700.

Dissolved N_2O in Southern Ocean fronts at 140˚E; production, consumption and budget

Boontanon, N.[a,d], **S. Watanabe**[b], **N. Yoshida**[a,c,d]

[a] Frontier Collaborative Research Center,
Tokyo Institute of Technology,
Yokohama,
Japan

[b] Japan Marine Science and Technology Center,
Kanagawa,
Japan

[c] Department of Environmental Science and Technology,
Tokyo Institute of Technology,
Yokohama,
Japan

[d] Also with SORST project,
Japan Science and Technology Agency,
Saitama,
Japan

Abstract. The distribution of dissolved N_2O in Antarctic Ocean along 140˚E was measured during the austral summer in the framework of the 43rd Japanese Antarctic Research Expedition (JARE-43). Surface dissolved N_2O was undersaturated (about 94% saturation) so far examined and the calculated mean sea-air flux rate was -3.68 ± 2.57 $\mu molm^{-2}d^{-1}$. The vertical distributions exhibited the N_2O maxima at around 150-300 m (ΔN_2O, 7.90-9.04 nM) below the chl. *a* maximum zone, which coincided with the oxygen minimum layer. The fact strongly suggested a relation between the N_2O productions/consumptions and AOU. In the deeper layer, the vertical movement of cold water around Antarctica should be one of the parameters that governed the intramolecular distribution of isotopic compositions of N_2O. The influence of the deep Southern Ocean N_2O during austral summer, 2002 on the global N_2O budget was estimated to be about 46.2 ± 5.32 $MgN_2O\text{-}Nd^{-1}$ which could escape to the atmosphere and take a part of the world ocean emission.

1. Introduction

Antarctic Ocean has some unique characteristics, as a major component of the world ocean, by its circum polar homogeneous nature of its physical and chemical variables, the immense expanse of cold surface water, as well as by the most pronounced seasonal variation at the sea surface as compared with other ocean basins [1]. N_2O was produced by biological processes of both nitrification and denitrification [2-6]. Under different redox conditions, N_2O is produced by uses a different inorganic nitrogenous compound (NH_3 or NO_3^-), with different isotopic fractionation factors. Isotopic signatures of N_2O are well recognized to provide constraints for relative source strength and information on reaction dynamics concerning its biological production pathways of N_2O under investigation. Furthermore, the isotopomers of N_2O contains more clearly biogeochemical information on its sources than in a conventional bulk ^{15}N and ^{18}O measurements [7]. We describe here the results of the first isotopomers studies of dissolved N_2O in the Antarctic Ocean, which is one of the most productive seas

in the world, to examine the origins of N_2O in the seawater and estimates of the inventory of N_2O to the atmosphere.

The collection of the samples was carried out in the framework of the 43rd Japanese Antarctic Research Expedition (JARE-43) during the 2002 Marine Science Cruise from February 6 to March 7, 2002 by R/V Tangaroa which was conducted for the purpose of understanding the biogeochemical cycle and biological processes in the Southern Ocean and their roles in the global environment (Fig. 1a). Details of the procedures of dissolved N_2O and its isotopomers analyzes will be shown elsewhere.

2. Results and discussion

At the surface, N_2O concentrations were everywhere lower than atmospheric equilibrium. The excess N_2O (ΔN_2O) increased significantly toward the continental margins with the mean ΔN_2O was -0.88 ± 0.39 nM (93.91%). The isotopic compositions of dissolved N_2O were also slightly enriched in the same direction, from 8.06 to 8.45‰ for $\delta^{15}N^{bulk}$ and 45.64 to 46.51‰ for $\delta^{18}O_{SMOW}$. The isotopomers result shows more variable than bulk $\delta^{15}N$, the site preference ($\delta^{15}N^{\alpha}$-$\delta^{15}N^{\beta}$) value of 18.36‰ at St.1 that appears to be nearly the same as N_2O in the troposphere [7]. While about 3‰ depleted was observed at the shallower region (St.8; Fig. 1d). Dissolved N_2O of the surface layers of the sea is usually at or near saturation while the N_2O concentrations of the Southern Ocean surface layer were found to be below atmospheric equilibrium, however, it is not surprising because similar phenomenon was also observed in the other ocean [8]. Since several processes can control the N_2O concentrations level in the surface water, furthermore, physical factors, mainly temperature and wind, can normally affect gas saturation values up to about 5% super or under saturation [9]. The decreasing in the surface equilibrium of N_2O in Southern Ocean is suggested to be associated with the increasing in the transfer velocity which related to the wind speed while the temperature around those areas is quite stable during sampling period. In the surface water, the isotopic composition of dissolved N_2O was governed by the gas exchange with the atmospheric N_2O. Inoue and Mook [10] reported that the kinetic fractionations factors during N_2O invasion and evasion result to the slightly heavier about 0.7‰ for $\delta^{15}N$ and 1.1‰ for $\delta^{18}O$ of dissolved N_2O than those in air.

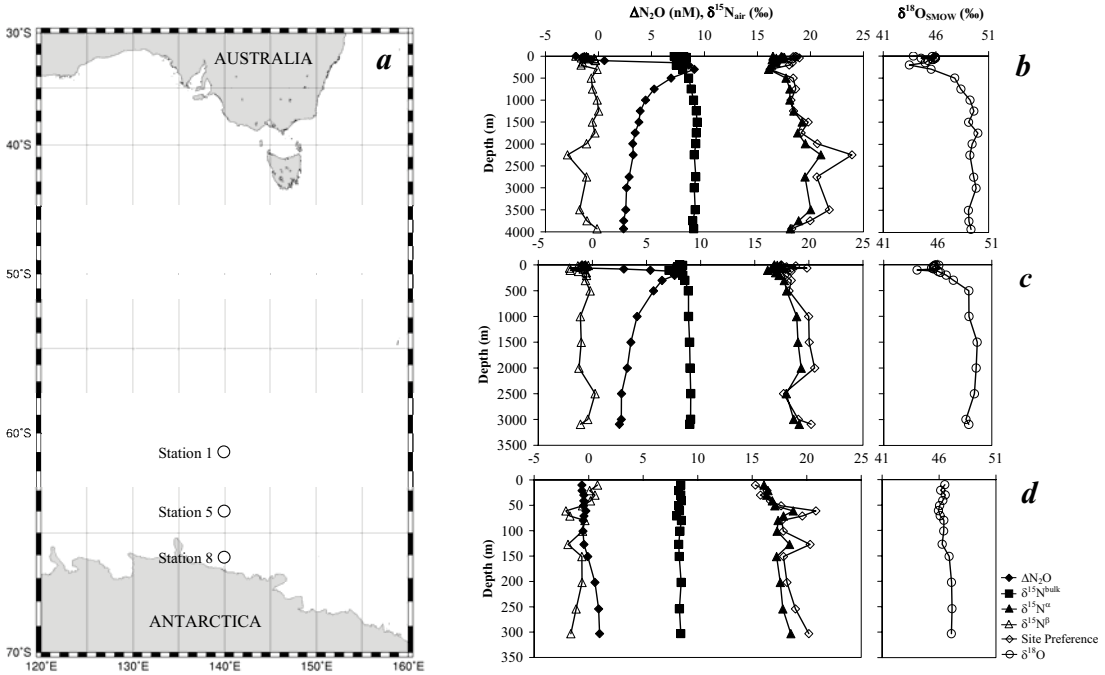

*FIG. 1. Location of sampling stations during JARE-43 Marine Science Cruise by R/V Tangaroa (**a**) and vertical profiles of the excess N_2O and isotopomers ratios ($\delta^{15}N^{bulk}$, $\delta^{15}N^{\alpha}$, $\delta^{15}N^{\beta}$ and $\delta^{18}O$) and site preference of N_2O observed at station 1 (61˚S; **b**), station 5 (64˚S; **c**) and station 8 (66.15˚S; **d**).*

The site preference was depleted from Sta.1 to Sta.8 associated with the enrichment of $\delta^{15}N^{\beta}$ while $\delta^{15}N^{\alpha}$ was much smaller variations which suggested that the β-site nitrogen heavier isotope ($^{15}N^{14}N^{16}O$) is slightly more soluble in the water than $^{14}N^{14}N^{16}O$. The former was caused by the significant difference in solute-solvent interaction (dispersion) energy between lighter and heavier molecules. The equilibrium fractionation of $\delta^{15}N^{\beta}$ in Southern Ocean were observed about +1.8 to +3.8‰ relative to the tropospheric $\delta^{15}N^{\beta}$-N_2O (~-3‰; [7]) and the fractionation is much larger than $\delta^{15}N^{bulk}$ (+1.06 to +1.45‰) which is the average of end and center nitrogen. These may caused by the kinetic fractionation of β-site nitrogen which much more active than center nitrogen during gas transfer across the gas-liquid interface, where the invasion process two processes have to be considered: dissolution and molecular diffusion near the surface, while for the evasion process only molecular diffusion from the water mass to the surface seems to exist [10].

Vertical distribution of dissolved N_2O was supersaturated from subsurface throughout the water column (Fig. 1b-d). The depth N_2O profiles show a concentration maximum (ΔN_2O maximum = 7.90-9.04 nM) between 100-200 m depth at the oxygen minimum layer. The ΔN_2O concentration generally decreased below 200 m at both, St.1 and 5, station. While St.8 profile did not show the N_2O maximum in subsurface, however, ΔN_2O concentration became supersaturated at the near bottom.

Bulk nitrogen and oxygen isotope ratios of dissolved N_2O at St.1 and 5 showed the subsurface minimum at the ΔN_2O maximum layer and both $\delta^{15}N^{bulk}$ and $\delta^{18}O$ maxima appeared at the bottom with a slight increase with depth. In the case of St.8, both $\delta^{15}N^{bulk}$ and $\delta^{18}O$ shows a constant value throughout the water column. Isotopomers of nitrogen, especially site preference, showed some vertical variation from subsurface to the deeper layers. Site preference decreased at the ΔN_2O maximum and slight increase with depth. Site preference maximum peak at St.1 appeared at about 2 200 m depth then decrease to the bottom. At St.5, site preference maximum were appear at about 2 000 m depth, and at the bottom. Although at St.8 the ΔN_2O and isotopic compositions did not shows their variation but site preference was much fluctuation throughout the water column. The maxima site preferences were appear at the depth of 60-140 m and also at the bottom. Subsurface N_2O was expected to be produced during the decompositions of sinking particles during summer season. In Southern Ocean that surrounds Antarctica, each summer, a phytoplankton bloom fueled by nutrient-rich waters leads to the growth of vast swarms of krill (*Euphausia superba*). During those phenomenon, the settling particles or fecal pellets may produce depend upon the life cycles of this krill, either directly or indirectly. The isotopic compositions of N_2O, +7.3 to +8.2‰ for $\delta^{15}N^{bulk}$ and +43.5 to +46.2‰ for $\delta^{18}O$, at the maximum layer were similar to the data obtained in the other oceans and freshwater ecosystem. The isotope ratios of N_2O suggested that N_2O was produced by the simultaneous occurrence of nitrification and denitrification processes of the sinking particles. With respect to the occurrence of redox conditions within an organic particle Kaplan & Wofsy [11] reported and suggested the occurrence of denitrification even in oxygenated water as long as large diameter of POM could provide to establish an anaerobic condition in the center of the particle. Since, N_2O produced during nitrification process in outer oxic layer could diffuse into inner layer and partly incorporated into denitrification processes. This kind of multi-occurrence of oxidation-reduction could provide the different isotopic signature of N_2O. In addition, $\delta^{15}N^{bulk}(N_2O)$ values became high and close to that of $\delta^{15}N(NO_3^-)$ (5-7‰ [12]), when N_2O was produced via denitrification processes. Ostrom et al. [13] reported the enrichment of ^{18}O by approximately 20‰ during nitrification process, since the $\delta^{18}O$ of dissolved O_2 was significantly high (+24.7‰) and produced N_2O is enriched in ^{18}O by +43 to +46‰ relative to seawater $\delta^{18}O$.

Since the site preference should be mainly dependent on production or consumption mechanisms, thus the relative considerations on the isotopomers of N_2O can further provide the constrain for the production mechanism of N_2O under investigation. In the above, the proposed N_2O production mechanism is considered by coupling of both nitrification and denitrification processes. Isotopic fractionation governed by kinetic isotope effects should occur during the reaction sequences for the outer layer while the oxidation of NOH does not involve a primary kinetic isotope effect and thus should not markedly affect site preference [14]. N_2O formed from dissimilatory nitrite reduction [15],

the N-N bond of N_2O is formed by nucleophilic attack of a second nitrite on a metal-coordinated nitrosyl species. The first N ultimately occupies the beta-position and fractionation could result in the process of nitrite binding to the ferrous heme following by nucleophilic attack of NO_2^- on the coordinated nitrosyl species resulting in the formation of the N-N bond can also lead to isotopic discrimination. These may results to the depletion of ^{15}N in center and terminal nitrogen of N_2O.

In the deeper layers, at the steady state, N_2O partly escaped with slightly enriched in $\delta^{15}N^{\alpha}$ while $\delta^{15}N^{\beta}$ shows only small fluctuation. Furthermore, in the deep water, the vertical movements of cold water from close inshore induced by the geopotential anomaly of the strong steering of the current by the ridge system around Antarctic, see [1 and 16], should be one of parameter to controls the isotopic compositions of N_2O (Fig. 2).

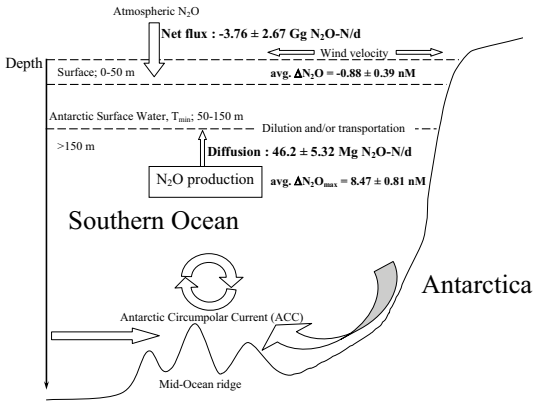

FIG. 2. Illustration summary of the results of dissolved N_2O in Southern Ocean during austral summer, 2002.

It is premature to calculate quantitatively the influence of Southern Ocean N_2O during austral summer, 2002 on the global N_2O budget. A conservation estimate shows that the N_2O flux found in this study would produce about 46.2 ± 5.32 $MgN_2O\text{-}Nd^{-1}$. This value is based on the assumption of upward N_2O flux and that the total surface area of Southern Ocean. This low production rate should be cause by the simultaneous occurrence of production-consumption of N_2O. However, these upward N_2O flux from N_2O maxima layer can be diluted or transferred by the current of fresh ice melting water. Thus, the emission of these N_2O may occur in the other areas depending upon the flow and diffusion rate. Furthermore, the existing data suggested that around the Antarctic Ocean is a large sinking spot of N_2O. We can estimate the sinking flux during austral summer, 2002 as about 3.76 ± 2.67 $GgN_2O\text{-}Nd^{-1}$ by using the sea-air flux and N_2O diffusion from N_2O maximum layer calculation.

REFERENCES

[1] LUTJEHARMS, J.R.E., "The oceanography and fish distribution of Southern Ocean", Fished of the Southern Ocean, (GON, O., HEEMSTRA P.C., Eds.), Smith J.L.B. Institute of Ichthyology, Grahamstown (1990) 6-27.

[2] DORE, J.E., et al., A large source of atmospheric nitrous oxide from subtropical North Pacific surface water, Nature **396** (1998) 63-66.

[3] KNOWLES, R., et al., Nitrous oxide concentrations in lakes: variations with depth and time, Limnol. Oceanogr. **26** (1981) 855-866.

[4] RYSGAARD, S., et al., Nitrification and denitrification in lake and estuarine sediments measured by the ^{15}N dilution technique and isotope pairing, Appl. Environ. Microbiol. **59** (1993) 2093-2098.

[5] SVENSSON, J.M., Emission of N_2O, nitrification and denitrification in a eutrophic lake sediment bioturbated by *Chironomus plumosus*, Aquat. Microb. Ecol. **14** (1998) 289-299.

[6] UEDA, S., et al., Accumulation of nitrous oxide in aerobic ground water, Water Res. **27** (1993) 1787-1792.

[7] YOSHIDA, N., TOYODA, S., Constraining the atmospheric N_2O budget from intramolecular site preference in N_2O isotopomers, Nature **405** (2000) 330-334.

[8] NAQVI, S.W.A., et al., Nitrous oxide in western Bay of Bengal, Mar. Chem. **47** (1994) 269-278.

[9] BIERI R.H., et al., Noble gas contents of marine waters, Earth Planet. Sc. Lett. **4** (1968) 329-333.

[10] INOUE, H.Y., MOOK, W.G., Equilibrium and kinetic nitrogen and oxygen isotope fractionations between dissolved gaseous N_2O, Chem. Geol. **113** (1994) 135-148.

[11] KAPLAN, W.A., WOFSY, S.C., "The biogeochemistry of nitrous oxide: a review", Advances in Aquatic Microbiology, (JANNASCH, H.W., WILLIAMS, P.J.B., Eds.), Academic Press, Florida (1985) 181-206.

[12] SIGMAN, D.M., et al., The $\delta^{15}N$ of nitrate in the Southern Ocean: Consumption of nitrate in surface waters, Global Biogeochem. Cycles **13** (1999) 1149-1166.

[13] OSTROM, N.E., et al., Mechanisms of nitrous oxide production in the subtropical North Pacific based on determinations of the isotopic abundances of nitrous oxide and di-oxygen, Chemosphere-Global Change Sci. **2** (2000) 281-290.

[14] POPP, B.N., et al., Nitrogen and oxygen isotopomeric constraints on the origins and sea-to-air flux of N_2O in the oligotrophic subtropical North Pacific gyre, Global Biogeochem. Cycles **16** (2002) 12-1.

[15] WEEG-AERSSENS, E., et al., Evidence from isotope labeling studies for a sequential mechanism for dissimilatory nitrite reduction, J. Am. Chem. Soc. **110** (1988) 6851-6856.

[16] ORIS, A.H., et al., On the meridional extent and fronts of the Antarctic Circumpolar Current, Deep-Sea Res.-I **42** (1995) 641-673.

Dynamics of a late spring phytoplankton bloom in the eastern Weddell Sea: short-timescale changes in $^{234}Th/^{238}U$ disequilibrium

Rodriguez y Baena, A.M.[a,b], J.C. Miquel[a], P. Masqué[c], J. La Rosa[a], E. Isla[d], T. Brey[e], J.A. Sanchez-Cabeza[c], S.W. Fowler[a]

[a] International Atomic Energy Agency,
Marine Environment Laboratory,
Monaco

[b] Dipartimento per lo Studio del Territorio e delle sue Risorse (DIP.TE.RIS.),
Universita' di Genova,
Italy

[c] Institut de Ciència i Tecnologia Ambientals,
Department de Física,
Universitat Autònoma de Barcelona,
Spain

[d] Institut de Ciències del Mar (CSIC),
Passeig Marítim de la Barceloneta,
Spain

[e] Alfred Wegener Institute for Polar and Marine Research,
Bremerhaven,
Germany

During the R/V "Polarstern" expedition ANT XXI/2 during November 2003-January 2004, short-timescale changes in $^{234}Th/^{238}U$ disequilibrium over a 25-day period were followed at a permanent station on the eastern Weddell Sea shelf (70°48.5 S, 10°44.0 W). The water column was sampled 16 times. At each sampling time, 2l-samples were collected at several (6 to 13) depths, spiked with ^{230}Th as a yield tracer, and precipitated according to the MnO_2 small volume technique [1]. Following beta counting, samples were alpha-counted for chemical recovery. Simultaneously, ^{234}Th fluxes were measured in sediment traps deployed in an adjacent region. According to CTD-fluorescence and plankton observations, a phytoplankton bloom was developing during the sampling period.

These results have been used for modelling ^{234}Th dynamics in the water column by a non-steady state distribution model [2]. Most measured total ^{234}Th activities in the water column were quite high compared to classically reported oceanic values. In some instances ^{234}Th may have been present in excess relative to its parent ^{238}U. One possible explanation for this imbalance could be the input of sea-ice algae, highly enriched in ^{234}Th, which typically occurs in this region due to sea-ice melting [3].

Sediment-trap measurements showed that ^{234}Th fluxes throughout the bloom matched well with the expected trends, with peaks coinciding with periods of high total mass fluxes.

This work will allow future assessment of POC and PON export by combining ^{234}Th fluxes with POC(PON)/^{234}Th ratios in sinking particles collected by *in-situ* pumping and sediment traps at the base of the photic layer. The radioisotope-based fluxes will be compared with organic carbon and nitrogen fluxes determined with sediment traps, as well as with the phytoplankton standing stock during the same period.

ACKNOWLEDGEMENT

The Agency is grateful for the support provided to its Marine Environment Laboratory by the Government of the Principality of Monaco.

REFERENCES

[1] BUESSELER, K.O., BENITEZ-NELSON, C., RUTGERS VAN DER LOEFF, M.M., ANDREWS, J., BALL, L., CROSSIN, G., CHARETTE, M.A., An intercomparison of small- and large-volume techniques for thorium-234 in seawater, Mar. Chem. **74** (2001) 15-28.

[2] COCHRAN, J.K., BUESSELER, K.O., BACON, M.P., WANG, H.W., HIRSCHBERG, D.J., BALL, L., ANDREWS, J., CROSSIN, G., FLEER, A., Short-lived thorium isotopes (^{234}Th, ^{228}Th) as indicators of POC export and particle cycling in the Ross Sea, Southern Ocean, Deep-Sea Research II **47** (2000) 3451-3490.

[3] RUTGERS VAN DER LOEFF, M.M., BUESSELER, K., BATHMANN, U., HENSE, I., ANDREWS, J., Comparison of carbon and opal export rates between summer and spring bloom periods in the region of the Antarctic Polar Front, SE Atlantic, Deep-Sea Res. II **49** (2002) 3849-3869.

OCEANS AND SEAS – POSTERS

GEOTRACES : An international program to study the global marine biogeochemistry of trace elements and isotopes

Jeandel, C.[a], R.F. Anderson[b], G. Henderson[c], R. Francois[d], M. Frank[e]

[a] LEGOS (CNRS/CNES/IRD/UPS),
Observatoire Midi-Pyrénées,
Toulouse,
France

[b] LDEO,
Columbia University,
Palisades, New York,
United States of America

[c] Department of Earth Sciences,
Oxford,
United Kingdom

[d] Woods Hole Oceanographic Institution,
Woods Hole, MA,
United States of America

[e] ETH,
Zurich,
Switzerland

GEOTRACES is a collaborative multi-national program to investigate the global marine biogeochemical cycles of trace elements and their isotopes. It is supported by the Scientific Committee for Oceanographic Research (SCOR).

Great advances in the analytical capabilities to measure trace elements and isotopes in the ocean have been made in the quarter century since the completion of GEOSECS, but much remains to be learned about the sources, transport, chemical speciation, biological availability, internal cycling and fate of the broad spectrum of trace elements and isotopes of interest to marine biogeochemists. Advances in chemical sensors, analytical instrumentation, and modeling make possible now research that could not have been envisioned even a decade ago. With the definition of a number of high priority research questions, and the availability of analytical techniques that permit sampling at high spatial and temporal density, the community of marine biogeochemists believes that the time is right to mount a major international research program to study the global marine biogeochemical cycles of trace elements and their isotopes.

Developing a full understanding of the distribution and biogeochemical behaviour of trace elements and their isotopes (TEIs) in seawater has the potential to provide unique insights into a wide range of oceanic processes: role of micronutrients in controlling the oceanic productivity, mechanisms controlling the fate of contaminants, quantifying key processes regulating the marine carbon cycle, insight into the mean velocity field and mixing processes in the ocean on very slow timescales, and paleo-oceanographic proxies.

The primary objectives for the GEOTRACES program are:

- To determine global distributions of selected TEIs in the ocean;

- To evaluate the oceanic sources, sinks, and internal cycling of these TEIs and thereby characterize more completely their global biogeochemical cycles;
- To build and maintain a core community of marine scientists who understand the chemical, physical and biological processes regulating the distribution and properties of trace elements and isotopes well enough to exploit them reliably in future interdisciplinary studies.

The establishment of a close and synergistic relationship between observations and modelling (forward and inverse) was also viewed as essential to streamline the field programs and optimise data interpretation.

We will elaborate on the goals of the program, describe the structure of the international coordination, and discuss the present status of the science and implementation plans.

Cadmium isotopic composition in the ocean

Lacan, F.[a], R. Francois[a], M. Bothner[b], J. Crusius[b], C. Jeandel[c]

[a] Woods Hole Oceanographic Institution (WHOI),
Woods Hole,
United States of America

[b] United States Geological Survey (USGS),
Woods Hole,
United States of America

[c] LEGOS (CNRS/CNES/IRD/UPS),
Observatoire Midi-Pyrénées,
Toulouse,
France

Recent developments in mass spectrometric techniques are allowing the systematic study of metal isotope fractionation in the environment. Cd isotopes have, as yet, received little attention, notwithstanding the well-documented involvement of Cd in biological cycling and its wide range of isotopic masses, which make it a prime candidate for fractionation.

We will present the first data in the ocean. A seawater profile from the North Pacific Ocean shows little yet probably significant variations. The later could result from water mass advection or biological processes or both. We will also present a seawater profile from the Mediterranean (Dyfamed site) and measurements in phytoplankton cultures. In addition we will present measurements carried out in a sewage treatment plant (where high bacterial degradation occurs).

If confirmed, Cd isotopic fractionation could have wide-ranging biogeochemical and paleoceanographic applications. In particular, it could lead to the development of a paleoceanographic tracer for bottom water oxygen concentration, a parameter that would provide important new constraints on the marine carbon cycle and deep ocean circulation during glacial periods.

Coral skeletons as proxy records: assessment of carbon isotopes in laboratory cultured corals and coral heads from French Polynesia

Liong Wee Kwong, L.[a], C. Ferrier-Pages[b], A.J.T. Jull[c], P. Povinec[a]

[a] International Atomic Energy Agency,
Marine Environment Laboratory,
Monaco

[b] Centre Scientifique de Monaco,
Musée Océanographique,
Monaco

[c] NSF Arizona AMS Laboratory,
The University of Arizona,
Tucson, Arizona,
United States of America

Scleractinian corals, particularly those living in warm shallow waters, continuously grow whereby generating annual density bands that can provide time markers for the development of long isotopic chronologies. Corals thus act like paleoclimate recorders and the geochemical tracers contained in their skeleton can be assessed very precisely. A very useful application concerns the determination of radiocarbon in the consecutive bands of their aragonite. As the radiocarbon activity reflects the seawater ^{14}C content at the time of deposition, it is thus possible to reconstruct the radiocarbon concentration of the surface ocean back in time, therefore, have access to several centuries of SST and salinity data.

Figure 1 is a photo of a coral slab, cut along the vertical growth axis, collected in Fangataufa atoll in 1997, when IAEA-MEL conducted a radiological survey that took place in the atolls of Mururoa and Fangataufa [1]. The density-banding pattern can be clearly observed and may be accentuated by irradiating with UV light.

A portion of coral is carefully sampled and the density bands are separated before being grounded to a fine powder. Fifty mg of this material is then hydrolysed with 5 ml H_3PO_4 under vacuum. Finally, pure

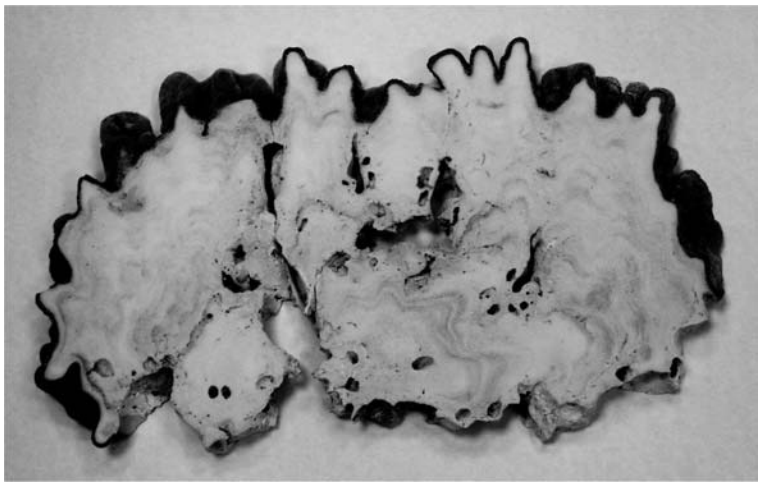

FIG. 1. A slice of a coral sample collected in Fangataufa Atoll.

CO_2 is cryogenically trapped before graphite synthesis [2]. The samples are currently being processed and the results will be available soon.

Screrochronology is based on the assumption that all the tracers, present in the seawater in which the coral is growing, be incorporated in the skeletal material. Several models put forward suggested the occurrence of isotopes kinetic fractionation during aragonite precipitation [3-5]. We propose to assess ^{13}C and ^{14}C in samples of corals that will be cultured under controlled laboratory conditions (temperature, light, salinity and food), at the Centre Scientifique de Monaco [6]. The main physiological parameters such as photosynthesis and growth will also be measured using PAM fluorimetry and the technique of buoyant weight respectively.

ACKNOWLEDGEMENT

The Agency is grateful for the support provided to its Marine Environment Laboratory by the Government of the Principality of Monaco.

REFERENCES

[1] POVINEC, P.P., et al., Marine radioactivity assessment of Mururoa and Fangataufa atolls, Sci. Total Environ. **237/238** (1999) 249-267

[2] LIONG WEE KWONG, L., POVINEC, P.P., JULL, A.J.T., Preparation of graphite targets from small marine samples for AMS radiocarbon measurements, Radiocarbon (2004) (in press).

[3] McCONNAUGHEY, T., ^{13}C and ^{18}O isotopic disequilibrium in biological carbonates: I. Patterns, Geochim. Cosmochim. Acta **53** (1989) 151-162.

[4] ADKINS, J.F., BOYLE, E.A., CURRY, W.B., Stable isotopes in deep-sea corals and a new mechanism for 'vital effects', Geochim. Cosmochim. Acta **67** (2003) 1129-1143.

[5] ROLLIN-BARD, C., CHAUSSIDON, M., FRANCE-LANORD, C., PH control on oxygen isotopic composition of symbiotic corals, Earth Planet. Sci. Lett. **215** 1-2 (2003) 275-288.

[6] REYNAUD-VAGANAY, S., GATTUSO, J.P., CUIF, J.P., JAUBERT, J., JUILLET-LECLERC, A., A novel culture technique for scleractinian corals: application to investigate changes in skeletal $\delta^{18}O$ as a function of temperature, Mar. Ecol. Prog. Ser. **180** (1999) 121-130.

^{137}Cs exchange processes in the Azov Sea

Matishov, D.G., G.G. Matishov, N.E. Kasatkina

Murmansk Marine Biological Institute KSC RAS (MMBI KSC RAS),
Murmansk,
Russian Federation

The aim of this paper is to establish current regularities of input, distribution and transformation of ^{137}Cs flow in the Azov Sea. Materials were water and bottom sediments samples collected in June 2003 in the Azov Sea during a complex MMBI expedition.

Current level of ^{137}Cs accumulation in the Azov Sea bottom sediments varies in the range of 6-76 Bq/kg dry weight (Fig. 1). In the Taganrog bay low ^{137}Cs (6.0 Bq/kg dry weight) concentrations are found in the coarse aleurite sands zone. The highest contents of the pointed out nuclide -50-76 Bq/kg is observed in the clayey silts of the central -the deepest part of the sea. In the Kerch strait fall-out ^{137}Cs activity in average is 20 Bq/kg dry weight.

^{137}Cs activity in the Azov Sea surface waters in June 2003 varies in the range 1.5-19.6 Bq/m^3 (Fig. 1). The highest concentrations of ^{137}Cs in the Azov Sea waters in 2003 were registered in the Kerch strait area (19.6 Bq/m^3). In the central part of the Azov Sea ^{137}Cs concentration is 8-11 Bq/m^3, in the Taganrog bay it lowers till 3-5 Bq/m^3, and in the river Don delta it is 1.5 Bq/m^3.

A weak correlation of the inverse proportional character is established between cesium accumulation in the bottom sediments and its concentration in the Azov Sea water masses.

Estimation of current flows of ^{137}Cs input and elimination in the Azov Sea is carried out. In 2003 0.03 TBq ^{137}Cs entered the Azov Sea with the Don river waters, 0.6 TBq ^{137}Cs entered from the Black Sea, thus, radio-nuclides deposing into the bottom sediments is a important factor of the Azov Sea waters self- purification.

General impression on the direction and transformation intensity of the ^{137}Cs ion run-off might be gained from the analysis of the migration of the dissolved form of this element in the estuary zone.

Dependency analysis of ^{137}Cs concentration in the Azov Sea water on salinity (Fig. 2) points out to the non- conservative behavior of ^{137}Cs in the Azov Sea. In the Kerch strait area solution in respect to the suspended phase is enriched with ^{137}Cs. But in the area from the Taganrog bay exit (salinity 8-10 PSU) there takes place a noticeable sorption of radio- nuclide on the suspension, as the result the suspension turned out to be enriched with ^{137}Cs in respect to the solution.

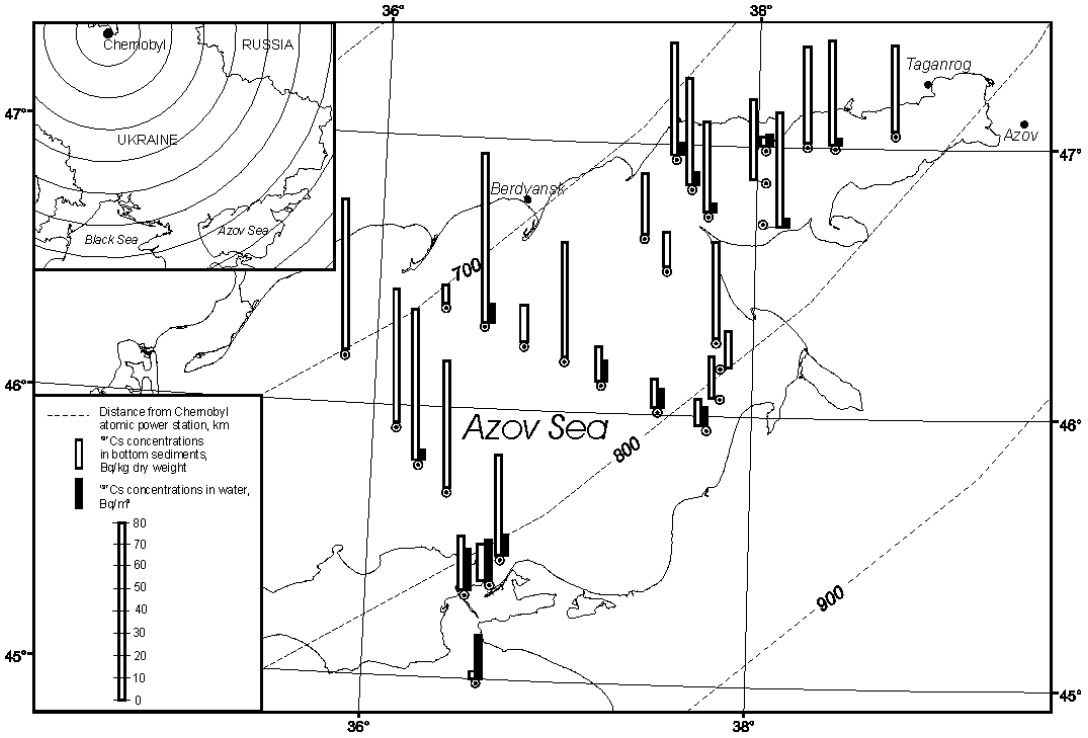
Chernobyl
RUSSIA
UKRAINE
Black Sea
Azov Sea
Taganrog
Azov
Berdyansk
Azov Sea
700
800
900
36°
38°
47°
46°
45°
Distance from Chernobyl atomic power station, km
137Cs concentrations in bottom sediments, Bq/kg dry weight
137Cs concentrations in water, Bq/m3
80
70
60
50
40
30
20
10
0

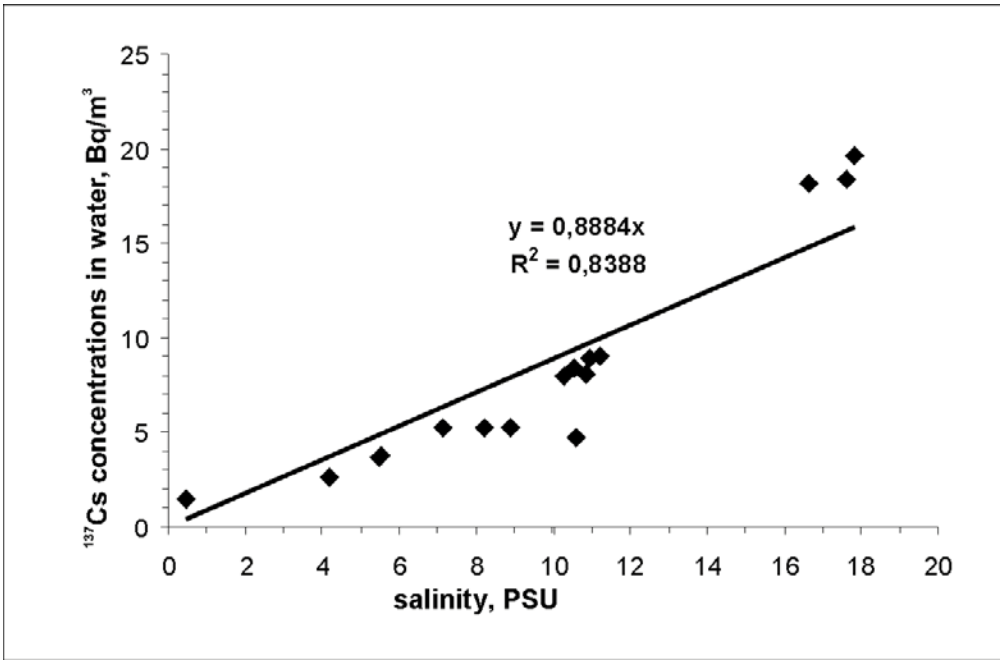
y = 0,8884x
R2 = 0,8388
137Cs concentrations in water, Bq/m3
salinity, PSU
0
5
10
15
20
25
0
2
4
6
8
10
12
14
16
18
20

Distributions of long-lived anthropogenic radionuclides (^{14}C, ^{129}I, and $^{239+240}Pu$) in coastal water columns off Sanriku, Japan

Shima, S., S. Gasa, K. Iseda, M. Kamamoto, H. Kofuji, T. Nakayama, K. Nishizawa, S. Mori, H. Kawamura

Japan Marine Science Foundation,
Mutsu,
Japan

The first commercial facility for reprocessing nuclear spent fuel in Japan is going to run in July 2006 and routine release of radionuclides to marine environment off Rokkasho will begin. Off Rokkasho area is located in the boundary where subarctic (Oyashio) and subtropical (Kuroshio) gyre mixes [1]. And the Tsugaru Warm Current (TWC) flows into this region through the Tsugaru Strait and originates in the Kuroshio flowing in the Sea of Japan/the East Sea (see Fig. 1). Those three water masses of different origins and coastal water mass coexist in the surface layer of this domain. So it is important to clarify the distribution of anthropogenic radionuclides and their behaviors in the coastal seawater.

Seawater samples were collected by use of CTD/Multi-Bottle Samplers (MBS) and large volume samplers (LVS) in October 2001 and June 2002. Carbon-14 and ^{129}I were analyzed by accelerator mass spectrometry (AMS) and $^{239,240}Pu$ was determined by the method of radiochemical separation and alpha spectrometry.

Th long-lived radionuclide concentrations for all samples were in the range -233 - 75‰ for $\Delta^{14}C$, not detected (N.D.) - 2.5×10^{7} atoms/Lfor ^{129}I, and N.D. - 0.025 mBq/L for $^{239,240}Pu$, respectively. The other anthropogenic radionuclides have the same concentration as those reported by the other organization. The vertical profiles of ^{14}C and ^{129}I decreased monotonically with depth as shown in Fig.2. On the other hand, $^{239,240}Pu$ profile have maximum at a depth of 500 – 700 m. The plots of potential density versus the concentrations designate that ^{14}C and ^{129}I virtually occurred in the water column lighter than the density of 26.6 - 26.8 and slightly penetrate into dense deeper layer. The maximum of Pu concentration existed at a density of 26.8 - 27.2.

There is no difference of ^{129}I concentration between two water masses (Oyashio and TWC) classified according to water temperature and salinity [2]. $\Delta^{14}C$ concentrations in TWC are higher than those in Oyashio, because TWC flows in sea surface over Oyashio [3].

ACKNOWLEDGEMENT

Part of this research was conducted under a contract with the Government of Aomori Prefecture.

REFERENCES

[1] TOMCZAK, M., GODFERY, J.S., Regional Oceanography: An Introduction (2001) pdf version 1.2, 391 pp.

[2] HANAWA, K., MITSUDERA, H., Variation of water system distribution in the Sanriku Coastal Area, J. Oceanogr. **42** 6 (1986) 435-446.

[3] SHIMA, S., et al., Distribution and Seasonal Change of the Tsugaru Warm Current water off Rokkasho (Proc. Int. Workshop Distribution and Speciation of Radionuclides in the Environment, Rokkasho, 2000) 289-296.

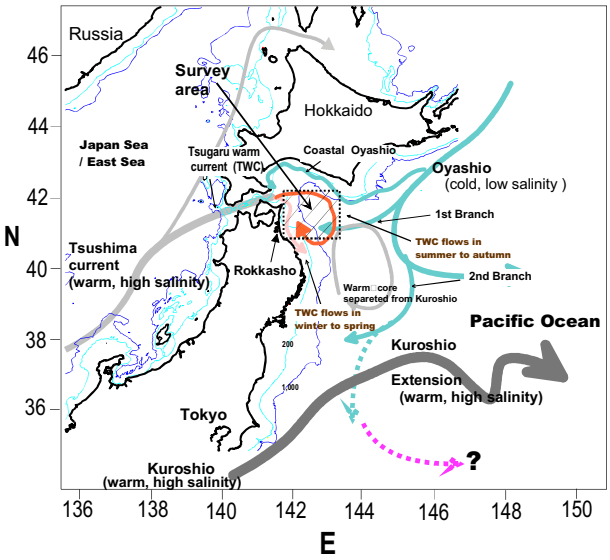

FIG. 1. Schematic distribution of water masses and flow pattern around the northern part of Japan.

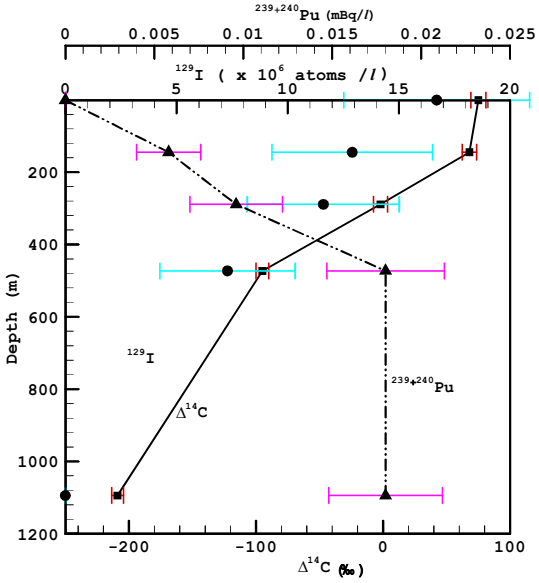

FIG. 2. Vertical profiles of radionuclides at Station 01W-2 (40°55.14' N, 142°19.89' E; Sampling date: Oct. 2001; bottom depth:1,130 m).

The Marine Information System (MARIS)

Povinec, P.P., P. Scotto, I. Osvath, H. Ramadan

Marine Environment Laboratory,
International Atomic Energy Agency,
Monaco

The IAEA's Marine Information System, a relational database based on a GIS (Geographical Information System), covering the distribution of radioactive and stable isotopes (and in the near future also other tracers and contaminants, such as organic compounds and trace metals) in the marine environment, as well as supporting oceanographic parameters (such as bathymetry, seawater temperature and salinity) has been developed in the Radiometrics Laboratory of the IAEA's Marine Environment Laboratory (IAEA-MEL) in Monaco. The first main objective of MARIS, building on the previously developed Global Marine Radioactivity Database (GLOMARD), is to provide information on radioactive contamination of the marine environment, by grouping and storing available data on the most important radionuclides in the world oceans and seas, in the open sea as well as in coastal zones, specifically in seawater, particulate matter, biota and sediment. Quantification of the sources of radionuclides in the world's oceans and seas, computer modelling of the dispersion of radionuclides and radiological assessment studies require that IAEA's Member States be provided with information on the past and present levels of radionuclides in the marine environment. The IAEA acts as a clearing-house for information on radioactive contaminants in the marine environment and makes data on marine radionuclide levels available to Member States for future assessment studies and the evaluation of trends in the contamination of the marine environment. In this respect IAEA-MEL has been acting as a central facility for the collection, synthesis and interpretation of data on marine radioactivity in the world ocean with the aim: (i) to provide immediate and up-to-date information on radionuclide levels and inventories in the seas and oceans; (ii) to provide a snap-shot of radionuclide levels at any time in any location; (iii) to investigate changes with time in radionuclide levels and inventories; (iv) to provide data for validation of models on the dispersion of radionuclides in the marine environment, (v) to provide bases for assessments of radiation doses to local, regional and global human populations and to marine biota, and (vi) to identify gaps in available information. The data provided by MARIS will be used as the international reference source on the radionuclide contamination of the marine environment so that any further contributions from nuclear industry, radioactive waste disposal sites, nuclear weapons test sites and possible nuclear accidents can be identified. The second main objective of MARIS is to provide information on distribution of radioactive and stable isotopes, trace metals and organic compounds in the world oceans and seas, which could be used as tracers for investigation of marine processes. This part of the database will be growing substantially in the near future, so that data on all important oceanic tracers will be available to IAEA's Members States for oceanographic investigations. The data stored in MARIS could be used for water and sediment dynamics studies, investigation of processes in the water column, seawater-sediment interactions, seawater-groundwater interactions, etc., as well as for validation of models used in climate change studies. Figure 1 illustrates a graphical product based on data, compiled from Member States' institutional databases and publications and included in MARIS, for ^{137}Cs in surface waters of North and Baltic Seas during the period 1986-1988. The on-line version of MARIS, containing validated datasets, is currently undergoing final tests, being available via the IAEA web site http://maris.iaea.org/.

ACKNOWLEDGEMENT

The Agency is grateful for the support provided to its Marine Environment Laboratory by the Government of the Principality of Monaco.

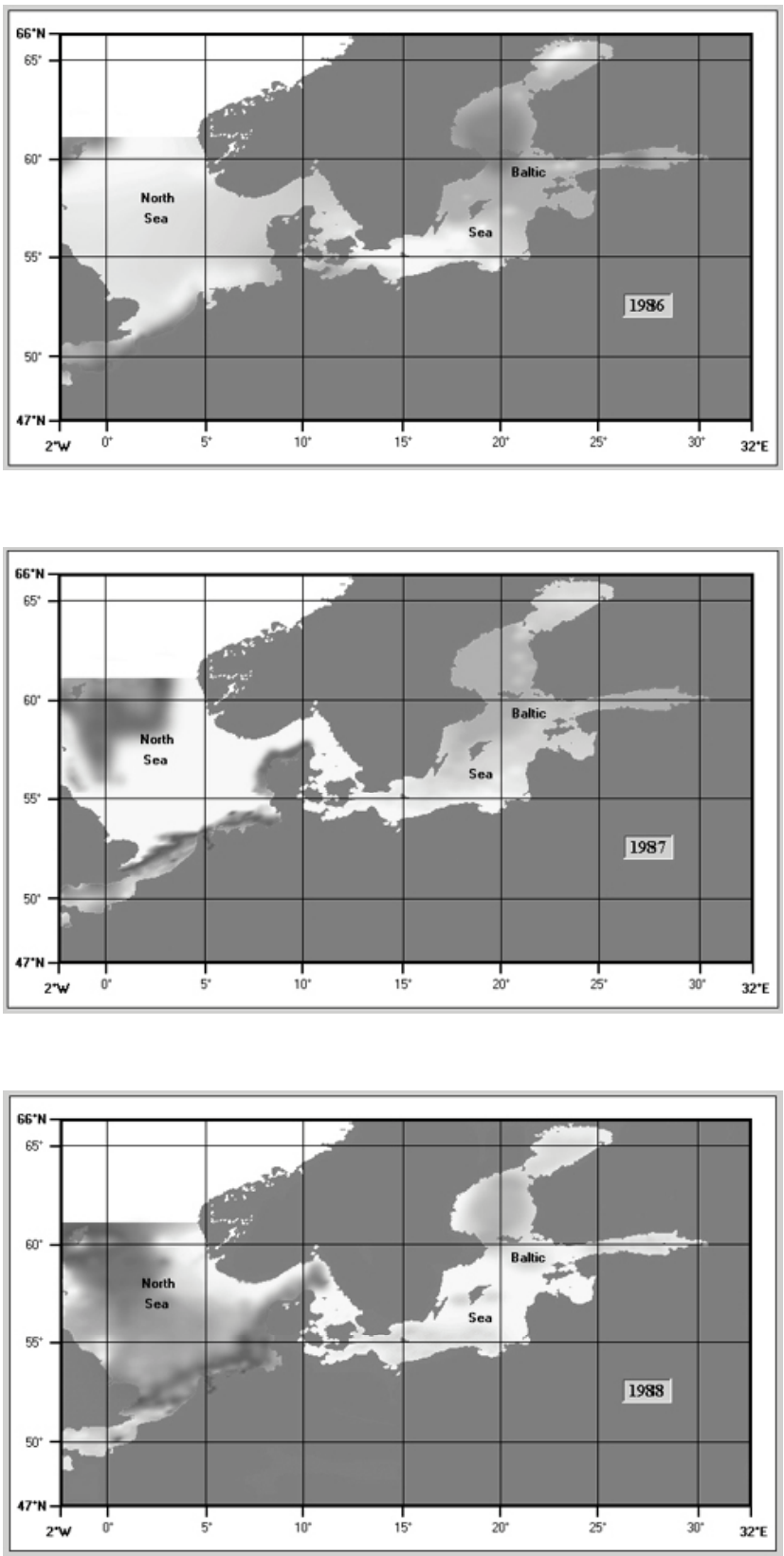

FIG. 1. ^{137}*Cs in surface waters (0 - 50 m) of North and Baltic Seas during 1986-1988, based on data from the MARIS database (Bq·m*$^{-3}$*).* **See ANNEX I, p. 660 for colour figure**

MEDITERRANEAN SEA

The Nile and the Levantine pump

Halim, Y.

Oceanography Department,
Faculty of Science,
Alexandria University,
Alexandria,
Egypt

Abstract. Basic characteristics of the Nile river and its impact on the Levantine Sea are presented and discussed. Both during the pre- and post-High Dam eras, the Nile was and still is one of the driving forces for the Levantine oceanographic system and presumably beyond, although in different ways.

1. Introduction

The summer of the year 1964, forty years ago, the Nile river was allowed for the last time to freely outflow into the Levantine sea before the Aswan High Dam became functional. An impetuous flood wave about 50 km^3 in volume spread by the end of summer over the south-east sub-basin with a climax in October (Fig. 1).

The periodical discharge of this large volume of river water with its heavy load of suspended sediments, dissolved and particulate nutrients had a drastic impact on the biological economy and the hydrography of the recipient basin. Its diluting effect is recorded up to Beirut and further north, in some years reaching up to the coast of Turkey [2] (Figs 2 and 3).

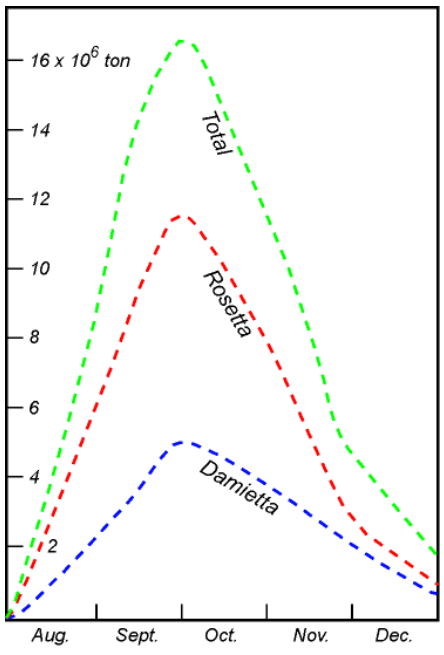

FIG. 1. Average monthly outflow of Nile waters for the five years 1959-1963 (Data modified from [1]).

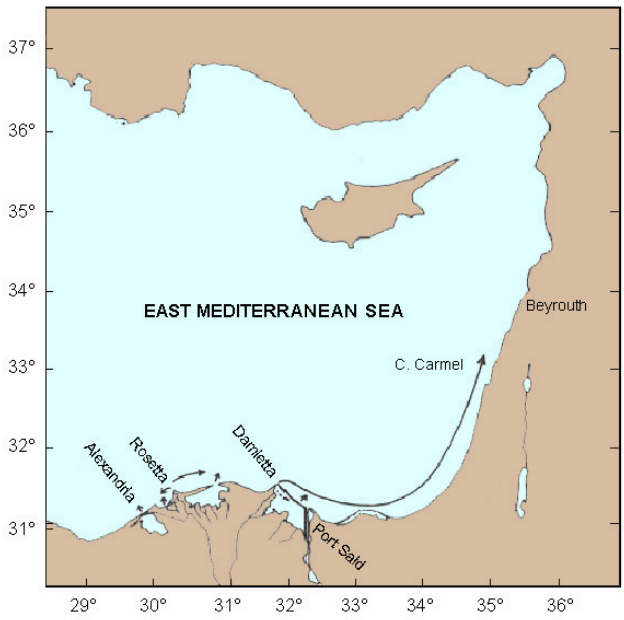

FIG. 2. Trajectory of the Nile stream (modified from [2]).

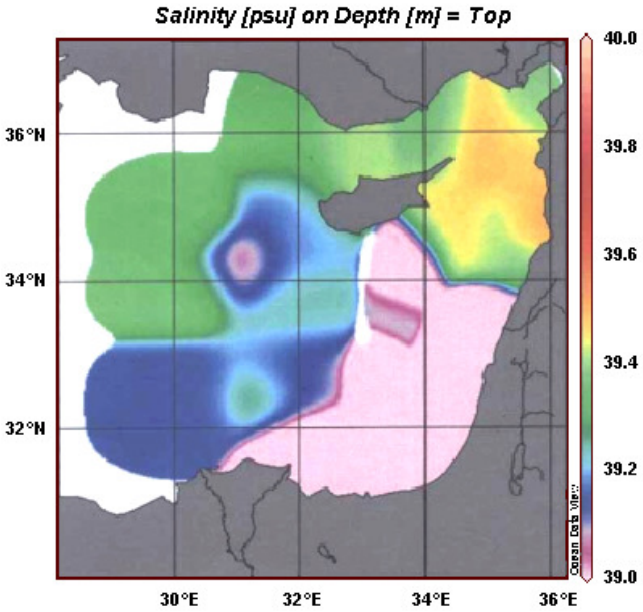

FIG. 3. Surface salinity for the eastern Levantine Sea, integrating all available data from 1900 to 1964. **See ANNEX I, p. 661 for colour version of figure.**

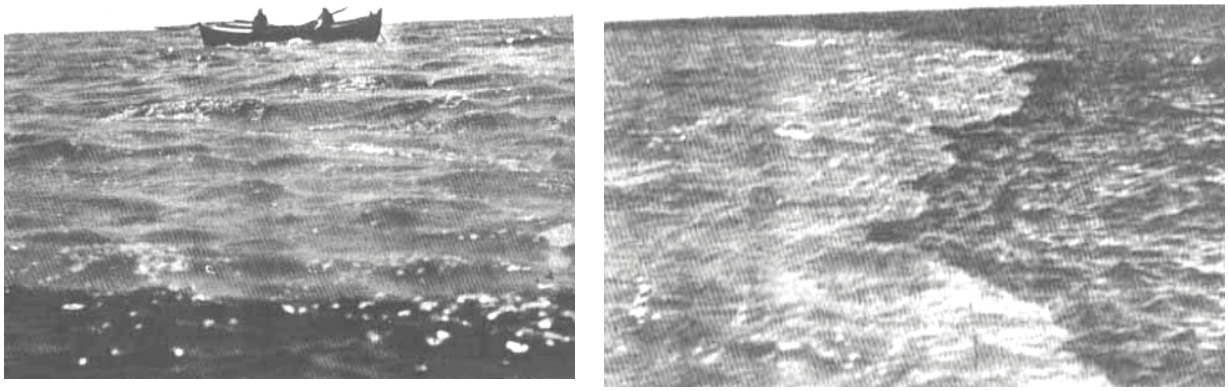

FIG. 4. The Stream front (after [3]) showing left: seawater in the foreground and the Stream in the background and, right: the stream to the left and seawater to the right.

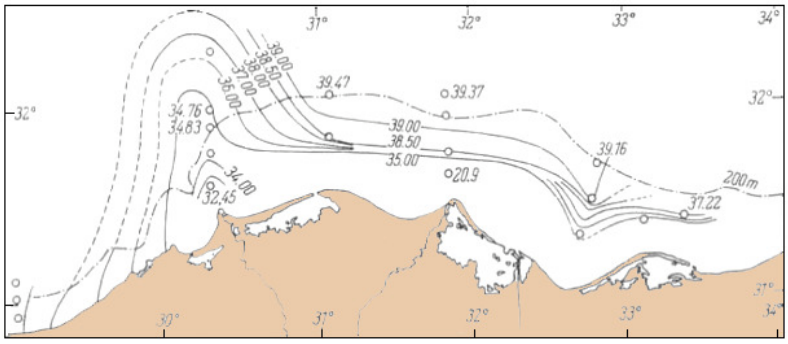

FIG. 5. Surface isohalines off the Nile Delta during October 1964 [1].

2. The Nile characteristics

In the vicinity of the two river outlets, the turbid floodwater could be seen as a well-defined "Nile Stream" sharply bounded by a discontinuity front along the 26 isopycnal line (Figs 4-6).

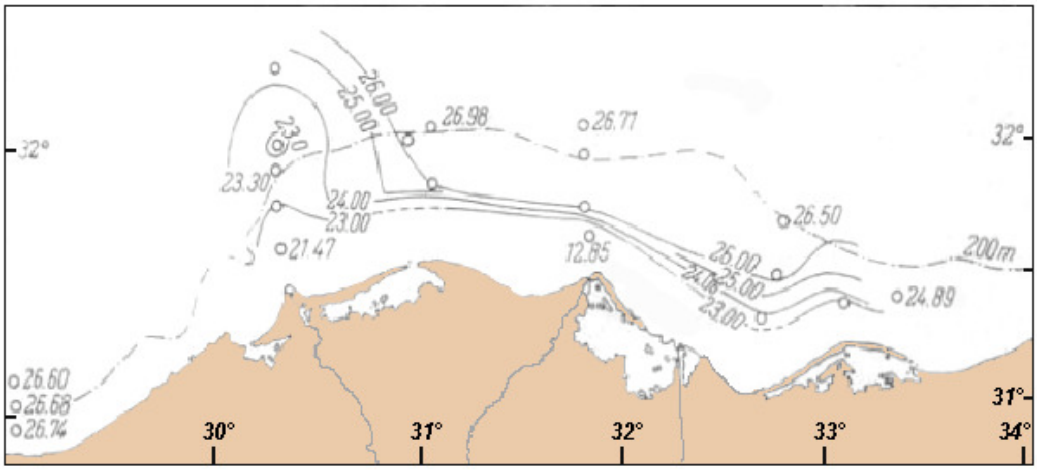

FIG. 6. Surface isopycnals off the Nile Delta in October 1964 [1].

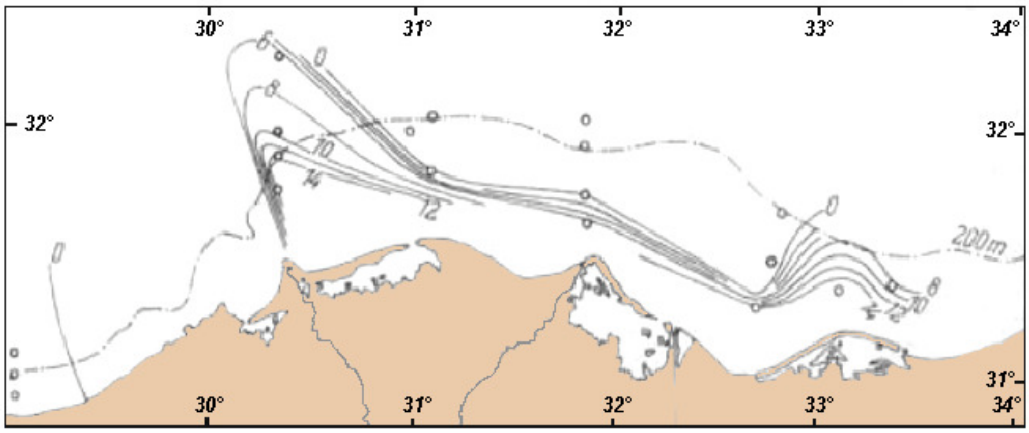

FIG. 7. Bathymetric topography of the 26-isopycnal surface [1].

The stream cut its way eastward along the Delta forming an elongated trough bounded at 14 to 18 m depth by the pycnoclyne layer. This layer of discontinuity acted as a riverbed on which sinking phytoplankton cells and silt particles accumulate, reducing dissolved oxygen (Fig. 7). Further east, with increasing distance, the stream waters gradually merge with Mediterranean waters.

Considerable amounts of nutrient salts, both dissolved and silt-adsorbed, were brought down and spread by the stream over its area of extension during the flood season. It has been estimated that about 8.2 x 10^3 tons of dissolved phosphate and 410 x 10^3 dissolved silicate were injected into the sub-basin during the flood season of 1964, an exceptionally high flood season [4], (Fig. 8).

The silt-adsorbed phosphate fraction was experimentally shown to be at least five times the dissolved fraction [5]. The adsorbed fraction is gradually released with dilution with poorer seawater as the stream travels eastward.

The flood outflow triggered the development of a massive bloom within hours from its release to the sea. Fuelled by the continued input of nutrients, the bloom extended over a vast area from the outlets to the front and remained active during the four months of the flood season. It was extensive in both space and time, in spite of heavy grazing by fish and zooplankton (Fig. 9).

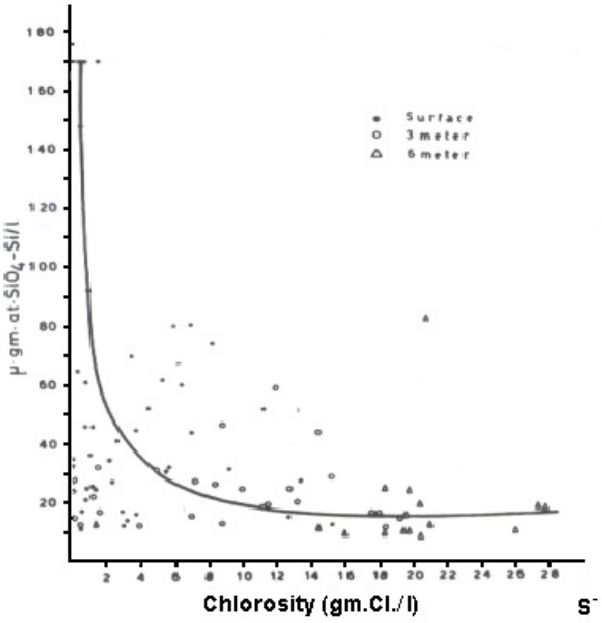

FIG. 8. Silicate-chlorosity relation for the Nile water at Rosetta estuary [6].

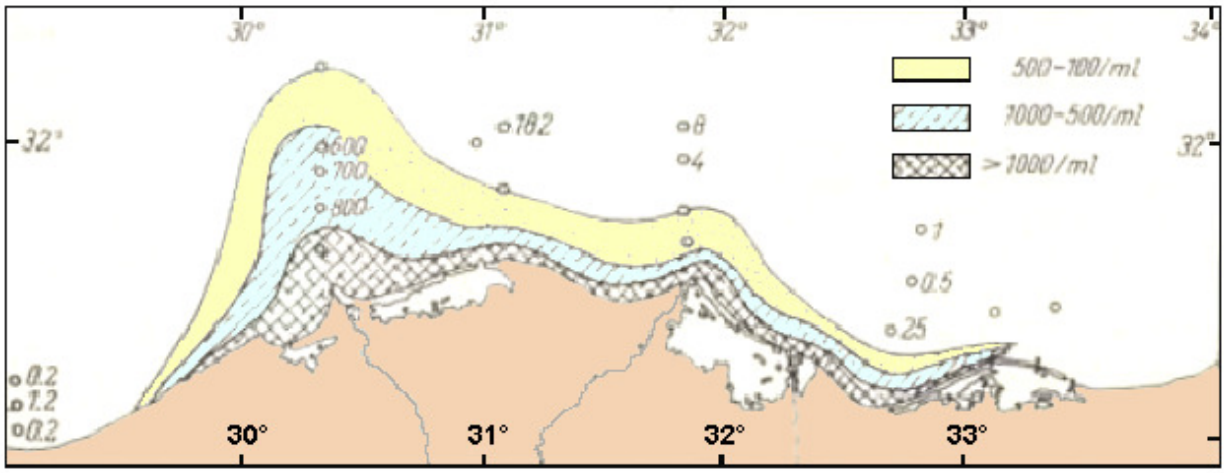

FIG. 9. The Nile bloom in October 1964 [1].

During this season, the notorious oligotrophy of the southern Levantine Sea gave way to a highly productive environment, one of the most productive environments of the Mediterranean basin. The food web was enhanced at all levels.

Before the Nile bloom the phytoplankton assemblage was relatively low in density but diversified, comprising Ebriidae, Dinoflagellates, and Diatoms. The Nile bloom is exclusively composed of Diatoms but it is not monospecific. This is a character which distinguishes such "natural" blooms from the so called "red tides" which, as a rule, are monospecific, and in most cases caused by the proliferation of a dinoflagellate species (Table I).

This was the main fishing season for pelagic and benthic filter-feeders and their predators. The bloom sustained an important Sardinella fisheries, which in this season only contributed about 20,000 tons, 40% of the total annual yield. The shrimp fisheries landed 7,000 tons.

Table I. Dominant Nile bloom species

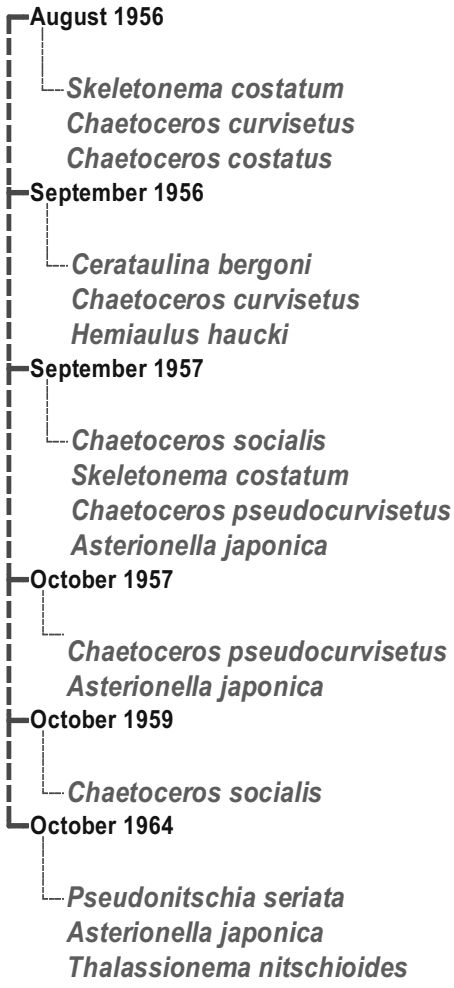

3. The post-damming conditions: decline and recovery of the fisheries

The completion of the Dam in 1967 was followed by the almost disappearance of the Nile bloom and a steady decline in fisheries. For 13 years, from 1967 to 1980 the catches remained at 10 to 25% of pre-dam levels. The Sardinella fisheries, which directly depend on primary production, were more impacted, dropping to less than 1,000 tons/year. The index "pelagic to demersal catch" dropped from 2.2 to 0.5 [4], (Fig. 10). This is not the only case of a drop in coastal zone productivity following damming of large rivers. As a matter of course, therefore, there is universal agreement that the quasi-collapse of Egyptian fisheries was caused by a single factor, the damming of the Nile. On closer inspection, however, at a greater resolution, this interpretation proves to be an over-simplification.

Both the decline and the remarkable recovery that followed provide one more example of the close interrelations between environmental and socio-political functions. The year 1967 witnessed both the completion of the dam and the June 1967 war. The recovery began with both increased agricultural runoff to the coastal zone following the regulation of the river, on one part, and with the peace treaty on the other.

After the events of mid-1967, military and security constraints on the movements of the fishing boats resulted in the shrinking of the fishing grounds. Fishing activities were only permitted in the inshore waters and by day-time. The waters off the Sinai coast became out of bounds for Egyptian fishermen. Furthermore, the available grounds became over-fished.

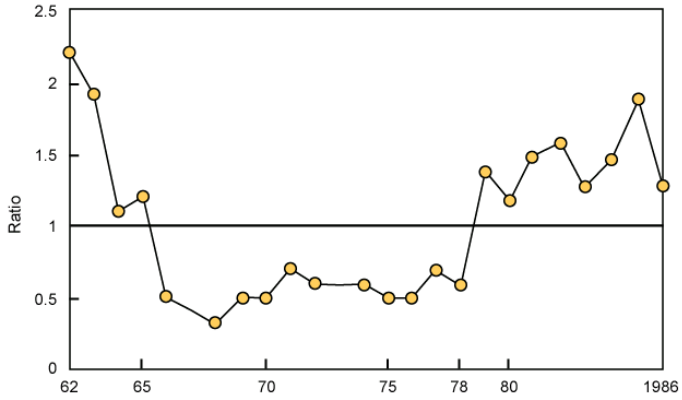

FIG. 10. Pelagic to demersal index from 1962 to 1986 [4].

The consistent declining trend was gradually reversed in 1978-1979. A phase of recovery begins and the catch rises to 52% of its pre-dam level by 1981. The upward trend was sustained in the following years. The recovery is to be interpreted as the result of a combination of factors, the restoration of normal conditions regarding fishing activities accompanied by a steady increase in the fishing effort and the use of improved fishing techniques.

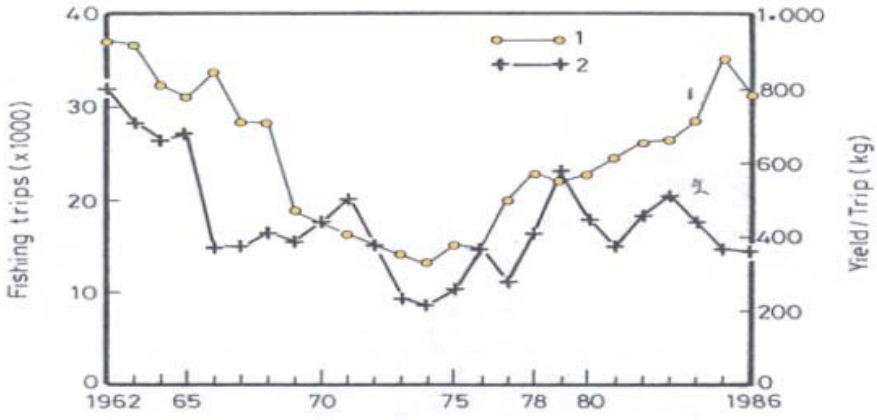

FIG. 11. Annual mean yield for mechanized boat, number of fishing trips (1) and yield per trip (2) [4].

The landing per fishing effort has also increased but with periodical fluctuations over several years, indicating over fishing (Fig. 11). A no less effective factor is the increased input of agricultural runoff to the coastal zone with the development of intensive agriculture following the greater availability of river water.

4. The post-damming flux

It would be misleading to think that the water input to the Delta coastal zone became restricted to the freshwater flux through the Rosetta outlet, now reduced to about 5-10% of the average pre-dam flux. There are eight large effluents from west to east, discharging agricultural drain water. This is Nile water that has undergone significant alterations. Irrigation water is collected in a system of ditches leading to drain canals which ultimately outflow into the coastal zone. Some outflow directly to the sea others through the coastal lagoons (Figs 12, 13).

In the ten years following the High Dam, land reclamation and more intensive agriculture have caused an increase of about 20% in the volume of drainage water in the Nile Delta. As a rule this water becomes enriched in nutrient salts and in dissolved humic materials and impoverished in oxygen. Soil silicate and nitrate from fertilizers dissolve in large amounts so that the silicate to phosphate and nitrate to phosphate ratios are abnormally high. The flux of agricultural drainage water through the

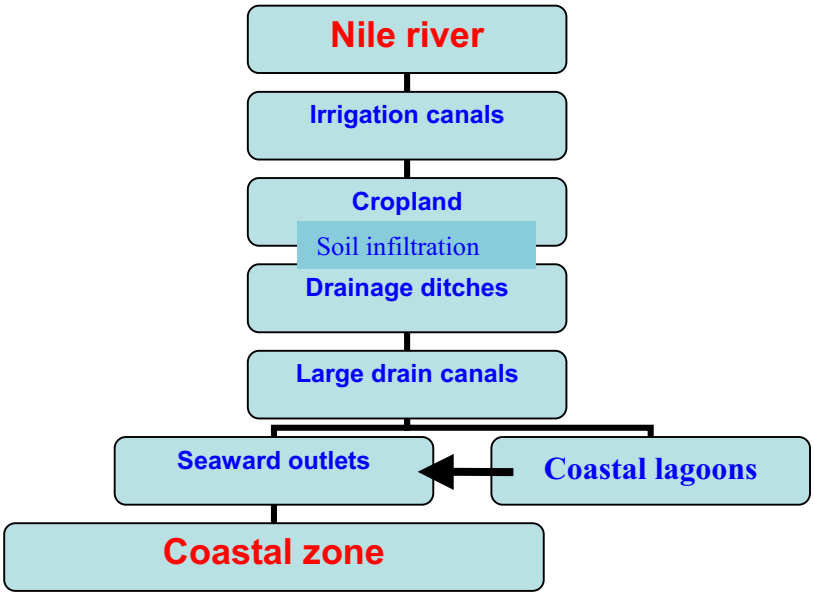

FIG. 12. Flow diagram: Nile water to drainage water to the coastal zone.

FIG. 13. The complex network of irrigation and drainage canals in northern Delta. From 1 to 8: effluent outlets.

eight effluents differs from the Nile flood in more than one aspect. The periodical pattern is replaced by a continuous one. While the impact of the Nile pulse was limited to three or four months, the drainage flux is continuous throughout the year.

Instead of two river outlets, the effluents are more or less equitably distributed from west to east along the coast. The level of dissolved nutrients is comparable, if not higher, but the total volume outflowing is smaller. Estimated at about 40% of the average pre-dam flow, it is devoid of suspended sediments.

A succession of localized bloom pulses throughout the year have replaced the massive autumn Nile bloom (Fig.14). As far as the fisheries are concerned, the post High Dam drainage pattern appears to have compensated the absence of the Nile input. The fisheries yield has recovered its pre High Dam level. These issues are also discussed by Nixon [7].

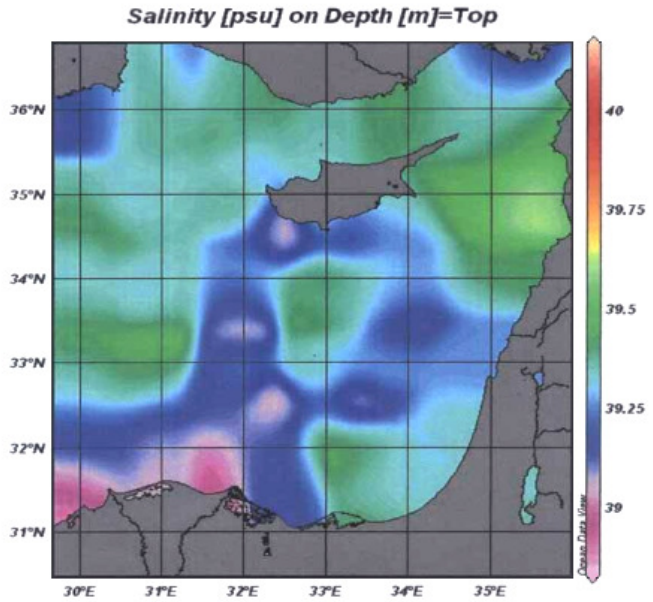

FIG. 14. Surface salinity of the eastern Levantine Sea, integration of all available data (1965-2000, October only). Showing localized dilution off the Nile Delta.

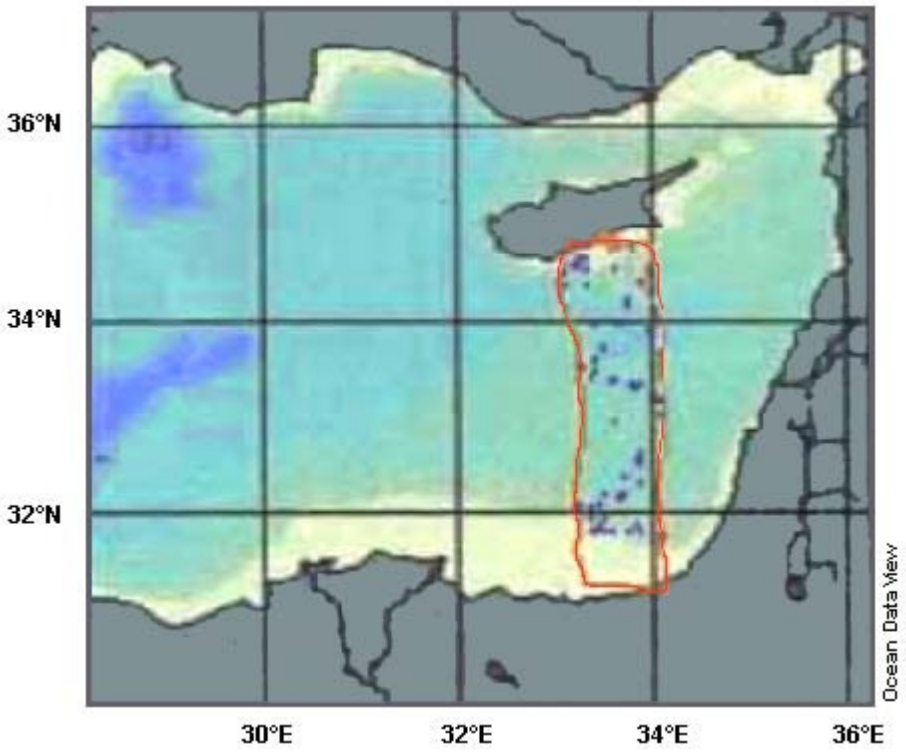

FIG. 15 a. Vertical profile, Egypt to Cyprus.

5. Impact of the high dam on the hydrography of the levantine sea. The "levantine pump"

The Mediterranean basin is known to be a concentration basin in an arid zone, where evaporation exceeds precipitation and river runoff. This is one of the main driving forces for its hydrographic system.

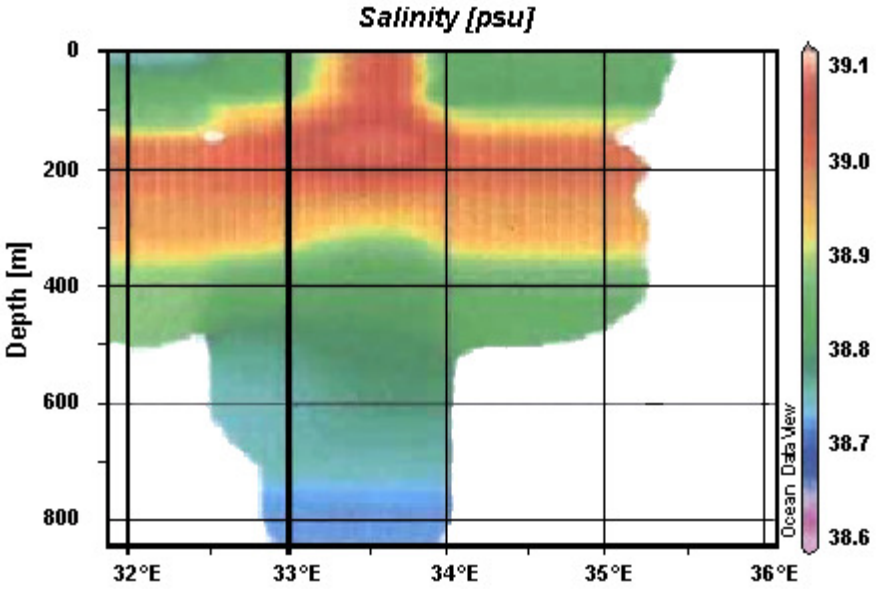

FIG. 15 b. The LIW, all available data 1900 to 1964 (end of winter).

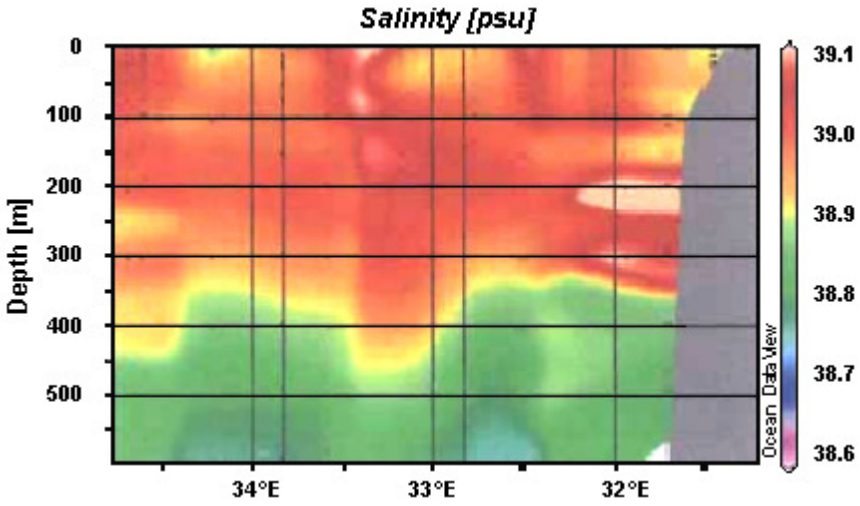

FIG. 15 c. The LIW, all available data 1965 to 2000 (end of winter).

The control of the river Nile has accentuated this process. Since the High Dam became functional, the salt content of the Levantine Sea has been on the increase, as shown by the data. The cumulative fresh water deficit for the past forty years comes to about 880 km^3, the drainage volume excluded. Winter vertical mixing is intensified by the rise in density that follows. A direct effect is to enhance the formation of the Levantine intermediate water, LIW. It is likely that several new source areas in the Levantine Sea contribute at present to its formation as already foreseen by Moreos [8]. The size of this water mass has actually been greatly magnified (Fig. 15 a, b, c).

It is not without interest to mention here the observation of Zore-Armanda [9]. She concluded that the increase in the Adriatic surface salinity is likely to be due to the deficit in the Nile fresh water input. The consequences are far reaching. The direct consequence will be an increase in the rate of what can be termed the "**Levantine pump**". The ultimate effect will be an acceleration of the rate of renewal of Mediterranean water. More Atlantic water will be pumped in and more Levantine Intermediate Water of higher salinity pumped out to the Atlantic ocean.

It can be concluded therefore, that both during the pre- and post-High Dam eras, the Nile was and still is one of the driving forces for the Levantine oceanographic system and presumably beyond, although in different ways.

ACKNOWLEDGEMENTS

The author is indebted to his colleague Prof. Ahmed El-Guindy for the data of Figures 3, 14, and 15. He is also very grateful to Miss Soha Shabaka who has given so much time and effort to produce the manuscript of this paper.

REFERENCES

[1] HALIM, Y., GUERGUESS, SH.K., SALEH, H.H., Hydrographic Conditions and Plankton in the Southeast Mediterranean during the Last Normal Nile Flood (1964), Int. Revue ges. Hydrobiol. **52** 3 (1967) 401-425.

[2] NIELSEN, J. N., Hydrography of the Mediterranean Sea and adjacent waters. Danish Oceanogr. Exped., 1908-1910, Vol 1 (1912) 77-191.

[3] HALIM, Y., Observations on the Nile bloom of phytoplankton in the Mediterranean, J. Conseil Intern. Explor. de la Mer. **26** 1 (1960) 59-67.

[4] HALIM, Y., MORCOS, S.A., RIZKALLA, S., EL-SAYED, M.KH., "The impact of the Nile and the Suez Canal on the living marine resources of the Egyptian Mediterranean waters (1958-1986)" Effects of reverine inputs on coastal ecosystems and fisheries resources, FAO Fisheries Technical paper **349** (1995).

[5] HALIM, Y., MORCOS, S.A., Le role des particules en suspension dans l'eau du Nil en crue dans la repartition des sels nutritifs au large de ses embouchures, Rapp.et Proces-verb., Comm. Int. Explor. Mer Medit., **28** (1966) 733-736.

[6] HALIM, Y., SAMAAN, A., ZAGHLOUL, F.A., Estuarine Plankton of the Nile and the Effect of Fresh-Water. Phytoplankton. In: Fresh-Water on the Sea. (Proc. Symp. Influence of Fresh-Water Outflow on Biological Processes in Fjords and Coastal Waters, 22-25 April 1974, Geilö, Norway), The Association of Norwegian Oceanographers, Oslo (1976).

[7] NIXON, S.W., Replacing the Nile: Are Anthropogenic Nutrients Providing the fertility once brought to the Mediterranean by a Great River? Ambio **32** 1 (2003) 30-39.

[8] MORCOS, S.A., "Sources of Mediterranean intermediate water in the Levantine Sea", Studies in physical oceanography, a tribute to Georg Wüst on his 80th birthday, (GORDON, A.L., Ed.) **2**, Gordon and Breach, New York (1972) 185-206.

[9] ZORE-ARMANDA, M., "Development of Mediterranean physical oceanography", Ocean Sciences Bridging the Millenia, A spectrum of historical accounts, UNESCO, Paris and China Ocean Press, Beijing (2004) 179-195.

The first decade of the big transient in the Eastern Mediterranean deep waters

Roether, W.[a], B. Klein[a], B.B. Manca[b]

[a] Institut für Umweltphysik,
University of Bremen,
Germany

[b] Istituto Nazionale di Oceanografia e di Geofisica Sperimentale-OGS,
Trieste,
Italy

Abstract. Using hydrographic and tracer data from four cruises of F/S METEOR, 1987 – 2001, we outline the changes in the deep waters of the Eastern Mediterranean that have occurred up to 2001. Aegean Sea output of highest-density waters was essentially restricted to 1992-94. While in the Levantine Sea, the distributions of temperature and salinity soon became fairly homogeneous laterally, those in the Ionian Sea were still highly non-uniform in 2001. The difference is ascribed to the special pathways of the Aegean-derived dense waters into and within the two seas, which are strongly controlled by bottom topography. Some relaxation of the original disturbance occurred after 1995, mostly by lateral water exchange, whereas significant bottom water formation did not resume until 2001. The deep waters have thus remained in a state far different from that of the classic situation, in which the Adriatic was the dominant source of the deep waters. Return to any quasi-steady state should take a century or longer. ^{3}He data taken in 1987, i.e., before the big event, demonstrate presence of helium released from the ocean floor in the deep and bottom waters of the Levantine Sea.

1. Introduction

The big changes in the hydrography and circulation of the Eastern Mediterranean that became evident during the year 1990 [1], now commonly termed the Eastern Mediterranean Transient (EMT), implied a shift of the production of deep and bottom waters from the Adriatic Sea to the Aegean Sea (Fig. 1). Starting from an enhancement of near-surface salinities in the Levantine Basin and the Cretan Sea (South Aegean) [2], the two extreme winters of 1991-92 and 1992-93 [3] induced the formation of particularly dense waters, which overflowed the sills of the Cretan Arc straits [4], mixing with and displacing the deep and bottom waters residing beyond [5, 6]. The total outflow has been estimated to amount to more than 7 Sverdrup·years (1 Sverdrup (Sv) = 10^6 m^3/s), replacing approximately 20% of the deep waters below 1600 m and lifting the deep waters upwards by up to about 500 m [1]. The Aegean production in its peak years thus exceeded several times that of the classical Adriatic source (~ 0.3 Sv [7, 8]). The changes up to 1995 have been addressed previously using data from two cruises of F/S METEOR in 1987 and 1995 [1, 6]. The present contribution deals with the further evolution of the EMT up to 2001, complementing other work [9, 10], and briefly looks into the future. It uses observations of four basin-wide cruises of F/S METEOR, 1987 – 2001, covering temperature, salinity, pressure (depth), and tracer measurements (chlorofluorocarbon-12 (CFC-12), tritium, ^{3}He). Relatively higher subsurface concentrations of tritium and CFC-12 point to an increased contribution of recently ventilated waters. Oceanic helium tends to equilibrate with atmospheric helium at the air-water boundary, but there are interior contributions of low-^{3}He release from the Earth's crust and high-^{3}He release from the mantle, and of ^{3}He generated by tritium decay ('tritiugenic' ^{3}He).

2. Tritium and ^{3}He pre-EMT sections (1987)

Figure 2 presents sections of tritium (Fig. 2a) and of δ^3He (Fig. 2b) along the East Mediterranean obtained during the 1987 METEOR cruise. Tritium concentrations, naturally, are largest in the upper waters. The elevated tritium evident at the base of the western slope reflects recent replenishment from

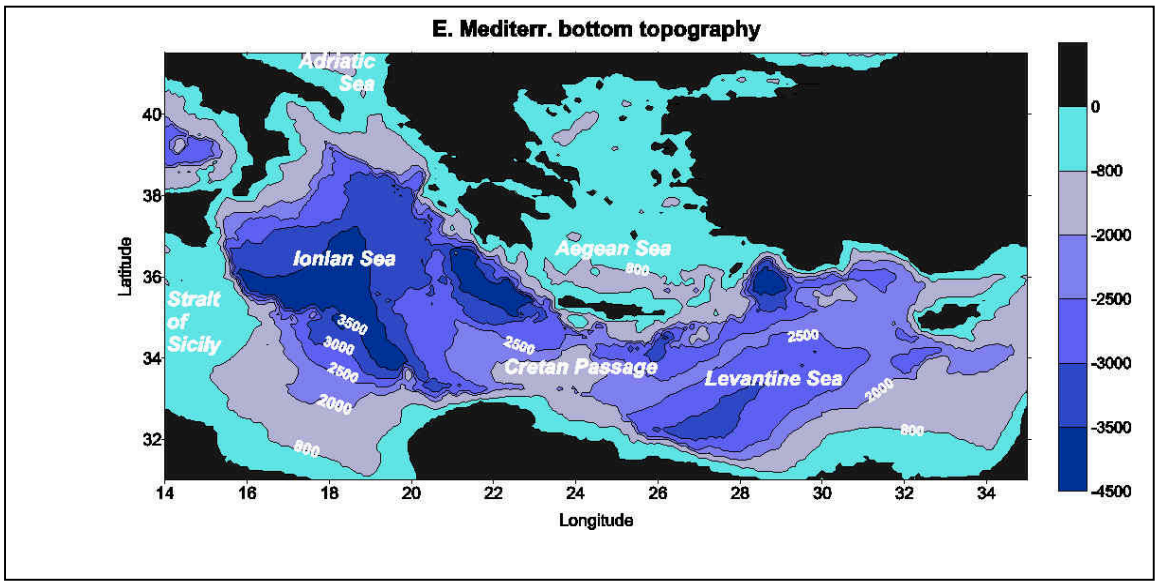

FIG. 1. Map of the East Mediterranean with geographic names and bathymetry. Otranto Strait (sill depth ~ 800 m) connects to the Adriatic, and Kasos Strait, east of Crete (~ 1000 m), provides the governing dense-water pathway out of the Aegean. The East Mediterranean Ridge separates the Hellenic Trench on its Cretan side from the rest of the East Mediterranean. The sill in the north of the passage is ~ 2700 m deep. The Strait of Sicily connects to the West Mediterranean. **See Annex I, p. 662 for colour version of figure.**

the Adriatic source. From here concentrations decrease eastward with a minimum at 1500 – 2000 m depth. Low tracer values extend upwards to roughly 600 m in the Levantine and to 1200 m further west. This distribution supports the classic notion that the deep waters are governed by a single convective cell fed by the Adriatic, and excludes penetration of Aegean-derived waters, and also of deep water formation within the Rhodes Gyre, to great depths in any significant amounts. Aegean outflow was rather apparent at several hundred m depth, causing the upper boundary of the convective cell to deepen south and west of Crete [11]. Other properties, such as CFC-12, entirely confirm this.

δ^3He (Fig. 2b) values at the surface approach equilibrium values with atmospheric helium ($\delta^3He_{equil} \approx$ -1.6%). Enhancement by tritiugenic ^{3}He is evident in a subsurface layer centered near 500 m depth and in the deeper waters wherever tritium concentrations (Fig. 2a) are sufficiently high. The maximum δ^3He values in the upper ^{3}He-rich layer toward the western slope and into Sicily Strait correspond to tritium/^{3}He 'ventilation' ages of approximately 12 years. A special feature is δ^3He values below δ^3He_{equil} in the Levantine deep and bottom waters, which arise from low-^{3}He release from the earth's crust. The release rate amounts to ~ 3 10^9 helium atoms/(m^2·s), with a mantle contribution of 5 % [12].

3. Observations during the EMT

Observations in 1995 of CFC-12 and other properties made clear that in the Cretan Passage and beyond, the deep-water tracer minimum of Fig. 2a had been filled in by dense, high-salinity waters released in large amounts from the Aegean Sea, that the release had lifted the 'old' deep waters upward by several 100 m, and that the tracer minimum had become weaker, indicating presence of recently ventilated Aegean outflow waters also at mid-depths [1]. In the west, pre-EMT (cf. Fig. 2a) and Aegean-derived elevated CFC-12 concentrations had merged. A 1999 survey found a horizontal relaxation of the CFC-12 distribution relative to that of 1995 [9], and further relaxation is evident in the observations of the 2001 METEOR cruise (not shown).

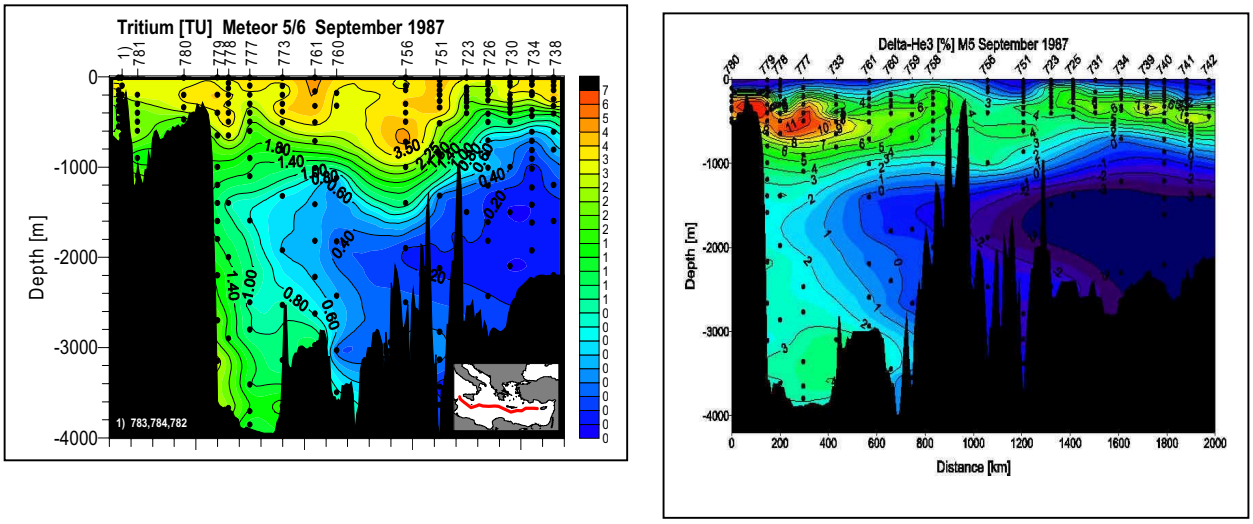

FIG. 2. Sections of tritium (TU; FIG. 2a, left) and of δ^3He (%; FIG. 2b, right) along the Eastern Mediterranean in Aug.-Sept. 1987 (METEOR cruise M5/6). Markings indicate data points, for tracks see inset map. δ^3He means the deviation of the ^{3}He/^{4}He ratio from that of atmospheric helium ($(^3He/^4He)_{atm} \approx 1.4 \cdot 10^{-6}$). Measurements by mass-spectrometer at Bremen [13]. **See ANNEX I, p. 662 for colour figure.**

Figure 3 shows temperature-salinity (T-S) diagrams of stations of the 2001 cruise that characterize the East Mediterranean at large, comparing with the pre-EMT situation in 1987. In that year, the T-S relationship was highly uniform in the deep waters (T_{pot} < 13.5°C), except for somewhat colder water toward the bottom for the Ionian station, which reflects near-bottom replenishment from the Adriatic. In the 2001 observations, density is higher by 0.02 – 0.03 units (we use σ_2 = density excess over 1000 kg/m^3, corrected adiabatically to 2000 dbar pressure), and salinity by 0.02 – 0.04 units, over the entire water column shown. It follows that in 2001 there were definitely no deep and mid-depth waters left that had escaped a significant imprint of the EMT. The 2001 Levantine station (Sta. 549) displays a pronounced inversion near density 37.8 (~ 1200 m depth), which is similarly found at all other Levantine stations (not shown). Near to that same density, the Ionian stations display a break toward higher salinities. Between approximately 1200 and 2500 m they show a large T-S variation, salinity being highest at Sta. 523 off Crete, to be ascribed to more direct exposure to replenishment from the Aegean. Corresponding data for 1995 (not shown) reveal ubiquitous EMT influence on the mid-depth and deeper waters already then. For the Ionian stations, the T-S relationship of 1995 was even more diverse than in 2001, with several stations showing salinity peaks close to the bottom. The T-S relationship at the Levantine stations, on the other hand, was quite similar to that in 2001, except that the salinity range below the inversion was larger and near-bottom densities a little higher. The CFC-12 distribution for 2001 (not shown) indicates absence of recent near-bottom renewal from the Adriatic, while at shallower depths signatures of such renewal are evident.

The temporal evolution of the deep and bottom waters through the EMT is illustrated by CFC-12 vs. density profiles of the four METEOR surveys in the S Ionian and the NW Levantine Seas (Fig. 4). Tracer concentrations and maximum densities increase markedly between 1987 and 1995, whereas the further changes up to 2001 are comparatively small. The bottom densities increase, from σ_2 = 37.79 - 37.808 in 1987, to 37.82 – 37.825 for the EMT profiles. The CFC-12 profiles consistently display a mid-depth minimum at σ_2 = 37.79 – 39.795, which densities however correspond to 1300 – 2000 m depth in 1987, but to only ~ 1000 m during the EMT. The jumps up to 1995 demonstrate that the major addition of Aegean-derived waters occurred prior to that year. Addition after 1995 has been comparatively moderate by volume, and never reached the density of the peak years. An example is the northwest Levantine tracer concentrations below the tracer minimum which down to about 3000 m were highest in 1999 [9], but decreased again up to 2001 (Fig. 4b). We note that by 1995, the Aegean

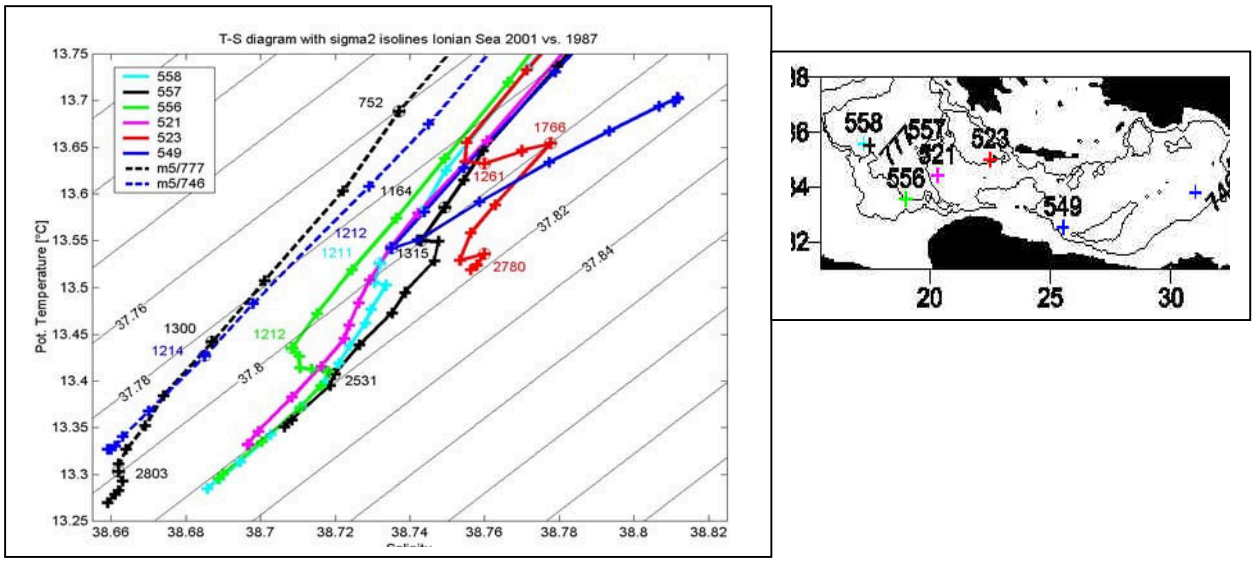

FIG. 3. Potential temperature-salinity diagram of the deep-water range based on bottle data for selected stations of cruise M51/2 (Oct-Nov. 2001; full lines) and M5/6 (1987; dashed lines). Markings indicate data points, density isolines are σ_2, for some data points depths (in dbar ≈ m) are noted, for station locations see map. Only one Levantine station is shown (Sta. 549).

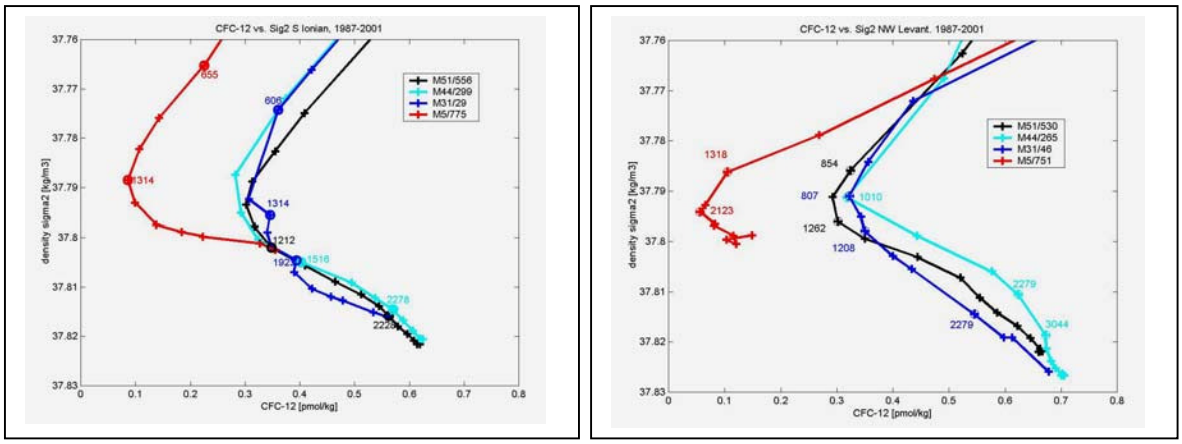

FIG. 4. CFC-12 (pmol/kg) versus density σ_2 (kg/m^3) in the South Ionian (Fig. 4a, left) and in the Northwest Levantine (Fig. 4b, right) according to observations in Aug.-Sept. 1987 (cruise M5/6), Jan. 1995 (M31/1), May 1999 (M44/4), and Oct.-Nov. 2001 (M51/2). Some depths (db) are marked. CFC-12 was measured on shipboard using techniques described previously [14, 15].

dense waters had not fully made it to the eastern Levantine, and that the situation in the western Ionian was more complex in comparison, because here the Aegean waters met pre-EMT waters that were already rather high in CFC-12 (cf. Fig. 2a). The waters upward of the tracer minimum have been generally more variable because shallower outflow from the Aegean and also from the Adriatic continued.

Whereas the T-S variation in Fig. 3 looks large, the total T and S ranges are, absolutely speaking, quite moderate, so that one has to rely on high data precision, including compatibility between cruises. The density range of the deep waters is also small, so that σ_2 (Figs 3 and 4) is a preferable measure of

vertical stability and of lateral density gradients, compared to the commonly used σ_θ (the potential-density excess referenced to ocean surface pressure).

4. Summary and conclusions

Although Aegean outflow began in 1989 [2, 4], outflow of the densest variety was restricted to a quite limited period of time, i.e., 1992-1994, considering that the period of the 1995 cruise (January) should have preceded any deep water formation in that year. Because Antikithera Strait, west of Crete, is about 400 m shallower than Kasos Strait in the east (Fig. 1), that Strait (possibly including Karpathos Strait, the next strait east of Crete) must be regarded as the principal pathway for outflow of the densest waters. Kasos Strait outflow filled, firstly, the adjoining parts of the Hellenic Trench north of the East Mediterranean Ridge (EMR; Fig. 1). From here the waters expanded eastward, crossed the EMR to feed the southern Levantine, and overflowed the northern sill in the Cretan Passage to the Ionian Sea. The eastward expansion was incomplete by 1995, but the southern Levantine was filled more swiftly, presumably because EMR bathymetry allowed overflow along much of its length. Transfer into the Ionian was subject to a delay because the northern channel is narrow, and the densest waters furthermore had to travel northward around the EMR, filling the deep parts of the Hellenic Trench downstream of the channel on the way, before entering the Ionian at large (~36°-37°N, 20.5°E; Fig. 1). Deep-water salinities and densities were raised across the entire Ionian by 1995, but the T-S relationship remained highly non-uniform even by 2001, mostly between densities 37.795 and 37.82 (~ 1300 – 2500 m). In that year the Aegean water influence was the lowest in the south (Sta. 556); the waters near density 37.805 here corresponded roughly to apparent 2:1 mixtures of pre-EMT waters and waters entering from east of the EMR (Sta. 523) and from the Levantine (Sta. 549; Fig. 3). The T-S relationship of the waters still deeper was rather uniform in comparison. Signatures of dense-water outflow from the Aegean and the Adriatic after 1994 are evident in mid-depth and deep waters, but up to 2001 density was never sufficiently high to replenish near-bottom waters to any significant degree.

A striking difference between the Levantine and the Ionian Seas is the largely uniform T-S relationship in the former Sea, in contrast to a wide range in the Ionian Sea. One cause for the latter is the mentioned delay of Aegean outflow to reach the Ionian west of the EMR, but further factors must be the deep recirculation and mixing field in that Sea, which are subject to strong topographic steering, and influence of the Adriatic. In the Levantine, vertical mixing caused a distinct shrinking of the salinity ranges below the T-S inversion between 1995 and 2001, accompanied by a decrease in near-bottom densities. As a result, near-bottom densities in 2001 were lower in the Levantine than in the Ionian (Fig. 3), where bottom densities changed much less. Much could be learned from investigating these and various further features in more detail, such as by reproducing them in dynamic ocean circulation models.

The deep hydrography and circulation of the East Mediterranean in 2001 was still highly transient and certainly far away from the pre-EMT situation. Looking to the future, one factor is that the current deep and bottom water densities exceed those of the pre-EMT era. New near-bottom replenishment must therefore either await erosion of that excess by vertical mixing, or another production of waters of elevated density. Even after bottom water renewal will have resumed, a speedy relaxation to the old or any new quasi-equilibrium state can hardly be expected, considering that in the classic situation the deep water renewal time scale was of the order of 100 years [7, 8]. A more detailed account of our findings will be the subject of a forthcoming publication.

ACKNOWLEDGEMENTS

We are grateful to the masters and crew of F/S METEOR and to numerous helpers at sea and in the home laboratories. The METEOR cruises were supported by the Deutsche Forschungsgemeinschaft, who also funded part of the tritium and ^{3}He measurements and of the data evaluation by one of the authors (B. K.). Our Mediterranean work was supported by EU grants MAS2-CT93-55 and MAS3-CT96-0051. B. B. M. acknowledges support by the Accordo di programma tra il CNR ed il MURST – Ecosistemi Marini, Legge 95/95.

REFERENCES

[1] ROETHER, W., et al., Recent changes in Eastern Mediterranean deep waters, Science **271** (1996) 333-335.

[2] MALANOTTE-RIZZOLI, P., et al., The Eastern Mediterranean in the 80s and 90s: the big transition in the intermediate and deep circulations, Dyn. Atm. Oceans **29** (1999) 365-395.

[3] JOSEY, S., Changes in the heat and freshwater forcing of the eastern Mediterranean and their influence on deep water formation, J. Geophys. Research **108** C7 (2003) 3237 doi:10.1029/2003JC001778.

[4] THEOCHARIS, A, et al., Climatic changes in the Aegean Sea influence the Eastern Mediterranean thermohaline circulation (1986-1997), Geophys. Res. Lett. **26** 11 (1999) 1617-1620.

[5] LASCARATOS, A., et al., Recent changes in deep water formation and spreading in the Mediterranean Sea: A review, Progr. Oceanogr. **44** (1999) 5-36.

[6] KLEIN, B., et al., The large deep water transient in the Eastern Mediterranean, Deep-Sea Res. I **46** (1999) 371-414.

[7] ROETHER, W., SCHLITZER, R., Eastern Mediterranean deep water renewal on the basis of chlorofluoromethane and tritium data, Dyn. Atm. Oceans **15** (1991) 333-354.

[8] ROETHER, W., WELL, R., Oxygen consumption in the Eastern Mediterranean, Deep-Sea Res. I **48** (2001) 1535-1551.

[9] THEOCHARIS, A., et al., Evolution and status of the Eastern Mediterranean Transient (1997-1999), J. Mar. Syst. **33-34** (2002) 91-116.

[10] MANCA, B.B., et al., Evolution of dynamics in the eastern Mediterranean affecting water mass structures and properties in the Ionian and Adriatic Seas, J. Geophys. Res. **108** C9 (2003) doi:10.1029/2002JC001664.

[11] ROETHER, W., et al., The Eastern Mediterranean tritium distribution in 1987, J. Mar. Systems **20** (1999) 49-61.

[12] ROETHER, W., et al., Component separation of oceanic helium, J. Geophys. Res. **103** C12 (1998) 27,931-27,946.

[13] SÜLTENFUß, J., et al., The Bremen mass spectrometric facility for the measurement of helium isotopes, neon, and tritium in water, Proc. Internat. Sympos. on Quality Assurance for Analytical Methods in Isotope Hydrology (2004), IAEA-CN-119/7 (in press).

[14] SCHLITZER, R., et al., Chlorofluoromethane and oxygen in the Eastern Mediterranean, Deep-Sea Res. I **38** (1991) 1531-1551.

[15] BULSIEWICZ, K., et al., A capillary-column chromatographic system for efficient chlorofluorocarbon measurement in ocean waters, J. Geophys. Res. **103** C8 (1998) 15,959-15,970.

Re-distribution of ^{137}Cs Chernobyl signal in the Aegean Sea

Delfanti, R.[a], C. Tsabaris[b], C. Papucci[a], H. Kaberi[b], R. Lorenzelli[c], V. Zervakis[d], M. Tangherlini[a], D. Georgopolous[b]

[a] ENEA-Marine Environment Research Centre,
La Spezia,
Italy

[b] Hellenic Centre for Marine Research (HCMR),
Anavyssos,
Greece

[c] ENEA-Brasimone Research Centre,
Camugnano,
Italy

[d] University of the Aegean,
Mytilene,
Greece

Abstract. The present levels of ^{137}Cs in the water column of the Aegean Sea are at all depths, significantly higher than in the pre-Chernobyl period. The concentrations in surface and intermediate water show a linear relationship to salinity, indicating that mixing of Black Sea Water with highly saline waters of Levantine origin is the main process controlling ^{137}Cs levels. The present ^{137}Cs concentrations in deep basins of the North and South Aegean (3.7 – 5.5 Bq m^{-3}) are the highest in the deep waters of the Mediterranean Sea. In the North Aegean the transfer of ^{137}Cs from the surface layers to the bottom took place through the dense water formation events in 1987 and 1993. The ^{137}Cs levels in the deep South Aegean are higher than expected, possibly in relation to a contribution of N-Aegean deep waters.

1. Introduction

The Chernobyl accident produced a patchy deposition of radionuclides over the Eastern and Northern basins of the Mediterranean Sea, that was superimposed over the previous fallout from atmospheric nuclear weapon tests. The deposition of Chernobyl-derived ^{137}Cs was particularly heavy onto the Black Sea (1.7 – 2.4 PBq) [1] and the Aegean – Ionian Seas along the Greek coasts (800 TBq) [2]. Moreover, the inflow of surface Black Sea water through the Dardanelles Straits still constitutes a point source of the conservative ^{137}Cs into the North Aegean Sea [3].

The objective of this study is to discuss the relationship between the re-distribution of ^{137}Cs Chernobyl signal in the Aegean Sea and water circulation in the area, with focus on the evolution in space and time and on the deep water formation processes.

2. Study area

The bottom topography of the Aegean Sea is characterised by an alternation of sills and shelves with deep basins (Fig. 1). The N-Aegean Basin is divided from the S-Aegean by the Cyclades Plateau and communication between the two basins is consequently restricted to the upper 400 m. The general water circulation is cyclonic, with warm, saline waters (mainly Levantine Surface Water, LSW and

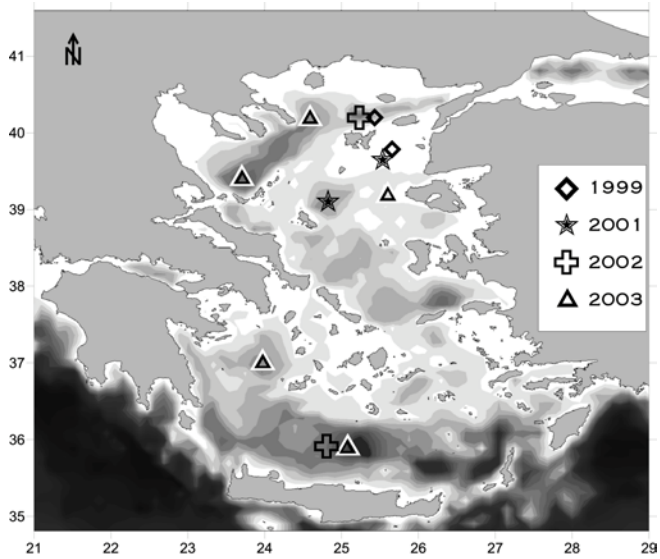

FIG. 1. The Aegean Sea and the sampling points.

Levantine Intermediate Water, LIW) entering from the Eastern Cretan Straits and flowing northward. Near the Dardanelles, low salinity waters form the 20-50 m thick Black Sea (BSW) layer at the surface, separated form the northward-flowing Levantine waters by a thermohaline front. The surface BSW layer gradually deepens and its low salinity increases through mixing with the underlying LIW along its pathway southward, along the coasts of the Hellenic peninsula. The deep basins are occupied by locally formed, very dense waters. In the S-Aegean Basin, below the surface water of Levantine origin, there are two types of dense waters, probably locally formed: the Cretan Intermediate Water (CIW) in the depth layer 100-400 m and the Cretan Deep Water (CDW) at the bottom of the basin, separated by a layer of Transition Mediterranean Water (TMW) coming from the Ionian and Levantine Seas, that during our study occupied the 600 to 750 depth interval [4].

3. Methods

Selected sampling was carried out in 1999, 2001, 2002 and 2003 by the Hellenic Centre for Marine Research and the Italian ENEA Marine Environment Research Centre during oceanographic campaigns designed for other purposes. Due to the limited shiptime available, particular attention was dedicated to gather information on the ^{137}Cs vertical profiles in the water column of selected sites (Lemnos and Skyros basin in the N-Aegean Sea, Mirtoan Basin and Cretan Sea in the South Aegean), where the signal of past events involving deep water formation is expected to be registered.

Seawater samples (20-40 L) were collected in the different water masses with a Rosette sampler, after a CTD cast. ^{137}Cs was preconcentrated by co-precipitation on 15 g of ammonium molibdophosphate (AMP) at pH 1.5. Chemical recovery was estimated by addition to the original sample of a known amount of ^{134}Cs. AMP samples were gamma counted on HPGe detectors (60% efficiency, 2.1 keV resolution at 1332 keV).

4. Results and discussion

The vertical profiles of ^{137}Cs have deeply changed with respect to the pre-Chernobyl period. As an example, we report in Fig. 2 the vertical profiles obtained by Florou [5] in 1984, decay corrected to present, and two of the vertical profiles obtained in this study, in the Northern Skyros Basin and in the Cretan Sea. ^{137}Cs levels are presently higher than the pre-Chernobyl ones at all depths in the water column. The concentrations increase from surface to the bottom. The present inventory in the Northern Skyros Basin is 4.1 kBq m^{-2}, almost 3 times higher than in 1984 (decay corrected to present) and most of the inventory (2.4 kBq m^{-2}) is now residing in the deepest part of the basin, below 500 m.

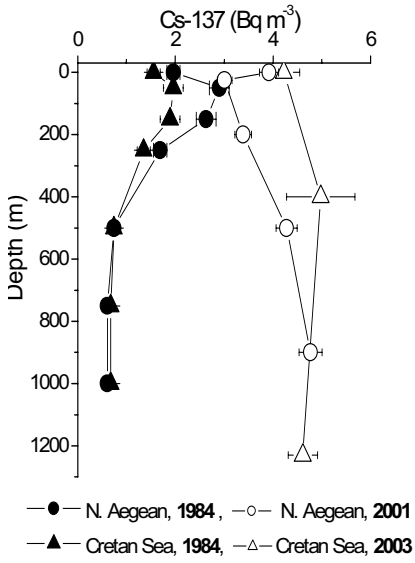

FIG. 2. Vertical profiles of ^{137}Cs in the water column of the North and South Aegean Sea. The original 1984 data are reported in [5] and have been decay corrected to 2001 (N. Aegean) and to 2003 (Cretan Sea) for comparison with recent profiles.

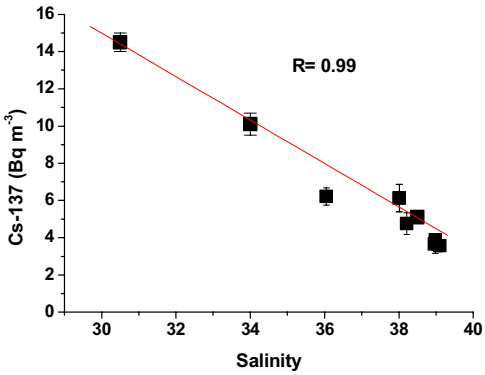

FIG. 3. ^{137}Cs concentrations vs. Salinity ‰ in surface water of the Aegean Sea.

The situation is similar in the Cretan Sea, where the inventory is 3.3 kBq m^{-2}, half of it in the depth layer 500 to 1000 m.

In the surface and intermediate layers there is a large variability in ^{137}Cs concentrations. In the surface water, the highest levels are found in the North Western Aegean. There is a clear trend of decreasing ^{137}Cs concentrations with increasing salinity (Fig. 3). Correspondingly, a linear relationship also characterises ^{137}Cs concentrations and salinity in intermediate water (200-400 m depth). It is evident that mixing/dilution of Black Sea Water, still containing relatively high ^{137}Cs concentrations, with highly saline Aegean waters is the dominant process determining the ^{137}Cs levels in surface and intermediate waters.

Also in the deep layers ^{137}Cs concentrations are much higher than in the pre-Chernobyl period: actually they are presently the highest in the deep waters of the whole Mediterranean Sea. In the North Aegean, the region of high ^{137}Cs concentrations at the surface due to the presence of the BSW layer, the transport of Chernobyl ^{137}Cs from surface to the deep layers took place through dense water formation events. Due to its low salinity, BSW acts as an insulation layer and, consequently, deep-water formation is rather infrequent in the North Aegean, taking place only at periods of exceptionally cold and dry winters and/or reduced Black Sea outflow. In the last 20 years there have been two major deep-water formation events: in winter 1987 (just after the Chernobyl accident), and in winter 1993 [6]. Present ^{137}Cs concentrations in the deep basins (4.1 – 5.5 Bq m^{-3}) must reflect those present in the intermediate and surface waters in 1993, modified by diffusion and mixing with the overlying water during the following stagnation period [7].

Also in the South Aegean ^{137}Cs concentrations in deep waters are quite high: 3.7 – 4.6 Bq m^{-3}. Historical observations and analyses suggest that the Cretan Sea is characterised by the formation of dense waters with variable characteristics, depending on the meteorological conditions and on the pre-conditioning of the water column. In the early nineties exceptionally dense, salty water started to fill

the deep Cretan Basin and to overflow the sills of the Cretan Arc straits [8], positioning at the bottom of the Ionian and Levantine Seas. Since 1995 the outflow of very dense Cretan water to the Levantine and Ionian basins has diminished, corresponding to a long stagnation period of the deep waters in the Cretan Sea. The present high ^{137}Cs concentrations in the deep basins of the South Aegean might reflect relatively high levels at the surface in the early nineties, when the deep waters were formed. At that time (early 90's) however, ^{137}Cs concentration in surface water of the Cretan Sea must have been significantly lower than in the North Aegean, under the influence of the ^{137}Cs-enriched Black Sea outflow. Consequently the deep waters formed locally in that period should have a ^{137}Cs content lower than in the North Aegean. In contrast, the values are very similar, suggesting a –possibly continued- contribution from the North Aegean to the deep water of the South Aegean basins.

5. Conclusions

The input of Chernobyl ^{137}Cs from the Chernobyl accident has been re-distributed among all the water masses of the Aegean Sea. The input through the Black Sea outflow strongly influences ^{137}Cs concentrations in surface and intermediate waters. The deep water formation events in 1987 and 1993 transferred significant quantities of ^{137}Cs to the deep basins of the North Aegean, where concentrations are now the highest among the deep waters of the whole Mediterranean Sea. Similar values are also found in the deep South Aegean Sea, suggesting that the deep waters residing in these basins could be partly originated in the North Aegean.

REFERENCES

[1] VAKULOVSKY, S.M., NIKITIN, A.I., CHUMICHEV, V.B., YU KATRICH, I., VOITSEKHOVICH, O.V., MEDINETS, V.I., PISAREV, V.V., BOVKUN, L.A., KHERSONSKY, E.S., Caesium-137 and Strontium-90 contamination of water bodies in the area affected by releases from the Chernobyl NPP accident: an overview, J. Environ. Radioactivity **23** (1994) 103-122.

[2] KRITIDIS, P., FLOROU, H., Estimation of the ^{137}Cs deposited in Aegean, Cretan and Ionian Seas after the Chernobyl accident, Rapp. Comm. Int. Mer Medit. **32** (1990) p. 318.

[3] EGOROV, V.N., POVINEC, P.P., POLIKARPOV, G.G., STOKOZOV, N.A., GULIN, S.B., KULEBAKINA, L.G., OSVATH, I., ^{90}Sr and ^{137}Cs in the Black Sea after the Chernobyl NPP accident: inventories, balance and tracer applications, J. Environ. Radioactivity **43** (1999) 137-155.

[4] ZERVAKIS, V., GEORGOPOULOS, A., KARAGEORGIS, A., THEOCHARIS, A., On the response of the Aegean Sea to climatic variability: a review, Int. J Climatology **24** (2004) 1845-1858, DOI: 10.1002/joc.1108.

[5] FLOROU, H., Distribution and behaviour of long-lived radionuclides in marine ecosystems (Greece), PhD thesis, Department of Zoology, University of Athens (1992) 253 pp.

[6] ZERVAKIS, V., GEORGOPOULOS, D., DRAKOPOULOS, P.G., The role of the North Aegean in triggering the recent Eastern Mediterranean climatic changes, J. Geophys. Res. **105** C11(2000) 26,103-26,116.

[7] ZERVAKIS, V., KRASAKOPOULOU, E., GEORGOPOULOS, D., SOUVERMEZOGLOU, E., Vertical diffusion and oxygen consumption during stagnation periods in the deep north Aegean, Deep-Sea Res. I **50** (2003) 53–71.

[8] THEOCHARIS, A., NITTIS, K., KONTOYIANNIS, H., PAPAGEORGIOU, E., BALOPOULOS, E., Climatic changes in the Aegean Sea influence the Eastern Mediterranean thermohaline circulation (1986-1997), Geophys. Res. Lett. **26** 11 (1999) 1617-1620.

$^{13}C/^{12}C$ isotope ratio and chemical composition of the organic matter forming mucilaginous aggregates in the Northern Adriatic Sea

Giani, M., V. Zangrando, D. Berto

Istituto Centrale per la Ricerca Scientifica e Tecnologica Applicata al Mare (ICRAM),
Brondolo,
Chioggia,
Italy

Abstract. Massive accumulation of mucilage have become quite frequent in the Northern Adriatic Sea during the last fifteen years. The origin of the organic matter forming the mucilaginous aggregates was investigated in order to find out if the organic matter of terrestrial origin is relevant in the aggregation process. The aggregates were sampled during summer 2000, 2001 and 2002 in many different areas of the Northern Adriatic and were subjected to the chemical characterisation and to the $\delta^{13}C$ analysis of the organic carbon both in bulk mucilages and in humic fractions. The organic matrix of the mucilages were found to have a completely marine origin when it is formed far from the estuarine mixing zone.

1. Introduction

In the Northern Adriatic Sea the frequency of occurrence of the massive formation of mucilaginous aggregates during summer has increased in the last fifteen years with respect to the previous period. Though the formation of mucilages on a basin scale is not recurrent every summer in recent years, two clusters of events were observed: one in 1988, 1989 and 1991, the second in 1997, 1998, 2000, 2001 and 2002. The aggregates can have different sizes, shapes and relative positions in water and can be classified as: macroflocs, stringers, ribbons, clouds, cob-webs, surface creamy layers and surface gelatinous layers [1, 2]. Different planktonic organisms contribute to the organic content of the mucilaginous aggregates: diatoms [3], dinoflagellates [4], cyanobacteria [5], and bacteria [6].

Riverine inputs are relevant in the Adriatic sea, where about one third of the freshwater reaching the Mediterranean Sea is discharged. After the phasing out in Italy of polyphosphates during the late '80s it has also been hypothesised that zeolites and polycarboxilic acids which were used in the formulation of detergents, could have played a role in enhancing the aggregation processes [7].

In order to establish the origin of the aggregates sampled during the summers of 2000, 2001 and 2002, the chemical characterisation and the $\delta^{13}C$ isotopic composition of organic carbon in different aggregates, plankton and humic substances were performed.

2. Materials and methods

2.1. Sampling

Mucilaginous aggregates were collected by scuba divers using 50 – 1500 mL plastic syringes or peristaltic pumps with PVC tubing depending on aggregates size. The sampling was performed both along the Italian and Croatian coasts and offshore during June-July 2000, July 2001 and June-July 2002. Aggregates were immediately frozen at –20°C. Before analyses, the aggregates were desalted by dialysis (Cellusep 3500 MWCO) against ultrapure Milli Q water and then lyophilised. Phytoplankton and zooplankton were sampled off the Po river delta by 30 and 200 μm nylon nets in January-March 2002. The plankton samples were separated by centrifugation, repeatedly washed with deionised Milli Q and then lyophilised.

2.2. Analytical methods

Total carbon, organic carbon, nitrogen and sulphur were determined by CHNS-O Analyser Fisons (Italy) model EA1108. Organic carbon was determined after removal of carbonates by concentrated HCl treatment in the tin cups. Inorganic carbon was calculated as the difference between total and organic carbon. The reproducibility of the method was lower than 2% and the accuracy was ± 4%.

Carbohydrates were determined spectrophotometrically by the MBTH (3-methyl-2benzothiazolinone hydrazone hydrochloride) assay after 1N HCl hydrolysis [8]. Protein contents in samples were determined by the Bradford method [9] after hydrolysis with 0.5N NaOH for 1h at 69°C. Results were expressed as albumin.

Humic fractions were separated using the method of International Humic Substance Society (www.ihss.gatec.edu) as humin fraction (insoluble in acids and bases), humic fraction (soluble in basic solution), fulvic fraction (soluble in acids and basic solutions). The UV-Visible spectra were performed by UV2 spectrophotometer ATI Unicam.

The $\delta^{13}C$ determinations were performed using Finnigam Delta Plus Isotope ratio Mass Spectrometer coupled with CHNS-O Analyser Fisons (Italy) model EA1108 and the results were expressed as deviation per mil (‰) from the international standard VPDB (Vienna Pee Dee Belemnite). The analytical precision of measurement was ± 0.2‰ and the reproducibility of the method was lower than 0.1‰. The $\delta^{13}C$ was determined after removal of carbonates by HCl treatment.

3. Results

3.1. Elemental composition of organic matter

The elemental composition of the aggregates analysed is reported in Fig. 1. The aggregates sampled were mainly composed of organic matter and secondarily of inorganic elements. The mean values for the different types of mucilages ranged from 11.1% to 32.3% for organic carbon, from 2.6% to 5.0% for inorganic carbon and between 0.74% and 4.32% for nitrogen. Sulphur content range from 0.3 to 3.8% for sedimented clouds and clouds respectively. High organic carbon was found in ribbons and clouds whereas false bottom and sedimented clouds had a high inorganic carbon content as a consequence of the entrapment of suspended matter rich in carbonates.

3.2. Organic matter composition: carbohydrates, proteins and humic substances

The composition of organic matter, expressed as the percentage of carbon in the fractions (proteins, carbohydrates, humin, humic and fulvic acids) relative to the total organic carbon content of the aggregates showed high variability (Fig. 2). Carbohydrates in the aggregates constitute 26.0 ± 11.2% of the organic carbon whereas proteins constitute 19.2 ± 14.2% with a decrease in surface aggregates and in sedimented clouds.

The humin incidence was more relevant in ribbon, clouds and sedimented clouds (31.4, 23.8 and 20.8% respectively), whereas lower values characterised the false bottom and the surface aggregates (Fig. 2). Humic fraction ranged from 2.7% to 6.3% of the organic carbon, fulvic fraction was quite variable in some aggregates, in clouds and ribbons it could not be extracted, whereas it constituted 3.1% in the surface aggregates and 20.3% in false bottom.

3.3. $\delta^{13}C$ of organic matter of mucilages and humic fraction

The $\delta^{13}C$ average value of the aggregates sampled in many different area of the Northern Adriatic was –19.2 ± 0.6‰ which falls in the range of natural plankton (from –19.7 to –24.1‰) and confirmed the marine origin of the bulk aggregates previous results found in mucilages sampled in the Gulf of Trieste in the summers of 1988, 1989 and 1991 [10].

The -20.8‰ $\delta^{13}C$ value of humic acid fraction extracted from sedimented cloud, sampled far from the estuarine zones, pointed out the marine origin probably deriving by plankton degradation [10] (Fig. 3) whereas other fractions extracted from coastal surface aggregates showed lower $\delta^{13}C$ values (–23.3‰), due to an inclusion of riverine organic matter in the aggregates.

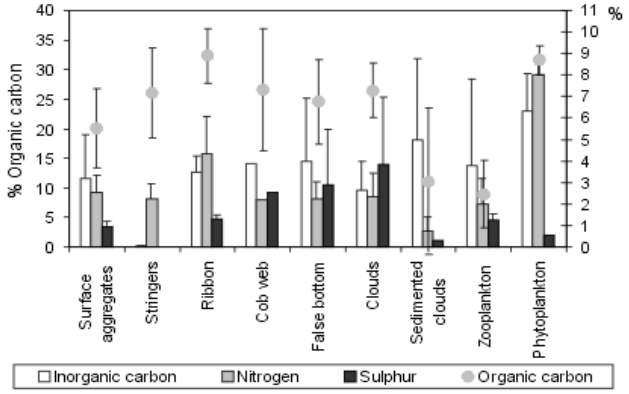

FIG. 1. C_{org}, C_{inorg}, N and S content, expressed as % w/w, in phytoplankton, zooplankton and different types of mucilages.

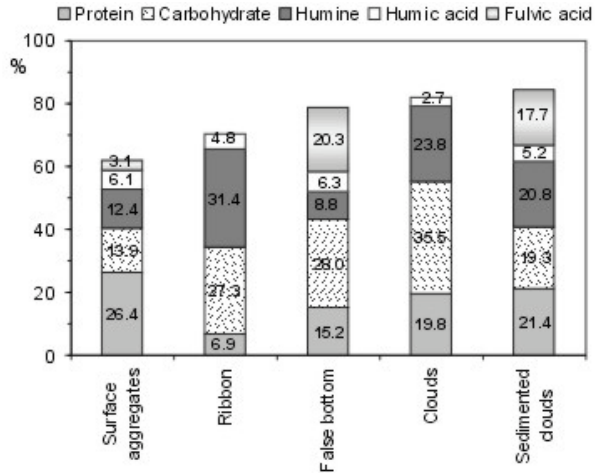

FIG. 2. Composition of the organic matter in different aggregates, expressed as percentage of carbon in the fraction (proteins, carbohydrates, humin, humic and fulvic acids) relative to the total organic carbon content in the aggregate.

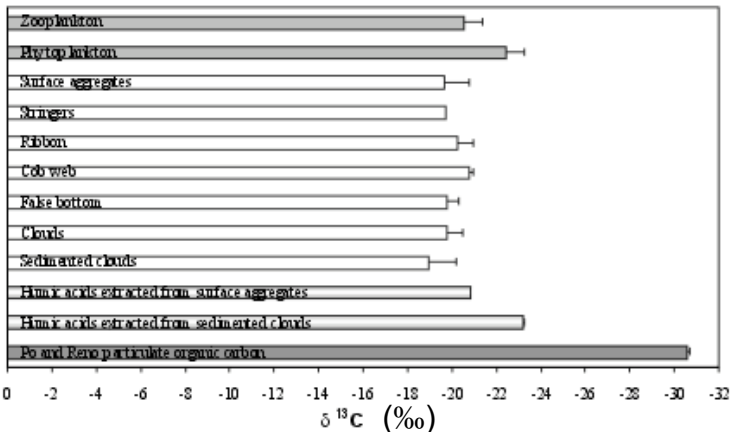

FIG. 3. $\delta^{13}C$ (‰) of organic matter in plankton, different types of mucilaginous aggregates, humic fractions extracted from mucilages and in riverine particulate organic matter.

REFERENCES

[1] STACHOWITSCH, M., FANUKO, N., RICHTER, M., Mucus aggregates in the Adriatic sea: an overview of stages and occurrences, Mar. Ecol. P.S.Z.N.I. **11** (1990) 327-350.

[2] PRECALI, R., GIANI, M., MARINI, M., GRILLI, F., FERRARI, C.R., PEČARA, O., PASCHINI, E., Mucilaginous aggregates in the northern Adriatic in the period 1999-2002: Typology and distribution, Sci. Tot. Environ. (submitted).

[3] NAJDEK, M., DEGOBBIS, D., MIOKOVIC, D., IVANCIC, I., Fatty acid and phytoplankton compositions of different types of mucilaginous aggregates in the Northern Adriatic, J. Plankton Res. **24** (2002) 429-441.

[4] POMPEI, M., MAZZIOTTI, C., GUERRINI, F., CANGINI, M., PIGOZZI, S., BENZI, M., PALAMIDESI, S., BONI, L., PISTOCCHI, R., Correlation between the presence of *Gonyaulax fragilis* (Dinophyceae) and the mucilage phenomena on the Emilia Romagna coast (Northern Adriatic sea), Harmful Algae **61** (2003) 1-16.

[5] KALTENBÖCK, E., HERNDL, G.J., Ecology of amorphous aggregations (marine snow) in the Northern Adriatic sea. IV. Dissolved nutrients and the eutrophic community associated with marine snow, Mar. Ecol. Prog. Ser. **87** (1992) 147-159.

[5] AZAM, F., FONDA UMANI, S., FUNERI E., Significance of bacteria in the mucilage phenomenon in the Northern Adriatic Sea. Ann. Ist. Super. Sanità **35** (1999) 411-419.

[7] PETTINE, M., PASSINO, R., CHIAUDANI, G., Le mucillaggini nei mari italiani. Dobbiamo ripensare la strategia anti-eutrofizzazione? Inquinamento **9** (1992) 54-64.

[8] JOHNSON, K., SIEBURTH, J., MCN. Dissolved carbhoydrates in seawater. A precise spectrophotometric analysis for monosaccharide, Mar. Chem. **5** (1977) 1-13.

[9] BRADFORD, M.M., A rapid and sensitive method for the quantification of microgram quantities of protein using the principal of protein-dye binding, Anal. Biochem. **72** (1976) 254-284.

[10] FAGANELI, J., KOVAČ, N., LESKOVŠEK, H., PEZDIČ, A., Source and fluxes of particulate organic matter in shallow coastal water characterized by summer macroaggregate formation. Biogeochemistry **29** (1995) 71-88.

[11] ISHIWATARI, R., Macromolecular material (humic substance) in the water column and sediments. Mar. Chem. **39** (1992) 151-166.

Carbon export assessed by sediment traps and ^{234}Th:^{238}U disequilibrium during the spring summer transition in the open NW Mediterranean

Miquel, J-C.[a], B. Gasser[a], A. Rodriguez y Baena[a], S.W. Fowler[a], J.K. Cochran[b]

[a] IAEA Marine Environment Laboratory,
Monaco

[b] Marine Sciences Research Center,
SUNY,
New York,
United States of America

Particle fluxes were measured at 200 m depth from January to July 2003 as part of the Dyfamed time-series observatory activities using moored Technicap PPS5 sediment traps. Water column was sampled for particulate and dissolved material at the same site (43°25'N; 7°51'E) with Challenger *in situ* pumps during four cruises of the Barmed and MedFlux projects (March, April, May and June 2003). Particulate matter was collected on a 70 μm polyamide prefilter followed by a precombusted GF/F filter (Ø 293 mm). The dissolved phase of ^{234}Th was extracted from the filtered water with MnO_2-impregnated wound fiber cartridges [1]. Particulate ^{234}Th was quantified on both fractions (>70 and 1-70 um) by non-destructive beta counting (Risø beta detector). The ^{234}Th activity of the dissolved fraction was measured in the ashed cartridges using a well-type high purity germanium detector (Canberra). Physical and fluorescence seawater data were obtained with a SeaBird SBE 911plus, and particulate organic carbon was analysed with a VarioEl elemental analyser.

Temperature profiles showed a mixed water column in March and April, and stratified in June. These profiles were contrasted by the fluorescence profiles which showed marked surface maxima in the first two months and a deep maximum typical for stratified waters in June. Particulate total and organic carbon profiles showed subsurface maxima at the beginning of the study (March) and, later on in May and June, a deep maxima at 50 m confirming the presence of a mixed surface layer in the upper 30 m which was well separated from the rest of the water column.

Total mass flux displayed a pronounced peak in mid-February and mid-March of approximately 400 mg $m^{-2}d^{-1}$. In January and from April to the end of June mass fluxes were always around 50 mg $m^{-2}d^{-1}$. Thorium-234 fluxes followed the same temporal trend, reaching 600 to 800 dpm $m^{-2}d^{-1}$ in February and March and less than 200 dpm $m^{-2}d^{-1}$ during the other periods. Thorium-234 activities in the water column mostly agreed with the particle distribution reflected in the POC profiles. In the upper waters, the $^{234}Th/^{238}U$ disequilibria became more pronounced from March through June. Both radionuclides reached equilibrium at around 150 m in March while it was above 100 m depth in June and slightly below in May.

In order to compare trap thorium fluxes with those predicted by the ^{234}Th activity in the water column the thorium deficit was integrated over the upper 200 m water depths. This yielded values from 800 dpm $m^{-2}d^{-1}$ to over 1000 dpm $m^{-2}d^{-1}$. Although the estimated flux in March corresponded to that measured in the sediment traps, overall, the water column derived ^{234}Th fluxes tended to be higher than those registered by the traps during the same time periods. POC export flux was calculated from the thorium flux by applying the $POC/^{234}Th$ ratio measured in large sinking particles [2]. This ratio (0.019 mg dpm^{-1} or 1.58 μmol dpm^{-1}) was measured in the particles >70 μm at 200 m depth, and yielded a POC flux in the range of 15 to 20 mg $m^{-2}d^{-1}$.

Our data show that ^{234}Th distribution traces fairly well the dynamics of particle distribution in the water column, and they confirm the applicability of this tracer in flux studies carried out over relatively short periods of time (weeks). The Th-derived data will be compared to POC sediment trap fluxes (data in process) and the variability of POC/^{234}Th ratio in our pumps and trap samples assessed.

ACKNOWLEDGEMENT

The Agency is grateful for the support provided to its Marine Environment Laboratory by the Government of the Principality of Monaco.

REFERENCES

[1] BUESSELER, K.O., COCHRAN, J.K., BACON, M.P., LIVINGSTON, H.D., CASSO, S.A., HIRSCHBERG, D., HARTMAN, M.C., FLEER, A.P., Determination of thorium isotopes in seawater by non-destructive and radiochemical procedures, Deep-Sea Res. **39** (1992) 1103-1114.

[2] COCHRAN, J.K., BARNES, C., ACHMAN, D., HIRSCHBERG, D.J., Thorium-234/Uranium-238 disequilibrium as an indicator of scavenging rate and particulate organic carbon fluxes in the Northeast Water Polynya Greenland, J. Geophys. Res. **100** C3 (1995) 4399-4410.

The benthic boundary layer: radioactivity and oceanographic data from the GEOSTAR-2 Observatory

Plastino, W.[a,b], M. Laubenstein[c], G. Etiope[b], P. Favali[b]

[a] Department of Physics,
University of Roma Tre,
Rome,
Italy

[b] National Institute for Geophysics and Volcanology,
Rome,
Italy

[c] National Institute for Nuclear Physics,
Gran Sasso National Laboratory,
Assergi,
Italy

GEOSTAR-2 (GEophysical and Oceanographic STation for Abyssal Research) is the first European deep-sea observatory for geophysical and environmental monitoring at seabed becoming operative in 2000. It was deployed in September 2000 from the Italian R/V Urania, in the southern Tyrrhenian Sea, between the Sicilian coast and the island of Ustica, at a depth of about 1900 m. After 206 days, in April 2001, the observatory was recovered. More than 4100 hours of data were recorded continuously. This mission represented the longest lasting experiment using a complex module, with an intelligent unit, deployed at great depth.

The sensors used for this mission (two magnetometers, a gravity meter, a hydrophone, a Doppler currentmeter, a single-point currentmeter, an automatic water sampler for laboratory geochemical analisys, a CTD and a transmissometer) were continuously controlled and managed by a data acquisition and control system able to trasmit the data via surface buoy and radio or satellite link to on-shore operators.

The seawater samples have been analysed for the following parameters:

- gas concentration: CO_2, CH_4, He, Ne
- helium isotopic composition: R/Ra ($^3He/^4He$ sample / $^3He/^4He$ atm)

CO_2 and CH_4 were analyzed by gas chromatography with micro-TCD. Helium analysis was carried out with a Perkin Elmer 8500 gas-chromatograph (Flame Ionization Detector and Hot Wire Detector; 5ppmv as detection limit; analytical errors of ± 5%). The $^3He/^4He$ isotopic ratio, was determined by a static mass spectrometer (VG5400TFT, VG Isotopes; typical uncertainties are about ±1% for $^3He/^4He$ ratios in the range of atmospheric values; below ±0.1% for high-^3He samples and below ±3% for low-^3He (radiogenic) samples).

The environmental radioactivity analyses of seawater samples, obtained by the automatic water sampler, has been performed in the framework of ERMES research project (Environmental Radioactivity Monitoring for Earth Sciences) to trace environmental changes in the Benthic Boundary Layer (BBL) seawater [1, 2].

The analysis of radionuclides was carried out by means of gamma spectrometry with coaxial high purity Germanium (HPGe) detectors having volumes ranging from 200 to 500 cm^3 and a total background rate in the energy range [(60÷2700) keV] varying from (221±2) to (980±10) counts/days depending on the detector [3]. Each seawater sample has been measured for about ten days using a polystyrene box of 70 mm diameter and 30 mm height [1, 2].

Oceanographic data evidenced ocean-lithosphere interactions in the 1900 m deep BBL, distinguishing two water masses with different origin and, possibly, benthic residence time. Environmental radioactivity analyses shown a BBL characterised by a colder Western Water (WW), which is episodically displaced by the cascading of the warmer Eastern Overflow Water (EOW) [4].

REFERENCES

[1] PLASTINO, W., LAUBENSTEIN, M., ETIOPE, G., FAVALI, P., Environmental radioactivity analysis in sea-water samples collected by GEOSTAR deep-sea observatory, Istituto Nazionale di Fisica Nucleare, Laboratori Nazionali del Gran Sasso, Annual Report (2002) 201-206.

[2] PLASTINO, W., LAUBENSTEIN, M., ETIOPE, G., FAVALI, P., GEOSTAR-2 observatory: the Benthic Boundary Layer dynamics by environmental radioactivity analyses, Istituto Nazionale di Fisica Nucleare, Laboratori Nazionali del Gran Sasso, Annual Report (2003) 203-208.

[3] ARPESELLA, C., A low background counting facility at Laboratori Nazionali del Gran Sasso, Appl. Rad. Isot. **47** (1996) 991-996.

[4] ETIOPE, G., FAVALI, P., FUDA, J.L., ITALIANO, F., LAUBENSTEIN, M., MILLOT, C., PLASTINO, W., The Benthic Boundary Layer: geochemical and oceanographic data from the GEOSTAR-2 observatory, Annals Geophys. (in press).

Black Sea radioactivity assessment and tracer studies: a Regional Technical Co-operation Programme

Osvath, I.[a], M. Samiei[b], A. Chupov[b], V. Egorov[c], G. Goktepe[d], A. Nikitin[e], S. Pagava[f], N. Panin[g], Gy. Ruzsa[h], K. Shimkus[i], B. Veleva[ij], O. Voitsekhovitch[k]

[a] IAEA - Marine Environment Laboratory,
Monaco

[b] International Atomic Energy Agency,
Vienna

[c] Institute of Biology of Southern Seas,
Sevastopol,
Ukraine

[d] Cekmece Nuclear Training and Research Centre,
Istanbul,
Turkey

[e] SPA "Typhoon",
Obninsk,
Russian Federation

[fi] Tbilisi State University,
Tbilisi,
Georgia

[g] National Institute of Geology and Geo-Ecology - GeoEcoMar,
Bucharest,
Romania

[h] National Institute for Environmental Research and Engineering,
Bucharest,
Romania

[i] P.P. Shirshov Institute of Oceanology – Southern Branch,
Gelendzhik,
Russian Federation

[j] National Institute of Meteorology and Hydrology,
Sofia,
Bulgaria

[k] Ukrainian Hydrometeorological Institute,
Kiev,
Ukraine

This paper summarises highlights of a recently finalised IAEA Regional Technical Co-operation Project, called "Marine Environmental Assessment of the Black Sea Region". This project aimed to complement other on-going regional programmes by addressing those gaps in regional capabilities, co-ordination and scientific investigations, which fall within the Agency's technical competence. The main objectives of the project were (i) to develop capabilities in the region to reliably assess Black Sea radioactive and non-radioactive pollution by using nuclear techniques; (ii) to implement a regionally co-ordinated monitoring programme for radionuclides in coastal waters; and (iii) to assess key processes controlling the fate of pollutants in the Black Sea by using radionuclides as tracers. The project was designed based on requests and proposals received from IAEA Member States and involved a nucleus of nine main counterpart institutes and twelve collaborating institutes/laboratories in the six riparian countries: Bulgaria, Georgia, Romania, the Russian Federation, Turkey and Ukraine. The IAEA contribution to the project amounted to $1.8 million over a period of 6 years (1995-2001), including the supply and commissioning of sampling and radiometric equipment and laboratory materials, expert visits, training courses, workshops, a seminar, fellowships, scientific visits, research vessel services and organisation of two Black Sea international scientific cruises, technical meetings, planning and co-ordination meetings and Ministerial meetings. The project thus had a strong capacity building component in support of national programmes and benefited in turn from commitment and considerable human resources, infrastructure and networking contributed by the national counterparts. Besides upgraded radioanalytical and assessment capabilities in the region, the project resulted in a large amount of new data, published so far in over 140 papers.

A programme for co-ordinated monitoring of coastal marine radioactivity was initiated at 15 stations around the Black Sea. Seawater, beach deposits (sand) and selected species of seaweed, mollusks and fish were collected once a year (twice yearly in the case of water) and analysed for ^{137}Cs by all laboratories and for additional radionuclides (^{90}Sr, ^{239,240}Pu, ^{210}Po) by a few laboratories.

Two international scientific cruises organized in 1998 and 2000 (Fig. 1) aimed to provide on-board training and to foster collaborative studies. Their main objectives were to assess contaminants in the marine environment, with a focus on anthropogenic radionuclides; to study particle fluxes, sedimentation, water mass mixing and eutrophication using radionuclides as tracers; and to perform trend monitoring at reference stations.

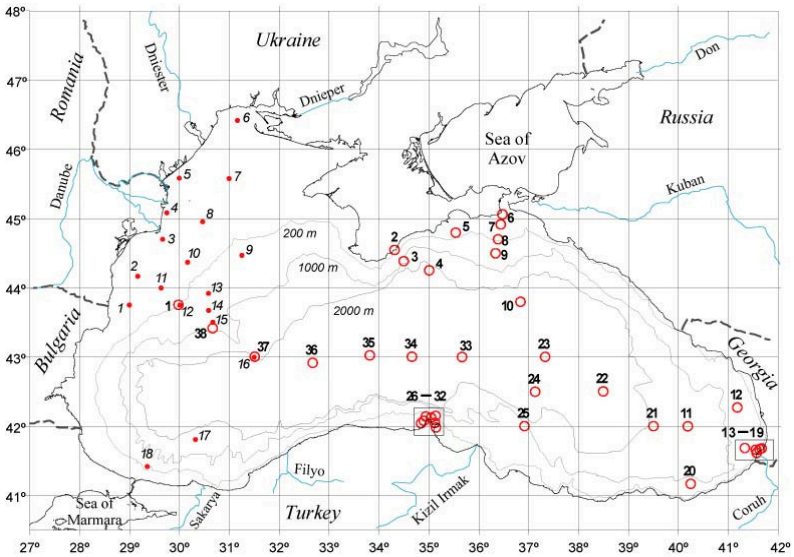

FIG. 1. Location of stations occupied during the IAEA Black Sea scientific cruises in 1998 (full circles, italics) and year 2000 (open circles, bold).

The field and laboratory work was carried out according to harmonized methodologies and supported through proficiency tests and intercomparison exercises.

Selected results will be presented in this paper and several other posters and oral presentations at this conference present details on subjects like ^{210}Po and associated doses, sedimentation and sediment inventories of radionuclides in the abyssal Black Sea and radiotracer chronology of metal pollution in the Eastern Black Sea.

ACKNOWLEDGEMENTS

This work was carried out in the framework of the IAEA Regional Technical Co-operation Project RER/2003 "Marine Environmental Assessment in the Black Sea Region". The Agency is grateful for the support provided to its Marine Environment Laboratory by the Government of the Principality of Monaco.

ISOTOPIC STUDIES

Reading the isotope language

Kutschera, W.

Institute for Isotope Research and Nuclear Physics,
University of Vienna,
Vienna,
Austria

"Reading the isotope language" means that we are following the various changes that affect isotope ratios. We know that in essentially all physical and chemical processes the relative abundance of isotopes within an element are subject to small changes. Most of these subtle changes are mass dependent (called mass fractionation), but mass-independent fractionations also occur occasionally.

In the current presentation we will walk through the seven large domains of our environment (atmosphere, biosphere, hydrosphere, cryosphere, lithosphere, cosmosphere, technosphere), "listening" to the isotope language and interpreting our world through this special window. An attempt will be made to point out the usefulness of this approach to gain a deeper understanding of the unique history of our physical world, and to get a glimpse at the human influence on its future.

Changes of stable isotope ratios through natural processes are quite small. For light elements (e.g. carbon, nitrogen, oxygen), where the relative mass differences between isotopes are large, mass fractionations are in the order of permil (‰). For heavier isotopes, the mass fractionations may even be one to two orders of magnitude smaller. Great progress has been achieved in measuring these minute changes of isotope ratios with various techniques, such as GMS (Gas Mass Spectrometry), TIMS (Thermal Ionisation Mass Spectrometry), SIMS (Secondary Ion Mass Spectrometry), and in recent years particularly with ICPMS (Inductively Coupled Plasma Mass Spectrometry). As a result, stable isotope ratios can now be measured with high precision and accuracy for essentially all elements.

In addition to mass fractionation which affects all isotopes, radioisotopes introduce an additional dimension. Their abundance may change considerably in the course of time (10 half-lives decrease a radioisotope-to-stable-isotope ratio by a factor of 1000). However, these isotope ratios are difficult to measure because of their extremely low values in natural settings (e.g. 10^{-12} to 10^{-15} for $^{14}C/^{12}C$ ratios). They require special methods such as AMS (Accelerator Mass Spectrometry), which currently dominates this field. Recently, also laser-based mass-spectrometric techniques (Resonance Ionisation Mass Spectrometry and Magneto-Optical Trap methods) are gaining ground in this field.

Taken together, we now have a multitude of versatile methods available to measure isotopic changes in essentially all sections of the environment. The continuing advances in reading the subtleties of the isotope language promises to help us to get a better view of our home planet and beyond.

^{15}N and unravelling the marine nitrogen cycle

Owens, N.J.P.

Plymouth Marine Laboratory,
Plymouth,
Devon,
United Kingdom

The marine nitrogen cycle is one of the most complex elemental cycles on earth, in which nitrogen 'cycles' between 8 oxidations states (-3 to +5), mediated predominantly by micro-organisms. The use of the stable isotope of nitrogen, ^{15}N, has been the most significant tool that has led to our current knowledge of this cycle.

From an historical context the introduction of ^{15}N can be traced back to parallel developments in two fields: a biogeochemical context and developments in isotope chemistry. In biogeochemistry the proposals of Liebig - "Liebig's Law of the Minimum" led to the recognition of the importance of nitrogen as a possible determinant of growth of living organisms. This was followed by early and important work of Brandt which initiated the study of nitrogen in the marine realm. The Founding Father's of marine chemistry Brand, Cooper and Harvey firmly established the nitrogen cycling into 'main-stream' marine science. The parallel developments in isotope chemistry initiated by Wien in the 1890s with the discovery of positive ions, through to the development of mass spectrometers by Thomson and the pioneering work on stable isotopes by Aston, Nier, Urey, Rittenberg and others was to lead ultimately to Hoering's seminal paper detailing the natural variations in ^{15}N in "natural materials". These dual developments led quickly to the use of ^{15}N in deliberate marine studies. Thus, Benson and Parker in 1961 used natural variations in ^{15}N to demonstrate unequivocally marine denitrification, and in 1967 Miyake and Wada published the first detailed study of variations in ^{15}N in marine organisms and foodchains. Alongside these developments there was landmark work being done by the use of ^{15}N as a deliberate tracer by Dugdale, Goering and others in the early 1960s which firmly established the use of ^{15}N as an important part of the marine 'armoury'.

As noted above ^{15}N can be used in two ways to help resolve the nitrogen cycle: study of the natural variation in its abundance in natural materials; use as a deliberate tracer by the addition of measurable concentrations under experimental conditions.

In the latter case the resolution of the form of nitrogen used by phytoplankton has led to the fundamental paradigm in biological oceanography of 'new' production. This was introduced in the 1967 by Dugdale and Goering and is important because it describes in effect the carrying capacity of any part of the marine environment. It thus sets the upper limit of the amount of carbon that can be sequestered by marine phytoplankton (of major importance in determining the role of the oceans in the context of global climate change); it also sets the upper limit of fish production (of major importance in the context of sustainable marine bioresources). Because of its importance a considerable amount of work has been conducted, using ^{15}N, over many years to establish the global level of 'new production'. A reasonably comprehensive study of the literature revealed over 70 studies since 1967 that when combined results in a global estimate of new production of 20GtC year-1; this estimate is of considerable significance for models of the global C cycle.

Turning to the use of variations in natural abundance of ^{15}N two examples serve to show its utility. First: the unequivocal demonstration that nitrogen fixation is of major importance in the marine environment. Many studies across the world-ocean have shown that components of the marine food-

chain are unusually 'light' in ^{15}N content; this could only occur if the basis of the nitrogen was from the atmosphere, which has a relatively low ^{15}N content. This finding is also of importance to global ecosystem models. Secondly, in resolving marine food-chains. The resolution of marine food-chains by ^{15}N is based on the observation and known theory of isotope fractionation as nitrogen is transformed from one form to another. Thus, as nitrogen moves up through trophic levels it is expected that consumers would progressively become 'heavier' in ^{15}N content. A large number of marine food-chains which otherwise would not be tractable to study have been resolved using this approach.

The above are limited examples of the use of ^{15}N but it is obvious that ^{15}N has been of enormous importance in resolving the marine nitrogen cycle. With the development of new techniques in molecular biology and the continuing development of more sensitive mass spectrometers we can expect a continuing development in its use and value to natural scientists.

Using stable isotopes (C, N) to constrain organics in sub-basement fossil soils (Ocean Drilling Program-Leg 197; N. Pacific): a possible example of isolated atmosphere-land-ocean systems

Bonaccorsi, R.

University of Trieste,
Dept. of Geological, Environmental, and Marine Sciences (DiSGAM),
Trieste,
Italy

Although the discovery of deep red-brown paleosols, or fossil soils, during Deep Sea Drilling Project (DSDP) and Ocean Drilling Program (ODP) legs dates back to the mid 1970s [1-3], the potential for preservation of organic matter in these igneous-derived silty-claystone units has been overlooked, and depositional settings have been inferred from only petrologic observations.

I present here naturally occurring stable isotopes of carbon and nitrogen ($\delta^{13}C_{org}$, $\delta^{15}N$) data of a well-preserved paleosol unit (Fig. 1) cored at Site 1206 (Koko Seamount) during the ODP Leg 197 (Emperor Seamounts, north Pacific Transect) [4-5]. The study of the sources and variation with depth of organic matter in sub-basement Fe-oxide-rich paleosol units from Leg 197 contributes to understanding the palaeoenvironmental history of the Emperor Seamounts prior to, during and after their burial and subsidence (ca. >48 to 55 Ma). Furthermore, preserved organic traces in such an isolated deep Earth system make them a useful test bed for future deep Earth's biosphere-relevant investigations [5-6].

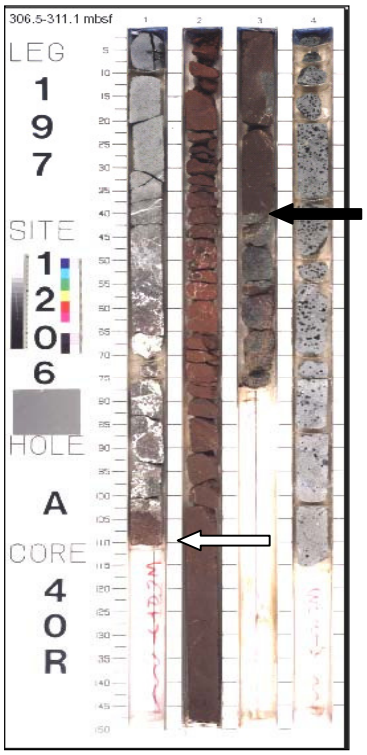

FIG. 1. Core 197-1206A-40R soil unit. This sequence develops for a total length of 234 cm and consists of a silty-clay red-brown material that becomes progressively lighter in color upward i.e., dusky brown (5YR 2/2) to very dusky red (10R 2/2).

This soil interval forms in the first part of Section 40R-3 (0-77 cm), it develops throughout the entire Section 40R-2, and ends as capped by a lava flow top at Section 40R-1, 104 cm. Throughout the fossil soil sequence two contacts are present: 1) the contact between the weathered lava flow top unit (white arrow), which represents the early/mid stage of soil formation; and 2) the contact between the top of the soil sequence (Unit 18A; [4]) and the overriding rock unit (black arrow) - i.e., the brecciated base of Unit 17 [4].

Measurements were made throughout Core 197-1206A-40R soil unit on organic-poor samples (C_{org} = 0.03-0.07%; 0.049 ± 0.011, n = 7) by using an Elemental Analyzer 1110 CHN coupled with a Finnegan Delta Plus MS-Conflo II.

This fossil soil system is characterized by a) the smallest difference for C ($\delta^{13}C_{org}$ =~1.5 delta ‰); b) the highest variability for N ($\delta^{15}N_{tot}$ = -9.5‰ to +2.5‰); c) even wider differences that occur between the fossil and the recent soils i.e., Hawaiian oxisols ($^{13}C_{org}$ = ~12 delta‰; ^{15}N =~18 delta‰) as counterparts.

More specifically, the $\delta^{13}C_{org}$ (bulk) values for the paleosol beds are –25.3‰ (at 307.54 mbsf) to -26.2‰ (at 308.92 mbsf) downcore. These values contrast to those obtained from an exposed Hawaiian oxisol sample (e.g., a Horizon-B sample at 100-105 cm-depth) with $\delta^{13}C_{org}$ = -23.0‰. Typical uncertainties for these measurements were ±0.1‰ to ±0.3‰.

First, $\delta^{13}C_{org}$ values of ca. -26‰ support a terrestrial, rather than marine source [7-8] of organics preserved in the paleosol interbeds from Core 197-1206A-40R. Thus, providing additional evidence for red claystone units as soil horizons subaerially formed on the top of Koko Seamount and buried by erupted lava flowing in a nearshore environment [1, 3-4]. The red soils probably underwent not only environmental changes (in paleolatitude and/or in paleoclimate) during formation, but also diagenetic changes after their burial.

However, $\delta^{13}C$ alone resulted inadequate at distinguishing among different carbon sources (i.e., microbials, algae and land plants, [e.g., 8]. Hence the need of adding ^{15}N data to constrain the source of organics in these interesting fossil soils.

Second, the isotopic composition of carbon and nitrogen would represent a complex signal from such history since late Palaeocene to early Eocene time [5]. Specifically, the stable isotope signature of C and N ($\delta^{13}C_{org}$ =~ -26‰; $\delta^{15}N_{tot}$ = -9.5‰ to +2.5‰) could reflect mixed sources of organics (i.e., plant and primary/secondary bacterial) and microbial-induced processes within the Carbon cycle and the Nitrogen cycle (e.g., nitrogen fixation, nitrification, and denitrification).

Finally, the geochemical divergence of these deeply buried fossil soils from their still exposed counterparts (with $\delta^{13}C_{org}$ =~-17 ‰ to ~ -23 ‰; $\delta^{15}N_{tot}$ = up to +8.5‰) would indicate a possible example of isolated atmosphere-land-ocean systems and deep Earth systems where to test for potential deep subsurface biospheres.

REFERENCES

[1] KARPOFF, A.M., Init. Repts. DSDP **55** Washington (1980) 707-711.
[2] Shipboard Scientific Party, Site 871, Proc. ODP, Init. Repts. **144** (1993) 41-103.
[3] HOLMES, M.A., Proc. ODP, Scientific Results, **144** (1995) 381-398
[4] Shipboard Scientific Party, Proc. ODP, Init. Repts. **197** (2002) College Station, TX
[5] BONACCORSI, R., et al., Abstract, IAU 2002 Bioastronomy Symposium (2002).
[6] FURNES, H., et al., Abstract, GSA 2001 Annual Meeting (2001).
[7] MEYERS, P.A., Chem. Geology, **144** (1994) 289-302.
[8] MEYERS, P.A., Org. Geochem. **27** 5/6 (1997) 213-259.

Hydrodynamic sorting of Washington margin sediments using SPLITT fractionation

Coppola, L.[a], Ö. Gustafsson[b], P. Andersson[a], M. Uchida[c], T.I. Eglinton[c]

[a] LIG, Swedish Museum of Natural History,
Stockholm,
Sweden

[b] Stockholm University,
Institute of Applied Environmental Research (ITM),
Stockholm,
Sweden

[c] Woods Hole Oceanographic Institution,
Department of Marine Chemistry & Geochemistry,
Woods Hole, MA,
United States of America

1. SPLITT fractionation

Sieving and SPLITT (split flow thin cell) fractionation were used to hydrodynamically sort surface sediments collected along an E-W transect from the mouth of the Columbia River, across the Washington continental margin, to the Cascadia Basin in the N.E. Pacific. Sediments were separated into various coarse (>250, 100-250, 63-100, 38-63 and <38 μm) and two fine (38->1m/d and 38-<1m/d) fractions. The sieve-SPLITT method was recently tested and validated by using a variety of natural sediments [1] and results indicated that many biogeochemical processes governed by particle dynamics could be examined using this approach.

2. Washington Margin results

Mass distribution of sieve fractions indicates that sediments from the Washington shelf are dominated by large particles (>250 μm) whereas fine particles (<38 μm) are predominant in slope and Cascadia Basin sediments. This is consistent with the natural grain size distribution occurring in Washington margin sediments [2]. The mass distribution is shown in Fig. 1.

Total Organic Carbon (TOC) contents of the sediments generally follow the same distribution as the mass. With the exception of inner shelf stations, most TOC resides in the fine fraction and ranges around 1.5-3%. Stable carbon isotopic measurements on TOC indicate an increase in $\delta^{13}C$ values from the shelf to the Cascadia Basin (from -34 to -20‰). Consistent with this, TOC/TON ratios decrease along the same transect (from 80 to 10), suggesting a transition from terrestrial to autochthonous marine sources.

These results will be completed by those from the splittate fractions. Results of other analysis of the sieve-SPLITT fractions (inorganic elements, surface area, mineralogy and Sr isotopes) will also be presented.

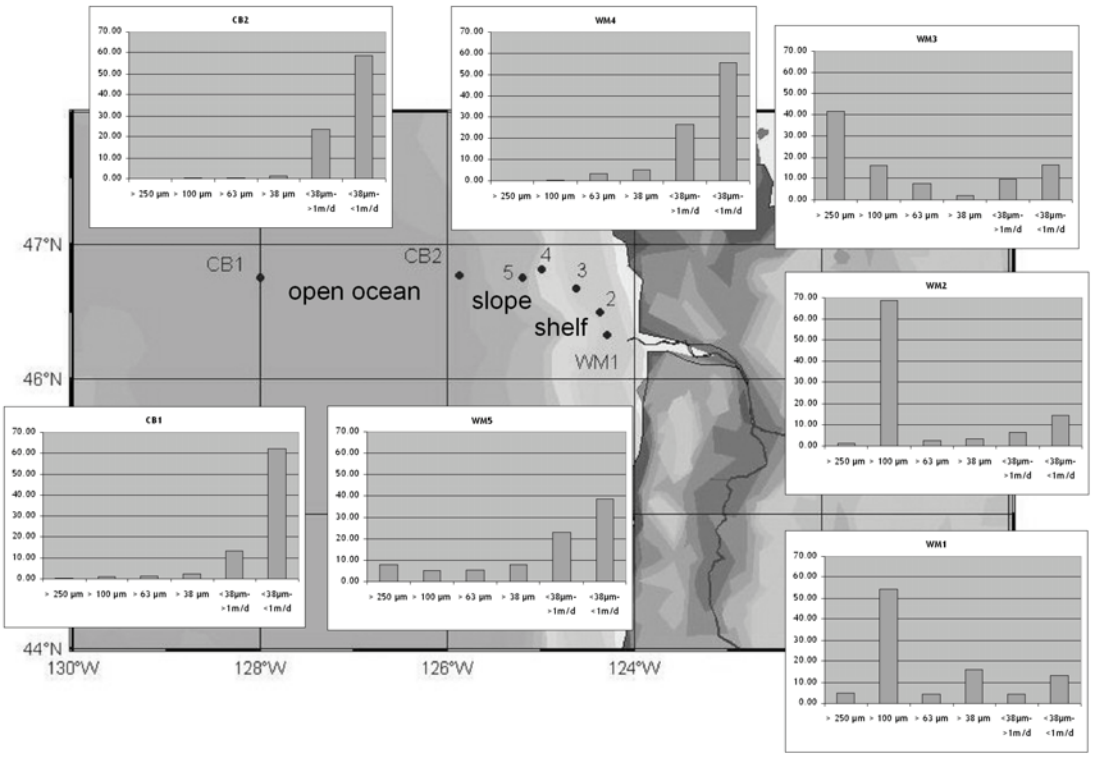

FIG. 1. Mass distribution of surface sediment fractions from sieve-SPLITT method in the Washington Margin area.

REFERENCES

[1] COPPOLA, L., GUSTAFSSON, Ö., ANDERSSON, P., LARSSON, J., AXELSSON, P., Water Res. (submitted).

[2] KEIL, R.G., TSAMAKIS, E., FUH, C.B., GIDDINGS, J.C., HEDGES, J.I., GCA **58** (1994) 879-893.

ISOTOPIC STUDIES - POSTERS

Sources of fine organic matter on the Southwestern Iberian continental shelf

Burdloff, D.[a], M.F. Araujo[a], J.M. Jouanneau[b]

[a] Instituto Tecnológico e Nuclear (ITN),
Sacavém,
Portugal

[b] UMR 5805 Environnements et Paléoenvironnements Océaniques,
Talence,
France

Elemental (organic carbon and total nitrogen) and isotopic ($\delta^{13}C$) record of fine-sized (< 63mm) particulate organic matter in Southwestern Iberian continental shelf sediments covering the last centuries is presented. This study was performed in order to estimate the contribution of terrestrial organic matter in marine sediments due to carried sediment load by the large Iberian river basins. Surface sediment samples were recovered from a Smith McIntyre grab sampler along three transepts located between mouths of Guadiana and Tinto-Odiel rivers. Moreover, two sediment cores (core 5 and core 8) were recovered from a vibro corer, located in the mud field on the Guadiana continental shelf at 72 m and 22 m water depth, respectively.

Organic carbon (OC), total nitrogen (TN) and $\delta^{13}C$ isotope ratios were measured, after carbonate removal, on the same sample aliquot by EA-IRMS (EuroVector 3028-HT Elemental Analyser on line with a SIRA 10 Isotope Ratio Mas Spectrometer). Results for isotope abundance are reported in per mil (‰) relative to Pee Dee Belemnite (PDB) standard for $\delta^{13}C$. OC and TN are reported in $mg.g^{-1}$ of dry sample.

Surficial sediments - The lowest $\delta^{13}C$ and the highest OC/TN ratios (averages ± 1s: OC/TN = 9.4 ± 0.9; $\delta^{13}C$ = -26.2 ± 0.2‰) of the most inner shelf sediments (adjacent to the Guadiana river) reflect organic matter derived from terrestrial C_3 plants (Fig. 2). In contrast, evidence of a changing source of organic matter is revealed both by the regular increasing trend of $\delta^{13}C$ values toward the outer shelf, and by the lowest OC/TN ratios for sediment below 70 m water depth (OC/TN = 8.8 ± 0.2; $\delta^{13}C$ = -24 ± 0.3‰). Any significant difference for elemental and isotopic records between the three transepts suggests that sedimentary organic matter is evenly distributed along the outer shelf.

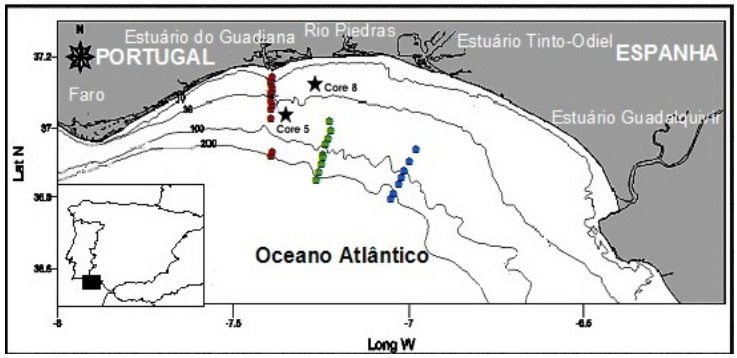

FIG. 1. Location of cores 5 and 8, and surface sediments sampled on the Southwestern Iberian continental shelf.

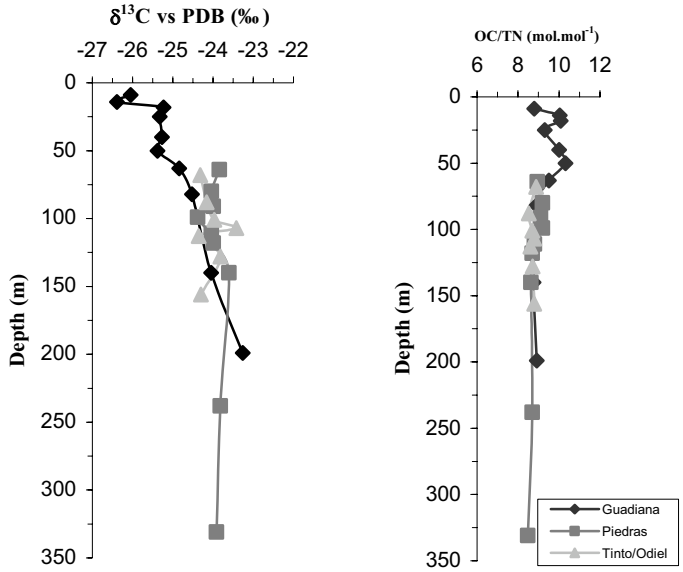

FIG. 2. OC/TN molar ratios and δ13C of fine (< 63 um) size fractions of surficial sediments from the Southwestern Iberian continental shelf.

Core 5 (Fig. 3) - The down-core variation of grain-size distribution indicate that fine fraction percentage (< 63 μm) decreases from 100% at the top to 55% at the bottom, suggesting a major change in sediment supply composition. The regular increase of OC and TN through the core suggests a gradual increase in fine-sized organic matter supply during the last centuries. The oscillations in the contents of both components may indicate a primary productivity variability on the continental shelf. Evidence of changing source of organic matter is also shown by the $\delta^{13}C$ values, ranging from –21.3‰ to –24.9‰. The highest $\delta^{13}C$ values are obtained for the most recent sediments. An average sedimentation rate of 0.12-0.13 $cm.yr^{-1}$ has been estimated using the ^{210}Pb-excess profile. The estimated sedimentation rate agrees well with the relative peak position of fallout nuclide ^{137}Cs. There is little evidence that particle reworking takes place in the upper sediments.

Core 8 (Fig. 4) - The down-core variation of grain-size distribution indicates that the fine fraction percentage (< 63 μm) is predominant (75 ± 5%) above 170 cm depth, contrasting sharply with the values displayed in the deeper part (45 ± 10%). This later depth corresponds to a major change in sediment supply composition. The regular increase of OC and TN toward the core top, from 6.6 $mg.g^{-1}$ and 0.8 $mg.g^{-1}$ to 15 $mg.g^{-1}$ and 1.7 $mg.g^{-1}$, respectively, suggests a gradual increase in fine-sized organic matter supply during the last centuries. Noticeable oscillations in the contents of both components above 170 cm depth are observed and may indicate a primary productivity variability on the continental shelf. Evidence of the changing source of organic matter is also shown by the $\delta^{13}C$ values, ranging from –26.3‰ to –23.7‰. The lowest $\delta^{13}C$ values are obtained for sediments above 170 cm depth.

Terrestrial versus marine sources of fine-sized organic matter (Fig. 5) - A first-order linear correlation can be drawn between $\delta^{13}C$ values and OC/TN ratios from cores 5 and 8. This relationship is usually interpreted as a mixing trend between terrestrial and marine sources of organic matter, providing depleted and enriched isotope ratios, respectively. The negative correlation indicates that the terrestrial source end-member is best approximated by core 8 samples, which have the most depleted in ^{13}C and nitrogen (high OC/TN) fine organic matter. The marine end-member would have an isotopic signature approached by the most enriched in ^{13}C and nitrogen core 5 samples. Assuming constant $\delta^{13}C$ end-member values for marine (-20‰) and terrestrial (-27‰) fine-sized organic matter supply along both cores, we can make a semi quantitative estimate of the continental contribution. According to our estimates, 55 to 90% and 20 to 70% of fine-sized organic matter is derived from terrestrial sources, respectively in core 8 and 5.

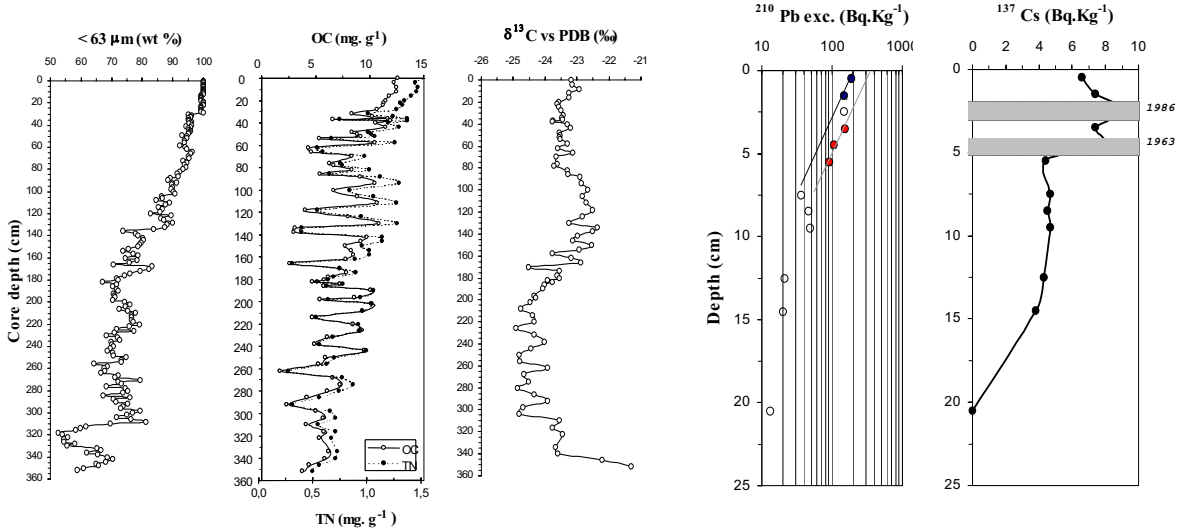

FIG. 3. Down-core variations of fine (< 63 µm) size fraction contents, OC and TN concentrations and $\delta^{13}C$, for fine size fractions of carbonate-free samples, and ^{210}Pb excess and ^{137}Cs activity profiles of core 5.

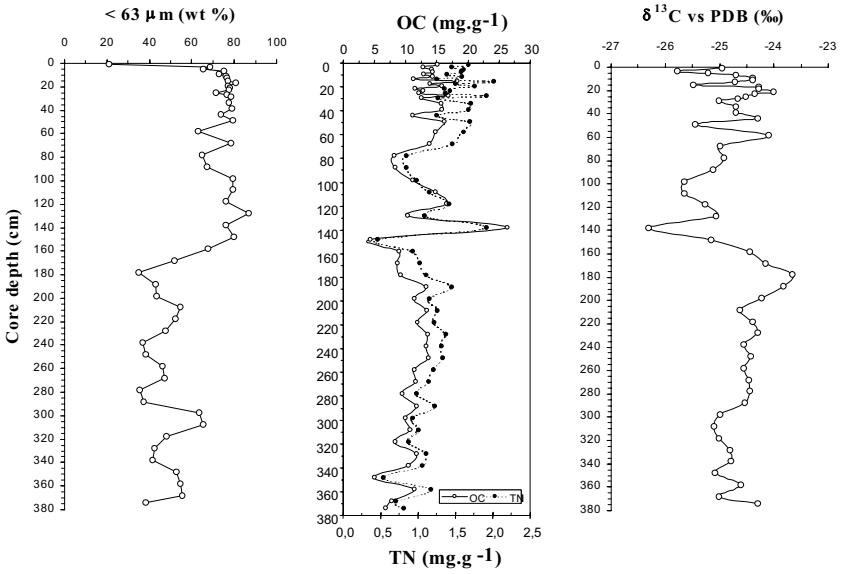

FIG. 4. Down-core variations of fine (< 63 µm) size fraction contents, OC and TN concentrations and $\delta^{13}C$, for fine size fractions of carbonate-free samples (core 8).

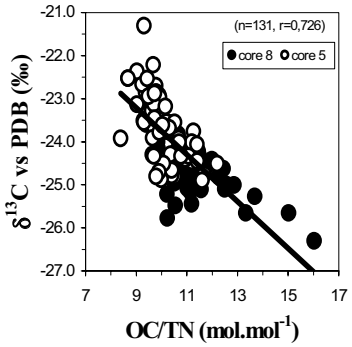

FIG. 5. $\delta^{13}C$ vs. OC/TN ratios, for fine size fractions of carbonate-free samples (core 5 and 8).

ACKNOWLEDGEMENTS

A part of this study is supported by the CRIDA project (PLE/8/00) through a financial support from FCT (Fundação para a Ciência e Tecnologia). We are grateful to FCT for supporting D. Burdloff through a postdoctoral fellowship (SFRH/BPD/6892/2001) at the ITN (Instituto Tecnológico e Nuclear).

Seasonal change of CO_2 recycling rate by understory vegetation in a cool-temperate forest in Japan

Kondo, M.[a], M. Uchida[b], H. Muraoka[a], H. Koizumi[a]

[a] Institute for Basin Ecosystem Studies,
Gifu University,
Gifu,
Japan

[b] Japan Agency for Marine-Earth Science and Technology (JAMSTEC),
Yokosuka,
Japan

Three main factors govern dynamics of CO_2 within a forest canopy: turbulent mixing with the atmosphere above canopy, photosynthesis and respiration. CO_2 released by respiration is either lost from the forest through turbulent mixing or refixed by photosynthesis within the canopy (CO_2 recycling). CO_2 concentration ($[CO_2]$) in a forest generally increases from canopy layer toward the soil surface due to the high $[CO_2]$ by plant and soil respiration. Therefore, the understory vegetation is capable of fixing the respired CO_2 through photosynthesis, and this process would highly influence the carbon dynamics within a forest.

In a temperate deciduous forest, stand structure is seasonally changed by the seasonal change of foliage biomass distribution and changes the environment factors in the forest understory such as light attenuation and soil temperature which affect photosynthetic activity of understory plants and respirations of plants and soil microbes. In this study, we examined how $[CO_2]$ and $\delta^{13}C$ of canopy profile change daily and seasonally in a cool-temperate deciduous forest at Takayama Experimental Site (36˚8'N, 137˚6'E, 1420 m a.s.l.) in Japan. We also estimated the percentage of respired CO_2 recycled by understory vegetation using a model developed by Sternberg (1989) [1]. At the Takayama Experimental Forest site, the understory is dominated by an evergreen dwarf bamboo grass (*Sasa senanensis* (Fr. Et Sav.) Rehdar).

There were dramatic changes in canopy foliage density and environmental conditions within the forest in only about five months of plants' growing season. There were clear diurnal changes in $[CO_2]$ within the forest ($[CO_2]_{canopy}$), especially on the soil surface, in mid-summer (August). $[CO_2]_{canopy}$ and $\delta^{13}C$ of CO_2 ($\delta^{13}C_{canopy}$)were vertically stratified in the forest, with maximum $[CO_2]$ (ca. 478ppm) and most negative $\delta^{13}C$ value (-12.5‰) near the soil surface (Fig. 1). The diurnal variations of $[CO_2]_{canopy}$ and $\delta^{13}C_{canopy}$ were also clearly observed in the forest; daytime $[CO_2]_{canopy}$ was considerably lower than that in night due to photosynthetically CO_2 uptake in daytime while respiratory CO_2 efflux and its accumulation occurred around the dense understory vegetation in night. The Sternberg's model [1] using, we calculated the fraction of respired CO_2 that was refixed photosynthetically by *S. senanensis*. The percentage of respired CO_2 refixed by *S. senanensis* ranged from 5 to 16% in summer depending on the diurnally fluctuated $[CO_2]_{canopy}$ in the understory. $[CO_2]_{canopy}$ and $\delta^{13}C_{canopy}$ showed small diurnal variation and small vertical difference in spring and autumn, reflecting reduced biological activities due to tree leaves fall (Fig.1). The percentage of respired CO_2 recycled by *S. senanensis* ranged from 22 to 26% in spring, and from 16 to 21% in autumn. These results were discussed in this study in terms of environmental and physiological factors as follows; (1) source CO_2 effects ($[CO_2]_{canopy}$ and $\delta^{13}C_{canopy}$) due to the seasonal change of soil respiration rate and turbulent mixing which depends on

forest canopy closure and (2) leaf photosynthetic discrimination effects influenced by the photosynthetic and stomatal responses to diurnal light incident patterns that are different between summer and spring (or autumn).

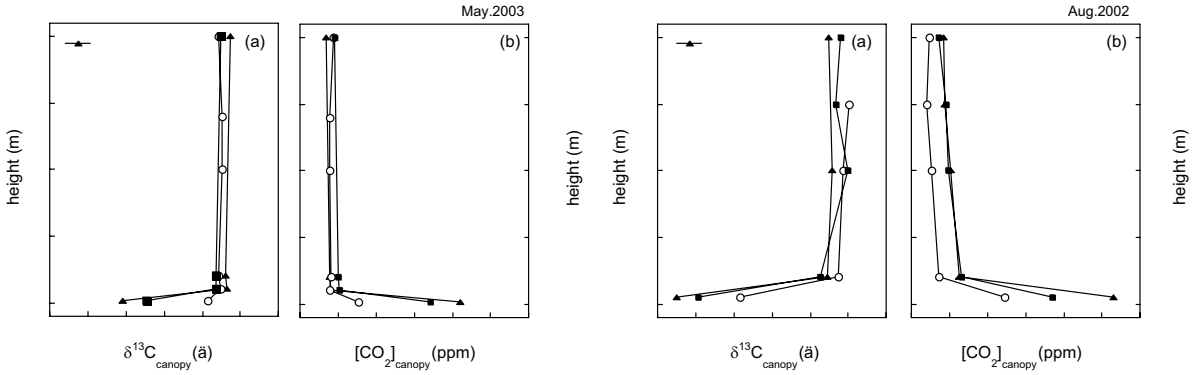

FIG. 1. Canopy profiles of $\delta^{13}C_{canopy}$ (a) and $[CO_2]_{canopy}$ (b) on August 2002 and May 2003.

REFERENCE

[1] STERNBERG, L., A model to estimate carbon dioxide recycling in forests using $^{13}C/^{12}C$ ratios and concentrations of ambient carbon dioxide, Agric. Forest Meteorol. **48** (1989) 163-173.

Photo- and chemo-synthetic organic carbon production and its fate in the Black Sea: use of isotopic techniques and tracing

Yilmaz, A.[a], Y. Coban-Yildaz[b]

[a] Middle East Technical University,
Institute of Marine Sciences,
Erdemli, Mersin,
Turkey

[b] Mersin University,
Department of Environmental Engineering,
Çiflikköy, Mersin,
Turkey

The Black Sea is a unique marine environment representing the largest land-locked/semi-enclosed and deep anoxic basin in the world. Its shelf region is generally narrow and it enlarges at the north western corner. It has a very large catchments area, receiving extraordinary amount of nutrients, pollutants as well as fresh water. The coastal waters of the Black Sea are principally fed by the river input and by the lateral/ vertical nutrient transport mechanisms. In the open ecosystem, which is dominated by the cyclonic eddies, primary production is mainly sustained by the influx of nutrients from the oxic/suboxic lower layers mainly by vertical mixing processes. However, the input from the anoxic layer is limited due to the presence of a permanent pycnocline in the Black Sea which coincides with the oxic-anoxic transition zone. Intense denitrification and redox-dependent processes within this zone limit nitrogen and phosphorus input to the productive layer (Fig. 1).

Multilayer systems having anoxia support multiple layers of biological production [1, 2]. In addition to photosynthetic production at the surface layer, microbial communities at the oxic-anoxic interface live on the residual chemical energy (i.e. H_2S, CH_4, NH_4^+, H_2) originate from anoxic waters. Photosynthetic and chemosynthetic production rates have been measured using ^{14}C isotopic technique in the Black Sea for 1998-2001 period and the results are presented in this synopsis.

The thickness of the euphotic zone was in the range of 15-35 m in the Black Sea during the study period. Photosynthetic production rates in this zone were in between 141 and 639 mg C m^{-2} d^{-1}. The lowest values were recorded in the central regions and the highest values were measured at the Turkish and Romanian shelf areas. Bioassay experiments showed that under optimum light conditions, the production is nitrogen limited in the Black Sea and NH_4 is preferable with respect to NO_3. In recent years, production in the Black Sea was more intense in autumn and less pronounced in spring.

Present data showed that, chemosynthetic production at O_2-H_2S interface is relatively high in the Black Sea and it is potential mid-water source of sedimentary biogenic particles for the basin related to the microbial activities and red-ox processes which are persistent features in the Black Sea ecosystem. Lateral transports of oxygenated waters from coastal areas possibly enhance the chemoautotrophic production. Indeed, the carbon produced at midwater depths may exceed the surface photosynthetic production. Arial chemosynthetic production for open region was 93.5 mg C m^{-2} d^{-1}, corresponding to 54% of the surface photosynthetic production. It was much higher (1951 mg C m^{-2} d^{-1} and 722% of the surface photosynthetic production) in coastal area, not only because of higher peak values, but also due to presence of thicker chemosynthetically active layer. For comparison, the range of chemo-autotrophic production in the Cariaco basin was 312-1884 mg C m^{-2} d^{-1} and this was equivalent to between 10% and 333% of its surface primary production [3].

Planktonic nitrogen productivity and relative importance of NO_3, NO_2 and NH_4 on productivity in the Black Sea were estimated using ^{15}N isotopic technique. Though the main nitrogen source utilised by phytoplankton was NH_4, annual 'f-ratio' was unexpectedly high, which could not be compensated by the estimated budget of new nitrogen input. Available estimations on new nitrogen input to the euphotic zone of the Black Sea corresponded to less than 20% of annual N-production rate estimated and the direct measurements revealed an f-ratio of 0.3-0.5. N_2 fixation seems to play a role in nitrogen supply and their potential contribution in supplying new nitrogen to the euphotic zone should be clarified.

Carbon and nitrogen natural isotopic ratios ($\delta^{15}N$ and $\delta^{13}C$) of suspended particulate organic matter (SPOM) produced in the water column of the Black Sea were also determined in the Black Sea. The results revealed important vertical and regional variations in terms of isotopic composition while the seasonality was less remarkable. SPOM of each layer possessed distinct isotopic composition associated with microbial decomposition and formation of organic matter. Isotopic signature of planktonic productivity in the euphotic zone, bacterial decomposition in the oxycline, chemo-auto- and –heterotrophic activities in the suboxic and anoxic layers were traced. C and N isotopic composition of Black Sea SPOM collected revealed that planktonic production and rapid recycling in the nutrient-poor surface layers. Dominance of 'old' partially decomposed fragments of SPOM dominated by lipids in the oxycline. Intense microbial activity in the suboxic/anoxic transition layer of especially coastal regions partially aerated by Mediterranean water.

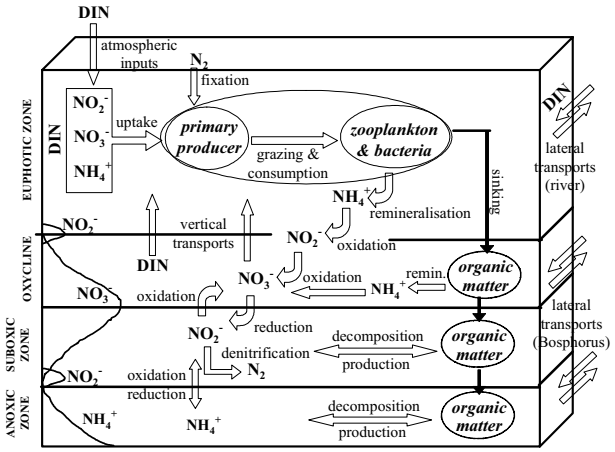

FIG. 1. Black Sea multi-layer system and processes in biogeochemical cycling.

REFERENCES

[1] JORGENSEN, B.B., FOSSING, H., WIRSEN, C.O., JANNASCH, H.W., Sulfide oxidation in the anoxic Black Sea chemocline, Deep-Sea Res. **38** (1991) S1083-S1103.

[2] SOROKIN, Y.I., The Black Sea- Ecology and Oceanography, Backhuys Publishers, UNESCO Venice Office, Leiden (2002) 875 pp.

[3] TAYLOR, G.T., IABICHELLA, M., HO, T.Y., SCRANTON, M.I., Chemoautotrophy in the redox transition zone of the Cariaco Basin: A significant midwater source of organic carbon production, Limnol. Oceanogr. **46** 1 (2001) 148-163.

ISOTOPE HYDROLOGY

Advances in isotope hydrology at the IAEA

Aggarwal, P.

International Atomic Energy Agency,
Vienna

More than one billion people do not have access to clean water. Three years after world leaders pledge in the UN Millennium Declaration to reduce this number in half by 2015, increasing access to safe water remains a great challenge. In our quest to increase water availability, it is likely in many cases that water resources are used before fully understanding their hydrology. Such "solutions" sometimes result in creating greater problems, such as in Bangladesh where the use of groundwater reduced the incidence of water-borne disease, but has led to a more difficult issue of arsenic poisoning. The fact that water on earth moves in a cycle has been known since ancient civilizations existed on different parts of the earth. However, appropriate water assessments at regional and national scale require quantitative understandings of space and time distribution of water and fluxes in different parts of the cycle. Isotope techniques have provided unmatched insights into the functioning of the water cycle. New areas of research at the IAEA include identification and assessment of moisture sources in precipitation, interactions between the water and carbon cycles, fossil groundwater assessment, and submarine groundwater discharge. This presentation will review recent advances in these fields.

Opportunities and challenges in research on ground-water modeling

Schwartz, F.W.

Department of Geological Sciences,
The Ohio State University,
Columbus,
Ohio,
United States of America

Since the inception of computer-based, ground-water modeling almost 40 years ago, there have tremendous scientific and technological advances. Virtually all problems of significance to the practice of ground water (contaminant transport, regional ground-water flow, and well-field development) have been solved. On the research side, new codes are pushing the frontiers to complex multiphase problems, coupled phenomena, and stochastic processes. Nevertheless, our recent bibliometric studies of papers in Water Resources Research suggest that many research strands are simply worn out. Researchers often remain content to tinker with twenty-year old codes, embellishing them with odd new subroutines, or new user interfaces. Others continue to be satisfied with incremental advancements in historically important strands of research related to modeling. Perhaps the greatest challenge facing the community of ground-water modelers is finding relevance in a scientific world that has changed and in many respects has left them behind. The realities are that modeling now is needed more than ever to help solve the most vexing of societal problems, for example the impact of global climate change on water resources systems. The opportunities open to those willing to work in this arena are as enormous as the new challenges stemming from needs to integration new tools (satellites, information technology) and new unconventional research teams (economists, social scientists). To an unprecedented degree, governments want more out of science than just ideas and new modeling techniques. Those researchers able to adapt to this paradigm shift will help lead modeling to the next logical step of solving important global and regional problems.

Tracing sources of organic matter and nitrate in the San Francisco Bay-Delta-River ecosystem using isotopic techniques

Kendall, C., S.R. Silva, B.E. Bemis, D.H. Doctor, S.D. Wankel

U.S. Geological Survey,
Menlo Park, California,
United States of America

Hypoxic conditions in rivers, wetlands, and coastal ecosystems can cause significant problems for fish and bird migrations, the local fishing industry, and for the usefulness of the water body for drinking water and recreational purposes. While it is usually obvious that the problem is excess nutrients, it is usually less obvious exactly what should be done to remediate the problem. This is because there are usually many different land uses that contribute nitrate and organic matter to the ecosystem, and it is often difficult to determine the dominant source of the nutrients and organic matter causing local problems -- such as low dissolved oxygen levels or the production of disinfection byproduct during water treatment -- with standard chemical and hydrologic mass balance methods. Isotopes often provide new insights into sources, and are a useful adjunct to conventional methods.

Therefore, we have analyzed the isotopic compositions of dissolved and particulate organic matter (DOM, POM), nitrate, and water samples from selected sites in the San Francisco Bay-Delta-River ecosystem since 2000. Organic matter and/or nitrate samples were collected at various times in 2000-2003 from ~20 sites on or near the San Joaquin River (SJR) and ~10 sites in the Delta. POM samples from Delta and SJR sites had similar ranges of $\delta^{15}N$ and $\delta^{13}C$ values. Main-stem SJR sites have nitrate-$\delta^{15}N$ ranging from +9 to +14‰ (avg. +11‰) whereas samples from drains, creeks, and tributaries that drain into the SJR range from 0 to +12‰ (avg. +6‰). POM samples from main-stem SJR sites have $\delta^{15}N$ values ~ 4‰ lower than the co-existing nitrate. Depending on season, the nitrate-$\delta^{15}N$ may increase or decrease up to 3‰ downstream, due to changing mixtures of sources, while nitrate-$\delta^{18}O$ almost always decreases downstream as the proportion of water in the SJR derived from the Sierra Mountains (which has water-$\delta^{18}O$ values of ~ -15‰) increases. C:N values of POM at main-stem SJR sites were usually <8, whereas C:N values from drains and creeks were usually >15.

The main conclusions from our preliminary investigations are: (1) POM at main SJR sites is mainly algal in origin except during major storms, whereas POM from the creeks and drains contains appreciable terrestrial detritus, (2) most of the algae in the SJR appears to be produced in situ, (3) groundwater is a significant source of nitrate to the river, (4) much of the nitrate in the SJR appears to be derived from animal or human waste, and (5) algae in the Bay in October 2002 (during a whole-system transect) seems to be N-limited. Interestingly, these isotope data often contradicted the conclusions from previous studies that used simple mass balance approaches to determine and quantify sources, resulting in the re-evaluation of some of the earlier interpretations. The value of isotopic techniques is that they use the natural isotopic “labels” of different sources of organic matter and nitrate to quantify the contributions from different sources. Hence, isotope data are an extremely useful adjunct to traditional methods for assessing and monitoring sources of organics and nutrients during ecosystem restoration programs.

Use of tritium time series to estimate physical parameters of hydrologic systems

Michel, R.L.

US Geological Survey,
Menlo Park, California,
United States of America

Tritium has been used as a tracer for the physical movement of water for the last five decades. After the major increases in the tritium world inventory produced by atmospheric nuclear weapons testing, its value as a tracer was quickly recognized [1]. The tritium transient has been applied to a large variety of environmental studies in hydrology, oceanography and atmospheric circulation. Tritium data frequently yield information on physical processes which can be difficult or impossible to obtain by other methods. As the tritium transient enters its sixth decade and the tritium concentrations are declining, the interpretation of tritium measurements has become more ambiguous. The tritium/^{3}He methodology has been developed and is of use in groundwater studies, but is of limited values for surface waters studies. One method, which is frequently overlooked, is the use of measurements made over long periods of time, either on a routine basis, or sporadically. With the use of a proper input function, the physical meaning of these data can often be unraveled.

A monthly tritium input function has been developed for a 2^{o} latitude by 5^{o} longitude grid for the continental United States for the period 1953-2001. The tritium concentrations for the grid are derived from a series of precipitation collection stations that have operated during the tritium transient [2]. For coordinates where no station was available, the data is interpolated between the nearest stations. No station operated prior to 1959 and many stations were discontinued during the 1970s and 1980s. To overcome these gaps in the data, correlations were carried out with the Ottawa, Canada station to f ill in gaps in the data for 1953 to 1987. Due to possible influences from local nuclear sources in Ottawa after 1987, correlations were carried out with the Vienna, Austria station for the period 1987-2001. Correlation coefficients relative to the Vienna station are given for each section on the grid for each month so that when more data becomes available on the IAEA website (http://isohis.IAEA.org) researchers can use it to extend the input function in time. This input function can then be used in modeling tritium time series.

An historical surface water data set has been compiled in cooperation with the IAEA consisting of surface water tritium concentrations measured since the 1940s. This data set consists of over 6000 surface tritium measurements made world-wide from prior to the beginning of atmospheric nuclear testing to 2004. There are many long-term data sets available in this group which furnish valuable data bases for understanding physical processes within the river basins. These data show the response of the surface water systems to the tritium transient over the past several decades. For many hydrologic systems, tritium concentrations in river water will be more important than concentrations in precipitation. This is frequently the case in studies involving irrigation and urban studies.

Figure 1 shows the response of the typical surface water system (Missouri River at Nebraska City, Iowa) to the tritium transient compared to that of the precipitation within the basin. The rise of tritium concentrations in surface waters is less than that found in precipitation, but the drop in concentrations is much slower. This is due to the residence times of the various reservoirs that contribute to the base flow of the river system. Mean residence times calculated for a series of different systems have shown variations from 1-2 years to approximately 20 years. These differences will have important implications for the response of different basins to pollution, and changes in land use and climate. The seasonal signal from release of spring melt and rains is also evident in the tritium concentrations for

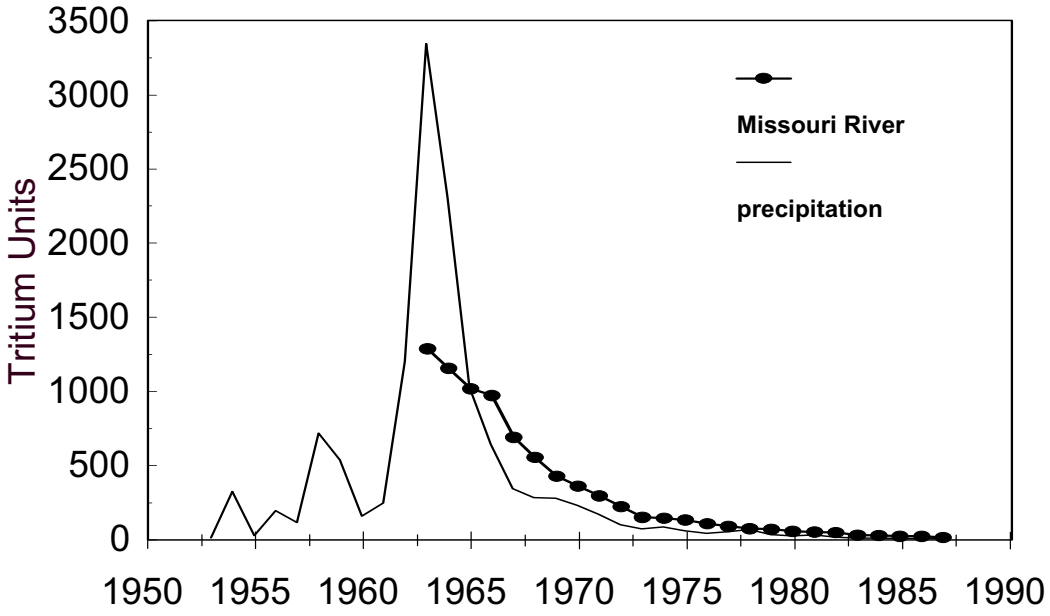

FIG. 1. Response of the Missouri River at Nebraska City, Iowa to the tritium transient compared to tritium concentrations in precipitation within the basin.

rivers for three to four years after the peak of the transient in 1963. These increases in concentration indicate the fraction of young water that makes up the flow during that period. As tritium concentrations in precipitation decreased this seasonal signal disappeared and cannot be used to determine the fraction of young water at the present time. These results indicate the importance of obtaining previous data for proper assessment of current data.

REFERENCES

[1] SUESS, H., Tritium geophysics as an international research project, Science **163** (1969) 1405-1410.

[2] MICHEL, R.L., Tritium deposition in the continental United States, 1953-1983, US Geological Survey Water Resources Investigations 89-4072 (1989) 45 pp.

Line-conditioned excess: a new method for characterizing stable hydrogen and oxygen isotope ratios in hydrologic systems

Landwehr, J.M., T.B. Coplen

U.S. Geological Survey (USGS),
Reston, Virginia,
United States of America

Abstract. Recent work characterizing the co-variation of stable isotope ratios in the large river systems of the United States has led us to develop a new mathematical method to express the relationship between stable hydrogen and oxygen isotope ratios in these systems. This method, entitled line conditioned excess, defines the offset between a meteoric water line and river water samples, with 0 indicating no difference between a river water sample and meteoric conditions, a positive value falling above the line and a negative one, below, in reference to a plot of δ^2H versus δ^{18}O. When the reference is to a local meteoric water line, the formulation is entitled 'lc-excess' and when to a global meteoric water line, 'LC-excess'. Line conditioned excess values reflect both source water differences as well as the full complexity of physical processes that produce surface waters. The method has proven useful in screening water samples with respect to meteoric conditions. It differs both in concept and in construct from the method of deuterium excess or d-excess.

1. Introduction

Our recent work characterizing the co-variation of stable isotope ratios in large river systems [1] has led us to define a new method to express the relationship between stable hydrogen and oxygen isotope ratios of waters in these systems. We have opportunistically obtained over 2000 samples from over 40 stations in several large river systems of the United States, including the Mississippi and major tributaries, the Rio Grande, the Colorado, the Columbia and the Yukon. Samples are taken on a quasi-monthly schedule for the U.S. Geological Survey's National Stream Quality Accounting Network (NASQAN) program [2]. Samples have been taken since 1997 through today, although not at all stations, and some stations have data from the 1980's as well. [3] Our challenge is to characterize the isotopic signatures of these large river systems and to understand the history by which the water arrived in the channel, including recent precipitation from different source air masses, seasonal evaporation patterns reflecting different conditions of temperature, relative humidity, and windiness, baseflow contributions from ground waters of possibly different ages, as well as upstream water contributions including possible dam releases.

2. Definitions and Discussion

The concept of a meteoric water line can be attributed to Craig [4] when he identified a linear relationship between the stable hydrogen and oxygen isotope ratios of water samples to be

$$\delta^2\mathrm{H} = 8\ \delta^{18}\mathrm{O} + 10$$

Craig described this relationship to be indicative of "waters which have not undergone excessive evapotranspiration." However, his samples included not only precipitation waters, but also water samples from rivers and lakes.

We reserve herein the term "meteoric water line" (MWL) to indicate a linear relationship based only on the stable hydrogen and oxygen isotope ratios from precipitation samples and the term "river water line" (RWL) for one based only on river water samples. Note that a RWL is not necessarily consistent with the appropriate region's MWL because a RWL reflects the full complexity of the terrestrial history of the surface channel water. Indeed, Kendall and Coplen [5] noted that there was generally a

lack of agreement between a local MWL (LMWL) for precipitation and a linear regression based on δ^2H versus δ^{18}O of the river water samples.

To determine how the isotopic values of river waters differ from their presumed source, namely regional precipitation, we defined the concept of "line conditioned excess" (lc-excess and LC-excess) to be the difference between the value of δ^2H from a water sample and a linear transform of the δ^{18}O from the same sample where the linear transformation reflects the relevant referenced meteoric water relationship. In particular, we define

$$\text{lc- excess} = \delta^2\text{H} - \text{a } \delta^{18}\text{O - b}$$

as the line conditioned excess where a and b are the coefficients of the local meteoric water line (LMWL) from the relevant region for the river water samples. Thus, if the river samples came from a region in east central Texas, USA, lc-excess could be defined from the LMWL for Waco, Texas with a = 6.52 and b = 4.58 [6] or if from south east Alberta, Canada, the LMWL for Calgary with a = 7.68 and b = -0.21 [7] could be used.

However, when dealing with river water samples from across the United States, we face two problems. First, the local meteoric water line may not be known for each specific regional situation. Second, for a large river basin such as that of the Mississippi, or when making comparisons between large river basins across the entire United States, no single LMWL represents an appropriate reference condition. Consequently, we defined an alternative formulation of line conditioned excess to reflect larger regional conditions using a Global Meteoric Water Line (GMWL). We called this formulation "LC-excess" and distinguish it from "lc-excess" which is based on a LMWL. We use here the GMWL as defined by Rozanski and others [8] based on the weighted average of precipitation at over 200 stations globally distributed. Thus,

$$\text{LC-excess} = \delta^2\text{H} - 8.20\ \delta^{18}\text{O} - 11.27$$

LC-excess expresses mathematically the offset between the GMWL and river water samples, with 0 indicating no difference between a river water sample and the GMWL, a positive value falling above the GMWL and a negative one, below.

We note here that line conditioned excess is neither the same concept nor the same construst as deuterium-excess, or d-excess, which was defined by Dansgaard [9] as

$$\text{d-excess} = \delta^2\text{H} - 8\ \delta^{18}\text{O}$$

Mechanically, d-excess is defined as an estimate of the intercept of the Craig relationship. Dansgaard interpreted d-excess to be an index of non-equilibrium in the simple condensation - evaporation of global precipitation, informing on kinetic evaporation conditions in the oceanic source area of the precipitation waters. That line conditioned excess is not the same construct as deuterium excess can be seen as follows. Suppose that the local meteoric water line is identical to the Rozanski et al. [8] GMWL and that the river waters are not highly altered after precipitating, so that the river samples accord with the relationship

$$\delta^2\text{H} \sim = 8.20\ \delta^{18}\text{O} + 11.27$$

Under these circumstances, the computed lc-excess values would be ~0 for all river water samples, indicating their close affinity to meteoric conditions, whereas the computed d-excess values would be

$$\text{d-excess} \sim = 0.20\ \delta^{18}\text{O} + 11.27$$

which varies with δ^{18}O, thus complicating the assessment of the relationship of interest herein, namely how consistent are the river samples with meteoric conditions.

To illustrate, we note that we obtained the following median LC-excess values for the major river basins: +1.9 ‰ in the Ohio, -1.6 ‰ in the mainstem Mississippi, -7.7 ‰ in the Missouri, -9.9 ‰ in the Rio Grande, -1.1 ‰ in the Upper Colorado, -9.1 ‰ in the Lower Colorado, -0.2 ‰ in the Columbia and -3.2 ‰ in the Yukon. The Columbia system, a coastal basin, had an LC-excess value that was indistinguishable from 0 (or the GMWL), whereas the more arid and mid-continental basins were most negative and furthest from 0 indicative of highly evaporative conditions (Rio Grande and Lower Colorado) or oxygen isotope depleted meteoric waters (Missouri). The positive value for the Ohio system may reflect the influence of the Great Lakes on precipitation in that basin.

Using the measurement uncertainties of the USGS Reston Stable Istopope Laboratory, namely 1‰ and 0.07 ‰ for δ^2H and δ^{18}O, respectively, we can derive the one standard deviation measurement uncertainty S for the line conditioned excess formulation to be

$$S = \{1^2 + (a\ 0.07)^2\}^{0.5}$$

where a is the slope coefficient from the MWL. Thus, for LC-excess using the Rozanski et al [8] coefficients, the value of S is 1.15 ‰.

We can make use of S to rescale the formula for line conditioned excess to assess significant departures from meteoric conditions. That is, we define

$$\text{lc- excess *} = [\delta^2\text{H} - a\ \delta^{18}\text{O} - b\ ] / S$$

and

$$\text{LC-excess*} = \{\delta^2\text{H} - 8.2\ \delta^{18}\text{O} - 11.27\} / 1.15$$

We derive LC-excess* for the median LC-excess values reported above to be, respectively, +1.6, -1.4, -6.7, -8.6, -1.0, -7.9, -0.2, and -2.8. Only those values for the Missouri (-6.7), the Rio Grande (-8.6), the Lower Colorado(-7.9) and possibly the Yukon (-2.8) river systems can be considered to be significantly inconsistent with the GMWL.

3. Summary

Line conditioned excess, specifically lc-excess (lc-excess*) and LC-excess (LC-excess*), directly indicates the offset of surface water samples from the relevant meteoric water line. Its interpretation is not complicated by varying with the oxygen isotope ratio as d-excess does. It is also an effective diagnostic method for distinguishing isotopic ratios between river basins.

ACKNOWLEDGEMENTS

This work was supported by the USGS National Research Program in Water Resources. We thank Joel Gat, Haiping Qi, Kinga Revesz, Martha Scholl, and Ike Winograd for helpful discussions.

REFERENCES

[1] LANDWEHR, J.M., COPLEN, T.B., The Oxygen and Hydrogen Ratios in Waters from the Largest River Systems of the United States, (Proceedings, Isotope Hydrology and Integrated Water Resources Management), IAEA, Vienna, IAEA-CN-104 (2004) 402-403.

[2] U.S.GEOLOGICAL SURVEY National Stream Quality Accounting Network, Monitoring the quality of the Nation's large rivers (last update 21 May 2004) http://water.usgs.gov/nasqan

[3] COPLEN, T.C., KENDALL, C. Stable Hydrogen and Oxygen Isotope Ratios for Selected Sites of the U.S. Geologcial Survey's NASQAN and Benchmark Surface-water Networks, U.S. Geological Survey Open-File Report **00-160** (2000) 409 pp.

[4] CRAIG, H., Isotopic Variations in Meteoric Waters, Science **133** (1961) 1702-1703.

[5] KENDALL, C., COPLEN, T., Distribution of oxygen-18 and deuterium in river waters across the United States. Hydrological Processes **15** (2001) 1363-1393.
[6] INTERNATIONAL ATOMIC ENERGY AGENCY, Statistical Treatment of Data on Environmental Isotopes of Precipitation, IAEA Technical Reports Series **No. 331** (1992) 436-440.
[7] PENG, H., MAYER, B., HARRIS, S., AND KROUSE, H.R., A 10-yr record of stable isotope ratios of hydrogen and oxygen in precipitation at Calgary, Alberta, Canada, Tellus **56B** (2004) 147-159.
[8] ROZANSKI, K., ARAGUAS-ARAGUAS, L., GONFIANTINI, R., Isotopic Patterns in Modern Global Precipitation (Climate Change in Continental Isotopic Records, Geophysical Monograph 78, ed.P.K. Swart, K.C.Lohmann, J.McKenzie,S.Savin), American Geophysical Union, Washington D.C., (1993) 1-36.
[9] DANSGAARD, W., Stable isotopes in precipitation, Tellus **16** (1964) 436-468.

Environmental tracers in groundwater of the North China Plain

Kreuzer, A.M.[a], C. Zongyu[b], R. Kipfer[c], W. Aesbach-Hertig[a]

[a] Institute of Environmental Physics,
University of Heidelberg,
Heidelberg,
Germany

[b] Institute of Hydrogeology and Environmental Geology,
Chinese Academy of Geological Sciences,
Zhengding,
Hebei,
China

[c] Institute of Isotope Geology,
Swiss Federal Institute of Technology (ETH),
Zürich,
Switzerland

Environmental tracers such as stable isotopes or noble gases in groundwater are important tools to study issues of water resources and to obtain palaeoclimate records. Applications of these methods to semi-arid regions are of particular interest. Old groundwaters in such places are not only climate archives, but in the first place water resources of high quality but finite quantity. The goal of our ongoing study is to investigate groundwater recharge and palaeo-climate in the semi-arid North China Plain. Here we present the first palaeoclimatic results.

The North China Plain consists of the deposits of the Yellow River and is the largest alluvial plain of eastern Asia. The plain is bordered on the west by the Taihang Mountains and fronts the Bohai Gulf in the east. It reaches up to the Yen Mountains in the north and to the Yangtze River in the south. The North China Plain is one of the most densely populated areas of the world. The plain has a temperate continental monsoon climate, with clear-cut seasons, dry winters and humid summers. The sediments of the plain contain four partly interconnected aquifers [1]. We focus here on results from the deepest aquifer, which has its recharge area near the mountains in the west and becomes deeper and confined to the east near the coast.

In March 2004 twenty-six wells along a transect from the recharge area near Shijiazhuang to the coastal area near Tianjin were sampled (see map Fig. 1, left panel). Each well was sampled for ^{14}C, ^{3}H, stable isotopes (^{2}H and ^{18}O) and noble gases. Because the ^{14}C measurements have not yet been performed, all results are preliminarily plotted versus the distance along the flow path from well No.1. The ages derived from wells that were already sampled by Zongyu et al. [1] show that the flow distance is a reasonable age proxy at least for the first 220 km of the flow path (mountain area to Cangzhou, see Fig. 1, right panel). Because the transect from Cangzhou to Tanggu was not dated before, it is uncertain whether this approach provides a reliable age scale at distances greater than 220 km. The right panel of Fig. 1 also shows the ^{4}He-concentration versus the distance along the flow path. The ^{4}He-concentration rises along the flow path as a result of accumulation of radiogenic ^{4}He, confirming that the groundwater age increases with distance.

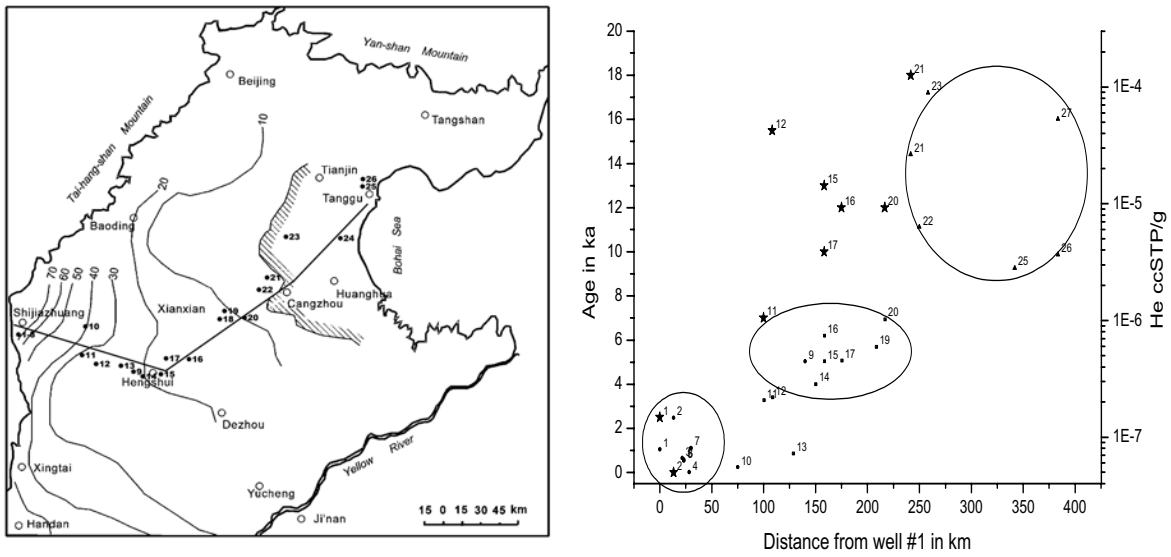

FIG. 1. Left: Map of the North China Plain, with contour lines of the pre-pumping hydraulic head. Filled circles with numbers indicate wells along the transect (bold line) from the outcrop area near Shijiazhuang to Tanggu near the sea. Right: Previously measured ^{14}C-ages from [1] (left scale, stars), and ^{4}He-concentrations (right scale, small symbols) versus the distance along the flow path. The circles show the grouping of wells (young, old and mantle-influenced) we refer to in the text.

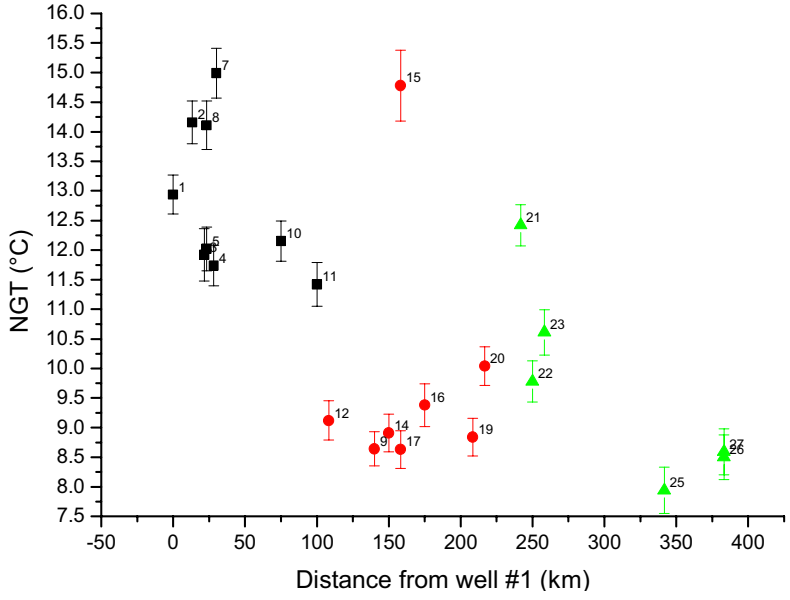

FIG. 2. Noble gas temperatures along flow distance. Three groups of young (squares), old (dots) and mantle-influenced (triangles) groundwater are distinguished. Points are labeled with well numbers.

Using additional information such as the ^{3}He/^{4}He-ratio and transient tracers, we distinguish three different groups of wells. The first group consists of wells with modern groundwater, from the region of Shijiazhuang (0 – 50 km flow distance). These wells were additionally sampled for SF_6 and ^{3}H and most of them were found to contain significant amounts of these transient tracers, proving that the groundwater in this region is very young.

The second group of wells ranges from 80 - 220 km of flow distance and consists of wells with old groundwater of higher ^{4}He-concentration. The results of Zongyu et al. [1] indicate ^{14}C-ages of 10 - 16 ka. The third group contains the wells 21-27 from the transect between Cangzhou and Tanggu. These

wells have the highest He-concentration and comparatively high $^{3}He/^{4}He$-ratios, clearly showing an addition of mantle-derived helium. A mantle helium signature has also been observed by Zhang et al. [2] in inclusions of the oil-bearing rocks in this area and has been related to several deep faults in this region. Due to the He isotope anomaly and the uncertain dating, the samples of the third group are treated separately in the interpretation of our results. The results from Wells 11 and 15 were also excluded from the analysis. Well 11 is thought to represent the transition between the first two groups, whereas Well 15 should belong to the old group but seems to be an outlier in the noble gas data.

Noble gas temperatures (NGTs) were calculated according to the model outlined by Aeschbach-Hertig et al. [3]. It provides very good fits to the data except for Well 13, for which no NGT was assigned. The NGTs are presented in Fig. 2 with different symbols for the three groups. The mean NGT of the first group (squares) is 13.0 ± 0.4°C, and although there is quite a big variation, the mean temperature closely reflects the modern mean annual air temperature in the area (13.4°C at Shijiazhuang). The origin of the relatively large scatter of NGTs in the young group is as of yet unclear. The mean NGT of the second group, which we interpret as the mean air temperature during the end of the last glacial period in the North China Plain, is 9.1 ± 0.2°C. Our best estimate for the glacial-interglacial temperature difference is therefore 3.9 ± 0.5°C. The last group of mantle-influenced groundwater samples varies strongly in NGTs, possibly because there may be admixing of a different water component than in the other two groups, related to the mantle He. Because we furthermore lack any information about the age of these wells, they are not interpreted at this point of time.

The simultaneous measurement of noble gases and stable isotopes in groundwater allows us to directly derive the slope of the $\delta^{18}O$-T relationship on the glacial-interglacial time scale. Fig. 3 shows the $\delta^{18}O$-values in respect to NGT. It shows the three groups of wells again, with the young group located around 13.0 °C and -8.3 ‰ and the old group located around 9.1 °C and -10.9 ‰. So the slope of the $\delta^{18}O$-NGT-line is 0.66 ‰ $°C^{-1}$. This is about twice the value obtained from modern precipitation at monitoring stations in China (0.35 ‰ $°C^{-1}$), based on which Zongyu et al. [1] derived a temperature difference of 6 - 9 °C between present and last glacial from their stable isotope data. The NGTs show that this estimate likely was too high.

Modern-day correlations between stable isotopes and temperature are often used to calculate paleotemperatures from measurements of stable isotopes in archives such as ice, speleothems, groundwater, and others. However, it is uncertain whether a $\delta^{18}O$-T relationship obtained from recent precipitation can be applied to glacial-interglacial time scales, where many boundary conditions have changed [4]. The combination of NGTs and stable isotope data from groundwater may provide a more reliable estimate of the regional long-term slope that may be useful in future stable isotope studies.

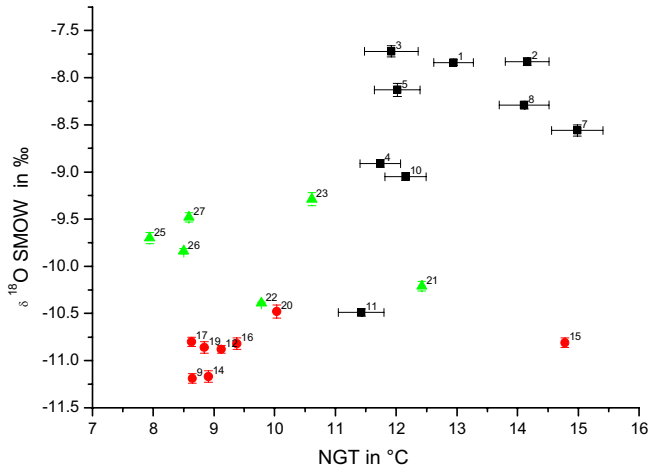

FIG. 3. Correlation between $\delta^{18}O$ and NGT. Symbols and numbering as in Fig. 2.

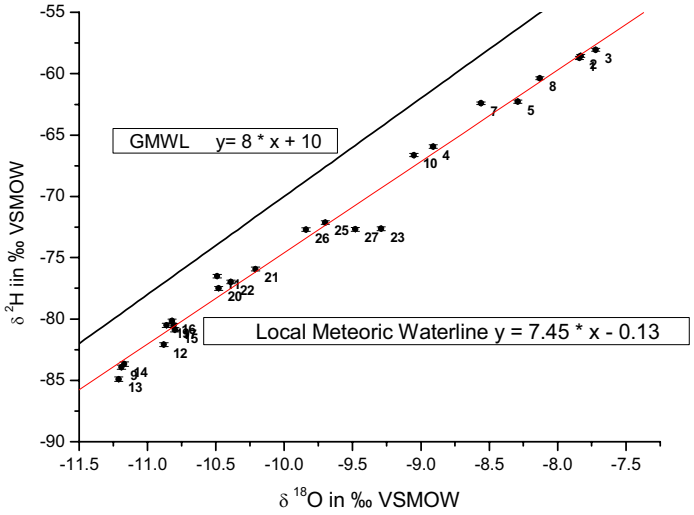

FIG. 4. Correlation between δ^2H and $\delta^{18}O$. Points are labeled with well numbers.

Yet, the reason for the discrepancy observed in this study still needs further investigation. In contrast to studies of polar ice sheets, in our case using the modern $\delta^{18}O$-T slope seems to over- rather than under-estimate the glacial-interglacial change. Comparing the stable isotope data to the global meteoric water line shows no obvious effects other than temperature. A fit through all data yields $\delta^2H = 7.45 \cdot \delta^{18}O - 0.13$ for the local meteoric waterline (Fig. 4). All data lie closely on this line, with no obvious difference in slope or deuterium excess between the young waters plotting in the upper right part and the older waters in the lower left. The mantle-influenced group lies somewhere in between. Evaporation would lead to deviations along lines with a lower slope, which does not seem to be the case. We can presently only speculate that part of the large glacial-interglacial changes of stable isotopes may be due to a different source of paleo-precipitation than today, when it is strongly dominated by summer monsoon rains.

ACKNOWLEDGEMENT

This work was financially supported by the National Science Foundations of Germany (DFG grant No. AE-93/1) and China (NSFC grant No. 40472125).

REFERENCES

[1] ZONGYU, C., JIXIANG, Q., JIANMING, X., JIAMING, X., HAO, Y., YUNJU, N., Paleoclimatic interpretation of the past 30 ka from isotopic studies of the deep confined aquifer of the North China plain, Appl. Geochem. **18** (2003) 997-1009.

[2] ZHANG, X., et al., Discovery and its geological significance of the mantle-derived helium in the inclusions of the Ordovician oil-bearing reservoir rocks in the Huanghua depression, China, Sci. in China Ser. D, Earth Sci. **47** (2004) 23-29.

[3] AESCHBACH-HERTIG, W., et al., Palaeotemperature reconstruction from noble gases in ground water taking into account equilibration with entrapped air, Nature **405** (2000) 1040-1044.

[4] FRICKE, H.C., O'NEIL, J.R., The correlation beween $^{18}O/^{16}O$ ratios of meteoric water and surface temperature: its use in investigating terrestrial climate change over geologic time, Earth Planet. Sci. Lett. **170** (1999) 181-196.

The relationship between the isotopic composition of lake and inflow waters and the limnology of a small carbonate lake in NW England

Fisher, E.H., S.F. Crowley, S. Barnes, K. Kiriakoulakis, J.D. Marshall

Department of Earth and Ocean Science,
University of Liverpool,
Liverpool,
United Kingdom

Abstract. Hawes Water is a carbonate-precipitating, monomictic, oligotrophic lake typical of many temperate, maritime, hard water lakes in NW Europe. Geochemical and isotopic studies show that lake hydrology is dominated by the local meteoric groundwater system, with little evidence of evaporative modification. The $\delta^{18}O$ of calcite precipitating from lake waters is consistent with temperature-dependent isotope fractionation relationships established by laboratory experiment. Minor differences between observed and predicted $\delta^{18}O_{calcite}$ result from a pH-dependent kinetic contribution to oxygen isotope fractionation in the natural lake environment. These observations show that: (a) climate information, in the form of summer water temperature and $\delta^{18}O$ of meteoric precipitation, is transferred quantitatively to the sediment record; and (b) ancient lake sediments preserve a recoverable record of past climate change.

1. Introduction

Oxygen isotope records recovered from carbonate-rich sediment cores collected from the Hawes Water lake basin (NW England) are being used to reconstruct Holocene and late glacial climate change. In order to confirm that environmental signals are transferred quantitatively to the sediment record a detailed study of the limnology of Hawes Water was carried out over a two-year period. The main objective was to examine the links between factors controlling the isotopic composition of lake waters and isotopic records preserved by carbonate lake sediment.

2. Methodology

Hawes Water is a small (8 ha), hard water lake located near Carnforth, NW England (54°10.9'N 2°48.0'W). The lake is situated at approximately 8m above sea level and occupies a localised depression within a karstic (Carboniferous) limestone aquifer. Water supply to the lake is controlled by groundwater (with smaller contributions from direct meteoric precipitation, surface drainage and semi-permanent springs), sourced from a catchment (~150 ha) dominated by low-lying limestone hills draped by thin (0-1.5 m) glacial diamicts and soils. The lake is characterised by a shallow (0-3 m) littoral fringe colonised by dense stands of reeds and aquatic macrophytes, and a deep (8-13 m), open water basin. The lake margin is separated from the deeper basin by a narrow zone (5-20 m wide) where lake bathymetry changes rapidly. Surface drainage occurs through an intensely modified (human intervention) peat bog (Hawes Water Moss) located at the southern end of the lake, but overall lake drainage is controlled by a natural continuation of the regional groundwater system.

Limnological observations were undertaken from April 1998 to April 2000. Water temperature was monitored continuously (2-hourly intervals) through the entire water column (1 to 3 m spacing) using *in situ* temperature data loggers. Water samples were analysed frequently (typically 3-4 week intervals). On-site measurements included temperature, pH, Σalkalinity and dissolved oxygen. Separate water samples were collected for laboratory analysis of cations and anions, nutrients ($\Sigma SiO_{2(aq)}$, P), chlorophyll, and stable isotope ratios ($\delta^{2}H$, $\delta^{18}O$). In addition, for one season (April-

October 1999), carbonate precipitates were collected for $\delta^{18}O$ analysis by suspending sheets of nylon mesh in the water column at 0, 1, 2, 4 and 6 m below lake level.

3. Results

Temperature: Temperature measurements (Fig. 1a) show that Hawes Water is a monomictic lake. Thermal stratification is initiated in early April and is fully developed – with a distinct thermocline located at a depth of ~6 m – from May to September. The stratification collapses progressively during late September and overturn of the water column is complete by late October.

Productivity: Hawes Water is a low productivity – oligotrophic – lake characterised by extremely low levels (<0.1 μg/mL) of dissolved phosphorous There is little evidence for anthropogenic modification of the lake nutrient cycle evident in many NW European lakes. Chlorophyll measurements provide evidence for a spring (early March) productivity event dominated by *Stephanodiscus* (diatoms) and a much less prominent autumnal (mid-September) bloom associated with the growth of *Chrysophyceae* (flagellates).

Dissolved oxygen: Levels of dissolved oxygen ($\%O_2$ saturation) show considerable seasonal and depth variation in response to thermal stratification and biological activity (Fig. 1b). The onset of thermal stratification coincides with a progressive increase in dissolved oxygen in the epilimnion and a reduction in the hypolimnion. These changes correspond with increasing photosynthesis in surface waters and increasing bacterial decomposition of organic matter deposited in lake basin sediment. During the mid-summer period a zone of intense oxygen enrichment (with peak $\%O_2$ saturation >200%) is developed at the thermocline in response to a localised seasonal growth of algae (*Bacillariophyceae*). Winter overturn of the water column, combined with the shut-down of significant biological activity, results in homogenization of dissolved oxygen levels and a return towards equilibrium with atmospheric pO_2.

pH, pCO_2, calcite saturation: In hard water lakes, dominated by bicarbonate alkalinity, pH, pCO_2 and calcite saturation are dependent variables and are strongly correlated (Fig. 2a). Figure 2b illustrates the variation in pH and calcite saturation for a 12-month period. Surface waters are permanently over saturated with respect to calcite; only in bottom waters, during late summer (July-September) when bacterial processes are most active, is pCO_2 sufficiently high to approach calcite undersaturation.

Qualitative observation from calcite precipitation on artificial substrates shows that carbonate precipitation is most intense in near-surface waters (0-4 m) and is effectively confined to summer months (June-August). Below 4 m the amount of calcite precipitation decreases sharply, with no precipitation occurring below the thermocline. No precipitation is observed to occur at any depth from mid-September to mid-April. These observations support CO_2 degassing and photosynthesis in the epilimnion as the driving mechanism for calcite precipitation.

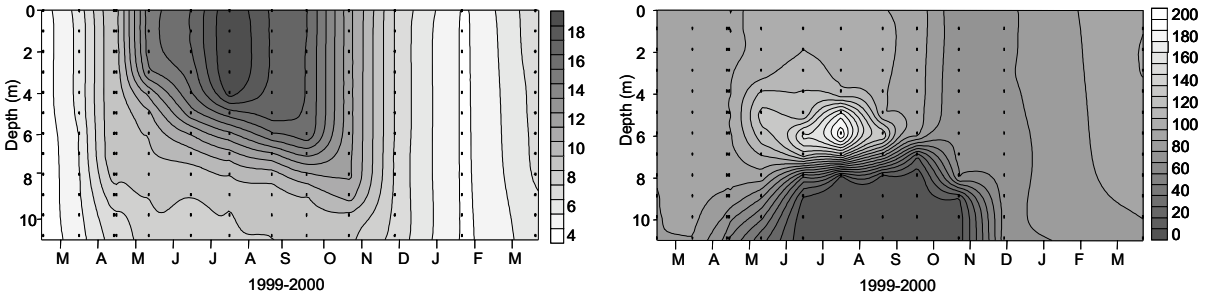

FIG. 1. Contoured depth-time plots: (a) temperature (°C); (b) dissolved oxygen (% O_2 saturation).

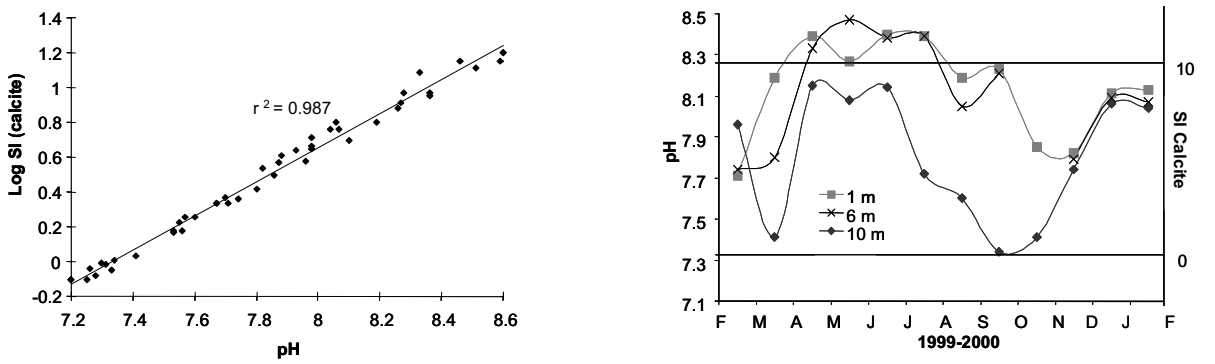

FIG. 2. (a) Correlation between calcite saturation index (log SI) and pH; (b) pH-time plot illustrating seasonal variation in pH and SI.

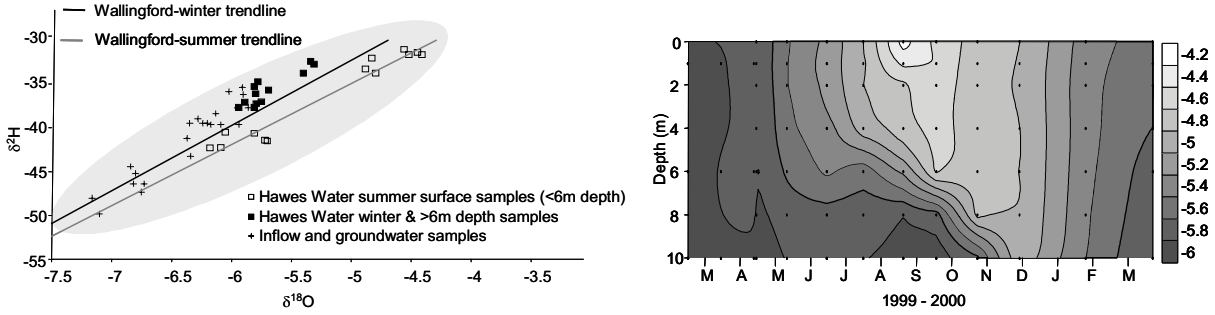

FIG. 3. (a) δ^2H-$\delta^{18}O$ plot showing the distribution of Hawes Water data with respect to the UK regional meteoric water line based on the GNIP site at Wallingford. Shaded area contains 95% of the data from the GNIP site; (b) Contoured depth-time plot for lake water $\delta^{18}O_{SMOW}$.

Hydrogen and oxygen isotopes: Comparison between a regional UK meteoric water line (MWL), (Wallingford GNIP site) and water samples collected from the local limestone aquifer and the lake basin (Fig. 3a) show that, in general, the Hawes Water hydrological system is dominated by meteoric input. The difference between the epilimnion and the deeper water can be attributed to seasonal differences in the composition of rainfall and a lack of mixing in the water column (Fig. 3b). Lake-level and water table measurements, combined with daily local rainfall records show a strong correlation between rainfall amount and Hawes Water base level. This suggests that the lake is very responsive to rainfall and implies that the changing isotopic composition of the epilimnion is dominated by seasonal changes in the isotopic composition of meteoric precipitation.

4. Oxygen isotope equilibrium – quantitative transfer of climate signals

A major objective of this study was to test the assumption that oxygen isotope records are transferred quantitatively to the calcite sediment deposited within the lake basin (cf. [1]). The $\delta^{18}O$ of calcite precipitated on artificial substrates located at fixed depths within the water column was compared directly with depth-equivalent temperature and $\delta^{18}O_w$ measurements. Data were plotted on a conventional $10^3 \ln\alpha$–temperature diagram (Fig. 4) and compared with an established temperature-dependent, calcite-H_2O, oxygen isotope fractionation relationship [2]. Small offsets between observed and predicted values – note that most data plot on the equilibrium trend within estimates of experimental error – can be attributed to errors associated with: (a) the averaging of environmental parameters (temperature, $\delta^{18}O_w$) over the monthly time intervals allowed for accumulation of calcite precipitates; (b) pH-dependent kinetic contributions to oxygen isotope fractionation [1, 3]; and (c)

possible kinetic artefacts associated with the use of artificial substrates to nucleate and collect precipitates. A small number of samples, collected at 6 m, are observed to depart significantly from the equilibrium trend. The reason for this is not yet understood.

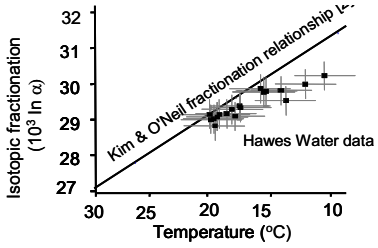

FIG. 4. Comparison between calcite-H_2O oxygen isotope fractionation ($10^3 ln\alpha$) and temperature for lake precipitates. Errors bars are based on cumulative uncertainties associated with observed ranges for temperature and $\delta^{18}O_w$ over monthly sampling intervals.

5. Conclusions

Hawes Water provides a natural laboratory for testing the transfer of climate signals to the sediment record in temperate, oligotrophic, maritime hard water lake systems. Hydrological investigation of the catchment and lake shows that Hawes Water hydrology is controlled by meteoric processes, with minimal modification of near-surface waters by seasonal evaporation. Geochemical and isotopic data obtained from lake waters and calcite precipitates are, in general, consistent with temperature-dependent equilibrium oxygen isotope fractionation. These observations show that carbonate sediments preserve a predictable and recoverable record of summer climate.

ACKNOWLEDGEMENTS

This research was funded by NERC grants. Site access was provided by English Nature.

REFERENCES

[1] TERRANES, J.L., et al., A study of oxygen isotopic fractionation during bio-induced calcite precipitation in eutrophic Baldeggersee, Switzerland, Geochim. Cosmochim. Acta **63** (1999) 1981-1989.

[2] KIM, S.T., O'Neil, J.R., Equilibrium and non-equilibrium oxygen isotope effects in synthetic carbonates, Geochim. Cosmochim. Acta **61** (1997) 3461-3475.

[3] USDOWSKI, E., HOEFS, J., Oxygen isotope exchange between carbonic acid, bicarbonate, carbonate, and water: a re-examination of the data of McCrea (1950) and an expression for the overall partitioning of oxygen isotopes between carbonate species and water, Geochim. Cosmochim. Acta **57** (1993) 3815-3818.

Stable water isotopes: revolutionary tools for global water cycle disturbance diagnosis

Henderson-Sellers, A.[a], P. Airey[a], D. Stone[a], K. McGuffie[b], A. Williams[a]

[a] ANSTO Environment,
Sydney,
Australia

[b] Applied Physics,
University of Technology,
Sydney,
Australia

Abstract. Here we assess the simulation of isotopic fluxes in basin-scale hydrology, focusing on the 'big leaf' representation of land surfaces in numerical models as the current mechanism for incorporating water isotopes. Applications of the simulation of stable isotopic behaviour simulated by global climate or earth system models, including river isotopic characterization of basin changes and plant-respired oxygen isotope 'tagging', to resolving uncertainty are limited until more basic criteria such as conservation, current mean climate and capture of observed variability are demonstrated. We find that surface water budgets are still rather poorly simulated and inadequately constrained at the scale of large basins; yet surface energy partition can be apparently well captured by models with inadequate land-surface parameterization.

1. Introduction

Coupled climate models, which integrate processes in the hydrosphere and biosphere into three-dimensional models of the atmosphere-ocean system are the most sophisticated tools available for understanding impact of various climate forcings on the climate system. The global water budget in these climate models is well simulated at a gross scale but, different model simulations applied to future or past climate changes result in differences in the details of the basin-scale hydrology ([8]). In addition to continuing to improve gross water flux measurements through coordinated measurement programs and using these to test models, there is also an opportunity to evaluate and potentially improve hydrological parameterizations at a basin scale using a novel data set: stable water isotopes.

Models of climate change and climatic variability are now being used to project water resources in large catchments and the more subtle aspects of these simulations of large basin hydrology still require validation. Stable isotopes of water have been used to interpret long-term temperature trends since Dansgaard [1] ([8]), and their systematic variations in the water cycle as a result of phase change and diffusion-derived isotopic fractionation have also been exploited in understanding the hydrological cycle in specific locations [2]. Sources of air masses and precipitation processes affect the relative amounts of isotopes present in precipitation while temperature-dependent equilibrium fractionation during evaporation and turbulent scale interactions in the atmospheric boundary layer increase the heavy isotope species in surface waters, [4, 5].

2. Hydro-climate processes

Stable water isotope characteristics of river discharge have provided information about basin-integrated hydro-climates where detailed measurements of the hydro-climate are impractical [9]. Features of models that require evaluation (and where isotopes could provide valuable assistance) include water re-cycling by the surface as a function of precipitation variability; evaporation sourcing (i.e. whether water vapour is from transpiration or evaporation from wetlands, soil, or the vegetation

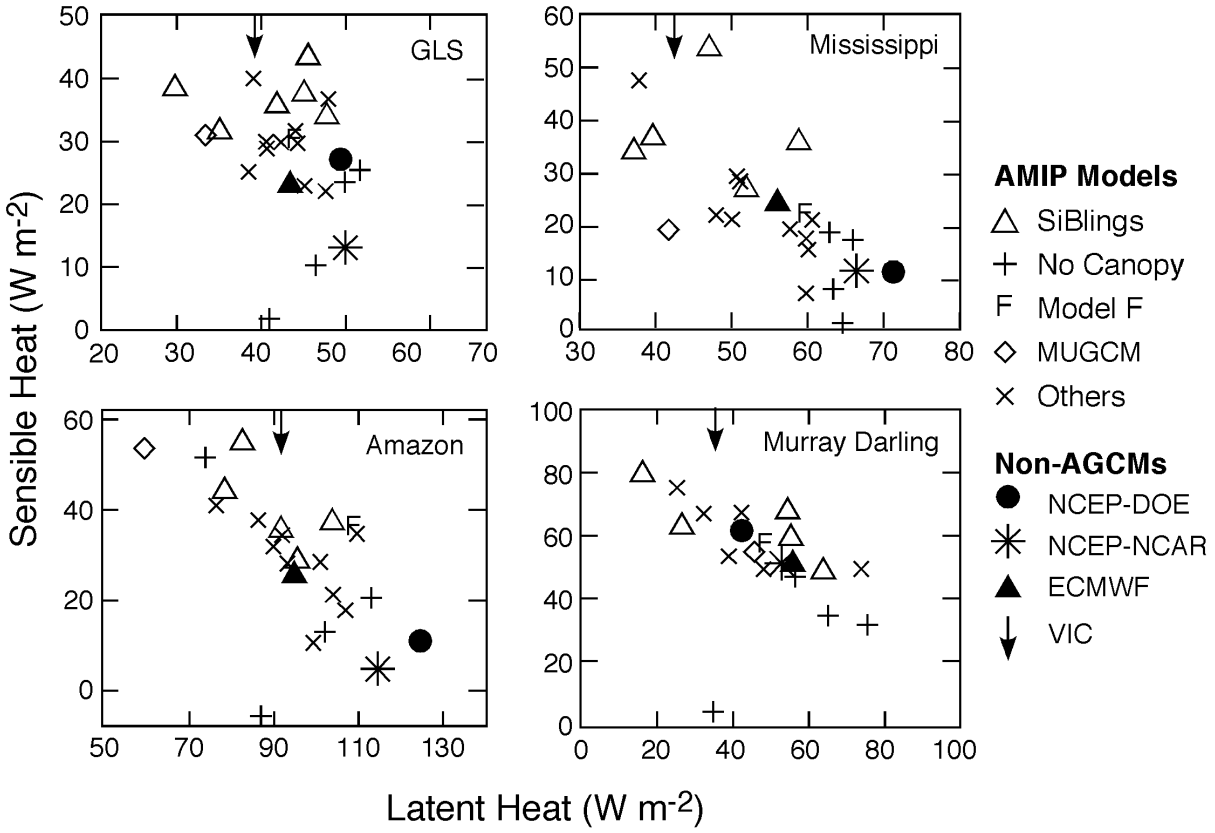

FIG. 1. Partitioning of surface energy between scaled sensible heat (SH) and latent heat (LH) for 20 AMIP II AGCMs (shown as three types: SiBlings, No Canopy and Others, includes Model F), the MUGCM (open diamond) and three re-analyses [NCEP-DOE (multi-point star), NCEP-NCAR (solid circle) and ECMWF (solid triangle)] for the global land surface (GLS) and the three basins: Amazon, Murray Darling and Mississippi. The vertical downward pointing arrow shows the LH calculated by VIC (after [14]).

canopy); and groundwater recharge/discharge processes including snow and glacier melt-water contributions. To utilize biological exchange of isotopes on a global scale, modellers must estimate photosynthetic discrimination of ^{18}O, the oxygen isotopic composition of plant and soil water over the continents and soil respiration [10].

Tracer techniques have not been widely employed in continental-scale water budgets, due to the lack of available isotope data for major components of the gross hydrological cycle, notably river discharge. Uncertainty regarding the capability of the approach is reducing and possible applications are being proposed [11]. Improvement of isotope monitoring in rivers and the development of new techniques for isotopic analysis of atmospheric vapour may support a wide range of multidisciplinary international programmes currently exploring water and energy budget methods and modelling [6, 7]. Stable water isotopes offer a means of monitoring the partitioning of water fluxes in the basin-integrated discharge signals of large cold climate basins [12]. Reducing the range of basin scale model predictions shown in Fig. 1 is a prime goal of climate modellers.

3. IPILPS

IPILPS is a new type of PILPS (http://pilps.mq.edu.au) experiment in which the process of international intercomparison will inform, illuminate and educate the land-surface scheme (LSS)

parameterization community while new aspects of LSS are being developed. Specifically, IPILPS is a component of the current initiative to add isotopic (stable and radioactive) representation to atmospheric and land-surface models. The scientific hypotheses to be tackled in IPILPS include:

- The ability of LSSs to reproduce isotopic components of the water and mass (carbon initially) budgets is directly related to their ability to reproduce gross water and mass budgets;
- Isotopic fluxes between the atmosphere and the land-surface depend more strongly on the land-surface parameterization than on the computed atmospheric conditions; and
- It is possible to generate 'adequately correct' isotopic pools and fluxes without adding complexity to the LSSs beyond a 'bucket' hydrology and a (one line) stomatal resistance term.

Isotopes offer a novel and unique tool with which to test and improve LSSs: as transpiration does not fractionate while evaporation does, the SWIs differentiate plant-effected vapourisation from non-plant processes.

The forcing data includes magnitudes of each isotope (i.e. $^{1}H_{2}^{18}O$ and $^{1}H^{2}H^{16}O$) in precipitation and in water vapour at the atmospheric lowest level plus all the standard (ALMA) meteorological forcing including 'regular' water ($^{1}H_{2}^{16}O$). Currently, REMOiso is the only functional RCM with SWI module worldwide, hence it is a crucial component of IPILPS [15, 16]. REMO uses the same physical schemes as the ECHAM-4, which provides its lateral boundary conditions. It runs on an Arakawa C grid with 0.5° resolution (~54 km), offering a factor of two improvement as compared with the highest resolution for ECHAM (T106 ~ 125 km). REMO can further be nested in itself, reaching a 1/6° resolution (~18 km). The SWI module computes the $H_{2}^{18}O$ and $HD^{16}O$ cycles identically to the standard $H_{2}^{16}O$ hydrological cycle. Fractionation processes are represented at all steps of the hydrological cycle: kinetic fractionation during open-sea evaporation, thermodynamical equilibration between vapour, liquid and ice phases according to convective and large-scale cloud microphysics, re-evaporation and kinetic equilibration of falling rain droplets and vertical diffusion through the planetary boundary layer. REMOiso has been applied and validated in several climatic environments including the three regimes selected for IPILPS.

Offline simulations need appropriate boundary conditions, i.e. input from a host model representing the atmospheric processes as close as possible to the actual meteorological conditions. Furthermore, both climatic and isotopic variables should be coherent. Even though the surface features are better represented in REMOiso than a GCM, running in a climatological mode does not permit reproduction of a specific synoptic meteorological situation. Reanalyses, on the other hand, assimilate all available meteorological observations and so are believed to provide the best estimation of the actual state of the atmosphere (cf. [13]). At present, no isotopic reanalysis information is available so to resolve this problem, Georg Hoffmann, Max Kelley and Kristof Sturm are developing a nudged version of ECHAMiso: leaving the (isotopic) water cycle untouched, the model dynamics is forced to match the reanalyses while conserving the water budget. Hence the simulated precipitation events correspond better to observed precipitation. This nudging technique applied to a SWI GCM is a unique feature, from which REMOiso will greatly benefit in the form of accurate lateral boundary conditions. Similar nudging will be applied to REMO in near future.

Under the IAEA CRP on "^{18}O in the Terrestrial Environment" Australia has agreed to make detailed observations at a site west of Canberra. Tumbarumba (35° 39' 20.6"S 148° 09' 07.5"E), which will be the Australian site, is located between Canberra and Wagga Wagga. The vegetation is classified as wet sclerophyll forest with the dominant species being *Eucalyptus delegatensis* and average tree height of 40 m. The site is 1200 m above mean sea level with mean annual precipitation of 1000 mm and temperature ranging between -10 to 30°C. A preliminary field effort using the Fourier Transform Infra-Red spectrometry (FTIR: University of Wollongong) will start in Jan/Feb 2005. We are very keen to obtain high quality observations of isotopic data in vapour, precipitation, soil and plant water and river run off. The IAEA archives some of these data within GNIP and GNIR as monthly averages.

Individual laboratories have similar data archived at higher temporal resolution. In the context of GEWEX prime focus on the diurnal cycle, it seems likely that monthly averaged data will be of only modest value.

REFERENCES

[1] DANSGAARD, W., Stable isotopes in precipitation, Tellus **16** (1964) 436-468.

[2] PETIT, J.R., JOUZEL, J., RAYNAUD, D., BARKOV, N.I., BARNOLA, J.-M., BASILE, I., BENDER, M., CHAPPELLAZ, J., DAVISK, M., DELAYGUE, G., DELMOTTE, M., KOTLYAKOV, V.M., LEGRAND, M., LIPENKOV, V.Y., LORIUS, C., PÉPIN, L., RITZ, C., SALTZMANK, E., STIEVENARD, M., Climate and atmospheric history of the past 420000 years from the Vostok ice core, Antarctica, Nature **399** (1999) 429–436.

[3] SALATI, E., VOSE, P.B., Amazon Basin: a system in equilibrium, Science **225** (1984) 129-137.

[4] CRAIG, H., Isotopic variations in meteoric water, Science **133** (1961) 1702-1703.

[5] GAT, J.R., Oxygen and hydrogen isotopes in the hydrological cycle, Ann.Rev. Earth Planet. Sci. **24** (1996) 225-262.

[6] MATSUI, E., SALATI, E., RIBEIRO, M.N.G., REIS, C.M., TANCREDI, A.C.S.N.F., GAT, J.R., Precipitation in the Central Amazon Basin: the isotopic composition of rain and atmospheric moisture at Belem and Manaus, Acta Amazonica **13** (1983) 307-369.

[7] ROZANSKI, K., ARAGUAS-ARAGUAS, L., GONFIANTINI, R., Isotopic patterns in modern global precipitation, Climate Change in Continental Isotopic Records Geophysical Monographs **78** (1993) 1-36.

[8] HOUGHTON, J.T., DING, Y., GRIGGS, D.J., NOGUER, M., VAN DER LINDEN, P.J., DAI, X., MASKELL, K., JOHNSON, C.A. (Eds.), Climate Change 2001: The Scientific Basis, Cambridge Univ. Press, Cambridge, UK (2001) 881 pp.

[9] GIBSON, J.J., EDWARDS, T.W.D., Regional water balance trends and evaporation-transpiration partitioning from a stable isotope survey of lakes in northern Canada, Global Biogeochemical Cycles **16** (2002) 10.1029/2001GB001839.

[10] RILEY, W.J., STILL, C.J., TORN, M.S., BERRY, J.A., A mechanistic model of $H_2{}^{18}O$ and $C^{18}OO$ fluxes between ecosystems and the atmosphere: Model description and sensitivity analyses, Global Biogeochemical Cycles **16** (2002) doi:10.1029/2002GB001878.

[11] GIBSON, J.J., AGGARWAL, P., HOGAN, J., KENDALL, C., MARTINELLI, L.A., STICHLER, W., RANK, D., GONI, I., CHOUDURY, M., GAT, J., BHATTACHARYA, S., SUGIMOTO, A., FEKETE, B., PIETRONIRO, A., MAURER, T., PANARELLO, H., STONE, D., SEYLER, P., MAURICE-BOURGOIN, L., HERZCEG, A., Isotope studies in large river basins: a new global rearch focus, EOS 83, **52** (2002) 613-617.

[12] GIBSON, J.J., Short-term evaporation and water budget comparisons in shallow Arctic lakes using non-steady isotope mass balance, J. Hydrology **264** (2002) 242–261.

[13] HENDERSON-SELLERS, A., IRANNEJAD, P., SHARMEEN, S., PHILLIPS, T.J., MCGUFFIE, K., ZHANG, H., Evaluating GEWEX CSES' simulated land-surface water budget components, GEWEX News **13** 3 (2003) 3-6.

[14] HENDERSON-SELLERS, A., MCGUFFIE, K., NOONE, D., IRANNEJAD, P., Using stable water isotopes to evaluate basin-scale simulations of surface water budgets, J. Hydrometeorol. **5** 5 (2004) 805-822.

[15] STURM, K., LANGMANN, B., HOFFMAN, G. AND STICHLER, W., Stable water isotopes in precipitation: a regional circulation modelling approach, Hydrological Processes (in press).

[16] STURM, K., VIMEUX, F. AND KRINNER, G., Seasonality in the water isotope signal over South America, J. Geophys. Res. (submitted).

Delineating sources of sulfate and nitrate in rivers and streams by combining hydrological, chemical and isotopic techniques

Mayer, B.[a], L. Rock[a], L. Hogberg[b], L. Jackson[b], M. Varner[c], J.B. Shanley[d], S.W. Bailey[e], M.J. Mitchell[f]

[a] Department of Geology & Geophysics,
University of Calgary,
Alberta,
Canada

[b] Department of Biological Sciences,
University of Calgary,
Alberta,
Canada

[c] Department of Physics & Astronomy,
University of Calgary,
Alberta,
Canada

[d] U.S. Geological Survey,
Montpelier, Vermont,
United States of America

[e] USDA Forest Service,
Northeastern Research Station,
Hubbard Brook Experimental Forest,
New Hampshire,
United States of America

[f] State University of New York,
College of Environmental Science & Forestry,
Syracuse, New York,
United States of America

There is an increasing number of studies published in the literature, which report on the isotopic compositions of sulfate ($\delta^{34}S$ and $\delta^{18}O$) and nitrate ($\delta^{15}N$ and $\delta^{18}O$) in headwater creeks, rivers, and streams. Many of these studies are, however, characterized by infrequent sampling and by a scarcity of accompanying hydrological or chemical data. This severely hampers the ability to relate the obtained isotope data to potential sources of sulfate and nitrate, or to processes which these solutes may have undergone in aquatic systems. We present a number of case studies, in which sulfate and nitrate from surface water systems were sampled repeatedly and the obtained $\delta^{34}S$, $\delta^{15}N$ and $\delta^{18}O$ values were interpreted in conjunction with hydrological and chemical data.

Using this approach in selected forested headwater catchments in New Hampshire and Vermont (USA), we were able to show that a significant portion of stream water sulfate during base flow may be derived from weathering of bedrock, particularly in catchments with sulfur-rich lithology. During storm events at the Archer Creek sub-catchments in the Arbutus Lake Watershed in the central

Adirondack Mountains of New York State (USA) in the fall of 2002, sulfate concentrations in stream water increased significantly and $\delta^{34}S_{sulfate}$ decreased to minimum values. This suggested that sulfate derived from oxidation of sulfide minerals, possibly in wetland areas or the hyporheic zone, contributed to the increased sulfate load in the streams following the storm events. Monitoring of stream water during spring snowmelt events in the Sleepers River Research Watershed (Vermont, USA) revealed elevated contributions of sulfate from pedospheric sources, but little direct contribution of sulfate from the melting snowpack. Also, nitrate was not derived from atmospheric inputs but primarily from nitrification processes in the soils.

In agriculturally used portions of a large watershed in southern Alberta (Canada), oxidation of pyrite in tills was identified as an additional source of riverine sulfate, indicated by increasing sulfate concentrations and decreasing $\delta^{34}S$ values. Furthermore, chemical and isotopic data showed that manure-derived nitrogen was responsible for increasing nitrate concentrations in the Oldman River and its tributaries, which drain agricultural land. Particularly in parts of the watershed with intensive irrigation, manure-derived nitrate appeared preferentially during the winter months in the irrigation canals, tributaries, and the Oldman River. This suggests that hydrological conditions control agricultural return flows to the surface water bodies in southern Alberta and impart significant seasonal variations on concentrations and isotopic compositions of riverine nitrate.

Using a combination of hydrological, chemical and isotopic techniques, we were also able to show that urban centers, such as Calgary in southern Alberta (Canada), have a significant impact on riverine nitrate and sulfate loads. Elevated nitrate concentrations were observed 30 to 50 km downstream of a large municipal sewage treatment plant, whereas $\delta^{15}N$ values indicated the presence of sewage-derived nitrate more than 60 km downstream of the point source. Sulfate concentrations also increased significantly in the Bow River downstream of the city of Calgary. Initially, it was speculated that this might be caused by the use of alum (aluminum sulfate) during drinking water treatment, but the changes in the isotopic composition of sulfate in river water below the city were inconsistent with this hypothesis. Therefore, we analyzed the sulfur isotope ratios of soluble sulfate released from a number of widely used detergents, soaps, and shampoos obtained from local supermarkets and determined an average $\delta^{34}S$ value of $+1 \pm 4‰$ ($n = 18$). Since sulfate released from the large municipal sewage treatment plant had similar $\delta^{34}S$ values, we concluded that the use of detergents and soaps in households is a major contributor to the increased sulfate load in the Bow River downstream of the city of Calgary.

In watersheds with forested, agricultural and/or urban land use, there are a number of different natural and anthropogenic sources of riverine sulfate and nitrate. Their relative contributions to sulfate and nitrate loads in rivers and streams can vary significantly depending on hydrological conditions and hence season. To identify these different sources and to asses their relative contributions, it is essential to repeatedly determine the isotopic composition of sulfate and nitrate obtained from several sampling sites along headwater creeks, rivers or streams. Interpretation of the trends of the obtained isotope data in conjunction with hydrological and chemical parameters will result in a significantly improved understanding of the sources of riverine sulfate and nitrate.

Isotope tracing of throughflow, residency and runoff to lakes for regional assessment of critical acid loadings to aquatic ecosystems

Gibson, J.J.[a], K. Bennett[b]

[a] National Water Research Institute,
University of Victoria,
Victoria BC,
Canada

[b] Department of Geography,
University of Victoria,
Victoria BC,
Canada

Mining, forestry and hydroelectric development are placing increasing stress on aquatic ecosystems of the Boreal Forest of Canada, particularly within the Athabasca Oil Sands Region of northeastern Alberta (near Ft. McMurray). Evaluation of the sensitivity of various aquatic ecosystems to such disturbances requires an improved understanding of the basic processes that control ecosystem health including water balance, biogeochemical interactions between lakes and their watersheds, acid sensitivity, and potential future modifications to these conditions under changing climate. One of the more pressing issues in Oil Sands development is the capacity of soils and water to buffer acidic emissions and deposition associated with mining and upgrading of bitumen. Current operations emit up to one tonne of SO_X and NO_x per thousand barrels of oil produced. Many new projects are improving on these emission rates, however, improvements are at considerable cost and future projections are still as much as 600 tonnes of SO_X and NO_x per day from operations near Ft. McMurray [1].

Sulfur and nitrogen emissions are oxidized in the atmosphere producing sulfate and nitrate anions, reducing the pH of atmospheric moisture and producing acid rain that is deposited on soils and vegetation. Positively charged cations are subsequently mobilized from the soil matrix and leach to surface waters with the deposited nitrate and sulfate reducing the buffering capacity of soils. While most of Alberta's soils have a large cation reserve and capacity to buffer acid deposition, a significant proportion of the landscape in the Ft. McMurray area contains soils with poor buffering capacity, which is expected to enhance the sensitivity of surface waters to acid deposition. The ability of surface waters to buffer acidic deposition is currently being evaluated using a steady state acid-loading model, the Henriksen model, although future efforts also include dynamic modelling.

The Henriksen model for predicting critical acidifying loads requires only two data inputs. One input, the base cation concentration, is currently obtained directly through routine sampling of lakes and is a relatively accurate measure of the buffering capacity in a lake. The second input, basin water yield, is estimated and is subject to significant errors, especially in complex, ungauged, low-relief drainage basins associated with the Boreal Plain of Alberta. The basin water yield is required to estimate the amount of buffering capacity delivered on an annual basis from the watershed. Error in water yield estimates limits the ability to determine the annually sustainable buffering capacity of both lakes and their watersheds.

This study demonstrates application of an isotope mass balance method for estimating basin water yield and other key hydrological parameters (throughflow, water residency) for acid sensitivity modelling in a network of 50 lakes in the region. Stable isotopes of water (oxygen-18 and deuterium) have been analysed from water samples collected during routine water quality surveys of the lakes.

Isotope composition of lakes in the region is controlled by isotope composition of precipitation input with predictable modifications by evaporation, so that the degree of isotopic enrichment can be used as a reliable indicator of lake flushing rates (throughflow), and water replacement rates. Basin water yield can subsequently be calculated from the replacement rate and volume of water in each lake. The isotope mass balance approach for estimating water balance parameters has been demonstrated in previous studies of open water bodies [2-8] and has been previously applied with success to characterize water balance of lakes in northern Alberta [9-11]. Required variables, practical limitations and successes of the approach in evaluating critical acid loadings are discussed.

REFERENCES

[1] GOLDER ASSOCIATES, Acid Deposition Sensitivity Mapping and Critical Load Exceedences in the Athabasca Oil Sands Region, Consultants Report to Alberta Environment (2002).

[2] INÇER, T., The use of oxygen-18 and deuterium concentrations in the water balance of lakes, Water Resour. Res. **4** (1986) 1289-1305.

[3] GAT, J.R., "Environmental isotope balance of Lake Tiberias", Isotopes in Hydrology, 1970, IAEA, Vienna (1970) 151-162.

[4] GAT, J.R., Lakes, in Stable Isotope Hydrology- Deuterium and Oxygen-18 in the Water Cycle, IAEA Techn. Rep. Ser. 210, IAEA, Vienna (1981) 203-221.

[5] GONFIANTINI, R., "Environmental isotopes in lake studies", Handbook of Environmental Isotope Geochemistry, Vol. **3** (FRITZ, P., FONTES, J. CH., Eds), Elsevier, New York (1986) 113-168.

[6] ZUBER, A., On the environmental isotope method for determining the water balance of some lakes, J. Hydrol. **61** (1983) 409-427.

[7] KRABBENHOFT, D.P., BOWSER, C.J., ANDERSON, M.P., VALLEY, J.W., Estimating groundwater exchange with lakes 1: The stable isotope mass balance method, Water Resour. Res. **26** (1990) 2445-2453.

[8] GAT, J.R., "Stable Isotopes of Fresh and Saline Lakes", Physics and Chemistry of Lakes (LERMAN, A., IMBODEN, D., GAT, J., Eds) Springer-Verlag, Berlin (1995) 139-165.

[9] GIBSON, J.J., PREPAS, E.E., MCEACHERN, P., Quantitative comparison of lake throughflow, residency, and catchment runoff using stable isotopes: modelling and results from a survey of Boreal lakes, J. Hydrol. **262** (2002) 128-144.

[10] MCEACHERN, P.M., PREPAS, E.E., GIBSON, J.J., DINSMORE, P., The forest fire induced impacts on phosphorus, nitrogen and chlorophyll-a concentrations in boreal sub-arctic lakes of northern Alberta, Can. J. Fish. Aquat. Sci. **57** 2 (2000) 73-81.

[11] PREPAS, E.E., PLANAS, D., GIBSON, J.J., VITT, D.H., PROWSE, T.D., DINSMORE, W.P., HALSEY, L.A., MCEACHERN, P.M., PAQUET, S., SCRIMGEOUR, G.J., TONN, W.M., PASZKOWSKI, C.A., WOLFSTEIN, K., Landscape variables influencing nutrients and phytoplankton communities in Boreal Plain lakes of northern Alberta: a comparison of wetland- and upland-dominated catchments, Can. J. Fish. Aquat. Sci. **58** (2001) 1286-1299.

Isotopic studies of environmental changes in the basins of the Caspian Sea and the Aral Sea

Ferronsky, V.I.[a], V.A. Polyakov[b], K. Froehlich[c], P.N. Kuprin[d], V.S. Brezgunov[a], L.S. Vlasova[a], Y.A. Karpychev[a]

[a] Water Problems Institute of the Russian Academy of Sciences,
Moscow,
Russian Federation

[b] All-Russian Institute of Hydrogeology and Engineering Geology,
Zeleny,
Moscow Region,
Russian Federation

[c] International Atomic Energy Agency,
Vienna

[d] Moscow State University,
Moscow,
Russian Federation

Abstract. During the last thirty years environmental changes in the Caspian and Aral Sea basins were studied measuring the isotopic composition of water and bottom sediments of the two seas, neighboring lakes and inflowing rivers. Results of these studies related to the impact of climate variations of the past and present-day hydrologic regime, water dynamics, sea level variation and sedimentation process are discussed in this paper. Evidence is given for eight short-periodic cycles of regression and transgression of the Caspian Sea in the Late Pleistocene-Holocene. The Caspian Sea was formed by two lakes separated by the natural Apsheron sill/dam. The discussion includes also the environmental conditions in the Aral Sea basin, especially the recent drying up of this Sea. Finally, the physical basis for understanding the nature of the short and long-periodic climate variation is emphasized by presenting the solution of the problem of rotation and oscillation of the Earth in its own force field.

1. Introduction

The aim of the paper is to summarize the results of the author's almost thirty year study of environmental changes carried out in the Caspian and Aral Sea basins. The selected region is well suited for studying environmental and climatic changes through isotope investigations including water and sediment of the sea. The study area represents a closed catchment basin of about $5 \cdot 10^6$ km^2 consisting of two sub-basins located in different climatic zones. One sub-basin belongs to a humid zone and including the catchment areas of rivers Volga and Ural, and also rivers from the eastern and northern slopes of the Caucasus and Elburs mountains. The second sub-basin is located in an arid zone occupying the widespread Turonean Lowlands, including the Aral Sea, and the Central Asian mountain slopes. The discharge of the first sub-basin reaches the Caspian Sea directly through the Caspian rivers, in the case of the second sub-basin indirectly through the Usboy River if the of the water level in the Aral Sea is higher than +56 m asl. Therefore, only during humid climate periods the Aral Sea catchment discharges into the Caspian Sea.

2. Objects of study and measured values

Since 1974 water and sediments of the following seas, lakes and rivers were investigated: Caspian and Aral Seas; Kara-Bogaz-Gol Gulf; Lakes Issyk Kul, Balkhash and Yaskhan; Rivers Volga, Amu Darya, Syr Darya, Chu and Ily.

The results of the studies were presented at a number scientific meetings and published in various proceedings and journals [1-8]. The investigations included (i) field work and sea cruises for sampling of water, coring of bottom sediments and in-situ measurements of oceanographic and hydrologic parameters, (ii) monitoring of isotopic composition of precipitation, and sea/lake and river water, and (iii) sample analyses in specialized laboratories. The following isotopic, sedimentologic, oceanographic, hydrometeorologic and chemical characteristics were measured and collected for evaluating the results in terms of environmental and climatic changes in the study area: ^{18}O and ^{2}H in water samples; oxygen and carbon isotopes of bulk carbonates; ^{14}C in sediments; lithology, petrography, granulometry, mineralogy of the sediments; X-ray and difractometry of carbonates and fine crystals; magnetic susceptibility, pollen, diatoms in the sediments; fossil remains of organisms and coarse-grained minerals; salt forming ions of pore water; $CaCO_3$ and $MgCO_3$ of the bulk sediments; salinity, temperature and density of marine water; bathymetric topography of the Apsheron Sill.

A database of the hydrometeorologic and oceanographic data was compiled. The evaluation of the data included modeling of the carbonate precipitation and formation of the isotopic composition of the carbonates.

3. The main findings

The hydrological, sedimentologic and oceanographic findings of the investigations include the following:

(1) Within the time interval from 24 to 11 ka BP the average sedimentation rate in the Middle Caspian Sea basin was about 0.12 mm/yr, whereas during the period of 11 to 6 ka, it was one order of magnitude higher (1.2 mm/yr). In contrast, in the southern basin of the Caspian Sea the average sedimentation rate during the period from 23 to 17.6 ka BP reached 0.9 mm/yr but only 0.19 mm/yr in the period from 17 to 6 ka [3, 4].

(2) The isotopic composition of oxygen and carbon of the carbonate fraction in bottom sediments shows that during the periods of increasing sedimentation rate in both Caspian basins isotopically light river water recharged alternatively from the south or the north [3, 4].

(3) The main salt forming ions in the pore water of the Caspian bottom sediments demonstrates that the water salinity of the basins varied asynchronously, only 22 ka BP the salinity of both basins reached the same value [3, 4].

(4) The accumulation of clastic particles of 1 to 0.63 mm size in the Caspian sediments shows that during the last 20 ka eight transgressive and regressive sea cycles occurred in each basin. About twenty or more short-periodic cycles can be derived by means of oxygen and carbon isotope records in the carbonates [3, 8].

(5) The present day water dynamics study using hydrogen and oxygen isotopes shows that the Caspian Sea level rise of 2.5 m in 1978-1995 has not been reflected by the water isotopic composition below a depth of 300 m. In 1996, in most of the southern basin sampling stations an increase of tritium content with depth below that level has been found. Tritium appeared to be the most sensitive tracer of vertical water exchange in the Caspian Sea [9].

(6) The investigation of sediment cores from the Kara-Bogaz-Gol Gulf demonstrates that within the period from 9.2 to 8.5 ka BP the reservoir was drying and sedimentation proceeded from fresh water discharged most likely by the Karyn-Zharyk River and its tributaries. This conclusion is

based on the fact that the δ^2H value in pore water was +6‰. That value suggests that the process took place in a drying up water body. And also concentration of Na^+ and Cl^- there was 2.5 to 3 g/L suggests that the gulf was a terminal lake without connection to the middle Caspian Sea. Around 8.5 ka BP the δ^2H value in water decreased up to -6‰, which indicates the beginning of dilution of the water in the former terminal salt lake by river runoff. During the period from 8.5 to 2.2 ka the value of δ^2H in the pore water decreased from -6 to -17‰, which points to an increase of the river runoff. The gulf was rapidly filled up and after ~3 ka BP periodically discharged water to the middle basin of the Caspian Sea. After the events of the New Caspian transgression at about 2.2 ka, the Karyn-Zharyk River system dried up and since that time the gulf is recharged by water from the Caspian Sea. All the measured values prove this conclusion [6].

(7) Four transgressive and three regressive periods during the Holocene history of the Aral Sea were found by study of the shore terraces and bottom sediments. The sea level rose from 53 m to 57 m asl and dropped from 44 m to 35 m asl. The sea level of 57 m asl indicates that at this time water from the Aral Sea discharged in the southern basin of the Caspian Sea through the Usboy river. Two peat layers of 0.2 and 0.4 m thickness with an age of 4,5 and 1.3 ka BP, respectively, were found in a sediment core. From 1.3 ka BP up to present time sedimentation continues at variable hydrological regimes with periodic rises and drops of the sea level. These findings are confirmed by alternate clay and sand lamination and salt crystal inclusions identified in the bottom sediment section [6].

(8) The results of isotopic, mineral and chemical analysis of bottom sediments from the Lake Issyk-Kul show that within 7.6 to 6 ka BP sedimentation was connected with steady recharge of cold water and discharge into the Chu River. Low concentrations of organic carbon, monohydrocalcite, $\delta^{18}O$ and Sr/Ca, and slightly increased concentrations of $CaCO_3$ and $MgCO_3$ at the upper boundary of the core interval prove the above conclusion. During the time interval from 6 to 4.3 ka BP, sedimentation continued at a reduced river water inflow, lower water level in the lake, increased salinity, and decreased sedimentation rate. This conclusion is proved by an increase in $\delta^{18}O$ in mollusk shells, a decrease in Mg^{2+} concentration in the deposited calcite, and an increase in concentration of organic matter and Sr/Ca ratio in shells. Within the upper interval from 4.3 to the present time periodic change in the lake regime was subject to periodic changes with deceases and increases of the lake level up to the Chu River bed through which the excess water was discharged [6].

(9) It was found by means of δ^2H, $\delta^{18}O$ and ^{14}C data, that the Yaskhan lens of fresh groundwater, which is located in the central part of the Karakumy desert in West Turkmenia (~40^o N, 63^o E) and has mineralization of less than 0.6 g/L and a ^{14}C contents of 17-22 pmc, has formed about 12 ka BP [1, 5].

(10) Impact of the pluvial epoch on the groundwater in the Central Asian and Near East region was demonstrated by isotope studies carried out in the Syr Darya, Amu Darya, Chu and Ily River basins and the Syrian desert [1, 5].

4. Environmental changes and natural events

On the basis of the above findings, the relationship between natural events and the most severe environmental changes in the Caspian and Aral basins can be described as follows:

(1) The opposite change in sedimentation rate between the southern and middle basin of the Caspian Sea accompanied by changes in isotopic composition of carbonates, salinity of water, chemistry and mineral contents of sediments, provides evidence of a change in the hydrological regime over the Central Asian and the European part of the catchment basin in the Late Pleistocene and Holocene. This change in the hydrological regime was caused by a drastic change of climate conditions, which started around 23-25 ka BP and finished about 10-12 ka BP. It was the latest long-periodic cycle of the Earth's climate evolution. As a result, the temperate humid climate in

the Central Asian region changed to hot semi-arid and arid climate, and the cold semi-arid climate in the Volga and Ural basins alternated to a temperate humid regime. The onset of aridity in the Central Asian region was accompanied by melting of the vast glaciers in the Pamir and Tien Shan and by runoff of enormous volumes of melt water to the Aral Sea and through the Usboy River to the Caspian Sea (Fig. 1). Judging by isotope data of carbonates and by salinity of pore water of the sediments, the process continued within 12 to 8 ka BP and periodically appeared later on.

(2) Extremely different sedimentation rate, salinity of pore water, changes of other measuring parameters in the southern and middle basin of the Caspian Sea and also the shape of bathymetric section of submarine part of the Apsheron Sill evidence that up to recent times the Caspian Sea was separated by the 30-50 km wide natural dam, the Apsheron Sill (Fig. 2). The geological history of the Apsheron Sill proves this conclusion [7]. Obviously, the merging of the lakes happened after the dam was washed out by water overflowing from one lake to another. The structure of the bathymetric section shows that the direction of the eroding flow was mainly from south to north. The measured data suggest that the unification of the two lakes was completed between 12 to 8 ka BP.

(3) The Aral Sea started to discharge water to the Caspian Sea after the Turonean Lowlands were filled in up to +56 m asl which is the mark of the Usboy River's outflow in the Kugunek Hills. From 23 to 8 ka BP the Turonean Lowlands were filled up to that mark forming an expansive low water Aral-Sarikamish Sea. During that period excess water discharged to the Caspian Sea by the Usboy River. At present a dry and highly eroded bed of the Usboy River at the foot of the Kopet-Dag Mountains evidences this (Fig. 2).

(4) The registered periodic change in contents of clay minerals in the Caspian bottom sediments mark at least eight transgression and regression cycles of changes in the hydrologic regime in each basin of the sea with a period of ~1.5-2 ka. More detailed records of oxygen and carbon isotopes in carbonates demonstrates periodicity in the runoff with shorter periods in the order of hundreds of years.

As follows from the available data on runoff, precipitation, temperature and sea level variation during the last 150 years, there are inter-annual changes in the hydrologic regime of the Caspian and Aral Sea basins, each 30-50 years the sea level amplitude reaches 1-2 m or more. That period of hydroclimatic variation seems to be important for human activities.

The above effects and also the same facts observed in other regions of the Earth encouraged the authors to search for the physical cause of short-periodic hydroclimatic change on the Earth by following Milancowich's astronomical theory of the long-term climate variation. In order to derive a possible short-periodic latitudinal effect in the variation of the solar energy flux we decided to treat the problem of the Earth's rotation and oscillation in its own force field. The results proved to be promising. A novel approach to studying climatic and water level changes in the Caspian and Aral Seas will be published elsewhere [10].

5. Conclusions

Isotope studies of environmental changes in the Caspian and Aral Sea basins give qualitative confirmation that short-periodic variation of the climate change is a natural process which has physical justification. The theoretical results summarized in this paper suggest that all other observed and proposed causes of global climate change are secondary effects in comparison to the primary effects discussed here. A further study of the connection between these physical causes and the observed climatic changes appears to be useful and could be carried out within the framework of an international project with the involvement of international organizations such as the IAEA and UNESCO.

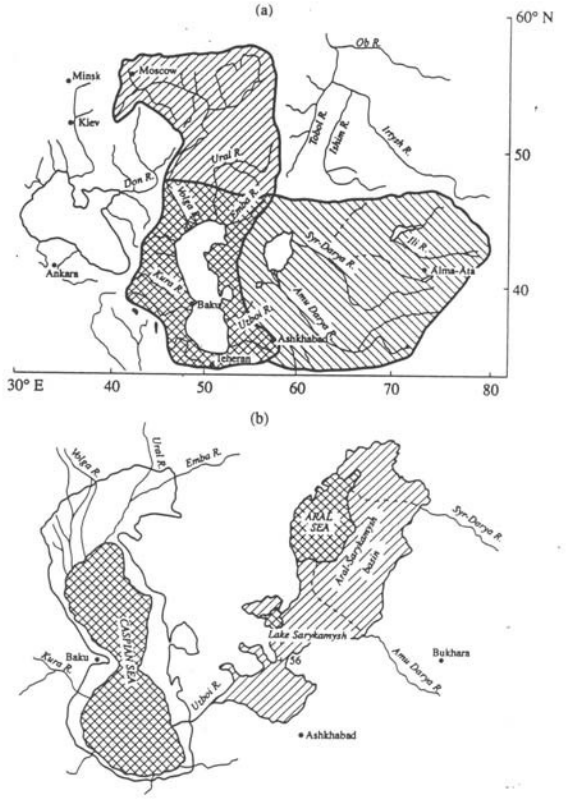

FIG. 1. Effect of latitudinal shift of the humid climate zone of the Caspian-Aral region. (a) Catchment basin change from the Volga-Ural to the Amu Darya -Syr Darya; (b) Regression of the Caspian and transgression of the Aral Seas during the transitional period of the climate zone shift.

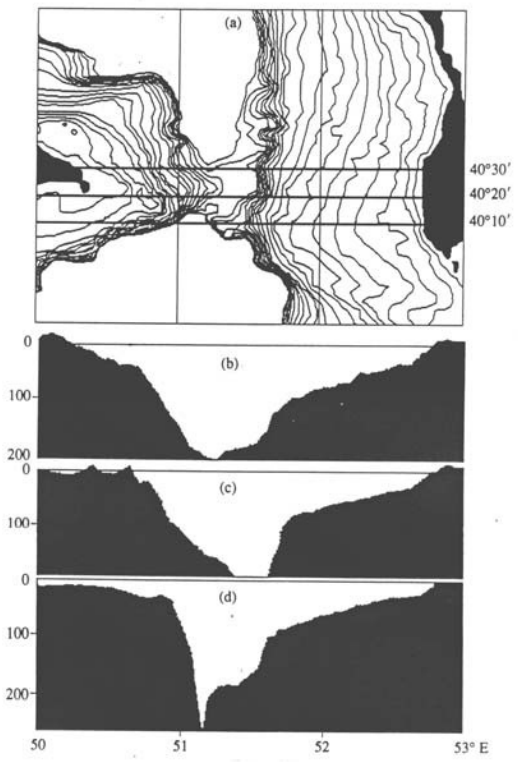

FIG. 2. (a) Bathymetric map of the Apsheron Sill with a 10 m isobathic interval and cross section of the Sill along latitudes (b) 40º 10', (c) 40º 20', (d) 40º 30'.

REFERENCES

[1] FERRONSKY, V.I., POLYAKOV, V.A., FERRONSKY, S.V., Isotope variation in water in hydrological cycle as a tool in a climate change mechanism study. In: Isotope Techniques in Water Resources Development 1991, Proc. Intern. Symp. IAEA, Vienna (1992) 567-586.

[2] FERRONSKY, V.I., POLYAKOV, V.A., FROEHLICH, K., LOBOV, A.L., BATOV, V.I., PIATROSIUS, R., KUPRIN, P.N., VARUSCHCHENKO, A.N., BOBKOV, A.F., Isotope studies of the Caspian Sea: Climate record from the bottom sediments (preliminary results). Proc. Intern. Symp. IAEA, Vienna (1998) 633-644.

[3] FERRONSKY, V.I., POLYAKOV, V.A., LOBOV, A.L., BATOV, V.I., FROEHLICH, K., GROENINGEN, M., Sedimentation rate record in the Caspian Sea bottom sediments as indicator of climate changes in the basin. In: Isotope Techniques in Water Resources Development and Management, Proc. Intern. Symp. Session 3, CD-ROM, IAEA, Vienna (1999).

[4] FERRONSKY, V.I., POLYAKOV, V.A., KUPRIN, P.N., LOBOV, A.L., The nature of variations in the level of the Caspian Sea (based on bottom-sediment data). Water Res. 26 (1999) 583-596.

[5] FERRONSKY, V.I., POLYAKOV, V.A.,.LOBOV, A.L., Isotope study of impact of climatic changes on hydrological cycle in Central Asian and Caspian arid region, IAEA TECDOC-1207, Vienna (2001) 59-76.

[6] FERRONSKY, V.I., BREZGUNOV, V.S., VLASOVA, L.S., KARPYCHEV, Yu.A., POLYAKOV, V.A., BOBKOV, A.F., ROMANOVSKY, V.V., JOHNSON, T., RICKETTS, D., RASMUSSEN, K., The Kara Bogaz Gol Bay, Lake Issyk Kul and Aral Sea sediments as archive of climate change in the Aral-Caspian basin, Proc. Intern. Conference, Vienna, IAEA (2002) 144-153.

[7] KUPRIN, P.N., Apsheron threshold and its role in the process of sedimentation and formation of hydrological regimes in the southern and middle Caspian basins, Water Res. **29** (2002) 473-484.

[8] KUPRIN, P.N., FERRONSKY, V.I., POPOVCHAK, V.P., SHLIKOV, V.G., ZOLOTOVA, L.A., KALISHEVA, M.V., Bottom sediments of the Caspian Sea as an indicator of changes in its water regime, Water Res. **30** (2003) 136-153

[9] FERRONSKY, V.I., POLYAKOV, V.A., BREZGUNOV, V.S., VLASOVA, L.S. POLYAKOV, V.A., FROEHLICH, K., ROZANSKY, K., Investigation of water-exchange processes in the Caspian Sea on the basis of isotopic and oceanographic data, Water Res. **30** (2003) 10-22.

[10] FERRONSKY, V.I., POLYAKOV, V.A., FROEHLICH, K., KUPRIN, P.N., BREZGUNOV, V.S., VLASOVA, L.S., KARPYCHEV, Yu.A., A novel approach to explain climatic and water level changes in the Caspian and Aral Seas (in preparation).

A geochemical and isotope hydrological study of eutrophication processes in the Plitvice Lakes, Croatia

Horvatinčić, N.[a], B. Obelić[a], J. Barešić[a], R. Čalić[b], S. Babinka[c], A. Suckow[d], I. Krajcar Bronić[a]

[a] Rudjer Bošković Institute,
Zagreb,
Croatia

[b] Watersupply Company,
Zagreb,
Croatia

[c] Leibniz Institute for Applied Geosciences (GGA),
Hannover,
Germany

[d] International Atomic Energy Agency,
Vienna

The Plitvice Lakes are a series of lakes, tufa barriers and waterfalls located in the Dinaric Karst in Central Croatia, where calcium carbonate precipitates very intensively forming tufa barriers in presence of macrophites and microphites. Therefore, the aquatic system of the whole area is very complex. Additionally, in the last decades an increase in the eutrophication process has been observed in some parts of the lakes and also in some tufa barriers. In our study, which is a part of the EU-Project ICA2-CT-2002-10009, we try to identify the source of the eutrophication process to see whether it is a consequence of anthropogenic pollution or process of naturally produced organic matter/humus in the lakes.

This ongoing study includes physico-chemical investigations of lake water, isotope hydrology studies in lake waters and karst springs (δ^2H and $\delta^{18}O$, Tritium/^3He, CFC/SF_6, $\delta^{13}C$ of dissolved inorganic carbon - DIC) and geochronology and geochemistry of lake sediments. Seasonal aquatic chemistry samples are complemented by monthly sampling for stable isotopes in water (δD, $\delta^{18}O$) at 15 sampling points including 4 springs, 5 lakes, waterfalls and streams between lakes. The ^{14}C and ^3H activity of monthly samples of atmospheric CO_2 and of precipitation, respectively, in this area is also recorded.

Parameters like temperature, pH, conductivity and dissolved oxygen are measured *in situ.* The isotope hydrological as well as the following chemical analyses of water are performed in the laboratory: dissolved organic carbon (DOC) and inorganic carbon (IC), nutrients as NO_2^-, NO_3^-, HPO_4^-, NH_4^+, additional anions F^-, Cl^-,SO_4^{2-}, HCO_3^-, cations Ca^{2+}, Mg^{2+}, Na^+, K^+, as well as trace elements (B, Al, Cr, Sr, Mn, Fe, Ni, Cu, Zn, As, Cd, Ba, Pb).

The results of physico-chemical measurements of water at 15 sampling points along a flow distance of about 12 km, including sites with very intense $CaCO_3$ precipitation, show the following:

1. Temperature, pH, concentration of calcium and bicarbonates (alkalinity), and hence the saturation index of $CaCO_3$ (I_{sat}), show significant change in downstream flow and also some seasonal variations. These results are compared with previous measurements (1). The results show that the carbon exchange process along CO_2–HCO_3^-–$CaCO_3$ plays an important role for tufa precipitation.

2. Concentration of DOC is higher in lake waters where eutrophication process is significant (1-2 mg/L) then in non-eutrophicated water, *e.g.* in spring waters (0.3-0.5 mg/L). Additionally, DOC values are also higher in some "clean" stream waters, where tufa does not precipitate in spite of otherwise favorable physico-chemical conditions for calcite precipitation, such as the high degree of supersaturation. In this case probably DOC inhibits tufa deposition.
3. The concentration of dissolved nutrient salts, as well as of trace elements in water, is very low for most of sampling points. No systematic difference in concentration of these species between "clear" and eutrophicated waters was observed.

$\delta^{13}C$ values of DIC in water of the Plitvice Lakes area steadily increase downstream from the karst springs ($\delta^{13}C$ is -12.5‰) to the river mouth ($\delta^{13}C$ is -10.0‰). Simultaneously, increase of ^{14}C activity of DIC in downstream flow in the same area was observed [2]. This is the consequence of the exchange process between the atmospheric CO_2 and DIC in water at rapids and waterfalls.

The first results for stable isotopes $\delta^{2}H$ and $\delta^{18}O$ in lake and stream waters plot above the global meteoric water line (GMWL) with a deuterium excess between 10 and 16. So most samples seem to have some influence from the Mediterranean area, where deuterium excess higher than 10 prevails. For the winter samples measured up to now evaporation from the lakes is not detectable from δD and $\delta^{18}O$ values. Earlier tritium samples of the karst springs have shown short residence times of several years [3]. New results from tritium, ^{3}He and CFC/SF_6 measurements confirm these results. Sediment dating of the first core from Lake Kozjak shows that the topmost 40 cm of sediment are younger than 40 years since ^{137}Cs is present in all samples. The resulting sedimentation rate of more than 1 cm/year contrasts with earlier findings using ^{14}C [4]. A possible reason could be the significant amount of organic matter mixed in carbonate sediment at this specific point.

The chemical and isotopic measurements of water indicate that the concentration of DOC is higher in the areas where the process of eutrophication is pronounced and that higher DOC concentration in water can inhibit the tufa/calcite precipitation. The preliminary chemical measurements of water do not indicate anthropogenic pollution of lake waters, and higher concentration of DOC in some sampling points can be a consequence of input of natural organic matter/humus to the lake water. Further investigations of geochemical and isotopic sediment-water interaction in the surface sediment at a total of 5 sampling points in the Plitvice Lakes area are in progress.

REFERENCES

[1] SRDOČ, D., HORVATINČIĆ, N., OBELIĆ, B., KRAJCAR, I., SLIEPČEVIĆ, A., Procesi taloženja kalcita u krškim vodama s posebnim osvrtom na Plitvička jezera (Calcite Deposition Processes in Karstwaters with Special Emphasis on the Plitvice Lakes, Yugoslavia) (English Abstract) Krš Jugoslavije (Carsus Iugoslaviae) **11** 4-6 (1985) 101-204.

[2] SRDOČ, D., KRAJCAR BRONIĆ, I., HORVATINČIĆ, N., OBELIĆ, B. The Increase of ^{14}C Activity of Dissolved Inorganic Carbon Along the River Course, Radiocarbon **28** (1986) 515-521.

[3] HORVATINČIĆ, N., KRAJCAR BRONIĆ, I., PEZDIČ, J., SRDOČ, D., OBELIĆ, B., The Distribution of Radioactive (^{3}H, ^{14}C) and Stable (^{2}H, ^{18}O) isotopes in Precipitation, Surface and Groundwaters during the Last Decade in Yugoslavia, Nuclear Instr. Meth. Phys. Res. B**17** (1986) 550-553.

[4] SRDOČ, D., HORVATINČIĆ, N., OBELIĆ, B. KRAJCAR BRONIĆ, I., MARČENKO, E., MERKT, S., WONG, H., SLIEPČEVIĆ, A., Radiocarbon dating of Lakes Sediments from two Karst Lakes in Yugoslavia, Radiocarbon **28** (1986) 495-502.

Determination of old and fresh water mixing in a Hungarian karstic aquifer using isotope methods

Molnár, M., L. Palcsu, É. Svingor, Z. Szántó, I. Futó, L. Rinyu

Institute of Nuclear Research,
Hungarian Academy of Sciences,
Laboratory of Environmental Studies,
Debrecen,
Hungary

The studied area is the part of the Aggtelek karst system, Hungary. The Pasnyag spring and the Lótusz spring are located one after the other nearby the Alsó-hill. The water of the Pasnyag spring applied as drinking water. From the local hydrogeological conditions it is possible that fresh and old ground water components are mixed in the springs (Figure 1). This fact is also confirmed by the water quality data.

The objective of this work was to determine the mixing ratio of the water of different origin in the springs. Repeated water sampling has been carried out around the site from the springs and two monitoring wells (F1 and F4) for two years. The F1 monitoring well is near at hand the Pasnyag spring, and the F4 well is between the two springs. The water quality of the Pasnyag spring and the nearby F1 well is significantly different.

Helium content and isotope ratio, tritium concentration (by ^{3}He ingrowth method), radiocarbon content of dissolved inorganic carbon (DIC), and δD, $\delta^{13}C$, $\delta^{18}O$ isotope ratios were measured from the water samples.

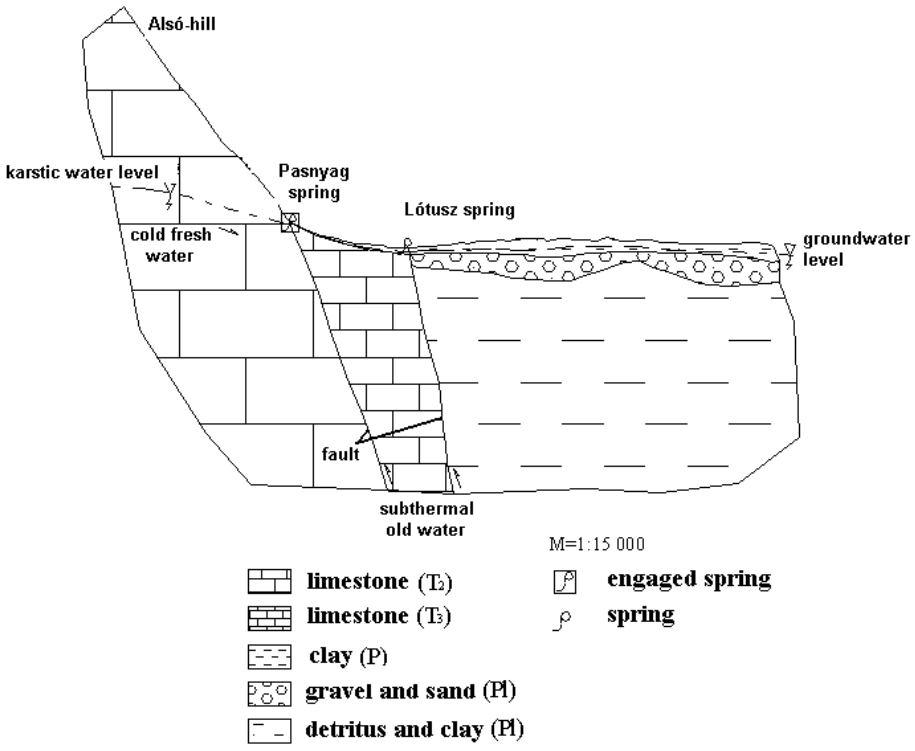

FIG. 1. Presumed hydrogeological scheme of the area.

On the basis of isotope measurements the water of the springs and the observed monitoring wells are composed of fresh and old components in different ratios. The fresh component is dominant in the Pasnyag spring. The tritium and radiocarbon concentration of this water show that it is fresh, young water directly from the karstic system, with only small amount of DIC from the limestone. The helium concentration and isotope ratio in the water of this spring also shows that the subthermal water component is not significant. Higher ratio of the fresh karstic water also detectable in the far F4 monitoring well, but it has slightly lower tritium and ^{14}C content. In the Lótusz spring and the F1 well (nearby the Pasnyag spring) higher ratio of the subthermal water was observed. The low tritium and radiocarbon content show together that these waters contain high amount of old water. The higher helium content and the higher radiogenic ^{4}He ratio of the water also indicate subthermal origin in these cases.

Estimation of groundwater recharge and vulnerability by tritium data in Hungary

Deak, J.

Water Resources Research Centre (VITUKI Plc),
Budapest,
Hungary

Tritium is an excellent tool for proving of the protected groundwater (containing no component younger than 50 years) and for estimation of infiltration and recharge rate.

Annual mean tritium record of precipitation revealing for Hungary shows that the present tritium content of the precipitation fallen before 1952, is not detectable (<1 TU) whereas all groundwaters infiltrated after 1952 are contaminated by tritium, originating from the nuclear weapon tests. The tritium less ("pre-bomb") groundwaters are protected against the pollutions originated from the surface in the last 50 years. This date corresponds well to the beginning of the intensive environment pollution of the agriculture and industry in Hungary. It means that micro-pollutants (including pesticides) originating from these pollutions should be found in the groundwaters containing detectable tritium and the tritium less groundwaters presumably do not contain them.

This very simple "to be or not to be" method allows developing a cost-effective groundwater quality monitoring network where the very expensive micro-pollutant analyses can be saved in the tritium less groundwaters. Furthermore routine chemical parameters should be analyzed less frequently (every 5 to 10 years) in the tritium less groundwaters. Appearance of tritium means the vulnerability, so tritium can be considered as an "early warning" of the pollutions from the last 50 years in the groundwaters. Case studies from Hungary proving this method will be presented.

The first use in practice: Hungarian Ministerial Decree of 21/2002 ordains for the public water supply companies to analyze periodically micro-pollutants in the raw water of the wells, excepting if the tritium content is less than 0,2 Bq/L (1,6 TU) because these groundwaters are protected against the pollutions of the last 50 years.

The effective infiltration rate of groundwater was estimated using the "tritium peak" method. Fundamental principle of this method is that the tritium content of precipitation was extremely high in 1963-64 years, in consequence of the nuclear weapon tests. Measuring the vertical tritium profile of groundwater or soil moisture, vertical flow velocity (v_z), infiltration rate (I) and the vertical hydraulic conductivity (k_z) were estimated by the present depth of tritium peak (h_{63}) and of zero tritium content (h_{52}).

According to our field studies in a recharge area of the regional groundwater flow regime of the Great Hungarian Plain the vertical flow velocity (Fig. 2.) was calculated as v_z = 200-250 mm/a. The infiltration rate was estimated as I = 40 to 50 mm/a, assuming n_o = 0.2 porosity. Vertical hydraulic conductivity looks be very low as k_z = (5 to 13) $*$ 10^{-8} m/s.

Same method was used for estimation of the vertical flow velocity and infiltration rate through the unsaturated zone in loess soil at the prospective nuclear waste disposal [1]. Tritium samples were extracted from the soil samples taken from dug-wells at the construction. Infiltration rates of 5 to 10 mm/a (1 to 2% of the total precipitation) and n_0 = 0,07 effective porosity were estimated by the method of tritium peak combined with tritium balance calculations.

Horizontal groundwater flow originating from the Danube with velocity arriving 500 m/a, was detected by the tritium peak method in 1992 in NW Hungary (Szigetköz area) in the more hundred meters thick gravel aquifer. Longitudinal dispersion coefficient of the gravel aquifer was estimated as 300 m by tritium and ^{3}He data [2, 3]. Repeating the tritium sampling five and ten years later the shift of the tritium peak provided useful information about the changes of the groundwater regime.

Groundwater flow velocities, infiltration rates and hydraulic conductivities can be estimated directly from tritium data but the main consume is the verification of hydraulic modeling [4].

REFERENCES

[1] HORVÁTH, I., DEÁK, J., HERTELENDI, E., SZŐCS, T., Hydrogeochemical investigations in the Tolna hills area, Ann. Report Geological Institute Hungary **II** (1996) 271-284.

[2] DEÁK, J., DESEŐ, É., BÖHLKE, J.K., REVESZ, K., Isotope Hydrology studies in the Szigetköz region, Northwest Hungary"", Isotopes in Water Resources Management, IAEA, Vienna (1996) 419-432

[3] STUTE, M., DEÁK, J., RÉVÉSZ, K., BÖHLKE, J.K., DESEŐ, É., WEPPERNING, R., SCHLOSSER, P., Tritium/^{3}He Dating of River Infiltration: An Example from the Danube in the Szigetköz Area, Hungary, Ground Water **35** 5 (1997) 905-911.

[4] FEHÉR, J., VAN GENUCHTEN, M.TH., DEÁK, J., Estimating long-term flow rates in the vadose zone using tritium measurements, (Proc. Sci. Colloquium “Porous or fractured unsaturated media: transports and behaviour” Monte Verita, Ascona, Switzerland October 5-9 1992).

Evolution of groundwater in a carbonate-bearing glacigenic aquifer, SW Finland: hydrochemical and isotopic evidence

Kortelainen, N.K.[a], J.A. Karhu[b], H. Lallukka[a], K. Lindqvist[a]

[a] Geological Survey of Finland,
Helsinki,
Finland

[b] University of Helsinki,
Department of Geology,
Helsinki,
Finland

Unusually high pH values, up to 9.5, are encountered in the glacigenic Virttaankangas aquifer, southwest Finland. This is in strong contrast to the pH values normally recorded in Finnish shallow groundwaters, averaging 6.4 [1, 2]. Chemical and isotopic (^{18}O, D, ^{13}C, T, ^{14}C) compositional parameters were determined in order to evaluate the origin of the unusual chemical composition of the groundwater at Virttaankangas. In addition, the mineralogical composition of the aquifer material was examined. The Virttaankangas groundwater formation has been studied extensively, because it has been selected as the site of an artificial recharge plant, intended to start operation in 2007. The project is the largest artificial groundwater scheme in northern Europe. The high pH values have been suggested to be related to the presence of carbonate minerals in glaciogenic sediments. However, only erratic carbonate boulders have been observed, and no outcrops containing carbonate rock have been discovered at the site.

The Virttaankangas aquifer is located in a NW-SE esker chain composed of Quartenary deposits. In the studied area of 54 km^2 the total thickness of sediments above the bedrock varies from 30 to 90 m. The formation of the stratigraphical succession occurred in three stages [3]. The core of the esker with coarse sand and gravel was deposited in the first stage. The second stage consists of an interlobate glaciofluvial ridge and fine-grained glaciolacustrine deposits. Locally the glaciolacustrine deposits form a confining interlayer holding a perched water table. The uppermost, third stage, is composed of sorted littoral sands formed during the regression of the former Baltic Sea. Accordingly, three distinct hydrogeological units can be identified: 1) an unconfined, highly conductive aquifer in the core of the esker, 2) a semi-confined aquifer, with fairly low hydraulic conductivity underlying the confining interlayer, and 3) an unconfined perched aquifer in the littoral deposit overlying the confining sediments.

The different hydrogeological units have distinct hydrochemical and isotope geochemical characteristics. The shortest residence time of groundwater is encountered in the perched aquifer of Unit 3, where seasonal $\delta^{18}O$ and δD variations are evident, and the tritium (ca. 10 TU) and radiocarbon (ca. 100 pmC) contents reflect those of recent precipitation. The perched water is highly unsaturated with respect to calcite ($\log SI_{calcite} << 0$). Chemically this water type is a typical shallow groundwater with a low pH value of < 7, low electric conductivity (EC) and low $\delta^{13}C$ of dissolved inorganic carbon (DIC) of < -20 ‰ (unpublished data). Oldest groundwaters are present in Unit 2, where some bomb tritium (ca. 21 TU) is still observed. None or minor seasonal variations are present in $\delta^{18}O$ and δD of Unit 1 and Unit 2. Groundwater in Unit 2 is saturated for calcite ($\log SI_{calcite} \approx 0$) and pH values are high, 9.2 – 9.5, exceeding values observed elsewhere in the aquifer. There is a small increase in the concentration of DIC from 0.2 mmol/L in Unit 3 to 0.4 mmol/L in Unit 2, suggesting dissolution of calcite. Existence of calcite as a source of DIC is confirmed by higher $\delta^{13}C$ (DIC) values in Unit 2,

ranging from –17 ‰ to –12 ‰. Concomitantly, the ^{14}C content of DIC has been lowered due to dissolution of old ^{14}C-free carbonate minerals. The $\delta^{13}C$ value of about –4.66 ‰ was measured from calcite in glacigenic sediments. In the unconfined aquifer (Unit 1), groundwater is slightly unsaturated for calcite (log $SI_{calsite} \leq 0$), however, the DIC content is approximately 0.5 mmol/L, which suggests slightly different evolution of DIC compared to Unit 2. Also pH is somewhat lower, 8.5 – 9.2. Both tritium (12-16 TU) and ^{14}C (80-90 pmC) concentrations are variable depending on the proportion of recent precipitation and the groundwater flow from Unit 2.

Mineralogical studies of the sediments in the Virttaankangas formation confirmed that very small quantities (0.5 % at most) of clastic, fine-grained (ca. 0.1 mm in diameter) calcite is present in the glacigenic units 1 and 2. However, the littoral sands of Unit 3 are nearly devoid of calcite. Calcite dissolution appears to be sufficient to explain the hydrochemical and isotope geochemical characteristics of the Virttaankangas aquifer. The reaction between groundwater and calcite in the Virttaankangas groundwater system was modelled using the PHREEQC program. A modelled evolution of DIC and pH in groundwater as calcite is dissolved to the point of saturation is in harmony with the chemistry of groundwaters collected from units 2 and 3 in the northeast side of the esker. The model represents closed system dissolution under conditions of a relatively low P_{CO2} of $10^{-2.65}$. In a closed system, pH increases significantly as calcite dissolves. It seems that dissolution of calcite under closed or partially closed system and relatively low CO_2 conditions explains the exceptionally high pH values in the Virttaankangas aquifer. Also the $\delta^{13}C$ values of DIC in groundwater are consistent with the origin of carbon from soil calcite and soil CO_2.

REFERENCES

[1] LAHERMO, P., ILMASTI, M., JUNTUNEN, R., TAKA, M., The Geochemical Atlas of Finland, Part 1, Espoo, Geological Survey of Finland (1990) 66 pp.

[2] TARVAINEN, T., LAHERMO, P., HATAKKA, T., HUIKURI, P., ILMASTI, M., JUNTUNEN, R., KARHU, J., KORTELAINEN, N., NIKKARINEN, M., VÄISÄNEN, U., Chemical composition of well water in Finland - main results of the "one thousand wells" project, (AUTIO, S., Ed.) Current Research 1999-2000, Geological Survey of Finland, Special Paper 31 (2001) 57-76.

[3] MÄKINEN, J., RÄSÄNEN, M., Early Holocene regressive spit-platform and nearshore deposition on a glaciofluvial ridge during the Yoldia Sea and the Ancylus Lake Phases of the Baltic Basin, SW Finland, Sed. Geol. **158** (2003) 25-56.

Tracing water-rock interactions: application to CO_2-rich and thermal mineral waters of the Forez graben, eastern French Massif Central

Gal, F., C.Y.J. Renac, D. Tisserand

Universite Jean Monnet,
Laboratoire Transferts Lithospheriques,
Saint Etienne,
France

The Forez graben, part of the French Hercynian Massif Central, is one of the Oligocene – Miocene graben surrounding the European Alpine belt. It's contoured by hercynian metamorphic rocks, ranging from schists – micaschists units to gneisses, and by numerous granites (Monts du Forez and Monts du Lyonnais). This graben is filled by clastic rocks (clay, sandy clay and sandstone) and few carbonate beds. Internal geometry tends to deepening eastward, reaching at least 500m deep. Some volcanic rocks are also present within the basin. As for lots of tertiary European grabens, numerous mineral water springs occur in or near the basin's limits. A majority is CO_2-rich and bicarbonate- sodium- rich, whereas other present a thermal bearing. Seven of those springs (both thermal and non-thermal) were studied during two years (monthly step sampling), using stable isotope (O, H and C), radiogenic isotopes (^3H and ^{14}C) and ions contents.

All waters are bicarbonate rich, from 500 to 3500 mg/L as HCO_3^-. Major cations are Na (150 to 1000 mg/L), Ca (10 to 200 mg/L), K (5 to 150 mg/L) and Mg (10 to 100 mg/L). Major anions [after HCO_3^-] are Cl (5 to 120 mg/L) and sulphate (7 to 50 mg/L). If assuming that contamination by surface water is of second importance, two events are highlighted by cations geothermometers calculations: first an interaction with surrounding rocks at moderate to high temperature, between 150 to 250°C and at low temperature c.a. 50 to 70°C. Nevertheless, all the waters appear to be immature regarding the fields defined by [1]. Inverse modelling (PhreeQC software, [2]) based on mass balance and isotopic compositions predicts dissolution of mineral species such as clays (illite, montmorillonite, kaolinite), oxides (hematite, goethite) and sulphates (gypse, anhydrite).

Based on oxygen and hydrogen isotope ratios (maximum $\delta^{18}O$ change: 1‰ ; δD change: 13‰ vs SMOW) of those mineral springs are preserved from actual atmospheric variations. Comparison with the local meteoric water line show a plot above the LMWL (taken at 400m asl; $\delta D=7.4\delta^{18}O+3.8$ ($r^2=0.96$)) for five springs, leading to a recharge area c.a. 100 to 200m above the actual basin level when assuming no changes in paleogeography. Moreover, episodic Tritium measurements were made. They show always values under 3 Tritium Units, except for one with a discharge in a river bed (5 TU), whereas present surface waters range from 6 to 9 TU.

Two springs plot far above the meteoric line, indicating a recharge upper in the surrounding topography. $\delta^{13}C_{DIC}$ measurements are different than surface waters (–16 to –22‰ PDB) and range from –3 to –5‰ PDB, except for a thermal spring (T_{mean}=29°C, $\delta^{13}C_{DIC}$ = –12‰ vs PDB).

Comparing ^{14}C and Tritium activities indicates that all the waters are between the "old" and "fossil" poles. Maximum ages calculated [3] are 8000 years BP for the thermal spring mentioned above and range between 19000 and 26000 years BP for the others. By taking into account ^{13}C ratios, alkalinity and water temperature, ages shift drastically to younger values: the thermal spring is then 2500 years BP.

So the studied waters fall within the surrounding “Monts du Forez” or “Monts du Lyonnais” between 2000 to 20000 years BP, infiltrate deep guided by inherited hercynian faults and experience two steps of interaction with rocks. Contamination or interaction with recent aquifers occurs during the rising up, as shown by Tritium content.

REFERENCES

[1] GIGGENBACH, W.F., Geothermal solute equilibria, Derivation of Na-K-Mg-Ca geoindicators, Geochim. Cosmochim. Acta **52** (1988) 2749-2765.

[2] PARKHURST, D.L., APPELO, C.A.J., User's guide to PHREEQC (Version 2) - a computer program for speciation, batch-reaction, one-dimensional transport, and inverse geochemical calculations: U.S. Geological Survey Water-Resources Investigations Report 99-4259 (1999) 312 pp.

[3] FONTES, J.C., GARNIER, J.M., Determination of the initial ^{14}C activity of the total dissolved carbon; a review of the existing models and a new approach, Water Resour. Res. 15 (1979) 399-413.

[4] KHARAKA, Y.K., LICO, M.S., LAW, L.M., Chemical geothermometers applied to formation waters, Gulf of Mexico and California basins, Am. Assoc. Petrol. Geol. Bull. **66** (1982) 588.

[5] KHARAKA, Y.K., MARINER, R.H., Chemical geothermometers and their application to formation waters from sedimentary basins : Thermal History of Sedimentary Basins, (NAESER, N.D., MCLOLLON, T.H., Eds) Springer Verlag, New York (1989) 99-117.

[6] FOURNIER, R.O., POTTER, R.W., An equation correlating the solubility of quartz in water from 25°C to 900°C at pressures up to 10 000 bars, Geochim. Cosmochim. Acta **46** (1982) 1969-1973.

Are oxygen isotopes of sulfate a useful tool for the quantification of sulfate reduction in a BTEX contaminated aquifer?

Knoeller, K.[a], C. Vogt[b], S. Weise[a]

[a] UFZ Centre for Environmental Research Leipzig-Halle,
Dept. of Isotope Hydrology,
Halle/Saale,
Germany

[b] UFZ Centre for Environmental Research Leipzig-Halle,
Dept. of Environmental Microbiology,
Halle/Saale,
Germany

The mineralization of organic contaminants to carbon dioxide and water by naturally occurring in-situ biodegradation is the basic concept of the natural attenuation of polluted aquifers. Sulfate reducing bacteria can contribute extensively to the biodegradation of organic contaminants. During the dissimilatory reduction of sulfate, the microorganisms produce sulfide to obtain energy for the oxidation of organic carbon provided by the contaminants. The preferential utilization of the lighter isotopes by bacteria usually results in the enrichment of the lighter isotope in the produced sulfide and of the heavier isotope in the remaining sulfate. For sulfur, the isotopic enrichment in the remaining sulfate has been used quite successfully for the identification and quantification of bacterial sulfate reduction (BSR). However, only little is known about the behavior of oxygen isotopes in sulfate during sulfate reduction under the specific conditions of an organic contamination. Therefore one goal of this study was to specify the fractionation mechanisms of sulfate oxygen closely related to biodegradation. The contamination of the investigated Quaternary aquifer is related to the operation of an industrial site that was originally set up in 1938 for the production of gasoline and upgraded for the production of benzene in 1960. During the operation from 1938 to 1990, numerous production accidents and leaks contributed to BTEX-contamination of the groundwater.

To obtain the basic fractionation parameters for sulfur and oxygen, experimental and field data were used. Microcosm experiments were inoculated with an enrichment culture from the study area. All experiments were conducted with toluene as the solely source of organic carbon. Groundwater samples were collected from multi-level sampling wells in a ca. 500 m^2 area within the contaminant plume. The sampling area was selected in order to avoid a mixing of sulfate from different sources. Groundwater and laboratory samples were analyzed for the content of dissolved sulfate and sulfide as well as for the isotopic composition of sulfate ($\delta^{34}S$, $\delta^{18}O$) and sulfide ($\delta^{34}S$).

The isotopic composition of sulfur in sulfate and sulfide from laboratory and groundwater samples are shown in Figs. 1 and 2, respectively. In both cases, the typical correlation between the fraction of the residual sulfate and the $\delta^{34}S\text{-}SO_4$ proves the occurrence of BSR. The average enrichment factors for ^{34}S were calculated from logarithmic fits of the respective data sets using a Rayleigh equation. While the experimental enrichment factor between SO_4 and S^{2-} was -23.4 ‰, a slightly smaller value of -17.5 ‰ was observed for field samples. Both values are consistent with previously reported data. $\delta^{34}S\text{-}S^{2-}$ values obtained during the laboratory experiments are in accordance with the expected values for the given enrichment factor in a system that is characterized by the accumulation of a product reservoir (Fig. 1). For groundwater samples the measured $\delta^{34}S\text{-}S^{2-}$ values do neither match the expected values for an accumulating product reservoir nor the values expected for an open system with H_2S-loss (Fig. 2).

As shown in Fig. 1, no correlation exists between the fraction of the residual sulfate and the δ^{18}O-SO_4. The absence of the typical ^{18}O-enrichment can be caused either by the interference of the kinetic isotope effect with an approaching isotopic equilibrium between oxygen in sulfate and water or by the superimposition of BSR by the bacterial disproportionation of S^0 to SO_4 and H_2S (BDS). A general lack of an oxygen isotope effect, e.g. due to the high load of organic contaminants, can be ruled out, since a significant oxygen isotope shift of more than 5 ‰ between the initial sulfate and the sulfate in the microcosm experiments was observed.

The oxygen isotopes of sulfate in groundwater samples show a much different behavior (Fig. 2) A strong correlation exists between the fraction of the residual sulfate and the measured δ^{18}O-SO_4. However, this correlation is rather of a linear type than of the logarithmic type that would be expected for BSR. Again, an interference of different processes, most likely BSR and BDS, seems obvious. Hydrochemical analyses showed that most groundwater samples contain a significant amount of elemental sulfur which supports the assumption of BDS occurrence.

In general, sulfur isotopes provide a very useful tool for the identification of BSR in BTEX contaminated aquifers. However, for the quantification of the process caution has to be used since a possible BDS can also affect the δ^{34}S of the remaining sulfate. Oxygen isotope data can also be quite useful as long as there is no interference with processes such as BDS or with an approaching equilibrium with water oxygen. But even in those cases, the unusual behavior of δ^{18}O-SO_4 helps recognize processes that have to be considered for the quantification of BSR using sulfur isotopes.

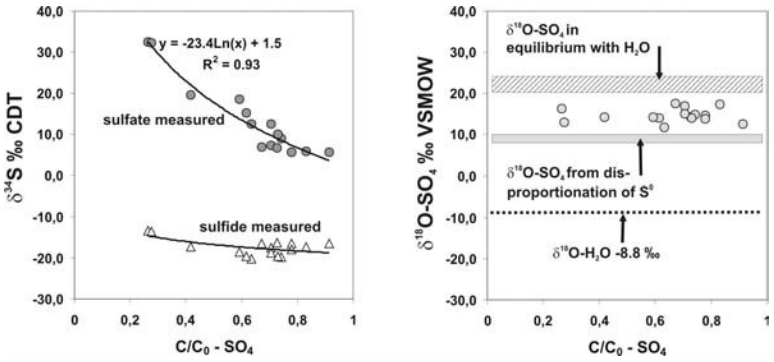

FIG. 1. Correlation between the remaining SO_4-fraction and the isotopic composition of SO_4 and S^{2-} in microcosm toluene degradation experiments.

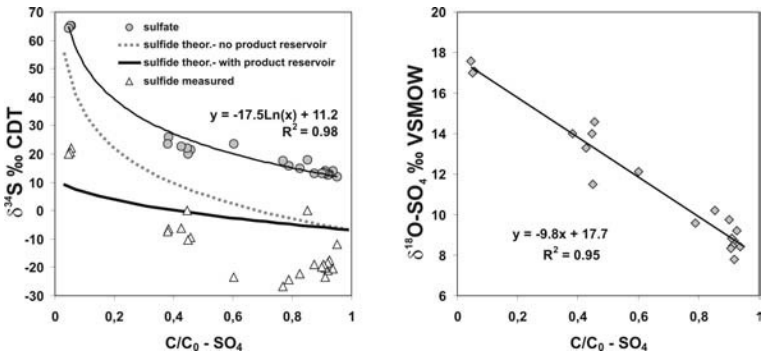

FIG. 2. Correlation between the remaining SO_4-fraction and the isotopic composition of SO_4 and S^{2-} in groundwater samples from the study area.

Stable isotope compositions of sedimentary organic carbon and nitrogen recovered from East African crater lake

Muzuka, A.N.N.

Institute of Marine Sciences,
University of Dar Es Salaam,
Zanzibar,
United Republic of Tanzania

Variation in the contents of organic carbon and nitrogen and stable isotopes composition of organic carbon for two cores (EMP LIV 2b and EMP LIV 4) recovered from the Empakai crater lake are used to deduce variability in sources of organic matter in the lake in relation to climatic changes. Also the stable isotopes of sedimentary nitrogen are used to assess effect of acid treatment on nitrogen stable isotopes. Cores EMP LIV 2b and EMP LIV 4 are 1 and 2 m long, and were recovered from water depths of 11 and 20 m respectively.

The Empakai Crater Lake (2°54'S; 35°50'E), which is a closed lake, is located in a semi arid environment about 10 kilometres south of the Oldonyo Lengai within the northeastern corner of the Ngorongoro Conservation Area Authority in northern Tanzania. Eight-accelerator mass spectrometer dates determined on total organic matter for core EMP LIV 4 indicate that the sedimentation rate in this lake is about 30 cm/ka for the late Pleistocene to early Holocene period.

Both $\delta^{13}C$ (average –24.0∀2.7λ) and $\delta^{15}N$ (8.2∀3.0λ) values for core EMP LIV 4 show a sharp change to lower values of about 4λ and 7λ respectively at around 8.7 ka uncorrected ^{14}C ages. Abrupt change in the stable isotopes compositions of organic carbon and nitrogen show major climatic changes to have taken place during the Pleistocene-Holocene period most probably changing from humid to drier conditions. The $\delta^{13}C$ values between 0 and 8.7 ka show small amplitude of downcore decrease, whereas that $\delta^{15}N$ values shows a general downcore increase an indication in changes in relative proportion of C_4 and C_3 material as well as climatic conditions. Between 8.7 and 11 ka, the $\delta^{13}C$ values depict slight downcore enrichment reaching peak during the Young Dryas. The lowermost part of the core shows depletion in ^{13}C centred at about 12 ka. Similarly, the $\delta^{15}N$ values show a downcore decrease between 8.7 and 12 ka. This may be an indication of increase in supply of phytoplanktonic material to the lake owing to increase in precipitation during the Pleistocene-Holocene transition.

Both cores have high contents of organic carbon and nitrogen an indication of preferential preservation. The contents of nitrogen (averaging 0.35∀0.25%) and organic carbon (averaging 6.9∀5.2%) for core EMP LIV 4 co-vary and are highly variable. Highest contents of organic carbon and nitrogen are confined between 10 and 12 ka. Furthermore, the C/N ratios, which average 21.4∀3.9, show a general downcore increase to the base of the core. The contents of organic carbon (averaging 4.8∀5.4%) and nitrogen (averaging 0.43∀0.47%) for core EMP LIV 2b shows a general downcore decrease to the base of the core with a sharp shift towards lower values at 35 cm. The C/N ratios values for core EMP LIV 2b that averages 12.7∀2.1 display 2 steps downcore increase.

Core EMP LIV 2b is chronologically poorly constrained with two available ^{14}C dates being reversed. The $\delta^{13}C$ values for core EMP LIV 2b, which averages -19.2∀2.2λ, shows a general downcore decrease with δ-values changing from -17λ to -21λ in the upper 30 cm. This trend is followed by a shift to higher values of about 5λ within 10 cm followed by a systematic downcore decrease to the base of the core. The $\delta^{15}N$ values for core EMP LIV 2b are highly variable and average 1.0∀3.6λ.

Generally, the stable isotope results indicate that climatic conditions have deteriorated since the middle Holocene. Furthermore, the results indicate that sources of organic matter in the Empakai crater lake has varied over time with more humid periods being characterized by material derived from phytoplankton and C_3 land plants. Also a difference in mean isotope values between shallower site (enriched) and deeper (depleted) site shows how heterogeneous the records can be even from the same area.

This study also assessed impact of sample treatment on the stable isotope compositions of nitrogen. Generally acidification processes cause isotope fractionation where treated particulate materials are depleted in ^{15}N relative to untreated fraction (Fig. 1). The difference in the stable isotope composition between treated and untreated samples is as high as 7‰. This could be attributed to hydrolysis effect where nitrogen rich compounds are removed. Thus, for the determination on nitrogen stable isotopes, untreated sedimentary materials are preferred over treated sediments.

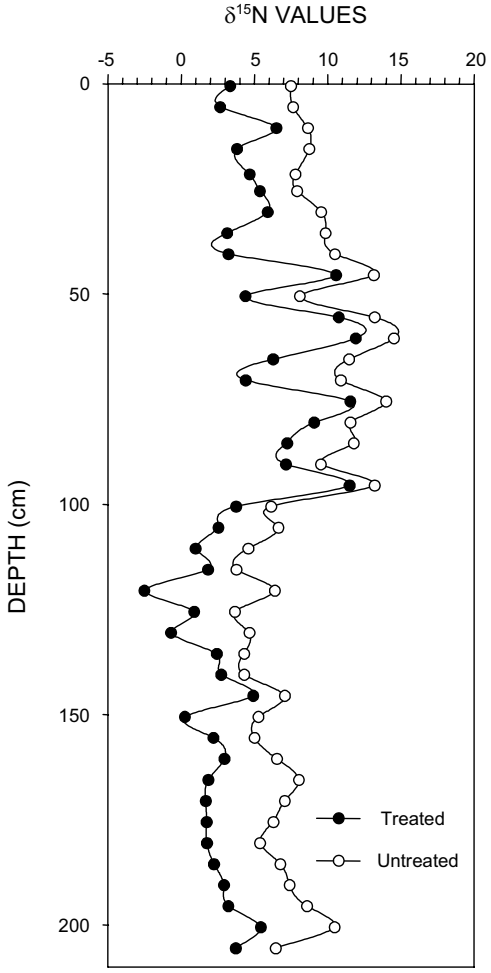

FIG. 1. A figure showing differences in stable isotopes composition of nitrogen between acidified (treated) and unacidified sediment samples.

Environmental isotopes and hydrochemistry approach to evaluate the source of recharge and pollution load in Manzala and Bardawil Lakes, Egypt

Aly, A.I.M.[a], M.A. Hamed[a], S.G. Abd El- Samie[a], E.A. Eweida[b]

[a] Egyptian Atomic Energy Authority,
Cairo,
Egypt

[b] Faculty of Science,
Cairo University,
Cairo,
Egypt

The present study has been conducted to evaluate the pollution load that has been exerted on two of the major lakes in Egypt; Bardawil and Manzala lakes. Bardawil lake is mainly sea water subjected to evaporation while Manzala lake is a mixture of saline water and fresh water and receives drainage water and effluents of different wastes. The study involves both environmental isotopes (^{18}O and D), major ions, nitrate and phosphate analysis of about 75 water samples collected through horizontal and vertical profiles in the two lakes.

Bardawil lake water (the average of TDS equals to 46521 ppm) is dominated by Cl, Na and Mg salts. The distribution of the ions is controlled by the inflow from sea water, the concentration by evaporation, the precipitation due to supersaturation and the specific gravity variations. The hydrochemical composition of Manzala lake water (average of TDS equals to 2554 ppm) is less homogenous than that of Bardawil lake water and reflects the effects of several factors and recharge sources; irrigation water / drainage water discharge, waste water load, sea water or groundwater inflow, bathometry and evaporation intensity. The concentrations of nitrate and phosphate acquire considerably high values in Manzala lake which indicate a high degree of pollution and eutrophication.

The isotopic content of Bardawil lake water has average values of 3.69‰ and 28.59‰ for $\delta\ ^{18}O$ and δ D, respectively. It has a relatively wide range of variation reflecting the effect of the different recharge sources (seawater, precipitation and seepage of groundwater) and the influence of the different hydrogeochemical conditions. The distribution of Bardawil lake water on $\delta\ ^{18}O$ *vs* δ D conventional diagram, (Fig. 1) follows a linear pattern.

$\delta D = 4.70\ \delta\ ^{18}O + 10.31$ of lower slope (4.70) than the meteoric line (slope = 8), [1]. This reflects the effect of evaporation on the occurring surface water in the lake. The starting points of the samples line (evaporation line) lie very close to Mediterranean Sea water which represent the original sources of lake water. The relative position of the water samples on the evaporation line and their deviation from the original points is a function of evaporation intensity.

The effect of evaporation on the isotopic composition of Bardawil lake water is also shown by the direct relationship between ^{18}O and TDS, (Fig. 2). This figure shows that the correlation coefficient is low particularly in the deeper zones (bottom water) than that of surface zones (surface water). This can be related to salt precipitation after stages of supersaturation in the surface water due to excessive evaporation processes which reaches about 1.6 m/y [2].

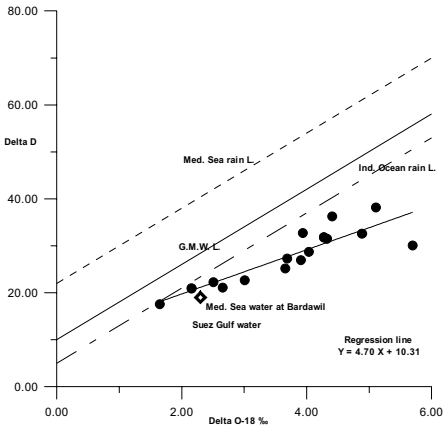

FIG. 1. $\delta^{18}O$ and δD relationship for Bardawil surface water.

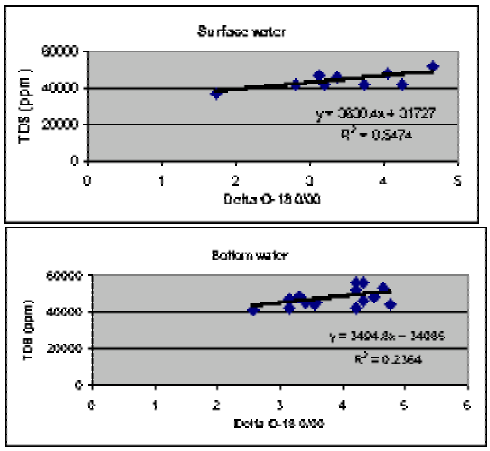

FIG. 2. TDS and delta O-18 relationship in Bardawil lake water.

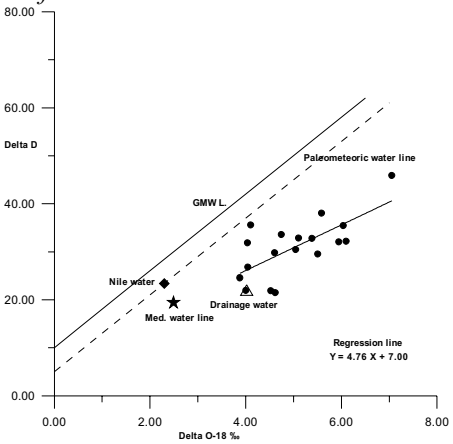

FIG. 3. $\delta^{18}O$ and δD relationship for Manzala surface water.

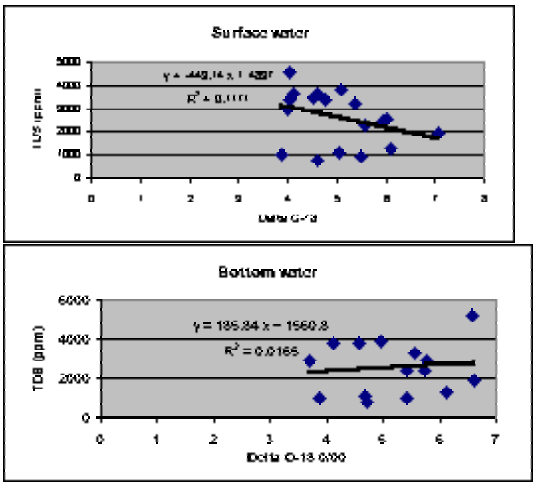

FIG. 4. TDS and delta O-18 relationship in Manzala lake water.

The isotopic content of Manzala lake water is characterized by average values of 5.07‰ and 29.79‰ for $\delta\ ^{18}O$ and δ D, respectively. The frequency distribution of the isotopic values reflects the multiplicity of the recharge sources (precipitation, seawater, drainage, irrigation and groundwater). The relationship between ^{18}O and deuterium for Manzala lake water is direct and follows a linear pattern of evaporation trend $\delta D = 4.76\ \delta\ ^{18}O + 7$, (Fig. 3). The isotopic contents of Nile water, seawater and drainage water (the recharging sources of the lake) lie close to the starting points of the evaporation line. The scatter of the points around the regression line is relatively high due to the variant proportion of the recharge sources and the different evaporation intensity. The relationship between ^{18}O and TDS, (Fig. 4), is very weak and the pattern is not easily defined. This can highlight on the great difference of salinity between the recharging sources (due to leaching, evaporation, dissolution etc.), while the isotopic content is not so variant.

REFERENCES

[1] CRAIG, H., GORDON, L., Deuterium and oxygen-18 variation in the ocean and the marine atmosphere, (TONGIORGI, E., Ed.), Stable Isotopes in Oceanographic Studies and Paleotemperature, Spoleto **9** (1965).

[2] FOSTER WHEELER, Italiana-Fosweco Div., Gebel El Maghara Rural Development Project, Final report submitted to the Governorate of North Sinai, Five volumes (1998).

Myall Lakes – isotope dating of short term environmental changes in a coastal lake system - anthropogenic pressures causing blue-green algae outbreaks in a national park

Flett, I.[a], H. Heijnis[b], K. Harle[c], G. Skilbeck[a]

[a] Department of Environmental Science,
University of Technology,
Sydney, NSW,
Australia

[b] ANSTO – Environment,
Sydney, NSW,
Australia

[c] CSIRO Sustainable Ecosystems,
Canberra, ACT,
Australia

The Myall Lakes system, 50 km North of Newcastle, Australia, is a barrier lake system covering 10000ha, and is brackish (ranging from Oligohaline to Mesohaline under the Venice System classification). The Myall Lakes system is far less disturbed than similar coastal lakes, and as an important migratory bird habitat, they are protected under the RAMSAR agreement. They are also fully encompassed by the Myall Lakes National Park, declared in 1972, and are important to the local tourism and fisheries industries. Only two small streams provide freshwater input therefore water-retention time is of concern, because any changes to nutrient regimes, or pollution in the catchment affecting the Lakes, may take a long time to be corrected. In recent summers a series of cyanobacteria blooms have occurred which may indicate that human activities such as agriculture and recreational boating and fishing are affecting the Myall Lakes.

Four sediment cores, up to 95cm long, were collected and sub-sampled for trace elements, palynological assemblages, sediment grain size and organic/carbonate content. Lead-210 (^{210}Pb) was used to determine sedimentation rates and construct a chronology. Fossilised algal remains, specifically the akinetes of cyanobacteria, were used to estimate previous algal populations in the lake system. This technique has the potential to be an important tool in not only historical environmental reconstruction but also in catchment management.

Results indicate that there have been cyclical fluctuations in the populations of aquatic plants and algae throughout recent history.

ISOTOPE HYDROLOGY – POSTERS

Temporal analysis of stable water isotopic characteristics in the Murray Darling Basin

Henderson-Sellers, A.[a], P. Airey[a], D. Stone[a], K. McGuffie[b]

[a] Environment,
Australian Nuclear Science and Technology Organisation,
Lucas Heights NSW,
Australia

[b] Department of Applied Physics,
University of Technology, Sydney,
Broadway NSW,
Australia

Abstract. In Australia stable water isotopes (SWIs) are being exploited in novel ways to establish objective validation of and improvement in existing water resource models. Three timescales have been used here to explore the role of stable water isotopes in refining climate and hydrological models of the Murray Darling Basin. Our goal here is to improve the dynamics of simulations of regional water cycles and, ultimately, reduce uncertainty in future water resource predictions.

The isotopic composition of water and carbon in e.g. ice cores, ground water and biomass has been recognized as relevant to hydro-climates on timescales from glacial [1] to extreme weather [8]. Over tens to thousands of years, we have examined the processes leading to the effective recharge of groundwater (Fig. 1(a)). The isotope data clearly indicate that in the warm arid/semi-arid regions, in contrast to the behaviour in cool temperate zones, effective recharge only occurs when the rainfall intensities exceed a threshold value. Isotopic estimates of this recharge threshold rainfall intensity could be applied to predictions of future groundwater resources.

Over years to decades, we have assessed the success of a range of atmospheric global circulation models in simulating key hydrological parameters over the AMIP II period including El Niño and La Niña forcing [2]. The results are rather poor for the majority (13 out of 20) AGCMs suggesting that further constraints on the basin's hydrology, such as from isotopes, may be valuable (Fig. 1(b)).

In our third approach, we have modelled minute to monthly isotope fluxes using (a) land surface schemes (LSSs) at particular grid points within the Murray Darling Basin and (b) a steady state (phenomenological) model of river hydrology. Modelling minute to monthly isotope fluxes using land surface schemes and a steady state (phenomenological) model of river hydrology allows comparison of the partitions of precipitation between transpiration, run-off and 'lake' evaporation with isotope observations from June 2002 to January 2003.

Model conservation, climatic variations and 'plausibility', all pre-requisites for good simulations, have been investigated here for the Murray Darling. I-GCM and I-LSS models' partitions of precipitation between transpiration, run-off and 'lake' evaporation have been compared with isotope observations from the Darling River from 2002 to 2004. We find that: (i) more work is needed on gross water fluxes first; (ii) simple isotopic models generate plausible values but more complex ones, as yet, do not; and (iii) isotopes have potential for evaluation of whether LSSs are (in)correctly recharging and accessing groundwater reservoirs and for evaluation of the partitioning of water into runoff cf. re-evaporation. Tests based around these concepts offer a novel addition to the traditional methods of validating climate models and their sub-components.

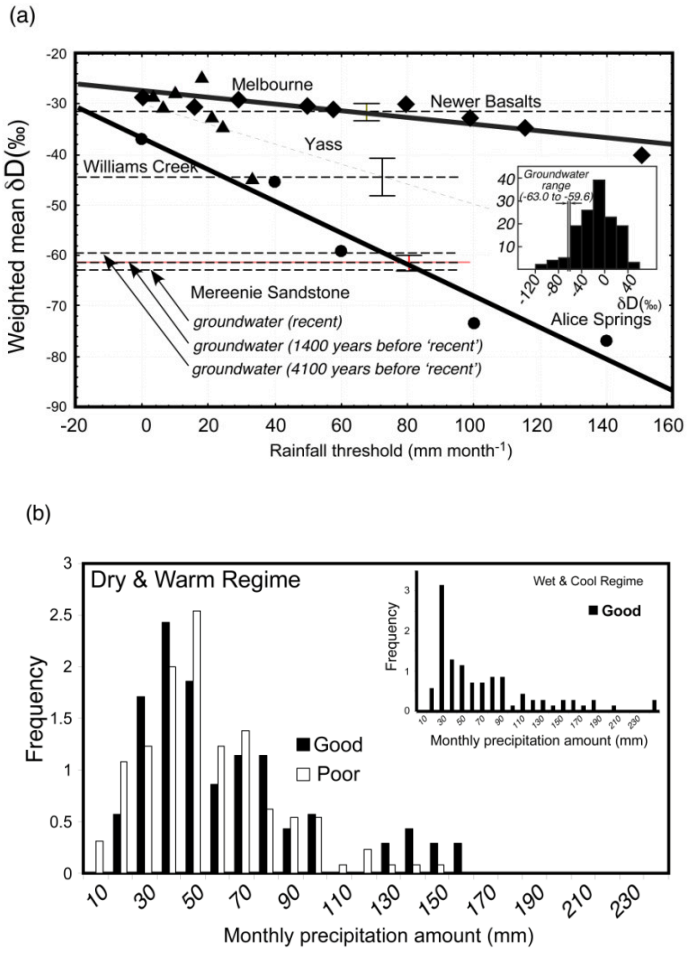

FIG. 1. (a) Variation of weighted mean δD‰ in rainfall exceeding threshold precipitation intensities as observed at Melbourne (monthly - diamonds), Yass (daily - triangles) and Alice Springs (monthly - circles) and the three dated Mereeni groundwaters plus the Williams creek and Newer Basalts groundwaters with (inset) for Alice Springs the GNIP-derived [4] δD in rainfall plus the groundwater δD from the Mereenie aquifer, and (b) frequency of monthly precipitation intensities from the 7 "good" and 13 "poor" AMIP II GCMs for El Niños (warm and dry) for the Murray Darling Basin and inset La Niñas (wet and cool) for 'good' models.

REFERENCES

[1] PETIT, J.R., JOUZEL, J., RAYNAUD, D., BARKOV, N.I., BARNOLA, J.-M., BASILE, I., BENDER, M., CHAPPELLAZ, J., DAVISK, M., DELAYGUE, G., DELMOTTE, M., KOTLYAKOV, V.M., LEGRAND, M., LIPENKOV, V.Y., LORIUS, C., PÉPIN, L., RITZ, C., SALTZMANK E., STIEVENARD, M., Climate and atmospheric history of the past 420000 years from the Vostok ice core, Antarctica, Nature **399** (1999) 429–436.

[2] LAWRENCE, J.R., GEDZELMAN, S.D., Tropical ice core isotopes: do they reflect changes in storm activity, Geophys. Res. Lett. **30** 2 (2003) 44-1 to 44-4, 10.1029/2002GL015906

[3] HENDERSON-SELLERS, A., MCGUFFIE, K., NOONE, D., IRANNEJAD, P., Using stable water isotopes to evaluate basin-scale simulations of surface water budgets, J. Hydrometeorology **5(5)** (2004) 805-822.

[4] GNIP WEB, Global Network for Isotopes in Precipitation. The GNIP Database. Release 3, (October 1999). URL: http://www.iaea.org/programs/ri/gnip/gnipmain.htm.

Application of stable isotope tracers to evaluate the hydrodynamic mechanisms of heavy metal mobilization in copper ore tailings

Knoeller, K.[a], M. Schubert[b]

[a] UFZ Centre for Environmental Research Leipzig-Halle,
Dept. of Isotope Hydrology,
Halle/Saale,
Germany

[b] UFZ Centre for Environmental Research Leipzig-Halle,
Dept. of Analytical Chemistry,
Halle/Saale,
Germany

The weathering and erosion of mining and ore processing residues may have a negative impact on local surface waters, which again is likely to be detrimental to groundwater quality. Assessing the environmental response and the dimension of the impacts requires understanding the interaction between the contaminant source and the involved flow systems. The paper presents results of a research on the potential of environmental isotope signatures ($\delta^{18}O$ and $\delta^{2}H$) to trace heavy metal emissions from a heap of processing residues via a spring situated at the foot of the heap.

The main goal of the investigation was to localize the source of contamination. The heap is considered to be a black box, with no indication given, if the heavy metals in the spring water, with concentrations of up to 2.000 mg/L, are predominantly leached from the processing residues by percolating rain water or by groundwater, entering the heap's base and reappearing at the spring. Knowledge of these processes is essential for the remediation of the site. Thus, the aim of the investigation was to distinguish spring water, which is dominated by local precipitation, from groundwater and to correlate the waters of different origin to the heavy metal contents of the spring water. High contaminant concentrations in the spring water did not allow distinguishing the waters by their chemical composition. In consequence, isotope signatures were used for differentiation.

Figure 1 displays the monitored data of spring discharge, rain, $\delta^{18}O$, and δD during a selected observation period in October 2003. In the course of that period, several lighter rain events occurred that did not significantly affect the spring discharge. Also, the isotopic composition of the rain water during the smaller events resembled the average isotopic composition of the spring water so that no significant temporal variation of the isotope data of the spring was observed.

In contrast to the minor variations during the lighter rain events, the discharge showed an immediate response to a heavier rain event. At its peak the discharge was about four times higher than before the event. However, the isotopic composition of the spring water, which is also shown in Fig. 1, indicates that only a part of the additional discharge directly results from percolating rain water. 30 minutes after the first significant increase of the discharge the additional discharge, which is about 100% above normal background values, only contains 30 % of rain water. At its peak, just 10% of the additionally discharged water is rain water. That means that only immediately after the rain event the spring discharge is directly influenced by percolating rain water.

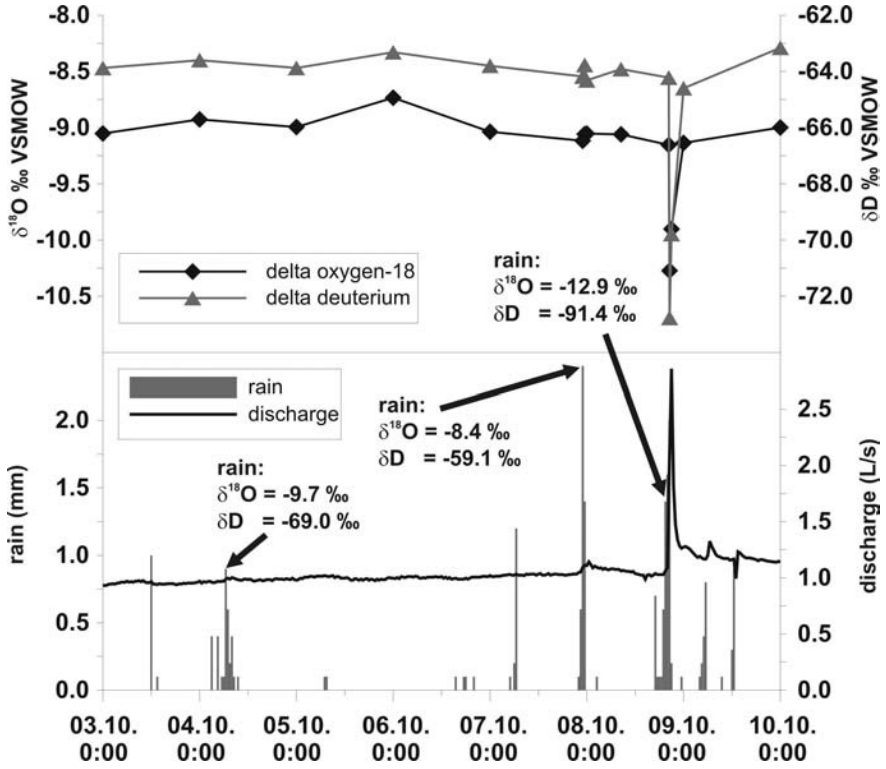

FIG. 1. Temporal variation of spring discharge, rain, and the isotopic composition of spring and rain water at the Stadtborn spring during a 8-day period in October 2003.

During the heavier rain event the lowest metal and sulfate concentrations are reached 30 minutes after the first increase of the discharge, i.e. when the influence of percolating rainwater is most pronounced. The Zn, Cd and SO_4 concentrations decrease to 45 % of the background concentration, Pb drops even down to 17 %. The decrease in concentrations can be explained by dilution. At the peak of the spring discharge, however, the concentrations begin to rise again. That indicates that as soon as the share of percolating rain water in the spring water decreases and the spring water is dominated by discharge from the aquifer, dilution becomes less relevant. This again shows that percolating rainwater only seems to cause a dilution of the contaminants, while the additional discharge of the aquifer triggers additional mobilization of the heavy metals, which occur mainly as sulfates.

The results indicate that the source of contamination seems to be located at the base of the heap. While percolating rain water does not mobilize significant amounts of contaminants, groundwater that emerges from the aquifer and migrates at the base of the heap has a strong impact on the heavy metal load of the spring water. Further studies, including those on $\delta^{34}S$ signatures along with tracer tests, are planned to verify that idea. If the additional data should confirm the present concept, it could be concluded, that covering the heap would not be an appropriate remediation measure.

^{210}Po in meteoric and surface waters at Corumbataí River Basin, São Paulo State, Brazil

Bonotto, D.M., J.L.N. De Lima

Instituto de Geociências e Ciências Exatas - UNESP,
Rio Claro,
São Paulo,
Brazil

^{210}Po is an intermediary member of the natural mass number (4n+2) ^{238}U decay series that finishes at the stable ^{206}Pb, according to the sequence: ^{238}U (4.49 Ga, α) → ^{234}Th (24.1 d, β$^-$) → ^{234}Pa (1.18 min, β$^-$) → ^{234}U (0.248 Ma, α) → ^{230}Th (75.2 ka, α) → ^{226}Ra (1622 a, α) → ^{222}Rn (3.83 d, α) → ^{218}Po (3.05 min, α) → ^{214}Pb (26.8 min, β$^-$) → ^{214}Bi (19.7 min, β$^-$) → ^{214}Po (0.16 ms, α) → ^{210}Pb (22.26 a, β$^-$) → ^{210}Bi (5 d, β$^-$) → ^{210}Po (138 d, α) → ^{206}Pb. Because some of the ^{222}Rn escape from the rocks and minerals to the surrounding fluid phase, such as air, ^{222}Rn emanating from land surfaces is responsible for ^{210}Pb and ^{210}Po present in the atmosphere. The average ^{222}Rn escape rates measured and calculated in the northern high latitudes are 0.18-0.53 atom cm^{-2} s^{-1} [1]. The oceans are not considered important sources of atmospheric ^{222}Rn, since the oceanic flux is about 1% of the continental one [2]. ^{210}Pb produced by ^{222}Rn is removed from the atmosphere by precipitation, being its concentration in rain of about 2 pCiL^{-1} [3]. The atmospheric ^{210}Pb returning to the earth's surface has been commonly referred to as unsupported (excess) ^{210}Pb, and neither ^{210}Po nor ^{210}Pb have been significantly investigated in atmospheric studies performed in South America.

The purpose of this investigation was to characterize the presence of ^{222}Rn and ^{210}Po in wet (rainwater) deposition occurring at a very important sedimentary basin located in São Paulo State, Brazil, i.e. the Corumbatai River Basin (Fig. 1). It is a sub-basin of the giant Paraná sedimentary basin (Paleozoic - Cenozoic) that extends over an area of 1,700,000 km^2. The Corumbataí River is the major river draining the area, and its water is extensively used by water supply systems in the basin. Since rainwater deposition has been recognized as a major source of dissolved species in rivers, surface waters from Corumbataí River were also collected at two sampling points, upstream and downstream from Rio Claro city, the principal municipality within the basin (Fig. 1).

Surface waters and rainwater samples for ^{210}Po and ^{222}Rn analyses were collected between January 1998 and January 1999. Volumes between 10 and 21 L were utilized for ^{210}Po analysis, whereas 1 L was used for evaluating ^{222}Rn in rainwater. A known amount (7.68 dpm/mL) of ^{209}Po spike was added to each sample for ^{210}Po analysis, and polonium co-precipitated with $Fe(OH)_3$. The recovered Po was plated onto a copper disc suspended in a 20% hydroxylamine hydrochloride + 25% sodium citrate solution heated to 85-90°C, and stirred during 75-90 min [4]. Conventional alpha spectroscopy with Si(Au) surface barrier detectors coupled to EG&G Ortec multichannel buffer was used to acquire the ^{210}Po activity concentration data. ^{222}Rn in rainwater was extracted by circulating a stream of Rn-free air through the sample container to purge the water phase of its dissolved/accumulated ^{222}Rn. The emanation procedure [5] consisting on its removal from the sample, its transfer to a scintillation flask, and its detection by alpha-scintillation counting was used to acquire the ^{222}Rn activity concentration data.

^{210}Po activity concentration in rainwater ranged between 0.04 and 1.19 dpm/L (average = 0.35 dpm/L) and between 0.07 and 0.46 dpm/L (average = 0.20 dpm/L) at the two investigated sampling points, whereas the ^{222}Rn activity concentration ranged between 40 and 479 dpm/L (average = 182 dpm/L). Thus, low ^{210}Po/^{222}Rn activity ratios corresponding to 0.0002-0.004 were determined, implying on the non-existence of secular radioactive equilibrium between these nuclides. This is, in fact, expected

since the ^{210}Pb half life is much higher than that of its parent ^{222}Rn. ^{210}Po activity concentration in surface waters collected upstream from Rio Claro city ranged between 0.06 and 0.75 dpm/L (average = 0.23 dpm/L), whereas in surface waters collected downstream from Rio Claro city ranged between 0.07 and 0.65 dpm/L (average = 0.26 dpm/L). A trend of decreasing ^{210}Po activity concentration in accordance with increasing rainfall was identified at both sampling sites, that is compatible with dilution effects in surface drainage during the more rainy periods. Traditionally, the drainage in the Corumbataí river basin has received along the time significant *in natura* emissions of municipal waste products and discharge of waste water, sludge, sewage, sanitary and industrial effluents, among others. Thus, the water quality downstream from Rio Claro city is much worse than that of upstream from Rio Claro city, but, despite this, the dissolved ^{210}Po activity concentration is practically the same at both sampling sites. This suggests that ^{210}Po is a conservative nuclide, potentially much important to be used as a natural tracer of hydrological systems, even in polluted areas.

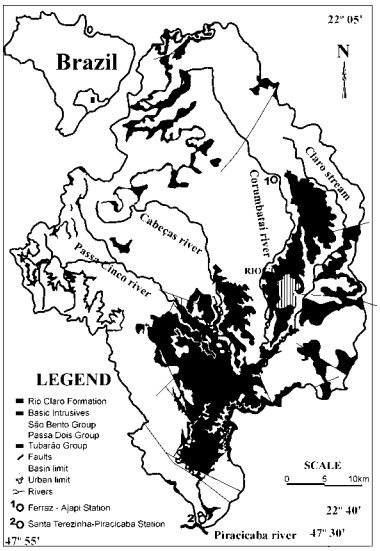

FIG. 1. Sketch map of the studied area and location of the sampling points for surface waters analysis.

REFERENCES

[1] BASKARAN, M., NAIDU, A.S., ^{210}Pb-derived chronology and the fluxes of ^{210}Pb and ^{137}Cs isotopes into continental shelf sediments, East Chukchi Sea, Alaskan Artic, Geochim. Cosmochim. Acta **59** (1995) 4435-4448.

[2] WILKENING, M.H., CLEMENTS, W.E., The ocean as a source of atmospheric radon-222, J. Geophys. Res. **80** (1975) 3828-3830.

[3] EAKINS, J.D., MORRISON, R.T., A new procedure for the determination of lead-210 in lake and marine sediments, Int. J. Appl. Radiation Isot. **29** (1978) 531-536.

[4] FLYNN, W.W., The determination of low levels of polonium-210 in environmental materials, Anal. Chim. Acta **43** (1968) 221-227.

[5] LUCAS, H.F., Improved low-level alpha-scintillation counter for radon, Rev. Scient. Instrum. **28** (1957) 680-683.

Residence times for surface waters in altered granite area : example of the "Furan" water catchment, east French Massif Central

Gal, F., C.Y.J. Renac, D. Tisserand

Universite Jean Monnet,
Laboratoire Transferts Lithospheriques,
Saint Etienne,
France

The topic of this study is to understand the behaviour of surface waters in a small catchment area (ca. 3300 ha – altitudes ranging from 550 m to 1300 m). Six springs located in the southern part of the French Massif Central have been studied for two years. The "Furan" watershed composed of metric arena overlays in a granitic and gneissic basement.

Oxygen and hydrogen stable isotope ratios were determined routinely. Tritium, carbon isotopes as well as alkalinity were punctually determined. Cations and anions were quantified using ICP-AES and ion chromatography. Further more, to better understand stable isotopes catchment's behavior, three years of daily rainwater sampling provide a well define local meteoric water line (collection at 400 m asl). Moreover, two other LMWL were established, at 770 m and 1100 m to quantify spatial and altitudinal changes.

Cations and anions content of springs are enriched regarding precipitation compositions (few mg/L), and the chemical content refers to low temperature reactions. Total dissolved ions range between 30 mg/L and 130 mg/L. Few alkalinity values were measured, from 1 to 7 mg/L as bicarbonate alkalinity, but there is no clear evidence that they match real values, sulphate content being higher. Ionic mass balance, based on pe redox equilibrium, were made using PhreeQC [1] and appears to be good for half of the springs (< –10%). The other half gives in first approach bad values, leading to break in the ammonium ion. Such NH_4^+ content might be related to agricultural impact. Inverse modelling suggests interaction with minerals such as kaolinite, chlorite, K-feldspar, underlining reactions between percolating water and altered granites.

From rainwater isotopic records, altitudinal variations are too small to modify both slope and D-excess of the LMWL. So the monthly mean of three years record is taken as representative of local rains and leads to $\delta D=7.4\delta^{18}O+3.8$ ($r^2=0.96$). During the year 2003 occurred a 40% decrease of pluviometry / mean annual pluviometry: high isotopes values recorded for these summer months lead to a depletion of –0.4 for the slope and 3.5‰ for D-excess. This may affect stable isotopes values for very near surface aquifers, and was slightly detected regarding sampled springs.

Stable isotopes ratios measured on those springs show no clear annual cycle: winter months are not always associated with depleted ratios. Maximum variations are ± 1‰ for $\delta^{18}O$ vs SMOW and ± 10‰ δD vs SMOW. Using isotopes ratios, these springs show an alignment along lines parallel to the LMWL, showing that they experiment little altitude and temperature gradient modifications along their flow path and that they infiltrate at heights ranging between 100 to 300 m above their outlet.

Modelling residence times in such aquifers was estimated using FlowPC [2] and O, H isotopes ratios. Two ways were examined: first taking the real precipitation input and second using elevated springs percolating downward. The first approach provides no good fit, despite an estimation of the evapotranspiration effect was taken into account (using Turc's formula). Soil effects (P_{CO2}) on $d^{18}O$

isotopic composition seem to have first order importance ($\delta^{13}C_{DIC}$ from –16 to –22‰ PDB, clearly related to C3 plant composition) and are in progress to improve input parameters. The second set of calculation eliminates such hypothesis and provides better results: transit time of ca. 2 months using dispersion model and 20% of aquifer stagnant water (efficiency > 75%), in agreement with the unique 2003 drought for 3 months.

Coupling isotopic geochemistry and major ion chemistry appears to be a good way to access surficial fluid circulation in small water catchment. Recharge areas can be located at c.a. 200 to 300 m above spring discharge, and times of aquifer recharge can be estimated for each spring. The percolation of rainwater into soil and subsurface aquifers leads to poor-content waters, that experiment little chemical interactions with surrounding rocks (granitic bearing) before discharge.

REFERENCES

[1] PARKHURST, D.L., APPELO, C.A.J., User's guide to PHREEQC (Version 2) - a computer program for speciation, batch-reaction, one-dimensional transport, and inverse geochemical calculations: U.S. Geological Survey Water-Resources Investigations Report **99-4259** (1999) 312 pp.

[2] MALOSZEWSKI, P., ZUBER, A., Lumped parameter models for interpretation of environmental tracer data. Manual on Mathematical Models in Isotope Hydrogeology, IAEA-TECDOC-910, IAEA, Vienna (1996) 9-58.

[3] FOURNIER, R.O., POTTER, R.W. II, An equation correlating the solubility of quartz in water from 25°C to 900°C at pressures up to 10 000 bars, Geochim. Cosmochim. Acta **46** (1982) 1969-1973.

Integrated forecast system atmospheric – hydrologic - hydraulic for the Urubamba River Basin

Metzger, L., M. Carrillo, A. Diaz, J. Coronado, G. Fano

Peruvian National Weather Service,
Lima,
Peru

During the months of December to March, Perú is affected by intense precipitations which generate every year land slides and floods mainly in low and middle river basins of the western and Eastern of the Andes, places that exhibit the greatest number of population and productive activities. These extreme events are favored by the steep slopes that characterize the Peruvian topography.

For this reason at the end of year 2000, SENAMHI began the design of a monitoring, analysis and forecast system, that had the capacity to predict the occurrence of adverse events on the low and middle river basins of the main rivers such as Piura river in the north of Peru and the Rimac river in the capital of the country.

The success of this system opened the possibilities of developing similar systems throughout the country and extend to different users or sectors such as: energy, water management, river transport, etc. An example of a solution prepared for a user (the gas extraction company Pluspetrol) was the implementation of a river level forecasting system in the Urubamba river to support river navigation in this amazonic river where water level variability turns risky the navigation during the dry season. The Urubamba catchment higher altitudes are famous because of the presence of the Machupicchu ancient city, downslope this city is characterized by the Amazon rainforest with scarce observation stations for water level and rainfall. A very challenging modelling and operational hydrology enterprise was developed.

The system implemented for the Urubamba river consist on running the atmospheric part of the global climate model CCM3, this model inputs Sea Surface Temperature forecasts from NCEP-NOAA. The global model was set on a T42 (300 km) grid resolution, this information was used as initial and boundary conditions for the regional model RAMS which provided a downscaled 20 Km grid resolution having as results daily precipitation forecasts.

Besides the global climate model a statistical forecast was developed using Empirical Orthogonal Functions (EOF), this methodology uses the Long Wave Radiation as a predictor for the precipitation occurrence in the study area. This model is based on an atmospheric-ocean teleconnection El Niño 3 region in the central tropical pacific and the observed rainfall over the Andes.

The information generated by the atmospheric model was used as input for the Sacramento hydrologic model originally developed by the National Weather Service River Forecast System (NWSRFS) which considers all the historical data (precipitation, flows and evapotranspiration), the model considers a perturbation in the form of a random variable which depends on the standard deviation and the mean, this algorithm allows to have not only one precipitation time series but the double or triple.

This is the basis on the hydrologic ensemble forecasting where each precipitation time series generates a flow time series and then using post processing codes we find the probabilistic forecasts of non excedance for different percentage of probability.

Finally the hydraulic model used was the HEC-RAS V.3.1 developed by the U.S Army Corps of Engineering which used all the cross sections available in the zone, manning values, contraction and expansion coefficients to convert the forecasted flow data into water level of the Urubamba river in four check points requested by the user: Malvinas, Nuevo Mundo, Sepahua and Maldonadillo.

SENAMHI provided of useful information for 2 years and was the result of a multidisciplinary systemic work that joined meteorologists, hydrologists, climatologists and system engineers. The information used by the Regional numerical model RAMS was assimilated from geostationary satellite GOES 8 and automatic stations located in strategic points considering the topography, accessibility, security, extreme rainfall conditions and consequent variability in the levels of the Urubamba river.

As a conclusion the work developed in the Urubamba river involves the ocean-atmosphere-hydrosphere interaction for generating precipitations and water levels in a virgin jungle basin in which has been established a hydrologic and hydraulic modelling system to give support and information to the river navigation in Amazonia.

Magmatic origin of CO_2 in the Surdulica Geothermal System

Miljevic, N., D. Golobocanin, A. Zujic

Vinca Institute of Nuclear Sciences,
Belgrade,
Serbia and Montenegro

The Surdulica geothermal aquifer, a complex granodiorite-granite system, situated in southeastern Serbia was hydrogeologically and geochemically studied using environmental isotopes [1]. The wide range of carbon isotopic compositions shows a complex carbon origin [2]. Cold water recharges under closed-system conditions with initial parameters, $\delta^{13}C$ = -27 ± 3‰ (regional organic carbon), pH_i = 5-6 reaching a value of –13‰ for $\delta^{13}C$ at the discharge. The concentrations of ^{13}C in geothermal water are significantly higher (up to 0‰), which indicate processes of intensive interaction between water and rocks (carbon mineral dissolution), isotopic exchange, and possible interior CO_2 source(s) (CO_2 liberated by thermal metamorphism of carbonate rocks and/or from the mantle). Since limestones have $\delta^{13}C$ values close to zero, it would be expected that on decarbonation the limestones would give off CO_2, with $\delta^{13}C$ values of about 5.0‰. However, most of the CO_2 sampled in studied geothermal area has negative $\delta^{13}C$ values (average about –1 to –5‰). This CO_2 can hardly be expected to be simply derived from the decarbonation of limestones. The aim of this paper was to estimate the contribution of deep-mantle CO_2 reservoir to hydrothermal system under investigation.

The $\delta^{13}C$ and $\delta^{18}O$ values of collected borehole rocks (granodiorite, amphibolites schist, granite, depth 104–999 m) and random surface marble samples gathered in two groups (Fig. 1). The first group is characterized with pretty uniform values close other carbonatites complexes (calcite, dolomite) world-wide [3] and close to most commonly observed mantle compositions ($\delta^{13}C$ = -5.0 to –7.0‰ and $\delta^{18}O$ = 5.0 to 8.0‰). The second one showed wide range of $\delta^{13}C$ values with very high $\delta^{18}O$ values.

Calculated value for dissolved CO_2 in the basin of 46 g/L and $\delta^{13}C$ between –4 and –5‰ in thermal waters cannot be explained solely by calcite and dolomite dissolution. We establish simple isotope mixing model for calculation of magmatic contribution of CO_2 in thermal waters according to relation

$$\delta^{13}C_{bicarbonate} = x\delta^{13}C_{mantle} + (1-x)\delta^{13}C_{calcite}$$

where x is the mole fraction of magmatic component. Using the average values for $\delta^{13}C_{bicarbonate}$ = -3.5‰ in thermal waters and carbon isotopic concentration of calcite ($\delta^{13}C_{calcite}$ = -3‰) and mantle ($\delta^{13}C_{mantle}$ = -6‰), the mantle CO_2 fraction has been estimated to be 20% under assumption that input amount of CO_2 in shallow cold water is negligible in respect to its deep source. A presented approach could be used as a preliminary investigation tool due to the more sophisticated open/closed-system models.

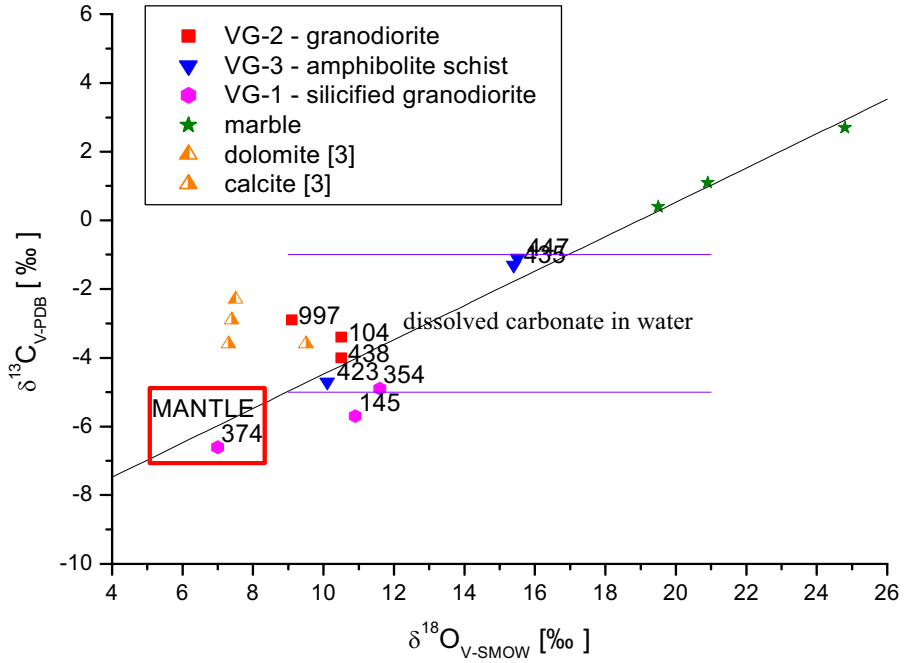

FIG. 1. Carbon and oxygen isotopic composition from borehole rocks (with indication of the depth) and random marble samples in the hydrothermal system Surdulica.

REFERENCES

[1] HADZISEHOVIC, M., DANGIC, A., MILJEVIC, N., SIPKA, V., GOLOBOCANIN, D., Geothermal-Water Characteristics in the Surdulica Aquifer, Ground Water **33** (1995) 112-123.

[2] HADZISEHOVIC, M., MILJEVIC, N., SIPKA, V., GOLOBOCANIN, D., POPOVIC R., Isotopic Analysis of Groundwater and Carbonate System in the Surdulica Geothermal Aquifer, Radiocarbon **35** (1993) 277-286.

[3] RAY, J.S., RAMESH, R., PANDE, K., Carbon Isotopes in Kerguelen Plume-Derived Carbonatites: Evidence for Recycled Inorganic Carbon, Earth Planet. Sci. Lett. **170** (1999) 205-214.

An oxygen isotope study in a lake-river system in Southern Finland

Sonninen, I.[a], E. Huitu[b], S. Mäkelä[b], L. Arvola[a]

[a] University of Helsinki,
Radiocarbon Dating Laboratory,
Finland

[b] University of Helsinki,
Lammi Biological Station,
Finland

The project "Nutrients from river basins – experimental and modelling approach" (NUTRIBA) is part of the Baltic Sea Research Programme (BIREME). The programme started in 2003 and runs for three years. The drainage basin of the River Kokemäenjoki in southern Finland running to the Baltic Sea is selected for study. The River Kokemäenjoki basin is the fourth largest water system in Finland with a total surface area of 27 000 km^2 and an average discharge of 230 m^3s^{-1}.

In connection to the larger research in the Kokemäenjoki river system stable isotope studies are carried out in a selected lake-river chain in the upper part of the water system. The site selected for study comprises of five lakes forming a chain. In addition to having a different hydrological position the lakes vary in their trophic status and the size of their drainage areas varies more than one order of magnitude. The theoretical residence time ranges from 0.1 to about 3 years. The surface area of the lakes varies from 1 to about 31.5 km^2, the catchment area from 116 to 1171 km^2, and the water volume of the lakes from 1.6 to 247x10^3m^3.

Water was sampled for isotope studies from the lakes at two depths and their in- and outlet river channels every second week during the ice free period and monthly during the ice covered period. The results from lake water samples collected during the first year show higher $\delta^{18}O$ values than those of regional mean precipitation and different degree of evaporation. Stratification formed in the deeper lakes and turn-over in spring and autumn were traced.

Variations of $\delta^{18}O$ values in lake waters during April-November ranged from c. 1 to 2‰ (Fig. 1). Mean seasonal variation found in $\delta^{18}O$ for the regional precipitation is 4-5‰.

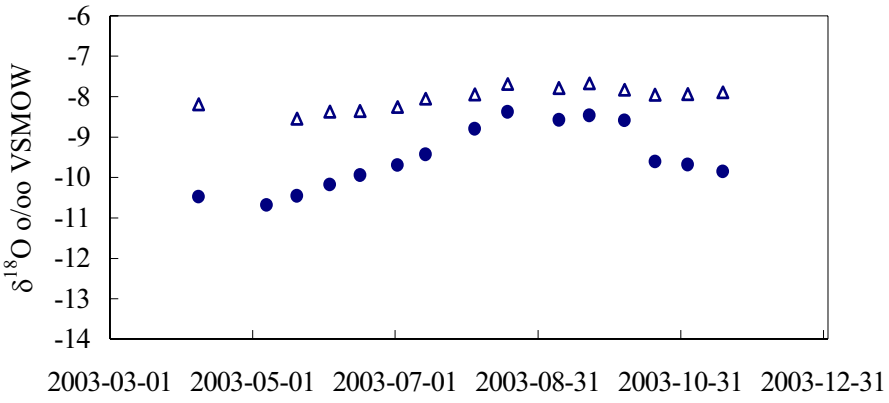

FIG. 1. Variations in $\delta^{18}O$ in surface (at 1 m depth) waters of two lakes, Lehee (●) and Iso-Roine (Δ), during sampling period from April to November 2003. Lehee is a small shallow through-flow lake and Iso-Roine the largest in the studied set of lakes.

Application of environmental isotopes of hydrogen (^{3}H), carbon (^{13}C & ^{14}C) and oxygen ($^{16}O/^{18}O$) in studies of groundwater-streamflow interactions

Stone, G., G. Jacobsen, C. Hughes, R. Szymczak

ANSTO Environment,
Menai NSW,
Australia

A current major effort in Australian water management is the conjunctive management of hydraulically connected Groundwater and Surface water systems, to provide the maximum benefit to water stakeholders. In particular Australia has a legislative limit on the amount of surface water that can be utilised in a particular catchment, but that is not the case for Groundwater, leading to tension amongst users in connected systems.

Groundwater and streamflow samples were collected during several studies in the Bega Valley and Murray-Darling Basin, NSW [1, 2]. Streamflow was sampled using a plastic bailer while groundwaters were withdrawn with the use of a Grundfos MP1 environmental sampling pump. They were analysed for stable isotopes ($^{2}H/H$, $^{18}O/^{16}O$) ratios, tritium (^{3}H), radiocarbon (^{14}C) and major and minor chemical species. Rainwaters were collected and analysed for stable isotopes only. Previous tritium in precipitation data were also utilised (Fig. 1). Ion Chromatography was used for the analysis of the anions while either ICP-MS or ICP-AES was used for cations. The tritium analysis was carried out by standard procedures of electrolytic concentration and liquid scintillation counting [3]. Analysis of the water samples for deuterium was conducted by CSIRO, Isotope Analysis laboratory using the zinc reduction method and a VG Isogas mass spectrometer (error; ± 0.8 per mil). Radiocarbon in groundwaters are measured using accelerator mass spectrometry (AMS). The water samples are filtered to 45 μm prior to CO_2 collection. Dissolved inorganic carbon (DIC) is separated by acidifying the water samples with 85% phosphoric acid, the resulting CO_2 is collected by sparging with He for 15 mins and cryogenic trapping. The CO_2 is purified by heating overnight to 600^{o}C in the presence of Ag wire. Graphite targets are then prepared by the reduction of the CO_2 using H_2 with an Fe catalyst at 600^{o}C. The resulting graphite/iron mix is measured in the ANTARES 10MV Tandem Accelerator. The determination of oxygen-18 was conducted at the University of Wollongong using the CO_2 gas equilibration method, purified using a Micromass Multiprep Unit and measured on a Micromass Prism III (error; ± 0.1 per mil).

A plot of tritium activity versus borehole location and depth (Figure 2), indicates that the Brogo River (Bega Valley, NSW) is not recharging the adjacent alluvium since the tritium is much lower than in the streamwater. The Bega river however is recharging the adjacent alluvium, both above and below its confluence with the Brogo river, since tritium values are similar in stream and alluvium.

Isotopes such as the stable and radioactive isotopes of water and carbon are particularly appropriate for the study of these connected water systems, providing a clear method of determining the source of groundwater, and hence the extent of mixing of nearby surface water (such as the local river), and the time frame for the mixing process. In particular the stable isotopes 2-H, 18-O, and 13-C provide a robust end-member analysis for the hydrographic separation of regional groundwater and any amount of river water which was replenished at a remote location; while the radioactive isotopes 3-H and 14-C are used to confirm the presence in groundwater of (isotopically modern) surface water, but also accurately determine the apparent rate of mixing at particular distances from the river.

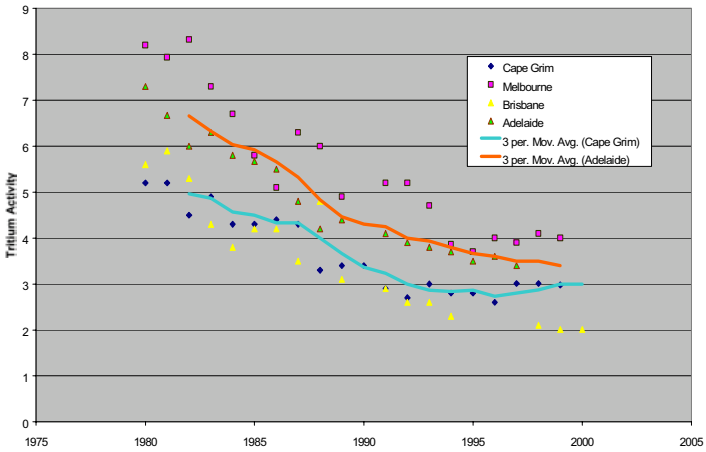

FIG. 1. Tritium in precipitation at selected stations in Southern Australia, 1979-2000.

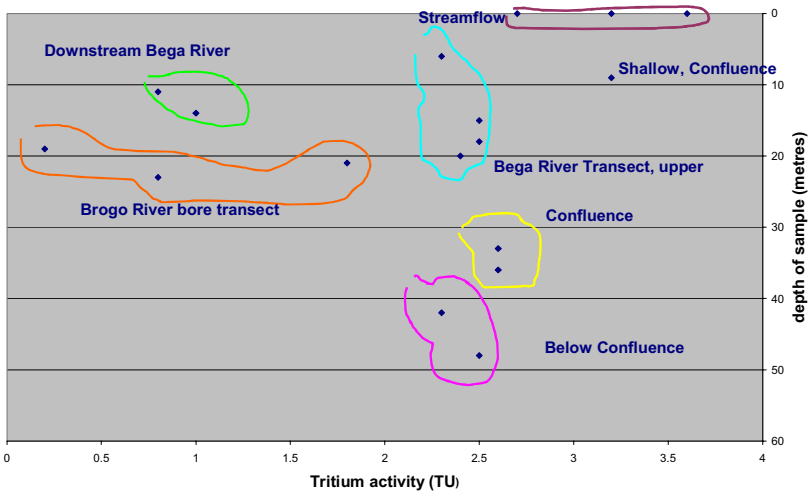

FIG. 2. Plot of tritium activity versus depth of sample for groups of bores in Bega Valley, NSW [1].

REFERENCES

[1] STONE, D.J.M., THOMAS, M., RUSSELL, G., Investigation of Groundwater-Streamflow interactions in the Bega alluvial aquifer using Tritium and Stable Isotope ratios (Proc. 4th Aust. Nuclear Assoc. Conf. on Nuclear Science and Engineering in Australia, Oct 2001) Sydney, Australia, (2001) 191-196.

[2] STONE, D.J.M., Streamflow-Groundwater interactions in the Murray Darling Basin determined by Tritium, 14-C and stable isotopes (Proc. 2004 Robertson Workshop on Environmental Geochemistry and Geochronology: Quaternary Chronologies Apr/May 2004) Ranelagh House, Robertson NSW (2004) 7.

[3] CALF, G.E., SEATONBURY, B.W., SMITH, L.W., The Measurement of Natural Levels of Tritium in Water (1975) AAEC /E373.

GROUNDWATER-SEAWATER INTERACTIONS

Measurement and potential importance of submarine groundwater discharge

Burnett, W.C.

Department of Oceanography,
Florida State University,
Tallahassee,
United States of America

While the major rivers of the world are reasonably well gauged and analyzed, thus allowing comparatively precise estimates of riverine inputs to the ocean, it remains very difficult to evaluate the influence of direct groundwater discharge into the ocean. In spite of the recognition that many land-sea interfaces of the world are characterized by "leaky" continental margins, it is unclear how important groundwater-derived springs and seeps are in terms of overall marine geochemical budgets.

The principal reason that groundwater estimates have not attained the precision base that is typically achieved of other oceanic inputs is that the direct discharge of groundwater into the coastal zone is inherently very difficult to measure. Concerted efforts are required to improve this situation by integrated application of hydrological and oceanographic techniques. Standard hydrological and oceanographic methodological approaches are quite different and have rarely been systematically compared by following a systematic scientific evaluation process. Hydrogeologists and oceanographers are literally approaching the same problem from different ends. In order to develop the scientific and technical knowledge that will enable these issues to be addressed with a higher degree of certainty, the IAEA together with UNESCO (IOC and IHP) is conducting a collaborative program which includes carefully designed intercomparison experiments in different coastal environments in order to provide a standardized methodology for assessment of SGD. Many of the methods being assessed are based on naturally-occurring radioisotopes that act as tracers of SGD. An important aspect of our program is to disseminate the results widely, to coastal managers and other relevant parties, in the hopes that national authorities will encourage the scientific community to investigate these phenomena properly. Thus far, we have conducted intercomparison experiments in Florida (August, 2000; karst hydrogeology); Western Australia (November, 2000; coastal plain); Sicily (volcanic and karst; March, 2002); Eastern Long Island (May; 2002; glacial till); and Ubatuba, Brazil (fractured crystalline rock). Results have generally shown good agreement between direct seepage meter measurements and estimates made via geochemical tracers. The agreement with hydrogeological models, however, has been more spotty. This may be a reflection of the models not including consideration of transient processes, such as tidal pumping, that force water through near-shore sediments. Plans for next year include an SGD assessment intercomparison experiment in the Mauritius Islands, Indian Ocean. It is becoming recognized that oceanic islands display disproportionately higher amounts of SGD compared to many continental areas.

Assessment of groundwater-seawater interactions in the Aral Sea basin

Kontar, E.A.[a], A.T. Salokhiddinov[b], Z.M. Khakimov[b]

[a] P.P. Shirshov Institute of Oceanology,
Russian Academy of Sciences,
Moscow,
Russian Federation

[b] National University of Uzbekistan,
Tashkent,
Uzbekistan

Abstract. We simulated the groundwater dynamics in three different aquifers of the Aral Sea region. The convenient analytical approach based on the water level equation and its solutions is applied to the analysis of the water balance of the Aral Sea, which now consists of two independent seas – the Large and Small Aral, and its temporal changes due to natural processes and anthropogenic impact. The estimates made by this approach show that preservation of the Large Sea at a level that is quite close to the current one requires an additional discharge of not less than 7.6 km^3/year, which may be in principle achieved by effective water conservation technologies. However, the Large Sea, in its turn, is close to being divided into two unequal and completely independent eastern and western parts. This process will be accelerated by annual fluctuations of the Amu Darya water flow together with difference between water level rise and fall rates. Therefore, the preservation of the sea as an ecological system with reasonable water volume cannot be achieved without providing independent water inflow to the western part of the Large Sea.

1. Introduction

The territory of the Aral Sea Region is known as an ecological disaster zone. Health specialists have identified high and increasing mineralisation of potable water, and also the abundance of highly toxic pollutants (mainly pesticides) in water, air and food, which contribute to the deterioration of the population's health. It is now obvious that, in order to provide reasonable living conditions to the population, it is first of all necessary to drastically improve the quality of the water dedicated to human needs. Due to their intensive pollution by industrial wastes and by drainage waters from irrigated fields, the Syr Darya and Amu Darya rivers can no longer be considered as a source of safe and sustainable water supply. In such a situation, a number of scientists consider that the population's water supply must be achieved through a more comprehensive use of fresh and even subsaline groundwater resources. According to the data obtained during our work on the INTAS 1003/1014 projects in 2003-2004, the Aral Sea coastal aquifers, intruding seawater through the free connection to the sea is mixed with and measurably diluted by groundwater derived from land drainage. Hydrological changes associated with poor water management, climate change and desertification in the Aral Sea region put question marks on long-term submarine groundwater discharge (SGD) development and the possibilities for its modeling and quantification. In order to meet this objective, we used, extend, compare and combine SGD results from different site-specific numerical simulations of groundwater outflow, and associated seawater intrusion and re-circulation in coastal aquifers.

As it is well known, because of intensive water diversions from the Amu Darya and Syr Darya rivers for irrigation of newly developed lands in Central Asia, the Aral Sea has shrunk to one-third of its surface area and divided into two parts – the Large and Small Seas, fed separately by the Amu Darya and Syr Darya rivers, respectively [1-6]. The current runoff delivered by the Syr Darya seems to be enough to keep the Small Sea in a quasi-stationary state. However, the Large Sea level is still declining and soon may reach a critical state, after which it would be impossible to take any

reasonable action for preserving it as an ecologically viable system. This depends not only on the water volume delivered by the Amu Darya to the sea, but also on the peculiarities of the Aral Sea's relief. Because the Large Sea, in its turn, has already divided into two, nearly-isolated, parts – eastern and western, water comes to the western part only through the eastern. Hereafter for the sake of convenience they will be called the East and West Seas, respectively. Further water level decline will lead to complete isolation of the West Sea from the East Sea, as a result the former, which now has more water than the latter, may eventually loss almost all this water due to evaporation. Up to the present, in order to resolve different aspects (hydrogeological, economical, ecological, political, etc.) of the Aral Sea crisis, at least 300 projects have been proposed [1-5, 8], including those well-known ones that suggest restoring the Sea at the expense of Russian north-flowing rivers or the Caspian Sea. However, only a few of these proposed projects are in fact being carried out. These minimal responses to the Aral Sea situation explicitly or implicitly assume that the Aral Sea cannot be preserved. Activities now are geared toward diminishing the possible consequences of its shrinkage.

Meanwhile, unless the Aral Sea is preserved at a reasonable level, preferably close to the current level, the effects of these attempts will apparently be minimal. A pessimistic view of the possibility of preventing the Aral Sea from further decline is also caused by the fact that it is practically impossible to reliably estimate each constituent such as real water fluxes to and from the sea, underground water discharge, and evaporated water of the Aral Sea water budget. This is because of the circumstances of the sea, e.g. significant water loss at the Sea's delta, the number of meteorological stations has decreased and those left are now quite far from the sea-shore, etc. Therefore, conventional approaches for analysis of the water balance, that rely on absolute values of these constituents, are not adequate for reliable estimation of either the current state of the Aral Sea or its behaviour in the future. A more convenient and reliable way to do this is through use of an equation for water level changes that can be monitored directly over time by modern altimetry techniques.

This paper presents the water-level equation-based approach [7] and its application for the analysis of the water balance of the Aral Sea and its temporal changes due to natural processes and anthropogenic impacts. The second section describes this approach, namely the water level equation, its solution, as well as a number of related equations. The third section is devoted to analysis of the Aral Sea's state and future behaviour using this approach. The results and role of the East and West Seas in the water balance of the Large Sea are discussed in the fourth section. The last section summarizes the results and main conclusions.

2. Theoretical approaches based on the water level equation

Changes of water level, h, of any basin can be described by the following equation [7]

$$\frac{dh}{dt} = \frac{a}{S(h)} - b, \tag{1}$$

where a is the resulting water discharge rate from all sources (rivers, ground water, etc) except precipitation; b is the evaporation rate from the current basin surface area, S, reduced by precipitations to this surface. The first term on the right side of Eq. (1) describes the elevation rate of the water level, and the second one – its rate of fall; in some time periods, off course, precipitation may dominate evaporation, then $b < 0$. All parameters in Eq. (1) are time dependent. The parameters a and b are subject to variations with respect to the seasons and time of day. These variations are complicated due to the irregularity of precipitation, as well as due to anthropogenic impacts. The surface area of the basin implicitly depends on time through its dependence on the water level, and this dependence may be also complicated.

Thus, the differential equation (1), in spite of its simplicity at first sight, does not have a closed form solution with respect to h. Off course, such solutions can be found for some specially chosen model systems or this equation can be integrated numerically by step by step approach for a given time dependence of a and b and $S(h)$. However, in this work we will be interested only in approximate

analytical solutions of Eq. (1), which are applicable for any system and, therefore, are much more valuable then specific solutions.

Note that an equation similar to Eq. (1) can be written for water volume changes too. Such an equation is often used in approaches (see, for instance, [2,3]) to water balance estimations, but its solutions, to our best knowledge, have not been obtained. It is clear that, apart from their greater complexity, they are of little interest, because water volume change itself is a derivable quantity to be estimated roughly using water level, surface changes, and hypsometry.

In contrast, the left side of Eq. (1) is directly and reliably measurable quantity. Therefore, this equation and its solutions enable one to extract such information on the state and dynamics of a basin, which is not possible in the case of equation for water volume changes. In particular, actual values of the parameters *a* and *b* at a given time also can be recovered by inverse approaches, mapping theoretical curves (solutions of Eq. (1)) onto actual water level changes. In this respect, it is worthwhile to note that, in most cases, experimental estimations with acceptable accuracy are not possible for every water budget constituent. Furthermore, such estimations may not always derive from the same time period (or this period may be too long) to use them safely for the period of interest.

In order to obtain solutions of Eq. (1), we introduce the following approximations. First, the period of time under consideration can be divided into a number of time intervals (days, months, seasons, years) and values of the variables *a* and *b* can be considered to be equal to their mean values in the corresponding intervals. Such an approximation, the accuracy of which can be systematically improved by decreasing of the length of the time intervals, is quite reasonable given the great uncertainty in experimental values of the water budget constituents and their possible irregular temporal changes. From this point of view, numerical integration, mentioned above, will not have any advantage in accuracy.

Second, the real water basin can be replaced by a convenient mathematical equivalent, elementary volume, such as a cone, a paraboloid of revolution, etc, that allows one to obtain simple solutions of Eq. (1), as well as water volume changes using only water level changes. Clearly, a real basin cannot be replaced by a single elementary volume for the entire range of possible water level changes. Therefore, the basin must be divided into parts, each of which can be defined by volume with appropriate parameters. For an elementary cone that we denote as Cup-2, the surface area-water level relation is

$$S = kh^2, \tag{2}$$

where $k = \pi / \mathrm{tg}^2\alpha$, α is the angle between the base and directrice of the cone. For a hyperbolic paraboloid of revolution, Cup-1, this relation reads

$$S = kh_c h, \tag{3}$$

where $k = 2\pi$, and h_c^{-1} is the curvature of the corresponding parabola. For the sake of completeness we must include in this family, at least, a volume resembling a swimming pool with $S = \mathrm{const}$, Cup-0.

These three volumes (in the sequence of Cup-0, Cup-1, Cup-2) mathematically correspond to the first three terms of a polynomial series in *h* approximating *S*. If one retains two terms in this series, one gets (3) by choosing an appropriate reference point for *h*; this point marks the bottom of the volume described by (3). A three-term series can be reduced to (2) in a particular case. The general case and series with more terms lead to solutions of ever increasing complexity. We will not be interested in such solutions, because there is no need to obtain a single solution for the whole range of possible water level changes in a particular basin, which would be rather inconvenient to use and non-transferable from a given basin to others. Instead, we will divide a given basin into limited intervals based on its depth, where simple models like Cup-1 and Cup-2 will be quite satisfactory. As one can

see below in the case of the Aral Sea, these intervals are few and not too narrow. In fact, they will be appropriate during quite long time periods. It is probable that other seas and lakes also need few elementary volumes with appropriate parameters (k and kh_c), as well, for adequate mathematical description.

Eq. (1) can be rewritten as follows

$$\frac{1}{b_0}\frac{dh}{dt} = \frac{a_0}{b_0 S} - 1 \tag{4}$$

or, accounting for the surface area-water level relations (2) and (3), as

$$\tau \frac{dH}{dt} = H^{-n} - 1 . \tag{5}$$

Here H is the dimensionless water level

$$H = \frac{1}{b_0 \tau} h , \tag{6}$$

Where τ is the time constant of the water basin

$$\tau_{Cup-1} = \frac{a_0}{k h_c b_0^2} \text{ and } \tau_{Cup-2} = \sqrt{\frac{a_0}{k b_0^3}} \tag{7}$$

for models Cup-1 ($n = 1$) and Cup-2 ($n = 2$), respectively; a_0 and b_0 are the mean values of parameters a and b for the given time interval.

Solutions of Eq. (5) for Cup-1 and Cup-2 are [7]

$$H = 1 + (H_0 - 1)\exp(H_0 - H - T) , \tag{8}$$

$$H = 1 + (H_0 - 1)\frac{(H+1)}{(H_0+1)}\exp[2(H_0 - H - T)] , \tag{9}$$

respectively, where $T = t/\tau$ is the dimensionless time; H_0 is the water level at the reference time, $t = 0$. Note that for each set of parameters a_0, b_0, k (or kh_c) there is a particular stationary water level, where $H_0 = 1$, that is $a_0 = b_0 S$. If these parameters have changed due to climatic and anthropogenic factors, then $H_0 \neq 1$, and the water level will tend to a new stationary state corresponding to the new values of the parameters.

It should be stressed that the equations (8) and (9) do not explicitly depend on the parameters a_0, b_0, k (or kh_c). Fig. 1 presents typical universal curves for a number of values of H_0, which are applicable for any water basin. As seen from this figure, the time for reaching the stationary state depends on H_0, τ and the type of volume and approximately equals to 5τ and 3τ for Cup-1 and Cup-2, respectively. Solution of Eq. (1) for Cup-0 ($S = S_0 = \text{const}$) is trivial:

$$h = h_0 + (H_0 - 1) b_0 t; \quad H_0 = a_0 / b_0 S_0 . \tag{10}$$

Here, if $H_0 \neq 1$, water level persistently rises ($H_0 > 1$) or falls unless all water volume in the basin disappears ($H_0 < 1$). Note that the models Cup-1 and Cup-2 (Fig. 1), unlike Cup-0, are asymmetric with respect to water rise and fall. This means that water level moves from one state to another and

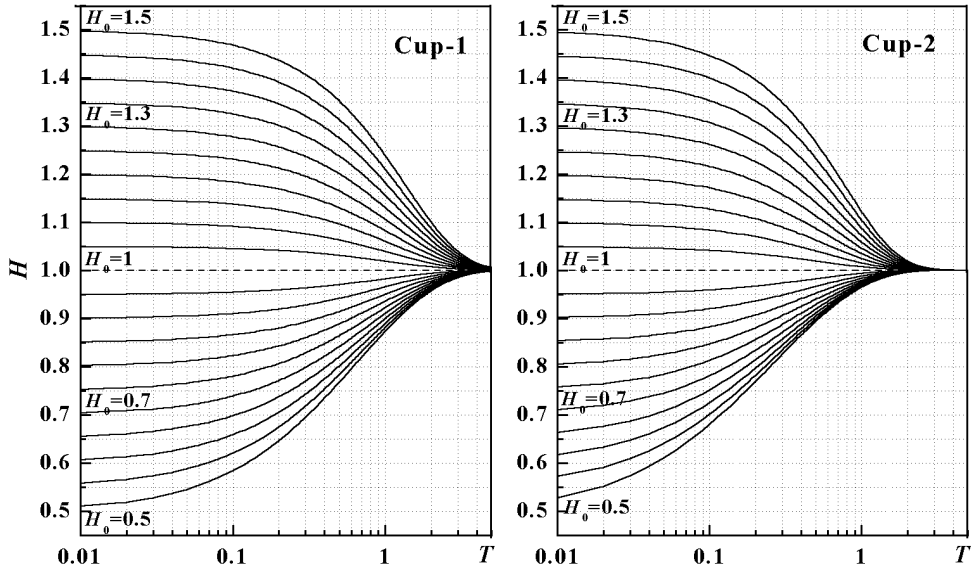

FIG. 1. Typical universal curves for predicting of water level temporal evolution for the water basin models of Cup-1 and Cup-2.

back in different time intervals; a water level rise takes more time than a fall of the same extent. Water volume change is $\Delta V(t) = \frac{kh_c}{2}[h^2(t) - h^2(0)]$ for Cup-1, (11)

$$\Delta V(t) = \frac{k}{3}[h^3(t) - h^3(0)] \text{ for Cup-2.} \quad (12)$$

Water deficit or excess for a given state of the basin can be obtained using known values of its surface and rate of water level variation as follows

$$\Delta a_0 = S(dh/dt + b_0) - Sb_0 = S(dh/dt), \quad (13)$$

which does not assume particular values of the water budget constituents or particular model of the basin.

The absolute value of the parameter a_0 is clearly

$$a_0 = b_0 S + \Delta a_0, \quad (14)$$

the uncertainty of which is defined by that of b_0. In principle, the parameter b_0 can also be recovered from water level changes.

Based on the current state and dynamics of the basin, the expected stationary water level, h_{st}, can be found from the following equation

$$h_{st} = h\left(1 + \frac{1}{b_0}\frac{dh}{dt}\right)^{1/n}. \quad (15)$$

The basin's time constant is related to h_{st}, $\tau = h_{st}/b_0$, and amounts to many years for realistic lakes and seas, because their level is much higher than the height of the water column evaporated during one year. However, from the fact that the evaporation rate varies not only during year, but also during the same day, one can conclude that water level never takes a truly stationary value, changing always around some value averaged over a quite long time period.

3. Conclusions

In summary, we have developed a convenient analytical approach for analysis of the water balance of basins (seas, lakes, and artificial water reservoirs) and their temporal changes, which is based on the water level equation and its solutions obtained by replacing the real basin by a set of elementary volumes with specified parameters. This approach has a number of advantages as compared to the usual approaches to water balance analysis. In particular, it enables one to avoid use of unreliable data or to estimate experimentally unavailable data from variations of water level.

REFERENCES

[1] GLAZOVSKII, N.A., Aralskiy krizis, Moskow, Nauka (1990).
[2] BORTNIK, V.I., CHISTYAEVA, S.P. (Eds), Aralskoe more, Leningrad, Gidrometeoizdat, (1990).
[3] CHUB, V.E., Izmenenie klimata i ego vliyanie na prirodno-resursniy potential Respubliki Uzbekistan, Tashkent, Glavgidromet RUz, (2000).
[4] UMAROV, U., KARIMOV, A.KH. (Eds), Vodnie resursi, problema Arala i okrujayushaya sreda (Tashkent, Universitet, 2000); MIRZAEV, S.SH., VALIEV, KH.I.. et al., Ekologicheskoe obosnovanie vedeniya selskogo i vodnogo khozyaystva, Tashkent, TIIIMSKH (2000).
[5] MICKLIN, PH.P., WILLIAMS, W.D., The Aral Sea Basin, NATO ASI Series, Partnership Sub-Series. Environment **12** Springer-Verlag (Proc. NATO Advanced Research Workshop, Tashkent, Uzbekistan, 1994).
[6] www-avico.cls.fr/html/applications/niveau/aral_uk.html; //www.dfd.dlr.de/app/land/aralsee.
[7] SALOKHIDDINOV, A.T., KHAKIMOV, Z.M., Uzb. J. Phys. **4** 3 (2001) 203-215.

Biogeochemical consequences of submarine groundwater discharge in the coastal ocean

Kim, G.[a], D.-W. Hwang[b], Y.-W. Lee[a], K. S. Park[b]

[a] School of Earth & Environmental Sciences,
Seoul National University,
Seoul,
Korea, Republic of

[b] Department of Oceanography,
Pukyong National University,
Busan,
Korea, Republic of

The nutrient inputs through the submarine discharge of fresh, brackish, and marine groundwaters may be comparable to the inputs through river discharge in the coastal ocean [1]. However, the biogeochemical influences of submarine groundwater discharge (SGD) in the coastal ocean are poorly understood. We present the biogeochemical and ecosystem changes in the coastal ocean due to the submarine discharge of nutrients in the South Sea of Korea.

We estimated SGD in a eutrophic semi-enclosed bay (Yeoja Bay) in the South Sea using radium isotopes (^{223}Ra, ^{224}Ra, and ^{226}Ra). The nitrogen, silicate, and radium concentrations in coastal groundwaters were in general much higher than those in seawaters offshore. Thus, the fluxes of new nutrients through SGD were higher than those through stream flow in this bay. This appears to result in the large input of excess nitrogen and silicate into the coastal ocean. In the offshore of this bay (red-tide areas), good correlations among ^{224}Ra, Si, and DIN (dissolved inorganic nitrogen) were observed, although phosphorus was almost completely depleted. Thus, the outbreak of red tides in this region seems to be due to the limited growth of diatoms under depleted DIP conditions, and the efficient utilization of DIN and DOP (dissolved organic phosphorous) by dinoflagellates. This case study indicates that nitrogen pollution in coastal groundwater and its subsequent discharge into the ocean may cause a significant ecological change that could trigger or facilitate harmful algal blooms.

In a volcanic island, Jeju, Korea, seepage rates were in the range 50-300 m/yr, which are much higher than those reported from typical continental shores. On the eastern shore of Jeju, almost all groundwater discharge is attributed to recirculating seawater, while fresh groundwater contributes about 20% of the total SGD on the western shore of Jeju. The measured radionuclides (^{228}Ra, ^{226}Ra, and ^{222}Rn) and nutrients in the groundwater suggest that the discharge of both fresh and recirculated seawater will have a significant influence on the economy of coastal nutrients and other chemical constituents in this region. This large discharge of natural chemical constituents appears to cause natural eutrophication in a semi enclosed bay of this volcanic island.

REFERENCES

[1] MOORE, W.S., Large groundwater inputs to coastal waters revealed by ^{226}Ra enrichments, Nature (1996) 612-614.

Contribution of environmental isotopes in the identification of groundwater salinization mechanisms in the Lower Tagus - Lower Sado Basin – Portugal

Carreira, P.M.[a], P.A. Galego Fernandes[b], D. Nunes[a], M.F. Araujo[a], M.O. Silva[b]

[a] Instituto Tecnológico e Nuclear (ITN),
Environmental Analytical Chemistry Group,
Sacavém,
Portugal

[b] Centro de Geologia,
Faculdade de Ciências da Universidade de Lisboa (FCUL),
Lisboa,
Portugal

Abstract. The role of environmental isotopes (δ^2H, $\delta^{13}C$, $\delta^{18}O$, ^3H and ^{14}C) in the identification of groundwater salinization mechanisms is discussed for the case of Lower Sado Basin in Portugal.

1. Introduction

The Lower Tagus – Lower Sado Basin is located in Setúbal-Lisbon region and represents an important water resource for a vast region. The highly populated urban and industrialized areas of Setúbal and Lisbon are supplied by this system, which has been extensively exploited over the last decades. In order to find out the source of salinization in the groundwater systems chemical (Cl^-, HCO_3^-, SO_4^{2-}, Ca^{2+}, Mg^{2+}, Na^+ and K^+) and isotopic analyses (δ^2H, $\delta^{13}C$, $\delta^{18}O$, ^3H and ^{14}C) were performed on groundwater samples collected in 39 boreholes. In the region under investigation there is a growing concern that these groundwater systems may be threatened by further exploitation (not controlled) due to mixing with the shallow aquifers (highly polluted), seawater intrusion processes in the coastal areas, or either by brine dissolution detected in depth by geophysical studies [1].

From the geological point of view the Lower Tagus – Lower Sado Basin is characterized by a synclinal structure composed by Tertiary sediments, mainly marine deposits. Three main groundwater systems can be identified in the region: a shallow quaternary aquifer constituted by alluvial deposits presenting high transmissivity values, underlied by the Pliocene and Miocene formations. Sandstones and limestones of marine origin related with different marine transgression and regression events compose the Miocene deposits. These deposits show an average thickness around 200 to 300 m, although in the central part of the basin these values increase up to 800 m. Fluvial terraces made of sands and clays represent the Pliocene layers (Fig. 1).

Geophysical studies performed in the region, reveal two important fault systems. The first located in the Lower Tagus valley with a N30ºE direction, and the other the so-called Setúbal - Pinhal Novo fault runs N-S and is responsible for a graben structure which allows the rising of a brine formation or ancient seawater trapped in the sediments (Fig. 2) [1].

2. Results and discussion

The hydrochemical evolution is characterized by a progressive increase in the total dissolved solids varying from 80 mgL^{-1} up to 2565 mgL^{-1} in the Pliocene aquifer while in the Miocene the mineralization varies between 200 mgL^{-1} to 7800 mgL^{-1}. In the central part of the basin, waters are used for public and agriculture supply, an increase of the water salinization was detected. The Cl^- and

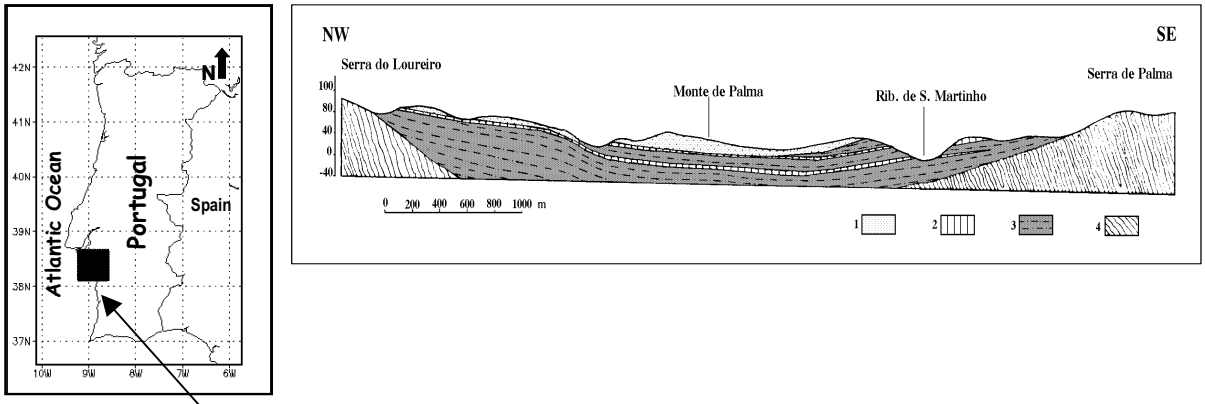

FIG. 1. Lower Tagus and Lower Sado basin cross section. (1) Silt-sandstone formation; (2) carbonate layers, marine Miocene; (3) sedimentary sequence of clay and sandstones (Miocene); (4) schist and greywacke (upper Devonian).

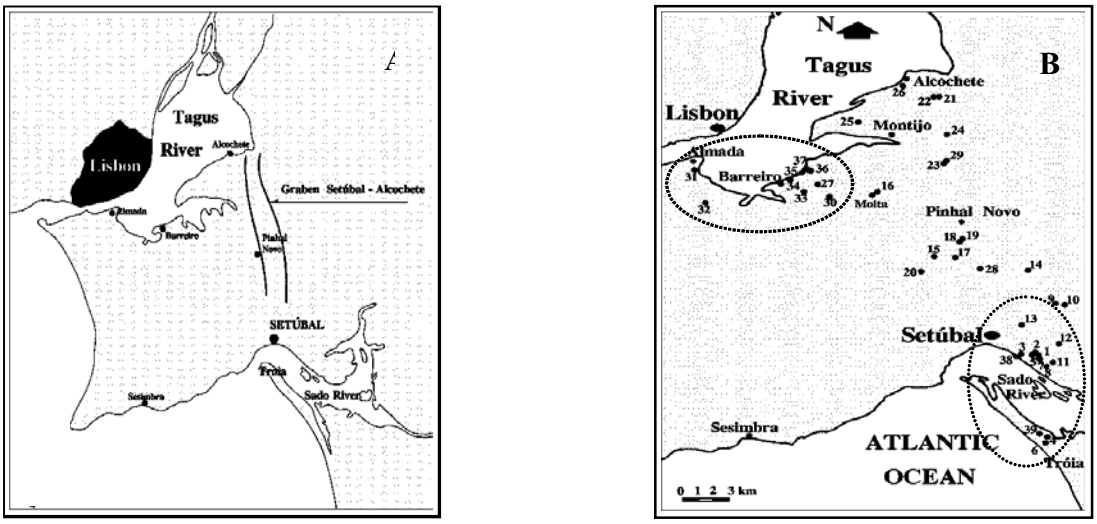

*FIG. 2. (**A**). Location of the graben structure detected in depth through geophysical studies. (**B**) Location of the sampled wells; two areas were identified with high increase of mineralization.*

Na^+ increase in the groundwater is most probably associated with the graben structure, responsible for the rising of the brine to minor depths. Two different evolution trends were identified in the ratio Ca/Na (Fig. 3): the first reflecting seawater mixing and the other with higher Ca content characterizing most probably the brine dissolution (Fig. 4).

No tritium was found in Miocene water samples. However in the shallow aquifer the ^3H content range from 1 to 3 TU. Radiocarbon was determined in 12 boreholes on the Total Dissolved Inorganic Carbon (TDIC). The range of values varies from 71.9 ± 0.7 pmc to 88 ± 0.8 pmc in the Pliocene, and from 2.9 ± 0.3 pmc to 45.6 ± 0.9 pmc in the Miocene.

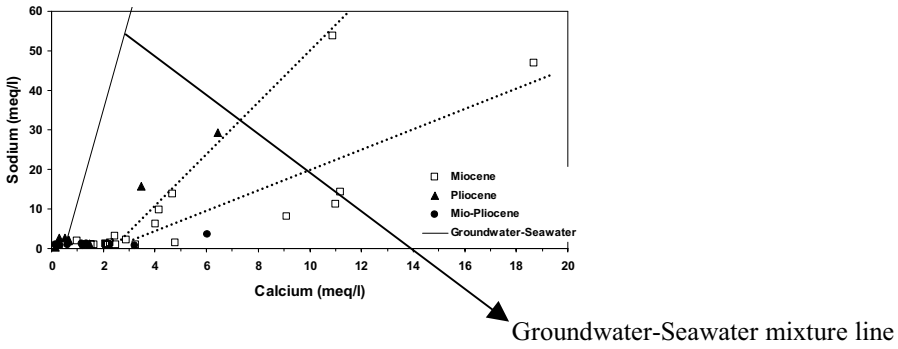

FIG. 3. Two different evolution trends were identified in the ratio Ca/Na. The groundwater samples with the highest mineralization are not plotted along the mixture line groundwater-seawater.

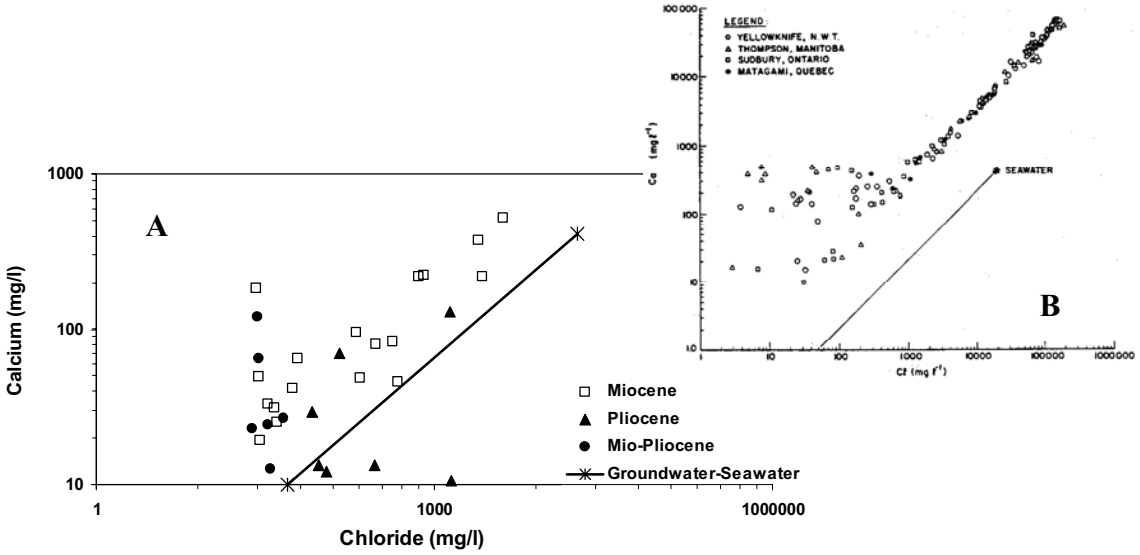

FIG. 4. Comparison between the Ca/Cl ratio of the groundwater samples from the Lower Tagus –Lower Sado Basin (A) with the Ca/Cl concentration in subsurface brines of Canadian Shield (Frape & Fritz [2].)

The apparent carbon-14 groundwater age was estimated using $\delta^{13}C$ values as correction factor (Table I) [3], and the apparent ages vary between modern (borehole 31 – sea water intrusion) and 25.4 ± 3.3 ka (borehole 3).

It is important to notice that all analysed water samples show a Saturation Index (SI) for calcite lower than –1.69, simultaneously the $\delta^{13}C$ measured in the TDIC of the groundwater samples is around $-10^{o}/_{oo}$. The observed relation, between the apparent carbon-14 groundwater age and the electrical conductivity or the Cl^- content, reveals an interesting pattern (Fig. 5). In fact, a dispersion of the borehole samples with the increase of salinization and apparent groundwater age can be observed, pointing out to brine dissolution mechanism (southern part of the basin) as the mechanism responsible for the deterioration of the water quality.

Table I. Apparent carbon-14 groundwater ages

Reference	Unit	E. Cond. (µS/cm)	$\delta^{13}C$ ($^{o}/_{oo}$)	^{14}C (pmc ± σ)	Apparent Age BP (ka)
3	Miocene	1636	-10.0	2.9 ± 0.3	25.4 ± 3.3
4	"	986	-12.1	5.9 ± 0.5	20.8 ± 2.9
31	"	1860	-10.5	45.8 ± 0.6	2.9 ± 2.6
38	"	2281	-10.0	10.8 ± 0.7	14.4 ± 2.9
39	"	919	-7.3	6.7 ± 0.6	16.1 ± 3.4
JK1	"	7650	-9.2	8.4 ± 0.8	15.9 ± 3.2
AC1	"	8010	-8.1	5.6 ± 1.2	18.3 ± 4.6
Frisado	"	3000	-10.4	12.9 ± 0.9	13.3 ± 2.9
5	Pliocene	4631	-17.9	88.1 ± 0.8	Modern
21	"	342	-17.6	71.9 ± 0.7	3.1 ± 2.3
27	"	2507	-10.0	85.6 ± 3.3	Modern
32	Mio-Pliocene	1112	-12.9	32.8 ± 0.5	7.2 ± 2.5

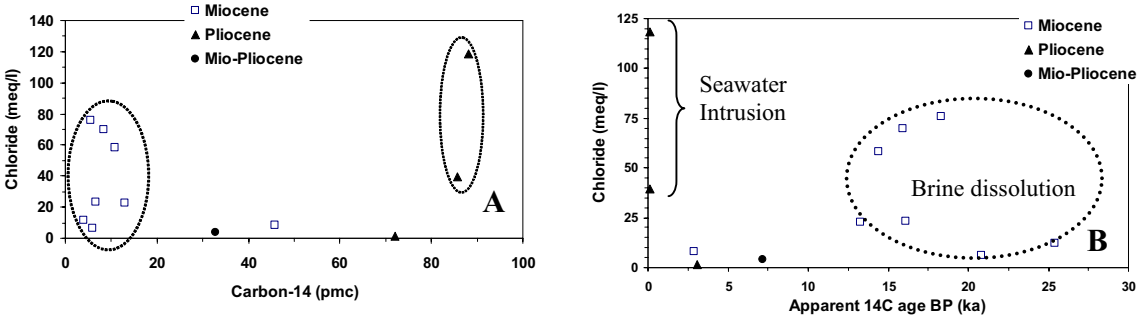

FIG. 5. Absence of a relationship between the increase of salinization and ^{14}C content in the southern part of the basin, point out to brine dissolution mechanism.

However, a different origin of the salinization was identified in Almada region (northern part of the basin): the results are pointing out to a recent seawater intrusion as the main mechanism responsible for the salts increase in the groundwater (Fig. 5B).

Small enrichment of about $2^{o}/_{oo}$ in deuterium and $0.2^{o}/_{oo}$ in oxygen-18 in Miocene groundwater samples was found, indicating that the recharge occurred under different climatic conditions (Fig. 6).

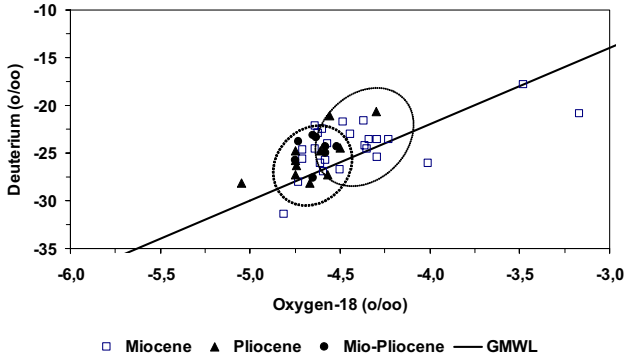

FIG. 6. $\delta^{18}O$ versus $\delta^{2}H$ of the groundwater samples from the Lower Tagus and Lower Sado basin. Small enrichment in heavy isotopes in Miocene groundwater samples.

REFERENCES

[1] ASTIER, J.L., Étude des resources en eaux souterraines de la Péninsule de Setúbal – Portugal. Geophysique – noveaux resultats de la prospection electrique, UNDP – UNESCO. Direcção Geral dos Serviços Hidráulicos 1979, Lisboa.

[2] APPELO, C.A.J., POSTMA, D., Geochemistry, groundwater and pollution, A.A. Balkema (1994) 6 pp.

[3] SALEM, O., VISSER, J.M., DRAY, M., GONFIANTINI, R., Groundwater flow patterns in the Western Libyan Arab Jamahiriya evaluated from isotopic data, arid-Zone Hydrology: Investigations with Isotope Techniques (Proc. Advisory Group Meeting), IAEA (1980) 165-179.

Salt water intrusion in aquifers of the south oriental coastal zones of Sicily

Aureli, A.[a], D. Fidelibus[b], A.M.G. Privitera[a], G.M.Zuppi[c]

[a] Palermo University,
National Group for the Defense from the Hydrogeological Catastrophes G.N.D.C.I.-C.N.R,
Palermo,
Italy

[b] Bari University,
Bari,
Italy

[c] Venice University,
Venice,
Italy

Abstract. The study of coastal aquifers deserves special attention in research and management of underground water resources. In this work we study the increase of salinity in coastal aquifers of south east Sicily, from Syracuse to Donnalucata, an area subject to intense overexploitation. Results of analyses of water samples collected in 2002-2004 in wells, springs and submarine springs are presented.

1. Introduction

Urban, industrial and agricultural developments in southern Sicily have provoked great environmental changes. Small fishing villages have become holiday resorts for large numbers of tourists. The petrochemical industry is contaminating coastal zones with organic compounds and heavy metals.

Thus, industry, agriculture and the tourist trade have increased the need for water. Thousands of wells have been drilled, thus depleting the aquifers and causing sea water intrusion into coastal aquifers up to about 10 km inland. Wells near the shore-line have been abandoned because of the presence of salt water [1]. The groundwater circulation follows a fractured drainage pattern over discontinuities constituted by bedding plans; the primary movement is vertical in unsaturated zones and horizontal in saturated zones [2].

On the coast, between Cassibile and Marina di Avola Rivers, numerous submarine springs were found in the past, evident testimony of discharge into the sea of deep aquifers. Recently these submarine springs have become smaller and only a few are visible, an example being the submarine spring near the source of the river Cassibile called “Balatone” (Fig. 1). The prevailing tendency in the Hyblean groundwater fluxes are springs observed in the sea and on the beach, at Marina di Avola (Fig. 1) and Donnalucata (Fig. 1). Their existence is due to the presence of a light covering of alluvial clays on the Ragusa Formation limestone. These springs have suffered from uncontrolled and irregular overexploitation of the underground aquifer in the hinterland. Their discharge has decreased and, in some cases they dry up for a few months each year. Their regime is conditioned by meteorological events that influenced aquifer recharge, and also water being drawn from the numerous wells [3].

FIG.1. Balatone, Tremoli and Donalucata springs.

All these phenomena and the decrease of a good part of the local water resources, triggered scientific investigations to better understand groundwater-seawater interactions in the region and to protect the remaining groundwater sources against salt-water intrusion.

Collaboration was established between the Italian universities of Palermo, Bari and Venice, and international agencies such as the IAEA and UNESCO. A project was developed with the main objective of studying the relationships between fresh water and seawater along the coast, with particular attention to the most qualified methodologies to probe and to improve the knowledge of hydraulic exchange phenomena, thermal exchanges, transfer of nutrients and contaminants from land to the sea, etc. Five zones with specific characteristics were selected in south-eastern Sicily, namely Zone A-Ciane; Zone B-Ognina; Zone C-Cassibile; Zone D-Avola; Zone E-Donnalucata (Fig. 2).

The area of this study is the Hyblean Plateau, primarily characterized by outcrops of carbonates and volcanites, connected to the tectonic activity in the zone from the Cretaceous to the Pliocene period. The presence of extensive aquifers directly connected to the sea, creates complex problems in the relationship between fresh water and seawater [4].

Research was carried out over three years (2002-2004) with periodic water sampling for analysis and geological, hydrogeological and geophysical controls. The differential time evolution study of submarine springs and wells water allowed to verify specific phenomena during the flood periods and shortage periods of the aquifer. As an example, chlorine concentration during June 2002 -March 2004 in Zone A - Ciane, in a spring and in two wells, is compared (Fig. 2).

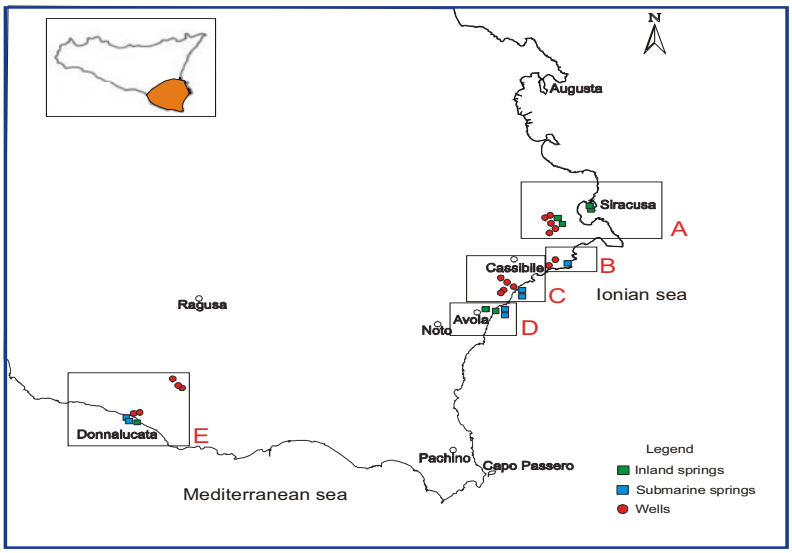

FIG. 2. Sampling zones.

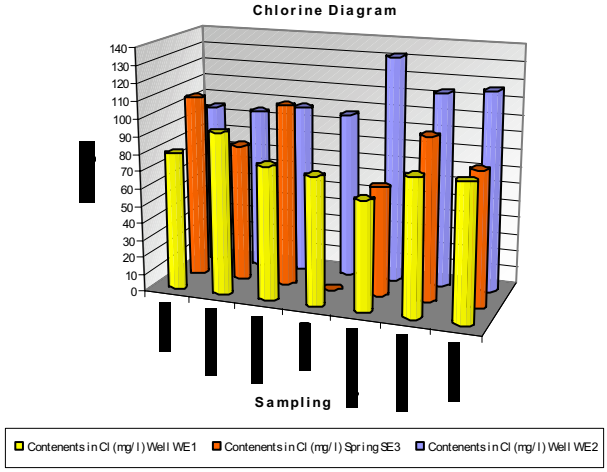

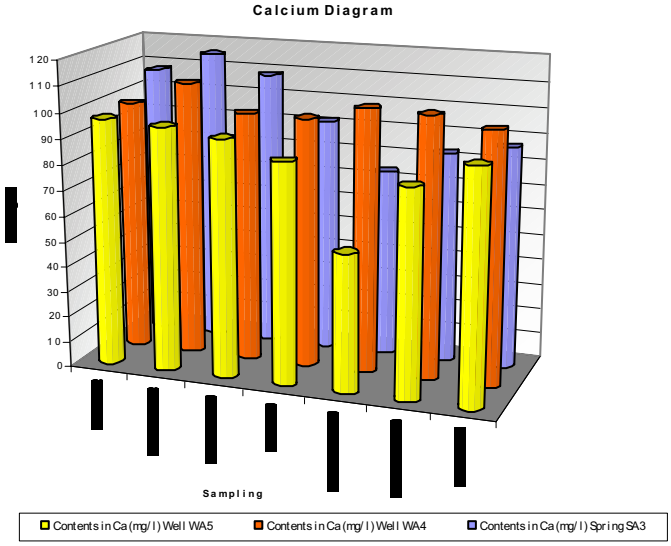

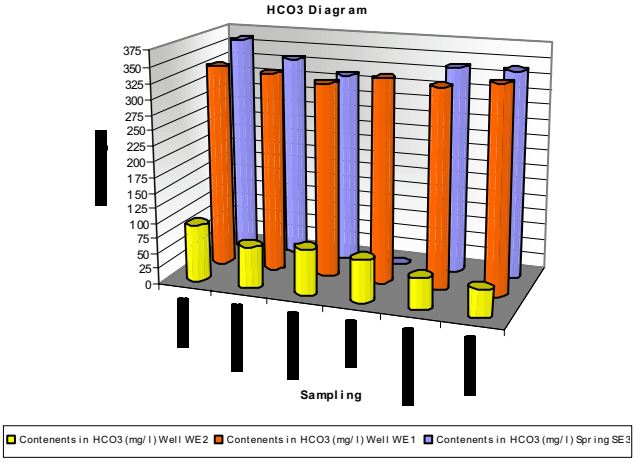

FIG. 3. Chlorine, Calcium and HCO_3 data.

In Spring SA3 and Well WA5 chloride evolution follows precipitation, increasing from June to October 2002, or during the arid and irrigation season. In September 2003, during an exceptional event, over 400 mm of precipitation fell during a period of a few hours provoking dilution of the chloride in water contained in Spring SA3 and Well WA5.

Although the two wells WA4 and WA5 are contiguous, the different chemical composition of their waters can only be explained by three-dimensional reconstruction based on the well stratigraphy and Vertical Electric Surveys [5]. The presence of a fault below quaternary coverage grounds facilitates underground flow of the infiltration water that in Well WA5. Well WA4 is influenced directly by salt-water intrusion (Fig. 2). Calcium, characteristic of the carbonate nature of the aquifer, is present. In the waters of spring SA3 and well WA5 the dilution effect of September 2003 rains is clearly observed, although in well WA4 salt-water intrusion prevails (Fig.3).

In well WE2 the exchange is almost negligible. Data allowed to follow the evolving salt water intrusion phenomenon in the coastal aquifer, to identify the preferential pathways of the salt water intrusion and to evaluate the risk. This aquifer, constituted by limestones, represents a fundamental element of the whole area, both where it is confined by upper pliocene material and where limestones outcrop and the aquifer is free [6].

The underground waters regime of this aquifer is very altered due to the uncontrolled construction of wells for drinking and irrigation water. The most negative effect resulted in the lowering of the piezometric levels. This has caused salt water intrusion up to 10 km from the coastline [7]. Many wells near the coast have become useless as sources of potable and irrigation water.

Considering the number of wells in the zone and the water quantities being subtracted, the quality of water contained in the deep aquifer has been negatively affected. The present work has allowed to disclose some interesting characteristics of salt-water intrusion phenomena and flow from the feeding basin to the depression caused by uncontrolled overexploitation.

REFERENCES

[1] AURELI, A., Esperienze e programmi di intervento in materia di ricarica delle falde, per contrastare l'intrusione marina in un acquifero carbonatico sovrasfruttato – IV Congresso di Ingegneria "Difesa e valorizzazione del suolo e degli acquiferi" Torino 10-11 Marzo 3, 1974 813-818 Ass. Mineraria Subalpina (1974).

[2] AURELI, A., Caratteristiche delle linee di flusso dell'intrusione marina influenzate dalla tettonica in area costiera ove gli acquiferi sono sovrasfruttati - Mem. Soc. Geol. Ital. n.37 Roma pp. 481-488 Publ. n.23 del G.N.D.C.I (1987).

[3] AURELI, A., Caratteristiche idrogeologiche e geomorfologiche di aree siciliane. Costiera del ragusano – CEMPA (1974).

[4] AURELI, A.,. L'influenza del carsismo ipogeo sulla morfologia e l'idrogeologia degli Iblei.Ragusa 14-16 Dicembre (1990).

[5] AURELI, A, GRIFEO, A. Salt water intrusion in a coastal aquiferf subject to overexploitation an to artificial recharge. 9th, Salt Water Intrusion Meeting, Delft May 1986-Delft Uniiversity of Tecnology (1986) 101-120.

[6] AURELI, A., CUSIMANO, G., CARRUBBA, S., DI PASQUALE, M., MAZZURCO, N., PRIVITERA, A.M.G., SILLUZIO, C., TOSTO, S., L'intervention des Organismes internationaux UNESCO-IAEA dans l'etude du programme de gestion du risque eau en pays semi-aride. Project Sicile, Colloque Franco Tunisien 21-22 May 2003 Tunis.

[7] AURELI, A, CARRUBBA, S., DI PASQUALE, M., MAZZURCO,N., PRIVITERA, A.M.G., SILLUZIO, C., TOSTO, S., Submarine Springs and salt water intrusion in fractured environment (Int. Conf. Groundwater in fractured Rocks 15-19 September 2003.)

Environmental isotope investigation of submarine groundwater discharge in Sicily, Italy

Aggarwal, P.K.[a], K.M. Kulkarni[a], P.P. Povinec[b], L-F. Han[c], M. Groening[a]

[a] International Atomic Energy Agency,
Vienna

[b] Marine Environment Laboratory,
International Atomic Energy Agency,
Monaco

[c] International Atomic Energy Agency,
Vienna

An important part of the continental water balance involves submarine groundwater discharge (SGD) [1]. Current estimates range from less than 10% to nearly 50% of the total riverine discharge into the oceans. As a result, SGD is increasingly being recognized as an important factor in the understanding and sustainable management of coastal freshwater aquifers in many areas of the world. In addition, SGD is a significant pathway for contamination of the near-shore marine environment from land-based activities.

Estimation of groundwater fluxes into the marine environment is complicated due to the fact that direct measurement is not possible by conventional means. Measurement of a range of isotopic tracers at the aquifer-marine interface provides the possibility to produce integrated flux estimates of discharge not possible by other non-nuclear methods. Within the framework of a coordinated research project of the IAEA and in cooperation with UNESCO, research work was initiated to develop isotope techniques for characterization of SGD. Together with the University of Palermo, Italy, the Sicilian coast was chosen for a pilot study based on various factors like availability of background information on geological setting, clear manifestation of SGD, local logistical support, and the Mediterranean Sea, which is a particularly vulnerable marine environment to fluxes of fresh and/or contaminated groundwater.

A reconnaissance sampling campaign was undertaken in 2001 and a few samples were collected and analysed for environmental isotopes. Twenty-three water samples from various sources like seawater, wells and springs were drawn in 2003 from different locations on the southwestern and southeastern parts of the Sicilian coast for isotope and chemical analyses. The samples were analyzed for ^{2}H, ^{18}O, $^{3}H/^{3}He$, ^{87}Sr, CFCs, etc. to better understand the submarine groundwater discharge process.

Figure 1 shows the plot of $\delta^{18}O$ versus $\delta^{2}H$ of Sicilian samples. Groundwater and some of the springs lie close to the Mediterranean meteoric water line with $\delta^{18}O$ values in the range of –4.5 to –6‰ (VSMOW). Coastal springs and wells, representing submarine groundwater discharge, have a value of about –2 to –3‰ $\delta^{18}O$ and fall on a mixing line between groundwater and seawater. These samples may consist of about 30 – 40% fresh groundwater, implying high submarine groundwater discharge in the coastal areas. Tritium content varies from 1.47 ± 0.24 to 4.08 ± 0.30. The residence time of groundwater in the limestone formations of Sicily, based on $^{3}H/^{3}He$ measurements and CFCs, is estimated to range from about 2 to 30 years.

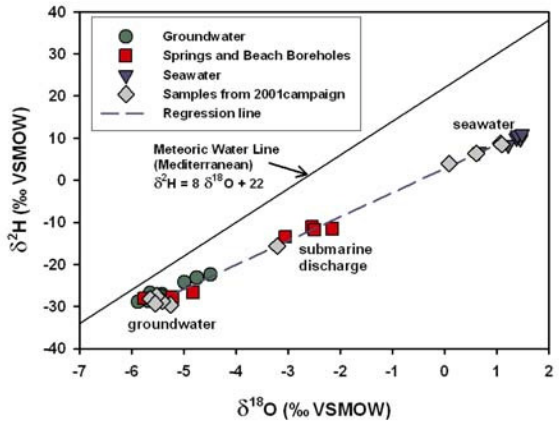

FIG. 1. Isotope studies suggest 30-40 % of fresh groundwater resource flows to sea as submarine groundwater discharge in Sicily.

ACKNOWLEDGEMENT

The Agency is grateful for the support provided to its Marine Environment Laboratory by the Government of the Principality of Monaco.

REFERENCE

[1] TANIGUCHI, M., et al., Investigation of submarine groundwater discharge, Hydrol. Process. **16** (2002) 2115-2129.

Radium isotopic tracers of submarine groundwater discharge into the Venice Lagoon

Garcia-Solsona, E.[a], P. Masqué[a], J. Rapaglia[b], H. Bokuniewicz[b], L. Zaggia[c], F. Collavini[c], J.K. Cochran[b], J.M. Zuppi[d], J.A. Sanchez-Cabeza[a], A. Beck[b]

[a] Institut de Ciència i Tecnologia Ambientals,
Universitat Autònoma de Barcelona,
Bellaterra,
Spain

[b] Marine Sciences Research Center,
Stony Brook University,
Stony Brook, NY,
United States of America

[c] Consiglio Nazionale delle Ricerche,
Istituto di Scienze Marine,
Venice,
Italy

[d] Dipartimento Scienze Ambientale,
Universita Ca Foscari de Venezia,
Venice,
Italy

Radium isotopes were used in conjunction with direct measurements to assess the discharge of groundwater across the northwest section of the Venice Lagoon floor about eight kilometers from the city (Fig. 1). This is an area of about 50 square kilometers of marshland dissected by channels. The lagoon sits atop a series of nine unconsolidated or semi-consolidated aquifers with a total thickness of about 1000 meters [1]. The surrounding land is of low relief, unlikely to support any substantial, water-table hydraulic gradient, but free-flowing artesian wells are found. Water samples for radium analysis were collected along three transects in May and June 2004. End-member samples were also collected in the Adriatic Sea, a nearby artesian well and two surface wells (near the Sile River) on the mainland. Over 250 direct measurements of submarine groundwater discharge were made over the course of nine months using benthic chambers vented to a plastic collection bag.

Up to two orders of magnitude of difference in short-lived radium (^{223}Ra and ^{224}Ra) activities were observed in surface waters. These values were comparable to those reported in coastal settings elsewhere where SGD has already been estimated [2]. Indeed, high activities were measured in a well sample from the marsh as well as in water collected from the benthic chambers. Enrichment was also observed in the artesian well. On the contrary, low levels of radium isotopes were determined in river, land wells and Adriatic waters. Overall, these results point to a substantial groundwater source to the lagoon. The surface water seems to be a mixture of at least four sources: the Adriatic, upward leakage from deep confined aquifers (the Artesian wells), near surface groundwater and rivers. A multiple end-member mixing model allows estimates of the contribution of each source. Direct measurements showed a high degree of variability with discharge rates ranging from five cm^3/cm^2/day to over 200 cm^3/cm^2.day. Higher discharge rates tended to be found deeper in the channels possibly where the channel cuts through a local aquitard. Nutrient analyses from the benthic chamber and ambient water samples show a concentration of ammonium in the seepage device water which is four to eight times

greater than that of ambient water samples. The average seepage device ammonium concentration was 325 ppb while it was 50 ppb in the ambient water. The circulation of groundwater through the marshes seems to be augmented with groundwater driven across the sea floor from deeper artesian aquifers that may be a significant source of ammonium to the lagoon. A second site in the industrial sector of the lagoon was also examined.

REFERENCES

[1] CARBOGNIN, L., GATTO, P., MOZZI, G., Guidebook to Studies of Land Subsidence due to Ground-Water Withdrawal, IAHS-AISH **121** (1977) 65-81.

[2] CHARETTE, M.A., BUESSELER, K.O., Submarine groundwater discharge of nutrients and copper to an urban subestuary of Chesapeake Bay (Elizabeth River), Limnol. Oceanogr. **49** 2 (2004) 376-385.

Hydrochemistry and isotopic characteristics of the submarine springs of south-eastern Sicily

Aureli, A.[a] , G. Barrocu[b], G. Cusimano[a], D. Fidelibus[c], L. Gatto[a], S. Hauser[d], M.A. Schiavo[d], L. Tulipano[e], G. M. Zuppi[f]

[a] Dipartimento di Geologia e Geodesia,
Università di Palermo,
Palermo,
Italy

[b] Dipartimento Ingegneria del Territorio,
Facoltà di Ingegneria,
Cagliari,
Italy

[c] Politecnico di Bari,
Bari,
Italy

[d] Dipartimento di Chimica Fisica della Terra (CFTA),
Università di Palermo,
Palermo,
Italy

[e] Facoltà di Ingegneria,
Università di Roma "La Sapienza",
Roma,
Italy

[f] Dipartimento di Scienze Ambientali,
Università Ca' Foscari di Venezia,
Venezia,
Italy

Karstic springs on Mediterranean environments are sensitive eco tops to hydrology in arid or semiarid areas and to paleohydrological changes during Holocene [1, 2]. Often these springs discharge below sea level, thus creating problems for a correct water resources management. A spectacular submarine spring row characterises the Southern Sicily offshore consisting of a wide carbonate plateau essentially formed by limestone and dolostones. Each single vent feature provides a unique opportunity to examine the onshore–offshore hydrogeologic processes, as well as point source submarine groundwater discharge. The marine carbonate of the Sicily Canal is one of the world's most productive aquifer systems. Parts of Sicily, Malta and other central Mediterranean islands almost entirely depend on this aquifer representing a reliable resource for municipal, agricultural and industrial water supply. The aquifer system in southern Sicily consists of interspersed limestone and dolomite strata. Impermeable beds confine the water-bearing zones under artesian pressure. Near the coast, Miocene and younger confining strata were eroded away, enabling direct hydrologic communication of carbonate ground water with coastal bottom waters. Mainland and offshore geology is illustrated by several geologic sections [3]. Groundwater is often under sufficient pressure. A relatively large volume of water is discharged from the aquifer system through terrestrial and

submarine springs, and this upward flow is expected to issue also along the seaward side of the land/sea margin, possibly even out to the shelf break. Groundwater, spring and seawater were analyzed for a suite of constituents that included major solutes (Cl, Na, SO_4, Mg, Ca, K, Sr, F, SiO_2), nutrients, select trace elements (Mn, Mo, Ba, U, V, Fe), and environmental isotopes (^2H, ^{13}C ^{14}C, ^{18}O). The upper gradient groundwater indicate a salinity of around 0.5 mSiemens, whereas the coastal groundwater depict a salinity higher than 1.5 mSiemens, which is a partial dilution by ambient seawater during advection/mixing.

Chemical data indicate that the meteoric waters mentioned above were at varying extents modified along the flow paths before issuing from terrestrial and submarine springs. Considering the consistency of individual water point water chemistry, the chemical interactions must approach chemical equilibrium or involve mineral reactions with very stable kinetics. Such chemical continuity is typical for groundwater with relatively long subsurface residence times. Waters discharging from these springs are presently at or near saturation with calcite.

Understanding the geochemical processes which lead to an increase in the TDS concentration of groundwater along the flow path and, for nutrients, to water pollution will enable better assessment and management of these coastal aquifers. At present, only some boreholes situated near the coast present significant fingerprint of marine intrusion.

In an attempt to identify the hydraulic connections between the various outlet points, groundwater was analyzed for stable and radioactive isotopes. The upgradient boreholes and springs are a mixture of present and older water on the basis of their relative low ^{14}C values (32.1 pmc). The older component contains an even lower amount of modern Carbon. However, the undersaturation of the mixture with respect to calcite, its high aqueous CO_2 content (up to 60 mg/L), and its enriched ^{13}C values (−1.8 to −3.1‰) suggest intensive water/rock interactions, which would contribute ^{14}C-devoid bicarbonates to the solution. Downgradient springs discharging along or below the Mediterranean coast contain groundwater contributions from higher altitudes, as evidenced by their depleted ^{18}O and D composition with respect to the local precipitation [4, 5] however, a larger portion of the recent water component could be contributed from direct precipitation on the carbonate.

The hydraulic behaviour of such a structure is obviously dominated by conduit flow conditions, i.e. fast flow and short groundwater residence time. The rapid flow conditions occurring in the infiltration zones, illustrated by tracing tests experiments, are the cause of the typically high time and space variability of their hydraulic and geochemical characteristics. Thus, these aquifers are relatively small, unconfined and characterized by groundwater residence times of years to tens of years. Consequently, these aquifers are fragile systems that respond rapidly to natural and anthropogenic processes. Groundwater quantities in these aquifers usually respond to short- and long-term climatic fluctuations influencing the amount of recharge and therefore the amount of groundwater available for use. Consequently, it is vital to understand processes influencing recharge to these aquifers more than discharge processes.

REFERENCES

[1] ANDREO, B., LIÑÁN, C., CARRASCO, F., JIMÉNEZ DE CISNEROS, C., CABALLERO, F., MUDRY, J., "Influence of rainfall quantity on the isotopic composition (^{18}O and ^2H) of water in mountainous areas", Application for groundwater research in the Yunquera-Nieves karst aquifers (S Spain), Appl. Geochem. **19** 4 (2004) 561-574.

[2] VANDENSCHRICK, G., VAN WESEMAEL, B., FROT, E., PULIDO-BOSCH, A., MOLINA, L., STIÉVENARD, M., SOUCHEZ, R., Using stable isotope analysis (D–^{18}O) to characterise the regional hydrology of the Sierra de Gador, south east Spain, J. Hydrology **265** 1-4 (2002) 43-55.

[3] CATALANO, R., DI STEFANO, P., SULLI, A., VITALE, F.P., Paleogeography and structure of the central Mediterranean: Sicily and its offshore area. Tectonophysics **260** 4 (1996) 291-323.

[4] CELLE-JEANTON, H., GONFIANTINI, R., TRAVI, Y., SOL, B., Oxygen-18 variations of rainwater during precipitation: application of the Rayleigh model to selected rainfalls in Southern France, J. Hydrology **289** 1-4 (2004) 165-177.

[5] LONGINELLI, A., SELMO, E., Isotopic composition of precipitation in Italy: a first overall map, J. Hydrology **270** 1-2 (2003) 75-88.

Groundwater inputs via ^{222}Rn and Ra isotopes off Ubatuba, Brazil

Burnett, W.C., R. Peterson, H. Dulaiova

Department of Oceanography,
Florida State University,
Tallahassee, FL,
United States of America

The principal reason that groundwater discharge estimates have not attained the precision that is typically achieved of other oceanic inputs is that the direct discharge of groundwater into the coastal zone is inherently very difficult to measure. Concerted efforts are required to improve this situation by integrated application of hydrological and oceanographic techniques. In order to develop the scientific and technical knowledge that will enable these issues to be addressed with a higher degree of certainty, UNESCO (IOC and IHP), together with the IAEA, has developed a 5-year program which includes intercomparison experiments in different coastal environments. An important aspect of our program is to disseminate the results widely, to coastal managers and other relevant parties, in the hopes that national authorities will encourage the scientific community to investigate these phenomena properly. We present here our isotopic results from the 3rd intercomparison experiment held in Ubatuba, Brazil November 16-22, 2003.

We used a combination of radioisotopic tracers (^{222}Rn and Ra isotopes) to estimate SGD fluxes and exchange rates during the Brazil intercomparison These tracers work because they display large concentration differences in groundwater relative to ocean water and behave conservatively (or nearly conservatively) in seawater. The short-lived radium isotopes (^{223}Ra and ^{224}Ra) are introduced near shore either by SGD or surface inputs and decrease away from shore as a result of radioactive decay and mixing. Since the decay terms are known precisely (the half-lives of ^{223}Ra and ^{224}Ra are 11 and 3.66 days, respectively), we can assess exchange rates by examination of the onshore-to-offshore distributions.

We measured the distribution of radon in the surface waters using a newly developed multi-detector radon system Three detectors were fed surface seawater from a submersible pump while being towed from a boat at an average speed of about 7 km/hr. Each detector is set to integrate counts over a 30-minute period and the detectors are run out of sequence by 10 minutes. Thus, a data point is recorded every 10 minutes. The results (Fig. 1a) show that there are definite areas of higher radon in the two embayments investigated. The highest area was along a rocky shoreline in the north central area of Flamengo Bay. We observed small springs in this area that consistently showed up as positive radon anomalies with lower salinities.

At the same time we were conducting the radon survey, we towed “Mn fibers” in a mesh bag behind the boat for periods of 30-40 minutes for determination of radium isotopes. The results for the ^{224}Ra/^{223}Ra activity ratio (Fig. 1b) show that there is a systematic trend from high ratios near shore and steadily decreasing ratios as one moves offshore. We consistently measured high ratios (~25) in the same area of north central Flamengo Bay where the high ^{222}Rn activities were observed.

The radium isotopic results may be used to estimate residence times of the water, assuming that the radium enters into the coastal waters with a constant isotopic composition:

$$\left[\frac{^{224}Ra}{^{223}Ra}\right]_{obs} = \left[\frac{^{224}Ra}{^{223}Ra}\right]_{i} \frac{e^{-\lambda_{224}t}}{e^{-\lambda_{223}t}}$$

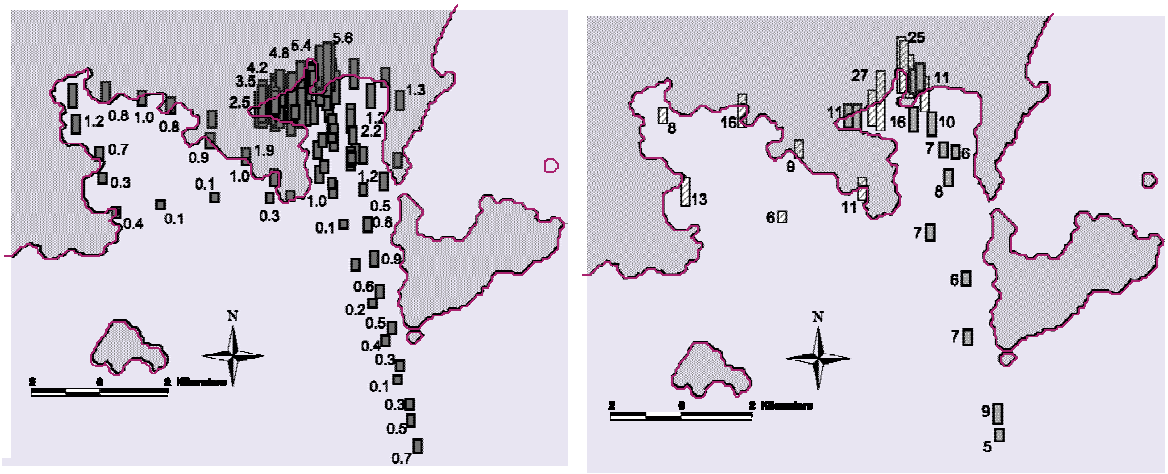

FIG. 1. Distribution of ^{222}Rn (left, dpm/L) and the $^{224}Ra/^{223}Ra$ activity ratio in surface waters off Flamengo Bay.

where $[^{224}Ra/^{223}Ra]_{obs}$ and $[^{224}Ra/^{223}Ra]_i$ represent the observed and initial activity ratios of the radium source water. Based on an initial activity ratio of 27 (the highest measured in Flamengo Bay) and a ratio of 5.3 near the end of our transect line at approximately 10 km offshore, we estimate a residence time of approximately 12.6 days.

We estimated SGD rates from continuous measurements of ^{222}Rn at a fixed location within the interior portion of Flamengo Bay. Net ^{222}Rn fluxes were determined by evaluating the change in inventories over each measurement interval after making appropriate allowances for tidal fluctuations and atmospheric evasion. Mixing with offshore waters is also accounted for and is estimated based on inspection of the calculated radon net fluxes or independently by use of short-lived Ra isotopes. The estimated SGD rates ranged from 0-15 cm/day and showed a similar pattern as seen by automated seepage meters that were also deployed in the area. It is clear from these results that the advection of pore water fluids across the seabed is not steady state but episodic with a period that suggests tidal forcing or modulation. Most of the seepage spikes we observed occurred during a transition from high tide to low tide. The highest flow events occurred on Nov. 17th, a period during which the highest rainfall was also recorded.

Submarine groundwater discharge into the Yellow Sea

Ryu, J.W., G. Kim

School of Earth & Environmental Sciences,
Seoul National University,
Seoul,
Korea, Republic of

While there have been increased observations of the magnitude of submarine groundwater discharge (SGD) at a few limited sites, many areas of the ocean have no information on SGD. In this study, we attempted to estimate SGD into a large continental margin, the Yellow Sea, using a ^{226}Ra mass-balance model.

The Yellow Sea is one of the largest continental shelves of the world, 4×10^5 km^2 in dimension, with a mean depth of 50 m. The seafloor of the Yellow Sea is deeper in the south than the north, and the gradient of the seafloor is steeper in the east than the west. It is semi-enclosed by the landmasses of China and Korean and one of the best examples of an epicontinental sea. Since the residence time of the Yellow Sea water is between 2-6 years [1], we thought that the estimate of SGD might be more accurate and environmental consequences of SGD are more important in the seawater.

The sources of Ra in this region can be divided into (1) the Changiang river water, (2) the Kuroshio surface water, and (3) the benthic (excess) inputs due to SGD and diffusion from bottom sediments. Using a mass-balance model of ^{226}Ra and ^{228}Ra, we calculated the excess ^{226}Ra and ^{228}Ra activities from benthic inputs and the residence time of seawaters. Then, the excess ^{226}Ra activity from SGD was calculated by subtracting the diffusive input (from bottom sediments) from the total excess activities. The SGD into the Yellow Sea was calculated on the basis of the residence time of seawater, excess ^{226}Ra inventory from SGD, and ^{226}Ra activity in potential brackish groundwater. Our estimate exhibits that SGD into the Yellow Sea is comparable to the river input in the Yellow Sea. Therefore, there may be important effects of SGD on the biogeochemistry and ecosystems of the Yellow Sea.

REFERENCE

[1] NOZAKI, Y., TSUBOTA, H., KASEMSUPAYA, V., YASHIMA, M., IKUTA, N., Residence times of surface water and particle-reactive ^{210}Pb and ^{210}Po in the East China and Yellow Seas, Geochim. Cosmochim. Acta (1991) 1265-1272.

Radium constraints on groundwaters and coastal waters dynamics in the Rhone Delta, France

Ollivier, P., C. Claude, O. Radakovitch, B. Hamelin

CEREGE, Europôle de l'Arbois,
Aix-en-Provence,
France

The Rhône delta is a natural protected area located nearby the largest French industrial center. This delta (Camargue) does host among the most numerous bird colonies in Western Europe. Ecological studies are undertaken to estimate the consequences of pollutant industries on the fauna and the flora. However, groundwater and coastal water dynamics are poorly documented. Geochemical tracers allow to investigate such dynamics that do control pollutant distribution within natural ecosystems. RESYST (created in 2002) is an environmental Research Observatory that offers a unique opportunity to study the response of a deltaic zone to natural and anthropogenic forcing. RESYST is leading a geochemical investigation coupling hydrological data with isotopic tracers to characterize fresh waters, groundwaters, and coastal waters [1].

Here we propose to use ^{226}Ra and ^{228}Ra as tracers of fresh or brackish water inputs to coastal zone by submarine processes [2]. Progressive movement of a salt front into an aquifer and discharge of the brackish water into the near shore should provide a source of radium isotopes to the coastal ocean. Once added to the nearshore waters, ^{226}Ra and ^{228}Ra should behave as conservative tracers. This isotopes allow both source and time constraints on coastal waters dynamics.

^{228}Ra (half-life of 5.75 years) and ^{226}Ra (half-life of 1602 years) isotopes are measured by TIMS at CEREGE in 1.5 l and 0.5 l of water respectively. In order to estimate the ^{226}Ra budget in the coastal zone, water samples have been collected from (1) deep groundwaters from the main water table(> 30 m), from (2) the largest lagoon of the Camargue area, (3) the Rhone river and (4) from surface coastal waters. The first results are presented here. In the deep groundwaters, salinity ranges from 2.5 to 38.8 g/l indicating that a process of salinisation is occurring, either directly through seawater intrusion or as a result of contamination with brackish waters. In these deep groundwaters, ^{226}Ra activities and ^{228}Ra/^{226}Ra activity ratios spread a large range of variations (72 – 2500 dpm/100kg and 1.5 to 26 respectively). Both ^{226}Ra and ^{228}Ra correlate positively with salinity in the aquifer but they are not conservative because of adsorption – desorption processes. They are not the result of mixing between the Rhone river and seawater.

These very high activities of both ^{226}Ra and ^{228}Ra suggest that groundwaters are a potential source of radium to coastal waters where several points are analyzed. Coastal water samples collected within to the Rhone mouth and further west generally display higher ^{226}Ra activity (mean and maximum values of 10.5 and 12 dpm/100kg respectively) than the Rhone river (10 dpm/100 kg) and than distal samples collected 50 km offshore the study area (mean value of 9.7 dpm/100 kg). Coastal waters are thus characterized by a small ^{226}Ra excess. The ^{226}Ra budget in the coastal zone is currently being conducted in order to estimate the influence of groundwaters in the coastal zone. The ^{226}Ra offshore record (9.7 dpm/100 kg) is in very good agreement with that of waters collected offshore Nice [3] that are thought to be representative of the Ligurian current value.

The ^{228}Ra budget is more difficult to estimate because of radioactive decay of ^{228}Ra. ^{228}Ra activity is determined on 1) samples characterized by a lower salinity that result from a significant influence of the Rhone river, 2) on coastal water collected further away from the Rhone plume and 3) on the Rhone river. We observe a significant negative correlation between the ^{228}Ra/^{226}Ra activity ratio and salinity

suggesting that in the coastal zone, ^{228}Ra behaves conservatively. This correlation reflects the mixing between coastal waters and the Rhone river. Exchange model shall be very useful to monitor pollutant transfer in the coastal environment.

REFERENCES

[1] OLLIVIER, P., CLAUDE, C., RADAKOVITCH, O., HAMELIN, B., Femtogram level of ^{226}Ra and ^{228}Ra measured by TIMS in water samples from the Rhone delta, France, Geophys. Res. Abstract **5** (2003) 09416.

[2] MOORE, W.S., Large groundwater inputs to coastal waters revealed by ^{228}Ra enrichments, Nature **380** (1996).

[3] SCHMIDT, S., REYSS, J.-L., Radium as an internal tracer of Mediterranean outflow water, J. Geophys. Res. **101** C2 (1996) 3589-3596.

RADIOECOLOGY

Recent trends in marine radioecology

Kershaw, P.J., K.S. Leonard, J.N. Aldridge, G.J. Hunt

The Centre for Environment, Fisheries & Aquaculture Science (CEFAS),
Lowestoft,
United Kingdom

This paper attempts to review some recent trends in the field of marine radioecology. It is focussed on the NW European continental shelf and NE Atlantic and is not intended to be comprehensive but rather consider some specific issues which it is hoped will have wider interest and application. Marine radioecology in the past decade, in a European context, has been undertaken against a background of largely declining trends: direct discharges from nuclear facilities have continued to be reduced overall (OSPAR undertaking); the marine impact of Chernobyl has lessoned; inputs of natural radionuclides from the phosphate industry, and other sources, have decreased significantly; and, in general concentrations of artificial radionuclides in environmental samples have decreased. There have been exceptions: some direct discharges have increased (e.g. ^{99}Tc and ^{129}I from reprocessing wastes); some existing sources (e.g. oil and gas) or potential sources (e.g. accidental releases, dumped waste in the Kara Sea) have received more attention.

Changes in waste treatment at La Hague led to a very significant increase in ^{129}I releases in the 1990s. This isotope has been promoted as an ocean tracer, particularly in combinaton with Accelerator Mass Spectrometry (AMS), providing low detection limits and high resolution. ^{129}I has been used to estimate transport rates in the Norwegian Coastal Current and in an elegant submarine-based study in the Arctic Ocean which showed an increase in the inflow of Atlantic Water. Releases of ^{129}I increased at Sellafield during the same period. In addition, there was a very significant increase in ^{99}Tc discharges in the mid-1990s. This too has been used as an ocean tracer, with some indication of variability in transport rates, across the shelf, linked to indicators of climate variability.

Observed concentrations of most artificial radionuclides in foodstuffs and indicator species have declined in the past decade, but at a lower rate than the reduction in the discharges. This illustrates the importance of past discharges which remain bioavailable. Concentrations of ^{241}Am have increased in some cases due to grow-in from ^{241}Pu. Concentrations of tritium (^{3}H) in marine species in the Severn Estuary (UK), associated with radio-pharmaceuticals manufacture, were higher than predicted. Over 90% was organic-bound with greater potential to transfer through the marine food chain from small organisms and to accumulate in fish. ^{99}Tc is readily absorbed by brown seaweeds and other biota. Regular sampling of *Fucus* sp. has provided an excellent marker of the transport of the ^{99}Tc 'pulse' across the NW European shelf. There is evidence that uptake by *Fucus* is affected by seasonal factors. In SW Sweden the relative bioavailability of ^{137}Cs and ^{99}Tc in *Fucus* illustrates the balance between the incoming Atlantic and outflowing Baltic Sea water. Predictably, higher environmental concentrations have led to higher critical group doses. The best-known example is lobster (*Homarus gammarus*), leading to socio-economic pressure to reduce the discharges. As a result of a new waste treatment process ^{99}Tc discharges are expected to decrease substantially by 2006.

In the Irish Sea the seabed and intertidal sediments, heavily contaminated in the past, provide a continuing source of ^{137}Cs and plutonium. Mixing processes have tended to dilute the radionuclide signal in the more mobile sediments, and made it harder to carry out an environmental inventory. However, in some sheltered environments, concentrations of ^{241}Am of > 10 kBq kg^{-1} have been preserved. Plutonium mobility in estuarine pore-waters has been linked to the seasonal cycling of Fe and Mn. At the extreme inland limits of saltwater penetration high levels of organic complexation have been observed in organic-rich soils. In offshore sediments, a recent study has indicated a much

larger proportion of plutonium is in a readiliy-exchangeable form than had previously been thought. The study paid great attention to sampling protocols and the careful application of selective extraction techniques. The findings have implications for estimating the bioavailability of the seabed source. The investigation of transuranics behaviour has also benefited from the application of AMS.

Computer models of radionuclide behaviour have tended to increase in sophistication, and a whole range is now available – from simple box models using equilibrium conditions to full 3D transport models incorporating 2 stage adsorption kinetics. Some have included a more elaborate representation of the seabed. What is interesting is that models using quite different approaches may produce similar outputs, illustrating the difficulty of using a single appproach to establishing a causal link and reinforcing the mantra that 'all models are wrong but some are useful'. Model simulations have allowed the relative contribution to dose from recent and 'historic' discharges to be distinguished. ^{99}Tc has been use to help validate a coupled ocean-ice model of the NE Atlantic and Arctic Oceans.

With a few exceptions, the justification for large-scale marine monitoring and associated research, on radiological grounds, has been harder to maintain in recent years. This has been matched with a decrease in the funding available for national and European programmes. This is unfortunate as it means researchers are less able to adequately address the legacy of past practises and the considerable uncertainties which remain in our understanding of the behaviour of radionuclides in the environment. It also ignores the contribution radioecology can make in describing how ecosystems function and means we are less able to participate in the 'ecosystem approach', being adopted by governments and regional conventions. However, against this rather subdued background there have been some significant advances, with an increasing effort to understand the mechanisms and kinetics of radionuclide transfer and behaviour.

Long-term behaviour of ^{137}Cs in Finnish lakes

Saxén, R.

STUK-Radiation and Nuclear Safety Authority,
Helsinki,
Finland

Abstract. Activity concentrations of ^{137}Cs in fish 18 years after the Chernobyl deposition still vary widely, in predatory fish by a factor of 300. Activity concentrations per unit deposition are clearly lower in eutrophic than in oligotrophic lakes. Average aggregated transfer factors of ^{137}Cs to pike in these two lake types were 0.004 and 0.03, respectively, with a large variation range for both during 1998-2002. CFs for perch in different lakes varied by a factor of 25. Ecological halftimes of ^{137}Cs in perch from the study lakes varied from 3 to 9 years.

1. Introduction

Following the Chernobyl accident ^{137}Cs was unevenly deposited in Finland (Fig. 1) [1]. This caused large variations in the ^{137}Cs contents of freshwater fish in Finnish lakes. Over time, environmental processes such as sedimentation, runoff, water flow and hydrological cycling, and factors such as the chemical characteristics (e.g. potassium levels) of the lake water, soil type and the topography of the catchment have affected the behaviour and transfer of ^{137}Cs in watersheds. Many Finnish lakes are oligotrophic and hence ^{137}Cs is highly accumulated in fish. High levels of humic substances are also typical of Finnish lakes.

2. Material and methods

About 6 000 freshwater fish samples from 350 Finnish lakes were analysed for ^{137}Cs from 1986-2003 [2-4]. Ten fish species were included in the samples. Sampling was focused on the central parts of Finland where the highest deposition of ^{137}Cs occurred, but samples from other areas were also analysed. Large lakes and small oligotrophic lakes, in which the highest ^{137}Cs contents were expected to be found, were included in the study. Over time the number of lakes and samples were gradually reduced. In 1998 and 2002, water samples from the 35 lakes then sampled for fishes were also analysed for ^{137}Cs. The results of this study revealed the large variation that still exists in the ^{137}Cs contents in both lake water and fish [5].

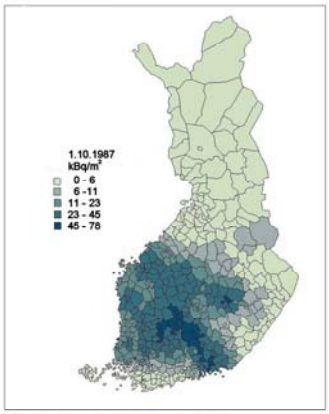

FIG. 1. Distribution of ^{137}Cs deposition in Finland after the Chernobyl accident [1].

3. ^{137}Cs in fish and lake water since 1986

The original distribution of the deposition has remained visible in the ^{137}Cs results from fish. The variation in ^{137}Cs contents in fish has been large throughout the years following the Chernobyl accident, especially in the areas with the highest deposition (Fig. 2). The year when the maximum contents were recorded in predatory fish in Finnish lakes was most commonly 1988. The variation range of ^{137}Cs in fish was still large in 2003, from 5 to 6400 Bq/kg (fresh weight).

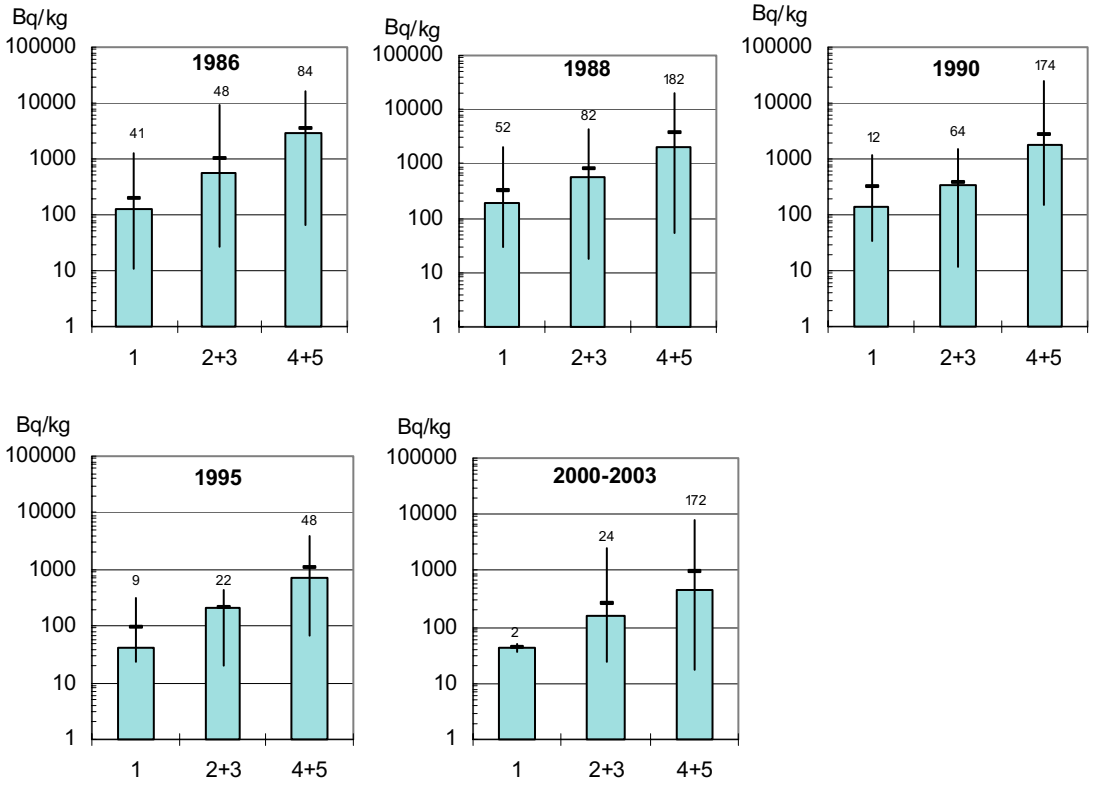

FIG. 2. Annual medians, arithmetic means and observed variation of ^{137}Cs in pike (Esox lucius) in different deposition areas in Finland in 1986, 1988, 1990, 1995 and 2000-2003. The number of samples is also given. The deposition areas 1, 2+3 and 4+5 refer to the areas shown in Fig. 1.

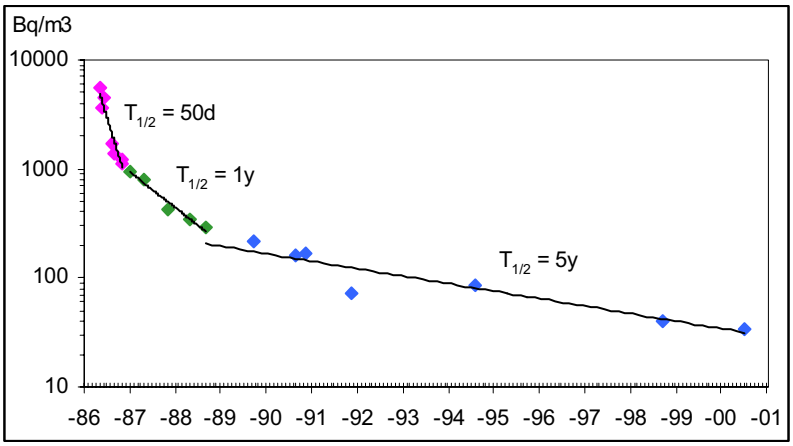

FIG. 3. An example of temporal changes in ^{137}Cs in the water of a large lake in deposition area 5.

The amount of ^{137}Cs deposited in a lake and in the nearby catchment was the dominant factor affecting the short term distribution of ^{137}Cs in fish and lake water after the deposition. Subsequently, several environmental processes have affected the transfer of ^{137}Cs and changed the distribution in different parts of the aquatic environment. Sinking with suspended material to the bottom sediment was one of the main mechanisms reducing the water contents of ^{137}Cs [6]. The effects of environmental processes on the behaviour of ^{137}Cs in lake water are reflected in the changes in its rate of decrease in lake water (Fig. 3). In 2002, ^{137}Cs in water from various lakes varied from 4 to 330 Bq/m^3 [5].

4. Transfer factors of ^{137}Cs from deposition to lake water and fish

Plotting ^{137}Cs in lake water (results from 1998 and 2002) against the original average deposition in the sampling municipality illustrates that there are numerous lakes where ^{137}Cs in water is much lower than in some others in relation to the amount of ^{137}Cs in the original deposition. The aggregated transfer factors of ^{137}Cs from the deposition to lake water, TF_w (Bq/m^3 in water / kBq/m^2 deposited), varied from 0.40 to 8.7, while the TF to pike varied from 0.002 to 0.04 in 1998. The values were highest in oligotrophic and lowest in eutrophic lakes (Fig. 4). Five lakes were included in both groups.

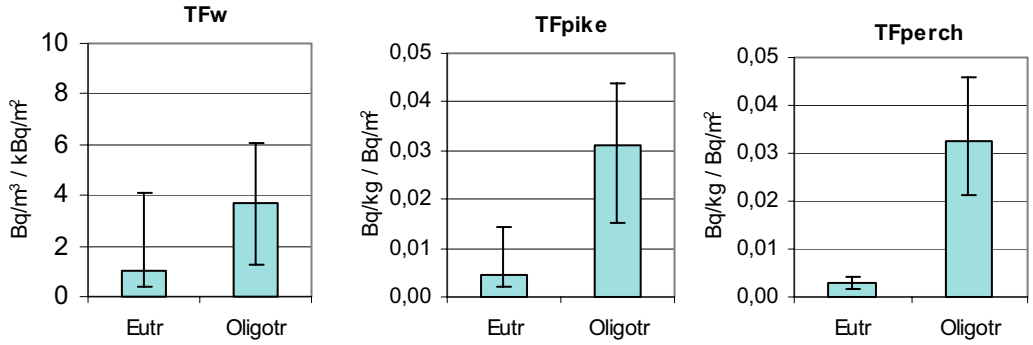

FIG. 4. Aggregated transfer factors from deposition to lake water (TF_w), to pike (TF_{pike}) and to perch (TF_{perch}) 12 years after the deposition in eutrophic and oligotrophic lakes. Both groups include five lakes. The original deposition in the sampling municipalities was corrected for the radioactive decay up to the sampling time of lake water or fish.

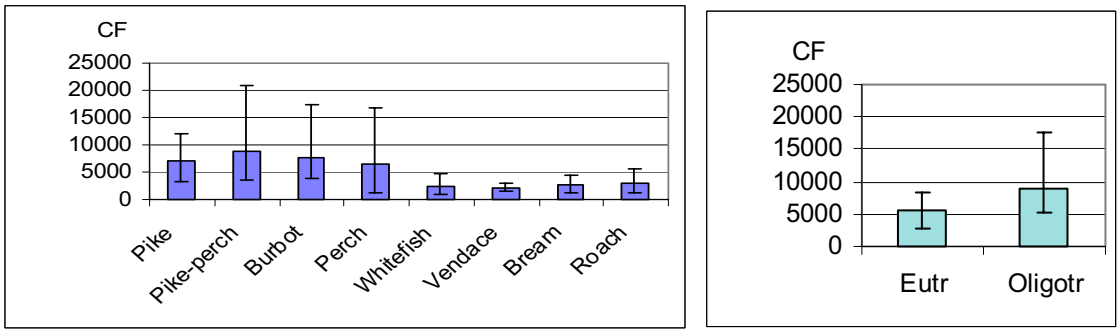

FIG. 5. Mean concentration factors of ^{137}Cs with variation for various fish species in Finnish lakes in 1998 and for perch in eutrophic and oligotrophic lakes.

5. Concentration factors of ^{137}Cs from lake water to fish

The correlation between ^{137}Cs in lake water and in fish was good in 1998 and 2002. Concentration factors, CF (Bq/kg in fish/ Bq/kg in water), were highest for predatory fish (pike, pike-perch, burbot, large perch) and varied from about 3 000 to 20 000 in various lakes in 1998. For nonpredatory fish, CFs were somewhat lower, varying from 1 000 to about 6 000 (Fig. 5).

6. Ecological halftimes of ^{137}Cs in fish

The rate of recovery of ^{137}Cs levels in fish has differed between lakes. The longest halftimes of ^{137}Cs in fish observed in this study were about 9 years for the period 1988-2002 and the shortest about 3 years (Fig. 6). There are some indications that a high content of humic substances decreases the uptake of ^{137}Cs by fish, but slows down the recovery of ^{137}Cs levels in fish, as in case of Lake 2 in Fig. 6.

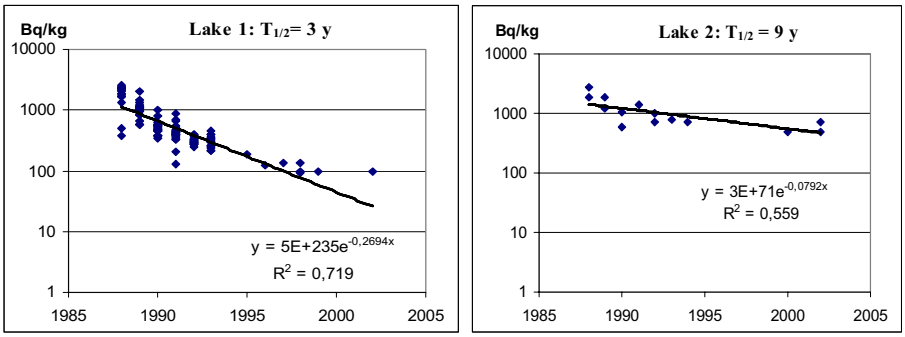

FIG. 6. Decline of ^{137}Cs in pike samples from two lakes and observed ecological halftimes for ^{137}Cs in pike in 1988-2002. Lake 1 is large and eutrophic and lake 2 is small with high content of humic substances in the water (colour > 200 mg Pt/l).

7. Summary

Although 18 years have elapsed since the Chernobyl deposition, large variations still exist in ^{137}Cs contents in both lake water and freshwater fish in Finnish lakes. ^{137}Cs in predatory fish varies by a factor of 300. Activity concentrations of ^{137}Cs in pike per unit deposition were by a factor of 10 lower in eutrophic than in oligotrophic lakes with a large variation range in both lake types in 2002. CFs for one species of fish (perch) in various lakes differed by a factor of up to 25, while activity concentrations varied by a factor of 200. Ecological halftimes of ^{137}Cs in pike varied from 3 to 9 years in 1988-2002. In the areas receiving the lowest deposition, ^{137}Cs contents have been at pre-Chernobyl level for many years, but in some oligotrophic lakes with a long ecological halftime in the area of the highest deposition it will still take years to reach the ^{137}Cs level of 100 Bq/kg in predatory fish.

REFERENCES

[1] ARVELA, H., et al., Mobile survey of environmental gamma radiation and fall-out levels in Finland after the Chernobyl accident, Radiation Prot. Dosimetry **32** 3 (1990) 177-184.

[2] SAXÉN, R., RANTAVAARA, A., Radioactivity of freshwater fish in Finland after the Chernobyl accident in 1986, Report STUK-A61, STUK-Radiation and Nuclear Safety Authority, Helsinki (1987).

[3] SAXÈN, R., KOSKELALINEN, U., Regional variation of ^{137}Cs in freshwater fishes in Finland, Proceedings of ECORAD 2001, Aix-en Provence, France, 3-7 September, 2001, F. Bréchignac Ed., Radioprotection-Colloques **37** (2002) C1 617-C1 620.

[4] SAXÉN, R., Transport of ^{137}Cs in large Finnish drainage basins. In: Dahlgaard H. (ed.). Nordic Radioecology. The transfer of radionuclides through Nordic Ecosystems to man, Studies in Environmental Science **62**, Elsevier, Netherlands (1994) 63-78.

[5] SAXÈN, R., KOSKELAINEN, U., ^{137}Cs in fishes and water in Finnish lakes - considerations for radiological risk assessment, ECORAD 2004, Aix-en-Provence, France, 5-10 September, 2004, a poster presentation, Radioprotection (submitted).

[5] SAXÉN, R., JAAKKOLA, T., et al., Distribution of ^{137}Cs and ^{90}Sr in the Southern part of Lake Päijänne, Radiochemistry **38** 4 (1996) 345-349, (translated from Radiochimiya **38** 4 (1996) 365-370).

The EPIC exposure assessment methodology – a case study for Arctic marine systems

Thørring, H., J.E. Brown, M. Iosjpe, A. Hosseini

Norwegian Radiation Protection Authority,
Østerås,
Norway

Abstract. For the EPIC impact assessment, the basic components of information that are required to derive dose-rates to organisms are: (1) the activity concentrations of radionuclides in reference organisms and their habitat, (2) dose conversion factors (DCFs), and (3) occupancy factors defining the time spent by biota in different representative locations within their habitat. To demonstrate this exposure assessment methodology, a case study was specified and total dose-rates to selected reference organisms were calculated.

1. Introduction

A framework for assessing the impacts of ionizing radiation in Arctic areas was developed in the project EPIC [1]. The derivation of dose-rates to biota is a fundamental part of this framework and the aim of this paper is to demonstrate the EPIC exposure assessment methodology for marine systems using a case study.

Since the starting point of the EPIC assessment for marine systems is unit concentrations of radioactivity in water and sediments, a release scenario needs to be specified with resultant activity concentrations in water and sediments before applying the exposure assessment methodology. Furthermore, the assessment requires the selection of a set of reference organisms that could act as representatives of the larger ecosystem. Thirteen marine reference organisms are considered in EPIC; these organisms have been specified based on an analysis of transfer pathways and the application of suitable selection criteria (e.g. ecological niche, radiosensitivity, amenability to research and monitoring).

2. Case study – release scenario and marine modeling

A hypothetical worst case release scenario at the Kola Nuclear Power Plant with a very large release of radionuclides to the atmosphere [2], was selected for the study. The activities of ^{137}Cs, ^{134}Cs, and ^{90}Sr released to the atmosphere were 14.0, 18.7, and 1.7 PBq, respectively. It was assumed that all of the released radioactivity was deposited in the Barents Sea.

The NRPA marine box-model [3] was used to simulate sea water and sediment activity concentrations of ^{137}Cs, ^{134}Cs, and ^{90}Sr in the Barents Sea during the first 20 years after the hypothetical accident.

3. Exposure assessment methodology

An overview of the main components of the exposure assessment methodology is given in Fig. 1.

Based on time-dependent sea water activity concentrations derived from the NRPA box-model, activity concentrations in marine reference organisms were calculated using equilibrium concentration factors (CFs) taken from [1]. Nuclide-specific internal dose conversion factors (DCFs) were used to convert the predicted activity concentrations in reference organisms to internal dose-rates (Eq. (1)).

$$\dot{D}_{int}^{j} = \sum_{i} C_{i}^{j} \cdot DCF_{int,i}^{j} \quad (1)$$

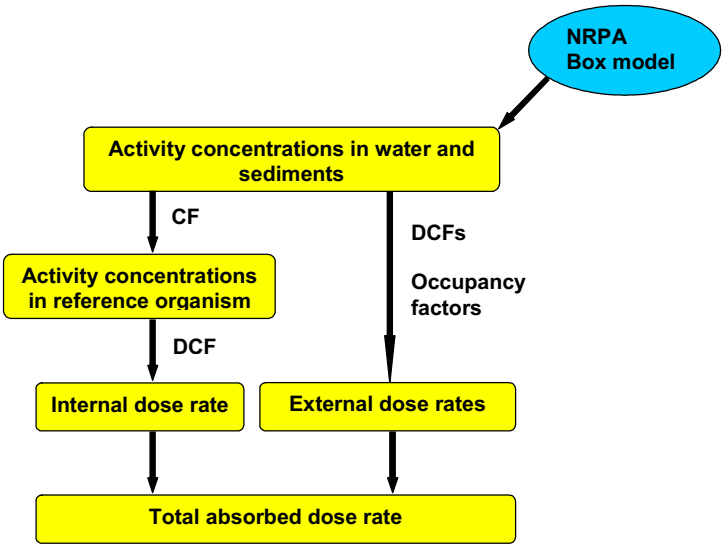

FIG. 1. Overview of the stages in the EPIC exposure assessment approach.

where

$\dot{D}_{int}^{j}$ is the internal dose rate received by reference organism *j* (Gy y^{-1}),

C_i^j is the average concentration of the radionuclide *i* in the reference organism *j* (Bq kg^{-1} FW),

$DCF_{int,i}^{j}$ is the radionuclide-specific dose conversion factor for internal exposure defined as the instantaneous dose rate per average activity concentration of radionuclide *i* in the reference organism *j* (Gy y^{-1} per Bq kg^{-1} FW).

External dose-rates were calculated from water and (when applicable) sediment activity concentrations using external DCFs and occupancy factors (Eq.(2)). The latter specifies the time spent by biota in various representative locations in its habitat (e.g. water surface, water column, sediment water interface) as defined in Ref. [1]. Relevant internal and external DCFs for reference organisms are also taken from [1].

$$\dot{D}_{ext}^{j} = \sum_{z} v_z \sum_{i} C_{zi}^{ref} \cdot DCF_{ext,zi}^{j} \quad (2)$$

where

$\dot{D}_{ext}^{j}$ is the external dose rate received by reference organism *j* (Gy y^{-1}),

v_z is the occupancy factor, i.e. fraction of the time that the organism *j* spends at a specified location z in its habitat,

C_{zi}^{ref} is the average concentration of the radionuclide *i* in the reference media of a given location z (Bq kg^{-1} (sediment) or Bq m^{-3} (water)),

$DCF_{ext,zi}^{j}$ is the radionuclide-specific dose conversion factor for external exposure defined as the instantaneous dose rate to reference organism *j* per average activity concentration of radionuclide *i* at location *z* (Gy y^{-1} per Bq kg^{-1} or Bq m^{-3}).

Furthermore, the total dose-rate (Eq. (3)) represents the sum of internal and external dose given by Eqs (1) and (2):

$$\dot{D}_{total}^{j} = \dot{D}_{int}^{j} + \dot{D}_{ext}^{j} \quad (3)$$

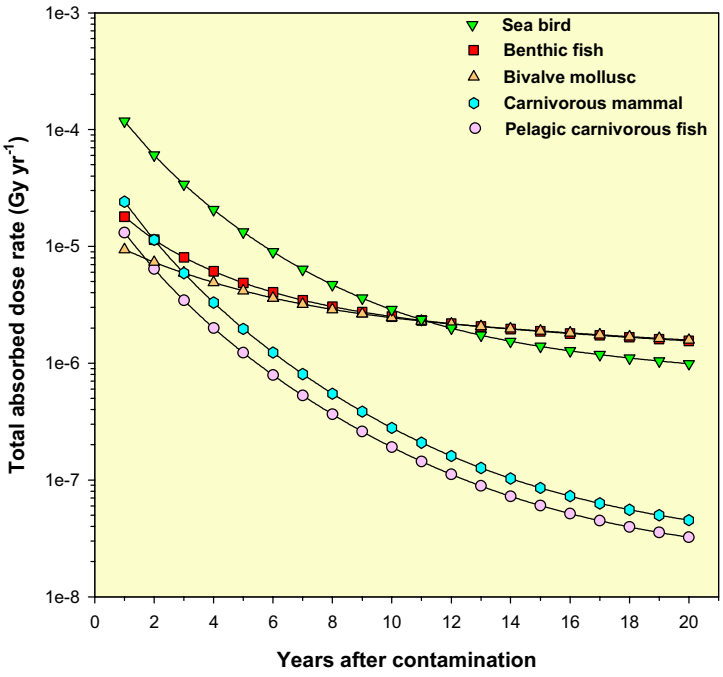

FIG. 2. Predicted total dose rates to reference organisms in the Barents Sea.

For the present study, five reference organisms are considered, namely: carnivorous pelagic fish, benthic fish, bivalve mollusc, sea bird, and carnivorous mammal. Simplifying assumptions were made with respect to occupancy factors for the considered case study: Bivalve molluscs and benthic fish were assumed to be present at the sediment-water interface at all times, whereas pelagic fish and marine mammals were assumed to be totally immersed in water at all times. Sea birds were assumed to spend 1/3 of their time on the water surface, 1/3 of their time in the inter-tidal zone, and the rest of their time in non-contaminated areas (e.g. in the air or on the ground).

4. Results and discussion

Total dose-rates from ^{137}Cs, ^{134}Cs, and ^{90}Sr to the five selected marine reference organisms calculated using Eqs (1)-(3) are shown in Fig. 2.

The concentration dynamics of radionuclides in the water column and sediment determine the dynamics of dose rates for all marine organisms. As shown in Fig. 2, sea birds receive the highest predicted doses for the first 10 years after the hypothetical accident, whereas benthic organisms (i.e. bivalve molluscs and benthic fish) become the most exposed group for periods in excess of 10 years. The large CF of caesium for sea birds seems to be of most importance for the relatively high predicted dose for this reference organism. Pelagic organisms (i.e. pelagic fish and sea mammals) receive total dose rates of comparable size to benthic organisms during the first years, but since doses to these organisms are only dependent on water concentrations, dose rates decrease quite rapidly. In contrast, total doses to benthic organisms level off due to external exposure from sediments.

In general, the predicted dose-rates to reference biota following the hypothetical “worst case” accident at Kola NPP are low. Sea birds receive the highest committed dose (20 years), followed by benthic organisms, while pelagic organisms receive the lowest doses.

5. Evaluation of dose rates

Interpretation of dose-rates in EPIC is limited to simple comparison with preliminary scales of dose-effect relationships as described in [4]. However, there are currently no dose limits in place that can be referred to when evaluating whether biota within Arctic environments are being protected from exposure to ionizing radiation. In order to assess the potential consequences of exposures to radiation on non-human biota two points of reference may be used: (a) Natural background dose rates and (b) Dose rates known to have specific biological effects on individual organisms.

ACKNOWLEDGEMENTS

The EPIC project was conducted under a contract (ICA2-CT-2000-10031) within the EC Inco-Copernicus research programme. Partners in the EPIC project were SPA TYPHOON (Russian Federation), Institute of Radiation Hygiene (Russian Federation), and Centre for Ecology and Hydrology (U.K.).

REFERENCES

[1] BROWN, J., THØRRING, H., HOSSEINI, A., (Eds.), The "EPIC" impact assessment framework: Towards the protection of the Arctic environment from the effects of ionising radiation, a Deliverable report for EPIC, Contract No: ICA2-CT-2000-10032, Norwegian Radiation Protection Authority, Østerås, Norway (2003) 175 pp.

[2] SKUTERUD, L., BERGAN, T., HOWARD, B., WRIGHT, S., (Eds.), Long-term consequences of potential radioactive contamination in the Northern areas: Northern Norway and Murmansk Region Summary Report, Joint Norwegian-Russian Expert Group (2002), 120 pp (ISBN 82-995962-1-1).

[3] IOSJPE, M., BROWN, J., STRAND, P., Modified approach for box modelling of radiological consequences from releases into marine environment, J. Environ. Radioactivity **60** 1-2, 91-103.

[4] SAZYKINA, T.G., JAWORSKA, A., BROWN, J.E. (Eds.), Dose-effects relationships for reference (or related) Arctic biota. Deliverable Report 5 for the EPIC project (Contract no. ICA2-CT-200-10032). Norwegian Radiation Protection Authority, Østerås (2003) 119.

Transfer of Chernobyl radionuclides in the aquatic systems

Zhukova, O.[a], M. Germenchuk[a], N. Shiryaeva[b], V. Drozdovich[b]

[a] The Republican Centre of Radiation Control and Environment Monitoring (RCREM),
Minsk,
Belarus

[b] The Institute of Radioecological Problems,
Minsk,
Belarus

Abstract. The concentrations of ^{137}Cs and ^{90}Sr in river waters of the Dnieper basin have decreased significantly and are now below maximum permissible levels set by national authorities and recommended by expert international organizations. Almost all the ^{137}Cs washed out of contaminated areas is immobilized in bottom sediments within the reservoirs of the rivers of Dnieper Basin. Lakes with no regular outflows present a radiological problem due to higher levels of ^{137}Cs in water and fish. The average total annual doses of inhabitants of settlements located in the Chernobyl accident areas, caused by environmental ^{137}Cs and ^{90}Sr, range from 0.1 to about 5 mSv. In many tens of settlements, the average annual exposure level still exceeds the national action level of 1 mSv.

1. Introduction

The hydrosphere plays an important role in the transfer of radioactive contamination from the places of ejection into the environment and further to a man. The river systems are the most moving parts of the hydrosphere. They favour more dynamic (after the atmospheric transfer) distribution of radioactive contamination during accidental ejection. During the initial period after the accident at the Chernobyl NPP the level dynamics of radioactive contamination was stipulated by radioactive fallouts on water bodies, by physico-chemical properties of aerosols and by hydrology. During the next years (for long-lived radionuclides) their concentration are determined mainly by secondary processes: washout from the contaminated watersheds, access with ground-water, wind carry from the contaminated dry land places on a water surface, interaction with bottom sediments. The processes of radioactive contamination runoff by rainwater and melt-water into the river basins are considered to be the most dynamical, long-term and dangerous. In watercourses and in reservoirs with running water the concentration of radionuclides is gradually decreased. At the same time in closed reservoirs and in the places of erosive material accumulation in the local negative structures of the hydrographic network and in closed falls of the relief such as lakes, ponds and reservoirs, the rise of radioactive concentration is observed.

2. Results and discussion

2.1. Results of radiation monitoring on the rivers of Belarus

The data of radiation monitoring of water bodies in Belarus show that the radiation situation on the rivers of the Dnieper and Pripyat basins was stabilised, the annual average concentration of ^{137}Cs during the period of observation 1987-2000 in large and medium rivers of Belarus have notably decreased. The exceeding of the National Permissible Level-99 (in drink water for ^{137}Cs – 10Bq/L and for ^{90}Sr – 0.37 Bq/L) in water of the rivers was not observed.

At present there is a distinct tendency to decrease ^{137}Cs fluxes by the rivers. The total ^{137}Cs fluxes by the rivers of Belarus for the period 1987-2003 has made for: the river Sozh (in Gomel) – 24.5·TBq, the

Dnieper (in Rechitsa) – 17.5 TBq, the Pripyat (in Mozyr) – 13.2 TBq, the Iput (in Dobrush) – 9.3 TBq, the Besed (in Svetilovitchi) – 1.9 TBq. From the total sum of ^{137}Cs activity which has been transferred by each river for 14 years (1987-2003), 85% has been transferred by the Iput for 2 years, 81% of activity has been transferred by the Sozh for 3 years, by Besed – for 4 years, by Pripyat – for 6 years and 71% of activity has been transferred by the Dnieper for 9 years.

The data analysis of surface water contamination levels by ^{90}Sr of the rivers of the Dnieper watershed shows the increased levels of this radionuclide in the river Besed in comparison with other inspected rivers. The dynamics of ^{90}Sr fluxes through the river sampling site shows that this radionuclide migrates mainly in a soluble state and is in instant dependence with the amount of water in the river. The total ^{90}Sr fluxes by the rivers of Belarus for the period 1990-2003 has made: the Sozh (Gomel) – 3.8 TBq, the Dnieper (Rechitsa) – 3.2 TBq, the Pripyat (Mozyr) – 4.5 TBq, the Iput (Dobrush) – 1.0 TBq, the Besed (Svetilovitchi) – 0.8 TBq [1].

Special attention should be paid to the surface waters of a group of small rivers and channels, which catchments are located on the territory of Chernobyl NPP exclusion zone, the largest of which are the Nizhnya Braginka River and Nesvich River. In these small rivers, a reduction in runoff of ^{137}Cs has been observed for several years, however, the concentrations of ^{90}Sr still exceed the national maximum permissible level during flood periods. For example, ^{137}Cs concentrations in the Nizhnya Braginka River were (0,03–4,2) Bk/L for period 1999-2004 and ^{90}Sr concentrations were (0.3–4.0) Bk/L.

The studies of the bottom sediments of the rivers of the Dnieper and Pripyat basins allow to find radiation dangerous places of radionuclides accumulation in the bottom sediments along the bed of the rivers and reservoirs. Practically on the whole part of the river Nizhnyaiya Braginka (Gden village) and below ^{137}Cs contamination levels of the bottom sediments in 23.08.2000 were from 12940 up to 49760 Bq/kg. Thus, they can be classified as a solid low-level radioactive waste (9630 Bq/kg). In the reservoir in front of Dobrush dam (the Iput river) in 15.10.1992 ^{137}Cs contamination levels of the bottom sediments were from 11400 up to 83600 Bq/kg.

High concentrations of mobile ^{137}Cs forms were found in the bottom sediments in some parts of the river Iput. The high concentration in the bottom sediments of the forms, which can exchange in the bottom-sediments-water system, is a potential danger of the secondary contamination of the rivers.

2.2. Transboundary migration of radionuclides in surface waters

One of the more serious long-term ecological effects of the Chernobyl fallout was the secondary run-off ("wash-off") of radionuclides from the initially contaminated areas through the river networks of Russia, Belarus and Ukraine, into the Dnieper reservoir system, thereby expanding the spatial scale of the accident and exposing millions of people who use the downstream resources of the Dnieper river.

Since the Chernobyl accident, water monitoring stations have been established within the Chernobyl exclusion zone and along the major rivers to determine the concentration of radionuclides and their total flow. Although these stations are not ideally suited to monitoring transboundary fluxes, estimates have been made for of ^{137}Cs and ^{90}Sr (Table I).

The transboundary migration of ^{137}Cs has decreased markedly with time. On the other hand, the transboundary migration of ^{90}Sr has fluctuated from year to year depending on the extent of annual flooding along the banks of the Prypiat river. Note, however, that the extent of wash out of radionuclides is only a very small percentage of the total inventory in the catchment area (Table I). The monitoring data from Belarus indicates that the radionuclide fluxes into the Dnieper river system have stabilized over the past 7-10 years and are now relatively low. The mean annual concentrations of ^{137}Cs during the period 1987–2003 in the water of large and medium rivers of Belarus was not too large. At present ^{137}Cs runoff from the Russia and Belarus watershed does not represent a substantial contribution to contamination of the Dnieper reservoirs on the territory of the Ukraine.

Table I. Estimates of transboundary transport of ^{137}Cs and ^{90}Sr by major rivers

	Observation period (years)	Iput	Besed	Pripiat	Dnieper
Section		Dobrush	Svetilovichi	Belaya Soroka*	Nedanchichi*
Border		Russia-Belarus	Russia-Belarus	Belarus-Ukraine	Belarus-Ukraine
^{137}Cs outflow, TBq	1987-1999	9.1	1.9	31.3	43.1
^{137}Cs, % catchment inventory		0.4	0.1	0.7	0.56
^{90}Sr outflow, TBq	1990-1999	0.9	0.7	52.6	34.3
^{90}Sr, % catchment inventory		2.2	1.9	4.3	3.6

*Data obtained by Ukrainian Hydrometeorological Institute.

The level of water contamination also does not pose any significant risks for water use because, according to the monitoring data of Belarus, the ^{137}Cs concentration in surface waters during the last 5 years remained on the level of 0.01-0.1 Bq/L, which is more than 10 times lower than the national limits for drinking water (10 Bq/L) for ^{137}Cs. Although the wash-off of radionuclides should continue to be monitored, there is no justification for remedial actions in the Upper Dnieper river system from a radiation safety viewpoint. Flaxes of ^{90}Sr increase markedly during times of high flooding. There is still transboundary transfer of radionuclides (mainly ^{90}Sr) by rivers within the Dnieper network The most important source is the flood plain of the Pripiat river within the Chernobyl exclusion zone.

2.3. Radioactive contamination of the lakes in Belarus

While ^{137}Cs concentrations in the surface waters of the Upper Dnieper River have reduced markedly, those in the lakes have remained high. Within the territory of Belarus there are several hundred such water-bodies of both natural and artificial origin. To date, detailed studies have been carried out on only a few lakes. Analysis of available data (see Table II) for lakes Svyatskoye (watershed of Besed' river) and Revucheye (watershed of Iput' river) show that the current levels of contamination in water are ^{137}Cs (8-9 Bq/L) and ^{90}Sr (0.4-0.6 Bq/L), These are close to the maximum permissible levels (^{137}Cs =10 Bq/L, ^{90}Sr = 0.37 Bq/L) according to the Radiation Safety Standards of Belarus (RDU-99). Lakes with no regular outflows still present a radiological problem due to higher levels of ^{137}Cs in water and fish.

In the lakes of the Dnieper river basin there are high levels of radioactive contamination by ^{137}Cs in fish. For example, in Svyatskoe lake contamination of ^{137}Cs in perch is 19410 Bq/kg, in pike 17430 Bq/kg, in roach – from 5800 to 2110 Bq/kg and in Revutee lake contamination of ^{137}Cs in pike – 4150 Bq/kg, in crucian – from 1940 to 3500 Bq/kg [2]. The concentration of ^{137}Cs in bottom sediments the Revuchee lake (10345-18260 Bq/kg) and the Svyatskoe lake (11618-16430 Bq/kg) are so great, that they can be attributed to lowlevel waste storage facilities (9630 Bq/kg). Such high levels of radioactive contamination of bottom sediments are secondary sources of pollution of water. Closed and hardly flowing surface water systems (lakes, ponds, etc.) due to erosion and sedimentation have been accumulating Chernobyl radionuclides. Water quality in some of these systems is almost equal to Intervention Level for fish has been already exceeded. The recommendations for monitoring of closed water systems are suggested.

2.4. Mathematical model of radionuclide transfer by river

In the framework of French-German Initiative the database on radionuclide transfer by surface runoff in heavily contaminated areas of Belarus, Russia and the Ukraine after Chernobyl NPP was prepared. Results of hydrological and meteorological observations were used for formation of input data files for validation of models accounting for wash-off from watersheds and r adionuclides transport in river

Table II. Contamination of water and bottom sediments by ^{137}Cs and ^{90}Sr in some lakes of Gomel region (the Dnieper river basin)

Lake	Date of sampling	^{137}Cs		^{90}Sr	
		Bottom sediments Bq/kg	Water solution, Bg/L	Bottom sediments, Bq/kg	Water solution, Bg/L
Svyatskoe	15.06.99	7067	9.0		0.007
		8399	8.0	33.4	0.02
	25.05.98	11618	4.7		0.3
		8917	5.8	133.3	0.4
		8473	5.7	54.6	0.4
	05.06.98	16430	1.5		
Revutee	09.07.97	5837			
		10345	5.4	28.0	
		6908	5.2		
		4544			
	05.06.98	18260	6.0	44.0	

systems; for formation of files of text data for validation of hydrological blocks of the model; for study of the relationship of radionuclides concentrations in the river water and its change in time as a function of hydrological and meteorological parameters [3]. On the basis of this database, the model for forecasts of radionuclides behaviour in the river system was tested. The model is verified using the data of radiation monitoring carried out on an experimental water catchment of the Iput river.

The model allows the following estimations: radionuclide concentration in soluble form, suspensions and with bottom sediments; radionuclide transfer though the control river site; coefficient of hard and liquid runoff of radionuclides into the river system. The forecast estimations of radioactive contamination of the surface water can be made during the local radionuclide access into the river system as well as during accidental radionuclide fallout onto the water surface. The test of the model of radioactive contamination transfer by river was made on the basis of the data, obtained on the experimental water catchment of the river Iput. The working efficiency of the model was tested by a range of calculation experiments for studying of radioactive contamination spread along the whole bed of the Iput [4]. The comparison of full-scale measurements, held for 1987-2000, and of the calculation results of the concentration in the water, on suspensions and in bottom sediments, which were referred to the last sampling site (Dobrush) were carried out. The calculations were made for hydraulically constant conditions for the whole time range. The agreement of experimental and calculated data for the Iput allows to conclude that the model passed the test satisfactory.

2.5. Dose assessment from the aquatic pathways: drinking water, direct exposure from shore, fish consumption

The external γ–exposure from radionuclides deposited on the ground and the ingestion of radiocesium are the main pathways of exposure to inhabitants of Belarus. To analyze contribution of aquatic pathways to exposure doses the following settlements have been considered:

- Svetilovichi with ^{137}Cs deposition density 1110 kBq·m^{-2}, placed near the lake Svyatskoe (basin of Besed river)
- Dubovy Log with ^{137}Cs deposition density 990 kBq·m^{-2}, placed near the lake Revuchee (basin of Iput river)

To assess effective dose from exposure pathways dosimetric models have been used [5]. Contributions of different pathways to the annual effective dose for 1998-1999 to standard population of settlements Svetilovichi and Dubovy Log, are:

- external exposure from radionuclides distributed in soil within the settlement (67 and 81%)
- external exposure from shore (0.8 and 0.9%)
- external exposure from water immersion during swimming (0.02 and 0.03%)
- internal exposure due to cesium ingestion with food (30 and 16.7%)
- internal exposure due to fish consumption (2.1 and 1.5%)
- internal exposure due to drinking water (0.1 and 0.2%)

Standard population is defining here as a population with standard (average) fish consumption and spending a small fraction of time near the lake. Contribution of aquatic pathways to the effective dose to standard population is rather small and lays in a range of 2.6-3.1%. The main contributor to the total effective dose among aquatic pathways is internal exposure due to fish consumption.

Contributions of different pathways to the annual effective dose for 1998-1999 to the critical group of population for the settlements Svetilovichi and Dubovy Log, accordingly are:

- external exposure from radionuclides distributed in soil within the settlement (50 and 64%)
- external exposure from shore (4.0 and 5.1%)
- external exposure from water immersion during swimming (0.01 and 0.02%)
- internal exposure due to cesium ingestion with food (24 and 13.7%)
- internal exposure due to fish consumption (21 and 15.2%)
- internal exposure due to drinking water (1.2 and 1.7%)

Contribution of aquatic pathways to the total effective dose to the critical group of population could lead up to 30%. For the critical group of population the main contributor to the total effective dose among aquatic pathways is internal exposure due to fish consumption. Contribution of external exposure from water immersion during swimming to the effective dose of critical group of population is negligible.

3. Conclusions

1. High levels of radioactivity remain within the Chernobyl exclusion zone. Important “hot spots” within this zone are the flood plain along the Prypiat river.
2. There is still transboundary transfer of radionuclides (mainly ^{90}Sr) by rivers within the Dnieper network. The most important source is the flood plain of the Prypiat river within the Chernobyl exclusion zone.
3. The concentrations of ^{137}Cs and ^{90}Sr in river waters of the Dnieper basin have decreased significantly and are now below maximum permissible levels set by national authorities and recommended by expert international organizations. Almost all the ^{137}Cs washed out of contaminated areas is immobilized in bottom sediments within the reservoirs of the rivers of Dnipier Basin.
4. Lakes with no regular outflows present a radiological problem due to higher levels of ^{137}Cs in water and fish.
5. Creation and actualization of database on water bodies contamination is necessary for development of specific scenarios for model testing and validation.

6. The average total annual doses of inhabitants of settlements located in the Chernobyl accident areas, caused by environmental ^{137}Cs and ^{90}Sr, range from 0.1 to about 5 mSv. In many tens of settlements, the average annual exposure level still exceeds the national action level of 1 mSv.

REFERENCES

[1] ZHUKOVA O.M., et al., Radioactive Contamination of Water Bodies on Territories of Bryansk-Gomel-Mogilev Chernobyl "Sport" and Improvement of Radiation Monitoring System, Natural resources **1** (2003) 82-86.

[2] OSTAPENYA, A.P., Behavior of cesium-137 in the lakes of different types. In: Lake Ecosystems: biological processes, anthropogenic transformation, water quality. Materials of the International Scientific conference, Minsk-Naroch (2000) 293-302.

[3] KONOPLEV, A.V., et al., Transfer of Chernobyl Cs-137 and Sr-90 by surface run-off, The Radioecology-Exotoxicology of Continental and Estuarine Environments (Proc. Int. Congress Aix-en-Provence, France), EDP Sciences **1** (2002) C1-315-C1-323.

[4] ZHUKOVA, O.M., et al., Model of Migration of Radionuclides in a River System, J. Eng. Phys. Thermophys **74** (2001) 936-945.

[5] MINENKO, V.F., DROZDOVITCH, V.V., TRETYAKEVITCH, S.S., Methodological approaches to calculation of annual effective dose for the population of Belarus, Radiation and Risk **7** (1996) 246-252.

Theoretical dose reconstruction along life-cycle for plaices (*Pleuronectes platessa)* living in the Northern Cotentin waters after 1966

Beaugelin Seiller, K., B. Fievet, J. Garnier-Laplace

Environmental and Emergency Operations Division,
Department for the Study of Radionuclide Behaviour in Ecosystems,
Institute of Radioprotection and Nuclear Safety,
St. Paul les Durance,
France

Abstract. Since 1966, the Northern Cotentin waters have been receiving low-level radioactive liquid releases leading to chronic exposure of wildlife to ionizing radiation. Considering the plaice (*Pleuronectes platessa*) trade value in the fishery, the corresponding potential detriment was estimated on the basis of dosimetric calculations and comparison to effects data found in the literature. For the whole fish life cycle, the radionuclide concentrations in water, sediment and fish were estimated from a former study. Dosimetric assessment was carried out with EDEN (Elementary Dose Evaluation for Natural environment), a tool developed at the IRSN allowing the estimation of dose rate to the biota per unit of radionuclide concentration. These calculations were performed for each radionuclide from each exposure source, internal as well as external, taking into account the plaice morphology and lifestyle for each of its development stage. On the basis of these two data sets, average annual doses were calculated. Their comparison to no effect value derived from the FASSET database led then to the risk estimation.

1. Introduction

The coastal ecosystem of the Northern Cotentin has been exposed to anthropogenic ionizing radiation since the launching of several nuclear industrial facilities. These waters have been receiving since 1966 low-level radioactive liquid releases produced mainly by the normal operation of the COGEMA reprocessing plant, combined later with releases from other nuclear installations (Fig. 1).

This situation led to the chronic exposure of wildlife to radionuclides released in this ecosystem. Considering the trade value of European plaice (*Pleuronectes platessa*) in the local fishing industry,

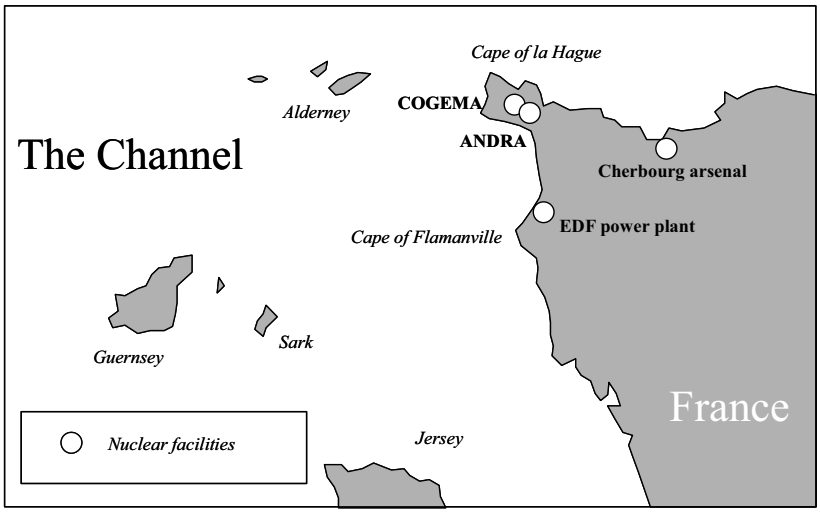

FIG.1. Situation map of the nuclear facilities (o) of concern.

the likelihood and magnitude of potential detriment due to radiological exposure along its whole life-cycle were estimated by applying a classical four-step environmental risk assessment (ERA) approach.

Some prerequisites, like a good knowledge about fish features (e.g. life span), constrained the duration of the reconstruction exercise and the corresponding period investigated for the ERA.

The first step of the ERA was the hazard identification, through the inventory of released radionuclides. In the second step, effects data were searched to investigate dose rate-effects relationships, aiming to estimate a Predicted No Effect Dose Rate (PNEDR), by analogy with the Predicted No Effect Concentration (PNEC) usual in chemical risk assessment. This value is then used as a benchmark for screening purpose that corresponds to the first phase of the ERA. The third step was the exposure analysis, to determine again the Predicted Environmental Dose Rate (PEDR). The fourth and last step of the ERA, the risk characterization, was realised through the comparison between the reconstructed dose rate and the effects data, expressed in its simplest way by applying the quotient method, as the ratio PEDR/PNEDR.

2. Fish features

The required data for the ERA are related to the plaice life-cycle, to determine among other parameters the study duration, the biometric aspects for the dosimetric calculation and the fish behaviour to characterize its exposure.

The European plaice, like most flat fish, presents a four-stage life cycle (egg, larvae, juvenile and adult) marked by a deep transition between the second and the third stages, the metamorphosis, that corresponds moreover with the fish settlement [1, 2]. The duration of each stage was determined from literature data [1-7], the average life span of the plaice being about 30 years. Shapes, sizes and weights are more or less described in the literature for each life stage of the plaice: eggs [4, 9, 10], larvae [4], [6], juvenile [9, 10], and adults [4, 7, 8].

3. Hazard identification

The inventory of the radioactive releases was already done, qualitatively (Table I) and quantitatively [11], in a former reconstruction exercise conducted by the Northern Cotentin Radioecology Group (GRNC). Data are then available from 1966 to 1997, that is to say duration of 31 years, equal to the average plaice life span. The ERA was consequently performed on this duration, to cover the whole life cycle of the fish.

Table I. Qualitative list of radionuclides released by nuclear facilities in the North Cotentin area considered in the dose reconstruction exercise for plaice

3H	59Ni	95Zr+Nb	121mSn	134Cs	233U	242Pu
10Be	63Ni	94Nb	126Sn	135Cs	234U	241Am
14C	65Zn	93Mo	124Sb	137Cs	235U	242Am
36Cl	75Se	99Tc	125Sb	144Ce+Pr	236U	242mAm
41Ca	79Se	103Ru+Rh	126Sb	147Pm	238U	243Am
54Mn	87Rb	106Ru+Rh	127Te	151Sm	237Np	242Cm
55Fe	89Sr	107Pd	127mTe	152Eu	236Pu	243Cm
57Co	90Sr+Y	110mAg	129I	154Eu	238Pu	244Cm
58Co	91Y	113mCd	131I	155Eu	239,240Pu	245Cm
60Co	93Zr	121Sn	133I	232U	241Pu	246Cm

4. Dose rate-effects relationships

Dose rate-effects relationships were investigated through the FASSET Radiation Effects Database (FRED, [12]), which contains more than 100 dose rate-effect data for plaice and chronic irradiation exposure. However this species-specific data set was to small and of a weak relevancy in terms of effects for this exercise. It was then decided to apply the Sensitivity Species Distribution technique to reproduction critical toxicity data (i.e. dose rate giving 10% of effect on reproduction endpoints derived by modelling on the primary FRED data set [13]). That leads to determine a corresponding PNEDR between 0.5 to 4 $mGy.d^{-1}$, the most probable value being about 1 $mGy.d^{-1}$. This value is one order of magnitude below 10 $mGy.d^{-1}$ for aquatic organisms [14].

5. Exposure analysis

The exposure analysis is dedicated to the assessment of the dose rates to which plaice was exposed, resulting from the multiplication of concentrations in radiation sources by adequate dose conversion coefficients. A deterministic and conservative PEDR is thus obtained by summing these products for the whole source term.

Yearly average concentrations from 1966 to 1997 were directly taken from the GRNC work [15], for each radionuclide in water, sediment and fish.

EDEN, a tool developed at the IRSN [16], permits dose coefficients calculation for any radionuclide, any organism and any user-defined exposure scenario. Its basic requirements are the source qualification (cf.§. 3), the biochemical composition of media and organisms (average data from the literature) and their geometrical description (cf.§. 2 for plaice, completed by picture analysis, a 5 m layer for water and a 1 m layer for sediments). For each radionuclide, a DPUC (Dose rate Per Unit of Concentration) is calculated with EDEN for each life stage (one per year for adult plaice), for internal and external exposures. Considering the combination of radionuclides, life stages and exposure scenario, about 9000 DPUCs were calculated, that can then not be reported here.

6. Risk characterization

The risk was evaluated by the ratio PEDR (cf.§. 5.) on PNEDR (cf.§. 4.), the variation range of which being considered. As a first screening approach, and with the assumptions of the study, no potential risk was identified for the plaice reproduction (Fig. 2).

The risk value evolution being closely related to those of the gamma releases, the weighting of the PEDR by Weighting Radiation Factors did not modify the outputs. At the end of the first year, the jump on the curve is explained by the settlement of the animal, the fish being later also exposed to sediment.

7. Conclusions

These results, obtained for a keystone fish in the “local” species, allow to estimate the order of magnitude of the risk associated to radionuclide releases performed for several decades of nuclear facilities operation.

The choice made to achieve this first screening study led to the estimation of no potential risk for plaices living in northern Cotentin waters from 1966 to 1997, the results being mainly determined by gamma releases and exposure to sediment (external irradiation). But numerous uncertainties have not be taken into account, that will be integrated for a more realistic ERA. For the PEDR, that means mainly to look at the uncertainties linked with the bioconcentration factors, the DPUC and the WRF. Concerning the PNEDR, the question of its assessment needs to be thoroughly explored particularly to take into account the background dose rate into the calculation.

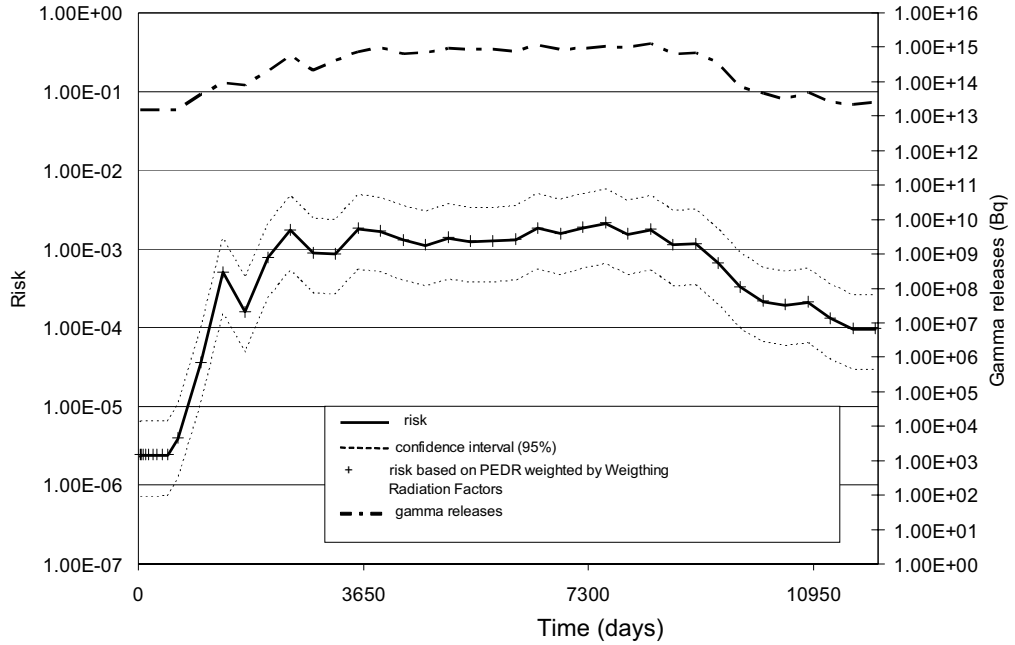

FIG. 2. Estimated risk on the whole plaice life cycle and gamma releases of the nuclear facilities.

Next steps are then to carry out a wider screening approach for a number of species present in the exposed ecosystem and to refine the risk assessment by combining more realistic and probabilistic analysis both for exposure and effects.

REFERENCES

[1] HYDER, K., NASH, R.D.M., Variations in settlement pattern of Irish Sea plaice (*Pleuronectes platessa*) as determined from a simulation model, J. Sea Res. **40** (1998) 59-71.

[2] WENNHAGE, H., GIBSON, R.N., Influence of food supply and a potential predator (*Crangon crangon*) on settling behaviour of plaice (*Pleuronectes platessa*), J. Sea Res. **39** (1998) 103-112

[3] NIELSEN, E., BAGGE, O., McKENZIE, B.R., Wind-induced transport of plaice (*Pleuronectes platessa*) early life-history stages in the Skagerrak-Kattegat, J. Sea Res. **39** (1998) 11-28.

[4] FISHBASE, Pleuronectes platessa (2004) http://www.fishbase.org/Summary/SpeciesSummary.cfm?ID=1342&genusname=Pleuronectes&speciesname=platessa

[5] CHRISTENSEN, M.N., KORSGAARD, B., Protein metabolism, growth and pigmentation patterns during metamorphosis of plaice (*Pleuronectes platessa*) larvae, J. Exp. Mar. Biol. Ecol. **237** (1999) 225-241.

[6] RYLAND, J.S., Observations on the Development of Larvae of the Plaice, *Pleuronectes platessa* L., in Aquaria, J. Cons. Perm. Int. Explor. Mer **30** (1966) 177-195.

[7] KUZNETSOVA, E.N., BONDARENKO, M.V., POLUEKTOVA, O.G., Long-term variability of the growth rate of Barents Sea plaice, J. Sea Res. (in press).

[8] SHERIDAN, R, Pleuronectes platessa (2004) (http://www.umh.ac.be/staff.Sheridan.Richard/inventaire/poi/htm/pleuronectes.htm).

[9] MINAMI, T., TANAKA, M., Life history cycles in flatfish from the northwestern pacific, with particular reference to their early life history, Neth. J. Sea Res. **29** (1992) 35-48.

[10] CHAMBERS, R.C., LEGGET, W.C., Possible causes and consequences of variation in age and size of metamorphosis in flatfishes (Pleuronectiformes): an analysis at the individual, population and species levels, Neth. J. Sea Res. **29** (1992) 7-24.

[11] NORTH-COTENTIN RADIOECOLOGY GROUP, (GRNC), Inventory of radioactive waste from nuclear installations, First mission, Work Group N°1 report (http://www.irsn.org/nord-cotentin).

[12] FASSET, FASSET Radiation Effects Database (FRED), EC 5th Framework Programme, Contract FIGE-CT-2000-00102 (http://www.fasset.org)

[13] GARNIER-LAPLACE, J., DENISON, F., GILBIN, R., DELLA-VEDOVA, C., ADAM, C., SIMON, O., BEAUGELIN-SEILLER, K., Bioavailability in ecological risk assessment for radionuclides, ECORAD 2004, Aix en Provence 6-9 septembre 2004.

[14] UNITED NATIONS SCIENTIFIC COMMITTEE ON THE EFFECTS OF ATOMIC RADIATION (UNSCEAR), Sources and effects of ionizing radiations report for the General assembly, United Nations, New York (1996).

[15] NORTH-COTENTIN RADIOECOLOGY GROUP, (GRNC), Models for the transfer of radionuclides in the environment, Work Group N°3 report (http://www.irsn.org/nord-cotentin).

[16] BEAUGELIN-SEILLER, K., GARNIER-LAPLACE, J., GARIEL, J.C., JASSERAND, F., E.D.E.N.: a tool for the estimation of dose coefficient equivalents for non-human biota, ECORAD 2004, Aix en Provence 6-9 septembre 2004.

Data synthesis for terrestrial gamma radiation level measured on the Japanese Islands and their adjacent ocean floor

Furukawa, M.

National Insitute of Radiological Sciences (NIRS),
Chiba,
Japan

Abstract. In order to design a suitable radiation protection system for the ecosystem, a database and several distribution maps of the terrestrial gamma radiation level in Japan and its adjacent sea floor have been compiled. Based on the database composed of about 2,300 data points, the average gamma radiation dose rate in and around Japan was estimated to be about 50 nGy/h. The minimum and maximum dose rates were estimated to be 0.1 nGy/h in the cold seepage in Sagami Bay, central Japan, and about 2,000 nGy/h in the hydrothermal vent field in Okinawa Trough, southwestern Japan.

1. Introduction

In planning the construction of a suitable radiation protection system for not only the public but also non-human species and ecosystems, it is especially important to know the real radiation levels in various environments. In this study, surveyed data for the terrestrial gamma radiation level from mountain areas to the ocean floor in and around Japan, mainly obtained or published over the past 25 years, have been collected as the basic information to design a suitable system. Based on the database, several distribution maps have been compiled to take an overview of the regional variation for the terrestrial gamma radiation level in the research area.

2. Data

Locations of the data points in and around Japan used in this study are shown in Fig. 1. An extensive field survey of the terrestrial gamma radiation level was conducted at about 800 points on the land surface of Japan by the National Institute of Radiological Sciences (NIRS) [1], and the outline of geographical distribution of the radiation level has been estimated [2]. In addition to the nationwide data, reported data from about 700 points obtained in Hokkaido, Aomori, Gunma, Gifu, Aichi, Mie, Nara, Ehime, Kochi and Fukuoka Prefectures [3-10] and Miyako Island in Okinawa Prefecture [11] were also used to make a more accurate distribution map in this study.

For the sea bottom, to find the gamma radiation level and to establish it in the database as fundamental measurement information for the oceanography, *in situ* measurements have been conducted since 1995 with deep-sea gamma radiation measurement systems installed on the manned submersibles “Shinkai 2000” and “Shinkai 6500” and a remotely operated submarine vehicle “Dolphin 3K” owned by the Japan Agency for Marine-Earth Science and Technology (JAMSTEC) [12]. Up to 2002, the measurements were operated at about 800 points on the sea bottom in the Pacific Ocean, the Japan, East China and Philippine Seas. This portion of the data was analyzed with the cooperation of NIRS [13]. All of these data, published on a JAMSTEC web site [14] were used in this study.

3. Results

A contour map of the terrestrial gamma radiation dose rate in air for the land was made by simple interpolation from the data obtained at 1,461 points. The distribution of the dose rate in air is shown in Fig. 2. Also the dose rates at the sea bottom are illustrated in Fig. 3.

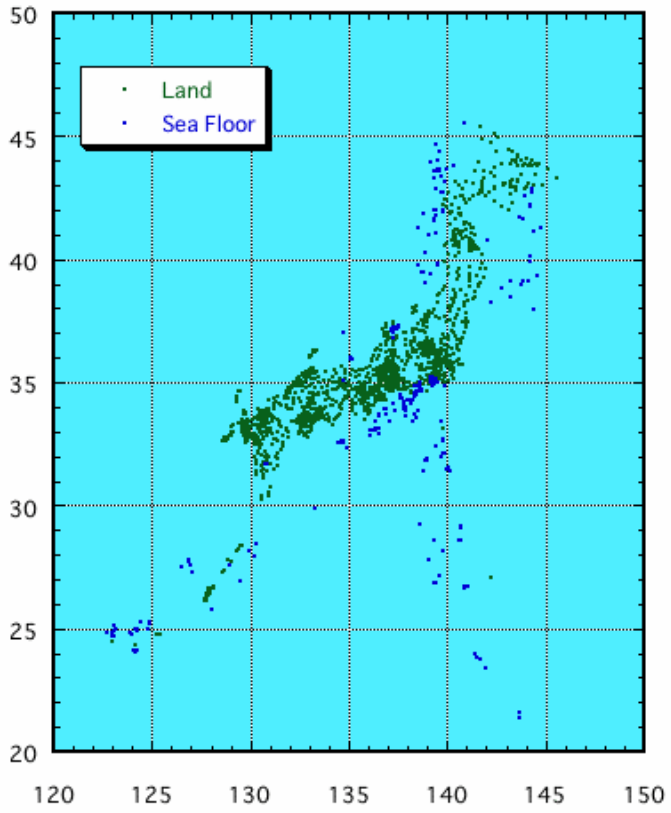

FIG. 1. Distribution of the data points in Japan and its adjacent sea floor.

The mean dose rate due to gamma radiation was estimated to be about 50 nGy/h. In general, the southwestern part of the research area has a higher dose rate compared with the northeastern part. This regional variation of the dose rate is mainly controlled by geological and geo-tectonic parameters. The terrestrial gamma radiation dose rates at the sea bottom are almost the same as the dose rates of the neighboring shore. For the land area, a maximum value of about 500 nGy/h was found around Tamagawa hot spring in Akita Prefecture in northeastern Japan. For the ocean floor, a relatively high dose rate of about 2,000 nGy/h was estimated at a hydrothermal vent field in Okinawa Trough, off Okinawa Islands situated in southwestern Japan. The minimum was estimated to be 0.1 nGy/h in the cold seepage in Sagami Bay, central Japan.

Although the number of data is limited, the above investigations provide valuable information in order to design a suitable radiation protection system for the wide variety of species and environments in Japan as well as in many East Asian countries. The data on natural radiation levels of the ocean floor is also valuable information for the study of unusual oceanic phenomena, such as submarine groundwater discharge, etc.

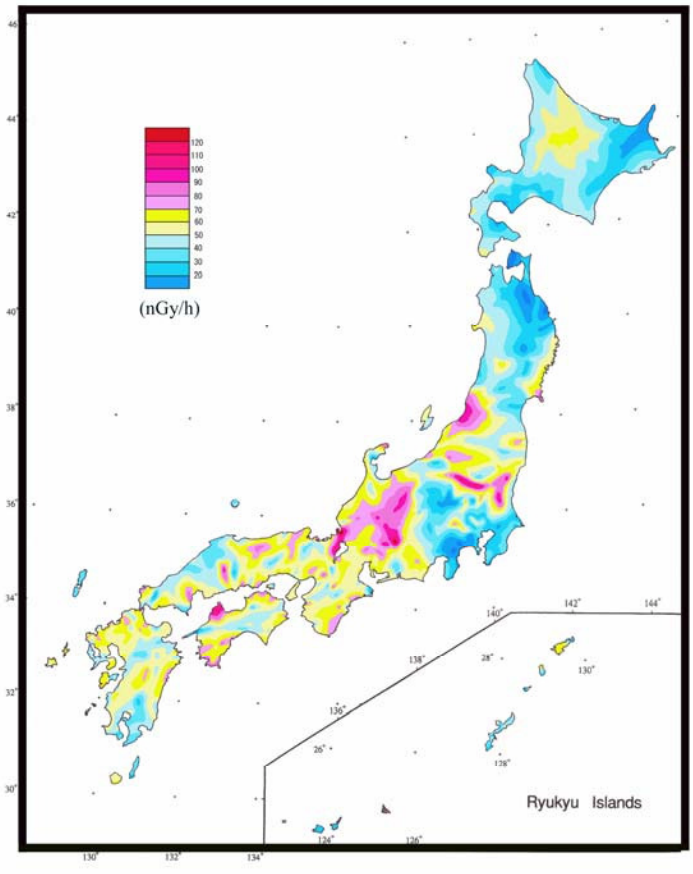

FIG. 2. Distribution of the absorbed dose rate in air due to terrestrial gamma radiation in Japan.
See ANNEX I, p. 663 for colour version of figure.

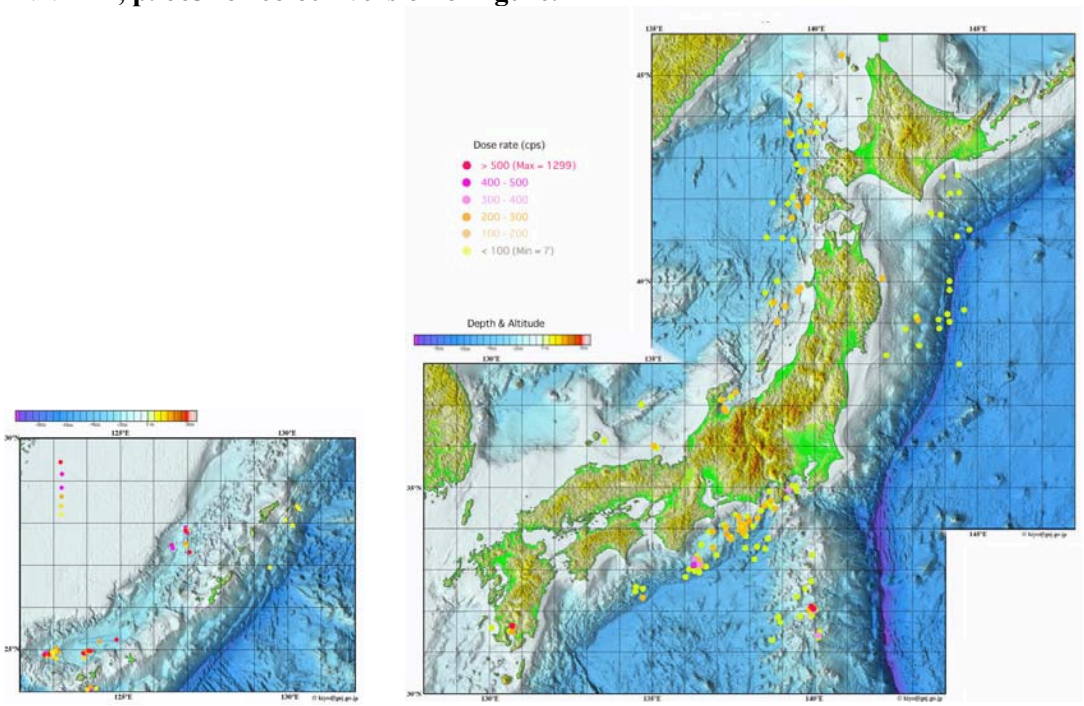

FIG. 3. Distribution of the absorbed dose rate due to terrestrial gamma radiation at the sea floor around Japan. The data are opened on a JAMSTEC website [14] 4 cps = approximately 1 nGy/h.

REFERENCES

[1] ABE, S., et al., Extensive field survey of natural radiation in Japan, J. Nuclear Sci. Technology **18** (1981) 21

[2] FURUKAWA, M., Natural radiation level in Japan Islands, Journal of Geography, **102** (1993) 865 (in Japanese with English abstract).

[3] SUGINO, M., et al., A survey of environmental radiation in southern Hokkaido, Bull. Gunma Pref. College of Health Sci., 4 (1997) 113 (in Japanese with English abstract).

[4] IYOGI, T., et al., Environmental gamma-ray dose rate in Aomori prefecture, Japan, Health Phys., **82** (2002) 521.

[5] SUGINO, M., SHIMO, M., Survey of environmental radiation dose rates and natural radionuclide concentrations in Gunma prefecture, Japan, Radioisotopes **51** (2002) 543 (in Japanese).

[6] SHIMO, M., et al., A survey of environmental radiation Aichi, Gifu and Mie prefectures, J. At. Energy Soc. Japan **41** (1999) 954 (in Japanese with English abstract).

[7] MINATO, S., et al., A survey of terrestrial gamma ray dose rates of Nara prefecture, Radioisotopes **52** (2003) 42 (in Japanese).

[8] Government of Ehime Prefecture, Japan, Results of the survey for natural radiations in Ehime prefecture (1996) 44p (in Japanese).

[9] CHIKASAWA, K., et al., Terrestrial gamma radiation in Kochi prefecture, Japan, J. Health Sci. **47** (2001) 362.

[10] HIRAI, E., et al., Measurement of natural background radiation in Fukuoka prefecture using ionization chamber and NaI (Tl) scintillation detector, Radioisotopes **44** (1995) 846 (in Japanese with English abstract).

[11] FURUKAWA, M., TOKONAMI, S., Distribution of absorbed dose rate in air because of terrestrial gamma radiation in Miyako-jima, Okinawa prefecture, Japan, Japanese, Health Phys. **36** (2001) 195 (in Japanese with English abstract).

[12] HATTORI, M., OKANO, M., In situ sea bottom gamma ray surveys by manned submersibles and ROV, JAMSTEC, Deep-Sea Res. **14** (1997) 639 (in Japanese with English abstract).

[13] FURUKAWA, M., Radiation environment of the Earth, Ionizing Radiation **29** (2003) 51 (in Japanese).

[14] Japan Agency for Marine-Earth Science and Technology (JAMSTEC), Sea Bottom Gamma Ray Database, http://www.jamstec.go.jp/gamma/page1.php3/.

Post depositional reactivity of the plutonium in marine sediments: new evidence from solid partitioning

Gouzy, A.[a], D. Boust[a], O. Connan[a], G. Billon[b], M. Agarande[c], L. Leon-Vintro[d], P.J. Kershaw[e]

[a] Laboratoire de Radioécologie de Cherbourg-Octeville, IRSN,
Cherbourg-Octeville,
France

[b] Laboratoire de Chimie Analytique et Marine,
Univ. Lille I,
Villeneuve d'Ascq,
France

[c] Laboratoire de Mesure de la Radioactivité de l'Environnement, IRSN,
Orsay,
France

[d] Department of Experimental Physics,
University College Dublin,
Dublin,
Ireland

[e] The Centre for Environment, Fisheries & Aquaculture Science (CEFAS),
Lowestoft,
United Kingdom

Plutonium remobilisation from bottom sediments of the Eastern Irish Sea has been evidenced and extensively documented [1]. Nevertheless, the processes by which the plutonium is released to the water column are still poorly understood. Data on the behaviour of this element during the diagenesis of marine sediments (e.g. [2]) are rather scarce. Previous works on the solid partition of plutonium have been proved to be unreliable [3].

To fill this gap, a thoroughly validated extraction protocol was designed and validated to study the solid partition of plutonium in anoxic sediments [3]; no significant dissolution of non-targeted geochemical phase was observed. Special care was brought to preserve the anoxic character of the sediments from sampling to the ultimate plutonium extraction from its carrier-phases and to prevent any resorption of plutonium by using a complexing agent. This protocol was used on different sediment cores recovered during the DIAPLU expedition (July 2002) in the Eastern Irish Sea. We report here the results obtained on a sediment core (25 cm long) collected at the depocentre of the so-called Eastern Mud-Patch, in the vicinity of the Sellafield plant outfall.

Sediment description and pH-Eh profiling were performed on board upon arrival on the deck then two subcores were prepared for further sedimentological and diagenetic studies, 10 cm and 16 cm inner diameter, respectively. They were carefully handled and stored to prevent any perturbation of the sediment column or water circulation. Back to the lab, the sediment core dedicated to geochemical analyses was sliced into 2 cm thick sections under a nitrogen atmosphere. Each of them was squeezed; pore water samples were acidified (except for alkalinity measurements which were carried out just after recovery) and squeezed sediment cakes were deep-frozen then stored for further analyses.

Unsqueeezed sediment subsamples were prepared for water content and particulate sulfide determination.

A number of parameters were determined on water samples (major and trace elements, sulfides, sulfates and dissolved organic carbon) as well as on sediments (some major and trace elements, particulate organic carbon, carbonate content, grain-size distribution, gamma-emitting radionuclides). Special attention was drawn to sulfide determination (acid volatile and chromium reducible sulfides: AVS and CRS) and to the solid partition of plutonium. The sequential extraction procedure dedicated to plutonium was applied to squeezed sediment sections. Five fractions were distinguished: exchangeable/readily oxidisable (pH8, including reactive sulfide - AVS), acid-soluble (pH5, including carbonates), reducible, oxidisable (organics and CRS sulfides), and residual fractions. Plutonium isotopes (^{239}Pu, ^{240}Pu, ^{241}Pu, ^{242}Pu) were measured in each fraction by ICPMS, using ^{244}Pu as yield tracer [4] together with a number of trace elements representative of the targeted phases (Ca, Sr, Mg, K, Fe, Mn, P, Al).

The sediments undergo active bioturbation and suboxic diagenesis (almost no oxygen penetration, subsurface peak concentrations of dissolved Fe and Mn, and negative Eh values). Peak values of both AVS and particulate organic carbon suggest that AVS could be produced by the anaerobic decaying of autochthonous organisms [5].

Plutonium is found to be mainly associated with the exchangeable/readily oxidisable (37±5%) and acid-soluble (40±4%) fractions. These results contradict many previous sequential extraction studies, e.g. [6], which took less care of preservation of the anoxic character of the sediment and of resorption of plutonium during the extraction. Consequently, a large proportion of the plutonium is liable to be actively recycled within the sediment column. It is actively concentrated into readily oxidisable sulfides (AVS; up to 100 000Bq.kg^{-1} in sulfide particles), potentially focusing its impact on biota, especially microorganisms. The inferred reactivity of plutonium during sediment resuspension should be reconsidered as well.

REFERENCES

[1] HUNT, G.J., KERSHAW, P.J., Remobilisation of artificial radionuclides from the sediment of the Irish Sea, J. Radiol. Prot. **10** (1990) 147-151.

[2] MALCOLM, S.J., KERSHAW, P.J., LOVETT, M.B., HARVEY, B.R., The interstitial water chemistry of ^{239,} ^{240}Pu and ^{241}Am in the sediments of the northeast Irish Sea, Geochim. Cosmochim. Acta **54** (1989) 29-35.

[3] LUCEY, J.A., GOUZY, A., BOUST, D., LEÓN VINTRÓ, L., BOWDEN, L., FINEGAN, P.P., KERSHAW, P.J., MITCHELL, P.I., Geochemical fractionation of plutonium in anoxic Irish Sea sediments using an optimised sequential extraction protocol, Appl. Rad. Isot. **60** (2004) 379-385.

[4] AGARANDE, M., BENZOUBIR, S., NEIVA-MARQUES, A.M., BOUISSET, P., Sector field inductively coupled plasma mass spectrometry, another tool for plutonium isotopes and plutonium isotope ratios determination in environmental matrices, J. Environ. Radioact. **72** (2004)169-176.

[5] ALLEN, R.E., Role of diffusion-precipitation reactions in authigenic pyritization, Chem. Geol. **182** (2002) 461-472.

[6] McDONALD, P., VIVES I BATTLE, J., BOUSCHER, A., WHITTALL, A., CHAMBERS, N., The availability of plutonium and americium in Irish Sea sediments for re-dissolution, Sci. Total Environ. **267** (2001) 109-123.

The extreme Rhone River flood of December 2003 (South East France) — consequences on the translocation of artificial radioactive contaminants onto the flooded areas

Eyrolle, F., C. Duffa, B. Rolland, C. Antonelli

IRSN/DEI/SESURE/LERCM,
St Paul Lez Durance,
France

In recent years, great progress has been made in reducing the direct emission of artificial radioactivity and other contaminants into the environment from industrial sources. However the transport and fate of previously-released pollutants is still of great concern. In particular, it is now recognized that certain natural sinks, such as soils and deposits of sediment in streams, rivers and oceans, can entrain the contaminants for long periods of time, only to serve as sources of contamination at some later date. Such a phenomenon was first observed in the Irish Sea after sharp decreases in releases from the spent fuel reprocessing plant in Sellafield [1, 2, 3]. In rivers, one of the primary mechanisms for the remobilization of contaminated deposits is thought to be major flood events [4, 5]. As a result of climate change, floods have become more abundant and more destructive in many regions of the globe including Europe [6]. Then substantial changes in risk of translocation of sediments and associated contaminants onto flooded areas is expected.

At the beginning of December 2003 an exceptional meteo climatic event led to an extreme Rhône River flood that flooded almost 500 km^2 of the low Rhône valley. Flooding waters entrained a large amount of sediments that have deposited on agricultural soils and urban areas. Therefore particle reactive contaminants such as radionuclides may have been partly translocated from the River onto a large terrestrial area through remobilisation of contaminated fluvial sediments [7]. The soils of the low Rhône valley are labelled with 2000 Bq m^{-2} for ^{137}Cs, 50 Bq m^{-2} for $^{239+240Pu}$ and 1.5 Bq m^{-2} for ^{238}Pu as mean values [8]. Based on our previous studies [9] we estimate than radioactive inputs onto flooded areas might reach about 500 Bq m^{-2} for ^{137}Cs. Nevertheless, a great spatial heterogeneity is expected depending on both the mass and nature of the sedimentary deposits. Several field cruises were performed until February 2004 to estimate the spatial spreading of sedimentary deposits. The deposit thinness were measured at almost 140 reference points within 3 main flooded areas whom one includes the Arles city. 87 samples were collected and are analysed for their sedimentary nature and organic matter content. About fifty percent of these samples are analysed regarding artificial radionuclides (gamma-emitters), organic contaminants and trace metals. Finally, a map of additional contamination of flooded areas during December 2003 is expected together with an evaluation of the consequences of such extreme flood events.

REFERENCES

[1] VIVES I BATTLE, J., Speciation and bioavailability of plutonium and americium in the Irish Sea and other marine ecosystems. PhD thesis. National University of Ireland, (1993) 347 pp.

[2] COOK, G.T., MACKENZIE, A.B., MCDONALD, P., JONES, S.R., Remobilisation of Sellafield derived radionuclides and transport from the north-east Irish Sea, J. Environ. Radioact. **5** (1997) 227-241.

[3] REMOTRANS EU PROJECT, Processes regulating remobilisation, bioavailability and translocation of radionuclides in marine sediments, EU Fifth Framework Programme, November 2000-October 2003, FP5-EURATOM.

[4] SMITH, P.P.G., 30 years of fluvial sediment studies within the Plynlimon experimental catchments, Wales, UK, 9th International symposium on the interaction between sediments and water, IASWS, 5-10 May 2002, Banff Springs, Canada (2002).
[5] EYROLLE, F., DUFFA, C., CHARMASSON, S., Inputs of plutonium isotopes from the Rhône River to the Gulf of Lion (North Western Mediterranean Sea) over the 1945-1998 period – mass balances, fluxes and predictive trend (Proc. Int. Conf. Radioactivity in the Environment, 1-5 September 2002, Monaco) (2002) 577-581.
[6] STARDEX EU PROGRAM, Statistical and Regional Dynamic Downscaling of Extreme for European Regions.
[7] EYROLLE, F., CHARMASSON, S., LOUVAT, D., Plutonium isotopes in the lower reaches of the River Rhone over the period 1945-2000 : Fluxes towards the Mediterranean Sea and sedimentary inventories, J. Environ. Radioact. SI **74** (2004)127-138.
[8] DUFFA, C., RENAUD, PH., CALMET, D., Activités de ^{238}Pu et $^{239+240}$Pu dans les sols cultivés de la basse vallée du Rhône, Comptes-rendus de l'Académie des Sciences, Sciences de la Terre et des Planètes **4** (2001) Fascicule a.
[9] ROLLAND, B., EYROLLE, F., BOURLÈS, D., Removal of sedimentary stocks and associated radioactivity in the lower Rhone River : preliminary results, 26-30 April 2004, EGU Nice, (2004) France.

Removal of sedimentary stocks and associated radioactivity in the lower Rhône River (South Eastern France)

Rolland, B.[a], F. Eyrolle[a], D. Bourlès[b]

[a] Institute for Radioprotection and Nuclear Safety (DEI/SESURE/LERCM),
S[t] Paul Lez Durance,
France

[b] CEREGE, Europôle Méditerranéen de l'Arbois,
Aix-en-Provence,
France

The Rhône River has drained for the last 40 years different sources of radioactive contamination (industrial releases, the Chernobyl accident, global fallouts due to the atmospheric nuclear tests).Since the drastic decrease of the industrial liquid releases of the Marcoule nuclear plant in the 1990s, artificial radioactivity from the global fallouts accumulated on the river catchments as well as artificial radioactivity from Marcoule releases accumulated in sediment storage may represent a non-negligible source term of radioactive contamination of Rhône River waters, especially during flood events [1].

In order to quantify the fluxes and the origin of radioactivity during floods, a suspended matter monitoring was set up on the Rhône River and its tributaries downstream all the rhodanian nuclear plants (in Arles). The artificial radionuclide ^{137}Cs and the natural radionuclides from atmospherically origin ^{7}Be ($T_{1/2}$=54 days) and $^{210}Pb_{xs}$ ($T_{1/2}$=20.4 years) were used as tracers for the particulate matter.

The monitoring results underlined the significance of floods in the transfer of suspended material and associated radioactivity towards the Mediterranean Sea. The 2 exceptional flood events of the autumn 2002 exported about 90% of the annual flux of suspended particulate material. At the same time, while 31±10 GBq of ^{137}Cs were carried by the Rhône River out of flood events (flow rate lower than 2500 $m^3.s^{-1}$), 115±10 GBq were exported during these 2 floods.

These results showed then a significant decrease of the particulate activity of ^{7}Be and $^{210}Pb_{xs}$ during the autumn 2002 floods as the flow-rate increases. This may be explained by the strong supply of material from the watershed soil leaching and/or by the removal of aged sediment storage, which dilute the ^{7}Be and $^{210}Pb_{xs}$ activities.

Furthermore, for flow-rates lower than 2500 $m^3.s^{-1}$, the particulate activity of ^{137}Cs measured in Arles is very variable and ranges from 10 to 65 $Bq.kg^{-1}$. This may be explained by the variability of the liquid releases of the Marcoule Nuclear plant. However, for flow-rates upper than 2500 $m^3.s^{-1}$ and increasing to 10000 $m^3.s^{-1}$, the particulate activity of ^{137}Cs ranges from 10 to 20 $Bq.kg^{-1}$ and is more or less constant. This range of activity is similar to the ^{137}Cs activities measured out of flood event downstream the Marcoule nuclear plant. This would show that the particulate material removed during floods originates mainly from the watershed soil leaching. The contribution of potential sediment storage with associated radioactivity originating from Marcoule would be then negligible.

Further investigations including the use of the plutonium isotopes ratios ($^{238}Pu/^{239,2340}Pu$ and $^{240}Pu/^{239}Pu$ ratios) will allow us to determine more accurately the contribution and the origin of the removed radioactivity during flood events. Moreover, due to their similar chemical behaviour, the $^{7}Be/^{210}Pb_{xs}$ ratio should correct for grain size and compositional variability of the particulate matter [2, 3]. The use of the $^{7}Be/^{210}Pb_{xs}$ ratio as tracer of the particulate matter will have to be discussed.

REFERENCES

[1] EYROLLE, F., et al., Plutonium isotopes in the lower reaches of the River Rhône over the period 1945-2000: fluxes towards the Mediterranean Sea and sedimentary inventories, J. Environ. Radioact. (2004).

[2] BONNIWELL, E.C., et al., Determining the times and distances of particle transit in a mountain stream using fallout radionuclides, Geomorph. **27** (1999) 75-92.

[3] CAILLET, S., et al., Factors controlling ^{7}Be and ^{210}Pb atmospheric deposition as revealed by sampling individual rain events in the region of Geneva, Switzerland, J. Environ. Radioact. **53** (2001) 241-256.

RADIOECOLOGY – POSTERS

Study of exposure to radiation in a lost wax foundry

Legarda, F., N. Alegría, M. Herranz, R. Idoeta

Department of Nuclear Engineering and Fluid Mechanics,
University of the Basque Country,
Bilbao,
Spain

Lost wax casting is an ancient method for making metal pieces. At the beginning of the process, the required metal piece is made in wax. After that, the wax model is covered with a silicaceous shell. When the silicaceous shell is finished, the wax is melted and replaced by liquid metal. As soon as the metal is cool the silicaceous shell is broken away. Finally a finishing process is made, and the piece is ready for utilization. The silicaceous shell is prepared with zircon sands containing varying concentrations of natural radionuclides: ^{238}U, ^{232}Th and ^{235}U together with their progenies. For that reason it is very convenient to assess the dose to workers, considering the tasks they perform and the exposure time during these activities over a year.

The first part of the study focuses on identifying the situations and areas where workers are exposed to radiation [1, 2, 3]. The exposure pathways are: inhalation of dust, ingestion of dust, inhalation of radon, skin contamination and external irradiation.

In a plant where this process is implemented the areas where workers are exposed are: the store, the shell building area, the foundry area, the shell or mold breaking area, and the waste area, including the areas close to the store. In these areas, workers are exposed while they work at their different tasks.

The second part of the study deals with dose assessment. In most of the areas, external irradiation is the dominant pathway, and in order to assess doses a Monte-Carlo simulation using MCNP-4C [4] code has been performed.

The photon fluxes thus obtained are multiplied by the conversion factor of flux to kerma for air [5], by conversion factor to Effective Dose by kerma unit [5], and by the number of emitted photons per disintegration of parent nuclide.

The application of this methodology to a given mill has produced the following results: Individual doses received by workers by area have a mean value of 5.9 μSv/y and a standard deviation of 7.7 μSv/y with an upper limit of 20.3 μSv/y and a lower limit of 0.2 μSv/y. The corresponding collective dose is 232.8 μSv/y and the distribution of dose by task being as follows:

- Maintenance: carrying the zircon sands from lorry to store (0.039 μSv/y), placing the zircon sand pallet on the shelf (0.012 μSv/y), exposure while the pallet is on the shelf (2.8 μSv/y), taking the pallet off the shelf (0.022 μSv/y), taking the pallet to the mold preparation area (0.39 μSv/y). The total collective dose associated to this task is 3.263 μSv/y
- Shell Making: shell preparation (58.2 μSv/y), shell cover (big trays) (76 μSv/y), shell cover (small trays) (9 μSv/y), exposures to molds (5.6μSv/y), loading the pieces on the wagon (2.1μSv/y), taking the wagon to the foundry area (7.4 μSv/y), taking the residues to the waste area (2.2 μSv/y), putting the pieces into the wax removing kiln (1.4 μSv/y). The total collective dose of this task is 161.91 μSv/y
- Mold preparation (35.2 μSv/y)

- Shell removal: waste material removal (0.4 μSv/y), and moving the cart from the foundry area (0.6 μSv/y)
- Finishing (28.6 μSv/y)
- Waste (0.00034 μSv)

Workers in shell making are the most exposed, but the value of the collective dose is less than 1 mSv/y.

Comparing with the levels of the graphical representation of the classification system [1, 2], we can conclude that the processes "do not need to consider regulation".

REFERENCES

[1] EUROPEAN COMMISSION, Reference levels for workplaces processing materials with enhanced levels of naturally occurring radionuclides, Radiation Prot. **95** (1999) E.C., Luxembourg.

[2] PENFOLD, J.S.S., MOBBS, S.F., DEGRANGE, J.P., SCHNEIDER, T., Establishment of reference levels for regulatory control of workplaces where materials are processed which contain enhanced levels of naturally occurring radionuclides, Radiation Prot. **107** (1999) E.C., Luxembourg.

[3] LEGARDA, F., ALEGRÍA, N., HERRANZ, M., IDOETA, R., Valoración de la Dosis recibida por el personal de Precicast Bilbao, S.A. como consecuencia de la utilización de arena de circonio, Dpto. Ingeniería Nuclear y Mecánica de Fluidos, Universidad del País Vasco, Informe INMF/07/03, Bilbao (2003).

[4] LOS ALAMOS NATIONAL LABORATORY, MCNP-4C Monte-Carlo N-Particle Transport Code System, versión 4C, LANL, New México (2001).

[5] INTERNATIONAL COMMISSION ON RADIOLOGICAL PROTECTION, ICRP Publication **74**, Pergamon Press (1997).

Artificial radionuclides in Black Sea sediments

Aliev, R.[a], St. Kalmykov[a], Yu. Sapozhnikov[a]

[a] Moscow State University,
Chemistry Department, Radiochemical Division,
Moscow,
Russian Federation

[b] Moscow State University,
Skobeltsyn Institute of Nuclear Physics,
Moscow,
Russian Federation

The present work is a summary of the Moscow State University's activities under the IAEA's RER 2/003 Project "Marine Environment assessment of the Black Sea Region". The Black sea is a highly-contaminated water body. The atmospheric nuclear tests in the 50-60s and the accident at the Chernobyl NPP (1986) are the main sources of man-made radionuclide contamination of the Black Sea. Some impact of the contemporary nuclear activities of European countries is possible as well. The aim of this work was to estimate the level and to reconstruct chronology of anthropogenic radioactive pollution of the Black Sea ecosystem.

Sediment samples (11 sediment cores) were collected by multicorer and gravity corer during the 55th Cruise of the RV "Professor Vodyanitsky" (2000) and during cruises of the RV "Akvanavt" (1997-2000) in the eastern part of the Black Sea and near Turkish, Russian and Ukrainian (Crimea) shores. Sediment samples were cut into 1 cm layers and analyzed for ^{137}Cs specific activity. The vertical distribution of ^{137}Cs in the Black Sea sediments in most cases has a sharp maximum, corresponding to the Chernobyl accident. Sometimes a second maximum caused by the atmospheric nuclear tests also occurs (corresponds to early 60s). The specific activity of ^{137}Cs in the bottom sediments of the Black Sea reaches the level of 200 Bq/kg of dry weight. Recently ^{137}Cs fluxes to marine sediments dramatically decreased. It means, that self-cleaning of water column takes part during the last years.

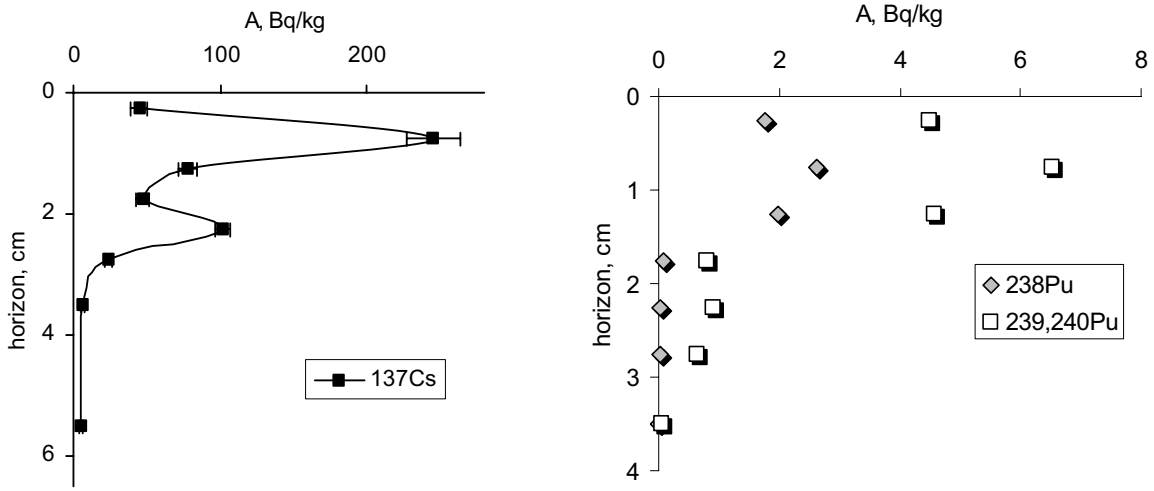

FIG.1. The vertical profiles of ^{137}Cs and Pu isotopes in the sediment cores from the Eastern Black Sea (Station BS-11 41°59.9' N 40°11.4' E), sea depth 1892 m.

In some cases the chronology of contamination by ^{137}Cs was proved by independent tracer – excess ^{210}Pb. In order to study the origin of the radioactive contamination the plutonium isotope ratios were used. The ^{241}Pu with a half-life period of 14.5 years served as sedimentation monitor together with $^{238}Pu/^{239,240}Pu$ and $^{241}Pu/^{239,240}Pu$ ratios [1]. The obtained data for Danube avandelta indicate that sediments are mixed and the radionuclides have both Chernobyl and fallout origin. The upper layers were mostly contaminated with Chernobyl plutonium whereas the relative content of fallout radionuclides increased in deeper layers. For the first time ^{237}Np specific activity data for the Black Sea sediments are presented [2].

REFERENCES

[1] ALIEV, R.A., KALMYKOV, ST.N., SAPOZHNIKOV, YU.A., "Man-made radionuclides in age-dated sediment cores from the Black Sea", Environmental radiochemical analysis II (WARWICK, P., Ed.), Royal Soc. Chem., Cambridge, UK, 254-262

[2] KALMYKOV, ST.N., ALIEV, R.A., SAPOZHNIKOV, D.YU., SAPOZHNIKOV, YU.A., AFINOGENOV, A.M., Determination of Np-237 by radiochemical neutron activation analysis combined with extraction chromatography, Appl. Radiat. Isot. 2004. **60** 2-4 (2004) 595-599.

Off-site environmental monitoring for radiological safety

Çelebi, N., G. Karahan, C. Özüag, B. Ataksor, E. Güngör, M. Taşdelen, M. Koçak

Çekmece Nuclear Research and Training Center,
Atatürk Airport,
İstanbul,
Turkey

Measurements of radioactivity in the environment for routine verification as well as in cases of emergency are very important for nuclear environmental safeguards. Radiological safety activities of Çekmece Nuclear Research and Training Center are provided as a part of the national program. Air samples from the environment were collected by the method of pumping air through the air filter for 1-day sampling to provide data on airborne activity concentration [1]. Measurements were done daily. Total alpha/beta radioactivity concentrations and gamma/beta dose rates at sample locations are measured. Air radioactivity concentrations are given in Table I. Water samples were taken monthly from Küçükcekmece Lake, the Marmara Sea and tap water and the radioactivity concentrations were evaluated with a Berthold gas proportional total alpha/beta counter. Annual average total alpha/beta radioactivity concentrations of environmental water samples are given in Table II. The concentrations of gamma emitters in air and water samples were determined by Canberra pure HPGe detectors with energies ranging from 50 keV to 2000 keV [2]. The software was prepared to create the data bank and the data management system. The input data in the software covers the period of 01.01.2003-01.02.2004.

Table I. Air radioactivity concentrations (Bq m^{-3})

Radioactivity type	Minimum	Maximum	Average
Alpha emitter	$1.89x10^{-3}$	$1.03x10^{-1}$	$1.24x10^{-2}$
Beta emitter	$1.92x10^{-3}$	$1.06x10^{-1}$	$1.36x10^{-2}$
Beta (after 7 days)	$1.05x10^{-4}$	$1.15x10^{-3}$	$7.02x10^{-4}$

Table II. Annual average total alpha/beta radioactivity concentrations of environmental water samples

Environmental water samples	Total Alpha Conc. (BqL^{-1})	Total Beta Conc. (BqL^{-1})
Rain Water	0.022±0.011	0.107±0.008
Snow water	0.015±0.009	0.092±0.014
Tap water (ÇNAEM)	0.006±0.002	0.054±0.015
Küçükçekmece Lake (Dock)	0.032±0.012	1.462±0.124
Küçükçekmece Lake (Kurtburnu)	0.025±0.014	1.425±0.545
Lake and Sea joint point	0.218±0.110	3.684±0.214
Marmara Sea (Florya)	0.207±0.009	4.344±0.322
Marmara Sea (Aksaray)	0.018±0.005	2.985±0.125

REFERENCES

[1] INTERNATIONAL ATOMIC ENERGY AGENCY, Measurement of Radionuclides in Food and the Environment, Technical Report Series **295,** IAEA, Vienna (1989).
[2] INTERNATIONAL COMMISSION ON RADIATION UNITS AND MEASUREMENTS, Gamma ray Spectrometry in Environment, ICRU Report **53,** Bethesda (1994).

Environmental monitoring of γ- and α- emitters in areas near Tomsk City (Siberia, Russia)

Choura, L.[a], G. Ardisson[b], V. Karataev[a], G. Barci-Funel[b], H. Michel[b], V. Barci[b]

[a] University Polytechnic of Tomsk,
Tomsk,
Russian Federation

[b] Laboratoire de Radiochimie, Sciences Analytiques et Environnement,
University of Nice Sophia-Antipolis,
Nice,
France

Nowadays, great attention is given to inspection of territories and estimation of existing radioactive situations. It is important to investigate territories about potential sources of radioactivity injections into a given environment, for example, such as the Siberian chemical complex (Tomsk - 7), which is located in the vicinity of Tomsk in the Southwest of Siberia.

Some of this potential sources of radioactive pollution are for example: the remnants of tests of nuclear weapons in the atmosphere (which began the sixties), the emissions of radioactive nuclides as a result of the Chernobyl accident, and the influence of the Siberian chemical complex. The complex was build in the middle of fifties and was intended to manufacture plutonium for industrial and military aims. During this time, in the complex there were some failures with emission of radioactive elements into the environment, the last one took place in 1993.

Our research focused on the inspection of the surrounding territory for man-made radionuclides. Soil samples were collected near to the sanitary - protective zone of the complex and about 55 km to the South. In the analyzed samples we measured the ^{137}Cs concentration by γ-spectrometry, $^{239,240}Pu$ and ^{238}Pu concentrations using radiochemical separation followed by α-spectrometry.

Our data on radionuclide concentrations and isotopic ratio allowed assessing the contamination sources of the area near the Tomsk city. Previous studies, performed in 1995, showed the absence of ^{134}Cs and therefore no influence of the Chernobyl accident. The higher concentrations of ^{137}Cs, $^{239,240}Pu$ is well as the isotopic ratio values near the complex allow asserting the influence of the Siberian chemical complex to the global activity of this region. However, in the territory far from the complex, the concentrations of made-man radionuclides are mainly due to the atmospheric tests of nuclear weapons.

Transport of radionuclides in and to Norwegian waters – 10 years of monitoring of the marine environment

Svaeren, I., H.E. Heldal, P. Alvestad, L. Føyn

Institute of Marine Research,
Bergen,
Norway

The Institute of Marine Research (IMR) is an advisory institute to the Norwegian Government on fisheries management, the marine living resources and the marine environment. In this capacity IMR conducts extensive monitoring of fish stocks, in particular, and the environmental conditions important for the various parts of marine life. Monitoring radioactivity is part of this, which comprises hydrography, contaminants, plankton, fish populations and demersal species as deep-water coral reefs. The monitoring of the various ecosystems allows us to consider a contaminant in a broader context than just the values and trend of that particular contaminant in itself. The history of monitoring radioactivity at IMR goes back to the late 1950s when atmospheric nuclear bomb tests took place in the eastern part of the Barents Sea and it was important for the Norwegian fisheries to have information on the possible radioactive impact to the Barents Sea fish stocks. The direct fall-out from the tests had a more or less immediate impact in fish, but mean values never exceeded 90 Bq kg^{-1} wet weight. The observations showed clear differences in uptake and seasonal differences between species [1, 2]. The atmospheric nuclear bomb tests ended in 1962 and IMR ended its monitoring programme in 1968, as it was believed at that time that radioactive contamination of the marine environment was something of the past. The Chernobyl-accident changed this picture, as did the accidents with nuclear submarines in the Barents Sea. Public awareness, and the fact that radioactive pollution became a political issue in Norway, released funding for new and more extensive monitoring in biota, sediments and water in areas important to Norwegian fisheries. In 1999 a national monitoring programme was established with the Norwegian Radiation Protection Agency (NRPA) as the coordinating institution.

The major sources for radioactive contamination in Norwegian waters are the nuclear industries in Europe, and Sellafield in particular, run-off from land to the Baltic Sea from Chernobyl fall-out and run-off to Norwegian fjords from areas in Norway contaminated by fall-out from the Chernobyl-accident. The transport routes from Europe, i.e. the southern North Sea, and the Baltic Sea follows the main currents, and contaminants are transported northwards along the coast mainly by the Norwegian Coastal Current into the Barents Sea and to the west of Spitsbergen and into the Greenland/Norwegians seas.

A much debated possible source for radioactive contamination is the sunken nuclear submarine “Komsomolets” situated at a depth of 1670 meters southwest of Bear Island at the entrance to the Barents Sea. IMR has monitored the site of the wreck regularly since 1992 without detecting any particular leaching from the nuclear devices in the wreck.

The fall-out from the Chernobyl-accident was unevenly distributed in the Nordic countries. The drainage of the areas around the Baltic Sea results in elevated values in the outflow from the Baltic Sea, through the Baltic Current, which continues along the Norwegian coast as the Norwegian Coastal Current. Some areas in Norway were particularly contaminated by the Chernobyl fall-out and this is now reflected in the sediments in the inner parts of the corresponding fjords.

Table I. Concentration of ^{137}Cs in marine organisms in samples from Norwegian waters 1992-2003.

Species	^{137}Cs Bq/kg dry wt.			^{137}Cs Bq/kg wet wt.			N. of samples	N. of individs.
	Min	Max	Mean	Min	Max	Mean		
Greenland halibut (*Reinhardtius hippoglossoides)*	0.8	2.30	1.6	0.2	0.6	0.4		102
Sprat *(Sprattus sprattus)*	0.8	6.20	2.1	0.3	2.1	0.6	18	
American plaice *(Hippoglossoides platessoides)*	0.8	1.3	1.0	0.2	0.3	0.2		195
Minke whale *(Balaenoptera acutorostrata)*	1.2	3.0	1.7	0.4	1	0.6		7
Withing *(Merlangius merlangus)*	1.9	8.9	4.0	0.4	2	0.9	6	
Haddock *(Melanogrammus aeglifinus)*	0.4	2.6	1.0	0.1	0.6	0.2		514
Salmon *(Salmo salar)*	0.4	6.5	2.2	0.2	2.3	0.7		146
Capelin *(Mallotus villosus)*	0.3	0.5	0.3	0.02	0.11	0.08	9	
Mackerel *(Scomber scombrus)*	0.7	2.8	1.2	0.13	0.5	0.2	6	
Harbour porpoise *(Phocoena phocoena)*	0.9	13.7	2.7	0.3	3.8	0.8		35
Arctic cod *(Boreogadus saida)*	nd	1.5	0.8	0.1	0.4	0.2	15	
Shrimp - mixed sample (Pandalus borealis)	<0.4	1.1	0.9	0.1	0.3	0.2	9	
Saithe *(Pollachius virens)*	1.1	5.8	1.7	0.2	1.2	0.3		81
Fry of saithe *(Pollachius virens)*	0.3	0.7	0.5				12	
Seal *(Phoca vitulina)*	1.5	3.4	2.3					10
Herring (Clupea harengus)	0.3	4.4	1.4	0.1	1.1	0.4	34	
Cod *(Gadhus morhua)*	0.6	6.8	1.4	0.1	1.2	0.3		940
Redfish *(Sebastes marinus)*	<0.3	2.0	1.1	0.1	0.4	0.3	13	
Stickleback (*Gasterosteus aculeatus*)			1.1			0.4	1	
Amphipods (*Themisto* sp.)			<0.8			0.1	7	
Cusk (*Brosme brosme*)						0.5	1	
Decapods *(Pandalus borealis*)						0.1	1	
Echinoderms (*Hippasteria phrygiana*)						0.3	1	
Leopardfish (*Anarhichas minor*)			1.1			0.2	1	
Squid (*Gonatus fabricii*)			<0.6				3	
Egg wrack (*Ascophyllum nodosum*)			0.6				2	
Atlantic catfish (*Anarhichas lupus*)			1.0			0.2	1	
Rat-tail (*Chimaera monstrosa*)			0.7			0.2	1	
Horse mackerel (*Trachurus trachurus*)	1.3	9.1	3.9	0.3	2.2	0.9	3	
Onion eye (*Macrourus berglax*)			1.4			0.3	1	
Starry ray (*Raja Amblyraja radiata*)			1.4			0.3	1	
Blue whiting (*Micromesistius poutassou)*			0.4			0.1	3	
Krill (*Euphausiacea*)			1.0			0.2	4	
Lemon dab (*Microstomus kitt*)			0.6			0.2	2	
Common hake (*Merluccius merluccius*)			5.2			1.1	1	
Lanternfishes (*Myctophidae*)			1.1			0.3	1	
Polychaetes (*Scalibregmidae*)						0.2	1	
Copepods (*Calanus finmarchicus*)			0.9				3	
Lumpfish (*Cyclopterus lumpus*)			<1.0				2	
Plaice (*Pleuronectes platessa*)			0.7			0.2	5	
Common dab (*Limanda limanda*)			0.9			0.3	5	
Juvenile herring (*Clupea harengus*)			0.5			0.2	4	
Sea cucumber (*Holothuroidea)*			<0.3			<0.1	1	
Starfish (*Asteriodea*)			0.1			nd	1	
Grey sole (*Glyptocephalus cynoglossus*)			<1.4			<0.4	1	
Deepwater redfish (*Sebastes mentella*)			0.7			0.2	4	
Poor cod (*Trisopterus minutus*)			1.7			0.1	1	
Tree-bearded rockling (*Gaidropsarus vulgaris*)			<3			<0.6	1	
Sandeel (*Ammodytes tobianus*)			0.5			<0.1	2	
Atlantic argentine (*Argentina silus*)			0.9			0.2	2	
Norway pout (*Trisopterus esmarki*)			0.8			0.2	5	
Vahls eelpout (*Lycodes vahli*)			<2.6			<0.5	1	

Table I shows data on radiocaesium in fish. The data covers the whole area of the regular fisheries surveys conducted by IMR and consist of both pelagic and demersal fish species. both commercial and non-commercial species. and in addition data from minke whales *(Balaenoptera acutorostrata)*. seals *(Phoca vitulina)* and harbour porpoise *(Phocoena phocoena)*. The highest ^{137}Cs values were found in one harbour porpoise. 13.8 Bq·kg^{-1} dry weight. in one whiting *(Merlangius merlangus)*. 8.9 Bq·kg^{-1} dry weight and in one horse mackerel *(Trachurus trachurus)* 9.1 Bq·kg^{-1} dry weight. The ^{137}Cs values determined in 940 cods *(Gadhus morhua)* ranged from 0.6 to 6.8 with a mean value of 1.4 Bq·kg^{-1} dry weight. All the mean dry weight values were found well below 5 Bq·kg^{-1}. For the corresponding wet weight mean values. they were all found to be below 1.5 Bq·kg^{-1}.

REFERENCES

[1] FØYN, L., Radioactive contamination in the Barents Sea. past and present status, uptake of radionuclides in fish and its impact on fisheries, ICES MEQC E **16** (1994).

[2] FØYN, L., SVÆREN, I., The Barents Sea its fisheries and the past and present status of radioactive contamination and its impact on fisheries (Int. Conf. Environ. Radioactivity in the Arctic, Oslo. Norway. August 21–25, 1995).

[3] FØYN, L., SVÆREN, I., Distribution and sedimentation of radionuclides in the Barents Sea, ICES J. Mar. Sci. **54** (1997) 333-340.

[4] HELDAL, H.E., VARSKOG, P., FØYN, L., Distribution of selected anthropogenic radionuclides (^{137}Cs, ^{238}Pu, ^{239,240}Pu and ^{241}Am) in marine sediments with emphasis on the Spitsbergen-Bear Island area, Sci Total Environ. **293** (2002) 233-45.

Management of GIS Database and multipurpose customization of computerized models of the contaminated aquatic and terrestrial ecosystems

Gheorghiu, D., R. Margineanu, D. Slavnicu

National Institute for Physics and Nuclear Engineering IFIN-HH,
Bucharest,
Romania

The experience of dealing with geographical and environmental data requests by different codes used for the assessment of radionuclide contamination and for the identifying the optimal remedial strategies for recovering the contaminated ecosystems conducted to the developing of an extended GIS database. This connects to the geographical features an Object Oriented database (OODB) comprising: population, land use, soil type and characteristics, hydrological networks (topologically defined, together with hydraulic parameters).

Two problems occurred during the process:

- The Price/Quality balance of the data: was solved using data source issued by profile research Institutes and the data acquiring with variable scale having higher resolution in the nuclear risk zones;
- The choice between Vector and Raster GIS data types: vector files were preferred, because these can be easily grid transformed.

The figures below present parts of source maps with attached database.

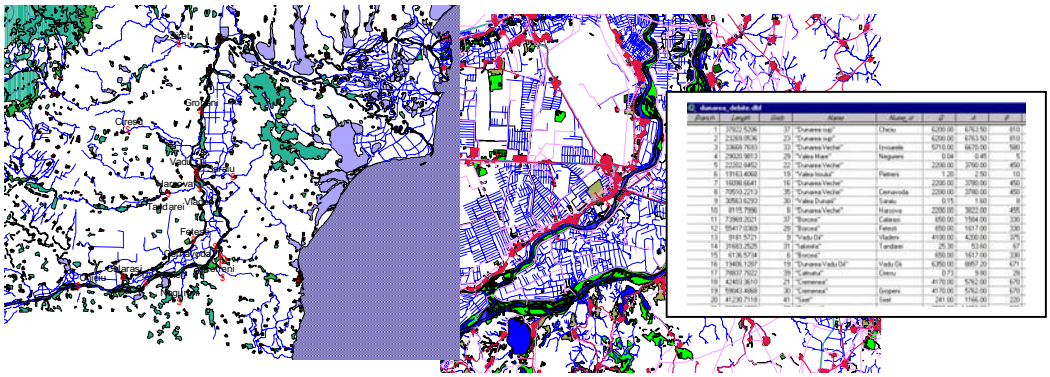

These GIS applications where used to extract, by SQL, necessary data for different environmental studies made in some projects:

EVANET-HYDRA Customisation of RODOS-Hydro [1] for Danube close to Romanian Cernavoda NPP:

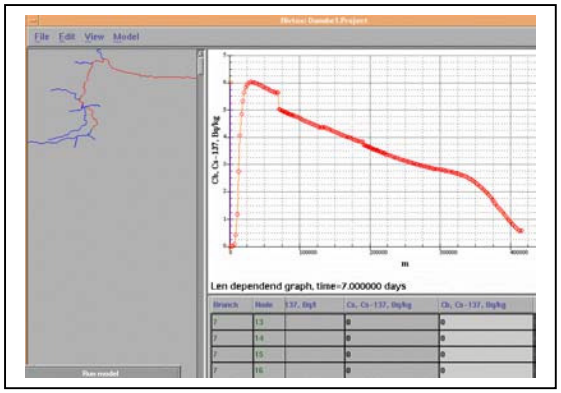

Cs-137 bottom concentration along the Danube river. RIVTOX Module.

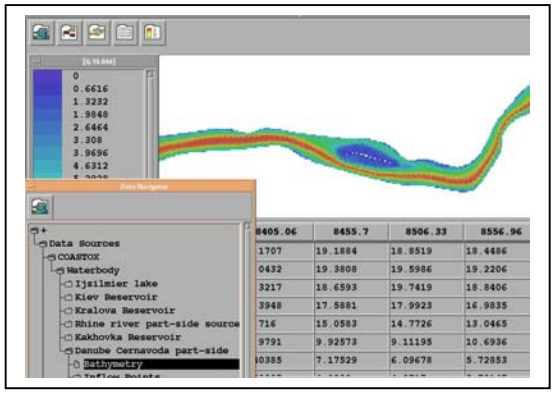

COASOTX module.

Customization of MOIRA [2]: A model-based computerized system for management support for restoring radionuclide contaminated aquatic ecosystems and drainage areas.

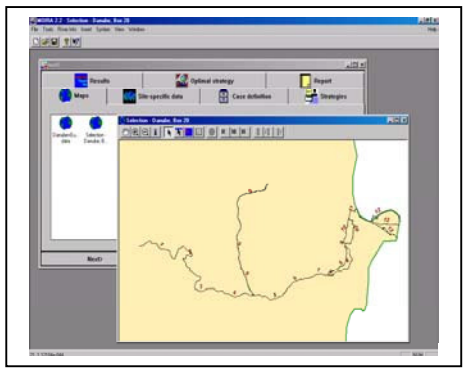

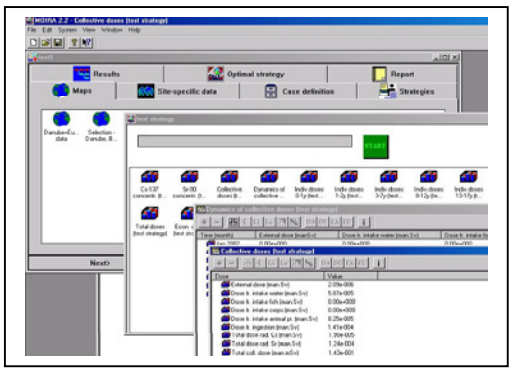

Using a common GIS database offers the possibility of intercomparison of simulated results of different models and codes.

REFERENCES

[1] HELING, R., RASKOB, W., POPOV, A., ZHELEZNYAK, M., Overview of Hydrological Dispersion Module-HDM of RODOS, RODOS-WG4-TN (99) 18.

[2] MONTE, L., Analysis of models assessing the radionuclide migration from catchments to waterbodies, Health Phys. **70** (1996) 227-237.

The prognosis of radioactive contamination of an environment of Belarus after catastrophe on Chernobyl NPP

Germenchuk, M., E. Shagalova, O. Zhukova

The Republican Centre of Radiation Control and Environment Monitoring,
Minsk,
Belarus

The area of contamination by ^{137}Cs after the Chernobyl accident higher than 37 kBq/m^2 amounts to 23.7% of the territory of Belarus, 7% of the territory of Ukraine and 1.5% of the European part of Russia. Most radioactive fallout was concentrated on the territory of the Republic of Belarus. In Belarus 46.45 thousand km^2 were contaminated with ^{137}Cs over 37 kBq/m^2. More than 3600 settlements including 27 towns are located in this area and 2.2 million people lived there. The important task in the post-accident period has been the estimation of the radioactive contamination of the territory of Belarus and the creation of specially oriented monitoring.

Radioactive contamination is non-uniform, having a "spotty" character even within the limits of one settlement. In Kolyban of Bragin district, Gomel region, the level of ^{137}Cs contamination varies from 170 to 2400 kBq/m^2. The maximum local level of the ^{137}Cs content in soil in the distant zone at the distance of 250 km has been registered in s.Chudyany of Cherikov district Mogilev region – 51000 kBq/m^2 (for local contamination).

Contamination by ^{90}Sr is of a more local character. Levels over 5.5 kBq/m^2 have been observed in an area of 21.100 km^2 that makes up 10% of the territory of the republic. The maximum levels of ^{90}Sr have been registered within the limits of 30-km from ChNPP and reach the level of 1800 kBq/m^2 in Khojniki district of Gomel region. The highest content in soils of the distant zone have been discovered at the distance of 250 km – in Cherikov district of Mogilev region and reaches up 29 kBq/m^2 and also in the north part of Gomel region in Vetka district – 137 kBq/m^2. Most ^{90}Sr contamination was concentrated on the territory of Gomel and partly Mogilev regions [1].

4.000 km^2 or about 2% of the territory of the republic have soil $^{238,239,240}Pu$ contamination exceeding 0.37 kBq/m^2. These territories are mainly situated in Gomel region and Cherikov district of the Mogilev region. So, the contamination of soil by plutonium isotopes from 0.37 to 3.7 kBq/m^2 has been registered in Gomel region. The content of plutonium in soil reaching 3.7 kBq/m^2 is characteristic of the 30-km zone of the Chernobyl NPP. The highest levels are observed in Khojniki district – more than 111 kBq/m^2. The numerical prognosis shows, that in Bragin town gamma exposure rates will be equal to level before the catastrophe on ChNPP approximately after 65 years, in Slavgorod and Chechersk towns – after 23-24 years.

The evolution of the extent of the area with ^{137}Cs contamination levels exceeding 37 kBq/m^2 was estimated using GIS:

- In 30 years (2016) the territory contaminated with levels in excess of 37 kBq/m² will be approximately 16%, i.e. a decrease with a factor 1,5 in comparison with 1986
- In 60 years (2046) contaminated surface will be approximately 10%, i.e. will decrease by a factor 2.4

Radioactive contamination of soils by ^{241}Am in Belarus is generally limited to the 30-km zone around the Chernobyl NPP. Maximum ^{241}Am levels will be reached in 2060 and will exceed the activity of ^{238,239,240} Pu approximately by a factor 2.

Research on the vertical migration of radionuclides in different soil types was carried out since 1992. Soil samples for analysis were sampled over a depth of 30 cm and radionuclides concentrations in different horizontal layers have been measured. Quasi-diffusion coefficients, mean diffusion coefficients and linear velocities for ^{137}Cs and ^{90}Sr were found with using two-component quasi-diffusion model of vertical migration of radionuclides. Prognosis of relative content of ^{137}Cs and ^{90}Sr in the depth of the soil profile for various types of soil was obtained.

Analysis of obtained data revealed that the main content of ^{137}Cs is located in 0-5 cm layer of turfy-podzolic, sandy-loam and loamy soil in case of low soil moisture, and of light unbogged (automorphous) soil. ^{137}Cs migration in moist light unbogged soil is approximately 10 cm deep. ^{90}Sr generally migrates faster than ^{137}Cs because of less strong bond with soil absorbing complex. The linear velocity and migration coefficients are shown in Table I.

^{137}Cs migration coefficients amounted to $(0.03\text{-}0.46)\cdot10^{-7}$ cm^2/s for a slow component, and for the fast one $(0.39\text{-}0.67)\cdot10^{-7}$ cm^2/s [4]. ^{90}Sr is characterised by higher migration rate. Correspondingly, the contribution of a fast-migrating component is more important, on average 30-60%. ^{90}Sr migration coefficients at the experimented sites amounted to $(0.07\text{-}0.58)\cdot10^{-7}$ cm^2/s for the slow component, and for the fast one $(0.64\text{-}1.28)\cdot10^{-7}$ cm^2/s. In comparison with ^{137}Cs, the more substantial ^{90}Sr transport from upper to lower soil layers is linked with a relatively high content of mobile forms (water-extractable, exchange, mobile). Even under conditions of limited humidification, the ^{90}Sr migration is faster [2].

Table I. Speed of linear migration V, and migration coefficients D_s, of ^{137}Cs and ^{90}Sr in soils of different genesis

Type of soil	Slow component		Fast component	
	V cm/y	Ds 10^{-7} cm^2/s	V cm/y	Ds 10^{-7} cm^2/s
^{90}Sr				
Soddy-podzolic and sandy-loam. sand-laid (automorphous)	0.17	0.07	0.53	0.64
Soddy-podzolic sandy and sandy-loam with redundant moistening signs; soddy-podzolic-gley (sandy. sandy-loam. gley-loam) as well as with alluvial humus horizon	0.42	0.39	0.66-0.72	0.91-1.28
Soddy-gley	0.46	0.58	0.70	1.17
Peaty-marshy	0.34	0.28	0.52	0.64
^{137}Cs				
Soddy-podzolic and sandy-loam. sand-laid (automorphous)	0.12	0.03	0.43	0.39
Soddy-podzolic sandy and sandy-loam with redundant moistening signs; Soddy-podzolic-gley (sandy. sandy-loam. gley-loam) as well as with alluvial humus horizon	0.35	0.18-0.28	0.46-0.52	0.47-0.64
Soddy-gley	0.23	0.10	0.50	0.53
Peaty-marshy	0.44	0.46	0.52	0.67

Table II. Prognosis of dynamics of average ^{137}Cs concentrations in some monitored rivers of Belarus for 2010

River, point of observation		Average ^{137}Cs concentration, Bq/L	
		Year 2000	Predicted 2010
1	Dnieper (t.Rechitsa)	0.016	0.001
2	Sozh (t.Gomel)	0.022	0.002
3	Iput (t.Dobrush)	0.048	0.004
4	Besed (s.Svetilovichi)	0.022	0.002
5	Pripyat (t.Mozyr)	0.015	0.002

The data from radiation monitoring of water bodies show that radiation situation on the rivers of Belarus has stabilized. The average concentration of ^{137}Cs in rivers of Belarus for the period 1987-2001 has considerably decreased. Average concentrations of ^{137}Cs in rivers in contamination territories for the period 1987-2001 were the following: for the Pripyat – (0.28–0.008) Bq/L, for the Dnieper – (0.27–0.01) Bq/L, for the Sozh – (1.6–0.016) Bq/L, for the Iput – (2.3–0.022) Bq/L, for the Besed – (0.7–0.013) Bq/L. Average concentrations of ^{137}Cs in all the controlled rivers are lower than Republican Permissible Levels for drink water [3]. Prognosis of dynamics of average ^{137}Cs concentrations in some rivers of Belarus for 2010 is given in Table II.

In conclusion we may say:

1. The analysis of the evolution of the area under contamination exceeding 37 kBq/m² for the period 1986-2046 shows, that in 30 years (2016) the territory contaminated with levels in excess of 37 kBq/m² will decrease to approximately 16%, i.e. a decrease by a factor 1.5 in comparison with 1986; in 60 years (2046) the contaminated surface will be approximately 10%, i.e. it will decrease by a factor 2.4.

2. Radioactive contamination of soils by ^{241}Am in Belarus is generally limited to the 30-km zone around the Chernobyl NPP. Maximum ^{241}Am levels will be reached in 2060 and will exceed the activity of ^{238,239,240}Pu by approximately a factor of 2.

3. Most of ^{137}Cs is located in the 0-5 cm layer of typical soils of Belarus.

4. The radiological situation of the rivers in Belarus has stabilized. The average concentrations of ^{137}Cs in rivers for the period 1987-2001 have considerably decreased. They are lower than the Republican Permissible Level for drinking water.

REFERENCES

[1] MATVEENKO, I.I., ZHUKOVA, O.M., GERMENCHUK, M.G., State and projection of the radiation on the territory of Belarus after Chernobyl accident, J. Radioanal. Nucl. Chem. **229** (1998) 19-21.

[2] SHAGALOVA, E., et al., Dynamics of radiation situation on the territory of Belarus and migration of radionuclides in different types of soils after Chernobyl catastrophe, J. Radioanal. Nucl. Chem **246** (2000) 521-525.

[3] ZHUKOVA, O., SHIRYAEVA, N., SHAGALOVA, E., Water migration of Chernobyl radionuclides in rivers of Belarus, The Radioecology-Ecotoxicology of Continental and Estuarine Environments (Proc. Int. Congress, Aix-en-Provence, France), EDP Sciences V.**II**. (2002) 723-728.

The annual variation of ^{238}U concentration and $^{234}U/^{238}U$, $^{235}U/^{238}U$ ratios in Greek rivers

Kehagia, K., S. Bratakos, V. Koukouliou, C. Potiriadis

GAEG,
Environmental Radioactivity Monitoring Department,
Athens,
Greece

In the framework of the environmental radioactivity monitoring in the country, systematic measurements are performed in river waters. Moreover, and because of, uranium mining activities performed in the past close to the northern Greek borders, measurements of the concentration of uranium isotopes are included in the measured parameters. In addition to that, the non-existence of depleted uranium (DU) in these rivers is verified, since an awareness of the Greek population exists as a consequence of the Kosovo conflict.

More specifically, a set of measurements of ^{238}U, ^{234}U and ^{235}U has been performed on a monthly basis, during the last three years, for the four rivers crossing the Greek northern borders (Table I). The water samples, collected always at the same sampling points, were measured by means of α-spectroscopic analysis after appropriate radioanalytical treatment. The source preparation was done by electrodeposition. The identification of the existence of DU is based on the determination of the concentration ratios of $^{235}U/^{238}U$ and $^{234}U/^{238}U$.

Since the ratio $^{235}U/^{238}U$ cannot be influenced by any physical or chemical process in nature, it is expected to be constant and independent of the origin of the sample. Any statistically significant difference from the natural ratio must be attributed to anthropogenic activities (e.g. DU). However, many measurement uncertainties exist due to the low activity concentration of the ^{235}U in samples containing natural uranium, in relation to the activity concentration of ^{238}U. For this reason, the variation of $^{234}U/^{238}U$ is used complementarily as an indicator of the existence of DU.

The ^{238}U concentration in river waters is relatively constant for each river, lying between (15.12-86.04) mBq/L or (1.22-7.03) μg/L, within the range of the values found in [1-3], with the exception of slightly increased concentration at the Strymonas river for the year 2003 (Table II). The determined $^{235}U/^{238}U$ ratio in this work was 0.048 ± 0.020, indicating as expected, the above-mentioned high uncertainty. As concerns the concentration ratio of $^{234}U/^{238}U$, the observed values in the present study are between 1.09-1.32, lying in the range of 0.8-10 as reported in [4] for natural waters.

Table I. General information on the rivers under examination

River	Area (ha)	Location	Flows from
Nestos	21.930	East Macedonian and Thrace, between Xanthi and Kavala	Bulgaria
Axios	11,808	North Greece, 20 km southwest of Thessaloniki	FYROM
Ardas-tributary of Evros	9.267	Trace-border with Turkey, 15km west site of Alexandroupolis	Bulgaria
Strymonas	1.500	Central Macedonia, near the city Serres	Bulgaria

Table II. Average concentration of ^{238}U measurements in four Greek rivers

Year	River	**Average Activity ^{238}U (mBq/L)**	**Range of ^{238}U activity(mBq/L)**	**$^{234}U/^{238}U$ (mBq/mBq) (range)**
2001	Nestos	49.40	27.54-78.66	1.10-1.19
2002	Nestos	30.65	12.34-52.33	1.09-1.27
2003	Nestos	40.89	17.85-61.12	1.10-1.18
2001	Axios	17.05	7.41-25.15	1.07-1.35
2002	Axios	15.12	8.04-23.89	1.15-1.43
2003	Axios	17.08	11.51-27.11	1.16-1.55
2001	Strymonas	37.10	19.04-52.41	1.00-1.15
2002	Strymonas	27.58	17.40-46.22	1.04-1.23
2003	Strymonas	86.04	19.68-340.00	1.00-1.20
2001	Ardas	13.44	8.65-20.05	1.16-1.37
2002	Ardas	14.40	12.49-17.04	1.16-1.40
2003	Ardas	15.78	12.75-19.03	1.22-1.42

In conclusion, systematic measurements in Greek rivers indicate that the ^{238}U concentration is in the natural range. Moreover, no DU contamination has been identified.

REFERENCES

[1] HESKETH, G.E., Natural Radioactivity in water, J. Soc. Radiol. Prot. **2** 3 (1982) 11-14.
[2] WANG, J.J., CHU, T.C., Radioactive Disequilibrium of Uranium and Thorium Nuclide Series in Hot Spring and River Water from Peitou Hot Spring Bain in Taipei, J. Nucl. Radiochem. Sci. **1** 1 (2000) 5-10.
[3] RAY, S.B., MOHANTI, M., SOMAYAJULU, B.L.K., Uranium Isotopes in the Mahanadi River-Estuarine System, India, Est. Coast. Shelf Sci. 40 (1995) 635-645.
[4] GOLDSTEIN, S.J., RODRIGUEZ, J.M., LUJAN, N., Measurement and Application of Uranium Isotopes for Human and Environmental Monitoring, Health Phys. **72** 1 (1997) 10-18.

Field study of sedimentation and radionuclide pollution of the Black Sea

Yesin, N.V., R.D. Kos'yan

The Southern Branch of the P.P. Shirshov Institute of Oceanology,
Russian Academy of Sciences,
Gelendzhik,
Russian Federation

The Black Sea is a unique semiclosed basin with a great surplus of fresh water, which flows, in the end, to the Marmara Sea through the Bosphorus. In Pleistocene-Holocene eras, when the level of the world ocean oscillated with the amplitude of 120 meters, regressive level of the Black Sea depended on the depth of the Bosphorus Strait, and it was always higher than that of the world ocean. Surplus of the fresh water promoted the sea water freshening during regressions. Sea salting took place during transgressions as a result of forming of countercurrents in the Strait. Periodic changes of sea water salinity and peculiarities of sedimentation in the Bosphorus strait promoted in Pleistocene the formation of alternated layers of coccolites and sapropels in a deep basin of the sea.

In view of great difficulties caused of varied conditions of sedimentation mechanism of terrigenic material transport to the sea abyssal in different stages of transgression and regression has not been completely studied till today, there are still no comprehensive data about the rate of sedimentation.

Research, fulfilled in expeditions within the project RER/2/003 by IAEA, afforded not only to study the process of the Black Sea bottom pollution by radionuclides after the nuclear weapon tests in atmosphere and the Chernobyl accident, but to obtain information concerning to the principal regularities of sedimentation. In this report the following questions are discussed: transport of radionuclides and their settling to the bottom: peculiarities of sedimentation within the abyssal plain, shelf and continental slope; modern rates of sedimentation according to the results of expeditions in 1998 and 2000.

The weight of solid particles in the upper sedimentary layer is 0.1 g. If we take into account density of water which fills the main volume of sample, then density of suspended matter is somewhat less (1.1 g/cm^3). The upper layer of the core is not a sediment yet, but it is a suspension flowing down the sea bottom. At the depth of 5 cm the weight of dry sediment in 1 cm^3 increases to 0.3 g/cm^3, and density of suspension, roughly to 1.28 g/cm^3, and this indicates the initial stage of the litification process.

When the depth becomes larger pressing of water from the sediment takes place under the pressure of upper layers and the decrease of sediment volume happens. As if sediment compression occurs with the simultaneous increase of its density. Thus, for instance, layer of sediment 1 cm thick, when it sinks down larger depth in the sedimentary strata, becomes thinner and the rate of sedimentation decreases. Therefore it is more expedient rate of sedimentation consider as the amount of solid sediment settling during the time unit for 1 cm^2 of the sea bottom area.

It seems to be possible to estimate a degree of compression of the upper sedimentary layer on the data of cores. As it is found, at the depth of 40 cm density of sediment increased in 1.08 times, as compared with the upper layer, 0.08 g/cm^3, and this points to an inconsiderable compression.

Available to the authors core material, 4/5 m long, sampled at the depth of 1935 m within the Russian section of the Black Sea, afforded to calculate maximum possible density of dry sediment. It turned

out to be from 2.6 to 3.1 g/cm^3 depending on mineral composition. Thus, the upper layer of sediment with density being 1.2 g/cm^3 in the moment of litification will be compressed from 2.2 to 2.6 times when the depth becomes greater. To compare modern rates of sedimentation and ancient ones it is necessary to enlarge the thickness of the ancient layer for 2.6 times depending on the depth.

We can estimate a mean rate of sedimentation on the shelf of the above mentioned region in the Holocene. An average velocity of the Black Sea level rise was 6 mm/year (120 meters for 20 thousand years). Therefore, at the depth of basic bottom being 60 m (modern), sea level was 10 thousand years later than the beginning of the transgression, and a process of sedimentation began here when the sea level rose for 20 m more, i.e. 3.3 thousand years later (20000 mm: 6 mm/year). Thus, the duration of sedimentation at this shelf section is 20 thousand years – 10 thousand years – 3/3 thousand years = 6.7 thousand years. During this period a sedimentary layer, 8 m thick, was formed here. Hence, a mean rate of sedimentation in Holocene was 8000 mm: 6700 years = 1.2 mm/year. But a modern rate, estimated on the data of RER/2/003 project, is from 4.5 to 5.5 mm/year (at the different sections of the shelf). If we take into consideration a coefficient of compression being 2.2. then we get the velocity of the bottom rise 7.3 years ago being 1.2 mm/year x 2.2 = 2.6 mm/year. This value of a mean rate of sedimentation is comparable with the modern rate of sedimentation (with regard to the fact that a value, taken as a basis of calculation, is not quite precise one). At the same time, there are grounds to conclude that during the last century rate of sedimentation at the given section increased. This may be explained by the intensification of economic activity on the shore, increase of land erosion and coast abrasion, increase of solid run-off and of rivers and piped drainage systems.

In conclusion it is possible to note, that the results of research within the RER/2/003 project afforded to reveal peculiarities of sedimentation process on the shelf, continental slope and abyssal plain. They show the presence of suspension flows everywhere on the shelf and continental slope.

Plutonium in components of the Techa – Ob river ecosystem

Kryshev, I.I., A.I. Kryshev

Scientific and Production Association "Typhoon",
Obninsk,
Russian Federation

The Techa River is part of the hydrological system Techa-Iset-Tobol-Irtysh-Ob, which belongs to the Kara Sea basin. The Techa River is 243 km long, and its catchment area is 7600 km^2. The river depth varies from 0.5 m to 2 m, and its width is, on the average, 15-30 m. The main sources of radioactive contamination of the Techa River were discharges of radionuclides during the period 1949-1956. To reduce the radionuclide transport, a system of bypasses and industrial reservoirs for storage of low-activity liquid wastes was constructed in the upper reaches of the Techa River during the period 1956-1965. The subject of this paper is the assesment of radioecological consequences from plutonium contamination in the Techa – Ob River ecosystem.

Data of observations on the ^{239,240}Pu content in components of the Techa River ecosystem were generalized, including activity concentrations of plutonium in water, bottom sediments, fish, floodplain soil and vegetation (Table I) [1-6]. Distribution of plutonium in the Techa ecosystem is not uniform. The highest activity concentrations of this radionuclide were observed at the upstream part of the Techa River. Floodplain of the upper river is major source of intake of radionuclides, as a result of wash-off of radionuclides from the floodplain soil and bottom sediments. Activity concentrations of ^{239,240}Pu in the Techa floodplain are maximum near the river-bed and decrease close to the background levels at the bounds of overflow. Activity concentrations of ^{239,240}Pu in floodplain soil (layer 0 – 20 cm) at the upstream part of the Techa River vary within the range 2 – 3300 Bq/kg d.w. Plutonium concentrations in floodplain soil at the middle and downstream parts of the Techa River are 10 and 30

Table I. Activity concentrations of ^{239,240}Pu in components of the Techa River ecosystem (1990 – 1995), Bq/kg

Component	Upstream part (0-40 km)	Middle part (40-120 km)	Downstream part (120-200 km)
Water	0.03 ± 0.02 (N=17)	0.009 ± 0.006 (N=8)	0.004 ± 0.003 (N=7)
Bottom sediments	290 ± 270 (N=32)	49 ± 41 (N=10)	1.8 ± 1.3 (N=10)
Aquatic plants	$15 \pm 2^*$	$3.8 \pm 0.2^*$	$0.35 \pm 0.04^*$
Fish	$0.026 \pm 0.003^*$	$0.008 \pm 0.002^*$	
Floodplain soil	310 (2-3300) (N=160)	29 (2-319) (N=56)	9 ± 8 (N=38)
Grass	62 ± 57 (N=9)	5.2 ± 1.8 (N=6)	$1.1 \pm 0.3^*$

* Data of single measurement. Activity concentration in bottom sediments, floodplain soil and grass are given in Bq/kg dry weight, in fish – in Bq/kg wet weight.

Table II. Contribution of ^{239,240}Pu to dose to biota of the Techa River (1990 – 1995), mGy/year

Organisms	Upstream part	Middle part	Downstream part
Fish	0.00068 (0.0136)	0.0002 (0.004)	
Aquatic plants	0.078 (1.56)	0.019 (0.38)	0.0018 (0.036)
Grass	0.48 (9.6)	0.04 (0.8)	0.0086 (0.172)

Assessments of exposure with w_r=20 for for α-radiation are given in brackets.

times lower , correspondingly, than those at the upstream part; at the same time they remain higher than the regional background level. Activity concentrations of plutonium in floodplain soil and bottom sediments of the Iset and Tobol Rivers (500 – 700 km from the upper Techa River) are close to the background level.

Plutonium content in bottom sediments, water and river biota decrease with a distance from the river head (dam of the technical water-body 11). Accumulation factor of ^{239,240}Pu in bottom sediments at upstream part of Techa is equal to 10000, whereas at middle part it is equal to 5000. Activity concentrations of ^{239,240}Pu in water is considerably (20 – 140 times) lower than the current permissible level 0.56 Bq/kg. Among the samples of river biota grass and aquatic plants have maximum content of plutonium.

Two variants of estimation of the ^{239,240}Pu contributions to dose to the river biota are presented in Table II: absorbed dose (α-particles were assumed to be totally absorbed within the organisms); and hypothetical analogue of equivalent dose evaluated with radiation weighting factor for α-particles w_r=20.

According to Ref. [7], internal doses to the Techa fish and aquatic plants from ^{90}Sr and ^{137}Cs in 1992 varied in range 1 – 10 mGy/year, which were considerably higher than the absorbed doses from plutonium. However, role of plutonium in exposure to vegetation in the upstream part of the Techa River become noticeable if we use in calculations the radiation weighting factor w_r=20 for α-particles.

ACKNOWLEDGEMENT

This work has been performed within the framework of ISTC Project 2558. The authors are grateful to ISTC for support of this study.

REFERENCES

[1] MARTYUSHOV, V.V., et al., Ekologia **5** (1997) 361-368.
[2] KRYSHEV, I.I., (Ed.), Environmental Risk Analysis for the Ural Radioactive Pattern. Moscow, Russian Nuclear Soc. (1997) 210 pp.
[3] NORWEGIAN RADIATION PROTECTION AUTHORITY, Sources contributing to radioactive contamination of the Techa river and areas surrounding the MAYAK Production Association, Urals, Russia (1997).
[4] TRAPEZNIKOV, A.V., et al., Problems of Radioecology and Boundary Branches **2** (1999) 20-66.
[5] ILYIN, L.A., GUBANOV, V.A., (Eds.), Major radiation accidents: their consequences and protection measures, Moscow, IzdAT (2001) 752 pp.
[6] AKLEEV, A.V., KISSELYOV, M.F., Medical-Biological and Ecological Impacts of Radioactive Contamination of the Techa River, Chelyabinsk, Urals Research Center for Radiation Medicine (2002) 88-92.
[7] KRYSHEV, I.I., et al., J. Environ. Radioactivity **38** 2 (1998) 195-209.

Mass accumulation rates and fallout radionuclides ^{210}Pb, ^{137}Cs and ^{241}Am inventories determined in radiometrically dated abyssal sediments of the Black Sea

Laptyev, G.V.[a], O.V. Voitsekhovitch[a], A.B. Kostezh[a], I. Osvath[b]

[a] Ukrainian Institute for Hydrometeorology (UHMI),
Kiev,
Ukraine

[b] Marine Environment Laboratory (MEL),
International Atomic Energy Agency,
Monaco

Five abyssal (deep-sea) sediment cores collected during the two international cruises onboard the R/V "Professor Vodyanitskiy" (RADEUX-1998 and RADEUX-2000) in the framework of the Regional Technical Co-operation Project RER/2/003 "Marine Environmental Assessment in the Black Sea Region" were subjected to detailed radiometric analysis. The sediments were dated using the radionuclides ^{210}Pb, ^{137}Cs and ^{241}Am and the results used to calculate a number of key parameters, e.g. radionuclide inventories, fluxes and sediment accumulation rates (Table I).

The sediment cores were collected using a MARK II-400 multi-corer (Bowers & Connelly) in both Western and Eastern sub-basins of the Black Sea. The cores were sliced on board with a resolution of 0.2 – 0.4 cm for the top 5 cm and 1-5 cm downward using an extruder that was specially designed to prevent loss of the uppermost fluff-layer, possible down-smearing and interlayer cross-contamination of the sediment. Dry bulk density (DBD) and cumulative dry mass (CDM) were calculated on a salt-free basis using direct determination of the salt contribution to the dry mass of the sediment. Calculations showed that in the near surface sediments, and particularly in the top fluff-layer, the salt dissolved in pore-water contributed up to 30-60% of the mass of dried sediments. Neglecting this correction could cause an erroneous interpretation of the ^{210}Pb activity profile, resulting in overestimation of both the average sedimentation rate and its recent temporal changes.

Sediment samples were analysed for ^{210}Pb, ^{226}Ra, ^{137}Cs and ^{241}Am by direct gamma assay in UHMI after 3 weeks equilibration in hermetically sealed plastic holders, using an EG&G Ortec (Ametek) HPGe GWL series well-type coaxial low background intrinsic germanium detector [1]. Correction was made for the effect of self-absorption of low energy γ-rays within the sample using attenuation parameters determined in [2].

Chronostratigraphical analysis of the data and sediment age calculation have been carried out by application of CRS and CIC dating models [3] to unsupported ^{210}Pb activity profiles which were calculated by subtracting ^{226}Ra activity from the total ^{210}Pb.

The results obtained suggest that the recent deposition history of the deep-sea sediments (last 100-150 years) is recorded in the upper 10 cm, which corresponds to the ^{226}Ra-^{210}Pb equilibrium depth. There were no statistically significant changes in the mass accumulation rates (MAR) over the last century, which ranged between 35-85 g m^{-2} y^{-1} at various sites.^{137}Cs and ^{241}Am activity profiles showed well resolved peaks for both bomb test and Chernobyl fallout, with the two maxima in activity corroborating that these deep-sea sediments are not being affected either by bioturbation or mechanical mixing. For the first time in a post-Chernobyl study ^{241}Am records were detected in the upper sediments, revealing a previously underestimated impact of the nuclear fuel component of the Chernobyl fallout on the Black Sea [4]. The ^{241}Am inventory almost doubled in both the western and

eastern sectors of the sea after Chernobyl, from 8-10 Bq m^{-2}, to 16-17 Bq m^{-2} by the year 2000. Taking into account the ingrowth of ^{241}Am due to the decay of its parent radionuclide ^{241}Pu, a further double increase of the ^{241}Am inventory in the following 60 years can be expected.

The increase of the ^{137}Cs inventory in Black Sea sediment after Chernobyl was up to 300-600 Bq m^{-2}. Comparing the results of ^{210}Pb chronology, ^{137}Cs total inventory and the relative position of peaks within the sediment cores in the present and previous studies [5, 6] yields an estimate of 3 to 6 years for the time required by particles carrying radionuclides to sink from the sea surface to the bottom (~2000 m).

Table I. MAR, ^{210}Pb flux and radionuclide inventories in Black Sea bottom sediment cores

Core	Depth (m)	MAR (g m^{-2} y^{-1})	^{210}Pb Flux (Bq m^{-2} y^{-1})	Radionuclide inventory (Bq m^{-2})		
				^{210}Pb	^{137}Cs	^{241}Am
BS98-15	1375	41	142 ± 3	4570 ± 109	192 ± 7	8.6 ± 1.0
BS2K-4	2147	35	177 ± 3	5690 ± 88	303 ± 6	10.9 ± 0.9
BS2K-11	1892	83	225 ± 3	7230 ± 106	598 ± 13	9.7 ± 1.1
BS2K-23	2168	41	173 ± 3	5543 ± 93	517 ± 12	16.1 ± 1.8
BS2K-37	2008	45	239 ± 4	7666 ± 125	610 ± 16	19.0 ± 1.1

ACKNOWLEDGEMENTS

The results presented were obtained in the framework of the IAEA Regional Technical Co-operation Project REP/2/003 “Marine Environmental Assessment in the Black Sea Region”. The authors are also very grateful to Prof. Peter G Appleby, Director of the University of Liverpool ERRC, for valuable discussions on ^{210}Pb dating techniques. The Agency is grateful for the support provided to its Marine Environment Laboratory by the Government of the Principality of Monaco.

REFERENCES

[1] APPLEBY, P.G., NOLAN, P.J., GIFFORD, D.W., GODFREY, M.J., OLDFIELD, F., ANDERSON, N.J., BATTARBEE, R.W., ^{210}Pb dating by low background gamma counting, Hydrobiologia **141** (1986) 21-27.

[2] APPLEBY, P.G., RICHARDSON, N., NOLAN, P.J., Self-absorption corrections for well-type germanium detectors, Nucl. Inst. Meth. B **71** (1992) 228-233.

[3] APPLEBY, P.G., OLDFIELD, F., The calculation of ^{210}Pb dates assuming a constant rate of supply of unsupported ^{210}Pb to the sediment, Catena **5** (1978) 1-8.

[4] BUESSELER, K.O., LIVINGSTON, H.D., "Natural and man-made radionuclides in the Black Sea", Radionuclides in the ocean: inputs and inventories, France, IPSN, Editions de Physique (1996) 199–217.

[5] BUESSELER, K.O., BENITEZ, C.R., Determination of mass accumulation rates and sediment radionuclide inventories in the deep Black Sea, Deep-Sea Res. I **41** 11/12 (1994) 1605–1615.

[6] GULIN, S.B., Recent changes of biogenic carbonate deposition in anoxic sediments of the Black Sea: sedimentary record and climatic implication, Mar. Environ. Res. **49** (2000) 319-328.

Multivariate statistics in the identification of unknown nuclear material

Nicolaou, G., N.F. Tsagas

Department of Electrical and Computer Engineering,
School of Engineering,
Demokritus University of Thrace,
Xanthi,
Greece

The identification, and hence origin determination, of unknown nuclear material that might be found undeclared away from designated locations in the nuclear fuel cycle, is an important task in the frame of nuclear forensics. Material with forensic importance can be found at the microscopic level, as particles in environmental samples, indicating possible clandestine production of fissile material, and as bulky samples in the case of illicit trafficking of nuclear material.

The objective of this work is to present, at a theoretical level, an isotopic finger-printing methodology which would determine the origin of unknown nuclear material with forensic importance. This is demonstrated for the case when the unknown nuclear material is spent nuclear fuel.

The methodology is based on multivariate statistics, such as cluster and factor analysis, complemented by spent fuel isotopic composition simulations using the zero-dimensional depletion computer code ORIGEN2 [1]. A major source of error in the calculation of the evolution of the fuel in a reactor is the burnup dependence of the cross-sections used. The cross-section libraries should accurately represent a given reactor-fuel system. The procedures followed and associated limitations are discussed.

The origin is determined from the characterisation of the material in terms of its initial enrichment, reactor type and burnup. The characterisation is based on the fact that the composition of spent nuclear fuel in individual nuclides is inherently consistent. A given composition of spent nuclear fuel, being the outcome of its initial composition, reactor type and irradiation history, should characterise uniquely the fuel and hence identify its origin.

The sought characterisation of the unknown spent nuclear fuel material is obtained from the comparison of its actinides and fission products content, with isotopics calculated with ORIGEN2 for a range of commercial spent fuels from PWR (UO_2 and MOX), BWR, CANDU and FBR. This comparison is performed through the cluster and factor analysis. Then, the origin of the set of calculated isotopics that closer resembles the unknown indicates the origin of the unknown.

Figure 1 shows a typical plot of factor analysis. The plot is demonstrated for a range of commercial spent fuels from PWR-UO_2 (var. 1 to 9) and PWR-MOX (var. 10 to 13). The term range refers to different initial enrichments and final burnup as encountered in nuclear power stations.

It is clearly seen that, on the basis of the actinide and fission product content which are calculated with ORIGEN2 for the range of fuels considered, two families of fuels are distinguished, namely those of UO_2 and MOX. This demonstrates that, on the basis of composition, same type of fuels are grouped together allowing the sought identification of unknown nuclear spent fuel when these are included in the analysis.

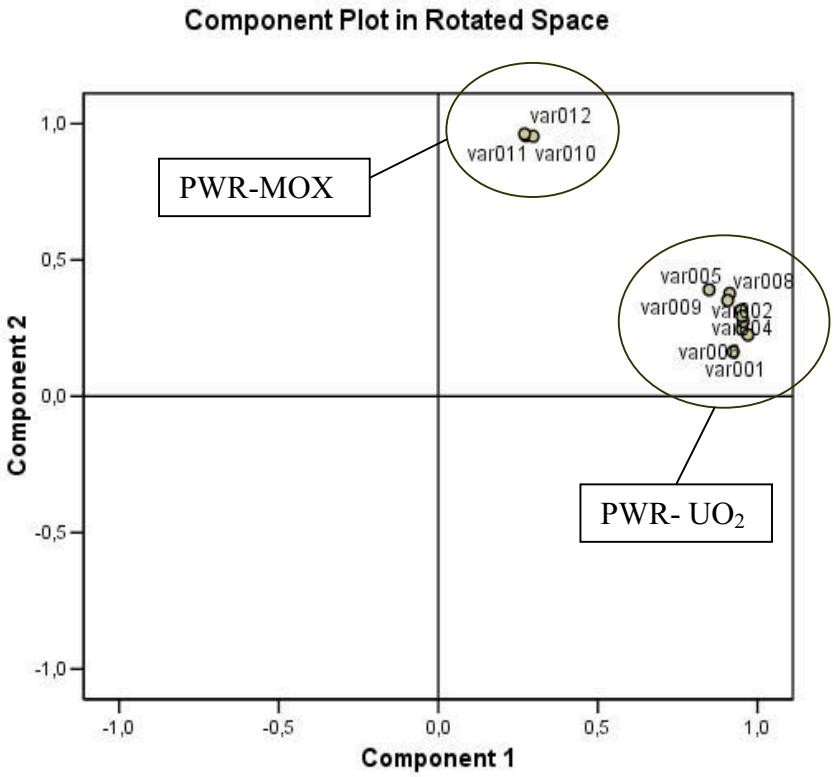

FIG. 1. Factor analysis plot.

REFERENCE

[1] CFOFF, A.C., ORNL/TM-7175, Oak Ridge National Laboratory (1980).

Radioactivity control of the Danube ecosystem

Pantelic, G.[a], I. Tanaskovic[a], V. Vuletic[a], P. Vancsura[b], A. Lengyel Varga[b]

[a] Institute of Occupational Health and Radiological Protection "Dr. Dragomir Karajović", Belgrade,
Serbia and Montenegro

[b] Environmental Protection Inspectorate Lower Danube Valley Region,
Baja,
Hungary

The samples from the Danube ecosystem were taken at the border profiles: Bezdan (Serbia) and Mohacs (Hungary), from 1997 to 1998 four times a year, and from 1999 six times annually [1].

The water samples were taken at three profiles of the Danube (left bank, middle, and right bank of the river), by peristaltic pump into plastic containers. The water sample is filtered through Quantitative ashes Advantec 0.45 μm filter-paper (11 cm in diameter) (suspended material). The filtrate is evaporated at the heating panel in crystallizer.

One by one kilogram of river sediment is taken by sampler and placed into plastic containers. The sediment is dried at 105^{o}C to constant weight, sieved through sieve and the fraction less than 250 μm is taken.

Depending upon the catch, the measurement is carried out in two kinds of fishes (catch of 3 kg each). The fish is dried at 450-500^{o}C to constant weight, fragmented and homogenized.

The algae are collected from the old boats being sunken in river water for a long time and from the docks of river ports. They are dried at 105^{o}C to constant weight, fragmented and homogenized.

Gross beta activity and gammaspectrometry were measured in the samples of filtrated water, suspended material, sediment, algae and fish. ^{90}Sr activity was determined in all samples but algae due to small quantity of the sample. Tritium activity was measured only in water samples.

The measurement of gross alpha and beta activity is carried out by α-β-proportional gas counter. The level of basic radiation is from 1 - 1.5 imp/min. The size of planchet is 2.3 in diameter. The performance of counter is defined by KC1 standard of the same thickness as the sample.

Tritium activity is determined in water sample which is filtered, distilled and electrolytically enriched. The water volume of 9 mL is added with 11 mL of scintillation solution. ^{3}H activity is measured by Liquid Scintillation spectrometer in plastic bottles of 20 ml. Immediately prior to measurement, the sample stands for a while in the counter for thermostasis.

Radiochemical method of ^{90}Sr separation is based on oxalate isolation of Ca and Sr, ignition to oxides and usage of aluminum as ^{90}Y carrier. The equilibrium is achieved in 18 days, and after that time ^{90}Y is isolated on $Al(OH)_3$ carrier, which is then ignited to oxide that is subsequently measured by α-β anti-coincidence counter. The size of planchet is 2.3 cm in diameter. The performance of counter is 24% and is determined by ^{90}Sr standard. Gammaspectrometry is carried out on pure germanium detector manufactured by EG&G "ORTEC", which is connected with multichannel analyzer (8192 channels) produced by the same manufacturer and with adequate computer facilities. Energetic calibration, as well as calibration of detector efficiency is performed by means of Amersham

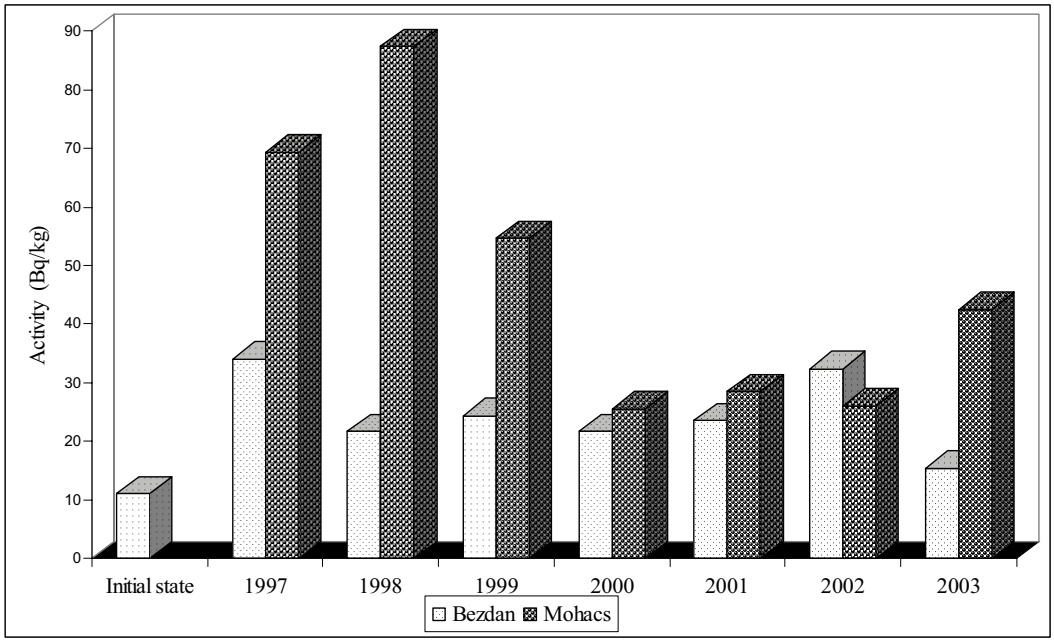

FIG. 1. ^{137}Cs activity concentration in the sediment.

radioactive standard. The time of measurement for a single sample is 60000 to 100000 s, while it is 250000 s for basic radiation.

The results of radioactivity measurements in samples of the Danube river, from 1997 to 2003, were compared to the measurements carried out for determination of the "initial state" (before the Paks Nuclear Power Plant started running). The results of measurements of gross beta activity (water, sediment, algae and fish), ^{3}H activity (water), ^{90}Sr activity (water, sediment and fish) and gammaspectrometry (water, sediment, algae and fish) reveal that the values are at the same level as they were before the Paks Nuclear Power Plant started running. The measurements of ^{137}Cs activity in sediment samples, from 1997 to 2003 (Fig. 1), show some increase of activity in relation to the "initial state", what could be assigned to contamination caused by Chernobyl Nuclear Power Plant accident in 1986.

Our results of measurements correlate well with the results of Hungarian part.

REFERENCE

[1] PANTELIĆ, G., EREMIĆ, M., PETROVIĆ, I., JAVORINA, L.J., TANASKOVIĆ, I., VANCSURA, P., LENGYEL VARGA, A., KÖVÁGÓ, J., Radioactivity control of the Danube at Yugoslav-Hungarian border area, Environmental Recovery of Yugoslavia, Monograph, Institute Vinča, Belgrade (2002) 193-201.

^{137}Cs fallout impact on forest soils and lake sediments in the Boreon area, Mercantour Massif, SE France

Rezzoug, S.[a], H. Michel[a], F. Fernex[b], G. Barci-Funel[a], V. Barci[a]

[a] Laboratoire de Radiochimie, Sciences Analytiques et Environnement,
University of Nice-Sophia Antipolis,
Nice,
France

[b] Department des Sciences de la Terre,
University of Nice-Sophia Antipolis,
Nice,
France

The Boréon area in the Mercantour Massif (Alpes-Maritimes) was contaminated by radionuclides after the Chernobyl accident in the first days of May 1986. In order to obtain ^{137}Cs and ^{210}Pb profiles, sediments from a small mountain lake in this area were collected, as well as forest soils in its vicinity, i.e. in a small valley and on the slopes. The ^{210}Pb flux was calculated from the inventory in a horizontal soil, at 1 km straight line from the lake, where the atmospheric ^{210}Pb (unsupported) is neither swept away nor enriched with lateral input; the ^{210}Pb flux is high in the area (0.09 Bq cm^{-2} y^{-1}) probably because of the great frequency of rain and uranium ores outcropping in the massif.

The ^{137}Cs soil profile in the valley (site A) (Fig. 1) displays a maximum activity (480 Bq kg^{-1}) at the top layer and a decrease as a function of depth. Two profile shapes were observed on the lateral slopes, one (site B) with downward decrease from the top where the activity is 1500 Bq kg^{-1}, the other (site D) with a maximum at 3.5 cm (455 Bq kg^{-1}). At the lower part of the slope (site E, below site B), the activity is highest at 3 cm with more than 2750 Bq kg^{-1}.

The comparison of the ^{137}Cs soil inventories and the unsupported ^{210}Pb allowed to estimate the ^{137}Cs fallout due to the Chernobyl accident in the study site (Boréon).

The recent lake sediments still undergo rather strong contamination by ^{137}Cs, and the sediment profiles show that the residence time of ^{137}Cs in the catchment area is long; only a small proportion is swept out every year by erosion.

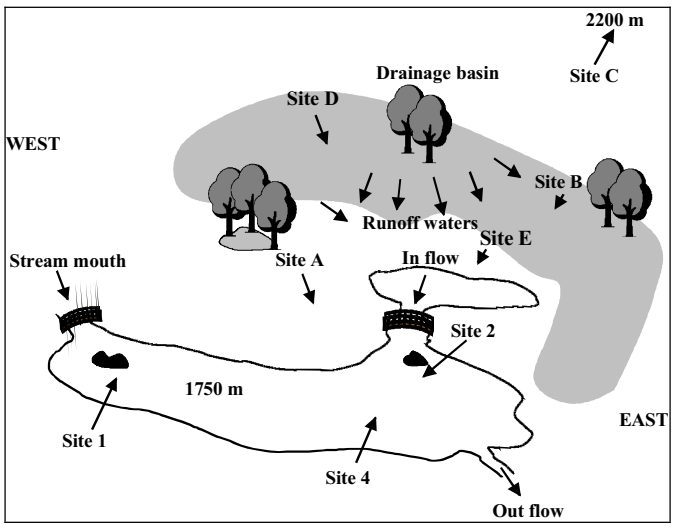

FIG. 1. Sampling locations.

Monitoring of radionuclides in the air: a radiation monitoring network of the Czech Republic

Rulik, P., J. Skrkal, J. Tecl

National Radiation Protection Institute,
Praha,
Czech Republic

The Radiation Monitoring Network (RMN) of the Czech Republic was established in 1986 after the Chernobyl accident. It is currently co-ordinated by the State Office for Nuclear Safety (www.sujb.cz) in co-operation with the National Radiation Protection Institute (NRPI, www.suro.cz). Activity of radionuclides in the atmosphere is continually monitored as a part of RMN activities at 12 sites. The aerosol is sampled on aerosol filters in one-week intervals with the help of sampling devices with throughput up to 900 m^3/h. Activity concentrations of ^{137}Cs, ^{7}Be and ^{210}Pb in the filters with sampled aerosol are established by gamma spectrometry. Besides these nuclides, atmospheric activity concentrations of ^{90}Sr, ^{238}Pu and $^{239+240}$Pu (in aerosols), ^{85}Kr and ^{14}C (in the gaseous phase), and ^{3}H (in atmospheric vapours) are also established at the Prague site. In the paper, some analyses are presented of data obtained from long-term monitoring of ^{137}Cs, ^{7}Be and ^{210}Pb in aerosols. Current data evaluations are published annually in the Reports on Radiation Situation on the Territory of the Czech Republic and on the NRPI website (www.suro.cz).

For 50% of determinations made in the Czech Republic, activity concentrations of ^{137}Cs are below the minimum significant activity levels, because only the Prague sampling site is equipped with a sampling device with sufficient throughput (900 m^3/h) that is required for reliable determination of activity concentrations lower than 10^{-6} Bq/m^3. All subsequent analyses refer to the Prague sampling site. The cumulative distribution of weekly values of ^{7}Be and ^{210}Pb activity concentrations in the period 1986-2003, as well as that of dust content, is approximately logarithmic-normal. Also the distribution of ^{137}Cs in the period 1993-2003 is logarithmic-normal because the activity concentration of ^{137}Cs has not changed significantly since 1993. Table I shows the corresponding values of geometric and arithmetic means and the tolerance interval. The mean values correspond with those established in neighbouring countries.

The analysis of time-dependent behaviour of ^{137}Cs in the atmospheric aerosol (and in fallouts) leads, in a simplified case, to a system of two differential equations with solution in the form of a sum of two exponential functions

$$A(t) = a_1 \cdot e^{-\frac{\ln 2}{T_1}t} + a_2 \cdot e^{-\frac{\ln 2}{T_2}t}$$

where $A(t)$ is the activity concentration as a function of time; a_1, a_2, T_1 and T_2 are constants that implicitly contain a combination of initial conditions and coefficients related to the fall out of aerosol from atmosphere on the soil surface, the re-suspension of aerosol with ^{137}Cs from soil surface to the atmosphere, the penetration of ^{137}Cs into the subsoil, and the half-life. T_2 represents the effective half-time of present diminution of activity in the atmosphere.

The time sequence of average annual activity concentrations of ^{137}Cs in aerosols and fallouts in Prague for the period 1987 - 2003, together with the function (1) corresponding to the data, is shown in Fig. 1. Due to the fluctuation of data, it is not possible to estimate the real rate of decrease of the activity in the atmosphere. However, the effective half-time of decrease will be longer than 15 to 20 years.

Table I. Geometric and arithmetic means and tolerance interval of ^{137}Cs, ^{7}Be and ^{210}Pb activity concentrations and dust content measured in Prague

	^{137}Cs [Bq / m^3]	^{7}Be [Bq / m^3]	^{210}Pb [Bq / m^3]	Dust content [g / m^3]
Geometric mean	8.52×10^{-7}	2.64×10^{-3}	3.81×10^{-4}	5.18×10^{-5}
GSD	1.84	1.64	1.86	1.65
Arithmetic mean	1.03×10^{-6}	2.97×10^{-3}	4.62×10^{-4}	5.86×10^{-5}
95% tolerance interval	2.42×10^{-7}	9.74×10^{-4}	1.07×10^{-4}	1.87×10^{-5}
(from - to)	2.99×10^{-6}	7.15×10^{-3}	1.35×10^{-3}	1.44×10^{-4}
Number of values	570	909	818	778

Note: ^{7}Be and ^{210}Pb, May 1986 – Dec. 2003; dust content, April 1988 – Dec. 2003; ^{137}Cs, Jan. 1993 - Dec. 2003.

A seasonal dependence of activity concentrations of ^{137}Cs, ^{7}Be, ^{210}Pb (activities both in Bq/m^3 and v Bq/g) and dust content at the significance level higher than 0.05 was identified by the analysis of mean values established for activities of all these radionuclides in individual months of 1993-2003.

It follows from the correlation tests that there is a significant mutual correlation between the activities of these radionuclides (activities both in Bq/m^3 and v Bq/g), and also the dust content, with value of t (Student's distribution) mostly higher than 4. The committed effective dose from inhalation is negligible; the highest one is that for ^{210}Pb which is below 20 μSv/year.

Determining the activity concentrations is a very sensitive procedure, with minimum detectable activities of ^{137}Cs in the on the level of 10^{-7} Bq/m^3. Specialists from NRPI are members of the European group RO-5 which is an informal group of experts specialized in monitoring of radionuclides in the atmosphere who are able to inform each other without delay (by e-mail) about changes in activity concentrations of artificial radionuclides.

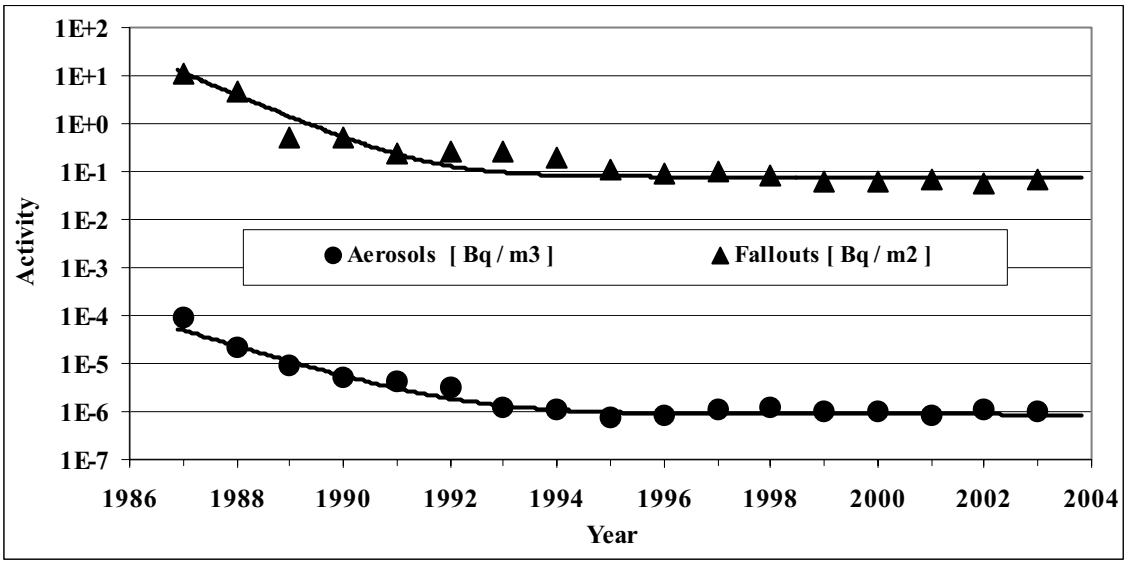

FIG. 1. Time course of average annual activity concentrations of ^{137}Cs in aerosols and fallouts in Prague for the period 1987 - 2003, together with the function (1) corresponding to the data.

Radiological assessment of the Egyptian Mediterranean Coast

El-Gamal, A.[a], I.H. Saleh[a], S. Nasr[a], M. Naim[b]

[a] Department of Environmental Studies,
Institute of Graduate Studies and Research,
Alexandria University,
Alexandria,
Egypt

[b] Department of Physics,
Faculty of Science,
Alexandria University,
Alexandria,
Egypt

On the basis of extensive sampling, gamma spectrometry, laboratory analyses, data evaluation and comparison with the reference data, the following assessment has been carried out. The radiological assessment has been done for a wide scale study area (about 1100 km) from El-Salloum in the west of the Mediterranean coast of Egypt to El-Arish in the east. The environmental radiological assessment steps are based on the criteria previously mentioned [1-2].

The sources of radioactivity possibly reach the Egyptian Mediterranean coast can be summarized as: primordial and radiogenic radionuclides (e.g. ^{40}K, ^{238}U and ^{232}Th series), cosmic rays and cosmogenic radionuclides (e.g. ^{7}Be), fertilizers (e.g. superphosphate), black sand (transported by the Nile River), fallout (either from nuclear testing or Chernobyl), seawater currents (transported either natural or man-made), Suez Canal (subject to receive a radioactive releasing and effluents from either nuclear power ships or submarines passing through the Canal), biological migration and sedimentary longshore movement (e.g. *Anguilla anguilla*), atmospheric radioactivity (e.g. ^{222}Rn and its daughters), domestic and medical sewage (minor source, short half-life), depleted uranium dust (possibly), satellite and aircraft accident (accidental) and rarely loss of industrial radioactive source (incidentally).

El-Salloum, Rashid and El-Gamil have been considered as concentrated basins for the majority of the radioisotopes. This suggestion was due to the special topographical features of these three stations, which make the accumulation of the radioactive isotopes possible.

Calculations of outdoor absorbed dose rate for human population at all stations under investigation from ^{238}U, ^{232}Th and ^{40}K were carried out. The calculated absorbed dose rate has been distinguished the coast into normal areas and Rashid black sand area as high background area. The range of calculated dose was 8.39-38.5 nGy/h. Good agreement was observed with NCRP absorbed dose rates 26 (17-40) nGy/h [3]. Calculations of gamma absorbed dose rate in Rashid black sand area collected in July 1998 recorded as 0.72 μGy/h. This value was considered as relatively high dose rate and it is remarkable of the high background radiation area at Rashid. Comparing with the reported gamma radiation dose rates in the others high background radiation areas, it was in agreement with Ramsar in Iran (0.7-50 μGy/h) and relatively lower than 1-2 μGy/h at Guarapari, Meaipe and Cumuruxatiba in Brazil [4].

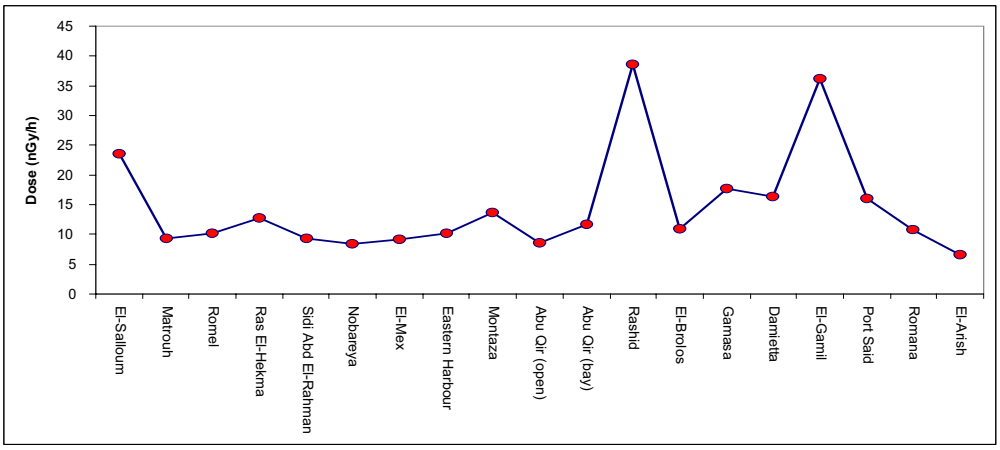

FIG. 1. Gamma absorbed dose rate (nGy/h) from sediments along the Egyptian Mediterranean coast (calculated from March 2000 data).

Annual intake radiation dose was achieved by estimation of the human intake of radioactivity due to fish consumption considering the Egyptian values. Using the mathematical calculation of annual dose per Bq, the total dose to a person, daily fed with 0.0136 kg fish, in one year was 10.3 µSv/y, which is mainly from ^{40}K.

The only man-made radionuclide detected in the Egyptian Mediterranean coast is ^{137}Cs with an average value 0.37 Bq/kg. This average value shows high agreement with the other referenced values in the world. The main source of ^{137}Cs is atmospheric fallout either from nuclear testing or Chernobyl. The marine transport from western Mediterranean could be considered as another source.

Surface seawater salinity showed a positive correlation with the concentrations of ^{40}K in surface seawater ($r = 0.64$). A mathematical model has been deduced to estimate the range of natural ^{40}K in surface seawater.

Assessment of radioactivity bioaccumulators was made among different biota collected from the Egyptian Mediterranean coast. It revealed that, *Patella* spp., *Anguilla* spp. and *Mytilus* spp were the best marine organisms for the capability to accumulate ^{40}K. Also, *Patella* spp., *Anguilla* spp. and the intermediate leaves of *Posidonia* spp. were found as good accumulators of both ^{214}Pb and ^{214}Bi. *Anguilla* spp. and *Mytilus* were found to be good accumulators of ^{228}Ac.

REFERENCES

[1] KRYSHEV, I.I., SAZYKINA, T.G., Radiological assessment of the impact of nuclear facilities on the marine environment in Russia, (Book Ext. Syn.. Int. Symp. Mar. Poll., Monaco, 5-9 October 1998) 237-238.

[2] POVINEC, P.P., Marine radioactivity assessment of Mururoa and Fangataufa Atolls, (Book Ext. Syn. Int. Symp. Mar. Poll., Monaco, 5-9 October 1998) 141-142.

[3] NATIONAL COUNCIL ON RADIATION PROTECTION AND MEASUREMENTS, Natural background radiation in the United States, NCRP Report **45** Washington (1975).

[4] GUY, S., An overview of natural background radiation sources, Part 1: external sources of radiation exposure, Natural background Radiation, Lecture 1 of 3 (1996).

Environmental monitoring at the Australian Nuclear Science & Technology Organisation (ANSTO)

Ferris, J., J. Harrison, E. Hoffmann, T.E. Payne, R. Szymczak

ANSTO Environment,
Menai NSW,
Australia

The Australian Nuclear Science and Technology Organisation (ANSTO) operates several facilities, including Australia's only research reactor, HIFAR, carrying out production of radiopharmaceuticals and research in nuclear science and technology. ANSTO is an agency of the Commonwealth of Australia. Most ANSTO facilities are at the Lucas Heights Science and Technology Centre (LHSTC), surrounded by a 1.6 km buffer zone, about 40 km southwest of Sydney. ANSTO also operates the National Medical Cyclotron (NMC), located on the grounds of Royal Prince Alfred Hospital in Camberdown, Sydney, which produces short-lived radioisotopes for medical investigations.

ANSTO is committed to undertaking its activities in a manner that protects human health and the environment and is consistent with national and international standards and our activities are regulated by the Australian Radiation Protection and Nuclear Safety Agency [1] under the *Australian Radiation Protection and Nuclear Safety Act (1998)*.

ANSTO has a comprehensive monitoring programme for the main pathways for potential exposure from routine and accidental releases for radioactivity. Annually, approximately 6000 samples are taken and some 10,000 analyses are performed. ANSTO monitors the amounts of airborne emissions, the radioactive and non-radioactive contaminants released to the sewer and subsequently to local coastal waters, the quality of stormwater leaving the site, the quality of groundwater and soils and sediment in the general vicinity.

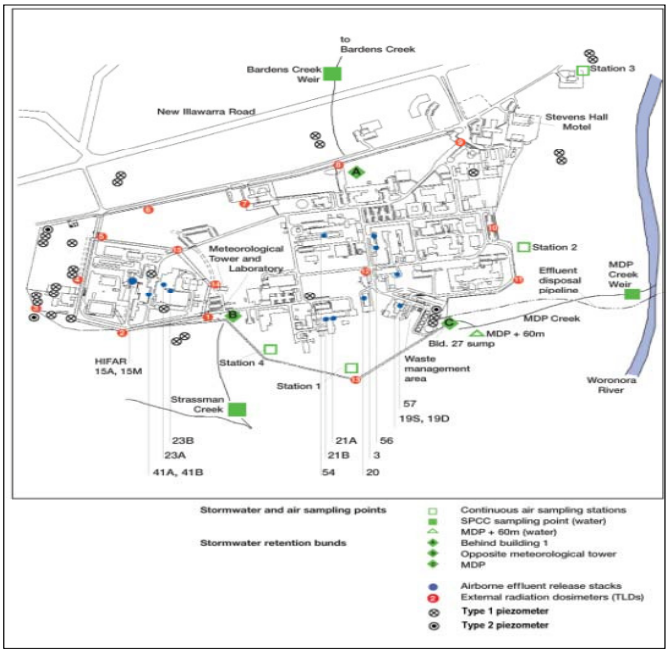

FIG. 1. Location of monitoring sites at the Lucas Heights Science & Technology Centre [3].

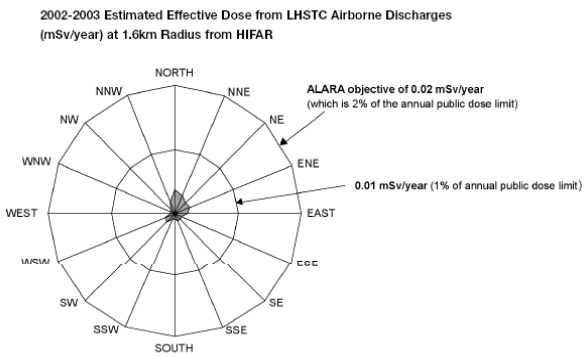

FIG. 2. Estimated Effective Dose from LHSTC airborne discharges 2002-03 [3].

The principal sources of potential radiation exposure to members of the general public from routine ANSTO operations at the LHSTC and National Medical Cyclotron are from airborne emissions and low-level liquid effluent discharges. The effective dose rate to a hypothetical individual potentially exposed to radiation in routine airborne discharges from the LHSTC during the 2002-03 fiscal year was less than 0.006 mSv/year, based on stack discharge data and concurrent meteorological information. This effective dose is well below the ALARA objective of 0.02 mSv/year and less than 1% of the public dose rate limit of 1 mSv/year for long term exposure that is recommended by the Australian Occupational Health and Safety Commission. It is also less than 1% of the natural background annual dose in Australia of about 1.5 mSv/year [2]. Thermoluminescent dosimeters placed around the LHSTC and at some local residences also demonstrate that the external gamma radiation levels at residential locations in the vicinity of the LHSTC were at normal background levels and not noticeably affected by ANSTO operations.

ANSTO operations at the LHSTC and the NMC make only a very small addition to the background radiation dose, even for the comparatively few members of the public identified as potentially exposed to radionuclides entering the environment from the ANSTO sites. The results of the monitoring programme are published annually in documents within the series *Environmental and Effluent Monitoring at ANSTO Sites* [3 and references therein], copies of which are available in the local Sutherland Shire Central Library and on request from the ANSTO Communications Manager.

The environmental and effluent monitoring programme at ANSTO is very much a team effort and acknowledgment goes to all associated staff for their valuable contributions.

REFERENCES

[1] ARPANSA, Recommendations for limiting exposure to ionizing radiation, republished as Rad. Prot. Series 1 (2002), Aust. Rad. Prot. Nucl. Safety Agency, Sydney.

[2] WEBB, D.V., SOLOMON, S.B., Background radiation levels and medical exposure levels in Australia, Radiation Protection in Australasia **16** 1 (1999) 7-14.

[3] HOFFMANN, E.L, FERRIS, J.M., MARCKICH, S.J., Environmental and Effluent Monitoring at ANSTO sites, ANSTO/E-752 (2003).

Radionuclides in the coastal environment of Indonesia

Umbara, H., H. Suseno

Radioecology and Marine Environment Section,
Radioactive Waste Management Development Center,
National Nuclear Energy Agency,
Serpong,
Indonesia

Present potential radiation risk in the coastal environment of Indonesia may result mainly from the presence of naturally occurring radioactive materials released to the aquatic environment from land-based sources, as some of the process industry uses large amounts of raw materials like ore, marl or clay which contains natural radionuclides. Therefore, in recent years we have been conducting radionuclide monitoring in Jakarta Bay with the aim to establish present levels of natural radionuclides in the coastal environment.

Further, we have also been developing methodologies for analysing fission products with the purpose of generating data on background levels of anthropogenic radionuclides in the coastal environment, important for planned construction of nuclear facilities in the region, so adequate radioecological risk assessment studies could be carried out in the future. Therefore radionuclide monitoring has been carried out at Muria peninsula as well, where the first Indonesian nuclear facility is planned to be constructed. Radionuclide monitoring results, both for natural and anthropogenic radionuclides in Muria Peninsula are presented in Table I.

Table I. Radionuclide concentrations in Muria Peninsula

Natural and Artificial Radionuclides Monitoring	
Radionuclide	Concentration (Bq/L)
Sea water	
Cs-137	2.98×10^{-3}
Sr-90	1.43×10^{-3}
Co-60	-
K-40	10.72
Rn-222	3.56
River water	
Cs-137	1.96×10^{-3}
Sr-90	2.23×10^{-3}
Co-60	-
K-40	6.34
Rn-222	2.16
Soil	Concentration, (Bq/Kg) dried weight
Cs-137	0.42
Sr-90	0.304
Co-60	-
K-40	35.36
Rn-222	3.6

Table I (cont'd). Radionuclide concentrations in Muria Peninsula

Sea sediment	
Cs-137	0.575
Sr-90	0.325
Co-60	-
K-40	67.86
Rn-222	-
Sea animal	Concentration, (Bq/g) ashed weight
1. Sea fish	
Cs-137	8.5×10^{-4}
Sr-90	-
2. Shrimp	
Cs-137	-
Sr-90	9.10×10^{-3}

Table II. Selection of marine mollusks as bio-indicators

Selection of Bio-indicator for Coastal Management		
Mollusk species		
Common Name	Scientific Name	Experimental Research using ^{109}Cd tracer
Cockle shell	*Anadara granosa*	CF_{ss} : 28.18 $T_{1/2b}$: 4.24 d
Ark	*Anadara inequivalvis*	CF_{ss} : 34.13 $T_{1/2b}$: 8.75 d
Reticulate Venus shell	*Eriqlyota reticulata*	On going
Hard clam	*Meretrix meretrix*	On going
Green mussel	*Perna viridis*	CF_{ss} : 65.72 $T_{1/2b}$: 11.75d
Blue green cat eye	*Turbo petholatus*	On going

We have also been developing experimental radiotracer techniques to determine bioaccumulation of key contaminants and their retention parameters for bioindicator organisms used in site-specific coastal pollution monitoring programmes, designed to furnish information on water quality. Candidates of marine mollusks as bioindicators are listed in Table II.

Determination of natural and artificial radioactivity levels in sediment in the Marmara Sea

Varinlioglu, A., R. Kucukcezzar, A. Kose

Çekmece Nuclear Research and Training Center,
Atatürk Airport,
İstanbul,
Turkey

The present paper reports the concentration levels of $^{239+240}$Pu, ^{137}Cs and ^{40}K in surficial sediment at 8 stations in the Marmara Sea of Turkey. The purpose of this paper is to follow up the earlier study and present results on the distributions of radionuclides in sediment of the Marmara Sea [1].

A major part of pollutants transported by current systems are normally adsorbed on fine grained particles in suspension. The dissolved radionuclides in the Marmara Region rivers are finally transported along the Marmara Sea coastal area to the Marmara Sea.

The sediment sample were collected on september 1998 – 2004. Result of the measurement for each station were compared between two sampling compaign in order to see the effect of the seasonal variations.

^{137}Cs and ^{40}K concentration levels were determined by gamma spectrometric method. $^{239+240}$Pu concentration level were determined by alpha spectrometric technique.

$^{239+240}$Pu concentration result varies between 0.45 ± 0.04 – 0.10 ± 0.01 Bq/kg. The ^{40}K content varies between 296 ± 47 – 437 ± 60 Bq/kg. The ^{137}Cs activity result varies between 12.6 ±2.6 – 44.1 ± 6.2 Bq/kg.

REFERENCE

[1] VARINLIOĞLU, A., KÜÇÜKCEZZAR, R., KÖSE, A., AKYÜZ, T., BAŞSARI, A., Determination of Natural and Artificial Radioactivity and Trace Element Level in Sediments in The Marmara Sea, Workshop of University of İstanbul, Institute of Marine Science (9 – 13. 06. 1997).

^{210}Po in the North-West Black Sea ecosystem

Lazorenko, G.E.[a], G. Polikarpov[a], I. Osvath[b]

[a] The A.O. Kovalevsky Institute of the Southern Seas,
National Academy of Sciences of Ukraine,
Sevastopol,
Ukraine

[b] Marine Environment Laboratory,
International Atomic Energy Agency,
Monaco

^{210}Po is a natural radionuclide which contributes 2-3 orders of magnitude more than anthropogenic radionuclides to doses received by humans from ingestion of seafood [1]. Data on ^{210}Po in the Black Sea were very scarce. This paper introduces an extensive set of data and related results obtained by the authors on ^{210}Po in water, bottom sediments, algae, macro- and mesozooplankton, mollusks and fishes from the Ukrainian area in the North-West Black Sea in the period 1998-2004. ^{210}Po concentrations in surface water of the open part of the sea in the summer season were around 1 Bq.m^{-3}. In the bottom sediments they ranged between 10 and 500 Bq·kg^{-1}dw, with maximum ^{210}Po concentrations in the area of the Western cyclonic gyre. Concentration factors for this radionuclide, estimated on a wet weight basis, had values of $1.5 \cdot 10^3$ for macrophytes, $4 \cdot 10^3$ for total zooplankton, 10^3-10^4 for entire fishes, depending on their ecological groups affiliation and $6 \cdot 10^4$ for mussels (*Mytilus galloprovincialis*). These values are comparable to those of similar species from other areas of the World Ocean [2]. Amongst the investigated species, the highest doses from ^{210}Po were estimated for the mussels [3]. Amongst the fishes, pelagic species (*Sprattus sprattus phalericus*, *Engraulis enchrasicolus ponticus*) are estimated to receive the highest doses from ^{210}Po (Fig. 1).

ACKNOWLEDGEMENT

This study has been carried out in the framework of the International Technical IAEA Project RER/2003 "Marine Environmental Assessment in the Black Sea Region". The Agency is grateful for the support provided to its Marine Environment Laboratory by the Government of the Principality of Monaco.

REFERENCES

[1] SOURCES OF RADIOACTIVITY IN THE MARINE ENVIRONMENT AND THEIR RELATIVE CONTRIBUTIONS TO OVERALL DOSE ASSESSMENT FROM MARINE RADIOACTIVITY (MARDOS), IAEA-TECDOC-838, IAEA, (1995).

[2] SEDIMENT DISTRIBUTION COEFFICIENTS AND CONCENTRATION FACTORS FOR BIOTA IN THE MARINE ENVIRONMENT, IAEA-TRS-422, IAEA (2004).

[3] LAZORENKO, G.E., POLIKARPOV, G., OSVATH I., The assessment of doses derived to Black Sea biota from ^{210}Po in natural conditions, UDK 546.79:594.124 (262.5) (in Russian).

Determination of γ radiation level and elemental composition in water, biota and sediments from Cayo Punta Brava, Morrocoy National Park, Venezuela

Castillo, J., J. Bermúdez, L. Sajo-Bohus, E. Greaves, D. Palacios

Universidad Simón Bolívar,
Caracas,
Venezuela

Natural and anthropogenic radionuclides and elemental composition in marine water, surface sediments, seagrass and macroalgae (*Padina sanctae-crucis*) from Cayo Punta Brava in Morrocoy National Park were analyzed.

Morrocoy National Park has an area of 32.090 hect. and it is conformed by several keys (Fig. 1). Its beautiful beaches make it a paradise for tourists. In 2004 Easter holidays Morrocoy received more than 572 thousands visitors [1]. Cayo Punta Brava is one of the most visited keys of the park (72000 tourists in 2004 Easter holidays) as it is connected to the mainland by a bridge and is thus more accessable to visitors.

Samples were collected in 10 locations along the coast. Seagrass and *Padina sanctae-crucis* were chosen for this study since they are widely distributed along coast and they can be easily collected. Measurements of radiations levels and elemental composition were carried out using high resolution γ spectrometry and total reflection X-ray fluorescence (TXRF) respectively.

Concentrations activity levels of uranium and thorium isotopes, ^{40}K and ^{137}Cs were determined using a HpGe detector (Canberra) of approximately 2 KeV resolution for the 1,33 MeV ^{60}Co peak and efficiency higher than 20% (supplied under the IAEA-Technical Co-operation project VEN-9-005).

TXRF spectrometer consist of a high voltage X-ray supply and fitted with a molybdenum anode X-ray tube operating at 45 KV and 20 mA, TXRF module fitted with a multilayer monochromator, 30 mm^2 Si(Li) (Canberra) detector of 180 eV energy resolution at the 5.9 KeV Mn Kα line and a PC-based multichannel analyzer (Canberra S-100). Standard addition techniques were used for elemental concentration quantification. Marine water was measured directly and sediments after a suspension preparation, following the procedure suggested by [2]. A vapor phase digestion (VPD) technique was required for seagrass and algae solutions preparations. Preliminary results indicate that the environment is suffering from low level pollution. This study will supply base-line data for determining unequivocally any future contamination.

FIG. 1. Morrocoy National Park Map.

FIG. 2. Cayo Punta Brava.

REFERENCES

[1] http://parquemorrocoy.blogspot.com/.

[2] CARIATI, F., FERMO, P., GILARDONI, S., GALLI, A., MILAZZO, A**.,** A new approach for archaeological ceramics analysis using total reflection X-ray fluorescence spectrometry, Spectrochim. Acta Part B **58** (2003) 177.

BIOMONITORS

Recent observations of ^{99}Tc in Finnish coastal waters

Ilus, E., V-P Vartti, T.K. Ikaheimonen, J. Mattila

STUK - Radiation and Nuclear Safety Authority,
Helsinki,
Finland

Abstract. This paper discusses the origin of ^{99}Tc detected in bladder wrack *(Fucus vesiculosus)* along the Finnish coast in 1999 and 2003, and in some other biota samples taken from an inland area of heavy Chernobyl fallout in Finland.

1. Introduction

In 1994, liquid discharges of ^{99}Tc from the British Nuclear Fuels (BNFL) reprocessing plant at Sellafield increased considerably when a new Enhanced Actinide Removal Plant (EARP) started operation. It is well known that traces of the releases were rapidly transported by ocean currents to the Scandinavian coast. By November 1996 the plume had reached the Norwegian south-west coast [1], and in June 1999, i.e. 4 years after the discharge, it was noted in the Danish Straits [2].

In 1998, Nordic Nuclear Safety Research (NKS) initiated a project in which one of the topics was the use of ^{99}Tc as a tracer of the transport of contaminated water masses from the Irish Sea to Nordic waters, including the Baltic Sea. In 1999, samples of bladder wrack (*Fucus vesiculosus*) were collected along the Finnish coast for ^{99}Tc analysis. The aim was to establish whether ^{99}Tc can be detected in Finnish coastal waters [3, 4]. The collection of *Fucus* and some other plant and animal samples was repeated in 2003 to monitor changes in the distribution pattern of ^{99}Tc, and to clarify the origin of ^{99}Tc found in *Fucus* along the Finnish coast.

2. Materials and methods

In 1999, samples of bladder wrack *(Fucus vesiculosus)* were collected at 30 stations along the western and southern coasts of Finland. In addition, samples of *Fucus* and some vascular plants *(Myriophyllum spicatum)*, mussels *(Macoma balthica* and *Mytilus edulis)* and a crustacean *(Saduria entomon)* were collected from the areas surrounding the Finnish nuclear power plants at Loviisa and Olkiluoto. The *Fucus* samples were generally taken from a depth of 1-3 metres by scuba diving [3]. One *Myriophyllum* sample was taken from an inland lake in southern Finland.

In 2003, sampling of *Fucus* was repeated at 16 of the same stations that were visited in 1999, and several samples of terrestrial *(Dryopteris carthusiana)* and aquatic plants *(Equisetum fluviatilis, Nymphaea candida, Nuphar lutea, Myriophyllum spicatum and Potamogeton natans)* were collected from an area in the Finnish Lake District (Mänttä) that was subjected to heavy Chernobyl fallout (70 kBq m^{-2} of ^{137}Cs) [5].

A new modification of the method for analysing ^{99}Tc in marine samples was developed. The method is based on extraction chromatography using a special reagent, TEVA resin. The method was tested in an intercomparison exercise arranged by the Risø National Laboratory, Denmark. Our results were in good agreement with those reported by the other laboratories. A detailed description of the method is provided by Ref. [4].

3. Results

Small amounts of ^{99}Tc were observed in all the *Fucus* samples collected in 1999; the activity concentrations ranged from 1.6 to 11.6 Bq kg^{-1} dry wt. (Fig. 1). The highest concentrations were found in two samples taken from the northernmost stations in the Quark, probably for biological reasons. Due to the low salinity of the water, *Fucus vesiculosus* is very slow-growing and small in this area, which is at the extreme limit of its permanent distribution range in the Baltic Sea. In seawater and in all other biota samples, the concentrations of ^{99}Tc were below the detection limit (Table I), which supports the use of *Fucus* as an indicator organism for ^{99}Tc in the brackish water environment of the Baltic Sea.

In 2003, the activity concentrations of ^{99}Tc were more evenly distributed in the *Fucus* samples, but again the highest value (6.7 Bq kg^{-1} dry wt.) was recorded in the Quark (Fig. 1). Small amounts of ^{99}Tc were observed in a terrestrial fern sample *(Dryopteris carthusiana)* and in four samples of aquatic vascular plants *(Equisetum fluviatilis, Nymphaea candida* (roots)*, Myriophyllum spicatum* and *Potamogeton natans)* in the inland area of Mänttä. The concentrations in Mänttä ranged from 2.1 to 2.6 Bq kg^{-1} dry wt. (Table I).

4. Discussion

Global fallout from atmospheric nuclear weapons tests carried out in the 1950s and 1960s is certainly the most important source of ^{99}Tc detected in *Fucus* along the Finnish coast and in the biota samples taken from the inland area of Mänttä. Another potential source of observations in *Fucus* could be discharges from the Sellafield nuclear fuel reprocessing plant in the 1970s and early 1980s as well as the mid- and late- 1990s, and their dispersal to the Baltic Sea by sea currents. However, some results may also point to the contribution of the Chernobyl accident.

Fucus samples and the other biota samples collected from the discharge areas of the Finnish nuclear power plants at Loviisa and Olkiluoto did not indicate any traces of local ^{99}Tc releases [3]. It was also difficult to find any clear indication of traces from Sellafield discharges along the Finnish coast. The timing does not correspond with the discharge history. The observations along the Finnish coast in 1999 do not match the fact that the transit time from the Irish Sea to the Danish Straits has been estimated to be 4 years [2, 6]. Moreover, the distribution pattern of ^{99}Tc in *Fucus* along the Finnish coast, with the highest values furthest to the north, does not lend support to the theory. In addition, it is clear that the ^{99}Tc found at the inland sites could not have originated from Sellafield via sea currents. A minor proportion of the ^{99}Tc in *Fucus* on the Finnish coast could in theory have earlier come from Sellafield, but this proportion should in each case be very small.

Prior to this study, Ref. [7] reported ^{99}Tc concentrations in *Fucus* from the Åland Islands (SW Finland) ranging from 1.9 to 3.3 Bq kg^{-1} dry wt. in 1983. They concluded that the most important source of ^{99}Tc on the east coast of Sweden (and probably also further to the north) was fallout from nuclear detonation tests. Ref. [8] concluded in their tracer study from 1986 that as the Baltic was the sea where the maximum water concentration of ^{99}Tc was most likely to occur after the Chernobyl accident, and as they were unable to detect any additional ^{99}Tc in the Baltic Sea water after the accident, the Chernobyl accident did not contribute significantly to ^{99}Tc levels in the north-eastern Atlantic Ocean.

However, some details in our results may support the theory that besides the global fallout, a small contribution from Chernobyl is possible. The activity concentrations of ^{99}Tc in *Fucus* from the Aland archipelago were somewhat higher in 1999 and 2003 than in 1983 [7]. In addition, there were several observations of ^{99}Tc in plant samples taken from the Mänttä area, which was one of the areas in Finland most contaminated by Chernobyl fallout. Furthermore, ^{99}Tc was not detected in the *Myriophyllum* sample taken from a lake in the lowest Deposition Zone 1 (Sammatti, 3 kBq m^{-2} of ^{137}Cs), while it was observed in the *Myriophyllum* sample taken from Mänttä, which belongs to the highest Deposition Zone 5 (70 kBq m^{-2} of ^{137}Cs). The distribution pattern of ^{99}Tc in *Fucus* along the

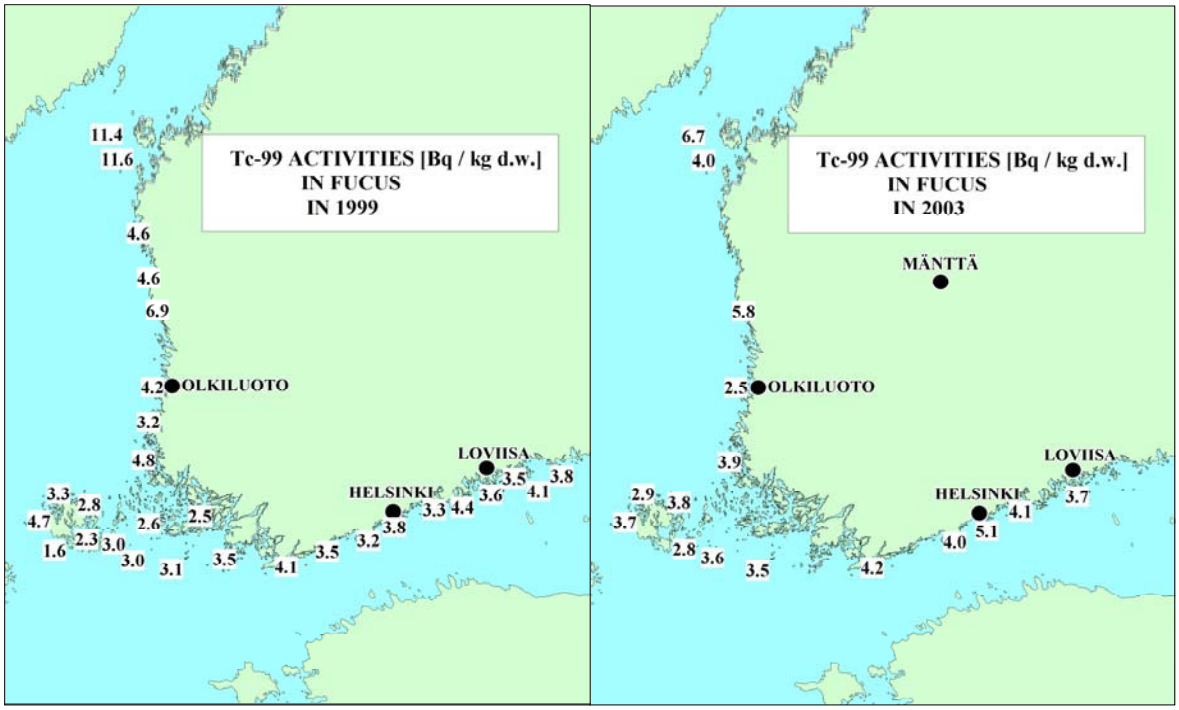

FIG. 1. Activity concentrations of ^{99}Tc [Bq kg^{-1} dry weight] in Fucus vesiculosus *collected in 1999 and 2003.*

Table I. Analyses of ^{99}Tc in other biota samples

Species	Character of area	Site	Year	Bq kg^{-1} d.w.	±1σ (%)
Periphyton	Coastal, NPP discharge area	Olkiluoto	2003	1.0	14
Ferns (terrestrial)					
Dryopteris carthusiana	Inland area	Mänttä	2003	2.1	13
Aquatic vascular plants					
Equisetum fluviatilis	Inland lake	Mänttä	2003	2.4	11
Nymphaea candida	Inland lake	Mänttä	2003	<0.9	
Nymphaea candida (roots)	Inland lake	Mänttä	2003	2.6	25
Nuphar lutea	Inland lake	Mänttä	2003	<0.8	
Myriophyllum sp.	Inland lake	Sammatti	1999	<1.2	
Myriophyllum spicatum	Coastal, NPP discharge area	Olkiluoto	1999	<0.7	
Myriophyllum spicatum	Coastal, NPP discharge area	Olkiluoto	1999	<0.6	
Myriophyllum spicatum	Inland lake	Mänttä	2003	2.5	21
Potamogeton natans	Inland lake	Mänttä	2003	2.2	15
Potamogeton natans	Inland lake	Mänttä	2004	<0.9	
Mussels					
Macoma balthica	Coastal, NPP discharge area	Olkiluoto	1999	<0.8	
Mytilus edulis	Coastal, NPP discharge area	Olkiluoto	1999	<0.7	
Mytilus edulis	Coastal, far from NPPs	Houtskari	1999	<0.6	
Mytilus edulis	Coastal, far from NPPs	Korppoo	1999	<0.6	
Mytilus edulis	Coastal, far from NPPs	Korppoo	1999	<0.6	
Crustaceans					
Saduria entomon	Coastal, NPP discharge area	Loviisa	1999	<0.9	

Finnish coast also supports the theory; the concentrations were on average lower in the Aland archipelago (which received less fallout) than in the Bothnian Sea and the Gulf of Finland.

Fucus was demonstrated to be an excellent indicator of ^{99}Tc in the brackish water environment of the Baltic Sea. Technetium was detected in many vascular plants in the Finnish Lake District, which receiver heavy Chernobyl fallout, not in vascular plants or benthic animals collected from the coastal areas, but in all the *Fucus* samples collected along the Finnish coast.

REFERENCES

[1] BROWN, J., KOLSTAD, A.K., LIND, B., RUDJORD, A.L., STRAND, P., Technetium-99 Contamination in the North Sea and in Norwegian Coastal Areas 1996 and 1997, Strålevern Rapport **3** (1998) 1-17.

[2] DAHLGAARD, H., HOU, X., NIELSEN, S.P., "Radioactive Tracers in Nordic Waters, ^{99}Tc, ^{137}Cs and ^{129}I" (S.E.Palsson, Ed.) Summaries of studies carried out in the NKS/BOK-2 project, Nordic nuclear safety research (2002) 129-133.

[3] ILUS, E., VARTTI, V-P., IKÄHEIMONEN, T.K., MATTILA, J., KLEMOLA, S., Technetium-99 in biota samples collected along the Finnish coast in 1999, Boreal Env. Res. **7** (2002) 91-97.

[4] IKÄHEIMONEN, T.K., VARTTI, V-P., ILUS, E., MATTILA, J., Technetium-99 in *Fucus* and seawater samples in the Finnish coastal area of the Baltic Sea, 1999, J. Radioanal. Nucl. Chem. **252** 2 (2002) 309-313.

[5] ARVELA, H., MARKKANEN, M., LEMMELÄ, H., Mobile survey of environmental gamma radiation and fall-out levels in Finland after the Chernobyl accident, Rad. Prot. Dosimetry **32** 3 (1990) 177-184.

[6] AARKROG, A., DAHLGAARD, H., HALLSTADIUS, L., HOLM, E., MATTSSON, S., RIOSECO, J., "Time trends of ^{99}Tc in Seaweed from Greenland waters" (Desmet, G., Myttenaere, C., Eds), Technetium in the environment, Elsevier Appl. Sci. Publ. (1986) 69-78.

[7] HOLM, E., RIOSECO, J., MATTSSON, S., "Technetium-99 in the Baltic Sea" (Desmet, G., Myttenaere C., Eds), Technetium in the environment, Elsevier Appl. Sci. Publ. (1986) 61-68.

[8] AARKROG, A., CARLSSON, L., CHEN, Q.J., DAHLGAARD, H., HOLM, E., HUYNH-NGOC, L., JENSEN, L.H., NIELSEN, S.P., NIES, H., Origin of technetium-99 and its use as a marine tracer, Nature **335** (1988) 338-340.

Water to swamp morning glory transfer of radium-226

Porntepkasemsan, B., K. Srisuksawad

Waste Assessment and Control Section,
Radioactive Waste Management Project,
Office of Atoms for Peace,
Bangkok,
Thailand

Abstract. Data obtained by 5 year-analyses were complied to explain the mechanism of radium-226 transfer from water to swamp morning glory *(Ipomoea Aquatica* Forsk.). Radium-226 uptake depends on its concentration in water as its concentration in the vegetables being a linear function of its concentration in water. Concentration factors *(CF_s)* for ^{226}Ra uptake from water into swamp morning glory ranged from 23 to 120, mean average 44. The *CF* or the rate constants of uptake and loss rate coefficient were found to be of first order kinetics and approximately equal to slope of the equation. Mechanism of ^{226}Ra transfer from water to swamp morning grown in uncontaminated zones can be expressed as an equation $C_p = a\ C_w^{\ b}$ where the parameter a and b are dependent on the aquatic plant species, in case of swamp morning glory a = 64.326, and b = 0.460.

1. Introduction

Radium-226 is one of health significance radionuclides. It is primarily a bone seeker, and has been associated with bone sarcoma. Information on the plant uptake of ^{226}Ra has tended to concentrate on areas of high natural background such as Kerala coast of India or the monazite sand and volcanic intrusive areas of Brazil [1]. There is still little information on the uptake from water of ^{226} Ra in uranium mining or processing areas where radionuclide in waste may have different chemical and biological properties. In terrestrial environment, the transfer and fate of ^{226}Ra from monazite sand processing operation is an important ecological concern. The greatest concern for the natural environment is the health implications of consuming produce from contaminated garden plots either terrestrial plant or aquatic plant.

The Office of Atoms for Peace (OAP) has located a semi-pilot scale facility for processing monazite sand, an unvalued ore tailings from tin mining. The process includes refining of uranium, thorium and rare-earth elements with the rejection of radium as a waste product. Effluent from the processes after being treated has been routine discharged into the Bangkhen canal where eventually connecting to the Chao Phraya River. Along the canal, a few farms growing aquatic plant, swamp morning glory (*Ipomoea Aquatica* Forsk.), can be found and these provide a unique opportunity for the field determination of water to aquatic plant *CFs*. Swamp morning glory is an important diet of the Thai population and is grown widespread in various canals throughout the entire year. Its consumption represents a significant pathway for the intake of radionuclides and for the delivery of the internal dose to man from those radionuclides.

This study aims at the determination of *CFs* for ^{226}Ra uptake by swamp morning glory grown in Bangkhen canal. Concentration of ^{226}Ra was measured in canal water and vegetable samples. These values were used to establish an equation for explaining the transfer mechanism of ^{226}Ra from water to swamp morning glory.

2. Method

Water and vegetable samples were collected four times a year (in January, April, July, and October) from 1998 to 2002 inclusive from four stations along the Bangkhen canal. The water samples were

taken at the mid depth of the canal and preserved with 1 ml of concentrated nitric acid per liter of sample. Swamp morning glory samples were restricted to the upper part and similar size. 5 liters of water sample were evaporated on the hot plate into 500 ml and occasionally rinsed with 0.6 M HNO_3 then filtered before further analysis. Vegetable sample was tap water washed to remove any traces of radioactive water, if any. It was dried in the oven at 60-100°C and incinerated in the muffle furnace at 400-450°C for at least 16 hours or until white ash was obtained. The ash was acid digested with addition of hydrogen peroxide to oxidize the organic material. Water and vegetable sample were determined on ^{226}Ra concentration by radiochemical separation.

3. Result and discussion

The magnitude of a radionuclide transfer from one compartment to the next, in this case from water to aquatic plant, is defined as the concentration factor, CF:

$$CF = C_p/C_w$$

Where C_p is the concentration of ^{226}Ra in the aquatic plant and C_w is its concentration in the water.

In this study, the concentration factors *(CFs)*, relative to fresh weight of vegetable, for ^{226}Ra uptake from water into swamp morning glory ranged from 23 to 120, mean average 44. In general, these data are comparable to the lower values found in the literatures. Rope and Whicker reported *CFs* for algae ranging from 1100 to 17 500 and for plants from 960 to 6900. Hesslein and Slavicek determined *CFs* for radium in macrophytes that ranged from 110 to 5000. The range of *CFs* for radium reported for phytoplankton, algae and macrophytes in the Animus River in Colorado-New Mexico was 400-1200, 200-2800, and 725-1200, respectively. However, one author has obtained concentration factors that agree with data from this study within an order of magnitude. SENES Consultants Limited reported *CFs* for twelve samples of macrophytes collected in the vicinity of uranium mining in Canada ranging from 10 to 330, geometric mean value 45 [cited in 2]. The low concentration factors obtained here may be due partly to the fact that the study area was an uncontaminated zone with little or no contamination by the OAP activity and swamp morning glory appeared to concentrate radium from the water to a lower degree than other aquatic plants.

No distinct seasonal variations have found even during monsoon periods. Mahon and Mathews [cited in 2] observed that CF_s for the yellow pond lily was seasonally dependent, ranging from 50 to 500 in samples collected in the summer, as compared with 900 to 2600 in samples taken in the spring. They attributed the differences to changes in the physiological state of the plant. Although many factors influencing seasonal variation, it can be assumed that the effect of Bangkhen canal flow rate was little difference among season and physiological state of swamp morning glory is stable causing by periodically harvesting.

A plot of ^{226}Ra concentration in water against ^{226}Ra values in plant give a linear relationship with slope approximately equal to the *CF*. The *CFs* or the rate constants of uptake and loss rate coefficient were found to be of first order kinetics (proportional to C_w^n, where n = 1). There is a clear trend of the increasing values for ^{226}Ra in swamp morning glory with increasing concentration in water. In order to express this trend quantitatively a linear regression analysis was carried out on the logarithm of the vegetable concentration versus the logarithm of the water concentration (Fig. 1), for each individual pair of values obtained.

A slightly significant correlation was found. Mechanism of radium-226 transfer from water to swamp morning glory grown in the study zones can be expressed as an equation

$$\log C_p = \log 64.326 + 0.46 \log C_w$$

or

$$C_p = 64.326\ C_w^{0.46}\ , \text{with } r^2 = 0.693, \text{ df} = 58 \text{ and } p < 0.05$$

Where C_p and C_w are ^{226}Ra concentrations in vegetable and water, respectively.

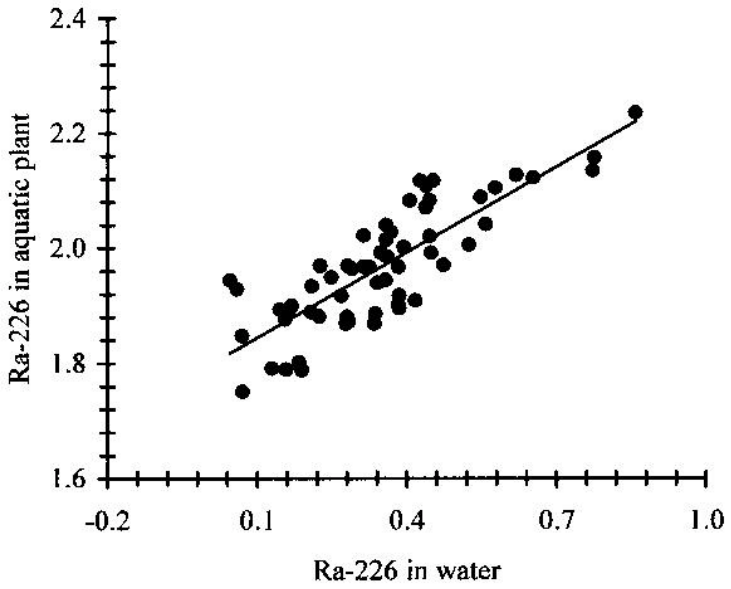

FIG. 1. Linear regression of the logarithm of ^{226}Ra concentration in swamp morning glory versus the logarithm of its concentration in water.

For the form function, C_p = a $C_w^{\ b}$ we find b = 0.46 which indicates non-linearity. Sheppard and Sheppard [3] use the linearity assumption for both essential and non-essential elements. They noted that plant readily uptake elements essential for their growth when substrate concentrations are low and that uptake of non-essential elements is generally constant at low substrate concentrations. A non-linear relationship between *CF* and water concentration, when this is low, in the case of non-essential element, could be explained if this element was simulating an essential one. On the other hand, at high substrate concentrations, plant uptake of essential and non-essential element can either be constant (no toxicity) or can decrease, avoiding toxicity and death. Data from this study are relatively sufficient enough to conclusively prove non-linearity of uptake. Therefore, uptake of ^{226} Ra in swamp morning glory depends on its concentration in water.

Aquatic plant uptake of radium from water is affected by numerous processes and factors. Some of influencing factors include: physico-chemical form of the radionuclide, type of vegetation, water characteristics, (such as pH, major ions, organic matter, suspended particle, and the presence of fertilizers, agricultural chemicals and chelating agents), the distribution of radionuclide within the water, and radium interchange between water column and the sediment [4]. Selected aquatic plant studied here is a freshwater vascular plant. It has a more complex structure than non vascular plant and can accumulate minerals from both water column and the sediment. However, it is not the aim of this work to perform an exhaustive study on the sediment and other parameters that influence the uptake of ^{226}Ra by swamp morning glory.

Water samples and swamp morning glory samples were also collected two times (in March and November 2003) from four reference stations in the Bangkhen canal. It is found that the concentration of ^{226}Ra in those stations fit the log-log line well enough. In general, the equation showed good agreement with ^{226}Ra concentrations in water and ^{226} Ra concentrations in vegetable.

The equation could be applied in a number of ways as it provides reliable estimates and economy in budget and time. It can be used for predicting the degree of dose enhancement due to ^{226}Ra contamination from the routine releases of effluent and together with dietary information assessing the health risk to resident.

Further work is needed to determine the influence of the effluents on drinking water, other aquatic biota, the population inhabiting the areas, and the canal sediment. In addition, the use of water

containing elevated levels of ^{226}Ra in any of irrigation system can result in the contamination of the vegetation, either directly or through uptake from soil contaminated through the irrigation process. In Thailand, rice culture and the long term health of paddy soil have high conservative value. Therefore, work on uptake in rice, a plant of great economic value needs to be examined further.

REFERENCES

[1] TRACY, B.L., et al., Transfer of ^{226}Ra, ^{210}Pb and uranium from soil to garden produce: assessment of risk, Health Physics **44** (1983) 469**.**

[2] HALBERT, B.E., et al., "Environmental Assessment Modeling", The Environmental Behaviour of Radium, Technical Reports Series No. 310, Vol. 2, IAEA, Vienna (1990) 345-389.

[3] SHEPPARD, M.I., SHEPPARD, S.C., The plant concentration ratio concept as applied to natural U, Health Physics **13** (1985) 1187.

[4] WILLIAMS, A.R., "Radium Uptake by Freshwater Plants", The Environmental Behaviour of Radium, Technical Reports Series No. 310, Vol. 1, IAEA, Vienna (1990) 487-503.

Phosphorus availability to ryegrass from urban sewage sludges assessed by isotopic labeling and dilution technique: effect of irradiation

El-Motaium, R.A.[a], C. Morel[b]

[a] Plant Research Dept., Nuclear Research Center,
Atomic Energy Authority,
Cairo,
Egypt

[b] National Institute for Agronomical Research,
Villenave d'Ornon,
France

Abstract. Urban sewage sludges are widely used as alternative P input because of their high P content. Irradiation of sewage sludge is developed in Egypt to make safe spreading of sludge on agricultural fields. In a pot experiment five different sludges were applied at 50 mg P kg^{-1} soil. In addition, water soluble super phosphate was included. The labeling of soil P by radioactive phosphate ions and the application of isotopic dilution principle were used to estimate the amount of P taken up by ryegrass grown in P deficient soil. Phosphorus derived from seeds represented 99% of the P taken up when no P was applied and 87% after applying 50 mg P-SSP (Single Super Phosphate) kg^{-1}. Sludge P participated by 98% to plant nutrition and 7.2% of the applied P was recovered. The sludge type and irradiation factors did not significantly affected sludge P availability assessed by both L value. The effectiveness of sludge P was about 6-fold greater than SSP.

1. Introduction

The utilization of treated sludge in agriculture land particularly to sandy soil has been an acceptable practice for recycling. The addition of sludge to soils has shown increase in soil available phosphorus and phosphorus uptake [1]. However, elimination of sludge contaminants (pathogens, toxic organic pollutants and heavy metals) is a must. Among the different methods used for sludge treatment, irradiation treatment is well recognized as an efficient method for improving sludge quality [2]. Precise knowledge of sludge P bioavailability is required to optimize the application rate and to meet plant requirement. The objectives of this study are: 1) to differentiate between the different sources that can potentially contribute to ryegrass P nutrition 2) to assess the effect of gamma irradiation on the plant-availability of sludge P 3) to compare the efficiency of sludge P to that of the water-soluble mineral P fertilizer 4) to evaluate plant available P (L-value).

2. Methods

Five different sludges were sampled from different wastewater treatment plants (WWTP) in Cairo:

1. raw domestic sludge from El-Gabal El-Asfar farm
2. primary and secondary treated domestic sludge from Zeneen WWTP
3. primary and secondary treated domestic + industrial sludge from Helwan WWTP
4. primary, secondary and anaerobiclly digested domestic sludge from El-Gabal El-Asfar WWTP
5. primary treated domestic sludge from Abou Rawash WWTP.

Each sludge sample was divided into two groups, one group was irradiated using (6 kGy) gamma irradiation " ^{60}Co source ", dose rate 5.7 kGy/h, the other group was not irradiated.

2.1. Analytical techniques

Ryegrass (*Lolium multiflorium* " var. Billion") seeds were swon in a pot experiment (1g/pot). The soil is classified as being sandy soil (Typic Torripsamments) [4]. The main characteristics of the soil were: texture class is sand (sand 95.0 %, 2.4 % silt and 2.6 % clay); the pH value is 8.0; the organic matter content is 0.1 g kg^{-1}; the total N content is 0.3 g kg^{-1} and the total P content is 9 mg kg^{-1}.

The soil was homogeneously labeled with a radioactive solution of carrier-free ^{32}P (about 3 MBq kg^{-1} soil). Sludge was applied at a rate of 50 mg kg^{-1} soil. Two treatments were also included: one is unamended soil and the other is a soil amended with 50 mg P kg^{-1} soil as commercial monocalcium phosphate (SSP). The twelve treatments were arranged in a randomized complete block design in a plastic greenhouse. The aerial part of the ryegrass was harvested every three weeks for a period of three month (four cuts). Hoagland nutrients solution [5] was added to each pot at the start of the experiment and after each cut. After each cut total P and ^{32}P was determined.

Certain weight of plant aerial part were ashed at 500^{o}C for 6 hours then dissolved in 0.2 M HNO_3. The ^{32}P counts, i.e. R0, r0, r and R values, were determined using a Liquid Scintillation Counter (Packard Tri-Carb-2700 TR). The total P content was determined in the same solution according to the green malachite method [6]. The total nitrogen content was determined in a different portion, using the C/N Analyzer (Elementar).

2.2. Determination of sludge P availability

The $^{32}PO_4$-labeling of soil P and the use of the isotopic dilution principle was applied to study P uptake. Let: R0, the amount of ^{32}P activity (carrier-free) added to unamended soil; P0 the P taken up by plant from the unamended soil; The r0 is the radioactivity taken up by plant from the unamended soil; IC0 is the isotopic composition of the P taken up by plant from the unamended soil, which is the ratio (r0/R0)/P0. R, the amount of P-32 radioactivity (carrier-free) added to soil before applying a given P source; P the amount of P taken up by plant from the amended soil; r the amount of radioactivity taken up by plant from the amended soil. The total P taken up by plant (Pt) from the amended soil is coming either from soil (Pso) or applied P (Pa) or seed (Pse) which gives:

$$Pt = Pso + Pa + Pse \quad [1]$$

$$(r/R)/Pso=IC0 \text{ and } Psoil=(r/R)/IC0 \quad [2]$$

by combining Eq. [1] and [2], the Pa value can be calculated:

$$Pa = Pt - Psoil - Pse = Pt - (r/R)/IC0 - Pse \quad [3]$$

The L value [3] was determined by applying the isotopic dilution principle giving: L0 = P0/(r0/R0)=1/IC0 for the unamended soil, and L = (Pt-Pse)/(r/R)=1/IC for the amended soil.

2.3. Statistical analysis

Two-way analysis of variance were conducted using SAS computer program to analyze the effect of sludge and irradiation factors. If a statistical effect is observed at 0.05 probability level, the means were compared using the Duncan's test.

The characteristics of the different types of sludges are presented in (Table I). The pH values are almost similar and in the neutral range (~ 6.4). The organic matter content in sludge ranged from 26.2% to 59.1%, being 6231 mg kg^{-1} in the raw sludge, but 13787 mg kg^{-1} in the digested sludge of El-Gabal El-Asfar WWTP. The total nitrogen in the sludges fluctuated between 1.72% to 3.56%. The

Table I. Main characteristics of the different sludges type before and after gamma- irradiation

Kind of Sludge	Irradiation	pH	Dry Matter (%)	OC (%)	O.M. (%)	Total P mg kg^{-1}	Total N (%)	C/N ratio	Available N g kg^{-1}	
									NH_4	NO_3
Raw	No	6.30	97.2	34.8	59.1	6559	2.79	12.5	0.43	8.51
Raw	Yes	6.42	97.3	34.5	58.7	6231	2.80	12.3	0.45	8.71
Secondary Zennen	No	6.45	97.7	31.2	53.1	7449	3.50	8.9	2.80	11.20
Secondary Zennen	Yes	6.83	93.0	31.5	53.6	7569	3.56	8.9	3.00	11.30
Secondary Helwan	No	6.70	96.7	27.5	46.8	8330	3.03	9.1	3.60	10.70
Secondary Helwan	Yes	6.60	96.5	25.7	43.6	7954	2.78	9.2	2.90	10.35
Digested	No	6.25	86.9	24.1	40.9	12761	3.01	8.0	2.40	0.21
Digested	Yes	6.31	86.6	25.1	42.7	13787	3.12	8.1	2.50	0.20
Primary	No	6.10	98.7	15.4	26.2	7852	1.72	9.0	0.56	1.53
Primary	Yes	5.91	98.2	18.1	30.7	7811	1.99	9.1	0.56	3.06

carbon to nitrogen ratio ranged from 8.0 to 12.5 in the different sludges. Radiation has no particular effect.

The two-way Anova did not show significant difference for both sludge types and irradiation on DMW (Table II). Sludges significantly increased DMW by (+44%) comparing to the no P treatment and by (+32%) comparing to the SSP application. This could be explained by the higher nitrogen content and uptake in sludge treatments. The relative increase in N uptake after sludge addition is +50% compare to the no P addition and +30% compare to SSP addition. Nitrogen recorded the highest values in sludge from Zeneen WWTP, which is associated with the highest P and N uptake and the highest P recovery by ryegrass aerial part. The low C/N ratio in Zeneen sludge (8.9) could enhance nitrogen mineralization. Sludge type affected significantly P-32 and total P uptake whereas gamma-irradiation did not.

The amount of P taken up by ryegrass from seed P was estimated to be 4.21±0.011 mg P kg^{-1} soil. Therefore, the total P taken up by ryegrass for all cuts were corrected by subtracting 4.21 mg P kg^{-1} soil.

The amount of P taken up from soil (Ps) was calculated using P-32 and P uptake and applying the isotopic composition principal determined on the unamended soil (Eq. [2]). The IC0 value is 4.2 mg P which give plant available soil P (L0 value) of 0.24 mg P kg^{-1} soil. This value is very low when it is compared to the L values range (12 to 278 mg P kg^{-1} soil) [7] even in soils considered as P-deficient.

Table II. Two-way analysis of variance for sludge and irradiation factors. Duncan's means comparisons at 0.05 probability level

Factors	DMW	P-32 uptake	P uptake[a]	IC	L value	Ps	Pa	Pdfsl	P recovery
	g kg^{-1} soil	Dimen-sionless	mg kg^{-1} soil	mgP^{-1} soil	mg kg^{-1} soil	Mg kg^{-1} soil	mg kg^{-1} soil	%	%
Sludge	NS	*	*	NS	NS	*	*	NS	*
Irradiation	NS	NS	NS	NS	NS	NS	NS	NS	NS
AddedP*Irradiation	NS	NS	NS	NS	NS	NS	NS	NS	NS
Mean	4.75	0.14	3.64	0.053	25.9	0.034	3.61	98.7	7.2
Root mean square error	0.98	0.04	1.47	0.043	10.7	0.0090	1.47	1.0	2.9
Sludge factor									
Raw	4.43	0.097b	2.9b	0.066	17.7	0.02b	2.85b	98.4	5.7b
Secondary, Zeneen	4.75	0.166a	4.6a	0.036	28.5	0.04a	4.56a	99.1	9.2a
Secondary,Helwan	4.89	0.155a	3.2ab	0.064	19.4	0.04a	3.15ab	98.5	6.2 ab
Digested	4.49	0.151a	2.8b	0.063	28.2	0.04a	2.76b	98.5	5.6 b
Primary	5.18	0.152a	4.7a	0.036	35.6	0.04a	4.66a	99.1	9.4a
Irradiation factor									
NI	4.75	0.147	3.2	0.066	21.6	0.035	3.2	98.4	6.4
I	4.74	0.142	4.1	0.039	30.2	0.034	4.0	99.1	8.1

[a] P uptake corrected for seed contribution

2.4. Sludge Phosphorus availability to ryegrass

The statistical analysis show significant differences in Pa and in %P recovery due to sludge type, but non-significant difference due to gamma irradiation. This effect in sludge types is explained by the general increase in P uptake due to interaction with the nitrogen associated with sludge. Neither sludge types nor gamma irradiation affected significantly the Pdfsl and the L value. The Pdfsl mean for sludges was very high, i.e. close to 99%, and identical to that of the SSP application. These Pdfsl values are up to 5 fold greater than many values previously published on water-soluble P [8]. Only half of 50 mg P kg^{-1} applied to soil was in L value. However, an even lower L value (14.9 mg kg^{-1} soil) was obtained with the SSP application showing that only 30% is plant-available. This could be due to the interaction between P and CaCO3 (2.4%) in sandy soil [10].

Sludge P can be evaluated in comparison to the water-soluble P by using availability coefficient ratio [10]. In this experiment, contrasting conclusions were obtained in Pa and %P recovery variables. The availability coefficient ratio showed that sludge is about 6 fold greater effective than SSP. By contrast, the ratio of the percentage of P derived from sludge to that of SSP is 1. This different conclusion is explained by differences in the amount and forms of N applied, between the different sludges and SSP, which had interacted on P uptake.

It is concluded from this study that the relative contribution of sludges to plant nutrition did not significantly depend on sludge type and irradiation factors. However, the amount of P taken up from sludges can significantly vary between sludges which was explained by differences in the amount and form of N added with the P application. As a consequence, the sludge P availability is equal to water-

soluble P, however the effectiveness of sludge P was about 6 fold greater than SSP when the percentage of P recovery was considered.

REFERENCES

[1] CONDRON, L.M., FROSSARD, E., NEWMAN, R.H., TEKELY, P., MOREL, J.L., "Use of 31P NMR in the study of soils and the environment", (Miner et al., Ed.) NMR epectroscopy in environmental science and technology, Oxford University Press (1996) UK.

[2] U.S. ENVIRONMENTAL PROTECTION AGENCY, Process design manual for sludge treatment and disposal, EPA 625/1-79-011, Center for Environmental Research Inform. Technical Transfer, Cincinnati, Ohio (1979) 1000 pp.

[3] LARSEN, S., The use of ^{32}P in studies on the uptake of phosphorus by plants. Plant and Soil **4** (1952) 1-10.

[4] SOIL SURVEY STAFF, Soil Taxonomy, Agric. Handbook No. 436, USDA, Washington D.C. (1975).

[5] HOAGLAND, D.R., ARNON, D.J., The water-culture method for growing plants without soil, Circ. Calif. Agr. Expt. Sta.. (1950) 347.

[6] OHNO, T., ZIBILSKE, L.M., Determination of low concentration of phosphorus in soil extracts using malachite green. Soil Sci. Soc. Amer. J. **55** (1991) 892-895.

[7] GUIVARCH, A., Plant-availability and relative fertilizing value of phosphorus in sewage sludge derived from different urban waste waters treatment plants, Ph.D Thesis, Institut National Polytechnique de Lorraine, Nancy, France (2001).

[8] MOREL, C., FARDEAU, J.C., Uptake of phosphate from soils and fertilizers as affected by soil P availability and solubility of phosphorus fertilizers, Plant and Soil **121** (1990) 217- 224.

[9] BADAWY, S.H., EL-MOTAIUM, R.A., Effect of irradiated and non-irradiated sewage sludge application on some nutrients heavy metals content of soils and tomato plants". (Proc. 1st Congress on: Recent Technology in Agriculture) Bull. Fac. Agric., Cairo Univ. Special Edition **IV** (1999) 728-744.

[10] BLACK, C.A., Soil fertility evaluation and control, Lewis publishers (1992).

Tolerance of fish to contaminated habitats: underlying mechanisms probed with isotopic tracers

Jeffree, R.A.[a], S J. Markich[b], J.R. Twining[c], S. Gale[d]

[a] Marine Environment Laboratory,
International Atomic Energy Agency,
Monaco

[b] Aquatic Solutions International,
Dundas Valley NSW,
Australia

[c] Environment Division,
ANSTO,
Menai NSW,
Australia

[d] University of Technology, Sydney,
Gore Hill Campus,
Gore Hill NSW,
Australia

Future scenarios indicate agricultural and industrial expansions in major river basins and enhanced world populations focusing in coastal watersheds [1], particularly in SE Asia. Such scenarios are consistent with increasing concentrations of various contaminants, including metals and radionuclides. It is important to assess the likely impacts on fisheries, their response and possible adaptability to enhanced contaminant levels and the implications for resulting transfer factors and contaminant levels in fisheries, that can be the major sources of subsistence and livelihood for coastal communities.

The likely future responses of fisheries to projected increases in contaminant loadings over broad geographical scales can be probed through the employment of currently highly contaminated aquatic environments. Such a system with these attributes, that we have investigated periodically since the early 1970s, is the Finniss River in tropical northern Australia, that has continued to receive acid mine drainage from the Rum Jungle U/Cu mine since the 1950s. Prior to mine-site remediation in the early 1980's measured loadings of Cu, Zn, Mn and sulfate caused severe impact to fish diversity and abundance, including fish kills observed in the main Finniss River and its East Branch. Following mine-site remediation and measured reductions in contaminant loadings, there has been recovery of fish communities in the main Finniss River and considerable recolonisation of the still highly contaminated region of the East Branch, that was virtually devoid of fish populations prior to remediation [2].

Following mine site remediation reductions in annual-cycle contaminant loads of sulfate, Cu, Zn, and Mn by factors of 3-7 were accompanied by an unexpected degree recovery in fish community structure in the contaminated region of the Finniss River, to the extent that they were not statistically ($P > 0.05$) distinguishable from unexposed environments [2]. However, these fish communities continue to be exposed to considerable annual tonnages of these contaminants, as well as the naturally-occurring radionuclides associated with uranium mine wastes. Hence their capacity to accumulate

contaminants under these conditions of long-term exposure and their adaptive response can be critically investigated, and is of concern to local stakeholders, both Aboriginal and European, who consume some of these fish species [3].

A more unexpected field observation was made in 1993 when five small fish species were found living in the East Branch of the Finniss River, where individual species penetrated the pollution gradient to varying degrees, but with one species (*Melanotaenia nigrans*) occurring at extremely high concentrations of Cu [4]. A laboratory-based study investigated the mechanisms of copper tolerance in *M. nigrans* from the polluted East Branch, compared to unexposed or reference populations. The bioconcentration of cyclotron-generated $^{64/67}$Cu in fish was used to investigate the mechanism of copper tolerance in exposed fish. In this short-term experiment Cu concentrations in all tissue sections were significantly (P<0.05) less (up to 50%) in exposed fish compared with the respective tissue sections of reference fish, when exposed to both low and elevated Cu water concentrations. The mechanism of copper tolerance was concluded to be reduced copper uptake in the gills, rather than increased binding or elimination. Initial and subsequent allozyme electrophoresis showed that heterozygosity was reduced in exposed fish compared with that of reference fish. Collectively, these results suggest that genetic selection may have occurred in the exposed fish population. This was the first study on the mechanisms of copper tolerance in a wild fish population that has been exposed to elevated copper concentrations [5].

A pilot study of Cu, U, Zn, Co, Ni, Pb, Mn, Ra and Po-210 in several edible species of fish that now occur in abundance in the region of the main Finniss exposed to mine effluents has shown the following. Each contaminant water concentration was enhanced in the contaminated zone at the time of sampling. Compared to unexposed control sites, flesh samples from two species [Bony bream (*Nematalosa erebi*) and Eel-tailed catfish (*Neosilurus ater*)] were not significantly (P>0.05) enhanced in mean concentrations of any of these contaminants, with some being actually reduced (P<0.05) in the most contaminated region. This pattern of reduced accumulation in the exposed populations under field conditions is comparable to that obtained experimentally for Cu uptake in *M. nigrans*.

ACKNOWLEDGEMENT

The Agency is grateful for the support provided to its Marine Environment Laboratory by the Government of the Principality of Monaco.

REFERENCES

[1] GESAMP, Protecting the Oceans from Land-based Activities; Land-based sources and activities affecting the quality and uses of the marine, coastal and associated freshwater environment, Rep. Stud. GESAMP No. **71** (2001) 162 pp.

[2] JEFFREE, R.A., TWINING, J.R., THOMPSON, J., Recovery of fish communities in the Finniss River, Northern Australia, following remediation of the Rum Jungle uranium/copper mine site, Environ. Sci. Technol. **35** (2001) 2932-2941.

[3] FERRIS, J., HOLDEN, P., The Finniss River Symposium: Rapporteurs' Report (Proc. Finniss River Symposium, August 23-24, 2001, Darwin), (MARKICH, S.J., JEFFREE, R.A., Eds) ANSTO E/748 (2002) 74-76.

[4] JEFFREE, R.A., TWINING, J.R., Contaminant Water Chemistry and Distribution of Fishes in the East Branch, Finniss River, following Remediation of the Rum Jungle Uranium/Copper Mine Site (Proc. 2000 Contaminated Site Remediation Conference, Melbourne, 4-8 December, 2000) 51-56.

[5] GALE, S.A., SMITH, S.V., LIM, R.P., JEFFREE R.A., PETOCZ, P., Insights into the mechanisms of copper tolerance of a population of black-banded rainbowfish (*Melanotaenia nigrans*) (Richardson) exposed to mine leachate, using $^{64/67}$Cu, Aquatic Toxicology **62** 2 (2003) 135–153.

Concentration factors for Tc-99 in lobsters (*Hommarus gammarus*) from Norwegian coastal areas

Rudjord, A.L.[a], A.K. Kolstad[a], H.E. Heldal[b]

[a] Norwegian Radiation Protection Authority (NRPA), Norway

[b] Institute of Marine Research (IMR), Norway

In the period 1994 to 2003, elevated levels of Tc-99 was discharged to the Irish Sea from the reprocessing facilities at Sellafield. Tc-99 is transported with ocean currents to the Norwegian coast, and earlier studies have shown that lobsters have a high ability to accumulate this radionuclide [1, 2].

A few lobster samples caught in 1997 as part of the Norwegian marine monitoring programme for radioactivity suggested higher concentration factors for lobsters along the Norwegian coastline compared to results reported from the Irish Sea [3]. A large variability in the Tc-99 concentrations in Irish Sea lobsters have been observed [4], which could perhaps be due to the relatively large variability of Tc-99 sea water concentrations in the Irish Sea. It is expected that sea water concentrations would be more homogenous further away from the source, giving concentration ratios between biota concentrations and sea water concentrations that corresponds somewhat better to the theoretical equilibrium concentration factors.

A more extensive sampling programme of lobsters (*Homarus gammarus*) in Norwegian Coastal areas was therefore carried out in the period 2001-2003, in most cases with simultaneous sampling of sea water. The sampling areas are shown in Figure 1.

FIG 1. Location of lobster sampling areas.

Table I. Concentration factors of ^{99}Tc in lobster (*Homarus gammarus*), Norwegian coastal areas, 2001-2003

Location (year)	Gender (F/M)	n	Organ	Concentration Factor mean ± 1 σ	median
Kvitsøy (2001)	F	4	Tail muscle	36,400 ± 5,200	34,200
	M	17	Tail muscle	7, 000 ± 4,100	5,800
Stefjord (2001)	F	1	Tail muscle	20,200	
	M	1	Tail muscle	2,800	
Værlandet (2002)	F	5	Tail muscle	17,800 ±12,600	12,700
	M	5	Tail muscle	3,000 ± 800	2,700
Flekkerøy (2002)	F	2	Tail muscle	11,800 ± 200	11,800
	M	4	Tail muscle	3,500 ± 3,300	2,100
Møre (2002)	M	6	Tail muscle	3,700 ± 2,900	2,600
Sandøya (2003)	F	8	Tail muscle	9,400 ± 5,700	8,500
	M	9	Tail muscle	2,500 ± 800	2,400

The lobsters were frozen, and their gender, wet weight, carapace length and total length were recorded. Radioanalysis was mainly performed on tail muscle tissue but results on individual organs will be reported later.

Simultaneous sea water samples were collected at Sandøya, Kvitsøy and Værlandet. Sea water concentrations were estimated based on monitoring results at Stefjord, Møre and Flekkerøy. Generally, the activity concentration of Tc-99 in the seawater varied in the range 0.95 to 2.1 Bq m^{-3}. Short term variations of this order can be expected within a geographical area due to various coastal effects, variations in currents or weather conditions.

The analysis results show a large variation in the activity concentrations of the lobsters, ranging from 2.2 Bq/kg wet weight and up to 62.2 Bq/kg w. w. In Table I, mean and median concentration factors (CF) obtained for each subsample are summarized. The concentrations are higher in female lobsters compared to males, with a factor ranging from 3.4 to 7.2 for the various subsamples, confirming earlier observations from the Irish Sea [4].

Individual concentration factors varied from 1,540 Bq kg^{-1}/ Bq L^{-1} to 13,500 Bq kg^{-1}/ Bq L^{-1} with a median value of 3100 Bq kg^{-1}/ Bq L^{-1} in males, and from 3800 Bq kg^{-1}/ Bq L^{-1} to a maximum of 44,000 Bq kg^{-1}/ Bq L^{-1} with a median value of 12,500 Bq kg^{-1}/ Bq L^{-1} in female lobsters.

The high accumulation of technetium-99 of lobsters compared to other crustacea is confirmed in this study, as well as the clear differences between males and females [4]. However, there is also a large variation in activity concentrations between lobsters collected at the same time in the same area and of the same gender. No clear correlation of concentration factor with carapace length or whole body fresh weight was observed. The most probable explanation for the large variations is food ingestion of Tc-99 or variations related to the molting/reproduction cycle of the lobsters.

REFERENCES

[1] SWIFT, D.J., The accumulation of ^{95m}Tc by juvenile lobsters (Homarus gammarus L.) J. Environ. Radioact. **2** (1985) 229-243.

[2] BUSBY, R., McCARTNEY, M., McDONALD, P., Technetium-99 concentration factors in Cumbrian seafood, Radioprotection-Colloques, **32** (1997) 311-316.

[3] BROWN, J.E., KOLSTAD, A.K., BRUNGOT, A.L., LIND, B., RUDJORD, A.L., STRAND, P., FØYN, L., Levels of Tc-99 in biota and sea water samples from Norwegian coastal waters and adjacent Seas, Mar. Poll. Bull. **38** 7 (1999) 560-571.

[4] SWIFT, D.J., NICHOLSON, M.D., Variability in the edible fraction content of Co-60, Tc-99, Ag-110m, Cs-137 and Am-241 between individual crabs and lobsters from Sellafield (North eastern Irish Sea), J. Environ. Radioact. **54** (2001) 311-326.

[5] SMITH, D.L., KNOWLES, J.F., WINPENNY, K., The accumulation, retention and distribution of ^{95m}Tc in crab (Cancer pagurus L.) and lobster (Homarus gammarus L.) A comparative study, J. Environ. Radioact. **40** 2 (1998) 113-135.

Bioaccumulation and retention of ^{210}Pb in the Mediterranean mussel *Mytilus galloprovincialis*

Boudjenoun, R.[a], J.-L. Teyssié[b], O. Cotret[b], J. Paganelli[b], S.W. Fowler[b], M. Warnau[b]

[a] Commissariat à l'Energie Atomique/CRNA,
Algiers,
Algeria

[b] Marine Environment Laboratory,
International Atomic Energy Agency,
Monaco

Pb is commonly reported as a pollutant of concern in the marine environment. Although severely regulated in the industrialised countries, global emissions are not showing a significant downward trend [1]. Therefore Pb will still cause problems because of its conservative nature and its increasing use in some industrial applications [2]. It is therefore important to develop tools to monitor the occurrence and abundance of Pb in coastal waters, particularly those in less-developed regions of the world where its use is not yet, or only poorly, regulated. Thus, the purpose of this study was to quantify Pb bioaccumulation in a widely distributed and abundant species along the Mediterranean coasts of North Africa, *viz*. the mussel *Mytilus galloprovincialis*, in order to assess the relevance of its use as a bioindicator species of Pb contamination [3, 4].

The experimental approach used highly sensitive nuclear detection techniques to investigate uptake and loss kinetics of the radiotracer ^{210}Pb in the mussels. Individuals were exposed experimentally to the radiotracer for 14 d via seawater (uptake phase). At the end of the exposure period, non-contaminated conditions were restored (clean flowing sea water) for 22 d and loss kinetics of ^{210}Pb from mussel tissues were determined (depuration phase) during that time. ^{210}Pb was found to be readily taken up according to linear uptake kinetics. At the end of the exposure period (14 d of exposure), calculated concentration factors reached values as high as 300 (Fig. 1). When mussels were exposed to increasing ^{210}Pb activities (0.25 to 2.5 Bq mL^{-1}), it was found that Pb bioaccumulation in the mussel tissues was directly proportional to ambient Pb concentrations in sea water.

Retention of the metal in mussel tissues was high with ca. 50% of incorporated Pb remaining in the tissues after 3 weeks of depuration (Fig. 2). Mussels displayed similar loss kinetics regardless the ^{210}Pb activity (0.25 to 2.5 Bq mL^{-1}) to which they were previously exposed. Estimated biological half-life (Tb½) of ^{210}Pb ranged between 23 and 28 days.

Overall, our results indicate that *M. galloprovincialis* could be a useful monitoring tool to assess Pb contamination of North African coastal waters and, thus, could be considered as a suitable bioindicator species for heavy metal monitoring programmes in this region.

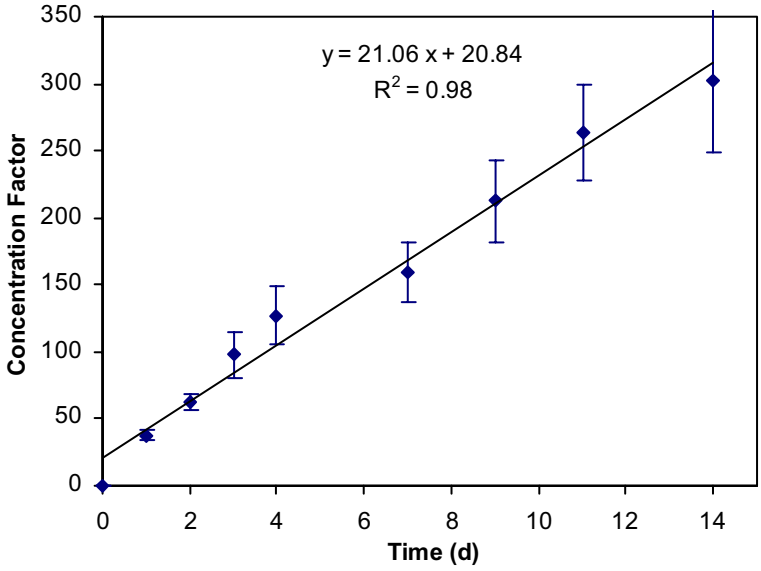

FIG. 1. Uptake kinetics of ^{210}Pb in Mytilus galloprovincialis *exposed via sea water (whole-body Concentration Factors; mean SD; n = 5).*

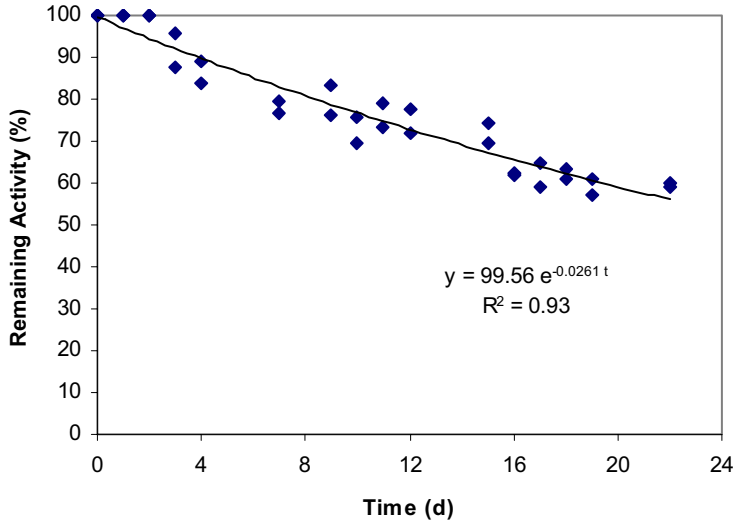

FIG. 2. Loss kinetics of ^{210}Pb in Mytilus galloprovincialis *previously exposed for 14 d via sea water (% of whole-body Remaining Activity).*

ACKNOWLEDGEMENT

The Agency is grateful for the support provided to its Marine Environment Laboratory by the Government of the Principality of Monaco.

REFERENCES

[1] SMITH, D.R., FLEGAL, A.R., AMBIO **24** (1995) 21.
[2] NSTF - North Sea Quality Status Report. Oslo and Paris Commissions, London (1993).
[3] STURESSON, U., Lead enrichment in shells of *Mytilus edulis,* AMBIO **5** (1976) 253-256.
[4] TRIPP, B.W., FARRINGTON, J.W., GOLDBERG, E.D., SERICANO, J., International Mussel Watch: the initial implementation phase, Mar. Poll. Bull. **24** (1992) 371-373.

Delineation of heavy metal uptake pathways (seawater, food and sediment) in tropical marine bivalves using metal radiotracers

Hédouin, L.[a,d], M. Métian[a], O. Cotret[a], J.-L. Teyssié[a], J. Paganelli[a], S.W. Fowler[a], R. Fichez[b], M. Warnau[a]

[a] Marine Environment Laboratory,
International Atomic Energy Agency,
Monaco

[b] IRD – Noumea Center,
New Caledonia

[c] LBEMB, UPRES-EA 3168,
La Rochelle University,
France

[d] Goro-Nickel,
New Caledonia

The SW lagoon of New Caledonia is subjected to intense heavy metal input from land-based mining industries exploiting metals such as Ni and, secondarily, Cr and Co [1]. However, as is the case for most tropical environments, little is known about the contamination status of this lagoon [1, 2]. In order to allow a better ecotoxicological characterization of the New Caledonian lagoon through monitoring of its seawater quality status, three locally common and abundant species were selected for laboratory radiotracer experiments. The objective of the study was to characterize and possibly validate their usefulness as bioindicator species in programmes for local pollution surveys and monitoring of the coastal zone.

The three species selected were the edible clam *Gafrarium tumidum*, and the oysters *Isognomon isognomon* and *Malleus regula*. Bioaccumulation and tissue distribution of six elements (Ni, Cd, Co, Cr, Zn, Ag) were determined following exposures via sea water, sediment and food using radiotracers (^{63}Ni, ^{109}Cd, ^{57}Co, ^{51}Cr, ^{65}Zn, ^{110m}Ag) and highly sensitive nuclear detection techniques (beta and gamma spectrometry).

Transfer from food was shown to be quite efficient; assimilation efficiencies (AE) of metals ingested with phytoplankton (*Isochrysis galbana*) ranged between 34 and 77%, and these ingested fractions of metals were retained for long periods of time (biological half-lives ranged between 20 and 400 days depending upon the element). In contrast, in terms of transfer efficiency, sediments were found to be a much less important pathway than sea water; for example, concentration factors from sea water estimated at steady-state, CF_{SS}, were three to five orders of magnitude higher that steady-state transfer factors from sediments, TF_{SS}. Nevertheless, metal concentrations in sediment are several orders of magnitude higher than those in sea water and, in terms of quantities of transferred elements, their impact on total metal accumulation may not be negligible.

Therefore, it was necessary to use a mathematical model [3] to estimate the relative contribution of each uptake pathway to the total bioaccumulation of metals in bivalves. The kinetic parameters measured in the different experiments investigating the exposure routes have been used to run the model. Computations suggest that sediment always accounts for only a minor part of the total bioaccumulation in the 3 bivalves (< 3%; except for Cd in the oysters: 20% in *I. isognomon* and 30%

in *M. regula*). In the clams, the predominant uptake route for all metals was found to be the food (95-99%). In contrast, both oysters accumulated Co and Cd mainly from food, whereas sea water was the predominant route for Zn accumulation. Interestingly, the two oysters displayed the same behaviour with respect to all the metals except Ag. The latter element was far more efficiently taken up and retained in the soft parts of *I. isognomon* than in *M. regula*. For this metal the bioaccumulation model indicated that *I. isognomon* took up Ag mainly from sea water (88%) whereas *M. regula* accumulated it principally from its food (90%). Furthermore, our results suggest that differing mechanisms (or induction threshold level) of Ag detoxification/storage occur in the two oyster species, and that the mechanism in *I. isognomon* is particularly sensitive and efficient.

In conclusion, food and, secondarily, sea water appear to be the predominant routes for the uptake of these metals in the three tropical bivalves investigated.

ACKNOWLEDGEMENT

The Agency is grateful for the support provided to its Marine Environment Laboratory by the Government of the Principality of Monaco.

REFERENCES

[1] LABROSSE, P., FICHEZ, R., FARMAN, R., ADAMS, T., New Caledonia (SHEPPARD, C.R.C., Ed.), Seas at the Millennium: An environmental evaluation, Pergamon Press, Amsterdam (2000) 723-736.

[2] BREAU, L., Etude de la bioaccumulation des métaux dans quelques espèces marines tropicales: recherche de bioindicateurs de contamination et application à la surveillance de l'environnement côtier dans le lagon sud-ouest de la Nouvelle-Calédonie. PhD. Thesis, La Rochelle University, France (2003) 282 pp.

[3] REINFELDER, J.R., FISHER, N.S., LUOMA, S.N., NICHOLS, J.W., WANG, W.X., Trace element trophic transfer in aquatic organisms: A critique of the kinetic model approach, Sci. Total Environ. **219** (1998) 117-135.

Po-210 and Pb-210 concentration factors for zooplankton and faecal pellets in the oligotrophic South-West Pacific

Jeffree, R.A.[a], R. Szymczak[b], G.A. Peck[c]

[a] International Atomic Energy Agency,
Marine Environment Laboratory,
Monaco

[b] ANSTO Environment,
Menai NSW,
Australia

[c] Department of Defence,
Joint Logistic Command,
Melbourne VIC
Australia

In a previous study on zooplankton sampled from very low productivity waters of French Polynesia [1], their Po-210 concentrations were found to be unexpectedly elevated, compared to values measured in marine zooplankton from various other geographical regions of the world. For the French Polynesian samples their Po-210 concentrations also increased appreciably as their biomass declined. A simple conceptual and mathematical model, that incorporated the established role of zooplankton faecal pellets in the removal of Po-210 and particle-reactive radionuclides and stable metals from the water column, could capture the shape of this empirical relationship between Po-210 concentration and their biomass and also explained the biomass-related mechanism that increases Po-210 concentrations in zooplankton [2]. Similarly, a field investigation in the Timor Sea showed that a range of particle-reactive elements showed elevated water concentrations as particle removal rates, as inferred from Th-234: U-238 disequilibria, reduced in the euphotic zone [3]. However, in these previous studies simultaneous *in situ* measurements of a range of parameters valuable in assessment of the role of zooplankton in the biogeochemical cycling of particle-reactive elements like Po-210 and Pb-210 were not made.

Here we report preliminary results of a field study, that was undertaken in the oligotrophic waters of the South-West Pacific between New Caledonia and Fiji, where we simultaneously measured a) zooplankton biomass and their faecal pellet production rates, b) Po-210 and its progenitor Pb-210 in water, zooplankton and their faecal pellets and c) particle flux rates using U-238:Th-234 disequilibria, to further assess the role of zooplankton in Po-210 and Pb-210 biogeochemistry in the euphotic zone of oligotrophic systems [4].

Zooplankton sampled from the oceanic region of the SW Pacific between Fiji and New Caledonia had biomasses ranging from 0.1 to 7.1 mg dw/m^3, with a median value of 3.6 and mean of 2.65 mg dw/m^3. Their faecal pellet production rates were measured on board and varied between $1.82.10^{-4}$-$3.78.10^{-3}$ g dry faecal pellet. g dry zooplankton^{-1}. hour^{-1}. Their measured Po-210 and Pb-210 concentrations were 830-2655 Bq kg dw^{-1} and 44-617 Bq kg dw^{-1}, respectively. Po-210 and Pb-210 concentrations in zooplankton varied between 565-1736 Bq kg dw^{-1} and 47-551 Bq kg dw^{-1}, respectively.

Po-210 concentration factors that only varied between 1.3–3.3. 10^5 were elevated compared to the IAEA recommended value of 3.10^4 based on previous values [5]. Similarly, Pb-210 concentration factors ranging from 0.9-9.1. 10^4, were considerably elevated compared to the IAEA recommended value of 1.10^3 [5], indicating the presence of a further concentrating mechanism.

Table 1. Po-210 and Pb-210 concentrations in samples of water, zooplankton and their faecal pellets. $^{\Omega}$ based on wet weight: dry weight conversion ratio of 7.5 [4]

Location	Date	Zooplankton biomass (mgDW/m^3)	Zooplankton concentration (Bq/KgDW)$^{\Omega}$		Water concentration [dissolved(mBq/L)]		Zooplankton faecal pellets (Bq/KgDW)		Concentration factors for zooplankton	
			Po-210	Pb-210	Po-210	Pb-210	Po-210	Pb-210	Po-210	Pb-210
Oceanic (OF1-14-03)	Mar 02	2.09	1736	266	0.70	1.67	2655	617	3.3. 10^5	2.1. 10^4
Oceanic (OF2-16-03)	Mar 02	7.12	1404	324	1.52	1.57	1389	438	1.2. 10^5	2.8. 10^4
Oceanic (OF3-19-03)	Mar 02	1.40	1039	187	0.47	1.72	2660	351	2.9. 10^5	1.4. 10^4
Oceanic (OF4-20-03)	Mar 02	2.22	998	209	0.92	3.19	2529	389	1.4. 10^5	0.9. 10^4
Oceanic (OF5-21-03)	Mar 02	4.68	1319	196	0.93	2.52	1784	419	1.9. 10^5	1.0. 10^4
Offshore 1	Nov 01	2.91	1285	302	1.23	0.81	830	115	1.4. 10^5	5.0. 10^4
Offshore 2	Nov 01	2.53	1348	551	0.68	0.81	1468	408	2.6. 10^5	9.1. 10^4
Offshore 3	Nov 01	2.66	1580	528	1.58	0.97	2578	390	1.3. 10^5	7.3. 10^4
Offshore 4a	Nov 01	0.7	1239	266	0.83	2.35	1734	431	2.0. 10^5	1.5. 10^4

Our results for Po-210 and Pb-210 show a consistency with published values [5, 6] in that the concentration factor for Po-210 is elevated relative to Pb-210, but contrast with previous reported values in both being elevated by about an order of magnitude. Their comparably elevated concentrations in faecal pellets suggest that enhanced concentrations in zooplankton are a reflection of the heightened concentrations in their dietary phytoplankton.

ACKNOWLEDGEMENT

The Agency is grateful for the support provided to its Marine Environment Laboratory by the Government of the Principality of Monaco.

REFERENCES

[1] POLETICO, C., TWINING, J.R., JEFFREE, R.A., Comparison of Concentrations of Natural and Artificial Radionuclides in Plankton from French Polynesian and Australian Coastal Waters (Proc. 9th Pacific Basin Conference, Sydney, Australia, 1-6 May) Trans. Am. Nucl. Soc. **70** 1 (1994) 989-993.

[2] JEFFREE, R.A., CARVALHO, F., FOWLER, S.W., FARBER-LORDA, J., Mechanism for enhanced uptake of radionuclides by zooplankton in French Polynesian oligotrophic waters, Environ. Sci. Techn. **31** (1997) 2584-2588.

[3] JEFFREE R.A, SZYMCZAK, R., Enhancing Effect of Marine Oligotrophy on Environmental Concentrations of Particle-Reactive Trace Elements, Environ. Sci. Techn. **34** 10 (2000) 1966-1969.

[4] JEFFREE, R.A, SZYMCZAK, R., PECK, G.A., Zooplankton concentration factors for Po-210 and Pb-210 in the Oligotrophic South-West Pacific (in prep.).

[5] INTERNATIONAL ATOMIC ENERGY AGENCY, Sediment Kds and Concentration Factors for Radionuclides in the Marine Environment, IAEA Technical Report Series TRS 247, Vienna (2003).

[6] NOZAKI, Y., THOMSON, J., TUREKIAN, K.K., The Distribution of ^{210}Pb and ^{210}Po in the surface waters of the Pacific Ocean, Earth Planet. Sci. Lett. **32** (1976) 304-312.

Distribution and interelement correlation between chemical elements and radionuclides in marine mammals from the southern Baltic Sea

Ciesielski, T.[a], M. Waszczuk-Jankowska[a], P. Fodor[b], Zs. Bertenyi[b], I. Kuklik[c], K. Skóra[c], R. Bojanowski[d], J. Namieśnik[e], P. Szefer[a]

[a] Department of Food Sciences,
Medical University of Gdansk,
Gdansk,
Poland

[b] Department of Applied Chemistry,
Faculty of Food Science,
Szent Istvan University,
Budapest,
Hungary

[c] Hel Marine Station,
University of Gdansk,
Gdansk,
Poland

[d] Marine Chemistry Laboratory,
Institute of Oceanology,
Polish Academy of Sciences,
Sopot,
Poland

[e] Department of Analytical Chemistry,
Chemical Faculty,
Gdansk University of Technology,
Gdansk,
Poland

Tissues of marine mammals (*Phocoena phocoena, Halichoerus grypus, Phoca hispida* and *Stenella coeruleoalba*) from the southern Baltic Sea were analysed for concentration of 26 elements (Al, As, B, Ba, Cd, Co, Cr, Cu, Fe, Ga, Li, Mn, Mo, Ni, Pb, Se, Si, Sr, Tl, V, Zn, Ca, K, Mg, Na, P) and radionuclides (^{137}Cs, ^{40}K, ^{210}Po). The trace and macroelements were determined by ICP-MS and ICP-AES while radionuclides using γ-spectrometry and α-spectrometry.

To find statistically significant relationship between hepatic concentrations of chemical elements and radionuclides, if any exist, the data obtained were processed by correlation analysis. Significant interelemental correlations ($p<0.05$) were found for the following assemblages: Al-Mg, Al-Mn, Ba-Ca-Sr, Ca-K-Mg-P, Cd-Fe, Fe-K, Fe-Se, K-Mn, K-Sr, Mg-Sr, Mg-Se, Mg-Zn, P-Se and P-Zn. Hepatic concentration of ^{137}Cs were negatively correlated with those of K and Si while ^{210}Po showed positive correlation with Mo.

The radioactivity data obtained in the present study are compared to those reported for marine mammals from the North Sea, Norwegian and Barents Sea (Fig. 1.). It is observed that levels of ^{137}Cs in porpoises from the southern Baltic are mostly attributable to the Chernobyl accident in 1986 while major source of this radionuclide in North Sea porpoises are discharges released from processing plants at Sellafield, England. Unlike the naturally occurring isotope ^{40}K, the ^{137}Cs displays tendency to accumulate significantly in mammals from Polish coast of the Baltic Sea.

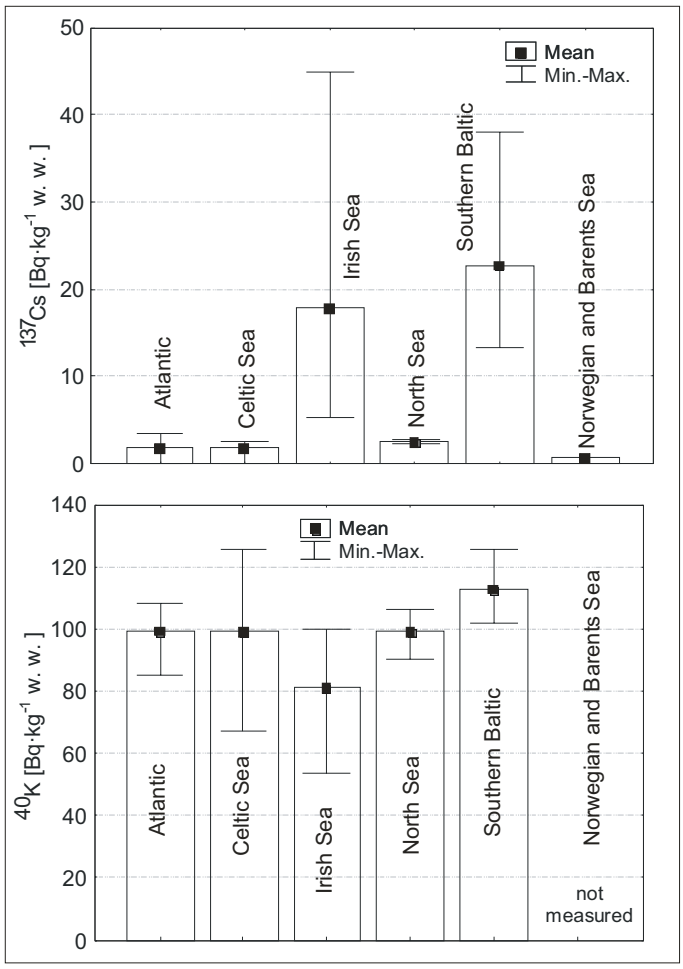

FIG. 1. Changes in the concentration of ^{137}Cs and ^{40}K in the muscle of harbor porpoises from different geographical regions.

Bioaccumulation of selected heavy metals in the brown alga *Lobophora variegata* : a radiotracer study

Metian, M.[a], L. Hédouin[a,b,c,d], E. Giron[a], E. Buschiazzo[a], V. Borne[a], J. Paganelli[a], R. Boudjenoun[e], O. Cotret[a], J.-L. Teyssié[a], S.W. Fowler[a], M. Warnau[a]

[a] International Atomic Energy Agency,
Marine Environment Laboratory,
Monaco

[b] IRD – Noumea Center,
New Caledonia

[c] LBEMB,
La Rochelle University,
France

[d] Goro-Nickel,
New Caledonia

[e] COMENA/CRNA,
Algiers,
Algeria

New Caledonia is a small South Pacific island whose main economic resources are derived from nickel exploitation. Local mining activities inevitably result in metal contamination of the surrounding environments. In particular, these long term activities are responsible for large inputs of metals into the SW lagoon and thereby constitute a threat to the local coastal marine ecosystems.

Available information on metal contamination in biota from New Caledonia is extremely scarce [1]. However, a recent study has screened metal contamination levels in a variety of local marine organisms in different locations of the SW lagoon [2]. This study showed that several species could be considered as potential bioindicators. Among these, the brown alga *Lobophora variegata* appeared as one of the most valuable candidates. Indeed, this species is abundant, widely distributed in the lagoon as well as in other tropical ecosystems, and displays high levels of metals within its tissues. The aim of this work was to investigate metal bioaccumulation kinetics in *L. variegata* in order to further assess its value as a sentinel species for identifying and monitoring environmental contamination.

Uptake and loss kinetics of six different metals (Cr, Co, Zn, Cd, Ag, and Ni) were determined using multi-element exposures with carrier-free or high specific activity radiotracers (^{51}Cr, ^{57}Co, ^{65}Zn, ^{109}Cd, ^{110m}Ag, ^{63}Ni) in order to carry out the experiments at realistic contaminant levels. In another set of experiments, mono-element exposures were carried out with five increasing concentrations of each metal (14d of exposure followed by 21 d of depuration) in order to assess the possible influence of ambient dissolved concentration on metal bioconcentration and retention capacity in the alga. The ranges of concentrations for each metal were selected in order to cover the range of dissolved concentrations encountered in the lagoon.

Results showed that all the metals tested were readily incorporated in the tissues of *L. variegata* and were concentrated according to linear kinetics. After 28 d of exposure, the alga attained concentration factors (CF) ranging from 585 to 6,530 depending on the element. Previously exposed algae were then

replaced in non-contaminated conditions for 2 months. Loss kinetics indicated that the metals were efficiently retained in the algae, and retention was characterized by biological half lives ($T_{b½}$) always longer than 33 d. Except for Zn, the CFs were independent of the ambient dissolved concentration of the metals. In the case of Zn, only the highest concentration tested had a lower CF observed. This was due most likely to a saturation of Zn binding sites at the highest ambient concentration used. Similarly, $T_{b½}$ was found to be constant over the whole range of dissolved concentrations tested.

In summary, *Lobophora variegata* appears to be an excellent bioindicator species that shows a rapid response time in metal uptake and therefore has a suitable potential to furnish valuable quantitative information on the contamination levels occurring in its surrounding environment.

ACKNOWLEDGEMENT

The Agency is grateful for the support provided to its Marine Environment Laboratory by the Government of the Principality of Monaco.

REFERENCES

[1] LABROSSE, P., FICHEZ, R., FARMAN, R., ADAMS, T., New Caledonia, (SHEPPARD, C.R.C., Ed.), Seas at the Millennium: An environmental evaluation, Pergamon Press, Amsterdam (2000) 723-736.

[2] BREAU, L., Etude de la bioaccumulation des métaux dans quelques espèces marines tropicales: recherche de bioindicateurs de contamination et application à la surveillance de l'environnement côtier dans le lagon sud-ouest de la Nouvelle-Calédonie, PhD Thesis, La Rochelle University, France (2003) 282 pp.

Anthropogenic radionuclides in fish, shellfish, algae and sediments from the Sudanese Red Sea coastal environment

Rifaat Babiker, H.K.[a], A.K. Sam[a], O.I. Osman[b], D.A. Sirelkhatim[a], J. La Rosa[c]

[a] Sudan Atomic Energy Commission,
Khartoum,
Sudan

[b] Chemistry Department,
Faculty of Science,
University of Khartoum,
Khartoum,
Sudan

[c] International Atomic Energy Agency,
Marine Environment Laboratory,
Monaco

The activity concentration of fallout radionuclides viz.^{238}Pu ,$^{239+240}$Pu, ^{241}Am,^{137}Cs and ^{90}Sr has been measured in some species of multicellular marine algae, coral fishes and shellfish, and surface sediments collected from the fringing reef at different locations along the Sudanese coast of the Red Sea. The measurements were carried out using alpha-particle spectrometry, high-resolution gamma spectrometry and gas-flow proportional counter.

In the sediments analyzed, the activity concentration averaged 2.65 ± 1.3 (^{238}Pu), 47.96 ± 26.3 ($^{239+240}$Pu), 19.1 ± 6.5 (^{241}Am), 273 ± 157 (^{137}Cs) and 140.8 ± 73.9 (^{90}Sr) mBq/kg dry weight. Activity concentration ratios were 0.066 ± 0.041 (^{238}Pu: $^{239+240}$Pu), 0.22 ± 0.04 ($^{239+240}$Pu:^{137}Cs), and 0.43 ± 0.1 (^{241}Am:$^{239+240}$Pu). These values are typical of those reported in the literature from the regions unaffected directly by nuclear accidents or nuclear reprocessing plant discharges and can thus be attributed to global fallout.

Average activity concentrations (mBq/gk Dry weight) in marine algae from different locations were found to be 20.1 ± 14.1, 21.6 ± 13.3 and 8.5 ± 3.8 ($^{239+240}$Pu), 6.2 ± 4.0, 11.7 ± 6.1 and 5.1 ± 3.5 (^{241}Am) and 688 ± 242, 868 ± 713 and 116 ± 14.8 (^{137}Cs) for brown, red and green algae, respectively. These results were found to be consistently decrease towards the south from Portsudan harbour (Fig. 1) and comparable to global fallout values. High levels of ^{137}Cs were observed in brown algae (*Cystoseria* species) and red algae (*Lauranthia* species). This possibly suggests their suitability to be used as bioindicators since algae are known to be effective bioindicators for monitoring the anthropogenic radioactivity in the marine environment.

Plutonium isotopes were measured in some species of coral fishes and shellfish samples from the fringing reefs area at Port Sudan. Activity concentrations of both ^{238}Pu ,$^{239+240}$Pu in fish are close to detection limits, while shellfish show values an order of magnitude higher relative to coral fish species. The lowest concentration for $^{239+240}$Pu was met in the molluscs species *Tridacnica* and the highest value was met in the coral species *Favites.*

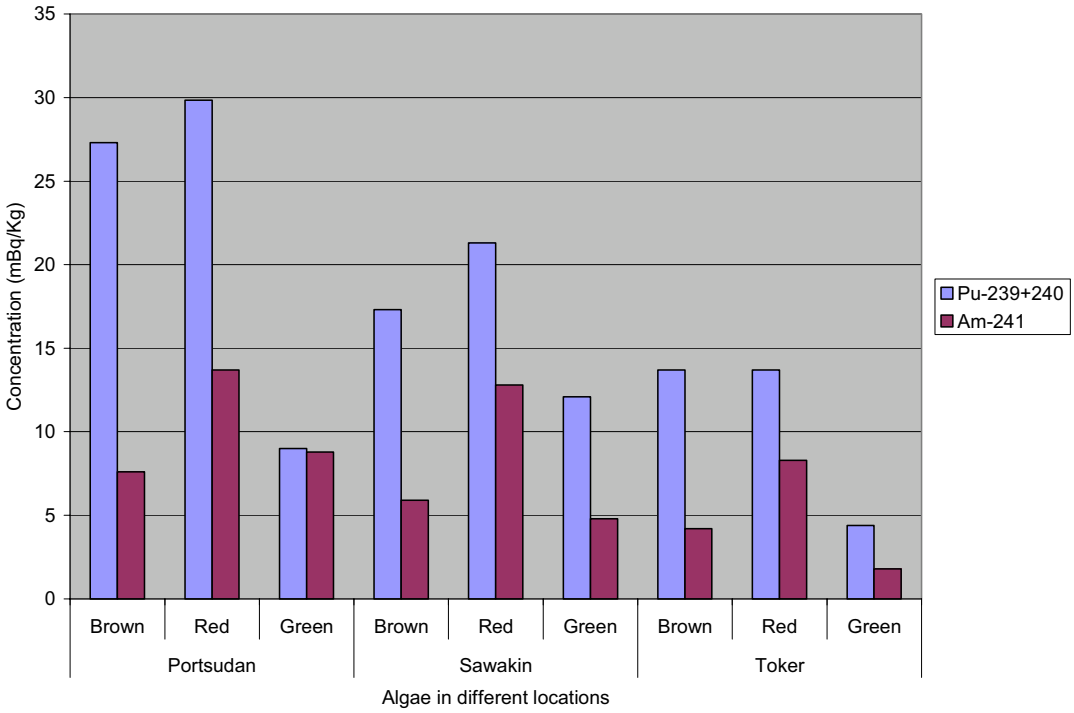

FIG. 1. Comparison of Pu and Am mean activity in mBq/kg in algae from different locations along the Red Sea coast.

ACKNOWLEDGEMENT

The Agency is grateful for the support provided to its Marine Environment Laboratory by the Government of the Principality of Monaco.

BIOMONITORS – POSTERS

Zinc uptake and behaviour in the scleractinian coral *Stylophora pistillata*

Boisson, F.[a], C. Richard[b], C. Ferrier-Pages[b]

[a] Marine Environment Laboratory,
International Atomic Energy Agency,
Monaco

[b] Centre Scientifique de Monaco,
Monaco

Zinc (Zn) is essential for organism growth as it is a cofactor of nearly 300 enzyme systems. In phytoplankton, carbonic anhydrase, a zinc-based metalloenzyme, is involved in the inorganic carbon acquisition from seawater. The activity of this enzyme has been shown to be dependent on the level of CO_2 and on the availability of zinc, thus conferring on zinc a key role in oceanic carbon cycling. Reef-building corals are autotrophic organisms, living in symbiosis with dinoflagellates called zooxanthellae. In the nutrient-poor tropical environment, concentrations of zinc might be low enough to limit photosynthesis and calcification in corals. A radiotracer technique was used to determine whether a scleractinian coral has the ability to efficiently bioaccumulate and retain the low in situ amounts of dissolved zinc required for its enzymatic activity determining its growth, and if there is any role played in this process by the symbiotic organism, the zooxanthellae.

To assess the Zn uptake and behaviour in *Stylophora pistillata*, two experiments were performed with 20 microcolonies each (culture method described in [1]). The corals nubbins were kept in the dark for the first experiment while they received 300 µmol photons m^{-2} s^{-1} in the second experiment at 8 different stable Zn concentrations in the experimental medium (5 nmoles l^{-1} being the natural zinc concentration measured in the seawater). Colonies were incubated 12 hours in 0.22 µm filtered seawater spiked with the radiotracer ^{65}Zn ($T_{1/2}$ = 244.3 days). The gamma emission of ^{65}Zn (506 KeV) in the skeleton, tissue and seawater was determined using a well type NaI detector. The chlorophyll fluorescence of the photosymbiotic components of the corals was measured using the underwater fluorometer Diving PAM (Walz, Germany).

The linear relationship (Fig. 1) obtained between concentrations of zinc incorporated in coral tissue and zinc concentration in the experimental medium ranging from environmental to high levels suggests that, (1) zinc diffuses through the coral tissue without any active transport process and, (2) almost the totality of zinc present in seawater is taken up by the coral tissue, the incorporation of zinc into the skeleton representing between 3 and 17% of the total zinc bioaccumulated in coral nubbins.

The uptake rates measured in coral tissues for the light/dark experiment (Fig. 2) ranged from 3.8 to 4.5 pmoles Zn (mg protein)$^{-1}$ h^{-1}. Zinc uptake rates were significantly higher for microcolonies of corals incubated under light conditions than values obtained in the dark (t-test, $p < 0.05$), while no significant difference was observed for Zn uptake rates in the skeleton (t-test, $p > 0.05$). These results indicate that zooxanthellae (located in the tissue of the corals) play a significant role in the incorporation of this metabolically essential metal. This is in agreement with the results of [2], who provided some evidence to suggest that zooxanthellae may have different metals loads than the coral tissue.

The results of the chlorophyll fluorescence of the photosymbiotic components of the corals further show that zinc enrichment in the marine environment stimulates the photosynthetic capacity of the corals through an enhancement of the activity of the coral's PSII. As a consequence, the calcification of corals should be also enhanced.

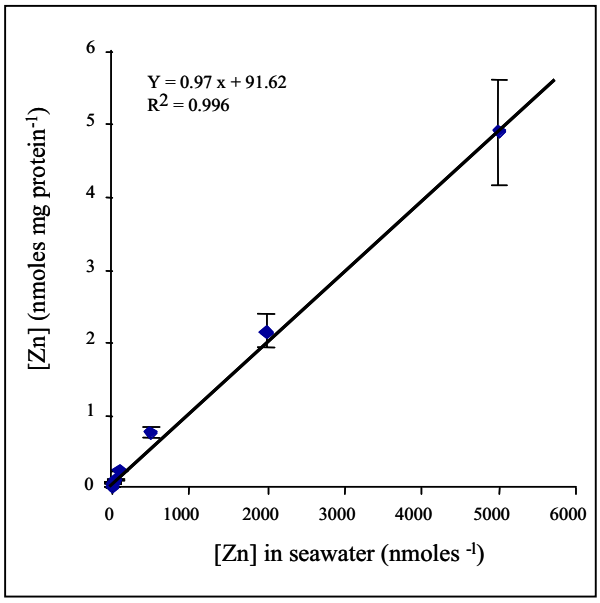

FIG. 1. Bioaccumulation of Zn in coral tissues as a function of [Zn] in seawater

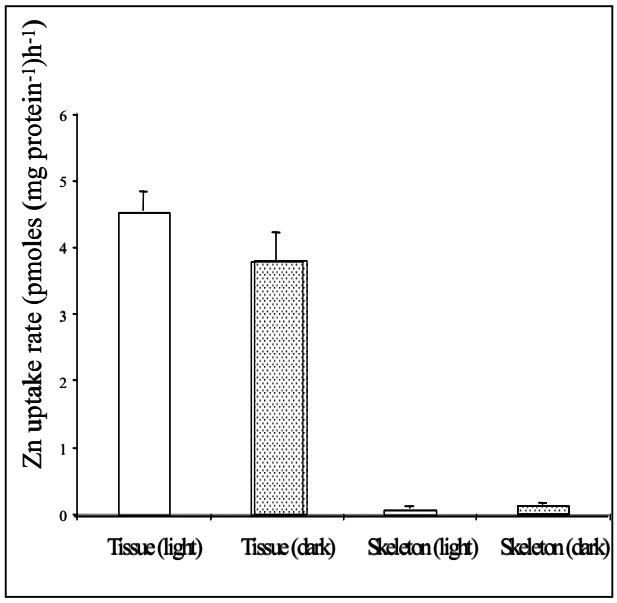

FIG. 2. Influence of light/dark regime on Zn uptake rate in coral tissues and in the skeleton

ACKNOWLEDGEMENT

The International Atomic Energy Agency is grateful for the support provided to its Marine Environment Laboratory by the Government of the Principality of Monaco.

REFERENCES

[1] TAMBUTTÉ, E., ALLEMAND, D., BOURGE, I., GATTUSO, J.P., JAUBERT, J., An improved ^{45}Ca protocol for investigating physiological mechanisms in coral calcification, Mar. Biol. **122** (1995) 453-459.

[2] MARSHALL, Occurrence, distribution and localisation of metals in cnidarians review, Microscopy and Technique **56** 5 (2002) 341-357.

Distribution of radioactive caesium, potassium and selected chemical elements in the macrophytes from the southern Baltic waters and application of factor analysis to study interelemental relationships

Zbikowski, R.[a], R. Bojanowski[b], P. Szefer[c], A. Latała[a]

[a] Institute of Oceanography,
Laboratory of Marine Plant Ecophysiology,
University of Gdańsk, Gdynia,
Poland

[b] Institute of Oceanology,
Polish Academy of Sciences,
Sopot,
Poland

[c] Department of Analytical Chemistry,
Medical University of Gdańsk,
Poland

Radioactive elements are specific kind of pollutants in aqueous environment. In Poland, the problem of radiological exposure has arisen since 1986 as a consequence of nuclear power station disaster in Chernobyl. Hence, a greater amount of isotope ^{137}Cs has been introduced into the Baltic Sea. Unfortunately, information on the concentrations of ^{137}Cs in macrophytes from the Polish economical zone waters following the Chernobyl accident are missing. The aim of the present investigations was to determine distribution and relationship of ^{137}Cs and ^{40}K content as well as selected macroelements (Ca, K, Na, Mg) and heavy metals (Cd, Cu, Ni, Pb, Mn, Zn) in benthic flora from the Southern Baltic waters (Gulf of Gdańsk and Vistula Lagoon) to find correlations and evaluate environmental quality of this areas.

The radionuclide contents were measured by gamma spectrometry. It was found in the present study that in the macrophytes from the Gulf of Gdańsk the average content of ^{137}Cs was 13.7 Bq/kg d.wt. Particularly high level of this element was noted in Ectocarpaceae, *Polysiphonia* sp., and *Myriophyllum spicatum*, from the Gulf of Gdańsk and in *Enteromorpha* sp. from the Vistula Lagoon. Comparing concentration factors (CF) of individual species it could be stated that they are several times higher in the macrophytes from the Vistula Lagoon than in those of the Gulf of Gdańsk. The content of ^{40}K in the benthic plants from the Gulf of Gdańsk (240 Bq/kg d.wt. on the average, range 82-423 Bq/kg d.wt.) was comparable to the values noted in the macrophytes from the Vistula Lagoon (322 Bq/kg d.wt. on the average, range 62-557 Bq/kg d.wt.). Ectocarpaceae and *Zostera marina* from the Gulf of Gdańsk as well as *Nuphar luteum* and *Ceratophyllum* sp. from the Vistula Lagoon were especially rich in ^{40}K. The values of ^{40}K concentration factors in the vascular plants from the Gulf of Gdańsk (range: 9-25) and in the Vistula Lagoon (range: 15-26) were similar. The comparison of ^{137}Cs content in 7 species of the benthic plants from the Gulf of Gdańsk to the analogous data obtained in 1973 does not reveal significant changes, with the exception of *Myriophyllum spicatum* where higher activities were found in the years 2000-2002.

The content of the selected metallic elements for the macrophytes was determined by flame atomic absorption spectroscopy (FAAS). The relationships and correlations between radionuclides and metallic elements contents in benthic plants from the Southern Baltic waters were determined using factor analysis with STATISTICA program.

High levels of natural radioactivity in biota from deep sea hydrothermal vents

Charmasson, S.[a], M. Agarande[b], D. Louvat[a], A-M. Neiva Marques[b], P-M. Sarradin[c], J. Loyen[b], D. Desbruyeres[c]

[a] Institut de Radioprotection et de Sûreté Nucléaire (IRSN),
DEI/SESURE,
La Seyne sur mer,
France

[b] IRSN/DEI/STEME,
France

[c] IFREMER Centre de Brest,
Département Environnement Profond,
France

Hydrothermal vent ecosystems are associated with areas of tectonic activities throughout the deep sea and are thus enriched in natural primitive radionuclides characterizing the magma source i.e. uranium-thorium series. However, the amount of data on radionuclide content in hydrothermal vent biota is very scarce. Here we present data from various archived biological samples collected on several hydrothermal vent site. Samples were collected by manned or unmanned submersibles on the East Pacific Rise (EPR) in 1996 and 2002 and on the Mid Atlantic Ridge (MAR) in 2001 (Table I).

Their concentrations in uranium and thorium isotopes were determined by isotope dilution mass spectrometry. Measurements were performed with a Sector field ICP-MS, the Axiom single collector from VG Elemental (Winsford, Cheshire, UK). ^{210}Po was determined through alpha spectrometry.

Table I. Characteristics of the locations and species sampled at various vent sites

Sampling dates	Site	Position		Depth (m)	Species
02/20/1996	Genesis EPR	12°48N	103°56W	2640	Polychaetes Alvinella
03/11/1996	Q vent EPR	09°51N	104°17W	2530	Polychaetes Paralvinella
06/28/2001	Rainbow MAR	36°13N	33°54W	2300	Crustacean Rimicaris
07/03/2001	Lucky strike MAR	37°17N	32°16W	1700	Mollusc Bathymodiolus
07/10/2001	Menez Gwen MAR	37°51N	31°31W	850	Mollusc Bathymodiolus
05/10/2002	Elsa EPR	12°48N	103°56W	2640	Vestimenfères Riftia
05/25/2002	Genesis EPR	12°48N	103°56W	2640	Polychaetes Paralvinella
05/25/2002	Genesis EPR	12°48N	103°56W	2640	Paralvinella Tubes + mucus

Table II. ^{234}U, ^{235}U, ^{238}U and ^{210}Po contents (Bq kg^{-1} dry weight) in various organisms from hydrothermal vents and in one crustacean sample from outside hydrothermal vent ecosystems (in italics)

Sampling dates	Species/Location	^{234}U	^{238}U	^{235}U	^{210}Po
06/28/2001	Rimicaris (MAR)	18.8 ± 1.1	16.9 ± 0.4	0.79 ± 0.05	na*
07/03/2001	Bathymodiolus (MAR)	106.7 ± 4.02	83.7 ± 2.4	3.8 ± 0.1	na
07/10/2001	Bathymodiolus (MAR)	10.5 ± 0.7	14.0 ± 0.3	0.43 ± 0.03	na
02/20/1996	Alvinella (EPR)	166.4 ± 8.9	199.8 ± 8.8	9.3 ± 0.5	na
03/11/1996	Paralvinella (EPR)	830.4 ± 106.3	660.3 ± 74.6	30.5 ± 3.8	na
05/10/2002	Riftia (EPR)	6.5 ± 0.8	39.5 ± 2.2	1.86 ± 0.14	100 ± 18
05/25/2002	Paralvinella (EPR)	1074.5 ± 132.7	856.0 ± 91.9	39.9 ± 4.9	na
05/25/2002	Tubes+mucus (EPR)	3566.7 ± 478.5	3041.8 ± 326.7	143.2 ± 18.7	16,000 ± 1300
08/04/2000	Orchomenella (Abyssal plain)	1.48 ± 0.06	5.21 ± 0.21	0.25 ± 0.02	na

*na: not analyzed

Results in Table II underline that high levels in uranium isotopes are found in polychaetes from the East Pacific Rise. The highest contents characterize their tubes plus mucus samples. On the contrary, the deep-sea amphipod sample (Orchomenella) collected outside hydrothermal vent areas exhibits the lowest values though direct comparison is difficult due to variability between species. ^{238}U contents in coastal marine organisms are generally in the range 1 to 5 Bq kg^{-1} dry weight. Comparison between sites (Atlantic vs Pacific) is not obvious since different species have been sampled on MAR and EPR but the highest levels characterize the samples from EPR. Some samples demonstrate $^{234}U/^{238}U$ ratios very close to the mean value for seawater (1.1 – 1.2) but four present lower ratios (i.e. one sample of Bathymodiolus, Paralvinella, Riftia and Orchomenella). This is certainly to be linked to an uptake of particulate uranium. ^{210}Po contents are very high in polychaetes tubes and mucus and are almost entirely supported by ^{210}Pb. This in agreement with what has been reported by Cherry et al. (1992) for polychaetes (Alvinella and Paralvinella) from EPR. These authors also reported highest levels for these elements in Paralvinella (i.e. 15113 and 19038 Bq kg^{-1} dry weight for ^{210}Pb and ^{210}Po respectively).

We are aware that this work is still based on too few data. A major work has to be done on this topic but these first results appear to be promising. The determination of vent organism concentrations for key elements in the uranium-thorium families has to be carried out in order to precisely determine the radiation exposure they are subject to. This appears especially important at the time where international bodies aim at promoting the development of criteria on the protection of the environment from effects arising from exposures to ionizing radiation.

ACKNOWLEDGEMENTS

The authors are grateful to the Chief Scientists of the various cruises, i.e. F. Gail (HOPE 1996), P.M. Sarradin (ATOS 2001) and N. Le Bris (PHARE 2002). Part of this work has been funded through the Ventox project EVK3 CT1999-2003 of the European Commission.

REFERENCE

[1] CHERRY, R., DESBRUYÈRES, D., HEYRAUD, M., NOLAN, C., High levels of natural radioactivity in hydrothermal vent polychaetes, C.R. Acad. Sci. Paris, t. 315, Série III (1992) 21-26.

Influence of ambient dissolved metal concentration on their bioaccumulation in two tropical oysters: a radiotracer study

Giron, E[a], E. Buschiazzo[a], L. Hédouin[a,b], M. Gomez Batista[c], M. Metian[a], V. Borne[a], O. Cotret[a], J.-L. Teyssié[a], S.W. Fowler[a], M. Warnau[a]

[a] International Atomic Energy Agency,
Marine Environment Laboratory,
Monaco

[b] IRD-Noumea Center,
Noumea,
New Caledonia

[c] CEAC,
Cienfuegos,
Cuba

The tropical coastal zone is presently experiencing increasing urban and industrial development. Subsequent socio-economic development results in increased production of wastes which finally reach the coastal environment where they constitute a possible threat for local marine ecosystems [1].

The SW lagoon of New Caledonia represents a tropical case study as it is subjected to large inputs of heavy metals mainly due to intense land-based mining activities. The metal contamination concerns essentially Ni (New Caledonia is the third world producer of Ni) but also other metals such as Cr, Co and Mn which occur at elevated concentrations in Ni ores. Although mining is a continuing activity in New Caledonia, available information about the contamination status of the marine environment is extremely scarce [2, 3]. Therefore, studies are needed to understand the behaviour and fate of metals in this region in order to be able to develop coastal zone monitoring programmes and improve local marine resource management.

In the framework of the "New Caledonia" Project funded by the French National PNEC Programme, the bioaccumulation of metals was investigated in two oyster species commonly found in the lagoon: *Isognomon isognomon* and *Malleus regula*. A recent field study indicated that these bivalves showed relatively high levels of metals in their soft tissues and that they were possible candidates as bioindicator species that could be used to discriminate between contamination levels in different locations.

Among the several pre-requisites that a bioindicator species should fulfil [4, 5], the one indicating that the organism should display body contaminant concentrations that reflect those occurring in the surrounding environment is rarely assessed. Nevertheless, this assumption is of prime importance. This is particularly the case for proper interpretation of monitoring data from the New Caledonia lagoon, since a wide range of dissolved concentrations of metals may be encountered in the field (e.g., Ni dissolved concentrations range from background levels off shore up to 1,340 ng L^{-1} in the most contaminated bays [3]).

The objective of this work was thus to investigate the bioaccumulation behaviour of the two selected oyster species under different contaminating conditions. Seven different metals (Co, Zn, Mn, Cd, Cr, As and Ni) were considered and their bioconcentration was studied using appropriate radiotracers (^{57}Co, ^{65}Zn, ^{54}Mn, ^{109}Cd, ^{51}Cr, ^{73}As and ^{63}Ni).

The selected organisms were exposed for 14 d to five increasing concentrations of one of the six selected metals and then held for 21 d under non-contaminated conditions. During these two periods, kinetics of metal uptake and loss were determined in whole-body individuals. In addition, tissue distribution of the metals was determined at the end of both exposure and depuration periods.

Uptake kinetics were expressed as the variation of the concentration factor (CF; ratio between radioactivity measured in the organism and in sea water) over time. Steady-state equilibrium was never reached during the observation period and uptake kinetics were always best described using a simple linear equation. Loss kinetics were expressed as the variation of the percentage of remaining activity (ratio between radioactivity in the organism at time *t* and at the beginning of the depuration period x 100) and were best described using a single-exponential equation.

In general, the results indicated that both oyster species took up and subsequently retained metals in direct proportion to the ambient dissolved concentration for all metals tested. Regressions between kinetic parameters (uptake rate constant, depuration rate constant, and assimilation efficiency of dissolved metal) and dissolved concentrations indicated that these parameters did not vary significantly with ambient metal concentrations over the entire range of concentrations that may be encountered in the waters of the lagoon.

The present study confirmed that both uptake and retention of the seven metals tested are proportional to their ambient dissolved concentrations in *I. isognomon* and *M. regula*. These findings are of prime importance, since they demonstrate that metal concentrations measured in both oysters actually reflect those occurring in their environment, and moreover validate the usefulness of these bivalves as bioindicator species for monitoring metal contamination in the New Caledonian lagoon.

ACKNOWLEDGEMENT

The Agency is grateful for the support provided to its Marine Environment Laboratory by the Government of the Principality of Monaco.

REFERENCES

[1] HATCHER, B.G., JOHANNES, R.E., ROBERTSON, A.I., Oceanogr. Mar. Biol. Annual Rev. **27** (1989) 337-414.

[2] LABROSSE, P., FICHEZ, R., FARMAN, R., ADAMS, T., New Caledonia, (SHEPPARD, C.R.C., Ed.), Seas at the Millennium: An environmental evaluation. Pergamon Press, Amsterdam (2000) 723-736.

[3] BREAU, L., Etude de la bioaccumulation des métaux dans quelques espèces marines tropicales : recherche de bioindicateurs de contamination et application à la surveillance de l'environnement côtier dans le lagon sud-ouest de la Nouvelle-Calédonie, PhD Thesis, La Rochelle University, France (2003) 282 pp.

[4] MOORE, N.W., A pesticide monitoring system with special reference to the selection of indicator species, J. Appl. Ecol. **3** (1966) 261-269.

[5] PHILLIPS, D.J.H., Use of macroalgae and invertebrates as monitors of metal levels in estuaries and coastal waters, Heavy Metals in the Marine Environment (FURNESS, R.W., RAINBOW, P.S., Eds) CRC Press, Boca Raton, FL (1990) 81-99.

Systematic model of metal and radionuclide bioaccumulation in crocodilian and molluscan calcified tissues

Jeffree, R.A.[a], S.J. Markich[b]

[a] International Atomic Energy Agency,
Marine Environment Laboratory,
Monaco

[b] Aquatic Solutions International,
Dundas Valley NSW,
Australia

Bioaccumulating organisms routinely concentrate a variety of contaminants from their aquatic medium. Discerning any underlying factors that explain patterns of accumulation in a systematic way improves both the theoretical basis of our understanding of bioacccumulation and our ability to correctly interpret environmental signals that are represented by a tissue concentration or set of contaminant concentrations. Operational predictors of variance between individuals in their contaminant tissue concentrations also enhance our ability to statistically demonstrate increases above background, allowing us to infer increased environmental exposure with more confidence.

Our recent investigations have focussed on concentrations of Pb in the osteoderms (dermal bones on the dorsal surface) of crocodiles in a study designed to monitor their contemporary and historical contamination status [1]. The associated environmental sampling program also provided the opportunity to more broadly investigate patterns of metal and radionuclide accumulation in this calcified vertebrate tissue. These studies on the estuarine crocodile (*Crocodylus porosus*) showed that both biotic and geographical factors can affect osteodermal and flesh concentrations for a variety of elements [2, 3].

A current study determined the metal concentrations and their predictors for the osteoderms of Australian freshwater crocodiles (*Crocodylus johnstoni*) from a single geographically restricted area, where each sampled individual was well characterised with respect to site fidelity, reproductive status and age, extending up to 63 years [4].

Crocodile size, age and osteoderm calcium concentration were highly significant ($P<0.001$) predictors of the osteoderm concentrations of a range of metals. Osteodermal metal concentrations were inversely related to both size and age, but positively related to osteoderm calcium concentration, that could explain up to 92% of variance between individuals. Relative to calcium concentration, the rates of metal accumulation in the osteoderms of *C. johnstoni* were inversely related to the solubility constant (log Ksp) of the metal as a phosphate. However, this relationship was not linear (Fig. 1 from [4]). This finding is consistent with that previously determined in the flesh of several species of freshwater bivalves [5], which like the crocodilian osteoderm, have a calcium phosphate repository viz. their extracellular granules in flesh.

The constancy of this relationship between rate of metal accumulation and the relative solubility of the calcium phosphate deposits, despite the contrasting Ca accumulation regimes and degree of taxonomic dissimilarity, strongly suggests an underlying principle that warrants further investigation in a greater range of biota [4].

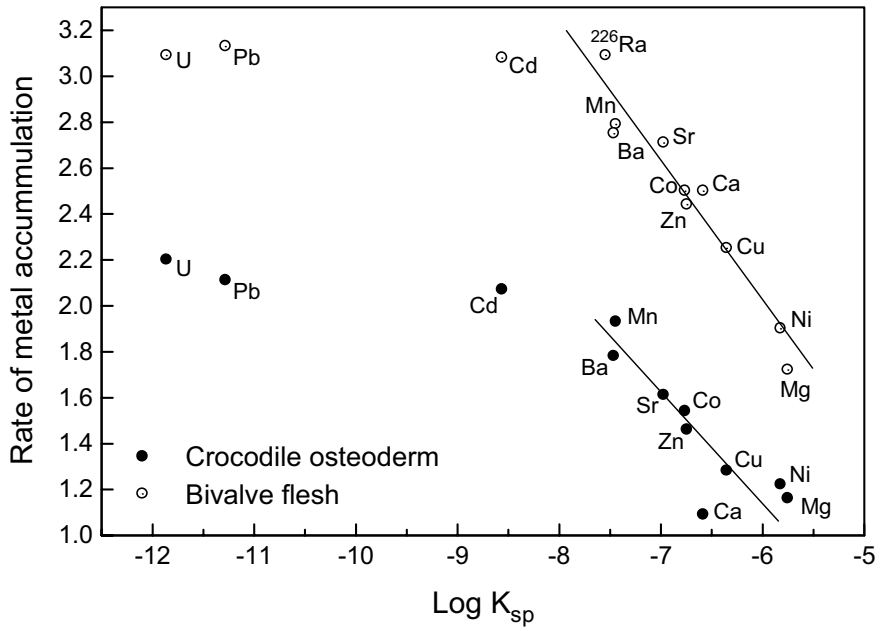

FIG. 1. Rate of accumulation for each metal plotted against its solubility constant (log_{10} K) as a phosphate for osteoderms of C. johnstoni and the flesh of a freshwater bivalve.

Furthermore, the range of predictive relationships that have been demonstrated, that explain much of the variance among individuals should provide a better capability to discern differences between populations in their contaminant status, for a variety of metals.

ACKNOWLEDGEMENT

The Agency is grateful for the support provided to its Marine Environment Laboratory by the Government of the Principality of Monaco.

REFERENCES

[1] TWINING, J., MARKICH, S., PRINCE, K., JEFFREE, R., Osteoderms of estuarine crocodiles record their enhanced Pb exposure in Kakadu National Park, Environ. Sci Technol. **33** (1999) 4396-4400.

[2] JEFFREE, R., MARKICH, S., TWINING, J., Metal concentrations in the flesh and osteoderms of estuarine crocodiles (*Crocodylus porosus*) from the Alligator Rivers Region, Northern Australia: Biotic and geographic predictors, Arch. Environ. Toxicol. Contam. **40** (2001) 236-245.

[3] MARKICH, S., JEFFREE, R., HARCH, B., Catchment-specific metal signatures in estuarine crocodiles (*Crocodylus porosus*) from the Alligator Rivers Region, Northern Australia, Sci. Total Environ. **287** (2002) 83-95.

[4] JEFFREE, R., MARKICH, S., TUCKER, A., Patterns of Metal Accumulation in Osteoderms of the Australian Freshwater Crocodile, *Crocodylus johnstoni*, Sci. Total Environ. (in press).

[5] MARKICH, S., BROWN, P., JEFFREE, R., Divalent metal accumulation in freshwater bivalves: An inverse relationship with metal phosphate solubility, Sci. Total Environ. **275** (2001) 27-41.

Bioaccumulation of arsenic and other heavy metals in the oyster *Crassostrea virginica* : a radiotracer study

Gómez-Batista, M.[a], M. Metian[b], E. Buschiazzo[b], J-L. Teyssié[b], O. Cotret[b], C. Alonso-Hernández[a], S.W. Fowler[b], M. Warnau[b]

[a] CEAC,
Cienfuegos,
Cuba

[b] International Atomic Energy Agency,
Marine Environment Laboratory,
Monaco

Arsenic is ubiquitous in the environment where it is present in soil, water and living organisms. The content of As in soil and water depends on natural geochemical factors as well as anthropogenic inputs such as combustion of hydrocarbons, production of fertilizers, and the use of arsenical pesticides. These anthropogenic inputs contribute to a significant portion of the total arsenic background levels in the marine environment. The harmful health effects of arsenic and its compounds on biological systems coupled with its widespread distribution have encouraged many investigators to closely monitor arsenic levels in the environment, especially in marine resources.

Cienfuegos Bay, situated in the southern part of Cuba, is a semi-enclosed bay divided into two well-defined hydrographic basins. The northern basin is subjected to important anthropogenic inputs from the outfall of Cienfuegos city (150,000 inhabitants), which is a major industrial pole of the country, as well as freshwater input from the Damuji and Salado rivers. The southern basin is subjected to lesser anthropogenic contamination originating from the Caonao and Arimao rivers. Part of the southern basin is a natural park which serves as a niche for many protected migratory birds and marine species.

Overall, the bay represents an important natural resource for the country due to industrial and artesian fishing activities, maritime transport, tourism, and its natural parks. During the last decade, important economic and social development around the bay has resulted in a significant increase in inputs of industrial and domestic wastes to its waters. Regarding As, direct inputs occurred from the nitrogen fertilizer factory which operated until 1989 and where two important accidental spills of As took place in 1979 and 2001.

Marine organisms represent an important component of the diet of the population of Cienfuegos; in particular people from the coastal areas of Castillo de Jagua, Las Minas and O'bourque ingest on average 51 kg of fish per year. Only few studies to date have investigated the total As content in marine organisms from Cuba. One of these studies measured total As in fish and crustaceans in Cienfuegos Bay in 1974 [2], before the first accidental spill. The results showed quite low As concentrations; e.g. mean values were 1.2 $\mu g\ g^{-1}$ dw in fish and 1.7 $\mu g\ g^{-1}$ dw in crustaceans which fall in the range of concentrations found in organisms from the western coast surveyed in the late 1980s (range: 0.01 to 4.82 $\mu g\ g^{-1}$dw; [3]). A more recent study has shown that total As concentrations in sediment and biota (fish, crustaceans and bivalves) have significantly increased in Cienfuegos bay during the last two decades [4]. Therefore, understanding the behaviour and fate of As in this region is of prime importance in order to be able to develop coastal zone monitoring programmes and improve local marine resource protection and management.

The objective of this work was to investigate the bioaccumulation behaviour of As and other co-occurring metals in the edible oyster *Crassostrea virginica,* a species that is abundant and widely

distributed in the Cienfuegos bay, and one that is frequently eaten by local populations. Seven different metals (As, Ag, Cr, Co, Cd, Mn and Zn) were examined and their bioconcentration was studied using γ-emitting radiotracers of the metals (^{73}As, ^{110m}Ag, ^{51}Cr, ^{57}Co, ^{109}Cd, ^{54}Mn and ^{65}Zn).

The organisms were exposed for 14 d in contaminated seawater to background concentrations of the seven metals and then held for 21 d under non-contaminated conditions. During these two periods, uptake and loss kinetics of the metal radiotracers were determined in whole individuals. In addition, tissue distribution of the metals was determined at the end of both uptake and depuration periods. In another experiment, *C. virginica* was exposed to four increasing concentrations of As dissolved in seawater in order to determine possible relationships between As bioaccumulation and ambient metal levels.

Uptake kinetics were expressed as the variation of the concentration factor (CF, ratio between radioactivity in the organism and in seawater) over time. After 14 d of exposure, CF reached mean values of 30-420 depending on the metal. Uptake kinetics of all metals except As were best described using a simple linear equation. For As a steady-state equilibrium was either reached or tended to be reached during the experimental period for all concentrations tested (CF_{ss} estimated at steady-state ≈ 10). In addition, no significant difference in bioaccumulation was found when oysters were exposed to increasing dissolved concentrations of As, except for the highest concentration tested (10 μg L^{-1}) where a slight decrease in concentration factor was observed.

Loss kinetics were expressed as the variation of the percentage of remaining activity (radioactivity in organism at time *t* / radioactivity at *t*=0 of depuration period) over time. The loss kinetics were generally best described using a single-exponential equation. Loss of ^{73}As, ^{110m}Ag, and ^{51}Cr was characterized by quite short retention times (Tb½ ≈ 4-5 d), whereas ^{57}Co, ^{109}Cd, ^{54}Mn and ^{65}Zn displayed much stronger retention (Tb½ > 30 d). No significant difference was found in As loss kinetics as a function of the initial exposure concentration.

In summary, our results demonstrate that *C. virginica* bioaccumulates metals efficiently. In the case of As, the oyster takes up the metal in direct proportion to the ambient dissolved As concentration and retains it to the same degree regardless of the initial exposure level. This indicates that *C. virginica* would be an excellent bioindicator species to monitor ambient levels of dissolved As. Furthermore, since this oyster rapidly reaches equilibrium concentrations of As and loses it quite rapidly from its tissues, *C. virginica* would be able to reveal short-term variations in As levels in the surrounding seawater.

REFERENCES

[1] ALONSO-HERNÁNDEZ, C.M., DIAZ-ASENCIO, M., MUÑOS-CARAVACA, A., SUAREZ-MORELL, E., AVILA-MORENO, R., J. Environ. Radioactivity **61** (2002) 203-211.

[2] CPHE, Informe de evaluación de las concentraciones de arsénico en la Bahía de Cienfuegos, Report, Provincial Center of Hygiene and Epidemiology, Cienfuegos, Cuba (1974).

[3] BELTRAN, G., SYMINTON, R., DOMINGUEZ, A., AMALIA, E., ROCH, R., (1988). Arsenic residues in marine products from the western zone of Cuba, Rev. Cubana Hig. Epidemiol. **26** (1988) 100-105.

[4] ALONSO-HERNÁNDEZ, C.M., GÓMEZ-BATISTA, M., MUÑOZ-CARAVACA, A., PÉREZ-SANTANA, S., DÍAZ-ASENCIO, M., ESTEVEZ-ALVAREZ, J.R., PUPO GONZÁLEZ, I., ALBERRO MACÍAS, N., Total arsenic in marine organisms from Cienfuegos Bay, Cuba (in prep.).

Use of fish biomarker response in the evaluation of the Black Sea and the Sea of Azov coastal ecosystem health

Rudneva, I., L.S. Oven, N.F. Shevchenko, E.N. Skuratuvskaya, T.B. Vahtina, O.S. Roshina

Institute of Biology of the Southern Seas,
National Ukrainian Academy of Sciences,
Sevastopol,
Ukraine

Environmental stress in the Black Sea and the Sea of Azov coastal zones resulted in very negative biological events of the ecosystem at various levels of its biological organization, from molecular to the community levels [1]. The peculiarities of the polluted responses should be applied for the assessment of stress factors and their effects. Fish populations are the most sensitive to anthropogenic impacts. Within the past 40 years the number of fish species in the Sevastopol coastal zone has declined 2-fold, and their storage 100-fold. Thus fish responses to stressors could be used for evaluation of the entire ecosystem health [2].

Highly distributed fish species *Scorpaena porcus* and *Neogobius melanostomus* were used as biomonitors for the evaluation of the status of coastal zones. Fish were collected from polluted and non-polluted bays in the Sevastopol region, and their study has included the analysis of various biological indicators (biomarkers).

Biochemical studies of antioxidant enzyme activities (catalase, SOD, peroxidase, glutathione reductase and glutathione-S-transferase), transaminases and aldolase in blood serum of fish caught in both seas showed the differences between the *N. melanostomus* inhabited in the Black Sea and the Sea of Azov coastal areas (Table I).

Table I. Blood antioxidant enzyme activities (per mg hemoglobin per min) in *N. melanostomus* inhabited coastal areas of the Black Sea and the Sea of Azov

Enzymes	Black Sea, n = 230	Sea of Azov, n = 166	p
Catalase, mg H_2O_2	0.76 ± 0.08	0.87 ± 0.08	n/s
SOD, arbitrary units	274.50 ± 29.00	472.30 ± 57.00	<0.01
Peroxidase, optical units	10.60 ± 0.74	6.00 ± 0.40	<0.01
Glutathione reductase nmol NADPH	10.30 ± 1.20	7.50 ± 0.70	<0.05
Glutathione-S-transferase nmol conjugate	69.20 ± 12.50	44.70 ± 6.10	n/s

n/s- not significant

The increase of the activity of the main antioxidant enzymes SOD and glutathione-S-transferase were demonstrated in fish blood collected in polluted areas, while the other parameters were not differed significantly. The integrated index of antioxidant enzyme activity of fish blood is presented in Table II. The highest values were detected in fish from high polluted areas, that demonstrated the induction of antioxidant system, as a response on environmental contamination.

Table II. The integrated index of antioxydant enzyme activities of fish blood (arbitrary units)

Pollution level	*N. melanostomus*		*S. porcus*
	Black Sea	Sea of Azov	Black Sea
Highly polluted	1919	-	67
Polluted	265	626	54
Non polluted	172	474	40

At the same time the lipid peroxidation level was higher in fish that inhabited contaminated areas, as compared with individuals from the non-contaminated bays. This was connected with oxidative stress induced by high concentrations of xenobiotics in the environment. Significant differences between the lipid concentration, the lipid composition and the law molecular weight antioxidants were not identified. Elelctrophoretical studies of blood serum proteins demonstrated the changes in the proteins composition and their variability in fish from polluted and non-polluted areas. Thus the most sensitive biochemical indicators in fish are blood antioxidant enzyme activities (SOD and GST), lipid peroxidation parameters as well as the serum proteins elelctrophoretic composition.

On the basis of the hystochemical data various anomalies were identified in fish gonads and in the process of their maturation. The violations of gametogenesis connected with the gypertrophic oocyts lost the success of maturation and reproductive process in fish from high contaminated areas.

In spite of the fact that the population characteristics of fish (mass, size, age, liver and gonad indices) are informative biological indicators to examine population experiences stress for evidence of long-term impact, we could not determine the significant changes between these parameters in both fish species from the studied bays. It could be connected with the high level of the anthropogenic impact and the contamination of Sevastopol bays. Thus, the most sensitive indicators to pollution are biochemical and hystochemical parameters. They could be used for evaluation of the marine coastal ecosystem health, and adapted for national and international marine monitoring programs.

REFERENCES

[1] RUDNEVA, I., "Environmental and security challenges in the Black Sea region", Environmental conflicts: Implications for Theory and Practice, (PETZOLD-BRADLEY, E., CARRIUS, A., VINCZE, A., Eds), Kluwer Academic Publications, Netherlands (2001) 189-207.

[2] ADAMS, S.M., SHEPARD, M.S., GREELY, J., JIMENEZ, B.D., RYON, M.G., SHUGART, L.P., McCARTHY, J.F., HINTON, D., The use of bioindicators for assessing the effects of pollutant stress in fish, Mar. Environ. Res. **28** 1-4 (1989) 459-464.

Microcalorimetry method for the evaluation of the pollution response of marine organisms

Rudneva, I.I., V.G. Shaida, N.S. Kuzminova

Institute of Biology of the Southern Seas,
National Ukrainian Academy of Sciences,
Sevastopol,
Ukraine

Studies of the metabolic responses of marine animals to pollution have been carried out using various analytical techniques, including respirometry, biochemical, physiological analysis and direct calorimetry, which is the preferred technique in this case because it permits to study metabolic rates *in vivo* [1].

The determination of heat produced by organisms using microcalorimetry is based on the fundamental relationship between the changes of the Gibbs energy (G), the enthalpy (H) and the entropy (S), which can be expressed using the following equations:

$$\Delta H = \Delta G + \Delta S \quad (1)$$

$$\Delta H + \Delta E = \Delta PV \quad (2)$$

where

ΔE is the change of the total system energy,
P is the pressure and
V is the volume.

In biological systems, the parameters T, V and P are constant and PV = 0. Thus, $\Delta H = \Delta E$ and $\Delta E = \Delta G + T\Delta S$. ΔG is the characteristic of the biological system, and reflects the catabolic/anabolic processes in the organism [2].

The goal of the present study was to analyze the heat production in some Black Sea organisms in different stages of their development and exposition to toxicants (PCBs and pesticides), and to study the influence of environmental pollution on this parameter.

The heat production of microalgae, highly distributed in hypersaline coastal lakes and bay crustacea *Artemia salina* nauplia, larvae of fish *Neogobius melanostomus*, *Atherina hepsetus* and *Atherina mochon pontica*, exposed to toxicants in experimental conditions, and metabolic rate of *Atherina hepsetus* larvae inhabited polluted and non-polluted areas were measured using the Biological Activity Monitor BAM 2277 (Thermometric, Sweden). The TAM was fitted with four channels, both containing measuring and reference cells (a twin calorimeter). The heat output signal was recorded by Digitam Data program on a PC and later analyzed by the Digitam Data Analysis program [3].

The obtained results showed that in all cases examined stressors led negative effects on testing marine organisms. They resulted in increased mortality and decreased heat production. The effect of PCBs (0.001 and 0.0001 μg per liter) on heat dissipation of *Artemia* and fish larvae is presented in Table I. In both cases the heat production in stressed larvae was significantly lower when compared with intact organisms. Additionally, the increase of the hatching time of *A. salina* and *N. melanostomus* eggs incubated in PCBs was demonstrated.

Table I. Heat production of *A. salina* and fish larvae exposed in different concentrations of PCBs (μWtper individual)

Species	Intact	PCB, 0.0001 μg per L	PCB, 0.001 μg per L
A .salina	0.15 ± 0.01	-	0.09 ± 0.01, p<0.01
A. hepsetus	14.78 ± 1.82	-	5.46 ± 0.40, p<0.01
N. melanostomus	14.28 ± 1.32	8.52 ± 0.59, p<0.01	9.30 ± 1.04, p<0.01

Table II. Heat production of *A. salina* and fish larvae *A. mochon pontica* exposed in different concentrations of cuprocsat (μWt per individual)

Species	Intact	0.625 mg/L	1.25mg/L	2.5 mg/L
A .salina	0.94 ± 0.14	0.45 ±0.15	0.45 ± 0.15	0.21 ± 0.02, p<0.01
A .mochon pontica	38.21 ± 1.53	15.52 ± 1.23, p<0.01	15.48 ± 0.86	8.65 ± 0.82, p<0.01

Table III. Heat production of *A. salina* and fish larvae *A mochon pontica* exposed in different concentrations of cyfoz (μWt per individual)

Species	Intact	0.625 mg/L	1.25mg/L	2.5 mg/L
A.salina	1.05 ± 0.04	0.75 ± 0.08	0.30 ± 0.05, p<0.01	0.35 ± 0.05, p<0.01
A .mochon pontica	38.21 ± 1.53	9.52 ± 0.20, p<0.01	9.85 ± 0.25, p<0.01	-

The metabolic rate of the *A. salina nauplia* exposed in Cu-containing pesticide cuprocsat (2.5 mg per L) decreased more than 2-fold. The phosphororganic pesticide cyfoz was more toxic and led to the decline of crustacea and fish larvae metabolic rates 4-fold at a concentration of 1.25 mg per L (Tables II and III). At a concentration of 2.5 mg/L all fish larvae died.

The metabolic rate of *A. hepstus* larvae caught in polluted area was significantly lower as compared with corresponding parameter of the larvae from non-polluted water. Thus the decrease of heat production in marine organisms exposed in different kinds of toxicants resulted in the damage of their metabolism and differences between energetic rate. The heat production is a very sensitive non-specific parameter for evaluation of organisms status exposed in different stressors and in inhabited polluted areas as compared with non-polluted.

REFERENCES

[1] MICROCALORIMETRY IN BIOCHEMISTRY AND BIOLOGY, Science Tools **19** 1 (1972) 1.

[2] KLOTZ, I., Energy of Biochemical Reaction, (1970) Mir, Moscow.

[3] NORMAT, M., GRAF, G., SZANIWSKA, A., Heat production in *Saduria entomoon (Isopoda*) from Gulf of Gdansk during experimental exposure to anoxic condition, Mar. Biology **131** (1998) 269-273.

A microbiological study on Rashid black sand sediments, Egypt

El-Gamal, A.[a], T. Zaghloul[b], I.H. Saleh[a], S. Nasr[a], M. Naim[c]

[a] Department of Environmental Studies,
Institute of Graduate Studies and Research (IGSR),
Alexandria University,
Alexandria,
Egypt

[b] Department of Biotechnology,
Institute of Graduate Studies and Research (IGSR),
Alexandria University,
Alexandria,
Egypt

[c] Department of Physics,
Faculty of Science,
Alexandria University,
Alexandria,
Egypt

A microbiological study was carried out to isolate and identify radio-tolerant bacteria present in a high radiation background area namely Rashid. Rashid is considered as one of the natural high radiation background areas in the world. It has been observed as the highest background radiation station along the Egyptian Mediterranean coast. This is due to the presence of black sand deposits in its sediments. Black sand contains monazite and zirconium minerals, which have uranium and thorium inclusions in their mineral structures. Gamma absorbed dose rate from Rashid black sand reached 0.72 μGy/h.

The microbiological examination of Rashid black sand revealed that, few bacterial strains, which are adapted and tolerant to this area were present. These strains were isolated, cultured and identified. Identification was carried out according to Bergey's manual [1]. Confirmatory identification was carried out using API-20E kits for *Enterobacteriacae* and Gram-negative isolates. Other Gram-positive isolates were partially identified based on the morphological features of colonies and cells. The identified strains were found to be *Pseudomonas fluorescens, P. putida*, *P. aeruginosa, Chryseomonas luteola, Xanthomonas maltophilia, Bacillus* spp., *Staphylococcus* spp., and *Micrococcus* spp (Table I).

The isolated bacteria could be used in several beneficial applications since other studies have proved that they can accumulate some radioactive materials [2-4]. Further studies are needed to construct an efficient, inexpensive and feasible method to remove uranium and other metals from an aqueous environment.

Table I. Cell morphology, assembly, gram stain and possible identification of some isolated bacteria from rashid black sand

Cell morphology	Assembly	Gram stain	Possible identification
Short rods	Single	Negative	*Pseudomonas fluorescens* *P. putida* *P. aeruginosa*
Very short rods	Single	Negative	*Chryseomonas luteola*
Rods	Single	Negative	*Xanthomonas maltophilia*
Rods	Single or in duplicate	Positive	*Bacillus* spp.
Cocci	Clusters	Positive	*Staphylococcus* spp.
Cocci	Mostly single	Positive	*Micrococcus* spp.

REFERENCES

[1] SNEATH, P.H.A., MAIR, N.S., SHARP, M.E., Bergey's Manual of Systematic Bacteriology **2** (1984) Williams and Wilkins, London.

[2] PREMUZIC, E.T., FRANCIS, A.J., LIN, M., SCHUBERT, J., Induced formation of chelating agents by *Pseudomonas aeruginosa* grown in presence of thorium and uranium, Arch. Environ. Contam. Toxicol. **14** 6 (1985) 759-68.

[3] LOVELY, D.R., PHILLIPS, E.J.P., GORBY, Y.A., LANDA, E.R., Microbial reduction of uranium, Nature **350** (1991) 413-416.

[4] SHAHAMAT, M., Sequestration of heavy metal by bacteria: Virture Newsletter, Science, March 2001, Virtue Science Meeting 2000, Microbiology.

Bioaccumulation of artificial radionuclides and dose assessment to biota in the Yenisei River (Russia)

Kryshev, A.I., T.G. Sazykina

Scientific and Production Association "Typhoon",
Obninsk,
Russian Federation

The Yenisei is a large river situated in Central Siberia (Russia). It flows northwards to the Yenisei Bay of the Kara Sea. The length of the Yenisei River is 3840 km, the average annual water discharge is 591 km^3. Since 1958, the Yenisei River is contaminated by the routine releases of radionuclides from the Krasnoyarsk Mining and Chemical Industrial Complex (KMCIC). Among the radionuclides presented in liquid discharges from KMCIC, radioisotopes of phosphorus, caesium and zinc are of major radioecological importance, since they are easily assimilated by the aquatic biota. Yenisei River is characterized by low concentrations of stable nutrients in water, particularly of phosphorus. This may be the reason for the intensive bioassimilation of radioactive phosphorus by organisms in the Yenisei River. The subject of this paper is reconstruction of accumulation of artificial radionuclides (^{32}P, ^{137}Cs, ^{65}Zn, ^{51}Cr, ^{54}Mn) by the Yenisei River biota during the 25-years period (1975 – 2000), and estimation of the internal dose rates to the river organisms. Among the radionuclides presented in the releases, ^{32}P is of particular importance.

Reconstruction of the radionuclide assimilation by the Yenisei biota was performed using the ECOMOD model approach. The model considers a radionuclide as a tracer, identical in its properties to a stable (analogous) element participated in the metabolism of aquatic organism. Radionuclide assimilated by an organism goes to the production of new biomass, and to compensation of metabolic losses of the analogous bioelement. Basic equations of the general ECOMOD approach were described in paper [1]. The model was adapted to the conditions of the Yenisei River and applied to calculate the dynamics of ^{32}P, ^{137}Cs, ^{65}Zn, ^{51}Cr, ^{54}Mn in the most typical Yenisei fish species: roach (non-predatory) and pike (predatory). Tables I and II show the reconstructed activity concentrations in roach and pike at the distances 16 – 80 km downstream the KMCIC. Activity concentrations of ^{32}P in the Yenisei fish were considerably higher comparing with other radionuclides. Activity concentrations of ^{32}P, ^{65}Zn, ^{51}Cr, ^{54}Mn in roach are higher than in pike, whereas activity concentrations of ^{137}Cs are higher in predatory species. Results of the model reconstruction were compared with the available data of measurements [2-3], and such comparison confirms adequacy of the model predictions.

Long-term dynamics of the internal exposure was estimated for the river organisms at the distances 16 – 80 km downstream the KMCIC. Average dose rates from incorporated γ-emitters were calculated taking into account geometric characteristics of organisms [4]; β-particles were assumed to be totally absorbed within the organisms. Average length of roach in the Yenisei River is 0.2 m, weight 0.17 kg; average length of pike in the Yenisei River is 0.52 m, weight 1.2 kg. Dose conversion factors for ^{32}P, ^{137}Cs, ^{65}Zn, ^{51}Cr and ^{54}Mn are shown in Table III. Annual average dose rates from incorporated radionuclides to the Yenisei biota are presented in Table IV. Maximum dose rates occurred in 1975 – 1980 and varied from 11 mGy/year (predatory fish) to 63 mGy/year (molluscs). These levels were several times higher than the background exposure to the Yenisei organisms, which was estimated as 0.7 – 4 mGy/year [2]. Major contributor to the internal exposure to the Yenisei biota is ^{32}P (up to 95%).

Table I. Annual average activity concentrations of radionuclides in non-predatory fish (roach) from the Yenisei River, model reconstruction

Years	Activity concentration, Bq/kg				
	^{32}P	^{137}Cs	^{65}Zn	^{51}Cr	^{54}Mn
1975 – 1980	5080 ± 2430	52 ± 46	76 ± 30	360 ± 150	24 ± 10
1981 – 1986	4240 ± 1850	26 ± 9	180 ± 60	320 ± 140	41 ± 16
1987 – 1992	3040 ± 1410	18 ± 7	81 ± 33	350 ± 150	33 ± 13
1993 – 2000	90 ± 40	6 ± 2	1.1 ± 0.5	3.5 ± 1.7	0.21 ± 0.17

Table II. Annual average activity concentrations of radionuclides in predatory fish (pike) from the Yenisei River, model reconstruction

Years	Activity concentration, Bq/kg				
	^{32}P	^{137}Cs	^{65}Zn	^{51}Cr	^{54}Mn
1975 – 1980	3050 ± 1460	68 ± 50	27 ± 11	230 ± 90	21 ± 9
1981 – 1986	2540 ± 1110	40 ± 13	76 ± 30	200 ± 80	36 ± 15
1987 – 1992	1830 ± 850	30 ± 10	39 ± 16	220 ± 90	30 ± 12
1993 – 2000	70 ± 30	10 ± 3	0.6 ± 0.4	2.2 ± 0.9	0.18 ± 0.15

Table III. Internal dose conversion factors for the Yenisei organisms

Organism	Dose conversion factor, Gy·day/Bq·kg				
	^{32}P	^{137}Cs	^{65}Zn	^{51}Cr	^{54}Mn
Roach	$9.6\cdot10^{-9}$	$3.9\cdot10^{-9}$	$5.8\cdot10^{-10}$	$5.0\cdot10^{-11}$	$8.8\cdot10^{-10}$
Pike	$9.6\cdot10^{-9}$	$4.3\cdot10^{-9}$	$8.8\cdot10^{-10}$	$7.5\cdot10^{-11}$	$1.3\cdot10^{-9}$
Molluscs	$9.6\cdot10^{-9}$	$3.5\cdot10^{-9}$	$1.7\cdot10^{-10}$	$1.5\cdot10^{-11}$	$2.6\cdot10^{-10}$

Table IV. Annual average dose rates from incorporated radionuclides to the Yenisei biota

Years	Internal dose rate, Gy/year		
	Roach	Pike	Molluscs
1975 – 1980	$(1.8 \pm 0.9)\cdot10^{-2}$	$(1.1 \pm 0.5)\cdot10^{-2}$	$(6.3 \pm 3.2)\cdot10^{-2}$
1981 – 1986	$(1.5 \pm 0.7)\cdot10^{-2}$	$(0.9 \pm 0.4)\cdot10^{-2}$	$(5.1 \pm 2.7)\cdot10^{-2}$
1987 – 1992	$(1.1 \pm 0.5)\cdot10^{-2}$	$(0.6 \pm 0.3)\cdot10^{-2}$	$(3.7 \pm 1.9)\cdot10^{-2}$
1993 – 2000	$(3.2 \pm 1.4)\cdot10^{-4}$	$(2.6 \pm 1.1)\cdot10^{-4}$	$(1.1 \pm 0.5)\cdot10^{-3}$

REFERENCES

[1] SAZYKINA, T.G., ECOMOD – An ecological approach to radioecological modelling, J. Environ. Radioactivity **50** 3 (2000) 207–220.

[2] KRYSHEV, I.I., RYAZANTSEV, E.P., Ecological safety of the nuclear energy complex of Russia, IzdAT, Moscow (2000) 384 pp. (in Russian).

[3] NOSOV, A.V., ASHANIN, M.V., IVANOV, A.B., MARTYNOVA, A.M., Radioactive contamination of the Yenisei River caused by the discharges from the Krasnoyarsk Mining and Chemical Industrial Complex, Atomic Energy **74** 2 (1993) 144–150.

[4] KRYSHEV, A.I., SAZYKINA, T.G., STRAND, P., BROWN, J.E., Radioecological model for dose estimation to Arctic marine biota,)Proc. 5th Int. Conf. Environmental Radioactivity in the Arctic and Antarctic, St.Petersburg, 16 – 20 June 2002), NRPA, Norway (2002) 326-329.

ATMOSPHERE

^{210}Pb, ^{210}Po and ^{7}Be in oceanic air from the North Pole to the Antarctic

Holm, E[a,b,c], P. Roos[b], M. Leisvik[c]

[a] Department of Medical Radiation Physics,
Lund University,
Sweden

[b] Risoe National Laboratory,
Roskilde,
Denmark

[c] UNIS,
Longyearbyen,
Svalbard,
Norway

Abstract. During the Swedish expedition SWEDARP, 1988-89 air filter samples were collected from Sweden to the Antarctic. In as similar way air filters were colleted at the SWEDARCTIC expedition 1991, from Sweden to the North Pole. The samples were analysed for ^{7}Be, ^{210}Po and ^{210}Pb. Our data for ^{7}Be show maximal concentrations between 45^{o}N and 45^{o}S, (2600-5100 μBq m^{-3}), and minima in the Arctic and Antarctic regions, 300 – 1100 μBq m^{-3} and 500 –1400 μBq m^{-3} respectively. The data show the strong convection of air close to the Equator bringing ^{7}Be to surface-level from the upper troposphere or even stratosphere. ^{210}Pb and ^{210}Po being the daughter products of ^{222}Rn depend on the sources of aerosols from the continents. The activity ratio ^{210}Po/^{210}Pb reflects the residence time in the troposphere. Our data show maximal concentrations in the equatorial regions, 60–150 μBq m^{-3} for ^{210}Po and 350-600 μBq m^{-3} for ^{210}Pb. The corresponding values for ^{210}Po in the polar regions, Arctic and Antarctic, are 5-80 μBq m^{-3} and 3-15 μBq m^{-3} respectively and for ^{210}Pb, 6-100 and 4-45 μBq m^{-3}. The activity ratio, ^{210}Po/^{210}Pb, between 45^{o}N and S are about 0.2-0.3 while they are as high as 0.7-1.1 in the Arctic and Antarctic regions. This shows that only small particles with long residence time reach the polar regions. The long residence time in the polar regions is due to low precipitation and low particle load.

1. Introduction

^{210}Pb and ^{210}Po being the daughter products of ^{222}Rn depend on the sources of aerosols from the continents The ^{210}Po/^{210}Pb activity ratio in air has been used for estimating their residence time [1]. The world average flux of ^{222}Rn to the atmosphere is about 15 mBq m^{-2} s^{-1} from continental soils and 0.2 mBq m^{-2} from ocean waters [2]. The winter fluxes are lower than summer fluxes. There are also other sources such as volcanic eruptions and industrial emissions but globally seen these sources are of minor importance. Long-range atmospheric transport is important for pollution in the Arctic.

^{7}Be is produced by spallation of nitrogen and oxygen in the stratosphere by energetic cosmic rays. Due to the relatively short physical half-life of ^{7}Be and the relatively long residence time in the stratosphere, most of the ^{7}Be does not reach the troposphere except during springtime, when there is an exchange between the stratosphere and troposphere at 45^{o}N an S. Since ^{7}Be is of cosmogenic origin, its flux to the earth has latitude dependence. The advantage of using a ship, as sampling platform is that resuspension from soil of previously deposited radionuclides is avoided.

2. Materials and methods

During the Swedish expedition SWEDARP, 1988-89 air filter samples were collected from Sweden to the Antarctic by an Andersen sampler (100 m^{3} h^{-1}) with membrane filters. In a similar way air filters were colleted at the SWEDARCTIC expedition, 1991, from Sweden to the North Pole. During this

expedition the sampler was calibrated for ^{7}Be ($T_{1/2}$ = 53.1 d) against a FOA sampler (1100 m^3 h^{-1}) with Microsorban filters. A second international intecalibration was performed in 1993 [3]. The samples were analysed for ^{7}Be by gamma spectrometry and for ^{210}Po ($T_{1/2}$ = 163 d) by alpha spectrometry after radio chemical separation. ^{210}Pb ($T_{1/2}$ = 21 a) was determined by studying the build-up of ^{210}Po from ^{210}Pb.

3. Results and discussion

^{210}Pb and ^{210}Po being the daughter products of ^{222}Rn depend on the sources of aerosols from the continents. The activity ratio ^{210}Po/^{210}Pb reflects the residence time in the troposphere. Our data (Figs 1 and 2) show maximal concentrations in the equatorial regions, 60-150 μBq m^{-3} for ^{210}Po and 350-600 μBq m^{-3} for ^{210}Pb. The corresponding values for ^{210}Po in the polar regions, Arctic and Antarctic, are, 5-80 μBq m^{-3} and 3-15 μBq m^{-3} respectively and for ^{210}Pb, 6-100 and 4-45 μBq m^{-3}. The data for ^{210}Pb are in excellent agreement with Atlantic data [4] and at Svalbard [5], especially considering the large daily and annual variations. The activity ratio, ^{210}Po/^{210}Pb, between 45°N and S are about 0.2-0.3 while they are as high as 0.7-1.1 in the Arctic and Antarctic regions. It is difficult to explain values over 1. The analytical difficulties are large at low concentrations. However there could be other explanations that other sources than exhalation from the ground with high ^{210}Po/^{210}Pb ratios play a role or the ^{210}Pb and ^{210}Po might have significant different deposition velocities. The residence time in the polar regions is long due to low precipitation and low particle load.

Our data for ^{7}Be (Figs 3 and 4) show maximal concentrations between 45°N and 45°S, (2600-5100 μBq m^{-3}), and minima in the Arctic and Antarctic regions, 300-1100 μBq m^{-3} and 500-1400 μBq m^{-3} respectively. There are no distinct maxima at 45°N or S, which is explained by that our samples were not collected during springtime but early to late summer. The data show the strong convection of air close to the Equator bringing ^{7}Be to surface-level from the upper troposphere or even stratosphere.

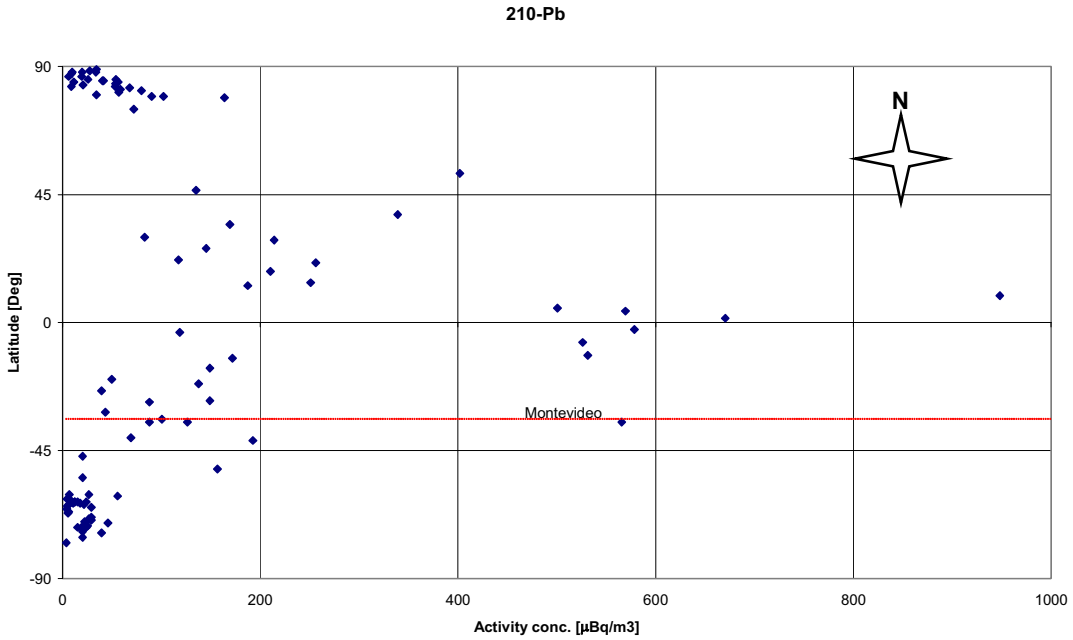

FIG. 1. Activity concentration of ^{210}Pb (μBq m^{-3}) in Atlantic surface air as a function of latitude.

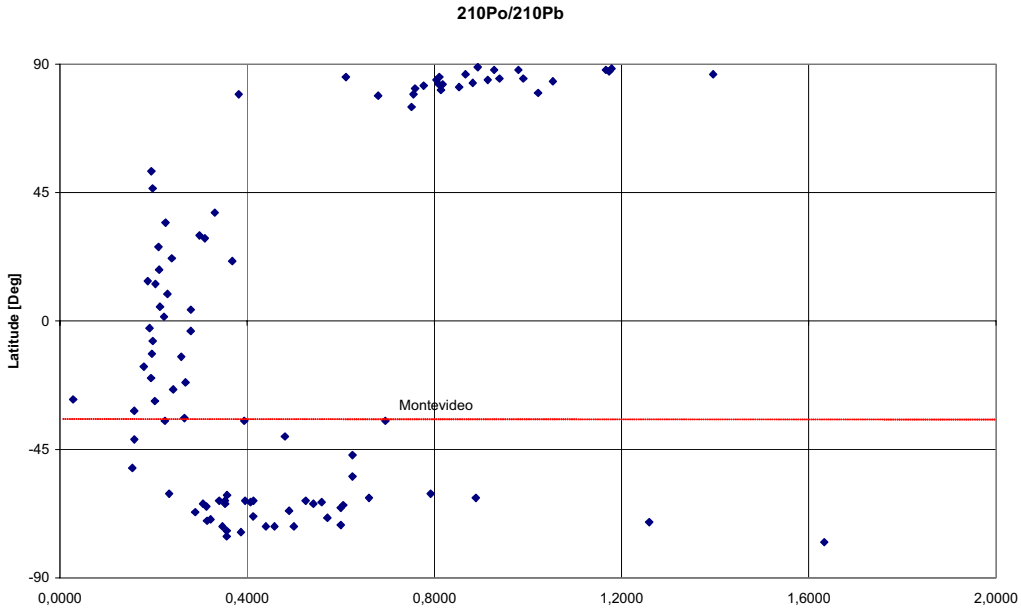

FIG. 2. The activity ratio $^{210}Po/^{210}Pb$ in Atlantic surface air as a function of latitude.

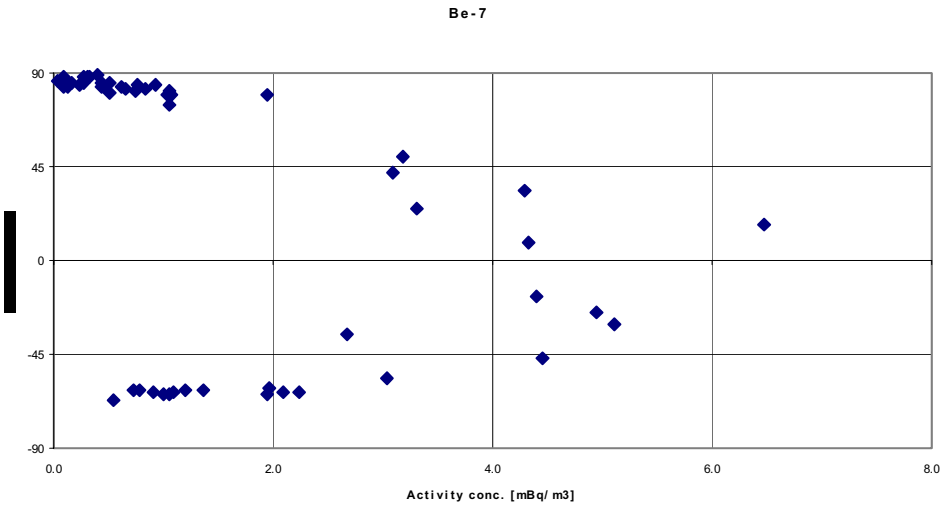

FIG. 3. Activity concentration of ^{7}Be ($\mu Bq\ m^{-3}$) in Atlantic surface air as a function of latitude.

3.1. Deposition velocity

The deposition velocity can be used to relate the total deposition flux to the atmospheric concentration. The deposition velocity in cm s^{-1} is $V_d = F/C_{air}$ where F is the deposition flux (Bq cm^{-2} a^{-1}) and C_{air} is the concentration in air (Bq m^{-3}). Using our data for air concentrations of ^{210}Pb in the Arctic and the Antarctic and deposition data from Ref. [6] we can calculate the deposition velocities. For the Arctic we find a values ranging from 0.7-13 cm s^{-1} with a mean of 2.0 cm s^{-1}.

For the Antarctic region the values range from 0.5-9.0 cm s^{-1} with a mean of 1.4 cm s^{-1}. We can from these possibly conclude that the deposition velocities for ^{210}Pb are slightly higher in the polar region compared to other regions with for example the Netherlands [7] and Germany [8], where the deposition velocity were 0.6-1.3 cm s^{-1} with a mean of 0.9 cm s^{-1} and 0.5-2 cm s^{-1} respectively, with maxima during summer.

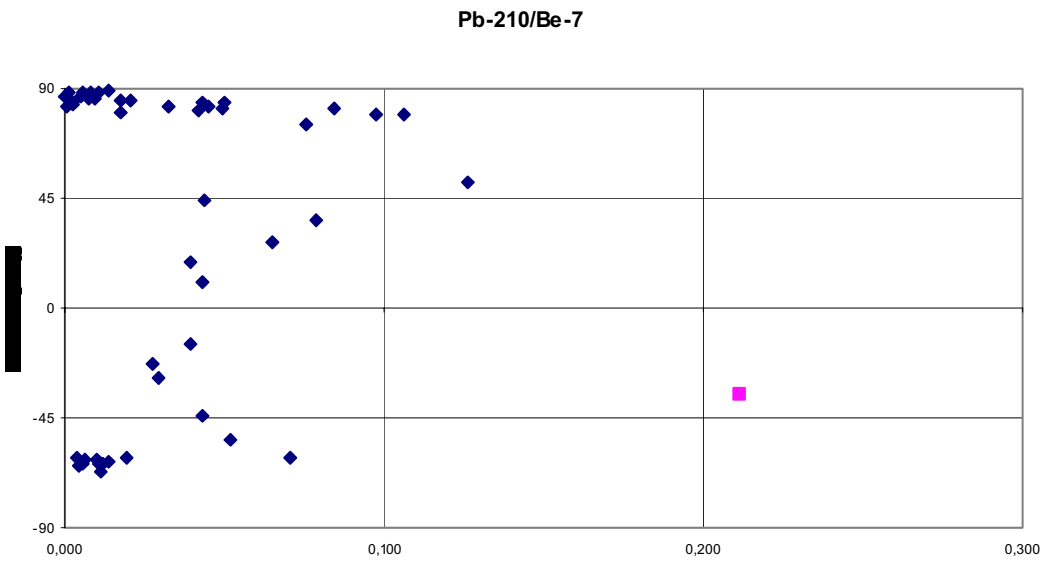

FIG. 4. The activity ratio $^{210}Pb/^{7}Be$ in Atlantic surface air as a function of latitude.

ACKNOWLEDGEMENT

We wish to thank the Swedish Polar Research Secretariat for their logistic support.

REFERENCES

[1] BASKARAN, M., SHAW, G.E., Residence time of arctic aerosols using the concentrations and activity ratios of ^{210}Po, ^{210}Pb and ^{7}Be, Aerosol Science **32** (2001) 443.

[2] SAMUELSSON, C., HALLSTADIUS, L., PERSSON, B., HEDVALL, R., HOLM, E., FORKMAN, B., ^{222}Rn and ^{210}Pb in the Arctic summer air, J. Environ. Radioact. **3** (1986) 35.

[3] VINTERSVED, I., Intercomparison of large stationary air samplers, In: Nordic Radioecology. The transfer of radionuclides through Nordic ecosystems to man (DAHLGAARD, H., Ed.), Elsevier, Amsterdam (1994) 385-405.

[4] PAATERO J., HATAKKA J., HOLMÉN, K., ENEROTH, K., VIISANEN, Y., Lead-210 concentration in the air at Mt. Zeppelin, Ny-Ålesund, Svalbard, Physics and Chemistry on the Earth **28** (2003) 1175.

[5] PREISS, N., MELIERES, M-A., POURCHET, M., Data base over Lead-210 concentrations in surface air, Lead-210 atmospheric deposition and water-sediment flux, Laboratoire de Glaciologie et Geophysique de l'Environnement, Saint-Martin-d'Heres, France (1998).

[6] BEKS, J.P., EISMA, D., van der PLICHT, J., A record of atmospheric ^{210}Pb deposition in The Netherlands, Sci. Total Environ. **222** (1998) 35.

[7] WINKLER, R., ROSNER, G., Seasonal and long-term variation of ^{210}Pb concentration in air, atmospheric deposition rate and total deposition velocity in south Germany, Sci. Total Environ. **263** (2000) 57.

Observation of airborne ^{210}Pb and ^{7}Be during the Arctic Ocean 2001 expedition

Paatero, J.[a], J. Hatakka[a], C. Leck[b], V. Aaltonen[a], Y. Viisanen[a]

[a] Finnish Meteorological Institute,
FI-00880 Helsinki,
Finland

[b] Stockholm University,
Department of Meteorology,
S-106 91 Stockholm,
Sweden

Abstract. Swedish Polar Research Secretariat arranged a multidisciplinary scientific expedition to the Arctic Ocean in 2001 with the Swedish icebreaker Oden. The aim of the atmospheric research programme was to study the chemical, biological, physical and meteorological processes that control the formation of nanometre-size aerosol particles and their influence on climate change especially in the Arctic region [1]. As a part of this programme airborne ^{222}Rn, ^{210}Pb and ^{7}Be and external radiation were measured for two purposes. These natural radionuclides can be used as tracers for air mass origin, and ionising radiation has been suggested to be the reason for the formation of aerosol particles in the air [2]. This report presents preliminary observations of airborne ^{210}Pb and ^{7}Be during the expedition.

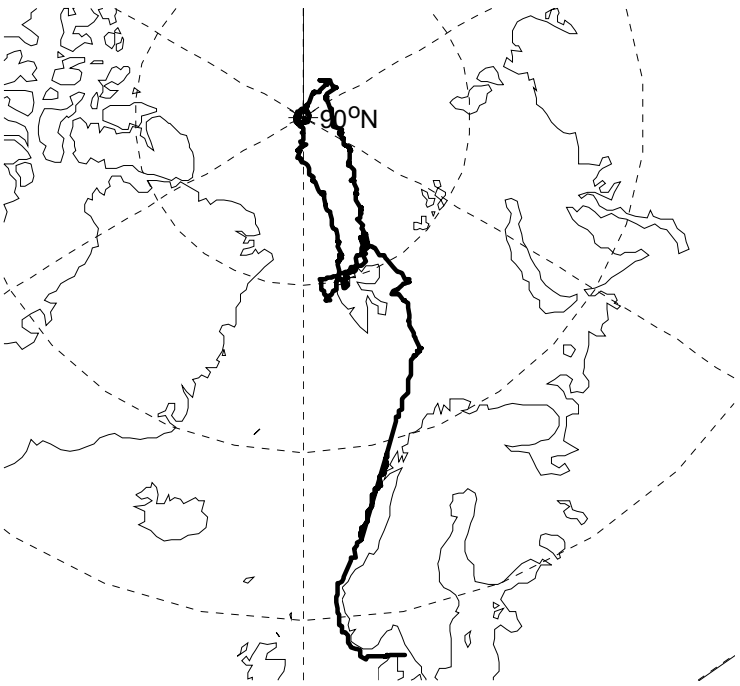

FIG. 1. Expedition route.

Table I. Sampling data and results (n.d. = not detected), Arctic Ocean 2001 expedition.

Start of sampling						End of sampling						Act. Conc.	
		Lat (N)		Lon (E/W)				Lat (N)		Lon (E/W)		µBq/m³	
Date	Time	°	min.	°	min.	Date	Time	°	min.	°	min.	Be-7	Pb-210
30/06	9.22	58	7	6	23 E	01/07	9.10	62	13	4	59 E	2000	54
01/07	9.28	62	16	5	3 E	02/07	9.04	66	46	10	34 E	~200	n.d.
02/07	9.20	66	49	10	38 E	03/07	8.54	71	30	18	10 E	~200	n.d.
03/07	9.06	71	32	18	14 E	05/07	11.43	77	52	29	45 E	1100	32
05/07	12.02	77	52	29	44 E	05/07	23.30	77	54	29	42 E	~300	n.d.
05/07	23.50	77	54	29	42 E	07/07	8.58	78	37	33	11 E	480	n.d.
07/07	9.11	78	37	33	11 E	08/07	8.54	79	19	32	6 E	1000	n.d.
08/07	9.12	79	22	32	1 E	09/07	5.51	82	3	25	58 E	~10	n.d.
09/07	6.06	82	3	25	58 E	10/07	15.55	82	0	25	58 E	560	32
11/07	6.18	81	20	24	22 E	12/07	11.31	81	12	25	20 E	~100	n.d.
15/07	13.58	79	9	8	0 E	16/07	13.59	80	33	13	19 E	~300	20
17/07	13.52	81	40	26	54 E	19/07	10.30	84	53	36	46 E	~1000	12
20/07	19.30	86	34	50	19 E	22/07	12.52	88	23	90	26 E	~100	23
22/07	12.59	88	24	91	1 E	23/07	12.58	88	20	127	0 E	370	27
23/07	13.07	88	20	127	0 E	24/07	14.09	87	42	134	36 E	220	n.d.
24/07	14.20	87	42	134	36 E	26/07	21.55	87	55	154	15 E	330	n.d.
26/07	22.03	87	55	154	16 E	27/07	22.37	87	52	154	44 E	~300	n.d.
27/07	22.47	87	52	154	44 E	29/07	19.37	88	28	152	21 E	400	n.d.
29/07	19.44	88	28	152	22 E	31/07	14.12	89	59	139	10 W	~300	17
31/07	14.23	89	59	139	9 W	02/08	13.10	88	56	1	48 W	~200	17
02/08	13.25	88	56	1	51 W	03/08	18.50	88	46	4	35 W	~500	n.d.
03/08	19.50	88	46	4	37 W	05/08	8.34	88	45	1	41 W	~100	n.d.
05/08	8.47	88	45	1	41 W	06/08	17.22	88	40	0	19 E	~300	22
06/08	17.36	88	40	0	20 E	07/08	19.12	88	37	3	16 E	~500	19
07/08	19.20	88	37	3	17 E	08/08	18.55	88	33	4	18 E	~100	n.d.
08/08	19.07	88	33	4	18 E	09/08	19.30	88	35	3	51 E	~200	n.d.
09/08	19.40	88	35	3	51 E	10/08	18.50	88	35	2	38 E	~200	n.d.
10/08	18.58	88	35	2	37 E	12/08	12.53	88	29	0	30 W	1800	29
12/08	13.02	88	29	0	30 W	13/08	17.25	88	24	1	45 W	~200	n.d.
13/08	17.36	88	24	1	46 W	15/08	12.40	88	21	2	14 W	~100	n.d.
15/08	13.48	88	21	2	14 W	16/08	17.05	88	16	5	32 W	~200	n.d.
16/08	17.17	88	16	5	33 W	17/08	17.16	88	15	7	26 W	~200	30
17/08	17.27	88	15	7	27 W	18/08	18.45	88	14	8	13 W	~400	n.d.
18/08	18.58	88	14	8	13 W	19/08	20.05	88	9	7	51 W	~100	n.d.
19/08	20.17	88	9	7	52 W	20/08	19.45	88	10	8	30 W	~1000	n.d.
20/08	20.00	88	10	8	31 W	21/08	16.58	87	49	2	59 W	~300	n.d.
21/08	17.08	87	48	2	57 W	22/08	16.43	86	3	11	1 E	~300	n.d.
22/08	16.51	86	3	11	17 E	23/08	17.45	85	33	15	20 E	~200	26
23/08	17.54	85	33	15	29 E	24/08	16.58	83	37	15	29 E	~600	n.d.
24/08	17.11	83	36	15	25 E	25/08	20.47	81	46	15	32 E	~200	n.d.

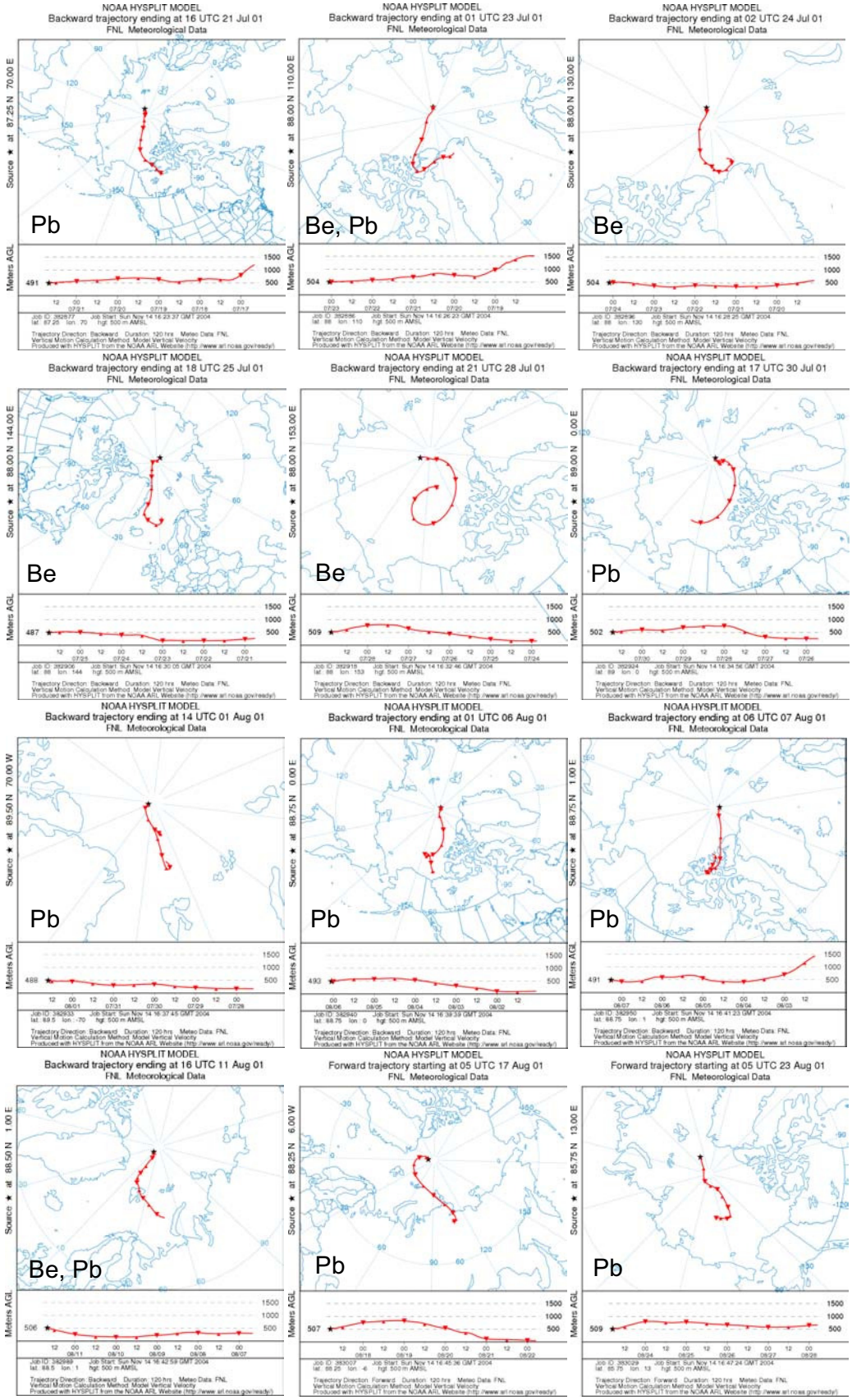

FIG. 2. HYSPLIT backward trajectories [5], length 120 hours, arrival height: 500 m above sea level, arrival time: median of the sampling period. The letters Be and Pb indicate which of these nuclides was/were observed.

The expedition started from Gothenburg, Sweden, on 26 June 2001 and ended at Svalbard on 29 August (Fig. 1). The expedition sailed first to Svalbard area, then NE to the Lomonosov ridge, the Makarov basin and to the North Pole. Most of the atmospheric programme was conducted during the ice drift experiment at the 88th latitude, while the icebreaker was moored to an ice floe and drifted for three weeks in August 2001. Aerosol samples were collected onto glass-fibre or quartz-fibre filters. After the return of the expedition the samples were assayed for ^{7}Be with semiconductor gamma spectrometry. Owing to the long delay between the sampling and the measurement most of the ^{7}Be had already decayed, thus in most cases only an estimate of the ^{7}Be concentration could be obtained. The ^{210}Pb contents of the samples was measured six months later by counting the alpha particles of the in-grown daughter nuclide ^{210}Po [3]. The detection limit for ^{210}Pb is about 10 μBq/m^{3}. According to air mass trajectories the ^{210}Pb activity concentrations above the detection limit north of the 85th latitude were often encountered with air masses having recent contacts with land areas (Figure 2). The highest ^{7}Be activity concentration was also observed in a similar meteorological situation, in agreement with an earlier study in northern Finland (Table I) [4, 5].

ACKNOWLEDGEMENTS

The authors would like to thank the Swedish Polar Research Secretariat, SwedArctic-2001 Programme, and Captain Mats Johansson and his officers and crew, Icebraker Oden, for logistical support. The financial support of Jenny and Antti Wihuri Foundation, Finland, is gratefully acknowledged. The authors would also like to thank NOAA/ARL, USA, for the access to HYSPLIT trajectory model.

REFERENCES

[1] LECK, C., TJERNSTRÖM, M., MATRAI, P., SWIETLICKI, E., BIGG, E.K., Can Marine Micro-organisms Influence Melting of the Arctic Pack Ice? Eos **85** (2004) 25-36.

[2] YU, F., TURCO, R.P., Ultrafine aerosol formation via ion-mediated nucleation. Geophysical Research Letters (2000) 27: 883-886.

[3] MATTSSON, R., PAATERO, J., HATAKKA, J., Automatic Alpha/Beta Analyser for Air Filter Samples - Absolute Determination of Radon Progeny by Pseudo-coincidence Techniques. Radiation Protection Dosimetry **63** (1996) 133-139.

[4] PAATERO, J., HATAKKA, J., Source Areas of Airborne ^{7}Be and ^{210}Pb Measured in Northern Finland, Health Phys. **79** (2000) 691-696.

[5] DRAXLER, R.R., HESS, G.D., An Overview of the Hysplit_4 Modeling System for Trajectories, Dispersion, and Deposition, Australian Meteorol. Mag. **47** (1998) 295-308.

Deposition rates of radionuclides in Monaco in 2002 and 2003

Pham, M.K., S-H. Lee, J. Gastaud, P.P. Povinec

Inernational Atomic Energy Agency,
Marine Environment Laboratory,
Monaco

Abstract. The monthly deposition rates of natural (^{7}Be and ^{210}Pb) and anthropogenic (^{137}Cs, $^{239+240}$Pu and ^{241}Am) radionuclides in 2002 were mainly influenced by wash-out of the atmosphere. The annual deposition rates of ^{7}Be and ^{210}Pb were 1190 and 250 Bq m^{-2} year^{-1}, respectively, comparable with annual deposition rates of ^{137}Cs, $^{239+240}$Pu and ^{241}Am, which were 2200, 110 and 40 mBq m^{-2} year^{-1}, respectively. An important contribution to the deposition of radionuclides in 2002 was the Saharan dust event in November 2002, when 1630, 90 and 35 mBq m^{-2} month^{-1} of ^{137}Cs, $^{239+240}$Pu and ^{241}Am was deposited, respectively, while only 320 mBq m^{-2} month^{-1} of ^{7}Be and 70 mBq m^{-2} month^{-1} of ^{210}Pb was deposited. On the contrary, in 2003 the monthly deposition rates of both natural and anthropogenic radionuclides were strongly influenced by dry deposition. The annual deposition rates of ^{137}Cs, $^{239+240}$Pu and ^{241}Am were 740, 14 and 5.9 mBq m^{-2} year^{-1}, respectively, compared to 840 Bq m^{-2} year^{-1} for ^{7}Be and 150 Bq m^{-2} year^{-1} for ^{210}Pb. The anthropogenic radionuclides in the Monaco atmosphere in 2002 and 2003 originated from global fallout.

1. Introduction

IAEA's Marine Eenvironment Laboratory (IAEA-MEL) in Monaco has been carrying out monitoring of radionuclides in the air over many years. Some radionuclides of natural origin (cosmogenic, radiogenic and primordial) and of anthropogenic origin have been monitored monthly (or daily in a case of an accident). Atmospheric input, controlled by a combination of dry and wet depostion with respect to the supply of natural (e.g. ^{7}Be, ^{210}Pb) and anthropogenic (e.g. ^{137}Cs, $^{239+240}$Pu and ^{241}Am) radionuclides has been considered as one of the most important sources of radionuclides in the marine environment. More than 90% of radionuclides in the atmosphere are removed by wet (precipitation, scavenging) processes [1]. The atmospheric input to the Mediterranean region has been strongly enhanced by Saharan dust deposition, resulting from atmospheric transport of particles from North Africa during cyclones [2]. Therefore Saharan dust events have been recognized as important pathways for particle deliveries into surface waters of the northwest Mediterranean Sea [3, 4]. The study of radionuclides and elemental composition of dust particles have been carried out for better understanding of the temporal behaviour of radionuclides in the atmosphere and their transport into the northwest Mediterranean Sea [5].

2. Experimental

The total (wet+dry) deposition was collected monthly using a 2 x 2 m^{2} collector, installed on the roof of the IAEA-MEL building in Monaco (43^{o}45'N, 07^{o}25'E). The collector system, consisting of three parallele polyethylene containers (200 liters each) has been designed to prevent evaporation of rainfall. A red colored-rainwater was collected in 7th June, 15th and 23/24th November 2002. This was due to special meteorological conditions when Saharan dust was transported from North Africa to Monaco. This phenomenon was less evident in May 2003 when a smaller quantity of red-particles was collected.

The radiochemical procedures used for sample preparation have already been described therefore they will not be presented in this paper [4-6]. For samples collected in 2003, the separation of dissolved and particulate phases of precipitation has been realized for the months with rain. For dry fall-out, no separation of dissolved and particulate phases has been done, the total activity of radionuclides was determined as in a previous year [5].

3. Results and discussion

3.1. Deposition rates of ^{7}Be and ^{210}Pb

The variation of monthly deposition rates of the cosmogenic ^{7}Be and the radiogenic ^{210}Pb in Monaco rain in 2002 is shown in Fig. 1. The deposition rate of ^{7}Be vary from 30 to 318 Bq m^{-2} month^{-1}, while for ^{210}Pb from 3.0 to 72 Bq m^{-2} month^{-1}. The monthly deposition rates of both radionuclides vary throughout the year in a similar way as the precipitation rate, as documented by high Pearson correlation coefficients (R) between ^{7}Be and ^{210}Pb, and the precipitation rate (R = 0.97 and 0.95, respectively). The temporal variations of ^{7}Be and ^{210}Pb are similar, although they have a different origin. The maximum of deposition rates for ^{7}Be and ^{210}Pb were found in February, May and November, where the precipitations were at maximum. The important signal of ^{7}Be and ^{210}Pb was observed in November, linked with two important events of Saharan dust deposition.

While for ^{7}Be the maximum concentration resulted essentially from washing out of the air, as the precipitation rate was at maximum, for ^{210}Pb except of washing out of local ^{210}Pb in the air, fine Saharan dust particles deposited during cyclones, with massic activities from 0.37 to 2.1 Bq g^{-1}, contributed to its high deposition rate.

The monthly deposition rates of ^{7}Be and ^{210}Pb in Monaco rain in 2003 is shown in Fig. 2. The total deposition rate of ^{7}Be varied from 1.6 to 170 Bq m^{-2} month^{-1}, while for ^{210}Pb from 1.0 to 33 Bq m^{-2} month^{-1}. We noticed that during this year, there was no rain for 4 months (February, March, June and July). As usually, the variation of ^{7}Be throughout the year has been following the precipitation rate (R=0.75) (Fig. 1). The variation of ^{210}Pb is irregullar throughout the year and no correlation has been observed between the ^{210}Pb deposition and the precipitation rate (R = 0.02).

The maximum ^{210}Pb deposition rate found in March 2003 has confirmed that the dry deposition may contribute significantly to the total deposition. On the contrary, deep minima in the ^{210}Pb dry deposition rate were observed in February and July. The observed variations in the ^{210}Pb dry deposition rate may result from different local conditions (e.g. radon emanation, resuspension, wind direction [7]).

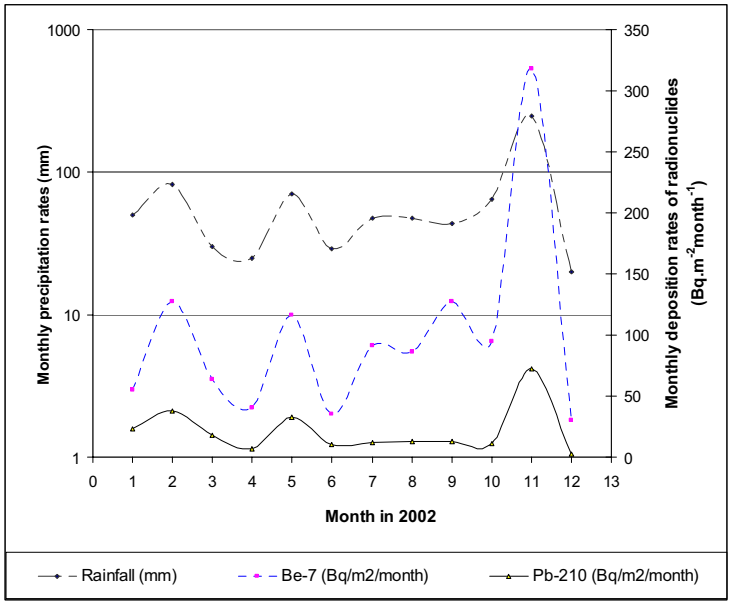

FIG. 1. Monthly precipitation, and deposition rates of ^{7}Be and ^{210}Pb in Monaco rain in 2002.

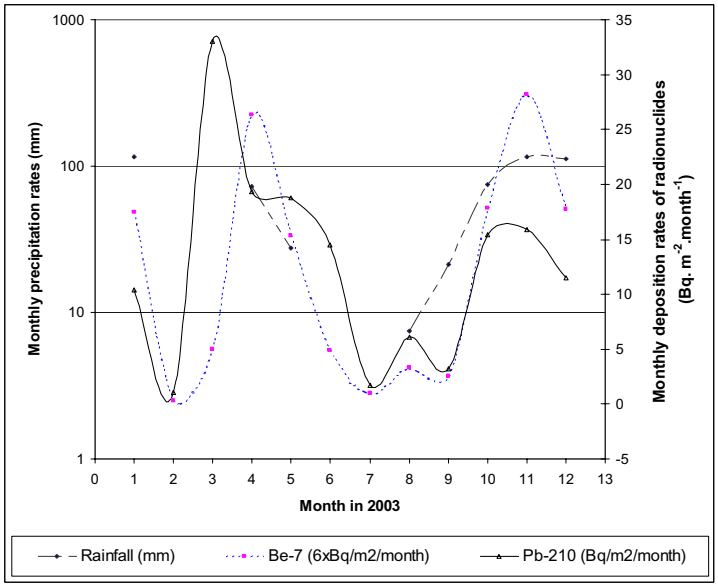

FIG. 2. Monthly precipitation, and deposition rates of ^{7}Be and ^{210}Pb in Monaco rain in 2003.

The ^{7}Be and ^{210}Pb concentrations in rain water obtained in two phases (dissolved and particulate) during seven months showed that both radionuclides have a low affinity to suspended particles (27% for ^{7}Be and 36% for ^{210}Pb).

3.2. Deposition rates of ^{137}Cs, $^{239+240}$Pu and ^{241}Am

The monthly deposition rates of anthropogenic ^{137}Cs, $^{239+240}$Pu, ^{241}Am in Monaco in 2002 are shown in Fig. 3. The total deposition rates of ^{137}Cs varied from 8.8 to 1630 mBq·m^{-2} month^{-1}, for $^{239+240}$Pu from 0.5 to 90 mBq m^{-2} month^{-1}, and for ^{241}Am from 0.25 to 35 mBq m^{-2} month^{-1}. The deposition of these radionuclides was carried out mostly by precipitation every month. The obtained correlation coefficients between these radionuclides and the precipitation rate were very high (R = 0.91).

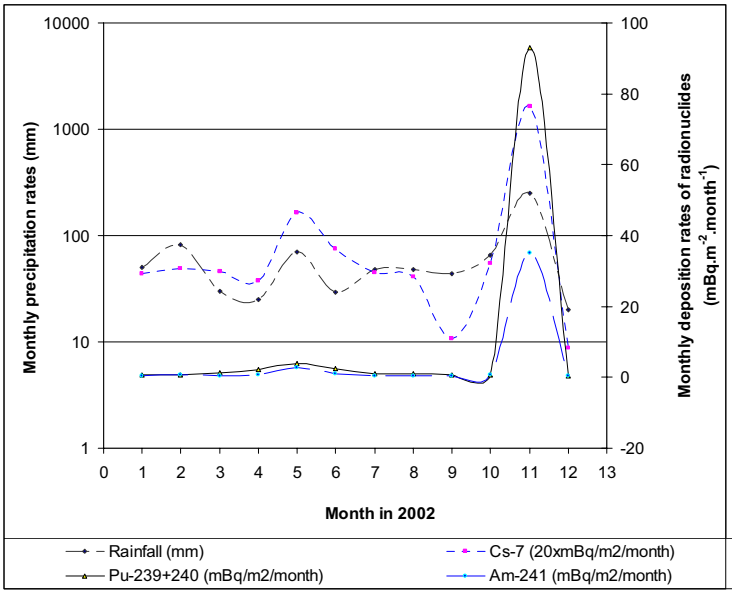

FIG. 3. Monthly precipitation, and deposition rates of ^{137}Cs, $^{239+240}$Pu and ^{241}Am in Monaco rain in 2002

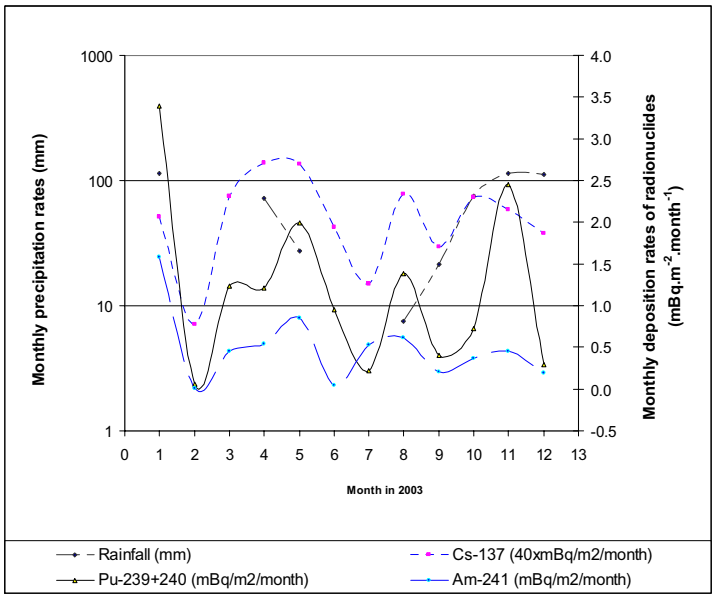

FIG. 4. Monthly precipitation, and deposition rates of ^{137}Cs, $^{239+240}$Pu and ^{241}Am in Monaco rain in 2003.

The highest total deposition rates of ^{137}Cs, $^{239+240}$Pu, ^{241}Am appeared in November 2002 when two important Saharan dust events influenced the radionuclide deposition rates. The annual deposition rates of Cs, Pu and Am in 2002 were 2200, 110 and 40 mBq m^{-2} year^{-1}, much higher than in previous years [8], as the Saharan dust event contributed about 74%, 86% and 82% to the total annual deposition rates of ^{137}Cs, $^{239+240}$Pu and ^{241}Am, respectively.

The average activity ratios of ^{241}Am/$^{239+240}$Pu (0.40±0.03) and $^{239+240}$Pu/^{137}Cs (0.025±0.003) in the precipitation are close to global fallout ratios (0.37 for ^{241}Am/$^{239+240}$Pu and 0.024 for $^{239+240}$Pu/^{137}Cs [9]). We therefore can conclude that the origin of these anthropogenic radionuclides in Monaco rainwater in 2002 is from global fallout.

The monthly deposition rates of ^{137}Cs, $^{239+240}$Pu and ^{241}Am in Monaco in 2003 are shown in Fig. 4. The total deposition rate of ^{137}Cs varied from 7 to 140 mBq m^{-2} month^{-1}, for $^{239+240}$Pu from 0.06 to 3.4 mBq m^{-2} month^{-1} and for ^{241}Am from 0.013 to 1.6 mBq m^{-2} month^{-1}. In constrast with 2002 data, when wash-out of these radionuclides was responsible for their total annual deposition rates, in 2003 dry depositions in February, March, June and July influenced their annual depositions rates. This is also confirmed by low correlation coefficients found between ^{137}Cs, $^{239+240}$Pu and ^{241}Am, and the precipitation rate (R = 0.03, 0.25 and 0.15, respectively).

Due to the weak signal of Saharan dust in May 2003, its contribution to the total annual deposition of ^{137}Cs, $^{239+240}$Pu and ^{241}Am is insignificant (in contrast to the important signal observed in November 2002). As a consequence, the total annual deposition rates of ^{137}Cs, $^{239+240}$Pu and ^{241}Am were 740, 14 and 5.9 mBq m^{-2} year^{-1}, respectively, i.e. much lower than in 2002.

The average activity ratios of ^{241}Am/$^{239+240}$Pu (0.37±0.04) and $^{239+240}$Pu/^{137}Cs (0.017±0.002) in the precipitation are close to global fallout ratios, similarly as in 2002.

The ^{137}Cs, $^{239+240}$Pu and ^{241}Am concentrations obtained in dissolved and particulate phases showed that the affinity of ^{137}Cs to the suspended particles is weaker (23-57%) than the affinity of $^{239+240}$Pu and ^{241}Am (46-91%), confirming that caesium is more soluble than plutonium and americium.

4. Conclusions

The monthly deposition rates of natural ^{7}Be and ^{210}Pb have been influenced principally by wash-out of the air, as supported by high correlation coefficients (0.90-0.96). The annual deposition rates of ^{7}Be and ^{210}Pb in 2002 were 1190 and 250 Bq m^{-2} year^{-1}, respectively. The main contribution to the deposition of anthropogenic ^{137}Cs, $^{239+240}$Pu and ^{241}Am in 2002 was the Saharan dust event, which occured in November 2002 and contributed 1630, 90 and 35 mBq m^{-2} month^{-1} for ^{137}Cs, $^{239+240}$Pu and ^{241}Am, respectively. The observed total annual deposition for ^{137}Cs, $^{239+240}$Pu and ^{241}Am was 2200, 110 and 40 mBq m^{-2} year^{-1}, respectively.

On the contrary, in 2003 the monthly deposition rates of both natural and anthropogenic radionuclides were strongly influenced by dry deposition. The annual deposition rates of ^{137}Cs, $^{239+240}$Pu and ^{241}Am were 740, 14 and 5.9 mBq m^{-2} year^{-1}, respectively, compared to 840 Bq m^{-2} year^{-1} for ^{7}Be and 150 Bq m^{-2} year^{-1} for ^{210}Pb. The anthropogenic radionuclides observed in the Monaco atmosphere in 2002 and 2003 originated from global fallout.

ACKNOWLEDGEMENT

The Agency is grateful for the support provided to its Marine Environment Laboratory by the Government of the Principality of Monaco.

REFERENCES

[1] BASKARAN, M., COLEMAN, C.H., SANTSHI, P.H., Atmospheric depositional fluxes of ^{7}Be and ^{210}Pb at Galveston and College Station, Texas, J. Geophys. Res. **98** (1993) 20555-20571.

[2] MOULIN, LAMBERT, C.E., DULAC, F., DAYAN, U., Control of atmospheric export of dust from North Africa by the North Atlantic Oscillation, Nature **387** (1997) 691-694.

[3] THEINS, M., BALLESTRA, S., YAMATO, A., FUKAI, R., Delivery of transuranic elements by rain to the Mediterranean Sea, Geochim. Cosmochim. Acta **44** (1980) 1091-1098.

[4] LEE, S-H., et al., Recent inputs and bugets of ^{90}Sr, ^{137}Cs, $^{239+240}$Pu and ^{241}Am in the northwest Mediterranean Sea, Deep-Sea Res. II **50** (2003) 2817-2834.

[5] PHAM, M.K. et al., Deposition of Saharan dust in Monaco rain 2001-2002, Physica Scripta **71** (2005) 1-4.

[6] LAROSA, J.J. et al., Separation of actinides, caesium and strontium from marines samples using extraction chromatography and sorbents, J. Radioanal. Nucl. Chem. **248** (2001) 765-770.

[7] IGARASHI, Y., et al., Resuspension: Decadal monitoring time series of the anthropogenic radioactivity deposition in Japan, J Radiation Res. **44** (2003) 319-328.

[8] LEE, S-H., PHAM, M.K., POVINEC, P.P., Radionuclide variations in the air over Monaco, J. Radioanal. Nucl. Chem. **254** (2002) 445-453.

[9] IKEUCHI, Y., et al., Anthropogenic radionuclides in seawater of the Far Eastern Seas, Sci. Total Environ. **237/238** (1999) 203-212.

Temporal and seasonal variations of stable isotopes (δ^2H and $\delta^{18}O$) and tritium in precipitation over Portugal

Carreira, P.M., P. Valerio, D. Nunes, M. F. Araújo

Instituto Tecnológico e Nuclear (ITN),
Environmental Analytical Chemistry Group,
Sacavem,
Portugal

Abstract. The Portuguese Network for Isotopes in Precipitation was initiated in 1988 by I.T.N. in collaboration with the I.A.E.A. and the Portuguese Meteorological Institute (I.M.). The network is composed of seven meteorological stations located in different regions of mainland Portugal (Fig. 1), as representative of the precipitation over this country (monthly basis). From 1988 to 2004 monthly precipitation samples were collected in these stations and the isotopic composition (deuterium, oxygen-18 and tritium) is being determined by the ITN through the Environmental Analytical Chemistry Group. Relevant meteorological and isotopic data from 1988 to 2003 is available and part has been submitted to the I.A.E.A. to incorporate in the GNIP database.

1. Introduction

From the climatic point of view**,** mainland Portugal is under north circulation regime and the water vapour moisture is mostly representing the Atlantic influence. Autumn and winter are the seasons of highest precipitation. Five meteorological stations from the National Network for Isotopes in Precipitation, Vila Real, Braganca, Penhas Douradas, Portalegre and Beja can be classified as continental stations, while Porto and Faro stations are located on the Atlantic coastline. The meteorological stations are located at different altitudes ranging from 9 m near the coastline**,** up to 1380 m in the interior (Fig. 1). This geographic situation leads to different climatic features that induce diverse isotopic compositions either in stable or radioactive isotopic contents.

The stable isotopic composition of precipitation is correlated with various environmental parameters, which characterize a given sampling point (e.g. the altitude above sea level, distance to the coast, air temperature, rain amount) [1, 2]. The distribution of $\delta^{18}O$ and δ^2H in precipitation mimics the topography of the regions**,** presenting depleted values at high altitudes, lower temperatures and with the increasing distance from the coast.

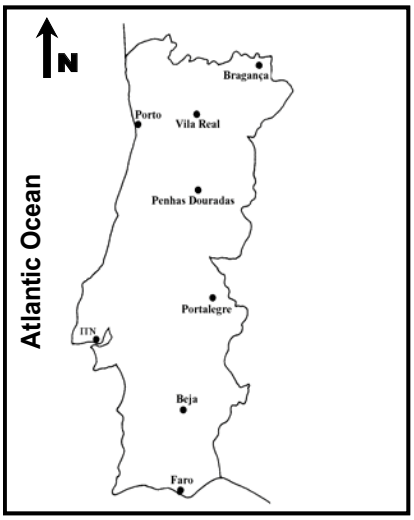

FIG .1. Location of the sampling stations of the Portuguese Network Isotopes in precipitation.

2. Results and discussion

In the Portuguese Network for Isotopes in Precipitation, part of this isotopic evolution observed in the precipitation water samples allows the identification of a gradual depletion of the Atlantic air masses from the coast through inland. This evolution is represented by the δ^2H and $\delta^{18}O$ values, which vary, respectively from –26.9‰ and –4.54‰ at Porto coastal station to –50.0‰ and –7.73‰ at Bragança inland station (Table I)).

Table I. Geographic, climatic and isotopic features of the meteorological stations of the Portuguese Network Isotopes in Precipitation

Station	Precip. (mm)	Temp. (ºC)	Altitude (m)	$\delta^{18}O$ (‰)	δ^2H (‰)	d-excess
Bragança	774	13.0	690	-7.73	-50.0	11.8
VilaReal	977	14.0	481	-6.40	-42.5	8.7
Porto	1042	15.2	93	-5.11	-30.7	10.3
PenhasDouradas	1411	9.7	1380	-8.11	-49.4	15.4
Portalegre	780	15.7	597	-6.23	-36.4	12.9
Portalegre	675	16.9	246	-5.84	-36.2	10.6
Faro	529	17.6	9	-4.70	-27.5	10.3

Seasonal variations in the stable isotopic composition of the precipitation water samples were also identified, characterized by the relation between the isotopic content**,** the mean monthly temperature and the precipitation amount (Fig. 2). These relations are described by the following equations:

$\delta^{18}O = (-0.21 \pm 0.02)\ T + (-8.59 \pm 1.07)$ $\quad r^2=0.74$

and

$\delta^2H = (-1.23 \pm 0.16)\ T + (-51.56 \pm 7.91)$ $\quad r^2=0.65$

$\delta^{18}O = (-0.01 \pm 0.003)\ Pp + (-4.46 \pm 1.36)$ $\quad r^2=0.50$

and

$\delta^2H = (-0.08 \pm 0.02)\ Pp + (-27.28 \pm 9.34)$ $\quad r^2=0.45$

The isotopic gradient with the altitude is often used in hydrology studies to estimate the recharge areas of the aquifers. In the studied meteorological stations the obtained gradients are $\Delta\delta^2H$ = -1‰ / 100 m and $\Delta\delta^{18}O$ = -0.2‰ / 100 m (Fig. 3).

A positive correlation was found between the altitude and the deuterium excess. Penhas Douradas station located at 1380 m presents the highest deuterium excess values observed in the network stations. The deuterium excess distribution within the hydrological year presents a similar pattern in all stations, which points out to the same origin of the air masses (Atlantic moisture), and to a similar isotopic evolution. However, an exception to this pattern is observed in Faro, a mixture of different air masses was identified in this station (coastal station at south of Portugal). This was revealed by a shift in the δ^2H and $\delta^{18}O$ values and consequently also in the deuterium excess values along the year (long term mean). This differentiation is probably due to a mixture of Atlantic air masses with the Mediterranean air moisture which presents δ^2H and $\delta^{18}O$ enriched values and higher deuterium excess at low altitude.

The regional meteoric water line (RMWL) for mainland Portugal (Fig. 4) was derived using weighted monthly averages of δ^2H and $\delta^{18}O$: $\delta^2H = (6.78 \pm 0.10)\ \delta^{18}O + (4.45 \pm 4.64)$, n= 405 and r= 0.95.

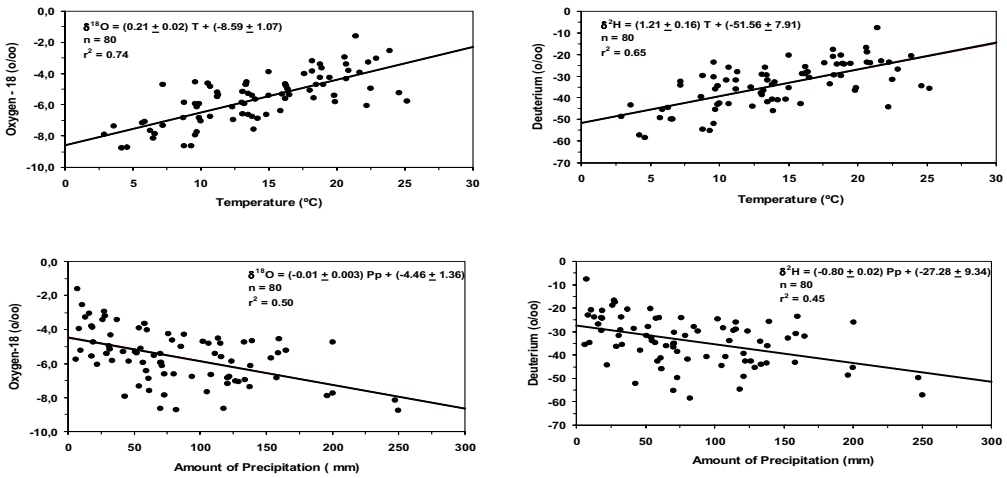

FIG. 2. Relationship between the isotopic composition and the mean monthly temperature and amount of precipitation.

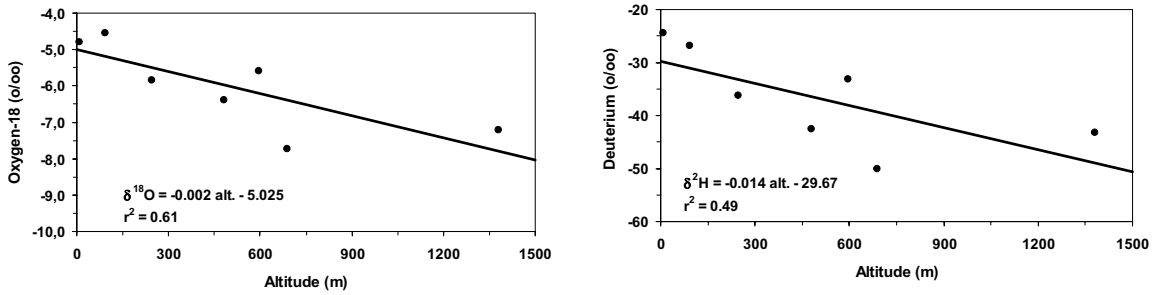

FIG. 3. Relationship between the mean isotopic composition and the sampling altitude.

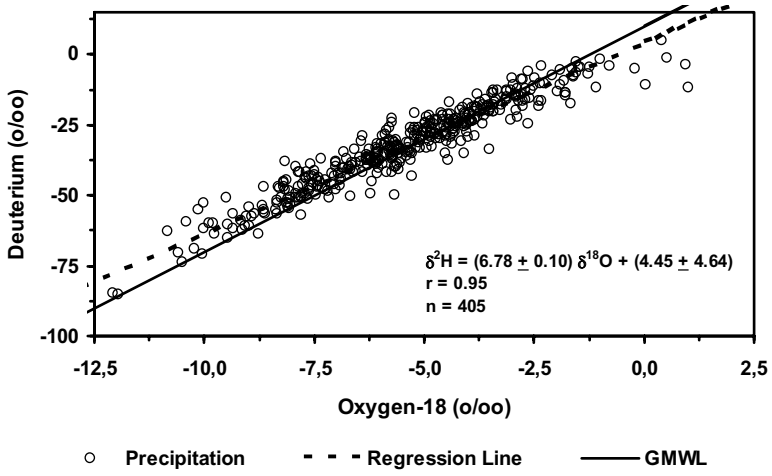

FIG. 4. Weighted $\delta^{18}O$ versus $\delta^{2}H$ in monthly precipitation collected in the Portuguese Network Isotopes in precipitation.

The tritium content determinations carried out in the monthly precipitation samples collected in the Portuguese Network for Isotopes in Precipitation, illustrate the seasonal variations: highest concentrations between June and July and the lowest values during autumn and winter time (Fig. 5).

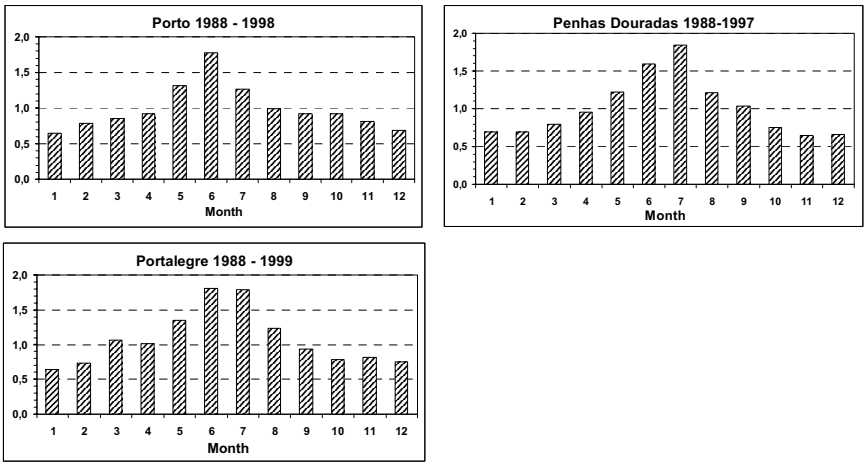

FIG. 5. Seasonal variation of the tritium content. Highest concentrations between June and July.

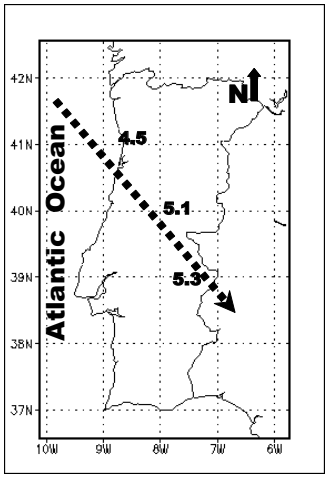

FIG. 6. Tritium concentration (TU) from coastal towards the hinterland stations. Dilution effect by oceanic water masses.

This trend can be related to the so-called "*spring leak effect*" – caused by the temporary mixing between the stratosphere and troposphere at high latitudes in early spring [3]. Also an effect similar to the "continental effect" for stable isotopes ($\delta^{18}O$ and $\delta^{2}H$) was found comparing the ^{3}H content of precipitation at different stations. The higher concentrations were found in the inland stations while the lower ^{3}H contents were determined near the ocean**,** due to the tritium dilution by the oceanic air masses. This dilution effect is evident in the arithmetic means of the weight annual mean from each station: $[^{3}H]_{Porto}$ = 4.5 TU; $[^{3}H]_{Penhas\ Douradas}$ = 5.1 TU and $[^{3}H]_{Portalegre}$ = 5.3 TU (Fig. 6).

REFERENCES

[1] ROZANSKI, K., SONNTAG, C., MUNNICH, K.O., Factors controlling stable isotope composition of European precipitation, Tellus **34** (1982) 142-150.

[2] ROZANSKI, K., ARAGUÁS-ARAGUÁS, L., GONFIANTINI, R., Isotopic patterns in modern global precipitation, Climate Change in Continental Isotopic Records, American Geophysical Union, Geophys. Monogr. **78** (1993) 1-36.

[3] GAT, J.R., MOOK, W.G., MEIJER, H.A.J., Atmospheric water, In: Environmental isotopes in the hydrological cycle. Principles and applications, UNESCO, IHP-V/Technical Documents in Hydrology **39** II, 113 pp.

Explanation of temporal changes of isotopic composition in precipitation in Hungary by meteorological data and satellite images

Palcsu, L.[a], E. Svingor[a], Z. Szántó[a], I. Futó[a], M. Molnár[a], L. Rinyu[a], R. Rozinai[a], Z. Dezső[b]

[a] Institute of Nuclear Research,
Hungarian Academy of Sciences,
Laboratory of Environmental Studies,
Debrecen,
Hungary

[b] University of Debrecen,
Department of Environmental Physics,
Debrecen,
Hungary

The aim of this work is to get a time series of the tritium content and delta values of oxygen and deuterium of precipitation characteristic for Hungary and to identify those factors, which have essential influence on the temporal changes. There are three main moisture sources, which determine the weather and the raining above Hungary. One of them is the Atlantic Moisture Source, which comes from the West bringing moisture from the mid-latitude Atlantic water vapour. The second main source of water is the Baltic Mositure Source. It brings moisture from the Arctic region over the Baltic Sea. The third source is the Mediterranean Moisture Source, which carries water from the South-West.

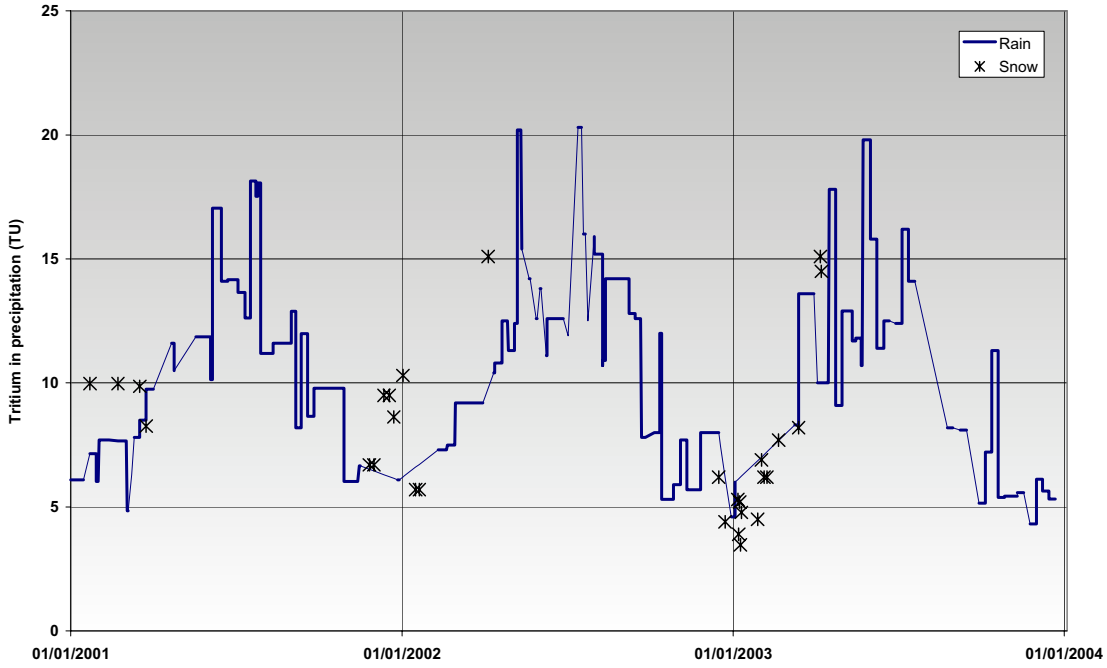

FIG. 1. Fast changes of tritium concentration in precipitation water (rain and snow) in East Hungary during the last three years

The rainfall events are continuously sampled in Debrecen, East-Hungary from December 2000. Tritium, deuterium, and oxygen-18 content of the precipitation samples are measured. We have found that the tritium content of the precipitation changed between 4.8 and 18.0 TU in 2001, between 4.4 and 20.3 TU in 2002, and between 3.5 and 19.8 TU in 2003 (see Fig. 1.), with an average of 10.4 ± 0.3 TU, 10.7 ± 0.3 TU and 8.7 ± 0.3 TU, respectively. The decreasing in the average tritium concentration of precipitation in 2003 was due to the very wet winter, while the year 2001 and 2002 were quite similar from the point of view of raining.

On the basis of satellite images (© EUMETSAT 2001-2004) and meteorological data we determine trajectories in order to decide which moisture source brings the water vapour. On the one hand the isotopic composition of precipitation depends on the moisture source, which provides the rainfall. On the other hand, the seasonal, continental and latitude effects have to be taken into account to explain the temporal changes. Sharp peaks (see Fig. 1.) in the tritium concentration of rain appear in early summer ("spring leak") as a consequence of the exchange between the troposphere and the stratosphere. We would like to understand better how this exchange mechanism works.

Cosmogenic ^{22}Na and ^{7}Be in ground level air in Kraków (Poland)

Grabowska, S., J.W. Mietelski

The Henryk Niewodniczański Institute of Nuclear Physics,
Polish Academy of Sciences,
Kraków,
Poland

Abstract. Although cosmogenic radionuclides emitting gamma radiation, such as ^{22}Na ($T_{1/2}$=2.6 y) and ^{7}Be ($T_{1/2}$=54 d) are mainly produced in stratosphere they are present in ground level air as well. The paper presents the variation of activity concentration for one week average for those nuclides in ground-level air and their activity ratio within one year period. Results are compared with measured previously average for cold and warm period for year from years 1996-2002. Obtained data support model of stratospheric air injection into troposphere.

1. Introduction

The cosmogenic radionuclides are produced in whole atmosphere, although the most intense processes goes in the stratosphere. One such radionuclide is ^{22}Na, which decays by beta plus decay with a half-life of 2.6 years, end emits gamma radiation of 1275 keV. Another is ^{7}Be, which is also a gamma-emitter (478 keV) and whose half-life is 54 days. Sooner or later all non-gaseous matter attaches to the aerosols. From the stratosphere cosmogenic radionuclides migrate to ground level air by means of different processes like diffusion, sedimentation, convection. Usually in ground level air the activity of ^{22}Na is on the level of a fraction of single μBq/m^3 may be studied by filtration of high volumes of the air and application of low-level gamma spectrometry. ^{7}Be is much more active, on the level of few mBq/m^3. In our previous study covering the years 1996-2002 (in half a year sets of samples) the cosmogenic ^{22}Na shows a strong seasonal variation (Fig. 1) with significant different mean values activity concentration between 0.333±0.095 μBq m^{-3} and 0.137±0.045 μBq m^{-3}, for summer and winter, respectively [1]. Moreover, the activity ratio for two cosmogenic radionuclides: ^{22}Na and ^{7}Be showed also changes with statistically significant seasonal differences (Fig. 2). The lower values were

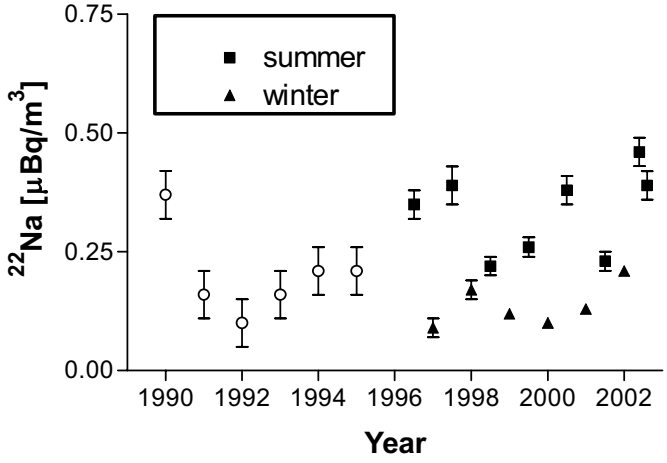

FIG. 1. The average one year (1990-1995) and half-a-year (1996-2002) ^{22}Na activity concentration in ground level air in Kraków [1].

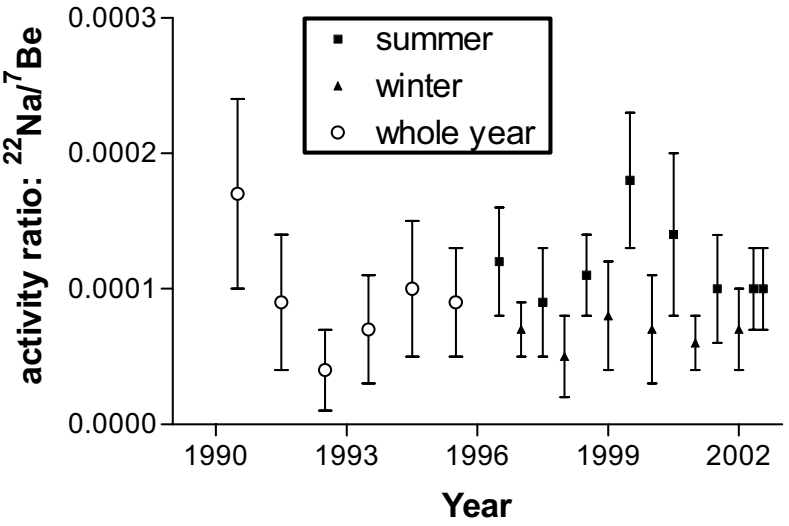

FIG. 2. Time evolution and seasonal variation of the ^{22}Na to ^{7}Be activity ratio in ground level air at Kraków [1].

found during winters. The conclusion was that transport of ^{22}Na from stratosphere to ground level air during summer seems to be so much effective, that results in kind of relative depletion of stratosphere with this nuclide. The aim of present investigation is to see the changes of ^{22}Na activity and of ^{22}Na to ^{7}Be activity ratio in more detailed way within a one year period.

2. Materials and methods

The Petryanov air filters from two ASS-500 aerosol sampling stations [2] (constructed by Polish Central Laboratory for Radiation Protection – Fig. 3) in weekly achieved filters exposed in Krakow during 2003 were analyzed for the presence of all gamma-emitters using a gamma-rays spectrometer with HPGe detector shielded with complex active and passive shields [3]. Samples were pressed down to a circular pellets of 50 mm diameter and 10 mm height. Calibration of the spectrometer was done using mix-radionuclides standard produced by PTB, Braunschweig, Germany. Each sample contains aerosols from more than 0.1 Mm^3 of air and was measured for about 6 days. Activities of all radionuclides were decay corrected for the middle of pumping period.

3. Results and discussion

Results on ^{22}Na activity are displayed in Fig. 4, and those for ^{7}Be in Fig. 5. Activities for ^{22}Na varies from 0.066±0.060 μBq m^{-3} to 0.739±0.093 μBq m^{-3}. Those for ^{7}Be were between 1269±72 μBq m^{-3} to 8469±424 μBq m^{-3}.

The time dependence of activity for both nuclides show maxima during warm part of the year and minima during cold part. However, the ^{22}Na to ^{7}Be activity ratio (Fig. 6) also show a time dependence with maximum during warmer part of the year. This result seems to confirm results obtained for a half of a year samples, namely that transport of ^{22}Na from stratosphere to ground level air during summer seems to be as effective that results in relative depletion of stratosphere with this nuclide. The stratospheric air injections might be such a process, therefore our results support hypothesis of common presence of stratospheric air injections [4, 5].

FIG. 3. A view on radiometric station of Institute of Nuclear Physics in Kraków. One of high volume aerosol sampling stations AAS-500 is visible on left side.

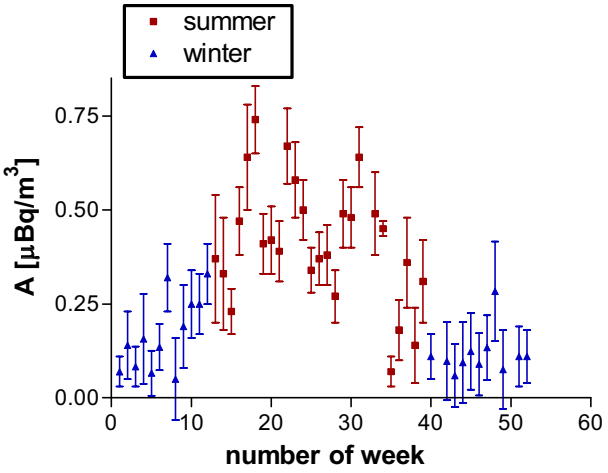

FIG. 4. ^{22}Na activity concentration in ground level air in Kraków (Southern Poland) during 2003.

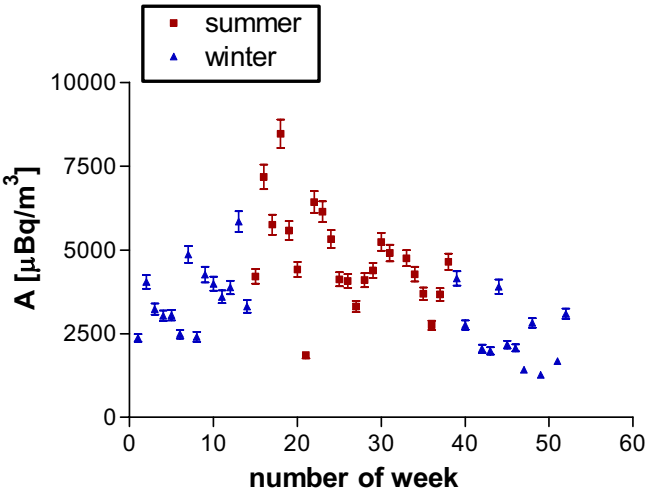

FIG. 5. ^{7}Be activity concentration in ground level air in Kraków (Southern Poland) during 2003.

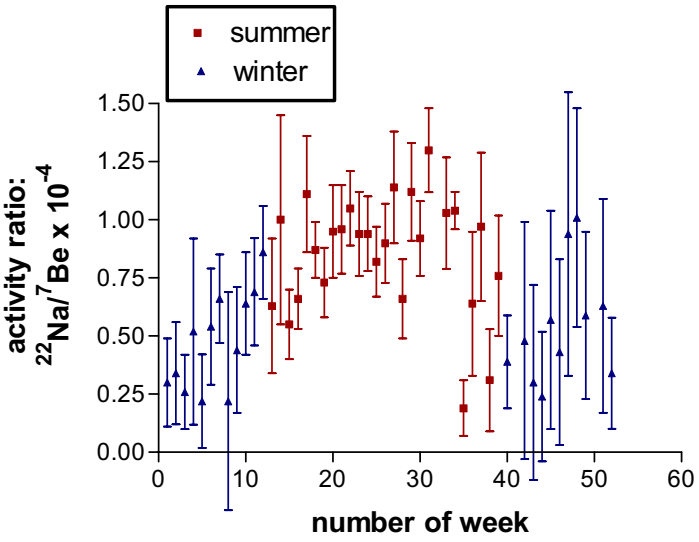

FIG. 6. ^{22}Na to ^{7}Be activity ratio for ground level air in Kraków during 2003.

REFERENCES

[1] GRABOWSKA, S., MIETELSKI, J.W., KOZAK, K., GACA, P., Gamma emitters on micro-becquerel activity level in air at Kraków (Poland), J. Atmos. Chem. **46** (2003) 103-116.

[2] JAGIELAK, J., BIERNACKA, M., ZARUCKI, R., The Method for Determination of Radionuclides Concentration in Ground Level Air Using the ASS-500 High Volume Sampler, (Book of Extended Synopses of Int. Symp. Environmental Impact of Radioactive Releases 8-12 May 1995) IAEA-SM-339/76P, IAEA, Vienna (1995) 216-217.

[3] MIETELSKI, J.W., HAJDUK, Z., HAJDUK, L., JURKOWSKI, J., Some Background Effects Observed with a Low-Level Gamma-Spectrometer with Muon Veto Detector (this volume).

[4] JANOSI, M., VATTAY, G., Soft Turbulence in the Atmospheric Boundary Layer., AIP Conf. Proc. Vol. 285, Noise in Physical Systems and 1/f Fluctuations, (HANDEL, P.H. CHUNG, Eds), AIP Press, New York (1993) 574.

[5] ROSNER, G., HöTZL, H., WINKLER, R., Continuous Wet-only and Dry-only Deposition Measurements of ^{137}Cs and ^{7}Be: an Indicator of Their Origin, Appl. Rad. Isotop. **47** (1996) 1135-1139.

FORSGC Network for isotopes in precipitation over the Monsoon Asia

Ichiyanagi, K.[a], K. Yoshimura[b], M. D. Yamanaka[a,c]

[a] Frontier Observational Research System for Global Change (FORSGC),
Japan Agency for Marine-Earth Science and Technology (JAMSTEC),
Yokohama,
Japan

[b] Institute for Industrial Sciences,
The University of Tokyo,
Tokyo,
Japan

[c] Graduate School of Science and Technology,
Kobe University,
Kobe,
Japan

The GNIP project provides the monthly data of stable isotopes in precipitation all over the world. For the validation of atmospheric water cycle by reanalysis datasets or GCM simulations, however, there are a few stations in Asia. Also, spatial and temporal variability of the stable isotope composition of precipitation in the Asia Pacific region was discussed based on the GNIP monthly dataset, and regional climatology and atmospheric circulation patterns. However, the relationship between isotope signature of precipitation and climate in tropics is not well understood, because the daily isotopic data in precipitation is limited.

Since 2000, the isotope group of the Frontier Observational Research System for Global Change (FORSGC) had been collecting the daily precipitation samples for stable isotopes over the Monsoon Asia, such as Siberia (3 stations), Tibetan Plateau (10 stations), Nepal (5 stations), Thailand (3 stations), Indonesia (5 stations), and Palau Island (1 station). In this study, we will introduce the FORSGC network for stable isotopes in precipitation database and show the short-term (monthly and daily) variability of precipitation isotopes observed in Thailand and Indonesia and so on.

The daily rainfall samples were collected during August to December 2001 at ChiangMai, Bangkok and Phuket stations in Thailand. These stations showed similar monthly variability in Oxygen-18, and most ranged from -15 permil to 0 permil. There were increasing trends in August and November, while decreasing trend in September. Daily variability, however, showed a different trend. A depletion of early-August at ChiangMai and a sudden enrichment around 10 October at Phuket were appeared. Considering relationships between Oxygen-18 and precipitation amount, there were positive correlations in three stations by the monthly basis. In general, isotopic compositions are heavy in low precipitation and light in high precipitation caused by the amount effect. The precipitation was small from August to early September and large from late September to early November. There was some correlations between $\delta^{18}O$ and precipitation if daily precipitation was less than 30mm, however, there was not significant if that was more than 30mm.

Also, the daily rainfall samples were collected during April to December in 2001 at Bukittinggi and Jambi stations which located western and eastern part of Sumatra Island, Indonesia. Most Oxygen-18 ranged from -15 permil to 0 permil in both stations. Only Jambi station showed seasonal variability

trend, that is, enrichment and depletion trends from April to August and from August to October, respectively. From November to December, there was depletion trend in both stations. The d-excess was ranged 10 to 15 permil in Bukittinggi, whereas sometimes ranged below 5 in Jumbi. This fact indicates the origin of rain water was much different between these two places. The daily rainfall variability was much different between them.

Furthermore, the time series in $\delta^{18}O$ and the origin of rain water was simulated using Isotope Circulation Model (ICM). The temporal and spatial resolution is daily time-scale and 2.5 degrees in latitude and longitude, respectively. Notice that this model devises to integrate all vertical atmospheric- and isotopic-physics in each grid. When water transit its phase among solid, liquid and gas, the evaluation of the isotopic composition is described by the Rayleigh distillation process. The atmospheric water budgets were calculated by using the variables from NCEP/NCAR renalysis. From the preliminary result of the ICM simulation, the time series of δ18O in two places were almost same pattern during May to December in 2001. However, the origin of rain water was much difference between these two places. Most of rain water in Bukittinggi was originated from the Indian Ocean through whole year. From a half to two third of rain water in Jumbi was originated from the Indian Ocean, and the remain was from Java Island and Java Sea. The mixing ratio of different original water was changed weekly or smaller time-scale. This results coincides with the observed d-excess variations.

ATMOSPHERE – POSTERS

Changes of methane and nitrous oxide in the atmosphere: New constraints from stable isotope analyses in polar firn and ice

Bernard, S.[a], T. Roeckmann[b], J. Kaiser[c], J. Chappellaz[a], J-M. Barnola[a], C.M. Brenninkmeijer[d]

[a] Laboratory of Glaciology and Geophysics of the Environment,
CNRS,
Grenoble,
France

[b] Max Planck Institute for Nuclear Physics,
Heidelberg,
Germany

[c] Department of Geosciences,
Princeton University,
Princeton,
United States of America

[d] Max Planck Institute for Chemistry,
Mainz,
Germany

Methane and nitrous oxide are two greenhouse gases playing a major role in atmospheric chemistry; methane largely affects the oxidative capacity of the atmosphere whereas nitrous oxide participates in many atmospherical chemical reactions in the stratosphere. A sharp increase in the mixing ratios of both gases has been observed since the beginning of the pre-industrial era, implying an increase of anthropogenic sources.

Although these gases are important in global climate changes, their budget remains poorly known. The evolution of their isotopic composition in the atmosphere brings additional constraints as it represents the final signature of their budgets and reflects changes in the relative contribution of sources and sinks.

We have measured isotopic composition of methane and nitrous oxide coming from polar firn air and enclosed in ice core bubbles. This is leading to mid term evolution of these gases (the last 200 years). A continuous flow technique is used at the Laboratory of Glaciology and Geophysics of Environment in Grenoble, France, to measure $\delta^{13}CH_4$, whereas a similar technique is used at Max Planck Institute for Nuclear Physics, In Heidelberg, Germany, to measure $\delta^{15}N_2O$, $^1\delta^{15}N_2O$, $^2\delta^{15}N_2O$ and $\delta N_2{}^{18}O$. Samples from both Antarctica (Berkner Island) and Greenland (North GRIP) were used. We will present these results and their tentative interpretation based on a diffusion model of gas isotopes in polar firn.

Seasonal variation of anthropogenic radionuclides in atmospheric samples from central radiation monitoring station in Korea

Chang, B.U., Y.J. Kim, C.S. Kim, H.Y. Choi, C.K. Kim, B.H. Rho, J.Y. Moon

Korea Institute of Nuclear Safety (KINS),
Daejeon,
Korea, Republic of

By reason of the rapid economic growth and industrialization, China is facing an unexpected increase of air pollution. Asian dust transport, known as "Yellow sand" in East Asia, originated from Chinese inland affects to neighboring countries. It has been a long time since the annually occurring "uninvited-guests", Asian dust and related air pollutants raised important environmental issue of not only it's own country, but also neighboring countries like Korea and Japan, and faraway countries, even the North American continent.

During the last three years (2001-2003), we have monitored the monthly variations of anthropogenic radionuclides in atmospheric samples collected from the Central Radiation Monitoring Station in Korea. After finishing the γ-ray measurement by HPGe, each sample was extracted by nitric acid with Sr and Cs carriers and Pu tracers. Pu, Sr and Cs in the acid extract were purified with the sequential separation method developed by our laboratory [1]. The activities of ^{137}Cs and ^{90}Sr were measured by a low background gas-proportional α/β counter (Tennelec Series 5, Oxford Instruments Inc.). Measurement for Pu radioactivity was performed using a PlasmaTrace2 sector field inductively coupled plasma mass spectrometry (Micromass, Manchester, UK).

The concentrations of ^{137}Cs, ^{90}Sr and Pu isotopes in the spring season showed relatively high values compared with those in other seasons. The so-called spring peak of ^{137}Cs, ^{90}Sr and Pu isotopes was observed in March. In sampling area, the total annual deposition of ^{137}Cs, ^{90}Sr and $^{239+240}$Pu in 2002, were 609, 242, 25.4 mBq/m^2, respectively. Especially, as the spring peak's total deposition (March, April, and May) of each radionuclide were 70, 55, 74% of total annual depositions of each radionuclide, respectively. These amounts were 12-15% higher than spring peak value in 2001. These increase of radioactivities caused by denser Asian dust in 2002 than 2001. In the contrary, the radioactivities of spring peak samples show relatively low in 2003. At this year, the occurrence frequency of Asian dust was very low.

These results indicate that the sources of anthropogenic radioactive elements in atmospheric samples are not the local resuspension but the transport from the source regions in Chinese inland.

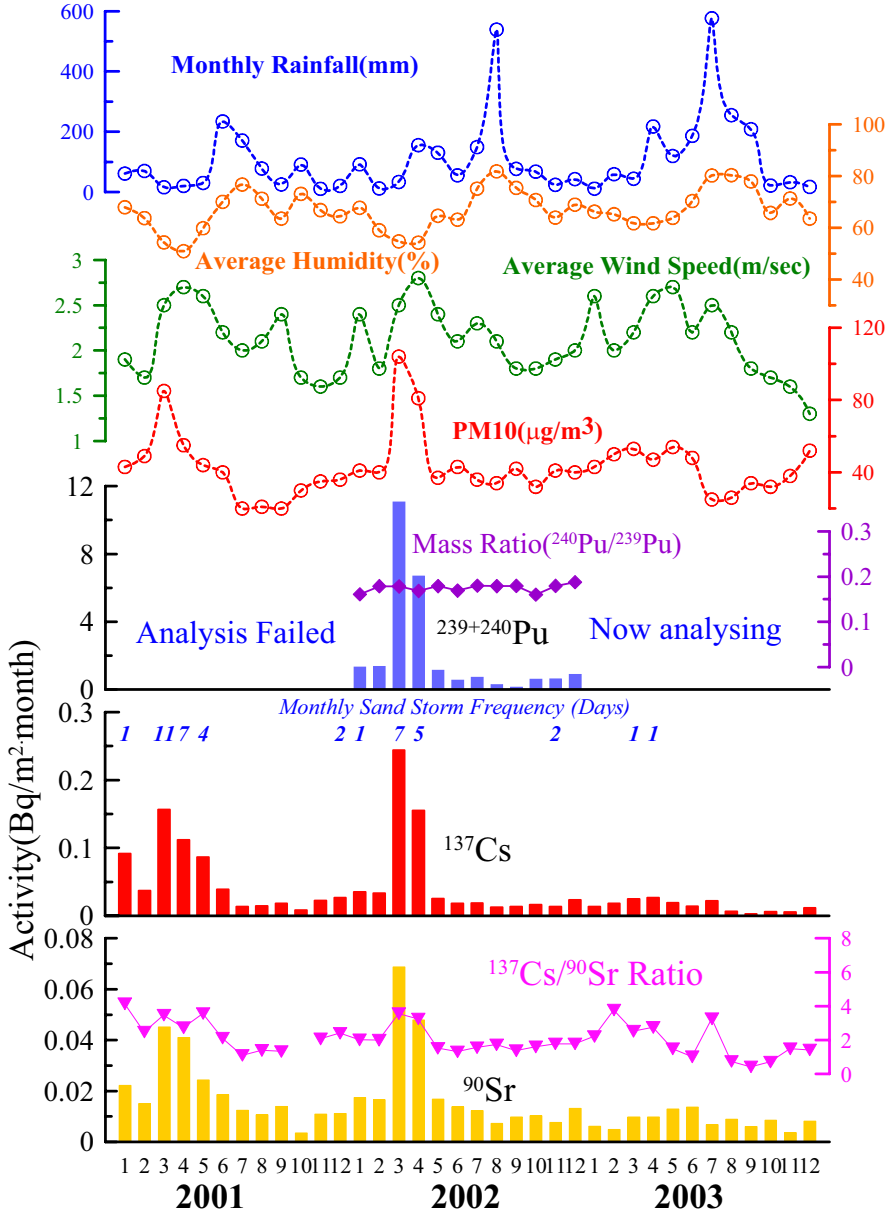

FIG. 1. Monthly variation of anthropogenic radionuclides in total deposition samples.

REFERENCE

[1] CHANG, B.U., KIM, Y.J., KIM, C.S., KIM, C.K., MOON, Y.J., Sequential Analysis of Artificial Radionuclides in Atmospheric Samples of Daejeon, Korea, IAEA-CN-98/5/15P (2002).

Surface mass balance of the East-Wilkes / Victoria region of Antarctica: an update

Magand, O.[a], C. Genthon[a], M. Frezzotti[b], M. Fily[a], S. Urbini[c], H. Gallee[a]

[a] Laboratory of Glaciology and Geophysics of Environment (LGGE),
UMR CNRS,
Grenoble,
France

[b] Ente per le Nuove Tecnologie, l'Energia e l'Ambiente (ENEA),
Roma,
Italy

[c] Instituto Nazionale di Geofisica e Vulcanologia,
Dipartimento per lo studio del Territorio e delle sue Risorse,
University of Genoa,
Genoa,
Italy

In spite of more than 2000 reported field measurements [1], there are 3 major difficulties to building an accurate observations-based full map of the Antarctic Surface Mass Balance (SMB): 1) Depending on measurements technique and time sampling, the reliability, accuracy and representability of a given report is highly variable and may be very poor; 2) There are still huge gaps in the spatial coverage of the available measurements, and much of the Antarctic SMB estimation currently relies on interpolation; and 3) Measurements sample various time periods and are time-inconsistent, so that real temporal variability can induce spurious spatial variability. Antarctica is a huge place (12.4 106 km²) and International programs as ITASE (International Trans-Antarctic Scientific Expeditions, [2]) are essential to obtain new high quality data to fill gaps and/or supersede older less reliable estimations of the SMB.

This work is focused on the East-Wilkes and Victoria (EWV) region (Fig. 1), in Antarctica (Section I), where new estimates of the Surface Mass Balance (SMB) have been recently produced thanks to Italian and French ITASE activities, in EWV in the 1998-2001 period [3-4]. Some of the most accurate dating techniques available, in particular, measurements of radioactive reference levels due to atmospheric thermonuclear tests (section II) and snow radar, have been used to obtain the new SMB data. More than 50 firn cores and/or snow pits, i.e. more than 1000 snow samples, have been dated using fifties and sixties horizons (Fig. 2). The detection of fission products (mainly ^{90}Sr, ^{90}Y and ^{137}Cs) was done with a low-level β counter, constituted by a surface-barrier silicon detector (Schlumberger type BEC 200-300 A) connected in anti-coincidence with a gas flow guard counter (proportional mode-parallel wires: Intertechnique type S30 A). The nuclear detection characteristics for global β radioactivity are described by [5].

These new SMB data make it possible to check, in this region, the Antarctic SMB maps built from compilation of older data and interpolations (Sections III and IV), here the map by Vaughan et al [6], henceforth referred to as the V-map, reports using 1860 field observations of various kinds, but none of the new data above, to build a full map of the Antarctica SMB. Microwave remote sensing was used as a semi-empirical tool to interpolate between the field reports. Figure 3 compares old field data with the SMB map in the EWV sector [6]. Except for a few outliers, the V-map is in good agreement with the older field data. This is an unsurprising result since these data were used to build the map.

Figure 4 compares the new data (ITASE firn cores) and Vaughan-map in the EWV sector. The V-map displays a distinctive structure of relatively high SMB in a region of otherwise very low accumulation south of 75°S. This structure is not confirmed by the new observations which suggest much more spatial homogeneity in this region. More generally, the V-map tends to overestimate the Antarctic SMB. The error in V-map relative to the new data reaches as much as 900% in the dry region.

The new data show that there is currently no proven method to interpolate across the huge gaps remaining between existing data. It is crucial that more and more accurate field determinations of the Antarctic SMB are obtained, in particular as part of ITASE.

ACKNOWLEDGEMENTS

Financial support from the French Ministry of Research, Italian Ministry of Research through PNRA Consortium, ACI Climate Change and Cryosphere is acknowledged for this work.

Field work in Antarctica was possible through the logistic support of the Italian Antarctic Program.

REFERENCES

[1] GIOVINETTO, M.B., ZWALLY, H.J., Spatial distribution of net surface accumulation on the Antarctic ice sheet, Ann. Glaciol. **31** (2000) 171-178.

[2] MAYEWSKI, P.A., GOODWIN, I.D., International Trans Antarctic Scientific Expedition (ITASE): 200 years of past Antarctic Climate and Environmental Change, Science and Implementation Plan, PAGES Workshop Report Series, **97-1** (1997) 48 p.

[3] FREZZOTTI, M., POURCHET, M., FLORA, O., GANDOLFI, S., GAY, M., URBINI, S., VINCENT, C., BECAGLI, S., GRAGNANI, R., PROPOSITO, M., TRAVERSI, R., UDISTI, R., FILY, M., Spatial and temporal variability of snow accumulation in East Antarctica from traverse data, Climate Dynam. (in press).

[4] MAGAND, O., FREZZOTTI, M., POURCHET, M., STENNI, B., GENONI, L., FILY, M., Climate variability along latitudinal and longitudinal transects in East Antarctica, Ann. Glaciol. (in press).

[5] POURCHET, M., PINGLOT, F., Radioactivity measurements applied to glaciers and lake sediments, Sci. Total Environ., **173-174** (1995) 211-223.

[6] VAUGHAN, D.G., BAMBER, J.L., GIOVINETTO, M., RUSSEL, J., COOPER, A.P.R., Reassessment of net surface mass balance in Antarctica, Jour. Climate, **12** (1999) 933-946.

Study of radionuclide concentration in the air at 11 km altitude using cabin filters from airliners

Mietelski, J.W., S. Grabowska, P. Gaca

Henryk Niewodniczański Institute of Nuclear Physics,
Polish Academy of Sciences,
Kraków,
Poland

Abstract. Results on ^{7}Be, ^{22}Na, ^{40}K, ^{137}Cs, ^{238}Pu, $^{239, 240}$Pu, uranium activities, thorium activity isotopic ratio for two samples from dust collected at cabin filters of airliner Boeing 767 exploited by LOT Polish Airlines at North Atlantic rout for two years are presented. Some details on the radiochemical procedure are presented.

1. Introduction

Radionuclides in ground-level air are often monitored at many locations all over the globe. Contrarily, the results on the high altitude concentrations of radionuclides are rather scarce. To learn more about radionuclides content at ca. 11 km altitude we decided to use cabin filters of airliners, which are a waste when removed from the airplane after about 2 years exploitation. It seems to be interesting to test to what extent the results on the radionuclides content obtained using this material could be comparable with the results obtained from purposely collected samples from much more expensive high altitude air-samplers which were especially installed on the airplanes [1] or balloons to investigate the radionuclides in the upper troposphere or low stratosphere.

The main objection may be that airplane intakes air through cabin filters also on ground, during take-off and landing, so not only at high altitude. Some air is re-circulated in ventilation system. We intended to study isotopic ratios to see if they are different from those typical at ground level air.

2. Materials and methods

We obtained two samples from Boeing 767 airliners exploited on the north Atlantic routs by LOT Polish Airlines. We looked for natural as well as artificial nuclides, which are gamma, alpha or beta emitters, especially for ^{7}Be, ^{22}Na, ^{40}K, ^{137}Cs, ^{238}Pu, $^{239, 240}$Pu, uranium and thorium. Dust was removed mechanically from surface of glass filter and put into a Marinelli beaker. Gamma spectrometric measurements were done using low-background system with veto muon detector and etruscian lead inner shield [2]. Then samples were incinerated.

It should be noticed that dust from filters contain mostly organic matter, after ashing in 600° C only about 20% of original mass remains. Alpha activity determination was performed using Silena AlphaQuattro alpha spectrometer with Canberra PIPS detectors. Alpha measurements were preceded by adequate, typical radiochemical separation processes with ^{236}Pu or ^{232}U tracers added. Plutonium was separated on Dowex-1 anion exchange resin from 8 M HNO_3 solution [3, 4] whereas U was separated also on Dowex-1 resin but from 9 M HCl [5]. No Th tracer was added, therefore results for Th are available only for isotopic activity ratios.

3. Results and discussion

Examples of obtained spectra are displayed in Figs. 1&2. Activity concentrations normalized to unit of dry dust are presented in Table I. Activity ratios for chosen radionuclides are presented in Table II.

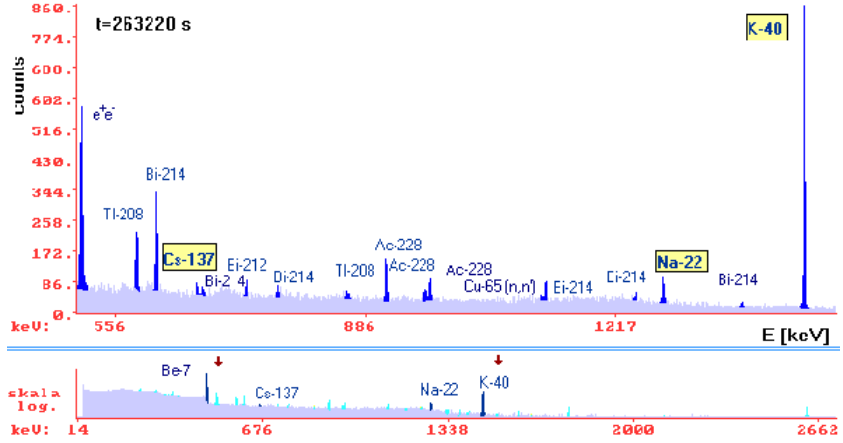

FIG. 1. Gamma spectrum of dust separated from Boeing 767 cabin filter.

Table I. Activity concentration for selected radionuclides in cabin filter dust.

Sample	Mass	Activity						
	[g]	kBq/kg	Bq/kg				mBq/kg	
		^{7}Be	^{22}Na	^{137}Cs	^{40}K	^{238}U	^{238}Pu	^{239,240}Pu
1	60.7	456±2	22.9±0.5	9.7±0.3	497±5	2.1±0.2	5.1±1.8	19.4±1.3
2	63.9	524±1	22.0±0.5	8.9±03	533±6	1.4±0.4	3.1±1.6	14.1±1.8

Table II. Some activity ratios observed in dust of cabin filters.

Sample	^{22}Na/^{7}Be	^{22}Na/^{137}Cs	^{238}Pu/^{239,240}Pu	^{235}U/^{238}U	^{234}U/^{238}U	^{230}Th/^{232}Th
1	(0.50±0.01)·10^{-4}	2.4±0.1	0.26±0.10	0.06±0.02	1.11±0.04	1.13±0.07
2	(0.42±0.01)·10^{-4}	2.5±0.1	0.22±0.13	0.06±0.03	1.10±0.02	1.05±0.06

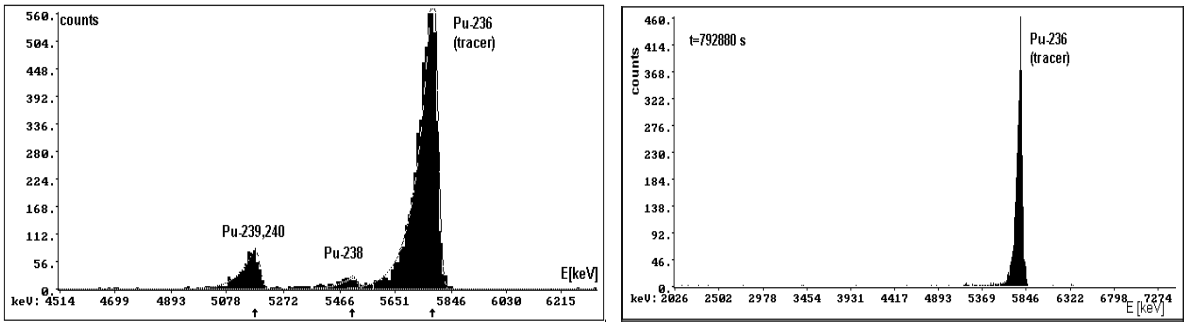

FIG.2. Alpha spectrum of plutonium fraction from dust separated from airliner cabin filter (left), 10 mBq of ^{236}Pu added as a tracer, measurement was lasting for three weeks. For comparison spectrum of blank sample is presented (right).

High values for ^{22}Na to ^{137}Cs activity ratio, equal to about 2.5, which is an order of magnitude higher than for ground level air, confirms that at least a lot of dust comes from high altitude dust. One of the questions was the plutonium activity and especially the activity ratio for plutonium alpha emitters ^{238}Pu and ^{239,240}Pu. Measured ^{239,240}Pu activity was 19.4+1.3 mBq/kg or 14.1+1.8 mBq/kg for dry dust, for first and second filters, respectively. Although with high relative uncertainty (due to tailing

of the tracer peak) the ^{238}Pu to ^{239,240}Pu activity ratio was found ranging from 22% to 26%. It was far more higher then the global fallout value of 0.03 or 0.04 [6]. The origin of this high ratio remains unclear, one of possible explanation is that traces of ^{238}Pu from US satellite SNAP 9A, crashed in 1964, are still present in the stratosphere. However, similar Pu ratio is a "hallmark" of discharge from Sellafield [7] nuclear fuel reprocessing plant. Observed uranium and thorium isotopic ratio are also close to those of seawater, therefore perhaps both Pu, U and Th come from a sea-spry of the North Sea.

REFERENCES

[1] KOWNACKA, L., JAWOROWSKI, Z., Sci. Total Environ. **144** (1994) 201-215.
[2] MIETELSKI, J.W., HAJDUK, Z., HAJDUK, L., JURKOWSKI, J., (this volume).
[3] LAROSA, J.J., COOPER, E., GHODS-ESPHAHANI, A., JANSTA, V., MAKAREWICZ, M., SHAWKY, S., VAJDA, N., J. Environ. Radioactivity **17** (1992) 183-209.
[4] MIETELSKI, J.W., WĄS, B., Appl. Rad. Isot. **46** (1995) 1203-1211.
[5] MIETELSKI, J.W., BAEZA, A.S., GUILLEN, J., BUZINNY, M., TSIGANKOV, N., GACA, P., JASIŃSKA, M., TOMANKIEWICZ, E., Appl. Rad. Isot. **56** (2002) 717-729.
[6] UNITED NATIONS SCIENTIFIC COMMITTEE ON THE EFFECTS OF ATOMIC RADIATION (UNSCEAR), Report with Annexes, United Nations sales publ. E.82.IX.8. New York (1982).
[7] KERSHAW, P.J., LEONARD, K.S., MCCUBBIN, D., ALDRIDGE, J.N., Plutonium in the Environment (KUDO, A., Ed.), Elsevier Science Ltd. (2001) 305-328.

The development of detailed climatic scenarios for the Central Asia Region

Normatov, I. Sh.

Institute of Water Problems,
Hydroenergetics and Ecology,
Academy of Sciences,
Republic of Tajikistan

In Tajikistan Republic over 10% of the territory is the zone of everlasting snow and glaciers. This territory requires strategic defence, as global anthropogenic increasing of temperature more perceptibly tells upon the regime of forming the river flow and activation of ice disintegration. Intense glaciers melting causes not only decreasing of the fresh water supply for Central Asia but also the formation of glacial lakes. Therefore there appears the danger of destructive mountain flows, which caused the human victims and land degradation not once. Under modern climatic conditions the area of the Pamirs and Alai's glaciers is decreasing annually by 1.2 sq. km. As a whole on region the tendency of decrease of emission of polluting substances from stationary sources in air pool is observed. If in 1990 the quantity of emission has made of 6793 thousand tons, by 1995 this size has decreased on 2084 thousand tons.

The maximal contribution to total amount of emissions of polluting substances in an atmosphere has of Kazakhstan – 68%. The share of other countries of Central Asia is distributed as follows: Uzbekistan – 18%, Turkmenistan – 10%, Kyrgyzstan – 2% Tajikistan – 2%.

In structure of manufacture of the electric power by Kazakhstan on a share of hydroelectric power station is 6-7%, dusty and coil – 79%, gas and fuel – oil – 12-13%.

In structure of generating capacities of power stations of Uzbekistan the densities of thermal power stations makes 87.4%, hydroelectric power stations – 12.6%. As power resources for manufacture of energy the share of gas makes 82.6%, black oil – 13%, coil – 4.4%.

The constant escalating of thermal capacities results in an aggravation of an ecological problem of region. Emissions of harmful substances by boiler of thermal power stations at development 1.0 GWt.h. is: Flying ashes and not burned down fuel – 4.6 thousand tons, oxides of sulfur – 4.4. thousand tons, oxides of nitrogen – 1.0 thousand t., thus are used about 850 thousand tons of atmospheric oxygen. It is necessary to note, that 1.0 tons oxide of nitrogen 1.0 thousand tons of a nitric layer, that results in decrease of absorbability of rigid ultra-violet space radiations. The decrease of absorption results in increase of intensity of rigid ultra-violet radiation in areas UV-AND (400-315 nm) and UV-IN (315-280 nm). The radiation has erythem, carcinogenic, antimythotic (lethal for a crate), mythogenic and other properties.

Recently published report on change of climate prepared within the framework of the convention UNO concerning change of climate, hydrometeoretical by a service of Uzbekistan, predicts negative consequences of influence of climate change on water resources. According to the given report for the period from 1957 for 1980, the glaciers in Central Asia have decreased by 19% in size.

The Aral crisis is most vivid example of an ecological problem with serious socio-economic consequences, to which directly or all states of Central Asia are indirectly connected. The crisis situation caused by drying of the Aral Sea, has developed as a result of an agrarian orientation of

economy on the basis of development of irrigation agriculture and growth irrevocable use of water on irrigation.

The essential river drain in deltas of Amu Darya and Syrdarya is insufficient for preservation ecological system. Since 1961 the sea level was constantly lowered with growing speed from 20 up to 90 sm. per one year. There is an intensive drainage and salting of grounds in deltas of these rivers, deep degradation of hydromorph ecological system. Former bottom of the sea became a source dusty and salty of carries on change of a temperature is observed. Moreover annually from dried up parts of bottom of the sea by a wind rises in air about 75 million tons of salt and sand, which are already found out at top of Pamir glaciers.

The observing network in Tajikistan Republic has a unique peculiarity, which differs it from similar networks in other countries. It is situated at the altitudes of 300 to 4,169 m, i.e. in the troposphere. All those stations were included into the world observing network.

In Tajikistan numerous scientific works require proper processing. Today it is necessary to make systematization and scientific analysis of hydrometeological data, accumulated for the last hundred years.

The foundation of the stations of the local and global monitoring of the greenhouse gases opens the wide perspective to establish the changing dynamics of green concentration according to the altitudes. It establishes the dependence of the snow and glaciers melting process and the formation of the river flows on the greenhouse gases concentration at the different heights, as well as the influence of the greenhouse gases on the flora and fauna.

The results of conducted measurements, observations of the greenhouse gases influencing the environment will generate the research and practical works in developing modern technologies, which provide the essential decrease in the greenhouse gases emission and the wide use of untraditional energy carriers instead of organic fuels.

Determination of mid-latitude radon-222 flux from the Southern Ocean using atmospheric radon-222 concentration measurements at an island ground station

Zahorowski, W., S. Chambers, A. Henderson-Sellers

Australian Nuclear Science and Technology Organisation,
Menai, New South Wales,
Australia

Terrestrial radon (radon-222) fluxes typically exceed oceanic fluxes by 2-3 orders of magnitude [1]. This sometimes leads to the oceanic flux being neglected in atmospheric models [2, 3]. However, direct comparisons between observed and simulated atmospheric radon concentration at remote sites with extended oceanic fetch would benefit from the inclusion of a realistic oceanic radon flux within models [4].

Existing estimates of oceanic radon fluxes are not well constrained, with values ranging over two orders of magnitude (0.0011 - 0.15 atoms $cm^{-2}s^{-1}$) [1, 5]. At present, the primary factors contributing to the poor characterisation of oceanic radon fluxes are the limited number of observations, and the representativeness of the published results. Previous studies have employed either the accumulation [1] or gradient methods [5]. Both methods are based on spot measurements and as such, are subject to local conditions. More importantly, it would be difficult, if not impossible, to relate such results to a wider range of environmental parameters such as wind speed and sea state, which have a significant effect on ocean-atmosphere exchange.

We present a method for the determination of regional oceanic radon fluxes. The method is applied to a subset of high sensitivity hourly atmospheric radon concentration observations from 1999 to 2003 made at Cape Grim, Tasmania (40°41'S, 144°41'E), a World Meteorological Organisation Global Atmosphere Watch (WMO GAW) station. A simple expression for an average oceanic radon flux is derived and applied using a subset of the observations considered to be representative of air parcels with an extended oceanic fetch.

We discuss the dataset using the notion of an 'oceanic event', which is defined here as any set of consecutive hourly observations coming from the oceanic sector. Typically, the duration of a single oceanic event will vary from a few hours to a few days. The intermittent nature of boundary layer wind fields can result in short-term transitions across the oceanic sector boundaries when the air mass has mixed origins. Since the terrestrial radon source is much stronger than the oceanic source, only oceanic events that persist on synoptic time-scales are likely to include hourly observations that are representative of a minimally perturbed oceanic fetch. The evolution of radon concentration in the composite oceanic event was examined. It was found that radon concentrations in the first 20-30 hours after change to the oceanic sector are strongly perturbed from oceanic values. After the initial 20-30 hours, mean radon concentrations in the composite oceanic event are within the 95% confidence interval. This suggests that radon concentrations from this portion of the composite oceanic event are minimally perturbed from typical oceanic values.

The lowest value in the range of estimated mean radon flux from the region of the Southern Ocean within the Cape Grim radon measurement fetch is about 0.0026 atoms $cm^{-2}s^{-1}$. This value is thought to constitute a lower limit estimate since it was obtained assuming negligible loss of radon from the marine boundary layer to the free troposphere. Taking into account the entrainment of radon from the

marine boundary layer to the lowest layer within the free troposphere, derived from airborne measurements of mixing of dimethyl sulphide and aerosol particles over the Southern Ocean, leads to an upper limit estimate of about 0.006 atoms $cm^{-2}s^{-1}$. Based on the 10 and 90 percentile radon concentration and wind speed observations, and assuming a mechanically driven mixing height, the regional oceanic radon flux may vary from 0.0014 to 0.008 atoms $cm^{-2}s^{-1}$ with changes in the sea state induced by wind and other environmental parameters.

Our findings support the common assumption that oceanic radon fluxes are 2-3 orders of magnitude lower than terrestrial radon fluxes, which are typically within the range 0.5-2 atoms $cm^{-2}s^{-1}$. Our values are lower than some experimental spot estimates of oceanic radon flux rates made in the seventies [1, 5]. However, they are in close agreement with more recent estimates of the flux derived from model evaluation studies and also with radon flux values assumed in an intercomparison of the convective and synoptic processes of 20 global atmospheric transport models sponsored by the World Climate Research Program [4].

The new method of oceanic radon flux derivation can be applied to other sites around the world where 'clean' ocean air can be clearly identified. The method offers an alternative to experimental local/spot estimates of oceanic radon flux such as the accumulation method and gradient methods. More importantly, it is representative of a large region and allows results to be related to a wider range of environmental parameters that influence sea state (e.g. wind speed), which have a significant effect on ocean-atmosphere exchange

REFERENCES

[1] WILKENING, M.H., CLEMENTS, W.E., Radon 222 from the ocean surface, J. Geophys. Research **80** 27 (1975) 3828-3830.

[2] MAHOWALD, N.M., RASCH, P.J., EATON, B.E., Transport of 222radon to the remo troposphere using the Model of Atmospheric Transport and Chemistry and assimilated win from ECMWF and the National Center for Environmental Prediction/NCAR. J. Geophys. R **102** D23 (1997) 28,139-28,151.

[3] DENTENER, F., FEICHTER, J., JEUKEN, A., Simulation of the transport of Rn-222 using on-line and off-line global models at different horizontal resolutions: a detailed comparison with measurements, Tellus **51B** (1999) 573-602.

[4] JACOB, J.J., PRATHER, M.J., RASCH, P.J., SHIA, R.-L., BALKANSKI, Y.J., BEAGLEY, S.R., BERGMANN, D.J., BLACKSHEAR, W.T., BROWN, M., CHIBA, M., CHIPPERFIELD, M.P., DE GRANDPRÉ, J., DIGNON, J.E., FEICHTER, J., GENTHON, C., GROSE, W.L., KASIBHATLA, P.S., KÖHLER, I., KRITZ, M.A., LAW, K., PENNER, J.E., RAMONET, M., REEVES, C.E., ROTMAN, D.A., STOCKWELL, D.Z., VAN VELTHOVEN, P.F.J., VERVER, G., WILD, O., YANG, H. AND ZIMMERMANN, P., Evaluation and intercomparison of global atmospheric transport models using ^{222}Rn and other short lived tracers, J. Geophys. Res. **102** D5 (1997) 5953-5970.

[5] PENG, T.-H., BROECKER, W.S., MATHIEU, G.C., LI, Y.-H., Radon evasion rates in the Atlantic and Pacific oceans as determined during the Geosecs program, J. Geophys. Res. **84** (1979) 2471-2486.

RADIONUCLIDE STUDIES OF SEDIMENTS

Latitudinal distribution and sedimentation of ^{90}Sr, ^{137}Cs, ^{241}Am and $^{239,240}Pu$ in bottom sediment of the Northwest Pacific Ocean

Lee, S-H.[a], P. P. Povinec[a], E. Wyse[a], G-H. Hong[b], C-S. Chung[b], S-H. Kim[b], H-J. Lee[b]

[a] Marine Environment Laboratory,
International Atomic Energy Agency,
Monaco

[b] Isotope Oceanography Laboratory,
Korea Ocean Research and Development Institute,
Ansan, Seoul,
Korea, Republic of

As a part of the Worldwide Marine Radioactivity Studies (WOMARS) of the International Atomic Energy Agency's Marine Environment Laboratory (IAEA-MEL) in Monaco, bottom sediment samples were collected along with water column samples in 1997 from the Northwest Pacific Ocean, and were analysed for ^{90}Sr, ^{137}Cs, $^{239,240}Pu$ and ^{241}Am contents in order to identify current distribution patterns and inventories, and to elucidate sources of these radionuclides in the region where the past US nuclear weapons tests were carried out. This study complements a previous reports on bottom sediments [1] and water column [2]. All the reported sediment data including data from 1997 cruise revealed that sedimentary $^{239+240}Pu$ and ^{241}Am concentrations peaked both in the latitudinal bands between 10-20^{o}N and 30-40^{o}N, and ^{137}Cs and ^{90}Sr in the latitudinal band between 30-40^{o}N (Fig. 1). The latitudinal bands between 10-20^{o}N and 30-40^{o}N correspond to the major areas affected by close-in fallout and global fallout, respectively. Sediment inventories of $^{239+240}Pu$ and ^{241}Am exceeded or nearly equalled their overlying water inventories near the Bikini Atoll, however, in mid latitudes, more than 70% of $^{239+240}Pu$ still remains in the water column. Sediment inventories of ^{137}Cs and ^{90}Sr account for about ten and less than five percent of the water column inventories, respectively. ^{241}Am inventories in sediments exceeded those of the water column. The activity ratios of $^{137}Cs/^{90}Sr$ and $^{241}Am/^{239,240}Pu$ in sediments were higher than of the global fallout ratios. ^{90}Sr content in the bottom sediments also appears to be controlled by the carbonate contents of the sea floor.

The relative contribution of global and close-in fallouts to the total $^{239,240}Pu$ was estimated using a two end-member mixing model based on the atom ratios of $^{240}Pu/^{239}Pu$. The contribution of close-in fallout in sediment appears to be about 56 % for the latitudinal belt 10-20^{o}N. It is not unexpected that close-in fallout Pu dominates in the bottom sediments near Bikini Atoll. ^{241}Am and ^{241}Pu age determination of the sediment slices was utilized to provide time constraint on a hiatus in the sediment accumulation in the Northwest Pacific Ocean.

ACKNOWLEDGEMENT

The Agency is grateful to the Government of the Principality of Monaco for its support of its Marine Enviornment Laboratory.

REFERENCES

[1] MOON, D.-S., HONG, G.-H., KIM, Y-I., BASKARAN, M., CHUNG, C-S., KIM, S-H., LEE, H.-J., LEE, S-H., POVINEC, P.P, Accumulation of artificial and natural radionuclides in the bottom sediments of the Northwest Pacific Ocean, Deep-Sea Res. II 50 17-21 (2003) 2649-2673.

[2] POVINEC, P.P, et al., IAEA'97 expedition to the NW Pacific Ocean-results of oceanographic and radionuclide investigations of the water column, Deep-Sea Res. II **50** 17-21 (2003) 2609-2637.

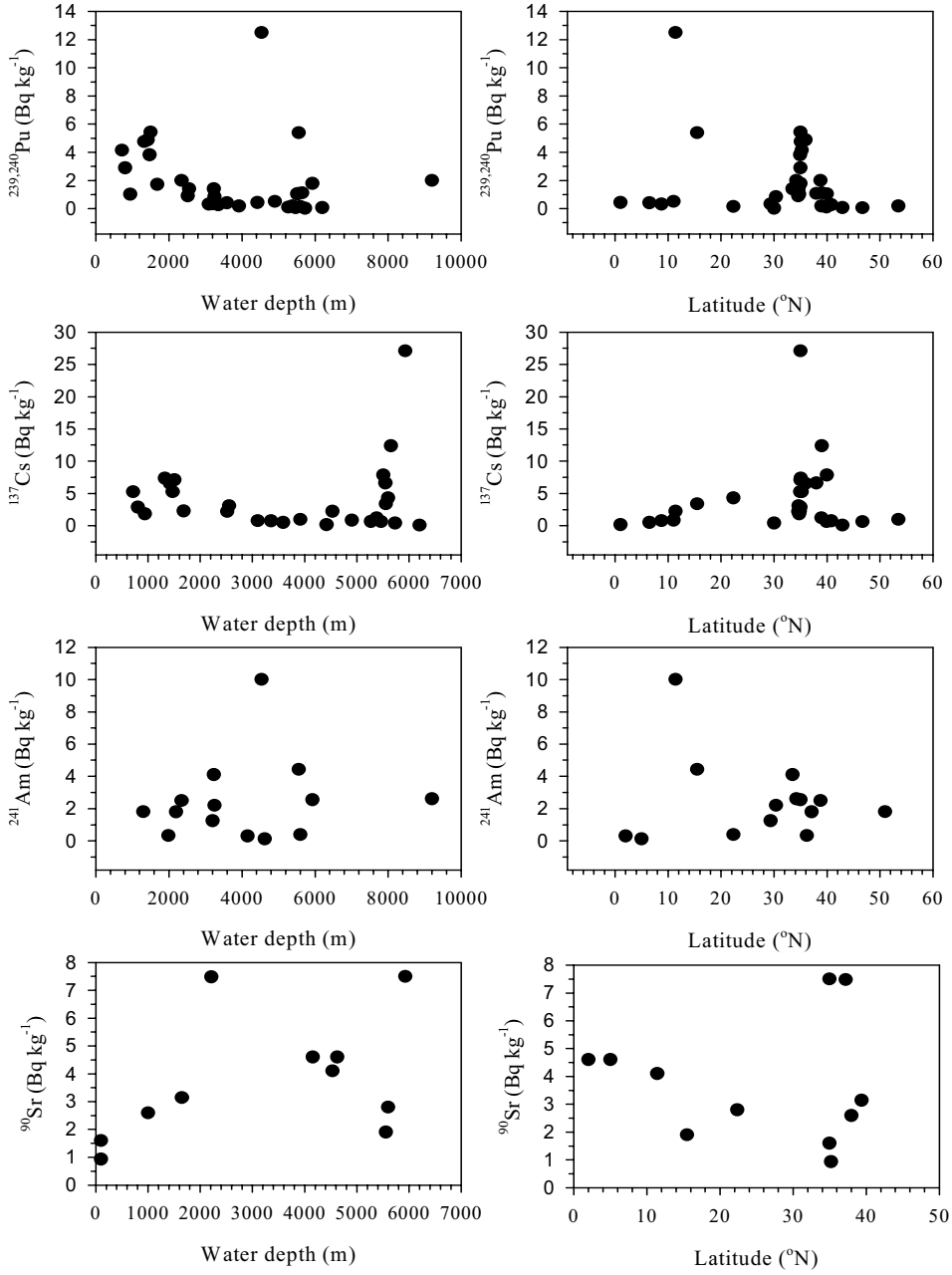

FIG. 1. Latitudinal distribution of anthropogenic radionuclides in the bottom sediment of the Northwest Pacific Ocean.

Radioactivity of Lake Sevan (Armenia) bottom sediments

Nalbandyan, A.G.[a], V.L. Ananyan[a], W.C. Burnett[b], J.C. Cable[c]

[a] Center for Ecological-Noosphere Studies of the National Academy of Sciences,
Yerevan,
Armenia

[b] Florida State University,
Tallahassee, Florida,
United States of America

[c] Louisiana State University,
Baton Rouge, Louisiana,
United States of America

Abstract. Paleo-radioecological investigations of bottom sediments of Lake Sevan, the second highest freshwater Alpine lake in the world, were performed in 2002 and 2003. Our research is the first paleolimnological study of Lake Sevan by sediment dating with ^{210}Pb and ^{137}Cs and geochemical analysis of sediment cores from the lake bottom. These sediments hold a valuable historical record of natural variations that occurred prior to the 1930s as well as anthropogenic changes that resulted from man-made intervention. Moreover the position of Lake Sevan in the high South Caucasus Mountains makes it an ideal location in the world for preserving radioecological record of global fallout.

1. Introduction

The major environmental issue in Armenia is Lake Sevan, "The Pearl of Armenia," located 1916 m above sea level. The lake is comprised of two sections, the Big Sevan (1032 km^2, maximum depth 37.7 m) and the Small Sevan (384 km^2, maximum depth 50.9 m). Some three dozen streamlets drain into Lake Sevan; but there is only one river that originates from the lake. Lake Sevan's catchment basin comprises 1/6 of Armenia's total area (29,800 km^2) and constitutes the primary water resource of the country. Thus, the lake has strategic importance, both geographically and politically, and it provides a significant source of freshwater to the whole South Caucasian region as well (Fig. 1).

Unfortunately, the water quality and ecology of the lake have suffered much from shortsighted management decisions made by the Soviet Government beginning from the 1930s [1, 2]. To provide additional water for irrigation, the lake water level was artificially lowered over the last century. Lake Sevan has also been an important source of hydroelectric power to Armenia. As a result, over a 40-year period lake volume decreased by 41% and the water level dropped by 19 m (Fig. 2). The entire nutrient balance of the lake is disrupted, eutrophication has started, and some formerly important fishes are now extinct.

2. Methods

Coring was accomplished during two cruises on the R/V *Hetazotogh* in September 2002 on the Small Sevan and August 2003 on the Big Sevan. Sediment cores up to ~1 m in length were collected with a Soviet-era gravity corer from 8 locations in the lake. All of the cores were sectioned onboard ship immediately after collection. Samples were stored until returned to the CENS laboratory the next day for processing. Bottom sediments were dried at 70^{0}C until a stable dry weight was achieved, subsequently homogenized, and split for concurrent radiochemical and chemical measurements.

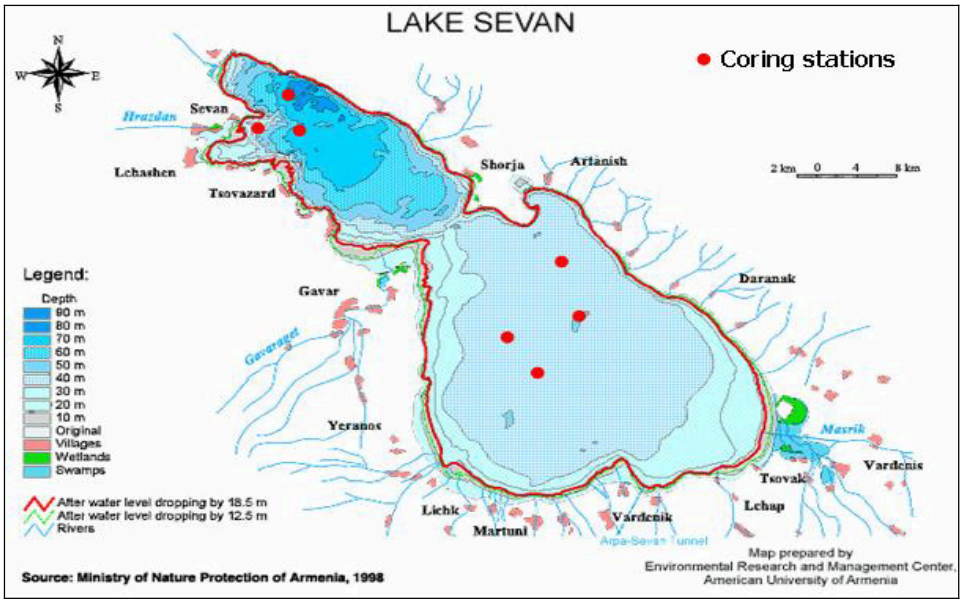

FIG. 1. Map of Lake Sevan with coring locations (closed circles).

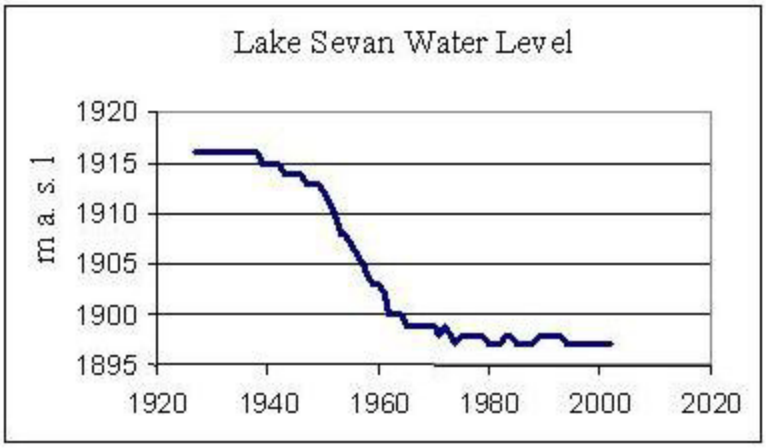

FIG. 2. Lake level variations (m asl) during the 20th Century.

Sediment dating was performed in environmental radioactivity laboratories at Florida State and Louisiana State Universities via analysis of ^{210}Pb and ^{137}Cs by direct gamma spectrometry with allowances being made for differences in self-absorption of the 46.5 keV photopeak from ^{210}Pb [3]. ^{226}Ra, ^{137}Cs, ^{40}K, ^{234}Th concentrations were determined at CENS through a low-background γ-spectrometer with a NaI detector. Analyses are still ongoing for most cores but we illustrate our results by showing the data from a core at station 2, located in the Small Sevan in the center of the northern, deeper lake.

In order to explore the possibility of ecological changes in the lake that may have been associated with the drastic water level fluctuations, we analyzed several ecological indicators in the lake sediments. Biogenic silica was analyzed through an ammonium molybdate method [5, 6], available phosphorus (AVP) by sulphuric acid digestion and ascorbic acid methods [4-6], $CaCO_3$ by acidimetric method [7], and organic carbon by Tyurin's acid digestion method [7].

3. Results

3.1. Age dating

An important part of this research is determining ages at each level in the cores. The "excess" or unsupported ^{210}Pb distribution displays a systematic drop off to about 25 cm down core with a much more rapid decline after that depth. While we detected ^{210}Pb throughout the core, ^{226}Ra levels were elevated in many deeper layers above that of ^{210}Pb and thus, no "excess" ^{210}Pb is reported for layers below 25 cm. The ^{137}Cs distribution shows two maxima, one at 7.5 cm and the other at 22.5 cm. We have interpreted these radiocesium peaks to represent fallout from the 1986 Chernobyl accident (7.5 cm) and from global bomb-testing fallout that reached a maximum in 1963 (22.5 cm). Based on these interpreted horizons, we adjusted the ^{210}Pb ages using the CRS (constant rate of supply) model [8] to coincide with the ^{137}Cs ages by addition of ^{210}Pb activity equal to an approximately 5-cm thick layer at the top of the core. We assume that this would represent sediment lost during the coring process (we are certain that some undetermined amount of material was lost due to the very high porosity in this region of the sediments). With this adjustment, the CRS ages match the ^{137}Cs age distribution interpretation nicely in the upper portions of the core. The ages for the lower sections are much more uncertain as there is no measurable excess ^{210}Pb below 30 cm. A summary of our excess ^{210}Pb and ^{137}Cs data, with the age interpretations is given in Fig. 3A. Several additional cores are being analyzed for dating purposes, and a more complete description of the age analysis will be presented later.

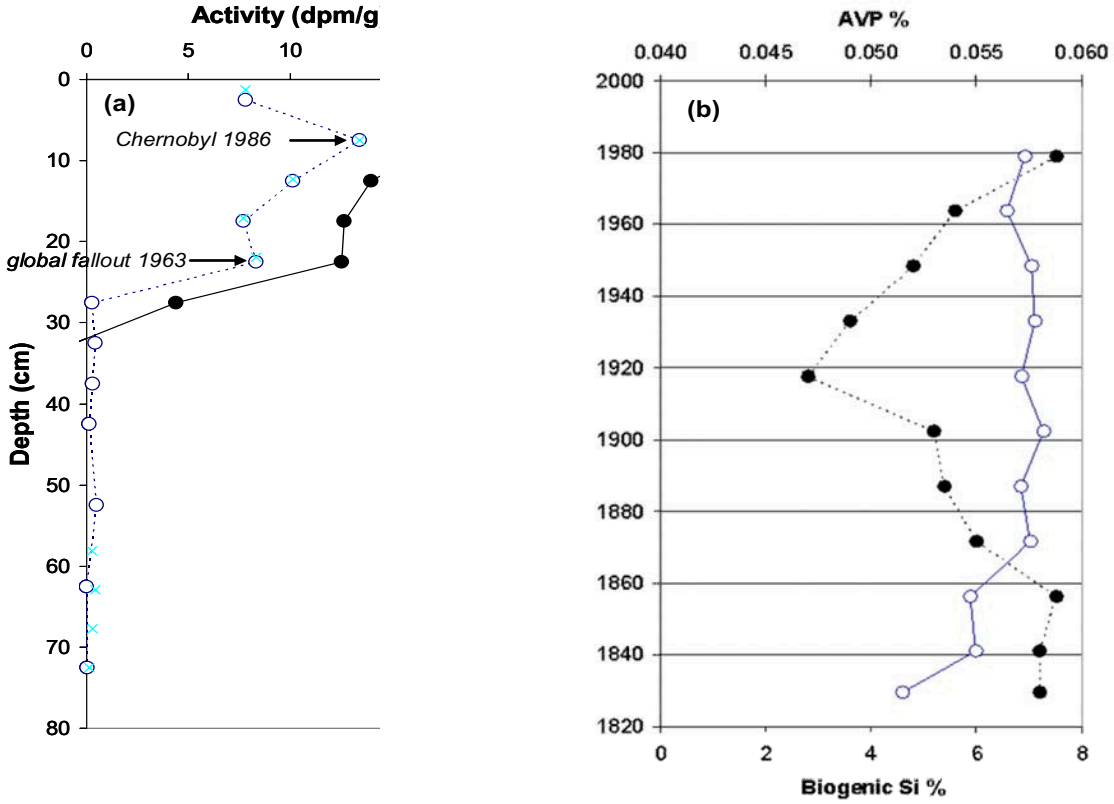

FIG. 3. (A) Activities of excess ^{210}Pb (closed circles) and ^{137}Cs (open circles) in core from station 2 show the ages of the sediments. (B) Down-core variations in biogenic silica (open circles) and available phosphorus (closed circles) are also shown for Station 2, where sediment ages are based on ^{137}Cs and excess ^{210}Pb profiles.

3.2. Ecological Factors

There are some substantial differences in the available phosphorus (AVP) and biogenic silica levels throughout this core (Fig. 3B). The AVP has a range of about 30% while the biogenic Si varies by almost 60%. AVP levels show a constant concentration during the early to middle 19th century, then displays a systematic decrease to the early 20th century when Soviet activities started, followed by a systematic increase to the highest level measured around 1980. Unfortunately, insufficient material was available for the uppermost section of this core to perform an AVP analysis.

The biogenic silica has the lowest concentration in the station 2 sediments in deepest layers analyzed, equivalent to early to middle 19th century. The remainder of this core shows fairly consistent levels around 7% for the rest of the period of record.

Several of the other cores we collected from Lake Sevan have finer-spaced intervals which should allow for more precise age and ecological interpretations. Work on these sediments is ongoing and will be available soon.

ACKNOWLEDGEMENTS

We would like to express our special thanks to the National Foundation of Science and Advanced Technologies (NFSAT) and the Civilian Research and Development Foundation (CRDF) (grant NFSAT EC 058-02/CRDF 12003) for funding this research. Our sincere thanks are extended to the American Association for the Advancement of Science WISC Program and the U.S. National Science Foundation NATO Fellowship Program. We wish to express our gratitude to Dr. Armen Saghatelyan, the director of CENS NAS RA for his kind assistance, our lab and fieldmates Armen Stepanyan and Armen Kyureghyan (CENS), Ricky Peterson (FSU), Elizabeth Dimitrova (LSU), Konstantin Pyuskulian (Armenian NPP) and Greta Afrikian (CENS), R/V *Hetazotogh* ship's crew, and all those who have contributed to this research.

REFERENCES

[1] OGANESSIAN, R.O., "Ecological problems of Lake Sevan", Ecological problems of Lake Sevan Conference Proceedings, Yerevan, Armenia **128** (1993) (in Russian).

[2] GULAKYAN, S.Z., WILKINSON, I.P., The influence of earthquakes on large lacustrine ecosystems, with particular emphasis on Lake Sevan, Armenia, Hydrobiologia **472** (2002) 123-130.

[3] CABLE, J.E., BURNETT, W.C., MORELAND, S., WESTMORELAND, J., Empirical assessment of gamma ray self-absorption in environmental sample analysis, Radioact. Radiochem. **12** (2201) 30-41.

[4] MURPHY, J., RILEY, J.P., A modified single method for determination of phosphate in natural waters, Anal. Chem. Acta **27** (1962) 31-36.

[5] SCHELSKE, C.L., CONLEY, B.J., STOERMER, E.F., NEWBERRY, T.L., CAMPBELL, C.B., Biogenic silica and phosphorus accumulation in sediments as indices of eutrophication in the Laurentian Great Lakes, Hydrobiologia **143** (1986)79-86.

[6] SOPs for determining Total Phosphorus, Available Phosphorus, and Biogenic Silica concentrations of Lake Michigan sediments and sediment trap material, Chapter 2, GLERL – SEB NUTRIENT **3** (1996) 3-307 to 3-312.

[7] ARINOUSHKINA, E.V., Manual for chemical analysis of soils, Moscow **487** (1970) (in Russian).

[8] APPLEBY, P.G., OLDFIELD, F., Application of Lead-210 to Sedimentation Studies (IVANOVICH, M., HARMON, R.S. Eds.), Uranium-Series Disequilibrium: Applications to Earth, Marine, and Environmental Problems, Second Edition, Chapter 14, Charendon Press, Oxford, UK (1992) 487-512.

Use of ^{137}Cs, ^{239,240}Pu and ^{210}Pb in sediment accumulation studies in the Baltic Sea

Mattila, J.[a], H. Kankaanpää[b], E. Ilus[a]

[a] STUK - Radiation and Nuclear Safety Authority,
Helsinki,
Finland

[b] Finnish Institute of Marine Research (FIMR),
Helsinki,
Finland

Abstract. Results from 99 sediment cores from various parts of the Baltic Sea and mostly from the accumulation bottoms were used to estimate sediment accumulation rates (SAR) and total amounts of ^{137}Cs activity and to characterize recent sediment accumulation. The results clearly illustrated the large range of SAR in the studied sea areas (60 - 6160 g m^{-2} y^{-1}), with the highest values generally observed in the northern part of the Bothnian Sea, in river estuaries and the eastern part of the Gulf of Finland. Bothnian Sea stations generally had median SAR values about two times higher than those in the Gulf of Finland and Bothnian Bay and about seven times higher than stations in the Baltic Proper. The total amounts of ^{137}Cs activity were also generally considerably higher at Bothnian Sea stations than in the Gulf of Finland and Bothnian Bay, and especially higher than at stations in the Baltic Proper. SAR values and total amounts of ^{137}Cs activity were highly correlated (Spearman rank correlation). Studies of variation within sedimentation basins and repeated sediment samplings showed that recent sediment accumulation in the Baltic Sea could have varied considerably, even within a short distance around the sampling locations. Unstable sedimentation in the Baltic Sea, horizontal movements of surface sediments and mixing processes could limit the use of these methods in sediment datings and in the estimation of SAR. The combination of several methods for dating recent sediment layers is recommended. The results of the present study emphasize that variation in sediment accumulation should be studied before monitoring is started, and that it is also important to keep the sediment sampling methods as standardized as possible during long term monitoring.

1. Introduction

The sediment accumulation rate (SAR) or net sedimentation is an essential parameter in contamination or monitoring studies and in budget calculations of seas. The vertical distribution of artificial radionuclides ^{137}Cs and ^{239,240}Pu and naturally occurring ^{210}Pb in sediments can be used in sediment dating and in the estimation of SAR. In the present study, results from several co-projects during 1995 - 2003 were summarized. The SAR results are based on time markers. These results were generally compared to those based on two ^{210}Pb models. The data were also used in studies of internal variation of SAR in some sedimentation basins and around some permanent monitoring stations. The repeatability of sediment sampling in practise was tested. Additionally, results obtained with two sediment corers have been compared. Bringing all these results together enables the mapping of SAR in the study area and evaluation of the practicability and sources of error of SAR estimation methods.

2. Materials and methods

In this study 99 sediment cores were collected from 69 stations (Fig. 1). Sediment samples were taken mainly during the cruises of the R/V ARANDA of the Finnish Institute of the Marine Research (FIMR). The majority of the samples were taken with Gemini (80 mm) or Gemax (90 mm) twin corers (core diameters in parenthesis). Cores were normally sliced into 1-cm subsamples to a depth of 10 - 20 cm and below that 2-cm slices were used. All sediment samples were frozen after sampling and freeze dried in the laboratory. ^{137}Cs profiles were analysed from each core, ^{239,240}Pu activities from 16 cores

and ^{210}Pb profiles were analysed from 56 cores. ^{137}Cs and ^{210}Pb activities were analysed by gamma-ray spectrometry, while ^{239,240}Pu analyses were performed with a radiochemical method [1]. In sediment datings the highest concentrations of ^{137}Cs or ^{239,240}Pu were used as a timemarker for the years 1986 and 1963, respectively [2]. With excess ^{210}Pb activities, CF:CS (constant flux : constant sedimentation) and CRS (constant rate of supply) models were used to estimate recent accumulation rates for the last 30 years [3]. The thicknesses of annually accumulated layers, AAL [mm y^{-1}], were resolved using SAR and porosities of the sediments, assuming a dry matter density of 2.5 g cm^{-3}.

3. Results and discussion

Estimated average SAR values for recent decades at the stations mostly representing accumulation bottoms were between 60 - 6160 g m^{-2} y^{-1}. The highest SAR values and highest total amounts of ^{137}Cs were observed in the northern part of the Bothnian Sea. At the southernmost station of the Bothnian Bay, the SAR and the total amounts of ^{137}Cs activity were high compared to other stations of that sea area. In the estuary of the River Paimionjoki in the southern Bothnian Sea, the average SAR was about 4900 and 900 g m^{-2} y^{-1} at 0-10 and 20-40 kilometers distance from the river mouth, respectively. At several stations in the eastern part of the Gulf of Finland and outer estuary of the River Kymijoki, SAR values clearly exceeded 1000 g m^{-2} y^{-1} with maximum values of over 2500 g m^{-2} y^{-1}. At about 10 and 20 km distance from the western mouth of the river Kymijoki, the SAR was about 1200 and 900 g m^{-2} y^{-1} respectively. At a station representing the sedimentation basin south of Åland, the estimated SAR value (3400 g m^{-2} y^{-1}) was significantly higher than the general level in the Baltic Proper (Table I). The highest values were related to bottom topography and water depth, an estuarine-type current system and flocculation of particulate material and abundant sources of accumulating material.

Generally, the median SAR value at Bothnian Sea stations was about two times higher than at those in the Gulf of Finland and Bothnian Bay and about seven times higher than at the stations of the Baltic Proper (Table I). Time-corrected total amounts of ^{137}Cs were three to four times higher at the Bothnian Sea stations than at those of the Gulf of Finland or Bothnian Bay and over 12 times higher than at the stations of the Baltic Proper (Table I). Correlation coefficients between the SAR values and the total ^{137}Cs amounts were high especially at the stations of the Bothnian Sea (Table I). There was also a positive correlation between SAR and estimated ^{210}Pb fluxes. These correlations can be explained by the high sediment/water distribution coefficients (K_d) of these metals in the brackish water environment [4].

In the cases of repeated samplings, considerable variation in the SAR and in total amounts of ^{137}Cs activities was observed at certain locations at different sampling times. In 1996, at the sedimentation basin of station JML (western Gulf of Finland), variation within a distance of about 170 metres was found to be small, while in the vicinity of station LL17 (Baltic Proper) the highest SAR values and total amounts of ^{137}Cs activity were about two to three times higher than the lowest within a distance of about 350 metres. These variations could mostly be related to uneven and unstable sediment accumulation in the Baltic Sea [5, 6, 7]. The results highlighted the importance of highly accurate position determination. Sediment sampling could have considerable effects on the results [8]. The present comparisons of sediment corers and sediment samplings clearly showed that the sampling methods should be standardized as much as possible during monitoring. Variations in sediment accumulation also need to be studied before permanent monitoring is started.

Timemarker-based estimation of the SAR was possible at most of the stations, but in 20% of cases the estimates were approximate and in a couple of cases the estimation was not attempted because of disturbed radionuclide profiles. There was generally a positive correlation between estimates that were based on timemarkers and ^{210}Pb models, but in about 40% of cases differences between the average SAR estimates exceeded 50%. In sediment datings and in the estimation of the SAR, fulfilment of the prerequisites of dating methods should be carefully considered for each core used. Recent sedimentation in the Baltic Sea has been unstable and there could be horizontal movements of poorly compacted surface sediments, or the surface sediments may be affected by mixing processes [6, 7]. These factors affect the radionuclide profiles and could limit the use of ^{137}Cs, ^{239,240}Pu and ^{210}Pb in

sediment datings and in estimation of the SAR. To ensure the validity of results in this kind of environment, sediment datings over longer periods of time (to 0 - 100 years) should be based on a combination of several dating methods. In this study, the radionuclide profiles and combined use of several methods proved to be a valuable tool in evaluating sediment accumulation and the practicability of the estimation methods.

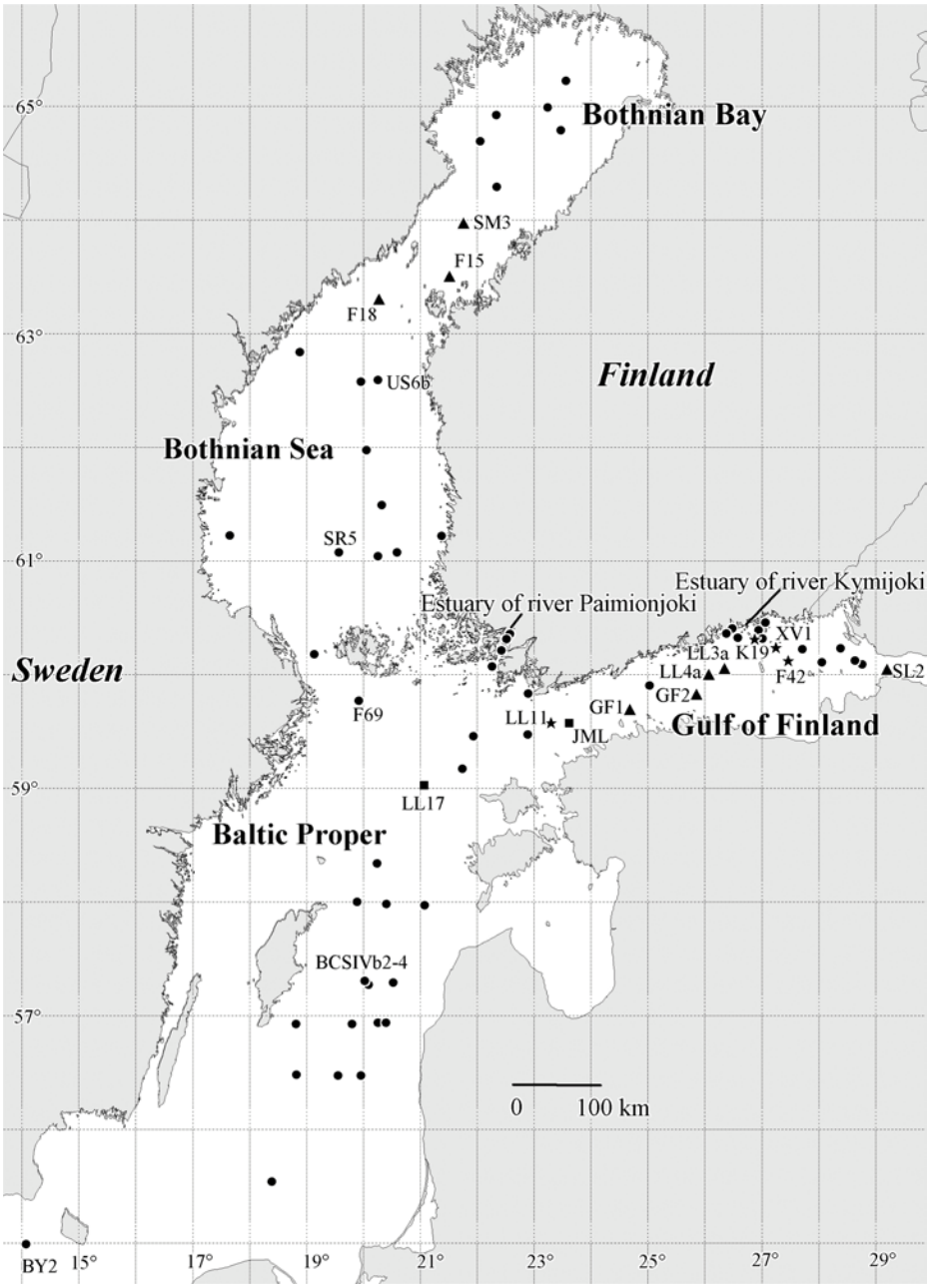

FIG. 1. Locations of sediment stations in the present study (1995 - 2003). Explanation of symbols: stations visited once (dots), more than once (triangles), sedimentation basins for local variation studies (squares) and stations where sediment sampling was also studied (stars).

Table I. Median values of SAR, thickness of the annually accumulating layer of sediment (AAL) to about 10 cm depth, total amounts of ^{137}Cs activity (^{137}Cs tot) and Spearman rank correlation coefficients (r_s) between the SAR and the total amounts of ^{137}Cs at sampling dates. To calculate median values for the sea areas, the total amounts of ^{137}Cs at each station were time-corrected to the year 2000. In the cases of several sediment cores at the same station at the same sampling date, average values of observations were used in calculations of SAR and AAL.

Stations of the	SAR [g m^{-2} y^{-1}]	AAL [mm y^{-1}]	^{137}Cs tot [Bq m^{-2}]	r_s
Bothnian Bay	500	1.9	9000	0.81
Bothnian Sea	1200	3.7	32400	0.93
Gulf of Finland	690	2.4	13200	0.73
Baltic Proper	180	0.8	2600	0.64

ACKNOWLEDGEMENTS

The authors wish to thank all the co-operators in the Finnish Institute of Marine Research, Finnish Environment Institute, National Public Health Institute (Department of Environmental Health) and Geological Survey of Finland. For financial support we are grateful to the Nordic Nuclear Safety Research, the Finnish Ministry of the Environment, the Academy of Finland and the Maj and Thor Nessling Foundation. We also thank the scientific staff and crew of the R/V ARANDA.

REFERENCES

[1] TAIPALE, T.K., TUOMAINEN, K., Radiochemical determination of plutonium and americium from seawater, sediment and biota samples, STUK-B-VALO 26, Helsinki (1985).

[2] HELSINKI COMMISSION, Radioactivity in the Baltic Sea 1992 - 1998, HELCOM, Baltic Marine Environment Protection Commission, Baltic Sea Environment Proceedings No. 85, Helsinki (2003).

[2 APPLEBY, P.G., OLDFIELD, F., “Application of lead-210 to sedimentation studies”, Uranium-series Disequilibrium: Applications to Earth, Marine and Environmental Sciences, 2nd edition (IVANOVICH, M., HARMON, R.S., Eds.), Clarendon Press, Oxford (1992) 731-778.

[4] INTERNATIONAL ATOMIC ENERGY AGENCY, Sediment K_ds and Concentration Factors for Radionuclides in the Marine Environment, Technical Reports Series No. 247, IAEA Vienna (1985).

[5] IGNATIUS, H., AXBERG, S., NIEMISTÖ, L., WINTERHALTER, B., “Quaternary geology of the Baltic Sea”, The Baltic Sea, (VOIPIO, A., Ed.), Elsevier (1981) 54-104.

[6] WINTERHALTER, B., Late-quaternary stratigraphy of Baltic Sea basins - a review. Bull. Geol. Soc. Finland 64, Part 2, (1992) 189-194.

[7] PERTTILÄ, M., et al., Contaminants in the Baltic Sea sediments. Results of the 1993 ICES/HELCOM Sediment Baseline Study, Meri. Report Series of the Finnish Institute of Marine Research No. 50 (2003).

[8] HELSINKI COMMISSION, Intercomparison of sediment sampling devices using artificial radionuclides in Baltic Sea sediments, The MOSSIE Report, HELCOM, Baltic Marine Environment Protection Commission, Baltic Sea Environment Proceedings No. 80, Helsinki (2000).

^{137}Cs accumulation in coastal sediments in Sweden

Pettersson, H.B.L.[a], I. Salih[a], J. Herrmann[b]

[a] Dept. of Radiation Physics,
Linköping University,
Linköping,
Sweden

[b] Federal Maritime and Hydrographic Agency,
Hamburg,
Germany

Abstract. Seabed sediment samples were collected in 1998, 2000 and 2001 at 20 sites located in the Baltic Sea and 4 sites in the Skagerakk. The objectives of the sampling campaigns were (i) to establish the coastal sediment distribution of ^{137}Cs, (ii) to evaluate the vertical core distribution of ^{137}Cs, (iii) to study the sediment accumulation rates, and (iv) to assess the sediment inventories of ^{137}Cs. The results show a large variation in ^{137}Cs concentrations and an almost 100-fold difference in inventories, showing the predominance of Chernobyl derived ^{137}Cs in the Baltic Proper compared to the western Baltic and the Skagerakk areas. Sediment accumulation rates were highly dependent on sediment types and ranged from 0.05 to 1.8 cm y^{-1}.

1. Introduction

Seabed sediment samples were collected during three cruise expeditions along the Swedish coast in June 1998 (GAUSS #320), July/August 2000 (GAUSS #352) and in June/July 2001 (GAUSS #369), (Fig. 1), organized by the German Federal Maritime and Hydrographic Agency. Six sites located in the Baltic Proper and 2 sites close to the Danish Straits were investigated in the 1st cruise. Five sites located in the Bothnian Sea of the Baltic Sea and 3 sites in the Baltic Proper were investigated in the 2nd cruise. In the 3rd cruise 8 sites were investigated, 1 site located on the southern part of the Baltic Proper, 3 sites located on the western coast in the Kattegat, and 4 sites situated in the Skagerakk.

The objectives of the sampling campaigns were (i) to establish the coastal sediment distribution of ^{137}Cs, (ii) to evaluate the vertical core distribution of ^{137}Cs, (iii) to study the sediment accumulation rates, and (iv) to assess the sediment inventories of ^{137}Cs.

2. Materials and methods

The sediment samples were collected by means of gravity corers and box-core samplers (sub sampling with cylindrical tubes) for sediment depths down to about 50 cm. The sediment cores were sliced on-board at 1 cm intervals and collected and sealed in plastic bottles. After freeze-drying in the home laboratory and determination of sample wet- and dry weights, the samples were homogenized and transferred to standard geometry plastic tubs (60 mL, 90 mL volume) for analysis by gamma spectrometry in a low-level underground laboratory. The sediment concentrations of ^{137}Cs and ^{226}Ra were assessed by using ^{137}Cs and ^{226}Ra standard solutions (traceable to NIST) thoroughly mixed in inactive sediment materials. The gamma spectrometry analyses were followed by radiochemical analysis of ^{210}Po. About 0.5-2 g dry sample material was used together with ^{208}Po standard solution for yield determination. The samples were wet ashed by microwave treatment using a standard protocol at approx 200^{o}C/12 bar. After dissolution and conversion into chloride form, Po was deposited spontaneously onto Ag discs using a standard protocol. The ^{208}Po and ^{210}Po content was assessed by alpha spectrometry using a Ortec Octete^{TM} system with PIPS detectors. The sediment accumulation of ^{210}Pb was then obtained by assessing the non-(^{226}Ra)-supported ^{210}Pb concentrations using the ^{210}Po

and ^{226}Ra data. The calculations were made from the assumption of constant rate of supply (CRS) of ^{210}Pb.

3. Results and discussion

The set of graphs in Fig. 2 show the depth distributions of ^{137}Cs and ^{210}Pb for 23 of the 24 sampling sites (site symbols A denote the 1998 cruise, B the 2000 cruise and C the 2001 cruise). The sediment depth distributions show in general a typical distinct peak concentration, ranging from the1st cm up to about 30 cm, followed by a monotone decline with depth. The depth of the mixing zone is much dependent on the sedimentation rate and organic content. In general, maximum ^{137}Cs concentrations are at least one magnitude higher in the Baltic Sea compared to the Skagerakk and Kattegat areas, showing the predominance of deposition from the Chernobyl accident release. The total input to the Baltic Sea from the Chernobyl accident amounts to about 4700 TBq, compared to the estimated deposition of 900 TBq from atmospheric weapons tests and about 250 TBq from European nuclear reprocessing releases [1]. The sediment accumulation rates (Fig. 2) show large variations, ranging from 0.05 to 1.8 cm y^{-1}. The sediments are of different types: sands, sandy mud, muddy sand, varved clays, pelitic muds, fine aleurite muds and moraine deposits. In addition, the organic content in the upper part of the sediments showed large variations. No clear correlation between accumulation rates and sediment type was observed. Neither is there an indication of expectedly higher deposition rates in deep basin areas or with water depth in general. However, the deposition rates show good agreement with literature data for the Baltic Sea [2, 3] and for the Gulf of Finland [4]. The sediment inventories of ^{137}Cs are displayed in the bottom figure, showing an almost 100-fold difference in inventories.

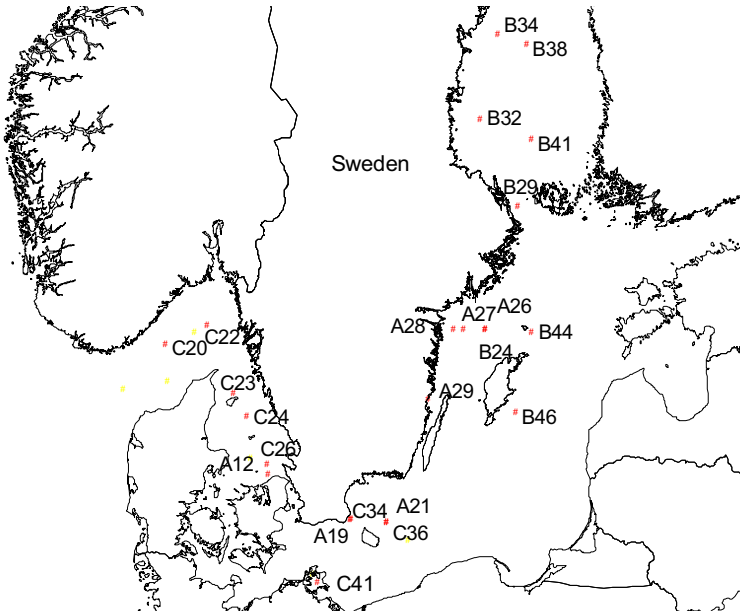

FIG. 1. Sampling sites.

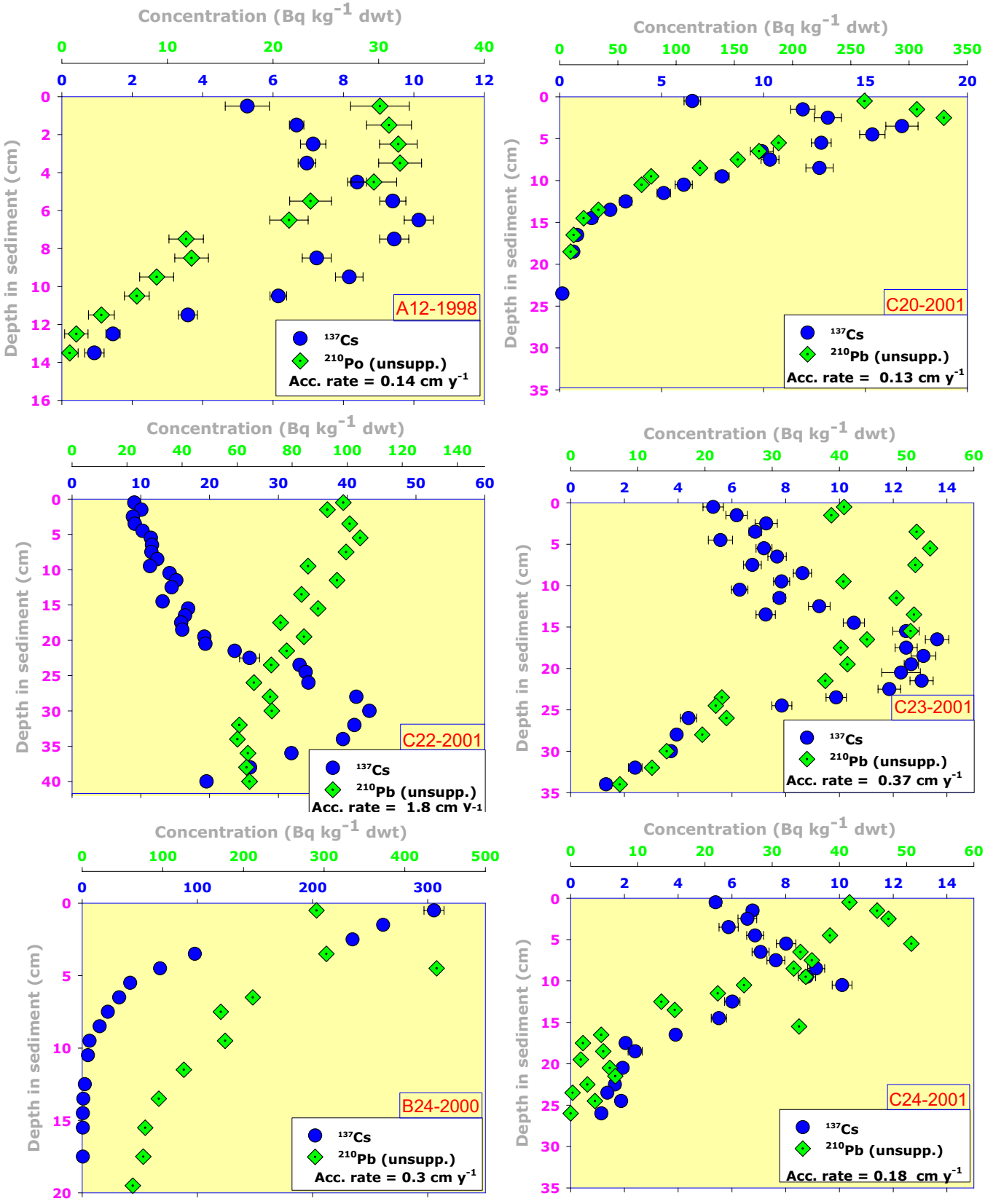
Concentration (Bq kg-1 dwt)
Depth in sediment (cm)
A12-1998
137Cs
210Po (unsupp.)
Acc. rate = 0.14 cm y-1
C20-2001
137Cs
210Pb (unsupp.)
Acc. rate = 0.13 cm y-1
C22-2001
137Cs
210Pb (unsupp.)
Acc. rate = 1.8 cm y-1
C23-2001
137Cs
210Pb (unsupp.)
Acc. rate = 0.37 cm y-1
B24-2000
137Cs
210Pb (unsupp.)
Acc. rate = 0.3 cm y-1
C24-2001
137Cs
210Pb (unsupp.)
Acc. rate = 0.18 cm y-1

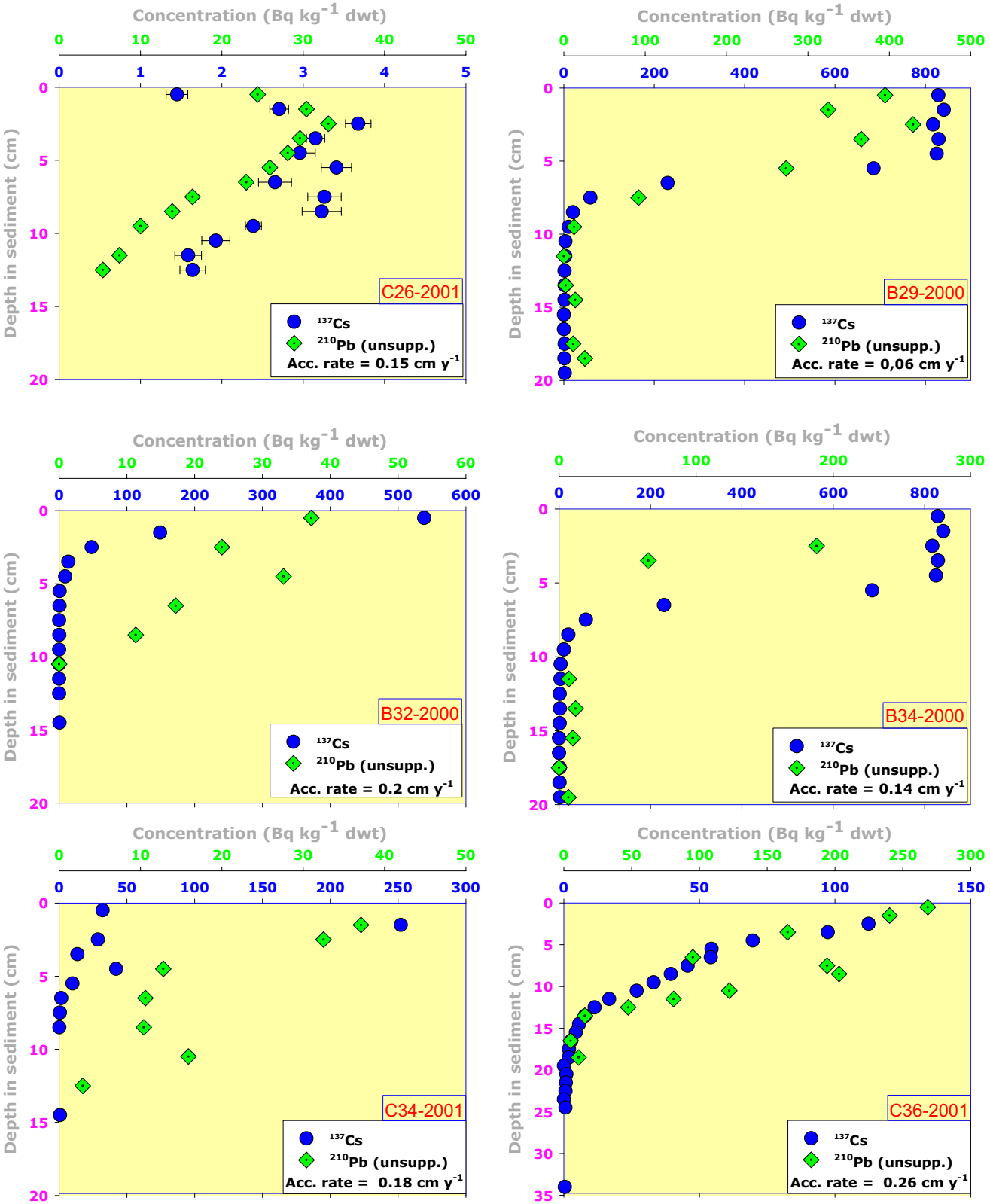
Concentration (Bq kg-1 dwt)
Depth in sediment (cm)
C26-2001
137Cs
210Pb (unsupp.)
Acc. rate = 0.15 cm y-1
B29-2000
Acc. rate = 0,06 cm y-1
B32-2000
Acc. rate = 0.2 cm y-1
B34-2000
Acc. rate = 0.14 cm y-1
C34-2001
Acc. rate = 0.18 cm y-1
C36-2001
Acc. rate = 0.26 cm y-1

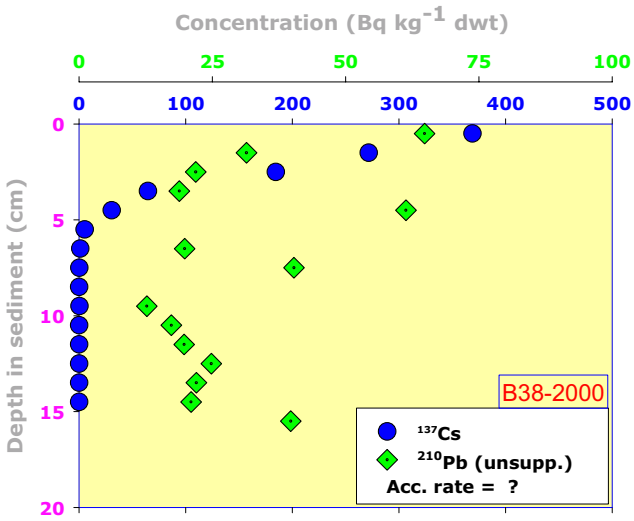
Concentration (Bq kg-1 dwt)
Depth in sediment (cm)
B38-2000
137Cs
210Pb (unsupp.)
Acc. rate = ?

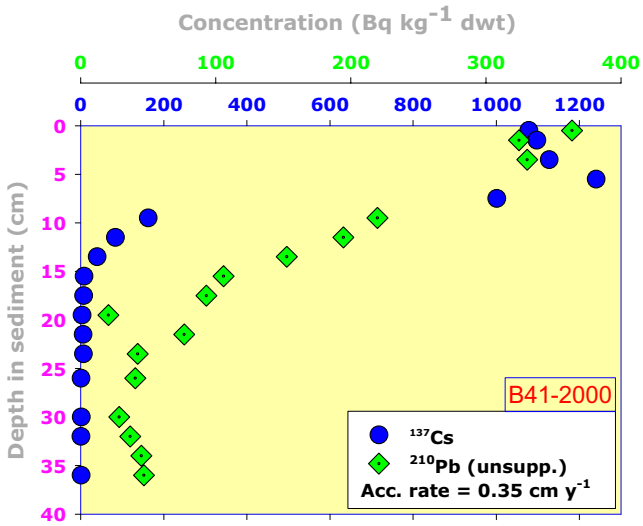
Concentration (Bq kg-1 dwt)
Depth in sediment (cm)
B41-2000
137Cs
210Pb (unsupp.)
Acc. rate = 0.35 cm y-1

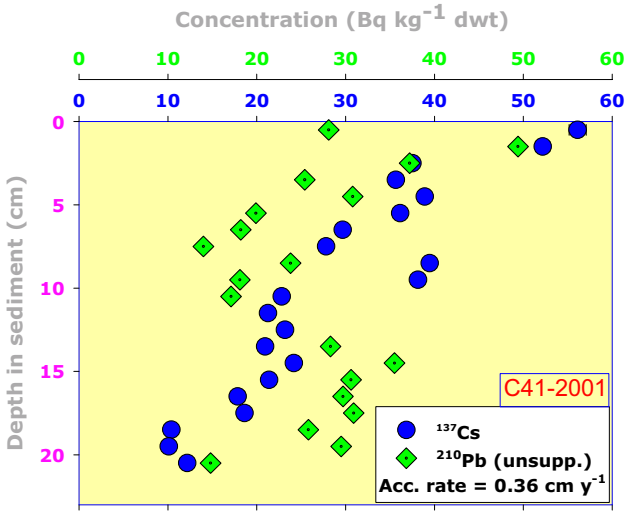
Concentration (Bq kg-1 dwt)
Depth in sediment (cm)
C41-2001
137Cs
210Pb (unsupp.)
Acc. rate = 0.36 cm y-1

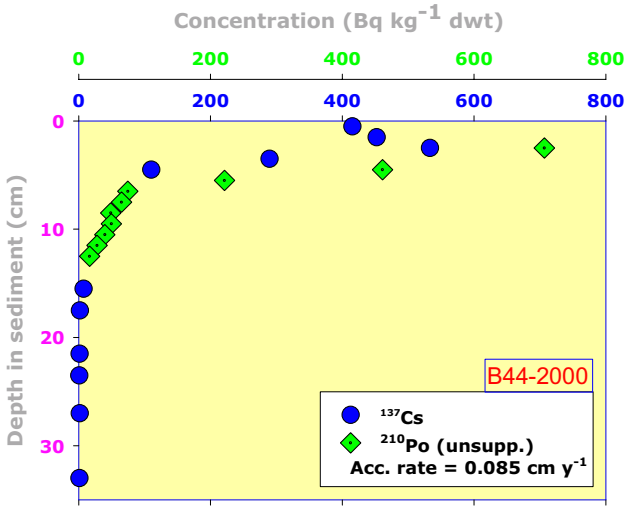
Concentration (Bq kg-1 dwt)
Depth in sediment (cm)
B44-2000
137Cs
210Po (unsupp.)
Acc. rate = 0.085 cm y-1

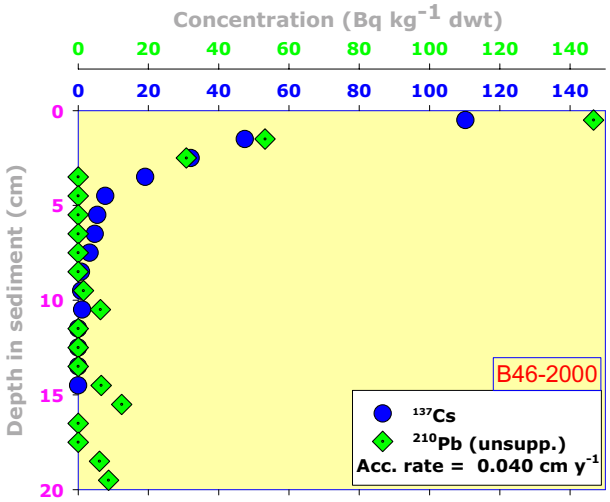
Concentration (Bq kg-1 dwt)
Depth in sediment (cm)
B46-2000
137Cs
210Pb (unsupp.)
Acc. rate = 0.040 cm y-1

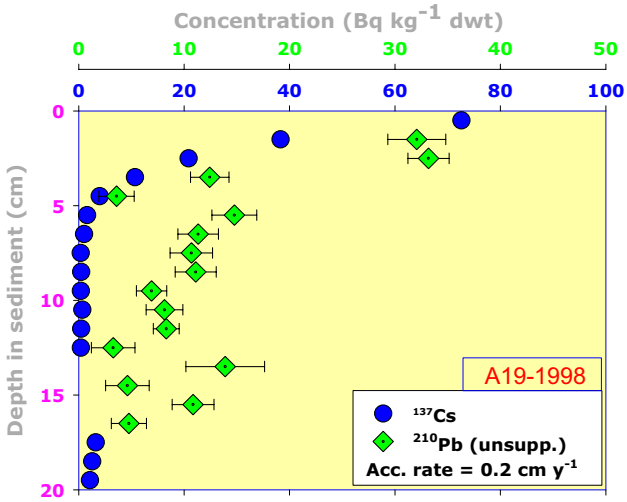
Concentration (Bq kg-1 dwt)
Depth in sediment (cm)
A19-1998
137Cs
210Pb (unsupp.)
Acc. rate = 0.2 cm y-1

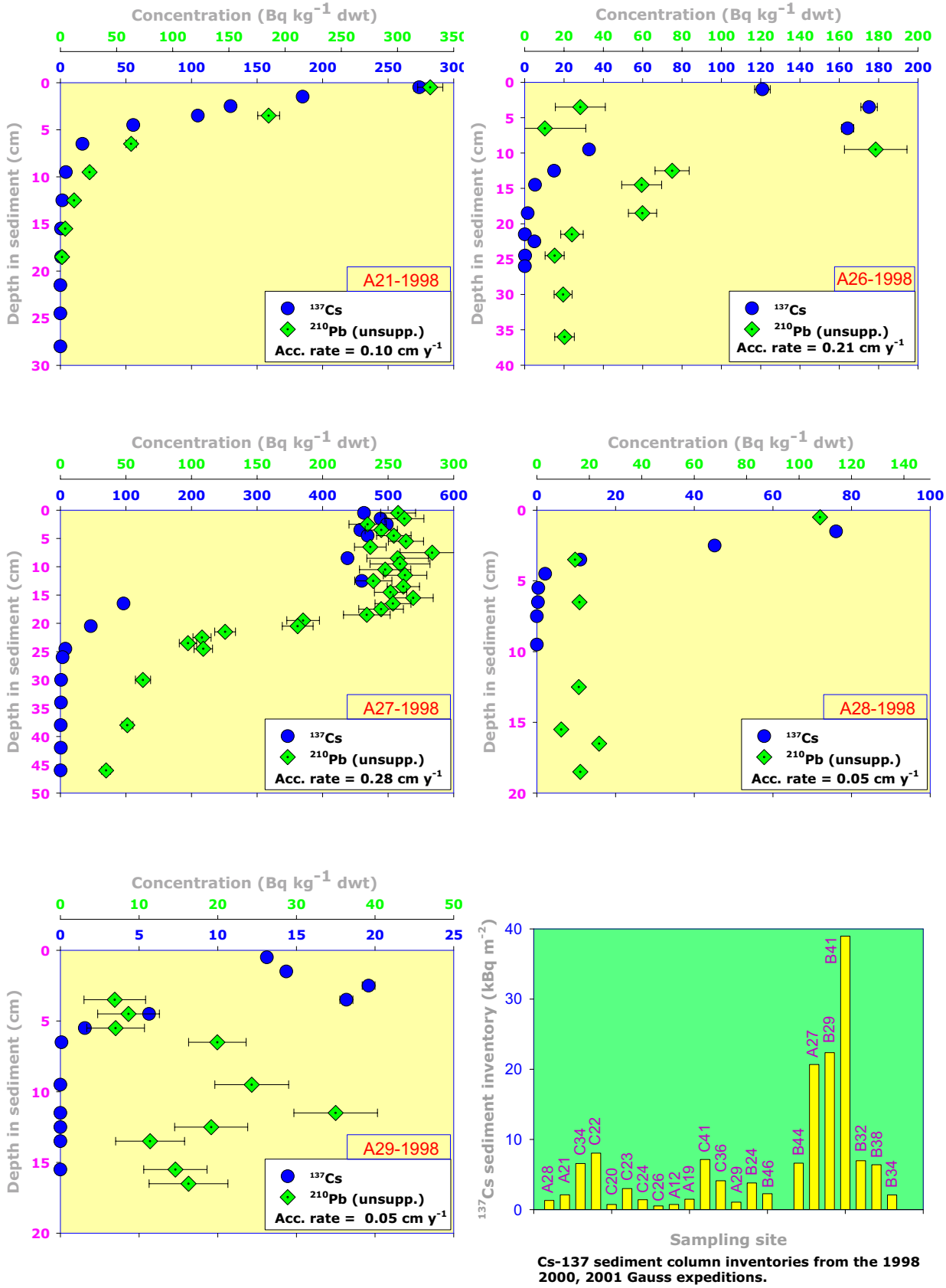

FIG. 2. Concentrations of ^{137}Cs and ^{210}Pb, sediment accumulations rates and ^{137}Cs inventories in Baltic Sea sediments.

ACKNOWLEDGEMENTS

The assistance from the R/V Gauss staff during the three expeditions in sampling, providing hydrological data and for the ship arrangements is greatly acknowledged. The work was financially supported by the Swedish Radiation Protection Authority.

REFERENCES

[1] EUROPEAN COMMISSION, The radiological exposure of the population of the European Community to radioactivity in the Baltic Sea. Radiation Protection. Radiation Protection Report No. 110. (1998) ISBN 92-828-7864-3.

[2] JONSSON, P., CARMAN, R., WULFF, F., Laminated sediments in the Baltic – a tool for evaluating nutrient massa balances, Ambio **19** (1990) 152-158.

[3] JONSSON, P., Large-scale changes of contaminants in Baltic Sea sediments during the twentieth century, Acta Univ. Ups. **407** (1992) ISBN 91-554-2997-1, 52 pp.

[4] VALLIUS, H., KANKAANPÄÄ, H., NIEMISTÖ, L., SANDMAN, O., Sedimentation and within-basin variations in the Gulf of Finland as determined by ^{137}Cs tracer (Proc. seminar, Dating of sediments and determination of sedimentation rate, Helsinki 2-3 April 1997) STUK A145 (E. ILLUS, Ed.) (1998).

Pollutant lead deposition in the Gulf of Lions over the last century reconstructed from sedimentary records

Miralles, J., A. Véron, O. Radakovitch, P. Deschamps, B. Hamelin

Université P. Cézanne,
Aix-en-Provence,
France

Abstract. Six sedimentary cores from the Gulf of Lions continental margin collected in the framework of the IVth MTP-MATER project were investigated for stable lead isotopes and ^{210}Pb aspects in order to determine the relevance of marine sediments as liable atmospheric fallout recorders. The mean sedimentary pollutant lead inventory is 110 ± 7 μg/cm^2 (102-121, n=6), in good agreement with atmospheric fallout over the last century established from salt marshes sediments study in Camargue. All sedimentary pollutant lead accumulations put back in time evidence maximum values in the mid 70s, in good agreement with anthropogenic emissions.

1. Introduction

In response to anthropogenic lead emissions, atmospheric lead concentrations increased to reach 18 times the natural level in 1979 [1]. This large enhancement of atmospheric lead concentration is traduced by public Health problems [2-5] that the European Union tried to reduce by restricting anthropogenic lead emissions. These policies immediately reduce the atmospheric lead concentration in urban and semi-remote areas [6-9].

The aim of this work is to evidence the capacity of marine sediments to be used as proxy to make a large-timescale characterization of pollutant lead atmospheric fallout by evidencing the actual degree of contamination (pollutant lead concentration down core measurements and calculating of pollutant lead inventories) and evidencing the phases of accumulation through time (determining geochronologies by ^{210}Pb analysis). Thus, we chose to investigate Gulf of Lions marine sediments since Western Mediterranean basin is rounded by countries members of the EU, and marine sediments are supposed to deliver a continuous signal through time. Furthermore, this western Mediterranean area has been largely studied giving us an efficient scientific background for lead inputs and accumulation [10, 11].

2. Analytical settings

About 20 cm length sediment cores were collected in the framework of the IVth MTP Project between the Planier and Petit Rhône canyons (Table I) using a multitube corer avoiding disturbances of the water-sediment interface. Sea campaigns have been made in the framework of the MTP-Mater program.

They were subsampled into 0.5 to 5 cm slices (depending on the depth in the core). Each layer was dried, homogenised and passed through a 2 mm sieve. Water contents were calculated from dry and wet weights of the samples and dry bulk densities were calculated assuming a mineral grain density of 2.6 g/cm^3. ^{210}Pb activities were measured by gamma-spectrometry with a semi-planar intrinsic Ge detector. It was calibrated by counting sediment standards of known activity. Stable lead isotopes (concentration and isotopic composition) were analysed by Thermal Ionisation Mass Spectrometry (TIMS) on a Finnigan MAT 262 at CEREGE (Université P. Cézanne, Aix-en-Provence, FRANCE). To avoid any contamination, all sample processing was performed in a clean room laboratory [12, 13]. Mass fractionation is corrected by external calibration against repeated analysis of SRM 981. Pb concentrations were measured by isotopic dilution involving ^{208}Pb spike.

Table I. Label, localization and water depth of each core

Core label	Open slope	Longitude	Latitude	Water depth (m)
HFF2	Planier-Marseille canyons	05°09'83	42°57'00	825
HFF3		05°12'67	42°51'75	1650
HFF5	Marseille – Grand Rhône canyons	04°59'41	42°52'79	780
HFF6		05°02'47	42°47'00	1240
HFF8	Grand Rhône-Petit Rhône canyons	04°45'75	42°47'00	732
HFF9		04°49'38	42°41'33	1280

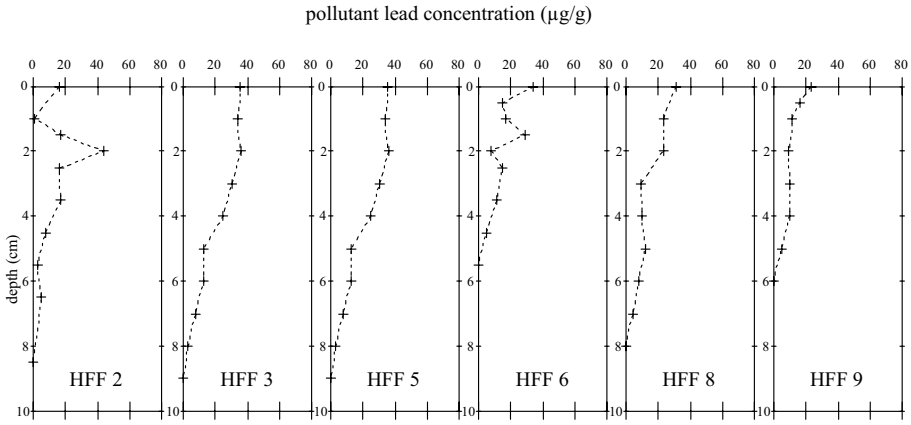

FIG. 1. Pollutant lead concentration (µg/g) in cores.

3. Pollutant lead in sediments

For a given sediment slice i, the determination of the pollutant lead inventories I_i (µg/cm^2) is based on the pollutant lead concentration, A_i (µg/g; Fig. 1) and ρ_i, the bulk density of sediment (g/cm^3) (Fig. 2).

$$I_i = A_i \, . \, \rho_i$$

The total pollutant lead inventory I_T is the sum of all I_i. along the core length. They range from 102 µg/cm^2 to 121 µg/cm^2, respectively HFF 8 and HFF 5, with a mean value of 110±7 µg/cm^2. This value is in good agreement with the estimate of total atmospheric lead fallout over the last century performed in this area [14]. Excepted HFF 9, they evidence a sub-surface pollutant lead accumulation maximum value (around 2 cm depth).

4. Geochronologies

Each core geochronology is made by applying a two-layers biodiffusive model where ^{210}Pbxs activity A at depth z is depending on mixing processes and sedimentation:

$$\frac{\partial A}{\partial z} = D_B \frac{\partial^2 A}{\partial^2 z} - S\frac{\partial A}{\partial z} - \lambda A$$

where

D_B is the mixing coefficient (cm^2/y),

S the sedimentation rate (cm/y) and

λ the decay radioactive constant of ^{210}Pb (22.3 y).

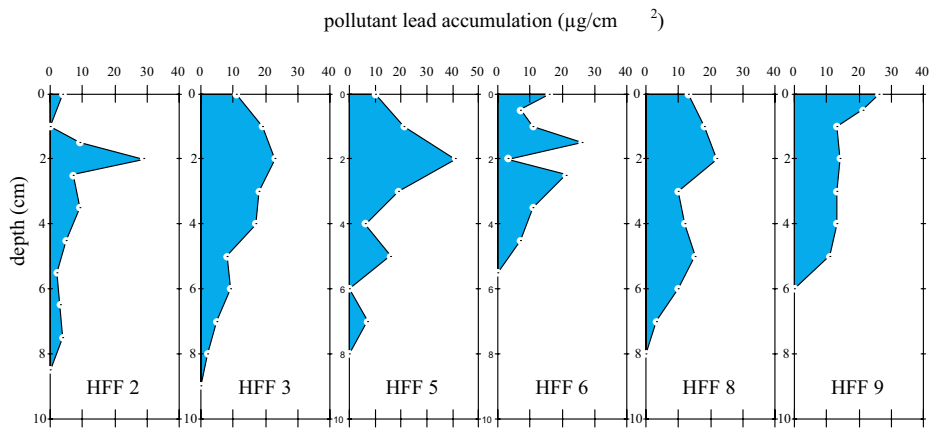

FIG. 2. Pollutant lead accumulation (µg/cm²) in cores.

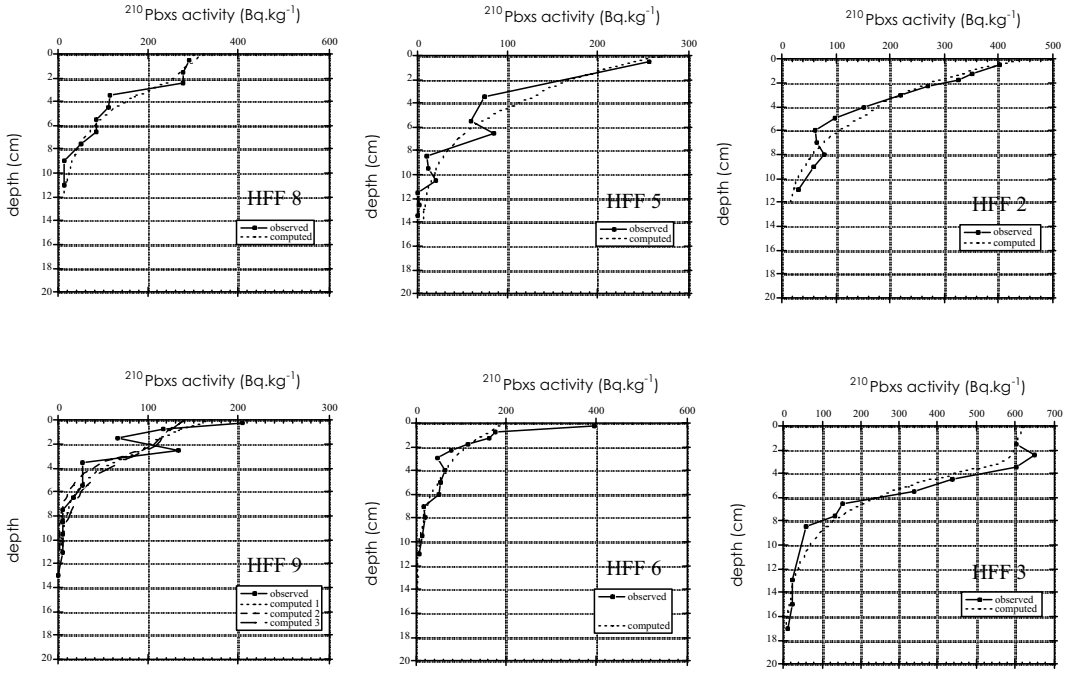

FIG. 3. Measured and theoretical ^{210}Pbxs activity (Bq/kg) profiles for each core.

The computation of the measured ^{210}Pbxs profile of each core (Fig. 3) give us the couple (D_B:S) solution of the previous equation and essential to determine the age of formation of each sediment slice:

$t = 1/\lambda * \mathrm{Ln}\ (A_o/A)$

where

t is the age formation of the slice,

A_0 the initial ^{210}Pbxs activity (Bq/kg) and

A the calculated ^{210}Pbxs activity (Bq/kg).

Modelling is efficient for five of the six cores, excepted for HFF 9 were the theoretical profile does not allow to obvious a solution-couple (D_B:S). Thus, this core is not considered in the following investigations upon time reconstruction of the pollutant lead deposition.

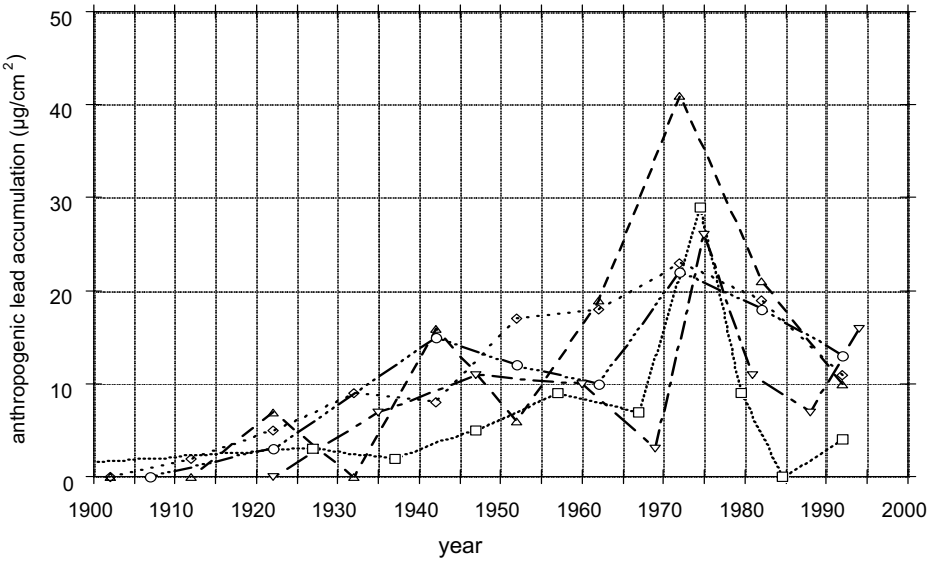

FIG. 4. Pollutant lead accumulation (µg/cm^2) in sediment over the last century.

5. Pollutant lead sedimentary accumulation through time

Respective pollutant lead accumulation and geochronologies are joined to evidence a general trend in the pollutant lead deposition in Gulf of Lions sediments through time (Fig. 4).

All investigated cores (i.e. excepted HFF 9 for which geochronology establishment was not satisfactory) present an accumulation peak in the 70s, more specially in 1973 ± 2, in good agreement with the pollutant lead emissions balance in France during the last century [15].

6. Conclusions

The coupling of stable isotopes and radionuclide studies enable to improve environmental studies. Investigations on lead isotopes, stable (^{206}Pb, ^{207}Pb) and radioactive (^{210}Pb), allow to characterize the atmospheric signal recording in the Gulf of Lions. Geochronologies and pollutant lead accumulation determinations performed on six cores (in fact, five of them) of the continental margin of the Gulf of Lions allow to reconstruct a pollutant lead accumulation trend through time with higher value in the mid-70s, in good agreement with known atmospheric deposition patterns. This work shows that marine sediments can be used as relevant proxies for time studies of contamination.

REFERENCES

[1] PACYNA, J.M., Estimation of the atmospheric emissions of trace elements from anthropogenic sources in Europe, Atmos. Env. **18** 1 (1984) 41.
[2] DAVIS, J.M., SVENDSGAARD, D.J., Lead and child development, Nature **329** (1987) 297.
[3] TRIPATHI, R.M., et al., Daily intake of heavy metals by infants through milk and milk products, Sci. Tot. Env. **227** (1999) 229.
[4] ZIETZ, B.P., et al., Epidemiological investigation on chromium toxicity to children exposed via the public drinking water supply, Sci. Tot. Env. **302** (2003) 127.
[5] LAKIND, J.S., et al., Environmental chemicals in human milk: a review of levels, infant exposures and health, and guidance for future research, Toxicol. App. Pharmacol. **198** 2 (2004) 184.
[6] OLIER, J.P., et al., Surveillance du Pb particulaire atmosphérique en sites urbains, Poll. Atm. **Janv.-Mars** (1990) 31.
[7] GRIMALDI, F., et al., Action du comité Marseille-Provence de l'APPA en matière d'étude des polluants métalliques de l'atmosphère, Poll. Atm. **139** (1993) 98.

[8] MIGON, C., et al., Évolution of atmospheric lead over the Northwestern Mediterranean between 1986 and 1992, Atm. Env. **27** 14 (1993) 2161.
[9] NICOLAS, E., et al., Abrupt decrease of lead concentration in the Mediterranean Sea: a response to antipollution policy, Geophys. Res. Let. **21** 19 (1994) 2119.
[10] FERRAND, J.L., et al., Isotopic tracing of anthropogenic Pb inventories and sedimentary fluxes in the Gulf of Lions (NW Mediterranean Sea), Cont. Shelf Res. **19** (1999) 23.
[11] ALLEMAN, L.Y., et al., Lead sources and transfer in the coastal Mediterranean: evidence from stable lead isotopes in marine particles, Deep Sea Res. II **47** (2000) 2257.
[12] VERON, A., et al., Isotopic evidence of pollutant lead sources in Northwestern France, Atm. Env. **33** (1999) 3377.
[13] VERON, A., et al., Evidence of recent lead pollution in deep Northeast Atlantic sediments, Nature **326** (1987) 278.
[14] Miralles, J., et al., Multitracer study of anthropogenic contamination records in the Camargue, Southern France, Sci. Tot. Env. **320** 1 (2004) 63.
[15] FERRAND, J.L., «Étude isotopique du cycle géochimique du Plomb anthropique et naturel en milieux marin et côtier, PhD Thesis, Univ. P. Cézanne, Marseille (1996).

Distribution Coefficients (K_ds) of naturally occurring radionuclides in river sediments

Al-Masri, M.S., S. Mamish, M.A. Haleem

Department of Protection and Safety,
Atomic Energy Commission of Syria,
Damascus,
Syrian Arab Republic

Information on distribution coefficients (K_ds) of natural and artificial radionuclides are most important for evaluation radionuclides transport pathways in marine and fresh water systems; K_d values are used in modeling radionuclides dispersion and addressing the problem of radioactive release [1-5]. It is also necessary for prediction of how efficiently sediments in suspension can remove contaminants from the water and the sorption potential of contaminants onto particulate matter. In addition, risk assessment modelers usually adopt mean K_d values reported in the IAEA Technical Report [1], which are only generic estimates and modelers has to use the values for a particularly system that is under investigation [4] and it was recommended to use K_ds ranges of values for specific element rather than single mean values be incorporated into model simulations of radionuclide dispersion [3, 4].

There is a lack of information on K_ds distribution coefficients of natural and artificial radionuclides in river and marine sediments of Syrian environment. Current risk assessment studies of the two main potential sources of enhanced naturally occurring radionuclides require K_d values in river sediments; viz. phosphate and oil industry. Emphasis has been placed on two areas, Orontos River near the phosphate factory and Euphrates River near the Syrian oil fields. Water, suspended particulates, and sediment samples were collected from several sites along the two rivers. Validated radioanalytical methods have been used for analysis. Laboratory K_d experiments were conducted for the following radionuclides discharged by these phosphate and oil industries: ^{226}Ra, uranium, ^{210}Po and ^{210}Pb. Variations of K_ds with aqueous phase composition and sediment composition have been studied using the batch sorption method. Correlations of K_ds values with some elements present in sediment have been established. *Kds* values were found to vary between $5.8 \times 10^3 - 2.3 \times 10^4$, $4.4 \times 10^3 - 1.1 \times 10^4$, $6.8 \times 10^2 - 1.6 \times 10^3$, $9.2 \times 10^2 - 2.8 \times 10^3$, for ^{210}Po, ^{210}Pb, ^{234}U and ^{238}U, respectively. These values agree with some minimum values given in the IAEA Technical report for marine sediment [1]. However, the data obtained in this study can be used for the radionuclides dispersion studies in the river system to assess risks to public due to discharges of the phosphate and oil industry.

REFERENCES

[1] INTERNATIONAL ATOMIC ENERGY AGENCY, Sediment K_ds and Concentration Factors for Radionuclides in the Marine Environment, Technical Report Series No. 247 (1985) IAEA, Vienna.

[2] MOORE, W.S., DEMASTERS, D.J., SMOAK, J.M., MCKEE, B,A., SWARZENSKI, P.W., Radionuclide Tracers of Sediment Water Interactions on the Amazon Shelf. Cont. Shelf. Res. **16** (1996) 645-665.

Natural gamma radionuclides in sediments of the Gulf of Mexico: an approach to radio-tracers transport and distribution of sediments in marine environments

Rodriguez-Espinosa, P.F.[a], V.M.V. Vidal L.[b], F.V. Vidal L.[b]

[a] Centro de Investigación en Ciencia Aplicada y Tecnología Avanzada,
Unidad Altamira,
Tamaulipas C.P.
Mexico

[b] Grupo de Estudios Oceanográficos,
Centro de Investigación en Ciencia Aplicada y Tecnología Avanzada,
Instituto Politécnico Nacional,
Cuernavaca, Morelos,
México

The following paper contains information of 23 cores collected nuclides in the Gulf of Mexico from 70 to 2,100 meters of depth. The cores were collected in Mexican Gulf of Mexico on OGMEX Oceanographic Campaigns between 1993 and 1995 (see Fig. 1).

Radiometric determinations were measured by the *Silena* gamma-spectrometer from 50 to 60,000 s at the Environmental Laboratory in Cienfuegos, Cuba. A database of 920 natural radio-nuclides from chains of ^{232}Th and ^{238}U [1], was obtained from 180 samples [2-4].

The most significant result was the geographic distribution of gamma radionuclides measured concentrations is regionally distinct. Finding a low ^{238}U gamma radio-nuclides concentration at low depth zones and high concentration in depth waters. While the already mentioned conditions are inverted for the ^{232}Th gamma radionuclides. As it is the case of ^{214}Pb and ^{212} Pb (see Fig. 2).

The discussion of results as here presented allows to assume a geographic distribution of natural gamma radionuclides under sedimentary material supplying conditions [5] by the hydrological basins which drain to the Gulf of Mexico and the marine currents transport those materials through the inside of the Gulf of Mexico [6, 7].

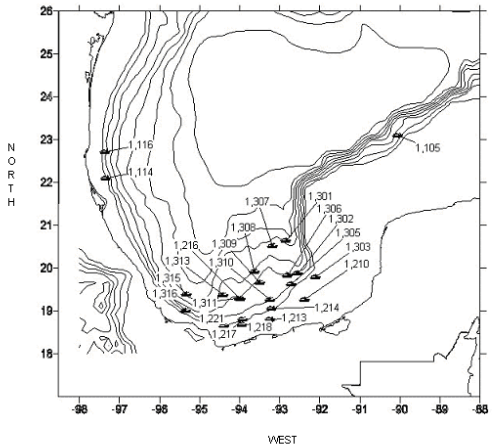

FIG. 1. Sediment samples collected in the Gulf of Mexico.

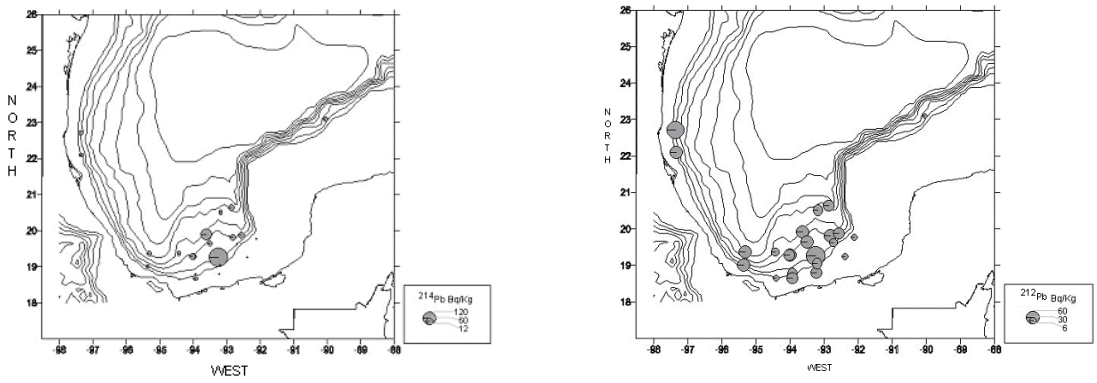

FIG. 2. Gamma radionuclides. As it is the case of ^{214}Pb and ^{212} Pb.

Associated results are shown to the rest of Gamma Radionuclides Natural that belong to the ^{238}U and ^{232}Th chains in order to permit corroborating associations in different proportions of these radionuclides in geological material of hydrological basins associated to the western slope in the Gulf of Mexico.

In conclusion the work as here presented allows the understanding and elucidation of the origin, transport and, deposition of sedimentary material by means of natural radionuclides tracers using low gamma spectrometry.

REFERENCES

[1] EISENBUD, M., Environmental radioactivity from natural, industrial and military sources, Academic Press Inc. NY. (1987) 475 pp.

[2] PAPUCCI, C., DELFANTI, R., Gamma spectrometry energy and efficient calibration, Notes of the International Training Course on Strategies and Methodologies for the applied marine radioactivity studies in Santa Teresa, Italy and Monaco, October 11–16, (1990) 6 pp.

[3] INTERNATIONAL ATOMIC ENERGY AGENCY, Reference Methods for Marine Radioactivity Studies 11, Technical Reports Series No. 169, IAEA, Vienna, (1975) p. 239.

[4] INTERNATIONAL ATOMIC ENERGY AGENCY, Measurement of Radionuclides in Food and The Environment, A Guidebook, Technical Reports Series No. 295, IAEA, Vienna, Austria (1989) 169 pp.

[5] RODRIGUEZ-ESPINOSA, P.F., VIDAL-LORANDI, F.V., VIDAL-LORANDI, V.M., Regionalization of natural and artificial radio-nuclides in sediments of the Mexican Gulf of Mexico environmental chains and radioactivity tracers conference – 6th South Pacific Environmental Radioactivity Association Conference Guidebook of Abstracts, June 19-23, 2000, Noumea, IRD Centre, New Caledonia, (2002) 66-67.

[6] RODRIGUEZ-ESPINOSA, P.F., VIDAL-LORANDI, F.V., VIDAL-LORANDI, V.M., Sources of environmental radioactivity in sediments of South of Gulf of Mexico, OIEA Proceedings (in press).

[7] VIDAL, V.M.V., VIDAL, F.V., MEZA-CONDE, E., ZAMBRANO-SALGADO, L., JAIMES DE LA CRUZ, B., Ring-slope interactions and formation of the western boundary current in the Gulf of Mexico, J. Geophys. Res. **104** C9 20 (1999) 523-20, 550.

Historical trend in heavy metal pollution in the sediments of Cienfuegos Bay (Cuba), defined by ^{210}Pb and ^{137}Cs geochronology

Alonso Hernandez, C.[a], S. Perez Santana[a], C. Brunori[b], R. Morabito[c], R. Delfanti[d], C. Papucci[d]

[a] Centro de Estudios Ambientales de Cienfuegos,
Cienfuegos,
Cuba

[b] ENEA-C.R.E. Casaccia,
PROT-CHIM,
Roma,
Italy

[c] ENEA-C.R.E. Casaccia,
PROT,
Roma,
Italy

[d] ENEA- Marine Environment Research Centre,
La Spezia,
Italy

Abstract. Investigations on the concentration level of heavy metals in the sediments of Cienfuegos Bay (Cuba) have been carried out, to reconstruct their "depositional history" by using radionuclide geochronology, to highlight the major changes occurred in the last century and to draw hypotheses on their origin. During two sampling campaigns (1999 and 2001) sediment cores and surficial grab samples have been collected in the two basins of the Bay. In this paper results on the horizontal and vertical distribution of arsenic, nickel and vanadium are discussed, along with data on concentrations of natural (excess ^{210}Pb) and anthropogenic (^{137}Cs) radionuclides, used as tools to "date" the sediment horizons. Results evidenced that important changes in the sedimentation regime of the Bay occurred in the last forty years, in relation to changes in land uses and to the effects of some extreme meteorological events. The distribution of the heavy metals shows the influence of the recent industrialisation of the area, as revealed by both the spatial and vertical concentration within the sediment horizons.

1. Introduction

The Bay of Cienfuegos, located in the southern-central part of Cuba (Fig.1), is an enclosed bay with a surface area of 90 km^2 and an average depth of 14 m. It is connected to the Caribbean Sea by a narrow channel 3 km long. The bay is divided in two well-defined hydrographic basins, due to the presence of a submerged ridge 1 m below the surface.

The northern basin receives most of the anthropic impact from the city sewage discharge, from the industrial area (thermoelectric power plant, fertilizer industry, oil refineries) and from the outflow of the Damuji and Salado rivers, that drain an area where intense agriculture has been developed in the last forty years. Wastewaters from the industrial pole and urbanic areas are, in some cases, untreated. The southern basin is subject to a smaller degree of anthropic pollution, mainly originated from the Caonao and Arimao rivers. Part of the southern basin is a natural park.

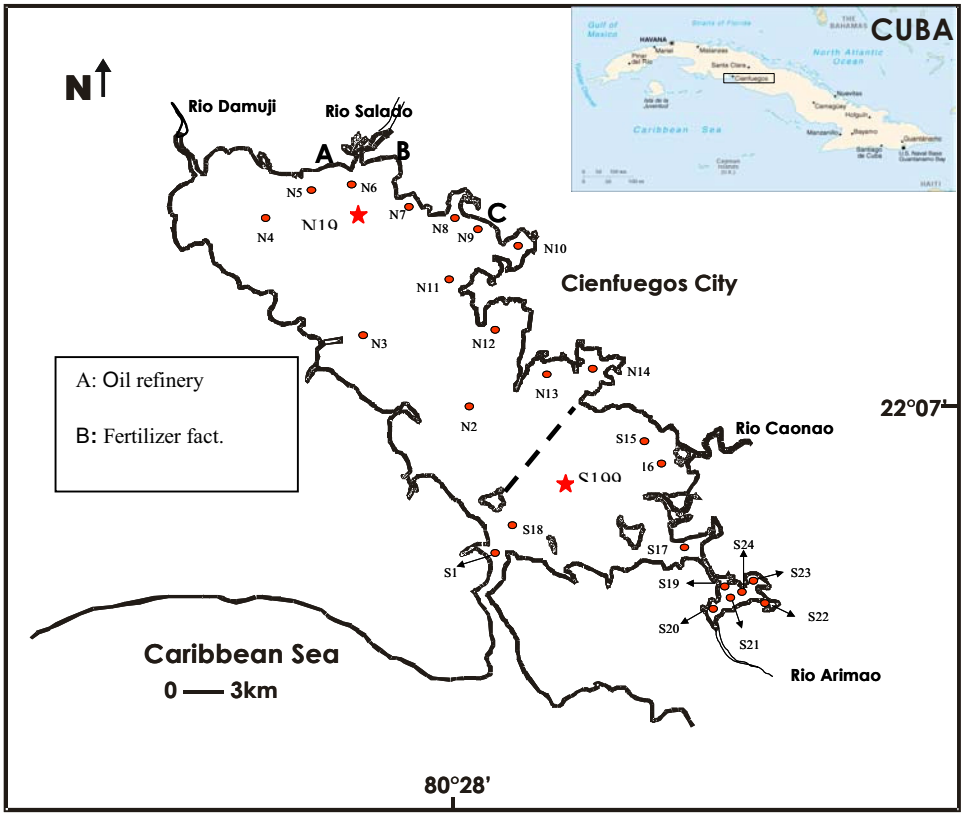

FIG. 1. Sampling stations (dots: grabs, 2001; stars: cores, 1999).

The hydrographic characteristics of the Bay are mainly controlled by enhanced thermohaline stratification due to the outflow of the rivers and by low tidal energy and limited exchanges with the open sea. Taking all these parameters into consideration, the Bay can finally be considered as an "accumulation area" for the contaminants (including heavy metals) introduced into the marine environment from many sources.

In the last three decades some deleterious ecological signals have been observed in the Bay: loss of marine biodiversity, shift in benthic communities, reduction in size and capture levels of commercial marine species, erosion of the coastline [1]. For these reasons a large environment research programme has been initiated, to define the main physical, chemical and biological characteristics of the bay, whose knowledge will constitute the basis for the correct management of the area.

As part of this programme, dating techiques based on the natural and antropogenic radionuclides (^{210}Pb and ^{137}Cs) and mineralogical distribution were applied by Alonso-Hernandez et al. [2] to study of the sedimentation regime in Cienfuegos Bay. This study showed that in the last 40 years significant changes have affected sedimentation processes in the Bay. These results were the base to evaluate the distribution of heavy metals in the bay.

The aims of the study are to identify the main processes responsible for the spatial and vertical distribution of heavy metals (As, V, Ni) in the sediments; to draw hypotheses on their origin; to reconstruct the pollution history, using natural and anthropogenic radionuclides as tools for dating the sediment horizons, and then to identify the major events related to the management of specific industries located in the Bay. The work is a result of a collaborative programme included in the bilateral scientific agreement 2000-2004 between Cuba and Italy.

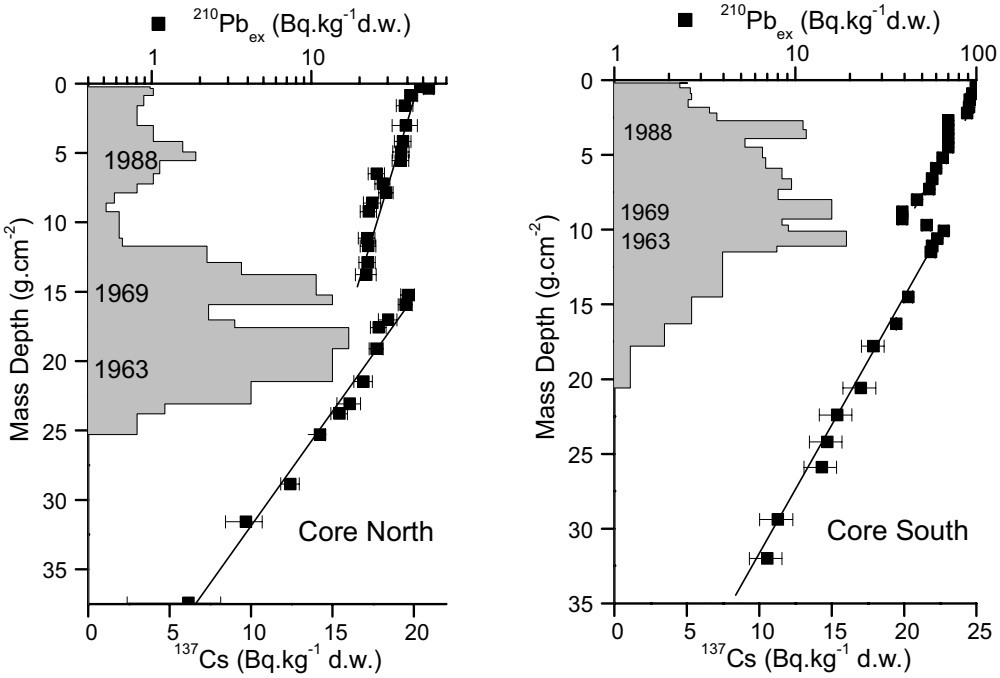

FIG. 2. Vertical profiles of ^{137}Cs and $^{210}Pb_{ex}$ in the northern and southern cores, 1999.

2. Materials and methods

Two sampling campaigns have been carried out in 1999 and 2001. The location of the sampling stations is reported in Fig.1. Surficial sediments have been collected in 24 stations, with a Petersen grab having a mean penetration depth of 5 cm. Sediment cores (N1999 and S1999) have been collected by a scuba diver carefully inserting a plastic tube, 12 cm in diameter and 100 cm in length, into the sediment.

Analytical procedure, calibration, and quality control of results are described elsewhere [3]. Briefly, the total dissolution of 0.5 g of sediment was performed using strong acids and a CEM microwave pressurized digestor. Determination of metals was carried out by ICP-MS (Perkin-Elmer ELAN 6000, equipped with a Ryton cross-flow nebuliser). Performance of the analytical procedure was checked analysing Certified Reference Materials (NIST 1646a, PACS-1, MESS-1). Sub-samples of the surficial sediments and of all core sections were analysed for ^{210}Pb, ^{226}Ra and ^{137}Cs contents by gamma-spectrometry, using low background intrinsic germanium coaxial detectors (60% relative efficiency, 2.1 keV resolution at 1333 keV) coupled with a multichannel analyser. Efficiency calibration was performed using a CANMET Standard U-Ore and QCY44 AMERSHAM Certified Solution. NBS and IAEA Reference Materials were used to check the accuracy of the results, that resulted within ± 10% of the certified values.

3. Results and discussion

3.1. Geochronology

The vertical profiles of ^{137}Cs in the cores collected in northern (N 1999) and southern (S 1999) basins have been used for "dating" specific sediment horizons. In the vertical profiles (Fig2), ^{137}Cs massic activities (in Bq kg $^{-1}$ dry weight, d.w.) were plotted versus "mass depth" (g cm^{-2}), instead of "depth" (cm), to avoid corrections for sediment compaction.

^{137}Cs was introduced into the Caribbean environment mainly by fallout from nuclear weapon testing in the atmosphere. The input function of ^{137}Cs at the latitude of Cuba is well defined [2], and shows a maximum in 1963: so it was realistic to attribute "1963" to the sediment layer corresponding to the

maximum ^{137}Cs concentration in the vertical profiles. The profiles show also two additional peaks between the maximum concentration and the surface, that we attributed to extra-inputs of ^{137}Cs-reach particles into the Bay. In fact, the calculated inventory of ^{137}Cs in the sediment cores (0.19 and 0.20 Bq cm^{-2}) are higher than the cumulative fallout deposition in the area, estimated from adjacent undisturbed soil (0.12 Bq cm^{-2}, [4]. This likely indicate a significant transport of ^{137}Cs from land to the bay. Moreover, two extreme meteorological episodes have been actually registered, after 1963, able to produce extra-input from the rivers : the hurricane "Camille", that crossed Cuba in 1969 with 500 mm of rain in 3 days and an exceptional period of heavy rain (1000 mm in 7 days) occurred in June 1988.

These events provided an extra-input of suspended load to the bay (carrying an enhanced ^{137}Cs content, associated to clay particles), from both the weathering of the catchment basins and the resuspension and transport of ^{137}Cs-rich sediment initially stored in the river bed. Finally, by crossing the data of the ^{137}Cs vertical profiles with those on the fallout deposition and with the meteo record for the region we reasonably hypothesised that the two extra-peaks could be dated at 1969 and 1988.

Results from the vertical profiles of $^{210}Pb_{ex}$ have been used to integrate those of ^{137}Cs dating and to derive information on the sedimentation regime in the last 100 years. The vertical profiles of $^{210}Pb_{ex}$ suggest significant variations in the sedimentation regime, both spatially and temporally. A remarkable discontinuity was observed in the profiles (Fig.2), corresponding to sedimentation processes occurred in the period 1963-1973. The CFCS/Constant Flux Constant Sedimentation model [5] was separately applied to the sediment layers below and above the observed discontinuity. While from the beginning of 1900 sediments were regularly accumulated at a rate of around 0.3 $g.cm^2.y^{-1}$, beginning from early Seventies the sediment accumulation rate almost doubled (0.5 $g.cm^{-2}.y^{-1}$) in the northern basin. In addition, corresponding to the caesium peaks, there are "packages of sediment" having the same age, supporting the hypothesis that ^{137}Cs peaks are correlated to the meteo events that produced enhanced supply of particles into the bay, in a very short period of time.

3.2. Nickel, vanadium, arsenic in sediments

In the case of nickel and vanadium particularly high concentrations were found, as expected, in the surficial samples collected in front of the thermoelectric power plant (Fig.1, point "C"). Concentration levels are twice (nickel) and three times (vanadium) higher than the average value found in the surficial sediments of the northern basin (Ni: 106 mg kg^{-1}, in respect to 50; V: 400 mg kg^{-1}, in respect to 137). This area can be considered as zone of preferential accumulation of the metals emitted by the plant, both in gaseous form and as wastewater. The plant was activated in 1939, but the substantial increase in power generation occurred in 1968.

The spatial distribution of Arsenic in 2001 is rather homogeneous in the two basins of the Bay, with concentrations around 5 $mg.kg^{-1}$.

Figure 3 shows the vertical profiles of vanadium, nickel and arsenic in the two cores. Actually the vertical profiles of vanadium and nickel in the sediment cores reveal enhanced concentrations in strata deposited after the early sixties. These differences are measured in both basins, demonstrating that the impact of the power plant has been redistributed on the whole bay territory, on a fifty years time-scale. On the contrary, the arsenic vertical profiles in the sediment cores gave an additional insight on impacts recently produced by the industry in the northern basin. While the profile gathered in the southern core shows values that can be considered as "background level", a significant increase in concentration (up to 88 mg kg^{-1}, more than one order of magnitude higher) was found down in the northern core, in strata corresponding to late-Seventies/early Eighties. This signal marks the management of a Nitrogen fertilizer industry, including the effect of a major accident occurred in 1979.

Summarizing, in fact, the re-distribution in the sediments is correlated a) to preferential pathways in wet and dry deposition for nickel and vanadium, initially dispersed into the atmosphere from the thermoelectric power plant located in the northern basin and b) to the water masses circulation and

sedimentation regime for the elements (like Arsenic, for instance) entering directly into the marine environment from factory and waste treatment. As a matter of fact, significant amounts of heavy metals have been introduced into the Bay, mainly in the northern basin, by authorized releases - and accidents - from the industrial complex. In addition, as important changes in land uses and random meteorological events produced additional inputs of suspended particle load (to which particle-reactive contaminants associate), an increased accumulation in the sediments was observed, both in terms of sediment accretion rate (g cm^{-2} y^{-1}) and concentration (g kg^{-1}) of metals.

4. Conclusions

(i) Cross-linking the studies on contaminants re-distribution processes and geochronology of sediments has been proved to be an essential method to elucidate the "history" of the relevant pollution. In this context, the use of appropriate natural and anthropogenic radionuclides as "clock" to evaluate the timing of the processes, constitute an efficient tool for dating the sediment horizons and for evidencing the changes occurred in the sedimentation regime.

(ii) The sedimentation regime in the Bay has changed in the last forty years. Sediment accumulation became faster and irregular. The most important reasons likely being: changes in land uses, including the development of intensive agriculture in late Fifties that resulted in enhanced deforestation in the area drained by the rivers, and in significant increase of the suspended load entering into the Bay; and, as described earlier, the period of heavy rain occurred in 1988, as well as during the hurricanes transits (remarkable was the effect of the hurricane "Camille" in 1969), that also led to enhanced supply of particulate material transported by rivers.

(iii) In the Bay of Cienfuegos, the pollutants introduced from the atmosphere (i.e. vanadium and nickel) are homogeneously distributed all over the two basins, on a time-scale of decades. The highest surficial concentrations are found close to their point source, likely the thermoelectric power plant, due to the leaching and (sometimes) the washing out of bottom ashes.

(iv) Arsenic, introduced directly into the sea by authorized releases of a fertilizer complex, sedimented in the northern basin, close to the point source. The vertical distribution in the

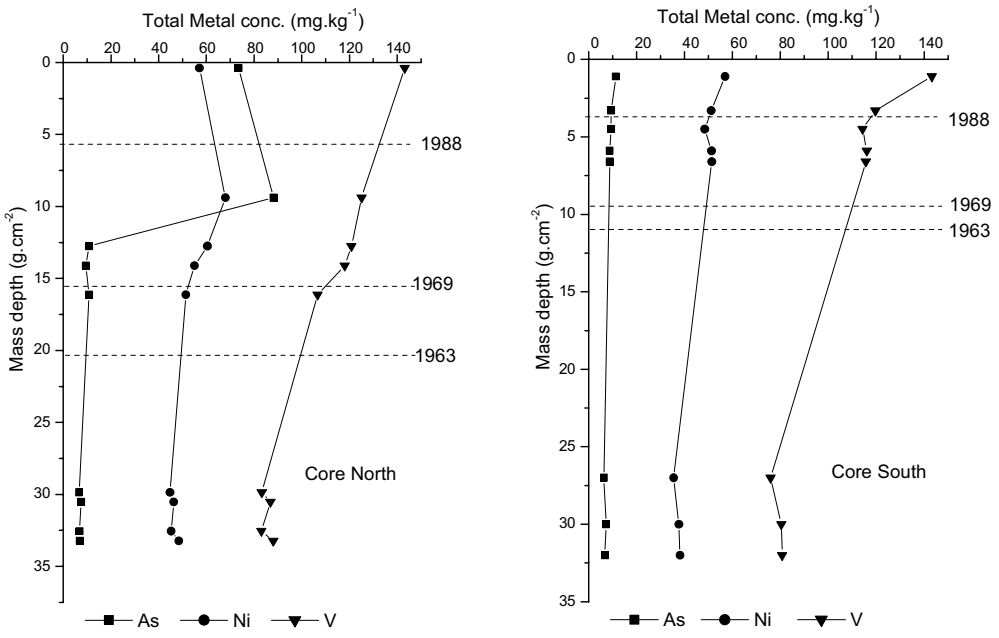

FIG. 3. Vertical profiles of arsenic, vanadium and nickel in the northern and southern cores, 1999.

northern sediment core reveals a sharp increase in strata corresponding to the late-Seventies, when a first major accident occurred with the sudden release into the Bay of liquid wastes with elevated arsenic concentration.

(v) The metals tend to remain in the bay environment for a long period: decades, at least.

(vi) Results from this study gave a first insight to support adequate strategies for the management of the Bay ecosystem and the surrounding area.

ACKNOWLEDGEMENTS

The work was partially carried out in the framework of the "Seventh Executive protocol of the Cultural and Scientific Agreement, 2001-2004" between Italy and Cuba, Annex 3/Environment/ Project no.6. The analytical activities have been supported by the International Centre for Theoretical Physics-Programme TRIL and by ENEA fellowships dedicated to developing countries.

REFERENCES

[1] MORALES-CLARO, R., Resumen de Investigaciones en la Bahia de Cienfuegos y Litoral Adyacente, Reporte de Investigacion, Academia de Ciencias de Cuba, Cienfuegos, **12** (1991)1-56.

[2] ALONSO-HERNANDEZ, C., CARTAS AGUILA, H., DIAZ-ASENCIO, M., MUNOS-CARAVACA, A., Reconstruction of ^{137}Cs signal in Cuba using ^{7}Be as tracer of vertical transport processes in the atmosphere, J. Environ. Radioact. **75** (2004)133-142.

[3] IPOLYI, I., BRUNORI, C., CREMISINI, C., FODOR, P., MACALUSO, L., MORABITO, R., Evaluation of performance of time-saving extraction devices in the BCR three-step sequential extraction procedure, J. Environ. Monitor. **4** (2002)541-548.

[4] SIBELLO-HERNANDEZ, R., ALONSO-HERNANDEZ, C., DIAZ-ASENCIO, M., CARTAS AGUILA, H., Caracterizacion radioactiva de los suelos y productos agricolas de la region central de Cuba, Centro Agricola **4** (2002)73-79.

[5] APPLEBY, P.G., OLDFIELD, F., IVANOVICH, M., HARMON, R.S., Application of ^{210}Pb to sedimentation studies (IVANOVICH, M., HARMON, R.S. (Eds.), Uranium-series Disequilibrium: Application to earth. Marine, and environmental Sciences, Clarendon Press, Oxford, 1992, pp. 731-778.

Western Tasmania - A reconstructed history of wide-spread aerial pollution in a formerly "pristine" area - the Use of ^{210}Pb & ^{226}Ra in retrospective monitoring of the environment

Heijnis, H.[a], K.J. Harle[b], J. Harrison[a]

[a] ANSTO – Environment,
Sydney, NSW,
Australia

[b] CSIRO Sustainable Ecosystems,
Canberra, ACT,
Australia

Using nuclear dating techniques and trace metal analysis of sediment cores an environmental history of Western Tasmania was reconstructed. Seven sites were selected to encompass a range of environments from highly human impacted to relatively pristine. They include sub-alpine tarns and coastal lowland lakes. Disturbed areas have been impacted by activities associated with logging, mining and colonial settlement while the near-pristine sites were located in areas with little disturbance, such as the Tasmanian Wilderness World Heritage Area.

Lead-210 (^{210}Pb) and radium-226 (^{226}Ra), both naturally occurring radioisotopes, were used to determine sediment accumulation rates and establish chronologies. Sediment cores collected from near pristine lakes were expected to reveal low and relatively constant trace metal concentrations consistent with areas subject to little to no human impact. However, evidence from these sediment cores revealed trace metal concentrations peaked in the 1960s and then began to decrease in the 1980s. This trend was also discovered, to a greater extent, in sediment cores collected from human impacted sites particularly those surrounding the Central Western mining area. Of all the metals investigated, lead (Pb), arsenic (As), tin (Sn) and copper (Cu) were found to show the most marked increases.

Temporal increases in metal concentrations were found to be a result of mining activities in Central Western Tasmania. Evidence for the most significant increase as shown by the trace metal profile coincided with the escalation of open cut mining while decreases in metal concentrations around 1980 coincided with the cessation of mining. Spatially, the dispersal was predominantly due to aerial pollution as concentrations of Pb, As, Sn and Cu were highest close to the mining areas although sites as far as 150 kilometres away showed marked metal concentration increases above background levels around 1960.

Application of neutron activatable tracers (NATs) for cohesive sediment transport studies in contaminated estuaries

Hollins, S.[a], R. Szymczak[a], P. Airey[a], W.L. Peirson[b], T. Payne[a]

[a] ANSTO Environment,
Menai NSW,
Australia

[b] Water Research Laboratory,
University of NSW,
Manly Vale NSW,
Australia

ANSTO and the University of NSW Water Research Laboratory (WRL) are investigating the migration of contaminants associated with cohesive sediments in Homebush Bay, Sydney. The study area is a highly urbanised and industrialised catchment with a long history of contamination [1]. Until 1890, when an ocean outfall was commissioned, domestic and industrial waste was discharged directly into Sydney Harbour [2]. Heavy metals and other hydrophobic pollutants have a distinct tendency towards solid phase partitioning. This means that the majority of heavy metals in the estuary are linked to particulates rather than occurring in the dissolved phase. Hence, in order to assess the impacts of the pollution and develop a scientific basis for remediation it is necessary to understand processes that resuspend and disperse the contaminated sediments.

The study approach involved the evaluation of the numerical model of the processes using activatable tracer techniques [3]. An ideal tracer binds to the material of interest with high integrity and is detected with high sensitivity and selectivity. Tracers can be used to study sediment transport over extended periods and are therefore ideally suited to observing the impact of extreme weather events on sediment mobilisation by monitoring the distribution of the label before and after the event. The tracer must not only adhere to the cohesive sediment with high integrity but must be detectable with high efficiency, high sensitivity and relatively low cost. Identification of the optimum activatable tracer involved an assessment of the nuclear (Table I) and sorption properties.

The implementation of the tracer study involved (a) labelling sediment from the study area with indium-115 in the laboratory and equilibrating for 3 weeks; (b) choosing a site where bathymetric surveys indicated significant recent accretion; (c) injection of the labelled sediment into an accurately located site in Homebush Bay (Fig. 1); (d) undertaking three surveys over the subsequent months; (e) analysis of samples via irradiation in the Fast Access Neutron facility in ANSTO's research reactor, HIFAR and gamma counting on a High Purity Germanium detector[3]; and (f) data processing, where the tracer concentrations were contoured using the Surfer© routine and interpreted in terms of advective and dispersive transport using a Gaussian approximation (Fig. 2). Information on vertical transport was obtained by coring.

These results are being used to evaluate a three-dimensional finite element model of the study area [4]. Estimates have been made of the aerial dispersion coefficients, of the surficial mixing due to bioturbation and of advective transport. This paper will focus on the optimum choice of the tracer for cohesive sediment transport studies and some early results.

Table I. Gamma ray intensities expressed as a percentage of the maximum value observed following the naa activation/cooling cycle [3]

Target Element	Product Nuclide	Activation time / Cooling time (seconds)				
		60/ 300	60/ 1200	300/ 300	300/ 1200	3600/ 82900
Samarium	Sm-155			**1.1**		
Rhenium	Re-188m	**1.2**		**5.6**		
Iridium	Ir-194					**1.1**
Gold	Au-198					**5.9**
Europium	Eu-152m1	**2.7**	**2.7**	**13.6**	**13.4**	**28.5**
Manganese	Mn-56	**1.6**	**1.5**	**7.7**	**7.3**	
Niobium	Nb-94m	**1.1**		**4.5**		
Indium	In-116m1	**20.5**	**16.9**	**100**	**82.6**	
Vanadium	V-52	**9.6**		**34.5**	**2.2**	

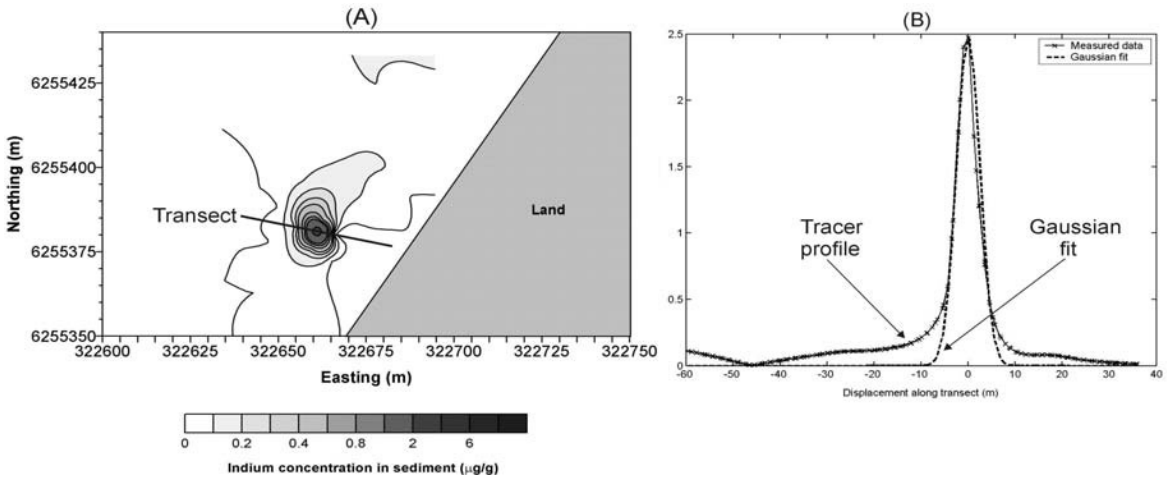

FIG. 1. (A) Distribution of labelled sediment on 7 Nov 2002 following injection on 22 May 2002; and (B) tracer profile along the transect, [3].

REFERENCES

[1] BIRCH, G.F., TAYLOR, S., Source of Heavy Metal Sediments of the Port Jackson, Australia, Sci. Tot. Environ. **227** (1999) 123-138.

[2] BIRCH, G.F., EYRE, B., TAYLOR, S.E., The distribution of nutrients in bottom sediments of Port Jackson (Sydney Harbour), Australia, Mar. Poll. Bull. **38** (1999) 1247-1251.

[3] HOLLINS, S., AIREY, P., SZYMCZAK, R., PAYNE, T., Optimising Activatable Tracers for Cohesive Sediment Transport Studies in Contaminated Estuaries. (Proc. 14th Pacific Basin Nuclear Conf., Mar. 2004), Honolulu, Hawaii (in press).

[4] SYDNEY PORTS CORPORATION - Coastal Section, Homebush Bay Hydrodynamics and Sediment Transport: preliminary model studies, Report No 96/01 (1996).

Sediment geochemical properties and dinoflagellate cyst distribution in Manila Bay, Philippines

Siringan, F.P.[a], R.V. Azanza[b], J.P. Duyanen[a], E.Z. Sombrito[c], N. Macalalad[a], P. Zamora[a], A. Yñiguez[d], E. Sta. Maria[c], A.D.M. Bulos[c]

[a] National Institute of Ge ological Sciences,
UP Diliman, Q.C.,
Philippines

[b] The Marine Science Institute,
UP Diliman, Q.C.,
Philippines

[c] Philippine Nuclear Research Institute,
Diliman Q.C.,
Philippines

[d] National Center for Caribbean Coral Reef Research,
Rosenstiel School of Marine and Atmospheric Science (RSMAS),
University of Miami,
Key Biscayne, Florida,
United States of America

One of the theories used to explain the initiation of harmful algal blooms (HAB's) is the release and germination of microalgal cysts from the sediments. Assessment of the sediment's geochemical properties and its correlation with past HAB occurrences could serve as a clue on the conditions favorable for the occurrence of HAB's. HAB's of *Pyrodinium bahamense* var. *compressum* seasonally occurred in Manila Bay, Philippines from 1988 to 1998. To help understand and manage this phenomenon, sediment cores were dated using Lead-210 and analyzed for cysts, grain size, total carbonate and organic matter, elemental concentrations and metals.

Lead-210 profiles indicated sedimentation rates of 1.2 to 2.5 cm/year while earlier periods ranged from 0.4 to 0.6 cm/yr. Such high sedimentation rates can dilute cyst counts which was apparent in this study. Shift in sedimentation rate could be attributed to the eruption of Mt. Pinatubo in 1991 which may have caused the burial of *Pyrodinium* cysts and subsequent non-occurrence of its blooms since 1998. Dating also showed the presence of *Pyrodinium* in the early 1950s and ensuing increase until 1988.

Autotrophic dinoflagellate cysts identified were: *Lingulodinium polyedra*, *Gonyaulax* spp., *Pyrophacus steinii*, *Protoceratium reticulatum* and *Pyrodinium bahamense* var. *compressum* while heterotrophs consisted of *Protoperidinium* and *Diplopsalis* species.

Cyst density fluctuated but showed overall increase through time. The increase was most significantly observed before 1991 which coincided with the Bay's first bloom in 1988. The fluctuations which implied cyclicity was found to be controlled by the overall abundance of heterotrophs. Autotrophs, however showed significant increase in abundance in younger sediments which could account for HAB's from 1988 to 1998.

Mud predominates in all of the cores which comprise of: clay (20% to 70%), silt (20% to 90%) and sand (0.6 to 3%). Major element profiles show an increase in Si/Al ratio and decrease of organic matter and total carbonates through time which is attributed to biogenic processes and increased

primary productivity of diatoms. Diatoms are primary prey of *Protoperidinium* species which were found to be highly abundant in the cores studied.

The geochemical scenarios on metal distribution and sourcing in space and time persisted, at least, during the last 10 years of the bay which show the well-defined distribution of potentially mobile metal loads in the bay's sediment system. This pattern may be salient to the correlation of the lateral distribution of the cysts and the metals in the sediments of the bay and the identification of sources of metals.

RADIONUCLIDE STUDIES OF SEDIMENTS - POSTERS

Determination of accumulation rates for organic carbon, carbonate, metal and sediment on the eastern continental margin of the Black Sea sediments during the Late Holocene

Güngör, E.[a], M.N. Çağatay[b], N. Güngör[a], B.G. Göktepe[a]

[a] Çekmece Nuclear Research Center,
Atatürk Airport, Istanbul,
Turkey

[b] Istanbul Technical University,
Geology Department,
Ayazağa, Istanbul,
Turkey

Accumulation Rates (ARs) in Black Sea samples for carbonate, organic carbon and some metals based on ^{210}Pb dating are determined and their interpretation is presented. The samples were collected during the international cruise (2000) organized by the IAEA as a part of the Marine Environmental Assessment of the Black Sea Region, Technical Cooperation Project RER/2/003. In this study one core (BS-23) located on the eastern continental margin of the Black Sea in water depth of 2168 m is examined. The sediment in this core consists of two units which are, from top to bottom, laminated coccolith marl and micro laminated sapropel units rich in organic carbon [3]. These units were formed after the flooding of the lacustrine Black Sea basin by Mediterranean waters via the Istanbul Strait at 7150 yrs BP [1, 2]. The total average AR for the last 125 years for this site was found to be 40.15 g.m^{-2}.yr^{-1} (26 cm.kyr^{-1}).

Considering the corrected AMS ^{14}C ages, the average linear sedimentation rate for core BS-23 over 2000 yrs is found to be about 1.5 times lower than those for the last 125 yrs determined from the ^{210}Pb data. This suggest that the sediment accumulation rate has significantly increased, probably in the last few hundred years, as a result of man's impact [4].

The average AR_{TOC} and AR_{CaCO3} in the upper three cm. of the core (Unit I) representing the last 125 yrs are 1.84 and 15.82 g.m^{-2}.yr^{-1}, respectively, whereas MAR_{TOC} and MAR_{CaCO3} values in Unit II are 2.79 and 3.74 g.m^{-2}.yr^{-1}, respectively. The high AR_{CaCO3} in Unit I is caused by the coccolithophore *E. huxleyi* which forms the white laminae (Table I).

Metals (Ba, Cu, Pb, Zn) show sharp increases in concentrations in the last about 50 years. In the upper part of the sediment Ba enrichment is 4-5 times the background, attesting to the increased eutrophication of the Black Sea. Similarly Pb, Zn and Cu exhibit very sharp increases in the top part of the core, reaching more than twice the background values and attesting to high metal inputs into the Black Sea during the last half century (Fig. 1).

Table I. Accumulation Rates (AR) for carbonate and organic carbon in core BS-23

UNIT (Section)	TOC (wt %)	CARBONATE (wt %)	SR+ (cm/kyr)	AR_{SED} (g.m^{-2}.yr^{-1})	AR_{TOC} (g.m^{-2}.yr^{-1})	AR_{CaCO3} (g.m^{-2}.yr^{-1})
Unit I	5.48	41.05			1.84	15.82
(0-3.5 cm)	4.38-6.84	29.2-49.2	26	40.15	1.15-2.32	4.92-24.15
Unit II	10.71	13.83			2.79	3.74
(31-37 cm)	8.14-12.21	5.77-24.59	16		2.10-3.32	1.43-7.20

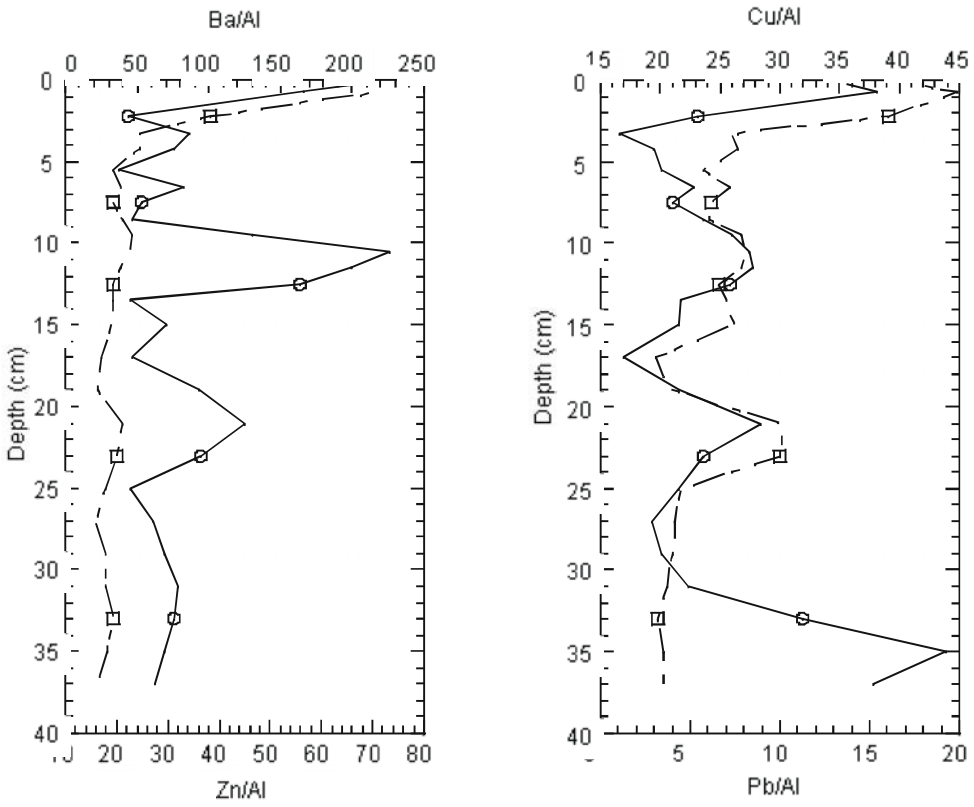

FIG. 1. Variation of Ba, Zn, Cu and Pb metal values versus depth.

ACKNOWLEDGEMENT

This work performed within the frame work of the IAEA Project RER/2/003 Marine Environmental Assessment in the Black Sea Region.

REFERENCES

[1] RYAN, W.B.F., PITMAN III, W.C., MAJOR, C.O., SHIMKUS, K., MOSKALENKO, V., JONES, G.A., DINITROV, P., GÖRÜR, N., SAKINÇ, M., YÜCE, H., An abrupt drowning of the Black Sea shelf, Mar. Geol. **138** (1997) 119-126.

[2] ÇAĞATAY, M.N., Geochemistry of the late Pleistocene-Holocene sediments of the Black Sea basin, In: Beşiktepe et al. (Eds.) Environmental Degradation of the Black Sea Challenges and Remedies, NATO Advanced Study Ser., Kluwer Academic Publishers (1999) pp. 9-22.

[3] ARTHUR, M.A., DEAN, W.E., Organic-matter production and preservation and evolution of anoxia in the Holocene Black Sea, Paleoceanography **13** (1999) 395-341.

[4] BUESSELER, K.O., BENITEZ, C.R., Determination of mass accumulation rates and sediment radionuclide inventories in the deep Black Sea, Deep-Sea Res. **41** (1993) 1605-1615.

Distribution of radionuclides and trace elements in marine sediments from coastal areas of Japan

Honda, T.[a], E. Suzuki[b]

[a] Atomic Energy Research Laboratory,
Musashi Institute of Technology,
Kawasaki,
Japan

[b] National Research Institute of Fisheries Science,
Yokohama,
Japan

^{137}Cs, ^{210}Pb and trace elements such as Sc, Mn, Sb, lanthanoids, Th and U were determined by gamma-spectrometry, instrumental neutron activation analysis (INAA) and low background beta-counting, coupled with radiochemical separation in marine sediment core samples (13-31 layers, 10cm φ, 2 cm thickness each) collected from 11 coastal areas (15 stations, 42°19′N-31°27′N, 141°19′E-130°30′E, 16-455 m of water depth) of Japan mainly facing the Pacific from 1985 to 1991.

In this work, the concentrations and inventories of ^{137}Cs, the ^{210}Pb sedimentation rates, the origin of the sediments and the sedimentary environment are reported using those data and vertical profiles obtained in the coastal areas of Japan.

The results obtained in this study are summarized as follows:

(1) The ^{137}Cs concentrations in the surface layer were 5.3 (1.9-10.8) Bq/kg-dry and estimated inventories at the sampling date were 697 (191-1441) Bq/m^2. These inventories are somewhat larger than those obtained from nearshore around Japan [1]. It can be seen that ^{137}Cs could be easily carried to the seabed and deposited there since the sediments analyzed in this work were collected from shallow areas compared with others. The UNSCEAR report (1993), however, estimates of the integrated deposition densities of 3.7-5.2 kBq/m^2 in 1990 for ^{137}Cs for latitudes of 30°-50°N and the observed inventories are rather smaller than those deposition densities because of the lack of those data for the water columns.

(2) The ^{210}Pb sedimentation rates were 0.361 (0.047-0.702) g/cm^2/y, which were clearly larger than 0.091 (0.049-0.140) g/cm^2/y (n=12) obtained from the coastal sediments (270-1860 m of water depth) facing the Japan Sea [1]. It seems to be caused by the difference of the water depth and topography of the seabed.

(3) In general, the abundance of Th is apparently higher in granitic rocks than andesitic rocks. On the contrary, that of Sc is higher in mafic rocks such as basalt. The Th/Sc ratio, therefore, reveals the proportion of granitic rocks to mafic rocks and gives important information of the origin of the sediments [2]. The Th/Sc ratios ranged from 0.0409 to 1.40 including six stations exceeded 0.5 in the surface layers. Those six stations are all in western Japan, which indicates that the origin of these sediments is mainly granitic detritus. Conversely, suggesting that in eastern Japan is mainly mafic since the lower Th/Sc ratios.

(4) The concentrations of Mn and Sb in the surface layer from Kagoshima Bay (31°27′N, 130°38′E) are several to ten times as large as those from other coastal areas of Japan. This fact suggests that those elements have been supplied from the ejecta from a volcano (Mt. Sakurajima) and the hydrothermal venting from a submarine volcano (Wakamiko Caldera) in the Bay.

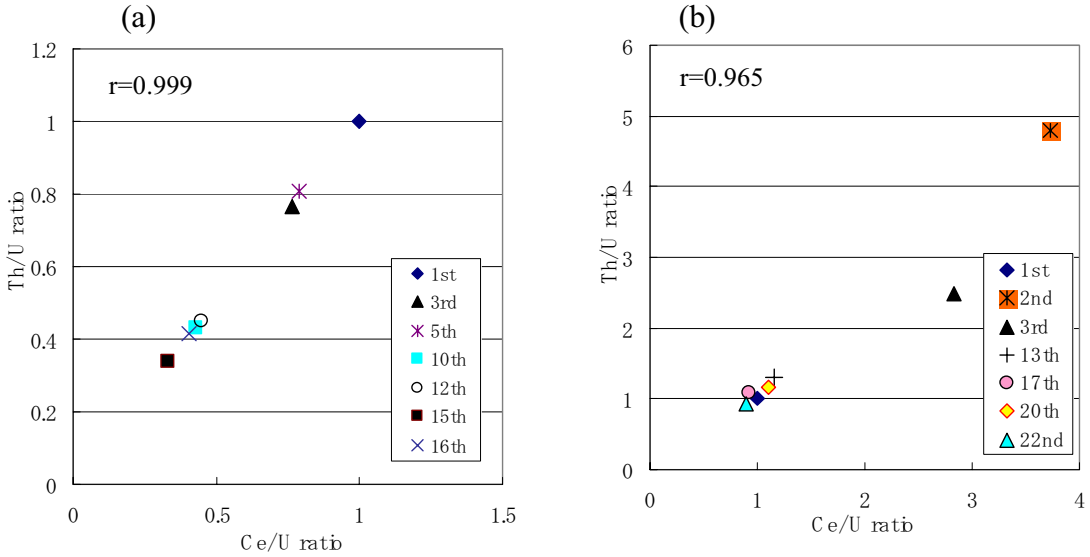

FIG. 1. Th/U-Ce/U plots (expressed in relative to a surface layer) in (a) Kagoshima Bay and (b) Shimabara Bay sediment cores. The symbol shows the order from the surface in the cores.

(5) In reducing conditions, the concentrations of Ce and Th would decrease in the sediment cores, whereas those of U would increase on the basis of the standard electrode potential. Both the Th/U ratios and the Ce/U ratios in the cores are expected to decrease in reducing conditions, conversely increase in oxidizing conditions. The Th/U-Ce/U plots expressed in relative to a surface layer are shown in the cores of (a) Kagoshima Bay and (b) Shimabara Bay (32°41′N, 130°30′E) as typical examples in Fig.1. As shown in Fig.1, in the cores of Kagoshima Bay (a), both the Th/U ratios and the Ce/U ratios except for a surface layer are fairly smaller than the unit (1.0) and decrease as going downward. Therefore, it is indicated that the cores below the surface are in reducing conditions, particularly in the lower cores. On the other hand, clearly that the second and third layers in (b) the Shimabara Bay cores are in strong oxidizing conditions since both ratios are still higher than the unit. The Th/U-Ce/U plot, *Honda plot*, introduced in this work is extremely useful to estimate the sedimentary environment such as redox conditions [2].

REFERENCES

[1] SUZUKI, E., ^{207}Bi and ^{137}Cs in Nearshore Marine Sediments. 1. Distribution of ^{207}Bi and ^{137}Cs in coastal marine sediments collected from the Japan Sea, Radioisotopes **42** 9 (1993) 503-510.

[2] HONDA, T., KIMURA, K., Distribution and Behavior of Major and Trace Elements in Tokyo Bay, Mutsu Bay and Funka Bay Marine Sediments, Bull. Soc. Sea Water Sci. Japan **57** 3 (2003) 166-180.

Sedimentation rates in reservoir and gullies derived from ^{137}Cs depth profile in the Moldavian Tableland - Romania

Margineanu, R.M.[a], I. Ionita[b], D. Gheorghiu[a]

[a] National Institute of R&D for Physics and Nuclear Engineering, IFIN-HH,
Bucharest,
Romania

[b] Faculty of Geography,
University of Jassy,
Romania

The Moldavian Plateau located in the Eastern Romania and extending about 25,000 square kilometers is considered as the broadest and most typical plateau of the country.

The radioactive fallout that has occurred after the Chernobyl accident was characterized by complex meteorological conditions in May 1986 [1, 2]. Consequently, the contamination of the soil surface was very non-uniform. One cannot possibly assume that, even for small areas of a few square kilometers, the initial deposition was uniform and subsequently the variations observed in inventory were caused by migration with and/or within the soil. Consequently, one should work on the assumption that, generally, the initial deposition remains unknown, practically everywhere in the area of interest. In special situation like those arising in the gullyheads, floodplain and reservoirs, from the total inventory of ^{137}Cs, the initial deposition due to the Chernobyl accident can be derived [3, 4].

In each investigated area, a pit was dug from which the samples were taken from surface up to 100-300 cm deep with an increment of 5 cm [5]. After conditioning, the samples were analyzed in the laboratory, using a Canberra MCA S100 system equipped with a Ge(Li) detector. The ^{137}Cs present in soil comes first from direct deposition and second from the redistribution of contaminated soils within watershed.

Fitting the profile distribution of ^{137}Cs in reservoir sediment and gully with a sum of gaussian functions, the position of the Chernobyl peak within sediments and the contribution of eroded soil to the total ^{137}Cs inventory in the investigated area was determined. The fitting function used is:

$$y = y_0 + \sum_i \frac{A_i}{w_i \sqrt{\pi/2}} e^{-2\frac{(x-x_{ic})^2}{w_i^2}}$$

In the investigated gullies and reservoirs, the profile distribution of ^{137}Cs in sedimented soil shows a complex pattern, the depth of ^{137}Cs due to Chernobyl deposition varies from 10 cm to 140 cm. The position of the maximum activity of ^{137}Cs in soil depends on erosion rate in the watershed.

In the area, the initial deposition from the Chernobyl accident ranges between 2 to 46 kBq/m^2. The data regarding some of the investigated reservoirs and gullies are summarized in Tables I and II. The position of maximum of the ^{137}Cs specific activity from Chernobyl deposition shows where the surface of bottom sediment was in 1986. The sedimentation rates for the investigated reservoirs are of 0.8 - 12 cm/year and for gullies from 0.8 – 3 cm/year. ^{137}Cs demonstrates to be very suitable for the assessing of long term erosion and sedimentation processes in the environment.

Table I. Sedimentation rates in Moldavian tableland reservoirs

Reservoir	River Basin	Chernobyl depth (cm)	Sedimentation rate (cm/year)
Bibiresti	Racatau	69.9	5.8
Antohesti	Berheci	57.3	4.8
Hutu-Gaiceana	Berheci	70.5	5.9
Puscasi	Racova	142.7	11.9
Pungesti-Garceni	Racova	30.9	2.6
Ras-Craesti	Barlad	35.0	2.9
Solesti	Vaslui	81.3	6.8
Popesti	Scobalteni	9.6	0.8
Doroscani	Scobalteni	23.0	1.9
Podul Iloaiei	Bahluiet	38.0	3.2
Ichimeni	Baseu	26.3	2.2

Table II. Sedimentation rates in moldavian tableland gullies

Gully	Gullyhead	Chernobyl depth (cm)	Sedimentation rate (cm/year)
Scranghita	4	8.4	0.8
Rapa Albastra	1	34.7	2.9
Gornei	2	12.1	1.1
Valea Timbrului	10	24.6	2.1

ACKNOWLEDGEMENTS

The authors express their gratitude to the IAEA, Vienna for its permanently support. The investigation was carried out during 1996 – 2000 in the framework of the IAEA Coordinated Research Program entitled “Soil Erosion and Sedimentation Assessment Studies by Environmental Radionuclides and their Application to Soil Conservation Measures”.

REFERENCES

[1] GALERIU, D., ONCESCU, M., MOCANU, N., “Radionuclide in soil: migration and dose assessment”, Seminars in Biophysics (FRANGOPOL, P.T., MORARIU, V.V., Eds), Vol. 5, CIP-Press, Central Institute of Physics, Bucharest (1988) 79-85.

[2] PAUNESCU, N., MARGINEANU, R., IORGULESCU, A., ^{90}Sr and ^{137}Cs fallout from Chernobyl in the Bucharest-Magurele area during 1986-1987, J. Radioanal. Nucl. Chem. (Letters) 128/4 (1988) 263-271.

[3] WALLING, D.E., QINPING, H.E., Interpretation of caesium-137 profiles in lacustrine and other sediments: the role of catchment-derived inputs, Hydrobiologia 235/236 (1992) 219-230.

[4] IZRAEL, YU.A., et. al., Atlas of caesium deposition on Europe after Chernobyl accident, CG-NA-16733-29-C (1998).

[5] IONITA, I., MARGINEANU, R., Assessment of the Reservoir Sedimentation Rates from ^{137}Cs Measurements in The Moldavian Plateau, Third IAEA RCM “Erosion and sedimentation processes assessment”, Barcelona 4-8 Oct. 1999, Spain.

Sedimentation rates in the Eastern Baltic Sea based on lead-210 dating

Mazeika, J.[a], R. Radzevicius[a], R. Dusauskiene-Duz[b]

[a] Institute of Geology and Geography,
Vilnius,
Lithuania

[b] Institute of Botany,
Vilnius,
Lithuania

Recently there has been renewed focus on the Baltic Sea. Not only because the Baltic is one of the world's largest estuarine systems but also because it is an area of focal importance for 15 countries as a transportation channel, recreational area and fishing ground. Study area is attributed to the Eastern Baltic Sea and comprises the Gulfs of Finland and Riga as well as the eastern Baltic proper.

Short Niemistö-type gravity corer (with inner diameter of 54 mm) was used to take the sediment cores (16 stations) mostly in 1989-1999. Sediment cores were usually sliced onboard into slices of different thickness (from 2 cm in recent cores to even 10-15 cm in earlier cores). Measurements of lead-210 activity in dried sediment samples were performed by two methods. The ^{210}Pb in earlier cores (1978-1992) was measured by low level beta counting of its daughter ^{210}Bi after classical radiochemical separation of ^{210}Pb carriers from the sample material. The cores of 1999 were examined by direct gamma-ray spectrometry using well-type detector (GWL-series) with a sensitive volume of 170 cm^3 and the well inside the germanium crystal of 16 mm. The calibration procedure of the system used in this study is described in [1]. A number of naturally occurring radioisotopes from the ^{238}U and ^{232}Th decay series, as well as man-made radioisotopes, e.g. ^{137}Cs, were determined.

Using thickness of wet sediment slices from earlier cores and unsupported ^{210}Pb activities, a constant rate of supply (CRS) model [2] was applied to calculate mean sedimentation rate and to construct a sediment chronology for the past 200 years of sedimentation. The unsupported ^{210}Pb activity was calculated by subtracting the supported activity, which was estimated by statistical calculations of total ^{210}Pb activity distribution in the lower slices. Using bulk sediment densities and unsupported ^{210}Pb activities, a constant rate of supply (CRS) model with variations [3] was applied to evaluate recent sedimentation for cores of 1999.

The unsupported ^{210}Pb activity was calculated by subtracting the supported activity, which was estimated from ^{226}Ra or any other gamma-emitting decay product (^{214}Pb). The ^{210}Pb dating results were compared and adjusted according to the occurrence of known ^{137}Cs main markers (Chernobyl, nuclear bomb testing) (Fig. 1) and are presented in Table I.

Sedimentation rates estimated vary between 0.3-2 mm/a with tendency to increase (3-7 mm/a) mainly after 1960. The similar values in adjacent areas are given in [4] (1-2 mm/a, sometimes 4-6 mm/a) and in [5] (0.2-4 mm/a, sometimes till 29 mm/a). Recent sedimentation is mainly determined by basement topography, the flux of material from rivers, coastal and submarine erosion of old sediments, plankton production, and by the hydrography (waves and currents) as the driving force of sediment transport.

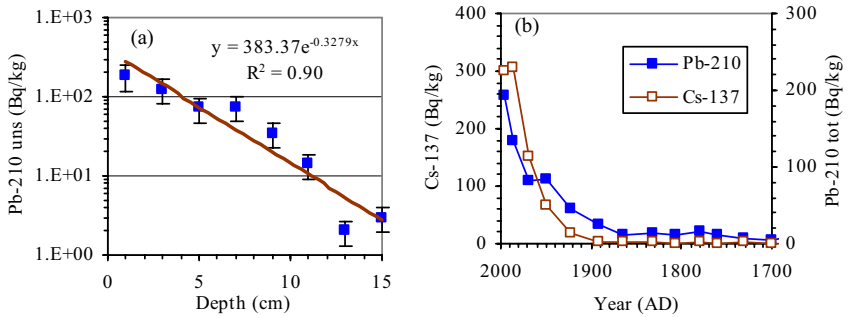

FIG. 1. Unsupported ^{210}Pb plotted vs. depth of the core (a) and total ^{210}Pb and ^{137}Cs plotted vs. calendar years (b) for gravity core 21/01.

Table I. Sedimentation rates estimated by lead-210 for short gravity cores

Core (original number)	Latitude	Longitude	Sea depth (m)	Core length (cm)	Slice No. in core	Prevailing lithology of mud	Mean sedimentation rate (mm/a)
17/1978	56°42'N	19°52'E	130	40	4	Fine aleuritic	2.7
33/1978	54°45'N	19°16'E	96	60	6	Pelitic	4.3
01/1986	59°37'N	27°05'E	70	200	14	Aleuritic-pelitic	1.5
07/1986	59°50'N	24°50'E	68	40	6	Pelitic	1.3
02/1987	59°50'N	25°38'E	77	24	6	Pelitic	1.2
05/1987	59°28'N	23°00'E	90	21	7	Pelitic	1.2
07/1987	57°31'N	20°34'E	145	20	6	Pelitic	1.2
10/1987	59°41'N	26°38'E	70	30	7	Pelitic	2.5
12/1987	59°40'N	25°24'E	93	13	7	Pelitic	0.3
14/1987	59°31'N	24°23'E	60	35	7	Fine aleuritic	2.5
13/1988	59°44'N	24°24'E	72	50	13	Aleuritic-pelitic	1.0
17/1988	59°54'N	26°37'E	64	70	9	Aleuritic-pelitic	6.5
13/1992	59°39'N	26°26'E	45	15	5	Aleuritic-pelitic	1.5
16/1992	59°28'N	23°57'E	75	17	6	Fine aleuritic	2.0
21/01-99*	55°34'520N	20°30'400E	68	41	20	Fine aleuritic	1.3
12/01-99*	55°36'970N	20°30'390E	64	33	16	Fine aleuritic	1.0

* ^{210}Pb dating results adjusted according to ^{137}Cs markers.

The spatial distribution of bed sediment types reflects the temporal integration of the various environmental influences. The fine-grained and light material (silt, clay, organic matter) is being deposited under low energy conditions, which are in the major basins. This context follows from the available sediment maps of the Baltic Sea.

REFERENCES

[1] GUDELIS, A., et al., Efficiency calibration of HPGe detectors for measuring environmental samples, Environ. Chem. Phys. **22** 3-4, Vilnius (2000) 117-125.

[2] ROBBINS, J.A., "Geochemical and geophysical applications of radioactive lead isotopes", Biogeochemistry of Lead (NRIAGU, J.O., Ed.) (1982) 285-393.

[3] BOLLHÖFER, A., MANGINI, A., LENHARD, A., WESSELS, M., GIOVANOLI, F., SCHWARZ, B., High-resolution ^{210}Pb dating of Lake Constance sediments: stable lead in Lake Constance, Environ. Geology **24** (1997) 267-274.

[4] KUNZENDORF, H., EMEIS, K-C., CHRISTIANSEN, C., Sedimentation in the central Baltic Sea as viewed by non-destructive Pb-210 dating, Danish J. Geogr. (1998) 1-9.

[5] HELCOM, Intercomparison of sediment sampling devices using artificial radionuclides in Baltic Sea sediments, the MOSSIE Report, Baltic Sea Environ. Proc. **80** (2000) 76 pp.

Residence time and sedimentation regime in Cienfuegos Bay, Cuba, with the use of ^{210}Pb and ^{137}Cs isotopes

Muñoz Caravaca, A., C. Alonso-Hernández, M. Díaz Asencio

Centro de Estudios Ambientales de Cienfuegos,
Cienfuegos,
Cuba

The combined atmospheric flux of ^{210}Pb and dating techniques based on natural and anthropogenic radionuclides ^{210}Pb and ^{137}Cs were applied to the study of the residence times and sedimentation regime in Cienfuegos Bay, Cuba.

Measurements of monthly atmospheric flux of ^{210}Pb in Cienfuegos, were conducted over a period of 3 years (1999 - 2004). The mean annual flux of ^{210}Pb for this period was 0.65 ± 0.05 Bq.cm^{-2}.yr^{-1}. Good agreement between atmospheric flux of ^{210}Pb and precipitations events are observed.

The accumulation rate, estimated through the ^{210}Pb dating technique, showed an increase during the last 40 years [1]. The recent sediment accumulation rates (0.40 - 0.45 g.cm^{-2}.y^{-1}) are almost double those estimated before 1965 (0.15 to 0.20 g.cm^{-2}.y^{-1}). The ^{210}Pb profiles contained significant deviations from a simple exponential decline and showed abrupt variations in the ^{210}Pb activity between 1966-1970. These irregularities match closely periods of anthropogenic changes (regimentation of the Arimao and Caonao rivers in the late 60s and early 70s) and exceptional natural events (Hurricane "Camille" in 1969 and the intense rainfall of 1988) which occurred in Cienfuegos. The ^{137}Cs and chlorite minerals profiles validate the results obtained from ^{210}Pb dating and confirm the effect of exceptional events and changes in the natural hydrological regimen of the bay in the past.

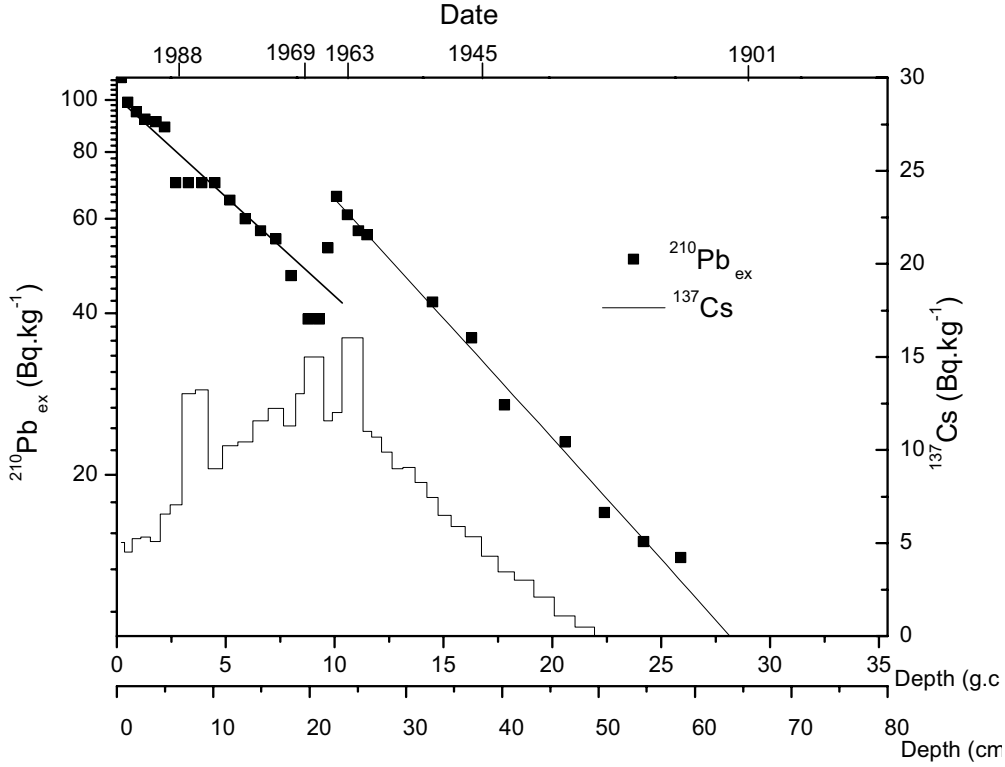

The residence time of ^{210}Pb in water column is near 20 days. This result could be use as a indicator of exchange processes between bay and the Caribbean Sea. Although ^{210}Pb is a non conservative tracer, its residence time express that this hydrodynamic property for Cienfuegos bay could be greater than for ^{210}Pb because this isotope has more losing factor, like radioactive decay and those concerning the sedimentation processes. Previous studies of this exchange processes based on tidal prims method indicated residence times of order of 90 days for a conservative pollutant [2].

The results obtained are applied for the Environmental Management Program of Cienfuegos Bay.

REFERENCES

[1] ALONSO-HERNANDEZ, C., et al., Recent changes in sedimentation regime in Cienfuegos Bay, Cuba, as inferred from ^{210}Pb and ^{137}Cs vertical profiles (in press).

[2] MUÑOZ CARAVACA, A., et al., Modelling transport processes in Cienfuegos Bay, Cuba (in press).

Baseline of ^{137}Cs and natural radionuclides in sediments along the Algerian coast

Noureddine, A., M. Menacer, R. Boudjenoun, A. Hammadi, M. Benkrid, M. Maache

Centre de Recherche Nucléaire d'Alger,
Algiers,
Algeria

The main sources of anthropogenic radionuclides are atmospheric fallout from nuclear weapons tests and discharges from nuclear reprocessing plants, from power reactors and nuclear accidents [1-3]. The major source is debris from atmospheric nuclear tests as global fallout, and fallout from the Chernobyl accident [4]. The aim of this work is to define a baseline of natural and anthropogenic radionuclides in sediment along the Algerian coast. A sampling campaign was organised during Sept.-Oct. 1999 by the laboratory of radiological impact studies staff (LEIR / CRNA), on board the M.S. Benyahia research vessel belonging to the "Institut des Sciences de la Mer et de l'Aménagement du Littoral" (ISMAL), to collect surface sediments and a sediment core along the Algerian coast. A total number of 41 superficial sediment were collected each 25 km along the coast from Ghazaouet station (N35°10.90-E 02°55.857) in the western part to El-Kala in the eastern part (N36°59.49-E08°26.93), at different depths ranging from the surface to 170 m, using a Van Veen Grab type. In addition to that, collection of a sediment core was carried out using a box corer at Annaba station in the eastern coast, at a depth of around 50 m. Multiparameter probe was also used to determine vertical profiles of temperature, salinity and pH in water column, where the sediment core was collected. On board, the sediment core was cut with a metallic sheet each 2 cm until a depth of 22 cm. All sediment samples were then stored in a freezer to be later analysed in the laboratory.

Samples were oven dried at 80°C, crushed, homogenised and put in appropriate plastic beakers. They were analysed by gamma spectrometry using a HP germanium detector. A computerised multichannel analyser (4096 channels), with interwinner software, was used to collect and analyse the spectra. Samples were separately put close in contact with the detector and counted to give statistically reliable results (24-48h). Detection efficiency was determined by preparation of a standard sample in the same conditions than samples, in which a liquid radioactive solution of ^{152}Eu was injected.

CTD data (temperature, salinity and pH) were recorded in the water column of the sediment core sampling location. Concentration of ^{137}Cs in surface sediment ranged from 0.29 ± 0.04 to 13.12 ± 0.50 Bq/kg d.w., with a mean value of 5.23 ± 0.21 Bq/kg d.w. Surface sediments were sampled from west to east from several depths starting from 13 m to 170 m, collecting therefore different sediment types

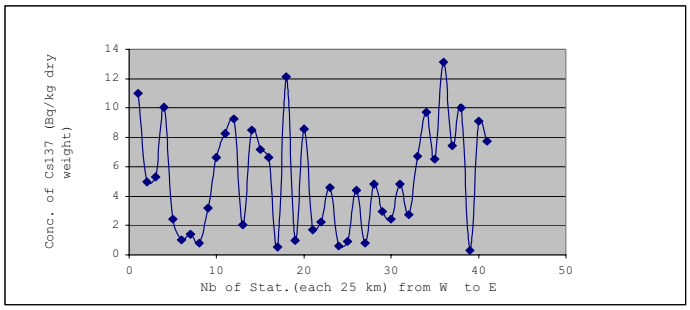

FIG. 1. ^{137}Cs concentration in surface sediment collected each 25 km along the Algerian coast.

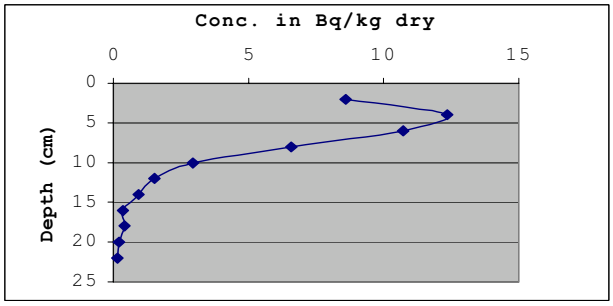

FIG. 2. ^{137}Cs profile in sediment core.

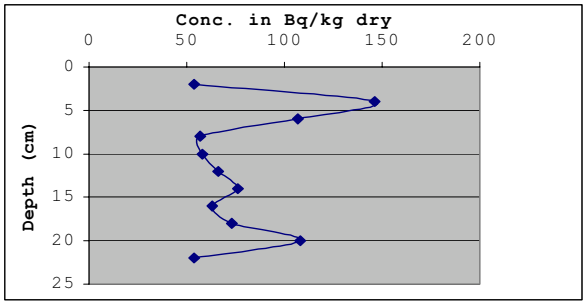

FIG. 3. ^{210}Pb profile in sediment core.

with a varied grain size. Variations of ^{137}Cs concentration in Bq/kg d.w. in surface sediment from the west to the east is seen to be slight. Concentration of ^{137}Cs is found to be depending on the nature of sediment and the perturbation of the sampling location (depth). According to these two parameters, ^{137}Cs concentration is relatively constant with possibly a slight increase from west to east. Comparison of these results (mean value: 5.23 ± 0.21 Bq/kg d.w.) with those obtained by other authors (mean value: 4.6 Bq/kg, for the whole Mediterranean Sea) indicates that there is similarity with small variation [5, 6], as shown in Fig. 2. Concerning ^{137}Cs in the sediment core, results are summarised in Table 2. Concentration levels ranged from 0.16 ± 0.014 Bq/kg d.w. to 12.36 ± 0.63 Bq/kg d.w. A ^{137}Cs peak was observed at 4 cm from the top with a concentration of 12.36 ± 0.63 Bq/kg d.w., decreasing to a concentration of (0.16 ± 0.014) Bq/kg d.w. at the bottom of the sediment core (22 cm). The corresponding profile is shown in Fig.3 and is similar to other profiles documented by other authors, with the exception of the ^{137}Cs peak position against depth and the concentration value [7-10]. The ^{137}Cs peak is believed to de due to the contamination produced by the Chernobyl accident. Concentration of ^{40}K, with a mean value of (370 ± 13) Bq/kg d.w., when plotted against each sampling station along the Algerian coast, show a very similar profile to that of ^{137}Cs. For the other radionuclides, equilibrium is seen between ^{214}Pb and ^{214}Bi, giving a concentration range of (5.53-37) Bq/kg d.w. for ^{214}Pb and (6.5-33) Bq/kg d.w. for ^{214}Bi, with mean values of 20.8 and 18.6 Bq/kg d.w. for ^{214}Pb and ^{214}Bi, respectively. The obtained results were compared to data reported by other authors and found to be in the same range [5, 11]. Regarding the sediment core, natural radioactivity was also determined through ^{40}K, uranium and thorium series. Values are higher than those obtained in surface sediment, mainly due to the nature of sediment which is more fine grain sized (muddy). In addition to that, ^{210}Pb concentration was determined and found to be in the range of 54 to 146 Bq/kg d.w., with a maximum value at 4 cm from the top. The ^{210}Pb profile is shown in Fig. 4. We can conclude that the Algerian coast was not directly affected by Chernobyl accident, and the measured ^{137}Cs is mainly due to nuclear global fallout. However, if there is even a low contamination, it should have resulted, after dilution, transport and distribution, from other areas contaminated by the Chernobyl accident.

The average concentration of ^{137}Cs is 5.2 ± 0.2 Bq/kg dry weight, close to values presented in the Mediterranean sea by other authors. A slight peak of ^{137}Cs is observed in the sediment core at about 4 cm at Annaba station, and is believed to be that of Chernobyl accident. Radioactive contamination is believed to represent mainly global fallout. Further studies should be carried out using more accurate equipment to achieve deeper depth. This is already undertaken under the IAEA regional project RAF/7/004 for the evaluation of contamination in the south Mediterranean Sea.

ACKNOWLEDGEMENTS

The authors wish to thank ISMAL staff represented by their Director M. Boulahdid, the scientific team and the crew who participated to the cruise, on board of M.S. Benyahia ISMAL research vessel, with all its facilities. Thanks are also due to the IAEA for the acquisition of sampling and counting equipment's through the TC projects ALG/2006 - 1995-1997, which were used in this oceanographic campaign and work.

REFERENCES

[1] BURTON, J.D., "Radioactive nuclides in the marine environment", Chemical Oceanography, 2nd ed. **3** (RILEY, J.P., SKIRROW, G.S., Eds), Academic press, London (1975).

[2] OECD, Marine Radioecology, the cycling of artificial radionuclides through marine food chains, Hamburg, 20th - 24th September 1971.

[3] NOUREDDINE, A., BENKRID, M., HAMMADI, A, BOUDJENOUN, R., MENACER, M., KHABER, A., KECIR, M.S., Radioactivity Distribution in Surface and Core Sediment of Central Part of the Algerian Coast; An Estimation of the Recent Sedimentation Rate, Mediterranean Marine Science **4** 2 (2003) 53-58.

[4] LEE, S.H., GASTAUD, J., POVINEC, P.P., HONG, G.H., KIM, S.H., CHUNG, C.S., LEE, K.W., PETTERSON, H.B.L., Distribution of plutonium and americium in the marginal seas of the northwest Pacific Ocean, Deep-Sea Res. II **50** (2003) 2727-2750.

[5] UNEP, Assessment of the state of pollution of the Mediterranean Sea by radioactive substances, Map Technical Reports Series 62, Athens (1992) 60 pp.

[6] HOLM, E., FUKAI, R., WHITEHEAD, N.E., Radionuclides in macroalgae at Monaco following the Chernobyl accident (Int. Conf. Environ. Radioactivity in the Med. Area, Baecelona, 1988) 439-451.

[7] SHOLKOVITZ, E.R., MANN, D.R., The pore water chemistry of ^{239,240}Pu and ^{137}Cs in sediments of Buzzards Bay, Massachussets, Geochim. Cosmochim. Acta **48** (1984) 1107-1144.

[8] IAEA - MEL, Monaco, Biennal report, 1989-1990.

[9] IAEA - MEL, Monaco, Report of recent activities (1994).

[10] IAEA, Training course series N° 7, Strategies and Methodologies for Applied Marine Radioactivity Studies, Vienna (1997).

[11] Natural Background radiation in the United States, recommendations of the Natural Council on radiation Protection and Measurements **15** (1975).

$^{197}Hg^{g}$ as radiotracer to study mercury methylation and demethylation processes in sediments and soils

Ribeiro Guevara, S.[a], M. Arribére[a], V. Jereb[b], S. Pérez Catán[a], M. Horvat[b]

[a] LAAN, Centro Atómico Bariloche,
Comisión Nacional de Energía Atómica,
Argentina

[b] Department of Environmental Sciences,
Jozef Stefan Institute,
Ljubljana,
Slovenia

The use of radioisotopes to trace different transport and transformation processes is widespread; in the case of mercury the most frequently used radiotracer is ^{203}Hg. However, when adequate facilities are available $^{197}Hg^{g}$ can be also employed successfully, as it was demonstrated in mercury methylation/de-methylation in soils and fresh water sediments performed at the Department of Environmental Sciences, Jozef Stefan Institute, and LAAN, Centro Atómico Bariloche. $^{197}Hg^{g}$ ($T_{½}$=64.14 h) can be produced in a research nuclear reactor by irradiating non-enriched Hg targets with thermal neutrons (for the $^{196}Hg(n,\gamma)^{197}Hg^{g}$ reaction σ_{th}=3080±180 b, production with epithermal neutrons is not relevant: I_{γ}=413±15 b [1]). $^{197}Hg^{m}$ ($T_{½}$=23.8 h) is also produced, and 93 % of its decay feeds the ground state, but with 30 times less probability (σ_{th}=109±6 b and I_{γ}=58.9±2.4 b [1]). $^{197}Hg^{g}$ has a production rate, for short irradiation periods, about 50 times higher than that of ^{203}Hg, and hence it is possible to produce it with high specific activity in shorter irradiations, in non-high flux reactors (10^{12} to 10^{13} $n.cm^{-2}.s^{-1}$), using non-enriched Hg. Another advantage of the use of $^{197}Hg^{g}$ to trace processes is that, because of its short half life, the cleaning of devices and tools of the $^{197}Hg^{g}$ contamination associated to their use or caused by accidents, can be done just letting the tracer to decay away, hence assuring no interference from previous experiments.

For the methylation/de-methylation experiments in soils and sediments mentioned in the last paragraph, $HgCl_2$ was irradiated to produce the $^{197}Hg^{2+}$ tracer, while $HgCH_3Cl$ was used to produce $CH_3{}^{197}Hg^{g}$. In both cases the tracer is ready to be used after a few hours of cooling time, to allow ^{38}Cl ($T_{½}$=37.24 m) to decay. $HgCl_2$ was dissolved in 3.2% HNO_3 after irradiation, and $HgCH_3Cl$ was dissolved in isopropanol. Since the $HgCH_3Cl$ decomposes during irradiation a purification has to be done immediately before each application. $HgCH_3^{+}$ and Hg^{2+} in 6M HCl solution were separated by anion exchange chromatography (Dowex 1x8 resin, Cl-form, 100-200 mesh) using minimal light conditions. The $HgCH_3^{+}$ is then collected and the solution neutralized for further tracer experiments.

The more relevant emissions associated to $^{197}Hg^{g}$ decay are X-rays 67.0 keV (21%), 68.8 keV (35%) 77.9 keV (12%) and 80.4 keV (3.3%), and γ-ray 77.3 keV (18%) [2]. Spectra obtained with HPGe detectors allow, in general, discriminating three main peaks by using usual peak fitting programs, namely 67.0 keV, 68.8 keV, and 77.3+77.9 keV. But the determination of areas manually in two regions, one including 67.0 and 68.8 keV X-rays, and the other including 77.3, 77.9, and 80.4 keV emissions, provide also accurate results since these kind of studies imply relative measurements with respect to a reference. Well, coaxial, and planar HPGe detectors were used in the experiments mentioned before.

Experiments consisted of amending triplicates sediment and soil samples, and incubating with labelled Hg for different time periods. In addition, blanks and samples in which microbial activity was inhibited by flash freezing just after inoculation ("killed control samples") were also assayed. $HgCH_3^{+}$

was extracted using toluene, which was then dried using anhydrous Na_2SO_4 [3]. A more extensive extraction procedure with thiosulphate was performed in some methylation experiments with lake sediments, in order to examine the possibility of Hg^{2+}carry-over. Total Hg inoculated in methylation experiments with sediments ranged from 50 to 100 $ng.g^{-1}$ wet sediment. The specific activity can be further improved with proper optimisation of the irradiation; for our experiments design an inoculation of 5-10 $ng.g^{-1}$ wet sediment can be achieved. The total Hg amounts of labelled Hg inoculated for the experiments performed are comparable to the amounts amended when ^{203}Hg and other non-radioactive tracers are used for this purpose. Methylation experiments performed on lake sediments by incubation of labelled Hg^{2+} showed $^{197}Hg^{g}CH_3^{+}$ recoveries as low as 0.105 ± 0.020 % to 0.133 ± 0.018 % for toluene extraction on "killed control samples", and 0.0354 ± 0.0078 % to 0.0716 ± 0.0035 %, also on "killed control samples" using the more extensive extraction (uncertainties reported are the standard deviations of triplicates).

REFERENCES

[1] MUGHABGHAB, S.F., DIVADEENAM, M., HOLDEN, N.E., Neutron Cross Sections, Vol. 1 and 2, Academic Press, New York, USA. (1981).

[2] BROWNE, E., FIRESTONE, R.B., (SHIRLEY, V., Ed.), Table of radioactive isotopes, John Wiley & Sons, New York, USA. (1986).

[3] MARVIN-DIPASQUALE, M.C., AGEE, J.J., BOUSE, R.M., JAFFE, B.E., Microbial cycling of mercury in contaminated pelagic and wetland sediment of San Pablo Bay, California, Environ. Geology **43** (2003) 260-267.

Spatial and temporal variations of uranium and thorium series along the Egyptian Mediterranean coast

Saleh, I.H.[a], A.A. El-Gamal[a], S.M. Nasr[a], M.A. Naim[b]

[a] Department of Environmental Studies,
Institute of Graduate Studies and Research (IGSR),
Alexandria University, Alexandria,
Egypt

[b] Department of Physics,
Faculty of Science,
Alexandria University, Alexandria,
Egypt

Uranium and thorium series are the two dominant radioactive decay chains in the environment. Sediment samples were collected bimonthly for two years from the area extending from El-Salloum to El-Arish. Gamma measurements have been carried out by means of high-resolution low background PC multi-channel spectrometer, using a coaxial HPGe detector. The highest U and Th series member's concentrations have been recorded at Rashid as one of the high background areas in the world. Except at Rashid, U and Th series concentrations were found to be at natural levels in all the other stations. The average concentrations along the coast during the monitoring period for ^{234}Th, ^{226}Ra, ^{214}Pb and ^{214}Bi as uranium series were 21.03, 19.49, 13.70 and 13.06 Bq/kg, respectively and for ^{228}Ac, ^{212}Pb, ^{212}Bi and ^{208}Tl as thorium series were 13.75, 10.40, 9.38 and 5.22 Bq/kg, respectively. The activity ratio of ^{228}Ac/^{208}Tl was approximately equal three for the majority of sediment samples. The concentration values of ^{212}Pb were shown to be close to the corresponding concentration values of ^{212}Bi and also between ^{214}Pb and ^{214}Bi. Moreover, the values of the Th series are looking lower than the values of the uranium series. Generally, the lowest Th series values have been detected mainly in the western sector stations except at El-Salloum. The concentration of uranium and thorium is depend on the calcium carbonate content, grain size composition of the sediments and marine biological activities [1].

Temporal variations have been distinguished for the four radioisotopes of the uranium series. The higher values observed at Rashid only during May, July and September 1998. The increase of specific activities was due to the contribution of the black sand in the samples during the first three campaigns. After September 1998, the flooding has been occurred in access in Nile River. High rate of sedimentation has been occurred due to the flooding by normal sand (lighter) instead of black sand (heavier) and this normal sand was covered the surface sediments over the original black sand. This may be the reason for decreasing the uranium concentration at Rashid during that period.

Figure 1 shows that seasonal variations can be distinguished for the uranium series member concentrations in sediments along the Egyptian Mediterranean coast. Relatively higher values of uranium series concentration have been detected in spring and autumn seasons. The percentages of seasonal distribution were 16%, 12%, 11%, 8%, 12% for spring 98, autumn 98, spring 99, autumn 99 and spring 2000, respectively.

Temporal variations of thorium series at Rashid have been represented. It is obvious that for the four radioisotopes, the higher values were detected during May, July and September 1998 as the same period of the detection of uranium high values. This is indicating that the main source of this increase either for U or Th series was the contribution of the black sand in the samples. Some random increases were monitored for ^{228}Ac during May and September 1999 and for ^{212}Pb in September 1999.

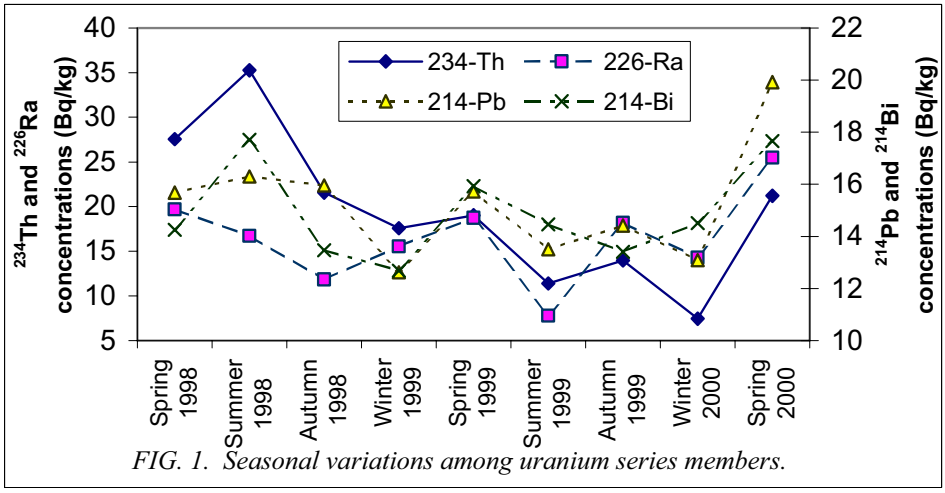

FIG. 1. Seasonal variations among uranium series members.

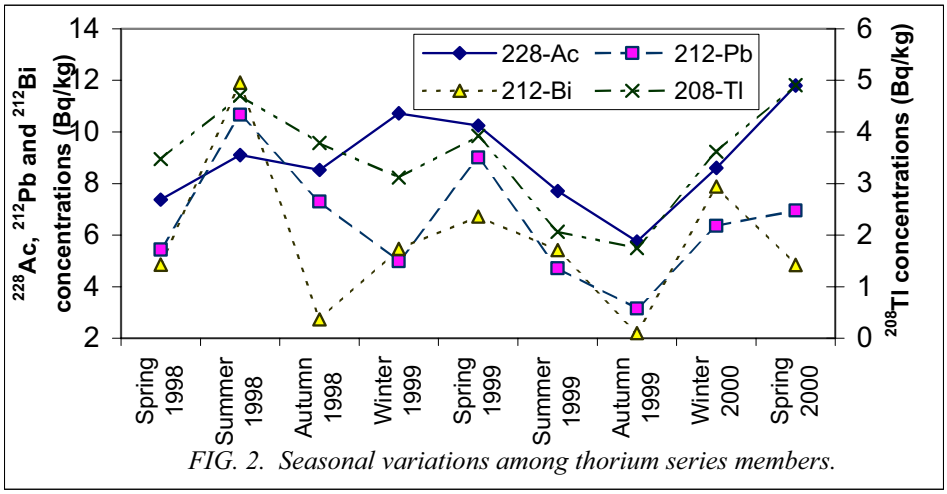

FIG. 2. Seasonal variations among thorium series members.

In most of thorium series member's seasonal variations have been distinguished as shown in Fig. 2. Autumn has been observed as the lowest concentrations season. This may be due to the low water period, which has insignificant discharge of suspended particle [2] that are rich in thorium series. This assumption could be confirmed by the presence of relatively high amounts of Th series activities at El-Gamil, which has very fine sand. Moreover, it may also be related to the biological activity during this season.

Lower seasonal distribution percentages of ^{228}Ac, ^{212}Pb, ^{212}Bi and ^{208}Tl have been detected in autumn seasons of 1999 and the values were 7.2%, 5.4%, 4.2% and 5.6%, respectively. On the other hand, relatively higher percentages of ^{228}Ac, ^{212}Pb, ^{212}Bi and ^{208}Tl were 12.8%, 15.4%, 12.9% and 12.5%, respectively detected in spring.

Mechanical analysis has been carried out for the sediment samples of the campaign of March 2000. The majority of sediment samples was fine gravelly sand as abundant size of the Egyptian Mediterranean coast. In order to obtain statistical parameters, plotting cumulative curves for the samples on probability papers was carried out. The western sector cumulative curves show that El-Salloum sediments have different origin than the other stations in this sector. This can be used as confirmatory statement for the difference of radioactivity concentrations in El-Salloum compared to the other stations in the western area. The other sediment samples from the other stations of the western sector showed approximately the same origin and distribution.

REFERENCES

[1] SWANSON, S.M., Food-chain transfer of U-series radionuclides in a northern Saskatchewan aquatic system, Health Phys. **49** (1985) 747-753.

[2] KANIVETS, V.V., et al., Riverine transport of Cs-137 and Sr-90 into the Black Sea after Chernobyl accident (data analysis and methodological aspects of monitoring), IAEA-SM-354/23, Int. Symp. Marine Pollution, Monaco, 5-9 October (1998) 44-51.

Estimation of sediment loading in Asian coastal area using ^{210}Pb inventory in mangrove sediment

Tateda, Y.[a], D.D. Nhan[b], N.Q. Long[b], N.H. Quang[b], N.H. Quy [b]

[a] Environmental Science Research Laboratory (CRIEPI),
Abiko,
Japan

[b] Institute of Nuclear Sciences and Technology (INST),
Hanoi,
Vietnam

Concentrations of ^{210}Pb in coastal sediment are generally controlled by local atmospheric ^{210}Pb flux and fine sediment input to coastal area, because the ^{210}Pb has high affinity to inorganic fine particles and ^{210}Pb inventory in coastal sediment is coincided with sediment loading to the area. Thus the ^{210}Pb level in coastal sediment is good index of sediment loading to coastal zones. However, in subtropical/tropical coastal area, such as S-E Asian coast, sediment loading is widely variable due to seasonal difference of precipitation and coastal sediment discharge among rainy/dry season. Secondly, the S-E Asian coastal areas are mostly covered with mangroves those entrap the sediment particle supplied from river to adjacent coastal waters. Since the entrapped fine sediment particles include not only the excess ^{210}Pb supplied from local atmosphere but also the accumulated sediment particles by terrestrial input, thus the ^{210}Pb inventory exceeds largely compared to the atmospheric supply. Thus the ^{210}Pb inventory balance in mangrove area is expected to reflect drastically the local sediment loading conditions in S-E Asia. We studied the ^{210}Pb balance in subtropical mangrove coastal water in Japan and found that the ^{210}Pb was useful natural tracer to evaluate the coastal sediment load [1]. However, limited data are reported about the mangrove coastal area [2, 3]. In this study, we collected mangrove sediment cores at the Japan and Viet Nam and analyzed the ^{210}Pb concentrations in sections of different depth and location. By comparing with the atmospheric flux, we estimate the balance of the ^{210}Pb in the area and evaluate the sediment loading to the studied mangrove area.

REFERENCES

[1] LYNCH, C., et al., Recent accretion in mangrove ecosystems based on ^{137}Cs and ^{210}Pb, Estuaries **4** (1989) 284-299.

[2] SMOAK, J., PATCHINEELAM, S., Sediment mixing and accumulation in a mangrove ecosystem: evidence from ^{210}Pb, ^{234}Th and ^{7}Be, Mangroves and Salt Marshes **3** (1999) 17-27.

[3] TATEDA, Y. Organic Carbon Supply and Accumulation in Mangrove Coastal Sediment, Nippon Suisan Gakkaishi **68** 5 (2002) 736-737.

Application of radionuclides to study recent changes in sediment accumulation rates in Adventfjorden, Svalbard

Zajączkowski, M.[a], W. Szczuciński[b], R. Bojanowski[a]

[a] Institute of Oceanology,
Polish Academy of Sciences,
Sopot,
Poland

[b] Collegium Polonicum,
Słubice,
Poland

Recent sediment accumulation rates in small subpolar fjord - Adventfjorden (Fig. 1) were determined by ^{210}Pb and ^{137}Cs dating. Modern rates in central basin decrease downfjord from 1.87 to 0.87 cm y^{-1} (2.5 to 1.14 g cm^{-2} y^{-1}).

Comparison of the modern values (1986–2001) with older ones (1963-1986) reveals a marked increase in sediment accumulation rates in the last decade (Table I). It correlates well with recent climate changes (warming and increase in precipitation). Comparison with published particulate matter flux data indicate, that a portion of sediment is bypassed to Isfjorden.

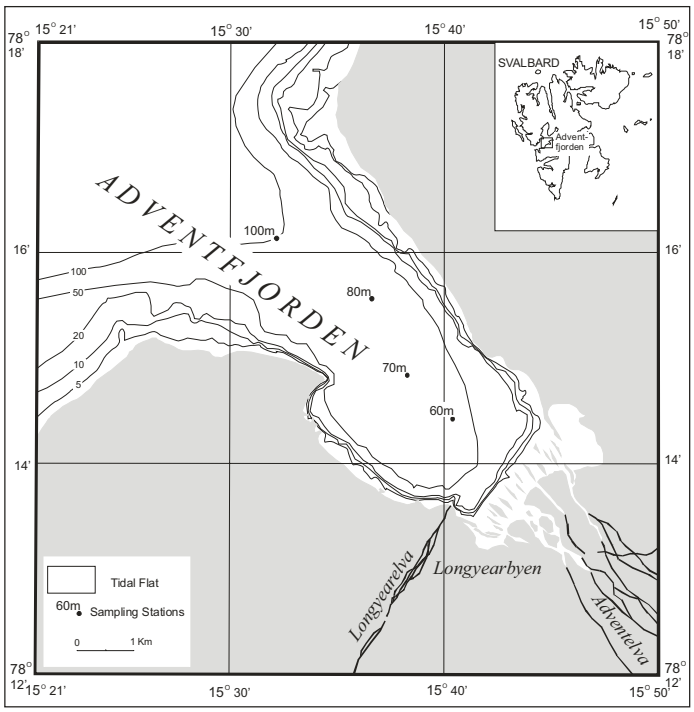

FIG. 1. Locations of coring stations in Adventfjorden.

Table I. The sediment accumulation rates in relation to distance from tidal flat. The rates are calculated from reference layers (1963 and 1986 peak) in ^{137}cs activity profiles. The creditability of the rates for 100 m core is discussed in the text. (LAR – linear accumulation rate; MAR – mass accumulation rate; NA – not available)

Station	Distance from tidal flat [km]	Depth of 1986 peak [cm]	Depth of 1963 peak [cm]		Accumul. rate 1986-2001	Accumul. rate 1963-1986	Accumul. rate 1963-2001
60m	1.2	29	NA	LAR [cm y^{-1}]	1.87	NA	NA
				MAR [g cm^{-2} y^{-1}]	2.50	NA	NA
70m	2.5	16	30	LAR [cm y^{-1}]	1.00	$\geq$ 0.58	$\geq$ 0.74
				MAR [g cm^{-2} y^{-1}]	1.29	$\geq$ 0.76	$\geq$ 0.96
80m	3.6	14	28	LAR [cm y^{-1}]	0.87	0.61	0.71
				MAR [g cm^{-2} y^{-1}]	1.14	0.79	0.92
100m	6.0	NA	7 (?)	LAR [cm y^{-1}]	NA	NA	0.07 (?)
				MAR [g cm^{-2} y^{-1}]	NA	NA	0.08 (?)

The use of a Cs-137 vertical migration model to study the temporal evolution of heavy metals in coastal sediments of the Bay of Cadiz (Spain)

Barrera, M.[a], R. A. Ligero[b], M. Casas-Ruiz[b]

[a] Departamento de Impacto Ambiental de la Energia,
CIEMAT,
Madrid,
Spain

[b] Departamento de Fisica Aplicada,
Universidad de Cadiz,
Cadiz,
Spain

The evolution of heavy metals (Zn, Cd, Pb, Hg) in sea bed sediments of the Bay of Cadiz (Spain) has been studied. Four sediment cores were collected from the Inner Bay zone (Fig. 1) where sediment textural composition is mainly formed by silt and clay with high organic content, showing a very high absorption capacity for the substances solved in the aquatic medium. The dating of the sediments has been performed using the fallout radionuclide ^{137}Cs as a tracer. Due to the high vertical mobility of this radionuclide in the sediment column, as a consequence of its molecular diffusion and the bioturbation existing in the area, the observed profiles are continuous and the 1963 maximum in fallout activity could not be assigned [1, 2]. The one dimensional diffusion-advection equation has been applied, considering the residence time of the radionuclide in the marshes zone, to develop a model that permits to interpret the profiles and to estimate the sedimentation rate, in order to infer the recent chronology of the sediment layers [1, 3]. By using the ^{210}Pb dating method with the CRS model in one station, it can be showed that the sedimentation rate could be assumed to be constant during a longer period of time. In consequence, the sediment dating has been extended up to 100 years backwards, allowing the study of the evolution of heavy metals during the last century. The sediment dating shows that the heavy metal pollution of the Inner Bay has been produced simultaneously in the whole zone, during the industrial development of the environment. The increase of heavy metals Zn and Cd started in the second half of the XX century, while the enhancement of Pb and Hg concentration started at the beginning of the XX century. Heavy metal concentrations reached maximum levels during the eighties decade, afterward a remarkable decrease in surface sediments has been observed, which could be attributed to the restrictive environmental measurements undertaken at the zone, in particular the control of industrial effluents and the decreasing use of leaded fuels [4].

REFERENCES

[1] BARRERA, M., Aplicaciones de técnicas de Espectrometría nuclear a columnas de sedimento en la Bahía de Cádiz, Ph. D. Thesis, Universidad de Cádiz (2002).

[2] LIGERO, R., BARRERA, M., CASAS-RUIZ, M., Levels of ^{137}Cs in muddy sediments of the seabed of the Bay of Cádiz, Spain, Part I: Vertical and spatial distribution of activities, J. Environ. Radioact. (in press).

[3] LIGERO, R., BARRERA, M., CASAS-RUIZ, M., Levels of ^{137}Cs in muddy sediments of the seabed of the Bay of Cádiz, Spain, Part II: Model of vertical migration of ^{137}Cs, J. Environ. Radioact. (in press).

[4] LIGERO, R., et al., Environmental Impact of unleaded gasolines in the Bay of Cadiz (Spain), Environ. Int. **30** (2004) 99-104.

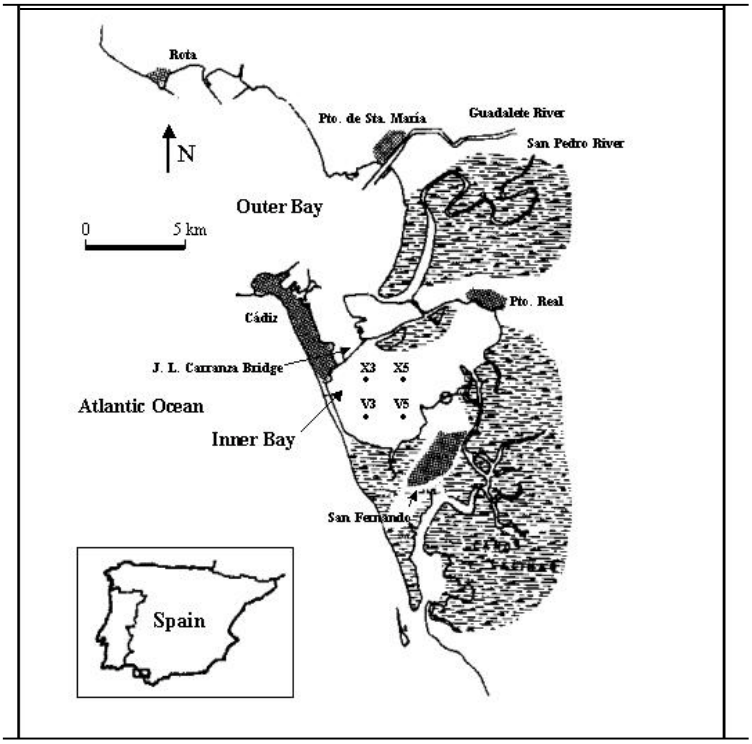

FIG. 1. The Bay of Cádiz and the sampling stations.

MODELLING

Modelling the oceanic Nd isotopic composition on a global scale

Arsouze, T.[a], C. Jeandel[a], F. Lacan[b], N. Ayoub[a], J-C. Dutay[c]

[a] LEGOS (CNRS/CNES/IRD/UPS),
Observatoire Midi-Pyrénées,
Toulouse,
France

[b] Woods Hole Oceanographic Institution,
Woods Hole, Massachusetts,
United States of America

[c] LSCE (CNRS/CEA) CE.
L'Orme des Merisiers,
Gif sur Yvette,
France

Since the end of the eighties, it is recognized that the Nd isotopic composition (expressed as ε_{Nd}) varies from ca –13 in the North Atlantic to ca –5 in the Pacific. It has been clearly established that far from any source of lithogenic material, ε_{Nd} is a conservative tracer of water mass mixing [1-5]. Since the range of ε_{Nd} values of the deep waters are imprinted in the metalliferous sediments, they are used by paleoceanographers to trace the past variations of the thermohaline circulation. However, many studies conducted in the present day ocean highlight that the Nd budgets based only on dust/riverine inputs were not able to reconcile the Nd content and ε_{Nd} variations between the 3 oceanic basins (the "Nd paradox"). The "missing source" was often suspected to be the oceanic margins but was quantified only recently [6-8].

This talk proposes modelling results of the Nd oceanic distribution (concentration and isotopic composition) on a global scale. For doing that, we first established an extensive compilation of the ε_{Nd} signatures of the world continental margins (deduced from more than 50 references, figure below). Then, we applied the rate of exchange of Nd between the continental margins and the oceans, deduced from Lacan and Jeandel (in rev.). This allowed to simulate lithogenic Nd inputs into a large scale circulation model (ORCA/OPA). Simulated vertical profiles are compared to those measured in the different oceanic basins.

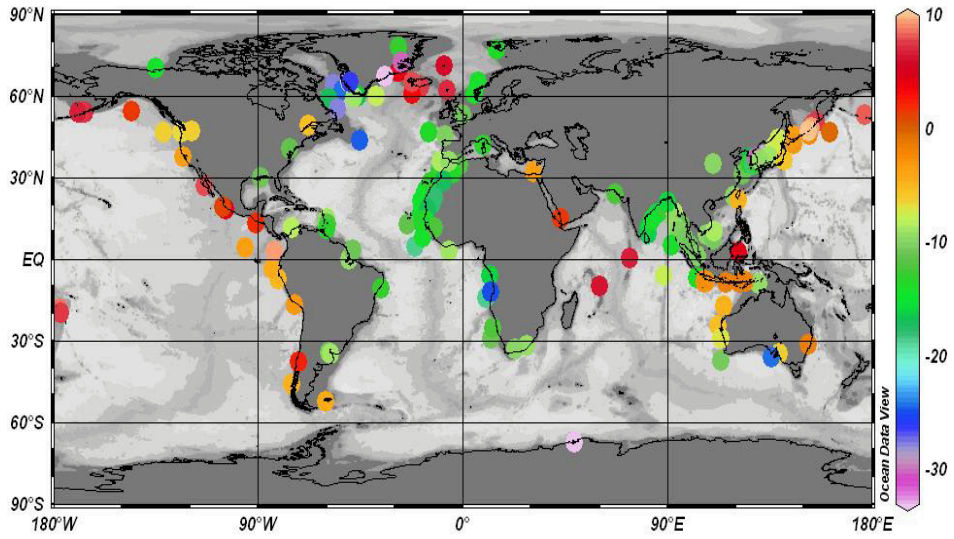

REFERENCES

[1] PIEPGRAS, D.J., WASSERBURG, G.J., Isotopic composition of neodymium in waters from the Drake Passage, Science **217** (1982) 207-217.

[2] PIEPGRAS, D.J., WASSERBURG, G.J., Rare earth element transport in the western North Atlantic inferred from isotopic observations, Geochim. Cosmochim. Acta **51** (1987) 1257-1271.

[3] JEANDEL, C., Concentration and isotopic composition of Nd in the South Atlantic Ocean, Earth Planet. Sci. Lett. **117** (1993) 581-591.

[4] JEANDEL, C., THOURON, D., FIEUX, M., Concentrations and isotopic compositions of neodymium in the eastern Indian Ocean and Indonesian straits, Geochim. Cosmochim. Acta **62** 15 (1998) 2597-2607.

[5] LACAN, F., JEANDEL, C., Subpolar Mode Water formation traced by neodymium isotopic composition, Geophys. Res. Lett. (in press).

[6] LACAN, F., JEANDEL, C., Tracing Papua New Guinea imprint on the central Equatorial Pacific Ocean using neodymium isotopic compositions and Rare Earth Element patterns, Earth Planet. Sci. Lett. **186** 3-4 (2001) 497-512.

[7] LACAN, F., JEANDEL, C., Neodymium isotopes as a new tool for quantifying exchange fluxes at the continent - ocean interface, Earth Planet. Sci. Lett. (under revision).

[8] TACHIKAWA, K., ATHIAS, V., JEANDEL, C., Neodymium budget in the modern ocean and paleoceanographic implications, J. Geophys. Res. **108** C8 (2003) 3254.

3-D Modelling technique of time-series ^{137}Cs concentration in coastal organisms in the case of short term introduction

Tateda, Y.[a], A. Wada[b]

[a] Environmental Science Research Laboratory,
Central Institute of Electric Power Industry,
Abiko, Chiba,
Japan

[b] Nihon University,
Tokyo,
Japan

Abstract. For the development of the modelling technique in predicting ^{137}Cs concentrations in marine biota, temporal and space distribution of ^{137}Cs concentrations in marine organisms are important especially in case of short-term introduction to coastal area. We developed a 3-dimensional model composed of nuclide transfer both from seawater and the food chain in an imaginary coastal area, expressing the temporal ^{137}Cs concentrations in marine organisms accompanied with the habitat location. The result of simulation by 3-D model in the case of short term introduction exhibits the following information: 1) the introduced ^{137}Cs in seawater is diluted and disappeared quickly by current advection and diffusion, while ^{137}Cs in organisms slowly increased even after the seawater is cleaned, mainly from the contribution from ^{137}Cs transfer through the food chain, 2) the ^{137}Cs concentration peak in fish appears approximately 3 months later, and the concentration ratio (^{137}Cs in organism / ^{137}Cs in seawater) at that time is larger than the biological concentration factor (BCF) in equilibrium state. This result indicates that i) monitoring of ^{137}Cs concentration in fish must be continued until 1 year after a 1 week acute input, and ii) the ^{137}Cs increase in seawater may have occurred during the previous 3 months in the case that a higher ^{137}Cs concentration ratio (organism / seawater) than 100 is observed in fish, because of the ^{137}Cs memory effect of local food chain ecosystem.

1. Introduction

Short-term estimation of released radionuclide behavior is necessary for decision-making in emergency situations. To predict radionuclide concentrations in marine organisms affected by short-term radionuclide introduction to coastal waters, the time series of ^{137}Cs transfer both from seawater and the food chain to marine organisms were studied [1, 2]. The model was developed for typical Japanese coastal waters including benthic food chain and planktonic food chain, with transfer parameter data set, such as uptake rate constant, excretion rate constants, gut transfer rates and food ingestion rates of ^{137}Cs, collected by many tracer experiment studies [3]. Marine radioecological studies established the ^{137}Cs Concentration Factor (CF, or BCF) as a transfer parameter to calculate nuclides concentration in marine organisms in equilibrium with seawater within marine ecosystems [4]. Furthermore, increasing demand of emergent prediction of time series ^{137}Cs concentration in marine organism in the case of unexpected accidental release of radionuclides from nuclear facilities calls for development of a dynamic model of ^{137}Cs transfer in marine environment for predicting temporal ^{137}Cs concentration in coastal organisms at transition state. However, modeling studies of the ^{137}Cs transfer especially in coastal biota has been limited through only a few steps in food chains [5-8].

A dynamic deterministic biological compartmental model of ^{137}Cs transfer in coastal ecosystems by [3] considers the ^{137}Cs transfer from seawater and through food chain in coastal waters, and was improved recently to be able to predict the short term temporal ^{137}Cs concentrations in coastal biota in the situation of short term deposition of ^{137}Cs to surface water, indicating that combining of ecological data sets and the ^{137}Cs uptake/excretion rate constant data sets is applicable for the dynamic biological model of the ^{137}Cs transfer through marine food chains in Japanese coastal waters. In this paper, we

upgraded this model to a 3-dimension, expressing the temporal ^{137}Cs concentrations in marine organisms accompanied with the habitat location. Using this 3-D prediction model, the computed temporal ^{137}Cs concentrations in Japanese coastal organisms are discussed in the condition of short underwater input to the coastal ecosystem.

2. Model structure, parameter, validation and simulation

The biological model of ^{137}Cs transfer in coastal ecosystems is a dynamic deterministic compartmental model that simulates ^{137}Cs transport through marine food webs in Japanese coastal waters. The main-model consists of 11 compartments (seawater, phytoplankton, zooplankton, detritus, detritus feeder, plankton feeding invertebrates, benthos feeding fish, algae, algae feeding invertebrates, plankton feeding fish, coastal carnivorous invertebrates and coastal carnivorous fish) and the detritus sub-model consists of 4 sub-compartments (terrigenous detritus, algal detritus, fecal detritus, molts). The compartment connection expressing the food chain relation is considered by food habitat studies of Japanese coastal organisms. In the biological model, the temporal ^{137}Cs concentration in each organism is determined by ^{137}Cs concentration in seawater and in food. The size effect on assimilation rate and daily feeding rate of predator enlarges those of juvenile stage prey organisms.

In the seawater and detritus compartment, the temporal evolutions of the ^{137}Cs concentrations in seawater, detrital matter in terrigenous detritus, algal detritus, fecal detritus and molts are computed. The source term can be given both as uniform to surface water or point source to underwater. Flux of re-dissolved ^{137}Cs from bottom sediment to bottom water column is also calculated. Assuming an ideal diffusion boundary, seawater compartment is defined as a 10 m layer. Diffusion coefficient of ^{137}Cs in water column can be selected as observed values at target coastal study sites.

The model was validated by temporal data sets of observed ^{137}Cs concentrations in Japanese coastal organisms and coastal waters both under steady state and non-steady state. The equilibrium ^{137}Cs concentrations in coastal biota and seawater calculated from empirical concentration factors (CFs) of ^{137}Cs in Japanese coastal organisms are used as steady state data sets. The result of the computed equilibrated values falling between the confidence intervals of the observed data, indicated that the model is acceptable under steady state. In contrast, the non-equilibrium ^{137}Cs concentration in coastal biota and seawater is recorded only in the case of temporal ^{137}Cs concentrations in coastal organisms and seawater in 1986, the year of the Chernobyl fallout. Open data of the Radioactivity Survey Data in Japan, National Institute of Radiological Science, were used as empirical non-steady data sets. The result of the calculated temporal ^{137}Cs activity profile falling between the confidence intervals of the observed data indicated that the model is acceptable also under non-steady state.

^{137}Cs introduction to a particular coastal ecosystem (45 km along shore, 15 km off shore, from 10 to 200 m depth) of Rokkasho, Aomori, Japan, was simulated as point introduction to underwater layer (23 km point, 3 km off shore, 30 m layer) approximately 1 week as total input of 1.9 TBq. Habitats of coastal biota were defined as observed in coastal area of Rokkasho, indicating that algae inhabits only at north coastal shore, while benthic organisms are living in bottom water, and swimming invertebrates and fishes distributed equally in the water column. Calculation conditions were given as winter and summer current and diffusive conditions.

3. Results and discussions

Computed temporal ^{137}Cs concentrations in benthic fish, algae, and squid living in an habitat area in the case of underwater point introduction (10 days) during summer in Rokkasho coastal waters are shown in Fig. 1. Three-D distribution of ^{137}Cs concentrations in benthic fish at 10, 20, 40, 90 days after acute introduction showed slow increase of ^{137}Cs concentrations in fish at the downcurrent area (south of the source). Although the ^{137}Cs in coastal water was cleaned by water advection and diffusion after 10 days, the ^{137}Cs concentrations in fish increased. The same distribution profile was computed for ^{137}Cs concentration in squid living down current in the area. However, ^{137}Cs concentrations in other organisms decreased after the stop of acute introduction. Macro algae inhabits

only rocky shore in the north area, thus the high ^{137}Cs concentrations in algae living near the source were computed, while decreasing trend of ^{137}Cs in algae after 10 days was computed as same as those obtained in squid.

Computed ^{137}Cs concentrations in surface water, benthic fish, algae and squid living at monitoring point of Rokkasho coastal water (Benthic fish: 15 km north from source, 1 km off shore, macro algae: 18 km south from source, 3 km off shore, squid: source point) are shown in Fig. 2. Time series of ^{137}Cs concentrations in surface water of winter and summer showed a similar temporal profile, demonstrating that simulated ^{137}Cs concentration peaks correspond to contaminated water plume advection. The ^{137}Cs concentrations in algae and squid increased correspondingly to ^{137}Cs increase in surface water, while those decreased gradually by metabolic excretion after clean water prevailed. In contrast, concentrations in benthic fish increased gradually and corresponded not strongly to the ^{137}Cs level in surface water. The calculated concentration peak in benthic fish was approximately 50 days later than the concentration peak in surface water.

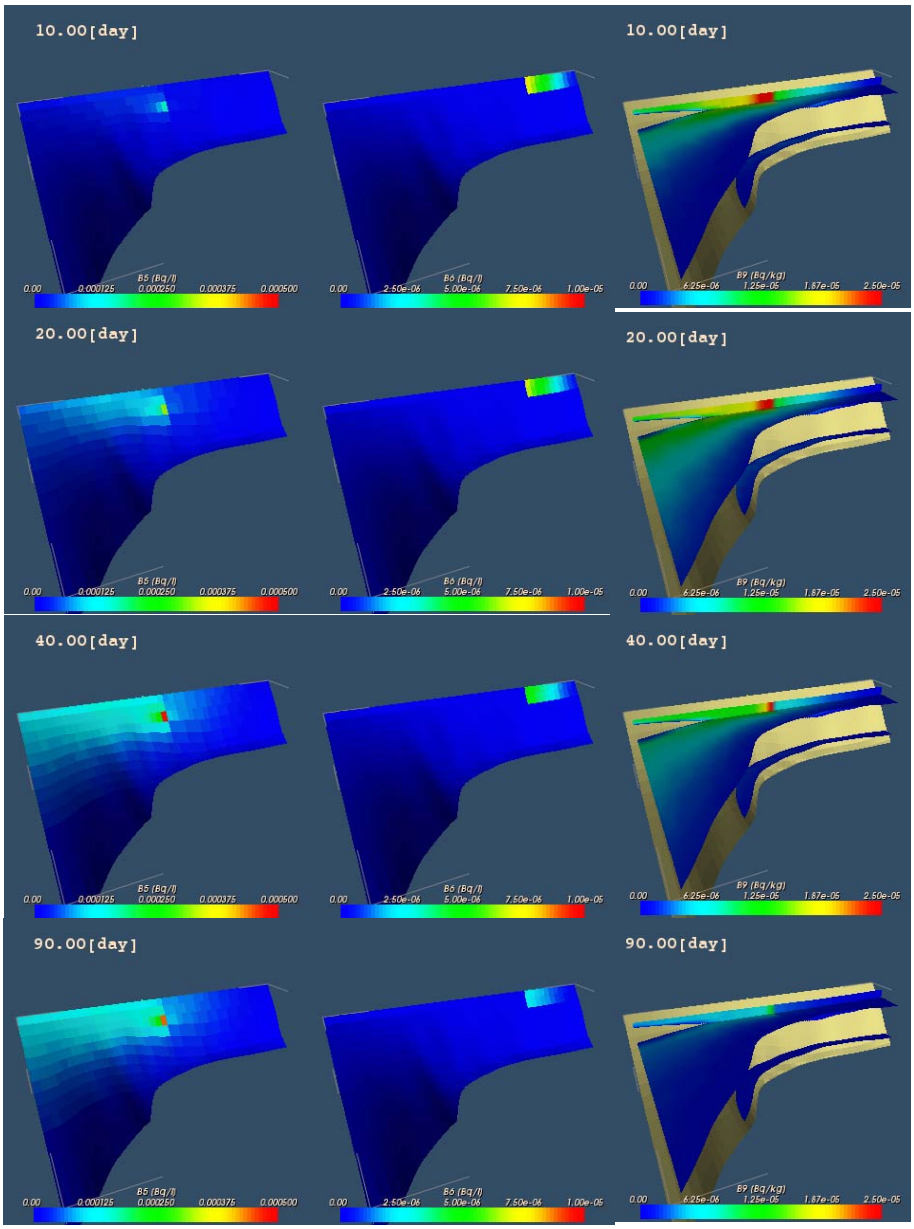

FIG. 1. Computed ^{137}Cs temporal concentration in benthic fish, macro algae and squid at Rokkasho coastal water (Centre circle:source. Shade:^{137}Cs concentrations). **See ANNEX I, p. 664 for colour figure**.

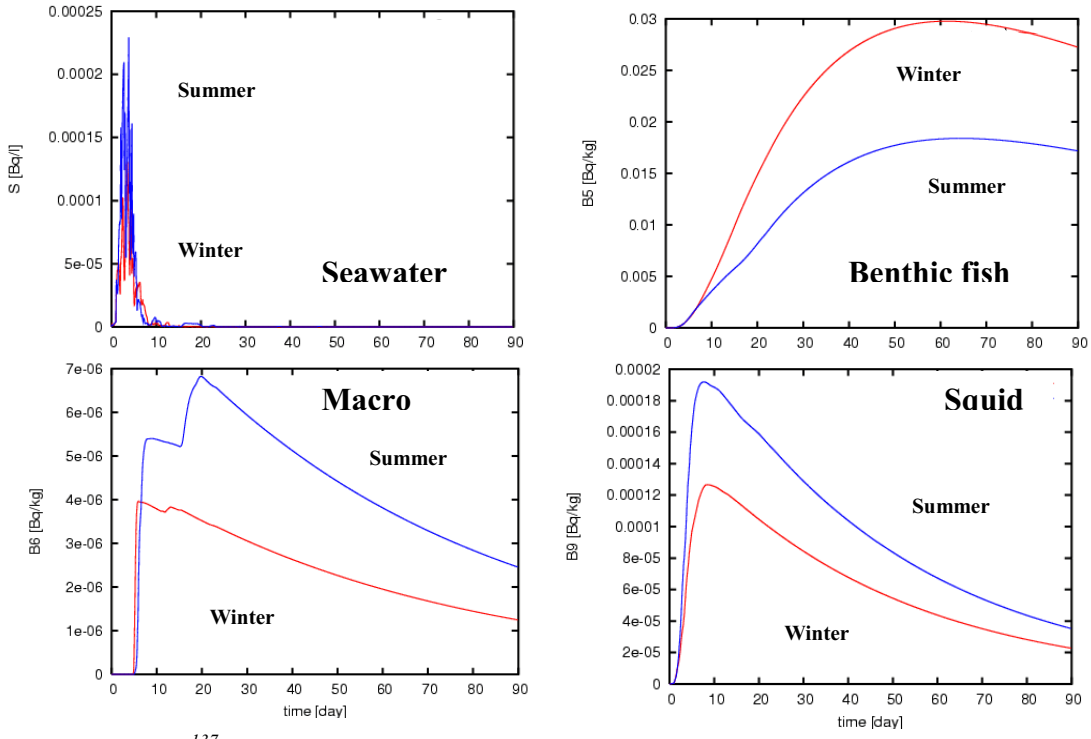

FIG. 2. Calculated ^{137}Cs temporal concentrations in benthic fish, macro algae and squid at monitoring point of Rokkasho coastal water.

The simulated results of temporal ^{137}Cs concentrations in biota decrease during living in clean water. The exceptional ^{137}Cs increase in organisms appeared in benthic fish even after the ^{137}Cs in water was decreased by clean water flushing. The input source of ^{137}Cs to fish was mainly from ^{137}Cs transfer from food organisms. The calculated delay of ^{137}Cs peak appearance is logically attributed to the slow metabolic rate of ^{137}Cs in fish. The magnitude of increase of ^{137}Cs concentration in fish was derived to be 30 mBq/kg of increase in case of 2 mBq/L increase of ^{137}Cs concentration in surface water by acute introduction during 10 days, 3 months before. The increase of ^{137}Cs concentration in other biota were calculated to be only 3 – 5 mBq/kg, not significantly different to background ^{137}Cs concentration variation in current Japanese biota (approximately 20 - 30mBq/kg). This result indicates that 1) monitoring of ^{137}Cs in fish must be continued until 1 year after a 1 week acute introduction, 2) undetected ^{137}Cs increase in seawater may have occurred during past 3 months in case of higher ^{137}Cs concentration ratio (organism / seawater) than 100 is observed in fish, because of the ^{137}Cs memory effect of the local food chain ecosystem

ACKNOWLEDGEMENT

Part of this research was financed by the Nuclear Safety Research Association (NSRA).

REFERENCES

[1] TATEDA, Y., Development of Basic Model for Dynamic Prediction of ^{137}Cs Concentration in Marine Organism, CRIEPI Rep. U94056 (1997) p. 57 (in Japanese).

[2] TATEDA, Y., Basic Model for the prediction of ^{137}Cs Concentration in the Organisms of detritus Food Chain, CRIEPI Rep. U97022 (1997) p. 28 (in Japanese).

[3] TATEDA, Y. et al., Modelling of ^{137}Cs concentration change in organisms of the Japanese coastal food chains, Intern. Symp. Marine Pollution, IAEA-SM-354, IAEA, Vienna (1998).

[4] INTERNATIONAL ATOMIC ENERGY AGENCY, Sediment Distribution Coefficients and Concentration Factors for Biota in the Marine Environment, Technical Reports Series No. 422, IAEA, Vienna (2004).

[5] AOYAMA, I., INOUE, Y., Estimation and evaluation of radioactive contamination through a food web in aquatic ecosystem (1), J. Radiat. Res. **14** (1973) 375-381

[6] NAKAMURA, R., M. NAKAHARA, SUZUKI, Y., UEDA, T., Relative importance of food and water in the accumulation of radionuclides by sea urchin *Strongylocentrotus nudus*, Bull. Jap. Soc. Sci. Fish. **52** (1986) 703-710.

[7] WANG, W-X., KE. C., YU, K.N., LAM, P.K.S., Modelling radiocesium bioaccumulation in a marine food chain, Mar. Ecor. Prog. Ser. **208** (2000) 41-50.

[8] HELING, R., LEPICARD, S., MADERICH, V., SHERSHAKOV, V., MUNGOV, G., CATSAROS, N., POPOV, POSEIDON, A., Final Report A module to predict the effects of radioactive discharges in the coastal regions, NRG Report IC15-CT98-0210 (2000) 47 pp.

Performance evaluation of the recently commissioned Worli submarine outfall, Mumbai, India, using radiotracer studies and mathematical modelling

Noble, J.[a], U.S. Kumar[a], U.P. Kulkarni[a], S.V. Navada[a], I. Gupta[b], R. Kumar[b]

[a] Isotope Applications Division,
Bhabha Atomic Research Centre,
Trombay, Mumbai,
India

[b] National Environmental Engineering Research Institute,
Mumbai,
India

Abstract. Three field tracer studies were performed using artificially produced ^{82}Br radioisotope to assess the functioning of a recently commissioned submarine sewage outfall at Worli, Mumbai, India under different tidal conditions. The first two injections were intended to understand the dispersion pattern of sewage near the outfall location during spring and neap ebb tides. The data obtained from the third study was used for the validation of various empirical and numerical near and far-field models, which are commonly used for the analysis and design of outfall systems. These studies revealed that, as the sewage is discharged through the outfall, it is adequately diluted by the entrainment caused by the outfall configurations and prevailing hydrodynamic conditions, thereby reducing any adverse impact on coastal waters. Also, the various dispersion characteristics including dilution factors predicted by the mathematical models compared well with those obtained from radiotracer studies.

1. Introduction

Coastal cities have the unique advantage of disposing the generated municipal and industrial effluents by discharging them into the adjacent coastal waters through long offshore outfalls to reduce any environmental concerns. The island city of Mumbai with a population of about 12 million currently experiences severe coastal pollution problems associated with the disposal of about 2225 million litres of untreated or partially treated sewage into the coastal waters every day. In order to improve the coastal water quality standards by dilution, dispersion and flushing, a few offshore sewage outfalls have been constructed at various locations and a few are underway. One such recently commissioned submarine outfall is located at Worli (Fig. 1a). Here, the collected wastewater is screened, degritted and then discharged into the tidal waters by gravity through a 3.4 km long offshore submarine outfall equipped with multi-port diffuser system aligned normal to the direction of tidal currents. Under normal operating conditions, the flow rate of sewage is about 7.2 m^3/s. To assess the functioning of the Worli outfall by studying the sewage dilution and dispersion processes, three radiotracer injections were carried out under various tidal conditions in the post commissioned regime.

Initial dilution being an outfall design parameter, is normally computed using various mathematical models. Other dispersion characteristics such as plume geometry, dilution factors, dispersion coefficients etc. can also be predicted using empirical models. These models generally developed for highly idealized flow conditions are rarely validated for complex field conditions. In the present study, the data obtained from radiotracer studies was also used for the validation of various empirical and numerical near and far-field models. Radioactive ^{82}Br ($t_{1/2}$ = 36 hrs) in the form of aqueous ammonium bromide was used as the tracer for all the injections in view of its excellent property for tracing the sewage discharge.

2. Radiotracer injections and monitoring

The first tracer injection was conducted at the onset of (spring) ebb tide. About 110 GBq of ^{82}Br was diluted in 15 litres of water and continuously injected along with the sewage for 1 hour at the rate of 250 ml/min. As the radioactive plume was established, the area downstream of the diffuser was tracked using submersible water proof γ-scintillation detector coupled to scaler/ratemeter. Integration of data from the plume monitoring program helped to construct 3D picture of the sewage field in the form of iso-activity contours (Fig. 1b). It was observed that the sewage movement is predominantly tide drifted and follows the current direction. At the near-field, the sewage comes out from the risers in the form of non-merging and surfacing plume. In the far-field, the plume was found to be confined to the top 1-2 m without mixing over the entire depth. The two observed surfacial plumes suggests that advection processes dominates over lateral mixing. Dilution factors and dispersion co-efficients were also estimated from the radiotracer data.

About 64 GBq of ^{82}Br was used in the second injection which was conducted during an (neap) ebb slack period. Counter clockwise movement of sewage plume was observed during flow reversals and the dispersion during slack periods are mainly controlled by the onshore winds (Fig. 1b).

In the third injection conducted during a flood tide, about 74 GBq of ^{82}Br was used. The obtained radiotracer data was utilized for the validation of commonly used near-and far field models.

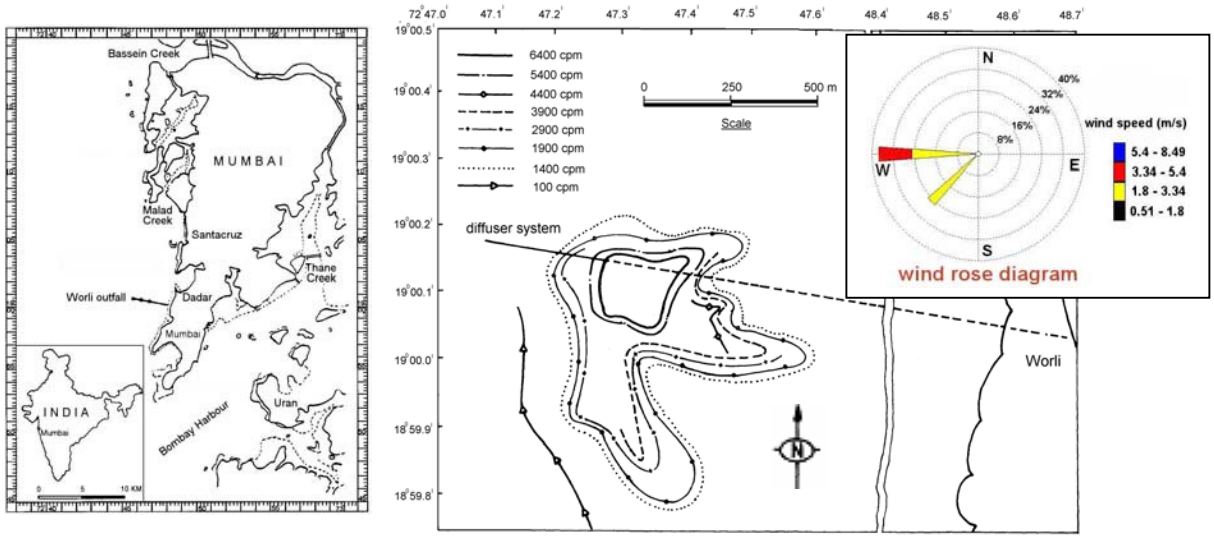

FIG. 1 (a) Location map of Worli submarine outfall, Mumbai (b) Isocount contour map showing the dispersion pattern of labeled sewage during neap ebb slack period.

3. Validation of mathematical models

3.1. Near field models

The validated near field models include: Cornel Mixing Zone Expert System (CORMIX) [1], 3D Lagrangian Jet Model (JETLAG) [2] and the empirical model suggested by Roberts and others [3]. Robert's empirical model for the estimation of various dispersion characteristics is as follows:

The average dilution at the end of the near field (S_1) is given by:

$$S_1 = 1.41.\frac{U.H}{\frac{Q}{L}}.0.58, \qquad 0.1 \le F \le 100 \tag{1}$$

where, Froude number F is given by: $F = \left(\frac{U^3}{b}\right)$ (2)

$$b = g^l \frac{Q}{L} \tag{3}$$

$$g^l = \left(g.\frac{\rho_a - \rho_{ef}}{\rho_a}\right) \tag{4}$$

where,

U is the current velocity (m/s),
H is the water depth at discharge point (m),
Q is the flow rate of sewage (m^3/s),
L is the diffuser length (m),
B is the total source buoyancy flux per unit diffuser length (m^3/s^3) given by Eq. (3),
g^l is the modified acceleration due to gravity given by Eq. (4) (m/s^2),
ρ_a is the density of ambient seawater at port level (kg/m^3),
ρ_{ef} is the density of effluent at port level (kg/m^3),

Length of the initial mixing region, (X_i) is given by $X_i = H.(0.566.F + 3.389)$ (5)

Width of the plume, (w_0) at the end of the near field is given by: $w_0 = 1.5.L$ (6)

The various plume dispersion characteristics computed using the above near-field models along with those obtained from radiotracer data is given in Table I. It is seen that the model predictions matches fairly well with those of radiotracer data. However, the slight variation in dilution factors near the outfall is because of the limitation of those models in representing the complex design of Worli outfall.

3.2. Far-field models

Far-field models like the empirical models proposed by Ref. [4] and Ref. [5] and a depth integrated 2D hydrodynamic and solute transport finite difference model, DIVAST [6] was also validated with radiotracer data.

According to Brooks's model, the centerline far-field dilution factors (S_2) and lateral dispersion coefficients (Dy) is given by the following equation:

$$S_2 = \frac{1}{erf\sqrt{\frac{1.5}{\left(1+\frac{2}{3}\beta.\frac{X_f}{w_0}\right)^3 - 1}}} \tag{7}$$

where, $\beta = \frac{12.Dy_0}{U.w_0}$ (8)

$$Dy_0 = \frac{0.01.(100.w_0)^{4/3}}{10^4} \quad (9)$$

$$X_f = X - X_i \quad (10)$$

X_f is the distance from end of near field to any specified location (m),

X is the distance between effluent discharge point and the specified location (m),

β is the dimensionless number defined by Eq. (8),

Dy_0 is the lateral dispersion coefficient at the beginning of far field (m^2/s).

The far-field dilution factors (S_2) derived from advection diffusion model with coefficients of turbulent diffusion given by Gardanov is:

$$S_2 = \frac{\left(w_0^{2/3} + 0.08\frac{X_f}{U} \right)^{3/2}}{w_0} \quad (11)$$

The numerical model (DIVAST), with three open boundaries (two flow and one elevation boundary), was initially calibrated with observed tidal elevations and velocity data. The model was simulated to predict the dispersion of radiotracer discharged through the Worli outfall. The predicted far-field dispersion characteristics were found to match fairly well with radiotracer data (Table II).

Table I. Comparison of near-field model predictions with radiotracer data

	Radiotracer	CORMIX	JETLAG	Roberts
Average dilution at the end of near field, S_1	50	68	55	60
Length of initial mixing zone, X_i (m)	11-20	7	14	5
Width of the plume at the end of near field, w_0 (m)	250-300	320		375

Table II. Comparison of far-field model predictions with radiotracer data

	Distance along plume axis (m)	Radiotracer	Brooks	Gardanov	DIVAST
Far field dilution, S_2	225	63	62	64	64
	625	90	70	81	108
	930	113	87	95	124
Width of the plume, w (m)	225	660	440		400
	625	642	555		600
	930	680	650		400
Lateral dispersion coefficient, Dy (m^2/s)		1.25	1.5		

4. Conclusions

From the study, it is concluded that, even though the outfall operational parameters have not yet been optimized by the operating agency, the sewage discharged through the Worli outfall is found to be adequately diluted by the entrainment caused by the outfall configurations and prevailing hydrodynamic conditions and thereby reducing any adverse impact on coastal waters. Also, the various dispersion characteristics including dilution factors predicted by the mathematical models compared well with those obtained from radiotracer studies.

REFERENCES

[1] CORNELL MIXING ZONE EXPERT SYSTEM (CORMIX), User's guide and documentation, http://www.cormix.info.

[2] LEE, J.H.W., CHEUNG, V., Generalised Lagrangian model for buoyant jets in current, J. Env. Engg. ASCE, **116** 6, (1990) 1085.

[3] ROBERTS, P.J.W., et al., Ocean outfalls II: Spatial evolution of submerged wastefield, J. Hydr. Engg. ASCE **115** 1, (1989) 26.

[4] BROOKS, N.H., "Diffusion of sewage effluent in an ocean current," (Proc. 1st Int. Conf. on Waste Disposal in the Marine Env.), Pergamon Press, N.Y. (1960).

[5] GARDANOC, T.V., Determination of the pollutant far-fields dilution using variable turbulent diffusion coefficients, Wat. Sci. Tech., **32** 7 (1995) 41.

[6] FALCONER R.A., A water quality simulation study of a natural harbour, J. Wat. Port, Coast. Ocean Engg. Div., ASCE **112** 1 (1986) 15.

Tracer studies with Arctic and subArctic coupled ice-ocean models: dispersion of radionuclides and oxygen isotopes

Karcher, M.J.[a], I.H. Harms[c], F. Kauker[a,b]

[a] Alfred Wegener Institute for Polar and Marine Research,
Bremerhaven,
Germany

[b] O.A.Sys - Ocean Atmosphere Systems GbR,
Hamburg,
Germany

[c] Institute for Marine Research, ZMAW,
University of Hamburg,
Germany

Natural and man-made soluble isotopes which enter the oceanic environment are advected by the ocean-currents or the ice-drift and are distributed over large areas far from their sources. By this they trace the dominant flow patterns and exchanges processes on timescales from years to decades.

By introducing such isotopes as tracers into coupled ice-ocean models used to study the climate system of the Arctic and Subarctic we receive progress in two areas: The intercomparison of model derived tracer distributions with observations offers the opportunity to validate the model experiments. If consistent with observations, the model experiments in turn may serve as an interpretative tool to understand the evolution of the observed distributions. The latter is especially valuable in areas like the Arctic Ocean, where the observations are sparse in time and space. We present examples from two projects introducing the natural isotope $\delta^{18}O$ as a tracer for river water in the Arctic and the man-made radionuclide Technetium-99, which has been emitted from west-European nuclear reprocessing facilities in increased amounts in the 1990s.

The natural isotope $\delta^{18}O$ enters the Arctic Ocean via the rivers carrying runoff from the Siberian and North American catchment areas. Since the signature of $\delta^{18}O$ for the rivers is markedly different from oceanic values it can serve as a tracer for the riverine component of freshwater. The investigation of the dynamics of freshwater in form of ice, ice-melt and river water in the Arctic Ocean is closely linked to a better understanding of the variability of the global thermohaline circulation. The latter is apparently influenced by the amount of freshwater released from the Arctic Ocean into the convective areas of the Nordic Seas and the Labrador Sea. The intercomparison of the modelled and observed patterns of $\delta^{18}O$ leads to better insight of the state of the large circulation systems which store and advect freshwater in the interior Arctic, namely the Beaufort Gyre and the Transpolar Drift, which have undergone significant changes in the last decade.

The man-made radionuclide Technetium-99 is emitted from the west-European reprocessing facilities in Sellafield and La Hague. Since 1994 the release has increased significantly and introduced an intense signal into the current system of the North Sea, the Nordic Seas and the Arctic Ocean. We simulate the dispersion of this radionuclide for the last decades. The results of this experiment feed into a Norwegian research project which aims an improvement of box-models used for assessment studies and monitoring strategies. At the same time an intercomparison of the simulated technetium signal with observations in the Nordic Seas and the central Arctic Ocean allows a better insight into the ventilation processes of those areas with respect to the inflowing water masses.

We will present recent advances in the described applications of isotopes in climate studies for the Arctic and subArctic domains and want to demonstrate the large potential of such combined model-observation studies with isotopes for the investigation of the climate system in the north, as well as for applied purposes like the dispersion of dissolved pollutants in the ocean.

Development of an atmosphere-land surface coupled isotope circulation model

Yoshimura, K., T. Oki

Institute of Industrial Science,
The University of Tokyo,
Tokyo,
Japan

Precipitation isotopes variability is dominantly controlled by large-scale atmospheric moisture transport processes. It was argued by Yoshimura et al. [1] with the Rayleigh-type isotope circulation model with the model reproduction of daily $H_2{}^{18}O$ variability over the sub-tropics, particularly Thailand, and monthly averages at global scales with GNIP (Global Network of Isotopes in Precipitation). However, there remain some discrepancies between the observation and the simulations. It probably implies that we cannot neglect some effect of land surface processes on the variability of precipitation isotopes; in particular. The effect on diurnal variaitons on precipitation seems quite large. To take a deeper insight on short-term variability of precipitation isotopes, including diurnal variability, the authors developed an isotope-incorporated land surface model coupled with the existed atmospheric isotope circulation model.

The original land surface model is MATSIRO (Minimal Advanced Treatments of Surface Interaction and Runoff) by Takata et al. [2]. In MATSIRO, evapotranspiration consists of three components; evaporation from bare soil, transpiration from vegetations, and evaporation of canopy-intercepted water. In MATSIRO-iso, isotopic behaviour of those components are individually estimated. For example, evaporation from bare soil (E_s) and its isotopic composition (R_{Es}) is calculated by using the following equation:

$$E_s = \rho C_{E_s} |V_a| \left(h_{soil} q_{s(T)} - q_a \right) \tag{1}$$

$$E_s{}^* = \rho C_{E_s}{}^* |V_a| \left(h_{soil} q_{s(T)} R_{soil} \alpha_{(T)} - q_a R_a \right) \tag{2}$$

$$R_{E_s} = \frac{E_s{}^*}{E_s} = \frac{C_{E_s}{}^*}{C_{E_s}} \left[\frac{h_{soil} q_{s(T)} R_{soil} \alpha_{(T)} - q_a R_a}{h_{soil} q_{s(T)} - q_a} \right] \tag{3}$$

where

ρ is concentration of waterC_{Es} and $C_{Es}{}^*$ denote bulk coefficients of water and the isotopes against water vapor, respectively, where the roughness that considers surface resistances is taken into account; the ratio of the bulk coefficients is known as the kinetic fractionation coefficient, and this study regards it as a function of wind speed [3]; h_{soil} is relative humidity of soil, q_s and q_a indicate saturated specific humidity and that of air vapor, respectively; R_{soil} and R_a denote isotopic composition of water in soil and air, respectively; T is temperature. For running the model, surface boundary conditions are required; specific humidity, wind speed, temperature, pressure, downward radiation, precipitation (convective and large scale), and isotope ratio of precipitation (convective and large scale) and vapor.

This study used surface variables from GAME reanalysis [4] and isotopic variables from the control run of Yoshimura et al. [1], as the boundary conditions. A vertical one-dimensional experiment in Chiangmai (18.8N, 99.0E), Thailand, for 1 April to 31 October in 1998 was carried out. Figures 1-4 show time series following: (Fig. 1) states of water storages in each of five soil layers, (Fig. 2) precipitation and runoff, (Fig. 3) isotopic compositions of soil water storages, precipitation, and

runoff, (Fig. 4) isotopic compositions of evaporation from bare soil, transpiration from vegetation, and evaporation from canopy-interception. The results indicate isotopes in surface soil layer are largely influenced by precipitation isotopes, but it is hardly affected below 25 cm. Moreover, isotopic values in evapotranspiration flux widely fluctuate with a little relation with that in precipitation. It should be noted that the common assumption in many isotopic models, evaporative isotopes is equal to precipitation isotopes, should be reconsidered.

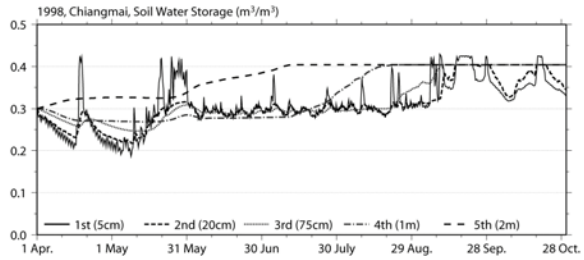

FIG. 1. Soil water storages in five layers.

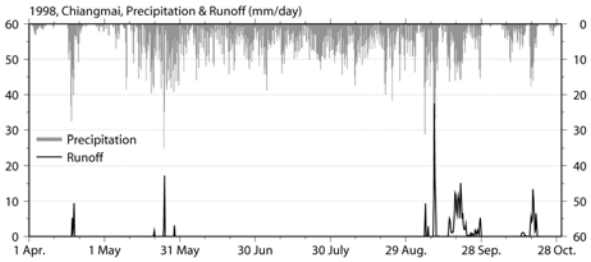

FIG. 2. Precipitation and runoff.

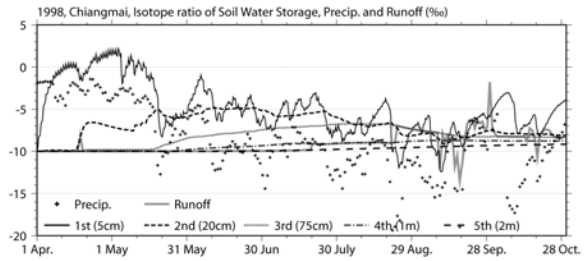

FIG. 3. Isotopic compositions of Figs. 1 & 2.

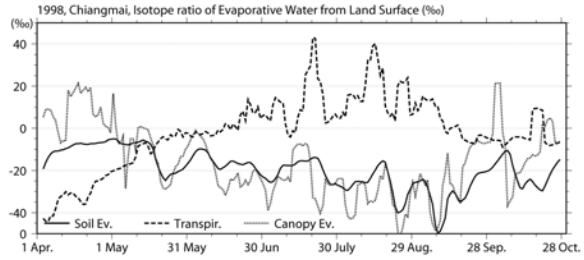

FIG. 4. Isotopic composition of three evap. fluxes.

REFERENCES

[1] YOSHIMURA, K., OKI, T., OHTE, N., KANAE, S., A quantitative analysis of short-term ^{18}O variability with a Rayleigh-type isotope circulation model, J. Geophys. Res. **108** doi:10.1029/2003JD003477 (2003).

[2] TAKATA, K., EMORI, S., WATANABE, T., Development of minimal advanced treatments of surface interaction and runoff, Glob. Planet. Change **38** (2003) 209-222.

[3] JOUZEL et al., Simulation of the HDO and $H_2{}^{18}O$ atmospheric cycles using the NASA GISS general circulation model: The seasonal cycle for present-day conditions, J. Geophys. Res. **92** (1987) 14,739-14,760.

[4] YAMAZAKI, N., KAMAHORI, H., TAKAHASHI, K., YATAGAI, A., On the GAME reanalysis, UCLA Trop. Meteorol. Newsl. **44**, Univ. of Calif., Los Angeles (2001).

MASS SPECTROMETRY

New directions for accelerator mass spectrometry technology

Kieser, W.E.[a], A.E. Litherland[a], X-L. Zhao[a], J.N. Smith[b], J. Cornett[c], L. Cousins[d], G. Javaheri[d], I. Tomski[d]

[a] IsoTrace Laboratory,
University of Toronto,
Toronto, Ontario,
Canada

[b] Atlantic Environmental Radioactivity Unit,
Fisheries and Oceans Canada,
Dartmouth, Nova Scotia,
Canada

[c] Radiation Protection Bureau,
Health Canada,
Ottawa, Ontario,
Canada

[d] Ionics Mass Spectrometry Group Inc.,
Concord, Ontario,
Canada

Abstract. The influence on accelerator mass spectrometry (AMS) of developments in other fields is reviewed and three examples are discussed in detail. The appropriate use of electric and magnetic analysers with small AMS systems (< 3MV) provides the ability to analysed heavier elements such as ^{129}I, for nuclear fuel monitoring and ocean circulation tracer studies. The inclusion of gas chromatography technology extends the capability of AMS to applications which require large numbers of samples with rapid turn-around. The adaptation of chemical reaction cell technology to negative ion beams adds new isobar selection capability to AMS and will permit analyses of isotopes such as ^{36}Cl on small AMS systems.

1. Introduction

The techniques used in Accelerator Mass Spectrometry (AMS) have often been made possible by developments occurring in other fields. Although several attempts to use accelerators for measurements of rare isotopes were made earlier [1, 2], it was only after the development of the caesium sputter negative ion source that AMS could become a routine analytical tool [3]. Caesium sputter sources were improved primarily by nuclear physics experimentalists to generate high current beams of many different negative ions. As these sources improved, they eventually could provide sufficient ion current from a small sample (mg of material such as graphite) so that rare isotopes, with abundance ratios as low as 1 part in 10^{15}, could be counted with appropriate statistics (for ^{14}C, a statistical precision of ±0.25%) [4] in a reasonable length of time (less than 30 minutes for ^{14}C ages less than 10,000 BP).

In this paper we will discuss three other advances in AMS technology, each at a different stage of its evolution.

1. The ability to analyse elements significantly heavier than ^{14}C with small (<3 MV) AMS systems became available when electric analysers were installed after the ion source and high resolution electric and magnetic analysers were appropriately combined in the post-accelerator section of the

spectrometer. The emergence of this technology coincided with the need to analyse ^{129}I as a monitor of nuclear fuel processing and waste storage and its development in this field soon led to the use of ^{129}I as a tracer for ocean circulation measurements.

2. Automated sample combustion systems have been available for a number of years, but their interface to AMS systems has been hindered by the significantly lower efficiency of earlier ion sources for C^- ion production from CO_2 gas rather than from solid graphite. The development of a high current CO_2 gas source by Oxford University [5, 6] and High Voltage Engineering Europa [7] has opened up a number of possibilities for fully integrated sample preparation and analysis systems [6, 8]. The development of a rapid ^{14}C analysis system for the analysis of ambient and higher levels of ^{14}C at IsoTrace is one example.
3. The use of chemical reaction cells has extended the range of applications for inductively coupled plasma mass spectrometry. The adaptation of this technology to AMS systems for isobar separation is fraught with many obstacles: e.g. conversion from positive to negative ions and large ion losses at even low AMS injection energies. However, studies with negative ions and chemical reaction cells have resulted in the recently funded project to integrate a reaction cell directly on the AMS injection line described in Section 4.

2. Heavy element analysis and iodine-129

2.1. Requirements for heavy element analysis

For any mass spectrometry system, as the atomic number of the element to be analysed increases, the number of possible interferences grows far more rapidly. This is particularly true for AMS where the rare ions have to be separated from beams of a related abundant ion, typically at ratios ranging from 10^{-10} to 10^{-15}. The equipment used to generate and transport the large ion beams necessary to measure very low concentrations, itself can contribute to the interference problem. One example of this is the caesium sputter source, which, while producing copious numbers of ions, gives the ions an energy distribution with tails both below and above the principal energy. Ions in the tail of the distribution from the abundant ion can have the same momentum as the rare ions at the peak of their distribution and therefore not be de-selected by magnetic analysis. A second example arises from the need to use a windowless gas canal in the high voltage terminal of the accelerator to change this ion charge from negative to positive. While this electron stripping canal also serves to destroy molecular interferences, small quantities of stripper gas degrade the vacuum in the high energy accelerator tube and cause a finite number of ions to change charge all along the high energy tube [8]. This gives rise to a continuum energy distribution of ions which can obscure the detection of rare ions at extremely low concentrations.

A solution to such problems involves the use of both electric and magnetic analysers: the former used to select a specific region from the energy spectrum of the ion beam (E/q) and the latter, a specific region from the momentum spectrum (ME/q^2), where E is the energy, M the mass and q the charge of the ion in question. The width of the energy distribution from the ion source can be limited very effectively by the insertion of a moderate resolution electric analyser between the source and the injection magnet of the system. The configuration used at IsoTrace is shown in figure 1 of ref. The interferences from the low abundance continuum of ions emerging from the accelerator requires a more complicated solution, when one considers that further scattering and charge changing in the residual gas of the vacuum system between the accelerator and the final detector. The number of continuum ions entering the detector varies inversely as the resolution of the high energy spectrometer magnet and the interleaving of electric and magnetic analysers reduces the contribution from post-accelerator scattering and charge changing [8]. The arrangement shown in figure 1 of ref. [8] has provided us with a very effective tool for the analysis of elements such as ^{129}I [2], but could be improved by the addition of a second magnet following the second electric analyser and better vacuum pumping.

2.2. Iodine-129 analysis and example

As a product of nuclear fission with a half life of 1.57×10^7 a, that is highly mobile in most environmental systems, ^{129}I has long been used as a tracer for monitoring the handling of nuclear fuel and waste material. With the ability to analyse very small samples by AMS [4], other applications based on the natural occurrence of uranium in the environment became possible: the study of groundwater flow in aquifers [5] and the characterization of oil reservoirs [6]. However, the advent of large scale nuclear fuel reprocessing, specifically at Sellafield, England and Cap la Hague, France, as a by-product, provided a unique opportunity for ocean circulation tracer measurements [7]. Collectively, these plants had maintained a relatively constant discharge rate of ~50 kg per year throughout the early 1990s, into the Irish Sea and the English Channel, respectively. Plumes from these points have been traced through the Norwegian Sea and beyond, into the Arctic Ocean [9] and over to the deep water formation regions east of Greenland [12]. In the mid 1990's the ^{129}I discharge rate was increased to > 200 kg per year [8], resulting in a pulse in the ^{129}I signal that will provide timing information for a number of circulation studies.

These studies are being continued, using the IsoTrace heavy element line, by J.N. Smith and his collaborators. The pulse associated the ^{129}I discharge increase has been traced through the Denmark Strait overflow waters into the Labrador Sea. Figure 1 shows the section between Labrador and Greenland with the stations where the sampling occurred; Figure 2, shows the distribution of ^{129}I in this region as a function of depth and location of the sampling stations. The penetration of the ^{129}I signal in the south-flowing deep Atlantic return current is evident. This plume will continue to be followed in collaboration with groups at Woods Hole Oceanographic Institution.

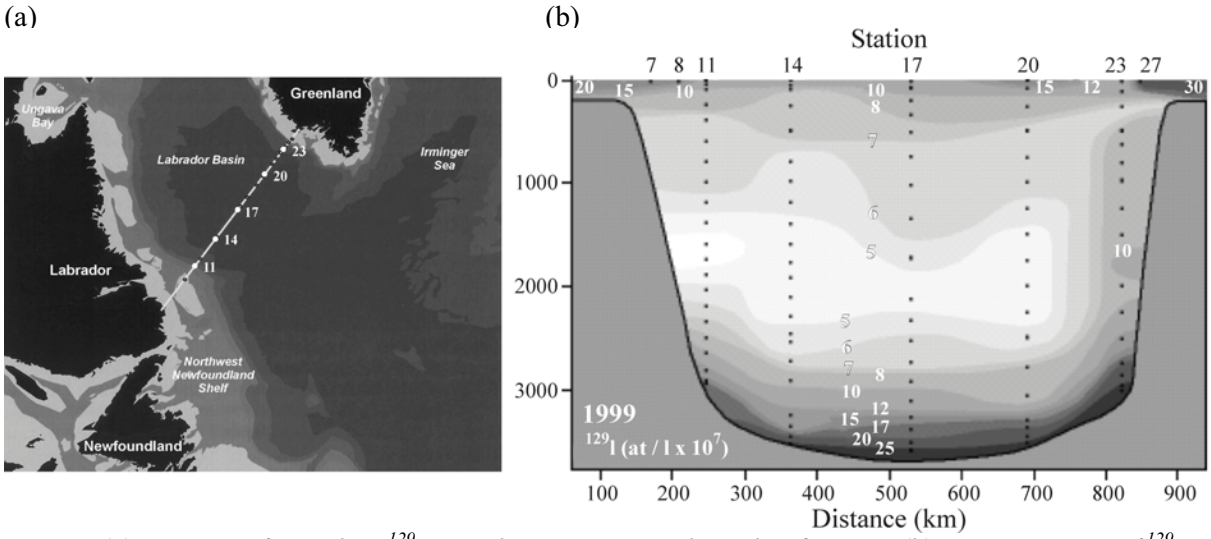

FIG. 1. (a)Location of sampling ^{129}I sampling stations in the Labrador Sea; (b) Concentration of ^{129}I as a function of depth and station location.

3. The rapid radiocarbon analysis project

3.1. Motivation

In addition to the uses of ^{14}C which derive from its cosmogenic formation, as a tool for dating and tracing the evolution of geologically recent natural processes and human history, ^{14}C is extensively used as a tracer in pharmaceutical and other biomedical research [13] and is produced anthropogenically and stored in significant quantities in a number of nuclear reactor systems [14]. Its long radiological half-life (5730 years) and low energy beta emission, make it very difficult to detect

at low levels in the field, using standard radiation survey instruments. Its biological residence time (~40 days in humans) [21] means that it can cause long-term health consequences if it is ingested or otherwise incorporated in human tissue, even at concentrations that are too low to measure with the conventional survey equipment. Hence, given the ready availability of ^{14}C, its accidental or malicious dispersal into the environment is a cause for concern for agencies in charge of national security and civil defense.

Assessing the aerial extent of a release of ^{14}C would require the analysis of a large number of easily obtained organic samples with a level of ^{14}C near and slightly above current ambient levels and the current methods for such analyses, both beta counting and AMS normally require which would hinder this process unacceptably under emergency conditions. However, the higher levels of ^{14}C present in such circumstances (between ambient and 1000 times ambient) require less critical sample preparation procedures than those needed for ^{14}C dating, where the levels can be as low as a factor 1000 below ambient and so these procedures are more amenable to automation. The development by Oxford Radiocarbon Accelerator Unit and High Voltage Engineering Europa of an AMS ion source capable of relatively high efficiency production of C^- ions from CO_2 gas [15] prompted the integration of this source (HVEE model SO-110-200) with automated combustion equipment at IsoTrace. This project is a collaboration between the Radiation Protection Bureau of Health Canada, the Atlantic Environmental Radioactivity Unit of Fisheries and Oceans Canada, High Voltage Engineering and IsoTrace, funded through the CRTI program [16] administered by Defense Research Canada.

3.2. Equipment

The rapid ^{14}C analysis system requires the integration of three components into the AMS system: the combustion unit, a transfer line that will match the output rate of the combustion system to feed rate of the ion source and permit parallel processing, and the SO-110 ion source itself. A schematic showing sample path through the essential components of all three units is shown in Figure 2.

3.2.1. The Combustion Unit

Rather than using a basic combustion unit which would provide an output stream of all combustion products, a decision was made to adapt and use an elemental analyzer in which gas chromatographic techniques are used to separate the combustion products. Of the available models, the Elementar Vario EL III was selected because of its somewhat larger sample capacity and its use of separate traps to isolate individual combustion products (SO_2, H_20 and CO_2). These traps can be individually released by electronic command, a feature which simplifies the design of the transfer line. In addition, the CO_2 production and trap unloading time is well matched to the anticipated AMS analysis time.

Initial tests of this unit have resulted in the replacement of some gas line fittings to reduce atmospheric leakage and an increase in the size of the water trap following the combustion column. Some modification to the control software is anticipated and as the elemental analyzer will be located in the spectrometer room, the function of weighing the samples before combustion will be separated and carried out offline.

3.2.2. The CO_2 transfer line

In order to maximize throughput and eliminate wastage of spectrometer time, parallel operation of the elemental analyzer and the ion source are necessary; i.e. while the ion source is analyzing a sample, the elemental analyzer is processing the following one. In addition, both the elemental analyzer and the ion source are designed for the use of helium as a carrier gas for the combustion products and the CO_2. However, the requirements of He pressure and flow rate are different for each device. Thus, the transfer line will consist of two parallel traps, one being loaded by the elemental analyzer while the second is being unloaded to the ion source.

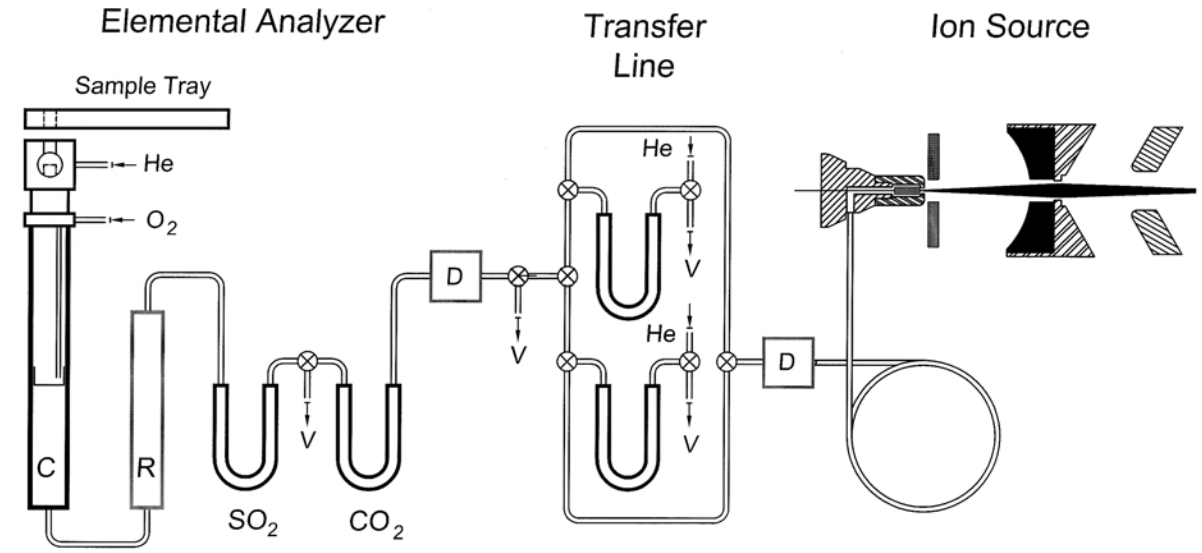

FIG. 2. Gas flow schematic for the three major components in the rapid ^{14}C system. To simplify the drawing, water traps are not shown. C *is the combustion tube,* R *is the reduction tube,* V *are vents,* D *are thermal conductivity detectors. The valves in the transfer line allow the elemental analyser to fill one of the traps while the other feeds gas to the ion source.*

3.2.3. The SO-110 CO_2 gas ion source

This ion source is based on the conventional high current negative ion caesium sputter source design in which caesium vapour is ionized by contact with a spherical tungsten ionizer at 1200°C and is focused onto a target in close proximity (~ 3 cm). Typical operating voltages are -2 to -4 kV from the ionizer to the target and 20 to 36 kV from the ionizer to ground, giving a total ion beam energy of up to 40 kV. To accommodate gas samples, the target holding assembly is designed to accept the gas feed at atmospheric pressure through a 0.25 mm diameter capillary and the target tip is modified to hold a titanium pellet (~2 mm diameter) inside a stainless steel shroud which partially contains the gas. Direct pumping of the ionizer and target vacuum system minimize the effect of the gas load.

As the titanium pellets acquire carbon atoms from the samples through adsorption and implantation by the sputtering process, they are changed for each sample. Hence, even in gas analysis mode, the 200 sample loading magazine is required. Experiments are now in progress to determine the optimum helium and CO_2 flow rates and to assess the possibility of using argon as a carrier gas. Analysis of the source control software is underway so that all three components can be operated in an unattended mode for production analysis.

4. Isobar separation using chemical reaction cells

Chlorine-36, produced in the atmosphere by the cosmic ray induced spallation or neutron activation of argon isotopes is an important tool for the study of groundwater. Its half life of 3.01×10^5 a, its conservative properties within groundwater and the lack of alternate sources of ^{36}Cl in most host rocks make it an ideal tool for determining the age of aquifers and tracing flow within them [23]. However, like a number of heavier elements it cannot be analysed with small accelerators simply by adding magnetic and electric spectrometers with higher resolution. Higher energy and thus larger accelerators (> 6 MV) are necessary so that range separation techniques can be used to remove the ^{36}S isobar [24, 25].

The addition of chemical reaction cells to inductively coupled plasma mass spectrometers has increased the selectivity of these instruments by using chemical reactions to remove interferences in

the positive ion beam through collisions with low pressure gas atoms or molecules in the reaction cell [26]. However, due to the low efficiency for conversion from positive to negative ions and the multiple scattering on conversion, it is impractical to adapt this technology to AMS (although it would be manageable if the charge changing canal were located near the entrance to the accelerator). Nevertheless, Fergusen and co-workers, in unrelated much earlier work, showed that similar chemical reactions could occur in a simple gas cell when using negative ions [27, 28]. With the realization that these reactions might be useful for solving the ^{36}Cl – ^{36}S isobar problem, these measurements were repeated and confirmed using Cl^- and S^- beams from an electrospray source and a radiofrequency quadrupole cell by Doupé [29], using equipment at Ionics Mass Spectrometry Group.

A collaboration between IsoTrace and Ionics MSGL has been funded to build a prototype system to demonstrate this capability on an actual AMS system. Figure 3 shows a schematic diagram of the path of the AMS low energy beam through the components that will be needed to separate the isobars. The beam from a high intensity sputter source, with energy ~30 keV, is magnetically analysed and the abundant ion species (^{35}Cl and ^{37}Cl) are collected in off-axis Faraday cups. The mass-36 beam is then decelerated to several hundred eV in a retarding lens, transferring the beam to the following components which are operated at a potential with respect to ground potential of several hundred volts less than the ion beam energy. A segmented RF ion guide, with a longitudinal DC gradient, will then be used to decelerate the beam from several hundred eV to approximately 1 eV. A short ion guide section containing an inert gas will then be used as a cooler, to minimizing lateral momentum and variations in the longitudinal momentum. This will be followed by an ion guide in a windowless gas cell where the charge transfer reactions take place. The final section is a standard RF quadrupole mass spectrometer to remove any interfering ions that might be scattered and emerge from the collision cell. The remaining mass-36 beam will then be re-accelerated to ~30 keV in a series of gap lenses for injection into the AMS system. The entire region between the gap lenses, operated at ~ –29 kV, will be pumped by two large cryopumps.

In the first year of its operation, this system will be used to optimize the many parameters that specify both the exact configuration of the ion guides and the operating conditions of the guides and reaction cell. Once these parameters are fixed and effectively a second prototype is built, validation and efficiency tests using blanks and reference materials will begin followed by the demonstration of the analysis of real hydrological and exposure age samples.

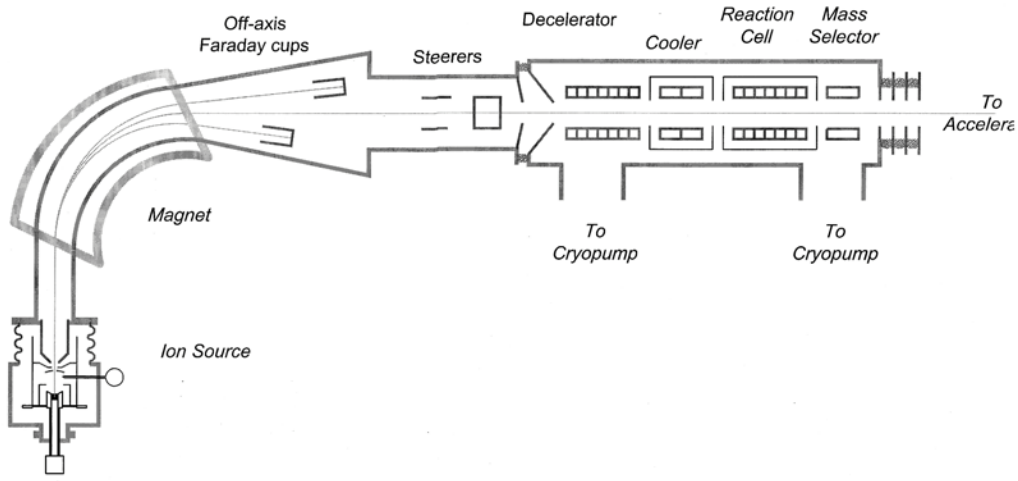

FIG. 3. Schematic drawing of the isobar selector as installed in the low energy end of an accelerator mass spectrometer. The unit containing the Decelerator, Cooler, Reaction Cell and Mass Selector is isolated and operated at a negative high voltage, several hundreds of volts less than the energy of the beam when it leaves the ion source.

5. Summary

Throughout the 27 year history of AMS, advances in this technology have often been made by introducing techniques and equipment from other fields. The ability to use less expensive, smaller accelerators in combination with additional electric and magnetic analysers has enhanced the widespread use of ^{129}I data for ocean circulation and other global transport studies. The use of gas chromatographic techniques in sample preparation and handling, with the availability of efficient gas fed ion sources, has already begun to open new avenues in ^{14}C analysis. Finally, the introduction of reaction cell technology as developed for ICP-MS, is showing a potential for expanding the capabilities of small AMS systems to a number of applications in which isobar elimination has been a problem.

ACKNOWLEDGEMENTS

Funding for part of the operation of the IsoTrace Laboratory and the research and development work discussed in this paper has been provided by the Natural Sciences and Engineering Research Council of Canada and the University of Toronto. Equipment and development of the rapid ^{14}C analysis system has been funded by the CRTI program [16] of Defense Research Canada. The authors also wish to thank the IsoTrace sample preparation technologists C. Soto and I. Ellis for their contributions to the ^{129}I and rapid ^{14}C programs respectively and R.P. Beukens and K. Leung for their work on the software and control systems.

REFERENCES

[1] ALVAREZ, L. W., CORNOG, R., ^{3}He in helium, Phys. Rev. **56** (1939) 379.
[2] MULLER, R. A., Radioisotope dating with a cyclotron, Science **196** (1977) 489-494.
[3] PURSER, K.H., LIEBERT, R.B., LITHERLAND, A.E., BEUKENS, R.P., GOVE, H.E., BENNETT, C.L., CLOVER, M.R., SONDHEIM, W.E., An attempt to detect stable N– ions from a sputter ion source and some implications of the results for the design of tandems for ultra-sensitive carbon analysis, Rev. Phys. Appl. **12** (1977) 1487-1492.
[4] STEIER, P., DELLINGER, F., KUTSCHERA, W., PRILLER, A., ROM, W., WILD, E.M., Pushing the Precision Limit of ^{14}C AMS**,** Radiocarbon **46** (2004) 5-16.
[5] BRONK RAMSEY, C., HEDGES, R.E.M., Hybrid ion sources: Radiocarbon measurements from microgram to milligram, Nucl. Instr. Meth. **B123** (1997) 539-545.
[6] BRONK RAMSEY, C., DITCHFIELD, P., HUMM, M., Using a Gas Ion Source for Radiocarbon AMS and GC-AMS**,** Radiocarbon **46** (2004) 25-32.
[7] MOUS, D.J.W., GOTTDANG, A., FOKKER, W., VAN DEN BROEK, R., KOOPMANS, R.B., The HVEE ^{14}C isotope ratio mass spectrometer for biomedical applications, *(*Proc. 15th Int. Conf. on the Application of Accelerators for Research and Industry, Denton, Texas, November 1998), AIP Conf. Proc. **475** (1999) 657.
[8] UHL, T., KRETSCHMER, W., LUPPOLD, W., SCHARF, A., Direct Coupling of an Elemental Analyzer and a Hybrid Ion Source for AMS Measurements, Radiocarbon **46** (2004) 65-75.
[9] KILIUS, L.R., RUCKLIDGE, J.C., LITHERLAND, A.E., Background Reduction for Heavy Element Acceleratory Mass Spectrometry, Nucl. Instr. Meth. **B31** (1988) 433-441.
[10] KILIUS, L.R., BABA, N., GARWAN, M.A., LITHERLAND, A.E., NADEAU, M-J., RUCKLIDGE, J.C., WILSON, G.C., ZHAO, X-L., AMS of Heavy Ions with Small Accelerators, Nucl. Instr. Meth. **B52** (1990) 357-365.
[11] KIESER, W.E., ZHAO, X-L., SOTO, C.Y., TRACY, B., Accelerator Mass Spectrometry of Iodine-129: Technique and Applications. J. Radioanal. Nucl. Chem. **262** (in press).
[12] ELMORE, D., GOVE, H.E., FERRARO, R., KILIUS, L.R., LEE, H.W., CHANG, K.H., BEUKENS, R.P., LITHERLAND, A.E., RUSSO, C.J., PURSER, K.H., MURRELL, M.T., FINKEL, R.C., Determination of ^{129}I using tandem accelerator mass spectrometry, Nature **286** (1980) 138-140.

[13] FABRYKA-MARTIN, J., DAVIS, S.N., ELMORE, D., Applications of ^{129}I and ^{36}Cl in hydrology, Nucl. Instr. Meth. **B29** (1987) 361-371.

[14] FEHN, U., TULLAI, S., TENG, T.E., ELMORE, D.E., KUBIK, P., Determination of ^{129}I in residues of two crude oils, Nucl. Instr. Meth. **B29** (1987) 380-382.

[15] YIOU, F., RAISBECK, GM., ZHOU, Z.Q., KILIUS, L.R., ^{129}I from Nuclear Fuel Reprocessing: Potential as an Oceanographic Tracer, Nucl. Instr. Meth. **B52** (1990) 436-439.

[16] SMITH, J.N., ELLIS, K.M., KILIUS, L.R., ^{129}I and ^{137}Cs tracer measurements in the Arctic Ocean, Deep-Sea Res. I **45** (1998). 959-984.

[17] EDMONDS, H.N., Tracer Applications of Anthropogenic Iodine-129 in the North Atlantic Ocean, Ph.D. thesis, Massachusetts Institute of Technology (1997) 186 pp

[18] RAISBECK, G.M., YIOU, F., ZHOU, Z.Q., KILIUS, L.R., KERSHAW, P.J., Marine discharges of I-129 by the nuclear reprocessing facilities of La Hague andSellafield, Radioprotection **32** (1997) 91-96

[19] VOGEL, J., Accelerator mass spectometry for human biochemistry: The practice and the potential, Nucl. Instr. Meth. **B172** (2000) 884-891.

[20] ALLSOP, P.J., JULIEN, J.P.S., Carbon-14 production and release in CANDU reactors, Atomic Energy of Canada Report **RC-1765**, Chalk River ON (1998).

[21] INTERNATIONAL COMMISSION ON RADIOLOGICAL PROTECTION: Annals **23** (1993) 141-167.

[22] **C**hemical, Biological, Radiological and Nuclear **R**esearch and **T**echnology **I**nitiative: http://www.crti.drdc-rddc.gc.ca/home_e.html.

[23] GOVE, H.E., Tandem-accelerator mass-spectrometry measurements of ^{36}Cl, ^{129}I and osmium isotopes in diverse natural samples, Phil. Trans. Royal Soc. London **A323** (1987) 103-119.

[24] ANDREWS, H.R., KOSLOWSKY, V.T., CORNETT, R.J.J., DAVIES, W.G., GREINER, B.F., IMAHORI, Y., MCKAY, J.W., MILTON, G.M., MILTON, J.C.D., AMS measurements of 36 Cl at Chalk River, Nucl. Instr. Meth. **B92** (1994) 74-78.

[25] SYNAL, H-A., BEER, J., BONANI, G., LUKASCZYK, C., SUTER, M., ^{36}Cl measurements at the Zúrich AMS facility, Nucl. Instr. Meth. **B92** (1994) 79-84.

[26] TANNER, S.D., BARANOV, V.L., BANDURA, D.R., Reaction Cells and Collision Cells for ICP-MS: Spectrochim. Acta **B57** (2002) 1361-1452.

[27] FEHSENFELD, F.C., FERGUSON, E.E., Further laboratory measurements of negative reactions of atmospheric interest, Planetary & Space Sci. **16** (1968) 701-702.

[28] DUNKIN, D.B., FEHSENFELD, F.C., FERGUSON, E.E., Thermal Energy Rate Constants for the Reactions $NO_2^- + Cl_2 \rightarrow CL_2^- + NO_2$, $Cl_2^- + NO_2 \rightarrow Cl^- + NO_2Cl$, $SH^- + NO_2 \rightarrow NO_2^- + SH$, $SH^- + Cl_2 \rightarrow Cl_2^- + SH$, and $S^- + NO_2 \rightarrow NO_2^- + S$, Chem. Phys. Lett. **15** (1972) 257-259.

[29] DOUPE, J., Assessment of Strategies for Measuring Cl-36 in Natural Samples, PhD Thesis, University of Toronto (2004).

^{53}Mn in ferromanganese encrustations

Korschinek, G.[a], M. Poutivtsev[a], T. Faestermann[a], K. Knie[a], G. Rugel[a], A. Wallner[b], J. Scholten[c], A. Mangini[d]

[a] Technische Universität München,
Garching,
Germany

[b] Universität Wien,
Vienna,
Austria

[c] Christian-Albrechts-Universität zu Kiel,
Kiel,
Germany

[d] Heidelberger Akademie der Wissenschaften,
Heidelberg,
Germany

Hydrogenetic deep-sea ferromanganese crusts reflect the changes of chemical composition of sea water on geological time scales. They grow extremely slowly with only a few mm/Myr and cover time spans up to 60 Myr. Therefore, they are an important archive for the reconstruction of paleo-oceanographic, paleogeographic, paleoclimatic, and even "paleoastronomic" [1] events.

Usually, ferromanganese crusts are dated radiometrically. The assumption of a known input of a radionuclide and the measurement of its decrease with depth allows a determination of the crust's growth rate and hence gives an age-to-depth relation. For time spans beyond about 1 Myr the cosmogenic nuclide ^{10}Be ($T_{1/2}$ = (1.51 ± 0.06) Myr) allows dating up to ~ 10 Myr [2].

However, the production rate of ^{10}Be depends on the magnitude of solar and geomagnetic fields, which reflect cosmic rays. Cosmic ray fluxes and thus ^{10}Be production rates in the past are not exactly known.

In this study the feasibility of dating with ^{53}Mn ($T_{1/2}$ = (3.7 ± 0.2) Myr) is being investigated, which is advantageous and/or complementary to ^{10}Be for different reasons:

i) ^{53}Mn has more than twice the half-life of ^{10}Be, thus dating of longer time-spans should be possible.

ii) ^{53}Mn is not significantly produced in the atmosphere (due to the lack of targets heavier than argon) but only in extraterrestrial dust particles. Therefore, its input is not influenced by geomagnetic field fluctuations. However, a constant flux of extraterrestrial matter has to be assumed.

We have measured several crusts originating from the Pacific Ocean. Near-continent crusts will be compared with far-continent crusts. The results will be shown and compared with ^{10}Be measurements.

REFERENCES

[1] KNIE, K., et al., Phys. Rev. Lett. **83** (1999) 18.
[2] SEGEL, M., et al., Nature **309** (1984) 540.

From bulk to particle analysis – a new challenge for radioecology

Betti, M., L. Aldave de las Heras, G. Tamborini

European Commission,
JRC, Institute for Transuranium Elements,
Karlsruhe,
Germany

Radioactivity may be introduced in the environment through a variety of systems and processes. Human activities involving nuclear weapons and nuclear fuel cycle (including mining, milling, fuel enrichment, fabrication, reactor operation, spent fuel stores, reprocessing facilities, medical applications and waste storage) are important, leading to a significant creation and release of radioactivity. Human technology also releases pre-existing natural radionuclides, which would otherwise remain trapped in the earth's crust. For instance, burning of fossil fuel (oil and coal) dominates direct atmospheric release at pre-existing natural radioactivity.

The distribution pattern of radioactive fallout depends on weather conditions (i.e. wet or dry) and on the nature of the surface and the physical-chemical form of the radionuclides, which may vary according to release and transport conditions as well as element properties. A general distinction can be made between gases, aerosols and particulate material. Particles with higher activity concentration, known as "hot particles", may result from atmospheric nuclear weapon tests or nuclear reactor accidents. Their activity is diluted as material is transferred to soil and water directly or via vegetation and movement through other biota. Therefore, for monitoring radioactivity in the environment it is necessary to analyse bulk samples from all biosphere compartments as well as single microparticles.

Analytical chemistry plays a determinant role for routine verifications as well as in case of radiological alarm to take decision for restoration of the environment and protection of the citizens.

The reference laboratory for the measurement of radioactivity in the environment (MaRE lab) at the Institute for Transuranium Element (European Commission, Joint Research Centre) provides scientific and technical support to the policy of the Directorate General for Transport and Energy (DG TREN) of the European Commission, both for the implementation of the requirements of environmental radioactivity surveillance (Art. 35-36 of the Euratom Treaty) and in the framework of the OSPAR (Oslo-Paris Convention) strategy with regards to radioactive substances for the protection of marine environment of the North-East Atlantic. MaRE lab provides also support to IAEA and Euratom for the detection of clandestine nuclear activities in the framework of nuclear safeguards and non-proliferation of nuclear materials.

In this lecture the role of the analytical techniques based, above all, on mass spectrometry and radiometry, is highlighted as applied to samples of different origin, for the determination of radionuclides (U, Np, Pu, Am, fission products) in bulk as well as in radioactive microparticles. The necessity to have complementary techniques in order to have independent results (in terms of Quality assurance/quality control) as well as to attain a complete inventory of the radioisotopes is shown.

Precise uranium isotopic measurements in groundwater around the CEA's Vaujours site

Baude, S., F. Pointurier, R. Chiappini

Commissariat à l'Energie Atomique (CEA),
DIF/DASE/SRCE,
Bruyères-le-Châtel,
France

Abstract. The French site Vaujours has undergone a number of explosion experiments involving some slightly depleted uranium material. The precise environmental assessment of this decommissioned facility was needed to answer questions from the local population. Since natural uranium is present at ppb levels in groundwater, we used high precision mass spectrometry and the resin bead technique to demonstrate that uranium migration is very limited.

1. Introduction

The CEA's (French Atomic Energy Commission) Vaujours site was selected in 1955 to conduct high explosive tests for research in explosives technology and safety studies. Experiments for understanding the physical interaction of materials with explosives were also performed. Between 1964 and 1992, about 2000 dry shots were made, mostly in a semi-containment configuration. These tests involved about 1200 kg of uranium. Although these experiments were conducted in accordance with health safety and environmental regulations, the decommissioning of the plant for the subsequent sale of the site led to the need for a precise environmental assessment to answer questions from the local population.

To carry out the environmental assessment, two main axes were chosen: first, to perform a radiological survey at the storage points where some waste materials were temporarily deposited after experiments; and second, to study the hydrogeology of the environment surrounding the site. The first point allowed to demonstrate the surface cleanliness after the decommissioning and to determine the actual source term from contaminated soils. The second point investigated the low uranium contamination of the underground and evaluates the short, medium and long term impacts of the storage activities.

2. Description of the site

The Vaujours centre is located in the region "Ile de France", 20 km north-east of Paris (Seine-Saint-Denis). The Fort of Vaujours was built at the end of the 19th century, on a hill. As described in Fig. 1 below, the Fort was built on a limestone layer forming the upper aquifer. To monitor the hydrogeology, this layer was equipped with several piezometers. A couple of rain water collectors were connected to the clay and gypsum layers. Note also the presence of springs.

3. Sampling and analytical techniques

In order to conduct the radiological survey, 34 soil sampling points were taken at 3 depth levels each, 4 rock cores were taken and 9 points were sampled for mosses. As for surface and ground waters, 17 sampling points were considered, including 9 piezometers, 5 rain water collectors and 2 springs.

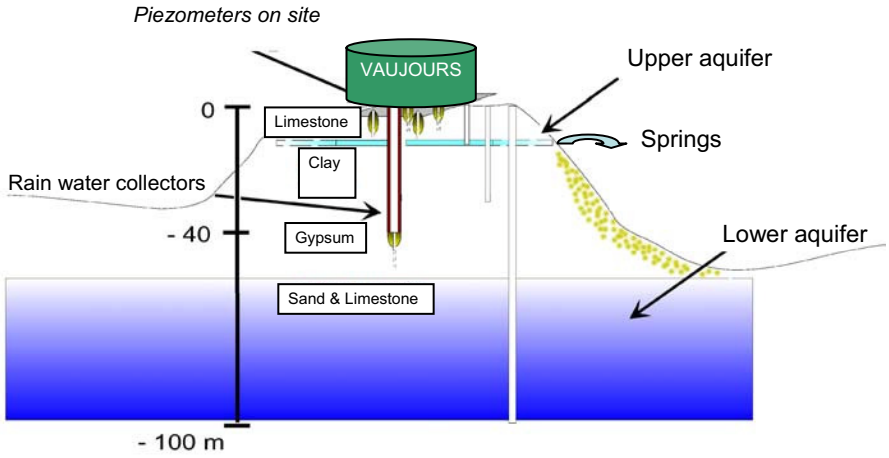

FIG. 1. Schematic of the hill under the Fort of Vaujours.

To reveal the migration of anthropogenic uranium in the environment, very precise isotopic ratio measurements are needed, due to the presence of natural uranium. Moreover, on this site, we determined the average value for the source term after measuring different contaminated soils and found a ratio $^{235}U/^{238}U = 0.0067$ (± 5%). This ratio is very close to natural uranium.

We therefore selected the sensitive and precise thermal ionization mass spectrometry technique using resin beads in association with a clean lab radiochemistry to have the lowest background [1-3].

3.1. Resin beads

400 µm beads of AG1X8 DOWEX resin (20-50 mesh) were selected. We rinsed the beads in ethanol and preconditionned them with hydrochloric acid. The beads were stored in diluted HCl.

3.2. Water samples

The samples are concentrated from about 100 mL to 50 µL. If the residue was small enough, we dried and added 5 µL of concentrated HCl and fixed the uranium with 2 or 3 beads overnight before loading on a rhenium filament (Cathodeon, U.K., Zone Refined). If the residue was too large, a small ion exchange column allowed uranium purification (fixing with nitric acid 8M and rinsing with HNO_3 0.1M).

3.3. Mass spectrometry

Filaments were measured using a single collector double focusing VG54-38 TIMS instrument (VG, U.K.). Peak jumping on a laboratory-built low background counting detector allowed about 1 million counts per second for total uranium signal from beads containing a few tens of picograms of U. Typical conditions were 4-5 amps corresponding to 1800°C. Figure 2 below shows a SEM picture of the resin beads on the Rh filament before and after the run.

4. Results

The measurements of the uranium concentrations in the waters around Vaujours were obtained for low and high waters conditions. As reported in Fig. 3, the uranium concentration ranged from 0.1 µg/L to 9.0 µg/L, where the average geological background for uranium is typically 2-3 µg/L.

The data for isotopic ratios are reported in Fig. 4. The correlation between $^{234}U/^{238}U$ and $^{235}U/^{238}U$ indicates that a large number of data are not significantly different from natural uranium.

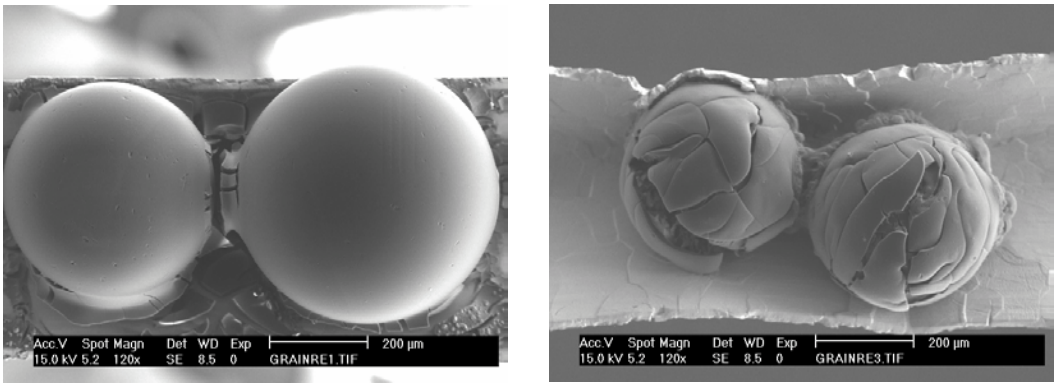

FIG. 2. SEM picture of the resin beads on the Rh filament before (left) and after (right) the run.

For the points that differ from natural uranium we can differentiate two main effects, the first is the depletion of ^{235}U due to anthropogenic uranium (mostly visible in rain water collector RWC P2).

The second effect is enrichment in ^{234}U due to leaching effects at the rock-water interface. This well-documented phenomenon results from a combination of α decay, chemical (U vs. Th) and physical (mass of ^{234}U vs ^{238}U) effects [4-5].

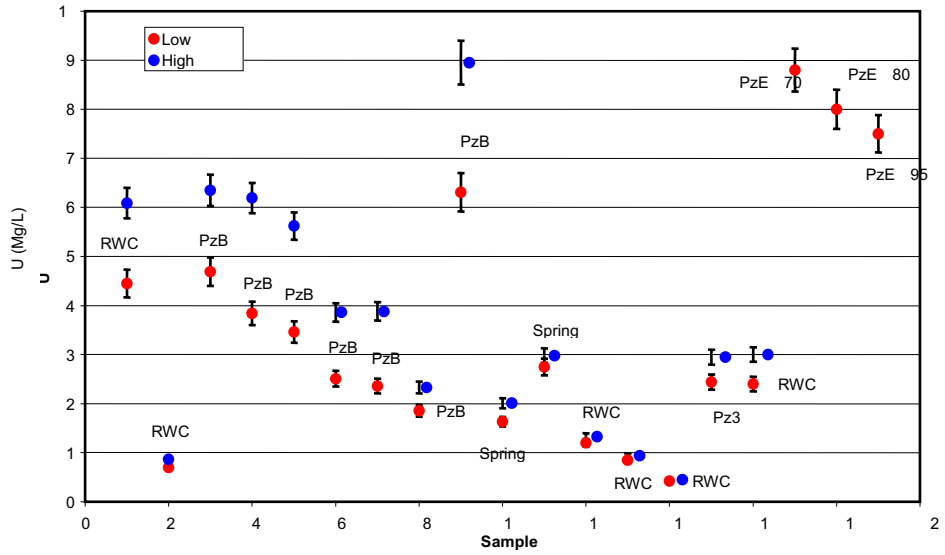

FIG. 3. Uranium concentration in ground waters (µg/L).

5. Conclusions

The authors made the environmental assessment of Vaujours center using the resin bead TIMS technique. The challenge was to demonstrate a very small contamination originating from anthropogenic uranium very close to natural levels. The technique revealed itself to be precise and sensitive. These measurements also show the important effect of deep waters-rock interface on the ^{234}U.

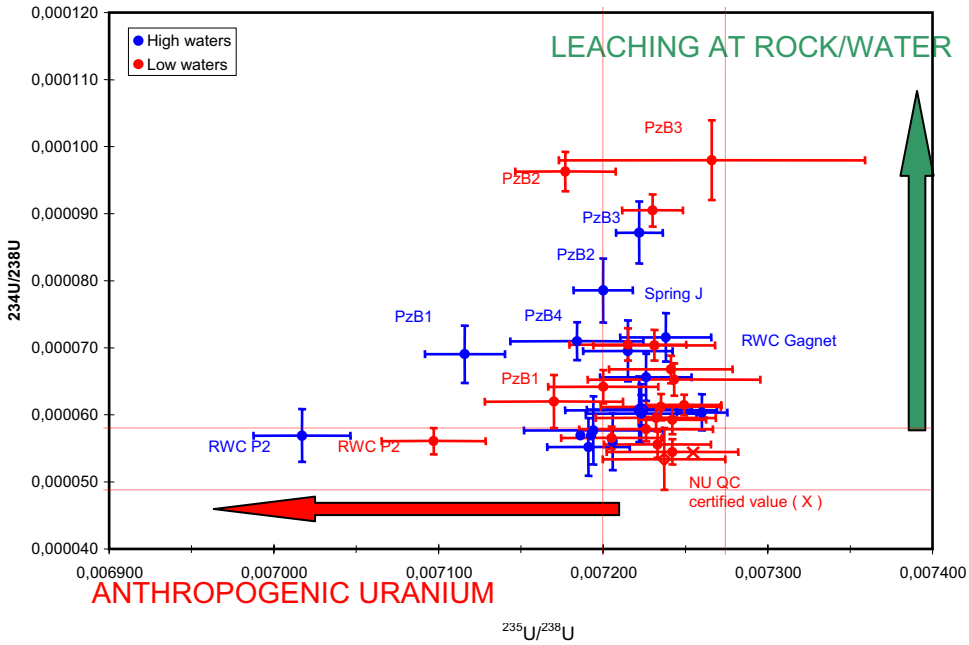

FIG. 4. $^{234}U/^{238}U$ vs. $^{235}U/^{238}U$ (atom ratios).

REFERENCES

[1] SMITH, D.H., CARTER, J.A., Int. J. Mass Spectrom. Ion Phys. **40** (1981) 211-215.
[2] POUPARD, D., JOUNIAUX, B., Radiochimica Acta **49** (1980) 25-28.
[3] POUPARD, D., JUERY, A., Radiochimica Acta **57** (1992) 21-24.
[4] REMY, M.L., LEMAITRE, N., Hydrogeologie **4** (1990) 267-278.
[5] CLANET, F., LECLERCQ, J., REMY, M.L., MORONI, J.P., CR Acad. Sci. **282** (1976) 804-810.

VERA, a versatile facility for accelerator mass spectrometry

Priller, A., M. Auer, R. Golser, W. Kutschera, P. Steier, C. Vockenhuber, A. Wallner, E.M. Wild, S. Winkler

VERA Laboratory,
Institute for Isotope Research and Nuclear Physics,
University of Vienna,
Vienna,
Austria

The Vienna Environmental Research Accelerator (VERA) is a center for accelerator mass spectrometry (AMS) at the University of Vienna based on a 3-MV tandem accelerator of the pelletron type. Since its opening in 1996 [1, 2], VERA has undergone a number of changes converting it to an AMS facility which can now measure almost all isotopes [3, 4]. A schematic layout of the facility in its present form is shown in figure 1. Although primarily built for AMS experiments, VERA will have in future also a PIXE setup (Proton Induced X-Ray Emission), both for internal and external proton-beam experiments.

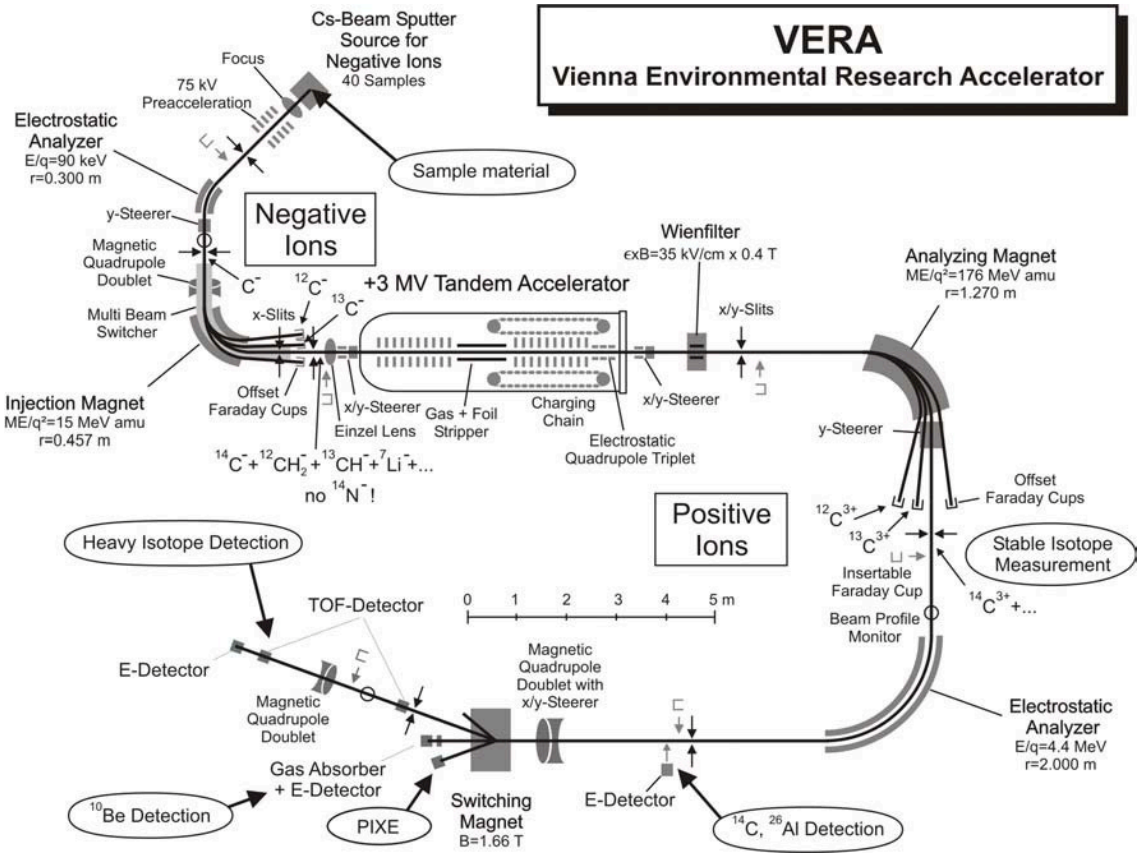

FIG. 1. Schematic layout of the VERA facility in its present form. The locations for the measurement of the three carbon isotopes for a ^{14}C AMS measurement is indicated. Other light radioisotopes (^{10}Be, ^{26}Al) are measured at the respective detector positions. Heavy radioisotopes (^{129}I, ^{182}Hf, ^{210}Pb, ^{236}U, and ^{244}Pu) are measured at the beamline including a TOF (time-of-flight) setup. The future PIXE position is also indicated.

VERA is operated in essentially three different modes: (1) AMS ^{14}C measurements are performed on a truly commercial basis for a company in the USA, and a full service including sample preparation, AMS measurement and ^{14}C calibration is offered for other customers (mostly for archaeological studies). (2) Cross disciplinary research programs employing ^{10}Be, ^{14}C, ^{26}Al, and ^{129}I are pursued in collaboration with experts from many different fields (e.g. archaeology [5], art, atmospheric transport and chemistry, botany, climatology, forensic medicine [6], geomorphology, high-mountain research, hydrology, ice core research). (3) Research programs involving both instrumental and new-isotope developments are also pursued. This includes the heavy isotope extension of VERA [3] to measure ^{182}Hf, ^{210}Pb, ^{236}U, and ^{244}Pu. Novel detector developments involve low-temperature calorimetric detectors [7] and natural diamond detectors [8].

VERA can be operated fully automated for "routine" measurements of ^{14}C, as well as manually for more exploratory experiments at the frontier of AMS. This presentation will concentrate on a few examples to demonstrate the large breadth of application with such a facility. One of these examples utilizes ocean sediments, where AMS measurements are under way to search for a possible signal from supernova-produced isotopes such as ^{182}Hf [9] and ^{244}Pu [10].

REFERENCES

[1] KUTSCHERA, W., COLLON, P., FRIEDMANN, H., GOLSER, R., HILLE, P., ROM, W., STEIER, P., TAGESEN, S., WALLNER, A., WILD, E., WINKLER, G., VERA: A New AMS Facility in Vienna, Nucl. Instr. Meth. Phys. Res. B **123** (1997) 47.

[2] PRILLER, A., GOLSER, R., HILLE, P., KUTSCHERA, W., ROM, W., STEIER, P., WALLNER, A., WILD, E., First Performance Tests of VERA, Nucl. Instr. Meth. Phys. Res. B **123** (1997) 193.

[3] VOCKENHUBER, C., AHMAD, I., GOLSER, R., KUTSCHERA, W., LIECHTEN-STEIN, V., PRILLER, A., STEIER, P., WINKLER, S., Accelerator Mass Spectrometry of Heavy Long-lived Radionuclides, Int. Jour. Mass. Spec. **223-224** (2003) 713.

[4] STEIER, P., GOLSER, R., KUTSCHERA, W., PRILLER, A., VOCKENHUBER, C., WINKLER, S., VERA, An AMS Facility for "All" Isotopes, Nucl. Instr. Meth. Phys. Res. B (in press).

[5] KUTSCHERA, W., MUELLER, W., "Isotope Language" of the Alpine Iceman Investigated with AMS and MS, Nucl. Instr. Meth. Phys. Res. B **204** (2003) 705.

[6] WILD, E.M., ARLAMOVSKY, K.A., GOLSER, R., KUTSCHERA, W., PRILLER, A., PUCHEGGER, S., ROM, W., STEIER, P., VYCUDILIK, W., ^{14}C Dating with the Bomb Peak: An Application to Forensic Medicine, Nucl. Instr. Meth. Phys. Res. B **172** (2000) 944.

[7] KRAFT, S., ANDRIANOV, V., BLEILE, A., EGELHOF, P., GOLSER, R., KISELEVA, A., KISELEV, O., KUTSCHERA, W., MEIER, J.P., PRILLER, A., SHRISVASTAVA, A., STEIER, P., VOCKENHUBER, C., First Application of Calorimetric Low-Temperature Detectors in Accelerator Mass Spectrometry, Nucl. Instr. Meth. Phys. Res. A **520** (2004) 63.

[8] LIECHTENSTEIN, V.K., EREMIN, N.V., GOLSER, R., KUTSCHERA, W., PASKHALOV, A.A., PRILLER, A., STEIER, P., VOCKENHUBER, C., WINKLER, S., Nucl. Instr. Meth. Phys. Res. A **521** (2004) 203.

[9] VOCKENHUBER, C., FELDSTEIN, C., PAUL, M., TRUBNIKOV, N., BICHLER, M., GOLSER, R., KUTSCHERA, W., PRILLER, A., STEIER, P., WINKLER, S., Search for Live ^{182}Hf in Deep-Sea Sediments, New Astron. Rev. **48** (2004) 161.

[10] WINKLER, S., AHMAD, I., GOLSER, R., KUTSCHERA, W., ORLANDINI, K.A., PAUL, M., PRILLER, A., STEIER, P., VOCKENHUBER, C., Anthropogenic ^{244}Pu in the Environment, New Astron. Rev. **48** (2004) 151.

Measurement of radioisotopes in marine samples by sector field ICP-MS

Wyse, E., S.-H. Lee, A. Rodriguez y Baena, S. Azemard, J.-C. Miquel, J. Gastaud, M.K. Pham, P.P. Povinec, S. de Mora

Marine Environment Laboratory,
International Atomic Energy Agency,
Monaco

Inductively coupled plasma mass spectrometry (ICP-MS) is renowned for its ultra-low limits of detection for measuring trace elements. Unlike other methods of elemental analysis, mass spectrometry separates and analyzes isotopes individually. With additional sensitivity for high-mass isotopes and virtually no spectral interferences in this mass range, ICP-MS is ideally suited for actinide analysis, and has been widely used in this capacity almost since its commercial inception in the mid-1980s.

The introduction of sector field ICP-MS has further increased its advantage and thus its application in radioecological studies. Improved ion transmission has dramatically enhanced both sensitivity and instrumental precision; limits of detection in the low pg L^{-1} range and isotope ratio precision of 0.1% RSD are routinely achievable, making the technique more sensitive than radiometrics counting methods for many of the longer-lived actinides.

The IAEA-MEL uses sector field (SF) ICP-MS for a variety of radioecological applications. Specific examples of these applications will be highlighted.

SF-ICP-MS has been used for measuring plutonium isotopes in seawater and sediments. Samples are spiked with ^{242}Pu as an internal quantitation standard before sample preconcentration. Special considerations include potential polyatomic interferences, which can be diagnosed via a decreased-mass peak shift. A desolvating nebulizer is used to minimize this effect. Higher resolution settings are also a possibility, however the sacrifice in sensitivity generally makes this option impractical. Table l lists as a typical example the analysis of ^{239}Pu and ^{242}Pu in IAEA reference materials for radionuclides in the marine environment.

SF-ICP-MS is also widely used for several projects requiring uranium information. Total uranium is typically measured in all kinds of environmental samples. A recent project investigating the transport of ^{234}Th in seawater to assess carbon export also attempted to confirm the correlation of total uranium with salinity, as has been proposed in other studies [1]. Optimal precision and accuracy was ultimately obtained by using isotope dilution with ^{236}U. On other projects, the $^{235}U/^{238}U$ ratio is often measured for determining possible inputs from either enriched (e.g., via the nuclear fuel cycle) or depleted (e.g., armor-piercing ballistics) sources. A special consideration for uranium isotopic analysis is the dead time of the detector, which must be accurately measured before beginning an analysis.

Table I. Pu isotopic ratios in IAEA Reference Materials (RMs) for radionuclides in the marine environment

RM	^{239}Pu Bq kg^{-1}	^{240}Pu Bq kg^{-1}	^{240}Pu/^{239}Pu mass ratio	Recommended $^{239+240}$Pu* Bq kg^{-1}
IAEA-134	9.8 ± 0.8	7.7 ± 0.6	0.212 ± 0.008	15 (13.8-16.2)
IAEA-135	127 ± 4	95 ± 4	0.196 ± 0.002	213 (205 -226)
IAEA-381	8.2 ± 0.3	7.1 ± 0.5	0.242 ± 0.022	14.2 (13.2 -15.2)
IAEA-384	103 ± 3	16 ± 1	0.049 ± 0.001	108 (105-110)
IAEA-385	1.9 ± 0.3	1.2 ± 0.1	0.178 ± 0.005	*Data not yet available*
IAEA-414	0.081 ± 0.008	0.049 ± 0.007	0.185 ± 0.005	0.120 (0.114-0.130)

* The recommended value (median) of the reference material represents the combined activities of ^{239}Pu and ^{240}Pu, measured by alpha-ray spectrometry. The 95% confidence interval is shown in parentheses.

ACKNOWLEDGEMENT

The Agency is grateful for the support provided to its Marine Environment Laboratory by the Government of the Principality of Monaco.

Environmental monitoring of long-lived radionuclides using multi-collector ICPMS

Gerdes, A., S. Weyer, G. Brey

Department of Mineralogy,
W Goethe-University,
Frankfurt,
Germany

Multi-collector Inductive Coupled Plasma Mass Spectrometry (MC-ICPMS) becomes increasingly important in monitoring environmental contamination, because it allows detection of long-lived radionuclides at ultra trace levels. High sample throughout combined with high precision and accuracy, low detection limits for most elements and simultaneous detection of up to 9 isotopes makes it prior to most other techniques. For homogeneous samples concentration and isotope composition can be determined with a precision and uncertainty of usually better than 0.5% using the isotope dilution method, e.g. isotope measurements relative to a well characterised ^{233}U tracer.

Exposure to low-level radioactive dust released into the environment accidentally or by the use of Depleted Uranium (DU) munitions in the military theatre demands precise screening of humans and local environment. Sensitive methods are also needed for monitoring and understanding the pathway of radionuclides in the biosphere and the human body. Using a method recently developed at our department it is for instance possible to detect urinary excretion of DU in the low fg/mL range or at fractions below 0.2% of the total urinary uranium concentration. This allows to monitor the inhalation of up to a few microgram of insoluble non-natural uranium particles in the lung several months or even years later.

As example we will show and discuss results from our study of the uranium isotope composition and concentration of surface water, topsoil and dust from different sites of Baghdad, Basra, and the Suweirah farming area. We also analysed urine from people living in these areas or stayed their for a relative short time. The samples, also including highly contaminated ones, such as wipes of tank top debris and penetrator channels, were collected from the Uranium Medical Research Centre field team after coalition operation Iraqi Freedom in early October 2003. Total soil samples, separated soil fine-fractions (< 100 micrometers), dust and evaporated water samples were spiked with an ^{233}U tracer of well-known composition and leached in hot aqua regia over more than 12 hours at about 100°C.

For the uranium-in-urine method about 500 mL were weighted, acidified with nitric acid to a pH < 2, and stirred at about 80°C on a hotplate. Uranium was co-precipitated with $Ca_3(PO_4)_2$ and the precipitate rinsed several time with ultra pure water, centrifuged and redissolved in 3:1 HNO_3:H_2O_2 mixture and heated to about 120°C for more than 12 hours in Teflon vessels in order to destroy remaining organic material. A ^{233}U tracer were added either during weighing of the total urine volume or to a 2 g aliquot, precisely weight to ± 0.5 mg. To minimize sample contamination we used only double-distilled acids, 18 Ohm MQ H_2O and reagents and beakers, which were thoroughly pre-cleaned before use. A beaker containing MQ H_2O instead of urine and an in-house urine standard were always processed alongside with the samples as procedural blank and reference monitor, respectively.

Uranium fractions of all samples were purified by ion-exchange chromatography using UTEVA resin before analysing with a double-focusing MC-ICPMS Neptune equipped with a retarding potential quadrupole lens and a secondary electron multiplier for ion counting. A Cetac autosampler and Aridus desolvating nebuliser were used for sample introduction. Reproducibility of the $^{235}U/^{238}U$, $^{234}U/^{238}U$

and $^{236}U/^{238}U$ (= 4.5 x 10^{-8}) for a 8ppb NBS950a solution (n=14) over two days were about 0.1, 0.4 and 5%, respectively. The recovery of U after chemical purification was usually better than 80% and analytical blanks for the entire soil and the urine method were below 1 and 6 picogram ^{238}U, respectively. Signal sensitivity of 0.3-0.4 V $ng^{-1}mL$, negligible $^{235}U^{1}H^{+}$ formation and ^{238}U tailing below 3 x 10^{-8} at m/z 236 enables precise detection of ^{236}U below 1 fg/g at $^{236}U/^{238}U$ ratios of below 3 x 10^{-8}. Using an enrichment factor of about 500 for urine the limit of detection for ^{236}U is about 2 x10^{-19} g/mL (0.2 ag/mL) and for ^{238}U about 1 x 10^{-14}g/mL urine. Accuracy and precision were monitored using NIST SRM NBL112a and SRM 950a as well as internal urine standards of natural and depleted uranium composition. The latter were prepared from natural urine very precisely mixed with uranium solutions made of pure metals. Errors were calculated by propagating the main error sources, such as uncertainties of all applied corrections and the reproducibility of the NBL112a.

Uranium and plutonium atom ratios and concentration factors in Reservoir 11 and Asanov Swamp, Mayak PA

Standring, W.J.F.[a], P. Børretzen[a], D.H. Oughton[b], L.K. Fifield[c]

[a] Norwegian Radiation Protection Authority,
Østerås,
Norway

[b] Department of Plant and Environmental Science,
Agricultural University of Norway,
Ås,
Norway

[c] Department of Nuclear Physics,
Australian National University,
Canberra, ACT,
Australia

Mayak Production Association, East Ural, Russia was established in the late 1940s to produce weapons-grade plutonium. Routine discharges and accidents at Mayak PA contaminated large areas with radionuclides, including the Techa River. When the scale of contamination became apparent a cascade of artificial reservoirs was constructed to store liquid wastes, hold back contamination and significantly reduce the amounts of radionuclides entering the Techa River. Reservoirs 10 and 11 (dams constructed in 1956 and 1963, respectively) are the largest: Russian total inventory estimates in 1993-1995 were 6.6 PBq and 1.2 PBq for Reservoirs 10 and 11, respectively [1]. These reservoirs are expected to have been influenced by more recent discharges from civil reprocessing. However, Techa sediments and riverbank soils, notably in the boggy Asanov Swamp downstream from Reservoir 11, are expected to contain artificial radionuclides from previous direct discharges associated with the production of weapons-grade plutonium.

The present work was designed to study atom ratios for U and Pu isotopes in water, soil, grass and aquatic biota samples collected in 1994 and 1996 from Reservoir 11 and the Asanov Swamp area. The study had three objectives: to generate new data in the form of $^{236}U/^{235}U$ atom ratios to help clarify the nuclide source characteristics in the studied areas; to confirm sediment and water $^{240}Pu/^{239}Pu$ atom ratios found in the literature for Mayak PA and supplement them with new ratios for biota samples; and lastly, to estimate concentration factors (CF) for the different biota in the studied area.

Atom ratios ($^{236}U/^{235}U$, $^{235}U/^{238}U$ and $^{240}Pu/^{239}Pu$) were determined using Accelerator Mass Spectrometry (AMS) to confirm radionuclide source characteristics and calculate activities and concentration factors for the studied samples. $^{236}U/^{235}U$ ratios give information about nuclear fuel burn-up time; $^{236}U/^{235}U$ ratios increase from weapons to civil sources. Plutonium isotope ratios vary with reactor type, nuclear fuel burn-up time, neutron flux and energy; and from weapon type and yield after nuclear detonations. $^{240}Pu/^{239}Pu$ atom ratios enable weapons grade Pu (ratio of 0.01-0.05) to be distinguished from civil reprocessing (ratio of 0.2-0.8) and global fallout (ratio of 0.17-0.19).

Our new data shows that Asanov samples had lower $^{236}U/^{235}U$ ratios than Reservoir 11 samples: 0.0005 - 0.0045 for Asanov compared with 0.0074 - 0.0153 for Reservoir 11 indicating that Asanov samples are affected by early discharges from weapons-grade Pu production. Results for Pu support

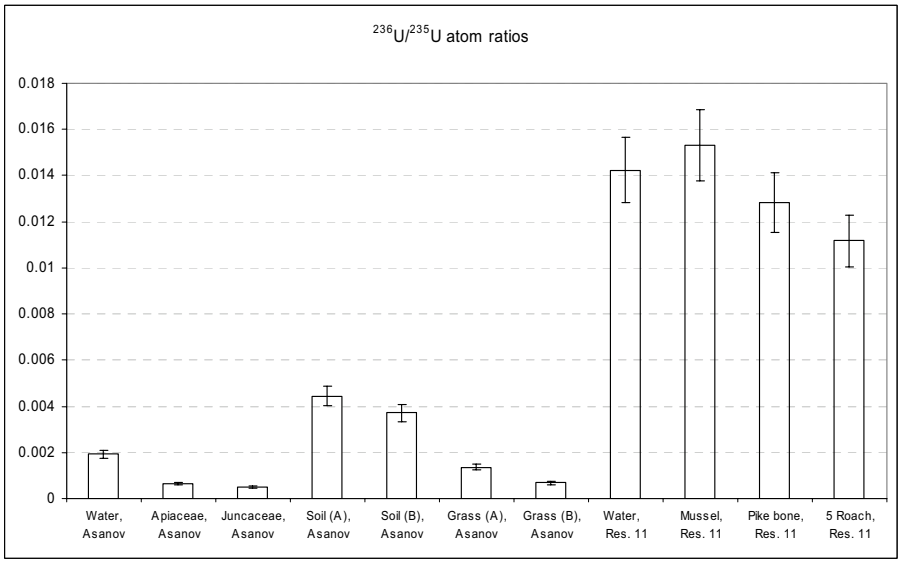

FIG. 1. Atom ratios for $^{236}U/^{235}U$. Error bars show 10 % uncertainty.

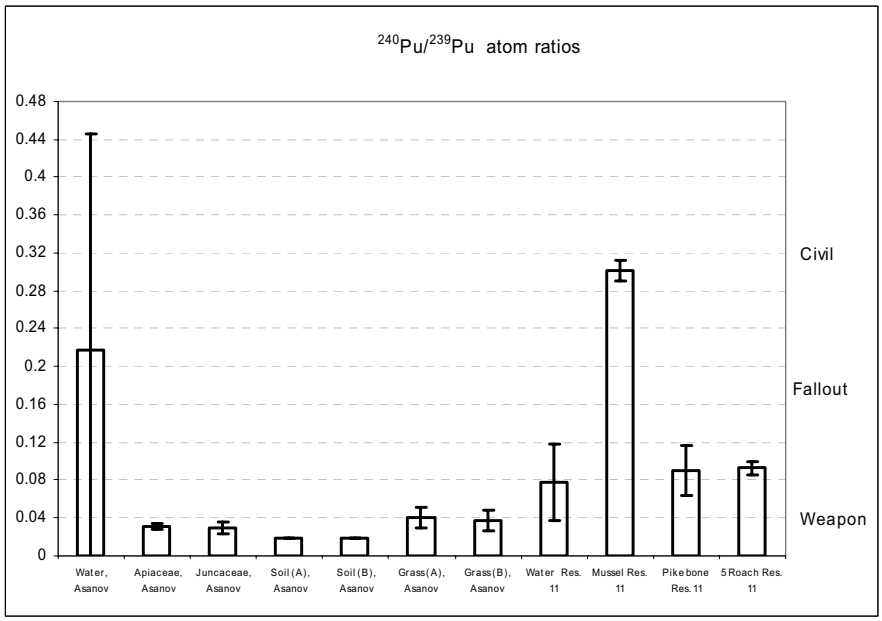

FIG. 2. Atom ratios for $^{240}Pu/^{239}Pu$: expected Pu ratio-ranges for weapon grade derived, fallout derived and civil reprocessing derived Pu are also indicated. Error bars based on ± 1 σ counting errors.

this: The lowest $^{240}Pu/^{239}Pu$ atom ratios were consistently found in Asanov Swamp samples (about 0.019) while $^{240}Pu/^{239}Pu$ atom ratios in Reservoir 11 were higher, indicating influence from more recent civil reprocessing. Uranium and plutonium concentration factors calculated for vegetation and biota samples at Mayak were comparable with corresponding values found in the literature.

[1] JOINT NORWEGIAN-RUSSIAN EXPERT GROUP (JNREG), Sources contributing to radioactive contamination of the Techa River and areas surrounding the 'Mayak' production association, Urals, Russia. Programme of the Joint Norwegian-Russian Investigations of possible impacts of the Mayak PA activities on radioactive contamination of the Barents and Kara Seas, JNREG, Østerås (1997).

Distribution of Pu and Am isotopes in BOMARC missile site soil

Lee, M.H., Y.J. Park, W.H. Kim

Nuclear Chemistry Research Division,
Korea Atomic Energy Research Institute,
Daejon,
Korea, Republic of

The activity concentrations as well as the activity and atomic ratios of the Pu and Am isotopes in different sizes of the soil sampled around BOMARC Missile Site were obtained by radiochemical analysis. The association pattern between the actinides and soil particles was investigated using a spherical model of a particle size with a variable radius. From the activity and atomic ratios of Pu and Am, the origin of the Pu and Am isotopes was identified in the BOMARC Missile Site soil.

Plutonium is one of the transuranic elements which is primarily present in the environment as a result of human activity, namely as the fallout from nuclear weapon testings during the late 1940s through to the early 1960s, and accidental releases due to military mishaps. One particular mishap occurred in 1960 at McGuire Air Force Base in New Jersey, when a Boeing Michigan Aeronautical Research Center (BOMARC) missile caught fire and the warhead was partially melted by the fire. Although the missile did not explode, subsequent fire fighting activities contributed to the dispersion of weapons grade plutonium into the local environment.

Soil samples around BOMARC site were taken to a depth of 2 inches by the U.S. Air Force Institute for Environment. The soil samples were blended and homogenized in a soil tumbler, and subdivided into approximately 20-gram samples. Grain size fractions were determined with sieves. Determination of ^{239,240}Pu, ^{238}Pu, ^{241}Pu, ^{241}Am and ^{238}U was performed using a radiochemical method. After adding ^{242}Pu, ^{243}Am and ^{232}U tracers, a total of a 2 g ashed soil sample was dissolved with concentrated HNO_3 and HF and evaporated to dryness. Dissolution in HNO_3/HF was repeated and again evaporated to dryness. The residue was dissolved in 9 M HCl. After filtration, the solution was passed over an anion exchange column (chloride form) to which the Pu was sorbed. The columns were washed with 9 M HCl followed by 8 M HNO_3. This effluent was evaporated to dryness and reserved for subsequent separation of the Am and U isotopes. Pu was eluted with 0.36 M HCl / 0.01 M HF. The Am and U residue was dissolved in 2 M HNO_3. Samples were loaded onto TRU Spec columns, after the TRU columns were conditioned with 2 M HNO_3. The columns were washed with 2 M HNO_3 and 9 M HCl. The Am fraction was eluted with 4 M HCl. U was eluted with 0.1 M ammonium oxalate solution. The Am fraction was purified with anion exchange resin that had been previously conditioned with 1 M HNO_3 – 93% CH_3OH. The purified Pu, Am and U isotopes were electroplated on stainless steel platelets and measured by an alpha spectrometer. For measuring the ^{241}Pu, Pu isotopes electrodeposited onto the stainless steel planchet were dissolved in 8 M HNO_3 and purified with an anion exchange column. The purified Pu isotopes were subjected to the ^{241}Pu measurement by a low background liquid scintillation counter. Also, the atomic ratios of ^{240}Pu/^{239}Pu were measured by a high resolution inductively coupled plasma mass spectrometry.

The activities of ^{239,240}Pu and ^{241}Am were apparently increased with a decreasing particle size of soil due to an increasing surface area, and the fitted values for these isotopes were correlated well with actual measured values (^{239,240}Pu; 0.994, ^{241}Am; 0.992). This result suggests that most of the Pu and Am isotopes are fixed to the soil as a surface coating. The fitted values of ^{238}U did not correlated well with the measured activities of ^{238}U (R^2 ; 0.588), which implies that a significant fraction of the U may be partitioned into the soil matrix rather than sorbed onto the particle surfaces.

The activity ratios of $^{238}Pu/^{239,240}Pu$ in different particle sizes of the BOMARC soil were found to be in the range of 0.018 to 0.033 with a mean value of 0.024, which is lower than the reported value (0.04) influenced by the SNAP-9A satellite accident in 1964. The activity ratios of $^{241}Pu/^{239,240}Pu$ and $^{241}Am/^{239,240}Pu$ were measured in the range of 2.87 to 3.52 and 0.15 to 0.24, respectively. These values are a little lower than the recently reported activity ratios influenced by the fallout from the nuclear weapons test. Also, the atomic ratios of $^{240}Pu/^{239}Pu$ in the BOMARC soil were found to be in the narrow range of 0.0559 to 0.0594 with a mean value of 0.0576, which is close to the value (0.05) of the weapon grades plutonium rather than the fallout value (0.18) influenced by the nuclear weapons test. Therefore, as a result of the activity ratios $^{238}Pu/^{239,240}Pu$ of $^{241}Pu/^{239,240}Pu$ and $^{241}Am/^{239,240}Pu$ as well as the atomic ratios of $^{240}Pu/^{239}Pu$, the Pu and Am isotopes detected in the BOMARC soil originated from the weapons grade plutonium rather than the nuclear weapon testings.

Detection of reprocessing activities through stable isotope measurements of atmospheric xenon by mass spectrometry

Pointurier, F., J.P. Fontaine, Ph. Hémet, N. Baglan, S. Baude, R. Chiappini

Commissariat à l'Energie Atomique (CEA),
DIF/DASE/SRCE,
Bruyères-le-Châtel,
France

Abstract. Noble gas stable isotope abundance measurements are a tool for detecting reprocessing activities of nuclear fuels. As a matter of fact, specific parameters such as burn-up and reactor type can be determined thanks to high precision mass spectrometers. However, these are costly instruments requiring skilful staff. The authors developed a simple method based on an inductively coupled plasma mass spectrometer which allows fast and accurate stable xenon isotope ratio measurements on air samples without xenon concentration. Relative standard deviations (RSD) are typically 0.4-0.5% for major isotopes and 1-2% for minor isotopes.

1. Introduction

It has been proved that noble gas stable isotope abundance measurements provide a tool for detecting reprocessing activities of nuclear fuels [1, 2]. Gas releases will significantly modify the natural isotopic ratio of xenon in the air surrounding the nuclear material. Moreover, it has been shown that specific parameters such as burn-up and reactor type can be determined thanks to high precision mass spectrometry [3, 4]. Nevertheless, these high cost instruments require skilful staff and tedious analytical procedures. On top of that, concentration of xenon from the air is needed as initial xenon concentration in the sample is below 100 ppb. Attempts at xenon isotopic measurements using commercially available quadrupole mass spectrometers with an electron impact source have not been successful [5, 6] because of lack of sensitivity and elevated background noise. The aim of the work presented here is to carry out simple, fast and accurate xenon isotopic abundance measurements on air sampled at atmospheric pressure (air grabbing) in the close vicinity or inside a nuclear facility, without purification and pre-concentration by gas chromatography and with a mass spectrometer available in our laboratory, easy to handle for us and at a reasonable cost. As induction plasma can be a powerful ionization source for noble gases [7], we tested an ICP-MS (Inductively Coupled Plasma - Mass Spectrometer), which is largely used in our laboratory for low-level actinide measurements. Gaseous samples are introduced through a home-made introduction line for gaseous samples.

2. Experimental device and methodology

A schematic of the gas handling system used for these experiments is given in Fig. 1 below. The 300 cm^3 bottles are filled with laboratory air or with sample and pressurized to 2 bars. Samples are initially at atmospheric pressure. The gas mixture is bled through the mass flow regulator so that a constant flow rate is maintained for a few minutes. A 1 ppm xenon standard is used to optimize sensitivity, stability and background of the mass spectrometer. Pure argon is used to rinse all the tubing. A more complete cleaning can be obtained thanks to a primary pump. The ICP-MS is a VG Elemental "PlasmaQuad2+" (Winsford, Cheshire, UK). Sensitivity is about 3.5×10^5 counts/s for ^{132}Xe with natural air flowing at 1 l/h. The xenon global ionization efficiency (dry plasma) can be estimated to be about 2×10^{-6}, which is about 4% of the uranium ionization efficiency, assuming total consumption of the sample using a micro-nebuliser.

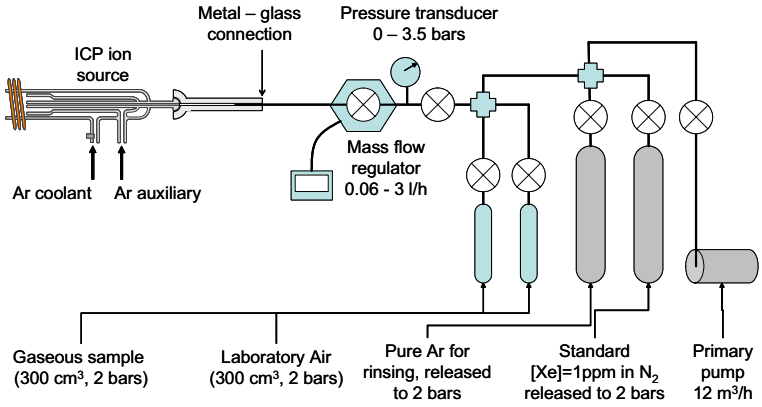

FIG. 1. Schematic of the gas handling system used for these experiments.

We correct for instrumental mass bias by bracketing each sample with a "xenon standard", which is actually a laboratory air sample. After measurement of each sample or standard, we rinse the introduction line with pure argon. Analysis of a sample typically lasts 10 minutes. No correction for isobaric or polyatomic interference is needed.

3. Results

Results of xenon isotope ratio measurements for a natural air sample collected around the laboratory are given in the Table I below. Results are compared with the values recommended by IUPAC for the natural xenon. The two sets of values are in very good accordance. Acceptable precision is obtained with typical RSD of 0.4-0.5% for major isotopes and of 1-2% for minor isotopes. It must be noted that these RSD are close to the ones associated to IUPAC natural xenon isotopic ratios.

Table I. Results of xenon isotopic ratio measurements for a natural air sample

Isotopic ratios	124/132	126/132	128/132	129/132	130/132	131/132	134/132	136/132
Lab air sample	0.00352	0.00335	0.07135	0.98467	0.15195	0.78697	0.38675	0.32949
SD	0.00008	0.00010	0.00056	0,00468	0,00097	0.00416	0.00158	0.00172
RSD	2.33%	2.88%	0.79%	0.48%	0.64%	0.53%	0.41%	0.52%
IUPAC nat. Xe	0.00357	0.00335	0.07136	0.98330	0.15173	0.78760	0.38825	0.32980
SD	0.00004	0.00004	0.00023	0.00390	0.00054	0.00280	0.00125	0.00096
RSD	1.06%	1.14%	0.32%	0.40%	0.36%	0.36%	0.32%	0.29%

4. Conclusion and future work

We developed instrumentation and methodology for fast (less than 20 minutes for sample + standards) and direct (air sample collected at atmospheric pressure, no xenon concentration) xenon isotope ratio measurements. We used for this a sensitive instrument (ICP-MS) normally dedicated to trace analysis in environmental samples and a home-made introduction line for gases.

Future works are: 1) measurement with a double-focusing sector-field ICP-MS, more sensitive and more precise for isotopic ratio measurement; 2) acquisition and use of a xenon isotopic standard (if one exists) and 3) test on real gas samples collected on the stack of a nuclear facility.

REFERENCES

[1] OHKUBO, M., Gaseous isotope correlation technique for safeguards at reprocessing facilities, IAERA-STR-240, International Atomic Energy Agency (1988).

[2] NAKHLEH, C.W., et al., "Noble gas atmospheric monitoring at reprocessing facilities, LA-UR-97-705, Los Alamos National Laboratory (1997).

[3] AREGBE, Y., et al., Detection of reprocessing activities through stable isotope measurements of atmospheric noble gases, Fresenius J. Anal. Chem. **358** (1997) 533-535.

[4] AREGBE, Y., et al., Release of anthropogenic xenon to the atmosphere: a large-scale isotope dilution, Int. J. of Mass Spectrometry and Ion Processes **154** (1996) 89-97.

[4] AREGBE, Y., et al., Comparative isotopic measurements on xenon and krypton, Int. J. Mass Spectr. and Ion Proc. **163** (1996) L1-L5.

[6] LEBRUN, A., et al., Faisabilité de la détermination du taux de combustion des assemblages au cours du cisaillage en tête d'usine de retraitement par la mesure des rapports isotopiques des gaz rares de fission, Note Technique CEA/DRN/DER/SSAE 97/0042 (1997).

[7] POTHS, J., CHAMBERLAIN, E.P., A high efficiency ion source for Kr and Xe isotopic measurements, Int. J. Mass Spectr. and Ion Proc. **146/147** (1995) 47-54.

Matrix effects during magnetic sector-field inductively coupled plasma mass spectrometry uranium isotope ratio measurements in complex environmental/biological samples

Quétel, C.R., E. Ponzevera, I. Tresl, E. Vassileva

European Commission Joint Research Centre,
Institute for Reference Materials and Measurements,
Geel,
Belgium

Sample matrix effects on mass discrimination during inductively coupled plasma mass spectrometry (ICP-MS) isotope ratio measurements are rarely reported. However, they can lead to errors larger than the uncertainty claimed on the ratio results when not properly taken into account or corrected for. For instance, up to 1% matrix specific effects were experienced during an isotope dilution mass spectrometry campaign we carried out for the certification of the Cd amount content in some food digest samples (7% acidity and salt content around 450μg g^{-1}) [1].

Specific nuclear safeguards programs were designed for the monitoring of declared and non-declared nuclear activities and important efforts are currently deployed to better understand the consequences on human health of the dispersion of depleted uranium in the environment. The interest in developing and/or improving measurement capabilities for uranium isotope ratios and uranium content in environmental and biological samples has therefore considerably increased in the last decade [2]. However, procedure validation is rarely addressed with these developments even though, for instance, non-disputable uncertainty statements are absolutely crucial to underpin correctly the important decisions of political, economical, military or medical nature that can arise from these results. This is why we produced simulated urine samples (complex matrix made of organic and inorganic components) with certified $n(^{234}U)/n(^{238}U)$, $n(^{235}U)/n(^{238}U)$ and $n(^{236}U)/n(^{238}U)$ ratios. These, which will eventually be commercially available for validation purposes, will first be used as test materials for an international interlaboratory comparison organised by IRMM and this exercise, named NUSIMEP-4 and open for participation to anyone [3].

This presentation will introduce magnetic sector-field inductively coupled plasma mass spectrometry (ICP-MS) uranium isotope ratio measurements on real human urine samples and in the NUSIMEP-4 test materials. These were carried out respectively with two different types of instruments, a single detector (SD) “high resolution” ICP-MS and a multiple collector (MC) ICP-MS. Our results illustrate the importance of carefully adapting the sample preparation and measurement calibration strategies to meet the uncertainties targeted for the end results. The analytical protocol originally developed included a microwave assisted acid digestion step, a matrix separation step by extraction chromatography on U-TEVA resin and an acquisition step by SD-ICP-MS using the IRMM-184 isotopic certified reference material to correct externally for mass discrimination effects. This combination proved to be fit for the purpose of getting ~ 2.5% combined uncertainty (U, k = 2) on $n(^{235}U)/n(^{238}U)$ ratio determination in real human urine samples at ultra low uranium levels (~ 5 – 20 pg g^{-1}) [2]. The same protocol was investigated for MC-ICP-MS measurements and simulated urine samples containing ~ 250 to 1000 times more uranium. Repeatability on MC-ICP-MS measurements can be as good as 0.02% (simultaneity of the signal acquisition) and thus the expectation was that this would result into an important reduction of the overall measurement uncertainty. However, our results show that it is not possible to get even 0.2% U. As described in the Figure below, this is mostly due to uncorrected small size matrix effects becoming “visible” thanks to the performance achievable with

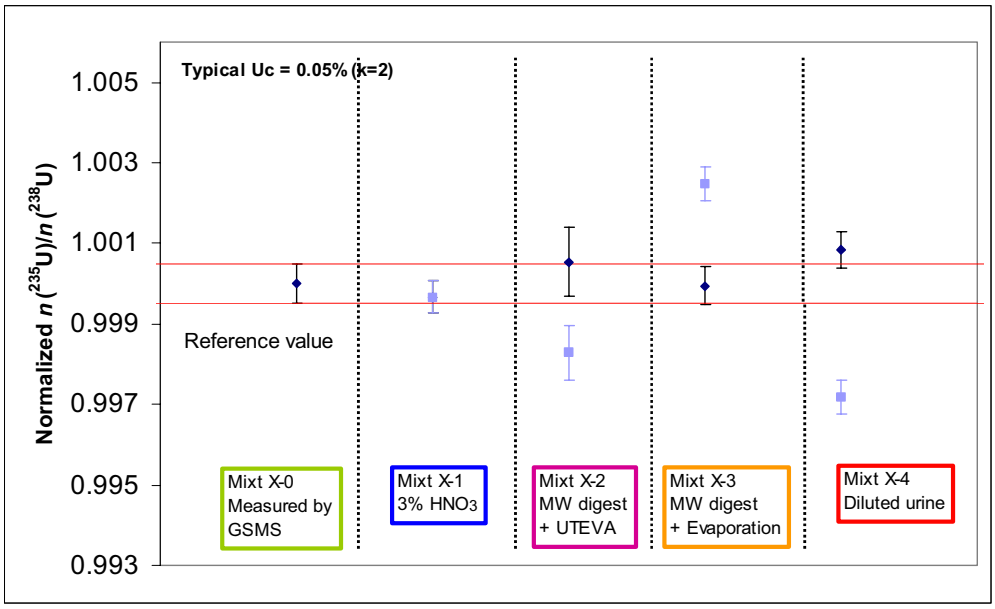

FIG. 1. Comparison of results obtained for different types of sample matrices, and corrected for mass discrimination in 2 different ways: first, with IRMM184 in matrix-matching conditions (black diamonds), second with IRMM184 in 3% HNO_3 matrix (blue squares). The two results obtained for Mixt-X1 are superposed.

the MC-ICP-MS. Hence, the strategy of sample preparation and/or of instrument calibration must be reviewed to account for these effects, correct for them and quantify the uncertainty arising from these corrections.

REFERENCES

[1] Spectrochim. Acta Part B **58** (2003) 1553-1565.
[2] Environ. Sci. Techn. **38** (2004) 581-586.
[3] WELLUM, R., et al., NUSIMEP: an external QC programme for measuring nuclear isotopes in environmental samples (these proceedings).

^{234}U and ^{230}Th determination by ID-FI-ICP-MS and application to uranium-series disequilibrium in marine samples

Godoy, M.L.D.P.[a], J.M. Godoy[b], R. Kowsmann[c]

[a] Instituto de Radioproteção e Dosimetria,
Comissão de Energia Nuclear,
Barra da Tijuca,
Rio de Janeiro,
Brazil

[b] Departamento de Química,
Pontifícia Universidade Católica do Rio de Janeiro,
Gávea, Rio de Janeiro,
Brazil

[c] PETROBRAS-CENPES,
Cidade Universitária,
Ilha do Fundão,
Rio de Janeiro,
Brazil

Abstract. A ^{234}U and ^{230}Th determination method based on an extraction chromatographic separation on a flow injection system coupled to a quadrupole ICP-MS was developed. Two millilitres UTEVA (Eichrom Company) cartridges were applied as separation tool and ^{236}U and ^{229}Th as spikes. Loading and washing steps were carried out in 3M HNO_3 solution and 0.05M ammonium oxalate applied to elute both uranium and thorium. The method was applied initially to the IAEA-327 soil reference sample and the obtained ^{234}U and ^{230}Th concentrations were in agreement with the reference levels. The method tested for marine shells and deep-sea sediment $^{230}Th/^{234}U$ dating. *Anadara notabilis* (Roding, 1798) shells dredged from the bottom of Araruama Lagoon, Rio de Janeiro, were obtained and ages between 2000 and 2900 years were found which are coherent with the lagoon formation history and with available ^{14}C ages. Samples from a deep-sea sediment core (2450 m water depth) were analyzed and the mean sedimentation rate of 2.8 cm ky^{-1} was calculated which fits with the value obtained using foraminifera ages (2.6 cm ky^{-1}).

1. Introduction

In wide scale, the hydrodynamics of the South Atlantic Ocean did not change, significantly, since the Late Oligocene/Recent Miocene. Therefore, the processes observed during the Quaternary can, in general terms, be extrapolated to those ages. This provides a good basis for the development of an analogous model probably valid for the Late Cenozoic, when the sand deposits in deep waters of the Campos Basin had been accumulated [1]. The presence of old and modern sand deposits in deep waters has always brought the interest of geoscientists and oil geologists. These sands are analogous of potential oil deposits and, consequently, they possess a great economic importance [1]. The bio-stratigrapy has been the basis of these studies. The presence and the frequency of certain foraminifera fossil are used as indicative of the occurred climatic changes during glacial and interglacial periods. The generated paleoclimatic curves, when compared with standard curves, allow sediment core dating. The methodology is well detailed in the work of Vicalvi [2] and is based on the paleoclimatic curve established by Ericson and Wollin [3] for the Atlantic Ocean. This methodology needs to be validated through absolute methods. In his work in the Campos Basin, Vicalvi [2] validated these curves for the period of up to 40000 years through dating with ^{14}C. Since 40000 years represents a practical limit of the ^{14}C technique, alternatives need to be applied, as the dating based on the pair $^{230}Th/^{234}U$, which

encloses periods of up to 350000 years [4, 5]. Additionally, as the bio-stratigraphy is based on a sequence of appearing/disappearing of certain species, the loss of intervals of the sediment core make impracticable the dating after this point. Additionally, the dating with $^{230}Th/^{234}U$ can be useful for the understanding of other events in Campos Basin as dating of authigenic carbonate nodules resultant of methane exudation [6] and deep-sea fossil corals dating.

One of the great disadvantages of the U and Th determination by alpha spectrometry, in this type of sample, is the large counting time necessary to achieve a good statistics and, consequently, a lower associated uncertainty. A way to face this difficulty is the use of the mass spectrometry, in particular, of the plasma inductively coupled mass spectrometry (ICP-MS). The ICP-MS technique is more adequate for the determination of ^{232}Th (1.39×10^{10} years) and ^{238}U (4.47×10^{9} years), long-lived radionuclides, but it can be applied, successfully, in the determination of ^{230}Th (7.52×10^{4} years) and ^{234}U (2.48×10^{5} years), in particular, if associated with a pre-concentration step. This pre-concentration can be carried out on-line using a flow injection system (FIAS) connected to the ICP-MS. In particular, for the determination of U and Th by FI-ICP-MS, the resins developed by the company Eichrom are quite popular, e.g. [7, 8]. Therefore, the aim of the present work was to develop an analytical method that is faster than the alpha spectrometry, for the application of the $^{230}Th/^{234}U$ dating of authigenic carbonate and deep-water sediments samples, taking into account the required accuracy and precision, and compare the calculated ages with those derivatives of the application of others techniques as the bio-stratigraphy.

2. Material and methods

The uranium and thorium elemental and isotope determinations were performed using a Perkin&Elmer ELAN 6000 ICP-MS. For the uranium and thorium separation, the system was coupled to a Perkin&Elmer flow injection system with a auto sampler. ^{236}U and ^{229}Th were used as spikes (Isotope Products Laboratories) and UTEVA (Eichrom Technologies Inc.) 2 mL cartridges were applied for uranium and thorium concentration and matrix separation. About 10 mL sample solution (3 M HNO_3) is pumped through the cartridge, follows a washing step, also with 3 M HNO_3, and uranium and thorium are eluted together using a 0.05 M ammonium oxalate solution.

The method was tested for ^{234}U and ^{230}Th determination in a standard reference soil sample (IAEA-327). Four 1 g aliquot samples were taken and completely dissolved by $HNO_3/HF/HClO_4$ and tetraborate fusion of the remaining residue. Samples taken from the PETROBRAS deep-sea sediment core 9821096 (water depth 2450 m) were obtained. One-gram aliquots were analysed for ^{234}U and ^{230}Th as described for the soil reference sample. *Anadara notabilis* shells dredged from the bottom of Araruama Lagoon, Rio de Janeiro, were obtained. The shells were cleaned as described by Mendonça and Godoy [9], ashed at 500 ^{o}C and crushed to fine powder on an agate mortar. Because of the expected low age and low uranium content, 5 g aliquots were taken, dissolved with 50 mL 3 M HNO_3 and the flow injection program modified accordingly.

3. Results and discussion

Six blank samples, including the ^{236}U and ^{229}Th spikes, were analysed and, based on the observed results, a detection limit of 0.35 and 0.05 mBq g^{-1} for ^{230}Th and ^{234}U, respectively, for one gram sample, was achieved. These detection limits seems to be adequate for a future $^{230}Th/^{234}U$ dating of fossil corals [10]. The ^{234}U and ^{230}Th obtained values for the IAEA-327 standard reference soil sample are shown in Table I. The ^{234}U is in agreement with the certificate value while ^{230}Th showed a tendency to lower values. The ^{230}Th determination was repeated and the same mean value was obtained. Comparing the ^{238}U certificate and the measured ^{234}U and ^{230}Th values, one could say that there is a radioactive equilibrium in the ^{238}U series in this soil sample. The achieved uncertainty for both radionuclides is similar to that expected for mass spectrometric measurements of these radionuclides [10].

Table I: Standard reference soil sample IAEA-327 obtained results for ^{234}U and ^{230}Th (Bq kg^{-1})

Radionuclide	Reference value	95% confidence interval	Mean value	SD
^{234}U	31.9	30.4-33.4	30.73	0.56
^{230}Th	34.1	32.4-35.8	31.52	0.65

The Araruana lagoon is a hypersaline lagoon, localised about 100 km from Rio de Janeiro city, and reached its actual stage about 3600 years ago [11]. Shell layers with radiocarbon ages between 2540 and 3450 years were observed on two sediments cores, sampled in the eastern part of the lagoon, below a 1.5-2.0 m thick organic mud layer [11]. Three shells were analysed, the detrital contribution to the uranium content in the 3M HNO_3 soluble phase ranged between 0.74 and 1.53%. The mean observed $^{234}U/^{238}U$ activity ratio (AR) was 1.17(0.03) and 1.18(0.04), and was obtained by alpha spectrometry, both in agreement with the AR observed in seawater. The obtained $^{230}Th/^{234}U$ ages were 2600(360, 95% IC), 2900(350, 95% IC) and 2000(240, 95% IC) ky, and are similar to the ^{14}C ages. According to malacologists of the Brazilian National Museum, *Anadara notabilis* were extinct in the Araruama lagoon some thousand years ago, which fits also with the obtained $^{230}Th/^{234}U$ ages.

For the 98210096 sediment core, the obtained $^{230}Th_{total}$, $^{234}U_{total}$, U and Th elemental concentration in the carbonate phase and U/Th elemental ratio in the residual phase, as well as the calculated $^{230}Th_{excess}$ are shown in Table II. The $^{238}U/^{232}Th$ ratio increases with depth, showing a higher detrital contribution for older ages. Two samples were twice analysed, 32 and 94 cm, and, as can be seen in both cases, the results were essentially equal. The $^{230}Th_{excess}$ was calculated according to the equation:

$$^{230}Th_{excess} = {}^{230}Th - {}^{230}Th_{residual} - {}^{230}Th_{authigenic} = {}^{230}Th - 0.0124\times Th_{carbonate}\times(U/Th)_{residual} - [(^{234}U - 0.0124\times Th_{carbonate}\times (U/Th)_{residual}) \times 1.45\times(e^{-\lambda 234.t} - e^{-\lambda 230.t})]$$

where, t = sediment layer age, which was estimated based on the foraminifera dates.

Since the complete sediment core was not available, only reference dates, the $^{230}Th_{excess}$ inventory was calculated as proposed by Oldfield and Appleby [12]. The calculated $^{230}Th_{excess}$ inventory was a factor of two higher than that obtained using the ^{230}Th flux to bottom sediments (F_{230Th}) according to Huh

Table II. Obtained $^{230}Th_{total}$, $^{234}U_{total}$, U and Th elemental concentration in the carbonate phase and the U/Th elemental ratio in the residual phase, as well as the calculated $^{230}Th_{excess}$ (values in Bq kg^{-1} or mg kg^{-1}, respectively)

Sediment layer depth (cm)	$^{230}Th_{total}$	$^{234}U_{total}$	U_{carb}	Th_{carb}	$(U/Th)_{res.}$	$^{230}Th_{excess}$
5	87.7	27.8	0.75	1.91	0.15	84.3
10	83.7	26.9	0.94	3.62	0.18	75.5
32a	98.4	32.6	0.67	4.05	0.17	89.8
32b	105.0	37.5				96.4
53	73.7	32.7	0.84	3.95	0.18	64.8
74	47.7	26.8	0.61	3.00	0.23	39.1
94a	42.4	35.3	1.06	2.88	0.22	34.5
94b	49.8	41.9				42.0
121	40.4	41.7	1.41	3.97	0.23	29.1
165	44.1	33.2	1.11	1.74	0.22	39.3
185	43.8	31.3	0.92	1.94	0.22	38.5
211	38.7	34.4	1.27	3.73	0.26	26.5
248	41.7	31.9	0.73	2.89	0.23	33.4
274	40.6	37.6	1.01	2.40	0.24	33.5
418	64.4	64.1	3.25	7.27	0.32	35.8

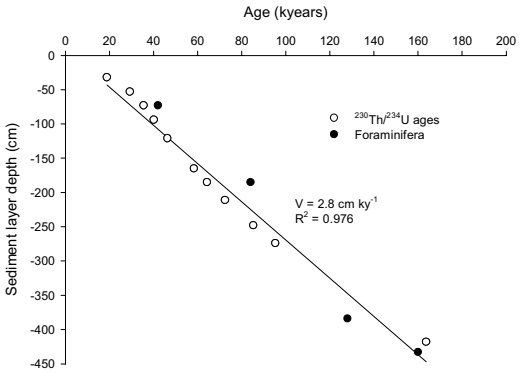

FIG. 1. 98210096 sediment core obtained $^{230}Th/^{234}U$ ages and foraminifera dates for comparation.

and Kadko [13], showing sediment focusing. A constant $^{230}Th_{excess}$ concentration was observed for the first 30 cm. The core description, performed by geologists from PETROBRAS also shows this mixing layer. Therefore, it was necessary also to include this factor on the age calculation. The mean residence time in the mixing zone was estimated in 18.8 kyears and its $^{230}Th_{excess}$ inventory in 2.8 Bq cm^{-2}. Figure I shows the obtained sediment layer depth versus CRS age profile, together is also shown the foraminifera datum. A mean sedimentation rate of 2.8 cm ky^{-1} was obtained similar to the mean sedimentation rate calculated using the foraminifera ages. However, additional sediment layers must be analysed, in particular at the end of the core, aiming to observe the sedimentation rate changes across the sediment core as expected based on the foraminifera ages. In order to test the CRS hypothesis, the $^{230}Th_{excess}$ flux between layers of known ages, based on the foraminifera dates, was calculated, according to Oldfield and Appleby [13], and compared to the integrated flux for the whole core. All values were in range of ±10% of the $^{230}Th_{excess}$ flux integrated for the whole care, showing be valid the use of the CRS model for this particular sediment core.

REFERENCES

[1] VIANA, A.R., et al., Hydrology, morphology and sedimentology of the Campos continental margin, offshore Brazil, Sedim. Geol. **115** (1998) 133-157.

[2] VICALVI, M.A., Zoneamento bioestratigráfico e paleoclimático dos sedimentos do quaternário superior do talude da Bacia de Campos, RJ, Brasil – B. Geoci. PETROBRAS **11** (1997) 132-165.

[3] ERICSON, D.B., WOLLIN, G., Pleistocene Climates in Atlantic and Pacific Oceans – A Comparison Based on Deep-Sea Sediments, Science, **167** (3924) (1970) 1483.

[4] THOMSON, J., et al., Implications for sedimentation changes on the Iberian margin over the two last glacial/interglacial transitions from Th-230 systematics – Earth Planet. Sci. Letters **165** (1999) 255-270.

[5] VEEH, H.H., et al., Glacial/interglacial variations of sedimentation on the Australian continental margin: constraints from excess Th-230, Mar. Geol. **166** (2000) 11-30.

[6] KOWSMANN, R.O., CARVALHO, M.D., Erosional event causing gas venting on the upper continental slope, Campos Basin, Brazil – Contin. Shelf Res. **22** (2002) 2345-2354.

[7] LEE, M.H., LEE, C.W., Radiochemical analysis of uranium isotopes in soil and sediment samples with extraction chromatography – Talanta **54** (2001) 181-186.

[8] PIETRUZKA, A.J., et al., Precise and accurate measurement of Ra-226/Th-230/U-238 disequilibria in volcanic rocks using plasma multicollector mass spectrometry. Chem. Geol. **188** (2002) 171-191.

[9] MENDONÇA, M.L.T.G., GODOY, J.M., Datação Radiocarbônica de Sítios Arqueológicos do Tipo Sambaqui pela Técnica de Absorção de CO_2: Uma Alternativa à Síntese Benzênica. Química Nova **27** (2003) 323-325.

[10] CHEN, J.H., et al., Mass spectrometry and application to uranium-series disequilibrium in: Uranium-series disequilibrium: Applications to Earth, Marine and Environmental Sciences 2nd edition, IVANOVICH M. and HARMON R.S. (editors), Oxford Science Publications, (1992) 174-206.

[11] TURCQ, B., et al., Origin and Evolution of the Quaternary Coastal Plain between Guaratiba and Cabo Frio, State of Rio de Janeiro, Brazil in: Environmental Geochemistry of Coastal Lagoon Systems, Rio de Janeiro, Brazil, (KNOPPER, B., BIDONE, E.D., ABRÃO, J.J. Eds), Universidade Federal Fluminense, Serie Geoquímica Ambiental **6** (1999) 25-46.

[12] OLDFIELD, F., APPLEBY, P.G., Empirical testing of ^{210}Pb dating models in: Lake Sediments and Environmental History, (HORWARTH E.Y., LUND J.G., Eds), Leicester University Press, (1984) 93-124.

[13] HUH, C.-A., KADKO, D.C., Marine sediments and sedimentation processes in: Uranium-series disequilibrium: Applications to Earth, Marine and Environmental Sciences 2nd edition (IVANOVICH, M., HARMON, R.S., Eds), Oxford Science Publications (1992) 460-486.

Determination of bromine stable isotopes in inorganic samples using continuous-flow isotope ratio mass spectrometry

Shouakar-Stash, O., R.J. Drimmie, S.K. Frape

Department of Earth Sciences,
University of Waterloo,
Waterloo, Ontario,
Canada

A new methodology for bromine stable isotope determination by Continuous-Flow Isotope Ratio Mass Spectrometry (CF-IRMS) was developed. The technique was investigated on inorganic samples. The system used in this study is an IsoPrime IRMS, with capabilities of both Dual-Inlet and Continuous-Flow modes coupled with HP 6890 Gas Chromatography (GC) and equipped with a CombiPAL autosampler.

Isotopic characterization of bromine isotopes could be a powerful tool of determining sources of formation waters and determining geological and hydrogeological processes especially if it is used in conjunction with other isotopes such as chlorine stable isotopes.

There are two different techniques currently used for bromine stable isotope determination, dual-inlet IRMS [1] and Thermal Ionization Mass Spectrometry (TIMS) [2]. This study represents the first attempt to measure bromine stable isotopes by using a CF-IRMS technology.

In this technique, the bromine isotopic composition is being determined by analyzing methyl bromide (CH_3Br) gas. CH_3Br gas is prepared by reacting 1 mg of silver bromide (AgBr) with 100 µL of methyl iodide (CH_3I) in 20 ml gas tight amber vials. CH_3I is added to the vials in a glove bag flushed with helium few times and kept filled with helium during the course of vial preparation by applying a steady flow of helium to the glove bag. Once vials are prepared, they are placed in an oven at 80°C for 48 hours for the reaction to occur. Once the reaction is completed, vials are moved to the autosampler tray and analyzed for bromine stable isotope determination. 400 µL of sample is injected into the GC, where CH_3Br is separated from CH_3I using a DB-5MS capillary column (Length 60 m, ID 0.32, Film 1µm). Separated CH_3Br gas is passed to the IRMS to be measured for bromine stable isotopes, while CH_3I is directed to the FID on the GC.

Due to the toxicity of the CH_3Br gas used for the analysis of bromine stable isotopes, one reservoir on the dual-inlet system was used to provide the reference gas, instead of a reference gas tank.

The precision achieved in this study using this new technique compares very well with the previous two techniques with a standard deviation better than 0.13 ‰.

REFERENCES

[1] EGGENKAMP, H.G.M., COLEMAN, M.L., Rediscovery of classical methods and their application to the measurement of stable bromine isotopes in natural samples, Chem. Geology **167** (2000) 393-402.

[2] XIAO, Y.K., LIU, W.G., QI, H.P., ZHANG, C.G., A new method for the high precision isotopic measurement of bromine by thermal ionization mass spectrometry, Int. J. Mass Spectrom. Ion Proc. **123** (1993) 117-123.

Critical evaluation of an isotope dilution ICP-MS method for the measurement of the Fe content in seawater

Petrov, I.I., C.R. Quétel, P.D.P. Taylor

European Commission Joint Research Centre,
Institute for Reference Materials and Measurements,
Geel,
Belgium

It is well known that direct analysis of seawater by means of inductively coupled plasma mass spectrometry (ICP-MS) is hardly possible because of the salt load in the samples. Determination of the element content at ultra-trace level in open-ocean water requires a separation from the matrix associated to significant concentration factors. For iron, an isotope dilution (ID) ICP-MS method was proposed [1] based on a multiple steps protocol, including a co-precipitation with magnesium hydroxide after ammonia loading and consecutive dissolution with hydrochloric acid. To be able to measure the iron content in the low pg g^{-1} range a correct assessment of the analytical procedural blank is of crucial importance. Not only this blank must be low, but also realistic (i.e. based on complete analytical sequence applied to real iron free seawater) and reproducible. This is particularly difficult considering the ubiquity of iron and the complexity of the seawater matrix and, despite years of experiments and publications, this remains a fundamental analytical challenge and a great source of complexity for the realisation of reliable profiles of dissolved iron data.

The present study considers different approaches we developed to assess, in a realistic way, the procedural blank of the IDMS method proposed by Wu and Boyle [1]. Our aim was to reproduce the full set of experimental steps involved in the determination of iron in seawater by IDMS at the nM level or below. Our results are evaluated in the light of those claimed by Wu and Boyle [1] who use ~4%-sample volume for their procedural blank determination. The results they present are rather convincing. However, downsizing by a factor of ~25 the sample volume not only minimises sample-tube contact and labware contribution to the blank, but results as well in a different set of operations and manipulations. These changes in the analytical protocol can easily lead to non-realistic procedural blank values. This is illustrated in the Figure at the end, where we reported our findings in term of relative contributions to our procedural blanks. Manipulations are by far the largest contributor as they contribute for ~ 50% of the total. Reagents, and particularly the nitric acid used to acidify the sample, and instrumental background come after with respectively nearly 25% and 20% of the contributions.

The ICP-MS measurements were performed by means of a single collector double focusing instrument ThermoFinnigan *Element2* at medium mass resolution, to resolve the isobaric interferences from argon-oxide based ions on iron isotopes. ‘Mass offset’ and ‘Lock Mass’ settings of instrument software were enabled. Obtained data were filtered by means of a spreadsheet program to remove peak spikes, which were not associated to the analyte but to matrix effects. Data were then further processed as described by Tresl et al. [2] to avoid generating biases associated to the software peak integration routine.

Apart from the centrifugation and the ICP-MS steps all the experiments were carried out under class-10 ultra-clean room conditions. Only ultra-pure reagents and water were used for sample preparation and treatment. Multisteps-procedure, including diluted ethanol, nitric and hydrochloric acid, and ultra-pure water, was applied for labware cleaning prior its usage for sample preparation.

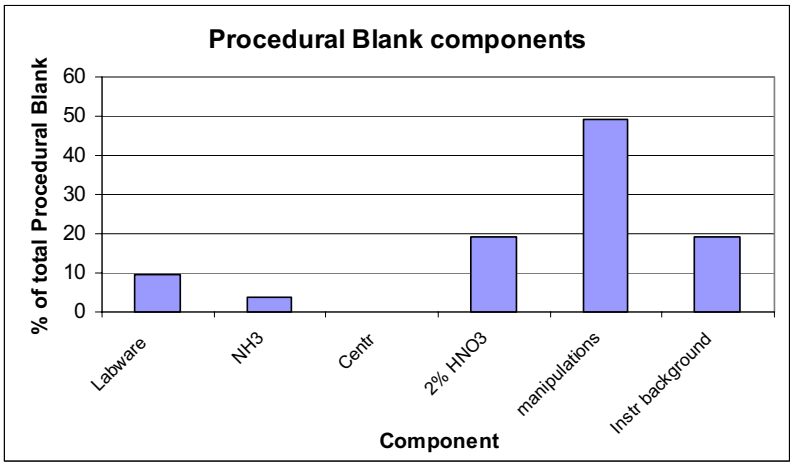

Component	% of total
Labware	9
NH3	4
Centr	0
2% HNO3	19
manipulations	49
Instr background	19

FIG. 1. Breakdown of the relative contributions to the blank corresponding to analytical procedure implemented for the determination of Fe in seawater.

REFERENCES

[1] WU, J., BOYLE, E.A., Determination of iron in seawater by high-resolution isotope dilution inductively coupled plasma mass spectrometry after $Mg(OH)_2$ coprecipitation, Anal. Chimica Acta 3**67** (1998) 183-191.

[2] TRESL, I., QUÉTEL, C.R., TAYLOR, P.D.P., Solution to data integration problems during isotope ratio measurements by magnetic sector inductively coupled plasma mass spectrometer at medium mass resolution: application to the certification of an enriched ^{53}Cr material by isotope dilution, Spectrochim. Acta B **58** (2003) 551-563.

Measurement of variations in stable mercury isotope ratios in the environment

Hintelmann, H., D. Foucher

Trent University,
Water Quality Centre,
Peterborough, Ontario,
Canada

Recent measurements have suggested that isotope signatures of mercury in different environmental compartments and among mercury ores from various sources may vary. However, it is still debated whether mercury from anthropogenic sources is isotopically different from geogenic mercury, which would allow tracing of mercury sources according to their isotopic fingerprint.

This presentation describes the use of an on-line mercury cold vapor technique (stannous chloride used as the reductant) to generate a continuous steady signal, which can be processed for precise isotope ratio measurements by multi-collector (MC)-ICP/MS. Special attention has been paid to ensure optimal MC-ICP/MS conditions allowing highly precise measurement of ratios (1 SD < 50 ppm, 0.005%), enough to be able to detect the anticipated small differences in mercury isotope ratios in nature. The method was applied to investigate the extent of mercury fractionation in a number of sediments from different environments.

The raw isotope ratios ($^{198}Hg/^{202}Hg$, $^{199}Hg/^{202}Hg$, $^{200}Hg/^{202}Hg$ and $^{201}Hg/^{202}Hg$) were determined as the average of a number of 300 measurements of 2 seconds integration time each, giving a global acquisition time of 10 minutes for a single sample. Due to the lack of a precisely characterized mercury isotope ratio standard, the accuracy of our method was checked by comparing relative per mil (‰) deviation (using the ∂-notation) of all our measurements to a common standard solution according to the formula :

$$\delta^{198/202}Hg = 1000x\left(\frac{^{198/202}Hg_{sample}}{^{198/202}Hg_{standard}}\right) - 1$$

with $^{198/202}Hg_{sample}$, the measured value of the sample and $^{198/202}Hg_{standard}$, the reference value of our in-house standard solution calculated as the average of one acquisition done before and after every sample. The external precision (1SD) of the measure for certified reference materials was determined from values obtained for replicate digests ($n \geq 6$).

The extent of mercury fractionation has been investigated in a variety of sediments from different locations for which sources of mercury have been identified. The samples consisted of (1) certified sediment reference materials obtained from natural or anthropogenically contaminated environments, (2) well characterized and dated sediment profiles from the Lake-658 of the Experimental Lakes Area, and (3) river catchments affected by gold or mercury mining.

An internal precision of 10 to 70 ppm (1SE) was obtained for all ratios and across the various sediment samples investigated. The external precision of the measurements for replicate sample digests ($n \geq 6$) was between 0.02 and 0.24‰ (1 SD), depending on the certified reference material. The range of ∂ values observed extended from 0.15 to 5.93‰ for the certified sediments and from 0.51 to 1.52‰ for the sediment profile (ELA, Lake-658). The magnitude of the mercury fractionation per amu was constant within one type of sample.

The isotopic signatures were significantly different (comparing values with internal or even external precision) among samples (certified materials) and, to a smaller extent, within near surface and deeper sediment of the single core. The surface sediment (0-10 cm), which shows elevated levels of mercury from presumably anthropogenic activities, appears to be enriched with lighter isotopes.

The measurements demonstrated the ability of the proposed method to detect significant differences in mercury isotope ratios within one type of samples (e.g. between different sediments) and so far have unequivocally shown that natural variations in mercury isotope ratios exist in nature. Future research will focus on the differentiation between natural and anthropogenic sources in the global mercury cycle. There is a need to get better understanding of the range of mercury isotope fractionation that can be expected in nature, i.e. among matrices (air/water/sediment/biota) and a single matrix (sediment cores). This information needs to be reconciled with observed differences to ultimately assess, whether variations in mercury isotope ratios are caused by natural fractionation processes or are a result of anthropogenic activity.

Recent achievements in increasing the electromagnetic separation efficiency of actinides

Vesnovskii, S.P.

Russian Federal Nuclear Center,
All Russian Scientific Research Institute for Experimental Physics,
Sarov,
Russian Federation

For more than 35 years the RFNC-VNIIEF laboratory has been engaged in electromagnetic separation of actinides. S-2 mass-separator equipped with a radiation protection system (a radiation shielding) enables to carry out separation of high-activity actinide materials such as uranium, plutonium, americium and curium. The basic characteristics of the S-2 mass-separator are presented in [1-3]. Recently this unique laboratory has been supplying products to foreign laboratories.

During the last three years the work concentrated on the improvement of the technology of electromagnetic separation with the aim to achieve stable characteristics of the S-2 mass-separator operation. Trichlorides of separated elements have been serving as a working substance. New technologies of production of pure trichlorides have been developed, including a technology of scattered material regeneration (when up to 85-90% of the material was possible to use in repeated cycles of separation), 100-% extraction efficiency and deep purification of accumulated isotopes from the collector boxes.

It can be seen that for the majority of isotopes unique levels of enrichment have been achieved. A set of Pu-239, Pu-241, Cm-243, Cm-245 isotopes is obtained using the process of double separation. Of course, the quality of products depends on the composition of separated mixtures. Uranium, plutonium, americium and curium were produced after a long irradiation of original materials in a nuclear reactor with high density of neutron flux.

For nuclear physics and other applications, thin standard layers of the enriched actinide isotopes are made by means of electrochemical and vacuum deposition. There are also available certified highly enriched isotope solutions which can be used as tracers or spikes in different areas of investigations. For the study of physical and chemical characteristics of isotopes in experiments with synthesis of heavy transactinium elements (carried out in the Laboratory of Nuclear Reactions of the Joint Institute of Nuclear Research in Dubna) we produced isotopic targets used in these experiments [5].

Table I. The nomenclature of available isotopes [4].

Main isotope contents (as atoms, %)									
Uranium		Neptunium		Plutonium		Americium		Curium	
U-233	99.97	Np-236	<0.01	Pu-238	99.6	Am-241	99.99	Cm-243	99.99
U-234	84.52	Np-237	99.99	Pu-239	99.997	Am-242m	85.6	Cm-244	99.3
U-235	99.9923			Pu-240	>99.9	Am-243	99.998	Cm-245	99.998
U-236	97.81			Pu-241	99.998			Cm-246	99.8
U-238	99.9990			Pu-242	99.99			Cm-247	90.2
				Pu-244	98.9			Cm-248	97.5

At present we are working on the preparation of plutonium-244 enriched up to 99.5%, even up to 99.99% [6]. We supply isotopes through JSC Tekhsnabexport – an organization associated with MinAtom that possesses a license for export of radionuclides. Usually the schedule for the specimens delivery from stock constitutes 3-6 months. Our transport containers have international certificates.

We have no doubts that our scientific and technological developments may be of interest to institutes working on heavy transactinide isotopes synthesis, as well as in applications of heavy isotopes as traces for studying environmental processes.

Recently we have also been working on increasing separation efficiencies for very expensive original isotopic materials using electromagnetic separation (from 5 to 15-20%). We are developing a new ion source as well as an electric power source with the aim to increase the operational temperature of the source, so the separated materials could be used in the form of metals and oxides. The high efficiency of the source will make it possible to use smaller amounts of original material for the production of the required mass of the material, and it will also improve radiation conditions for carrying out the works with separating highly active isotopic mixtures.

REFERENCES

[1] ABRAMYCHEV, S., BALASHOV, N., et al., Electromagnetic separation of actinide isotopes, Nucl. Instr. Meth. B**70** (1992) 5.

[2] VESNOVSKII, S., POLYNOV, V., Highly enriched isotopes of uranium and transuranium elements for scientific investigation, Nucl. Instr. Meth. B**70** (1992) 9.

[3] VESNOVSKII, S., POLYNOV, V., NIKITIN, E., VJACHIN, V., Quality and availability of actinide isotopes from the All-Russian Scientific Research Institute of Experimental Physics in Arzamas-16, Nucl. Instr. Meth. A**334** (1993) 37.

[4] VESNOVSKII, S., RFNC-VNIIEF capabilities to production high pure isotopes for scientific and medical applications, J. Radionanal. Nucl. Chem. **257** 1 (2003) 27-31.

[5] OGANISSEAN, Yu., PATIN, J., IL'KAEV, R., VESNOVSKII, S., et al., Measurements of cross sections and decay properties of the isotopes of elements 112, 114 and 116 produced in the fusion reactions ^{233,238}U, ^{242}Pu, and ^{248}Cm + ^{48}Ca, Phys. Rev. C. (in press).

[6] DERON, S., VESNOVSKII, S., Development of technology for high-purity ^{244}Pu production by method of electromagnetic separation, Nucl. Instr. Meth. A**438** (1999) 20-22.

MASS SPECTROMETRY - POSTERS

Nuclear geophysiology: isotopes in Australian environmental analysis

Henderson-Sellers, A., D. Stone, S. Hollins, M. Hotchkis, D. Fink

Australian Nuclear Science and Technology Organisation,
Lucas Heights, NSW,
Australia

Abstract. Lovelock [1] introduced the term 'geophysiology' to describe the holistic study of the Earth systems. By analogy with medicine, and the corresponding field of nuclear medicine, 'nuclear geophysiology' describes the application of nuclear techniques to Earth system science. Injections of radioisotopes into the Earth's systems occur naturally and continuously, while artificial radionuclides have been injected at times as a result of human activities. Here, we provide some examples of Australian investigations into the physiology of the Earth derived from the study of these isotopes.

1. Isotopic tracers and metal uptake in biota in Sydney Harbour

As part of an ANSTO/University of Technology, Sydney collaborative investigation into the trophic transfer of metals in a Sydney estuarine system, the uptake and depuration of ^{75}Se and ^{109}Cd by the crab *H. cordiformis* from seawater (and particulates) was examined in a preliminary scoping study prior to using the animals as prey in studies of contaminant transfer to fish. Uptake of ^{75}Se appeared to reach equilibrium by 150 h (Fig. 1a) with an equilibrium concentration factor (CF) of approximately 30. A first-order kinetic model indicated that the biological half-life ($T_{½}$) of ^{75}Se was 18 h. The CF of ^{109}Cd at the end of the uptake phase was approximately 9 and did not reach equilibrium (Fig. 1a). The $T_{½}$ could not be calculated from this data. After 165 h of depuration, approximately 50% of ^{75}Se and 70% of ^{109}Cd remained in *H. cordiformis* (Fig. 1b).

2. Australian hydrology

The results indicate that although ^{75}Se had greater bioavailability than ^{109}Cd to *H. cordiformis* in a seawater system in the short-term, it was also more readily lost from the organism. This suggests that Cd may be more persistent than Se in estuarine trophic systems.

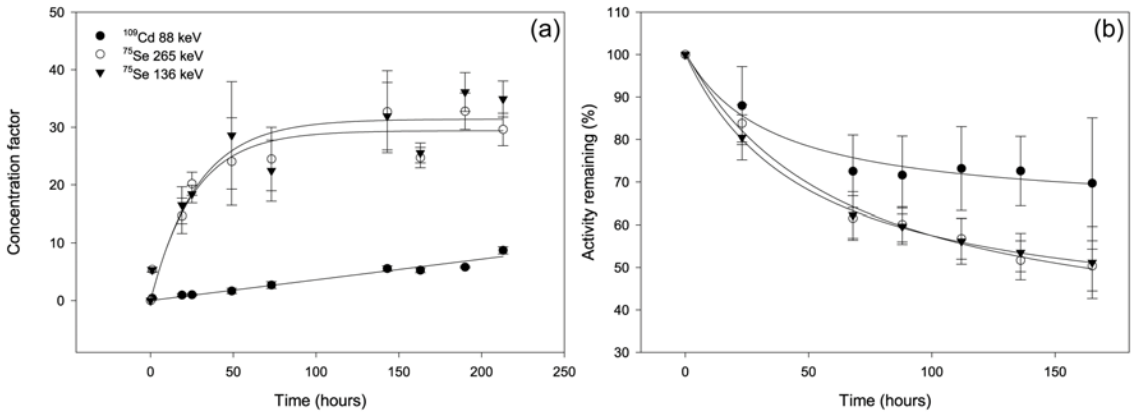

FIG. 1. (a) Concentration factors over the uptake phase in H. cordiformis exposed to ^{75}Se and ^{109}Cd in seawater (mean ± SE). (b) Depuration (%) of ^{75}Se and ^{109}Cd by H. cordiformis (mean ± SE).

Isotopes such as the stable and radioactive isotopes found in water are particularly appropriate for the study of the dry Australian landscape with its connected water systems, providing a clear method of determining the source of groundwater, and hence the extent of mixing of nearby surface water and the time frame for the mixing process [8]. In particular, the stable isotopes ^{2}H, ^{18}O, and ^{13}C provide a robust end-member analysis for the hydrographical separation of regional groundwater and any amount of river water which was replenished at a remote location; while the radioactive isotopes ^{3}H and ^{14}C are used to confirm the presence in groundwater of (isotopically modern) surface water, but also accurately determine the apparent rate of mixing at particular distances from the river.

3. Cosmogenic radioisotopes – ^{14}C, ^{10}Be, ^{26}Al

Earth scientists have long sought an analytical technique that would provide the chronology of exposed bedrock surfaces and hence the timing of major geomorphologic processes. Such a technique is now developing based on the in-situ production of long-lived cosmogenic radionuclides (CRNs). The radioisotopes ^{10}Be ($T_{1/2}$=1.5Ma), ^{26}Al (0.7Ma) and ^{36}Cl (0.3Ma) are produced by cosmic ray bombardment of exposed rocks, in the first metre or so of the Earth's crust. Although the rate of in-situ production in surface rocks is extremely low, ultrasensitive technique of Accelerator Mass Spectrometry (AMS) (detection limit of ~10,000 atoms) can now be applied to as little as ~10 grams of a quartz rock sample exposed at sea-level for times as short as a few thousand years. Radioisotopes with half-lives ranging from 0.3 to 1.5 Ma, are ideally suited to study Quaternary geomorphology and palaeoclimate change. In addition to providing 'simple model' ages for glacial moraine deposits and bedrock erosion rates, CRNs are now applied to more complex scenarios, such as soil production rates, burial histories, regolith accumulation rates, escarpment retreat and river incision rates, large scale (regional) sediment tracing and catchment evolution processes.

4. Anthropogenic radioisotopes – ^{129}I, uranium, plutonium

ANSTO Environment is playing a pioneering role in developing new methods for monitoring adherence to the Nuclear Non-proliferation Treaty. Working with the IAEA Department of Safeguards, new analytical procedures have been developed to assist with their environmental monitoring programme. Signatures of nuclear activities, in the form of trace amounts of radioisotopes in environmental samples, can be used to identify undeclared nuclear facilities or undeclared activities at declared facilities. At ANSTO we have developed the use of Accelerator Mass Spectrometry (AMS) for analysis of ^{236}U in environmental samples. ^{236}U is a sensitive indicator of irradiated uranium. AMS is also used to detect the long-lived fission product ^{129}I and Plutonium at extremely low levels. The presence of ^{129}I can be a signature of reprocessing. ANSTO performs analyses of these radioisotopes as an accredited member of the IAEA Safeguards network of analytical laboratories.

Australian soldiers on duty in the Gulf risk possible exposure to depleted uranium. Depleted uranium is the by-product of uranium enrichment. Due to its high density, it is the ideal material for use in armour-piercing ammunition and in armour for fighting vehicles. Depleted uranium may enter the body through inhalation of the dust-like particles, ingestion of contaminated food or through wounds. At ANSTO, a sensitive analytical technique based on isotope dilution and inductively coupled plasma mass spectrometry (ICP-MS) was used to detect depleted uranium in urine samples. By addition of known quantities of ^{236}U (isotope dilution) to the urine samples and measuring the relative abundances of different isotopes (^{236}U, ^{235}U and ^{238}U) of uranium by ICP-MS, we are able to quantify (quantification limit of 20 ng/L) and distinguish between natural and depleted uranium.

REFERENCES

[1] LOVELOCK, J.E., The Ages of Gaia, Oxford University Press, Oxford (1988).

[2] HENDERSON-SELLERS, A., MCGUFFIE, K., NOONE, D., IRANNEJAD, P., Using stable water isotopes to evaluate basin-scale simulations of surface water budgets, J. Hydrometeorol. **5** 5 (2004) 805-822.

AMS measurement of ^{129}I and its application as an oceanographic tracer

Suzuki T., T. Kitamura, S. Kabuto, O. Togawa, H. Amano

Japan Atomic Energy Research Institute (JAERI)
Marine Research Laboratory
Minato-matchi, Mutsu,
Aomori
Japan

An iodine beam line had been set up at Accelerator Mass Spectrometry facility of the Japan Atomic Energy Research Institute (JAERI-AMS) [1]. Two nuclear fuel reprocessing plants in Europe, La Hague (France) and Sellafield (England), have released ^{129}I to the marine environment [2]. It has been used as an oceanographic tracer in the north Atlantic and/or Arctic Oceans [3]. In Japan, a new nuclear fuel reprocessing plant will be operated at Rokkasho in the near future. We intend to investigate not only the migration of ^{129}I in the marine environment, but also the potential use of ^{129}I as an oceanographic tracer in the North Pacific Ocean, using ^{129}I released from the Rokkasho facility.

JAERI-AMS which is manufactured by High Voltage Engineering Europa (HVEE) has a 3MV accelerator and two independent beam lines. One is optimized for ^{14}C measurement and the other is for ^{129}I.

The precision test for the iodine line was carried out using the IsoTrace Lab. Standard ($^{129}I/^{127}I=1.1x10^{-10}$). Five samples were measured during four runs. The mean value of the obtained $^{129}I/^{127}I$ ratios for 20 measurements (5targets x 4runs) was $(7.89\pm0.09)x10^{-11}$. The relative standard deviation was 1.1%. This demonstrated that iodine isotopic ratio could be measured with a precision of about 1% at the level of 10^{-10} isotopic ratio. The differences between standard ratio and obtained one suggested that the transmission efficiency from the magnet to the TOF detector was approximately 70%.

Standard samples having a variety of iodine isotopic ratios were diluted from the NIST 4949C and another one which was provided by Dr. Imamura. The results of the standard samples measurement are shown in Fig. 1. This demonstrated that iodine beam line had a good linearity between 10^{-10} and 10^{-12} isotopic ratio.

The background level of the ^{129}I beam line was estimated by measuring commercial AgI, which was measured to be $^{129}I/^{127}I = (3.9\pm0.3) \times 10^{-13}$. Since our measured TOF detector spectrum did not exhibit any counts underneath ^{129}I peak, we concluded that the detection limit was at least one order of magnitude lower than the measured ratio.

We think that our high-sensitivity ^{129}I beam line is a powerful tool for new marine environmental research.

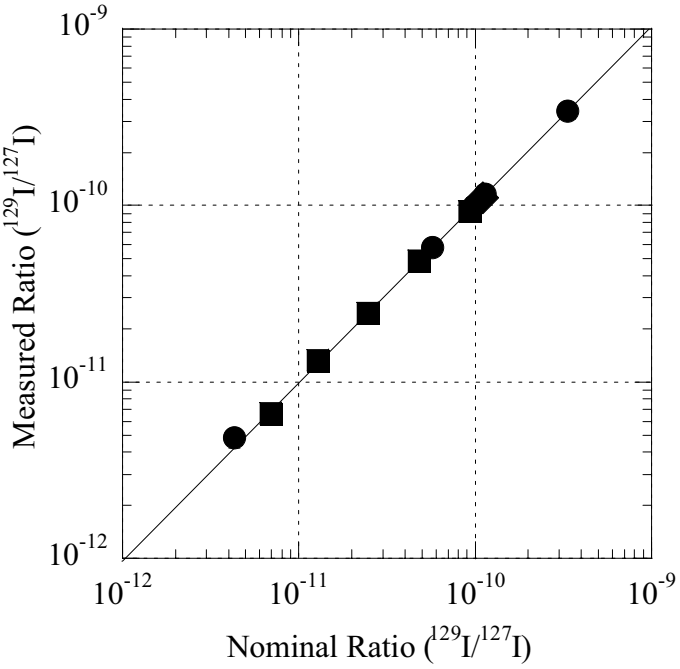

FIG. 1. Results of ^{129}I standard measurement. The x-axis indicates nominal ratio and y-axis indicates measured ratio of each standard. All data was normalized to IsoTrace Lab. Standard which has a nominal ratio $^{129}I/^{127}I = 1.1x10^{-10}$.

To measure iodine isotopic ratio in seawater samples by AMS, it is necessary to convert iodine species to silver iodide. The sample preparation for AMS target was performed by an extraction method. An iodine carrier (2-3 mg) was added to a seawater sample after filtering it. After iodate was reduced to iodide by sodium sulfite under sulfuric acid solution, iodide was oxidized for the extraction with carbon tetrachloride. And then back-extraction was performed by the addition of sodium bisulfite and sulfuric acid solution. Silver nitrate was added to the extracted iodine solution to precipitate iodine as AgI.

REFERENCES

[1] SUZUKI, T. et al., Performance of the new iodine-129 beamline at JAERI-AMS, Nucl. Instr. and Meth. B **223-224** (2004) 87-91.

[2] RAISBECK, G.M. et al., ^{129}I from nuclear fuel reprocessing facilites at Sellafield (U.K.) and La Hague (France); potential as an oceanographic tracer, J. Marine. Syst. **6** (1995) 561-570.

[3] SMITH, J.N. et al., ^{129}I and ^{137}Cs tracer measurements in the Arctic Ocean, Deep-Sea Res. I **45** (1998) 959-984.

RADIOMETRICS

Low level gamma-ray spectrometry at the PTB underground laboratory UDO

Neumaier, S., D. Arnold

Physikalisch-Technische Bundesanstalt,
Braunschweig,
Germany

Abstract. A new ultra-low background (ULB) gamma-ray spectrometry system has been installed 925 m below ground at the underground laboratory "UDO" of the Physikalisch-Technische Bundesanstalt, Braunschweig. This new system, consisting of a 95% coaxial HPGe-detector and a passive shielding (20 cm of low-activity lead, 10 cm electrolytic copper and radon suppression by N_2-flushing), will be described. Most of the peak count rates are less than 1 count per day and the integral background count rate in the energy range from 40 keV to 2750 keV is about 20 h^{-1}. This system was especially used to determine very small activity concentrations of ^{60}Co in environmental samples from Hiroshima and Tokai-mura and very small concentrations of long-lived radionuclides in meteorites. Results from these applications will be reported.

1. Introduction

In 1991, the Physikalisch-Technische Bundesanstalt (PTB), the national institute for science and technology in Germany, established an underground laboratory for dosimetry and spectrometry (UDO) in the Asse salt mine near Braunschweig (Germany). Due to the depth of 925 m below ground (≅ 2100 m of water equivalent), the cosmic-ray muon intensity in this facility is reduced by more than 5 orders of magnitude compared to ground level. In addition, the low specific activity of the pure rock salt (2-4 Bq/kg) and a moderate activity concentration of radon in air (10-20 Bq/m^3) result in an extremely low ambient dose equivalent rate of less than 1 nSv/h. The UDO facility is, therefore, well suited for dosimetry at very low dose rates, as well as for other applications which require low radiation levels and/or a very low muon intensity, such as low-background gamma-ray spectrometry. UDO is the deepest underground installation for scientific and technological studies in Germany. World-wide it is even the only underground laboratory which provides a calibration facility for dose and dose rate meters at very low dose rates (i.e. between 10 nSv/h to 100 nSv/h) [1]. Since its installation in 1991, international intercomparisons of dose and dose rate meters [2], a few radiobiological investigations and a considerable number of detector tests have been performed at the UDO facility. In 1998, a low-background gamma-ray spectrometry system was installed [3]. Meanwhile, there are three low-background gamma-ray detectors in operation. In this paper, an ultra-low background (ULB) gamma-ray detector system, operated at UDO since 2002, as well as first applications of this system, will be described.

2. The underground laboratory UDO

The Asse salt mine near Braunschweig, operated by GSF (National Research Centre for Environment and Health in Germany), was used to study the disposal of radioactive waste by permanent storage deep underground. These activities ceased in 1992, and the subterranean cavities are now being backfilled and access to the Asse mine is assured only for another 7 years. The measurements described in this paper were all performed at the UDO laboratory located on the lowest floor of the Asse mine at 925 m below ground, where the ambient dose equivalent rate is one of the lowest world-wide. To preserve this low radiation level, the UDO building itself (dimensions:14 x 3.6 x 2.8 m^3) was made from well selected materials of low intrinsic activity (< 2 Bq/kg). An air-conditioning system

with filters reduces the outside air temperature of 35°C to 21°C inside the UDO-lab and assures sufficient protection against the penetration of salt dust. In addition, a slight overpressure reduces the diffusion of unfiltered air into the laboratory. A detailed description of UDO is given in [3]. After 12 years of operation, in July 2004 the UDO facility had to be removed from the 925 m level due to the progressive backfilling of the Asse mine and was shortly afterwards reinstalled at a higher floor at 490 m below ground, where it will remain for another seven years, until its final shut-down.

3. Low-level gamma-ray spectrometry at UDO

Commercially available low-level gamma-ray spectrometry systems usually consist of high-purity (HP) germanium detectors with a passive shielding. At ground level, the background spectra of such dedicated low background devices are dominated by contributions originating from cosmic ray interactions. There are two main options to reduce these contributions: (I) the use of "active shieldings" (veto-counters) and (II) the operation of detector systems, in subterranean laboratories, sufficiently shielded against cosmic radiation (especially muons), by thick layers of matter.

The main limitations of Method (I) are insufficiencies in the suppression of the background due to time-delayed particles produced by cosmic ray interactions (e.g. neutrons) outside the coverage of the active shielding. Method (II) requires access to laboratories deep underground [4], located e.g. in long subterranean tunnels (like e.g. the Gran Sasso laboratory) or in mines (like e.g. the UDO laboratory).

At UDO, several low-background detector systems are operated. A low-background (LB) detector system consisting of a coaxial "extended range*" HPGe-detector (1.95 kg, 88% relative efficiency, FWHM 2.0 keV at 1.33 MeV) of low intrinsic activity with an end cap of very pure aluminium ("KryAl") with an entrance window 0.5 mm in thickness, housed inside a passive shielding, composed of a 20 cm outer layer of low-activity lead (^{210}Pb: 5-6 Bq/kg), and a 1 cm inner layer of pure electrolytic copper. The inner part of the shielding is flushed with N_2 to reduce the concentration of radon and its progenies. The continuous background in the background spectrum of the LB detector system at UDO is reduced by a factor of 30 (at low energies of about 100 keV) and a factor of 100 (at energies higher than 1 MeV) compared to measurements performed with the same system at ground level. A detailed description of this detector system is given in [3]. Using this detector system, it has been possible to measure very low activities of environmental samples, intrinsic activities of detector components (e.g. from highly sensitive dosemeters) and various samples from interdisciplinary applications.

4. The ULB detector system

In order to achieve lowest detection limits in gamma-ray spectrometry, an ultra-low background detector (coaxial p-type "extended range", 95% relative efficiency, FWHM 2.15 keV at 1.33 MeV) was built in 1999 by Canberra Industries. The end cap of the ULB detector is made of electrolytic copper with a carbon-epoxy window (∅=86 mm) 0.5 mm in thickness. The following precautions were taken to reduce the intrinsic background of the detector itself:

- no air transportation of the crystal or any other detector component to avoid activation due to spallation reactions caused by fast neutrons (e.g. ^{70}Ge(n,2p4n)^{65}Zn, ^{63,65}Cu(n,xnyp)^{57,58,60}Co).
- use of fresh electrolytic copper (to avoid activation due to spallation reactions). The electrolytic copper used for the inner shielding of the ULB detector system was produced by Norddeutsche Affinerie in Hamburg. In total, it remained only 14 days at ground level, including the time of the electrolytic process itself (7 days), the time for the melting process and the time for manufacturing at the PTB workshop (part of the manufacturing work was done at the workshops of the Asse salt mine, deep underground).
- selected materials for all detector components (e.g. old ship steel).

*[1] "Extended range" detectors (Canberra Industries) are p-type crystals (having a good energy resolution and high peak-to-Compton ratio) with an extremely thin insensitive zone at the front face. At this face, the efficiency remains high, even for very low energies of only a few keV ("n-type behaviour"). This feature allows "extended range" detectors to be simultaneously used for both high and very low energies.

The ULB detector system was accommodated in a shielding consisting of an outer layer of 10 cm of lead (^{210}Pb: < 6 Bq/kg), an intermediate layer of 10 cm of very pure lead (^{210}Pb: < 2 Bq/kg), and an inner layer of 10 cm of very fresh electrolytic copper. To minimise the diffusion of radon and its progenies into the system, the full set-up is housed in a glove box. With the ULB detector at UDO, the following net count rates of background lines, attributed to intrinsic activities of the detector or shielding, were measured: 46.5 keV (^{210}Pb): 1.9 d^{-1}; 186 keV (^{226}Ra/^{235}U): 1.8 d^{-1}; 352 keV (^{214}Pb): 7 d^{-1}, 511 keV (annih.): < 0.3 d^{-1}; 662 keV (^{137}Cs): < 0.3 d^{-1}; 911 keV (^{228}Ac): 0.3 d^{-1}; 1332 keV (^{60}Co): 0.7 d^{-1}; 1461 keV (^{40}K): 10 d^{-1}; 2615 keV (^{208}Tl): 0.2 d^{-1} (the relative uncertainties of these count rates vary from 10% to 25%). Within an energy range of 40 keV to 2750 keV, the ULB detector system at UDO shows an overall count rate of 22 h^{-1}.

The peak count rate of ^{40}K is still unsatisfactory. Measurements of the carbon epoxy as well as the glue, both used for the entrance window of the end-cap, show that the ^{40}K is most probably due to these two materials. It is therefore intended to remove the end-cup used at present and replace it by a pure Kryal one.

5. Applications and results

The ULB detector system has successfully been used to determine very small activity concentrations of ^{60}Co in environmental samples from Hiroshima and Tokai-mura and to determine very small concentrations of long-lived radionuclides in meteorites.

5.1. Hiroshima and Tokai-mura

Neutrons from the atomic bomb explosion in Hiroshima induced ^{60}Co in steel. 57 years after the explosion (this means more than 11 half-lives of ^{60}Co) it was still possible to measure ^{60}Co without any pre-concentration in steel samples of some 100 g collected at distances up to 1200 m from the point of explosion of the bomb [5]. The ^{60}Co-activities measured allow the fluence of neutrons to be reconstructed, as was the case for the criticality accident at Tokai-mura in 1999, where the ^{60}Co-activity in spoons was measured 2 years after the event [6].

5.2. Meteorites

The cosmic radiation interacts with extra-terrestrial material and produces a large variety of radioactive isotopes by nuclear reactions. If such kind of material reaches the earth (e.g. meteorites), the atmosphere stops the production of new radioactive atoms and if it can be identified and brought into a laboratory, measurements of the radioactive isotopes allow the age of such material to be determined. ^{26}Al is one of the long-lived radionuclides which is routinely measured in meteorites.

In 1999, PTB participated in an intercomparison to determine the ^{26}Al-activity in four different meteorites [7]. The aim was to compare different measurement techniques (e.g. accelerator mass spectrometry and underground gamma-ray measurements). In spring 2004, PTB received two stone samples collected in Spain which were measured immediately with the ULB detector. Figure 1 shows the spectrum of one of them which has a mass of about 400 g and was measured for 20 days.

The radioactive isotopes produced by cosmic radiation are indicated in the spectrum. Some of the isotopes have very short half-lives below 100 days. The result of the measurement, together with the typical surface structure and the collecting point in Spain, confirm that the stones are part of a

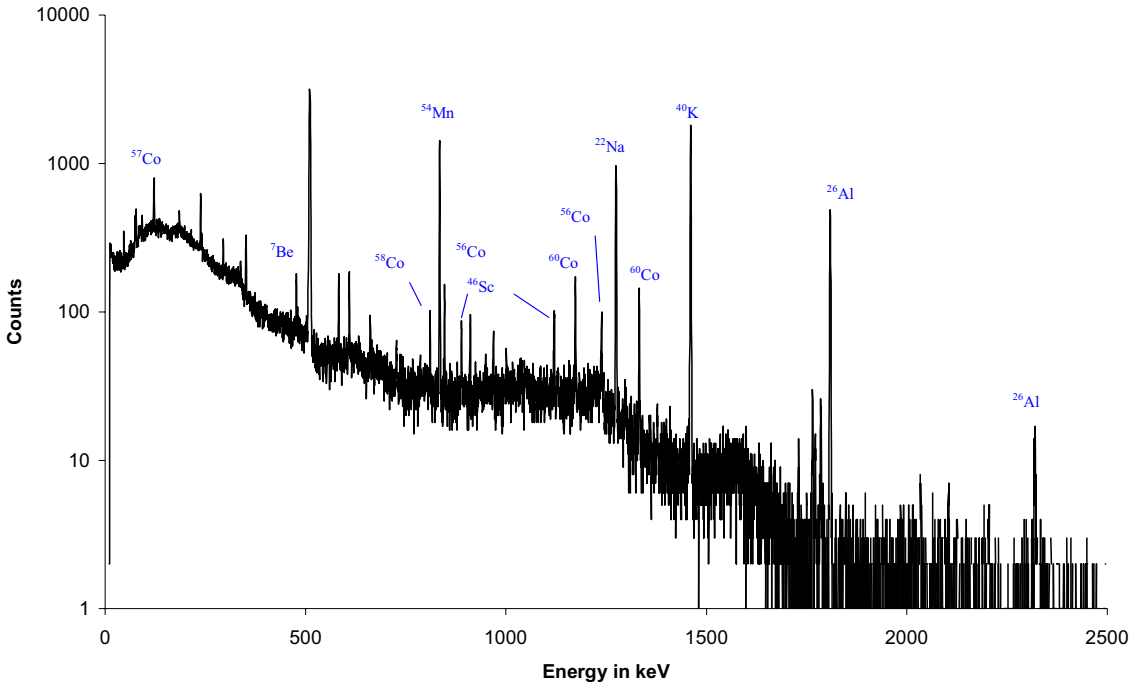

FIG. 1. Spectrum of a meteorite sample, activated by cosmic radiation, a few month after its entrance into the earth atmosphere. Details are described in 5.2.

meteorite whose fall was observed in Spain in January 2004. It has to be pointed out that most of the short-lived radionuclides could be measured only due to the very low background in the underground laboratory.

6. Summary

The Asse salt mine is being backfilled and will presumably be definitely closed in 2013. Due to this progressive process, in July 2004, the UDO-laboratory had to be removed from the lowest floor at 925 m below ground. The reinstallation of the UDO building at a higher floor (490 m below ground) of the Asse mine was finished in October 2004, and the measurement programs will start again in spring 2005. Access to the 490 m level is guaranteed until 2011. For this short period of seven years, UDO remains a unique facility for low-level experiments in Germany. It provides e.g. exceptionally good conditions for dosimetry at very low dose rates, as well as for ultra-low-level gamma-ray spectrometry. A new detector system for ultra- low background gamma-ray spectrometry at UDO improves the detection limits for most gamma-ray emitters by more than one order of magnitude compared with conventionally available low-background systems with passive shielding operated at ground level. The detection limits are still significantly lower than those obtained at ground level using actively shielded detectors. Therefore, it is still convenient to perform low-level gamma-ray spectrometry deep underground. The underground facility UDO of PTB is member of the CELLAR network of European underground laboratories. Part of the results presented were achieved in co-operation with other CELLAR members. In the remaining seven years, UDO shall continue to take an active part in the scientific program of the CELLAR network. In addition, UDO and its facilities are accessible to customers from science and industry, and PTB is open to co-operate with other scientific or technological institutions.

REFERENCES

[1] NEUMAIER, S., et al., The PTB contribution to the 1999 EURADOS intercomparison of national early warning systems, Radiat. Prot. Dosim. **92** 1-3 (2000) 101–108.

[2] SAEZ-VERGARA, J.C., et al., Lessons learnt from an international intercomparison of national network systems used to provide early warning of a nuclear accident having transboundary implications, Radiat. Prot. Dosim. **103** 3 (2003) 197-210.

[3] NEUMAIER, S., et al., The PTB underground laboratory for dosimetry and spectrometry, Appl. Radiat. Isot. **53** 1-2 (2000) 173-178.

[4] LAUBENSTEIN, M., et al., Underground measurements of radioactivity, Appl. Radiat. Isot. **61** 2-3 (2004) 167-172.

[5] HULT, M., et al., Deep underground measurements of ^{60}Co in steel exposed to the atomic bomb in Hiroshima, Appl. Radiat. Isot. **61** 2-3 (2004) 173-177.

[6] GASPARO, J., et al., Measurements of ^{60}Co in spoons activated by neutrons during the JCO criticality accident at Tokai-mura in 1999, J. Environ. Radioactivity **73** 3 (2004) 307-321.

[7] ARNOLD, D., et al., Deep underground gamma-spectrometric measurement of Al-26 in meteorite samples, Appl. Radiat. Isot. **56** 1-2 (2002) 405-408.

Background effects observed with a low-level gamma-spectrometer with muon veto detector

Mietelski, J.W., Z. Hajduk, L. Hajduk, J. Jurkowski

Henryk Niewodniczański Institute of Nuclear Physics,
Polish Academy of Sciences,
Kraków,
Poland

Abstract. A low background gamma spectrometer was constructed a few years ago at Krakow's Institute of Nuclear Physics. The spectrometer consists of a low-background HPGe detector housed in an aluminium-free cryostat, a passive shield which includes also Etruscan lead and an active shield – a veto Charpak chamber sensitive for muons on the top. The spectrometer is now in routine operating. In the article some influence of the active and passive shield on the observed background effects especially to those attributed to the neutrons are discussed. Introduction of a paraffin – cadmium element inside the shielded area makes the system very sensitive for neutron flux.

1. Introduction

A low background, ground level gamma spectrometer was constructed few years ago at Krakow's Institute of Nuclear Physics. The spectrometer was designed for the environmental studies in the Environmental Radioactivity Laboratory, Department of Nuclear Physical Chemistry. Among others it was applied for the study of ^{22}Na in the atmosphere [1] and in a course of study on Antarctic and Arctic radioactive contamination (not yet published). The aim of the article is to discuss some influences of the active and passive shield on the observed background effects especially to those attributed to the neutrons [2-5] since part of the spectrometer time was used for studying such background effects.

2. Instruments

The germanium detector, constructed by one of us (J.J.) is a true-coaxial p-type HPGe one with the nominal efficiency of 25%. It has "U" type aluminium-free cryostat. The aluminium was excluded due to the presence of traces of uranium in all examined by us aluminium alloys. The endcup of detector is made of stainless steel. After a few years of exploitation a composite foil window made of carbon fibre which supports a capon foil covered with ultra thin aluminium foil was added from the very top of the endcup. The window has 3.5 cm of diameter. The inner holder of germanium crystal is made of pure electrolytic copper. The resolution is 2.3 keV for 1173 keV, the ^{60}Co peak. Spectrometric electronics modules were manufactured by Silena (mod. 7329 and 7411) and Canberra (mod. 2022 and 3106). The passive shield (Fig. 1) consists of (from outside-to-inside): 8 cm (all sides and bottom) and 12 cm (top) of paraffin, 10 cm of standard lead, 2 mm of cadmium, 5 cm of 2500 years old, Etruscan lead (Plombum Ltd) and 1 cm pure electrolytic copper. Specific activity of ^{210}Pb in old lead was assessed at PTB, Braunschweig (Germany) and it was said to be within range of 6-8 mBq/g. The inner shielded volume of spectrometer is flushed with liquid nitrogen vapours, to reduce radon daughters contribution to the spectra. The multiwire Charpak's chamber (constructed by two of us: Z.H. & L.H.) is a muon detector. It is situated on the top of the spectrometer. To enlarge the solid angle it is situated between the parts of a passive shield (Fig. 1). Detector has two active layers, with volume of 70×70×2 cm^3 each. It is flushed by a mixture of 80% Ar + 20% CO_2 (technical gas known as Corgon), the flush rate is about 0.5 l/h. Chamber is polarized with 2 kV of high voltage. It has 160 anode wires, which are made of tungsten coated with gold, the cathodes are from aluminized mylar. Anode wires are grouped in 4

sections in each layer, 20 wire in one section. All sections are parallel each to other. Signals from anode wires from each section go to appropriate discriminating amplifiers (one of eight) where they are converted to fast, NIM-like signals. Those signals are standardized to full NIM standard in a second discriminator and then they go to a logic unit. Various logical configurations of sections were tested to optimize the effectiveness of the shielding. Initially it was the coincidence between sum of two layers, then sum of coincidence in sections, which are situated one above another, and finally, sum of signals from all sections. This resulting signal is transformed to a 19 μs long TTL pulse, which is used as a veto for spectrometer's ADC. Timing and duration of TTL pulse were also optimized to achieve highest possible effectiveness. The chamber gives the count rate equal to about 3500 cpm in coincidence of layers mode and about 11000 cpm in sum of all sections mode. The active shield does not affect badly the dead time. Even in highest count rate, finally chosen "sum of the all sections" logical configuration, the spectrometer's dead time is increased by less then 0.5%.

3. Results

Background spectra obtained with active shield turned on is displayed in Fig. 2. Some details of the effectiveness of muon chamber on continuous background and selected lines are presented in Table I. Achieved reduction of count rate for a broad window from 50 keV to 2.7 MeV is 56% (52% for window from 80 keV to 3 MeV: from 0.88 cps to 0.46 cps). The continuous background is reduced almost evenly in all parts of spectrum. Namely, similar reduction rate was also observed for 511 keV annihilation line. Similar reduction factor was observed for (n, γ) lines caused [3, 4] by inelastic scattering of neutrons (see Table II). The active shield is obviously not affecting ^{40}K line (1461 keV). Introduction of the thin, composite window was done to make detector sensitive for low energies.

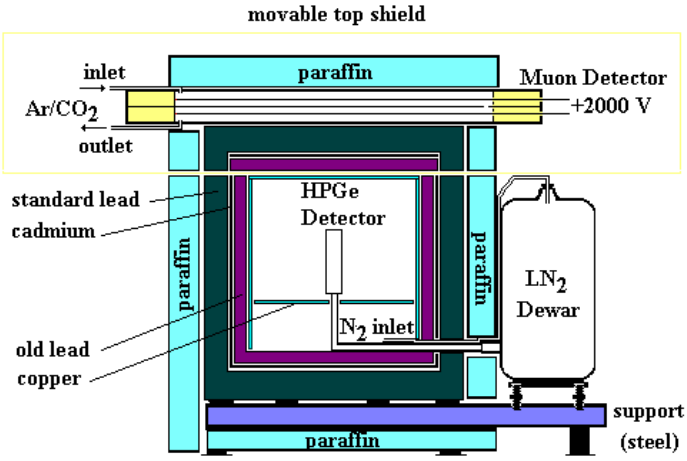

FIG. 1. A scheme of construction of low-level gamma spectrometer shield.

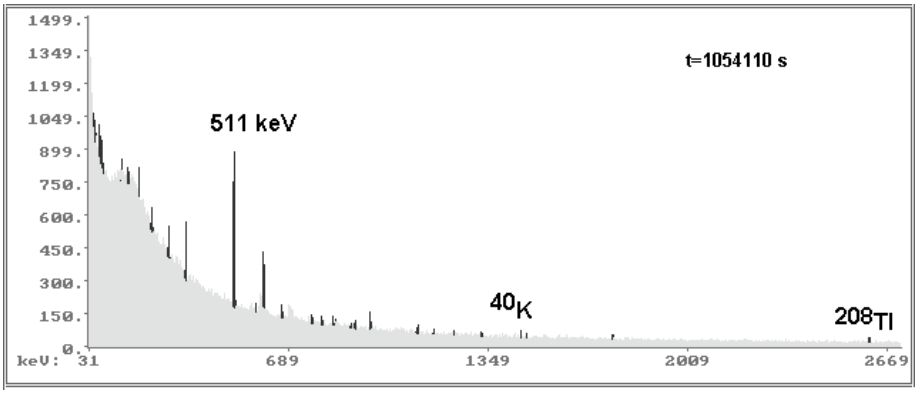

FIG. 2. Background of spectrometer described here (veto "on").

Table I. Effectiveness of gamma spectrometer background count rate reduction after usage of veto chamber, all counts in [cps]. Data prior to introducing composite window.

Description	symbol	Σ(50-500) keV	Σ(0.5-1) MeV	Σ(1-2.7) MeV	511 keV	1461 keV
No veto	A	0.6106	0.1986	0.1655	0.01036	0.00029
Veto on, AND*	B	0.5417	0.1761	0.1424	0.00777	0.00025
Veto on, OR*	C	0.3402	0.1128	0.0854	0.00519	0.00032
reduction rate	B:A	0.887	0.887	0.860	0.75	0.86
reduction rate	C:A	0.557	0.568	0.516	0.50	1.10

* - logic product (AND, coincidence) or logic sum (OR) of signals from two layers.

Table II. Count rate reduction observed for asymmetric gamma lines induced by neutron inelastic scattering in spectrometer background, with and without application of active shield (veto detector).

Energy [keV]	reaction	Count Rate [cps]	
		veto off	veto on
595.9	Ge(n,γ)	0.00287	0.00160
691.3	Ge(n, γ)	0.00221	0.00150

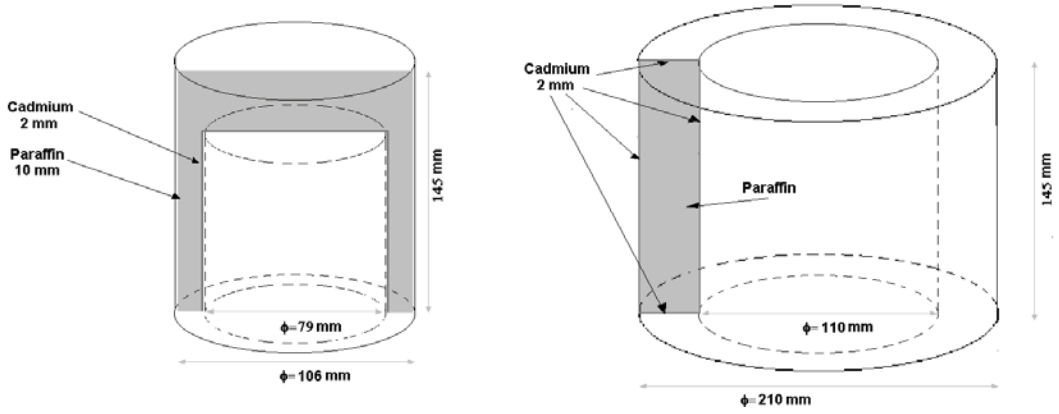

FIG. 3. Shape of two cadmium-paraffin elements used for detection of neutrons with HPGe detector.

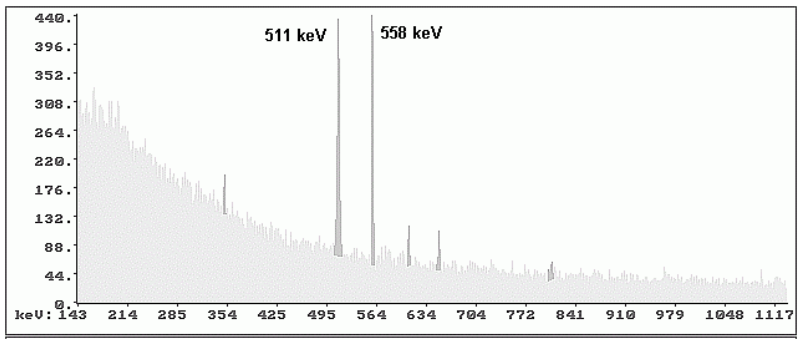

FIG. 4. Gamma rays spectrum of background with both simple devices presented in Fig. 3 (left and right) placed inside the shield of spectrometer.

Table III. Results for 558.5 keV intensity in neutron field for described here spectrometer in which two paraffin/cadmium devices were put inside the shield. Details in text.

Conditions	cps
Background (no neutron source)	$(2.9 \div 4.7) \cdot 10^{-3}$
Cf neutron source situated:	
Directly on outside of passive shield	2.90
Inside lead shield, above copper lining	22.0

Many effects are observed due to nuclear reaction caused by neutrons. To make neutron effects easier to observe, simple devices were introduced by one of us (J.W.M.). One was just a plastic Marinelli beaker of 0.5 dm^3 volume, the bottom and inner sides were lined with 2 mm thick cadmium plate, and the whole volume was filled with paraffin (Fig. 3a). Second device was a torus-like cane made of 2 mm cadmium plate and filled with paraffin (Fig. 3b). After introducing any or both of some additional gamma lines appear, of which the 558.4 keV $^{113}Cd(n,\gamma)^{114}Cd$ [5] is the most intense. Example of a part of background spectrum with cadmium - paraffin element inside is presented in Fig. 4. The sensitivity for detection of neutrons was proofed using an old weak Cf neutron source. During this experiment both Cd/paraffin devices were inside detector shield. Results are presented in Table III. The presence of the neutron source enlarged count rate by 3 orders of magnitude, and by another order of magnitude, when it was closer to the detector. However, the same cadmium/paraffin elements gives an order of magnitude lower count rate than for described here spectrometer, when it was put inside standard gamma-ray spectrometer with HPGe detector, equipped only with passive shield made of 10 cm lead and 2 cm copper and 2 mm cadmium between them. It is not shielded by paraffin. The biggest difference between passive shields is in thickness of lead so in their masses. This is a factor of at least 50%. The thicker shield is a more effective target for cosmic muons. This suggests, that what is registered as 558 keV line in background (with Cd+paraffin devices inside) is not caused by neutrons from the background directly, but most likely by muons. Muons interact only by electromagnetic forces and by weak interaction. They do not interact by strong nuclear forces. Since probability of weak processes is very low, one has to assume that neutrons are most likely originating from secondary nuclear processes induced by charged particles. At present we are trying to understand these processes better by Monte-Carlo simulations, however the work has not been finished yet.

The most interesting effects for low-level counting are perhaps n, γ processes which occur not in construction materials but in the sample matrix. A deionised water matrix show the 2.223 MeV hydrogen neutron capture line [2]. Observation of deuterium synthesis line shows the synthesis occurred in sample inside the shield. It occurs also in certain low intensity in any surface or sea waters. Besides appearance of such as above new lines intensities of some background lines can change. In Table 4 an influence on background line obtained for this water sample is presented. Since water acts as moderator processes induced by fast neutrons has lower counts rates, but some others induced by thermal neutrons occurs more often. The count rate for annihilation line is not affected, and those for Rn daughters (for example 609 keV of ^{214}Bi) is lower – Rn is removed from direct distance of detector. Generally the count rates with for pure water sample are higher than for spectrometer background: it is about 10% increase below 1 MeV and 27.5% increase between 1 MeV and 2.7 MeV.

4. Conclusions

The low-background system constructed in our Institute seems to have reasonable low background for such devices operating at ground-level laboratories. A simple tool for studying the neutron field inside shield of gamma spectrometer was introduced. It was proofed that it is sensitive for neutrons. Applying gamma-spectrometry for low-level counting the effects induced by non-radioactive sample matrix on gamma spectrum should be taken into consideration. The main origin of these effects is related not

directly to neutron background in measurement room, but to neutron background inside the shield, caused by muons. This neutron field inside shield seems to be more intense than outside. The studies on this field will be continued.

Table IV. Influence on chosen background gamma rays intensities of water sample (0.5 dm^3 Marinelli).

Energy [keV]	Process	Count rate for water sample [cps]	Count rates ratio (Water to Background)
139	$^{74}Ge(n,\gamma)^{75}Ge$	0.00096(12)	2.14(0.59)
198	$^{70}Ge(n,\gamma)^{71}Ge$	0.00105(13)	1.72(0.38)
511	e^+e^-	0.00413(11)	1.04(4)
596	$^{74}Ge(n,n')$	0.00127(13)	0.91(0.12)
609	^{214}Bi	0.00057(6)	0.64(7)
692	$^{72}Ge(n,n')$	0.00097(10)	0.79(10)
669	$^{63}Cu(n,n')$	0.00013(5)	0.58(23)
2223	$H(n,\gamma)D$	0.00022(3)	>24
50-500	sum of all	0.3528(6)	1.1044(9)
500-1000	sum of all	0.0996(3)	1.1089(5)
1000-2700	sum of all	0.0989(3)	1.2749(4)

ACKNOWLEDGEMENTS

We want to express our many thanks for our co-workers, who helped a lot in this construction, especially Dr. M. Jasińska, Mr. R.Hajduk, Mr. J. Michałowski and Dr. K. Kozak. Professor M.Wójcik of Jagiellonian University is also warmly acknowledged for his valuable discussion during the design phase.

REFERENCES

[1] GRABOWSKA, S.,MIETELSKI, J.W., KOZAK, K., GACA, P., J. Atm. Chem. **46** (2003) 103-116.
[2] HEUSSER, G., Nucl. Inst. Meth. Phys. Res. A **369** (1996) 539-543.
[3] NÚÑEZ-LAGOS, R., VIRTO, A., Appl. Rad. Isotop. **47** (1996) 1011-1021.
[4] ŠKORO, G.P., ANIČIN, I.V., KUKOČ, A.H, KROMPTIĆ, D.J., ADŽIĆ, P., VUKANOVIĆ, R., ŽUPANČIĆ, M., Nucl. Inst. Meth. Phys. Res. A **316** (1992) 333-336.
[5] HEUSSER, G., Nucl. Inst. Meth. Phys. Res. B **83** (1993) 223-238.

Remote sensing of intertidal sediment bound radionuclide storage, remobilization and deposition: Case study in the Ribble estuary

Tyler A.N.[a], R. Wakefield[a], P. McDonald[b], M. Rainey[a], P. Atkin[b]

[a] School of Biological and Environmental Sciences,
University of Stirling,
Stirling,
United Kingdom

[b] Westlakes Scientific Consulting Ltd,
Westlakes Science & Technology Park,
Moor Row,
Cumbria,
United Kingdom

Abstract. Intertidal environments of the Irish Sea are spatially complex and dynamic systems. The ability to understand and monitor these environments is fundamental to a variety of industrial, regulatory and government bodies. Intertidal estuarine environments often represent sinks and sources for industrial discharges. The ability to map the fate of these discharges through remote sensing provides a powerful tool in environmental monitoring and is critical in understanding their redistribution. This study focuses on the Ribble estuary, Lancashire, UK, which is accumulating elevated radionuclide concentrations discharged under license from BNFL Sellafield and Westinghouse Springfields. This paper presents the results from a series of investigations which demonstrate: i) that conventional airborne remote sensing using the Airborne Thematic Mapper (flown by the UK's Natural Environment Research Council) combined with sophisticated image analysis and ground truthing can be used to quantitatively map intertidal specific activity concentrations of anthropogenic radionuclides derived from BNFL Sellafield (r^2>0.8); and ii) that time series imagery flown over tidal sequences can be used to identify sources of radionuclide bearing sediments, characterise the hydrodynamic features of the estuary and quantify fluxes of sediment and radionuclides over tidal cycles.

1. Introduction

Estuaries represent a critical interface between the marine and terrestrial environment and can act as a sink or a source for contaminants discharged to the aquatic environment. The distribution of fine sediment particles is particularly critical to the transport and retention of pollutants such as the anthropogenic radionuclides discharged under license from British Nuclear Fuels plc (BNFL) Sellafield plant since 1952 [1]. Given the substantial decrease in radionuclide effluent discharged since the mid 1970s and the lower projected levels of radionuclides entering estuaries [2, 3], coupled with issues of coastal squeeze from sea level rise, evaluating the fate and behaviour of these current coastal reservoirs of radionuclides is of increasing importance.

Whilst point sampling and monitoring can provide analytically detailed information for spatially isolated locations, absolute interpretation on the data derived from the samples may be limited without a spatial or temporal context. Characterising the heterogeneity of intertidal areas through point sampling is commonly time consuming, expensive and often unrepresentative [4]. Direct measurement of gamma emitting radionuclide concentrations through in-situ gamma spectrometry provides a more rapid and spatially representative means for measuring radionuclide concentrations and has been successfully demonstrated in salt marsh environments [5, 6, 7]. However, covering the intertidal

environment is time consuming and limited by issues of inaccessibility. Airborne gamma ray spectrometry offers greater and more rapid spatial coverage [8], but is gained at the expense of spatial resolution (footprint *c* 300 m across at flying altitude of 75 m), a resolution too coarse to provide detailed measures and mechanistic interpretation of contaminant distribution [4].

Conventional airborne remote sensing has the ability to provide synoptic information across the whole estuarine environment. Much work has already been undertaken on the mapping of intertidal surfaces using 'soft' classification at Stirling, demonstrating for the first time that airborne thematic mapper (ATM) image data is capable of quantitatively mapping intertidal sediment grain size, in particular percentage clay content [9, 10, 11]. Mapping suspended particulate matter, in particular suspended sediment concentrations is also a well established technique in remote sensing [12, 13, 14].

The paper demonstrates how airborne remote sensing combined with ground reference data collection can be used to map intertidal radionuclide concentrations and sediment bound radionuclide fluxes within the estuaries.

2. Study site, data acquisition and processing

The Ribble Estuary in Lancashire UK, shown in Fig. 1, is 31 km in length, lying in an east-west orientation from Preston to Lytham St. Anne's (Fig. 1). Re-engineering of the main channel at the turn of the 20th century coupled with the cessation of dredging in the 1980s has lead to rapid slat marsh development and estuary siltation. The sand and silt accumulating in the channel and the salt marshes is predominantly supplied from the Irish Sea via the action of an asymmetrical tidal system. These sediments are contaminated by historical licensed discharges from the British Nuclear Fuels plc (BNFL) Sellafield site.

Airborne data acquisition has the distinct advantage of enabling data to be collected at specified times and for time series data acquisition and the temporal frequencies required. Collection of intertidal image data was optimised to occur following a period of exposure and drying to maximise the spectral contrast between sand and clay dominated sediments [10]. The ATM imagery was processed using linear spectral mixture modelling to provide relative sub pixel abundances of sand mud, moisture and microphytobenthos. These spectral end member components were recombined through multivariate regression analysis with ground reference data to derive percentage clay. This methodology is detailed in [11]. In addition to grain size analysis, intertidal samples were also analysed by gamma spectrometry.

A series of nine flight lines with Compact Airborne Spectrographic Image (CASI) data wrer collected over a flood tide sequence. The CASI instrument was programmed to measure reflectance values in optimised bands following preliminary in-situ spectral characterisation [12]. The images were calibrated from concomitant ground reference data. Water samples were filtered for gamma spectrometry analysis and the determination of suspended sediment concentration (SSC).

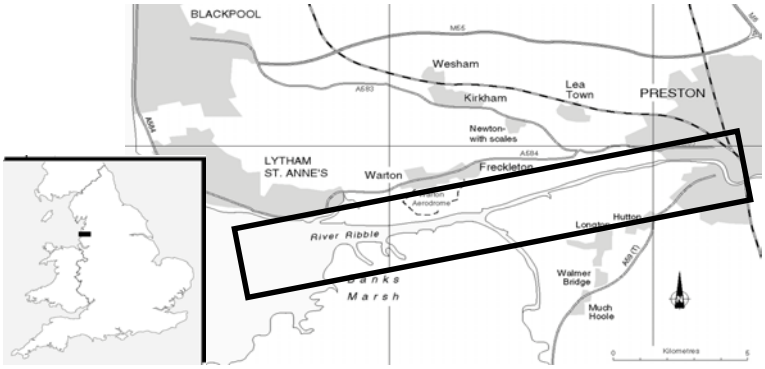

FIG. 1. Map of the Ribble Estuary showing the main CASI and ATM flight path.

3. Results and Discussion

3.1. Intertidal radionuclide concentrations

Figure 2 shows an example of the calibrated percentage clay intertidal image. Comparison between ground reference and image data data was good ($r^2 > 0.8$). A well established relationship between percentage clay and radionucide concentrations was established over a series of summer sampling trips and across the whole of the intertidal area. The relationship between ^{137}Cs and percentage clay is shown in Figure 3 [16].

This synoptic approach also yields valuable information for estuarine modelling and radioecology. Sediment stability is controlled by sediment composition and a surface covering of microphytobenthos. Current research is predicting sediment erosivity from image information. In addition, the distribution of sediment type and cover is an indicator for grazing of benthic fauna and wildfowl. In addition, the presence of microphytobethos may be important in the remobilisation of radionuclides from sediments back into the water column.

3.2. Sediment flux

Time series analysis of the nine CASI flight lines demonstrates how the data can be used for time series analysis, important in understanding the hydrodynamics of the estuarine system. In addition, similarly strong relationships between SSC and ^{137}Cs have been established [12] and validated by further sampling. Images of suspended sediment (Fig. 4), coupled with estimates of water volume, derived from 2 dimensional hydrodynamic model, and depth-profile validated assumptions of the vertical stratification and mixing of SSC has enabled estimates of the total suspended sediment load and radionuclide concentration to be established. By building up a time series profile, it is possible to establish the total amount of sediment eroded and deposited in the estuary over the flood tide. Figure 5 illustrates the concept of erosion and deposition. For the time series data collected in August 1997, around 20% more sediment was deposited than eroded over the flood tide only. This equates to about 20,000 tonnes of sediment or *c.* 6 GBq of ^{137}Cs. A proportion of this sediment will then be lost over the ebb tide sequence. This is currently being investigated further to estimate the total net sediment and radionulide deposition following the ebb tide sequences.

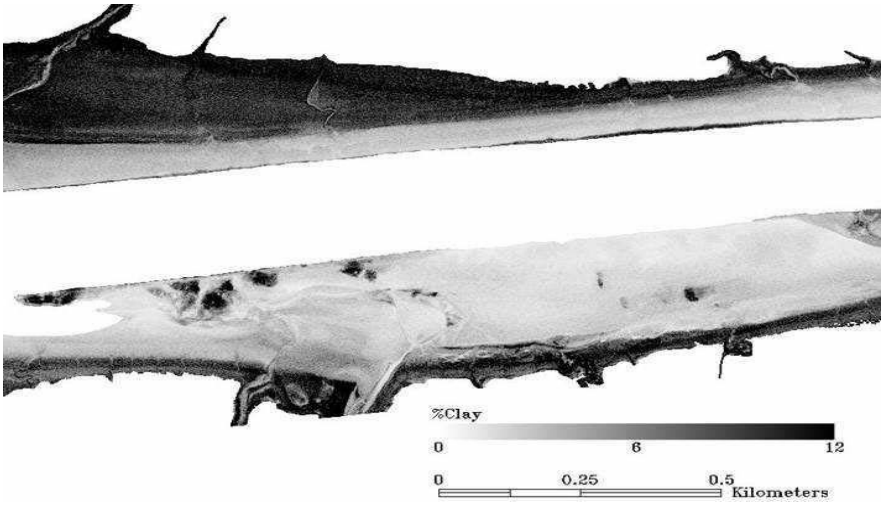

FIG. 2. Subset of the percentage clay map, May 1997, after [11, 15].

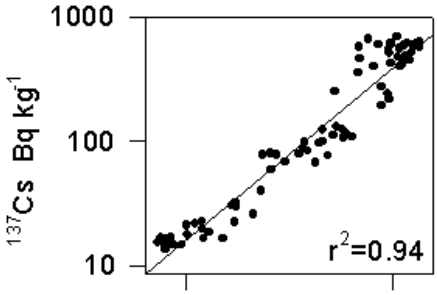

FIG. 3. Relationship between pecent clay and ^{137}Cs [15, 16].

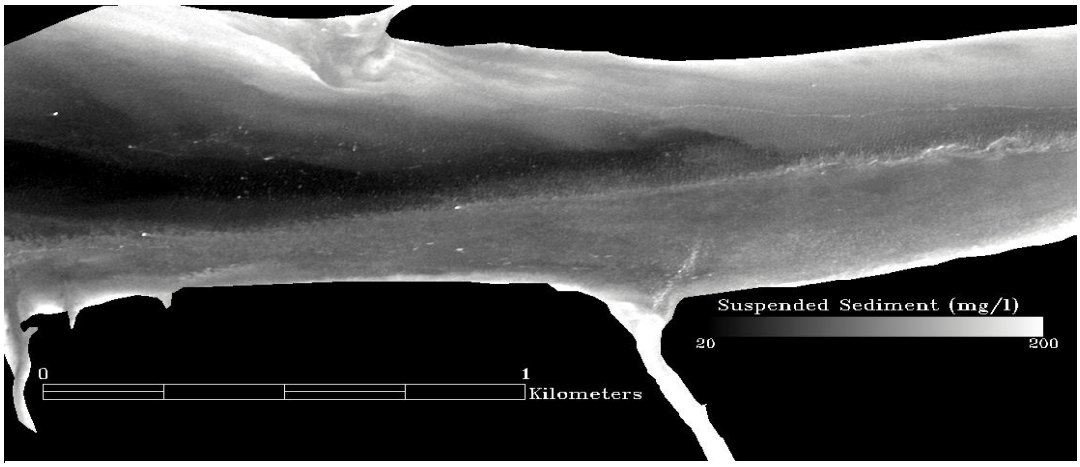

FIG. 4. Subsection of a SSC over a flood tide April 2003.

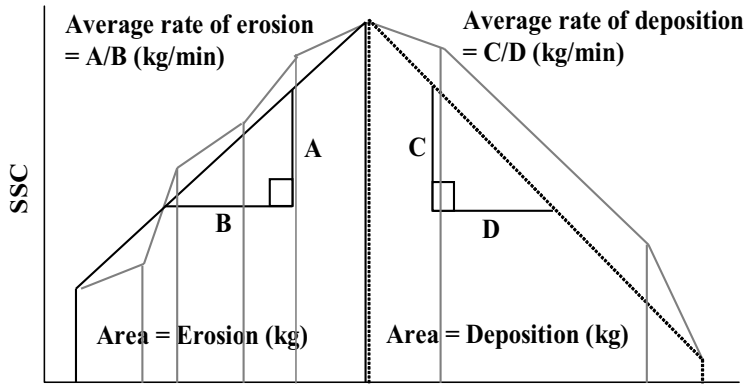

FIG. 5. A schematic representation of the trapeziums, areas and gradients used in the calculation of net deposition from image data.

ACKNOWLEDGEMENTS

This research was funded by the Natural Environment Research Council (NERC), BNFL, Westlakes Scientific Consulting and the University of Stirling. NERC also provided the remote sensing data.

REFERENCES

[1] MACKENZIE, A.B., et al., Sediment Radionuclide Profiles: Implications for Mechanisms of Sellafield Waste Dispersal in the Irish Sea, J. Environ Radioact. **23** (1994) 39-69.
[2] COOK, G.T., et al., Remobilization of Sellafield-derived radionuclides and transport from the NE Irish Sea, J. Environ. Radioact. **35** (1997) 227-241.
[3] MACKENZIE, A.B., et al., The influence of mixing timescales and re-dissolution processes on the distribution of radionuclides in northeast Irish Sea sediments, J. Environ. Radioact. **39** (1998) 35-53.
[4] TYLER, A.N., et al., Investigations of Spatial Variability and Fields of View in Environmental Gamma Ray Spectrometry, J. Environ. Radioact. **33** 3 (1996) 213-235.
[5] TYLER, A.N., High accuracy in situ radiometric mapping, J. Environ. Radioact. **72** (2004) 195-202.
[6] TYLER, A.N., Monitoring Anthropogenic Radioactivity in Salt Marsh Environments through in situ gamma ray spectrometry, J. Environ. Radioact. **45** 3 (1999) 235-252.
[7] TYLER, A.N., et al., Estimating and Accounting for ^{137}Cs Source Burial through In-situ Gamma Spectrometry in Salt Marsh Environments, J. Environ. Radioact. **33** 3 (1996) 195-212.
[8] SANDERSON, D.C.W., et al., Demonstrating the European capability for airborne gamma spectrometry: Results from the ECCOMAGS exercise, Rad. Protect. Dosimetry **109** (2004) 119-125.
[9] BRYANT, R., TYLER, A.N., et al., A preliminary investigation into the VNIR spectral characteristics of inter-tidal sediments, Int. J. Remote Sensing **17** 2 (1996) 405-412.
[10] RAINEY, M., TYLER, A.N., et al., The influence of surface and interstitial moisture on the spectral characteristics of intertidal sediments: Implications for airborne image collection and processing. Int. J. of Remote Sensing **21** (2000) 3025-3038.
[11] RAINEY, M., TYLER, A.N., et al., Mapping Estuarine Intertidal Sediment Size Fractions through Airborne Remote Sensing, Remote Sensing of the Environment **86** (2003) 480-490 12.
[12] ATKIN, P., Investigating Radionuclide Bearing Suspended Sediment Transort Mechanisms in the Ribble Estuary using Airborne Remote Sensing, PhD Thesis, University of Stirling, UK (2000).
[13] SVAB, E.M., TYLER, A.N, et al., Characterising the spectral reflectance of algae in lake waters with high suspended sediment concentrations, Int. J. of Remote Sensing (in press).
[14] SVAB, E.M., TYLER A.N, et al., Remote sensing of Lake Balaton, Hungary: A mixture modelling approach to quantifying blooms of phytoplankton in water characterised by high-suspended sediment, Int. J. of Remote Sensing (submitted).
[15] RAINEY, M.P.R., Airborne Remote Sensing of Estaurine Radionuclide Concentrations, PhD Thesis, University of Stirling, UK (1999).
[16] TYLER, A.N., et al., Deriving accurate intertidal radionuclide concentrations at high spatial resolution through airborne remote sensing (in prep.).

Device development for marine gamma survey of seabed on Azerbaijani section of Caspian Sea

Bayramov, Z.

Azerbaijan National Aerospace Agency,
Baku,
Azerbaijan Republic

To explore the potential of isotope techniques for studying water balance and dynamics of the Caspian Sea two research training cruises were carried out, in late summer of 1995 and 1996, respectively, within the framework of an IAEA technical co-operation project [1]. Unfortunately during these expeditions there is a highly important aspect of the problem of maintaining of ecological balance which is covered insufficiently. This is a composition of seabed's radiational situation map. This question gains the special importance for exploitation of closed systems, which include also the Caspian Sea. The problem is that the Caspian Sea unlike to other water basins possessing rich deposits of hydrocarbon raw materials (e.g. the Mexican Gulf, the North Sea, the Persian Gulf), is a closed type bio-ecological system, where the rigid balance of hydrosphere, biosphere and especially of geological structure of seabed is existed. The violation of any of these components can lead to practically irreversible processes, and as a result, to ecological catastrophe. Realization of gamma survey of seabed makes it possible to determine initial background of seabed's gamma field at the beginning of well drilling work. Further periodical monitoring of radiational situation will be based on results of initial condition of seabed's gamma-field. By this purpose we developed an original complex for determination of percentage content of major components of gamma field, namely, of natural radio-nuclides U-238, Th-232 and K-40 in three working energetical windows: 1.65-1.85 MeV 2.5-2.8 MeV and 1.35-1.55 MeV using calibration on isotope Cs-137 (0.662 MeV) (Fig. 1). Complex will consist of two parts; underwater part and ship s part (Fig. 1).

The detection unit is standard scintillation block developed on the basis of monocristal NaJ (Tl). having sizes ∅150 x 200 mm, protected by sealed water-tight underwater housing made of sheet of steel, having width equal to 10 mm, designed for pressure up to 100 atm, i.e. for depth nearly equal to 1000 m. A cable-rope with length equal to 1000 m connects this underwater housing with ship's winch. The underwater housing is mounted on the carrying frame of transportation structure, pulled by towing cable-rope along the seabed. Gamma survey is carried out on the basis of landscape map of seabed of determined area /2/. An on-board computer carries out detailed processing of information about percentage content of U, Th and K at the given point, received from the seabed. Reliability and possibility of long time period of continuous work of proposed device allows to carry out mapping of area's radiational situation at the sea conditions along predetermined route, the coordinates of which are determined by high-precision navigational satellite system DGPS. Data received from synchronous measurements of radiational background and geodesy coordinates are brought in to on-board computer's date base. The special software of processing make it possible to develop the map of radiational situation of pre-arranged scale for determined area and to record the initial condition of environment at the moment of measurement.

As a result, these maps make it possible to decide two problems. The first is an ecological problem. Successful introduction of oil contracts last years, on the other hand, create the conditions for sharp increase of the deep oil platform’s refuses to the Caspian Sea. But that, in its turn, become the reason of an increase of seabed’s natural radioactive background. The second is oil and gas deposits exploration. Researches have shown that natural radioactive background existing over the oil and gas deposits contours is approximately 3-5 times low than that of other areas. The reason is that speed of

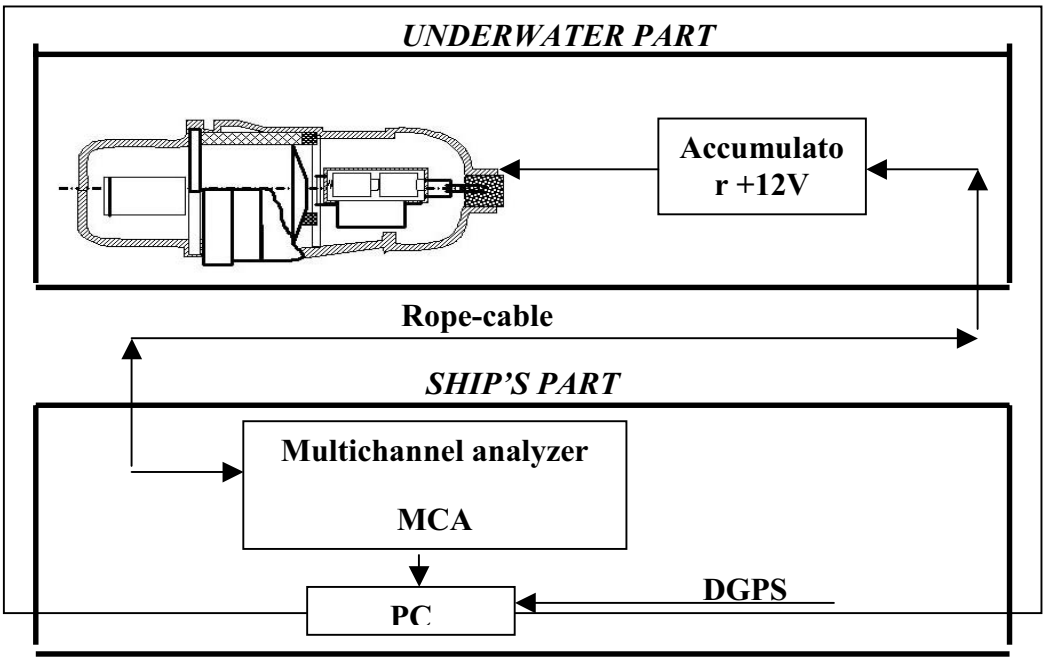

FIG. 1. Structure of underwater gamma-spectrometer.

leakage of radionuclides to upper layers in oil, is comparatively low. This process causes the shortage of such natural radionuclides as uranium, potassium and thorium, in upper layers of seabed. The contours of oil and gas deposits situating in depth of seabed may be accurately determined using developed maps [3].

REFERENCES

[1] FROEHLICH, K., ROZANSKI, K., POVINEC, P., OREGIONI, B., GASTAUD, J., Isotope studies in the Caspian Sea, Sci. Total Environ. **237/238** (1999) 419-427.

[2] BAYRAMOV, Z.T., "Devices Designed for Radiation Monitoring and Marine Gamma Survey in the Azerbaijan National Aerospace Agency", II Eurasian Conference on Nuclear Science and Its Application Abstracts, NATO Advanced Research Workshop: Environmental Protection Against Radioactive Pollution, Almaty, Republic of Kazakhstan, September 16-19, 2002.

[3] AGAYEV, F., BAYRAMOV, Z.T., RZAYEV, E.A., FRANTSEVA, V.V., KERIMOV, F.N., Marine Gamma Survey (Proc. ASPG/EAGE Int. Conf. Petroleum Geology and Hydrocarbon Potential of the Caspian Sea & Black Seas Region, Baku, May 2002).

Low background germanium detector technology from Canberra

Verplancke, J.[a], M. Berst[b], M.O. Lampert[b], O. Tench[c]

[a] Canberra Semiconductor N.V.,
Olen,
Belgium

[b] Canberra Eurisys SA,
Lingolsheim,
France

[c] Canberra Industries Inc.,
Meriden,
United States of America

Since Eurisys Mesures and Canberra merged into one company under the wings of Cogema-Areva in February 2001, decades of know-how and experience in building Germanium detectors for low level gamma ray analysis have been brought together. This vast experience means that Canberra can offer a large variety of "low level detectors" depending on the application. The complexity and cost of these detectors increase with the decreasing detection limits that our customers want to obtain.

In this paper we give a short overview of the various categories of "low level HP Ge detectors" that we produce. We present some examples of detection limits that can be obtained with each of these and we show what measures are taken to come to the next lower limit of detection. The spectroscopist should be aware, however, that the detection limit that can be obtained with a particular source and isotope mix depends in the first place on the choice of the detector element geometry and size, and on the geometry of the cryostat and source. Reference [1] discusses this aspect of the optimum counting conditions. The choice of the shielding and the location of the detector-shield combination (above or below ground level) comes in second place. The precise design and choice of materials for the cryostat – the subject of this paper – are generally only the third factor of importance [2, 3].

The simplest low level gamma counting system that we consider in this paper consists of a standard high purity germanium detector in a standard lead shield. The cryostat materials used for these standard detectors are selected mainly for their mechanical properties and cost. Selection of the cryostat materials for their radio-purity comes only in the second place. The contribution of their activities to the background in the spectrum is neglectable since the measuring times are usually limited (typically 1 hour) and the background coming from the room and from the sample is generally higher. Detection limits that are aimed for in this category are in the order of 0.5 to 1 Bq per kg (for Cs-137 in a water sample and one hour counting time [4]). This is still one order of magnitude lower than when no lead shield is used [5].

When lower detection limits are aimed for, for instance by applying longer counting times, the background activity coming from the radio-isotopes present in the cryostat construction materials of standard detectors become more important. This is particularly true when radioisotopes of interest are present in these construction materials: ^{60}Co, ^{40}K, ^{137}Cs, ^{232}Th, ^{235,238}U and their daughters. At this level, also the activity generated by (n,γ) and (n, n'γ) reactions by cosmogenic neutrons on construction materials in the system may become a nuisance. These applications constitute 90% of the low level, environmental sample analysis applications. For these, Canberra developed standardized

"ultra-low-background" (ULB) cryostats. Construction materials are replaced by materials that are practically free of radioactivity that may become visible after a few hours of counting. Materials that have large cross sections for interactons with cosmic particles are avoided. Detector parts that cannot be replaced by radio-pure alternatives (electronic components, molecular sieves, PCBs, …) are moved away from the detector element, outside the lead-shield and not in line of view with the detector element. The lead shields used with these detectors generally have the facility to flush the inside with nitrogen boil-off gas to minimize the background coming from Radon in the air.

The overall background level obtained with these detectors is not much lower than with the previous category of "low background detectors" (typically some 10%). However, most of the strongest photopeaks disappear from the blank spectrum, allowing measurement of virtually any isotope with good statistics down to a level below 1 Bq/kg (for 100 % abundance and 1 hour counting time).

Applications that require much lower detection limits and much longer counting times, are mainly hindered by artifacts that are created by the interaction of the counting system with cosmic particles. A solution that is used then is to place the shield and detector in a deep underground location or with a cosmic-veto shield on top of the lead shield. At these levels, other phenomena become visible that are otherwise obscured by the cosmic background:

- trace-amount of radio-impurities in the construction materials, such as activity in the front-end electronic components, ^{210}Pb activity coming from the solderings used, etc…
- activation products of copper and germanium that have grown in during their stay above ground.

The measures to overcome these "contaminants" can go very far, including avoiding soldering, detector assembly in extreme clean room environments and hiding electronic components behind massive internal shielding or using very special materials like ultra-high purity endcaps and holders, very old steel and lead parts and using only fresh germanium and copper that is stored deep underground at all (practical) times.

These solutions are engineering intensive, require the input and help from the user, and are obviously much more expensive that the standard ultralow-background solutions.

Other papers on this conference [6] show that using such extreme measures, detection limits as low as a few μBq per kg of material can be obtained.

REFERENCES

[1] VERPLANCKE, J., About Shapes and Geometries of high purity germanium detectors, presented at the Nucl. Phys. Conf., Madrid, Aug. (1999).

[2] CEUPPENS, M. et al., Low Background Germanium Detectors; from environmental laboratory to underground counting facility, (Proc. Workshop "Methods and Applications of Low Level Radioactivity Measurements"), Rossendorf, Nov. (1996).

[3] VERPLANCKE, J., Low Level Gamma Spectroscopy; low, lower, lowest, Nucl. Instr. Meth. A312 (1992) 174-182.

[4] CANBERRA document: Application Note: Gamma Analyst Performance Characteristics (MDAs) (1997).

[5] TOIVONEN. H., Development of in-field monitoring techniques, Report on Task FIN A845 on the Finnish Support Programme to IAEA Safeguards, Dec. 1994.

[6] HEUSSER G. et al., these proceedings.

The Gran Sasso National Laboratories (L.N.G.S.): status and outlook

Laubenstein, M.

Laboratori Nazionali del Gran Sasso,
Assergi (AQ),
Italy

The Gran Sasso National Laboratories (L.N.G.S.) are world-wide one of the biggest underground laboratories (e.g. [1]). They are located about 100 km east of Rome in Italy along the highway, in the Gran Sasso Range of the Italian Abruzzi. Their mission is strictly connected to the fields of particle and astroparticle physics, where the experiments located underground have given an enormous and very important contribution for their understanding. The underground laboratories are located at 1400m depth (equivalent to an overburden of 3800 m of water). In the past years a change took place during which the first generation experiments have gradually been replaced by a new generation of experiments.

Some of the experiments which have given important results during the past 15 years are GALLEX, MACRO, and, more recently, DAMA, the Heidelberg-Moscow double beta decay experiment and the LUNA experiment. GALLEX was the first experiment measuring the pp-neutrino flux coming from the sun and confirming the solar neutrino deficit registered by the other solar neutrino experiments. MACRO gave a very valuable contribution to the understanding of the cosmic ray attenuation and induced reactions in the earth mantle, pushing at the same time the limit for the predicted flux of magnetic monopoles further down. DAMA, instead, is world-wide the first experiment, which is giving a possible signal of dark matter particles. The Heidelberg-Moscow double beta decay experiment has given the best limit on the neutrino less double beta decay for ^{76}Ge. In the end, LUNA has measured nuclear reactions of astrophysical interest, approximately close to the energy range of the reactions in the sun.

The new generation of experiments consists above all in the very ambitious project of the CERN Gran Sasso neutrino beam. On their way through the earth mantle the neutrinos, generated in the CERN accelerators, could change their flavour. This flavour changing, commonly referred to as oscillation, is already confirmed for the neutrinos coming from the sun, but it is important to know, whether this process is taking place also on the medium range, which is important for the determination of the neutrino mass parameters. The experiments at the L.N.G.S. which will perform this detection are currently under construction. They are OPERA and ICARUS. OPERA is using an emulsion technology. It consists of thousand of photographic emulsions, which do not detect the neutrino directly, but the reaction products. ICARUS, instead, is a huge detector working with 600 t of liquid argon, working as a time projection chamber. Then there are several new initiatives of smaller experiments, aiming either at the detection of dark matter with new methods and larger detectors (CRESST, WARP), or at the confirmation/refusal of double beta decay (CUORICINO, an enhanced and enlarged ^{76}Ge experiment).

Apart from the primary mission in fundamental physics experiments, the unique position of the underground laboratories inside a mountain, close to an active seismic fault, gives also rise to geophysics and geology experiments (e.g. [2]). Those experiments are collecting very useful information, e.g. about the behaviour of the groundwater reservoir, and the precursor events of micro- and macro-seismic activity.

Last but not least, the almost complete absence of cosmic rays and the very low radioactivity of the surrounding environment give the possibility of refining and improving the instrumentation for low-level experiments. The L.N.G.S. are housing one of the biggest low-level research facilities underground (e.g. [3]). It is equipped with eight high purity Germanium detectors with one of them having the lowest background ever measured with such a type of detector. Recently was installed a low background liquid scintillation counter. It was found in the past years that for this kind of detectors the location deep underground is greatly enhancing their performance, increasing the signal stability and lowering the background. An enlargement of the low background facility is under way, because the request of space for new applications is high, and it is surely worthwhile to pursue this street for the sake of interdisciplinary applications. For example in the near future the L.N.G.S. underground will host also the prototype of a new gravitational wave experiment, LISA, which will be sent in a few years from now in its mission around the sun.

In conclusion, the L.N.G.S. are a unique and large underground facility giving the possibility for a wide range of researchers, physicists, geophysicists, geologists, biologists and many others to widen their knowledge, to develop new detectors and interconnect various field of research for the benefit of all.

REFERENCES

[1] BETTINI, A., Neutrino physics at Gran Sasso Laboratory, Nucl. Phys., B. (Proc. Suppl.) **100** (2001) 332.

[2] PLASTINO, W., et al., Radon groundwater monitoring at underground laboratories of Gran Sasso (Italy), Geophys. Res. Lett. **28** 14 (2001) 2675.

[3] ARPESELLA, C., A Low Background Counting Facility at Laboratori Nazionali del Gran Sasso, Appl. Rad. Isotop. **47** (1996) 991.

Neutron fluence measurements using underground HPGe-detectors

Hult, M., J. Gasparro

EC-JRC-IRMM,
Geel,
Belgium

IRMM performs gamma-ray spectrometry in the underground laboratory HADES located at a depth of about 500 m water equivalent at the premises of the Belgian nuclear centre SCK•CEN in Mol and operated by Euridice. By performing gamma-ray spectrometry with HPGe-detectors deep underground one can reduce the background counting rate with a factor of 1000 compared to a low background detector above ground [1]. Underground HPGe-detectors are being employed in an increasing number of different fields. One field in which the use of underground HPGe-detectors has proven to be particularly useful is in the field of neutron fluence measurements. It is useful at this stage to point out that according to the ISO guides [2, 3] the entities particle flux, fluence and fluence rate are used together with the units s^{-1}, m^{-2} and $m^{-2}s^{-1}$, respectively. The name flux density can be used as synonym to fluence rate.

Measurement of neutrons (energy and fluence) is a delicate task in nuclear measurements. By making use of underground gamma-ray spectrometry it is possible to extend the present use of the so called foil activation technique (a common technique to measure neutron fluxes in nuclear reactors) to encompass very low neutron fluences (even environmental neutron fluences) as well. As we started working on this technique a couple of years ago, 4 interesting applications have evolved and will be briefly described below.

Application #1, ALARA principle and benchmarking: Around nuclear installations like accelerators and reactors there is generally an enhanced neutron field. The neutron dose meters used for monitoring purposes are often not reliable at very low doses. By using metal discs of various materials it is possible to measure also only slightly enhanced neutron flux levels. This can be used to better implement the ALARA principle. Such work has been carried out at the IRMM Van de Graaff accelerator as well as at the BR-1 reactor of SCK•CEN [4]. The neutron field near medical accelerator is often overlooked. We aim at studying this in the future.

Application #2, use of fast neutron induced reactions: An accurate neutron energy spectrum can be produced using unfolding techniques in combination with activation foils/discs. Although the activation technique is very sensitive to thermal neutrons it is not so sensitive to fast neutrons due to the generally low activation cross sections for high energy neutrons. The use of threshold reactions and underground gamma-ray spectrometry allows us to produce a neutron spectrum with relatively high resolution, which is useful for benchmarking of other (on-line) neutron monitors or machine (accelerator/reactor) properties.

Application #3, retrospective neutron fluence measurements: In 1999 there was a criticality accident at the JCO fuel factor in Tokai-mura. The accident was characterised by:

- High release of neutrons (for 20 hours) to the surroundings
- Only negligible amounts of fission products were released
- Poor neutron monitoring facilities outside the plant

In order to understand the effects of the accident, activated samples (table salt, gold items, steel spoons etc.) were collected from houses in Tokai-mura by the Japanese investigation team headed by Prof.

Komura [5]. Some of these items had low activities due to either too large distance from epicentre and/or long time (in relation to the half-life in question) between activation and measurement [6].

Man's knowledge of the effect of ionising radiation on the human body is to a large extent based on follow-ups of Hiroshima/Nagasaki victims. In a project similar to the "JCO-measurements", IRMM measured steel activated by the A-bomb in 1945 in order to better quantify the dose received by the population [7]. At present the dose is calculated using computer models and measurements are necessary to verify these models.

Application #4, environmental neutron flux inside various material: With thin discs/foils it is possible to measure the neutron flux inside various materials with high depth resolution. This is important for example in geoscience, which relies on cosmogenically induced activation in order to make e.g. age determinations and erosion histories.

REFERENCES

[1] LAUBENSTEIN, M., et al., Underground measurements of radioactivity, Appl. Radiat. Isot. **61** (2004) 167-172.
[2] ISO, Quantities and units – Part 9: Atomic and nuclear physics, ISO 31-9 (1992) (E).
[3] ISO, Quantities and units – Part 10: Nuclear reactions and ionizing radiation, ISO 31-10 (1992) (E).
[4] MARTINEZ CANET, M.J., HULT, M., KÖHLER, M., AIT ABDERRAHIM, H., MARLOYE, D., Metal discs as very low thermal neutron flux monitors in reactor environment, ASTM technical Publication 1398 (2001) 761-768.
[5] KOMURA, K., et al., The JCO criticality accident at Tokai-mura, Japan: an overview of the sampling campaign and preliminary results, J. Environ. Radioact. **50** (2000) 3-14.
[6] GASPARRO, J., et al., Measurements of ^{60}Co spoons activated by neutrons during the JCO criticality accident at Tokai-mura in 1999, J. Environ. Radioact. **73** (2004) 307-321.
[7] HULT, M., et al., Deep underground measurements of ^{60}Co in steel exposed to the Hiroshima atomic bomb explosion, Appl. Radiat. Isot. **61** (2004) 173-177.

RADIOMETRICS - POSTERS

Determination of Th, U, Pu and Am radionuclides in soil and marine samples

Benkrid, M.[a], S. De Figueiredo[b]

[a] Centre de Recherche Nucléaire d'Alger,
02 Bd. F. Fanon, B.P. 399,
Alger-Gare,
Algeria

[b] Technical University of Vienna,
Vienna,
Austria

A combined procedure was used for the determination of actinides Th, U, Pu and Am radionuclides in Mediterranean sediments, IAEA reference samples, intercomparison material and Monaco seawater. The analysis was based on anion exchanges and UTEVA and TRU columns for separation and purification of the specific actinides.

The radiochemical procedure was based on Pu and Th separation by a strong basic ion exchange resin in 8M HNO_3 and 10M HCl respectively after oxidation state adjustments to Pu(IV). Then the uranium was retained in a tributyl phosphate (TBP) phase and separated from any Th traces by extraction chromatography on an UTEVA resin. The Americium was pre-concentrated by co-precipitation with calcium oxalate. It was separated from rare earths by extraction chromatography on TRU resin. For alpha measurements, the sources were prepared by the NdF_3 electrodeposition and co-precipitation method as illustrated in Figure 1showing the flow scheme of the radiochemical-separation procedure for the actinide elements.

The actinides of interest are emitting alpha particles in the region of 3.95MeV (^{232}Th) to 8.8MeV (^{212}Po). It is not possible to find any significant variation of the detector efficiency in the energy interval ranging from 2.5 to 8.8 MeV, which makes the quantitative evaluation of alpha particles spectra much simpler than in the case of gamma ray ones. The energy resolution improves with increased detector bias which is individually specified for each detector. The evaluation of the energy resolution of alpha peaks (FWHM= Full-Width at Half Maximum) is not straight forward due the fact that most alpha particles are not emitted at only one energy level.

The PIPS (Passivated Implanted Planar Silicon) detector has an extremely thin layer window which means less energy loss and better resolution. To ensure correct identification and quantification of alpha-emitting nuclides, it is necessary to calibrate the system for both energies, with mixed alpha standard ($^{239+240}$Pu, ^{241}Am and ^{244}Cm) and efficiency by means of a highly polished stainless steel disc electrodeposited source (^{241}Am). A relationship between the channel-energy and the determination of the effective detector efficiency for the chamber can be provided. The background of the detectors is generally low. The detectors tend to be contaminated especially with ^{210}Po (by evaporation) and by recoil nuclei (as ^{224}Ra from ^{228}Th).

A very wide range of values were obtained depending on the sample. The $^{239+240}$Pu and ^{238}Pu concentrations varied from 0.7 to 14.8 Bq kg^{-1} dry weight and from 0.016 to 2.74 Bq kg^{-1} dry weight respectively. The ^{238}U and ^{234}U concentrations ranged from 27.0 to 63.6 Bq kg^{-1} dry weight and 24.6 to 69.2 Bq kg^{-1} dry weight respectively. The ^{232}Th concentration ranged from 1.23 to 63.50 Bq kg^{-1} dry weight.

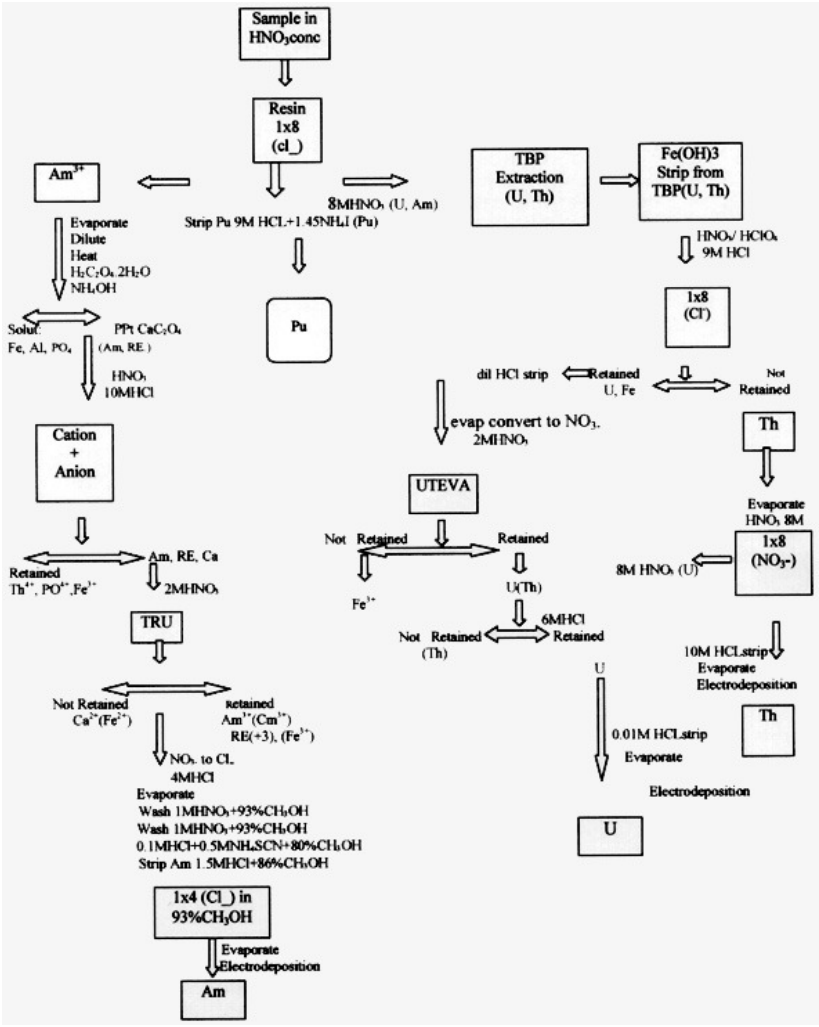

FIG. 1. Flow scheme of the radiochemical separation procedure for the actinide elements.

The radiochemical separation of the actinides for (Th, U, Pu and Am) follows almost the same procedure in environmental samples. There were great advantages of using extraction chromatography (TRU and UTEVA Eichrom materials) and Bio-rad resins for the radiochemical separation in environmental samples.

REFERENCES

[1] LA ROSA, J.J., BURNETT, W., LEE, S.H., LEVY, I., GASTAUD, J., POVINEC, P.P., Separation of actinides, caesium and strontium from marine samples using extraction chromatography and sorbents, J. Radioanal. Nucl. Chem. **248** 3 (2001) 765-770.

[2] MORENO, J., VAJDA, N., DANESI, P.R., LA ROSA, J.J., ZEILLER, E., SINOJMERI, M., Combined procedure for the determination of ^{90}Sr, ^{241}Am and Pu radionuclides in soil samples, J. Radioanal. Nucl. Chem. **226** 1-2 (1997) 279-284.

[3] HOLM, E., Review of alpha-particles spectrometric measurements of actinides, J. Appl. Radiat. Isot. **35** 4 (1984) 285-290.

[4] STEINHÄUSLER, F., GASTBERGER, M., HUBMER, A.K. SPANO, M., RANALDI, L., STRONATI, L., TESTA, A., Assessment of the radiation dose due to nuclear tests for residents in areas adjacent to the Semipalatinsk test-site «polygon» (Kazakhstan).

Validation of alpha-spectrometric methods for ^{226}Ra measurements using a double tracer technique

Bojanowski, R.[a], Z. Radecki[b]

[a] Polish Academy of Sciences,
Institute of Oceanology (PAS),
Sopot,
Poland

[b] International Atomic Energy Agency,
Vienna

Determination of ^{226}Ra by alpha-spectrometry is always associated with some loss of the analyte, because radiochemical operations are never quantitative. All radiochemical procedures must, therefore, include some steps to enable these losses to be quantified and accounted for in subsequent calculations.

^{133}Ba and ^{225}Ra are the most commonly used radionuclides for monitoring ^{226}Ra recovery but both have some flaws. The barium does not follow exactly the behaviour of ^{226}Ra in some radiochemical reactions, which makes the assumption of their equivalence as yield determinands questionable. As for ^{225}Ra, its usefulness is limited by inconvenient nuclear properties combined with a complex decay scheme, which makes it difficult to maintain a stock calibrated solution in a radiochemically pure state for long-term use.

We have developed a simple ^{225}Ra generator, which enables to milk it from its parent ^{229}Th radionuclide at any time for immediate use. It is based on removal of thorium and actinium from the mother liquid by extraction with N-Benzoyl-N-phenylhydroxylamine in chloroform at pH 8 – 9. Alternatively, 5,7-dichlor-8-hydroxychinoline can be used with the same effect, but it is less stable than the former reagent.

The ^{225}Ra tracer has been used in parallel with the ^{133}Ba to examine the performance of selected radiochemical procedures on real samples and to elucidate sources of discrepancies in analytical results obtained on some IAEA`s reference materials.

Interaction of plutonium with humic acid

Génot, L., H. Michel, G. Barci-Funel, V. Barci

Laboratoire de Radiochimie,
Sciences Analytiques et Environnement,
Université de Nice-Sophia Antipolis,
France

Humic substances are naturally occurring organic compounds of high molecular weight. They are capable of interacting with metals by complexation or redox process. Therefore the behavior of trace elements, especially anthropogenic radionuclides, in soils or sediments is greatly influenced by humic substances[1, 2]. We have studied complexation of plutonium by Aldrich humic acid in solution at different values of ionic strength.

Purification of humic acid

The commercial sodium salt was purified in order to eliminate mineral impurities and non-humic substances. The method used was adapted from Ref. [3]. Humic acid is treated with HF-HCl to dissolve mineral impurities. The residue is dissolved in NaOH solution and precipitated in acidic conditions (HCl) to eliminate fulvic acids and humines. Then the humic acid is dialysed against distilled water until chloride free and shaken with a cationic resin in H^+ form to remove metallic impurities. After freeze-drying we obtained purified humic acid in protoned form.

Potentiometric titration of humic acid

Acid-base properties of humic acid (AH) were investigated by potentiometric titration in the pH range 4-9 for three different ionic strength. Experiments were carried at 25±1°C under argon atmosphere. The charging of the molecule was calculated for each point of the titration curve according to the charge balance of the solution [4]:

$$Q = \frac{C_{NaOH} - C_{HNO3} + 10^{-pH} + 10^{pH-pKe}}{C_{AH}}$$

Charge of the humic acid is plotted against pH in Fig. 1.

Interactions with plutonium

Complexing abilities of humic acid were studied at trace plutonium concentration (below 10^{-10} $mol.L^{-1}$). To evaluate the concentration of free and complexed forms or plutonium in solution, the equilibrium dialysis method [5] and the ion exchange resin method[6] were used. The performances of the two methods were compared.

Plutonium was quantified by alpha spectrometric measurement after electrodeposition on a stainless steel disc [7].

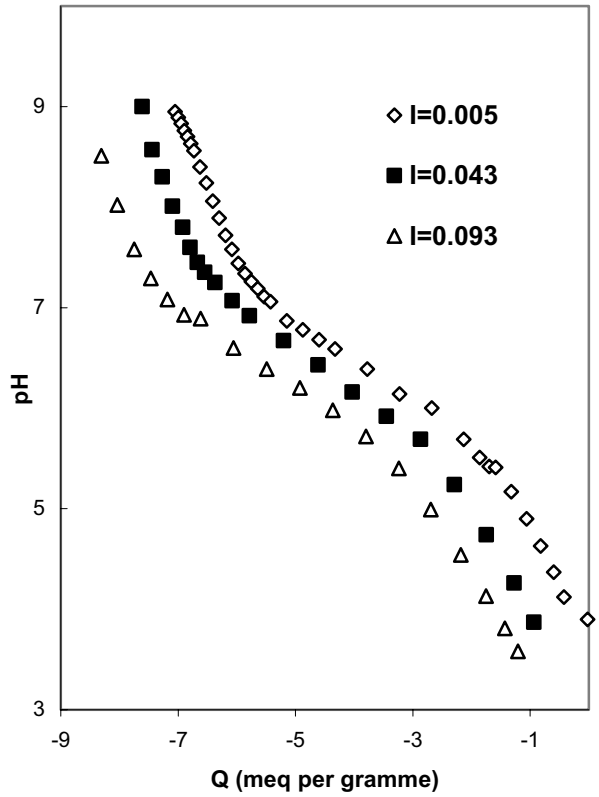

FIG. 1: Potentiometric titration of humic acid. C_{AH} : 400 mg. l^{-1} , C_{NaOH} echantillon : $4x10^{-3}$ mol.L^{-1}, Titrant : HNO_3 0.01 mol.L^{-1}, Temperature : 25±1°C.

REFERENCES

[1] WOOD, S.A., The role of humic substances in the transport and fixation of metals of economic interest (Au, Pt, Pd, U, V), Ore Geol. Rev. **11** (1996) 1.

[2] JONES, M.N., BRYAN, N.D., Colloidal properties of humic substances, Adv. Coll. Interface Sci. **78** (1998) 1.

[3] VERMEER, A.W.P., VAN RIEMSDIJK, W.H., KOOPAL, L.K., Adsorption of humic acid to mineral particles 1: Specific and electrostatic interactions, Langmuir **14** (1998) 2810.

[4] FUKUSHIMA, M., TANAKA, S., HASEBE, K., TAGA, M., NAKAMURA, H., Interpretation of the acid-base equilibrium of humic acid by a continuous pK distribution and electrostatic model, Anal. Chim. Acta **302** (1995) 365.

[5] GLAUS, M.A., HUMMEL, W., VAN LOON, L.R., Trace metal-humate interactions. I. Experimental determination of conditional stability constants, Appl. Geochem. **15** (2000) 953.

[6] WENMING, D., HONGXIA, Z., MEIDE, H., ZUYI, T., Use of the ion exchange method for the determination of stability constants of trivalent metal complexes with humic and fulvic acids, Part I: Eu^{3+} and Am^{3+} complexes in weakly acidic conditions, Appl. Radiat. Isot. **56** (2002) 959.

[7] TALVITIE, N.A., Electrodeposition of actinides for alpha spectrometric determination, Anal. Chem. **44** (1972) 280.

Sorption of cesium on bentonite: the role of calcite

Hurel, C.[a], A. Delisse[b], N. Marmier[a], F. Fromage[b], A.C.M. Bourg[c]

[a] Laboratoire de Radiochimie,
Sciences Analytiques et Environnement,
University of Nice Sophia Antipolis,
France

[b] Groupe de Recherche en Chimie Inorganique University of Reims,
Champagne Ardenne,
Reims,
France

[c] Environmental Hydrogeochemistry Group, UMR 5034,
University of Pau,
France

Since bentonite is investigated for its use in Engineered Barriers Systems as backfill material, many studies of their surfaces properties have been performed in the past years to qualify and quantify adsorption on their surfaces, which can be one of the major processes limiting migration of radionuclides away from a disposal site. Nevertheless, most of these studies concerned simplified systems, such as Na-montmorillonite in mono-electrolyte solution. As ion-exchange processes are of importance in water-clays interactions, adsorption of natural major ions has also to be taken into account for natural systems.

The aim of this work is (i) to quantify the sorption of the natural major cations on the montmorillonite surface, (ii) to compare the sorption of cesium, in two different systems, a simple one (Na-montmorillonite in $NaNO_3$ 0.05 $Mol.L^{-1}$) and a complex one (natural bentonite in a synthetic natural water) and then (iii) to assess the influence of the natural major ions on this sorption, and to identify the role of the calcite phase present in bentonite.

The methodology used consists in several batch experiments, first considering a very simple solution ($NaNO_3$), then using mixtures of two different electrolytes, and lastly using a synthetic natural water. A surface complexation model, describing the surface of clays as a mixture of ion-exchange and complexation surface sites, is used to provide interpretations and quantifications of the sorption processes.

Observed results indicate that affinity for the montmorillonite surface is greatest for Ca, then Mg and then K. The sorption of cesium is strongly affected by the presence in solution of Ca, witch can come from the partial dissolution of calcite.

ACKNOWLEDGEMENT

This study is one part of a work supported by ANDRA on the retention properties of bentonite materials.

Caesium sorption–desorption behaviour in bottom sediments

Lujanienė, G.[a], B. Šilobritienė[a], K. Jokšas[b]

[a] Institute of Physics,
Vilnius,
Lithuania

[b] Institute of Geology and Geography,
Vilnius,
Lithuania

The objective of this study is to focus on the sorption and desorption behavior of Cs in the complex heterogeneous system of bottom sediments in order to better understand the cesium behavior during the Baltic Sea water flooding events to the Curonian Lagoon and transport of suspended particles from the Curronian Lagoon to the Baltic Sea. Three sorption and desorption experiments were carried out.

Kinetic tracer experiments were performed in order to better understand the sorption of ^{137}Cs on bottom sediments during the intrusions of sea water to the Curonian Lagoon and ^{137}Cs sorption on the suspended particles because similar particles are transported to the Baltic Sea from the Curonian Lagoon and that rather long time is required to reach equilibrium. These experiments indicated that particles can display intensive and selective sorption towards the Cs ions in marine water.

A sample of bottom sediments collected in Curronian Lagoon was used for sorption experiments. Total carbon (TC) and total organic carbon (TOC) were determined using a LECO CS-125 analyser. The stable Cs concentration was determined using ICP–MS, and clay minerals were identified by X–ray diffraction. Filtered sea water of 7.0 salinity labelled with ^{134}Cs was used for the sorption experiment. The total concentration of Cs in solution was 0.04ppb. The solids were separated by centrifugation at 4000 rpm after different contact time between solution and sediments. Details of the experiment are described in [1]. The modified Tesser sequential extraction method was used to study association of Cs in sediments. ^{137}Cs and ^{134}Cs activities were measured using an intrinsic germanium detector. The precision of ^{134}Cs measurements by gamma spectrometry was <3% at $\pm 1\sigma$.

Results of sorption of ^{134}Cs in sediments after different contact time indicated that more than 70% of ^{134}Cs tracer was sorbed during the first three days. Similar results were obtained during the second experiment. The decrease in the caesium amount in the exchangeable fraction desorbed by NH_4^+ possibly corresponds to the decrease in the number of frayed edge sites available for Cs sorption. The decrease in the sorption rate accompanied by an increase in association of ^{134}Cs with carbonate fraction can be attributed to the effect of coatings that are usually present in natural heterogeneous sediments. In the sediment sample used for the sorption experiment, a high content of carbonate was determined. The carbonate coatings can inhibit the caesium uptake by clay minerals. The caesium ions need some time to diffuse through carbonate coating to the clay particles where they can be sorbed on the available sorption sites. Cs^+ forms soluble carbonates as do the other alkali elements. Cs in solution is trapped in calcite insignificantly because its ionic radius greatly exceeds the radius of Ca^{2+}. A negligible amount of Cs usually observed in carbonate fraction after the sequential extraction can be considered as traces of Cs^+ incorporated in calcite during co–precipitation and/or Cs^+ sorbed on regular exchange complex sites under carbonate coatings.

The comparative analyses of ^{134}Cs fraction distribution after 241 and 375 days of the sorption experiment with that of the ^{137}Cs distribution, determined in the same sediment sample before the

sorption experiment, indicated that after 375 days of sorption the equilibrium was not fully reached, but distribution was found to be close to equilibrium.

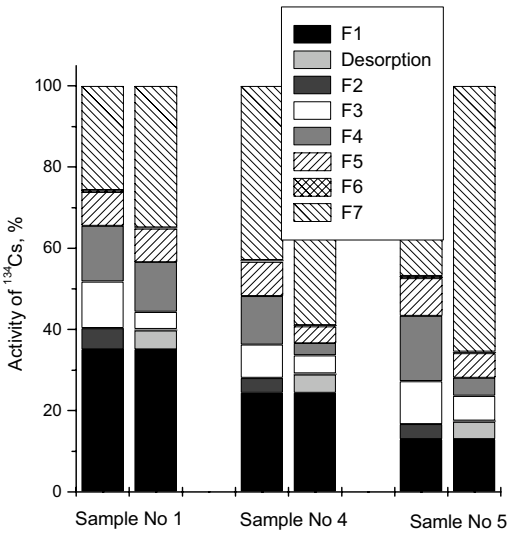

FIG. 1. Comparison of fraction distribution before and after desorption (2nd experiment) (F1-contact solution, F2-exchangeable ($MgCl_2$), F3-exchangeable (NH_4Cl), F4-carbonates, F5-organic, F6-oxides, F7-residue).

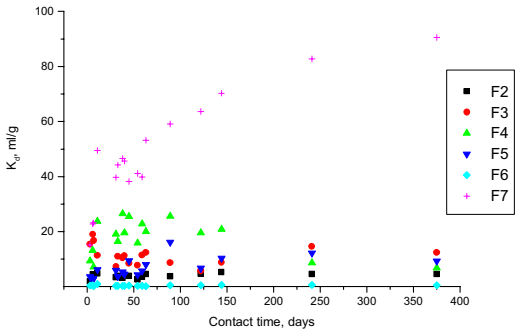

FIG. 2. K_d for ^{134}Cs (first experiment) in different fractions as a function of contact time for sediments (sediment/sea water ratio 1 : 10), (F2- exchangeable ($MgCl_2$), F3- exchangeable (NH_4Cl), F4 - carbonates, F5 -organic, F6 - oxides, F7-residue).

The short-term desorption experiments indicated an insignificant release of Cs^+ from the regular exchange complex (Fig. 1). The remobilization of "fixed" caesium was not observed, on the contrary, the redistribution of caesium towards its fixation in clay minerals was observed, and on a time scale its fixation kinetics was comparable with that of the sorption experiment. Experiments have shown the double effect of coatings on sorption of Cs on bottom sediments: at primary stage of sorption, coatings inhibit sorption of Cs, however, later they can inhibit the release of Cs to the surrounding solution.

Data obtained from these experiments were used to calculate the K_d coefficients both for total bottom sediments and different geochemical sediments phases (Fig 2). It can be seen that residual fraction, which reflects the Cs sorption on clay minerals, is the most important in Cs incorporating to bottom sediments, while the role of other geochemical phases is relevant only during two months of the sorption experiment.

This study indicated that flooding events of sea water contaminated with caesium can cause a significant accumulation of caesium in the bottom sediments of the Curronian Lagoon and result in the redistribution of ^{137}Cs activity concentration in the bottom sediments from one area to another.

ACKNOWLEDGEMENTS

This work was partly performed under the auspices of IAEA under the project LIT/7/002 and the Lithuanian State Science and Studies Foundation project No C-19/2003.

REFERENCE

[1] LUJANIENĖ, G., ŠILOBRITIENĖ, B., JOKŠAS, K., Effect of coatings on caesium sorption-desorption behaviour in bottom sediments, Environ. Chem. Phys **25** 3 (2003) 129.

Pre-concentration and determination of ^{210}Pb in water by liquid scintillation spectrometry

Merešová, J., M. Vršková, K. Sedláčková, Z. Jakubčová

Water Research Institute,
Bratislava,
Slovakia

A method for ^{210}Pb determination in water samples is described. The nuclide is pre-concentrated on ion-exchanger and then measured via liquid scintillation spectrometry. The efficiency of pre-concentration method and of measurement was assigned. The method was tested on several bottled mineral waters.

A liquid scintillation technique is rarely used for the determination of environmental ^{210}Pb because of the low environmental ^{210}Pb activities. This problem can be solved by using of the low-background liquid scintillation spectrometer and the appropriate radiochemical sample preparation (pre-concentration, suitable scintillation cocktail, etc.).

^{210}Pb is a daughter product of a gaseous ^{222}Rn, which originates from ^{238}U decay chain. It is beta emitter and beta decay is attended by emitting of gamma quantum. The half-life of ^{210}Pb is 22.2 y. ^{210}Pb enriched in the human body through the food chain remains in the skeleton long enough to produce the highest skeletal dose of any natural radionuclide under conditions of average background exposure. On the other hand, the short life of ^{210}Po relative to that of ^{210}Pb, as well as its short biological half-life of 50 days, makes ^{210}Pb in the body the most important source of high energetic (E_α = 5.3 MeV) ^{210}Po under normal conditions [1]. Significant concentrations of ^{210}Pb and its decay products ^{210}Bi and ^{210}Po can be expected in waters with higher ^{226}Ra or ^{222}Rn activities.

According to the recommendation of ICRP, the highest permissible level of annual intake of the ^{210}Pb is 2.10^4 Bq [1]. The limit concentrations of the radionuclides in water are given by regulation of Ministry of the Health of the Slovak Republic [2]. The derived intervention level for the ^{210}Pb is 0.8 Bq L^{-1}. The drinking water is divided into three types with respect to the usage of the water. Exceed of these limits demand the proper safety precaution.

In two litres of the sample are added 40 mL of buffer solution acetate into pH = 5.5 and the 0.2 mL of the carrier $Pb(NO_3)_2$, with the concentration of lead 2 mg L^{-1}, is added into. The separation of lead is carried out on ion-exchanger DOWEX® with volume 4 mL. The DOWEX® was chosen from six different types of ion-exchangers. They were compared for the ability to remove Pb^{2+} ions from the complex sample matrices. The yield of Pb^{2+} was found to be strongly dependent on the type of ion exchanger and markedly influenced by the sample's pH and exchanger volume/weight too. Subsequently, ion-exchanger with captured lead is dripped through with 3M HNO_3 to concentrate into 25 mL volumetric flask. Then 10 mL of the concentrate is taken into vial and 10 mL of liquid scintillator ULTIMAGOLD™ is added. Another two types of scintillators INSTAGEL™ and OPTIFLUOR O™ were tested. ULTIMAGOLD™ showed the best qualities for this purpose. Sample prepared with this method is measured via liquid scintillation counting (LSC). In our laboratory we are using Tri-Carb® 2900TR. For the calculation of volume activity of ^{210}Pb is used the energetic window from 0 to 30 keV and the count of background is deducted. Measured time is 30 minutes in 25 cycles.

The efficiency of pre-concentration and of the measurement was determined with four calibration points (Fig. 1.). The value of efficiency is 0.203 ± 0.003 and the limit of detection is 0.04 Bq L^{-1}.

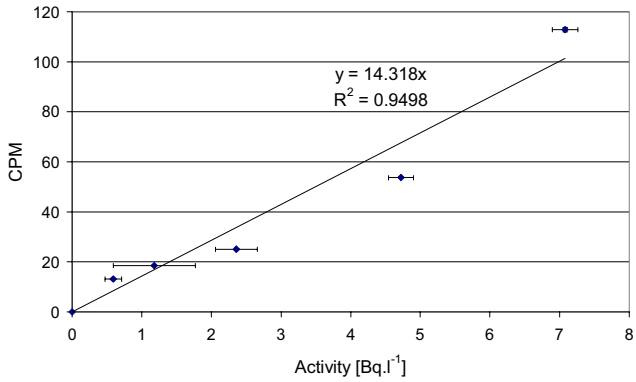

FIG. 1. Calibration curve.

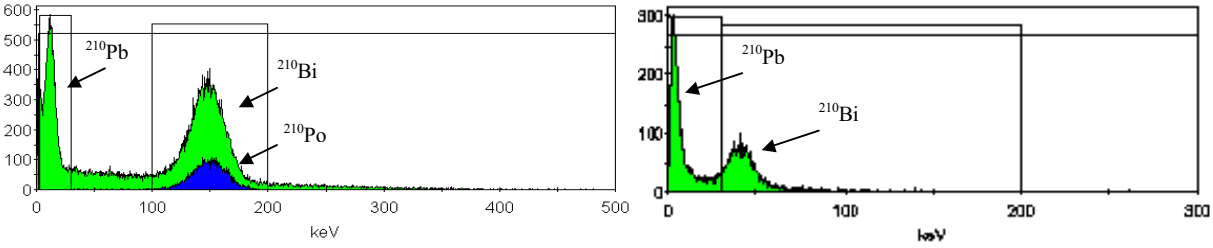

(a) *(b)*

FIG. 2. Comparison of measured spectra.

Figure 2 (a) shows a spectrum of the sample of ^{210}Pb, where the alpha peak from ^{210}Po (blue colour) and beta peak from ^{210}Bi (green colour) can be seen. This sample was not pre-concentrated. On the other hand, Fig. 2 (b) shows a spectrum of the pre-concentrated sample of ^{210}Pb. The alpha peak from ^{210}Po is not observable, because polonium was not extracted from the ion-exchanger. As a result of quenching, the spectrum is shifted to lower energies.

The technique was tested on the several bottled mineral waters distributed on Slovak market. The measured values are in Table I. Almost in all real samples the measured activities of ^{210}Pb were under the intervention level 0.8 Bq.L^{-1}, except the sample of Cígeľka. This mineral water is used for its healing powers, it is not for daily use.

Table I. Concentrations of ^{210}Pb in bottled mineral waters

Mineral water	^{210}Pb [Bq L^{-1}]
Čerínska	0.38 ± 0.02
Salvator	0.48 ± 0.02
Fatra	0.12 ± 0.01
Slatina	0.35 ± 0.02
Radenska	0.30 ± 0.01
Mítická	< 0.04
Budiš	0.31 ± 0.02
Santovka	0.38 ± 0.02
Cígeľka	1.29 ± 0.03

REFERENCES

[1] LEBECKA, J., CHALUPNIK, S., Method of determination on ^{210}Pb by liquid scintillation technique In: Rare Nuclear Processes (POVINEC, P., Ed), Sci. World, Singapore (2000) 336-342.

[2] REGULATION OF MINISTRY OF THE HEALTH OF THE SLOVAK REPUBLIC No. 12/2001 on Standards to Assign Radiation Protection.

Implications of radiochemical purity of ^{99}Mo/^{99}Tc generator eluates for the determination of low levels of ^{99}Tc in seawater

Selnæs, Ø.G.[a], M. Dowdall[b], C. Davids[b], J.P. Gwynn[b]

[a] Norwegian Radiation Protection Authority,
Svanhovd Environmental Centre,
Svanvik,
Norway

[b] Norwegian Radiation Protection Authority,
Polar Environmental Centre,
Tromsø,
Norway

The determination of sub-Becquerel levels of the long-lived fission product ^{99}Tc in environmental matrices in general and seawater in particular presents analytical challenges, not least with respect to the selection of an appropriate and practicable tracer for calculation of radiochemical yield. Although a number of isotopes (^{97}Tc, ^{95m}Tc and ^{97m}Tc) have been proposed for this purpose, ^{99m}Tc, eluted from easily available ^{99}Mo/^{99m}Tc generators, is currently a commonly used tracer due to its availability, convenient assay and practicability [1]. For the analysis of low levels (< 1Bq/m^3 or kg) of ^{99}Tc in seawater samples, attention must be focused on the radiochemical purity of the tracer solution in relation to isotopic contamination with both ^{99}Tc and other radionuclides.

Isotopic contamination of eluates from ^{99}Mo/^{99m}Tc generators can arise during manufacture and reported impurities include ^{99}Mo, ^{131}I, ^{132}I, ^{106}Ru, ^{90}Sr, ^{90}Y, ^{89}Sr and ^{103}Ru [2]. Of more consequence for the analysis considered here is the presence of ^{99}Tc in such eluates. A cursory examination of the decay scheme of ^{99}Mo indicates that there are two different routes by which ^{99}Tc can be produced within a ^{99}Mo/^{99m}Tc generator. Any ^{99}Tc within the eluate will inevitably pass through the analytical sequence and contribute to the final analytical signal. Initial consideration of the problem indicates that correction for the ^{99}Tc contribution is possible knowing the activity and history of the particular generator although the findings of [3] indicate that such procedures may be invalid.

To investigate the possible impact of ^{99}Tc contamination on the analysis of low activity seawater samples, a series of investigations were conducted. The generators used in the study were of nominal activity of 25 GBq ^{99}Mo at the time of original calibration and were 2-3 weeks old before use, at which point the ^{99}Mo activity was of the order of 10-20 MBq. Before that time, the generators had been used for their intended radio-pharmaceutical purposes. Prior to use for tracer provision the generators were eluted three times with 0.9% NaCl to purge any build-up of Tc within the generators. Generators were then left for at least 12 hours to allow ingrowth of ^{99m}Tc, before tracer production. The tracer was used in the analysis of ^{99}Tc in 50 and 100 l seawater samples from the Arctic seas by a radiochemical procedure [4]. Tracer solutions were also analysed for ^{99}Tc content using the same radiochemical technique as well as being counted for gross beta without radiochemical separation and bulked tracers were analysed by high resolution gamma ray spectrometry to detect gamma emitting impurities.

Tracer solutions that were counted without separation produced anomalous beta activity relative to purified tracer solutions due to the presence of ^{103}Ru which was confirmed by gamma spectrometry. All tracer solutions produced a positive response for ^{99}Tc with levels of the nuclide in the tracer solutions of the order 1-10 mBq/g, while no signal was detected in any of the distilled water samples. Typically, 0.3-0.8 grams of tracer solution is required to insure a detectable signal at the end of the

purification process. This implies that for samples containing activities in the order of 8-10 mBq, interference from ^{99}Tc produced by the generator is significant. The extent of this interference for a series of real samples indicates that ^{99}Tc contamination from the eluate can result in overestimation of activity in low level samples by factors of up to 30%.

REFERENCES

[1] CASTRONOVO, F.P., Technetium-99m: basic nuclear physics and chemical properties, Am. J. Hosp. Pharm. **32** 5 (1975) 480-488.

[4] CHEN, Q., AARKROG, A., NIELSEN, P., DAHLGAARD, H., LIND, B., KOLSTAD, A.K., YU, Y., Procedures for determination of ^{239,240}Pu, ^{241}Am, ^{237}Np, ^{234,238}U, ^{228,230,232}Th, ^{99}Tc, ^{210}Pb and ^{210}Po in environmental materials, Riso National Laboratory, Roskilde, Denmark, Riso-R-1263.

[3] HOLLAND, M.E., DEUTSCH, E., HEINEMAN, W.R., Studies on commercially available ^{99}Mo/^{99m}Tc radionuclide generators – II. Operating characteristics and behaviour of ^{99}Mo/^{99m}Tc generators, Appl. Radiat. Isot. **37** 2 (1986) 173–180.

[2] VESELY, P., CIFKA, J., Some chemical and technical problems connected with technetium-99m generators, Nuclear Research Institute, Pez, Czechoslovakia, UJC 2414-Ch. (1970) 21 pp.

Development of a procedure for the determination of ^{226}Ra, ^{228}Ra and ^{210}Pb in produced water

Sidhu, R., K. Ostmo, T. Bjerk, R. Nordvi, E. Stralberg

Institute for Energy Technology (IFE),
Kjeller,
Norway

Large amounts of produced water (120 Mm^3 in 2002) are discharged to the sea in connection with oil and gas production on the Norwegian Continental Shelf. This water contains elevated levels of some natural radionuclides, mainly ^{226}Ra and ^{228}Ra. Determination of natural radionuclides in produced water from the Norwegian continental shelf has so far only concentrated on ^{226}Ra using the emanation technique. However, in OSPAR the Radioactive Substance Committee (RSC) is working on a strategy to reduce discharges from all industries. Further work was therefore commissioned to more accurately establish the radionuclide composition and activity concentrations in the wastes arising from the extractive industry sector. In 2003, the Norwegian Radiation Protection Authority therefore asked the oil and gas companies to collect monthly samples of produced water from all discharge points for six months (a total of 260 samples). The samples were to be analysed for ^{228}Ra and ^{210}Pb in addition to ^{226}Ra.

To avoid the use of time-consuming radiochemical separations, it was decided to perform the determination of ^{226}Ra, ^{228}Ra and ^{210}Pb using gamma spectrometry. Since the amount of uranium in produced water is quite low, interference from ^{235}U gamma can be neglected and ^{226}Ra can be determined using its 186 keV gamma. ^{228}Ra can be determined via the gammas of its progeny ^{228}Ac, and ^{210}Pb can be determined using its 46 keV gamma. A direct determination of these radionuclides in untreated produced water is although not feasible, both due to the inhomogeneity of the sample (oil, water, particles) and due to the relatively high detection limit of germanium detectors.

A method was therefore developed based on permanganate treatment of the produced water under acidic conditions, followed by MnO_2 co-precipitation of the analytes at elevated pH. The precipitated MnO_2 together with oil and suspended particles was then collected by filtration, dried and mixed with Al_2O_3 to a fixed geometry and the gamma analysis performed using HPGe detectors. A self-absorption correction of the ^{210}Pb activity was made using the method proposed by Ref. [1] and tested in our laboratory [2]. The chemical yield was checked using ^{133}Ba as a tracer. The method was checked by analysing three produced water test samples added known amounts of ^{133}Ba, ^{226}Ra and ^{210}Pb. On average the Pb, Ra and Ba recoveries were 89 ± 17%, 91 ± 15% and 89 ± 13% (±2 σ). The results indicate that the procedure is effective, giving high chemical yield, and that ^{133}Ba can be used as tracer for both Ra and Pb.

The method was therefore adopted for the analysis of real samples. It proved to be successful for most of the samples, giving a chemical yield of above 80% for more than 50% of the samples (n=134), but in about 25% of the samples, the yield fell below 30% (Fig. 1). Those samples that showed low chemical yield (n=59) were evaporated to dryness, and the activity determined directly on the remaining salts.

Several tests were performed to elucidate the cause for this. One possible explanation could be the presence of complexing agents, for example production chemicals as scale inhibitors (e.g. phosphonates and polycarboxylates). These chemicals are effective in complexing Ra at elevated pH, and thereby preventing its precipitation. At low pH the chemicals are protonated and hence cannot complex metals or provide particle growth inhibition.

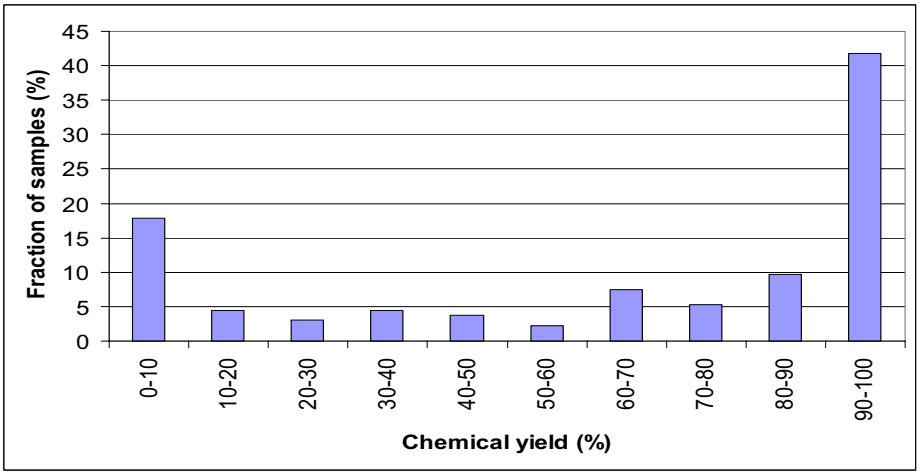

FIG. 1. Fractional yield of the tracer (^{133}Ba) when utilising MnO_2 co-precipitation for Ra and Pb preconcentration from 2 litre produced water (n=134).

A new procedure, combining Ba and Pb sulfate precipitation at low pH was therefore developed. In this procedure a 2 L sample is transferred to an appropriate jar and the sample container washed using 1 M HNO_3. The sample is then added ^{133}Ba tracer, 1 gram $KMnO_4$ and 30 grams Na_2SO_4 and stirred. The solution is then heated for an hour. Then 0.3 grams $BaCl_2 \cdot 2H_2O$ and 1.2 grams $Pb(NO_3)_2$ dissolved in water are added slowly. Solid $Na_2S_2O_5$ is then added if the sample contains MnO_4^- that has not been reduced to MnO_2. The solution is then cooled to room temperature and the precipitate collected on glass fiber filter. The precipitate is then dried and homogenised with Al_2O_3 to a fixed geometry. The sample is left for three days to achieve secular equilibrium between ^{228}Ra and ^{228}Ac, and the activities of ^{210}Pb, ^{226}Ra, ^{228}Ra and ^{133}Ba determined as mentioned earlier.

This method was tested on 6 produced water samples added known amounts of ^{226}Ra and ^{210}Pb. On average the ^{210}Pb, ^{226}Ra and ^{133}Ba recoveries were 84 ± 24%, 101 ± 20% and 109 ±1 4%, respectively. This rapid method provides a detection limit of below 1 Bq/L for all the analytes. Our test of 260 samples (both precipitated and evaporated) shows that the produced water from Norwegian Continental Shelf contains low levels of ^{210}Pb (below the detection limit), while ^{226}Ra and ^{228}Ra are detected in almost all samples.

REFERENCES

[1] CUTSHALL, et al., Direct analysis of ^{210}Pb in sediment samples: Self absorption corrections, Nucl. Instr. Meth. **206** (1983) 309-312.

[2] SIDHU, R., STRÅLBERG, E., Self-absorption correction in the gamma analysis of low energy gamma emitters in LSA scale, 3rd Dresden Symposium on Radiation Protection, Enhanced Naturally Occurring Radioactivity, ENOR III, Dresden (2003).

Design of a low background ZnS(Ag) alpha counter for water samples using a plastic veto setector

Ardid, M.[a], J.L. Ferrero[b]

[a] Departament de Física Aplicada,
E.P.S. de Gandia,
Universitat Politècnica de València,
València,
Spain

[b] Institut de Ciència dels Materials de la Universitat de València Estudi General,
València,
Spain

We have developed a high-efficient ZnS(Ag) alpha counter with large area of detection, low background, easy operation, monitoring and control, and low cost of operation. These features make this detector very suitable for the analysis of large solid residuum water samples like in the case of water from the seas or rivers. The main difficulty of this kind of detectors is to achieve a reasonable low background. It is assumed that the background comes from natural sources (mainly radon), and there is no contribution from cosmic, beta or gamma rays since the efficiency for these sources is low. However, in a recent study we have shown that the cosmic ray contribution can be very important (up to 50%). Therefore, it is worthwhile to take out this contribution. With this purpose, we have developed an alpha counter which consists basically of a 5" diameter ZnS(Ag) and opposite to it, there is a plastic veto detector of the same dimensions. Both scintillation detectors are read out by two photomultipliers. This anti-coincidence equipment reduces significantly the background, and, therefore, less time of measurement is required to achieve the same limit of detection, which is a crucial aspect in the analysis of environmental samples.

Gas detectors or scintillation discs are widely used for the measurement of alpha radioactivity in environmental samples. However, we consider that usual commercial equipment has some drawbacks like the cost of operation and the difficulty of supervision. These aspects motivated us to develop a high-efficient alpha counter with little cost of operation and easy monitoring. Our solution consists of a 5'' diameter, 0.1 mm thickness ZnS(Ag) scintillation disc glued to a light-guide and read out by a photomultiplier of 3'' diameter phototube. All the electronics required for the operation and data acquisition of the equipment are easily controlled by means of a computer, and the alpha spectra and the settings are monitored in the screen, which allows the detection of a failure immediately. Since the samples are not in direct contact with the detector, it has little cost of operation because disposable discs or gas supply are not necessary. The efficiency remains high enough (larger than 35%) and there is a reasonable background considering the large sensitive area (around 10^{-3} Bq) [1]**.** These features make possible to do alpha analysis of environmental samples in relatively short time and it is very suitable for large solid residuum water samples like in the case of water from the seas or rivers. Moreover, it is being used for fast alpha analysis of water from the pools of nuclear power plants before evacuating the water to the river [1].

In order to enhance the capabilities of this technique we have recently designed new equipment that reduces considerably the background using a plastic veto detector. It is assumed that the background in ZnS(Ag) alpha counters comes from natural sources and there is no contribution from cosmic, beta or

gamma rays since the efficiency for these sources is below 0.001%. However, Bosley and Simpson have shown that the gamma contribution could be important if the gain of the alpha counter is high enough [2]. Moreover, in a recent study we have shown that the cosmic ray contribution can be very important (up to 50%) [3]. Then, in our opinion it is worthwhile to take out this contribution. With this purpose, we have developed an alpha counter that consists basically of the detector above described and opposite to it, a plastic scintillation veto detector of the same diameter and 0.5 mm thickness. A scheme of the equipment and a picture of it are presented in Fig. 1.

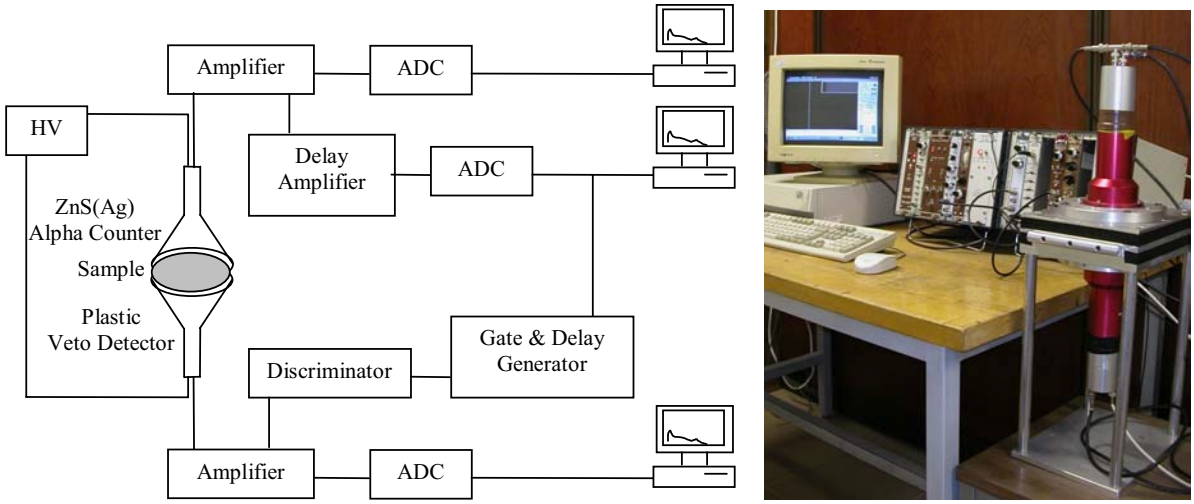

FIG. 1. Scheme and picture of the alpha counter using a plastic scintillation veto detector.

In this section we show the advantages of using the veto detector from previous equipment by comparing the time needed to measure the total alpha radiation in drinking water. In particular, we look at the time needed for the measurements in drinking water from Valencia, which has a solid residuum of approximately 1.0 g/l, to achieve a limit of detection equal to 0.025 Bq/l, which is the value required by the Spanish authority "Consejo de Seguridad Nuclear" for the laboratories of the "Red de Estaciones de Muestreo" program. Using the alpha counter alone a measurement of nine hours is needed, whereas the time is reduced to only six hours with the plastic veto detector. From our measurements and calculations we can conclude that this anti-coincidence equipment reduces significantly the background, and, therefore, less time of measurement is required to achieve the same limit of detection value, which is a crucial aspect in some cases of analysis of environmental samples.

REFERENCES

[1] SANZHEZ, J.D., ARDID, M., FERRERO, J.L., Determinación rápida de la actividad alfa total en muestras líquidas con el equipo ALF-3. Aplicación a los vertidos de C.N. Cofrentes, 30 Reunión Anual de la SNE, Alicante (2004) (in Spanish).

[2] BOSLEY, R.B., SIMPSON, J.A., Choice of alpha-probe operating voltage to suit a wide range of conditions, Journal of Radiological Protection **22** (2002) 293.

[3] ARDID, M., FERRERO, J.L., HERRERO, A., Use of the anti-coincidence technique to reduce the background on a ZnS(Ag) alpha counter, Radiation Measurements (2004) (submitted).

Determination of Ra-224, Ra-226 and Ra-228 by gamma-ray spectrometry with radon retention

Herranz, M., R. Idoeta, A. Abelairas, F. Legarda

Department of Nuclear Engineering and Fluid Mechanics,
University of the Basque Country,
Bilbao,
Spain

The purpose of this work is to improve the determination, through gamma-ray spectrometry, of radium isotopes ^{228}Ra, ^{226}Ra and ^{224}Ra in water. This improvement has been developed after the participation in the IAEA Proficiency test: "Determination of radium and Uranium radionuclides in water" in December 2002, and applied to the same samples of this proficiency test.

The aim of this new procedure is the determination of ^{228}Ra, ^{226}Ra and ^{224}Ra activities by measuring the gamma-ray emissions of their decay products ^{228}Ac, ^{214}Pb and ^{212}Pb, respectively.

In the search for these activities, radiochemical separation of radium and lead are required. A co-precipitation method with stable barium and lead was carried out to obtain two different precipitates, both of them as sulphate [1].

However emanation of unknown quantities of ^{222}Rn and ^{220}Rn is produced from the fine precipitate of the radium sulphate obtained [8] which leads to wrong determinations of ^{224}Ra and ^{226}Ra activities. To avoid this radon exhalation effect the mentioned deposit, once the chemical yield has been calculated, is dissolved with EDTA and the resulting liquid incorporated into charcoal, and then it is dried and introduced into a suitable container. Afterwards the container is sealed and stored in a freezer.

Different configurations of charcoal sizes and types as well as containers have been analysed. To perform this analysis several samples of those mentioned above containing ^{226}Ra were used in order to test its equilibrium with the progeny, ^{214}Pb and ^{214}Bi, through gamma-ray spectrometry. The following results for contaminated samples with less than 50 Bq of ^{226}Ra and using 30 ~ 50 g of charcoal have been obtained:

- There is a slight tendency to obtain better results using metallic containers rather than plastic ones
- In general, specific activated charcoals, prepared to retain radon or noble gases allow better results than unspecific charcoals, but cannot be considered as better in a clear way
- For the activities of radium used in this work no improvement in radon retention was observed when employing higher quantities of activated carbon

We have considered that the equilibrium of radium isotopes and their decay products starts growing at the moment of sealing. The daughters of the different radium isotopes present at that moment have been considered as unsupported.

In accordance with the particular radioisotopes the following considerations have to be made:

- ^{226}Ra: measurement should be made at about 21 days after sealing in order to assure its secular equilibrium with its progeny ^{214}Pb and ^{214}Bi.

- ^{228}Ra: the equilibrium with its daughter ^{228}Ac is quickly obtained (about 2 or 3 days)
- ^{224}Ra: in order to obtain transient equilibrium (with a factor of 1.14) between ^{224}Ra and its product ^{212}Pb about 3 days are needed after sample sealing. At this moment the activity of ^{224}Ra produced from the ^{228}Ra in the sample is negligible (less than 0.2%) and the unsupported ^{212}Pb that will have decayed (produced from the time of sealing) is only of 0.85%.

Therefore the following temporal scheme is proposed: after the sealing of the sample in its container, 2 measurements are carried out: the first one on the 3rd day to assess ^{228}Ra and ^{224}Ra and the second one the 21st day in order to determine ^{226}Ra. Our measurements have been made using high-purity Ge detectors with 24 hours of counting time. Counts from ^{212}Pb have to be corrected taking into account the counting time and its transient equilibrium with ^{224}Ra.

This measuring procedure has been applied firstly to standard solutions codes 023 and 097 of ^{228}Ra and ^{226}Ra, respectively, supplied by the IAEA for year 2002 proficiency test. The results are in very good agreement (accuracy and precision) with test results supplied by IAEA [2].

Secondly, the same procedure has been applied to samples IAEA-422 and 423 that are synthetic waters and to IAEA-428, natural water, which have very different activities of ^{228}Ra and ^{226}Ra. Comparative analysis of the measured activities and the IAEA values show very close agreement (accuracy and precision) between them.

After these essays, we can conclude that the proposed method for the retention of the radon that comes from the precipitate containing radium works correctly and leads to results that agree very well with the reference values of radium.

ACKNOWLEDGEMENTS

The authors are grateful to NORIT, NUCON International and CHEMVIRON companies for providing their activated charcoals for this work.

REFERENCES

[1] SUAREZ, G., DEL REY, J.A. et al., Determinación radioquímica conjunta de Radio-224, Radio-226, Ra-228 y Plomo-210, Ministerio de Industria y Energía ITN/TR-14/R-88, Madrid 1988.

[2] JURADO VARGAS, M., A model to explain simultaneously the ^{222}Rn and ^{220}Rn emanation from thin electrodeposited sources, Nucl. Instr. Meth. A **447** (2000) 608-613.

[3] RADECKI, Z., Preliminary evaluation of the exercise AQCS PT "Determination of Ra and U Isotopes in Water", IAEA, Vienna (2003).

Application of analytical methods for evaluation of natural radionuclides in the vicinity of water discharges into the sea

Jerez Veguería, S.F.[a], J.M. Godoy[a,b]

[a] Depto. de Química,
Pontifícia Universidade Católica,
Rio de Janeiro,
Brazil

[b] Instituto de Radioproteção e Dosimetria,
Comissão Nacional de Energia Nuclear,
Rio de Janeiro,
Brazil

Abstract. In the present paper the application of analytical methods for environmental evaluation of natural U, ^{226}Ra, ^{228}Ra and ^{210}Pb in produced water, sea water and sediment around the effluent discharges offshore oil industry were studied. The sedimentation rate in the studied sites was determined by dating with ^{210}Pb. The obtained results showed that the concentrations of this radionuclides are at normal background levels.

1. Introduction

Elevated activities of naturally occurring radioactive materials (NORM), such as ^{226}Ra and ^{228}Ra, are often found in the produced waters of oil and gas industry. In this work the analytical methods for the determination of natural U, ^{226}Ra, ^{228}Ra and ^{210}Pb in produced water, seawater and sediment around the effluent discharges of offshore oil industry were studied.

2. Materials and methods

2.1. Environmental region of study

The offshore oil industry in the Bacia de Campos is located 60 km from the coast of the State of Rio de Janeiro. For this study, two fixed production platforms and a Station of Treatment of Effluent in Macaé were selected. In order to evaluate the environmental impact from discharges of produced water into the sea, the seawater and sediment samples were collected at distances from 250 m to 1000 m around the platforms.

2.2. Uranium determination

Uranium determinations in produced water and seawater were performed by Inductively Coupled Plasma Mass Spectrometry (ICP-MS) with ultrasonic nebulizer in quantitative mode (external calibration) using ^{205}Tl as internal standard. The samples (salinity ≥ 3.5% p/v) were diluted 1:100 with Milli-Q water and acidified with HNO_3 sub-distilled [1].

2.3. Determination of ^{226}Ra, ^{228}Ra and ^{210}Pb

Using one liter of produced water and twenty liter of seawater, after radiochemical separation, ^{210}Pb was determined by beta counting of ^{210}Bi, and ^{226}Ra and ^{228}Ra were determined by gross alpha and beta counting using a proportional 10-channel low-level proportional counter. Another method to determine radium concentration in seawater was implemented: a 400 L seawater sample was percolated through cellulose cartridges and then ^{226}Ra and ^{228}Ra activities were determined by γ-ray

spectrometry with a high-purity Ge detector of ^{214}Bi and ^{228}Ac, respectively [2]. ^{226}Ra and ^{228}Ra were determined in surface sediments sampled around the effluent discharges, either their total content by γ-ray spectrometry of ^{214}Bi and ^{228}Ac respectively, either by gross alpha and beta counting after leaching with EDTA [2]. The total ^{210}Pb activities in sediment samples were determined by γ-ray spectrometry with auto-absorption correction. The sedimentation rate in the studied sites was determined by dating with ^{210}Pb using the the Constant I.

3. Results and discussion

A total of 21 samples of produced water, 42 of sea water, 22 of marine sediment and 3 of sediment samples with ten layers of 1 cm each for the dating with ^{210}Pb, were analyzed. The results of ^{226}Ra, ^{228}Ra and ^{210}Pb concentrations in the produced waters are shown in Table I.

The implemented method for the determination of uranium in sea water showed a good performance with a detection limit of 0.06 μg L^{-1}. The average uranium concentration in sea water was 3.07 ± 0.27 μg L^{-1}, compatible with the value reported for oceanic waters. The method was validated with the certificated sea water CASS-3 (2.8 μg L^{-1}) and was observed a good agreement with the reference value: 2.7 μg L^{-1} (± 20%). Using 20-l seawater samples, the data obtained for ^{226}Ra, ^{228}Ra and ^{210}Pb were below the detection limit of the method used (5 mBq L^{-1}). The method of preconcentration of radium isotopes from 400-l samples in the cellulose cartridges coated with MnO_2 showed better sensibility and the concentrations were 0.95 - 1.73 mBq L^{-1} for ^{226}Ra and 0.75 - 3.00 mBq L^{-1} for ^{228}Ra. This results are in agreement with literature values reported for unpolluted seawater. Radium, in the form of co-precipitated barium sulfate, could not be detected in the suspended particle fraction.

The results of ^{226}Ra, ^{228}Ra and ^{210}Pb concentrations in the surface sediments are shown in the Table II.

The results of leached ^{226}Ra and ^{228}Ra were < 0.09 Bq kg^{-1} and < 0.20 Bq kg^{-1}, respectively. The content of radium isotopes in sediment samples didn't show any evidences of contamination in the areas studied. The sedimentation rates in the site of the two studied platforms were of 0.08 cm/yr and 0.28 cm/yr. In the first case this value is coherent for an area of low deposition of sediments as the area of the continental platform. In the second case the increment of the sedimentation rate can be attributed to the contribution of particulate material of fluvial origin (Rio Paraíba River) in this region.

4. Conclusions

The analytic techniques used in this work showed a good performance for the environmental evaluation of natural radionuclides in the vicinity of the produced water discharges into the sea. The results showed that, in spite of elevated concentration of radium in produced water, the obtained concentrations in the sea water and sediment samples are at normal background levels.

Table I. Dissolved and particulate ^{226}Ra and ^{228}Ra in the liquid effluent of oil offshore platforms

Produced water	^{226}Ra (Bq L^{-1})	^{228}Ra (Bq L^{-1})	^{210}Pb (Bq L^{-1})
Dissolved	0.01 - 6.00	0.05 - 12.00	0.04 - 1.94
Particulate	0.02 - 6.24	0.04 - 9.65	0.03 - 0.57

Table II. Concentration of ^{226}Ra, ^{228}Ra and ^{210}Pb in total sediment in the studied sites

	^{226}Ra (Bq kg^{-1})	^{228}Ra (Bq kg^{-1})	^{210}Pb (Bq kg^{-1})
Surface sediments	< 8 - 345	16 - 955	< 23 - 638

REFERENCES

[1] JEREZ VEGUERIA, S.F., Estudo da Emissão de Metais Traço e Radionuclídeos Relacionados à Produção de Petróleo na Bacia de Campos, Doctorate thesis, PUC-Rio, Rio de Janeiro (2002).

[2] JEREZ VEGUERIA, S.F., GODOY, J.M., Environmental Impact studies of Barium and Radium discharges by Produced Water from the "Bacia de Campos" Oil-Field Offshore Platform, Brazil, J. Environ. Radioact. **62** (2002) 29-38.

Evaluation of the infinite radius of a radioactive water environment

Kedhi, M.

Institute of Nuclear Physics,
Tirana,
Albania

The value of the infinite radius of gamma rays in a uniform radioactive aquatic environment is calculated by two ways. By the first method, for Am-241, I-131, Au-198, Cs-137 and Co-60 the infinite radius was calculated using the number of the counts that a detector gives in air and in water for different source detector distances. The detector used was SGSR 54-IO with NaI(Tl) crystal (38 mm x 25 mm) and threshold 50 keV. The build up factor as a function of the source detector distance was fitted with a parabola. The number R of the counts given by the detector, settled in the center of a spherical uniform radioactive aquatic environment, was calculated by integrating the counts given by an aquatic volume dv over the whole volume of the sphere. This calculation was done also for a sphere considered as a real infinite, too. The values of the infinite radius for different gamma ray energies are fitted with a power function. The infinite radius for Am-241, Cs-137, K-40, Bi-214 and Tl-208 nuclides was calculated also by Monte Carlo simulation.

The uniform radioactive water environment is considered as infinite when the response of a detector inside it gives at least 99 percent of the value of such geometrical infinite environment [1]. In a lot of radioactive methods applications in hydrology [2] and industry and, also, in the study of marine radioactive contamination by underwater gamma spectrometry using Monte-Carlo simulation [3], the value of the infinite radius is required. The measurements of build up factor for five radioactive nuclides and the Monte-Carlo simulation for five nuclides were used for this evaluation. The measurements of the build up factor were carried out in a big tank filled with water. The SGSR 54_IO NaI(Tl) (38 mm * 25 mm) detector was used.

The detector response dR for *n* quanta emitted within the unit time by environmental volume dv that strike the detector case area *dS* under the angle θ with the surface normal (Fig. 1), is:

$$\mathrm{dR} = \frac{n\,dS\cos\theta}{4\pi r^2}\,\varepsilon B'(r)\exp\left(-\mu r - \frac{\mu' d}{\cos\theta}\right)\mathrm{dv}, \qquad (1)$$

where: ε, the detector efficiency, μ and μ', linear attenuation coefficients of water and of the detector case that has the thickness d, r is the distance of dv from the detector centre and B'(r) is the build up factor of these quanta in water. The total detector response is given by:

$$\mathrm{R} = \frac{n}{4\pi}\int_S dS \int_\varphi d\varphi \int_\theta \cos\theta\sin\theta\exp\left(-\frac{\mu' d}{\cos\theta}\right)d\theta \int_r \varepsilon B'(r)\exp(-\mu r)\,dr \qquad (2)$$

The counts build up factor B(r) we calculated by the equation $N_w = N_a B(r)\exp[-\mu(r)r]$, where Nw and Na are the number of counts in water and air, respectively, corrected for their backgrounds. For monoenergetic radiations we have μ (r) = const. Co-60 was considered as a monoenergetic source with E = 1250 keV. For the other nuclides we calculate:

$$\mu(r) = \frac{1}{r}\ln\frac{\sum_i I_i}{\sum_i I_i \exp(-\mu_i r)}, \qquad (3)$$

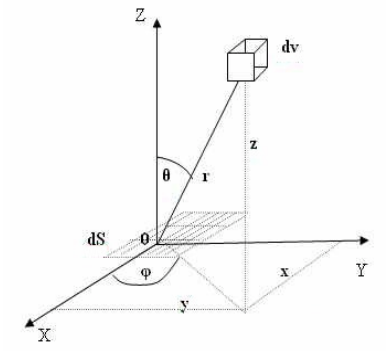

FIG. 1. Position of an aquatic volume dv and detector area ds.

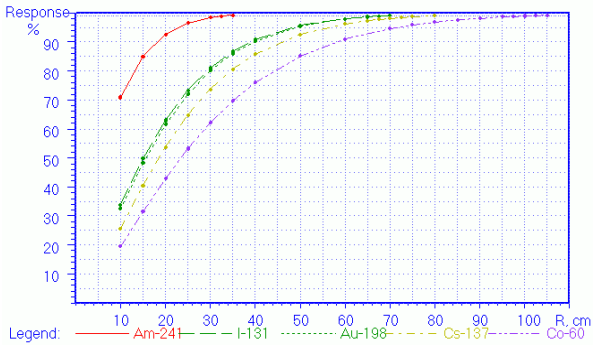

FIG. 2. The detector response for some nuclides as a function of the source detector distance.

where μ_i is the linear attenuation coefficient for the energy with the yield I_i%. The found values of $\mu(r)$ were fitted with the function $\mu(r) = a * r^b$. We found B(r) by fitting the measured values with the function $B(r) = 1 + \alpha[\mu(r)r] + \beta[\mu(r)r]^2$. This function, found experimentally, includes the efficiency $\varepsilon = \varepsilon(E)$, so B(r) represents, with a constant proximity, the product $\varepsilon B'(r)$ in equations (1) and (2). By equation (2) we calculated the detector response R_∞ for a real infinite radius (such was considered the distance 3 m for Co-60 and 2 m for others, in these ranges the γ-quanta narrow beam is attenuated 10^8 times) and R_r for spheres of different radiuses. The value r for which the ratio R_∞/R is 0.99 was taken as the infinite radius of the nuclide in the aquatic environment. The calculation of the infinite radius by Monte Carlo simulation was done according this schema: we calculated the flux intensity, that means the number of gamma quanta emitted in the spherical aquatic environment of radius R, for different values of R, that strike within the unit time, the unit area of the detector, which was considered as a sphere of radius r settled in the centre.

The found values of R_∞ for Am-241, I-131, Au-198, Cs-137 and Co-60 are 35 cm, 70 cm, 72 cm, 80 cm, and 100 cm, respectively. The values of R_∞ for different γ - ray energies are fitted with the function $R_\infty = a * E^b$. The values of the coefficients are a = 9.9557 and b = 0.3222. The fitting results are very good. The values of R_∞, calculated by Monte Carlo simulation for the nuclides Am-241, Cs-137, K-40, Bi-214 and Tl-208, are 35 cm, 85 cm, 105 cm, 115 cm and 120 cm, respectively. All these data are presented in Figs 2 and 3.

The evaluation of infinite radius of gamma radiation in an uniform radioactive environment is given by two methods: by measuring in a big tank of build up factor (for Am-241, I-131, Au-198, Cs-137 and C0-60 nuclides) and by Monte Carlo simulation (for Am-241, Cs-137, K-40, Bi-214 and Tl-208). For common nuclides the found values are the same. The dependence of this radius from the energy of gamma nuclides is given, too. From this can be found the infinite radius of other energies.

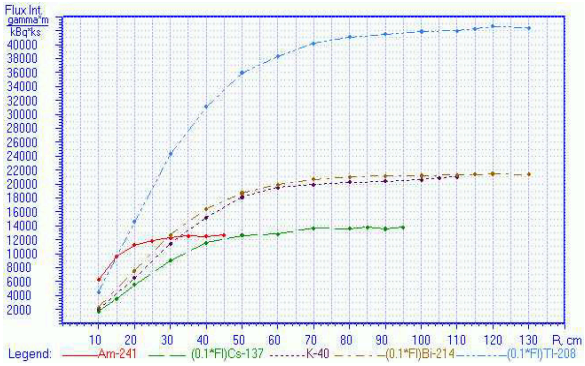

FIG. 3. Flux intensity in the centre of a seawater spherical environment for some values of R.

REFERENCES

[1] GASPAR, E., ONCESCU, M., Radioactive Tracers in Hydrology (1972) 299-304.
[2] GUIZERIX, J., et al., "Les mesures de debit effectuées en France à l'aide de traceurs radioactifs par la méthode d'integration", Radioisotopes in Hydrology, IAEA, Vienna, (1963) 255.
[3] ARCIBASHEV, B.A., Jaderno-geologiceskaja razvedka, Moskva, Atomizdat (1972).

Development of monitor for multiple beta-ray nuclides in liquid radioactive wastes

Kim, C.S.[a], B.H. Rho[a], U.W. Nam[b], K.I. Seon[b], C.K. Kim[c]

[a] Korea Institute of Nuclear Safety(KINS),
Daejon,
Korea, Republic of

[b] Korea Astronomy Observatory (KAO),
Daejon,
Korea, Republic of

[c] Seibersdorf Laboratories,
International Atomic Energy Agency,
Seibersdorf,
Austria

A new liquid scintillator system was developed to measure the multiple beta-labeled mixture. The signal processing system consisted of two photomultiplier tubes and coincidence count circuit which had 50% background rejection rate. An algorithm using least square method was developed for simultaneous radioassay of multiple beta-emitters. The characteristics of the system were analyzed using 4 beta-labeled samples(^{3}H, ^{14}C, ^{36}Cl and ^{90}Sr).

Recently, the safety management of radioactive isotopes has been emphasized by the increase of radioactive isotope application in areas of medical, industrial and scientific research along with industrialization. Most radionuclides used in the medical diagnosis and scientific research are beta-emitters. Not only careful handing of radionuclides in the nuclear facilities but also the management of radioactive liquid waste from medical utility is very importance with a view to protecting the environment. The current method being used in monitoring the radioactive waste, however, is difficult for continuing operation and further the sample preparation is very cumbersome. In addition, when the sample is mixed with several beta-emitters, each nuclide should be separated chemically and then analyzed using different analysis procedure. Therefore, a new monitoring system to solve these problems was developed.

An automatic sample mixer system was designed for continuous monitoring, which consisted of the following 4 stages: 1) automatic sample transfer, 2) capping and uncapping the sample bottle, 3) sample preparation system and 4) its attachment to the detector. This monitoring system can be operated on-line, as an option, through RS-232 communication protocol with the integrated operating software installed in main control computer.

A new liquid scintillator system for the measurement of multiple beta-emitters was developed and its characteristics were investigated. The signal processing system consisted of two photomultiplier tubes and a coincidence count circuit which had 50% background rejection and pulse amplitude comparison (PAC) reduce about 12% in background count rate [1]. An algorithm using least square method used by was developed for simultaneous radioassay of multiple beta-emitters [2, 3].

The reliability was examined by 4 beta-ray standard mixture (^{3}H, ^{14}C, ^{36}Cl and ^{90}Sr) and the analytical results were in good agreement with the reference values within 7% relative error. A few minutes measurement demonstrated that the detection limits achieved for all those nuclide except ^{90}Sr satisfied

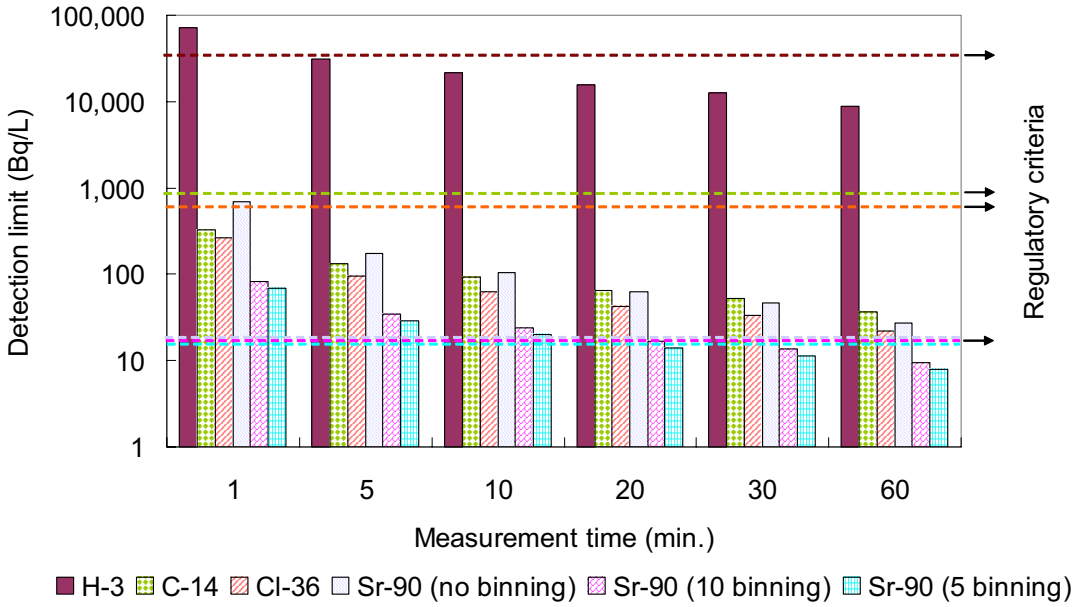

FIG. 1. Detection limit and regulation criteria for liquid radiowaste.

the regulatory criteria for effluent discharge. For ^{90}Sr, the detection limits was satisfied increasing the detection time to around 20 minutes together with the application of binning method (Fig. 1).

REFERENCES

[1] NAM, W.U., et al., Development of prototype liquid scintillator system for monitoring liquid radioactive waste, Korean Asso. for Rad. Protec. **28** 3 (2003) 173.

[2] TAKIUE, M., et al., A new approach to analytical radioassay of multiple beta-labeled samples using a liquid scintillation spectrometer, Nucl. Instr. Meth. A**293** (1990) 596.

[3] SEON, K.I., et al., Radioassay of multiple beta-labeled mixtures using least-square method, Korean Asso. for Rad. Protec. **26** 4 (2001) 375.

Development of an in-situ fission track analysis for detecting fissile actinides in soils and sediments contaminated with actinides

Lee, M.H.[a], H.Y. Pyo[a], Y.J. Park[a], K.Y. Jee[a], S.B. Clark[b]

[a] Nuclear Chemistry Research Division,
Korea Atomic Energy Research Institute,
Daejon,
Korea, Republic of

[b] Washington State University,
Department of Chemistry and Nuclear Radiation Center,
Pullman,
United States of America

A fission track analysis (FTA) and an alpha track analysis (ATA) were developed to identify hot particles in contaminated soil or sediment. With the FTA techniques, the track image of the grid coated with Th and fissile nuclides on the Lexan detector was so clearly recorded that the location of the fissile particles was easily identified in the soil or sediment contaminated with the actinides. With the ATA techniques, many of the hot particles contaminated with Pu were discriminated from the U on the track detector due to the different sensitivity of the ^{239}Pu and ^{235}U on the CR-39 detector.

Conventional analytical methods used for determining concentrations and distributions of hot particles emitting alpha radiation involve a complex chemical processing and need intensive manpower. In recent years various FTA and ATA techniques with nuclear track detectors have been applied directly to highly contaminated soil without a radiochemical analysis. FTA and ATA techniques provide direct information for detecting nuclides with high fission cross sections such as ^{235}U and ^{239}Pu in contaminated environmental samples.

For the FTA, thorium was electroplated onto the SEM grid with electrodeposition solution. The current was adjusted to 0.85 A and held for 1 hour. After the SEM grid electroplated with Th was put on the track detector, contaminated soil particles collected from BOMARC missile facilities (McGuire Air Force Base, New Jersey) were sprinkled on the Lexan detector and then taped together to immobilized the soil particles. The samples were irradiated with a thermal neutron flux of 2.92 x 10^{12} $cm^{-2} \cdot s^{-1}$. After the samples were unpacked, the detectors were etched in a solution of 6 M NaOH at 70 ± 1°C for 10 minutes. For the ATA, soil particles were sprinkled on the CR-39 detector and then taped for immobilizing the soil particles. The samples were exposed for a minimum of two weeks to create detectable alpha tracks. After the samples were unpackaged, the detectors were etched in a solution of 6.25 M NaOH at 75 ± 1°C for 5 hours. Fission and alpha tracks were observed using an optical microscope.

An image of the fission tracks by the grid electrodeposited with thorium was clearly recorded on the track detector. The image generated by the fissile nuclides can be distinguished from the image of the outline of the SEM grid. The fission tracks were not distributed randomly within the detector, but rather were arranged in a distinct “star-burst” shape. The fission tracks from the highly fissile nuclides were correlated with the fission tracks from the grid coated with thorium. By using the fission track image, the fissile particles within the grid electroplated with thorium were easily identified and could be separated from the sample matrix for the analysis of speciation of the single particles.

Alpha tracks of the contaminated BOMARC soil particles were recorded randomly on the CR-39 track detector. Various bundles of alpha tracks were recorded on the CR-39 detector, depending on the activity concentration of the fissile nuclides. The "agglomerated drops" shape of the alpha tracks on the CR-39 is a little different from the "star-burst" shape of the fission tracks on the Lexan. Most of the alpha tracks recorded on the CR-39 detector were likely generated from ^{239}Pu not ^{235}U, because the alpha tracks generated by ^{239}Pu are more active on the CR-39 detector than those by ^{235}U due to the different half-lives. This infers that many of the hot particles in the BOMARC soil may be contaminated with plutonium isotopes. This verification was supported from the results of the radiochemical analysis that the activity concentration of ^{239,240}Pu in the BOMARC soil, approximately 4.56 Bq/g, was determined to be about two orders of a magnitude higher than the natural level of the ^{235}U concentration. Also, for obtaining information of the speciation of the hot particles, the fissile particles can be further studied by microscale techniques such as SIMS (secondary ion mass spectrometry) and SXMA (synchrotron x-ray microprobe analysis), after separating the hot particles from the contaminated soil with the FTA techniques.

Radon alpha and gamma-ray spectrometry with YAP:Ce scintillator

Plastino, W.[a,b], P. De Felice[c]

[a] Department of Physics,
University of Roma Tre,
Rome,
Italy

[b] National Institute for Nuclear Physics,
Section of Roma Tre,
Rome,
Italy

[c] ENEA,
National Institute for Metrology of Ionizing Radiations,
Rome,
Italy

The detection properties of a YAP:Ce scintillator ($YAlO_3$:Ce crystal) for radon and radon daughters alpha and gamma-ray spectrometry were investigated.

The crystal response has been studied under severe extreme conditions to simulate environments of geophysical interest, particularly those found in geothermal and volcanic areas. Tests in water up to a temperature of 100°C and in acids solutions such as HCl (37%), H_2SO_4 (48%) and HNO_3 (65%) have been performed.

The experimental array consisted of a bare cylindrical crystal of YAP:Ce optically coupled to a Hamamatsu H5784 photomultiplier with standard bialkali photocatode. The crystal size was 8 mm diameter and 30 mm height. The crystal was positioned at the geometrical center of a 6 l stainless steel light- and gas-tight vessel equipped with gas input/output and a pass-through electrical connectors.

Output signals were integrated with a charge preamplifier, shaped with a spectroscopy amplifier (ORTEC-450) and processed by a multichannel analyzer card (ORTEC-Trump). The collected pulse-height spectrum was managed by a suitable MCA emulation software (ORTEC-Maestro32).

The device was serially connected to the radon Reference Measurement System (RMS) developed at the National Institute for Metrology of Ionizing Radiations (INMRI-ENEA) [2]. The RMS is routinely used for calibration and testing of radon measuring instruments and it provided the reference radon-in-air activity concentration needed for efficiency calibration of the YAP:Ce radon spectrometer. The RMS is based on a cylindrical electrostatic cell with a Si detector. It is used for the alpha spectrometry of the electrostatically collected polonium ions produced in the decay of radon. The radioactive source section consisted in a 35 cm^3 glass bulb filled with about 15 kBq radon in air. The internal volume of the whole circuit was about 10 L.

The energy calibration curves of the device were obtained irradiating the crystal by means of a set of radioactive point sources of different radionuclides (^{133}Ba, ^{241}Am, ^{57}Co, ^{22}Na, ^{137}Cs) positioned at 5 cm source-detector distance. These provided a number of photons with well spaced gamma-ray energies up to about 700 keV.

The measurements with standard radon sources provided by the INMRI-ENEA have emphasized the non-hygroscopic properties of the scintillator and a small dependence of the light yield on temperature and HNO_3.

The data collected have pointed out that the YAP:Ce scintillator can allow high response stability for radon alpha and gamma-ray spectrometry in environments with large temperature gradients and high acid concentrations.

REFERENCES

[1] PLASTINO, W., DE FELICE, P., DE NOTARISTEFANI, F., Radon gamma-ray spectrometry with YAP:Ce scintillator, Nucl. Instr. Meth. A **486** 1-2 (2002) 146-149.

[2] DE FELICE, P., MYTEBERI, XH., The ^{222}Rn Reference Measurement System developed at ENEA, Nucl. Instr. Meth. A **369** 2-3 (1996) 445-451.

Nuclear and physical methods of monitoring the content of technogeneous (Pu, Am) and natural (Rn) radionuclides in the environment, used in Belarus

Zhuk, I.V., O.I. Yaroshevich, V.A. Bryileva, M.K. Kievets, E.M. Lomonosova

Joint Institute of Power and Nuclear Research (JIPNR),
National Academy of Sciences of Belarus,
Minsk,
Belarus

The paper presents a description of some techniques developed or modified in JIPNR to measure transuranium elements and radon content.

For express determination of Pu and ^{241}Am content in the territories contaminated as a result of heavy accident on NPP'S the technique was developed that allowed determining content of all Pu-isotopes (^{238}Pu, ^{239}Pu, ^{241}Pu, ^{241}Pu) in the samples by means of measuring of ^{241}Am activity with x-γ- modified spectrometry method and calculating of composition of fuel in the reactor by the time of the accident. The necessary algorithms and software for the calculation of Pu content are described. Here, it is supposed, that the radionuclides released from different parts of the reactor's core mixed in the air well [1] and fell down on the surface of the ground with the average composition formed in the reactor by the moment of the accident. It is also accepted that the relative content of Pu isotopes is preserved (with the account of the radioactive decay) in the migration process in the environment after release from the reactor. The approach specified gives the possibility to exclude practically labour-consuming radiochemical analyses of soil samples on Pu content. The comparison of the results of this express calculation-experimental method with the results of traditional radiochemical analyses for territories at the distance of 8 to ~ 50 km from the Chernobyl NPP is presented in Table I.

For the measurements of Pu and ^{241}Am in soils and sediments a modified x-γ- spectrometry technique was used, based on measurement of γ-radiation of ^{241}Am with E_γ=59,6 keV using planar HPGe-detectors with large surface (1000-2000 cm^2) and standard sources made of sand, impregnated with standard ^{241}Am solution. Two variants of this technique were used: (i) direct measurement of x- γ-radiation from the investigated samples and (ii) the measurement after simple chemical procedures

Table I. Comparison of the results of specific activity determination (Bq/kg) of ^{241}Am and Pu isotopes in soil samples

Isotope	**^{241}Am**	**$^{239+240}$Pu**	
Point of Resettlement, Distance from ChNPP/ Soil Type	Experiment (γ-χ-spectrometry technique)	Experiment (radiochemistry analysis, α-spectrometry)*	Calculation by the measured activity of ^{241}Am
Masany, 8 km/turf-podzol	230 ± 40	240 ± 40	245
v. Kryuki, 20 km/sandy	110 ± 35	105 ± 30	117
Dernovichi, 33 km/peat-bogged	21 ± 7	18 ± 6	22
Lomatchy, 48 km/turf-podzol	22 ± 8	20 ± 6	23

*Radiochemical analyses as to $^{239+240}$Pu content in soil samples have been carried out by V.P. Kudrjashov and V.P. Mironov (Institute of Radiobiology NASB).

(i.e. co-precipitation Pu and Am with oxalic salts for purification of investigated samples from the interfering radionuclides Cs and Sb first of all). The minimum detectable activity A_{min} is 1,0 Bk/kg for ^{241}Am and 80 Bk/kg for ^{238,239,240}Pu. The cost and time of such analysis is less in several times than for radiochemical analysis with the following alpha-spectrometry. Technique is described in detail [2].

To carry out large-scale radon measurements in air of building the method was applied, based on using passive integral radonometers with solid state nuclear track detectors (SSNTDs) and allowed to obtaining results averaged vs. long time interval (up to 3 months) and thus taking into account temporal variation of radon exhalation from soil and real regime of ventilation of building. The nitrocellulose KODAK film LR-115 was used as the SSNTD. The equipment used allowed performing subsequent chemical treatment of large amount of SSNTDs (up to 100) after its exposition and automatic electrospark accounting of tracks.

In this paper we describe equipment and some results of indoor radon measurements carried out using this technique. The radon chamber, used as a standard radon source, is also described.

The reliability of the results obtained is verified by interlaboratory comparisons. The results of measurements of radon volumetric activity are presented, obtained in the framework of the program of interlaboratory comparisons in Belarus.

REFERENCES

[1] ORLOV, M.YU., SNYKOV, V.P., KHVALENSKYJ, YU.A., et al., Radioactive contamination of the territory of Belarus and Russia after the Chernobyl NPP accident, Atomic Energy, **72** 4 (1992) 371-376.

[2] BUSHUEV, A.V., ZUBAREV, V.N., PETROVA, E.V., et al., Development of gamma ray/x-ray spectrometric methods for monitoring the contamination of soil with ^{241}Am and Pu, Atomic Energy **82** 2 (1997) 116-123.

In-situ gamma ray spectrometry with the K-A-TE-RINA submersible detector

Tsabaris, C.[a,b], Th. Dakladas[c]

[a] Hellenic Centre for Marine Research,
Anavyssos,
Greece

[b] Hellenic Army Academy,
Vari,
Greece

[c] Ministry of National Defense,
Mesogion 151,
Greece

A new detection system, named K-A-TE-RINA (Innovative Sensor for Artificial Radioactivity), has been developed for radioactivity measurements in the marine environment. The system is based on a NaI scintillator housed by special plastic material capable for operation in open sea. The efficiency of the detection system is measured in the laboratory using two reference gamma ray sources: ^{40}K and ^{137}Cs. The developed electronics offer proper adjustment of the maximum detection energy in order to apply the system in different key-environments, focusing to a special requested radionuclide. The low power consumption and the gain stabilization of the output voltage make the developed system reliable for long-term measurements. Many tests were also made in order to check the linearity of electronics in case of long-term measurements. In future, the system will be installed on a specific application buoy together with other detectors (like salinity, rain-gauge, temperature and wind direction), for the correlation of radioactivity variation with those magnitudes.

In situ gamma ray spectrometry is widely used for monitoring natural as well as anthropogenic radioactivity in the marine environment. The sensitivity of such detection system has to be very high due to the dilution factor of the sea. Although various spectrometric methods based on scintillation spectrometry [1] and spectrum deconvolution [2] have been used for monitoring of the marine environment, the NaI-detection systems are not capable of measuring low -level volumetric activity (a few Bq/m^3). In addition the poor energy resolution makes the deconvolution procedure not applicable when the energy difference of the involved gamma rays is less than 50 keV at 662keV gamma ray energy. In the present work a newly developed system is presented, named KA-TE-RINA [3]. The system was calibrated in a tank for the energy, energy resolution and efficiency. The specifications of the system as well as the improvements for optimal operation are described below.

The new system monitors gamma rays in the energy range from a threshold to 5000 keV. The radioactivity sensor of the system consists of a 3”x3” NaI detection crystal, with built-in photomultiplier tube and a preamplifier (developed by Canberra). A watertight enclosure, which resides the sensor and the electronics, is also developed [3]. The sensor has been energy calibrated and tested for its stability to temperature variations for continuous monitoring. Particularly, the energy and energy resolution calibration has been performed in the lab by using reference γ-ray sources. The underwater measurements of the detector efficiency and absolute calibration have also been made. For this purpose a calibration tank of 5.5m^3 volume, filled with water has been used. The sensor was mounted in the middle of the tank. An electric pump was placed for circulating the water assuring

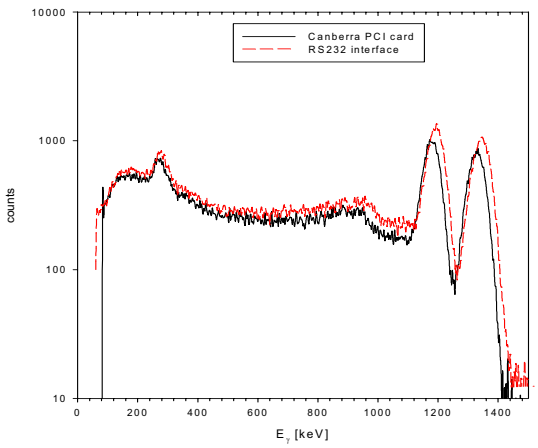

FIG. 1. The acquired spectra with the PCI card and with the developed electronics (RS232 interface).

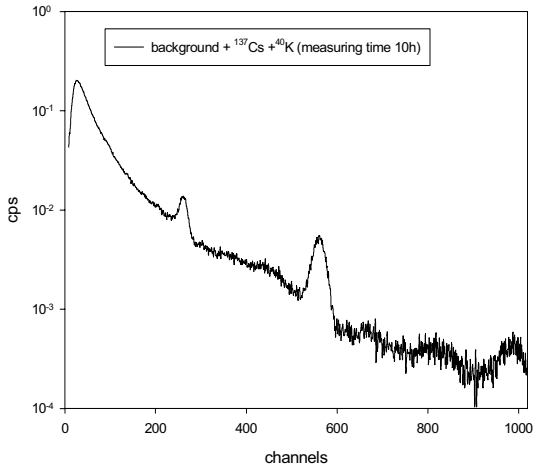

FIG. 2. The acquired spectrum with the calibration reference sources ^{40}K and ^{137}Cs.

sedimentation avoidance, good water mixing with the appropriate reference sources and homogenous conditions.

First, the NaI sensor was set up using the PCI-slot card (ASA 100) developed from Canberra Company. The optimum operating voltage was 1000 V and the amplification gain was adjusted for detecting gamma rays until 2800 keV. A typical spectrum is shown in Fig. 1, measured in the laboratory using a ^{60}Co reference source. Measurement with the same geometry and the same source (^{60}Co) is also performed for validating the developed electronic devices. The acquired spectrum is shown in Fig. 1. The comparison of the two spectra is very satisfactory, in the entire energy range. Both spectra have been energy calibrated, using two photopeak energies of ^{60}Co reference source and presuming the linearity of electronics. In addition the FWHM was measured for ten energies in the energy interval between threshold and 1500 keV. An improvement of the system was that, the FWHM was reduced by a factor of 1.5 compared to other systems. More specifically at 662 keV the FWHM is 35 keV instead of 60 keV which is the energy resolution of the RADAM system [4]

The efficiency calibration of the detector in the tank was calculated by integrating the net 661 and 1461 keV photopeaks, using two reference sources: ^{40}K and ^{137}Cs [5]. The acquired spectrum is shown in Fig. 2. The analysis of the spectra has been performed with the "SPECTRG" software package [6]. The efficiency of the new system is about 30% higher compared with a similar underwater system [4]. The gain stabilisation of the system (voltage drift elimination) was performed using the 1461 keV of ^{40}K, the 2615 keV of ^{208}Tl and the 50 keV of the seawater threshold. The linearity of the system was checked measuring the emission of other nuclides, like ^{214}Bi and ^{214}Pb. The non-linearity of electronics is very low, i.e. the non-linear amplification coefficient is of the order of 10^{-9}.

The derived efficiency and the decrement of the FWHM will improve the detection limit in comparison with similar system (RADAM) used in the POSEIDON network [2, 4]. In future, the integration of the developed system on a real-time data-forwarding sea surface buoy will complete the aim of this work. This is consistent to the further idea of building an operational and low cost buoy network, for monitoring radioactivity levels at the open sea. Additionally a similar system could be applied in rivers and lakes as an early alarm system for possible water pollution.

REFERENCES

[1] OSVATH, I., POVINEC, P.P., Seabed γ-ray spectrometry: application at IAEA-MEL, J. Environ. Radioact. **53** (2001) 335.
[2] TSABARIS, C., BALLAS, D., On line gamma ray spectrometry at open sea, Appl. Radiat. Isot. (2004) (accepted (ARI 3094)).
[3] TSABARIS, C., THANOS, I., DAKLADAS, TH., The development and application of an underwater γ- spectrometer in the marine environment, Radioprotection Suppl. EDP Sciences (2004) (in press).
[4] HANSEN, S.E., STEL, J.H., Elsevier Oceanogr. Ser. **62** (1997) 137-147.
[5] NTZIOU, I., Master Thesis, National Technical University of Athens (2004).
[6] KALFAS, C., SPECTRG- Software Package for Analysis of Gamma-Ray Spectra". Personal communication (2000).

Optimisation of sample geometry for gamma spectrometric measurements through Monte Carlo simulation

Dovlete, C., I. Osvath

Marine Environment Laboratory,
International Atomic Energy Agency,
Monaco

Gamma-ray spectrometry of environmental samples is generally a low-level counting technique, therefore it is important to minimise the external (background) radiation to the detector, using an adequate shield, and to maximize the detection of radiation emitted by the sample itself, using an adequate measurement geometry. The optimum sample geometry depends on the sample quantity available, sample density, energy of interest and the size and shape of the detector. A modelling approach allows the determination of the optimum sample geometry with respect to various criteria and also the estimation of uncertainties, complementing effectively a rather laborious purely experimental approach.

Commonly utilised geometries in environmental measurements are cylindrical and Marinelli type. Cylindrical geometries were studied for several types of matrices, sample volumes and HPGe detectors in use in the laboratory. The optimisation criteria selected refer to maximising detection efficiency by changing the aspect ratio of the sample geometry (diameter to height ratio) and minimising systematic errors related to small deviations from the prescribed geometry. Simulations were carried out using the GESPECOR software package for the range of energies of usual interest for environmental measurements: 46.5 keV (^{210}Pb line), 59.5 keV (^{241}Am), 661.6 keV (^{137}Cs) and 1460.7 keV (^{40}K).

Figure 1 presents results of efficiency calculations for sediment (ρ = 1.6 g·cm^{-3}) samples of 10 cm^3, 49 cm^3, 98 cm^3 and 140 cm^3 volume, in polypropylene (ρ = 1.1 g·cm^{-3}) cylindrical containers, measured on a 170 cm^3 HPGe detector. It can be seen that for small samples (10 cm^3) a 0.5 – 0.8 cm sample height corresponds to maximum detection efficiency, sensitivity to sample height reaching however also a maximum here for the lower energy range. For high energies (1460.7 keV) an increase of the sample height from 0.8 to 2.8 cm results in a detection efficiency decrease of only 20%. Usually the measurement accuracy is the key criterion, therefore a well defined measurement geometry is preferable, i.e. one with a low aspect ratio. This generally results in lower measurement efficiencies, except for large volume samples and the higher energy range. For example, in the case of a 140 cm^3 sample, sample heights between 2 and 4 cm ensure both high detection efficiency and lower contribution to combined uncertainties related to uncertainties in sample height.

The Monte-Carlo simulations thus permitted a quantitative determination of the optimum sample geometries so as to maximise detection efficiencies and minimise measurement uncertainties.

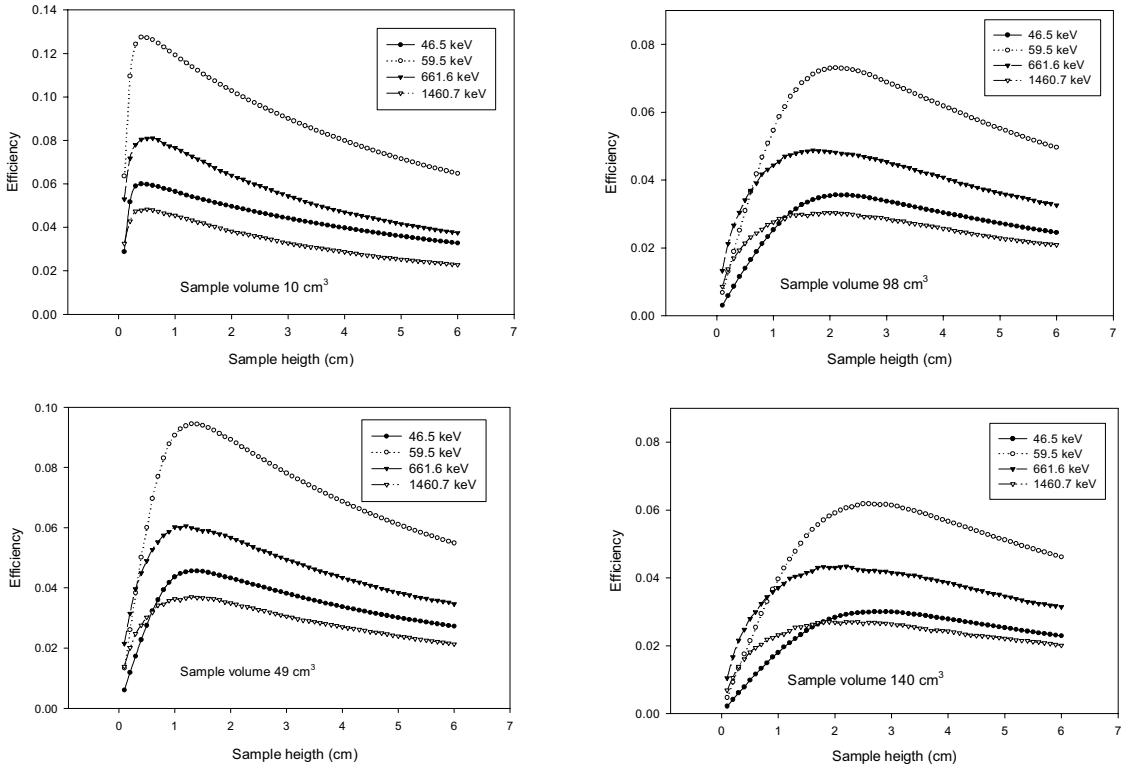

FIG. 1. Calculated detection efficiency as a function of sample height for various sample volumes and gamma-ray energies (sediment sample, density ρ=1.6 g·cm^{-3}, on coaxial HPGe detector of 170 cm^3 volume).

ACKNOWLEDGEMENT

The Agency is grateful for the support provided to its Marine Environment Laboratory by the Government of the Principality of Monaco.

QUALITY ASSURANCE

NUSIMEP: an external QC programme for measuring nuclear isotopes in environmental samples

Stolarz, A., L. Benedik, A. Alonso, T. Altzizoglou, W. De Bolle, H. Kühn, A. Moens, E. Ponzevera, C. Quétel, A. Verbruggen, R. Wellum

European Commission, Joint Research Centre,
Institute for Reference Materials and Measurements (IRMM),
Geel,
Belgium

Abstract. External quality control programmes are necessary for laboratories to demonstrate their capabilities of carrying out high quality measurements. The NUSIMEP programme is addressed to laboratories active in the nuclear environment field. Measurements of uranium isotopic ratios in a simulated biological matrix and uranium, plutonium and caesium isotopic ratios in a saline matrix are the subjects of the comparison campaigns presently being organised by IRMM.

1. Quality control programmes of measurements

Delivering good quality information is of major importance in the present world. Such information includes the results of various analytical measurements as these are important for the quality and often the safety of our lives. External quality control programmes are needed for laboratories to demonstrate their capabilities of carrying out high quality chemical analysis measurements. Through participation in such comparison campaigns, laboratories can ascertain their degree of equivalence on the international scene.

The Isotope Measurements Unit at the Institute of Reference Materials and Measurements organises quality control comparison campaigns within the frame of 3 programmes. Two of these programmes, the Nuclear Signature Interlaboratory Measurements Evaluation Programme (NUSIMEP) and the Regular European Interlaboratory Measurements Evaluation Programme (REIMEP) are addressed to laboratories active in the nuclear field and one, the International Measurements Evaluation Programme (IMEP), to laboratories from the non-nuclear field.

All three comparison campaigns share the same concepts and principles:

(a) **Laboratories receive** well-characterised **samples,** certified amounts of the measured elements or isotopes, **with undisclosed values**. The certified values, established as far as possible at IRMM, are disclosed to laboratories upon receiving their results.

(b) Full **confidentiality is guaranteed** with respect to the link between result and participant identity.

(c) **Campaigns are open to all interested laboratories**.

(d) Participating **laboratories are asked to perform the measurements working under routine conditions** using the techniques, procedures and instrumentation of their own choice.

(e) Participating laboratories should supply a best estimate of the expanded measurement uncertainty on their results. This uncertainty should be a range which laboratories claim contains the value under investigation.

(f) Individual measurement results of participants are compared against the certified reference value provided by IRMM. The certified reference value has a demonstrated uncertainty evaluated according to international guidelines and demonstrates traceability to the SI.

(g) Programmes are focused as much as possible on ‘real-life’ samples.

2. NUSIMEP campaigns

NUSIMEP has started relatively recently and is directed towards measurements of isotopic ratios of trace amounts of nuclear elements in the environment. The programme was established to support the growing need to measure the isotopic abundances of the elements characteristic for the nuclear fuel cycle and appearing in trace amounts in the environment. Such measurements are required not only for Safeguards, as part of the Additional Protocol for tracing non-declared nuclear activities but also for the implementation of the Non-Proliferation Treaty.

In the first three campaigns uranium isotopes were to be measured in: an aqueous solution (NUSIMEP 1) [1], as a dry uranium nitrate (NUSIMEP 2) [2] and in saline media (NUSIMEP 3) [3].

Over recent years the need to control the use of recycled nuclear waste material has become very important. The war in Kosovo, where considerable amounts of ammunition made of material containing depleted uranium were used, triggered the recognition of the need to control possible environmental contamination. In such studies not only the total amount of uranium but also its isotopic ratios are of great concern as the change of isotopic ratios characteristic for natural uranium reflects the degree of contamination of the environment either by enriched or depleted uranium.

Measurement of the uranium content and isotopic ratio in urine can provide a measure of the exposure of the individual to uranium contamination in the environment. A large part of the normal daily uptake of uranium (0.9-1.5 μg) from food, drink and by inhalation is filtered by the kidneys and excreted in the urine. Contamination of the environment either by enriched or depleted uranium (in the case of depleted uranium from shells and other munitions) should be reflected in changed uranium isotopic ratios measured in the urine. The ratios of natural and typical depleted uranium samples are given in Table I.

Table I. Uranium isotopic ratios in natural and depleted uranium

	natural ratio	in depleted U (example)
$n(^{234}U / ^{238}U)$	$5.54\ 10^{-5}$	$8.80\ 10^{-6}$
$n(^{235}U / ^{238}U)$	$7.25\ 10^{-3}$	$2.00\ 10^{-3}$
$n(^{236}U / ^{238}U)$	$1.2\ 10^{-11}$ - $5.6\ 10^{-10}$	possibly > 10^{-4} (dependent on the source of the uranium)

Two inter-laboratory comparison campaigns for isotopic ratio measurements of uranium in simulated urine are being organised by IRMM in 2004: one under the auspices of the Comité Consultatif pour la Quantité de Matière Métrologie en Chimie, CCQM – Pilot Study 48 and one, open to all laboratories, within the frame of NUSIMEP campaigns.

The presently ongoing and planned NUSIMEP campaigns are described below: NUSIMEP 4 for measurement of uranium isotope ratios in simulated urine and NUSIMEP 5 for uranium, plutonium and caesium isotope ratios in a saline matrix, which will start in 2005.

3. NUSIMEP 4 campaign: uranium isotopic ratios in a simulated biological matrix

In NUSIMEP 4, laboratories are invited to demonstrate their capability of carrying out precise measurements of uranium isotopic ratios in a matrix similar to urine. Carrying out such measurements is a very challenging analytical task because of complex matrix effects and low amounts of uranium as well as the low abundance of the isotopes of mass 234, 235, 236. Urine is a difficult but important matrix for measurements of uranium isotopic ratios, especially for showing the presence of, and therefore exposure to, enriched or depleted uranium.

Two samples with slightly depleted or slightly enriched uranium dissolved in a matrix simulating urine and at a concentration of 5 ng/g solution will be delivered to participants in screw-cap polypropylene bottles. In this campaign the specific concentration is only indicative and participating laboratories are requested to measure the isotopic ratios. The stated uranium concentration is also considerably higher than expected in 'real' urine samples. The reasons for this are to ensure no losses of uranium during storage and transport but also to allow laboratories to measure the minor isotope ratios relatively easily.

3.1. Sample preparation

The uranium isotopic mixtures were prepared by mixing in the gas phase two or more samples of UF_6 with certified isotopic abundances. The samples were certified by carrying out measurements on the bulk samples by Gas Source Mass Spectrometry for the ratio $n(^{235}U)/n(^{238}U)$ and Thermal Ionisation Mass Spectrometry for the ratios $n(^{234}U)/n(^{238}U)$ and $n(^{236}U)/n(^{238}U)$. This combination of methods yields isotopic ratios with low uncertainties and has been applied successfully at IRMM for previous NUSIMEP and REIMEP campaigns.

After conversion to the nitrate form and dissolution in nitric acid medium, the certified uranium materials were diluted before use with ultra-clean nitric acid and stored in pre-cleaned polypropylene bottles until use.

The uranium isotopic ratios of the final solutions were certified from the measured values of the ratios of the bulk material taking into account possible effects from traces of natural uranium in the matrix solution and from blanks in the preparation procedure. These blanks were kept to very low levels by consistent use of clean laboratory conditions for cleaning laboratory ware and by use of sub-boiled acids and water.

A simulated urine matrix consisting of a saline solution and urea dissolved in 0.5 M nitric acid was used. Prior to preparation of the matrix solution, its components were analysed for their uranium content and as a result of this the saline mixture was purified from traces of natural uranium.

The purification was performed by passing the saline solution through *Eichrom Industries* U-TEVA columns. A set of parallel columns was designed and built at IRMM to perform the purification of the large volume of solution needed for both programmes, CCQM – P48 and for NUSIMEP 4, as well as for the forthcoming NUSIMEP 5 campaign. In designing the set-up the consideration that the saline solution under cleaning should have no contact with the air during the whole cleaning process down to the collecting container was taken into account. Moreover, to ensure no re-contamination by natural uranium present in the air, the purification process was performed in Ultra-Clean Chemical Laboratory (UCCL) class 10 at IRMM.

The 3 M nitric acid of the solution was found to be sufficient to reach nearly 100% (> 99.5%) uranium retention as proved by subsequent measurements of the uranium concentration performed by ICP-MS, although it is reported by Eichrom [4] that the highest retention coefficient is reached from the solution of above 5 M nitric acid.

The saline solution was diluted and adjusted to 0.5M in nitric acid and the urea then added to make the simulated urine matrix solution.

Before delivering the samples to participants the quality of the pre-cleaned polypropylene bottles used as sample containers was tested. The quality test included a leak test as well as measurement of uranium leached from the material of the container after storing under acidic conditions for several weeks.

3.2. Participation in NUSIMEP 4

For the first time the NUSIMEP campaign will be operated via the Internet through a web link **www.irmm.jrc.be/imep/nusimep.html**. The MILC (Metrological InterLaboratory Comparison) web based informatics tool, previously developed for IMEP comparison campaigns, has been adapted to support other IRMM comparison campaigns including NUSIMEP. It allows participants to register and submit results via a web URL link that is unique for each campaign. Confidentiality is assured by allocating a personal key code to each participant to be used for the on-line results reporting.

At the time of reporting, the solutions have been finished and the certification measurements, comprising isotopic measurements of the bulk material together with measurements of trace amounts of uranium from the matrix solution and other sources, are completed. Registration is planned to be closed by the end of November 2004 and solutions will be shipped to the participants before the end of the same year. Results are expected to be delivered by the participants by the end of February 2005 and the collection of the results and publication of the Report to the Participants is planned to take place before July 2005.

4. NUSIMEP 5 campaign: uranium, plutonium and caesium isotopic ratios in a saline matrix

NUSIMEP 5 is planned to start in 2005 and is designed to present similar analytical problems for the measurements of uranium, plutonium and caesium in typical aqueous environmental samples. Laboratories will be requested to measure the isotopic composition of uranium, plutonium (sub-Bq levels) and of Cs (^{134}Cs plus ^{137}Cs) in a 1 % saline solution. This matrix was chosen to provide some difficulty for the measurements: a chemical separation will normally be needed for the measurements of uranium and plutonium. The uranium concentration, as in NUSIMEP 4, is planned to be at the 5 ng/g (5 ppb) level as this has found to be a good compromise between sample preparation, i.e. avoiding cross-contamination from outside sources of uranium, and providing a test for the measurement capability of the laboratories. The enrichments of uranium materials, as in NUSIMEP 4, is planned to range from slightly depleted to slightly enriched (ca. 2%).

It is understood that not all laboratories will be able to measure all nuclides but both Pu and Cs are valuable indicators of nuclear activity and therefore are regularly measured in environmental samples. The chosen isotopic compositions of plutonium allow the measurement of the alpha ratio of ^{238}Pu/(^{238}Pu + ^{240}Pu) although the isotopic content of the Pu will be certified by TIMS. The Cs isotopic mixture will be prepared by metrological mixing of certified solutions of the two nuclides.

As mentioned above, the matrix solution was prepared while purifying the saline solution for urine preparation. Before application for NUSIMEP 5 the γ-ray emission was checked by low-level γ-ray spectrometry performed in the low-background laboratory, HADES at IRMM. The results confirmed only the presence of natural potassium: no Cs contamination was found.

The campaign is in an advanced state of preparedness. Control measurements are being carried out on the stability of Pu in this matrix and it is expected that the campaign will be opened for participation later in 2005.

5. Conclusions

The NUSIMEP campaigns are filling a need for external QC for laboratories measuring in particular isotopic ratios of materials in the environment resulting from nuclear activities. The problems of measuring uranium isotopic composition in urine samples are addressed in NUSIMEP 4; this campaign is expected to be finished in mid 2005. The following campaign, NUSIMEP 5, covers the measurement of uranium, plutonium and caesium isotopic ratios in natural waters and will be opened when NUSIMEP 4 is completed.

REFERENCES

[1] MAYER, K., PERRIN, R.E., DE BOLLE, W., AGARANDE, M., OVASKAINEN, R., ALONSO, A., De BIÈVRE, P., Certified Reference Materials for Quality Control of Environmental Measurements; ESARDA 17th Annual Sym. on Safeguards and Nuclear Material Management, Aachen, Germany, 9-11 May, 1995.

[2] HELD, A., ALONSO, A., De BOLLE, W., VERBRUGGEN, A., WELLUM, R., NUSIMEP 2: Uranium isotopic abundances, EUR 19744/EN (2001).

[3] WELLUM, R., ALONSO, A., De BOLLE, W., HELD, A., VERBRUGGEN, A., NUSIMEP 3: an External QC Campaign for the measurement of Uranium Isotopic Ratios in Saline Solutions, Advances in Destructive and Non-destructive Analysis for Environmental Monitoring and Nuclear Forensics, ITU, Karlsruhe, Germany; 21-23 October 2002.

[4] HORWITZ E.P., et al., Separation and preconcentration of uranium from acidic media by extraction chromatrography, Analytica Chimica Acta **226** (1992) 25-37 (HP392).

Accreditation in university environmental radioactivity laboratories

Llauradó, M.[a], C. Navarro[b], I. Vallés[c]

[a] Laboratori de Radiologia Ambiental (LRA-UB),
Departament de Química Analítica,
Universitat de Barcelona,
Barcelona,
Spain

[b] Unitat de Garantia de Qualitat (UGQ-UB),
Serveis Científico Tècnics,
Universitat de Barcelona,
Barcelona,
Spain

[c] Laboratori d'Anàlisis de Radiaoctivitat (LARA-UPC),
Institut de Tècniques Energétiques,
Universitat Politècnica de Catalunya,
Barcelona,
Spain

The experimental work performed in university laboratories comes from many different fields and it is assumed to be of high quality. In general, the results are published in national or international journals or presented at conferences. Only a few laboratories have a clear understanding of the importance of implementing Quality Assurance Systems and the accreditation of their activities according to the international standards, such as ISO 17025. Today, few universities include this issue in their programmes. Most laboratories associate quality assurance with the fact that referees before publication have revised their works.

Here the authors describe their experience in two university laboratories involved in environmental radioactivity control. Both laboratories have implanted a Quality Assurance System based on ISO 17025, the standard used for accreditation of the technical competence of laboratories. One of them (LARA-UPC) belongs to a research institute and the other (LRA-UB) belongs to a university department with different logistic organisation. Both laboratories provide services to public and private institutions along side their teaching and research activities.

The Quality Assurance Unit (UGQ-UB) is responsible for activities related to technical support in implementation and assessment in quality systems. In the case of these laboratories this UGQ performs internal audits.

Accreditation is particularly important in environmental radioactivity analysis, where objective evidence of the quality of the data is required. Moreover, the results of radioactivity analysis are important: e.g. quality of water for human consumption (Directive 98/83/CE), environmental surveys (PVRA, Art. 35 of the Euratom Treaty for EU members), imports of agricultural products (Directive 99/1661/EC), export certificate required for agricultural products (2001/1621/EC), measurements in support of health and safety. It is important to assure the accuracy and precision of the results to guarantee that decisions are based on reliable data.

On the basis of accreditation, laboratories can demonstrate their capabilities to customers and give assurance that their analyses will be carried out according to internationally accepted standards.

According to our experience the accreditation system has the following advantages:

- Better organisation of laboratories
- Increased confidence in the results
- Personnel qualified and trained for their specific tasks and permanent monitoring of their performance
- Definition of performance criteria
- Permanent monitoring for procedures that need changing
- Permanent records of instrument performance, which provides a basis for planning repair and replacement needs
- Continuous assessment of the quality of the data generated by the analyst
- Traceability of results
- Improvement of reliability of research results
- Transmission of experience about laboratory quality assurance to students
- Availability as reference laboratory in low-level radioactivity tests

The accreditation system suffers from the following limitations:

- High cost for university laboratories and poor recognition by the scientific community. For university laboratories accreditation is not a competitive factor, but is rather seen as a commercial strategy
- It is not an added value for all users
- It increases the cost of the service
- High degree of bureaucracy and low logistic support
- Difficulty or retaining stable and qualified personnel
- The fact that the methods must be applied strictly sometimes hinders the research activity
- The scope of the analysis is normally limited, and generally does not include all the analyses the laboratory offers
- Difficulty out of carrying out research activities together with teaching and service activities using the same technical personal, facilities and equipment

In spite of the differences between the organisational structure of the two university laboratories, the advantages and limitations of the accreditation are similar.

The implementation of Quality Systems in university laboratories produces a high benefit not only for activities related to services but also in teaching and research.

Evaluating a laboratory's performance in drinking water samples

Romero, M.L.[a], R. Salas[b]

[a] Departamento de Impacto Ambiental de la Energia,
CIEMAT,
Madrid,
Spain

[b] Consejo de Seguridad Nuclear (CSN),
Madrid,
Spain

The radiological protection of the environment and the population requires from all states to have laboratories with internationally comparable quality levels. To meet these requirements laboratories must establish quality assurance programs to ensure that can produce data of the required quality. Laboratories can provide objective evidence of their performance through participation in external quality assessment exercises.

The management of the radiological environmental monitoring programs (REM) in Spain is responsibility of the CSN (Nuclear Safety Council), and their performance is carried out with the collaboration of laboratories in autonomic regions (Fig. 1) which provide the radioanalytical results in compliance with general criteria established by the CSN.

The reliability of the assessment obtained from these programs requires that laboratories producing the analytical data be able to demonstrate the accuracy and comparability of their results, as well as their traceability to International Standards. To this end the CSN organises in collaboration with CIEMAT periodical inter-laboratory test comparisons, using samples similar in composition and activity levels to the ones routinely analysed in the programs.

Following the issue of the European Community Drinking Water Directive [1] concerning the quality of water for human consumption and its implementation by the Spanish Government [2], the last inter-comparison exercise was organised by using a water sample, in an attempt to evaluate the performance of the laboratories analysing the required radioactivity parameters (H-3, alpha and beta activity). The sample (a *synthetic drinking water*), was prepared at the National Laboratory for Ionising Radiation's Standards (CIEMAT), and contained the following radionuclides H-3, Pu-(239+240), Am-241, Sr-90, Cs-137 and K-40, results from gross Alpha, gross Beta and Residual Beta activity were also requested to participants.

The organisation and the assessment of the laboratory's performance were achieved according to the recommendations of the ISO-43 guide [3] and the ISO/IUPAC/AOAC international protocol [4]. A total of thirty-nine laboratories participated in the exercise and the evaluation of the laboratories performance is presented and discussed in this paper.

FIG. 1. Laboratories.

REFERENCES

[1] COUNCIL DIRECTIVE 98/83/EC on the Quality of Water Intended for Human Consumption.

[2] REAL DECRETO 140/2003 por el que se establecen los criterios sanitarios de la calidad del agua de consumo humano.

[3] INTERNATIONAL ORGANIZATION FOR STANDARDIZATION (ISO) ISO/IEC 43-1, 2 ISO, Geneva, Switzerland (1997).

[4] THOMPSON, M., WOOD, R., The international harmonized protocol for the proficiency testing of (chemical) analytical laboratories, Pure Appl. Chem. **65** 9 (1993) 2123-2144.

SI-traceable measurement of methylmercury in tuna by species-specific isotope dilution with a ^{202}Hg isotopically enriched methylmercury reference material

Snell, J.P., C.R. Quétel

Institute for Reference Materials and Measurements,
Joint Research Centre - European Commission,
Geel,
Belgium

The Comité Consultatif pour la Quantité de Matière, CCQM, from the International Committee for Weights and Measures, has the tasks to co-ordinate the activities of national metrology laboratories in establishing traceability of measurements to the SI and to stimulate understanding of the concept of uncertainty and assignment of uncertainty statements to measurements. CCQM working groups develop and execute international comparisons to establish the technical basis for the mutual recognition of measurement capabilities. In 2003, IRMM, the metrology institute of the European Commission, launched CCQM pilot study 39 on the measurement of As, Se, Pb, Hg and CH_3Hg in tuna. The aims were to strengthen the comparability of measurements EU member states are obliged to make under EC regulation 466/2001 (monitoring of contaminants in food) on the total element contents, and to evaluate the comparability of CH_3Hg measurement with new measurement techniques. At the CCQM level, it is necessary to produce measurements for all analytes through processes with established traceability to the SI and with uncertainty statements.

The IRMM contribution to CCQM-P39 for the determination of the tuna's CH_3Hg amount content was based on species specific isotope dilution mass spectrometry applied as a primary method of measurement. IRMM-670, a newly developed ^{202}Hg enriched CH_3Hg isotopic reference material, was blended to the tuna sample, from which Hg species were extracted and derivatised to non-polar forms. Gas chromatography inductively coupled plasma mass spectrometry, GC-ICP-MS, was used for Hg species separation and detection of the $n(^{200}Hg)/n(^{202}Hg)$ ratio in the CH_3Hg of the blended material. The SI-traceable CH_3Hg amount content was then obtained through comparison using an IDMS equation with the IRMM-670 reference CH_3Hg amount content (including the isotopic compositions of natural Hg recommended by IUPAC, and certified for CH_3Hg in IRMM-670). IRMM-639, a natural-like Hg reference material with certified isotopic composition, was used to calibrate the GC-ICP-MS by monitoring extracts of this material, between sample measurements. The traceability to the SI of the IRMM-670 certified values is described elsewhere [1].

The uncertainty associated to the result was estimated according to ISO/GUM. It combined the individual uncertainty contributions attached to all identified experimental steps involved in the measurement. Effects studied included detector dead time correction and instrumental background correction for transient signal measurement, the degree to which the spike material equilibrated with incipient CH_3Hg in the tuna and the moisture content of the tuna. As shown in the table, identification of the relative uncertainty contributions from each of the experimental processes allowed optimisation of the measurement procedure, as well as being considered one method of validating the procedure, according to ISO17025.

Table I. Contributory factors to the uncertainty of the measured ch_3hg mass fraction

factor	% of total U
Isotope equilibration factor	51.1
CH_3Hg amount content of IRMM-670	8.1
GC-ICP-MS blend ratio measurement	24.3
Deadtime correction	4.0
Moisture content, oven-drying	3.3
Natural Hg amount fractions (IUPAC)	2.4
GC-ICP-MS K-factor ratio measurement	4.1
Certified $^{200}Hg/^{202}Hg$ in IRMM-670	1.0
Certified $^{200}Hg/^{202}Hg$ in IRMM-639	0.6
Background correction	0.4
Other factors	0.7

The mass fraction of Hg in the form of CH_3Hg, in the tuna, with expanded combined uncertainty (k=2) was 3.95 (25) · 10^{-6} kg(Hg)·kg^{-1}, which corresponds to a total expanded uncertainty of 5.6 %. The 9 CCQM-P39 participants that measured CH_3Hg by SSID provided results with a standard deviation of 1.9 % (n=8, excluding 1, 2s outlier). Of these, 6 used IRMM-670 certified values, without re-characterisation of the material. The value submitted by IRMM lay 0.4 % from the mean, which provided an additional validation of the IRMM-670 certification process, as well as the tuna measurement.

REFERENCE

[1] SNELL, J.P., QUÉTEL, C.R., A new ^{202}Hg isotopically enriched methylmercury reference material for isotope dilution measurements in biological and environmental samples (these proceedings).

QUALITY ASSURANCE – POSTERS

ISO 9001 accreditation in an R&D environment - is it possible?

Szymczak, R., A. Henderson-Sellers, R.T. Lowson, R. Chisari

ANSTO Environment,
Menai NSW,
Australia

The Australian Nuclear Science and Technology Organisation (ANSTO) is Australia's national nuclear organisation and its centre of Australian nuclear expertise. ANSTO is in the process of replacing its 1950's, 15 MW, high flux (up to 10^{15} n cm^{-2} s^{-1}) reactor with a new reactor which will allow it to continue its cutting edge nuclear science and radiopharmaceutical production well into the 21st century. A ministerial requirement for licensing the facility is ISO 9001 accreditation of its quality management system. The accreditation process has been staggered at ANSTO. Individual divisions are attaining ISO 9001 accreditation separately, leading up to site-wide accreditation of an overarching ANSTO Business Management System.

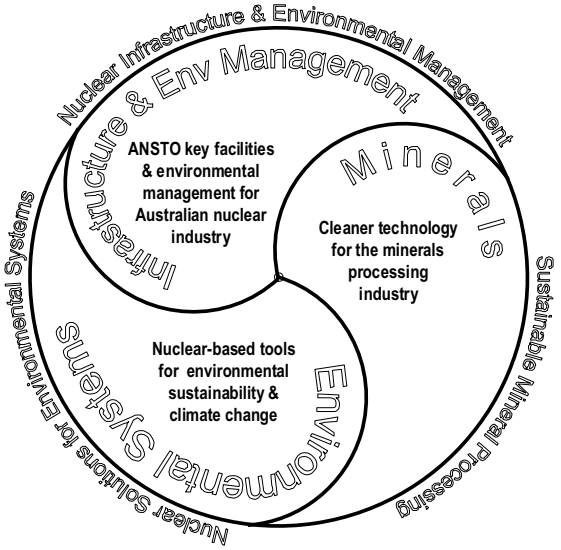

FIG. 1. Structural orientation schematic for ANSTO Environment.

ANSTO Environment is the largest multidisciplinary environmental research group in Australia and the largest R & D unit at ANSTO, comprising around 150 biologists, chemists, engineers, geophysicists, meteorologists, microbiologists, oceanographers, physicists, and technicians (Fig. 1). ANSTO Environment operates and maintains a wide range of advanced nuclear and analytical facilities including three particle accelerators, a 10 MV Tandem accelerator, a 3 MV Van de Graaff accelerator and a newly acquired 2MV HVEE tandetron; a high current 50 kV Metal Vapour Vacuum Arc Ion Implantation (MEVVA) Facility; a Secondary Ion Mass Spectrometer (SIMS); and many other laboratory and field-based facilities.

The objective of ANSTO Environment is to carry out a problem-focused, balanced program of strategic and applied research and development, using its nuclear science-based core expertise and closely-related techniques, to:

- assist the Commonwealth Government to further its national and international initiatives, and to protect and conserve the natural environment through sustainable development
- assist industry in advancing Australia's competitive position in the world economy
- ensure that environmental monitoring of nuclear facilities is effective in assuring operational adherence to sound environmental protection principles

“Make everything as simple as possible, but not simpler”

Albert Einstein

In February 2000 ANSTO Environment successfully acquired ISO 9001:2000 accreditation of its quality management system and was amongst the first organisations to adopt the new 2000 revision of the international ISO 9001 standard. The new standard allows a much more flexible and less prescriptive format for quality management systems however, in the absence of examples of accreditation in the R & D area, presented a challenge in concept, definition of process, buy-in by staff and subsequent maintenance of the successful certification. The ANSTO Environment Manual of Good Management Practice [1] outlines our identity, our vision, our core values, our responsibilities, our operational processes and our commitment to continual improvement via internal and external review.

This paper is a description and discussion of the elements, concepts and process for achieving staff buy-in in the face of initial opposition. This included identifying those necessary elements of a good management system, rejection of pejorative dogma associated with ‘Quality’ and ownership of the process by all the staff.

REFERENCE

[1] AUSTRALIAN NUCLEAR SCIENCE AND TECHNOLOGY ORGANIZATION, Environment Manual of Good Management Practice, Ver 3, ANSTO, Australia (2003) 8.

The quality control system in environmental water radioactivity laboratories

Camacho, A., I. Vallés, X. Ortega

Institut de Tècniques Energètiques,
Technical University of Catalonia (UPC),
Barcelona,
Spain

In this paper, the quality control (QC) program used at the Environmental Radioactivity Analysis Laboratory are presented and internal and external quality control programs are discussed. Internal quality control program involves the preparation of duplicates, the use of certified reference materials, the preparation of blank samples and instrument performance charts. The external quality control is based on the participation in inter-comparison tests and proficiency testing programs of radioactivity in water.

The Environmental Radioactivity Analysis Laboratory (LARA) located at the "Institut de Tècniques Energètiques (INTE)" of the Technical University of Catalonia in Barcelona (Spain) has been measuring radioactivity in water samples for approximately twenty years. The laboratory was accredited in June of 2002 according to the ISO 17025 Standard [1] for 16 procedures associated with the determination of low-level radioactivity in water. The LARA has been developing a quality control system for monitoring the validity of radioactivity measurements in water. This monitoring includes external and internal quality control.

LARA quality control program is based on internal and external QC programmes. Internal QC [2] involves the preparation of duplicates, the use of certified reference materials, the preparation of blank samples and instrument performance charts.

In order to verify internal laboratory precision for each procedure a minimum of one sample for every 20 samples is analyzed in duplicate. The results are evaluated by the relative percentage difference test (RPD) in samples exceeding ten times the detection level and by the spooled counting error (SCE) in the other samples.

The following equations are used to calculate RPD and SCE:

$$RPD = \frac{R_1 - R_2}{\overline{R}} \cdot 100 \qquad |R_1 - R_2| \leq 3\sqrt{s_1^2 + s_2^2} \text{ (SCE)},$$

where:

R_1, R_2 and $\overline{R}$ are the activities in the primary sample, in the duplicate sample and the mean value, respectively.

s_1 and s_2 are the counting errors associated with laboratory measurement of the primary sample and the duplicate sample.

The results are considered acceptable when the RPD is lower than 20% or the SCE condition is verified.

Certified reference materials are evaluated by control charts (CC). Agreement of the measured value with ± 20% of the expected value indicates validity of the calibration curve.

The instrument performances are checked measuring weekly or monthly the background and the efficiency of the detectors. Data from background and efficiencies measurements are statistically evaluated to assign control limits and control charts are drawn for each detector.

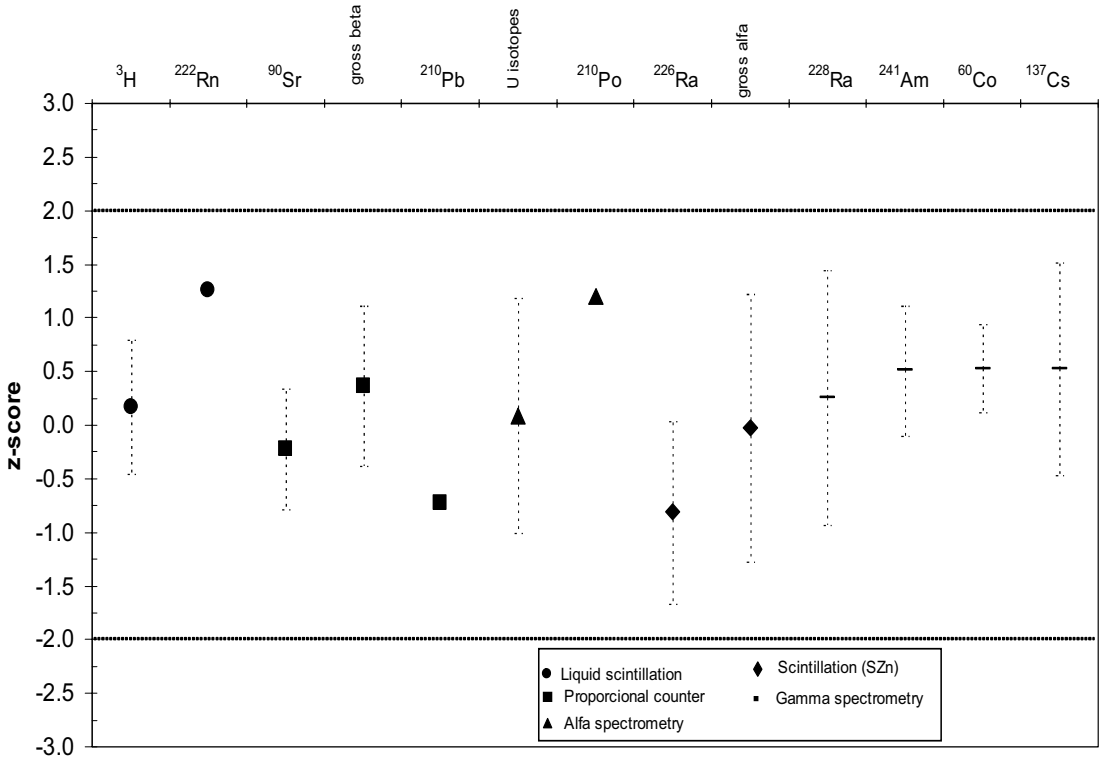

FIG. 1. z-score [3] numbers obtained in the inter-comparison tests. Points show the mean value and bar the range.

The external quality control is based on the participation in inter-comparison tests, proficiency testing programs of radioactivity in water and samples exchange programs between accredited laboratories. These tests have been organized by the Environmental Protection Agency (EPA), the International Atomic Energy Agency (IAEA), the Spanish Nuclear Safety Board (CSN), the World Health Organization-International Reference Center for Radioactivity (OMS-IRC), Environmental Resource Associates (ERA) and some Spanish universities. Figure 1 shows a summary of the z-score numbers obtained in the inter-comparison tests.

The quality control program provides continuous control assurance that assays and measurement systems are performing satisfactorily. Corrective actions are initiated if data lied outside the control range. Permanent records of instrument performance provides a basis for planning repair and replacement needs. The proposed quality system ensures the reliability of laboratory measurements.

REFERENCES

[1] ISO-17025, General Requirements for the Competence of Testing and Calibration Laboratories, (1999).
[2] EPA-600/7-77-088, Handbook for analytical quality control in radioanalytical laboratories, (1977).
[3] ISO-43-1, Proficiency testing by interlaboratory comparisons, Part 1 (1997).

Development of a laboratory information management system at IAEA-MEL

Bartocci, J., H. Ramadan, I. Osvath, P.P. Povinec

Marine Environment Laboratory,
International Atomic Energy Agency,
Monaco

In order to deal with an increasing number of incoming samples and/or to follow more closely their life cycle within an analytical laboratory, a computerized system is generally used to increase trackability and to support Good Laboratory Practice. The System for Laboratory Information Management (SLIM) which is under develoment at IAEA-MEL is a computerized system designed to suit the sample processing and analytical operations specific to a marine environment laboratory running a wide range of projects involving measurement of radioactive and non-radioactive contaminants and tracers and global-scale support to analytical quality. The system is custom-taylored to IAEA-MEL needs yet it is flexible enough to be adaptable for use in other environmental analytical labs.

The design of the SLIM database structure was the first step of the system development. While no changes are foreseeably needed in the developed backbone structure, the database implementation can evolve with software, hardware and communication-related options, one key area being that of analytical instrument-computer interface.

The structure of the database can be divided into three distinct parts:

i) collection of information

ii) sample tracking

iii) reporting results

These different parts show the different laboratory activity areas covered by the SLIM database. The structure (tables and fields) of the database were designed, and at present the implementation is being planned as a multiple step process, starting with basic functions i) and ii), and building upon these gradually. The implementation of SLIM will support increased trackability and efficiency and will facilitate laboratory management.

Figure 1 shows the principal structure of the SLIM database, distinguishing its three main parts: the **collection of information**, the **sample tracking** and the **reporting of results**.

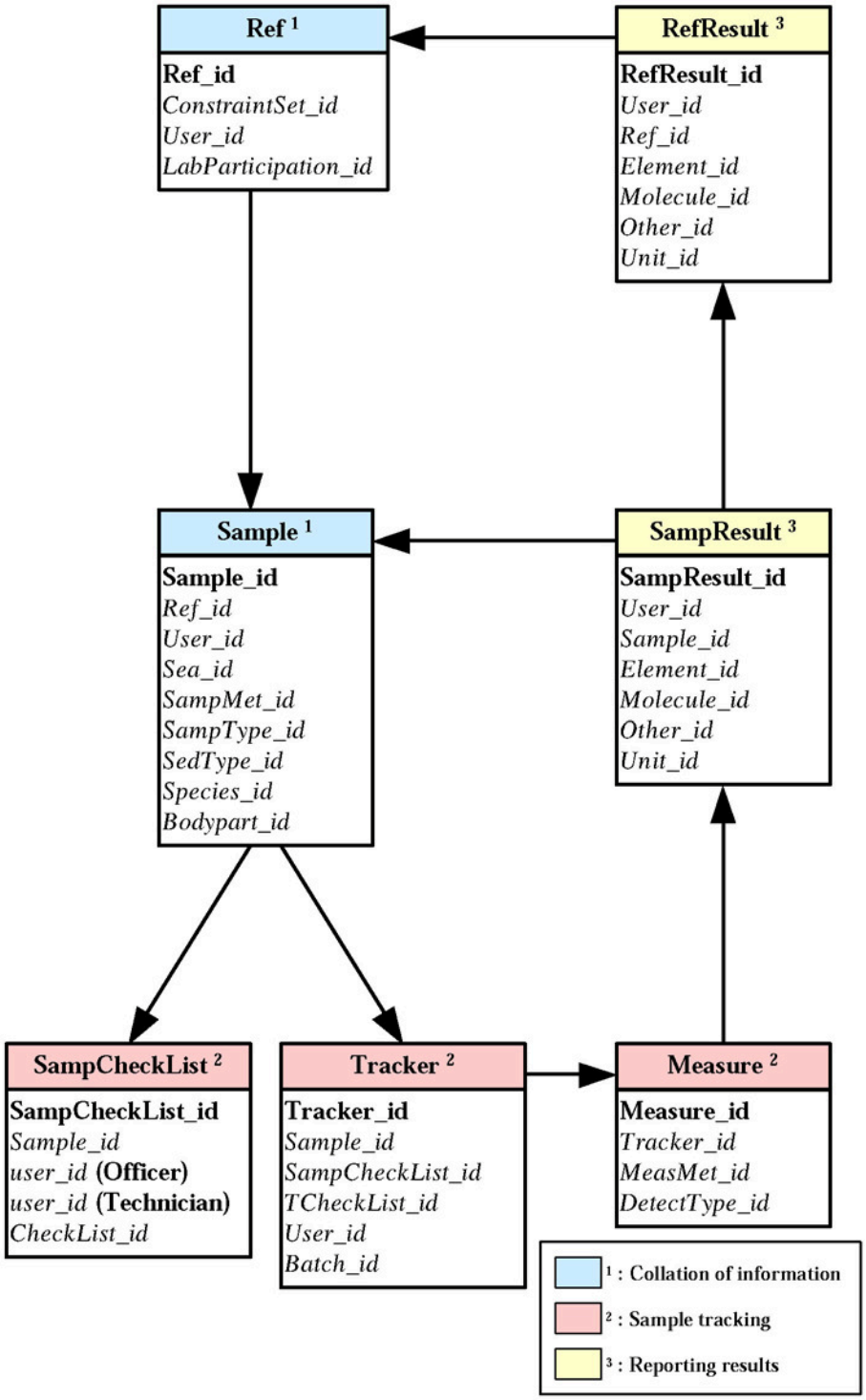

FIG. 1. The principal structure of the SLIM database.

A new ^{202}Hg isotopically enriched methylmercury spike material with SI-traceable reference values for isotope dilution measurements in biological and environmental samples

Snell, J.P., C.R. Quetel

Institute for Reference Materials and Measurements,
Joint Research Centre,
European Commission,
Geel,
Belgium

HgO enriched in ^{202}Hg was used for the preparation of a solution of ^{202}Hg enriched CH_3Hg. The CH_3HgCl was synthesised by reaction with a Grignard reagent and a subsequent comproportionation reaction between dimethylmercury, $(CH_3)_2Hg$, and $HgCl_2$, that was optimised to give a high yield of the product, pure from other Hg species and by-products of the synthesis reaction. To prepare the CH_3HgCl for use as an IDMS spike, it was dissolved in 2 % ethanol. The spike was thereby maintained in a relatively reactive form without solution preservatives that might alter its chemical behaviour compared to incipient CH_3Hg in a sample. Aliquots were sealed in quartz ampoules and a 1-year stability study was undertaken by storing a series of ampoules under different temperature conditions to all be measured on the same occasion (an isochronous study) and by retaining a portion of the solution in a closeable bottle under recommended storage conditions, with measurements at 3-month intervals.

The Hg amount content in the form of CH_3Hg was obtained by subtraction of the inorganic Hg amount content (determined by gas chromatography inductively coupled plasma mass spectrometry, GC-ICP-MS) from the total Hg amount content (determined by blending with IRMM-639, a natural Hg isotopic certified reference material, ICRM, and isotope dilution mass spectrometry of the digested material). Only CH_3Hg and inorganic Hg were detectable in the reference material with inorganic Hg in <2 % of the total amount. GC-ICP-MS was also used to confirm that the isotopic composition of Hg in the form of CH_3Hg was identical to that of IRMM-640, an inorganic Hg ICRM prepared from the same ^{202}Hg enriched HgO, within enlarged uncertainty statements. These processes allowed the SI-traceable certification of both the amount content of CH_3Hg and its isotopic composition, accompanied by combined uncertainty statements estimated according to ISO/GUM.

The final uncertainty on the Hg amount content in the form of CH_3Hg (3.5 % relative, k=2) included a contribution covering for potential changes over 2 years of shelf-life. No degradation of the CH_3Hg content or isotopic composition was statistically observable over the storage period, so this contribution was extrapolated from the uncertainty in measurement repeatability of the isochronous study.

Ampoules are now available for distribution as an ICRM, named IRMM-670, with the certified reference values listed in Table I.

Table I. Ampoules available for distribution as an ICRM, named IRMM-670, with the certified reference values

Material :	$CH_3{}^{202}HgCl$ in 2 % ethanol/water	
amount content	Certified value	Uncertainty [1]
mol $(CH_3(^{202}Hg)Cl) \cdot g^{-1}$	$171.0 \cdot 10^{-9}$	$6.1 \cdot 10^{-9}$
mol $(CH_3HgCl) \cdot g^{-1}$	$175.1 \cdot 10^{-9}$	$6.2 \cdot 10^{-9}$
Isotope amount ratios of Hg in the form of CH_3HgCl	Certified value	Uncertainty [1]
$n(^{196}Hg)/n(^{202}Hg)$	0.000 018	0.000 013
$n(^{198}Hg)/n(^{202}Hg)$	0.000 623	0.000 050
$n(^{199}Hg)/n(^{202}Hg)$	0.001 603	0.000 096
$n(^{200}Hg)/n(^{202}Hg)$	0.005 50	0.000 22
$n(^{201}Hg)/n(^{202}Hg)$	0.013 35	0.000 53
$n(^{204}Hg)/n(^{202}Hg)$	0.002 60	0.000 16
molar mass of Hg in the form of CH_3HgCl	Certified value	Uncertainty [1]
$g \cdot mol^{-1}$	201.944 66	0.000 76

1) All uncertainties are expanded uncertainties, with a coverage factor, $k = 2$

NON- RADIOACTIVE CONTAMINANTS - POSTERS

Chronology of metal pollution offshore Coruh Mouth, Eastern Black Sea

Secrieru, D.[a], S. Gulin[b], I. Osvath[c]

[a] GeoEcoMar Institute of Geology and Geo-Ecology,
Constanta,
Romania

[b] Institute of Biology of Southern Seas,
Sevastopol,
Ukraine

[c] Marine Environment Laboratory,
International Atomic Energy Agency,
Monaco

Among the areas investigated during two international cruises organised by the IAEA in the Black Sea in 1998 and 2000, two areas were singled out, on the NW Shelf and offshore the Coruh mouth, as having the highest levels of heavy metals in sediment. The River Coruh drains mountainous regions of Turkey and Georgia, having a high transport energy. Offshore its mouth, Cu reaches up to 340 μg/g and Ba up to 2350 μg/g in sediment. These maximum levels are about 7, respectively 10 times higher than "background" values measured in Black Sea sediments. It can be noted that at two of the four locations in the studied area Cu exceeded the ERL concentration for marine sediments (270 μg/g), indicating a likely impact on marine biota at the respective sites. Most of the other heavy metals (Co, Ni, Pb, Zn, Cd, Cr and V), the major component Fe_2O_3 and the minor component TiO_2 were also enriched, to a lesser degree, in the area offshore the Coruh mouth. Ba and Cu were related here by a significant linear correlation (r_{Ba-Cu}=0.905), indicating a common origin for both metals. At the same time both metals were significantly correlated ($\alpha \leq 0.01$) with Pb, Cd and Zn, Ba being also significantly correlated with Cr. All these metals have no significant correlations with any potential normalizing component. The general enrichment of these elements points to a substantial input from a region characterized by the presence of polymetallic and barite mineralizations, the paragenesis being specific for porphyry copper deposits. Deposits of this type are present in both Georgia and Turkey and both countries are mining them. Both natural erosion and transport and anthropic activities can contribute to the measured enrichment and it is of interest to identify and characterize the sources and the processes and timescales involved in transport and deposition as well as the post-depositional processes. The spatial distribution of Cu and Ba surface sediment concentrations offshore the Coruh mouth clearly confirms the river as the source of input of heavy metals. The vertical distributions of copper concentrations are characterized by ample fluctuations (Fig. 1 illustrates the profile at one of the sampled sites). ^{137}Cs was used to derive down-core chronology and, until further insight will be obtained on post-depositional processes, the observed variations in the Cu profile were tentatively attributed to variations in the input resulting from copper industry upstream Coruh. The most likely source lies in the Artvin area, where a major Cu processing center, Murgul-Artvin, is located, about 60 km from the mouth of the river. The most likely source for the increased Ba concentrations is the Cerattepe high-grade gold ore deposit near Artvin, where gold is located in oxidized barite rich units and the mining and processing of the ore results in a great quantity of Ba rich wastes. No detailed production data are at this stage available for these industries, however global data were available for Cu mining in Turkey since the early 1960s. The timeline corresponding to the measured Cu profile in Fig. 1, when taking into account transport, deposition and post-depositional processes, matches fairly well key time points such as: significant growth of the mining industry in the mid 1930s; actions to

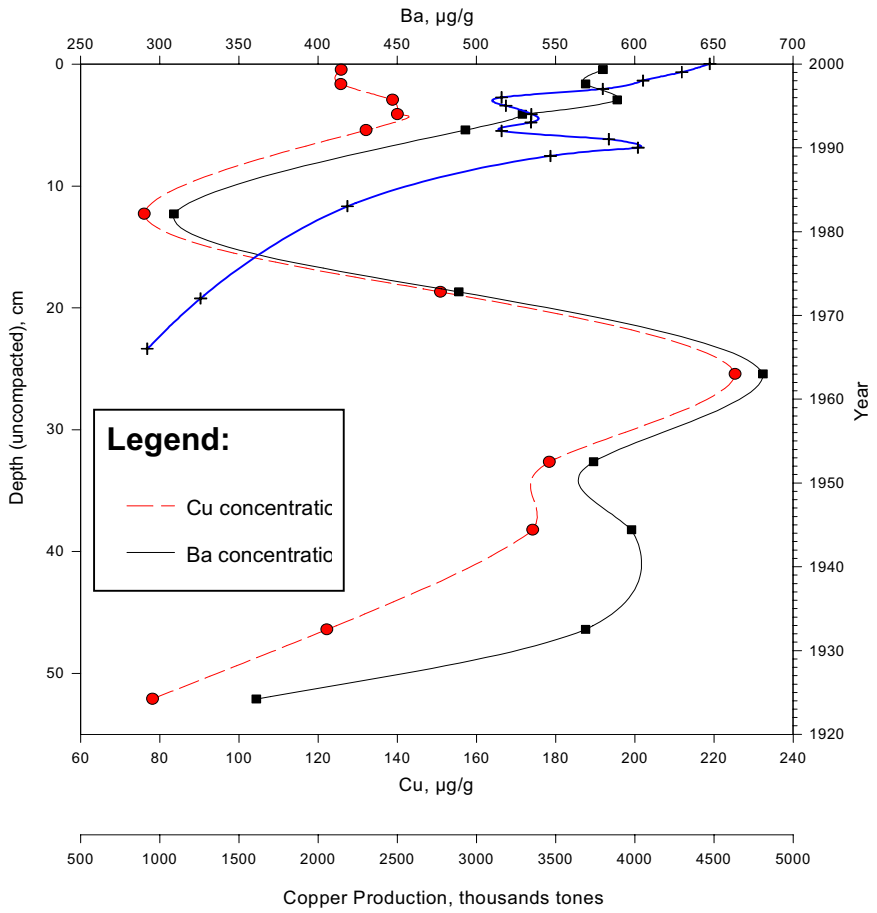

FIG. 1. Cu and Ba concentrations in sediment at a location situated offshore the mouth of River Coruh (Station BS2K-17, 41°39'656 N, 41°33'231, 70 m water depth, sampled on 01.10.2000) and ^{137}Cs-based geochronology. Cu production in Turkey is also represented.

address environmental concerns starting to be implemented in the 1970s and being consolidated with the Turkish Environmental Law coming into force in 1973. Further detailed studies and additional information will be required to make a complete assessment of the site's contamination, to trace the burying of the sub-surface Cu peak, to corroborate chronologies using additional tracers and to identify effects of post-depositional processes. Combined with previous results obtained by the authors on the buffering capacity of this river's watershed, this study could improve the predictive capabilities concerning the fate of contaminants released in or deposited on the basin.

ACKNOWLEDGEMENTS

This study was carried out in the framework of the IAEA TC Project RER/2003 "Marine Environmental Assessment in the Black Sea Region". The Agency is grateful for the support provided to its Marine Environment Laboratory by the Government of the Principality of Monaco.

Content of toxic elements in fish species of the Black Sea

Zubachenko, V., S. Omelchenko, G. Shimchuk

Crimean Regional Research and
Production Centre for Standardization, Metrology and Certification,
Sevastopol,
Ukraine

Chemical pollution of the Black Sea including toxic elements and organic compounds conduct to negative ecological consequences. The basic sources of toxic elements are coastal deep outlets of the black and nonferrous metallurgy enterprises, port zones and household waters. High concentration of copper, lead, zinc, chromium, arsenic is exhibited in the sewage water spewing out into the Black Sea ecosystem, especially in the coastal region [1]. These contaminants result in very negative changes in biocenose as they move through the food chains and are collected in marine organisms, leading to their death, decline in health and recession of biodiversity [2].

On this basis the purpose of the present work is to study the contents of toxic elements in some fish species from two Sevastopol bays distinguished by level of anthropogenous load.

Mesogobius bathrachocephalus, Scorpaena porcus and *Merlangus merlangus euxinos* from Martynova and Karantinnaya bays served as the research material in order to determine toxic elements. The toxic elements content was determined using the classic polarography method per State Standards 26930-26934-86 [3]. The arsenic content was determined using the photocolorimetry method, mercury - by way of flameless atomic absorption on "Yulia-2" analyzer. The received results were compared with the maximum limiting values. The received data for the toxic elements contents is exhibited in Tables I and II.

Table I. The toxic elements contents in the fish species from two bays of the Black Sea

Bay	Martynova						Karantinnaya					
Toxic Elements / Research Objects	Cu	Pb	Cd	Zn	As	Hg	Cu	Pb	Cd	Zn	As	Hg
Mesogobius bathrachocephalus	0.5	0.02	0.03	3.9	1.02	0.06	0.3	0.08	-	1.8	1.21	0.08
Scorpaena porcus	1.2	0.03	-	2.3	0.35	0.06	0.3	0.10	0.05	2.4	0.69	0.05
Merlangus merlangus euxinos	0.3	0.04	-	3.2	1.0	0.04	0.2	0.01	-	1.6	0.61	0.05
Max. limiting values	10	1	0.2	40	5.0	0.4	10	1	0.2	40	5.0	0.4

It is obvious that the content of the toxic elements in fish species of both bays varies over a wide range, thus not exceeding maximum limiting values. The contents of zinc in *Merlangus merlangus euxinos* and *Mesogobius bathrachocephalus* is two times higher in the Karantinnaya bay in comparison with the Martynova one. Cadmium was determined in two cases only. Lead concentration was inconsiderable in all samples thus proving literature data [4].

Table II. Relative concentration of the toxic elements in fish species from the two Black Sea bays, %

	Bays											
	Martynova						Karantinnaya					
Toxic elements Research object	Cu	Pb	Cd	Zn	As	Hg	Cu	Pb	Cd	Zn	As	Hg
Mesogobius bathrachocephalus	9.04	0.36	0.54	70.5	18.44	1.08	8.64	2.31	-	51.87	34.87	2.3
Scorpaena porcus	30.45	0.76	-	58.4	8.88	1.52	8.36	2.78	1.39	66.85	19.22	1.39
Merlangus merlangus euxinos	6.5	0.87	-	69.9	21.83	0.87	8.1	0.4	-	64.8	24.7	2.0

The results of the study performed permitted to demonstrate that the quantity of toxic elements in the studied species of fishes populating two of the Sevastopol Bays varied within a broad range with no maximum permissible concentrations exceeded. The largest quantity of zinc was detected in the *Merlangus* of the Martynova Bay. This value exceeded twofold the respective value in the *Merlangus* of the Karantinnaya Bay.

The level of toxic elements in the fishes populating the two Black Sea bays can be expressed in terms of percentage in ascending powers as follows: cadmium → lead → mercury→copper→arsenic→zinc.

Therefore, the results of the study performed permit the following conclusion: despite a relatively favourable situation in the content of toxic elements in the common fish species populating the Black Sea, regular biomonitoring of the Black Sea basin should be conducted with a view to forecasting eventual ecological risks and dangers for human health.

REFERENCES

[1] RUDNEVA, I., "Impacts of metallurgical industry on the coastal ecosystem of Black Sea countries" Approaches to Handling Environmental Problems in the Mining and Metallurgical Regions (FILOH, L., BUTORINA, I., Eds), Kluwer Academic Publishers, Netherlands (2003) 27-33.

[2] MOISEENKO, T., Evaluation of ecological risk in the cases of metal pollution in water, Water Res. **2** 2 (1999) 186-197 (in Russian).

[3] GOSTY 26930-26936-86.

[4] BUDNIKOV, G.K., Heavy metals in ecological monitoring of the water systems, Biology Kazan, KGU (1998).

Trace metal distributions in the water column and surface sediments of İzmit Bay (Turkey) after the Marmara (İzmit) Earthquake

Balkis, N.[a], E. Senol[b]

[a] Istanbul University, Institute of Marine Science and Management,
Vefa, Istanbul,
Turkey

[b] Turkish Naval Academy,
Department of Basic Science,
Tuzia, Istanbul,
Turkey

İzmit Bay is a semi-enclosed water body situated in the NE of the Marmara Sea with a length of 50 km, width varying between 2 and 10 km and has an area of 310 km^2. The Bay and its surroundings are one of the most heavily industralized and populated regions of NW Turkey with the growth of industry increasing since 1960. İzmit Bay has been subjected to pollution problems [1] including eutrophication of the water and inputs of toxic industrial and domestic effluents. Total organic matter load of industrial discharges has been reduced to 80% within the last 10 years, whereas domestic organic loads have been increased twofold [2]. The earthquake with a magnitude of 7.4 occurred on 17^{th} of August 1999, destroying the eastern Marmara Region. The surface waters of the Bay were partly covered by the thick petroleum layers and partly by a film [3, 4]. Balkis [5] investigated the consumption of DO and formation of DHS in the lower layer of the Bay after the earthquake.

Dissolved heavy metal concentrations (Fe, Mn, Pb, Cu and Cd) were measured by atomic absorption spectrophotometer (AAS) following preconcentration with ammonium 1-pyrrolidinedithiocarbamate (APDC) in an organic extraction [6]. The surface sediments Al, Fe, Mn, Cu, Zn, Co and Cr contents were determined by atomic absorption spectrophotometer (AAS) after a "total" digestion, involving HNO_3 + $HClO_4$ + HF acid mixture [7].

The distribution of metal (Fe, Pb, Cu, Zn, Co, Cr and Cd) concentrations in both the water column and surface sediments shows the influences of anthropogenic inputs in the Bay. The results are summarized in Tables I and II. The Mn enrichment in the lower layer water of the central and eastern basins originates from the occurring anoxic conditions after the Marmara (İzmit) Earthquake.

Table I. Metal concentrations along the water column of the İzmit Bay (mg/L)

Element	October 1999	December 1999	February 2000	May 2000	August 2000
Fe	7-15	<4-4	<4-13	<4	<4
Mn	<1-4	1-7	2-4	4-12	<1-13
Pb	<0.8-1	<0.8-0.9	0.9-1	<0.8-2	<0.8-1
Cu	0.5-0.7	0.5-0.9	0.4-0.8	<0.4-0.6	<0.4-0.8
Cd	<0.1	<0.1	<0.1	<0.1	<0.1

Table II. Range of metal concentrations of bulk surface sediments of İzmit Bay

Element	Average shale (Krauskopf, 1979)	Gulf of İzmit min - max	Gulf of İzmit mean - SD
Cu (ppm)	50	11 - 42	23 ± 9
Zn (ppm)	90	84 - 306	149 ± 57
Fe (%)	4.7	4.6 - 7.1	6.1 ± 0.6
Mn(ppm)	850	139 - 494	327 ± 89
Co(ppm)	20	6 - 20	12 ± 4
Cr (ppm)	100	34 - 77	58 ± 11
Al (%)	9.2	2.3 - 11.4	7.4 ± 2.5

REFERENCES

[1] OKAY, S.O., LEGOVIÇ, T., TÜFEKÇİ, V., EGESEL, L., MORKOÇ, E., Environmental impact of land-based pollutants on İzmit Bay (Turkey): short-term algal bioassays and simulation of toxicity distribution in the marine environment, Archives Environ. Contam. Toxicology **31** (1996) 459-465.

[2] MORKOÇ, E., OKAY, S.O., TOLUN, L., TÜFEKÇİ, V., TÜFEKÇİ, H., LEGOVIÇ, T., Towards a clean İzmit Bay, Environmental Int. **26** (2001) 157-161.

[3] GÜVEN, K.C., SUR, H.İ., OKUŞ, E., YÜKSEK, A., UYSAL, A., BALKIS, N., KIRATLI, N., ÜNLÜ, S., ALTIOK, H., TAŞ, S., ASLAN, A., YILMAZ, N., MÜFTÜOĞLU, A.E., GAZİOĞLU, C., CEBECİ, M., İzmit Körfezi'nin Oşinografisi, 17 Ağustos 1999 Depremi sonrası İzmit Körfezi'nde Ölçme ve İzleme Programı. Technical Report. T.C. Çevre Bakanlığı. Deniz Bilimleri ve İşletmeciliği Enstitüsü, Istanbul Üniversity (2000) (in Turkish).

[4] OKAY, S.O., TOLUN, L., TELLİ-KARAKOÇ, F., TÜFEKÇİ, V., TÜFEKÇİ, H., MORKOÇ, E., İzmit Bay (Turkey) Ecosystem after Marmara Earthquake and Subsequent Refinery Fire: the Long-term Data, Mar. Poll. Bull. **42** (2001) 361-369.

[5] BALKIS, N., The effect of Marmara (İzmit) Earthquake on the chemical Oceanography of İzmit Bay, Turkey, Mar. Poll. Bull. **46** (2003) 865-878.

[6] BRULAND, K.W., COALE, K.H., Mart, L., Analysis of seawater for dissolved cadmium, copper and lead: an inter comparison of voltametric and atomic adsorption methods, Mar. Chem. 17 (1985) 285-300.

[7] LORING, D.H., RANTALA, R.T.T., Manuel for the geochemical analyses of marine sediments and suspended particulate matter, Earth-Sci. Rev. **32** (1992) 235-283.

A survey of metal pollution in mussels *Mytilus galloprovincialis* (L.1758) from the northern coast of the Turkish Aegean Sea

U. Sunlu

Ege University,
Faculty of Fisheries,
Department of Hydrobiology,
Bornova-Izmir,
Turkey

Marine organisms generally, mussels and benthic fish are selected as suitable indicator species of coastal pollution, as they give complementary information on chemicals bio-available in the water column and sediments, respectively. Bioaccumulation patterns of the different pollutants vary substantially among species. Habitat, season and food web play a key role on the bioaccumulation process. Filter feeder organisms accumulate most of the pollutants at more higher levels than those found in water column so that they permit to reflect the quality of coastal environments. Mediterranean mussels *Mytilus galloprovincialis* (L.1758) have criteria of ideal bio-monitors as sedentary and easy to sample over Mediterranean coastal zones[1, 2].

The aim of this study was to investigate the present status of the distribution of heavy metal levels in economically important bivalve from Northern coast of Turkish Aegean Sea.

The mussels were collected by hand on rocks along the coastal zones at 5 sampling locations during the period of November 2002-April 2003. The 5 sampling stations are shown in Fig. 1 below.

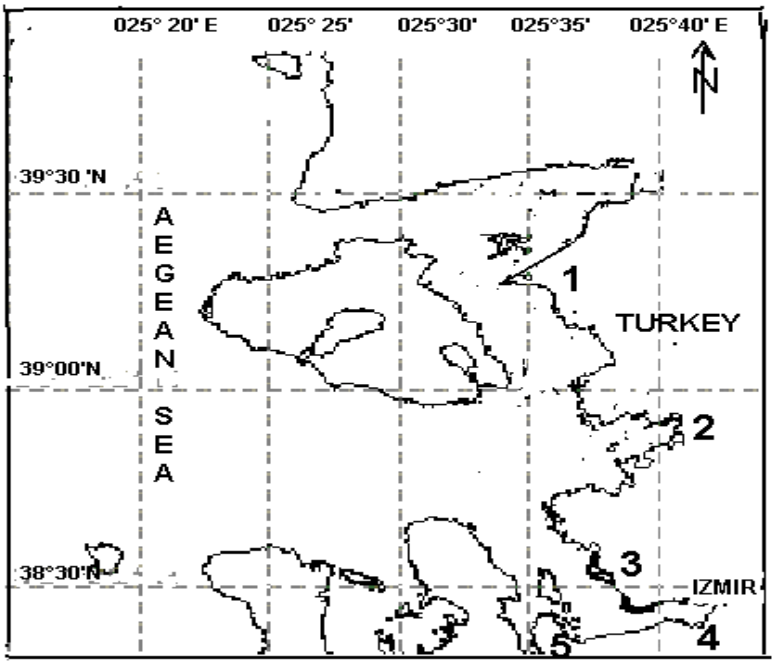

FIG. 1. Sampling stations for mussel collection.

All samples transported daily to the laboratory. Edible soft tissues of mussels were removed from the shells on the day of sampling and were kept at frozen at –30°C until the analysis. The collected

mussels were divided in two groups according to their size (small size 3-4 cm. and big size 7-8 cm.).The composite samples of soft mussel tissues were wet–ashed by nitric and percloric acid. Solutions of tissues were analysed by 2380 Perkin–Elmer AAS. Inter-calibration homogenate sample (IAEA –142/ TM) was used as a quality control for the analytical methodology [3].

The concentrations of some heavy metals (Pb, Cu, Zn) in the soft tissues of *M. galloprovincialis* were determined separately from different regions of Northern Turkish Aegean Sea. The Average levels of heavy metals in mussels are given in Table I.

Table I. The average concentrations of some heavy metals in *m. Galloprovincialis* from different regions of northern turkish aegean sea ($\mu g g^{-1}$ wet weight)

Stations	Pb	Zn	Cu
Ayvalık (1)	0.40 ± 0.04	18.22 ± 0.61	0.95 ± 0.09
Candarli (2)	0.60 ± 0.03	25.60 ± 1.87	1.50 ± 0.18
Homa (3)	1.40 ± 0.14	22.59 ± 1.77	1.60 ± 0.15
Inciralti (4)	1.70 ± 0.17	35.45 ± 4.21	1.82 ± 0.21
Urla Iskele (5)	0.80 ± 0.08	20.15 ± 1.20	1.45 ± 0.10

It can be seen from the table that there are significant differences in metal concentrations according to the localities. The maximum heavy metal concentrations measured in station 4. In this station, a dominant source of metal concentration is from urban and industrial activities Station 2 and 3 are affected by the heavy polluted rivers (Gediz and Bakircay) For each sampling location the highest concentrations of heavy metals was found in small size mussels while the smallest concentrations were found in big size mussels. An inverse relationship metal concentration and animal size.

Concentrations of lead, copper and Zinc in mussels collected in the Northern Turkish Aegean Sea coast are of the same order of magnitude as those which were reported for other places in this area of the Mediterranean Sea [2-5].

REFERENCES

[1] PORTE, C., ALBAIGES, J., Spatial and Temporal Trends in the Distribution of Contaminants and Their Biological Effects in the NW Mediterranean, Med. Mussel Watch Workshop Document (2002) 57-58.

[2] UGUR, A., YENER, G., BASSARI, A., Trace Metals and ^{210}Po (^{210}Po) Concentrations in Mussels (*Mytilus galloprovincialis*) Consumed at Western Anatolia, Appl. Rad. Isotop. **57** (2002) 565-571.

[3] BERNHARD, M., Manual of Methods in Aquatic Environment Research, FAO Fisheries Technical Paper FIRIT/T **158** (1976) 1-123.

[4] VEGLIA, A.A., Survey of Heavy Metals in Mussels (Monaco 1989-1996), IAEA-TECDOC-1094, IAEA, Vienna (1998) 593-595.

[5] SUNLU, U., Comparison of Heavy Metal Levels in Native and Cultured Mussel *Mytilus galloprovincialis* (L.1758) from The Bay of Izmir (Aegean Sea-Turkey), Med. Mussel Watch Workshop Document (2002) 69-72.

Benthic foraminiferal response to heavy metal pollution in Izmir Bay (Eastern Aegean Sea)

Bergin, F.[a], F. Kucuksezgin[b], E. Uluturhan[b], I.F. Barut[c], E. Meric[c], N. Avsar[d]

[a] Bosphorus University,
Cultural Heritage Museum,
Bebek, Istanbul,
Turkey

[b] Dokuz Eylul University, Institute of Marine Sciences and Technology,
Inciraltı, Izmir,
Turkey

[c] Istanbul University,
Institute of Marine Sciences and Management,
Vefa, Istanbul,
Turkey

[d] Cukurova University,
Faculty of Architecture and Engineering,
Dept. of Geology Engineering,
Balcalı, Adana,
Turkey

Benthic foraminifera are increasingly used as environmental bio-indicators especially in polluted environments where their sensitivity to pollutants may be expressed by a modification of their test structure and by the change of the assemblages. The Gulf of Izmir is located in western Turkey and surrounded by a densely populated community. It has been contaminated by numerous heavy metals, geochemical analyses have shown that metals are significant pollutants in the inner part of the bay. Outer and middle sections showed low levels of heavy metal enrichments except for the estuary of the Gediz River.

Foraminifera (class Foraminifera, phylum Granuloreticulata) are among the more abundant protozoa in marine and brackish water habitats. They are unicellular protista that construct shells of one and many chambers. Their sizes range from 100 microns to 20 cm. Studies of pollution effects on benthic foraminifera were initiated by Resig [1] and Watkins [2]. The effects of heavy metals pollution on foraminifera are studied especially by [3-5].

Sediment samples were collected from 16 stations in the Gulf of Izmir (Fig. 1) during the *R/V K.Piri Reis* cruise in November 2002 in the framework of the Gulf of Izmir Marine Research Project. Sediment samples were taken using Van-Veen Grab sampler that collects sediment over a surface of about 400 cm^2. A constant volume of 50 cm^3 of sediment was taken from the upper 1 cm of each sample.

The samples for metal analyses were dried in a freeze dryer, homogenized and reduced to a fine powder. Samples were digested in a microwave digestion system (Milestone 1200) with a HNO_3-HF-$HClO_4$-HCl acid mixture solutions and were analyzed by flame and graphite furnace AAS (Varian Spectraa-300 plus).

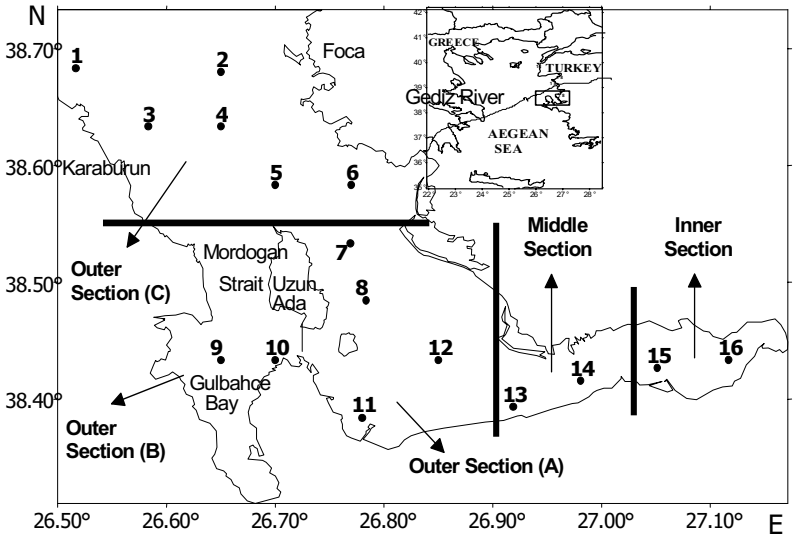

FIG. 1. Location map of sampling points in Izmir Bay.

The foraminifera are identified according to the criteria laid down by [6] and [7]. A total of 16 sediment samples were used for this study from the Gulf of Izmir. For foraminiferal research 20 grams of dry sediment were treated with 17% H_2O_2 and left for 24 hours within it. The samples were stained with Rose Bengal to help recognize the living individuals. After drying and sieving the residues through a 250 mm mesh, the foraminifers were picked up and examined under a binocular microscope.

- We identified 67 foraminifer and 22 ostracod species
- The most polluted area is the Inner Bay where the number of species decreases
- The most abundant species at the study area are *Ammonia tepida, Elphidium crispum, Ampicoryna scalaris, Noniella turgida* and *Nonion depressulum*. The last two species have been already identified in the Northern Aegean and these species were found in the Gulf of Izmir in this study due to northern Aegean waters flowing into the Gulf of Izmir
- Test deformities are observed in *Ammonia tepid* and *Adelosina mediterranensis*
- Living specimens are limited in number
- *Elphidium crispum* is correlated with Hg (R= 0.844), while negative correlation was found between *Elphidium crispum* and Cr (R= -0.637). Positive correlations were observed between Ni-*Amphycoryna scalaris* (R= 0.484), and Ni-*Noniella turgida* (R= 0.455), Mn-*Noniella turgida* (R= 0.558)
- The factors determining the distribution of Foraminiferal assemblages are organic pollutants. The high species number at Gülbahçe Bay and Gediz River effluents verify this conclusion

REFERENCES

[1] RESIG, J.M., Foraminiferal ecology around ocean outfalls off southern California. In: Person, E. (Ed.), Disposal in the Marine Environment, Pergamon Press, London (1960) 104-121.

[2] WATKINS, J.G., Foraminiferal ecology around the Orange Country, California, ocean sewer outfall, Micropaleontology **7** (1961) 199-206.

[3] YANKO, V., AHMAD, M., KAMİNSKİ, M., Morphological deformities of benthic foraminiferal tests in response to pollution by heavy metals: Implications for pollution monitoring, J. Foraminiferal Res. **28** 3 (1998) 177-200.

[4] DEBENAY, J.P., TSAKIRIDIS, E., SOULARD, R., GROSSEL, H., Factors determining the distribution of foraminiferal assemblages in Port Joinville Harbor (Ile d'Yeu, France): The influence of pollution, Mar. Micropaeontology **43** (2001) 75-118.

[5] ARMYNOT DU CHATELET, E., DEBENAY, J.P., SOULARD, R.,Foraminiferal proxies for pollution monitoring in moderately polluted harbors, Environ. Poll. **127** 1 (2003) 27-40.

[6] LOEBLICH, J.R., TAPPAN, H., Foraminiferal genera and their classification, Van Reinhold Company **970** (1988) 842.

[7] MERIC, E., AVSAR, N., BERGIN, F., Benthic foraminifera of Eastern Aegean Sea (Turkey) systematics and autoecology, Turkish Marine Reseach Foundation and Chamber of Geological Engineers of Turkey, Publication **18** (2004) 306.

Speciation of mercury and tin in marine sediments and biological matrix

Mzoughi, N.[a], M. Brava[b], T. Stoichev[b], M. Dachraoui[c], G. Lespes[b], D. Amouroux[b], M. Potin-Gautier[b], O.F.X. Donard[b]

[a] Institut National des Sciences et Technologie de la Mer,
Laboratoire Milieu Marin,
Salammbô,
Tunisia

[b] Laboratoire de Chimie Analytique Bio-Inorganique et Environnement,
CNRS,
Université de Pau et des Pays de l'Adour,
Pau,
France

[c] Laboratoire de Chimie Analytique et Electrochimie,
Faculté des Sciences de Tunis,
Tunisia

The aim of this study was to investigate for the first time, the distribution of mercury and tin compounds in marine sediments and mussel tissues collected in Bizerte lagoon, Tunisia during two seasons (summer and winter).

Butyl-, Phenyl- and octyltin compounds were determined using a rapid speciation method. This analytical procedure is based on one-step simultaneous ethylation/extraction with sodium tetraethylborate in aqueous phase. Gas chromatography interfaced to Pulsed Flame Photometric Detection (GC-PFPD) was used to perform quantitative determination [1].

Analysis of methylmercury MMHg and inorganic mercury Hg^{2+} was performed by hyphenated system combining ethylation and/or hydride generation on-line with Cryogenic trapping, gas chromatography and atomic fluorescence spectrometry [2].

Validation of methods was performed using a certified sediment and biological reference material.

Results of organotin species cannot allow to establish any significant difference between the seasonal levels of contamination. The high values found in the South East of the lagoon and specially in the region of Menzel Bouguiba can be related to the intense industrial activities in this area. The predominance of butyl- and phenyltins comes probably from antifouling paints on boats and piers [3]. Indeed tributyl- and triphenyltins contained in these paints are directly released into the environment. Results show the predominance of butyltin compounds for all stations, and of monosubstituted compounds during summer.

Among all the organotins, the trisubstituted ones and specially TBT have quite high concentrations, which are widely due to releasing from antifouling paints, since an important maritime traffic exists in the lagoon.

The increasing of mono- and disubstituted compounds is attributed to the biodegradation phenomenon, which conducts to the successive desalkylation or desarylation of all the organotins since the concentrations of monoorganotins are slowly increasing.

Organotin contamination of biomass probably limited because concentrations observed in mussel tissues are rather low compared to those found in other coastal living organisms.

Results for speciation of mercury suggest that a fraction of the inorganic mercury load in the sediments of the lagoon undergoes methylation pathways. The MMHg produced is assimilated in the mussels more readily than the Hg^{2+}.

However, anthropogenic sources of inorganic mercury Hg^{2+}, most probably from metallurgy or tire production industries have been evidenced. One part of Hg^{2+} is methylated in the sediments and is assimilated by the mussels from the lagoon of Bizerte more readily than do Hg^{2+}. Finally, MMHg contamination of biological organisms is probably limited because concentrations observed in mussels tissues are rather low when compared to other coastal environments [4].

Consequently, for filter-feeding organisms, such as mussels, the concentrations of mercury and tin species determined in Bizerte Lagoon do not present significant toxicological risk for human consumption.

REFERENCES

[1] CARLIER-PINASSEAU, C., LESPES, G., ASTRUC, M., Appl. Organometal. Chem. **10** (1996) 505-512.
[2] TSENG, C.M., AMOUROUX, D., ABRIL, G., TESSIER, E., ETCHEBER, H., DONARD, O.X.F., Environ. Sci. .Technol. **35** (2001) 2627-2633.
[3] MAKKAR, N.S., KRONICK, A.T., COONEY, J.J., Chemosphere **18** (1989) 2043.
[4] COSSA, D., CLAISSE, D., Le methylmercure dans les mollusques du littoral Français, (1999) Ifremer, France.

Accumulation of heavy metals in shellfish from the coast of Tunisia

Chouba, L.[a], N. Langar-Zamouri[a], A. El Abed[a], M.S. Romdhane[b],

[a] National Institute of the Sciences and Technologies of the Sea (INSTM), Tunisia

[b] National Institute of Agronomy (INAT), Tunisia

The Tunisian coast is the site for many industrial and tourist activities that may affect the environmental quality and living marine resources of coastal zones. Several shellfish species are prospected but clams and mussels are the only ones that are actively exploited. Studies related to toxicity and pollutant impacts in Tunisia on marine fauna and flora have been reported in several works [1-3]. However, very few works were conducted on quantification of heavy metals in consumables or non-exploitable shellfish in the Tunisia coast. The main objectives of this study are:

(i) to estimate the levels of heavy metal pollutants such as cadmium (Cd), lead (Pb) and mercury (Hg);

(ii) to identify an indicator of the marine ecosystem chemical quality.

Samples were collected from various sites, selected according to the degree of pollution along the coastline area of Tunisia (Fig. 1).

The studied species and their numbers were: Tapes decussates(160), Mytilus galloprovincialis(80), Crassostrea gigas(60), Pinctada radiata(40), Solen marginatus(60), Mactra corallina(80), Donax trunculus(160) and Venus verrucosa(60). Each sample was measured and weighed, then the totality of the flesh was recovered in adequate small bottles. After homogenization, lyophilization and grinding, samples were mineralised at 90 °C by nitric acid on a hot plate during three hours. The Cd and Pb

FIG. 1. Study area with sampling locations.

concentrations were determined by graphite furnace Atomic Absorption Spectrometry (AAS, Varian model 220 Z), using an L'Vov platform, a matrix modifier and correction for non specific absorption by the Zeeman effect [4]. For Hg, the concentrations were measured by cold vapor AAS technique, using stannous chloride as a reducing agent [5]. The accuracy of the AAS and validity of the processes were tested with a reference material (ROMP).

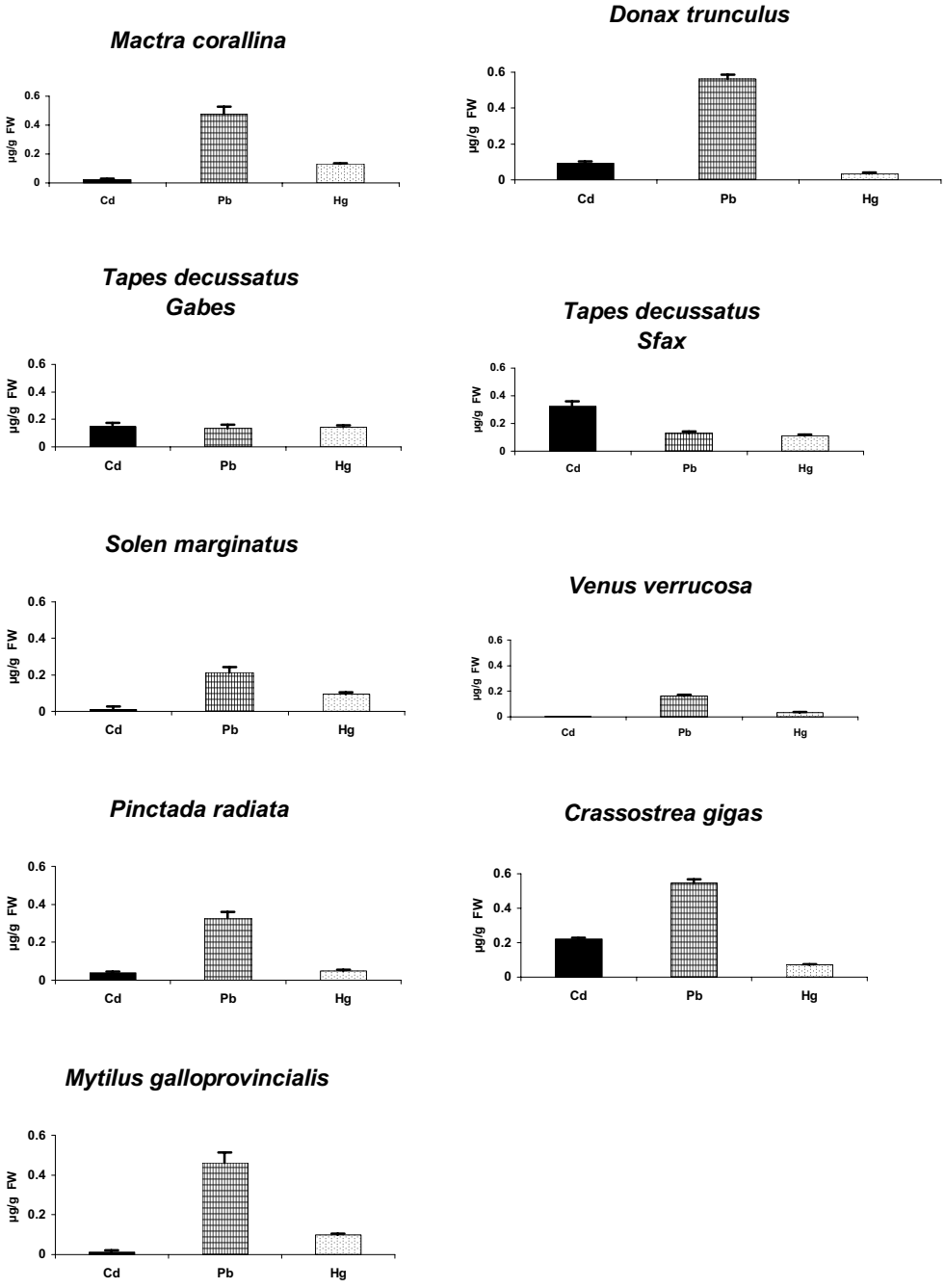

FIG. 2. Average concentration of trace metals (Cd, Pb, Hg) in different shellfish species. Error bars denote standard deviation.

Metal concentration in a tissue was presented as µg/g fresh weight (FW) and plotted on histograms (Fig. 2). Cd, Pb and Hg measured in different species ranged from 0,003 to 0,222, from 0,127 to 0,562 and from 0,033 to 0,131 µg/g FW, respectively. The concentrations of Pb, Cd and Hg determined in the flesh of three Bivalve species (*Mactra corallina*, *Donax trunculus* and *Solen marginatus*) sampled in northern area of Tunisia were relatively similar. This is can be explained by the fact that these species have the same bioaccumulation capacity for each metal, with less assimilation for lead by *Solen marginatus*. On the other hand, *Venus verrucosa* sampled in the same area showed a lower bioaccumulation capacity than that of other species. If we compare the bioaccumulation of metals between regions and within species, we found that the highest cadmium levels were recorded in clam flesh collected from Gabes and Sfax and in oyster flesh collected in Bizerte lagoon. Similar lead concentrations were obtained within all studied species in the different areas, except for clams collected from the south and "warty venus" collected from the north. Mercury accumulation were low compare to those found in Mediterranean shellfish. Concentrations recorded are dependent of shellfish species and locations.

The accumulation of metals depends on their availability in the ecosystem. The degree of ecosystem contamination is correlated to the amount of anthropogenic discharges. However, all concentrations remain lower than the thresholds recommended by the World Organization of Health (WHO). This preliminary work contributed to the study of bioaccumulation of three toxic metals such as Cd, Pb and Hg in some species of Bivalves collected along the Tunisian coasts. At the same time, these results give an idea about the ecosystem chemical quality. In future work, in order to compare and identify a new bioindicator, we will study other shellfish species (e.g. carnivores) coming from the same regions.

REFERENCES

[1] CHOUBA, L., AMARA, H., EL ABED, A., Heavy metals (Cd, Pb, Hg) in marine organisms from north Tunisian Coast, (Proc. Fifth Int. Conf. Mediterranean Coastal Environment, MEDCOAST) 1-3 (2001) 523 p.

[2] KHESSIBA, A., AISSA, P., Effet du lindane sur certains biomarqueurs de stress chez la moule (*Mytillus galloprovincialis*) originaire de la lagune de Bizerte (Tunisie), ctes des 5èmes Journées Tun. Scien. de la Mer Bull. INSTM, N. Spécial **7** (2002) 132-135.

[3] M'ZOUGHI, N., STOICHEV, T., DACHRAOUI, M., EL ABED, A., AMOUROUX, D., DONARD, O.F.X., Inorganic mercury and methylmercury in surface sediments and mussel tissues from a microtidal lagoon Bizerte, (Tunisia), J. Coastal Conserv. **8** (2002) 141-145.

[4] SHNITZER, G., PELLERI, C., LOUET. C., Apport des micro-ondes à la minéralisation humide d'un produit biologique en vue du dosage du Hg par SAA. *Bu*ll. Lab. Vét. N° 25, (1987).

[5] UNEP/IAEA/FAO, Determination of total cadmium, zinc, lead and copper in selected marine organisms by atomic absorption spectrophotometry. Reference Methods for Marine Pollution Studies N° 11 Rev. 11 49 (1990).

[6] UNEP/IAEA/FAO, Determination of total mercury in selected marine organisms by cold vapour atomic absorption spectrophotometry, Ref. Meth. Mar. Poll. Studies **8** 1 (1984).

Total arsenic in marine organisms from Cienfuegos Bay, Cuba

Alonso-Hernandez, C.[a], M. Gómez Batista[a], A. Muñoz-Caravaca[a], S. Pérez-Santana[a], M. Díaz-Asencio[a], J. Estévez Alvarez[b], I. Pupo González[b], N. Alberro Macías[b]

[a] Centro de Estudios Ambientales de Cienfuegos,
Ciudad Nuclear,
Cienfuegos,
Cuba

[b] Centro de Aplicaciones Tecnológicas y Desarrollo Nuclear,
Ciudad de la Habana,
Cuba

Levels of total arsenic were determined in muscle tissues of species of finnish, crustaceans and molluscs from Cienfuegos Bay, Cuba. The arsenic contents in the samples were determined using an Energy Dispersive X Ray Fluorescence (EDXRF) method. The highest values of Total arsenic were found in crustaceans. Averages found for fish, crustaceans and molluscs were 10.2, 26.5 and 22 μg g^{-1} dry wt, respectively. These results are considered to be characteristic for normal or naturally altered areas.

Cienfuegos Bay, situated in the Southern part of Cuba, is a semi-enclosed bay with a surface area of 90 km^2 and an average depth of 14 m. It is connected to the Caribbean Sea by a narrow channel 3 km long. The bay is divided in two well defined hydrographic basins, due to the presence of a submerged ridge 1m below the surface. The Northern basin receives most of the anthropic impact from the outfall of Cienfuegos city (150,000 inhabitants), industrial pole in the country, and the freshwater input of Damuji and Salado rivers. The Southern basin is subjected to a smaller degree of anthropic pollution originating from the Caonao and Arimao rivers. Part of the Southern basin is a natural park, which represents a niche for protected migratory birds and marine species.

The bay represents the most important natural resource in the province, due to fishing activities, maritime transport, tourism industry and natural parks. During the last decade it has acquired an important economic and social development, resulting in an increase of industrial and domestic wastes which are discharged into the bay. Direct input of Arsenic to Cienfuegos bay occurs through the Nitrogen Fertilizer Factory, which was authorized to release Arsenic residuals up to 1981 and where two accidental As spills took place in 1979 and 2001.

Marine organisms represent an important component of the diet of the population of Cienfuegos. In particular, people from the coastal areas of Castillo de Jagua, Las Minas and O'bourque have an average ingestion rate of fish of 51 kg yr^{-1}, varying from 21 to 116.

Only a few studies have investigated the total As content in marine organisms from Cuba. In particular, a survey of marine products from the Western coast, displayed concentrations of Arsenic ranging from 0.01 to 4.82 μg g^{-1}d.w. [1]. Total Arsenic in fish and crustaceans was also measured in Cienfuegos Bay in 1974 and results showed low concentrations of this compound (1.2 μg g^{-1} d.w. in fish and 1.7 in crustaceans).

Sixteen species of fish, two of molluscs and three of crustaceans were caught in Cienfuegos Bay. The target species were selected among those of dietary importance for the population.

The arsenic contents in the samples were determined using an Energy Dispersive X Ray Fluorescence (EDXRF) method (Si/Li detector with 180 eV for Mn Kα and Cd-109 annular source. The elaboration of the spectra and quantitative analysis was carried out using the QSAX System [2]. Compton peak was used for the matrix effects correction. Several Biological Certified Reference Materials (NRCC DOLT-2 Dogfish Liver, NRCC TORT-2 Lobster Hepatopancreas, NIES CRM-9 Sargasso, NRCC DORM-1 Dogfish Muscle and IAEA-140/TM Seaweed *Fucus sp.*) were measured for calculating the As concentrations in the samples.

The highest values of Arsenic were found in crustaceans, which showed a mean value of 26.5 μg g^{-1} d.w. (values ranging from 6.9 to 53.9). These levels are in agreement with others found in literature for shrimps and marine crabs captured in estuaries and enclosed bays [3-5]. The higher Arsenic content in tissues of bottom dwellers such as shrimps and crabs, can be attributed to their habitat being close to the sediment. Sediments are always higher in Arsenic than water and bottom water usually contains higher As concentration than surface water [6, 7]. When comparing the obtained values from this study with those reported in 1974 for shrimps from Cienfuegos bay, we observed that the mean value of Arsenic in crustaceans was 18 times higher than at the time. This could be explained through the increase of antrophic activity in the area during the last decades, when artificial sources of As were established in the coastal zone. In particular, the routine and accidental release of Arsenic residuals from the Nitrogen Fertilizer Factory could be responsible for the observed pattern.

In the fish muscle, the mean As concentration was 10.21 μg g^{-1} d.w. (values ranging from 2 to 42.6). These results are considered to be characteristic for normal or naturally altered areas. The international reports consulted [8, 3, 9] indicate that marine fish can reach total As contents up to 150 μg g^{-1} d.w., without any risk for the population that consumes it. However, as for the crustaceans, the Arsenic levels obtained in this study are 12 times higher than those reported in fish from Cienfuegos bay in 1974, and are considerably larger that those reported by [1] in fish captured from Western Cuba.

REFERENCES

[1] BELTRAN, G., SYMINTON, R., DOMINGUEZ, A., AMALIA, E., ROCH, R., Arsenic residues in marine products from the western zone of Cuba, Rev. Cubana Hig. Epidemiol. **26** (1988) 100-105.
[2] INTERNATIONAL ATOMIC ENERGY AGENCY, Manual for QXAS, Quantitative X-Ray Analysis System (version 3.2), IAEA, Vienna (1995).
[3] SUÑER, M.A., DEVESA, V., MUÑOZ, O., LOPEZ, F., MONTORO, R., ARIAS, A.M., BLASCO, J., Total and inorganic arsenic in the fauna of the Guadalquivir estuary: environmental and human health implications, Sci. Tot. Environ. **242** (1999) 261-270.
[4] STEPHAN, SATHY, (2000).
[5] XIU-SHENG et al., (2001).
[6] BYRD, J.T., The seasonal cycle of arsenic in estuaries and near shore waters of the South Atlantic Bight, Mar. Chem. **25** (1988) 383-394.
[7] TREMBLEY, G.H., GOBEIL, C., Dissolved arsenic in the St Lawrence Estuary and the Saquenay Fjord, Canada, Mar. Poll. Bull. **21** (1990) 465-431.
[8] RONAL EISLER, (1981).
[9] KHUDRE, M.A., ZAMIL, M., RAWDAH, T.N., TAWABINI, B.S., Levels of Arsenic in Fish from the Arabian Gulf, Mar. Poll. Bull. **24** (1992) 94-97.

Arsenic accumulation by ferns from the iron quadrangle, Minas Gerais, Brazil

Palmieri, H.E.L.[a], H.A. Nalini Jr.[b], M.Â. de B. C. Menezes[a], J.B.S. Barbosa[a], J. dos S.J. Pereira[a], L.V. Leonel[a]

[a] Nuclear Technology Development Centre,
National Commission for Nuclear Energy (CDTN/CNEN),
Belo Horizonte,
Minas Gerais,
Brazil

[b] Federal University of Ouro Preto,
Geological Department,
Ouro Preto,
Minas Gerais,
Brazil

The Iron Quadrangle, located in the Brazilian state of Minas Gerais, is considered one of the richest mineral-bearing region in the world [1, 2]. It is well known for the occurrence of iron and gold ores. A great number of active and ancient gold mines can be found in this region. The gold ore is rich in arsenic with the As/Au ratios ranging from 300 to 3000 [3]. In the past companies produced As-oxide as a byproduct in Nova Lima and Passagem de Mariana regions. Dressing materials were usually stored along the rivers or simply thrown in the drainage (e.g. Carmo river in Passagem de Mariana). Nowadays, big dams have been built to store the tailings and the effluents are being treated according to environmental regulations [3].

Ma et al. [4] and Francesconi et al. [5] have demonstrated that the fern species, *Pteris vittata* and *Pityrogramma calomelanos* are arsenic hyperaccumulate plants and recommend them for use in the remediation of arsenic-contaminated soils. These species were suggested for phytoremediation due to their high bioaccumulation factors, short life cycle, high propagation rates, wide distribution, large shoot mass and their ability to tolerate high arsenic concentrations in soils [6]. Phytoremediation, an emerging plant-based technology for the removal of toxic elements from the soil and water has been receiving renewed attention.

The aim of this work was to evaluate the uptake of arsenic by the ferns *Pteris vittata* and *Pityrogramma calomelanos* collected in an area of the Iron Quadrangle that might be suffering influence from contaminated arsenic waste from old gold mines. These ferns are commonly found in this region.

Fern samples and the soil within the root mass were collected in February and March 2003. The samples (*Pteris vittata*) were divided into leaves and rhizoids. The leaves and rhizoids were washed thoroughly with tap water, rinsed with deionized water and sliced in small pieces. After freeze dried, the samples were ground and sieved (< 5 mm) to be analyzed. The soil samples were air-dried, sieved and the finest–grains < 250 mesh, consisting of silt and clay, were used for analysis.

Arsenic concentration in the soil and fern tissue was determined using neutron activation analysis (NAA) specifically the k_0-standardization method and the energy dispersive spectrometry technique (EDS). A KEVEX RAY with Am^{241} as photons source, was used. The irradiation was performed in the reactor TRIGA MARK I IPR-R1 at CDTN, at 100 kW, under a thermal flux 6.6 10^{11} neutrons. cm^{-2} s^{-1}.

Table I. Arsenic concentration in soil and fern tissue

Site	UTM coordinates	Sample	Arsenic ($\mu g\ g^{-1}$ dry mass)
01	676 762 / 7 749 122	Soil	12
		Pteris vittata (rhizoid)	55
		Pteris vittata (leaves)	102
02	658 496 / 7 755 208	Soil	12
		Pteris vittata (rhizoid)	263
		Pteris vittata (leaves)	373
03	658 395 / 7 755 080	Soil	100
		Pteris vittata (rhizoid)	128
		Pteris vittata (leaves)	202
04	663 945 / 7 746 302	Soil	957
		Pteris vittata (leaves)	2585
		Pityrogramma calomelanos (leaves)	1710

The gamma spectroscopy was performed in a HPGe detector 15% of efficiency. The gamma spectra were obtained and evaluated by HyperLab PC software and the concentration calculated using the KAYZERO/SOLCOI software.

As shown in Table I, the results obtained confirm literature data. The ferns *Pteris vittata* and *Pityrogramma calomelanos* actually extract arsenic from the soil and translocate it into its fronds with higher arsenic concentration in the leaves than in the rhizoids. The highest value of arsenic was found in the soil and ferns collected at site 04. In the past this region was the local where waste from the Passagem de Mariana mine used to be thrown.

Further studies on arsenic accumulation by these ferns are necessary to evaluate the use of the phytoremediation in Brazilian arsenic-contaminated soils.

REFERENCES

[1] BRAZIL GOLD'91 – The economics, geology, geochemistry and genesis of gold deposits. Proceedings...Symposium Brazil Gold'91, 13 – 17 May 1991, Belo Horizonte.

[2] MATSCHULLAT, J., BORBA, R.P., DESCHAMPS, E., FIGUEIREDO, B.R., GABRIO, T., SCHWENK, M., Human and environmental contamination in the Iron Quadrangle, Brazil, Appl. Geochem. **15** (2000) 181-190.

[3] BORBA, R.P., Arsênio em ambiente superficial: processos geoquímicos naturais e antropogênicos em uma área de mineração aurífera. PhD Thesis, State University of Campinas, Geoscience Institute, São Paulo (2002).

[4] MA, L.Q., KOMART, K.M., TU, C., ZHANG, W., CAI, Y., KENNELLY, E.D., A fern that hyperaccumulates arsenic, Nature **409** (2001) 579.

[5] FRANCESCONI, K., VISOOTTIVISETH, P., SRIDOKCHAN, W., GOESSLER, W., Arsenic species in a hyperaccumulating fern, Pityrogramma calomelanos: a potencial phytoremediator of arsenic-contaminated soils, Sci. Tot. Environ. **284** (2002) 27-35.

[6] VISOOTTIVISETH, P., FRANCESCONI, K., SRIDOKCHAN, W., The potential of Thai idigenous plant species fort he pytoremediation of arsenic contaminated land, Environ. Poll. **118** (2002) 453-461.

Occurrence of Butyltin compounds in sediment and bivalve from three harbour areas (Ho Chi Minh, Da Nang and Hai Phong) in Viet Nam

Dang, D.N.[a], D.T. Loan[a], I. Tolosa[b], S.J. de Mora[b]

[a] Institute for Nuclear Science and Technology,
Hanoi,
Vietnam

[b] Marine Environmental Studies Laboratory,
Marine Environment Laboratory,
International Atomic Energy Agency,
Monaco

Organotin compounds (OTs) such as butyl- and phenyltin were widely used in the past as stabilizers in PVC production and in antifouling paints for marine vessels of all types. Ecotoxicity of these compounds was proven to cause imposex in marine snails and shell malformation in oysters [1, 2]. The occurrence of OTs has been well studied for coastal South Korea, Japan, China, Thailand, and Malaysia [3, 4]. In these areas, TBT was measured in marine sediments, seawater, and biological samples at higher concentrations than its metabolites monobutyltin (MBT) and dibutyltin (DBT). Shipyard activities were the main source of OTs in these regions.

Viet Nam, located along the South China Sea, has a coastline of 2,000 km where the shipbuilding industry was intensively developed many years ago. It is believed that a large amount of OTs was used in antifouling paints for vessel hulls in the yards and dry docks. Only limited data exist regarding the level of organotin contamination in the marine environment of Vietnam [5,6]. This study aims to improve the regional database for OTs in the marine environment.

The study was conducted in 2003 with sediment and bivalve (*Meretrix meretix*) samples. Sediment was taken from dry docks in Ho Chi Minh and Hai Phong cities and from cargo harbours in Ho Chi Minh (south), Da Nang (centre) and Hai Phong (north) (Figure 1). The clams were bought from local fishermen cruising around the harbours, as well as near dry docks in Ho Chi Minh and Hai Phong. OTs compounds: tributyltin (TBT), monobutyltin (MBT), and dibutyltin (DBT) were analysed using a previously reported procedure [7].

TBT, DBT and MBT were found in all the samples. The concentration of ΣBTs was highest (122 ng Sn g^{-1} d.w) in sediment from Song Cam (Hai Phong), where 7 shipbuilding and vessel repair yards are located. The lowest concentration of ΣBTs (21-22 ng g^{-1} d.w) was found in sediment from cargo ports (Da Nang, and Hai Phong). This implies that the main source of BTs in the marine environment in Viet Nam is the shipbuilding activities. For the clam (*Meretrix meretrix*), the concentration of ΣBTs varied in the range 11-60 ng Sn g^{-1} wet wt. There was a good correlation (R^2=0.85) between total organic matter- (TOM) normalised ΣBTs in sediment and hexane extractable organic matter- (HEOM) normalised ΣBTs in clam soft tissue. The mean Biota Sediment Accumulation Factors (BSAFs, organic carbon/lipid) for MBT, DBT and TBT in clam's soft tissue were found to be 1.83±0.66, 1.44±0.23 and 1.16±0.47, respectively, indicating that sediment-bound OTs might be an important source of contamination for the clam. The ratio of TBT to Σ(MBT + DBT) in sediment was 0.67± 0.03 for all the sampling sites indicating the recent use of TBT in Vietnam. Although, legislation to control the use of butyltin compounds in the country started only in 2003, further studies on the occurrence and environmental behaviour of these chemicals in the tropical marine environment are required.

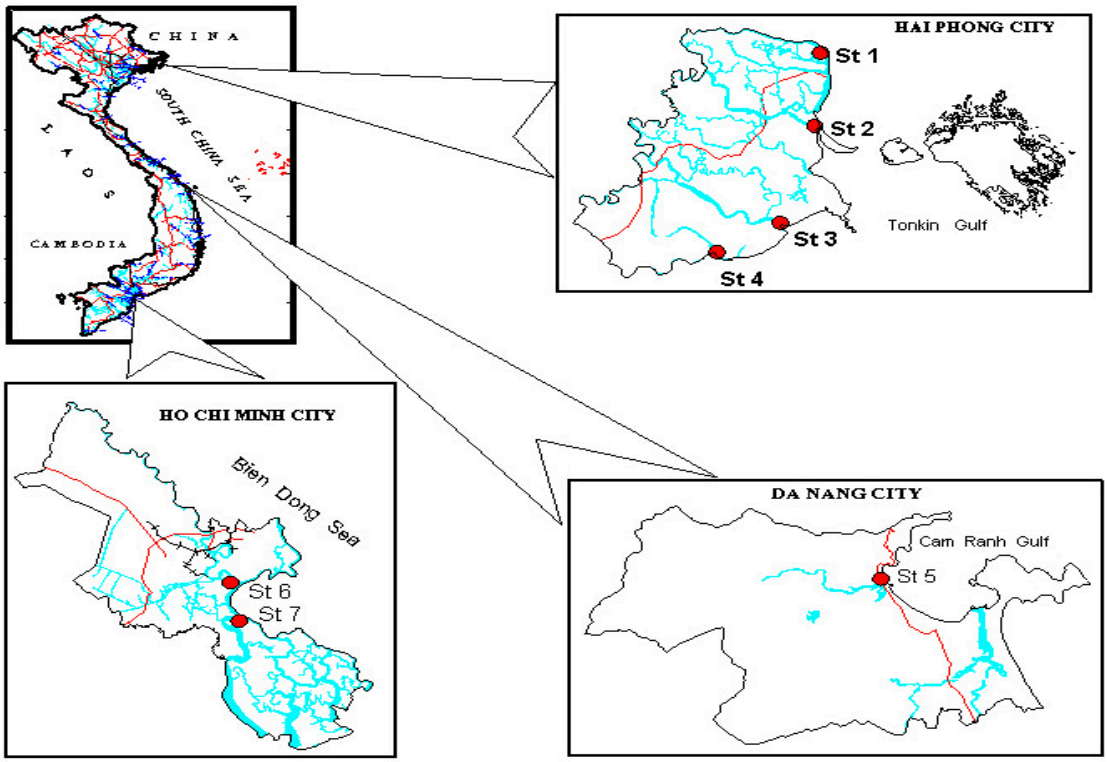

FIG. 1. Map showing sampling locations: St 1: Nam Trieu mouth, St 2: Song Cam mouth, St 3: Hai Phong cargo port, St 4: Lach Tray mouth, St 5: Da Nang cargo port, St 6: Ba Son shipyard, St 7: Sai Gon cargo port.

ACKNOWLEDGEMENT

The Work has been carried out with financial support from IAEA Research Contract No.11823/RBF. The Agency is grateful for the support provided to its Marine Environment Laboratory by the Government of the Principality of Monaco.

REFERENCES

[1] ALZIEU, C., et al., Tin contamination in Arcachon Bay. Effects on oyster shell anomalies, Mar. Poll. Bull. **17** (1986) 494.

[2] HALLERS-TJABBES, C.C.T., et al., Imposex and organotin concentrations in *Buccinum* and *Neptunea antiqua* from the North Sea: relationship to shipping density and hydrographical conditions, Mar. Environ. Res. **55** (2003) 203.

[3] HYAE-KYUNG, H., et al., Butyltin residues in blue mussels (*Mytilus edulis*) and arkshells (*Scapharca broughtonii*) collected from Korean coastal water, Environ. Poll. **117** (2002) 475.

[4] BECH, M., Imposex and tributyltin contamination as a consequence of the establishment of a marina, and increasing yachting activities at Phuket Island, Thailand, Environ. Poll. **117** (2002) 421.

[5] KANNAN, K., et al., Butyltins in muscle and liver of fish collected from certain Asian and Oceanic countries, Environ. Poll., **90 (**1995) 279.

[6] MIDORIKAWA, S., et al.,Concentrations of organotin compounds in sediment and clams collected from coastal areas in Vietnam, Environm. Poll. **131 (**2004) 401.

[7] CASSI, R., et al., Organotin speciation analyses in marine biota using sodium tetraethylborate ethylation and gas chromatography with flame photometric detection, Appl. Organom. Chem. **16** (2002) 355.

Nuclear detectives - reconstructing histories of toxic dinoflagellates & blue green algae in coastal lakes and estuaries

Heijnis, H.[a], A. McMinn[b], G. Hallegraeff[b], K. Srisuksawad[c]

[a] ANSTO Environment,
Menai NSW,
Australia

[b] University of Tasmania,
Hobart,
Australia

[c] Office of Atoms for Peace,
Bangkok,
Thailand

Using isotopic, geochemical and microfossil analyses of sediment cores, it is possible to reconstruct pre and post-colonial environmental conditions of coastal lakes and estuaries and their catchments. This is an important management tool, not only for determining the base line 'natural' conditions of these ecosystems but also identifying the nature and extent of changes they have experienced through time, including the influx of pollutants and changes in sedimentation regimes. Such information is generally not available from historic records.

Practical examples includes the following case-studies:

1) Tasmania & South Australia - Over the past couple of decades “alien species” have been introduced to the coastal waters of Australia and of Tasmania in particular, such as the toxic dinoflagellate *Gymnodinium Catenatum.* Careful dating and reconstruction of sediment archives have revealed the time and nature of this arrival.

2) NSW Blue Green Algae in the Great Lakes Area: The occurrence of blue-green algal blooms in the Great Lakes area of NSW have now been linked with catchment changes and the dynamics of this coastal system, using reconstructed histories from sediment cores.

These detailed histories span the last 60 – 80 years, and cover the post World War II coastal population & development expansion.

Occurrence and availability of prioritary compounds (chlorinated pesticides, polybrominated diphenyl ethers, alkylphenols and heavy metals) in freshwater sediments and fish

Lacorte, S., E. Martínez, D. Raldúa, A. Navarro, D. Barceló

Department of Environmental Chemistry,
IIQAB-CSIC,
Barcelona, Catalonia,
Spain

The aim of this work was to determine priority organic and inorganic compounds in river sediments and fish and to study their availability. Twelve organ chlorinated compounds (OC), 40 polybromodiphenyl ethers (PBDEs), 2 alkylphenols (nonylphenol and octylphenol) (AP), and 9 heavy metals (HM) were investigated in samples taken in 20 locations along the Ebro river, in north east Spain. Sediment samples represent a stable matrix which indicate recent pollution episodes, whereas fish samples are good sentinels to monitor bioavailability and bioaccumulation. Compound selection was based on their inclusion in European priority lists (Directives 76/464/CEE and 60/2000/EU). The study area covered the Ebro hydrographic basin which is the main tributary in Spain and flows through large agricultural areas characterized by wines, corn and maize and represents an important water source for the many industrial and urban activities settled along its course. To control the quality of the river basin, and in accordance with EU Directives, priority pollutants have been determined in sediment and fish to determine most ubiquitous compounds, geographical distribution and bioavailability of pollutants to two different fish species. For such purpose, different analytical methods were developed to analyse all the above mentioned chemical species in the upper 2 cm sediment layer and in whole fish (*Barbus graellsii, Cyprinus carpio)*. Among compounds studied, hexachlorocyclohexane, pentachlorophenol, aldrin, dieldrin and isodrin, and trichlorobenzene were never detected. All samples contained organic pollutants at total levels between 134 and 3199 µg/Kg-dw and total HM from 60.9 and 5131 mg/kg-dw, depending on sample location. For 18 of the 20 samples points, a correlation of 0.53 was found between total organic and total inorganic concentration. In sediment samples, among the 4 chemical groups studied, HM were present at levels between 0.17 and 4036 mg/kg dry weight (dw), being Hg detected at a high concentration downstream from an important chemical industry and Cu, Pb and Zn showed highest levels at the river source and at the river outlet. It is relevant that octylphenol was found in the totality of sediments analysed at a concentration from 48.5 to 152.1 µg/kg-dw whereas nonylphenol was detected in 8 samples out of 18 analysed but at much higher concentration, from 160.6 to 3000 µg/kg-dw, being the levels highest in industrialized areas (in river source, close to Zaragoza city, in the industrialized area of Monzón and in the city of Tortosa). 2,4 and 4,4-DDT, DDD and DDEs were also detected in all sediments with total levels between 4.7 to 240.9 µg/kg-dw. In most locations, the levels of DDTs were higher than DDEs or DDDs, indicating a slow degradation or a still recent input. In other cases, only DDT was encountered. Highest levels were in the city of Tortosa, located just before the estuary and characterized by both agricultural and industrial activities. PBDEs were found in 16 samples at a concentration range between 0.04 and 20.9 µg/kg-dw, being the main congeners encountered BDE 47 and BDE 99, as reported in other sediment samples [1]. In some locations, high levels of DDT were correlated also with high levels of PBDEs, indicating point source pollution of these two families of compounds.

Fish samples followed a similar picture as regards to the fact that all fishes contained levels of organic and inorganic compounds, as indicated in previous works (2). However, despite 2 species were collected from each site, no correlation was found between the levels of organic nor inorganic compounds, probably due to the fact that although they corresponded to the same trophic level, the

biology is different. Among the organic compounds studied, hexachlorobenzene, DDT and metabolites, AP and PBDEs were detected. HM were detected at levels between 0.04 and 68.9 mg/kg ww, being in all cases lower than the levels found in sediments. Only in one site close to an industrial area, Hg was found at highest levels (up to 1.89 mg/kg-dw) and this correlated with high levels of hexachlorobenzene in the same fish (up to 169 µg/kg-dw). In contrast to sediment samples, OP was detected in only one sample at a level of 6.9 µg/kg-dw whereas NP was detected in 2 stations at levels from 74.5 to 146.4 µg/kg-dw. No correlation was found between AP levels in sediment and fish, indicating that sediments was not a source of AP to fish or that fish may metabolise such compounds.

On the other hand, total DDTs and total PBDEs, concentration was higher in fish than in sediment, with levels from 5.1 to 2447.4 µg/kg-dw for the former and between 0.1 and 218.5 µg/kg-dw for PBDEs. For total DDTs total PBDEs, good agreement was found among levels in sediment and in fish, indicating that these compounds can be bioaccumulated in freshwater fish. Fish with highest loads were situated close to big urban areas or with important agricultural activities.

It can be concluded that DDTs and PBDEs, which account for the more persistent organic compounds, have been encountered in practically all samples analysed and that levels in fish are higher than in sediment, indicating that sediment can be a drainage of persistent pollutants and a source to biota.

REFERENCES

[1] LACORTE, S., GUILLAMON, M., MARTINEZ, E., VIANA, P., BARCELÓ, D., Occurrence and specific congener profile of 40 polybrominated diphenyl ethers in river and coastal sediments from Portugal, Environ. Sci. Techn. **37** (2003) 892-898.

[2] VIVES I BATLLE, J., GRIMALT, J.O., LACORTE, S., GUILLAMÓN, M., BARCELÓ, D., Polybromodiphenyl Ether (PBDE) Flame Retardants in fish from lakes in European high mountains and Greenland, Environ. Sci. Techn. **38** (2004) 2338-2344.

Fate of alkylphenols, chlorophenols and bisphenol A in the Lake Shihwa, Korea

Oh, J.R., D. Li

South Sea Institute,
KORDI,
Geoje,
Korea, Republic of

Surface water, suspended particles in surface water and sediment samples from the brackish lake, Shihwa, and its surrounding creeks were collected during Aug. 2001 to May 2004 in Korea. Representative endocrine disrupting chemicals (EDCs) such as alkylphenols, chlorophenols and bisphenol A, were determined from each matrix by GC/MS [1]. Among them, alkylphenol compounds were recorded as the major pollutants affecting Lake Shihwa water quality [2, 3].

High concentration of alkylphenols were measured in those matrices in and around industrial complexes. The levels decreased gradually with distance from the industrial areas. Though alkylphenols concentration in sediment varied from that of water and suspended particle, high concentrations were generally found in industrial area and in central part of the Lake Shihwa. Concentrations of nonylphenol from industrial area were similar or higher than US and EU regulatory value which is 1 μg/L. Spatial and seasonal variation of alkylphenol in dissolved water and suspended particulate were similar but not in the sediment. The alkylphenol concentration was the highest in summer and the lowest in winter. There is no annual correlation on the levels of alkylphenol in water and particulate. Phenolic compounds are continuously discharged into Lake Shihwa from surrounding industries and hence the input of alkylphenols increases in time. Alkylphenol compounds were continuously produced by biodegradation of alkylphenol polyethoxylate and it was accumulated in the sediments by adsorption. Nonylphenol and bisphenol A were the major endocrine disrupting chemicals determined in the Lake Shihwa. The contents of nonylphenol and bisphenol A in dissolved water, suspended particle and sediment are 60, 70, 90% and 35, 25, 8%, respectively. The levels of these chemicals measured in creeks were about 25 times higher than those in Lake Shihwa.

In order to identify the source and behavior of alkylphenols in the environment, the relationship between nonylphenol and water quality parameters such as salinity, pH, DO, COD, TN and TP were studied. Those parameters point to industrial input as the principle source of alkylphenol pollution to Lake Shihwa.

In order to investigate vertical distribution profile of alkylphenols in the sediment, two sediment cores were collected from Lake Shihwa. The concentrations profile indicates that the lowest concentration were at the surface layer and the highest at the bottom. The degradation rate of nonylphenol in the seawater was lower than it's parent compounds namely nonylphenol diethoxylate. Detailed study is underway in our laboratory to understand this fully.

REFERENCES

[1] LI, D., OH, J.R., PARK, J., Silyl derivatization of alkylphenols, chlorophenols and bisphenol A for simultaneous GC/MS determination, Anal. Chem. **73** (2001) 3089-3095.

[2] LI, Z., LI, D., OH, J.R., JE, J-G., Seasonal and spatial distribution of nonylphenol in Shihwa Lake, Korea, Chemosphere **56** (2004) 611-618.

[3] LI, D., KIM, M., OH, J.R., PARK, J., Distribution characteristics of nonylphenols in the artificial Lake Shihwa, and surrounding creeks in Korea, Chemosphere **56** (2004) 783-790.

An investigation of the important parameters used for application of chemical reaction model at environmental soils in Egypt

Kamel, N.H.M.

Radiation Protection Department,
Nuclear Research Center,
Atomic Energy Authority,
Cairo,
Egypt

Aquatic sediments are principally derived from weathering process. The Industrial wastes and mining activities are the potential sources of pollution. Uranium is a common element in the earth, it has moved and will be moved by naturally occurring geochemical process. Phosphates are usually from naturally and/or synthetic wastes. The objective of our research was to test of the environmental soils and/or sediments as an adsorbent media for the removal of uranium and phosphate compounds from environmental sediment samples. The coastal line sites such as Sharm El-Sheikh, Taba, Dahab and Hardgea attract over one millions tourists every year. Contamination by phosphates and uranium represented a great hazardous effect on the tourism industries. Studying of the pollution by the phosphate compounds especially with uranium is very important. The experimental procedures in this study were carried out using the above mentioned marine sediments and other fresh water sediments from other parts along the River Nile in Egypt. mineralogical investigations were carried out with X-ray diffraction technique. The sediment samples showed that it contained of the major kaolonite mixed with feldspar and quartz minerals. Chemical analyses of the sediments showed that the environmental sediments contain, 60 to 85% SiO_2, 9 to 25% Al_2O_3 and 2 to 5% Fe_2O_3. carbonates were found 9 – 13% and the organics % are < 5%. Concentrations of the PO_4^{3-} at the environmental sediments in aqueous distilled water was found 0.1 to 1.3 * 10^{-3} mg/kg, PO_4-^{3} ions in the aqueous phase was found > 1.5 and 2 mg/kg at Port-Said and Rashid samples. Concentrations of the soluble UO_2 was found less than 0.5 mg/kg at all the investigated samples. The pH of the soils in distilled water was found from 7.8 to 8.1, the pH of the Rashid sample was found to be 6.2. In order to obtain the limitation of the solubility of phosphate compounds .Different concentrations of PO_4 were equilibrated with the fixed weights of the solid samples volume of the aqueous phosphate solutions ranged from 0.2 to 2 ppm were added to the dried sediment samples. Concentrations of PO_4^{3-} remained at the aqueous phase were determined by the stannous chloride photometric method. The solid surfaces of environmental sediment and soils are amphoteric has a certain surface charge depends on the solution hydrogen ion concentrations. At a certain pH value, the solid surface has a net zero charge, in which the solid surface has no charge. The point of zero charge of the sediment samples were determined by the salt effect [1]. The PZC was found 7 to 8 for all the samples. Figure 1 shows an example of the determination of the PZC of sample (Dahab). The constant capacity model was used for the determination of the specific PO_4^{3-} in equilibrium with solid phase. When a certain volume of distilled water were added to the environmental sediment samples, the slightly adsorbed phosphate and uranium ions were released, and sometimes phosphate only without uranium were released. Concentrations of the phosphates and uranium released depending on the pH of the solid in water. The species and the equilibrium constants of PO_4^{3-}in water – sediment system at a certain pH value. According to the mass action law was given as:

$$\equiv SOH + H^+ \Leftrightarrow SOH_2^+ \quad (1)$$

$$SOH \Leftrightarrow SO^- + H^+ \quad (2)$$

$$\equiv SOH + H_3PO_4 \Leftrightarrow \equiv SH_2PO_4 + H_2O \quad K_1 = 10.5 \quad (3)$$

$$\equiv SOH + H_3PO_4 \Leftrightarrow \equiv SH_2PO_4^- + H^{+\cdots\cdots} \quad K_2 = 5.00 \ . \quad (4)$$

$\equiv SOH + H_3PO_4 \Leftrightarrow SH_2PO_4^{2-} + H_2O + 2\,H^+ \quad K_3 = -1.16$ (5)

the possibility of the presence of the uranuyl phosphate species in water and their equilibrium constants Ka_1, Ka_2, Ka_3 were given by the following Equations 6-8 as follows:

$UO_2HPO_4 \Leftrightarrow UO^{2+} + HPO_4^{2-}$ ……Ka1 = -8.41 (6)

$UO_2H_2PO_4^+ \Leftrightarrow UO_2^{2+} + HPO_4^{2-} + H^+ \quad Ka_2 = -10.23$ (7)

$UHPO_4^{2+} \Leftrightarrow U^{4+} + HPO_4^{2-} \quad Ka_3 = -12.05$ (8)

Neglecting of the other uraniyl phosphate species because it has a low equilibrium constants. By applying the constant capacity model (CCM) and the intrinsic equilibrium constants. Eq. 9 is an example of that was applied for the reaction 1 as [2] :

$$K_{s1}\,(in) = \frac{\left[SOH_2^+\right]}{\left[SOH\right]\left[H^+\right]}\exp\left(F\psi o / RT\right) \quad (9)$$

by similar way the intrinsic equilibrium constant was applied for the other chemical reactions (2-8). The state of the different species, SOH_2+, SO^-, $\equiv SH_2PO_4$, $\equiv SH_2PO_4^-$, $\equiv SHPO_4^{2-}$, $UO_2H_2PO_4$, $UO_2H_2PO_4^-$, $UHPO_4^{2+}$ at pH 7.8 to 8.1 were determined.

The results showed, by the ion activity products (IAP). The saturation index (SI) was calculated and equal log(IAP/Keq.), so, when SI = 0, the phosphate compound was in equilibrium with the solid phase, when, SI has a negative value, the phosphate compound will dissolve and when SI has a positive value, the phosphate compound will precipitate. Keq was used from the reactions of the Eq. 1-8. The results showed that, phosphate ions was in equilibrium with the solid phase at phosphate concentration $1.3 * 10^{-3}$ mg/kg, PO_4^{3-} ions was soluble at the concentrations 0.01 to $0.1 * 10^{-3}$ mg/kg, PO_4^{3-} ions was precipitated at the concentrations > $1.5 * 10^{-3}$ mg/kg and uranium was soluble at the concentrations < $0.5 * 10^{-3}$ mg/kg. Phosphate compounds at most of the sediments of the River Nile, Agamy, Port-Said and Rashid samples are over saturated that is mean that these sites are more polluted and the uranyl phosphate compound has a great hazardous effect on the living organisms.

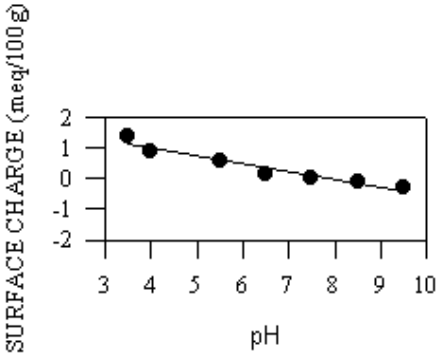

FIG. 1. The point of zero charge of Dahab sample.

REFERENCES

[1] WERNER, S., Chemistry of the Solid – Water Interface John Wiley & Sons, Inc. (1992).

[2] URE., A.M., DAVIDSON, Chemical Speciation in the Environment, Blackie Academic & Professional (1995).

Reconstruction of water purification system using soil - sorption of refractory DOM and phosphate ion to soil beads under static and dynamic water flow conditions

Fujikawa, Y.[a], T. Hamasaki[b], G. Prasai[b], R. Imada[b], E. Ikeda[b], H. Ozaki[b], M. Sugahara[b]

[a] Kyoto University Research Reactor Institute,
Kumatori,
Osaka 590-0494,
Japan

[b] Osaka Sangyo University,
Daito-shi,
Osaka 574-8530,
Japan

High flow-rate soil percolation system was developed using soil beads processed out of loam. In the present report, removal of refractory dissolved organic matter (DOM) and phosphate ion by sorption to soil under static and dynamic water flow condition were compared.

The soil tested was Akadama soil (loam from Kanuma, Japan, parent material: tephra) and Kuroboku soil (Andosol from Hiroshima, Japan, parent material: tephra). Sorption isotherm of phosphate ion, fulvic acid, and high molecular weight DOM (>1000 Dalton) was obtained for the soil samples at 25℃. Potassium hydrogen phosphate solution was used to test the sorption of phosphate ion. The fulvic acid, originally the impurity in Aldrich humic acid, was extracted from the humic acid and was desalinated by gel filtration with Sephadex G-25. The DOM was recovered from wastewater from a stock farm by tangential flow ultrafiltration (Pellicon-2 Mini, Millipore). The fulvic acid and the DOM from wastewater were not biodegradable in the 28 day biodegradability test.

Prior to the column test and pilot scale test, Akadama soil (purchased as powder) was processed into beads using a turbulent granulating machine and was later baked at 600℃ to make it water-resistive. Kuroboku soil was granulated using bentonite clay as a binder but without baking. Column experiment was vertical upflow system at a flow rate of 2 mL/min (1.5 m/day), with the soil beads packed in the 5 cm diameter column made of acrylic resin to the height of ca. 15 cm. Approximately 50 mL of concentrated fulvic acid (20 mg weight as organic carbon) was instantaneously injected to the column with simulated river water. The effluent was periodically collected using a fraction collector, and DOC (dissolved organic carbon) concentration, pH and EC of the effluent was monitored. Pilot scale test was done at the site in Hiroshima adjoining a stock farm. Akadama and Kuroboku soil beads were packed in two sets of 80 cm × 120 cm steel bath to the height of 50 cm, respectively, and the wastewater from the stock farm, after passing it through a gravel pit for prefiltration, was continuously pumped to the soil system at the flow rate of 2m/day. The influent of the pilot scale test contained ca. 4 mg/L of dissolved T-P (total phosphorus) and 14 mg/L of DOC. BOD_5 of the influent was mostly below the detection limit (<4 mgO_2/L), and the biodegradability test showed that ca. 90% of DOC there was recalcitrant. The influent and effluent from the pilot scale test were collected every two weeks, and were analyzed for T-P (dissolved and total), DOC, COD-Cr, pH and EC.

Results of the sorption isotherm test are summarized in Table I. Sorption isotherm of DOM and fulvic acid was linear when the amount of OM sorbed was the order of 10^3 mg-organic carbon/kg-soil or less.

Table I. Parameters obtained from the sorption isotherm plot

Soil	Phosphate ion*[1]		DOM recovered from wastewater from the stock farm		Fulvic acid*[3]	
	k_d(mL/kg)	pH*[2]	k_d	pH*[2]	k_d	pH*[2]
Kuroboku beads (binder: bentonite)	509.8	(6.2)	-	-	39.7	(6.1)
Kuruboku soil	545.7	(6.2)	4.3	(6.5)	8.8	(6.9)
Akadamia beads 600°C	192.2	(6.8)	25.9	(6.7)	81.3	(6.4)
Kanuma beads 600°C	522.7	(7.1)	28.3	(7.0)	104.1	(6.5)

*[1] Sorption data was fitted to the linear istotherm when the amount of phosphate ion sorbed was of the order of <125 mg (as total phosphorus)/kg-soil.
*[2] pH of the soil solution when sorption isotherm was obtained.
*[3] Sorption data was fitted to the linear isotherm when the amount of organic matter sorbed was of the order of $<10^3$ mg (as organic carbon)/kg-soil.

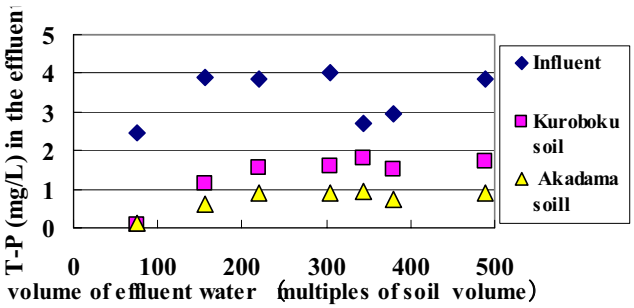

FIG. 1. Breakthrough curve of T-P (pilot scale test).

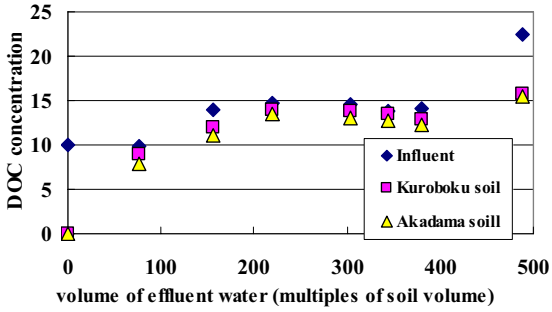

FIG. 2. Breakthrough curve of DOC (pilot scale test).

The sorption isotherm of phosphate ion could be approximated with linear isotherm when the amount of T-P sorbed was <ca. 10^2 mg-P/kg-soil while it was compatible with the Freundlich isotherm when the amount of T-P sorbed was the order of 10^4 mg-P/kg-soil or less (Sugahara *et al*., this issue).

The results of the column test showed that in the column packed with Akadama soil which exhibited higher sorption of fulvic acid compared to Kuroboku soil in isotherm test, significant retardation of injected FA relative to Kuroboku soil was observed. Also ca. 50% loss of the fulvic acid injected into the column was observed for Akadama soil, which was attributed to the slow biological decomposition of the fulvic acid once sorbed to the soil.

The results of the pilot scale test (Figs. 1 and 2) were in accordance with the theory of sorptive solute transport in aggregated soil. The elongated tailing of breakthrough curves of T-P and DOC shows that the diffusion of the solute to internal pores of soil beads and sortion was effective. The removal of T-P was higher in Kuroboku soil unit than Akadama soil unit, as opposed to the sorption isotherm results. An investigation is under way to clarify the cause.

Basic experimental research for the reconstruction of water purification system using soil - sorption isotherm of fulvic acid and phosphate ion for selected materials under different pH

Sugahara, M.[a], Y. Fujikawa[b], R. Imada[a], H. Ozaki[a], G. Prasai[a], T. Hamasaki[a]

[a] Osaka Sangyo University (OSU),
Daito-shi, Osaka,
Japan

[b] Kyoto University Research Reactor Institute (KURRI),
Kumatori, Osaka,
Japan

A series of sorption experiments was conducted for the establishment of water purification technique using soil and the other materials as a sorbent. Materials that showed comparatively high sorption of dissolved organic matter (DOM) and phosphate ion were selected among more than 100 soil and sludge samples collected from Japan, based on the results of batch sorption experiment using fulvic acid (FA hereafter) and phosphate ion as sorbate (Table 1). Materials that had high FA sorptivity were rarer than those with high phosphate ion sorptivity. Sorption isotherm of phosphate ion and FA was obtained for the selected sorbent under different pH conditions.

The obtained sorption isotherm parameters are shown in Tables 2 and 3. The results could be summarized as follows: (1) sorption of fulvic acid could be approximated by linear isotherm (Langmuir isotherm) when the amount of DOM sorbed was $< 10^3$ mg-organic carbon/kg-soil (10^4 mg-organic carbon/kg-soil), (2) sorption of phosphate ion could be described by linear isotherm (Freundlich isotherm) when the amount of phosphorus sorbed was $< 10^3$ mg-P/kg-soil ($< 10^4$ mg-P/kg-soil), (3) sorption of fulvic acid and phosphate ion varied with pH of the soil solution, (4) K_d (slope of the linear sorption isotherm) of FA was smaller at higher concentration of fulvic acid. Obviously, the type of soil used, and pH and the concentration of the sorbate in the water to be treated significantly influences the performance of the soil percolation system regarding the removal of pollutants in dissolved form.

Table I. Materials from Japan that showed high sorption of fulvic acid and phophate ion

High sorption of fulvic acid	High sorption of phosphate ion
apatite (reagent)	volcanic ash soil (subsoil from Amagase, Oita)
calcium phsophate (reagent)	volcanic ash soil ('Akadama soil' from deeper layer, Tochigi)
Andosol (Koga, Shiga)	volcanic ash soil (fine grained 'Kanuma soil', from Tochigi)
charcoal made out of wood	silt from Sakishima, Osaka
volcanic ash soil ('Akadama soil' from Tochigi)	vocanic ash soil ('Shirasu' from Kagoshima)
Andosol (Santo, Shiga)	sludge from water treatment plant in Shiga
sludge from a WTP in Shiga	calchium phosphate (reagent)
limonite (goethite from Kumamoto)	limonite (goethite from Akamizu, Kumamoto)
goethite (Gifu)	Andosols from Santo, Shiga
charcoal made out of bamboo	sludge from water treatment plant in Shiga
volcanic ash soil (Andosol from Ibaragi)	coal fly ash mixed with gypsum
bentonite	Andosols from Mt. Sanbe, Shimane

Table II. Sorption isotherm parameters obtained from the experiment (sorbate: fulvic acid)

sample name	pH	DOM sorbed mg-OC/kg *1	K_d (mL/g) of fulvic acid	q_m *3	b *3
charcoal	7.8	< 900	443.9	-	-
apatite (reagent)	7.5	$<1.1\times 10^4$	54.8	-	-
limonite	6	<900	53.8	-	-
Andosol (Santo, Shiga)	6	<900	14.7	-	-
Andosol (Hiroshima)	6.4	$<10\times 10^3$	54.3	-	-
Akadama soil (Tochigi)	6.5	$<10\times 10^3$	141.2	-	-
Kanuma soil (Tochigi)	6.5	$<10\times 10^3$	104.1	-	-
Andosol (Hiroshima)	5.2	$<1.1\times 10^4$	(28.3) *2	1.4×10^4	0.013
Andosol (Hiroshima)	6.9	$<4.0\times 10^3$	(8.8) *2	-	-
Andosol (Hiroshima)	7.2	$<9.7\times 10^3$	(17.8) *2	1.4×10^4	0.008
Akadama soil (Tochigi)	5.3	$<1.9\times 10^4$	(62.9) *2	2.0×10^4	0.63
Akadama soil (Tochigi)	7.2	$<1.6\times 10^4$	49.3	-	-
Akadama soil (Tochigi)	7.5	$<1.5\times 10^4$	(46.7) *2	2.0×10^4	0.018
Kanuma soil (Tochigi)	5	$<1.5\times 10^4$	(36.3) *2	1.7×10^4	0.05
Kanuma soil (Tochigi)	7.1	$<1.0\times 10^4$	(24.8) *2	1.4×10^4	0.008
Kanuma soil (Tochigi)	7.7	$<1.1\times 10^4$	(34.8) *2	2.0×10^4	0.005

*1 the observed range of the amount of solute sorbed by the sorbent

*2 slope of the quasilinear isotherm

*3 Parameters of Langmuir isotherm $q=q_mbc/(1+bc)$ where q is the amount of solute sorbed per unit mass of sorbent, c is the concentration of solute in the liquid phase at equilibrium.

Table III. Sorption isotherm parameters obtained from the experiment (sorbate: phosphate ion)

sample name	pH	T-P sorbed mg-P/kg *1	K_d (mL/g) of phosphate ion	k *2	n *2
limonite	3.8	$<1.2\times 10^2$	230.7	–	–
Andosol (Hiroshima)	6.2	$<3.8\times 10^3$	286.7	–	–
Akadama soil (Tochigi)	6.3	$<3.6\times 10^3$	3347.7	–	–
Kanuma soil (Tochigi)	7.1	$<2.9\times 10^3$	621.3	–	–
Andosol (Hiroshima)	5	$<9.4\times 10^3$	–	2.3×10^3	0.40
Andosol (Hiroshima)	6.3	$<8.4\times 10^3$	–	1.5×10^3	0.38
Andosol (Hiroshima)	7.5	$<7.0\times 10^3$	–	9.6×10^2	0.42
Akadama soil (Tochigi)	5.5	$<6.9\times 10^3$	–	2.2×10^3	0.36
Akadama soil (Tochigi)	6.5	$<7.0\times 10^3$	–	1.3×10^3	0.36
Akadama soil (Tochigi)	7.5	$<6.5\times 10^3$	–	1.7×10^3	0.30
Kanuma soil (Tochigi)	5	$<9.7\times 10^3$	–	2.4×10^3	0.34
Kanuma soil (Tochigi)	6.8	$<6.2\times 10^3$	–	8.6×10^2	0.40
Kanuma soil (Tochigi)	7.5	$<5.2\times 10^3$	–	8.3×10^2	0.38

*1 the observed range of the amount of solute sorbed by the sorbent

*2 Parameters of Freundlich isotherm $q=kc^n$ where q is the amount of solute sorbed per unit mass of sorbent, c is the concentration of solute in the liquid phase at sorption equilibrium.

Basic experimental research for the reconstruction of water purification system using soil - changes of sorption of fulvic acid and phosphoric acid by heating processing

Hamasaki, T.[a], Y. Fujikawa[b], R. Imada[a], M. Nagatomo[a], M. Sugahara[a], H. Ozaki[a]

[a] Osaka Sangyo University,
Osaka,
Japan

[b] Research Reactor Institute,
Kyoto University,
Osaka,
Japan

Sorption ability of pollutants such as organic matters and nutrient salts is necessary to soils for water purification system. Sorption experiments were conducted on the sorption of fulvic acid (a form of humic substances, designated as FA hereafter) and phosphoric acid, promising soils and solid wastes were found for the system [1, 2].

These materials should have permeability and water resisting with keeping sorption ability of pollutants. For this reason, it is necessary to process into beads and strengthen against water flowing. However, FA sorption of some materials was blocked by processing into beads. The reason may be attributable to leaching of organic matter from a soybean extract as binder material added upon processing of the soil into beads [3].

The purpose of this study is to conduct an experiment of heating processing of promising materials for the system to confirm changes of FA and phosphoric acid sorption. Two volcanic soils (Akadama-soil and Kanuma-soil) discharged from manufacturing and four kinds of sludge from water treatment plants (hereinafter referred to as WTT) were preferred to promising materials. Two kinds of sludge of water source are grand water, two others are river water.

Heating Processing was conducted each material sieved under 2 mm diameter at 200, 400, 600, 880 and 1200 deg. C, 30 minutes in a muffle furnace.

The sorption experiment of heated and unheated materials was conducted at 25 deg. C in a dark place, at the solid to liquid ratio of 1: 2.5. The amount of added FA and phosphoric acid was equivalent to 33 mg/L DOC (dissolved organic carbon) and 2 mg/L T-P (total phosphorus).

K_d (sorption coefficient) was calculated as an index of sorption from the equation assuming linear sorption isotherm:

$$K_d=(V/m)\ ((C_b+C_0)/C-1)$$

where C_0 (mg/L) and C (mg/L) are the respective added and measured DOC (or T-P) concentrations in the liquid phase; C_b (mg/L) is the DOC (or T-P) concentration in the sample blank, and m (g) and V (L) respectively are the mass of sorbent and the volume of the solution in each flask.

The result of FA and phosphoric acid sorption is shown in the following figure. Most samples of both sorptions descend at 200 and 400 deg. C, and ascend at 600 deg. C. The reason may be concentration of organic matter which easy to liquate out are decreased by combustion at 600 deg. C, and organic matter is easy to liquate out by heating at 200 and 400 deg. C. WTT sludge of Osaka North and Osaka South is sourced from grand water, unheated and 600 deg. C of their FA sorption are higher than FA sorption of sludge of Aichi and Kyoto sourced from river water. Concentration of iron in four kind of sludge is Osaka North 23.7%, Osaka South 13.8%, Aichi 3.7% and Kyoto 3.2%; iron concentration may be one of the reasons for the different FA sorption. Peak of FA sorption is around 600 deg. C. FA sorption of two kind of sludge at 880 and 1200 deg. C is decreased compared with the sorption at 600 deg. C.

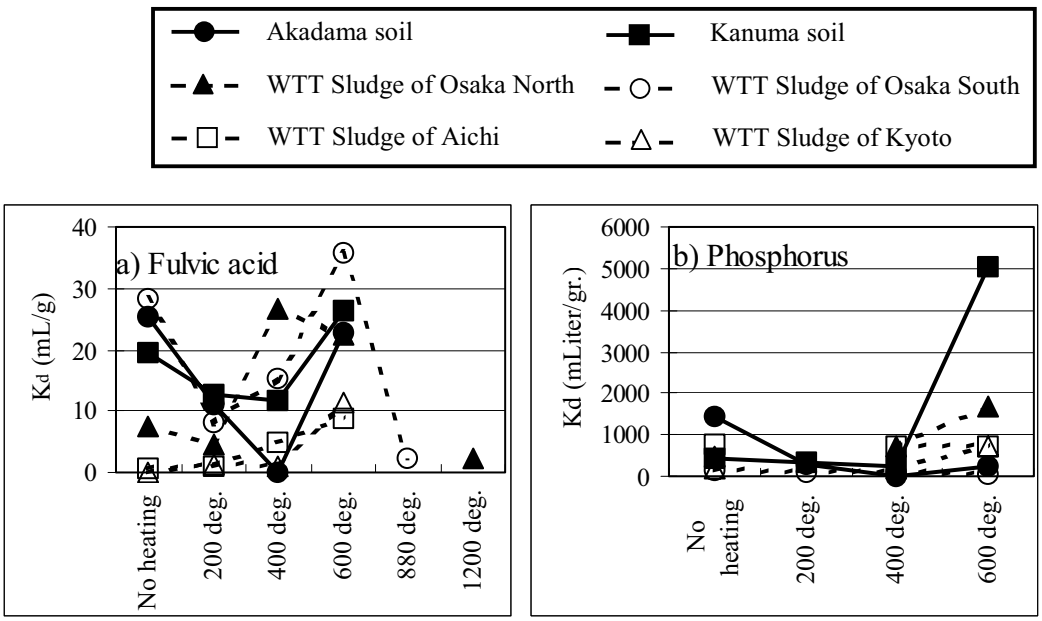

FIG. 1. Correlation between sorption coefficient and heating processing.

Heating processing makes strength against water flowing. This study indicates sorption of FA and phosphoric acid keep even heating at 600 deg. C as no heating. As the result of this sorption experiment, heating processing is the one of effective methods for strength against water flowing.

For construct the next water purification system using soil, mechanism of sorption changes by heating processing should be solved, and an experiment with pilot scale plant using these materials should be also conducted.

REFERENCES

[1] FUJIKAWA, Y., et al., Characterization of Japanese soil and other geological materials based on the sorption of humic substances (Proc. Int. Conf. Radioactivity in the Environment) (2002) 619-623.

[2] FUJIKAWA, Y., et al., Re-evaluation and Re-construction of Water Purification System Using Soil I: Assessment of Soil as a Sorbent of Humic Substances and Phosphorous Acid, ECOHAZARD 2003, International Water Association (IWA) (2003).

[3] HAMASAKI, T., et al., Re-evaluation and Re-construction of Water Purification System Using Soil II: Mechanisms of Removal of Pollutants from Infiltrating Water, ECOHAZARD 2003, International Water Association (IWA) (2003).

ANNEX I

COLOUR FIGURES

Bomb-radiocarbon: distribution, inventory, and change

Key, R.M.

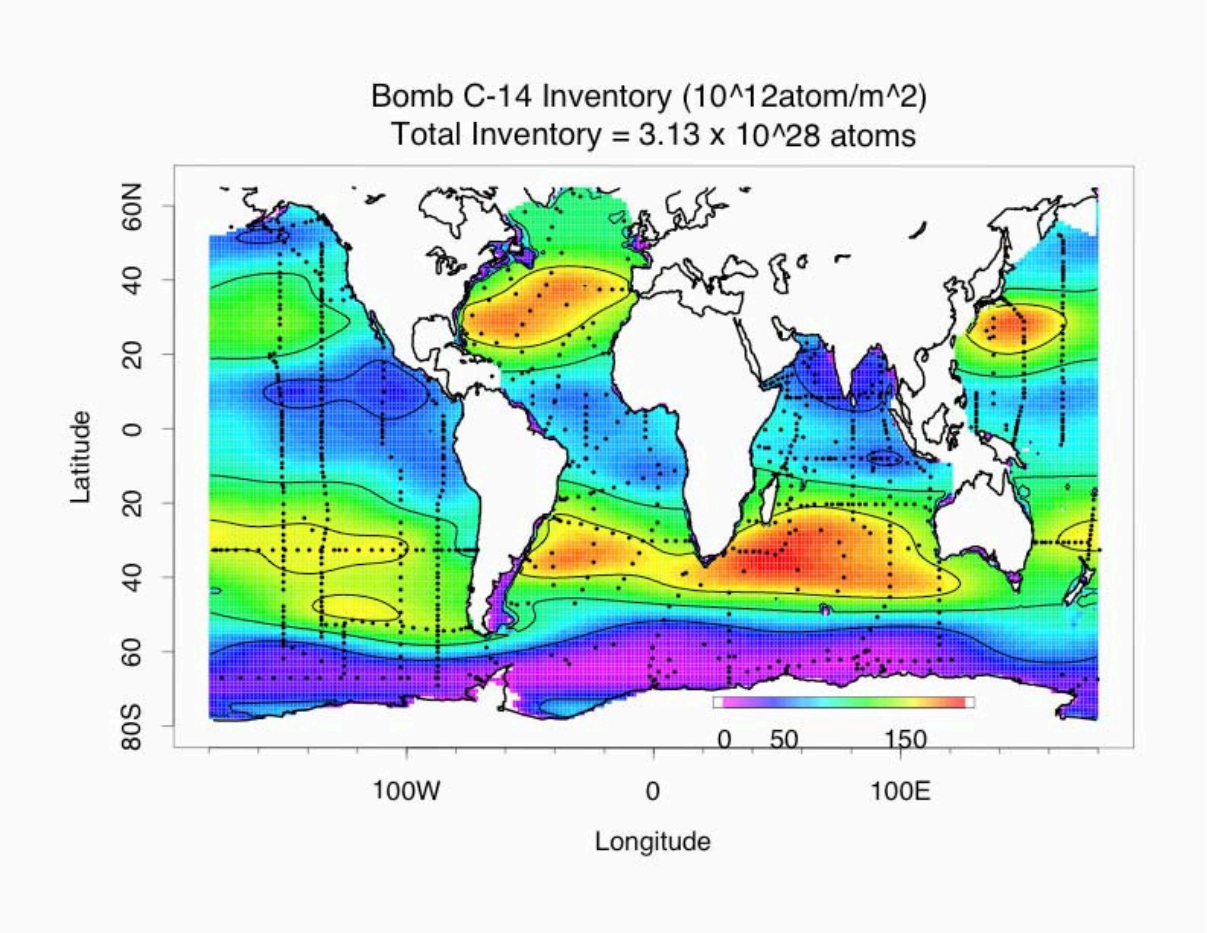

FIG. 1. Bomb C-14 inventory based on GEOSECS and WOCE data. Highest inventories are observed in the North Atlantic, in the regions of formation of North Pacific Intermediate Water and in the southern hemisphere.

IAEA-CN-118/120, p. 36

The Marine Information System (MARIS)

Povinec, P.P., P. Scotto, I. Osvath, H. Ramadan

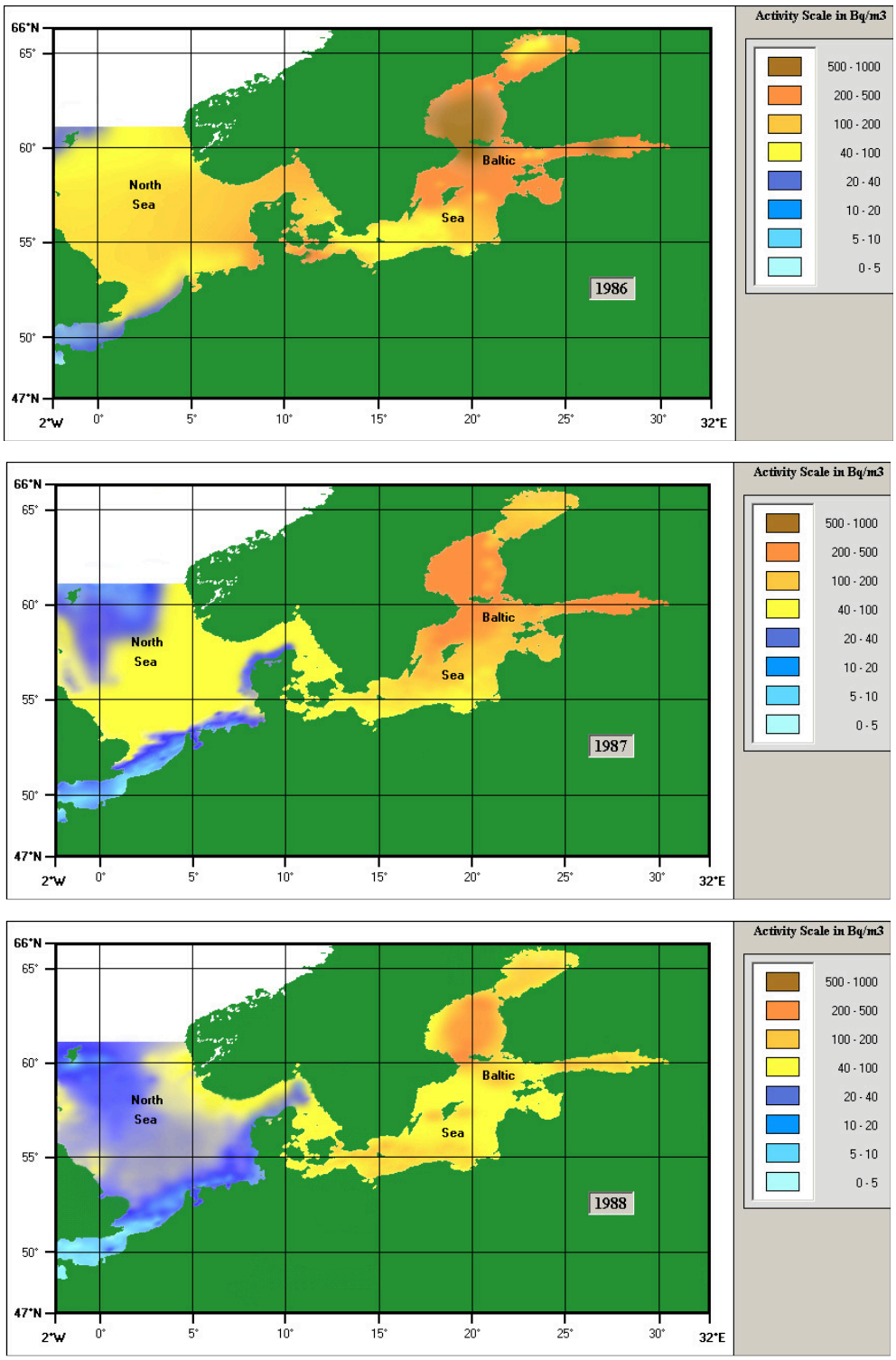

FIG. 1. ^{137}Cs in surface waters (0 - 50 m) of North and Baltic Seas during the period 1986-1988, based on data from the MARIS database (Bq·m-3).

IAEA-CN-118/6P, p. 69

The Nile and the Levantine pump

Halim, Y.

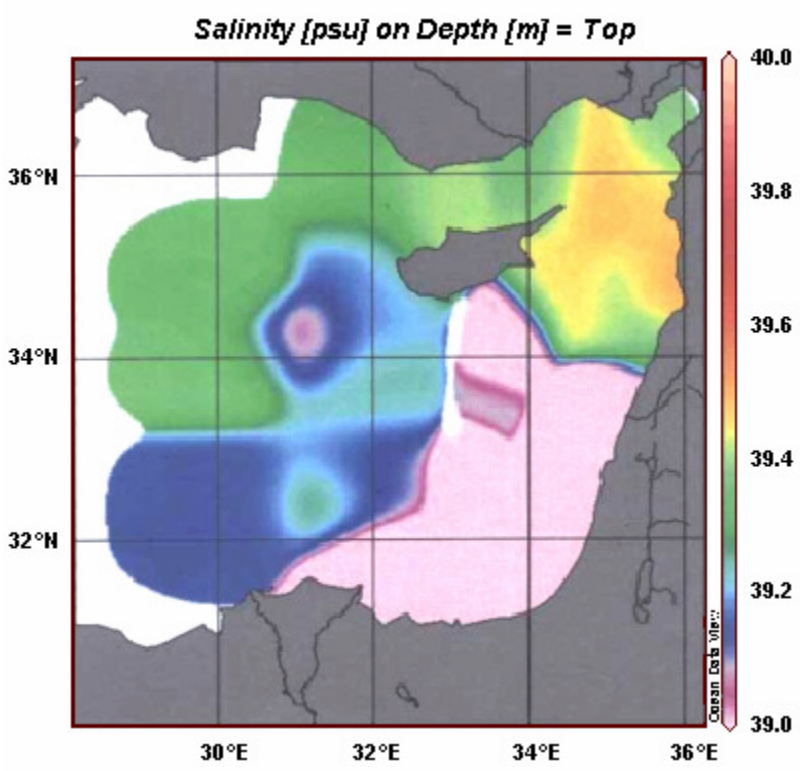

FIG. 3. Surface salinity for the eastern Levantine Sea, integrating all available data from 1900 to 1964.

IAEA-CN-118/183, p. 74

The first decade of the big transient in the Eastern Mediterranean deep waters

Roether, W. B. Klein, B.B. Manca

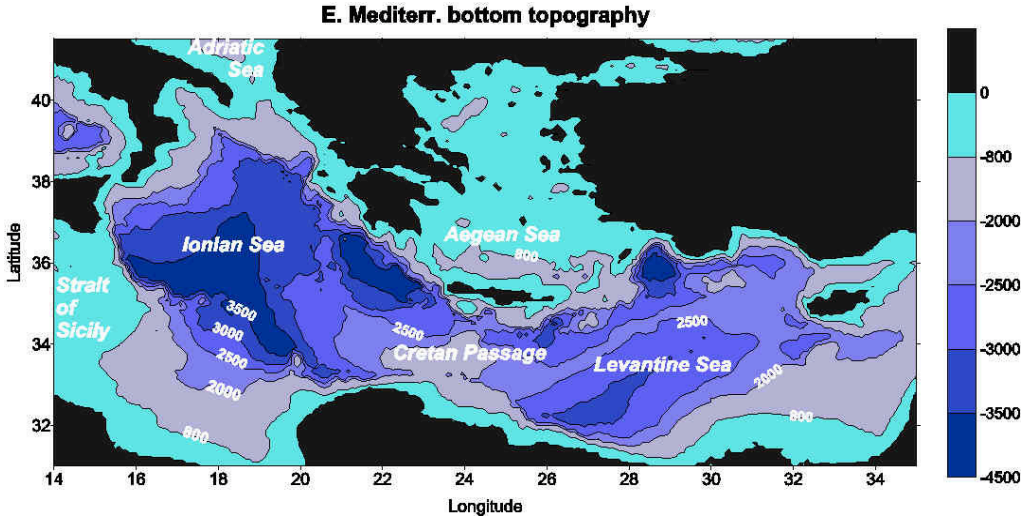

FIG. 1. Map of the East Mediterranean with geographic names and bathymetry. Otranto Strait (sill depth ~ 800 m) connects to the Adriatic, and Kasos Strait, east of Crete (~ 1000 m), provides the governing dense-water pathway out of the Aegean. The East Mediterranean Ridge separates the Hellenic Trench on its Cretan side from the rest of the East Mediterranean. The sill in the north of the passage is ~ 2700 m deep. The Strait of Sicily connects to the West Mediterranean.

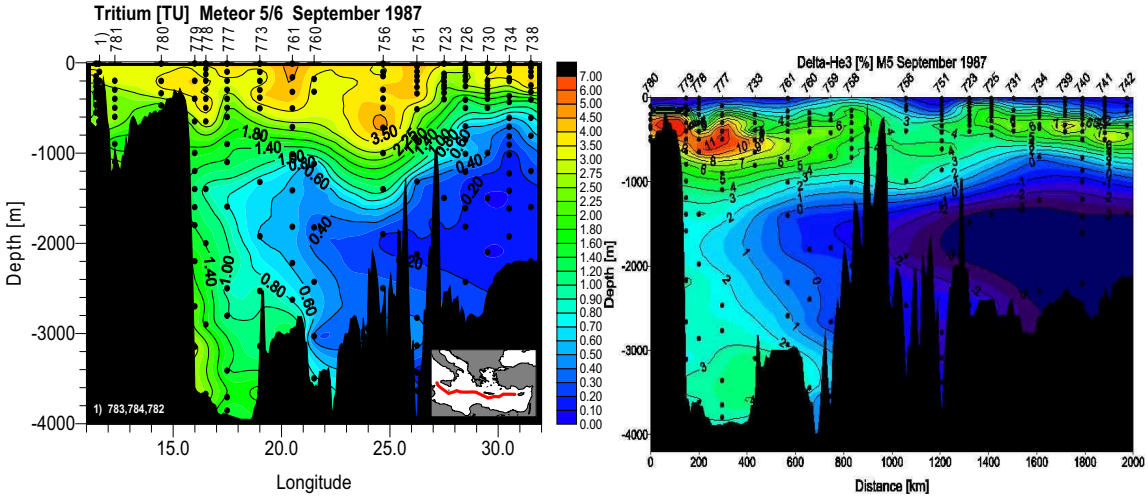

FIG. 2. Sections of tritium (TU; Fig. 2a, left) and of δ^3He (%; Fig. 2b, right) along the Eastern Mediterranean in Aug.-Sept. 1987 (METEOR cruise M5/6). Markings indicate data points, for tracks see inset map. δ^3He means the deviation of the $^3He/^4He$ ratio from that of atmospheric helium ($(^3He/^4He)_{atm} \approx 1.4 \cdot 10^{-6}$). Measurements performed mass-spectrometrically at Bremen [13].

IAEA-CN-118/184, pp. 84, 85

Data synthesis for terrestrial gamma radiation level measured on the Japanese Islands and their adjacent ocean floor

M. Furukawa

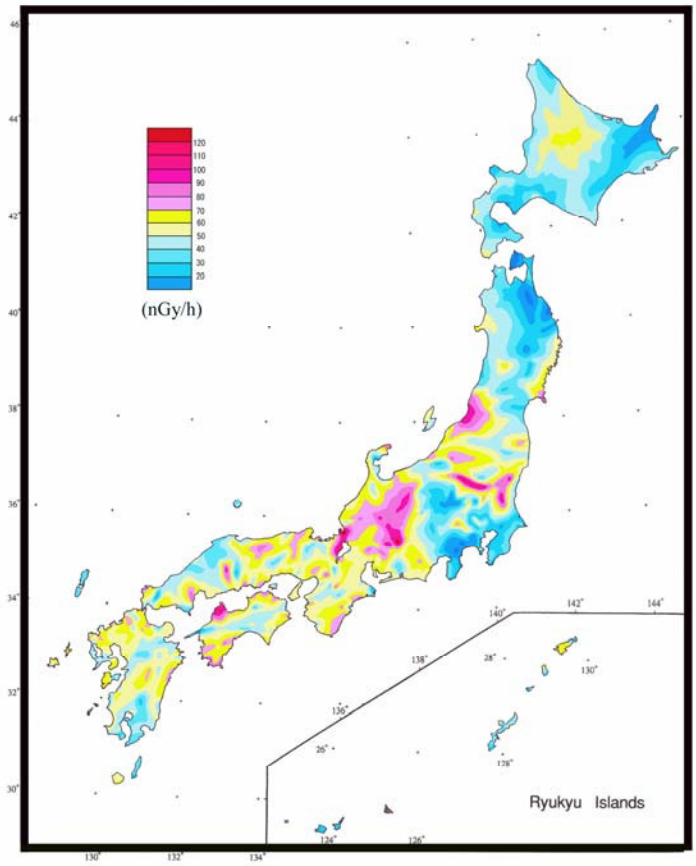

FIG. 2. Distribution of the absorbed dose rate in air due to terrestrial gamma radiation in Japan.

IAEA-CN-118/39, p. 250

3-D Modelling technique of time-series ^{137}Cs concentration in coastal organisms in the case of short term introduction

Y. Tateda, A. Wada

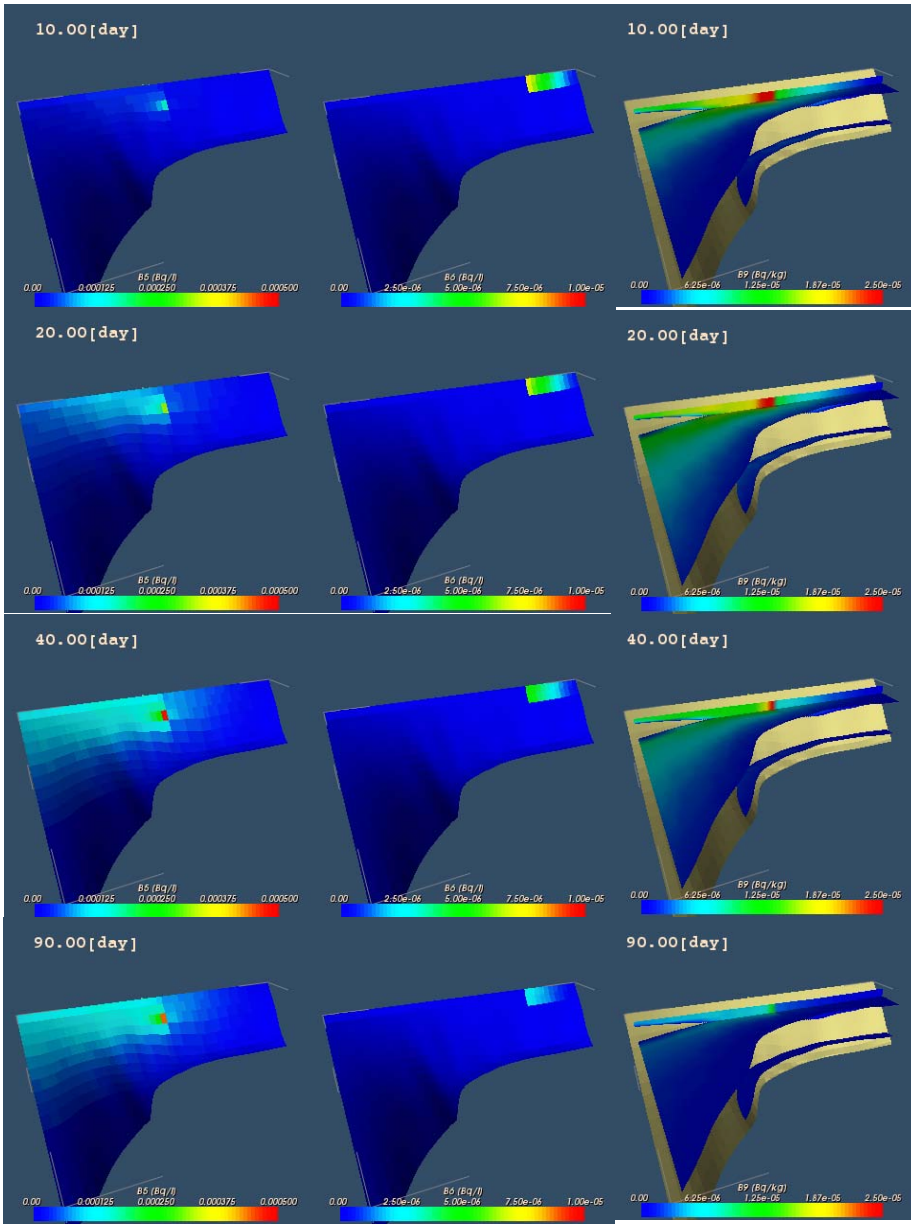

FIG. 1. Computed ^{137}Cs temporal concentration in benthic fish, macro algae and squid at Rokkasho coastal water (Central circle: source. Shade: ^{137}Cs concentrations).

IAEA/CN-118/52, p. 467

CHAIRPERSONS OF SESSIONS

Plenary Session I	M. Betti R.F.C. Mantoura	Germany IAEA
Plenary Session II	N.J.P. Owens W. Kutschera	United Kingdom Austria
Plenary Session III	P. Schlosser J.J. Gibson	United States of America Canada
Plenary Session IV	A.J.T. Jull W.E. Kieser	United States of America Canada
Plenary Session V	R. Key A. Priller	United States of America Austria
Plenary Session VI	P.K. Aggarwal C. Papucci	IAEA Italy
Parallel Session 1.1	M. Boisson J. Readman	Monaco United Kingdom
Parallel Session 1.2	R. Delfanti P. Masque	Italy Spain
Parallel Session 2.1	R. Dunbar E.R.M. Druffel	United States of America United States of America
Parallel Session 2.2	J.W. Beck D. Fink	United States of America Australia
Parallel Session 3.1	P.J. Kershaw V. Barci	United Kingdom France
Parallel Session 3.2	D. Boust H. Pettersson	France Sweden
Parallel Session 4.1	J. Vives i Battle M. Iosjpe	United Kingdom Norway
Parallel Session 4.2	C. Jeandel M. Karcher	France Germany
Parallel Session 5	E. Boaretto L. Coppola	Israel Sweden
Parallel Session 6	K. Komura H. Florou	Japan Greece
Parallel Session 7.1	C. Kendall F.W. Schwartz	United States of America United States of America

Parallel session 7.2	R.L. Michel I. Carmi	United States of America Israel
Parallel Session 7.3	V.I. Ferronsky N. Horvatincic	Russian Federation Croatia
Parallel Session 8.1.	G. Korschinek P. Roos	Germany Denmark
Parallel Session 8.2	D.L. Biddulph Y. Ikeuchi	United States of America Japan
Parallel Session 8.3	E. Holm	Sweden
Parallel Session 9	C. Tsabaris J.W. Mietelski	Greece Poland
Parallel Session 10.1	S. Charmasson S.W. Fowler	France IAEA
Parallel Session 10.2	J. Carroll R. Jeffree	Norway IAEA
Parallel Session 11.1	W. Burnett E. Kontar	United States of America Russian Federation
Parallel Session 11.2	H. Bokuniewicz G.M. Zuppi	United States of America Italy
Parallel Session 11.3	J. de Oliveira	Brazil
Parallel Session 12	S. de Mora A. Henderson-Sellers	IAEA Australia
Parallel Session 13	K. Hirose N. Yoshida	Japan Japan
Parallel Session 14.1	M. Hult G. Heusser	Belgium Germany
Parallel Session 14.2	M. Hult D. Arnold	Belgium Germany
Parallel Session 15	G.H. Hong G. Gungor	Korea, Republic of Turkey
Parallel Session 16	M. Aoyama T. Honda	Japan Japan

SECRETARIAT OF THE CONFERENCE

Scientific Secretary: P.P. Povinec, IAEA

Conference Services: C. Coolbaugh, IAEA

M. Solarik-Leahy, IAEA

Scientific Advisory Committee: R.F.C. Mantoura, IAEA

P.K. Aggrawal, IAEA

A. Aureli, IHP, UNESCO

M. Boisson, CSM

F. Briand, CIESM

K.R. Sreenivasan, ICTP

U. Unluata, IOC, UNESCO

LIST OF PARTICIPANTS

Aeschbach-Hertig, W.	Institute for Environmental Physics im Neuenheimer Feld 229 D-69120 Heidelberg Germany Fax: +496221546405 EMail: aeschbach@iup.uni-heidelberg.de
Aggarwal, P.K.	International Atomic Energy Agency P.O. Box 100 A-1400 Vienna Austria
Al-Alem, E.A.	Marine Environment Laboratory International Atomic Energy Agency MC-98000 Monaco
Al Hassani, S.R.S.	United Arab Emirates Armed Forces P.O. Box 23752 Al Ain United Arab Emirates Fax: +97125854678 EMail: alhassanis@hotmail.com
Alegria, N.	Escuela de Ingeniros de Bilbao Dto. Ing. Nuclear y Mec. De Fluidos Alemeda Urquijo, s/n E-48013 Bilbao Spain Fax: +34946014159 EMail: inbalgun@bi.ehu.es
Allemand, D.	Centre Scientifique de Monaco Avenue Saint-Martin MC 98000 Monaco Fax: +37792167981 EMail: allemand@centrescientifique.mc
Al-Masri, M.S.	Atomic Energy Commission of Syria P.O. Box 6091 Damascus Syrian Arab Republic Fax: +963116112289 EMail: msmasri@aec.org.sy
Alonso-Hernández, C.M.	Centro de Estudios Ambientales de Cienfuegos Ap5 Ciudad Nuclear 59350 Cienfuegos Cuba Fax: +53432511889 EMail: carlos@ceac.perla.inf.cu

Al-Rousan, S.
University of Jordan & Yarmouk University
Marine Science Station
P.O. Box 195
77110 Aqaba
Jordan
Fax: +96232013674
EMail: s.rousan@ju.edu.jo

Alvestad, P.
Havforskninbinstitutet (IMB)
PB 1580 Nordes
5817 Bergen
Norway
EMail: pennyl@imr.no

Aoyama, M.
Geochemical Research Department
Meteorological Research Institute
Nagamine 1-1
305-0051 Tsukuba
Japan
Fax: +81298538728
EMail: maoyama@mri-jma.go.jp

Araujo, M.F.D.
Instituto Tecnologico e Nuclear
Estrada Nacional No 10
2686 953 Sacavem
Portugal
Fax: +351219941455
EMail: Faraujo@itn.mces.pt

Ardid Ramírez, M.
Escuela Politécnica Superior de Gandia
Universitat Politècnica de Valéncia
Carretera Nazaret-Oliva
s/n E-46730 Gandia
Spain
Fax: +34962849309
EMail: mardid@fis.upv.es

Arkaah, A.B.
University of Ghana
Dept. of Oceanography & Fisheries
P.O. Box LG 99
University of Ghana
Legon
Ghana
Fax: +23321513976
EMail: amaarkaah@yahoo.com

Arnold, D.
Physikalisch-Technische Bundesanstalt
Department 6.1 Radioactivity
Bundesallee 100
D-38116 Braunschweig
Germany
Fax: +495315926120
EMail: dirk.arnold@ptb.de

Ata, L.	Koeberg Nuclear Power Station Melkbosstrand, Cape Private Bag X10 Kernkrag 7440 South Africa Fax: +27215505117 EMail: laurence.ata@eskom.co.za
Azanza, R.	Marine Science Institute University of the Philippines Diliman, Quezon City 1101 Philippines Fax: +6329215967 EMail: rhod@upmsi.ph
Azemard, S.	Marine Environment Laboratory International Atomic Energy Agency MC 98000 Monaco
Babiker, R.	Sudan Atomic Energy Commission P.O. Box 3001 Khartoum Sudan Fax: +249912869321 EMail: rifaatk@yahoo.com
Balkis, Mehmet	University of Istanbul Institute of Marine Science and Management Istanbul 34470 Turkey EMail: mbal@istanbul.edu.tr
Balkis, N.	Institute of Marine Sciences and Management Istanbul University Müsküle Sokak No. 1 TR-34470 Vefa- Istanbul Turkey Fax: +902125268433 EMail: nbal@istanbul.edu.tr
Ballestra, S.	Marine Environment Laboratory International Atomic Energy Agency MC 98000 Monaco
Barci, V.	Laboratoire Radiochimie, Sciences Analytiques, Environnement UNSA 28 avenue Valrose F-06108 Nice Cedex 2 France Fax: +33492076364 EMail: barci@unice.fr

Barci-Funel, G.
Laboratoire de Radiochimie Sciences Analytiques et Environnement
Faculté des Sciences
28 avenue de Valrose
F-06108 Nice Cedex 2
France
Fax: +33492076364
EMail: gbarci@unice.fr

Barci, V
Laboratoire Radiochemie, Sciences Analytiques et Environnement - Fac. Sciences,
Parc Valrose
06108, NICE
France
Fax: 33 (0) 4 92 07 63 64
EMail: barci@unice.fr

Barrera, M.
CIEMAT
Avda. Complutense 22
E-28040 Madrid
Spain
Fax: +34913466121
EMail: manuel.barrera@ciemat.es

Bartocci, J.
Marine Environment Laboratory
International Atomic Energy Agency
MC 98000 Monaco

Baude, S.
Commissariat a l'Energie Atomique (CEA)
P.O. Box 12
91680 Bruyeres-le-Chatel
France
Fax: +33169267065
EMail: stephane.baude@cea.fr

Bayramov, Z.
Azerbaijan National Academy of Sciences
Azerbaijan National Aerospace Agency
159 Azadlig Avenue
AZ1106 Baku
Azerbaijan
Fax: +99412621738
EMail: bayramov_z@yahoo.com

Beaugelin-Seiller, K.
Environment and Emergency Operations Division
Department for the Study of Radionuclides
Bat. 159-BP 3
13115 Saint-Paul-Les-Durance
France
Fax: +33 4 42 25 62 92
EMail: karine.beaugelin@irsn.fr

Beck, W.J.
University of Arizona
Physics Department
Building #81
Tucson, Arizona 85721
United States of America
EMail: wbeck@physics.Arizona.edu

Benkrid, M.
Commissariat à l'énergie atomique
Centre de recherche nucléaire
2, boulevard Frantz Fanon
B.P. 399
16000 Alger-gare
Algeria
Fax: +21321648242
EMail: m_benkrid@hotmail.com

Benmansour, M.
Centre national de l'énergie, des sciences et des techniques nucléaires
B.P. 1382
10001 Rabat, RP
Morocco
Fax: +21237803277
EMail: benmansour@cnesten.org.ma

Bergin, A.F.
Bogazici University Museum
34342 Bebek
Istanbul
Turkey
Fax: +902122656357
EMail: berginfu@boun.edu.tr

Berglund, M.
EC-JRC Institute for Reference Materials and Measurements
Retieseweg 111
B-2440 Geel
Belgium
Fax: +3214571863
EMail: michael.berglund@cec.eu.int

Bermúdez, J.
Laboratorio de Física Nuclear
Universidad Simón Bolivar
Apto 89000
Caracas 1080 A
Venezuela
Fax: +582129063590
EMail: judilka@hotmail.com

Bernard, S.
LGGE CNRS / UMR 5183
Domaine Universitaire 54
rue Moliere
BP 96
F-8402 Saint Martin d'Heres
France
Fax: +330476824201
EMail: bernard@lgge.obs.ujf-grenoble.fr

Betti, M.
EC-JRC
Institute for Transuranium Elements
P.O. Box 2340
D-76125 Karlsruhe
GERMANY
Fax: +497247951186
EMail: betti@itu.fzk.de

Biddulph, D.
The University of Arizona
Physics Department
1118 East Fourth Street
PAS 81, Room 236
Tucson, AZ 85721
United States of America
Fax: +15206269348
EMail: biddulph@physics.arizona.edu

Boaretto, E.
Weizmann Institute of Science
76100 Rehovot
Israel
Fax: +972 8 9346062
EMail: elisabetts.boaretto@we12mann.ac

Bode, A.
Instituto Español de Oceanografía
Centro Oceanográfico de A Coruña
Apdo. 130
E-15080 A Coruña
Spain
Fax: +34981229077
EMail: antonio.bodo@co.ieo.es

Boisson, F.
Marine Environment Laboratory
International Atomic Energy Agency
MC 98000 Monaco

Boisson, M.
Centre Scientifique de Monaco
16 bd de Suisse
MC-98000 Monaco
Fax: +37792167981
EMail: mboisson@centrescientifique.mc

Bojanowski, R.
Polish Academy of Sciences
Institute of Oceanology
Ml. Powstanicow Warszawy 55
81712 SOPOT
Poland
Fax: +485855121130
EMail: rbojan@iopan.gda.pl

Bokuniewicz, H.J.
Marine Sciences Research Center
Stony Brook University
Stony Brook, NY 11794-5000
United States of America
Fax: +16316328820
EMail: hbokuniewicz@notes.cc.sunysb.edu

Bonaccorsi, R.
University of Trieste (DiSGAM)
Via E. Weiss 2
(c/o Comprensorio di S. Giovanni)
34127 Trieste
Italy
Fax: +398405582048
EMail: bonaccor@univ.trieste.it;
bonaccorsi.rosalba@excite.com

Bonotto, D.M.
IGCE - Instituto de Geociências e Ciências Exatas
UNESP - Universidade Estadual
Paulista Julio de Mesquita Filho
Rua 10, No. 2527- C.P. 178
BR-13506-900 Rio Claro - SP
Brazil
Fax: +551935249644
EMail: dbonotto@rc.unesp.br

Boontanon, N.
Frontier Collaborative Research Center
Tokyo Institute of Technology
(Yoshida Lab, G5-203)
4259 Nagatsuta, Midori-ku,
Yokohama, Kanagawa 226-8502
Japan
Fax: +81459245517
EMail: bnarin@depe.titech.ac.jp

Boudjenoun, R.
Marine Environment Laboratory
International Atomic Energy Agency
MC 98000 Monaco

Boust, D.
Laboratoire de Radioecologie de Cherbourg Octeville IRSN
BP 10
F-50130 Cherbourg Octeville
France
Fax: +33233014130
EMail: dominique.boust@irsn.fr

Briand, F.
CIESM
16 boulevard de Suisse
MC 98000 Monaco

Burdloff, D.
Instituto Tecnologico e Nuclear
Estrada Nacional No 10
2686 953 Sacavem
Portugal
Fax: +351219941455
EMail: burdloff@itn.mces.pt

Bürger, S.
Institut für Kernchemie
Universität Mainz
Fritz-Strassmann-Weg 2
D-55099 Mainz
Germany
Fax: +4961313925253
EMail: buers002@mail.uni-mainz.de

Burkart, W.
Department of Nuclear Sciences and Applications
International Atomic Energy Agency
P.O. Box 100
A-1400 Vienna
Austria

Burnett, W.C.
Department of Oceanography
Florida State University
Tallahassee, FL 32306
United States of America
Fax: +18506442581
EMail: wburnett@mailer.fsu.edu

Camacho, A.
Institut de Tecniques Energetiques
Universitat Politecnica de Catalunya
Etseib, Diagonal 647
08028 Barcelona
Spain
Fax: +34934017149
EMail: antonia.camacho@upc.es

Carmi, I.
Tel-Aviv University
Faculty of Exact Sciences
Department of Geophysics and Planetary Sciences
P.O. Box 39040
69978 Tel Aviv
Israel
Fax: +97236409282
EMail: carmiisr@post.tau.ac.il

Carreira Paquete, P.M.M.
Instituto Tecnologico e Nuclear
Estrada Nacional No 10
2686 953 Sacavem
Portugal
Fax: +351219941455
EMail: carreira@itn.mces.pt

Carroll, J.
AKVAPLAN-NIVA AS
Polar Environmental Centre
N-9296 Tromso
Norway
Fax: +4777750301
EMail: jc@akvaplan.niva.no

Cassi, R.
Marine Environment Laboratory
International Atomic Energy Agency
MC 98000 Monaco

Castillo, J.
Laboratorio de Física Nuclear
Universidad Simón Bolivar
Apto 89000
Caracas 1080 A
Venezuela
Fax: +582129063590
EMail: jcmleo@hotmail.com

Cattini, C.
Marine Environment Laboratory
International Atomic Energy Agency
MC 98000 Monaco

Chang, B.U.
Korea Institute of Nuclear Safety
19 Guseong
Yuseong
Taejeon 305-338
Korea Rep. of
Fax: +82428680556
EMail: hafadai@kins.re.kr

Charmasson, S.
IRSN
Ifremer Centre
B.P. 330
83507 La Seyne sur Mer Cedex
France
Fax: +33494304416
EMail: sabine.charmasson@ifremer.fr

Charuratna, A.
Groundwater Monitoring Section
Department of Groundwater Resources
Rama VI Road Phyathai
Bangkok 10400
Thailand
Fax: +6622466137; +6625613013
EMail: adisai54@hotmail.com

Chiappini, R.
Commissariat a l'Energie Atomique (CEA)
P.O. Box 12
91680 Bruyeres-le-Chatel
France
Fax: +33169267065
EMail: remo.chiappini@cea.fr

Chouba, L.
Institut National des Sciences et Technologies de la Mer
Port de Pêche
TN-2060 La Goulette
Tunis
Tunisia
Fax: +2161732622
EMail: lassaad.chouba@instm.rnrt.tn

Choura, L.
Laboratoire Radiochimie et Environnement
UNSA
28 avenue Valrose
F-06108 Nice Cedex 2
France
Fax: +33492076364
EMail: choura@unice.fr

Claude, C.
CEREGE
Europôle Mediterranéen de l'Arbois
B.P. 80
F-13545 Aix-en-Provence
Cedex 04
France
Fax: +33442971545
EMail: cclaude@cerege.fr

Collins, J.M.
AWE
Aldermaston, Reading
Berkshire, RG7 4PR
United Kingdom
EMail: jane.collins@awe.co.uk

Comanducci, J-F.
Marine Environment Laboratory
International Atomic Energy Agency
MC 98000 Monaco

Coppola, L.
Laboratory for Isotope Geology
Swedish Museum of Natural History
Frescativaegen 40
Box 50007
S-104 05 Stockholm
Sweden
EMail: laurent.coppola@nrm.se

Cotret, O.
Marine Environment Laboratory
International Atomic Energy Agency
MC 98000 Monaco

Cunha, I.I.L.
Radiochemistry Division
IPEN-CNEN-SP
rua Manoel Alonso Esteves
66 Jardim Bonfiglioli
Sao Paulo cep 05589020
Brazil
Fax: +551137356552
EMail: iedacunha@ig.com.br

Dakladas, Th.
Ministry of National Defense
15500,
Mesogion 151
Greece
EMail: tdak33@in.gr

Dang, Duc Nhan	Institute for Nuclear Science and Technology 5T-160 Hoang Quoc Viet St. Cau Giay, Hanoi Vietnam Fax: +8448363295 EMail: ddnhan@mail.vaec.gov.vn
Davulienė, L.	Institute of Physics Savanoriu Str. 231 2300 Vilnius Lithuania Fax: +37052602317 EMail: arlauske@ktl.mii.lt
De Mora, S.	Marine Environment Laboratory International Atomic Energy Agency MC 98000 Monaco
De Oliveira, J.O.	Instituto de Pesquisas Energéticas Nucleares Centro de Metrologia das Radiaçoes Av. Prof. Lineu Prestes 2242 BR-05508-900 São Paulo, SP Brazil Fax: +551138169118 EMail: jolivei@ipen.br
Deák, J.	Water Resources Research Center (VITUKI PLC) Kvassay Jenö út 1 H-1095 Budapest Hungary Fax: +3613495131 EMail: deak3@iaxelero.hu
Delfanti, R.	ENEA - Marine Environment Research Centre Forte di Santa Teresa Pozzuolo di Lerici I-19032 Lerici (la Spezia) Italy Fax: +390187978213 EMail: roberta.delfanti@santateresa.enea.it
Dennis, P.	Stable Isotope Laboratory School of Environmental Sciences University of East Anglia Norwich NR4 7TJ United Kingdom Fax: +441603507719 EMail: paul.dennis@dmtechnology.co.uk
Dody, A.	Nuclear Research Centre (NEGEV) P.O. Box 9001 Beer Sheva 84190 Israel Fax: +97286567690 EMail: dodik@bgu.ac.il

Dovlete, C.
Marine Environment Laboratory
International Atomic Energy Agency
MC 98000 Monaco

Drimmie, R.J.
Environmental Isotope Laboratory
Department of Earth Sciences
University of Waterloo
Waterloo, Ontario N2L 3G1
Canada
Fax: +15197467484
EMail: rdrimmie@uwaterloo.ca

Druffel, E.
University of California Irvine
Dept. of Earth System Science
3224 Croul Hall
Irvine, California, 92697-3100
United States of America
Fax: +019498243874
EMail: edruffel@uci.edu

Duffa, C.
Institute for Radioprotection and Nuclear Safety
IRSN/DEI/SESURE/LERCM,
BP 3
F-13115 St-Paul-lez-Durance
France
Fax: +33442256373
EMail: celine.duffa@irsn.fr

Dunbar, R.
Stanford University, GES
Stanford CA 94305-2115
United States of America
Fax: +016507250979
EMail: dunbar@stanford.edu

El-Motaium, R.C.
Plant Research Department
Nuclear Research Center
Atomic Energy Authority
Inshas
13759 Cairo
Egypt
Fax: +2023859406
EMail: rawiac@yahoo.com

Eyrolle, F.
Institute for Radioprotection and Nuclear Safety
IRSN/DEI/SESURE/LERCM,
BP 3
F-13115 St Paul-lez-Durance
France
Fax: +33442256373
EMail: frederique.eyrolle@irsn.fr

Fernex, F.
Département des sciences de la terre
Université de Nice – Sophia Antipolis
28 avenue Valrose
F-06108 Nice Cedex 2
France
Fax: +3392076816
EMail: fernex@unice.fr

Ferrier-Pagès, C.
Centre Scientifique de Monaco
c/o Musée océanographique
Avenue Saint-Martin
MC-98000 Monaco
Fax: +37792167981
EMail: ferrier@centrescientifique.mc

Ferronsky, V.I.
Water Problems Institute of the Russian Academy of Sciences
Gubkin Street 3
RU-119991 Moscow
Russian Federation
Fax: +70951355415
EMail: ferron@aqua.laser.ru

Fichez, R.
Centre d'Oceanologie de Marseille
Station Marine d'Endoume
rue de la Batterie des Lions
13007 Marseille
France
Fax: +33491041635
EMail: fichez@com.univ-mrs.fr

Fink, D.
Australian Nuclear Science and Technology Organisation
PMB 1
Menai 2234 NSW
Australia
Email: D.Fink@anso.gov.au

Fisher, E.H.
Department of Earth and Ocean Sciences
Jane Herdman Building
University of Liverpool
4 Brownlow Street
Liverpool L69 3GP
United Kingdom
Fax: +441517945196
EMail: e.h.fisher@liverpool.ac.uk

Florou, H.
Institute of Nuclear Technology and Radiation Protection
Aghia Paraskevi 153 10
P.O. Box 60228
GR-15A310 Aghia Paraskevi
Athens
Greece
Fax: +3012106513050
EMail: eflorou@ipta.demokritos.gr

Fórizs, I.
Laboratory for Geochemical Research
Hungarian Academy of Sciences
Budaörsi út 45
H-1112 Budapest
Hungary
Fax: +3613193137
EMail: forizs@geochem.hu

Fowler, S.W.
Marine Environment Laboratory
International Atomic Energy Agency
MC 98000 Monaco

Føyn, L.
Institute of Marine Research
P.O. Box 1870
Nordnes
N-5817 Bergen
Norway
Fax: +4755238584
EMail: lars@imr.no

Fujikawa, Y.
Division of Nuclear Engineering Science
Research Reactor Institute
Kyoto University
2-1010 Asashironishi
Kumatori-cho, Sennan-gun Osaka 590-0494
Japan
Fax: +81724512620
EMail: fujikawa@rri.kyoto-u.ac.jp

Fukai, R.
Marine Environment Laboratory
International Atomic Energy Agency
MC 98000 Monaco

Furukawa, M.
National Institute of Radiological Sciences
4-9-1 Anagawa, Inage-ku
Chiba 263-8555
Japan
Fax: +81432064098
EMail: m_furu@nirs.go.jp

Gafvert, T.
Norwegian Radiation Protection Authority
P.O. Box 55
N-1332 Østerås
Norway
Fax: +4767147407
EMail: torbjorn.gafvert@nrpa.no

Gal, F.G.
Universite Jean Monnet
Laboratoire Transferts Lithospheriques
23 rue Paul Michelon
42023 Saint Etienne cedex 2
France
Fax: +33477485108
EMail: frederick.gal@unie-st-etienne.fr

Garcia Solsona, E.
Universitat Autonoma de Barcelona (ICTA-UAB)
Facultat de Ciencies
08193 Bellaterra
Spain
Fax: +34935813331
EMail: esther.garcia@uab.es

Garnaga, G.
Marine Environment Laboratory
International Atomic Energy Agency
MC 98000 Monaco

Gastaud, J.
Marine Environment Laboratory
International Atomic Energy Agency
MC 98000 Monaco

Gelle, K.A.
Environmental Research & Wildlife Development Agency
P.O.Box 45553
Abu Dhabi
United Arab Emirates
Fax: +97126815010
EMail: kgelle@erwda.gov.ae

Genot, L.
Laboratoire de Radiochimie, Sciences Analytiques et Environnement
Université de Nice Sophia Antipolis
28 avenue de Valrose
F-06108 Nice Cedex 2
France
Fax: +33492076364
EMail: genot@unice.fr

Gerdes, A.
Department of Mineralogy
J.W. Goethe University
Senckenberganlage 28
D-60054 Frankfurt am Main
Germany
Fax: +496979828066
EMail: gerdes@em.uni-frankfurt.de

Gheorghiu, D.
National Institute for Physics and Nuclear Engineering "Horia Hulubei"
407 Atomistilor
R-077125 Magurele
Bucharest
Romania
Fax: +40214574440
EMail: dorina.gheorghiu@ifin.nipne.ro

Giani, M.
Central Institute for Scientific and Technological Research, ICRAM
Localita Brondolo (Chioggia)
I-30015 Venezia
Italy
Fax: +390415547897
EMail: m.giani@icram.org

Gibson, J.J.
Water & Climate Impacts Research Centre (WCIRC),
National Water Research Institute
c/o Department of Geography
University of Victoria
P.O. Box 3050
Victoria BC V8W 3P5
Canada
Fax: +12504725167
EMail: john.gibson@ec.gc.ca

Godoy, J.M.
Instituto de Radioprotecao e Dosimetria
Comissao de nacional de Energia Nuclear
Caixo Postal 37750
22780-160 Rio de Janeiro,
Brazil
Fax: +442392768150
EMail: jmgodoy@ird.gov.br

Godoy, M.L.
Instituto de Radioproteção e Dosimetria
Comissão de nacional de Energia Nuclear
Caixo Postal 37750
22780-160 Rio de Janeiro
Brazil
Fax: +552124421950
EMail: malu@ird.gov.br

Goktepe, B.G.
Adviser to the President
Head, Nuclear Information Branch
Eskisehir Yolu, 9 Km
06530 Ankara
Turkey
EMail: gul.goktepe@taek,gov.tr

Gooding, M.R.
DSTL Radiological Protection Services
Institute of Naval Medecine
Crescent Road
Alverstoke, Gosport PO12 2DL
United Kingdom
Fax: +442392768150
EMail: mrgooding@dstl.gov.uk

Grabowska, S.
The Henryk Niewoknicyanski Institute of Nuclear Physics
Radzikowskiego 152
31342 Kraków
Poland
Fax: +48126628458
EMail: sylwia.grabowska@ifi.edu.pl

Gungor, E.
Çekmece Nuclear Research and Training Centre
Health Physics Department
P.O. Box 1
Ataturk Airport, Istanbul
Turkey
Fax: +902125482230
EMail: emingungor@nukleer.gov.tr

Gungor, N.
Çekmece Nuclear Research and Training Center
P.O. Box 1
Atatürk Airport
TR-34149 Istanbul
Turkey
Fax: +902125482230
EMail: nurdangungor@hotmail.com

Gurriaran, R.
Institut de radioprotection et de sûreté nucléaire, IRSN
Bâtiment 501,
Bois des Rames
F-91400 Orsay
France
Fax: +33169855841
EMail: rodolfo.gurriaran@irsn.fr

Gutierrez, D.
Instituto del Mar de Peru
P.O. Box 22
Callao
Peru
EMail: dgutierrez@imarpe.gob.pe

Hadiasmoro, R.R.
The Agency for Marine and Fisheries Research
Jakarta
Indonesia

Haikin, N.
Israel AEC Nuclear Research Centre, NEGEV
P.O. Box 9001
Beer-Sheva 84190
Israel
Fax: +97286567690
EMail: nitsah@nrcn.org.il

Halim, Y.
Alexandria University
Faculty of Science
Department of Oceanography
Alexandria 21511
Egypt
Fax: +2035457611
EMail: youssefhalim@hotmail.com

Hamajima, Y.
Low Level Radioactivity Laboratoy
Kanazawa University
Wake, Tatsunokuchi
Nomi-gun
Ishikawa 923-1224
Japan
Fax: +81761515528
EMail: hama@cacheibm.s.kanazawa-u.ac.jp

Hamasaki, T.
Osaka Sangyo University
3-1-1 Nakagaito, daito-shi
Osaka 574-8530
Japan
Fax: +81728711259
EMail: hamasaki@due.osaka-sandai.ac.jp

Hamed, M.A.
National Centre for Nuclear Safety and Radiation Control
Egyptian Atomic Energy Authority
3 Ahmed El-Zomor Street, P.O. Box 7551
Nasr City, Cairo 11762
Egypt
Fax: +2022740238
EMail: mhamed754@yahoo.com

Hedouin, L.
Marine Environment Laboratory
International Atomic Energy Agency
MC 98000 Monaco

Heijnis, H.
Australian Nuclear Science and Technology Organisation
PMB 1
Menai NSW 2234
Australia
EMail: henk.heijnis@ansto.gov.au

Henderson-Sellers, A.
Environment Division
Australian Nuclear Science and Technology Organisation
PMB 1
Menai NSW 2234
Australia
EMail: ahssec@ansto.gov.au

Herut, B.
Israel Oceanographic & Limnological Research
Tel-Shikmona
P.O. Box 8030
31080 Haifa
Israel
Fax: +97248511911
EMail: barak@ocean.org.il

Heusser, G.
Max-Plank-Institut fuer Kernphysik
P.O. Box 10389
69029 Heidelberg
Germany
Fax: +496221516607
EMail: gerd.heusser@mpi-hd.mpg.de

Hintelmann, H.
Trent University
1600 West bank Drive
Department of Chemistry
Peterborough ON K9J 7B8
Canada
Fax: +7057481625
EMail: hhintelmann@trentu.ca

Hirose, K.
Meteorological Research Institute
Nagmine 1-1, Tsukuba
Ibaraki 3050052
Japan
Fax: +81298538728
EMail: khirose@mri.jma.go.jp

Holm, E.
Department of Medical Radiation Physics
Lund University Hospital
S-221 85 Lund
Sweden
Fax: +4646127249
EMail: elis.holm@radfys.lu.se

Homs, G.H.
Institut de Tecniques Energetiques
Universitat Politecnica de Catalunya
Etseib, Diagonal 647
08028 Barcelona
Spain
Fax: 34 93 4011749
EMail: GABRIEL.HOMS@UPC.ES

Honda, T.
Musashi Institute of Technology
Atomic Energy Research Laboratory
971 Ozenji, Asao-ku
Kawasaki-shi Kanagawa 215-0013
Japan
Fax: +81449556071
EMail: honda@atom.musashi-tech.ac.jp

Hong, G.H.
Korea Ocean Research and Devlopment Institute
Ansan P.O. Box 29
Kyonggi 425600
Korea Rep. of
Fax: +82314084493
EMail: ghhong@kordi.re.kr

Horvatincic, N.
Ruder Boskovic Institute
Bijenicka 54
P.O. Box 180
10002 Zagreb
Croatia
Fax: +38514680239
EMail: nada.horvatincic@irb.hr

Hult, M
EC-JRC-IRMM
Radionuclide Metrology
Retieseweg
B-2440 Geel
Belgium
Tel.: +32-14-571269
Fax.: +32-14-584273
EMail: mikael.hult@cec.eu.int

Huynh-Ngoc, L.
Marine Environment Laboratory
International Atomic Energy Agency
MC 98000 Monaco

Ichiyanagi, K.
Institute of Observational Reseach for Global Change
3173-25 Showa-machi Kanazawa-ku
Yokohama-city, Kanagawa 236-0001
Japan
Fax: +81457785706
EMail: kimpei@jamstec.go.jp

Idoeta, R.
Escuela de Ingenieros de Bilbao
Dto. Ing. Nuclear y Mec. De Fluidos
Urquijo, s/n
E-48013 Bilbao
Spain
Fax: +34946014159
EMail: inpidher@bi.ehu.es

Ikaheimonen, T.K.
Radiation and Nuclear Safety Authority (STUK)
P.O. Box 14
00881 Helsinki
Finland
Fax: +358975988589
EMail: taria.ikaheimonen@stuk.fi

Ikeuchi, Y.
Japan Chemical Analysis Center
295-3 Sanno-cho, Inage-ku
Chiba-shi
Chiba 263-0002
Japan
Fax: +81434235326
EMail: y-ikeuchi@jcac.or.jp

Ilus, E.
Radiation and Nuclear Safety Authority (STUK)
P.O. Box 14
00881 Helsinki
Finland
Fax: +358975988589
EMail: erkki.ilus@stuk.fi

Iosjpe, M.
Norwegian Radiation Protection Authority
Grini Naeringspark 13
P.O. Box 55
N-1332 Østerås
Norway
Fax: +4767147407
EMail: mikhail.iosjpe@nrpa.no

Jeandel, C.
LEGOS
Observatoire Midi-Pyrenees
14 avenue Edouard Belin
31400 Toulouse
France
Fax: +33561253205
EMail: catherine.jeandel@cnes.fr

Jeffree, R.
Marine Environment Laboratory
International Atomic Energy Agency
MC 98000 Monaco

Jerez Vegueria, S.
Universidade Federal Fluminese (UFF)
Instituto de Quimica,
Departameno de Quimica Analitica outeiro de Sao Joao
R Batista
Rio de Janeiro
Brazil
Fax: +552131141314; +552126292143
EMail: sfjerez@rdc.puc-rio.br

Jia, G.
APAT
National Environmental Protection Agency
Via Castel Romano, 100
I-00128 Roma
Italy
Fax: +39065050519
EMail: jia@apat.it

Jordan, N.
Laboratorire de Radiochime, Sciences Analytiques et Environment
Faculté des Sciences
28 avenue Valrose
F- 06108 Nice
France
Fax: +33492076364
EMail: jordan@unice.fr

Jull, A.J.T.
The University of Arizona
Physics Department
1118 East Fourth Street
PAS 81, Room 236
Tucson, AZ 85721
United States of America
Fax: +15206219619
EMail: jull@email.arizona.edu

Kaberi, H.
Hellenic Centre for Marine Research
P.O. Box 712
GR-19013 Anavyssos
Greece
Fax: +302291076347
EMail: ekaberi@ath.hcmr.gr

Karcher, M.J.
Alfred- Wegener-Institute for Polar and Marine Research
Columbusstrasse
D-27515 Bremerhaven
Germany
Fax: +4947148311797
EMail: mkarcher@awi-bremerhaven.de

Kasatkina, N.
Murmansk Marine Biological Institute
Kola Scientific Centre
Russian Academy of Sciences
17 Vladimirskaya St
183010 Murmansk
Russian Federation
Fax: +78152253994
EMail: icd@mmbi.info

Kedhi, M.
Institute of Nuclear Physics
P.O. Box 85
Tirana
Albania
Fax: +3554362596
EMail: mkedhi@sanx.net

Kehagia, K.K.
Greek Atomic Energy Commission
P.O. Box 60092
GR-153 10 Aghia Paraskevi
Attiki
Greece
Fax: +302106506748
EMail: kkehagia@eeae.gr

Kendall, C.
U.S. Geological Survey
345 Middlefield Road
MS 434 Menlo Park
California 94025
United States of America
Fax: +16503295590
EMail: ckendall@usgs.gov

Kershaw, P.J.
The Centre for Environment, Fisheries and Aquaculture Science
Pakefield Road
Lowestoft, Suffolk NR33 0HT
United Kingdom
Fax: +441502524546
EMail: p.j.kershaw@cefas.co.uk

Key, R.M.
Atmosheric and Oceanic Science Program
Princeton University
Forestal Campus
Princeton, NJ 8544
United States of America
Fax: +16092582850
EMail: key@princeton.edu

Kieser, W.E.
IsoTrace Laboratory
University of Toronto
60 Saint-George Street
Toronto, Ontario, M5S 1A7
Canada
Fax: +14169784711
EMail: liam.kieser@utoronto.ca

Kim, B-K.
Department of Technical Co-operaion
International Atomic Energy Agency
P.O. Box 100, A-1400 Vienna
Austria
Fax: +43126007
EMail: b-k.kim@iaea.org

Kim, C.K.
Seibersdorf Laboratories
Department of Nuclear Sciences and Applications
2444 Seibersdorf
Austria

Kim, C-S.
Korea Institute of Nuclear Safety
19 Kusung-Dong, Yusong-ku
Taejon 305-338
Korea Rep. of
Fax: +82428619945
EMail: cskim@kins.re.kr

Kim, G-B.
School of Earth and Environmental Sciences
Seoul National University
NS80 Shinlim-dong, Kwanak-gu
Seoul 151-742
Korea Rep. of
Fax: +8228766508
EMail: gkim@snu.ac.kr

Kits, J.
Eurostandard CZ Ltd.
Radiova 1
10200 Prague 10
Czech Republic
Fax: +420266029499
EMail: kits@eurostandard.cz

Knoeller, K.
Department of Isotope Hydrology
UFZ - Centre for Environmental Research
Theodor-Lieser-Strasse 4
D-06120 Halle/Saale
Germany
Fax: +493455585559
EMail: kay.knoeller@.ufz.de

Koehler, M.
VKTA
Verein fuer
Kernverfahrenstechnik und
Analytik Rossendorf e.V.
PF 510119
01314 Dresden
Germany
Fax: +493512603190
EMail: koehler@vkta.de

Kolstad, A.K.
Norwegian Radiation Protection Authority
Grini Naeringspark 13
P.O. Box 55
N-1332 Østerås
Norway
Fax: +4767147407
EMail: trine.kolstad@nrpa.no

Komura, K.	Low Level Radioactivity Laboratory Kanazawa University Wake, Tatsunokuchi, Nomi-gun Ishikawa 923-1224 Japan Fax: +81761515528 EMail: komura@yu.incl.ne.jp
Kondo, M.	Institute for Basin Ecosystem Studies Gifu University 1-1 Yanagido 501-1193 Gifu Japan Fax: +81582932062 EMail: k-miyuki@green.gifu-u.ac.jp
Kontar, E.A.	P.P.Shirshov Institute of Oceanology 36 Nakhimovskty Prospekt Moscow 117851 Russian Federation Fax: +7951245983 EMail: ekontar@ocean.fsu.edu
Korschinek, G.	Fachbereich Physik E15 Technische Universität München G-85748 Garching Germany Fax: +498928914280 EMail: korschin@ph.tum.de
Kortelainen, N.M.	Geological Survey of Finland P.O. Box 96 02151 Espoo Finland Fax: +3582055012 EMail: nina.kortelainen@gsf.fi
Kos'yan, R.	The Southern Branch of the P.P. Shirshov Institute of Oceanology Russian Academy of Sciences Bluebay RU-353467 Gelendzhik-7 Russian Federation Fax: +78614128089 EMail: kosyan@sdios.coast.ru
Kreuzer, A.	Institute for Environmental Physics im Neuenheimer Feld 229 D-69120 Heidelberg Germany Fax: +496221546405 EMail: andreas.kreuzer@iup.uni-heidelberg.de

Krom, M.D.
University of Leeds
School of Earth and Environment
Leeds LS2 9JT
United Kingdom
Fax: +441133433167
EMail: m.d.krom@earth.leeds.ac.uk

Kryshev, A.I.
Scientific and Production Association "Typhoon"
82 Lenin Avenue
RU-249038 Obninsk
Kaluga Region
Russian Federation
Fax: +70843940910
EMail: ecomod@obninsk.com

Kryshev, I.I.
Scientific and Production Association "Typhoon"
82 Lenin Avenue
RU-249038 Obninsk
Kaluga Region
Russian Federation
Fax: +70843940910
EMail: ecomod@obninsk.com

Kutschera, W.
Institute for Isotope Research and Nuclear Physics
University of Vienna
Währingerstrasse 17
A-1090 Vienna
Austria
Fax: +43142779517
EMail: walter.kutschera@univie.ac.at

Lacorte, S.
IIQAB-CSIC
Jordi Girona 18-26
E-08034 Barcelona
Spain
Fax: +34932045904
EMail: slbqam@cid.csic.es

Landwehr, J.M.
U.S. Geological Survey
National Center MS431
12201 Sunrise Valley Drive
Reston, VA 20192
United States of America
Fax: +17036485274
EMail: jmlandwe@usgs.gov

Lascaratos, A.
University of Athens
Department of Applied Physics
University Campus, Bld PHYS-V
157 84 Athens,
Greece
Fax: +30210 7295 281

Laubenstein, M.	National Institute for Nuclear Physics S.S. 17/BIS KM 18,910 I-67010 Assergi (AQ) Italy Fax: +390862437570 EMail: Matthias.Laubenstein@lngs.infn.it
Lavrova, T.	Department of Monitoring of Radioactivity in the Environment Ukrainian Institute for Hydrometeorology 37, Prospekt Nauki 03028 Kiev Ukraine Fax: +330442655363; 2651130 EMail: lavrovat@yahoo.co.uk
Lee, M.H.	Korea Atomic Energy Research Institute Nuclear Environmental Reserch Division Taejon 305353 Korea Rep. of Fax: +82428611761 EMail: mhlee@kaeri.re.kr
Lee, S-H.	Marine Environment Laboratory International Atomic Energy Agency MC 98000 Monaco
Levy-Palomo, I.	Marine Environment Laboratory International Atomic Energy Agency MC 98000 Monaco
Liong Wee Kwong, L.	Marine Environment Laboratory International Atomic Energy Agency MC 98000 Monaco
Livingston, H.D.	Marine Environment Laboratory International Atomic Energy Agency MC 98000 Monaco
Llaurado, M.	Departement de Química Analítica Facultat de Química Universitat de Barcelona Diagonal 647, 3 Planta E-08028 Barcelona Spain Fax: +349340212333 EMail: montse.llaurado.@ub.edu
Lujanienė, G.	Institute of Physics Savanoriu Ave 231 2300 Vilnius Lithuania Fax: +37052602317 EMail: lujaniene@ar.fl.lt

Magand, O.
LGGE CNRS / UMR 5183
Domaine Universitaire 54
rue Moliere
BP 96
F-8402 Saint Martin d'Heres
France
Fax: +330476824201
EMail: magand@lgge.obs.ujf-grenoble.fr

Mantoura, R.F.C.
Marine Environment Laboratory
International Atomic Energy Agency
MC 98000 Monaco

Margineanu, R.M.
National Institute of R&D for Physics and Nuclear Engineering
"Horia Hulubei"
407 Atomistilor
R-077125 Magurele, jud. llfov
Romania
Fax: +40214574440
EMail: romulus@ifin.nipne.ro

Mashiatullah, A.
Radiation and Isotope Application Division
Pakistan Institute of Nuclear Science and Technology (PINSTECH)
Nilore, Islamabad
Pakistan
Fax: +92519290275
EMail: azhar@pinstech.org.pk

Masqué, P.
Universitat Autonoma de Barcelona (ICTA-UAB)
Facultat de Ciencies
08193 Bellaterra
Spain
Fax: +34935813331
EMail: pere.masque@uab.es

Masson, O.
IRSN-Cadarache
Bat. 153 / BP 3
13115 Saint Paul Lez Durance
France
Fax: +33442256373
EMail: olivier.masson@irsn.fr

Matishov, G.
Murmansk Marine Biological Institute
Vladimirskaja st. 17
RU-183010 Murmansk
Russian Federation
Fax: +78152253994
EMail: icd@mmbi.info

Mattila, J.K.
Radiation and Nuclear Safety Authority (STUK)
P.O. Box 14
00881 Helsinki
Finland
Fax: +358975988589
EMail: jukka.mattila@stuk.fi

Mayer, A.
IDPA-CNR
Istituto Per La Dinamiga Dei Processi Ambientali-Consiglio Nazionali Delle Ricerche
Via Mario Bianco, 9
Milano
Italy
EMail: Adriano.MayerAIDPA.CNR.IT

Mayer, B.
Department of Geology and Geophysics
University of Calgary
2500 University Drive NW
Calgary, Alberta T2N 1N4
Canada
Fax: +14032208514
EMail: bmayer@ucalgary.ca

Mazeika, J.
Institute of Geology & Geography
Sevcenkos 13
LT-2600 Vilnius
Lithuania
Fax: +37052104695
EMail: mazeika@geo.lt

McGuffie, K.
Department of Applied Physics
University of Technology Sydney
PO Box 123
Broadway NSW 2007
Australia
Fax: +61295142219
EMail: kendal.mcguffie@uts.edu.au

Meresová, J.
Water Research Institute
NABR. L. Svobodu 5
SK-81249 Bratislava 1
Slovakia
Fax: +421254418047
EMail: j.meresova@pobox.sk

Metian, M.
Marine Environment Laboratory
International Atomic Energy Agency
MC 98000 Monaco

Metzger-Terrazas, L.A.
SENAMHI
Jr. Cahuide, 785
Jesus Maria
Peru
EMail: lmetzger@senamhi.gob.pe

Michel, H.
Laboratoire de radiochimie, Sciences Analytiques, Environnement
Universite de Nice – Sophia Antipolis
28 Avenue Valrose
06108 Nice
France
Fax: +33492076364
EMail: hmichel@unice.fr

Michel, R.L.
U.S. Geological Survey
345 Middlefield Road
MS 434, Menlo Park, California 94025-3591
United States of America
Fax: +16503294547
EMail: rlmichel@usgs.gov

Mietelski, J.W.
The Henryk Niewoknicyanski Institute of Nuclear Physics
Radzikowskiego 152
31342 Kraków
Poland
Fax: +48126628458
EMail: jerzy.mietelski@ifi.edu.pl

Migeon, S.
Geosciences Marines
Port de la Darse
F-06230 Villefranche
France
Fax: +33492942610
EMail: migeon@geoazur.obs-vlfr.fr

Miljevic, N.M.
VINCA Institute of Nuclear Sciences
P.O. Box 522
11001 Belgrade
Serbia And Montenegro
Fax: +381114447207
EMail: emiljevi@rt270.vin.bg.ac.yu

Miquel, J-C.
Marine Environment Laboratory
International Atomic Energy Agency
MC 98000 Monaco

Miralles, J.
IRSN - DEI/SESURE/LERCM,
Base Ifremer
BP 330
83507 La Seyne / Mer
France
Fax: +334 91 30 44 16
EMail: jerome.miralles@ifremer.fr

Möbius, S.S.
Forschungszentrum Karlsruhe GmbH
Fortbildungzentrum für Technik und Umwelt (FTU)
Hermann von Helmholtz Platz 1
D-76344 Eggenstein-Leopoldshafen
Germany
Fax: +497247824857
EMail: siegurd.moebius@ftu.fzk.de

Molnár, M.
Institute of Nuclear Research of the Hungarian Academy of Sciences
Bem Tér 18/c
H-4026 Debrecen
Hungary
Fax: +3652416181
EMail: mmol@atomki.hu

Muñoz Caravaca, A.
Laboratorio de Vigilancia Radiológica Ambiental del Centro
AP. 5
CP 59350 C. Nuclear Cienfuegos
Cuba
Fax: +53432511889
EMail: alain@ceacgrn.perla.inf.cu

Muzuka, A.N.N.
Institute of Marine Sciences
University of Dar Es Salaam
P.O. Box 668
Zanzibar
United Republic of Tanzania
Fax: +255242233050
EMail: muzuka@ims.udsm.ac.tz

Mzoughi, N.
Institut National des Sciences et Technologies de la Mer
Laboratoire Milieu marin
28, rue 2 mars 1934
TN-2025 Salammbo
Tunisia
Fax: +21671732622
EMail: nadia.mzoughi@instm.rnrt.tn

Nakano, M.
Environmental Protection Section
Japan Nuclear Cycle Development Institute
4-33 Muramatsu, Tokai-mura
Naka-gun
Ibaraki 319-1194
Japan
Fax: +81292823838
EMail: mnakano@tokai.jnc.go.jp

Nalbandyan, A.
Center for Ecological Noosphere Studies
National Academy of Sciences
68 Abovian street
375025 Yerevan
Armenia
Fax: +3741580254
EMail: ecocentr@sci.am ; annagg@yahoo.com

Neumaier, S.
Physikalisch-Technische Bundesanstalt
Department 6.3
Radiation Protection Dosimetry
Bundesallee 100
D-38116 Braunschweig
Germany
Fax: +495315926262
EMail: stefan.neumaier@ptb.de

Nicolaou, G.
Demokritus University of Thrace
School of Engineering
Department of Electrical and Computer Engineering
Lab. of Nuclear Technology
12 Vas. Sofias Str. G-R67100 Xant
Greece
EMail: nicolaouee.duth.gr

Noble, J.
Isotope Applications Division HIRUP
Bhabha Atomic Research Centre
Trombay, Mumbai 400 085
India
Fax: +912225505151
EMail: noblej@magnum.barc.ernet.in

Noureddine, A.
Commissariat à l'énergie atomique
Centre de recherche nucléaire d'Alger
A 2, boulevard Frantz Fanon
B.P. 399
16000 Alger-gare
Algeria
Fax: +21321434280
EMail: noureddine_abdelkader@hotmail.com

Nuñez-Lagos, R.
University of Zaragoza
Departamento de FisicaTeorica
Faculdad de Ciencias
c/Pedro Cerbuna 12
E-50009 Zaragoza
Spain
Fax: +34976762483
EMail: nlagos@unizar.es

Ogrinc, N.
Jozef Stefan Institute
Jamova 39
SI-1000 Ljubljana
Slovenia
Fax: +38615885346
EMail: nives.ogrinc@ijs.si

Oh, J.R.
South Sea Institute, KORDI
391 Jangmok-Ri
Jangmok-Myon
Geoje
Gyungnam 656830
Korea Rep. of
Fax: +82556398689
EMail: jroh@kordi.re.kr

Omoto, K.
Department of Geography
College of Humanities and Sciences
Nihon University
25-40 Sakurajosui-3Chome
Setagaya-Ku
Tokyo 156-8550
Japan
Fax: +81353179429
EMail: omoto@chs.nihon-u.ac.jp

Onabid, M.A.
University of Glasgow
Department of Statistics
15 University Gardens
Glasgow
United Kingdom
Fax: +441413304814
EMail: mathias@stats.gla.ac.uk

Oregioni, B.
Marine Environment Laboratory
International Atomic Energy Agency
MC 98000 Monaco

Osvath, I.
Marine Environment Laboratory
International Atomic Energy Agency
MC 98000 Monaco

Owens, N.J.
Plymouth Marine Laboratory
Prospect Place
The Hoe
Plymouth, Devon
United Kingdom
EMail: njpo@pml.ac.uk

Paatero, J.P.
Finnish Meteorological Institute
Sahaajankatu 20E
00880 Helsinki
Finland
Fax: +358919295403
EMail: jussi.paatero@fmi.fi

Palcsu, L.
Institute of Nuclear Research of the Hungarian Academy of Sciences
Bem Tér 18/c
H-4026 Debrecen
Hungary
Fax: +3652416181
EMail: palcsu@atomki.hu

Papatryphonos, S.
Water Development Department
Ministry of Agriculture, Natural Resources and Environment
1409 Nicosia
Cyprus
Fax: +35722304539
EMail: spap@avacom.net

Papucci, C.
ENEA
Marine Environment Research Centre
Forte di Santa Teresa
Pozzuluolo di Lerici
19032 Lerici (La Spezia)
Italy
Fax: +390187978236
EMail: carlo.papucci@santateresa.enea.it

Petrov, I.I.
Institute for Reference Materials and Measurements
Joint Research Centre
European Commission
IRMM-JRC-EC
Retieseweg 111, 2440 Geel
Belgium
EMail: ivan.petrov@cec.eu.int

Pettersson, H.
Department of Radiation Physics
Linköping University Hospital
S-581 85 Linköping
Sweden
Fax: +4613222895
EMail: hakan.pettersson@lio.se

Pham, M.K.
Marine Environment Laboratory
International Atomic Energy Agency
MC 98000 Monaco

Plastino, W.
University of Roma Tre
Department of Physics
Via della Vasca Navale, 84
I-00146 Roma
Italy
Fax: +39065579303
EMail: plastino@fis.uniroma3.it

Porntepkasemsan, B.
Office of Atoms for Peace (OAEP)
16, Vibhavadi Rangsit Road
Chatuchak
Bangkok 10900
Thailand
Fax: +6625613013
EMail: boonsom@oaep.go.th

Povinec, P.
Marine Environment Laboratory
International Atomic Energy Agency
MC 98000 Monaco

Priller, A.
Institute for Isotope Research and Nuclear Physics
University of Vienna
Waehringer Str. 17
A-1090 Vienna
Austria
Fax: +43142779517

Privitera, A.M.G.
viale Benedetto Croche 50
95122 Catania - Sicily
Italy
EMail: agataprivitera@inwind.it

Quetel, C.R.
Institute for Reference Materials and Measurements
Joint Research Centre
European Commission
IRMM-JRC-EC
Retieseweg 111, 2440 Geel
Belgium
EMail: christophe.quetel@cec.eu.int

Raisbeck, G.
Centre de Spectrometrie Nucléaire et de Spetrometrie de Masse/IN2P3/CNRS
Bât 108
F-91405 Campus Orsay
France
Fax: 33169155268
EMail: raisbeck@csnsm.in2p3.fr

Ramadan, H.
Marine Environment Laboratory
International Atomic Energy Agency
MC 98000 Monaco

Rapaglia, J.
G1 Ridgeland Manor
Rye, New York 10580
United States of America
EMail: jrapagli@icsunysb.edu

Readman, J.
Plymouth Marine Laboratory
Prospect Place
The Hoe
PL1 3DH Plymouth
United Kingdom
Fax: +441752633101
EMail: jwre@pml.ac.uk

Reynaud, S.
Centre Scientifique de Monaco
c/o Musée océanographique
Avenue Saint-Martin
MC-98000 Monaco
Fax: +37792167981
EMail: sreynaud@centrescientifique.mc

Rezzoug, S.
Laboratoire de Radiochimie, Sciences Analytiques et Environnement
Université de Nice – Sophia Antipolis
28 avenue Valrose
F-06108 Nice
France
Fax: +33492076364
EMail: rezzoug@unice.fr

Risica, S.
Technology and Health Department
Istituto Superiore di Sanità
Viale Regina Elena 299
I-00161 Rome
Italy
Fax: +390649387075
EMail: serena@iss.it

Rodriguez Espinosa, P.F.
Goelogía y Radioquímica Marina
Centro de Investigación en Cienca Aplicada y Tecnología
Avanzada del Instituto Politecni Nacional
km. 14.5 Carretera Tampico
Puerto de Altamira Tamaulipas
89600 México
Mexico
Fax: +18332649302
EMail: prodrigueze@ipn.mx

Rodriguez y Baena, A.
Marine Environment Laboratory
International Atomic Energy Agency
MC 98000 Monaco

Roether, W.
University of Bremen
Bibliothekstrasse1
D-28359 Bremen
Germany
Fax: +494212187018
EMail: wroether@physik.uni-bremen.de

Rolland, B.
Institute for Radioprotection and Nuclear Safety
IRSN/DEI/SESURE/LERCM, BP 3
13115 St Paul Lez Durance
France
Fax: +33442256373
EMail: benoit.rolland@irsn.fr

Romero, M.L.
CIEMAT
Avda. Complutense 22
E-28040 Madrid
Spain
Fax: +34913466121
EMail: lourdes.romero@ciemat.es

Roos, P.
Risoe National Laboratory
Department of Radiation Research
NUK-204, P.O. Box 49
DK-4000 Roskilde
Denmark
EMail: per.roos@risoe.dk

Rudjord, A.L.
Norwegian Radiation Protection Authority
Grini Naeringspark
P.O. Box 55, N-1332 Østerås
Norway
Fax: +4767147407
EMail: anne.rudjord@nrpa.no

Rulik, P.
National Radiation Protection Institute
Srobaroba 48
10000 Prague
Czech Republic
EMail: petr.rulik@suro.cz

Ryu, Jae-Woong
School of Earth and Environmental Sciences
Seoul National University
NS80 Shinlim-dong, Kwanak-gu
Seoul 151-742
Korea Rep. of
Fax: +8228766508
EMail: gryu4506@snu.ac.kr

Saleh, I.H.
Institute of Graduate Studies and Research
Alexandria University
163 Horreya Avenue
P.O. Box 832, El-Shatby
Alexandria
Egypt
Fax: +2034285792
EMail: ihindawy@yahoo.com

Salih, A.
University of Sydney
Australian Key Centre for Microscopy & Microaalysis
Madsen Building FO9
Sydney NSW 2006
Australia
EMail: anya@emu.usyd.edu.au

Sanchez-Cabeza, J.A.
Marine Environment Laboratory
International Atomic Energy Agency
MC 98000 Monaco

Saxen, R.L.
Radiation and Nuclear Safety Authority (STUK)
P.O. Box 14
00881 Helsinki
Finland
Fax: +358975988589
EMail: ritva.saxen@stuk.fi

Schertz, M.
Laboratoire de Radiochemie, des Sciences Analytiques et de l'Environnement
Universite de Nice – Sophia Antipolis
28 Avenue Valrose
06108 Nice
France
EMail: schertz@unice.fr

Schlosser, P.
Lamont-Doherty Earth Observatory
Columbia University
61 Route 9W, P.O. Box 1000
Palisades, NY 10964
United States of America
Fax: +18453658176
EMail: schlosser@ldeo.columbia.edu

Schubert, M.
UFZ Centre for Environmental Research
Permoserstrasse 15
D-04318 Leipzig
Germany
Fax: +493412352002/2625
EMail: michael.schubert@ufz.de

Schwartz, F.
Department of Geological Sciences
The Ohio State University
125 South Oval Mall
Columbus, OH 431210
United States of America
Fax: +016142927688
EMail: schwartz.11@osu.edu

Scotto, P.
Marine Environment Laboratory
International Atomic Energy Agency
MC 98000 Monaco

Shima, S.
Mutsu Marine Laboratory
Japan Marine Science Foundation
4-24 Minato-machi, Mutsu-shi
Aomori 035-0084
Japan
Fax: +81175229112
EMail: hima@jmsfmml.or.jp

Shouakar-Stash, O.
University of Waterloo
Department of Earth Sciences
200 University of Waterloo
University Avenue West
Waterloo Ontario, N2L3G1
Canada
Fax: +15197467484
EMail: orfan@uwaterloo.ca

Sidhu, R.S.
Institute for Energy Technology
P.O.Box 40
N-2027 Kjeller
Norway
Fax: +4763812561
EMail: rajdeep.sidhu@ife.no

Sihra, K.
National Radiological Protection Board
Chilton, Didcot,
Oxon, OX11 ORQ
United Kingdom
Fax: +441235833891
EMail: kamaljit.sihra@nrpb.org

Skilbeck, G.
University of Technology of Sydney
Broadway
Sydney NSW 2006
Australia

Snell, J.P.
Institute for Reference Materials and Measurements
Joint Research Centre
European Commission
Retieseweg 111, 2440 Geel
Belgium
EMail: james.snell@cec.eu.int

Sonninen, E.
Radiocarbon Dating Laboratory
University of Helsinki
P.O. Box 64
FI-00014 Helsinki
Finland
Fax: +358919150741
EMail: eloni.sonninen@helsinki.fi

Standring, W.J.
Grini Naeringspark 13
The Norwegian Radiation Protection Authority
P.O. Box 55
N-1332 Østerås
Norway
Fax: +4767147407
EMail: william.standring@nrpa.no

Stiller, M.
5 Haem street
Rishon Le Zion 75240
Israel
Fax: +97239641159
EMail: stiller@alumni.technion.ac.il

Stolarz, A.
Institute for Reference Materials and Measurements
Joint Research Centre
European Commission
Retieseweg 111
B-2440 Geel
Belgium
Fax: +3214571863
EMail: anna.stolarz@cec.eu.int

Stralberg, E.
Institute for Energy Technology
P.O. Box 40
N-2027 Kjeller
Norway
Fax: +4763812561
EMail: elisas@ife.no

Sugahara, M.
Osaka Sangyo University
3-1-1 Nakagaito, daito-shi
Osaka 574-8530
Japan
Fax: +81728711259
EMail: sugahara@duc.osaka-sandai.ac.jp

Sunlu, U.
Ege University
Faculty of Fisheries
Department of Hydrobiology
TR-35100 Bornova-Izmir
Turkey
Fax: +902323883685
EMail: sunlu@sufak.ege.edu.tr

Suzuki, T.
Japan Atomic Energy Research Institute
4-24 Minato-Machi
Mutsu, Aomori
Japan
Fax: +81175224213
EMail: iodine@popsvr.tokai.jaeri.go.jp

Svaeren, I.
Institute of Marine Research
P.O. Box 1870 Nordnes
N-5817 Bergen
Norway
Fax: +4755238584
EMail: ingrid.svaeren@imr.no

Szymczak, R.
Australian Nuclear Science and Technology Organisation
Private Mail Bag No.1
Menai, NSW 2234
Australia
EMail: rsx@ansto.gov.au

Tateda, Y.
Environmental Science Research Laboratory
Central Research Institute of Electric Power Industry
1646 Abiko, Abiko-shi
Chiba 270-1194
Japan
Fax: +81471827922
EMail: tateda@criepi.denken.or.jp

Teyssie, J-L.
Marine Environment Laboratory
International Atomic Energy Agency
MC 98000 Monaco

Thingstad, F.
Department of Microbiology
University of Bergen
Jahnebk, 5
N-5020 Bergen
Norway
Fax: +4755589671
EMail: freed.thingstad@im.uib.no

Thorring, H
Norwegian Radiation Protection Authority
P.O. Box 55
N-1332 Østerås
Norway
Fax: +4767147407
EMail: havard.thorring@nrpa.no

Tolosa Bertral, I.
Marine Environment Laboratory
International Atomic Energy Agency
MC 98000 Monaco

Toole, J.
UKAEA
Building D2003/10
Dounreay, Thurso
Caithness KW14 7TZ
United Kingdom
Fax: +441847806901
EMail: joe.toole@ukaea.org.uk

Tsabaris, C.
Hellenic Centre for Marine Research
P.O. Box 712
GR-19013 Anavyssos
Greece
Fax: +302291076323
EMail: tsabaris@ncmr.gr

Tyler, A.N.
School of Biological and Environmental Sciences
University of Stirling
Stirling, FK9 4LA
United Kingdom
Fax: +441786467843
EMail: a.n.tyler@stir.ac.uk

Ugur, A.
Ege University
Institute of Nuclear Sciences
TR-35100 Bornova-Izmir
Turkey
Fax: +902323886466
EMail: aysun@bornova.ege.edu.tr

Umbara, H.
Radioactive Waste Management Development Center
National Nuclear Energy Agency
Kawasan Puspiptek,
Serpong Tangerang 15310
Indonesia
Fax: +62217560927
EMail: umbara@batan.go.id

Vallés, I.
Institut de Tècniques Energètiques
Universitat Politècnica de Catalunya
Etseib, Diagonal 647
E-08028 Barcelona
Spain
Fax: +34934017149
EMail: isabel.valles@upc.es

Vas, D.
Marine Environment Laboratory
International Atomic Energy Agency
MC 98000 Monaco

Verplancke, J.M.A.
Canberra Semiconductor N.V.
Lammerdries 25
B-2250 Olen
Belgium
Fax: +3214221991
EMail: jverplancke@canberra.com

Vesnovskii, P.
All Russian Scientific Research Institute for Experimental Physics
37 Mira Street
Sarov
607190 Nizhni Novgorod Region
Russian Federation
Fax: +78313045569
EMail: vesnovskii@expd.vniief.ru

Villeneuve, J-P.
Marine Environment Laboratory
International Atomic Energy Agency
MC 98000 Monaco

Vives i Batlle, J.
Westlakes Scientific Consulting
The Princess Royal Building
Westlakes Science and
Technology Park
Moor Row, Cumbria CA24 3LN
United Kingdom
Fax: +441946514091
EMail: jordi.vives@westlakes.ac.uk

Voitsekhovitch, O.
Department of Monitoring of Radioactivity in the Environment
Ukrainian Institute for Hydrometeorology
37, Prospekt Nauki
03028 Kiev
Ukraine
Fax: +380442655363
EMail: voitsekh@voi.vedos.kiev.ua

Warnau, M.
Marine Environment Laboratory
International Atomic Energy Agency
MC 98000 Monaco

Weinstein, Y.
Department of Geography
Bar-Ilan University
52900 Ramat-Gan
Israel
Fax: +97235344430
EMail: weinsty@mail.biu.ac.il

Wellum, R.
Institute for Reference Materials and Measurements
Joint Research Centre
European Commission
Retieseweg 100
B-2440 Geel
Belgium
Fax: +3214571863
EMail: roger.wellum@cec.eu-int

Whitehead, N.E.	Whitehead Associates 54, Redvers Drive Lower Hutt 6009 New Zealand Fax: +6445650263 EMail: whiteh@paradise.net.nz
Witek-McManus, M.C.	DM Technology Ltd. 17 Spinney Way Cudham Kent TN14 704 United Kingdom EMail: moira.mcmanus@dmtechnology.co.uk
Wyse, E.	Marine Environment Laboratory International Atomic Energy Agency MC-98000 Monaco
Yoshida, N.	Tokyo Institute of Technology Frontier Collaborative Research Center 4259, Nagatsuta, Midori-ku Yokohama 226-8502 Japan Fax: +81459245506 EMail: naoyoshi@depe.titech.ac.jp
Yoshimura, K.	Institute of Industrial Science University of Tokyo 4-6-1 Komaba, Meguro-ku Tokyo 153-8505 Japan Fax: +81354526383 EMail: kei@iis.u-tokyo.ac.jp
Zhukova, O.M.	The Republican Centre of Radiation Control and Environment Monitoring 110 A Skorina Av. 220023 Minsk Belarus Fax: +375172639562 EMail: us206@zad.by.mecom.ru
Zubachenko, V.L.	Crimean State Scientific & Research Center of Standardization, Metrology and Certification Krymskaya Pravda str. 61 Simferopol 25000 Crimea Ukraine Fax: +380652446961 EMail: standart@mail.strace.net

INTERNATIONAL ATOMIC ENERGY AGENCY
VIENNA
ISBN 92–0–111205–X
ISSN 1563–0153